

RPP-ENV-58782, Rev. 0

6.0 ANALYSIS OF PERFORMANCE

This PA provides an assessment of the long-term human health impacts following the closure of the WMA C facility in the 200 East Area of the Hanford Site. This section provides an overview of the methodology developed to assess the scenarios and pathways and describes the conceptual models of facility performance and the development and implementation of the mathematical models used to estimate the impacts from the proposed closure action. It also integrates the information presented in earlier sections that forms the basis for the conceptual and mathematical model of the WMA C facility following closure. The information related to the analysis and modeling approach is presented in the following subsections:

- 6.1 Overview of Analysis
- 6.2 Conceptual Model of Facility Performance
- 6.3 Mathematical Models
- 6.4 Model Validation.

6.1 OVERVIEW OF ANALYSIS

The method of analysis used to assess the long-term performance of WMA C is briefly described in this section, with more detailed information presented in later sections. The analysis incorporates key elements of the disposal system called *safety functions* that are deemed important in assessing the system performance. The safety concept of the closed tank farm is that various features of the closed facility have specific attributes that contribute to the ability of the system to meet performance objectives. These attributes are called *safety functions* in this PA. Safety functions are identified from basic understanding of the projected behavior of the system in the post-closure period. These safety functions and their behavior are used to identify specific analysis cases that show the robustness and defense-in-depth of the closed facility.

Facility performance is defined in terms of the onsite and offsite exposures and doses from radionuclides that may be inadvertently contacted and/or that might migrate from the disposal facility. All of the calculated exposures in the PA are hypothetical, and depend on a future member of the public engaging in activities on the Central Plateau without knowledge of the prior existence of the Hanford Site and its disposal activities. Exposure calculated in this way is higher and occurs at earlier times than potential exposures off the Hanford Site, and therefore provides a more stringent set of exposure conditions than potential offsite exposures.

The various pathways of potential exposure are illustrated in Figure 6-1. The most important exposure pathway for hydrologic transport is groundwater use for drinking water, irrigation, livestock watering, and biotic transport. In the groundwater pathway, the analysis is focused on meteoric water from rain and snowfall, which enters the subsurface, contacts contaminants that have diffused from the grouted residual waste, and carries these contaminants to the unconfined aquifer. The surface water pathway is omitted from this PA because surface water does not exist within the 100 m (328 ft) point of analysis distance from the WMA C boundary. Potential atmospheric exposures are included as a separate analysis; however, their impact is expected to be limited because only a few radionuclides (e.g., tritium, ^{14}C , ^{129}I , and ^{222}Rn) that are present in

RPP-ENV-58782, Rev. 0

the residual waste inventory can partition into the gas phase. As a result, the main focus of this PA is on evaluating the groundwater pathway.

The analysis of the groundwater pathway comprises evaluations directed at two different performance objectives. The first is an all-pathway dose contribution to a hypothetical receptor that consumes contaminated groundwater, leafy vegetables and produce that were irrigated with contaminated groundwater, and milk and meat from animals that consume contaminated water and pasture grass irrigated with contaminated groundwater. The second is a groundwater protection performance objective, which limits concentrations in groundwater, regardless of use or potential exposure by humans.

The strategy for the WMA C PA is to define and analyze both a base case and a suite of sensitivity and uncertainty cases. The base case is a single deterministic evaluation of future dose to the public as a result of the anticipated retrieval and closure actions taken at WMA C. It represents the scenario in which the safety functions behave as expected as the facility evolves into the future. The base case assumptions and parameters generally are based on best available information, but some parameter estimates related to future conditions may have a conservative bias. The results of the base case are used to evaluate compliance with the DOE O 435.1 all-pathways performance objectives. Additional sensitivity cases and uncertainty analyses were defined to explore the effect of uncertainties in the models, assumptions, and parameter ranges. The sensitivity cases were defined to evaluate the consequences associated with either the full or partial loss of a safety function. In this way, the PA is specifically structured to evaluate the key elements of the disposal system that contribute to its long-term safety. Uncertainty analyses were conducted to evaluate the effect of parameter uncertainty on potential exposures. The uncertainty analyses were undertaken using an abstraction model so that a large number of analyses can be performed within a limited time.

Confidence in the data, assumptions, and methods used in the analysis was developed through the following approaches.

- Many data were based on WMA C-specific site characterization, sampling, measurements and interpretations, including those for contaminant inventory, geology, hydrology and geochemistry. When data specific to WMA C were not available, data from nearby sites, such as vadose zone hydraulic property data and information developed from soil samples collected in the vicinity of the IDF or comparable conditions, as well as data reported in the literature, were used.
- Data were upscaled to represent field-scale processes using scientifically-accepted approaches that have been published in peer-reviewed journals. Upscaling techniques use information from small, core-scale measurements to develop parameters that are applicable to large, field-scale models.
- The process-based modeling software, STOMP[®] code (PNNL-12030, “STOMP Subsurface Transport Over Multiple Phases Version 2.0 Theory Guide”; Pacific Northwest National Laboratory, Queried 12/18/2015, [STOMP User Guide], http://stomp.pnnl.gov/user_guide/STOMP_guide.stm; PNNL-11216, “STOMP

RPP-ENV-58782, Rev. 0

Subsurface Transport Over Multiple Phases Application Guide”), has been benchmarked and deemed suitable for use in this PA. The STOMP[®] code is the pre-authorized modeling software at the Hanford Site for vadose zone and near-field groundwater modeling (Internal memorandum 1301789, “Modeling to Support Regulatory Decisionmaking at Hanford”). The STOMP[®] code has previously been qualified for simulation use at Hanford by CH2M HILL Plateau Remediation Company (CHPRC) (CHPRC-00269, “STOMP Requirements Traceability Matrix CHPRC Build 4”).

- The system-level modeling software, GoldSim[®] (“GoldSim Contaminant Transport Module User’s Guide” [GoldSim Technology Group 2014a]; “GoldSim Distributed Processing Module User’s Guide” [GoldSim Technology Group 2014b]; “GoldSim Probabilistic Simulation Environment User’s Guide” [GoldSim Technology Group 2014c]), has been deemed suitable based on its wide usage and acceptance in the various PAs across the DOE complex. GoldSim[®] was the principal code used for systems-level and uncertainty analysis modeling in this PA effort. The GoldSim[®] software is an example of additional simulation software that may be used at Hanford as long as DOE and Environmental Management software quality requirements are met.
- Sensitivity and uncertainty analyses were conducted to evaluate the effect of parameter uncertainties and alternative conceptual models on the overall performance of the system.

Results using the models and values are presented in Section 7.0 for the groundwater and air-pathway scenarios and in Section 8.0 for intruder scenarios. Section 9.0 also presents the comparison to performance objectives.

6.2 CONCEPTUAL MODEL OF FACILITY PERFORMANCE

The WMA C PA methodology uses conceptual models that are based on the physical system and expected contaminant migration pathways. Figure 6-2 provides a schematic representation of both WMA C at closure and the contaminant migration into the environment along the various pathways evaluated in this PA. The WMA C site is composed of both man-made and natural components. The man-made components of the system that influence contaminant migration include a closure surface barrier, the WMA C tanks, pipelines, and infrastructure, and the distribution of waste in those components. The natural components of the system that influence contaminant migration are a number of mostly horizontal to slightly dipping (to the northeast) stratigraphic layers within the saturated and unsaturated zones, net infiltration resulting from rainfall, and any antecedent moisture conditions (and contaminants) within WMA C or from adjacent sites. For the base case, Figure 6-3 illustrates the major stratigraphic units for the WMA C site that form a thick vadose zone ranging from 75 to 85 m (246 to 280 ft) thick. The water table is located within the undifferentiated Hanford formation and Cold Creek gravels with a predominantly south/southeastwardly groundwater flow.

Figure 6-4 shows an aerial view of WMA C, and surrounding disturbed, undisturbed, and resurfaced areas. Also shown is the location of A Complex, where the 100 m (328 ft) point of analysis downgradient of WMA C is located. This location represents the assumed location of a

RPP-ENV-58782, Rev. 0

hypothetical well that supplies water for drinking and irrigation in the all-pathway dose scenario calculations.

Several key safety functions and related FEPs characterize the conceptual models for release and transport of radionuclides in WMA C and are discussed in Appendix H (Safety Functions and Features, Events, and Processes) for the post-closure period. The conceptual models and relevant parameters for fate and transport modeling are developed for the following four time periods:

- Pre-operations and initial construction period (before 1945) representing the time when the tank farm ground remained undisturbed from the Hanford Manhattan Project mission
- Operations period representing tank farm construction, current, and immediate future conditions of the tank farm (1945 to 2020)
- Closure and post-closure period during the assumed design life of the intact surface barrier (2020 to 2520) when the tanks become grouted and radionuclides begin to diffuse out of the grout
- Post-closure period beyond assumed design life of the surface barrier (2520 to 12120) when the performance of the surface barrier is assumed to degrade.

A 1,000-year post-closure period is considered in the WMA C PA for the purpose of evaluating compliance with DOE O 435.1 performance objectives; a 10,000-year post-closure period is considered for the purpose of evaluating uncertainty in the results because of the slow travel time through the vadose zone under post-closure conditions. Peak concentrations for many of the radionuclides evaluated occur between 1,000 and 10,000 years.

In the WMA C PA analysis, net infiltration is controlled by the Modified RCRA Subtitle C barrier. This barrier has a design life of 500 years, and this time period is used in the base case. However, the surface barrier may potentially last longer or shorter than the design life, depending on how the site evolves in the post-closure period. Sensitivity analysis cases evaluate alternative future behavior patterns in the infiltration rate due to uncertainty in the design life. Contact of infiltrating water with the residual waste is also limited by the tank structure, by the grout infill, and by the tank shell. There is substantial uncertainty about how long the tank wall may last before physical and chemical degradation occurs and allows water to flow through it. However, the tank structure and infill grout together will form a low-permeability barrier to flow. Evaluations of the durability of this material and the longevity of its function to reduce water flow indicate very long lifetimes for the cementitious features of the tanks, such that they produce very low flow rates through the residual wastes for more than 10,000 years (see Section 6.2.1.2, Evaluation of Tank Stability). Under these conditions, releases from the residual wastes only occur by diffusion through the base mat and into the vadose zone below the tanks. Sensitivity analyses evaluate alternative conditions when advective releases occur at earlier times.

Figure 6-1. Overview of the Dose Calculations for Exposure Along the Groundwater Pathway and Air Pathway for the Waste Management Area C Performance Assessment.

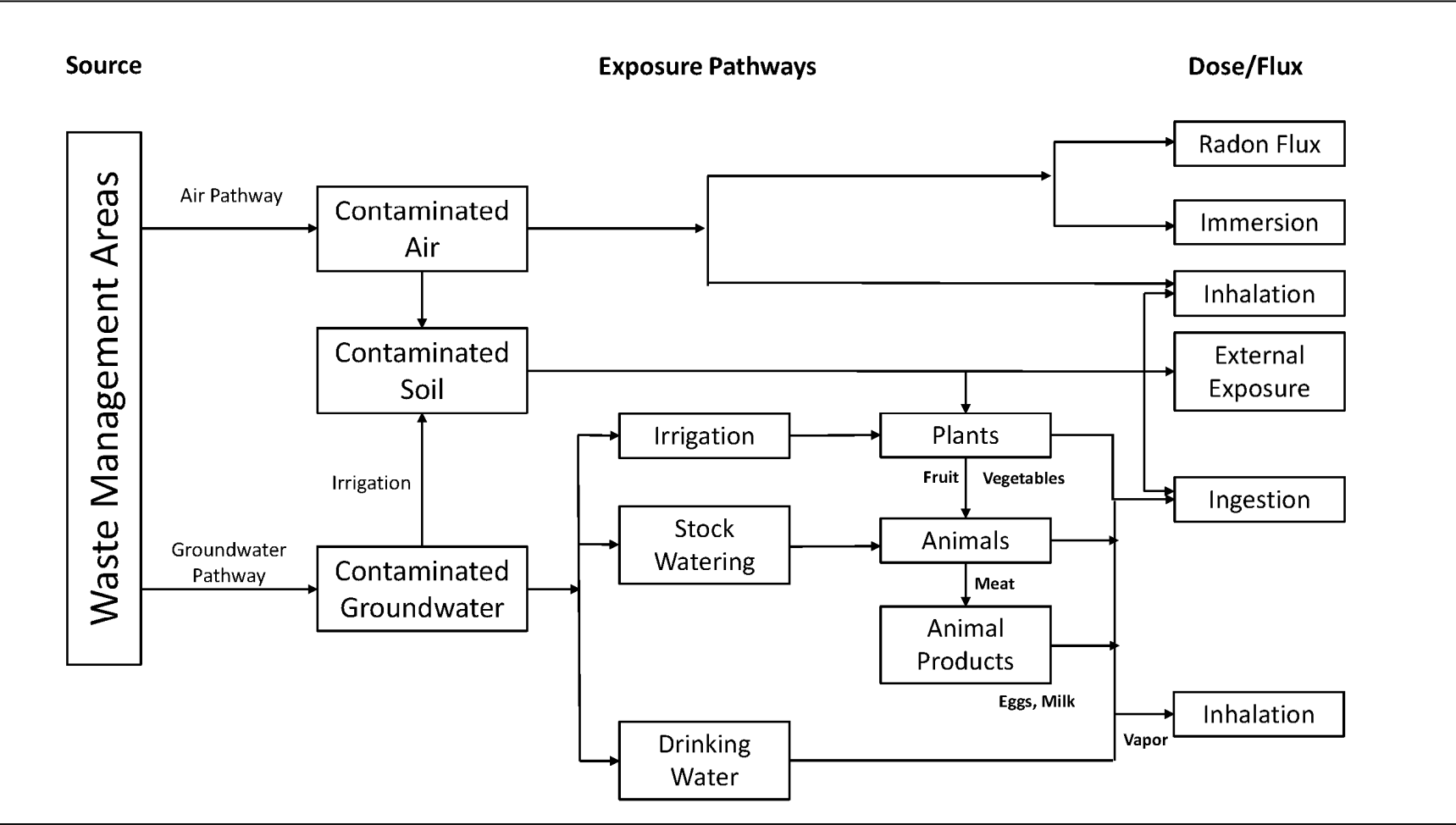
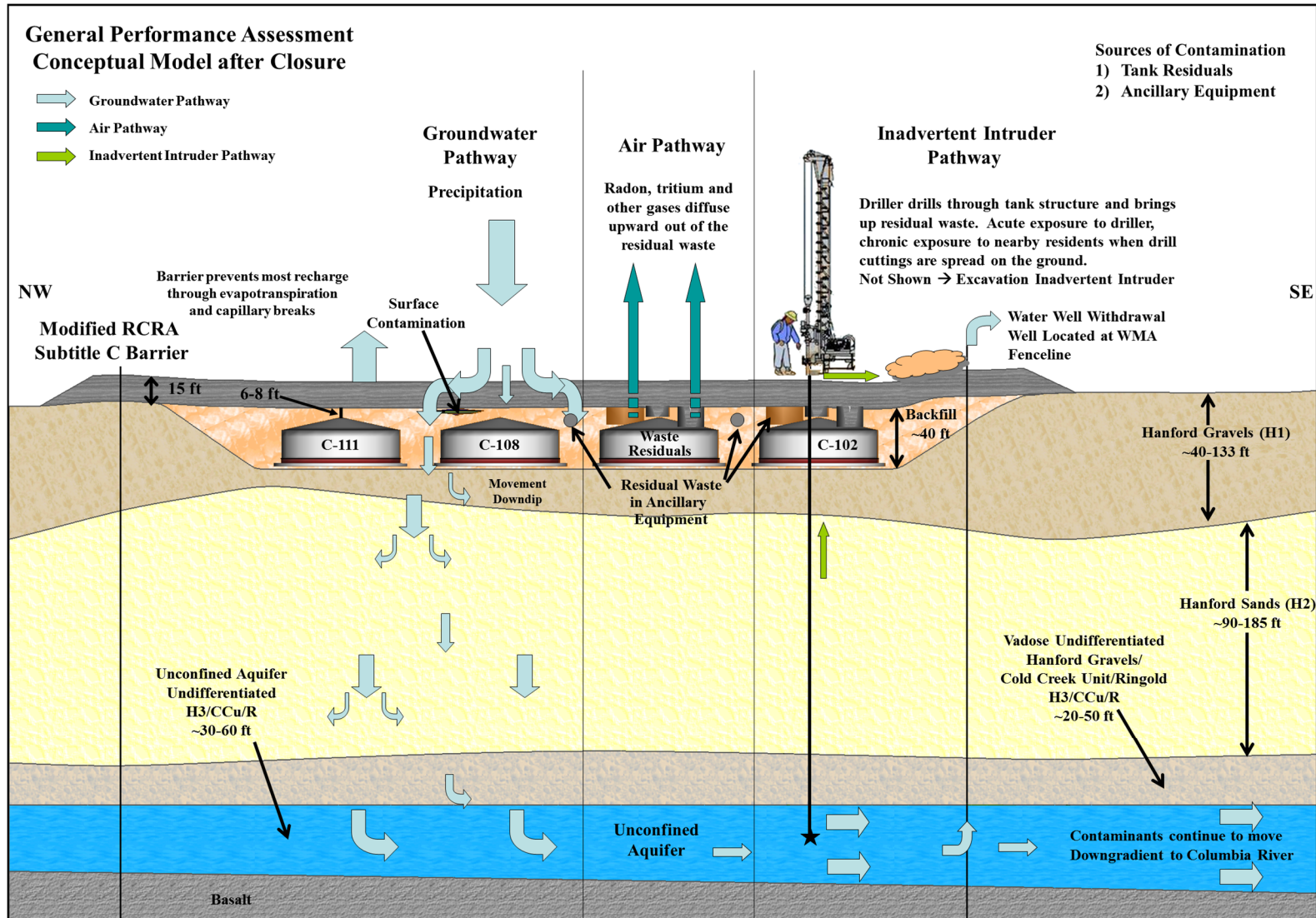


Figure 6-2. Schematic Conceptual Representation of Waste Management Area C and Contaminant Migration into the Environment along the Various Pathways Evaluated in the Performance Assessment.



RCRA = Resource Conservation and Recovery Act of 1976

WMA = Waste Management Area

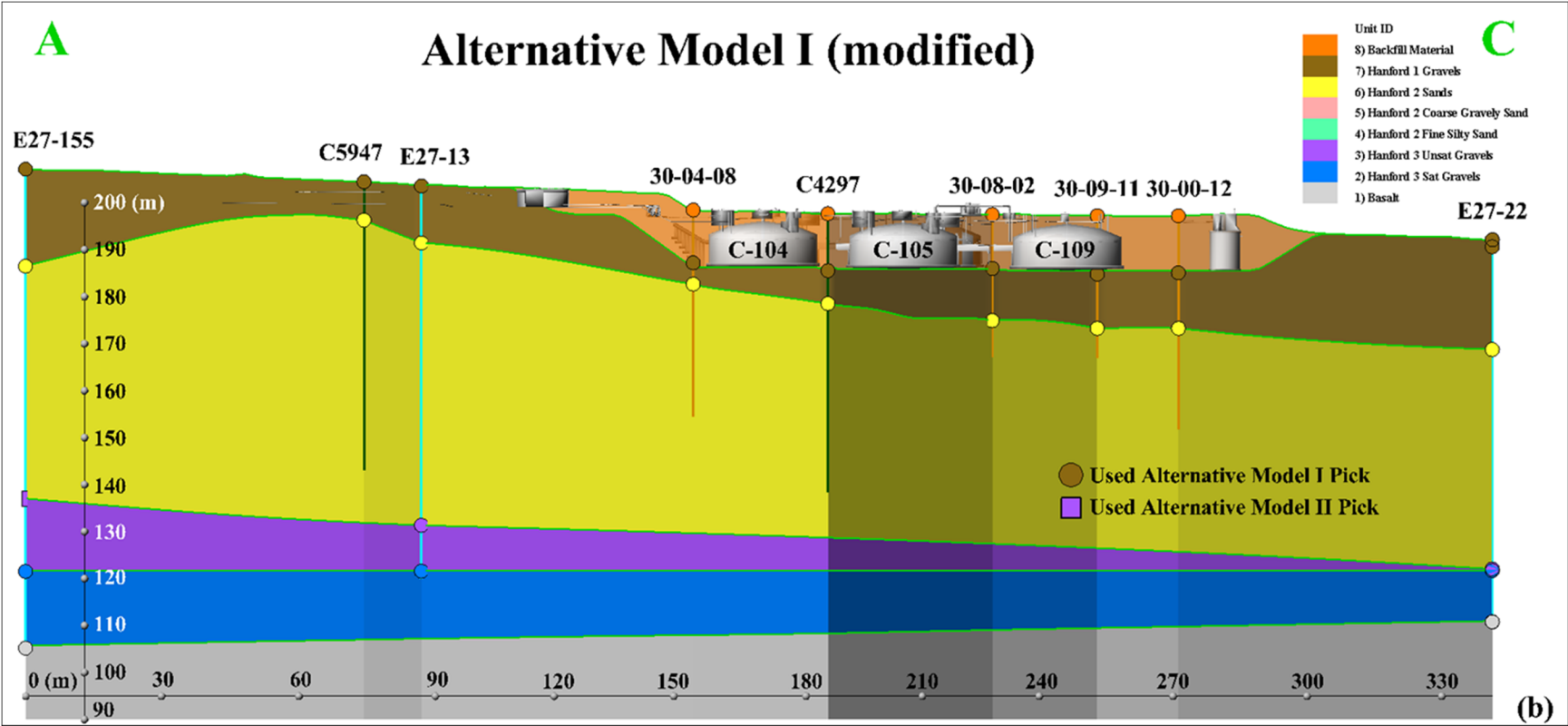
Figure 6-3. Conceptual Model of the Waste Management Area C Site Showing Stratigraphy.

1
2
3
4

6-7

5
6

RPP-ENV-58782, Rev. 0



RPP-ENV-58782, Rev. 0

Figure 6-4. Aerial View of Waste Management Area C Showing Surface Features and the Surrounding Area.



WMA = Waste Management Area

RPP-ENV-58782, Rev. 0

For WMA C vadose zone modeling, small-scale laboratory measurements provide the basis for hydraulic properties used to predict the large, field-scale flow behavior (Appendix B). Each heterogeneous geologic unit is replaced by an equivalent homogeneous medium (EHM) with macroscopic flow properties. With each heterogeneous unit assigned its upscaled or effective hydraulic properties, the simulated flow fields predict the bulk or mean flow behavior at the field scale. Upscaling, in effect, accounts for the differences in scale between small, core-scale measurements and large, field-scale modeling. The radionuclides travel through the vadose zone until they reach the water table and the unconfined aquifer. The unconfined aquifer is also treated as an EHM, and an equivalent saturated hydraulic conductivity is estimated for the undifferentiated Hanford gravels and CCU sediments (Appendix C). In the final step of the analysis, the exposure scenario dose conversion factors are applied to the estimated groundwater concentrations at a 100 m (328 ft) downgradient location to determine total equivalent dose.

6.2.1 Source Term and Engineered Features

The source term considers processes associated with release of contaminants from residual waste into the natural environment. Separate source terms are considered for each of the twelve 100-series tanks, four 200-series tanks, C-301 catch tank, 244-CR vault, and pipelines, resulting in 19 separate source terms. The inventory used in the source term model includes the current estimate of the inventory and residual volume (Tables 3-13 through 3-15). Source terms for pits and diversion boxes are not explicitly considered but are incorporated as part of the pipeline source term.

Both mineral phase solubility-limited and matrix degradation rate-limited processes are considered for release of contaminant from the waste. These conceptual models are based on observations made through multi-year leaching tests and identification of mineral phases as presented in Section 5. The following release mechanisms are considered based on experimental results:

- a matrix-degradation-rate-based release of ^{99}Tc , and
- solubility-controlled releases of uranium.

The engineered features that are considered in the source term calculations are the tank structure, pipeline area,¹ infill grout material, and the emplaced surface cover at closure. The modified RCRA Subtitle C barrier reduces the net infiltration that will eventually percolate to the buried tank structures and ancillary equipment. The infill grout material provides not only structural stability to the tank configuration, but also provides a relatively impermeable barrier to flow leading to flow diversion around the tank, as long as the grout is not physically degraded. The infill grout material also controls the chemical conditions of the pore water that contacts the residual waste through mineral phase dissolution and precipitation (e.g., dissolution of portlandite and precipitation of calcite).

The source term processes that are considered in the post-closure period include releases of contaminants from residual waste, and their transport to the underlying vadose zone via either

¹ Individual pipelines are not treated as separate sources. Instead, the inventory associated with the pipeline source term is distributed uniformly over the area at WMA C that contains pipelines.

RPP-ENV-58782, Rev. 0

diffusion or advection. Conceptually, the key processes expected to affect contaminant releases from tank residuals include:

- Leaching of contaminants from the tank waste residual layer into the pore water associated with the tank residuals
- Diffusive transport of contaminants through the tank wall grout and concrete layer, along the tortuous continuous connections, to vadose zone soil outside the tank
- Ongoing chemical and physical degradation of the tank wall concrete and grout layer
- Ongoing dissolution and degradation of emplaced grout in the tank leading to eventual formation of cracks
- Once a sufficient number of cracks form in the engineered barriers, the potential exists for advective flow of water to begin to influence the source term.

Not all processes that are considered conceptually are included in the numerical models. Data from laboratory testing on the concrete samples provide a basis for the degradation of the concrete structure.

6.2.1.1 Conceptualization of Source Term. The distribution of residual waste volume within the retrieved tanks has been estimated by a variety of techniques that have involved video observations and computer/CAD modeling (e.g., RPP-CALC-54266, “Post-Hard Heel Retrieval Camera/CAD Modeling System Waste Volume Estimate for Tank 241-C-108”). The result of one such attempt is presented in Figure 6-5. The green and brown areas indicate the distribution of residual waste over the tank bottom while the blue area represents waste water remaining in the tank. Spatial distribution of residual waste volumes are estimated for the tank dish bottom, tank walls and stiffener rings, and in-tank equipment for the retrieved tanks, and are summarized in RPP-RPT-42323, Rev. 3. The estimates indicate that the majority of residual waste is located in the tank dish bottom (>80% for the 100-series tanks and >50% for the 200-series tanks), with minor amounts associated with the in-tank equipment.

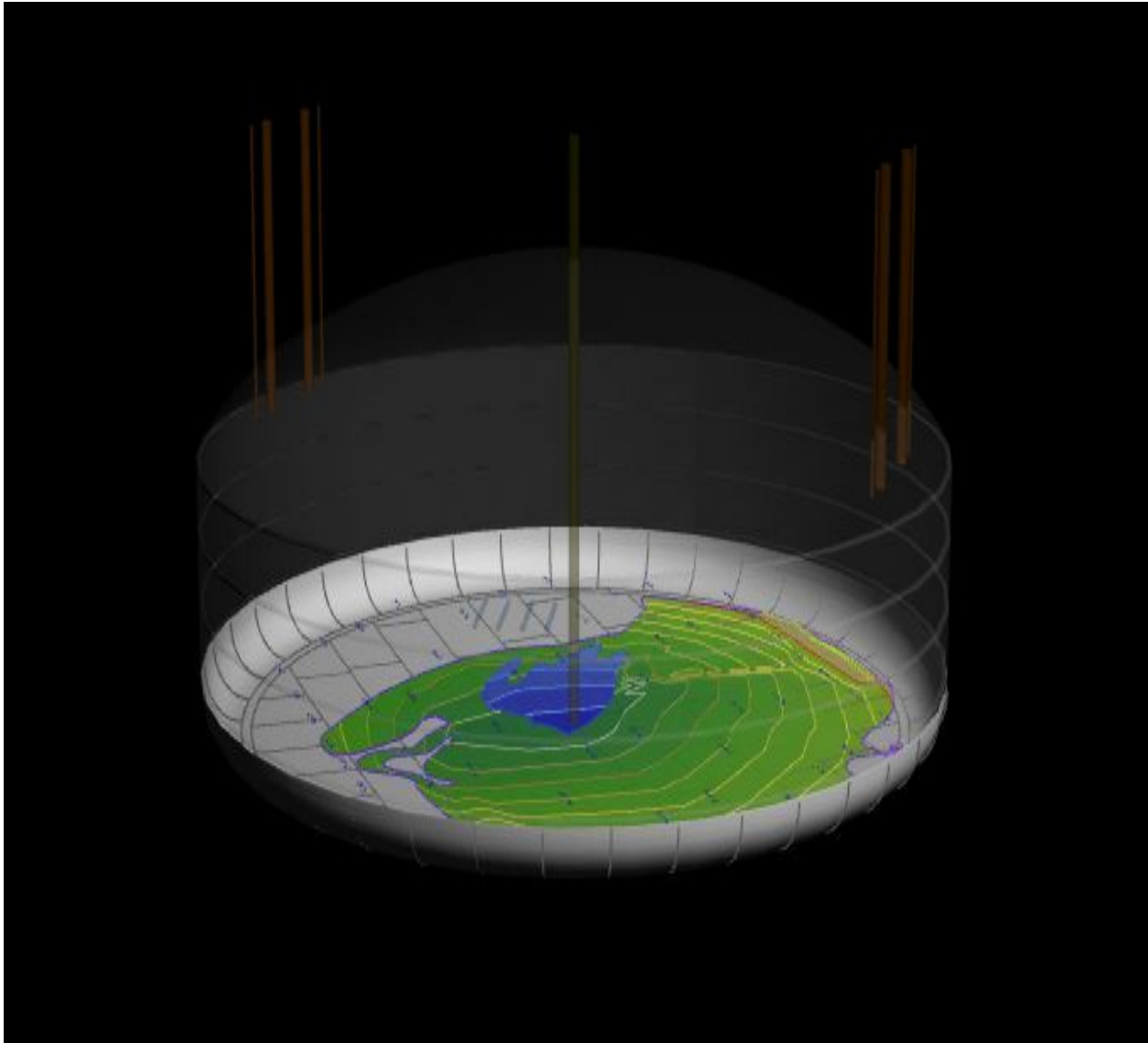
For the purpose of developing a source release model for tanks and 244-CR vault, the residual waste volume is conceptualized to be present as a thin layer at the base of the tank (Figure 6-6). The estimated residual waste volume is assumed to be spread across the circular tank dish bottom area. The residual waste is conceptualized to be sludge-like, with a texture similar to a hardened paleosol. It is assumed to be fully saturated with a porosity of 40% based on evaluation of sludge waste phase from the retrieved tanks (TWINS, Queried 02/10/2014, [WMA C Tanks, wt% water in sludge/solid waste type], <http://twins.pnl.gov/twins.htm>). The variability associated with residual volume is considered in the uncertainty analysis.

While the tank is intact, it will divert any water that infiltrates through the surface cover. Therefore, the transport mechanism for release of contaminants from the residual tank waste to the underlying vadose zone is primarily diffusive. The dissolved concentration of contaminants in the residual waste pore volume is controlled by the waste characteristics, such as waste form

RPP-ENV-58782, Rev. 0

1 degradation and dissolution of solubility-controlling mineral phases. The presence of continuous
2 water connections is assumed across the grout and concrete layers for the diffusive transport to
3 occur in the aqueous phase.

4
5 **Figure 6-5. Computer-Aided Modeling Results Showing Distribution of Residual Waste**
6 **for a Retrieved Tank.**
7

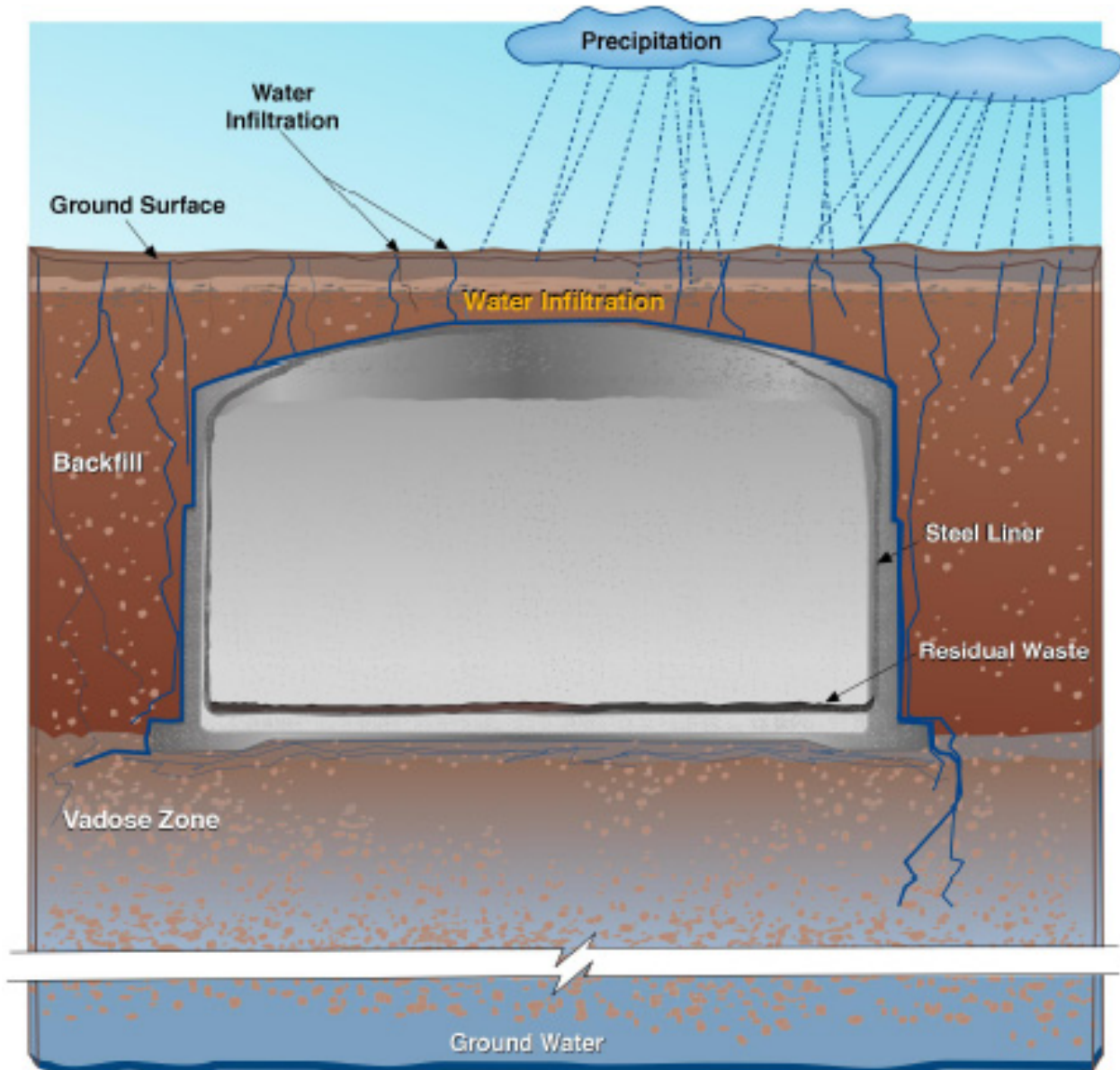


8
9
10 The source release model for the pipelines is quite different from the tanks. Instead of modeling
11 discrete source terms, a single source area reflective of the approximate areal distribution of the
12 waste transfer pipelines is considered. This is the assessed area of the tank farm where pipelines
13 are generally present. The estimated residual inventory is uniformly spread over this area.
14 Unlike tanks, the pipelines are assumed not to be filled with grout at closure, and due to limited
15 information on the condition of the pipeline material, the pipeline walls are assumed to be absent
16 (i.e., no structural integrity). Therefore, both advective and diffusive releases are considered
17 from the pipelines. More details related to the source conceptualization are discussed below.

RPP-ENV-58782, Rev. 0

Only those aspects of the engineered features that are used in developing parameters for source term modeling are presented.

Figure 6-6. Conceptual Model of Tank after Site Closure.



6.2.1.1.1 100-Series Tanks. The C-100-series tanks consist of a concrete base slab with a steel-plate lining. They have an inside diameter of 22.9 m (75 ft) and an internal height of 5.5 m (18 ft) from the bottom metal sheets to the top of the metal side plates, which is also the spring line for the dome. The tanks are buried underground with ~2.1 m (7 ft) of backfill over the top of the dome to provide shielding from radiation exposure. The details of the engineered structure at the base of the C-100-series tanks are shown in Figures 6-7 and 6-8. The structures were built by installing a reinforced-concrete base that is at least 0.15 m (6 in.) thick followed by 0.05 m (2 in.) of additional grout on top, over which carbon steel liner was emplaced. Following the

RPP-ENV-58782, Rev. 0

completion of the bottom of the tank, the sidewalls of the metal liner were welded together and the liner was encased in sidewall concrete ~0.3 m (1 ft) thick. A concrete dome ~0.38 m (1.25 ft) thick was erected on top of the tank with a 3-ply waterproof membrane applied to the top of the dome.

The carbon steel liner thickness varies, from 0.95 cm (0.375 in.) thick at the base of the tank to 0.64 cm (0.25 in.) thick along the sides. As shown in Figure 6-6, the residual waste layer is conceptualized to be located on top of the carbon steel liner. Although the carbon steel liner was designed to hold the waste in place and act as a barrier to transport of contaminants, the liner is assumed to be absent due to lack of information on its present condition. Recent studies related to characterization of the corrosion behavior of the carbon steel liner (WHC-EP-0772, "Characterization of the Corrosion Behavior of the Carbon Steel Liner in Hanford Site Single-Shell Tanks") determined several likely corrosion processes within the tank environment that could lead to degradation of steel. Some of the likely corrosion processes are pitting and crevice corrosion, stress corrosion cracking, general corrosion, and galvanic cell corrosion. These are discussed in more detail in RPP-RPT-46879. These processes lead to uncertainties regarding the state of the carbon steel liner; consequently, it is assumed to be absent in the model. As a result, the residual waste layer is conceptualized to overlie the 0.05-m (2-in.)-thick grout layer that is underlain by the 0.15-m (6-in.)-thick base slab concrete layer. The source term model represents the shortest possible vertical diffusive transport path length from residual waste layer to outside of the tank, which is the combined thickness of grout and base slab concrete layer of 0.2 m (8 in.). The diffusive area is taken to be the base area of the tank. The aqueous concentration of contaminants in the residual waste provide the upstream boundary concentration for diffusive transport with a zero concentration boundary being applied in the far-field (at the water table depth). The source term release calculations are performed using the system model.

6.2.1.1.2 200-Series Tanks. The details of the engineered structure at the base of the C-200-series tanks is presented in Figure 6-9. The 200-series tanks have an internal diameter of 6.1 m (20 ft) and an operating depth of 7.3 m (24 ft). Other than the difference in dimensions, the basic construction of the 200-series tanks is similar to the 100-series tanks. The 200-series tanks also have a base concrete slab over which a grout layer and a steel liner is present. The thickness of the base concrete slab is 0.15 m (6 in.), while the grout layer is 0.025 m (1 in.), leading to a combined thickness of 0.178 m (7 in.). Because the thickness differences are minor between the 100-series and 200-series tanks, a constant thickness of 0.2 m (8 in.) is applied to all the tanks for simplifying the diffusive transport calculations. Note that this thickness is conservative for diffusive release calculations as it ignores thickness of overlying steel liner (or steel corrosion products) and the residual waste (sludge) layer.

6.2.1.1.3 244-CR Process Tank Vault. The configuration of the 244-CR vault that is located in the southwest corner of the C Farm complex is shown in Figure 6-10 (with additional details shown in Figure 3-40). The vault is a two-level, underground, reinforced-concrete structure. The lower level consists of four cells, each equipped with a concrete sump. The exterior walls and dividing walls between the cells are 0.61 m (2 ft) thick, with each cell housing a steel tank. The cells housing tanks CR-011 and CR-001 are each 7.9 m (26 ft) long by 6.7 m (22 ft) wide. The cells housing tanks CR-002 and CR-003 are each 6.1 m (20 ft) long by 4.9 m (16 ft) wide.

RPP-ENV-58782, Rev. 0

Although the cells are distinct, for the purpose of source term modeling their inventory is assumed to be uniformly distributed over the rectangular footprint of the 244-CR vault of ~28-m (92-ft) length and 5.8-m (19-ft) width. The residual waste layer is conceptualized to be present over the grouted base of the tank, and the diffusive thickness is assumed to be 0.2 m (8 in.) to be consistent with the path lengths assumed for the 100-series and 200-series tanks.

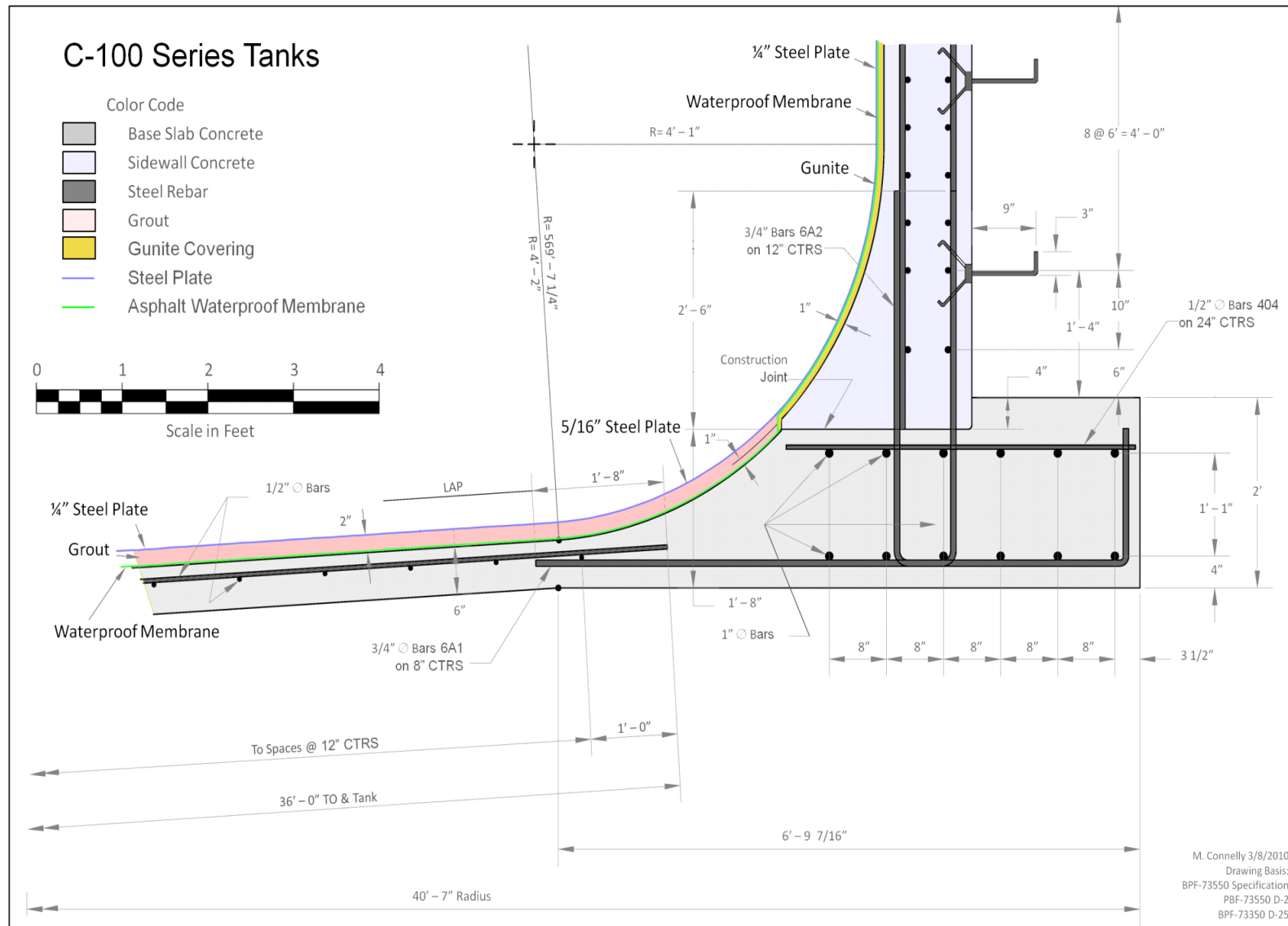
6.2.1.1.4 Pipelines. An extensive network of transfer lines connects the various components of the tank farms. These pipelines carried a variety of process wastes, typically in a slurry form. The initial tank farm waste-transfer pipelines installed in 1944 to 1945 were direct-buried (not encased) pipelines, with some on concrete slabs. Typical burial depth was 1 m (3 ft). After 1947, all pipelines installed were either concrete encased or pipe-in-pipe encased. The primary pipe used was typically carbon or stainless steel. Figure 6-11 shows the areal extent of active and existing pipelines in WMA C during the 1961 to 1978 time period.

As discussed in RPP-PLAN-47559, ~11.2 km (7 mi) and 200 separate pipelines with different diameters and lengths comprise the abandoned pipelines in WMA C. Appendix A of RPP-PLAN-47559 compiles the information on various pipeline segments, indicating that the pipeline diameters typically vary from 0.05 m (2 in.) to 0.15 m (6 in.), with 0.076 m (3 in.) pipe diameter being the most common.

The residual pipeline inventory is based on the assumption of eight fully plugged cascade lines, one known plugged pipeline, and remaining pipelines assumed to be 5% full (RPP-PLAN-47559). Although the source inventory within the pipeline is spatially variable, for the purpose of the source release calculations the pipeline residual inventory is assumed uniformly distributed over a square area of side length 150 m (492 ft). This square area of areal extent 225,000 m² (0.09 mi²) roughly coincides with the pipeline extent area shown in Figure 6-11. The contaminated thickness in the vertical direction is 0.076 m (3 in.), which is the most common pipeline diameter. The residual inventory is uniformly distributed within this volume mixed in with the bulk soil (backfill). Even though the pipeline material (carbon steel or stainless steel) or any pipe grout-fill (that may occur in the future) may act as a barrier, it is not considered in the model and the mass release from pipeline is both advective and diffusive.

6.2.1.1.5 Gas-Phase Diffusive Flux. While the infill grout is intact, upward gaseous diffusion of volatile contaminants is modeled from the residual waste layer towards the atmosphere. The air content within the infill grout is assumed to be 6% based on characterization information for possible Hanford grout (WSRC-TR-2005-00195, "Summary of Grout Development and Testing for Single Shell Tank Closure at Hanford"). Upward diffusive gas phase transport through the tank occurs along a 10-m (32.8-ft)-long pathway towards the land surface. This pathway is split into a lower 5-m (16.4-ft) thickness composed of infill grout material followed by another 5-m (16.4-ft) thickness of soil overburden. The porosity and saturation of the infill grout and soil overburden for the purpose of diffusive release calculations are fixed over time. The surface barrier that will be emplaced at closure over the tank farm will provide additional depth to the waste. For performing the air pathway calculations, this thickness is conservatively ignored.

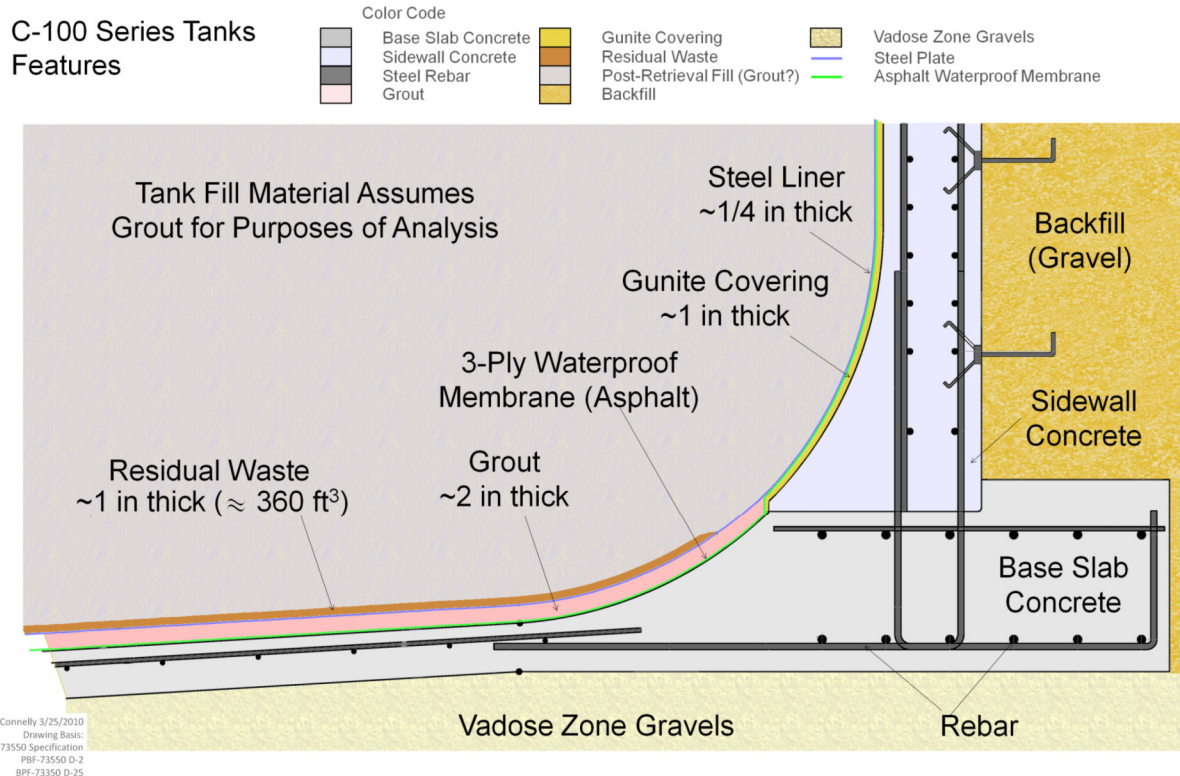
Figure 6-7. Engineered Structure at the Base of the C-100-Series Tank.



RPP-ENV-58782, Rev. 0

Reference: BPF-73550, "Specifications For Construction of Composite Storage Tanks Bldg. No. 241 Hanford Engineer Works Project 9536."

RPP-ENV-58782, Rev. 0

Figure 6-8. C-100-Series Tank Corner Features.

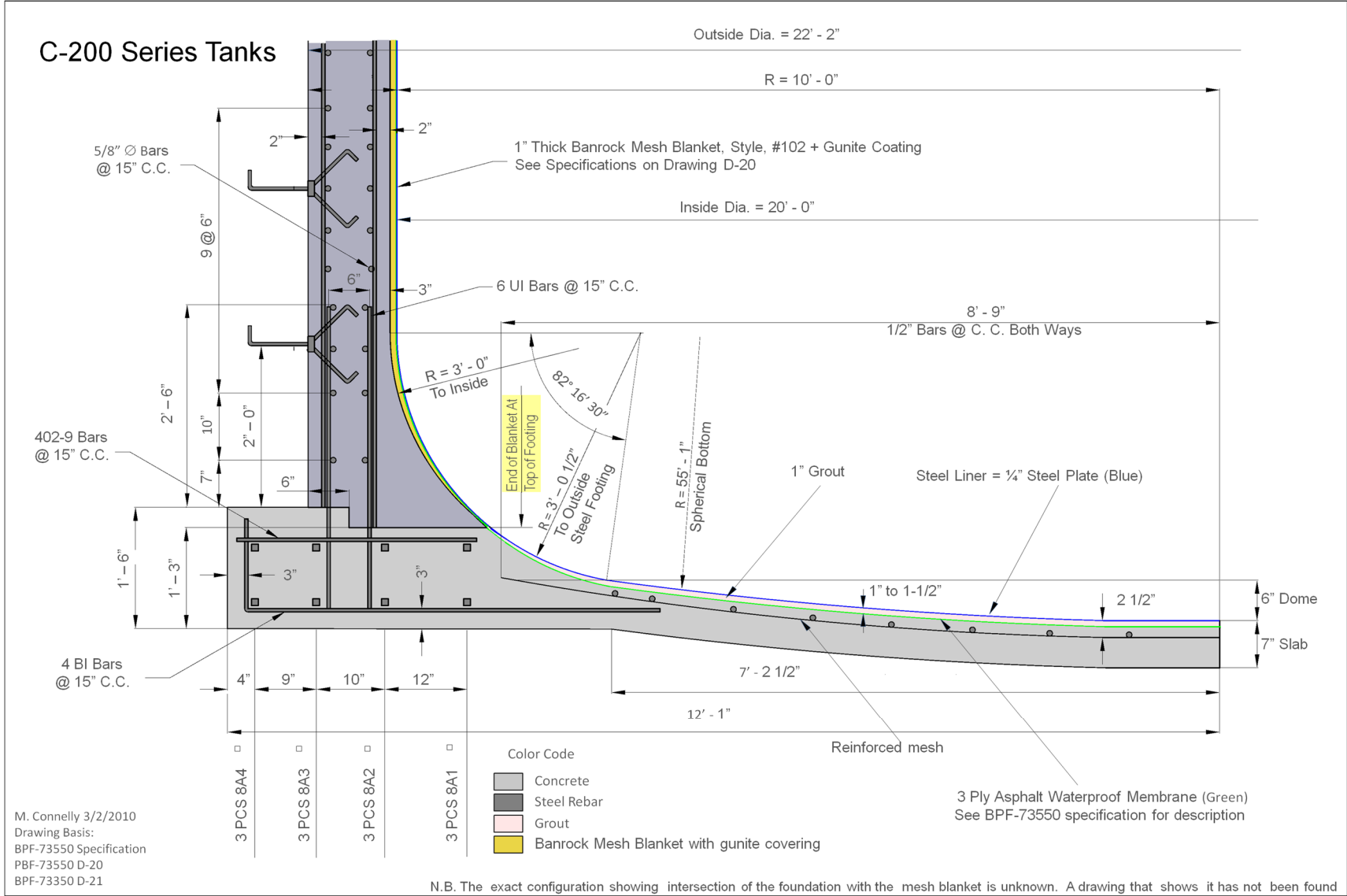
Reference: BPF-73550, "Specifications For Construction of Composite Storage Tanks Bldg. No. 241 Hanford Engineer Works Project 9536."

6.2.1.2 Evaluation of Tank Stability. At closure, the tanks will be filled in with grout to provide structural and chemical stability and low permeability. During the placement of grout, the tank structure itself acts as a form into which the grout is poured. If the placement is not significantly interrupted, and if the grout mixes meet the placement specifications, the result will be a large monolith of emplaced grout. The PA model calculations assume a 5-m (16.4-ft) thickness of the infill grout.

As the grout is not yet specified, reasonable assumptions are made about its likely composition and behavior. A possible tank fill is described in WSRC-TR-2005-00195 as consisting of three layers of grout: free flowing layer, structural stability layer, and a high compressive strength layer. The grout is anticipated to be formulated to meet the following core functions of the tank fill materials:

1. To confine residual waste through limitation of flow and through chemical stabilization of the residual material
2. To provide stability and minimize maintenance
3. To reduce potential for infiltration or inadvertent intrusion.

Figure 6-9. C-200-Series Tank Cross-Section.

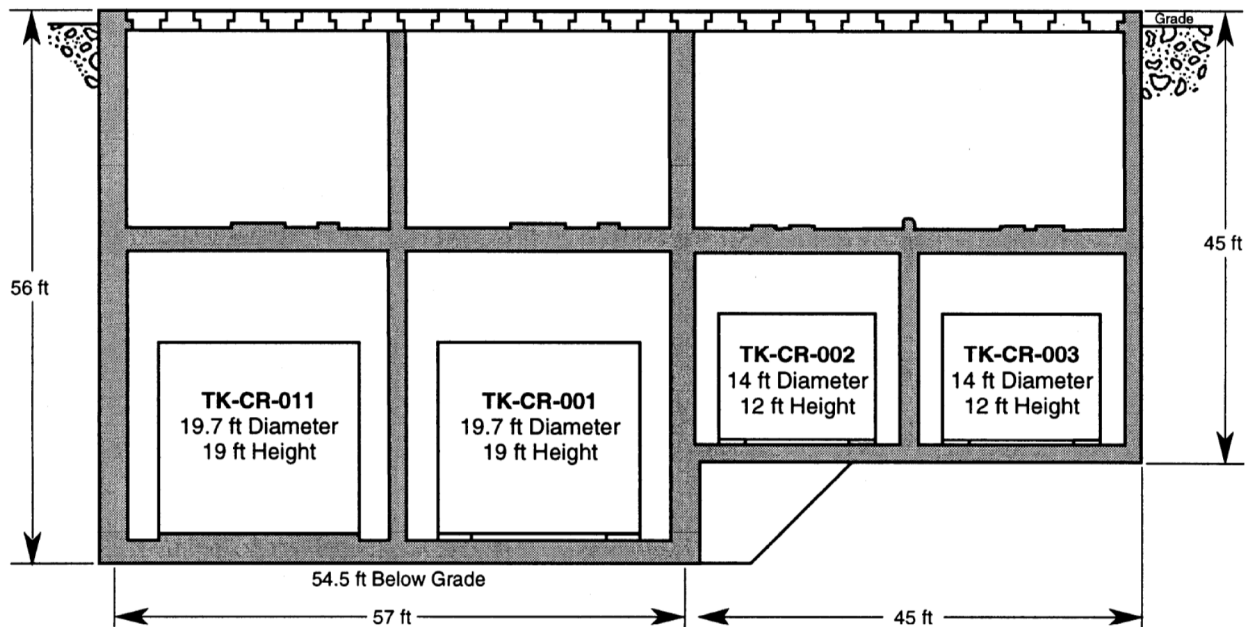


Reference: BPF-73550, "Specifications For Construction of Composite Storage Tanks Bldg. No. 241 Hanford Engineer Works Project 9536."

RPP-ENV-58782, Rev. 0

RPP-ENV-58782, Rev. 0

Figure 6-10. Schematic of the 244-CR Process Tank Vault in Waste Management Area C.



The exact composition of grout is currently unknown, but it is likely to provide a significant barrier to flow through the tank, thereby restricting the release from the residual waste to be diffusive controlled. Once the grout meets compressive strength to resist deformation, limited physical damage is expected since the tank structure is below ground and will be protected by lithostatic (overburden) pressure. Degradation due to freezing and thawing is not likely to be significant either, due to depth of the tanks and ancillary equipment being below the freeze zone (deeper than 0.61 m [24 in.]). In addition, the geochemical conditions in the Hanford vadose zone are favorable for preventing concrete degradation. The Hanford soil pore waters are alkaline and are at or near saturation with calcite; therefore, any meaningful decalcification (acid attack) is unlikely. The tank wall and grouted infill material is expected to undergo slow chemical and physical degradation. Therefore, the monolith is likely to remain an effective hydrologic barrier for a very long time as discussed in Section 6.2.1.2.3.

6.2.1.2.1 Grout Degradation. After closure, the tank concrete and grout is exposed to a combination of physical and chemical processes. Some processes may be beneficial (for example, continuing hydration and self-sealing of cracks), while others may create deleterious changes, such as shrinkage and thermal cracking. Although the geochemical conditions at the Hanford Site are favorable to preventing grout and concrete degradation, there are potential chemical degradation mechanisms that under certain conditions could lead to degradation of concrete forming the tank wall and the tank infill grout material. These key chemical degradation mechanisms are discussed and evaluated below along with the reasoning as to why these mechanisms are not carried forward into the numerical modeling.

Carbonation. Carbonation is the process where the CO_2 available in the soil-gas reacts with the calcium hydroxide in concrete to form calcium carbonate. This process is shown in Figure 6-12,

RPP-ENV-58782, Rev. 0

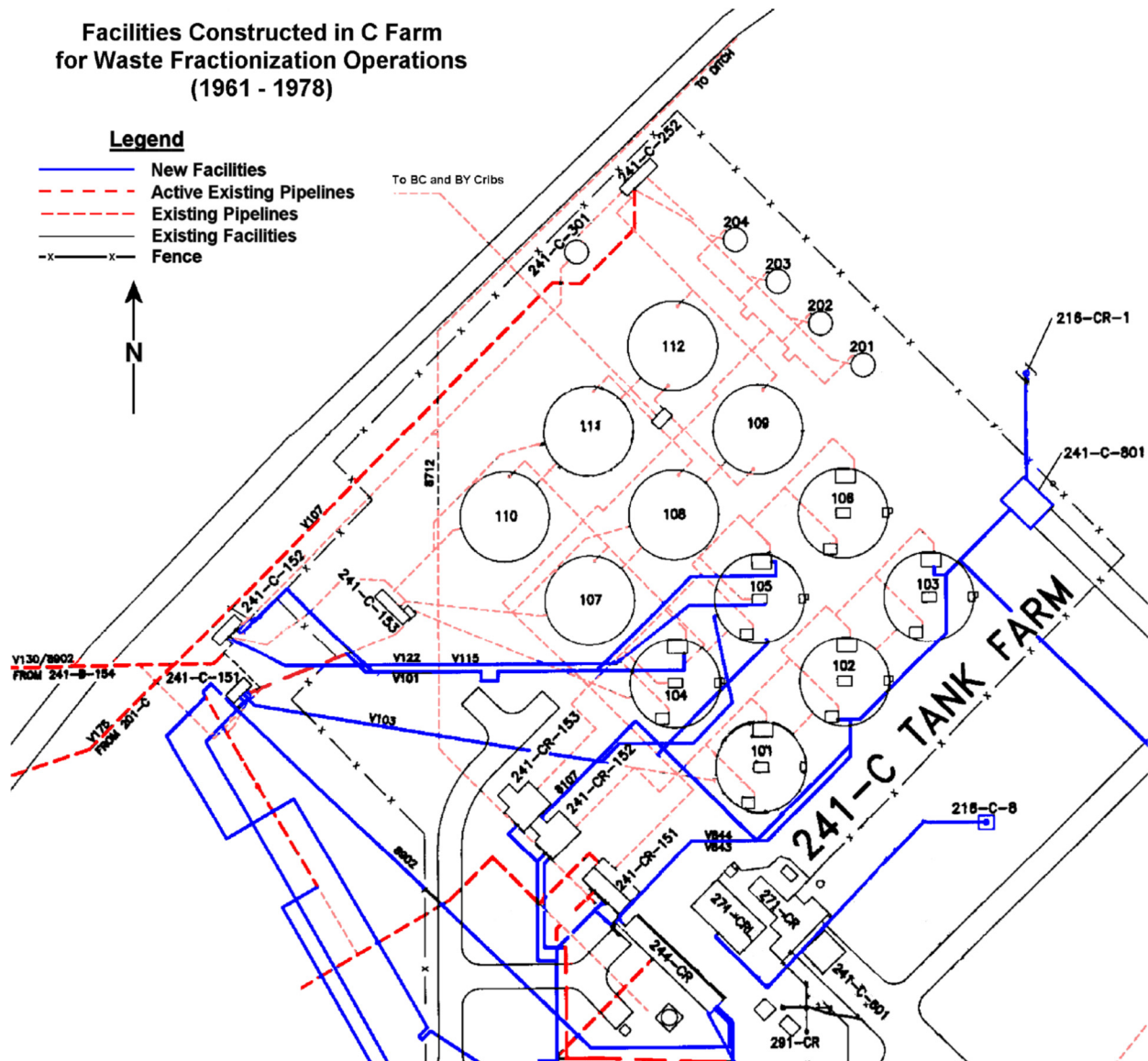
1 where the CO_2 (g) is supplied by gaseous diffusion through the soil column. The carbonation
2 reaction front is defined as the interface where the $\text{Ca}(\text{OH})_2$ actively reacts with CO_2 gas and
3 where the pH transitions from >12 [reflecting $\text{Ca}(\text{OH})_2$ equilibrated pore water] to pH of 9
4 (reflecting CaCO_3 equilibrated pore water). Carbonation of concrete is a slow and continuous
5 process that progresses from the outer surface inwards but slows down with increasing diffusive
6 length. Detailed studies have indicated that movement of a carbonation front is typically
7 proportional to the square root of exposure time. Carbonation has two effects: it increases
8 mechanical strength of concrete by reducing permeability and reducing porosity (calcite has
9 higher molar volume than portlandite), but it also decreases alkalinity, which is essential for
10 corrosion prevention of the steel liner and other reinforcement steel. Below a pH of 10, the
11 steel's thin layer of surface passivation dissolves and corrosion is promoted. Depending on the
12 amount of steel present and its role in maintaining structural integrity of the tank, the stability of
13 the tank can be compromised. Unlike normal reinforced concrete where significant amounts of
14 rebar are present, the WMA C SSTs have relatively little equipment (and therefore steel)
15 incorporated into the grout.

16
17 The process of carbonation continues until all of the $\text{Ca}(\text{OH})_2$ is dissolved. At this point, the
18 dissolution chemistry is controlled by other hydrated calcium silicate and aluminate phases.
19 When all of the $\text{Ca}(\text{OH})_2$ has been leached away, other constituents become exposed to chemical
20 decomposition. This decomposition eventually leaves behind silica and alumina compounds,
21 which have little or no strength.

22
23 **Sulfate attack.** Sulfate attack represents a complex set of chemical and physical processes
24 where the hydrated and unreacted phases in portland cement react with sulfate ions to form solid
25 phases. This can lead to increased cracking due to formation of sulfate-bearing phases such as
26 ettringite and gypsum, with considerable local expansion. Sulfate attack is typically managed by
27 minimizing the reactive component (tricalcium aluminate) in the cement. The source of sulfate
28 can be external (infiltrating water) or internal (from the concrete/cement itself). Delayed
29 ettringite can form from an internal sulfate source such as sulfate present in the tank residuals.
30 Although there may be some sulfate in the tank residuals, this amount is generally small
31 (compared to the amount of grout infill) due to extensive washing and cleaning steps undertaken
32 to remove the sludge. In addition, the grout is produced using low sulfate water with aggregate
33 (fine sand) that is low in sulfate. The external source of sulfate is going to be slowly infiltrating
34 waters, which have low sulfate content. Due to limited availability of sulfate, the impact from
35 sulfate attack is not expected to be important for grout degradation in Hanford SSTs.

36
37 **Alkali-aggregate Attack.** The alkali-aggregate reaction occurs when aggregates containing
38 reactive silica react with sodium and potassium oxides in the portland cement to form an
39 alkali-silica gel. This gel can absorb water, which in turn can lead to expansion and cracking of
40 the grout. In the mixes for Hanford tank fill, non-reactive quartz sand will likely be used. In
41 addition, it is known that substitution of fly ash and blast furnace slag for some of the portland
42 cement will mitigate the impact of the alkali-aggregate reactions. Finally, portland cements
43 produced today intentionally have low amounts of alkali content to avoid alkali-aggregate
44 reaction. Therefore, it appears unlikely that cracking due to alkali-aggregate reaction would
45 occur in the Hanford SSTs.

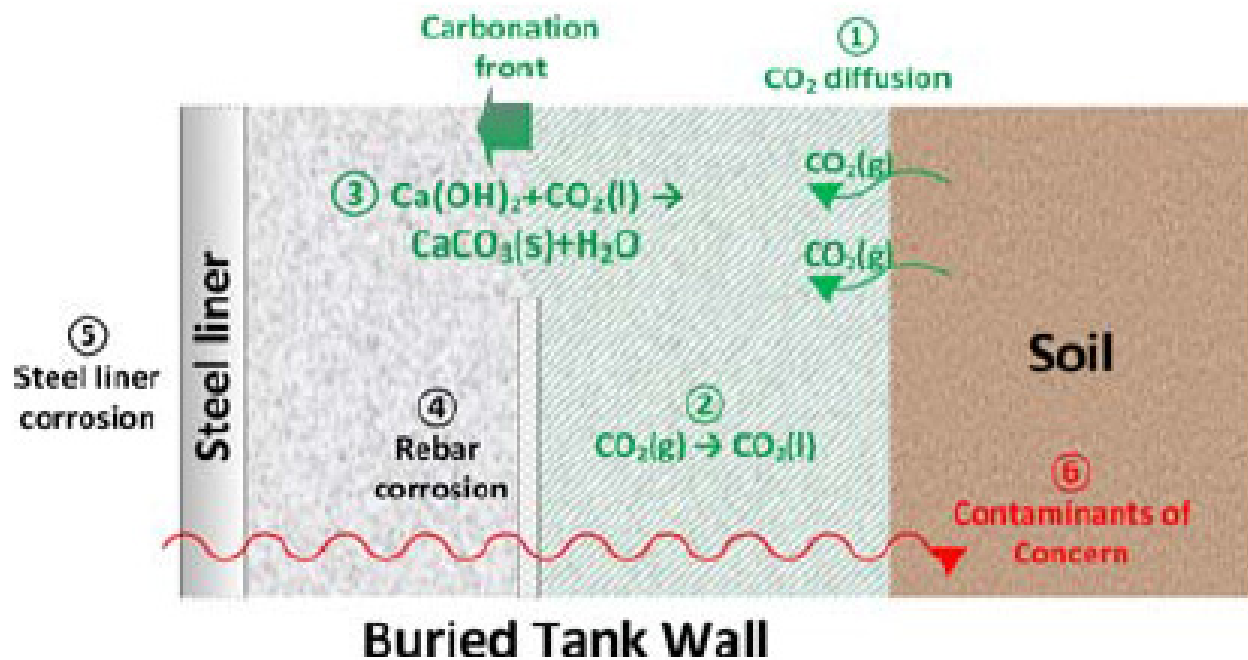
Figure 6-11. Location of Active and Existing Pipelines Along with New and Existing Facilities for Waste Fractionization Operations (1961 to 1978).



Acid Leaching (Decalcification). Acid leaching or decalcification refers to leaching of calcium ions (coupled with hydroxide ions) from pore solutions and dissolution of calcium hydroxide, C-S-H, and hydrated calcium aluminate phases in cementitious materials [WSRC-STI-2007-00607, “Chemical Degradation Assessment of Cementitious Materials for the HLW Tank Closure Project (U)”]. This form of degradation occurs when concrete is in contact with acidic water for long periods of time. The ultimate residue produced by decalcification consists of hydrous forms of silica (silica gel), alumina (alumina gel), and iron oxide. The rate of attack depends on the flow rate and the chemistry of water. Since ambient Hanford pore waters have high alkalinity and are at near saturation with calcite mineral phase, the process of decalcification is likely to be very slow, if it occurs at all.

RPP-ENV-58782, Rev. 0

Figure 6-12. Carbonation Process Acting on the Buried Tank Wall.



Current evaluations of chemical conditions inside the tank (based on residual waste chemistry) and outside the tank (based on pore water chemistry) indicate very benign conditions with regard to chemical degradation of concrete and tank-fill grout material. Consequently, the degradation due to chemical processes will progress at a very slow rate. Among the processes evaluated, carbonation was identified as the most likely chemical degradation mechanism, which will proceed naturally due to availability of CO_2 via gaseous diffusion.

6.2.1.2.2 Grout Monolith Stability. During scale-up testing for tank infill material, two monolith structures were created and tested for strength. The details are presented in WSRC-TR-2005-00195. Figure 6-13 shows the two monolith structures produced by placing three layers of grout into 4.6-m (15-ft)-diameter swimming pools during scale-up testing. These monoliths remained after the swimming pool structures were removed. The layered monoliths displayed significant strength, as demonstrated by the difficulty encountered in breaking them apart. In fact, the bulldozer and the heavy-duty forklift shown in the figure were unable to turn over the monoliths. Both monoliths were repeatedly lifted on one side and dropped without breaking. Eventually, the bulldozer was able to break the monoliths along horizontal planes by ramming the bulldozer blade at the level of the interfacial areas. These tests indicate substantial increase in strength even though these monoliths were in initial phase of curing (only 5 days after the capping grout had been poured, and about 8 total days since the pouring of the first stabilization layer). Compressive strength measurements confirmed this and indicate that significant strengthening likely continues to occur out to 90 days of curing.

6.2.1.2.3 Hanford Tank Concrete Evaluation. As part of the initiative to evaluate the structural integrity of the tanks (called Single-Shell Tank Integrity Project or SSTIP), a 1.4-m (55-in.)-diameter reinforced concrete dome "Plug" was removed from tank C-107 in December 2010. More recently, an 11.6-m (38-ft) sidewall concrete core was removed from

RPP-ENV-58782, Rev. 0

1 tank 241-A-106 (located in the WMA A-AX south of WMA C) in May 2014. Results from
2 inspection, physical testing, and petrographic examination of the concrete cores are reported in
3 RPP-RPT-50934 and RPP-RPT-58254. These analyses are very important in predicting the tank
4 wall degradation because they provide direct empirical evidence on the state of concrete wall
5 material after being left underground for 60 to 70 years. The results of analyses that are relevant
6 for the PA are discussed below.

7
8 The 1.4-m (55-in.)-diameter concrete section ("Plug") removed from the center of the dome of
9 tank C-107 is shown in Figure 6-14. It was removed using a combination of high-pressure water
10 and garnet abrasive. Fourteen cores were taken from the concrete "Plug," each 10.7 cm (4.2 in.)
11 in diameter. Of those 14 cores, 12 underwent mechanical testing and 2 underwent petrographic
12 examination. No cracks or large air voids were found during the inspection process.
13 Additionally, the protective asphaltic membrane and mortar layers that were laid out during the
14 construction were found to be intact. The average compressive strength of all of the tested cores
15 was about 55,158 kPa (8,000 psi), more than 2.5 times the original 28-day design strength
16 specified at the time of construction. Based on the results of petrographic examination, the
17 concrete represented by the cores was in good condition. No distress (cracking or excessive
18 microcracking) was observed in either core. The concrete showed no evidence of chemical
19 attack, significant alkali-aggregate reactions, or other deleterious mechanisms involving
20 aggregates and/or paste constituents. The concrete in both cores exhibited good physical paste
21 properties. Apart from localized softer paste at the immediate top surface, the paste in the cores
22 was hard and dense through the depth of the concrete. Distribution of aggregates and other paste
23 constituents was uniform. Macroscopically, the cores were well consolidated (no large voids).
24 The cement was nearly completely hydrated. The depth of carbonation from the top surface of
25 both cores was reported to be 1 to 2 mm (0.04 to 0.08 in.).

26
27 Sidewall coring of tank 241-A-106 was completed over two weeks in May 2014. Over 11.6 m
28 (38 ft) of concrete core (8.4-cm [3.3-in.] diameter) was successfully removed to a depth
29 approximately halfway through the tank footing. This tank was chosen due to its high heat load
30 history and concerns over the thermal degradation of the concrete from heat exposure. The
31 collected concrete cores are shown in Figure 6-15. Physical testing for structural integrity
32 indicated favorable results, with values generally greater, and in many cases significantly greater,
33 than expected. It is concluded that the effects of thermal degradation on the mechanical
34 properties of the concrete appear to be negligible. No deficiencies were found with regard to the
35 structural integrity of the tank. Petrographic analyses determined that the concrete is in overall
36 good condition, with a minor amount of microcracking and minor evidence of deleterious
37 mechanisms that do not appear to have significantly affected the overall quality and integrity of
38 the concrete (RPP-RPT-58254). The concrete was composed of siliceous natural gravel coarse
39 aggregate and natural sand fine aggregate uniformly distributed in a portland cement paste
40 binder. The paste appeared to be of good quality, although some degree of paste alteration
41 (leaching of calcium hydroxide from the paste) was observed, along with a small amount of
42 secondary ettringite mineral, possibly from sulfate containing impurities in the paste. Only one
43 crack and very few microcracks were observed in the examined core segments. A very minor
44 degree of alkali-silica reaction (ASR) had occurred in the concrete; however, no deterioration (no
45 associated cracks or microcracks) was observed. Given the age of the concrete and current
46 degree of ASR, further reaction and/or associated expansion is deemed unlikely. The depth of

RPP-ENV-58782, Rev. 0

1 carbonation was found to be shallow and about 1 to 4 mm from outer surface in some core
2 segments (RPP-RPT-58254).

3
4 Results of material properties tests of concrete cores from the haunch and wall of
5 tank 241-SX-115 (SX-115) and 202-A PUREX Canyon Building have been evaluated and
6 documented in RHO-RE-CR-2, "Strength and Elastic Properties Tests of Hanford Concrete
7 Cores – 241-SX-115 Tank and 202-A Purex Canyon Building." Both structures were built in the
8 1953 to 1954 time frame using the same concrete mix design. Compression strength and tensile
9 strength tests on concrete samples taken from tank SX-115 in year 1981 indicated a pattern of
10 possible decreasing strength with depth, but all samples were above the design value
11 (compressive strength of 20,680 kPa [3,000 psi]). Material property tests were conducted on
12 17 specimens from the 202-A PUREX Building under three temperature conditions: unheated,
13 heated to 93.3 °C (200 °F), and heated to 93.3 °C (200 °F) and then cooled to ambient
14 temperature. The rate of heating was set at 23.9 °C/day (75 °F/day) to determine if the heat-up
15 rate was significant in affecting the strength. The compressive strength for samples tested after
16 heating to 93.3 °C (200 °F) showed a small decline compared to the unheated samples.
17 However, for samples that were heated to 93.3 °C (200 °F) and then allowed to cool to ambient
18 temperature, some strength recovery was observed with values falling well within the range of
19 strengths measured for the unheated concrete. The compressive strengths of the 202-A PUREX
20 Building concrete specimens were in excess of 20,680 kPa (3,000 psi) design value in all cases.

21
22 Visual inspection of 37 concrete core samples from tank SX-115 and 17 concrete core samples
23 from 202-A PUREX Building indicated that most of the samples had no visible signs of concrete
24 deterioration. However, four tank farm cores and two PUREX Building cores were found to
25 have visible cracks, ranging from ~5 to 25 cm (2 to 10 in.) in length, possibly from coring
26 activities.

27
28 A number of tests have been performed to evaluate the strength and elastic properties of the
29 Hanford Tank Farm concrete core materials for temperatures varying from 22.2 °C to 121.1 °C
30 (72 °F to 250 °F) (RHO-RE-CR-2). These tests were conducted on 7.6 cm by 15.2 cm (3 in. by
31 6 in.) cylinders fabricated from core materials from the 241-A, 241-S, 241-T, and 241-U Tank
32 Farms. The 241-A Tank Farm concrete compressive and tensile strengths were about
33 45% greater than those values obtained from tank SX-115 concrete; however, the elastic
34 properties were essentially equal. This could be due to variations between concrete batches or
35 the fact that SX-115 tank wall concrete was subjected to higher temperatures during tank farm
36 operations than the dome concrete in the 241-A Tank Farm. In no case did compressive strength
37 of any tank SX-115 specimen fall below 20,680 kPa (3,000 psi). The lowest strength measured
38 was 26,372 kPa (3,825 psi).

39
40 These results indicate that the concrete walls within WMA C tanks are likely to be structurally
41 stable and in relatively good condition. The elevated temperatures experienced due to heat
42 generated from radioactive decay and chemical reactions within the tank are unlikely to cause
43 any appreciable decline in strength of the concrete in the tank walls.

RPP-ENV-58782, Rev. 0

Figure 6-13. Demolition of (a) Pool 1 Monolith and (b) Pool 2 Monolith after Only 5 Days after the Capping Layer had been Poured.
Note that monolith from Pool 2 is in the foreground in (a). Also note the vertical crack in the Pool 2 monolith that occurred during the demolition.

(a)

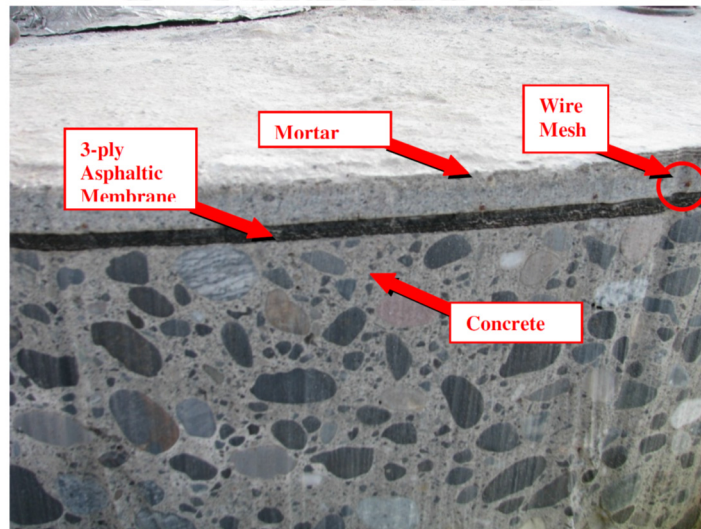


(b)

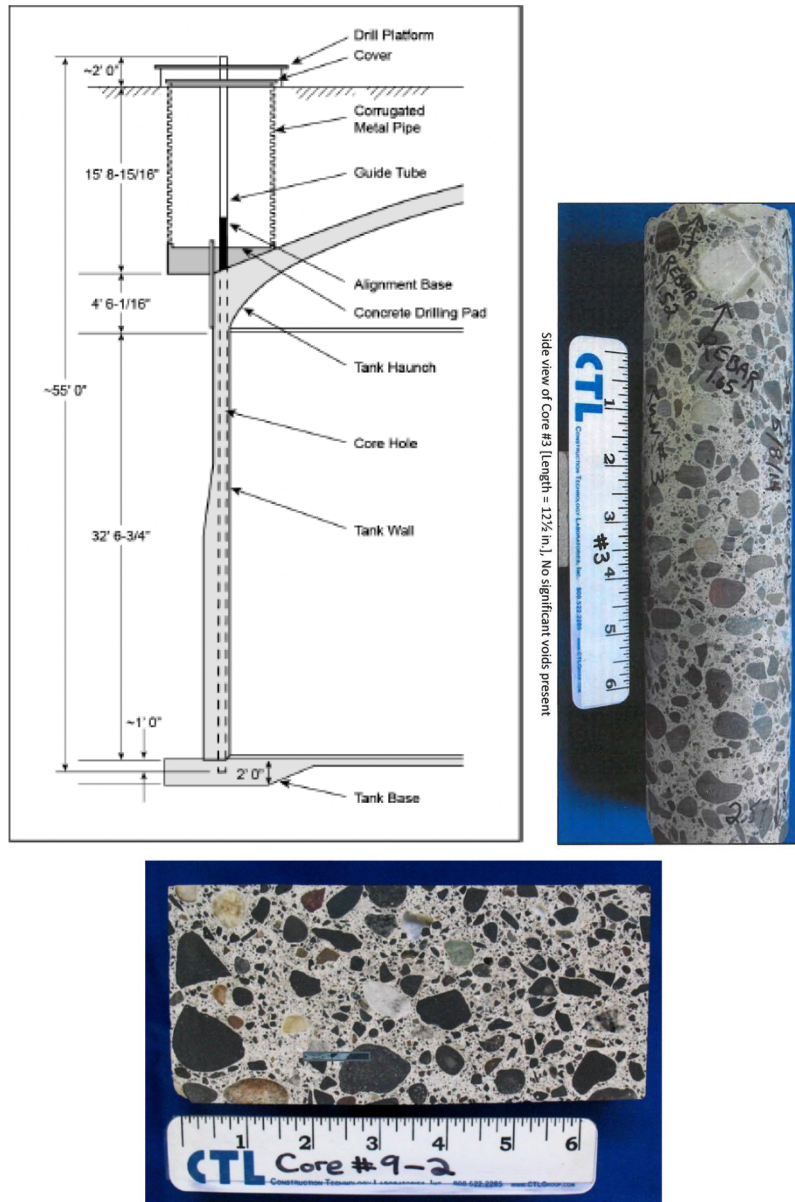


RPP-ENV-58782, Rev. 0

Figure 6-14. Evaluation of 55-inch Diameter Reinforced Concrete Dome Plug from Tank 214-C-107.



RPP-ENV-58782, Rev. 0

Figure 6-15. Evaluation of Sidewall Concrete Core from Tank 241-A-106.

Aboveground Concrete Structure Evaluation. In addition to the concrete samples taken from SSTs, some information on chemical degradation is also available from concrete cores taken from aboveground concrete structures on the Hanford Site. PNNL-23841, "Radionuclide Migration through Sediment and Concrete: 16 Years of Investigations" summarizes the characteristics of three concrete cores from aboveground structures that have been exposed to Hanford weather for 14, 28, and 57 years. The characterization summary is presented in Table 6-1. A minor degree of microcracking is noticeable, along with a moderately tight paste-aggregate bond. Ettringite is observed in the void spaces. The depth of carbonation increases with increasing age of the concrete. In the oldest specimen (213J), the carbonation had extended ~50 mm (1.97 in.) into the concrete wall. Given the limited data, the rate of

RPP-ENV-58782, Rev. 0

carbonation of concrete at the Hanford Site can be estimated at ~0.3 to 0.9 mm (0.01 to 0.04 in.) per year. This carbonation rate provides an upper bound value that can be expected for a concrete under Hanford Site conditions.

Table 6-1. Characteristics of Concrete Cores from Aboveground Structures at the Hanford Site.

Characteristic	Field Lysimeter Test Facility Sample	622C Sample	213J Sample
Age	14	28	57
Carbonation Depth (mm)	1 – 10	2 – 8	48 – 53
Air Content (%)	4 – 5	2 – 4	1 – 2
Water/Cement Ratio	0.5 – 0.55	0.5 – 0.55	0.52 – 0.57
Secondary Deposits	Abundant ettringite lining voids	Ettringite lining voids	None in outer 50 mm – minor ettringite lining voids
Microcracks	Minor	Minor	Common in outer 50 mm
Steel	#4 ~103 mm cover	None	#4 ~80 mm cover
Unit Weight (pcf)	153	152	148
Aggregates	Well-graded siliceous gravel, 19 mm top size	Well-graded siliceous gravel, 23 mm top size	Well-graded siliceous gravel, 21 mm top size
Paste-Aggregate Bond	Moderately tight	Moderately tight	Moderately tight to moderately weak

Reference: PNNL-23841, “Radionuclide Migration through Sediment and Concrete: 16 Years of Investigations.”

Observations of the cores for buried Hanford tanks indicate the carbonation depth ranges from 1 to 4 mm (0.04 to 0.16 in.). Considering about 60 to 70 years of burial time, the carbonation rates are calculated to be ~0.01 to 0.07 mm/yr (0.0004 to 0.0028 in./yr). For the aboveground concrete structure, the carbonation rate is expectedly much higher and calculated to be about 0.3 to 0.9 mm/yr (0.01 to 0.04 in.). However, the rate of carbonation would be affected by several factors, such as concrete composition, porosity, and the degree of exposure to weathering.

Simplifying carbonation as a sharp moving front, a simple analytical expression for the location x_c (mm) of the carbonation front when Relative Humidity exceeds 50% can be given as follows (Brown et al. 2013, “Modeling Carbonation of High-Level Waste Tank Integrity and Closure”):

$$x_c = A\sqrt{t}$$

where A is proportionality constant and a function of initial CO₂ concentration, effective diffusivity of CO₂, etc., while t is exposure time.

Experimental results have confirmed this non-linear relationship between the carbonation front and square root of exposure time. For the sake of simplicity, and in order to do a bounding

RPP-ENV-58782, Rev. 0

calculation, one can assume that the maximum depth of carbonation within the buried concrete tank structure is 10 mm (0.39 in.) (instead of the observed 1 to 4 mm [0.039 to 0.157 in.]). Next, considering 70 years of exposure time (burial time of SST in WMA C), the proportionality constant (A) can be calculated from the above equation to be 1.2 mm (0.05 in.) per square root of time in year. This Hanford Site-specific proportionality constant can then be used to calculate the depth of carbonation front as a function of time. Depths of carbonation front are calculated for arbitrary time periods in Table 6-2. Considering that a 0.2 m (8 in.) minimum thickness of concrete (and grout) layer exists at the base of the tank, the time for the carbonation front to propagate through this thickness will take over 20,000 years. The actual time frames would be even longer, since the observed depth of carbonation is 1 to 4 mm (0.039 to 0.157 in.) instead of assumed 10 mm (0.39 in.) for this calculation.

Table 6-2. Bounding Depth of Carbonation for Buried Concrete Calculated For Different Exposure Times Under Hanford-Specific Conditions.

Elapsed Time (yr)	Depth (mm)	Depth (inches)
1,000	37.8	1.5
5,000	84.5	3.3
10,000	119.5	4.7
20,000	169.0	6.7
50,000	267.3	10.5
100,000	378.0	14.9

The above calculated time does not include carbonation through the infill grout material, which will also have to undergo chemical degradation (likely carbonation) before tank integrity can be assumed to be lost. A simple calculation—using 5.5 m (18 ft) grout thickness in the tank, and assuming carbonation front propagating from both top and bottom directions, and assuming a bounding 0.1 mm/yr (0.004 in./yr) linear carbonation rate—shows that the grout will not be fully degraded for another 27,500 years. As a result, the total time for the carbonation front to move through both the concrete wall and the infill grout can easily exceed 50,000 years. Results from recent modeling conducted by Brown et al. (2013) under Hanford subsurface conditions (assuming 2.4% CO₂ in soil gas at 90% concrete saturations) indicates that the carbonation front propagation rate is < 0.1 mm/yr (0.004 in./yr).

The information presented above indicates that it is highly unlikely for the tank degradation to occur within the modeled time period of 10,000 years. As a result, the water entry in the tank is likely to be very slow or nonexistent altogether. For the purpose of the PA analysis, the infill grout is conceptualized to be located above the thin residual waste layer and separated from the grout/concrete layer at the base of the tank. While the infill grout is intact, no water can flow through the residual waste, and therefore the primary contaminant transport pathway is by diffusion through water in the pore spaces to the base of the tank and into the underlying vadose zone.

RPP-ENV-58782, Rev. 0

Natural Analogues. A way to gain insight into the longevity (durability) of grout, concrete, and mortar is through consideration of some of the well-studied ancient structures such as the Pantheon in Rome, Hadrian's Wall in Scotland, the Roman Aqueducts system, etc. Their durability is discussed in WSRC-TR-2005-00195. Such ancient structures that use pozzolanic materials in conjunction with hydrated lime $[\text{Ca}(\text{OH})_2]$ best simulate modern day concrete, grout, and mortar. Some of these ancient structures have existed for over 2,000 years despite being subjected to weather, abrasion, wars, and neglect. The longevity of these ancient structures, which is attributable to materials selection and placement techniques, suggests that the lifetimes for the grout monoliths within the protected, underground SSTs at Hanford could also extend into the thousands of years.

6.2.2 Radionuclide Transport

This section discusses the conceptual model of the projected transport of radionuclides from the source term through the environment to the points of exposure and identifies the mechanisms included in the analysis for groundwater, atmospheric, and biotic transport pathways.

6.2.2.1 Conceptual Model for Groundwater Pathway. This section provides an overview of major features that affect flow and transport of radionuclides within the vadose zone and saturated zone underlying WMA C. Estimates of radionuclide concentrations in environmental media are used to estimate doses to a hypothetical individual based on an assumed exposure scenario. Analysis of performance therefore requires estimates of (1) the inventory of radionuclides in the facility, (2) the release rates of these radionuclides from the tank and pipeline residual waste, and (3) the migration rates and concentrations of radionuclides released from the residual waste in environmental media (air, soil, and water).

The conceptual model of the groundwater pathway considers a diffusion-controlled release of radionuclides from the grouted tanks and ancillary equipment and an advection-controlled release from the pipelines, vertical transport through the vadose zone to the water table, and then transport laterally through the aquifer to a hypothetical well located 100 m (328 ft) downgradient. These features and processes reflect safety functions that serve as barriers to exposure in the context of defense in depth for protection of hypothetical receptors. The grouting of the tanks represents an engineered safety function or barrier to exposure, because one of the purposes of the grout is to limit the release of radionuclides from the tanks to the vadose zone. The modified RCRA Subtitle C barrier represents a hybrid barrier to exposure, because while it is an engineered structure it eventually evolves into part of the natural system. The vadose zone beneath WMA C can also be viewed as a natural barrier. Once contaminants enter the vadose zone, the low recharge (infiltration rate) controlled by the surface cover system, the thickness of the vadose zone between the base of the tanks and the unconfined aquifer, and the soil-contaminant interaction, prevent all but the least-reactive contaminants from reaching the unconfined aquifer for thousands of years. As leachate containing contaminants enters the aquifer from the vadose zone, it mixes with groundwater flowing within the saturated zone (aquifer) beneath WMA C to make concentrations of contaminants in groundwater more dilute. This dilution in concentration lowers the exposure point concentration and consequent dose to a receptor. Thus, the transport of radionuclides to the groundwater is a complicated process that depends on data and assumptions relevant to the following physical systems: (1) engineered

RPP-ENV-58782, Rev. 0

features of WMA C, (2) surface features of WMA C, (3) the vadose zone beneath WMA C, and (4) the saturated zone (groundwater) beneath WMA C.

First, this section describes the facility features important to modeling the release of contaminants from the source areas. This is followed by descriptions of the temporal evolution of the WMA C surface, the vadose zone stratigraphy, and the geochemical effects that impact radionuclide transport. Next is an overview discussing the basis for the saturated zone flow and transport used in the WMA C PA. The final section provides a detailed justification of important assumptions and simplifications of the vadose zone flow and transport model.

6.2.2.1.1 Waste Management Area C Facility Structures. Section 3 provides a description of WMA C and the planned surface engineered cover system. The physical system includes the closure barrier and the complex structures that make up the closed facility. The WMA C sources consist of twelve 2,006,000-L (530,000-gal) 100-series tanks, four 208,000-L (55,000-gal) 200-series tanks, a 136,000-L (36,000-gal) catch tank, a vault with two 57,000-L (15,000-gal) and two 151,000-L (40,000-gal) tanks, and an estimated 12.8 km (8 mi) of pipeline (RPP-50233, “Waste Management Area C Closure Conceptual Design Support Report”). RPP-RPT-49701 identifies the following four phases associated with the closure of WMA C.

- Facility Closure – All below-grade tanks and equipment are grouted to stabilize residual waste and void spaces.
- Demolition and Decommissioning (D&D) Activities – All above-grade facilities, equipment, utilities, and tank farm features are dispositioned, and all existing drywells and groundwater wells are decommissioned.
- Closure Cap Construction – The long-term surface barrier over the tank farm is constructed.
- Post-Closure Monitoring and Maintenance – Monitoring using a closure-related monitoring network continues as necessary to ensure the performance of the closure cap and to provide verification that the tank farm closure is satisfying the DOE O 435.1 performance objectives.

The grouting of the tanks and ancillary equipment is intended to stabilize these structures (prevent collapse) and to minimize the release of radionuclides by keeping the release controlled by diffusion processes. Contaminant releases from the grouted tanks and ancillary equipment are expected to remain diffusive, with no (or negligible) advection occurring through the tanks and ancillary equipment because sufficient degradation of the tank-wall and infill grout material is unlikely to occur within the simulated time period of 10,000 years. Chemical degradation rates are expected to be the same as carbonation rates, and it is estimated that for the carbonation front to propagate through the minimum wall thickness of a tank (~200 mm [~8 in.]), it will take ~30,000 years. This calculated time excludes grout material inside the tank, which will also have to undergo carbonation before tank integrity could be assumed to be lost.

RPP-ENV-58782, Rev. 0

6.2.2.1.2 Temporal Evolution of Waste Management Area C Surface. Net infiltration, deep percolation, and recharge of water are the major transport mechanisms for moving contaminants from the closed system to the groundwater. In arid and semiarid regions with thick vadose zones, such as the Hanford Site, long-term factors like climate change, changes in the annual precipitation rates, and changes in vegetation structure and community are necessary to influence the deep vertical water fluxes. In these regions, large seasonal fluctuations in soil water potential are generally contained within the upper few meters of soil, and the spatially and temporally varying moisture fluxes even out within the deep subsurface above the water table.

With expected changes to the land cover over time due to growth of vegetation, several time periods have been conceptualized (Table 6-3) to represent the changes in recharge rates and hydrologic conditions at WMA C. Each of these time periods is characterized by a different recharge rate that will be discussed in Section 6.3.2. Following is a discussion of two assumptions that pertain to recharge: (1) that net infiltration through the thick, heterogeneous vadose zone in the 200 Areas dampens the effect of discrete events, and therefore episodic precipitation events can be replaced by an average annual recharge rate; and (2) that impacts resulting from plausible climate change that may occur during the evaluation period do not adversely impact the performance of the surface or vadose zone as a barrier.

Multi-year evaluations of soil moisture content data collected from vegetated desert soils throughout the United States indicate that water potentials remain very low and relatively invariant below depths of 2 to 5 m (6.6 to 16.4 ft) ("Ecohydrological Control of Deep Drainage in Arid and Semiarid Regions" [Seyfried et al. 2005]). In response to intermittent years of elevated precipitation such as those caused by El Nino in the southwestern United States, the biomass usage of water by deep-rooted xeric vegetation increases, depleting the excess water, and no net increase in groundwater recharge occurs ("Global synthesis of groundwater recharge in semiarid and arid regions" [Scanlon et al. 2006], Analysis of Techniques for Estimating Potential Recharge and Shallow Unsaturated Zone Water Balance near Yucca Mountain, Nevada [Leary 1990]). Simulation results representing the impact of a 20-year period of temporally varying precipitation on a surface barrier and a clean, graveled surface indicate that the temporal variation in drainage can effectively be ignored, and that an average value can be used with little loss of accuracy (WHC-EP-0332, "Simulations of Infiltration of Meteoric Water and Contaminant Plume Movement in the Vadose Zone at Single-Shell Tank 241-T-106 at the Hanford Site," pp. 18-21).

The sensitivity-uncertainty period of analysis extends to 10,000 years. Therefore, impacts to the performance of the vadose zone as a barrier caused by climate change during the evaluation period are plausible. However, climate change is not likely to affect the performance of the vadose zone as a barrier appreciably. Recharge rates applied to the design and post-design periods of the modeling are likely to remain unchanged, even if the precipitation increases as a consequence of climate change. Long-term climate studies (see Section 3.1.2.6, Climate Change) indicate that for the last 10,000 years precipitation ranged from 0% to 50% less than current levels, and ranged between 75% and 128% of modern levels during the glacial period before the Holocene (PNNL-13033). The average annual precipitation (172.2 mm [6.78 in.]) at the Hanford Site for 1981 to 2010 is actually less than the lower end of the range typically associated with sagebrush-dominated ecosystems (200 to 500 mm/yr [7.87 to 19.69 in.],

RPP-ENV-58782, Rev. 0

U.S. Department of Agriculture, Natural Resources Conservation Service, Queried 12/18/2015, [Fact Sheets & Plant Guides/*Artemisia tridentata* ssp. *tridentata*], http://plants.usda.gov/plantguide/pdf/pg_arttrt.pdf). Thus, the sagebrush community appears capable of exploiting any increases in soil moisture caused by increases in the annual precipitation consistent with or even in excess of the previous glacial period.

Table 6-3. Timeline Considered for Representing the Evolution of Waste Management Area C.

Phase	Conditions	Duration	Conceptual Half Cross Section of the Waste Management Area C Area
Pre-operations	Before construction of Waste Management Area C	Until steady-state moisture conditions are achieved for the year.	<p>Natural</p>
Construction and Operations	Current conditions	1945 to 2020	<p>Natural Disturbed and/or Resurfaced Construction and Operation</p>
Early Post-Closure	Transition to conditions of restricted recharge due to modified RCRA C Subtitle C barrier	2020 to 2520	<p>Natural Reclaimed and/or Revegetated Modified RCRA C Surface Barrier First 500 Years</p>
Late Post-Closure	Degraded surface barrier conditions	2520 to 12020 (end of sensitivity and uncertainty analysis evaluation period)	<p>Natural Reclaimed and/or Revegetated Modified RCRA C Surface Barrier Beyond 500 Years</p>

RCRA = Resource Conservation and Recovery Act of 1976

Pre-operations. Hydrologic conditions prior to the facility construction (1945) control the initial moisture content and the matric potential in the vadose zone. To estimate the initial conditions, a pre-operations phase is considered, which produces initial moisture conditions for subsequent temporal changes conceptualized at WMA C. A vegetation cover representative of natural conditions is assumed over the whole domain during this period.

Construction and Operations. The operations period (current condition) is considered to represent the WMA C construction phase along with operations until closure of the WMA. This period starts in 1945 and is assumed to end in 2020 when a surface barrier is placed over the

RPP-ENV-58782, Rev. 0

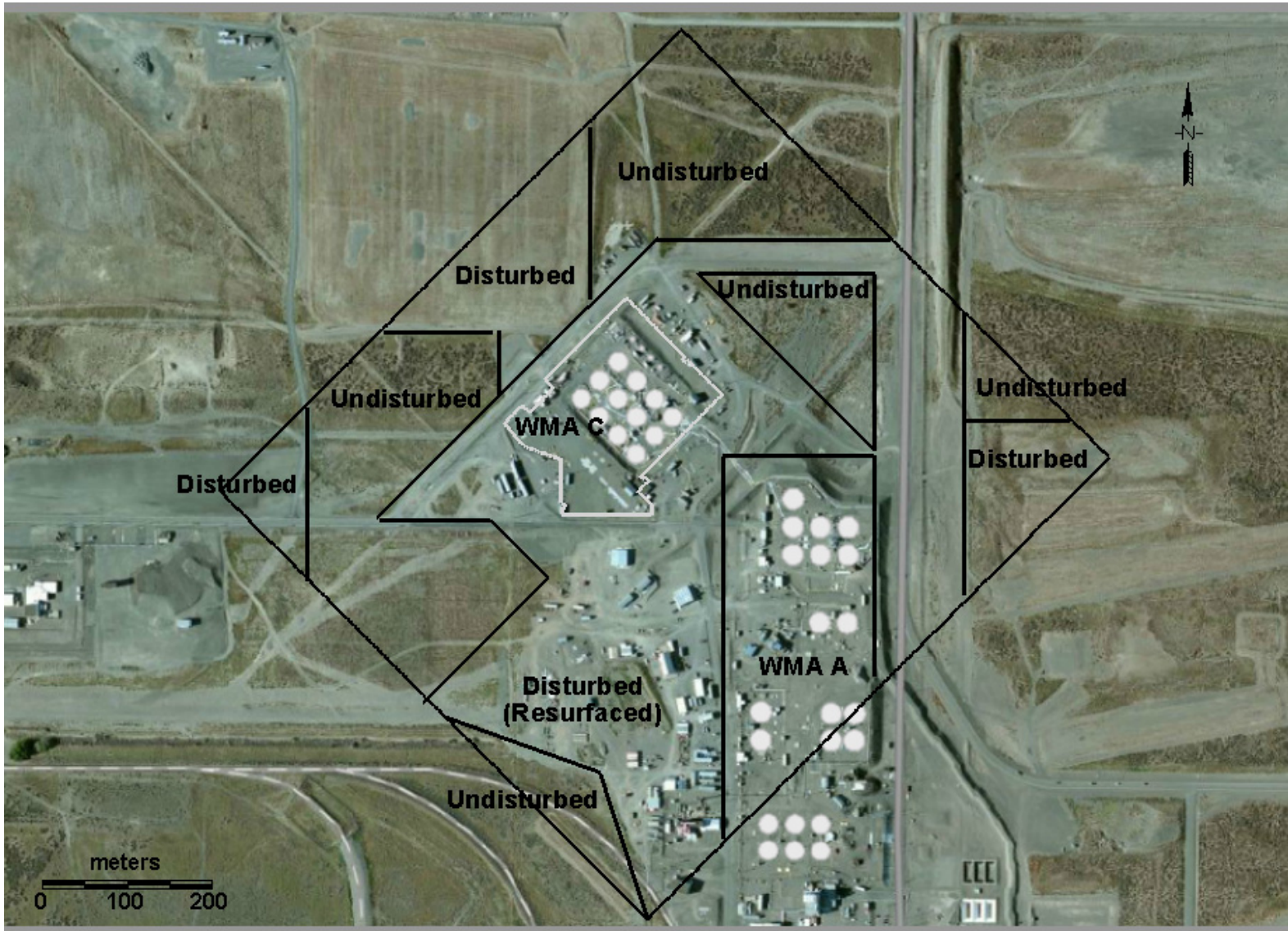
1 facility. A distinct recharge rate will be assigned to the following four different zones during this
2 period (Figure 6-16):

- 3
- 4 • The undisturbed zone around the facility characterized by a native vegetation cover
- 5
- 6 • The disturbed zone around the facility that has scant, deep-rooted vegetation but
- 7 extensive grass cover
- 8
- 9 • The resurfaced zone around the facility that has no vegetation cover
- 10
- 11 • The WMA A-AX zone that corresponds to the tank farm gravel backfill that is not
- 12 covered by vegetation
- 13
- 14 • The WMA C zone that corresponds to the tank farm gravel backfill that is not covered by
- 15 vegetation.
- 16

17 **Early Post-Closure.** At the end of the construction period, the early post-closure period is
18 considered to represent the time when the modified RCRA C barrier functions according to its
19 design specifications for 500 years according to DOE/RL-93-33. The closure barrier functions to
20 limit the flow of infiltrating moisture into the system by its water storage capacity and built-in
21 engineered capillary breaks. During this period, distinct recharge rates are assigned to
22 five spatially distinct zones (Figure 6-17):

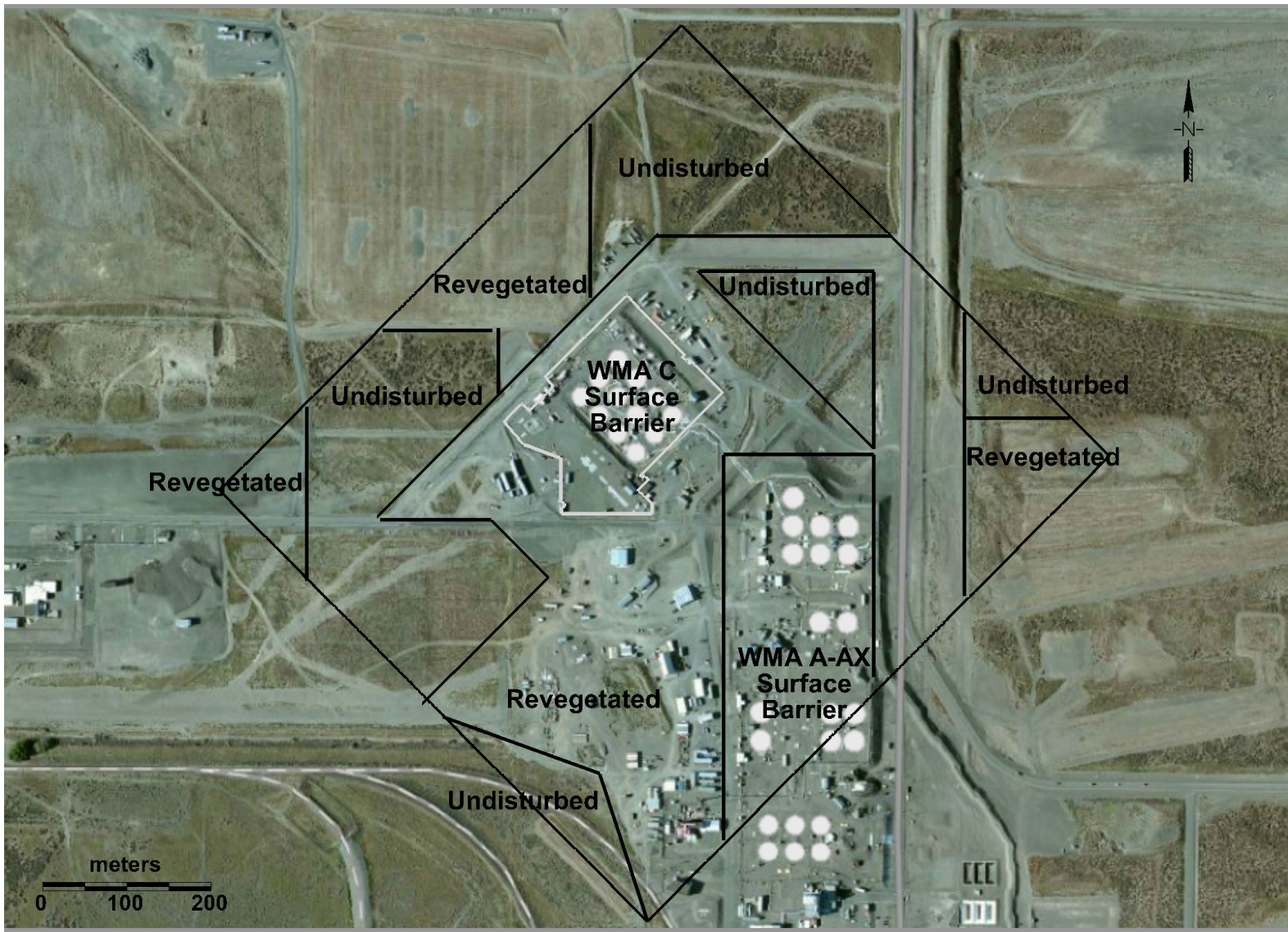
- 23
- 24 • The undisturbed zone, away from the WMA C surface barrier and the surrounding berm,
- 25 characterized by an undisturbed native vegetation cover
- 26
- 27 • The disturbed zone, away from the WMA C surface barrier and the surrounding berm,
- 28 characterized by an artificially-introduced vegetation cover attempting to reclaim the
- 29 surface with native vegetation species
- 30
- 31 • The resurfaced zone, away from the WMA C surface barrier and the surrounding berm,
- 32 characterized by an artificially-introduced vegetation cover attempting to reclaim the
- 33 surface with native vegetation species
- 34
- 35 • The zone beneath the extent of the WMA A-AX surface barrier that is designed to
- 36 minimize infiltration of meteoric waters
- 37
- 38 • The zone beneath the extent of the WMA C surface barrier that is designed to minimize
- 39 infiltration of meteoric waters.
- 40

1 **Figure 6-16. Surface Conditions In and Around Waste Management Area C during the Construction and Operations Period.**
2



WMA = Waste Management Area

Figure 6-17. Inferred Surface Conditions In and Around Waste Management Area C during the Post-Closure Period.



WMA = Waste Management Area

RPP-ENV-58782, Rev. 0

Late Post-Closure. Finally, a late post-closure period is considered to represent the functioning of a degraded surface barrier. This period will start at the end of its assumed design life expectancy of the surface barrier (year 2520) and will continue through the rest of the simulated time period. A distinct recharge rate will be assigned to three different zones during this period (Figure 6-17):

- The undisturbed, disturbed, and resurfaced zones away from the WMA C barrier characterized by undisturbed or reclaimed native vegetation cover
- The degraded WMA A-AX surface barrier fully covered with vegetation that has undergone reclaiming soil and ecological processes
- The degraded WMA C surface barrier fully covered with vegetation that has undergone reclaiming soil and ecological processes.

6.2.2.1.3 Vadose Zone Beneath Waste Management Area C. The vadose zone underlying WMA C consists of heterogeneous layers of sedimentary units that vary in thickness at different locations (see Section 3.1.9.1).

Conceptually, and for the purpose of simplification, each heterogeneous sedimentary unit is defined as an EHM having macroscopic flow properties as discussed in Appendix B. The porous media continuum assumption, an extended form of Darcy-Buckingham Law for vadose zone applications and the soil relative permeability/saturation/capillary pressure relations, provides the basis for vadose zone flow and transport modeling. In the model domain, the hydraulic properties describing flow and transport characteristics associated with each geologic layer are approximated by average up-scaled values. The upscaled hydraulic property values used in the flow and transport model for each EHM are derived from small- and micro-scale (sample) measurements (Appendix B). Each EHM unit thus possesses different flow and transport parameters (hydraulic conductivity, bulk density, and dispersivity). For each heterogeneous HSU having spatially variable hydraulic properties, moisture-dependent anisotropy represents the bulk behavior for the EHM (“Application of Stochastic Methods to Transient Flow and Transport in Heterogeneous Unsaturated Soils” [Polmann 1990]). The model thus describes the bulk (or mean) flow and contaminant transport behavior in the vadose zone that is applicable and appropriate to the evaluation and estimation of overall and eventual contaminant impacts to groundwater. Appendix B provides details on the approach for developing the effective (upscaled) flow and transport parameters for the vadose zone.

Features such as clastic dikes, sills, and tectonic structures can allow water and contaminants to bypass vadose zone continuum fate and transport processes. Clastic dikes (subvertical linear features composed of fine-textured sediments), discussed in Section 3.1.4.2.3, Clastic Dikes, do occur in the vadose zone, extend up to tens of meters in length, and crosscut the major layers. Within the Central Plateau, there is little evidence of enhanced transport in these preferential pathways in arid and semiarid climates with low-water flux in the vadose zone, particularly where soils are coarse-grained such as in Hanford formation sediments (“Influence of Clastic Dikes on Vertical Migration of Contaminants at the Hanford Site” [Murray et al. 2007]). While these features may form preferentially faster flow pathways under saturated conditions, under

RPP-ENV-58782, Rev. 0

unsaturated flow conditions these features tend to act as barriers to transport. Precipitation at arid sites is usually too low (in relation to saturated hydraulic conductivity) to invoke preferential flow. Much of the water in the dry soils is simply retained on grain surfaces by capillary forces and does not move along preferential pathways (Murray et al. 2007; “Hydrologic Mechanisms Governing Fluid Flow in a Partially Saturated, Fractured, Porous Medium” [Wang and Narasimhan 1985]).

6.2.2.1.4 Aquifer System Beneath Waste Management Area C. The integrated, saturated-unsaturated, 3-D WMA C PA model calculates concentrations of radionuclides in groundwater downgradient of the WMA C fenceline. For these calculations, flow and transport parameters need to be estimated for the unconfined aquifer because, as recharge containing contaminants enters the aquifer, the leachate mixes with groundwater and becomes more dilute. The flow and transport parameters needed for unconfined aquifer calculations are saturated hydraulic conductivity, specific storage, effective porosity, hydraulic gradient, depth to water table, and dispersivity.

A fundamental difference exists as to how the large-scale macroscopic parameters are derived for saturated media versus unsaturated media. First, in a highly heterogeneous flow domain such as WMA C exists a hierarchy of length scales that needs to be recognized (Appendix C, Figure C-1) and an increase in parameter estimates with an increase in flow domain is noticeable. The evolving heterogeneities at various length scales result in a scale dependence of effective parameters such as saturated hydraulic conductivity and dispersivity. For WMA C PA saturated media modeling, the flow domain of interest is the “Field Scale,” which is shown on the right of Figure C-1. The unconfined aquifer is treated as an EHM, and an equivalent saturated hydraulic conductivity is estimated for the undifferentiated Hanford gravels (Appendix C).

For the large-time, large-scale PA modeling applications, the macro-scale parameterization for saturated media effective parameters depends on the configuration of the heterogeneous media, as well as the establishment and setup of the local boundary conditions. This is unlike the WMA C vadose zone parameterization wherein the effective parameters at the large and macro scale are derived from properties at the small and micro scale using upscaling methods. Instead, the effective parameterization for WMA C saturated media hydraulic conductivity, for example, is best achieved via a field-scale calibrated groundwater model, which accounts for appropriate local-scale boundary conditions, flow configuration, and history matching. Estimates of hydraulic properties are based on the groundwater flux in the aquifer around WMA C according to the Central Plateau groundwater model calibration reported in CP-47631, “Model Package Report: Central Plateau Groundwater Model Version 6.3.3.” Flux is a rate measurement defined as the flow through a defined area. It is well suited for the PA because the emphasis of its evaluation is the contaminant mass conveyed through the aquifer to a PoCal aligned with the direction of groundwater flow. Thus, the hydraulic property values derived from the calibrated Central Plateau groundwater model fluxes are applied to the WMA C PA flow model domain.

6.2.2.1.5 Radionuclide Transport in the Environment. The geochemical and sorption conceptual model primarily concerns the movement and retardation of contaminants in the vadose zone. For the PA analysis, the empirical equilibrium sorption-based approach is assumed to approximate contaminant sorption during transport. The focus of the modeling is on far-field

RPP-ENV-58782, Rev. 0

transport, away from WMA C, with the bulk of the residence time of contaminants likely to be in the thick vadose zone. Concentration-dependent sorption/desorption of radionuclides, development of reaction fronts from dissolution and precipitation of mineral phases, and variable soil vapor pressures are possible at or very close to the tanks, vault, and pipelines. But away from these structures, due to mixing and continued buffering by mineral-water reactions, residual waste-derived water is expected to become similar to the ambient pore water within a short distance from the base of WMA C. The effluent concentrations from the base of the tank are likely to be so low that they cannot appreciably diminish the thick vadose zone's substantial capacity for sorption and buffering.

The use of the linear isotherm (constant K_d model) is assumed to be generally applicable when: (1) contaminants are present at low concentrations, (2) the geochemical environment being modeled is not affected by large spatial or temporal changes, and (3) the possible sorption sites occupied by the contaminant remain much less than the sorption capacity over the scale of transport. K_d values are chosen assuming low-salt, near-neutral waste chemistry. It is acknowledged that the K_d values used in fate and transport models are effective K_d values representing the effective combinations of processes contributing to the overall contaminant retardation and/or release behavior. The advantage of the empirical linear adsorption model or K_d approach is that it is easy to implement and generally deemed sufficient for modeling contaminant transport in the far-field through thick sediment column (DOE/RL-2011-50, Regulatory Basis and Implementation of a Graded Approach to Evaluation of Groundwater Protection).

6.2.2.1.6 Summary of Assumptions. The integrated, saturated-unsaturated, 3-D WMA C PA model calculates concentrations of radionuclides in groundwater downgradient of the WMA C fenceline. For the conceptual model, the following simplifying assumptions were made for the base case:

- WMA C closure occurs in 2020
- Release of radionuclides contained within the grouted residual waste is controlled by the process of diffusion, and remains diffusive with no advection occurring through the tank during the simulated time period of 10,000 years
- The impact of the varying size and shapes of waste material within the grouted tanks and ancillary equipment was ignored
- Moisture flow within the grouted tanks and ancillary equipment is negligible
- Episodic precipitation events and net infiltration through the thick, heterogeneous vadose zone in the 200 Areas can be approximated by an average annual recharge rate
- Impacts resulting from plausible climate change that may occur during the evaluation period do not adversely impact the performance of the surface or vadose zone as a barrier

RPP-ENV-58782, Rev. 0

- The modified RCRA Subtitle C barrier functions according to its design specifications for 500 years
- The impact of the closure barrier on moisture flow was approximated by an assumed recharge rate into the facility
- Flow in the vadose zone occurs in accordance with the porous media continuum assumption
- The hydrostratigraphy of the vadose zone is adequately represented by the delineation of equivalent homogeneous units for evaluating bulk (or mean) flow and contaminant transport
- Vadose zone hydraulic property values upscaled from small- and micro-scale (sample) measurements apply to the field scale for the equivalent homogeneous units
- The inclusion of moisture-dependent anisotropy functions allows the homogeneous HSUs to adequately approximate the effects of heterogeneity
- Features such as clastic dikes, sills, and tectonic structures that can allow water and contaminants to bypass vadose zone continuum fate and transport processes are not consequential to the analysis
- Effective parameterization for WMA C saturated media is best achieved via a field-scale calibrated groundwater model (Appendix C).

6.2.2.2 Conceptual Model for Air Pathway. Gases and vapors can potentially diffuse upward from the residual waste in the WMA C tanks and ancillary equipment to the ground surface. The principal mechanism by which contaminants migrate from the waste to the ground surface is gaseous diffusion along the air-filled pore spaces that are assumed to be continuous.

Of the contaminants contained in WMA C wastes at closure, four of them could potentially originate as gas from the residual wastes:

- Carbon-14 as CO₂ gas
- Hydrogen-3 as H₂ gas
- Iodine-129 as I₂ gas
- Radon-222 as radon gas.

Due to the small inventory of these radionuclides in the tank residuals, the dose contribution from the air pathway is expected to be small (relative to the groundwater pathway). Since tanks will be fully grouted at closure and the residual waste layer is conceptualized to be present near the base of the tank, it is assumed that grout will behave as a porous medium, and gases could slowly emanate and diffuse through the tortuous pathway along the gas-filled pore space. The

RPP-ENV-58782, Rev. 0

releases are driven by the partitioning of the radionuclides among the aqueous phase, solid phase, and gaseous phase, and therefore modeled by considering the following equilibrium coefficients:

- K_d for solid/water phase partitioning
- Henry's law constant (K_h) for air/water partitioning.

The atmospheric transport pathway calculations are conducted in two steps. The first step calculates the diffusive flux from the residual waste to the ground surface, while the second step calculates the transport in air to the receptor location. The details of each step are described below.

1. Gaseous fluxes emitted from each source term (tanks and ancillary equipment) are calculated by assuming a zero concentration boundary at the surface. This is conceptually equivalent to having a large enough wind speed near the ground surface of WMA C that the air parcel is renewed constantly, thereby maximizing the diffusive gradient.

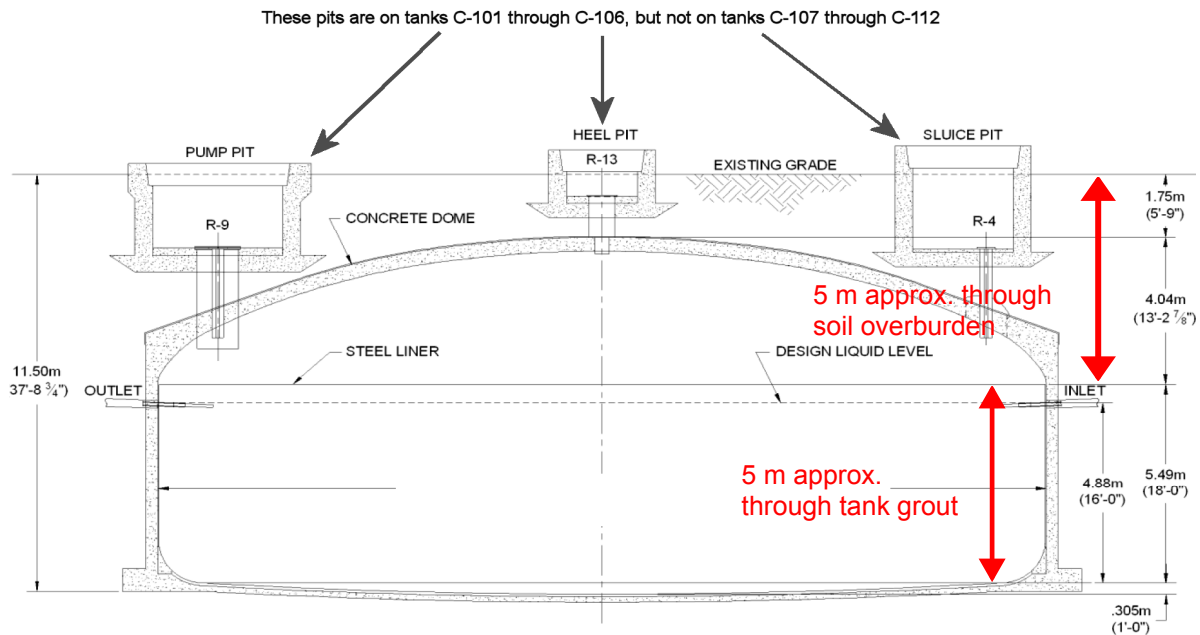
Upward diffusive gas phase transport through the SSTs, 244-CR vault, and C-301 catch tank is modeled to occur along a 10-m (32.8-ft)-long pathway towards the land surface. This pathway is split into a lower 5-m (16.4-ft) thickness composed of infill grout material, followed by another 5-m (16.4-ft) thickness of soil overburden (Figure 6-18). The diffusive area is the base area of each source term, consistent with the calculations described in Section 6.2.1. A surface barrier that will be emplaced at closure over the tank farm will provide additional diffusive pathway length to the surface but, for performing the air pathway calculations, this thickness is ignored. The diffusive length chosen is the minimum thickness over which gas-phase diffusion is likely to occur through the tortuous air-filled pore volume (defined by the air content). The 5-m (16.4-ft) thickness through the infill grout only considers the thickness up to the top of the steel liner, which is likely to remain as the minimum path length.

The air content within the infill grout is assumed to be 6% based on characterization information for possible Hanford grout (WSRC-TR-2005-00195). The air content of the soil overburden is calculated by taking the difference in the backfill porosity and soil moisture content that varies as a function of time. The air content of the infill grout for the purpose of diffusive release calculations is fixed over time, even though studies have indicated that chemical transformation of initial grout material will likely cause porosity reduction over time due to increased molar volume of the newly formed mineral phases. The effective diffusion coefficient for each gas is calculated separately by taking its binary diffusion coefficient in free air, under atmospheric pressure of 1 atm and a temperature of 20 °C (68 °F), and multiplying by the gas tortuosity.

The calculations consider equilibrium partitioning of contaminants among solid, water, and air phases. Assumed grout K_d values are applied for the 5-m (16.4-ft) diffusive pathway calculations within the infill tank grout material, while no sorption is assumed for the 5-m (16.4-ft) pathway length considered through the soil backfill material.

RPP-ENV-58782, Rev. 0

Figure 6-18. Conceptualization of Air Pathway Diffusive Release from the Tank to the Surface.



241-C-100 SERIES SST
530,000 GALLON CAPACITY

For the pipelines, the gas phase diffusive calculations are performed in a similar manner to that described above, except for consideration of the 5-m (16.4-ft) diffusive path length along the grout infill material. For pipeline analysis, only the 5-m (16.4-ft) diffusive path length along the soil overburden is considered.

- The gas-phase diffusive mass flux arriving at the surface for each source area (twelve 100-series tanks, four 200-series tanks, CR-Vaults, C-301 catch tank, and the pipelines) is captured and then transported (except for radon), assuming advection and dispersion via wind movement to the receptor placed 100 m (328 ft) downwind from the WMA C fenceline. The air mixing height is assumed to be 2 m (6.6 ft). Horizontal air dispersion is considered along the transport pathway, which is based on the expected air turbulence in and around WMA C.

The calculated air concentrations at the receptor location are used for evaluating air pathway dose, and are compared to the performance objective of 10 mrem/yr atmospheric release dose limit. On the other hand, the ^{222}Rn flux emanating at the surface from each source is compared to the performance objective of 20 pCi m⁻²s⁻¹ atmospheric release flux limit.

RPP-ENV-58782, Rev. 0

6.2.3 Exposure Pathways and Scenarios

This section discusses the exposure scenarios that are developed to meet DOE O 435.1 PA requirements.

An exposure pathway can be described as the physical course that a COPC takes from the point of presence in a specific environmental media to a receptor. The route of exposure is the means by which a COPC enters a receptor. An exposure scenario includes data and exposure parameters that describe how exposure occurs. The receptor is assumed to reside 100 m (328 ft) downgradient of the facility fenceline.

To meet the DOE O 435.1 requirements, an all-pathways farmer scenario is implemented to calculate the total effective dose equivalent for comparison to the performance objective of 25 mrem, which is the total effective dose equivalent in a year from all exposure pathways, excluding the dose from radon and progeny in air. In this scenario, calculations are performed based on predicted radionuclide transport through the groundwater pathway and atmospheric pathway, and exposure at the point of contact.

For the groundwater transport pathway, the single family farmer is assumed to reside 100 m (328 ft) downgradient from the facility fenceline and draw contaminated water from a well. The receptor is an adult who is assumed to use the water to drink, irrigate crops, and water livestock. The receptor is assumed to receive dose from the following exposure routes:

- Ingestion of water
- Ingestion of fruits and vegetables grown on the farm
- Ingestion of beef raised on the farm
- Ingestion of milk from cows raised on fodder grown on the farm
- Ingestion of eggs from poultry fed with fodder grown on the farm
- Ingestion of poultry fed with fodder grown on the farm
- Incidental ingestion of contaminated soil
- Inhalation of contaminated soil (dust) in the air
- Inhalation of water vapor
- External exposure to radiation.

The equations associated with each exposure route are implemented in the system model. The exposure parameter values used in the equations, along with element-specific bioconcentration factors (transfer coefficients), are based on guidance provided in various guidance documents from EPA, National Council on Radiation Protection and Measurements, International Atomic Energy Agency, and International Commission on Radiological Protection. The dose conversion factors (effective dose coefficients) on a radionuclide basis are taken from DOE guidance documents (DOE-STD-1196-2011 and EPA-402-R-93-081, Federal Guidance Report No. 12, External Exposure to Radionuclides in Air, Water, and Soil), respectively.

RPP-ENV-58782, Rev. 0

For the atmospheric transport pathway, the following three exposure routes are considered for the receptor residing 100 m (328 ft) downgradient of the facility fenceline:

- Air immersion
- Inhalation of dust
- External exposure to radiation from the contaminated ground surface.

DOE M 435.1-1 Change (Chg) 1 IV.P.(2) states that the PA shall include an assessment of impacts calculated for a hypothetical person assumed to inadvertently intrude for a temporary period into the LLW disposal facility. Inadvertent intruder scenarios are discussed in detail in Section 9.

To evaluate protection of water resources, radionuclide concentration in groundwater 100 m (328 ft) downgradient from WMA C fenceline is compared to drinking water standards specified by Title 40, CFR, Part 141, “National Primary Drinking Water Regulations,” Subpart G—National Primary Drinking Water Regulations: Maximum Contaminant Levels and Maximum Residual Disinfectant Levels, §141.66 Maximum contaminant levels for radionuclides (40 CFR 141.66) over the compliance period. Several separate comparisons are required to evaluate compliance with drinking water standards, as follows.

- Combined ^{226}Ra and ^{228}Ra – concentrations are added and the sum must be less than 5 pCi/L.
- Gross alpha activity (excluding radon and uranium) – the sum of concentrations for each radionuclide that decays by alpha particle emission must be less than 15 pCi/L.
- Beta and Gamma Emitters – the sum of all radionuclides that emit either a beta particle or gamma radiation must be less than 4 mrem/yr to the total body or any internal organ. The dose must be calculated assuming an individual who drinks 2 L/day (0.5 gal/day) of the contaminated water.
- Strontium-90 – concentrations must be less than 8 pCi/L.
- Tritium – concentrations must be less than 20,000 pCi/L.
- Total uranium (metal) – concentrations must be less than 30 $\mu\text{g/L}$ (3.0×10^{-5} oz/ft³).

6.3 MATHEMATICAL MODELS

This section presents development and implementation of mathematical models that are used to evaluate flow and radionuclide transport and long-term human health and environmental impacts. Mathematical models and their implementation into process-level or system-level models are described for the following components of the conceptual model of the closed WMA C facility including 1) source-term and engineered system (Section 6.3.1); 2) radionuclide

RPP-ENV-58782, Rev. 0

transport along the groundwater and atmospheric pathways (Section 6.3.2); and 3) exposure and dose analysis (Section 6.3.3).

6.3.1 Source Term and Engineered Features

The processes associated with the release of contaminants into the pore waters of the material in the tank and ancillary equipment, and their migration from the residual waste matrix through the surrounding engineered barriers, are denoted as the source term in this PA.

The experimental observation and conceptualizations related to each of these processes has been presented in Sections 5 and Section 6.2.1. The objective of this section is to present the mathematical description of the processes implemented for modeling the release of contaminants from the waste form (source) through the engineered features (tank) to the near-field just outside the tanks and ancillary equipment.

While the tank (and ancillary equipment) infill material remains intact, it is assumed that releases occur by diffusion through the base of the tank base mat, consisting of grout and concrete layers. For volatiles released from the residual wastes, it is assumed that their transport through the tank infill grout material and the soil overburden is controlled by upward diffusion.

Both mineral phase solubility-limited and matrix degradation rate-limited processes are considered for the key analytes. These have been studied in detail in the laboratory, and the laboratory results have been incorporated in the source term analysis. In particular, the following release models are used, which are based on empirical evidence:

- a matrix-degradation-rate-based release of ^{99}Tc
- solubility-controlled releases of uranium.

In the two subsections that follow, the empirical evidence for the release models for ^{99}Tc and uranium is established. Multi-year leaching studies have been conducted on tank residual samples focused on leaching behavior of key contaminants such as ^{99}Tc and uranium. Based on evaluation of the results, models based on solubility control or matrix degradation are implemented in the PA calculations for ^{99}Tc and isotopes of uranium, as discussed below. For all other radionuclides evaluated in this PA, conservative source-term calculations are performed whereby all of the radionuclides are assumed to be instantly and completely available in solution within the residual waste volume, and available for an immediate diffusive release.

The next two subsections discuss the basis for the diffusion coefficients for the aqueous and air pathways, and the basis for the sorption of contaminants in the grout/concrete layer. Finally, in the last subsection, the basis is presented for considering diffusive releases for the source term when the tank structure and infill grout material are intact.

6.3.1.1 Source Release Model for Technetium-99. The matrix-degradation-rate-based release model developed for ^{99}Tc is based on the results of the SPFT experiments conducted on C-103, C-202, and C-203 tank residual waste. The experimental setup and analyses results are presented in PNNL-20616, "Contaminant Release from Hanford Tank Residual Waste – Results

RPP-ENV-58782, Rev. 0

of Single-Pass Flow-Through Tests” and in Cantrell et al. 2013. These tests were conducted under low flow conditions (~ 0.1 mL/hr [0.06 in.³/hr]) for a period of about six months with no stirring of residual waste in the solution. The initial solution-to-solid weight ratio is 120 (based on 0.06 L [0.016 gal] of initial solution in contact with 0.5 g [0.018 oz] sample), and the residence time of the solution in the reaction vessel was calculated to be 25 days. The initial concentrations of ^{99}Tc reported in the samples were: 0.23 $\mu\text{g/g}$ (0.0081 oz/ton) for tank C-103, 0.23 $\mu\text{g/g}$ (0.0081 oz/ton) for tank C-202, and 0.11 $\mu\text{g/g}$ (0.0039 oz/ton) for tank C-203. Appendix A of PNNL-20616 provides the complete tabulation of the analytical results that are relevant to the PA for the three leachates—namely, deionized water, CaCO_3 saturated solution, and 0.005 M $\text{Ca}(\text{OH})_2$ solution. The results of the leaching for the three tank residual waste samples are presented in Figure 6-19. The ^{99}Tc concentrations in all three leachates are very similar, with the concentrations appearing to drop off exponentially with increasing solution-to-solid ratio. The initial sample concentration was low because the leachate solutions contained no ^{99}Tc .

The results of the SPFT experiments were further analyzed to quantify the fractional leaching rate of ^{99}Tc using the 0.005 M $\text{Ca}(\text{OH})_2$ solution, since it is expected that infill grout will condition the chemistry of incoming waters for a very long time period.

- a) The results presented in Table A of PNNL-20616 in terms of solution-to-solid ratio are first converted to elapsed time (in days), based on 25 days of residence time in the reaction vessel being equivalent to 120 initial solution-to-solid ratio.
- b) The initial concentration of ^{99}Tc in the residual waste sample is used, along with the mass of the sample, to estimate the initial ^{99}Tc mass (in terms of grams).
- c) Based on reported ^{99}Tc concentrations ($\mu\text{g/L}$) in the effluent, the cumulative mass of ^{99}Tc leached is calculated and then converted to fraction of initial mass leached. From this, the fraction of mass remaining in the solid sample is calculated as a function of time.
- d) An exponential trend line is fitted to the fraction remaining (as a function of time) and the rate constant is derived (in units of day^{-1}), which represents a first-order release rate from the solid to the solution. The trend line is fitted to the dataset following flushing of resident vessel volume (approximately 25 days) and while the concentrations are above the detection limit.

The fraction remaining for ^{99}Tc along with the fitted trend line results are presented in Figures 6-20 through 6-22. The results indicate that the first-order reaction rate constant defining the release of ^{99}Tc from the residual waste varies over a narrow range of 5×10^{-4} to 8×10^{-4} day^{-1} . This rate constant reflects the longer-term rate of release of ^{99}Tc following the initial release as noted by the early spike in concentration in Figure 6-19 (a-c). The percent ^{99}Tc leached from the various SPFT experiments varies from 4.5 to 15% (as noted in Table 5-3), and is influenced more by the particular sample type than by the type of the leachate.

Figure 6-19. Technetium-99 Concentration in Single-Pass Flow-Through Leachates for (a) Tank 241-C-103, (b) Tank 241-C-202, and (c) Tank 241-C-203 as a Function of the Total Volume of Leachate that has Contacted the Waste in Terms of Leachate Solution to Solid (Initial) Weight Ratio. (1 of 3 sheets)

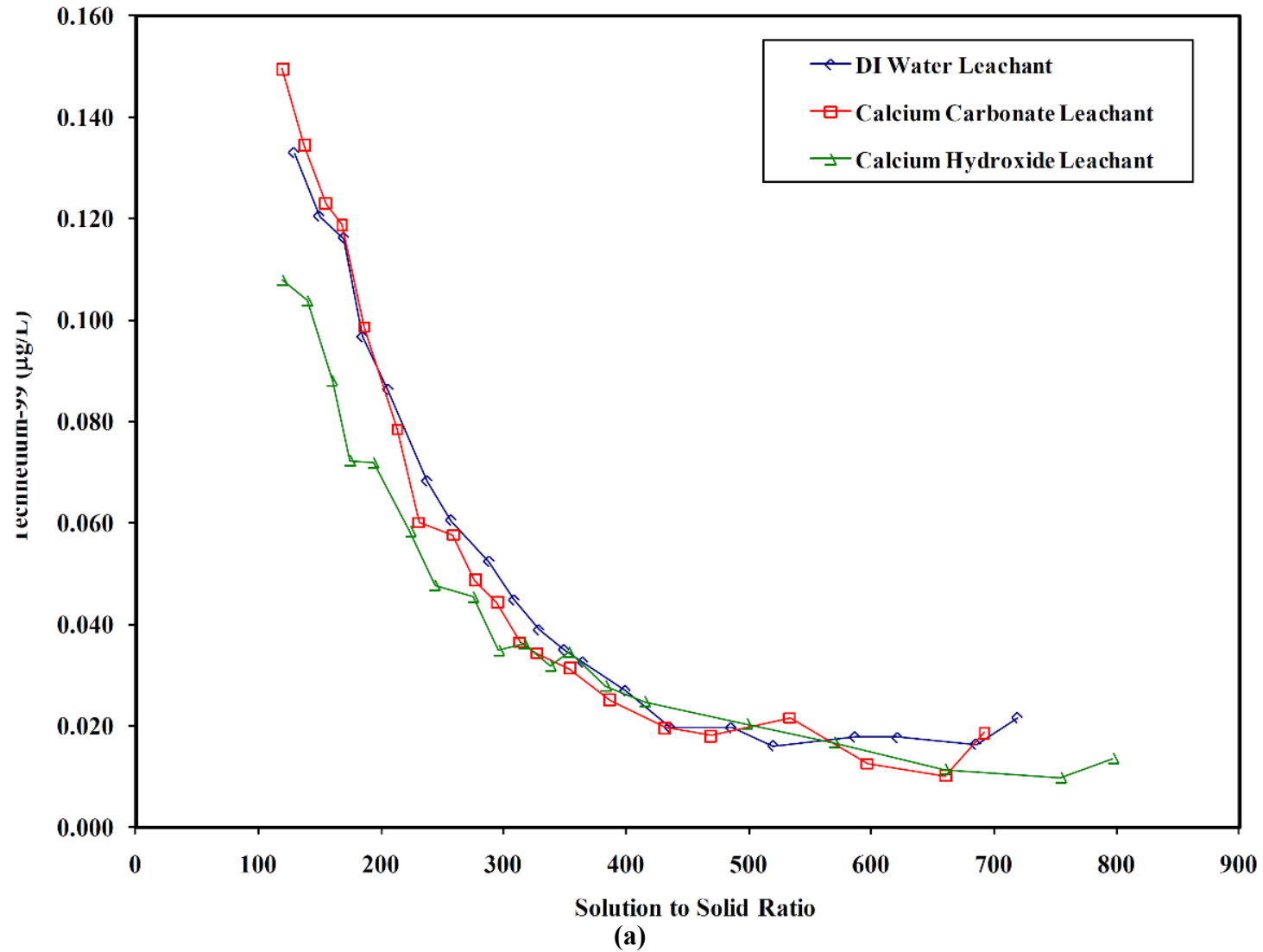


Figure 6-19. Technetium-99 Concentration in Single-Pass Flow-Through Leachates for (a) Tank 241-C-103, (b) Tank 241-C-202, and (c) Tank 241-C-203 as a Function of the Total Volume of Leachate that has Contacted the Waste in Terms of Leachate Solution to Solid (Initial) Weight Ratio. (2 of 3 sheets)

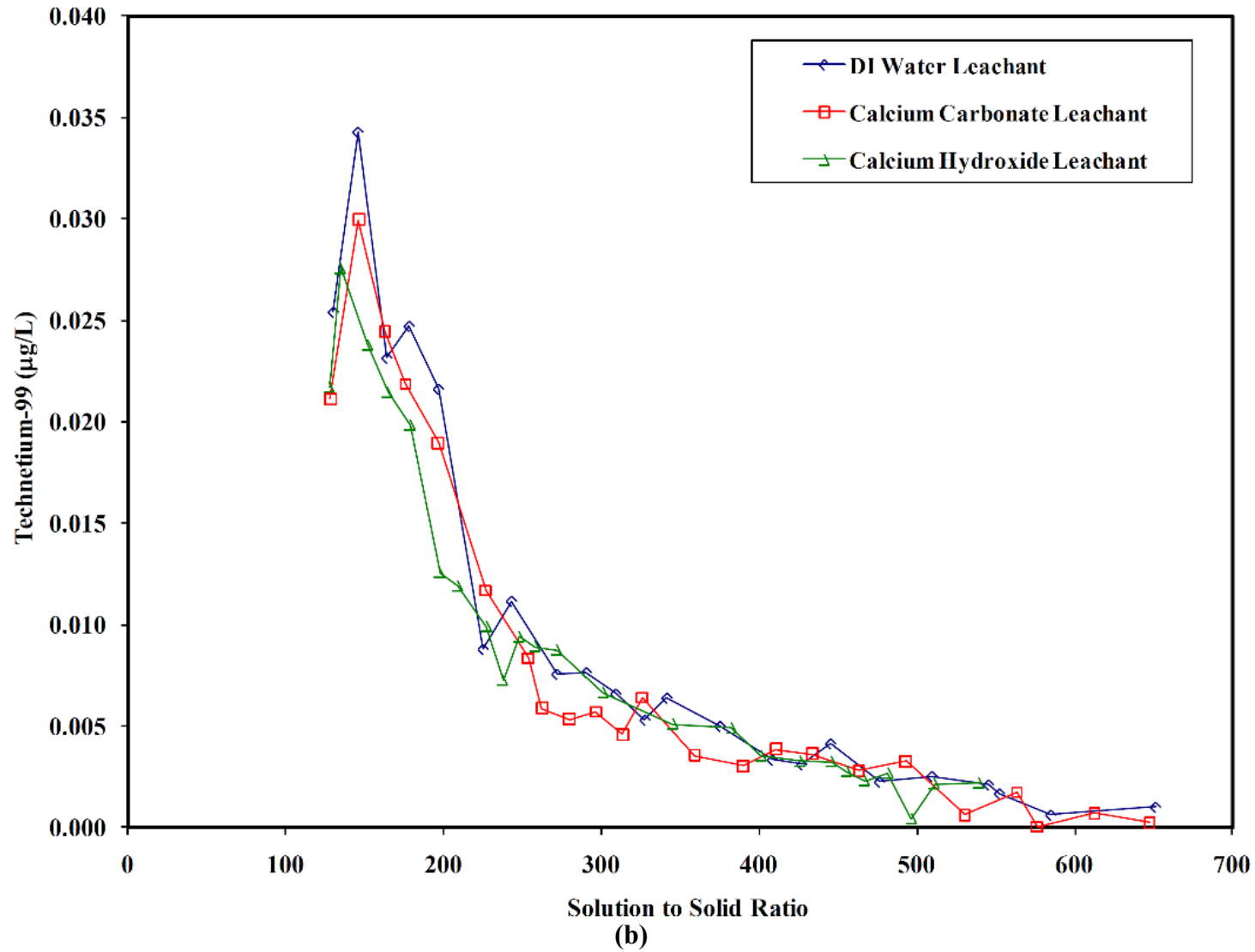
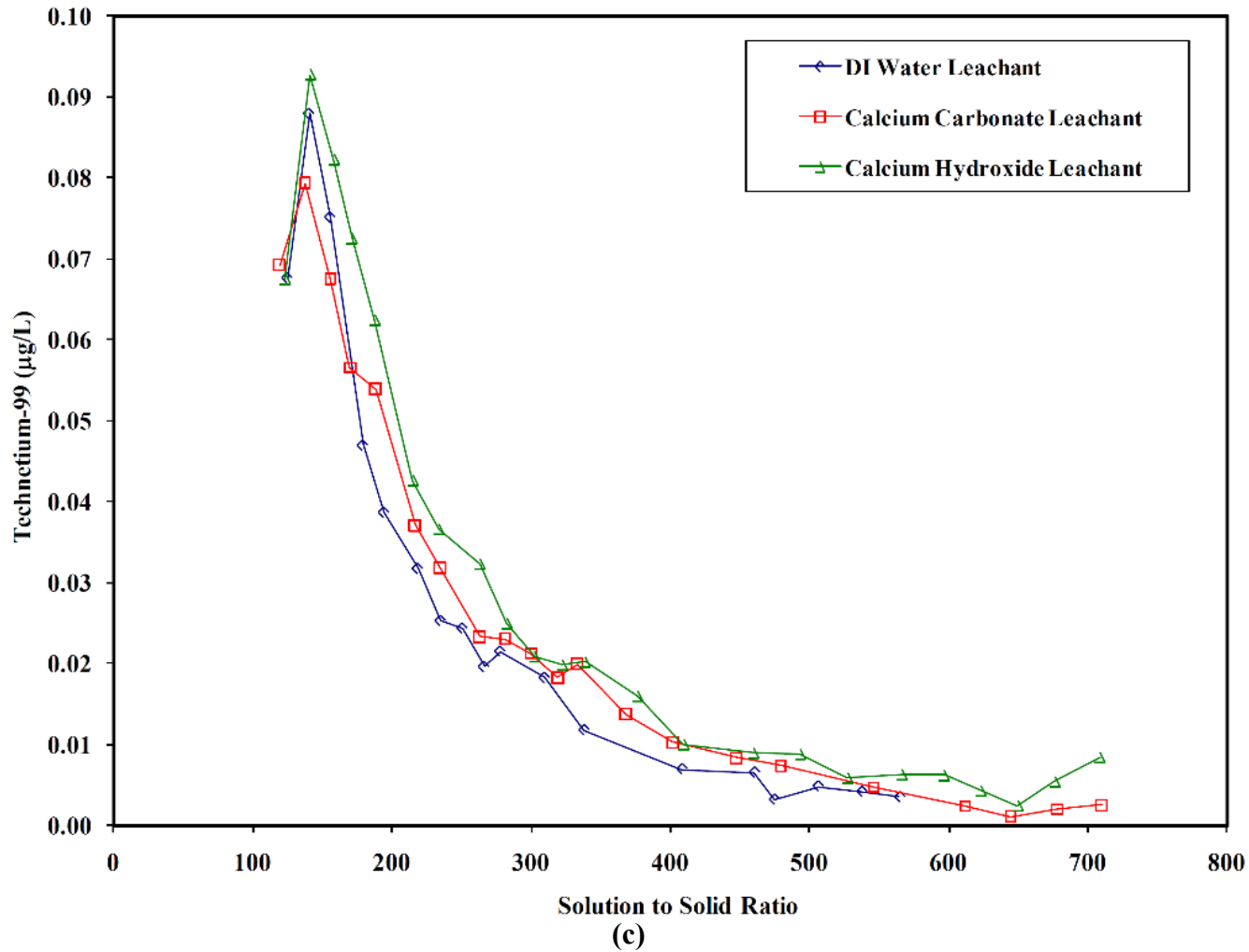


Figure 6-19. Technetium-99 Concentration in Single-Pass Flow-Through Leachates for (a) Tank 241-C-103, (b) Tank 241-C-202, and (c) Tank 241-C-203 as a Function of the Total Volume of Leachate that has Contacted the Waste in Terms of Leachate Solution to Solid (Initial) Weight Ratio. (3 of 3 sheets)

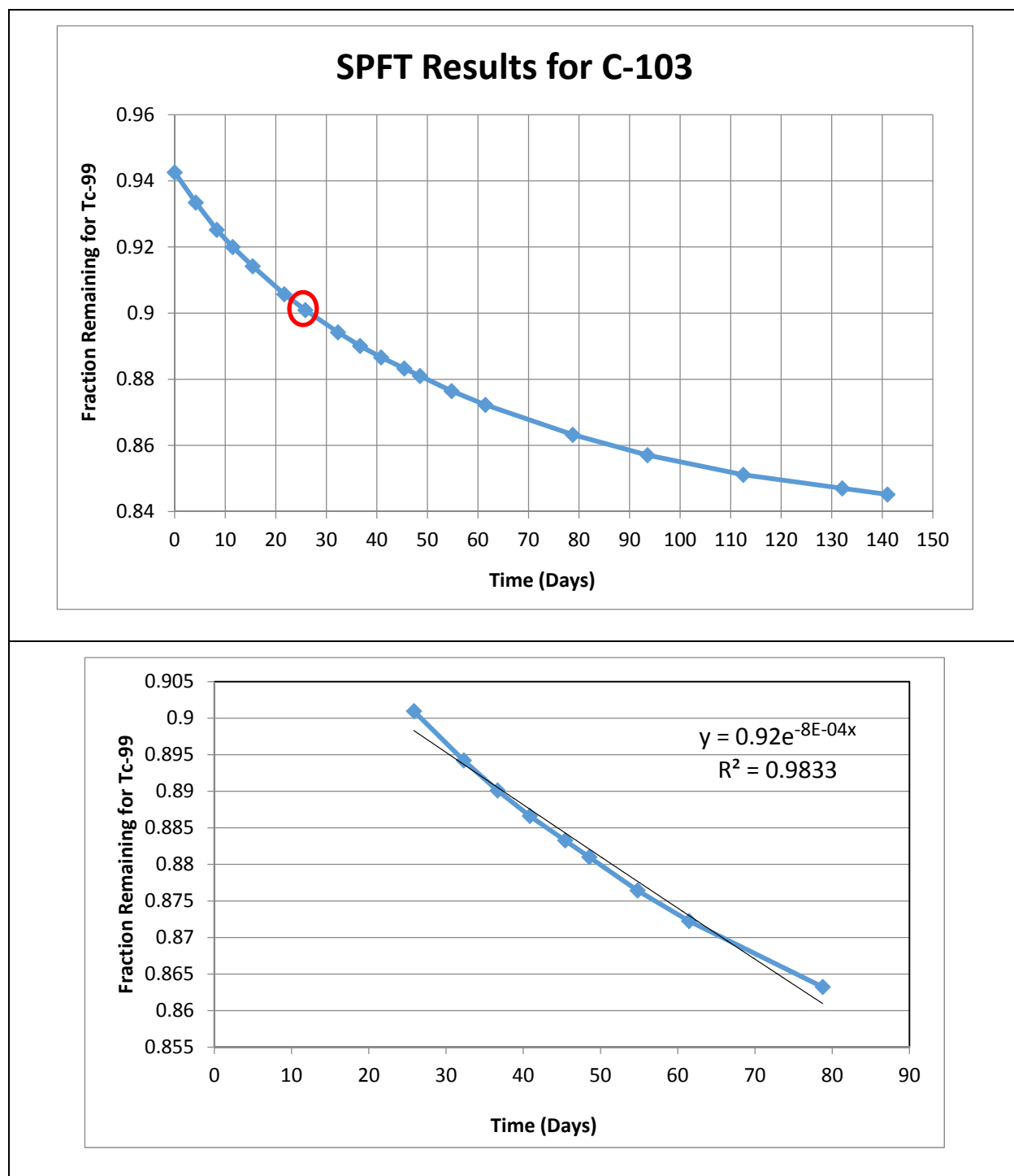


DI = deionized

Source: PNNL-20616, "Contaminant Release from Hanford Tank Residual Waste – Results of Single-Pass Flow-Through Tests."

RPP-ENV-58782, Rev. 0

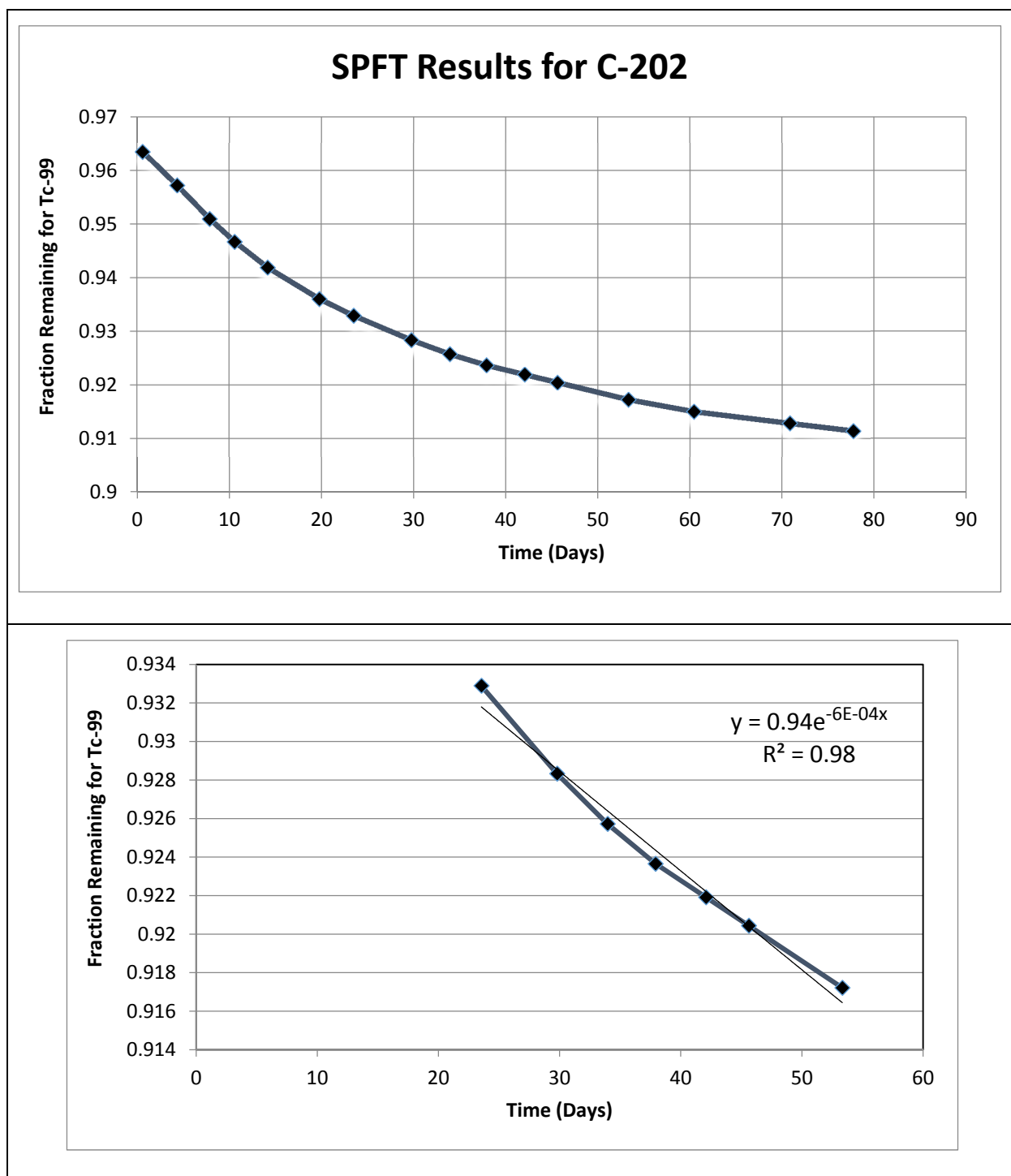
Figure 6-20. Fractional Release of Technetium-99 for Single-Pass Flow-Through Experiments from Tank 241-C-103 Along with the Estimate of the First-Order Reaction Rate Constant of 8E-04 day⁻¹.



1 SPFT = Single-Pass Flow-Through
2

RPP-ENV-58782, Rev. 0

Figure 6-21. Fractional Release of Technetium-99 for Single-Pass Flow-Through Experiments from Tank 241-C-202 Along with the Estimate of the First-Order Reaction Rate Constant of 6E-04 day⁻¹.

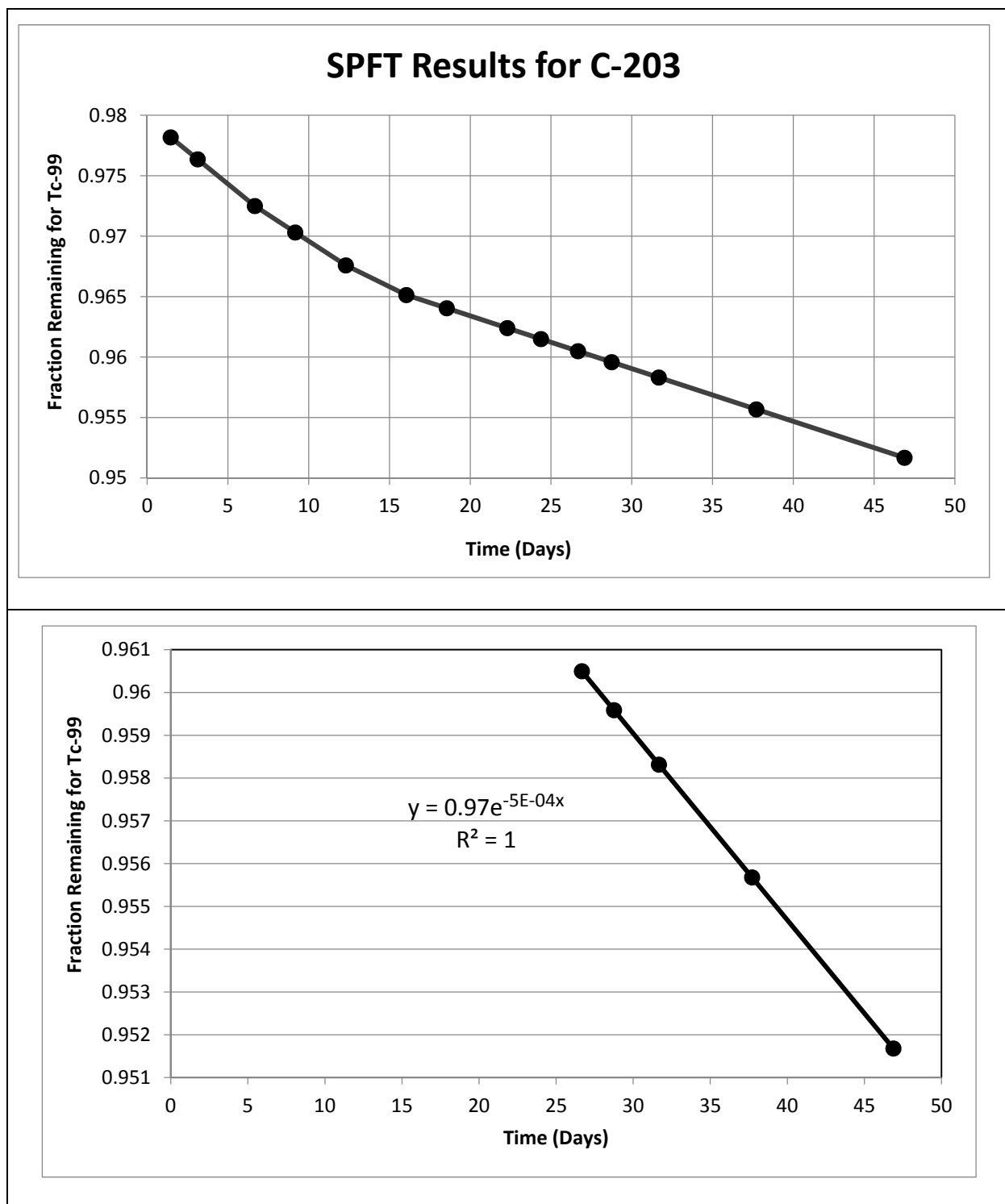


1 SPFT = Single-Pass Flow-Through

2

RPP-ENV-58782, Rev. 0

Figure 6-22. Fractional Release of Technetium-99 for Single-Pass Flow-Through Experiments from Tank 241-C-203 Along with the Estimate of the First-Order Reaction Rate Constant of 5E-04 day⁻¹.



1 SPFT = Single-Pass Flow-Through

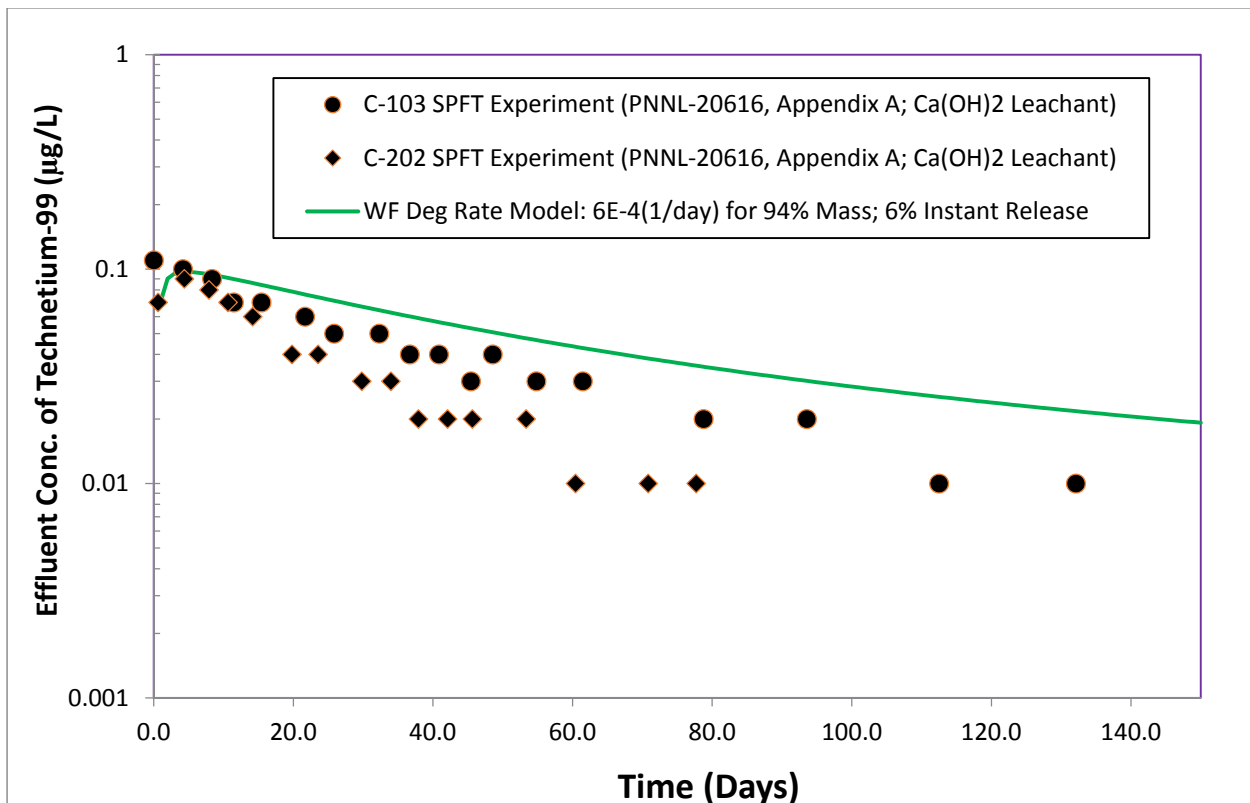
2

RPP-ENV-58782, Rev. 0

To make the source release model for ^{99}Tc consistent with the observations, an initial 6% fraction of the ^{99}Tc inventory is considered to be instantaneously available for release, while the remaining 94% fraction undergoes relatively slower release at the fractional rate of $6 \times 10^{-4} \text{ day}^{-1}$. These estimates of parameters are implemented in the base case. The uncertainty in the initial release fraction and the fractional release rate is evaluated separately (see Section 8).

In order to evaluate the adequacy of the ^{99}Tc release model, a calculation is performed using the base case estimate parameters to simulate the release of ^{99}Tc from the SPFT experiments, which are then compared to the observed concentration in C-103 and C-202 tank effluents. The calculation setup is similar to the reactor vessel volume and flow rate used for doing the SPFT experiments. The results of the calculations are presented in Figure 6-23, indicating that the base case parameters capture the release of ^{99}Tc and lead to conservative dissolved concentrations for calculating the diffusive flux.

Figure 6-23. Simulated Versus Observed Effluent Concentrations of Technetium-99 ($\mu\text{g/L}$) from the Single-Pass Flow-Through Experiments Conducted on Tanks 241-C-103 and 241-C-202 Residual Waste. The simulated concentrations are based on best estimate release parameters from residual waste.



SPFT = Single-Pass Flow-Through

Reference: PNNL-20616, "Contaminant Release from Hanford Tank Residual Waste – Results of Single-Pass Flow-Through Tests."

RPP-ENV-58782, Rev. 0

6.3.1.2 Source Release Model for Uranium. As discussed in Section 5, laboratory leaching tests have been conducted on residual waste samples from various tanks. Cantrell et al. (2013) provided the analysis of residual waste following leaching with three different leachates—namely, DI (deionized) water, CaCO_3 saturated solution, and 0.005 M Ca(OH)_2 solution. These three leachates represent a range of possible water types contacting the residual waste. The CaCO_3 saturated solution was used to simulate a leachate produced by aged carbonate cement or a typical Hanford vadose zone pore water, 0.005 M Ca(OH)_2 solution was used to represent the likely influence of interaction of infiltrating vadose zone pore water with portlandite [Ca(OH)_2] in the grouted tanks, and the DI water was used as a baseline for the leach tests to evaluate the influence of waters that have not been altered by reactions with the Ca(OH)_2 and CaCO_3 leachates.

The general trends in uranium leachate concentrations for the C-103, C-202, and C-203 tank residual wastes are very similar. The results are presented for tank C-202 in Figure 5-4. The leached uranium concentration using DI water and CaCO_3 saturated solution are significantly higher than those in the 0.005 M Ca(OH)_2 leachates. This is attributed to forming Ca-rich precipitates (Ca phosphate and calcite) on the surfaces of the waste particles when using Ca(OH)_2 leachate, inhibiting dissolution of the underlying uranium phases in the waste. Since the tanks are planned to be grouted prior to closure, the primary leachate is expected to be Ca(OH)_2 saturated solution (Deutsch et al. 2011), which is likely to reduce the leaching of uranium.

To investigate this leaching behavior, thermodynamic equilibrium modeling was conducted. The saturation indices (SIs) calculated for the tank C-202 SPFT effluents for the three leachates indicated that DI water and CaCO_3 saturated leachate give similar SI results, while the Ca(OH)_2 leachate SI results are quite different. Results from DI water and CaCO_3 saturated leachates indicate that $\text{NaUO}_2\text{PO}_4 \cdot x\text{H}_2\text{O}$ is near equilibrium while Ca-containing phases (such as calcite and hydroxylapatite) were all undersaturated. The SI results for the Ca(OH)_2 leachates indicate all uranium-bearing phases to be highly undersaturated but are near-saturated or oversaturated with respect to Ca-containing phases. Calcite was near saturation, while hydroxylapatite and fluorapatite were consistently highly oversaturated.

These results are consistent with the observed leaching behavior of uranium. It is hypothesized that precipitation of Ca-rich phases resulted in coatings on the waste particles that could have temporarily inhibited dissolution and attainment of equilibrium for any uranium phase in contact with Ca(OH)_2 leachate solutions.

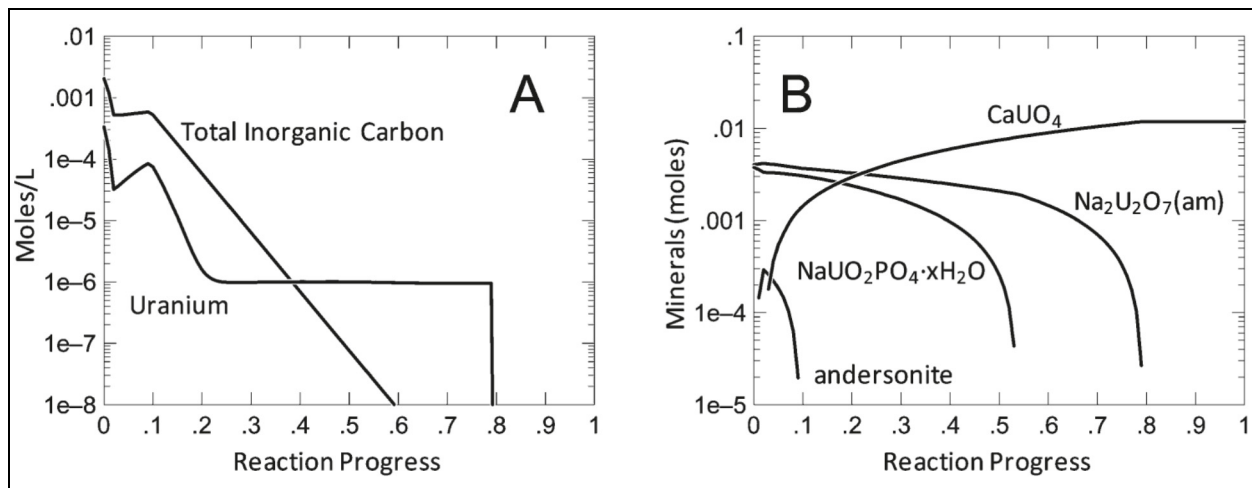
These results indicate that as long as the infiltrating water though the tank passes through the infill grout material, it will be conditioned to be similar to a dilute Ca(OH)_2 leachate solution and the uranium dissolution will remain inhibited (Cantrell et al. 2013). At some distant time in the future when the tank is assumed to be sufficiently degraded such that large open fractures develop that do not allow appreciable residence time for infiltrating waters to contact and equilibrate with the grout material, the leachate would be similar to the CaCO_3 saturated water, and at that time the uranium concentrations may increase when the residual waste is contacted.

RPP-ENV-58782, Rev. 0

Reaction-path modeling was undertaken in “Thermodynamic Model for Uranium Release from Hanford Site Tank Residual Waste” (Cantrell et al. 2011) to evaluate the uranium release under the $\text{Ca}(\text{OH})_2$ and CaCO_3 saturated waters by applying an infiltration rate of 1 mm/yr (0.039 in./yr) through the tank material over 10,000 years. The steel of the tank itself was assumed to have no impact on the hydrology or system chemistry, and the waste was assumed to be uniformly distributed at the bottom of the tank. The results of this reaction-path modeling are summarized below.

For $\text{Ca}(\text{OH})_2$ saturated water, the tank was assumed to be filled with cementitious material (i.e., concrete or grout), and the composition of the simulated pore water was assumed to be 0.015 M $\text{Ca}(\text{OH})_2$ and 1×10^{-5} M SI. The results of the reaction progress in terms of the uranium and total inorganic carbon (TIC) concentrations and the paragenetic sequence of uranium phases over the course of 10,000 years are shown in Figure 6-24. Initially, high uranium concentrations occur in solution ($\sim 3 \times 10^{-4}$ M) because of high carbonate complexation of uranium, but decline rapidly and rebound somewhat as a small amount of andersonite $[\text{Na}_2\text{CaUO}_2(\text{CO}_3)_3 \cdot 6\text{H}_2\text{O}]$ first precipitates and then dissolves. As the reaction progress continues, $\text{NaUO}_2\text{PO}_4 \cdot x\text{H}_2\text{O}$ dissolved preferentially to $\text{Na}_2\text{U}_2\text{O}_7(\text{am})$. As carbonate continues to leach from the waste, uranium concentrations continue to decline until a plateau is reached at approximately 1×10^{-6} M. This occurs at the approximate point where CaUO_4 becomes the dominant phase. A dramatic reduction in uranium concentrations occurs when $\text{Na}_2\text{U}_2\text{O}_7(\text{am})$ dissolved completely, leaving CaUO_4 as the only phase to control uranium release concentrations. A reaction progress of 1.0 is equivalent to 1 mm/yr (0.039 in./yr) of flow for 10,000 years, and therefore represents 10,000 mm (394 in.) of flow.

Figure 6-24. Uranium and Total Inorganic Carbon Concentrations (A) and the Paragenetic Sequence of Uranium Phases Present in the Waste (B) as a Function of Reaction Progress for the $\text{Ca}(\text{OH})_2$ Saturated Water Scenario.
A reaction progress of 1 is equivalent to 10,000 years of infiltration at 1 mm/yr.



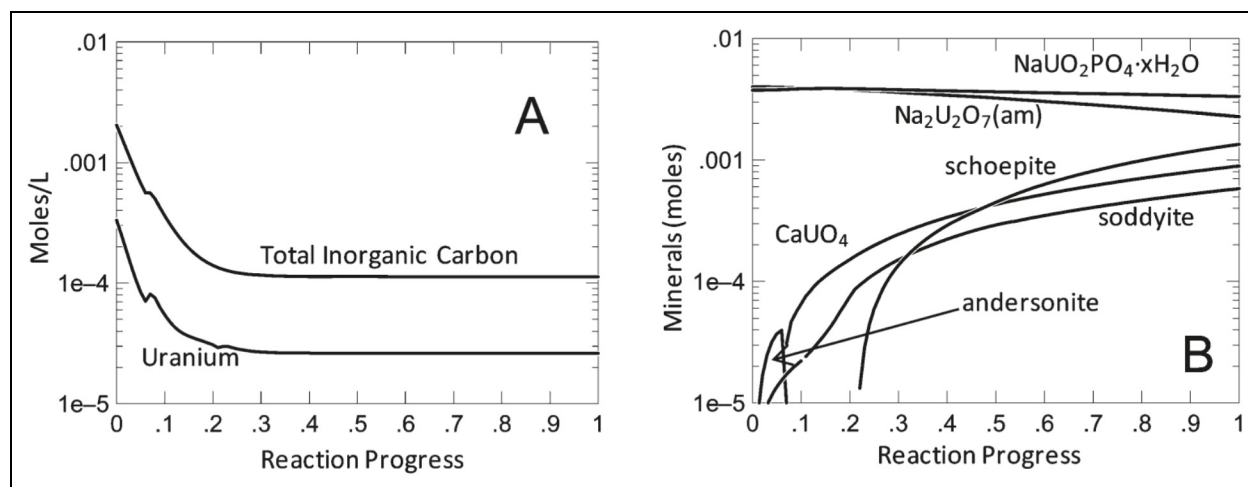
A similar reaction progress modeling calculation for the CaCO_3 saturated waters is shown in Figure 6-25. Initial high uranium concentrations in solution ($\sim 3 \times 10^{-4}$ M) occur because of high carbonate complexation of uranium due to soluble Na_2CO_3 or cejkaite $[\text{Na}_4(\text{UO}_2)(\text{CO}_3)_3]$. As

RPP-ENV-58782, Rev. 0

very soluble carbonate phases dissolve, the uranium concentration of $\sim 2.6 \times 10^{-5}$ M is maintained primarily by dissolution of $\text{NaUO}_2\text{PO}_4 \cdot x\text{H}_2\text{O}$ and $\text{Na}_2\text{U}_2\text{O}_7(\text{am})$, although schoepite ($\text{UO}_3 \cdot 2\text{H}_2\text{O}$) also becomes important.

Figure 6-25. Uranium and Total Inorganic Carbon Concentrations (A) and the Paragenetic Sequence of Uranium Phases Present in the Waste (B) as a Function of Reaction Progress for the CaCO_3 Saturated Water Scenario.

A reaction progress of 1 is equivalent to 10,000 years of infiltration at 1 mm/yr.



Over the course of these simulations, 2% of the uranium in the waste is calculated to be dissolved in the $\text{Ca}(\text{OH})_2$ saturated water, compared to 6.4% for the CaCO_3 saturated water. This is attributed to the formation of relatively insoluble CaUO_4 phase under high Ca and high pH conditions.

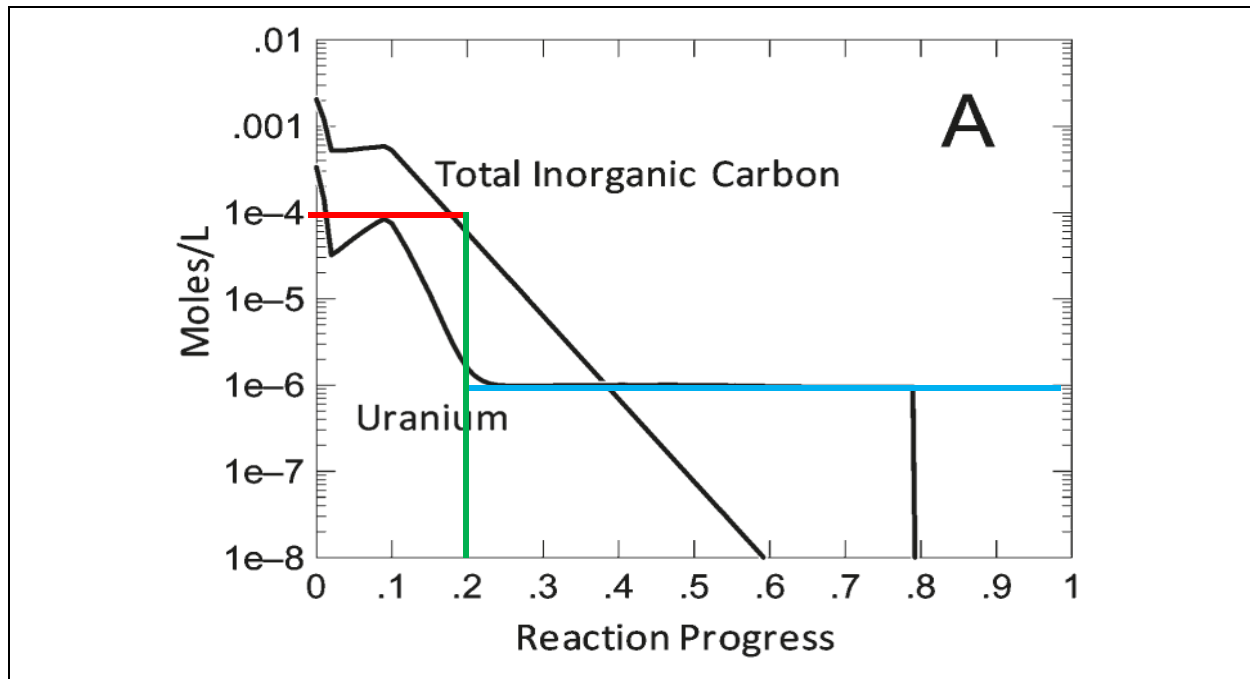
The results of the reaction progress modeling are used to impose solubility limits for uranium. As a conservative calculation, it is assumed that the infill grout is not a barrier to flow through the tank, and the recharge rates imposed on the backfill material (0.5 mm/yr [0.019 in./yr] for the first 500 years and 3.5 mm/yr [0.138 in./yr] afterwards) are also the flow rates through the tanks, even though the rates are likely to be far lower due to lower permeability. Given these flow rates, it is calculated that in the 1,000-year post-closure compliance time period, a total of 2,000 mm (78.7 in.) of water would flow ($0.5 \text{ mm/yr} [0.019 \text{ in./yr}] \times 500 \text{ years} + 3.5 \text{ mm/yr} [0.138 \text{ in./yr}] \times 500 \text{ years}$). This is equivalent to a reaction progress of 0.2 presented in Figures 6-24 and 6-25. Using this information, the following solubility controls are imposed on the uranium concentrations for the base case, as shown in Figure 6-26.

- Apply solubility limit of 1×10^{-4} M for 1,000 years (equivalent to reaction progress of 0.2) based on the assumption that amorphous uranium mineral phases such as $\text{Na}_2\text{U}_2\text{O}_7(\text{am})$ control the solubility.
- After 1,000 years, apply the solubility limit of 1×10^{-6} M, assuming CaUO_4 as the solubility-controlling mineral phase under $\text{Ca}(\text{OH})_2$ saturated conditions (infill grout saturated and intact-tank conditions).

RPP-ENV-58782, Rev. 0

- If and when the tank is assumed to be degraded such that flow rates are fast enough not to equilibrate with the infill grout material and rather are CaCO_3 saturated (vadose zone water), then apply a solubility limit of 1×10^{-4} M for 1,000 years. Beyond this time, apply solubility limit of 2×10^{-5} M based on the long-term uranium concentrations shown in Figure 6-25, assuming minimal influence of $\text{Ca}(\text{OH})_2$ water.

Figure 6-26. Uranium Solubility Model Implemented with Solubility Limits Varying with Time.
Reaction progress of 0.2 is equivalent to 1,000 years of flow under base case recharge conditions through the backfill material.



The reaction progress modeling calculations are performed under relatively static conditions. The SPFT tests discussed in Section 5 can be considered as analogous to column flow-through experiments. These are conducted under low flow conditions (~ 0.1 mL/hr [0.06 in.³/hr]) for a period of about six months (at the sediment mass-to-solution ratio of 0.5 g [0.02 oz] to 0.06 L [3.66 in.³]) with no stirring of the waste form in the solution. Even under these conditions, the application of the initial high solubility limit of 1×10^{-4} M is conservative for the 1,000-year time period. The SPFT test conducted on tank C-202 residuals (Figure 6-27) indicates that peak uranium concentrations for the CaCO_3 saturated water reached the solubility limit 1×10^{-4} M for a short duration at an early time, but later dropped to much lower numbers, and therefore represents a likely bounding uranium solubility value under all conditions at WMA C. This solubility limit is imposed for pipeline releases as well, where the releases are likely to be advectively dominated. This assumption is justified by the same logic about flow rates presented above.

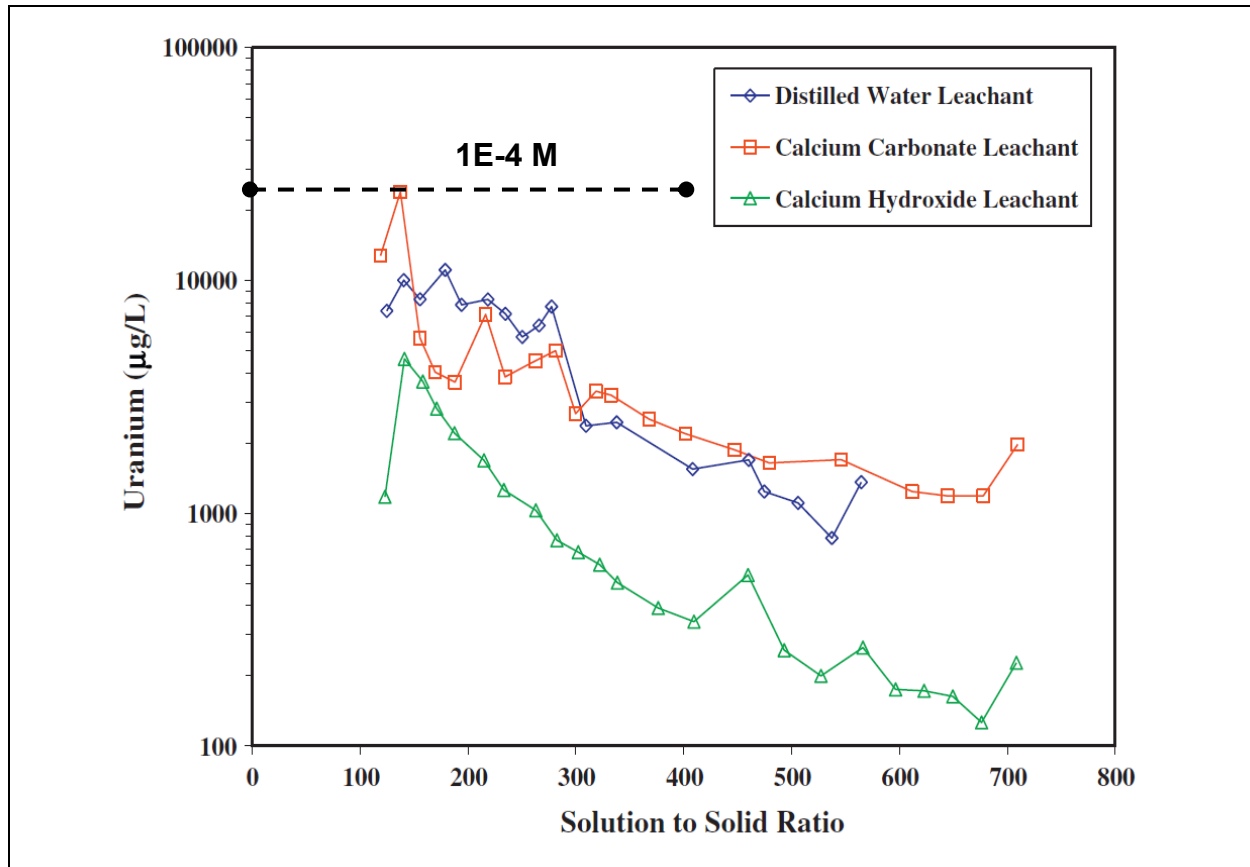
6.3.1.3 Effective Diffusion Coefficient for Transport Through Tank Structure.

Observations of retrieved tanks show that the residual waste is primarily distributed on the tank

RPP-ENV-58782, Rev. 0

bottoms (see Section 5.2 of RPP-RPT-42323). Consequently, the residual waste is represented as a uniform layer at the base of the tank. Under the likely scenario, where tank wall integrity is maintained and the infill grout is not physically degraded (Section 6.2.1.2), the primary contaminant transport process will be diffusive. The shortest diffusive pathway for release to the near-field environment is through the base of the tank as presented in Figure 6-28. The diffusive thickness being considered is the 20 cm (8 in.) combined thickness of concrete and grout layer located at the base of the tank (ignoring the steel plate). The aqueous phase diffusive transport will occur along the water phase within the pore spaces of the grout and concrete layer. The effective diffusion coefficient (which includes effects of tortuosity), concentration gradient, and sorption behavior within the grout and concrete layer control the diffusive mass flux.

Figure 6-27. Comparison of Initially Imposed Uranium Solubility Limit of 1×10^{-4} M to the Observed Concentrations during the Single-Pass Flow-Through Conducted on 241-C-202 Tank Residual.



The effective diffusion coefficient of mobile contaminants (such as ^{99}Tc) through the combined grout and concrete base mat is considered a key parameter that controls the diffusive flux. Over the past decade, several experiments have been conducted to determine the effective diffusion coefficient through concrete for relatively mobile contaminants under unsaturated conditions. The results of various experiments are presented in PNNL-23841. Of particular interest are the sediment-concrete half-cell experiments conducted in Year 2008 (for a period of 351 days) with ^{99}Tc and stable iodine.

6-58

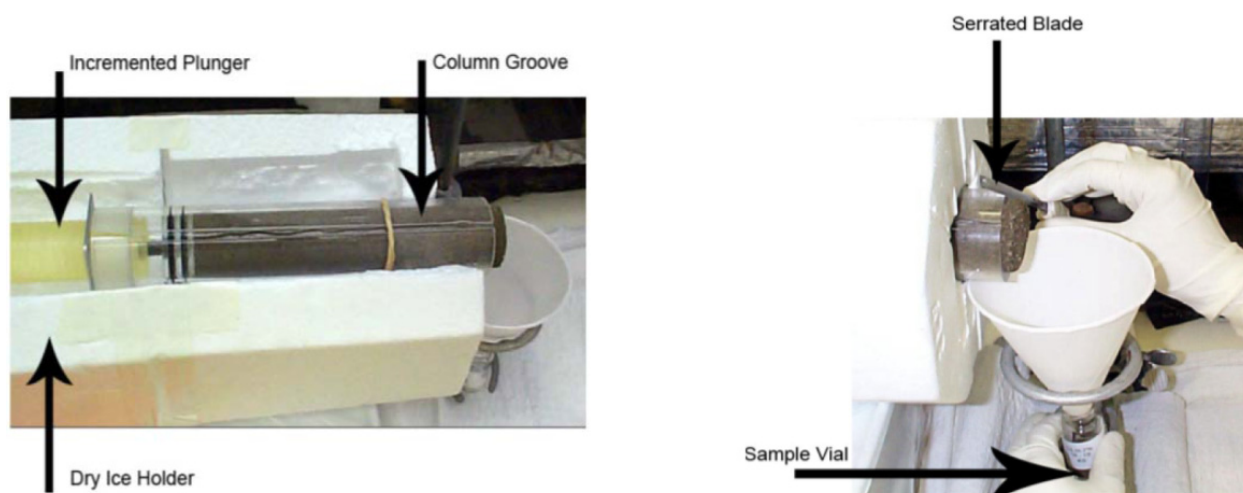


RPP-ENV-58782, Rev. 0

Laboratory-scale concrete mixtures were prepared by omitting coarse aggregates and using 40 to 60 mesh size sand instead. The concrete mix prepared consisted of mainly Type I/II sulfate resistant portland cement (27%), Class F fly ash (4%), sand (51%), and steel fiber (4%). The water-to-cement ratio was 0.5.

The experiments were conducted using cylindrical cells made of Schedule 40 PVC pipe (Figure 6-29). Caps were machined to fit into both ends of the PVC pipe and fitted with O-rings to minimize moisture loss during the test. For the sediment-concrete half-cells, the cell containing contaminant-spiked sediment was placed in contact with the non-spiked concrete monolith. The diffusion tests were run horizontally and undisturbed, with periodic rotation of the cell by 90 degrees. At the completion of the experiment, the concrete half-cells were sectioned parallel to the sediment-concrete interface. The concrete slices were then ground and two-to-one extracts (due to small sample size) by mass were performed on concrete fractions using the distilled deionized (DDI) water.

Figure 6-29. Set-Up of the Diffusive Half-Cell Experiment Contacting Contaminant-Spiked Sediment (or Concrete) Sample with the Non-Spiked Sediment (or Concrete) Sample.



The concentration profiles developed in the concrete are analyzed by fitting the analytical solution to Fick's second law, with the assumption of zero concentration downstream boundary condition, and deriving a bulk diffusion coefficient for the media. This bulk diffusion coefficient implicitly incorporates the effects of porosity and tortuosity due to diffusion that primarily occurs along the water films in the concrete. For the purpose of modeling mass transport along the water (liquid) phase the effective diffusion coefficient in the water phase is needed (instead of bulk diffusion coefficient), which can be derived by multiplying bulk diffusion coefficient with the moisture content. Since the moisture content of the base mat concrete and grout material is not known and would likely change with time due to slow but steady physical and chemical degradation, the effective diffusion coefficient is chosen conservatively to be the same as the measured bulk diffusion coefficient for the purpose of source-term modeling. In other words, the reduction due to multiplying with moisture content is not applied for calculating the

RPP-ENV-58782, Rev. 0

diffusive flux. Note that the effective diffusion coefficient incorporates the effects of tortuosity resulting from transport along water films in the porous media.

Sediment-concrete diffusion experiments were initiated to investigate the effect of sediment moisture, concrete iron content, and concrete carbonation on the diffusivity of ^{99}Tc from sediment into concrete (PNNL-23841, Section 4.2.2). Sediment half-cell specimens were spiked with ^{99}Tc (4.2×10^{-4} mg ^{99}Tc /g sediment) to achieve a measurable diffusion profile in the concrete part of the half-cell. Hanford fine sand was used for the sediment half-cell. In these experiments, iron content was varied in the concrete specimens from 0% to 12%, sediment moisture content was varied (4%, 7%, or 15%), and half of the concrete monoliths were carbonated prior to preparing the half-cells. The characteristics of the concrete half-cells are listed in Table 6-4. Half-cell sampling was conducted at 351 days. Figure 6-30 presents the concentration profile developed in the concrete.

The calculated effective diffusion coefficients of ^{99}Tc derived from the experimental results are presented in Figure 6-31 and tabulated in Table 6-4. They range from 6.6×10^{-9} cm²/s to 1.6×10^{-7} cm²/s (1.0×10^{-7} in.²/s to 2.5×10^{-6} in.²/s), with a median value of $\sim 3 \times 10^{-8}$ cm²/s (4.7×10^{-7} in.²/s). No particular measurable trend exists to indicate whether the effective diffusion coefficient varies with moisture content of the sediment. The highest ^{99}Tc diffusivities were predominantly observed in the non-carbonated concrete cores contacting spiked sediments. A clear effect from the addition of iron was not observed. In general, the increased carbonation reduced diffusion coefficients.

Similar experiments, as described above, were performed using stable iodine in 2008, where the sediment half-cell specimens were spiked with stable iodine at concentrations of ~ 7 mg of iodine per gram (246.9 oz/ton) of sediment (PNNL-23841, Section 4.1.2). The concentration profiles developed in the concrete half-cells were evaluated and the effective diffusion coefficient was determined for iodine, which ranged from 1.4×10^{-8} cm²/s to 9.7×10^{-8} cm²/s (2.17×10^{-7} in.²/s to 1.50×10^{-6} in.²/s) with a median value of 2.6×10^{-8} cm²/s (4.03×10^{-7} in.²/s). The non-carbonated samples exhibited a larger depth of diffusion compared to the carbonated samples, similar to the observations made for ^{99}Tc . The range of effective diffusion coefficient (and the median value) for iodine in concrete is very similar to that for ^{99}Tc .

Experiments were also performed to assess the effect of fractures in the concrete on diffusion of ^{99}Tc and iodine. For this purpose, the concrete monoliths were wrapped in shrink-wrap (to prevent the formation of rubble), and the end of the flathead screwdriver was placed directly in the center of the core and stuck once. Each fractured concrete monolith had a single midline fracture that penetrated the length of the core. A set of sediment to fractured concrete diffusion half-cell experiments were conducted, by varying the iron content using both carbonated and non-carbonated concrete but keeping the moisture content in the sediment half-cell constant at 4%. The sediment half-cell specimens were spiked with ^{99}Tc at a concentration of 3.24×10^{-4} mg per gram (0.011 oz/ton) of sediment. The derived effective diffusion coefficient ranged from 1.9×10^{-9} cm²/s to 2.5×10^{-8} cm²/s (2.94×10^{-8} in.²/s to 3.88×10^{-7} in.²/s). Similar experiments conducted using stable iodine (spiked at 7 mg per gram [246.9 oz/ton] of sediment) resulted in effective diffusion coefficient that ranged from 4.7×10^{-9} cm²/s to 8.4×10^{-8} cm²/s (7.29×10^{-8} in.²/s to 1.30×10^{-6} in.²/s). These ranges are similar to the ranges calculated for diffusion in the unfractured concrete monolith.

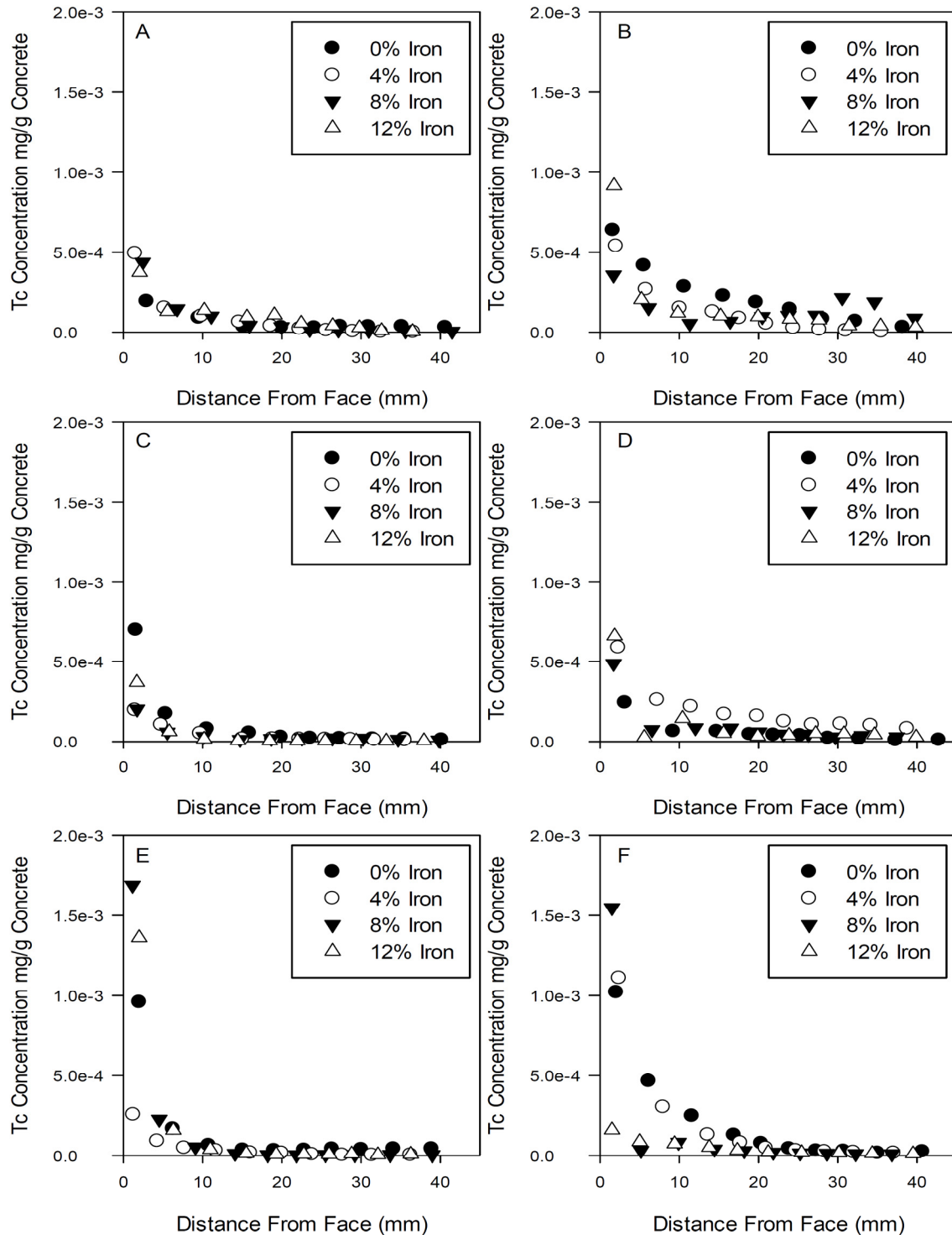
Table 6-4. Characteristics of Concrete Specimens Used in Sediment-Concrete Half-Cell Experiments Along with Derived Bulk Diffusion Coefficient of Technetium-99 for the Concrete.*

Core ID	Length (cm)	Diameter (cm)	Surface Area (cm ²)	Volume (cm ³)	Weight (g)	Density (g/cm ³)	Iron (wt%)	Carbonated	Initial Sediment Moisture Content (%)	Technetium-99 Diffusivity (cm ² /s)
C-08-3-0-325	4.09	4.33	84.97	60.1	131.44	2.19	0	N	4	7.08E-08
C-08-3-0-329	4.32	4.33	88.13	63.53	139.5	2.2	0	N	7	6.55E-08
C-08-3-0-330	3.85	4.33	81.77	56.65	123.5	2.18	0	N	15	3.51E-08
C-08-3-0-332	4.33	4.32	88.09	63.48	139.65	2.2	0	Y	4	2.23E-08
C-08-3-0-333	4.35	4.33	88.57	64	140.79	2.2	0	Y	7	2.25E-08
C-08-3-0-334	4.07	4.32	84.56	59.67	130.55	2.19	0	Y	15	1.22E-08
C-08-3-4-350	3.84	4.32	81.43	56.28	127.25	2.26	4	N	4	3.21E-08
C-08-3-4-351	4	4.33	83.92	58.96	132.78	2.25	4	N	7	1.57E-07
C-08-3-4-353	4.01	4.33	83.99	59.04	133.38	2.26	4	N	15	3.09E-08
C-08-3-4-357	3.9	4.32	82.19	57.11	128.77	2.25	4	Y	4	3.09E-08
C-08-3-4-359	3.83	4.32	81.25	56.09	126.5	2.26	4	Y	7	1.07E-08
C-08-3-4-360	4.11	4.33	85.47	60.64	136.11	2.24	4	Y	15	3.26E-08
C-08-3-8-401	4.07	4.32	84.4	59.5	135.91	2.28	8	N	4	7.76E-09
C-08-3-8-402	3.81	4.32	81.02	55.84	127.31	2.28	8	N	7	2.85E-08
C-08-3-8-403	4	4.33	83.87	58.91	133.35	2.26	8	N	15	1.62E-08
C-08-3-8-404	4.05	4.33	84.61	59.71	133.69	2.24	8	Y	4	5.34E-08
C-08-3-8-405	3.86	4.33	81.77	56.65	126.96	2.24	8	Y	7	9.25E-09
C-08-3-8-406	3.94	4.33	83.08	58.05	130.61	2.25	8	Y	15	6.61E-09
C-08-3-12-425	4.33	4.27	87.54	62.88	143.44	2.28	12	N	4	1.07E-07
C-08-3-12-426	4.33	4.33	88.35	63.76	145.77	2.29	12	N	7	1.31E-08
C-08-3-12-427	4.33	4.22	86.94	62.23	141.71	2.28	12	N	15	8.21E-08
C-08-3-12-432	4.02	4.32	83.83	58.88	134.09	2.28	12	Y	4	4.6E-08
C-08-3-12-433	4.15	4.33	85.81	61.01	139.8	2.29	12	Y	7	6.95E-09
C-08-3-12-435	3.88	4.33	82.22	57.12	130.04	2.28	12	Y	15	7.09E-09

*Note: For the purpose of source-term calculations, the bulk diffusion coefficient is considered to be the same as effective diffusion coefficient.

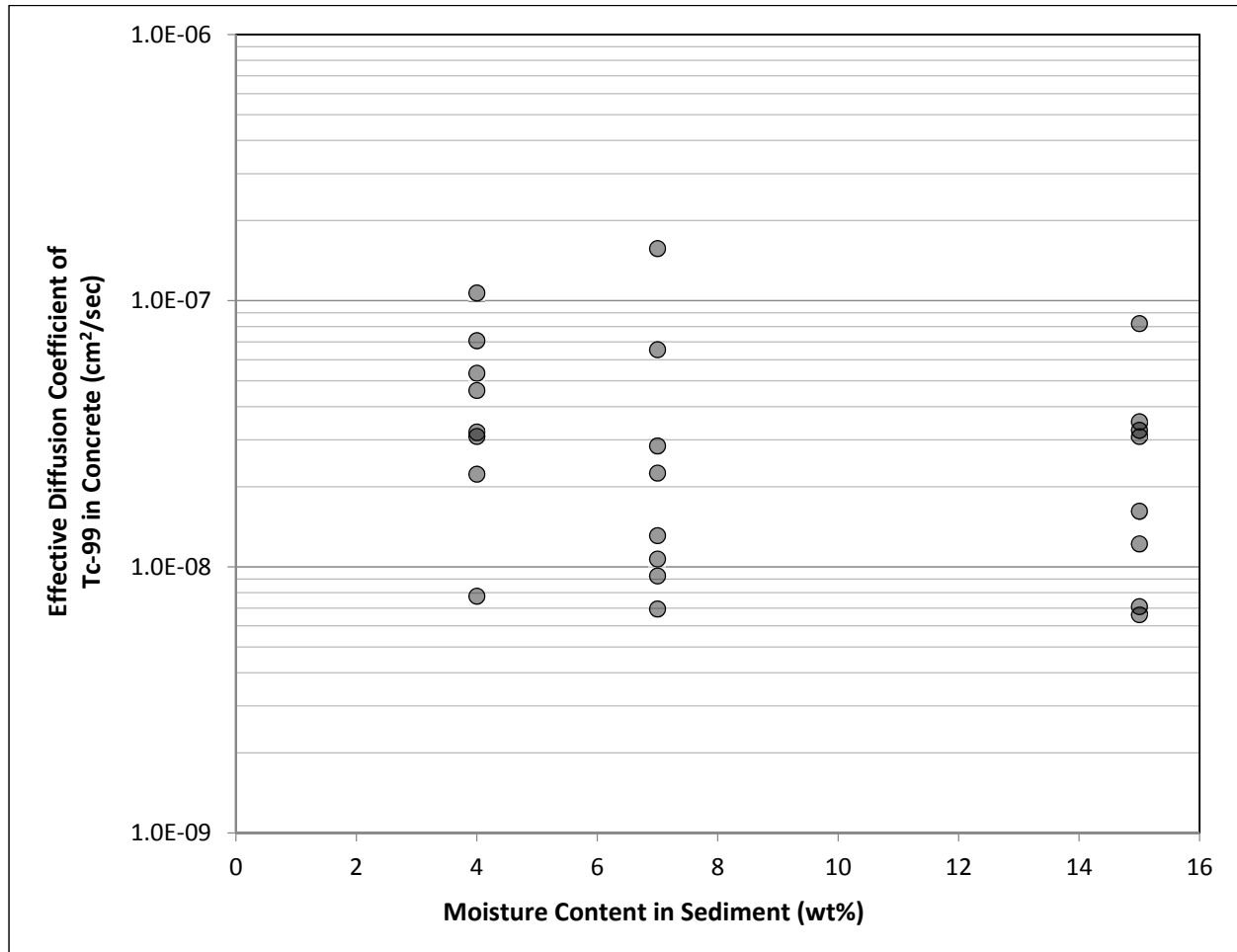
RPP-ENV-58782, Rev. 0

Figure 6-30. Technetium-99 Concentration Profiles in Concrete from Sediment-Concrete Half-Cell Experiments Conducted on (A) 4% Sediment Moisture, Carbonated Monoliths, (B) 4% Sediment Moisture, Non-Carbonated Monoliths, (C) 7% Sediment Moisture, Carbonated Monoliths, (D) 7% Sediment Moisture, Non-Carbonated Monoliths, (E) 15% Sediment Moisture, Carbonated Monoliths, and (F) 15% Sediment Moisture, Non-Carbonated Monoliths.



RPP-ENV-58782, Rev. 0

Figure 6-31. Effective Diffusion Coefficient of Technetium-99 in Concrete Based on Experiments Conducted Using Sediment-Concrete Half-Cells.



Reference: PNNL-23841, "Radionuclide Migration through Sediment and Concrete: 16 Years of Investigations."

For the purpose of the PA base case calculations, the experimental median value of $3 \times 10^{-8} \text{ cm}^2/\text{s}$ ($4.65 \times 10^{-7} \text{ in.}^2/\text{s}$) is chosen as the best estimate for the effective diffusion coefficient in concrete. This value is applied to all species diffusing through the concrete. Based on the range presented in Figure 6-31, an uncertainty range with a minimum and maximum value of $6 \times 10^{-9} \text{ cm}^2/\text{s}$ and $2 \times 10^{-7} \text{ cm}^2/\text{s}$ ($9.30 \times 10^{-8} \text{ in.}^2/\text{s}$ and $3.10 \times 10^{-6} \text{ in.}^2/\text{s}$) will be evaluated in Section 8 (Uncertainty Analysis).

6.3.1.4 Sorption of Contaminants to Grout and Concrete. A linear sorption isotherm (using a K_d approach) is considered for determining sorption within the grout and concrete layer for various contaminants as they undergo diffusive (and advective) transport through the tank. The K_d values are presented in Table 6-5 in terms of best estimate and the uncertainty range that are derived from relevant published literature for chemical conditions that are likely to exist within the grout/concrete layer within the tanks.

RPP-ENV-58782, Rev. 0

Table 6-5. K_d Values (mL/g) for Grout/Concrete Used for Waste Management Area C Performance Assessment.

Element	Best	Minimum	Maximum	Reference
Ac	1.00E+05	3.00E+03	3.30E+05	NAGRA NTB 02-20
Al	0.00E+00	0.00E+00	0.00E+00	No relevant information
Am	1.00E+03	2.00E+02	5.00E+03	SKB R-05-75
B	0.00E+00	0.00E+00	0.00E+00	No relevant information
C	2.00E+02	1.00E+02	4.00E+03	SKB R-05-75
Cd	4.00E+01	2.00E+00	8.00E+02	SKB R-05-75
Cm	1.00E+03	2.00E+02	5.00E+03	SKB R-05-75
CN	0.00E+00	0.00E+00	0.00E+00	No relevant information
Co	4.00E+01	4.00E+00	4.00E+02	SKB R-05-75
Cr	0.00E+00	0.00E+00	0.00E+00	No relevant information
Cs	1.00E+00	1.00E-01	1.00E+01	SKB R-05-75
Eu	5.00E+03	1.00E+03	2.50E+04	SKB R-05-75
F	0.00E+00	0.00E+00	0.00E+00	No relevant information
Fe	0.00E+00	0.00E+00	0.00E+00	No relevant information
H	1.00E-01	7.10E-02	1.40E-01	NAGRA NTB 02-20
Hg	0.00E+00	0.00E+00	0.00E+00	No relevant information
I	3.00E+00	3.00E-01	3.00E+01	SKB R-05-75
Mn	0.00E+00	0.00E+00	0.00E+00	No relevant information
Nb	5.00E+02	1.00E+02	2.50E+04	SKB R-05-75
Ni	4.00E+01	8.00E+00	2.00E+02	SKB R-05-75
NO ₂	0.00E+00	0.00E+00	0.00E+00	No relevant information
NO ₃	0.00E+00	0.00E+00	0.00E+00	No relevant information
Np	1.00E+02	7.10E+01	1.40E+02	NAGRA NTB 02-20
Pa	1.00E+02	7.10E+01	1.40E+02	NAGRA NTB 02-20
Pb	5.00E+02	3.60E+02	7.10E+02	NAGRA NTB 02-20
Pu	1.00E+02	7.14E+01	1.40E+02	NAGRA NTB 02-20
Ra	5.00E+01	5.00E+00	5.00E+02	SKB R-05-75
Rn	0.00E+00	0.00E+00	0.00E+00	No relevant information
Se	6.00E+00	1.00E-01	4.00E+02	SKB R-05-75
Sm	5.00E+03	1.00E+03	2.50E+04	SKB R-05-75
Sn	5.00E+02	2.50E+01	1.00E+04	SKB R-05-75
Sr	1.00E+00	5.00E-01	5.00E+01	SKB R-05-75
Tributyl phosphate	0.00E+00	0.00E+00	0.00E+00	No relevant information
Tc	1.00E+00	7.10E-01	1.40E+00	NAGRA NTB 02-20
Th	3.00E+04	1.00E+03	1.00E+06	NIROND-TR 2008-23 E
U	2.00E+03	1.40E+03	2.80E+03	NAGRA NTB 02-20
Zr	1.00E+04	3.00E+03	3.30E+04	NAGRA NTB 02-20

References:

NAGRA NTB 02-20, "Cementitious Near-Field Sorption Data Base for Performance Assessment of an ILW Repository in Opalinus Clay."

NIROND-TR 2008-23 E, "Review of sorption values for the cementitious near field of a near surface radioactive waste disposal facility, Project near surface disposal of category A waste at Dessel."

PSI Bericht Nr. 95-06, "Sorption Databases for the Cementitious Near-Field of a L/ILW Repository for Performance Assessment."

SKB Rapport R-05-75, "Assessment of uncertainty intervals for sorption coefficients SFR-1 uppföljning av SAFE."

RPP-ENV-58782, Rev. 0

1 Development of a sophisticated sorption model depends on the availability of complete sets of
2 experimental data, including measurement of isotherm, and dependence on solid-to-liquid ratio
3 under conditions that are applicable to the near-field environment. Presently the vast majority of
4 sorption data on cementitious material are based on single-point measurements, and information
5 on uptake mechanisms and uptake controlling phases in cement systems are lacking to a large
6 extent (NAGRA NTB 02-20, "Cementitious Near-Field Sorption Data Base for Performance
7 Assessment of an ILW Repository in Opalinus Clay"). Until studies are performed at the
8 molecular level to discern uptake processes, sorption databases, in conjunction with scientific
9 expertise, can be used to select site-specific sorption values.

10
11 As described below, selections for sorption values (K_d) have been made based on review of past
12 reports that are focused on developing internally consistent cement sorption databases for
13 cementitious near-field material (hardened cement paste) based on the composition of cement
14 porewaters and stage of cement degradation.

- 15
16 • Conditions in the closed tank farm are expected to be moderately oxidizing, owing to the
17 position of the waste in unsaturated conditions. Where data are available to differentiate
18 between oxidizing and reducing conditions, K_d values under oxidizing conditions are
19 preferentially selected, as it leads to lower K_d values relative to reducing conditions.
20
- 21 • Composition of the cementitious material (grout or concrete) may have different
22 chemical compositions, and therefore differ in contaminant uptake mechanisms and
23 cement phases. Due to lack of information, the differences in sorption between various
24 types of cements and concrete are ignored.
25
- 26 • The selected K_d values are based on assumption of $\text{Ca}(\text{OH})_2$ saturated waters contacting
27 the waste, and therefore represent the so-called stage II of the chemical degradation of
28 cementitious material. In this stage, chemical composition of the alkali-depleted cement
29 pore water is controlled by the solubility of portlandite. The impact on K_d values during
30 evolution of chemical conditions from stage I (higher alkali content and pH) to stage II is
31 expected to be minor and incorporated within the uncertainty range.
32
- 33 • The reviews of SKB R-05-75, "Assessment of uncertainty intervals for sorption
34 coefficients, SFR-1 uppföljning av SAFE" and NIRON-TR 2008-23 E, "Review of
35 sorption values for the cementitious near field of a near surface radioactive waste
36 disposal facility, Project near surface disposal of category A waste at Dessel" are more
37 recent, and represent critical reviews and independent data from NAGRA NTB 02-20 and
38 PSI Bericht Nr. 95-06, "Sorption Databases for the Cementitious Near-Field of a L/ILW
39 Repository for Performance Assessment." Where appropriate values are available from
40 these more recent references, they are preferred to the older ones.
41
- 42 • When K_d values are absent from these references, a value of zero has been assumed for
43 the analyte since chemical equivalences between similar analytes have not been
44 performed to justify nonzero K_d values. As necessary, chemical equivalences suggested
45 by SKB R-05-75 may be used to update K_d values in future iterations of the PA
46 modeling.

RPP-ENV-58782, Rev. 0

- When there was significant disagreement between literature sources, the lower (less sorptive) K_d value has been chosen. For example, K_d values under oxidizing conditions were selected over those measured under reducing conditions.

The K_d values were compared to values used in Savannah River F and H tank farm PAs (WSRC-STI-2007-00369, “Hydraulic and Physical Properties of Tank Grouts and Base Mat Surrogate Concrete for FTF Closure” and WSRC-STI-2007-00607). The values used for WMA C are generally consistent with or more conservative than comparable values used for the facility-specific grout used at Savannah River. When WMA C values are more conservative, it has been for one of the following two reasons.

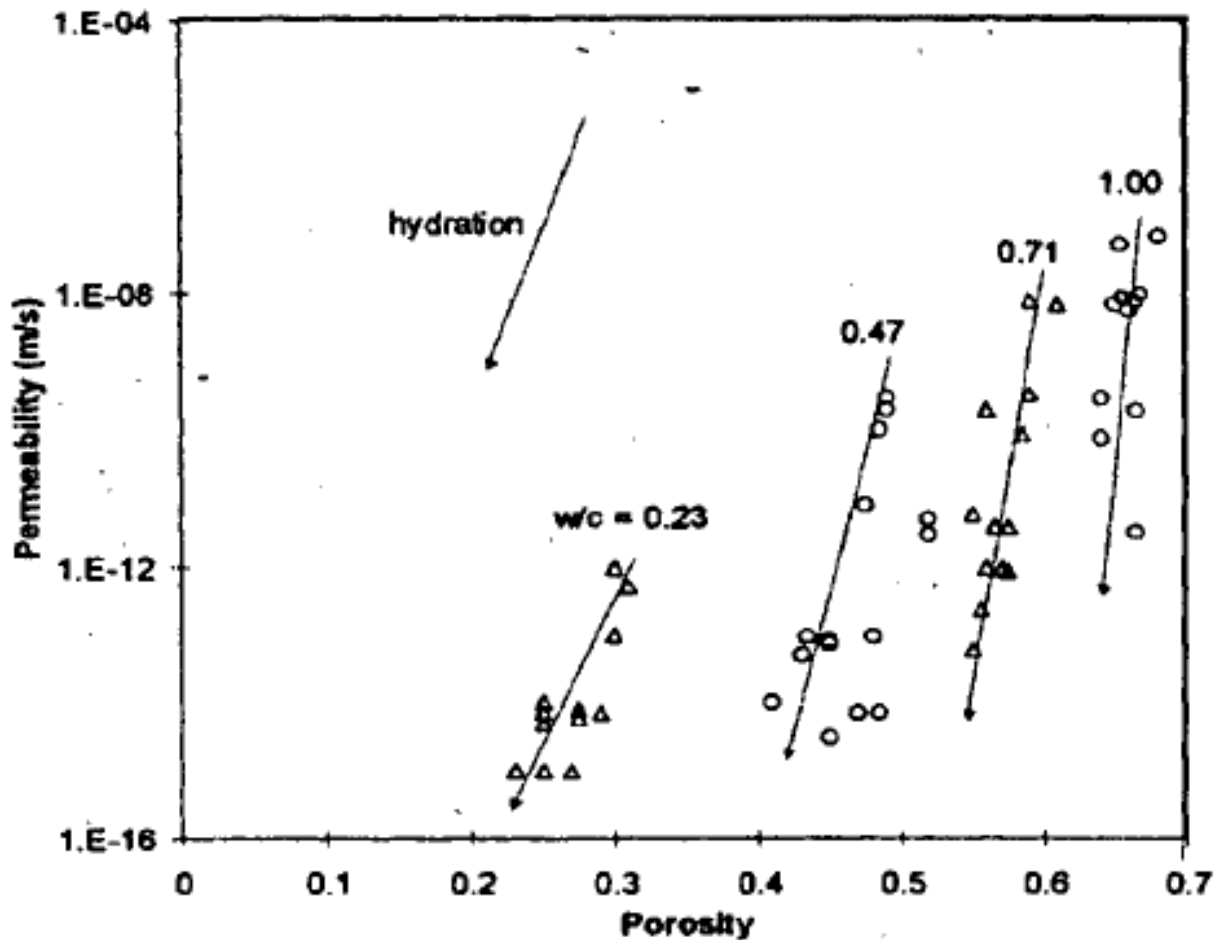
- The grout used at Savannah River produces reducing conditions. In the absence of a specific grout formulation for WMA C, it has been assumed that oxidizing conditions will exist in the grout, which leads to lower (more conservative) K_d values for some radionuclides of interest.
- The disposal system at WMA C is very robust with respect to meeting performance objectives. As a result, when data were ambiguous or insufficient in any way, it was more efficient to make a conservative assumption about K_d than to spend resources to resolve the value in greater detail. So, for instance, when data are lacking for a contaminant it is assigned a value of zero.

6.3.1.5 Evaluation of Diffusive Release Assumption for Intact Tank Condition. Based on the tank infill grout and concrete degradation mechanisms discussed in Section 6.2.1.2, it was determined that tanks are not likely to be fully degraded within the modeled time period of 10,000 years. Due to the unlikely development of continuous fracture pathways within the infill grout over the 10,000 years, advective flow is likely to be very slow, to the extent that it is negligible. Therefore, the primary contaminant transport process will be diffusion (in the aqueous phase), where concentration differences across the grout and concrete tank base mat provide a gradient leading to diffusion. The predominance of diffusion with negligible amount of advection, if any, is based on the following reasoning.

1. The backfill material surrounding the tank structure will provide a preferential pathway for any water infiltrating through the surface cover. Due to large contrast in relative permeability (several orders of magnitude) between gravel-dominated backfill material and grout monolith inside the tank under ambient conditions, most of the infiltrating water will flow around and bypass the tank structure.
2. The capillary forces within the grout micropores are much larger than surrounding backfill soil. Therefore, initially when the grout is emplaced in the tank, the grout will wick water from the surrounding material and hold it in place, much like a clay lens within a sand body. With increasing degree of hydration over time that leads to formation of calcium silicate hydrate (C-S-H) gel, the amount of interconnected pore space is known to reduce, and some capillary pores will become discontinuous. This is likely to further reduce the permeability appreciably (“Relationships between permeability and pore structure of hardened cement paste” [Nyame and Illston 1981]) as shown in Figure 6-32.

RPP-ENV-58782, Rev. 0

Figure 6-32. Porosity-Permeability Relationship as a Function of Hydration and Water-to-Cement Ratio.



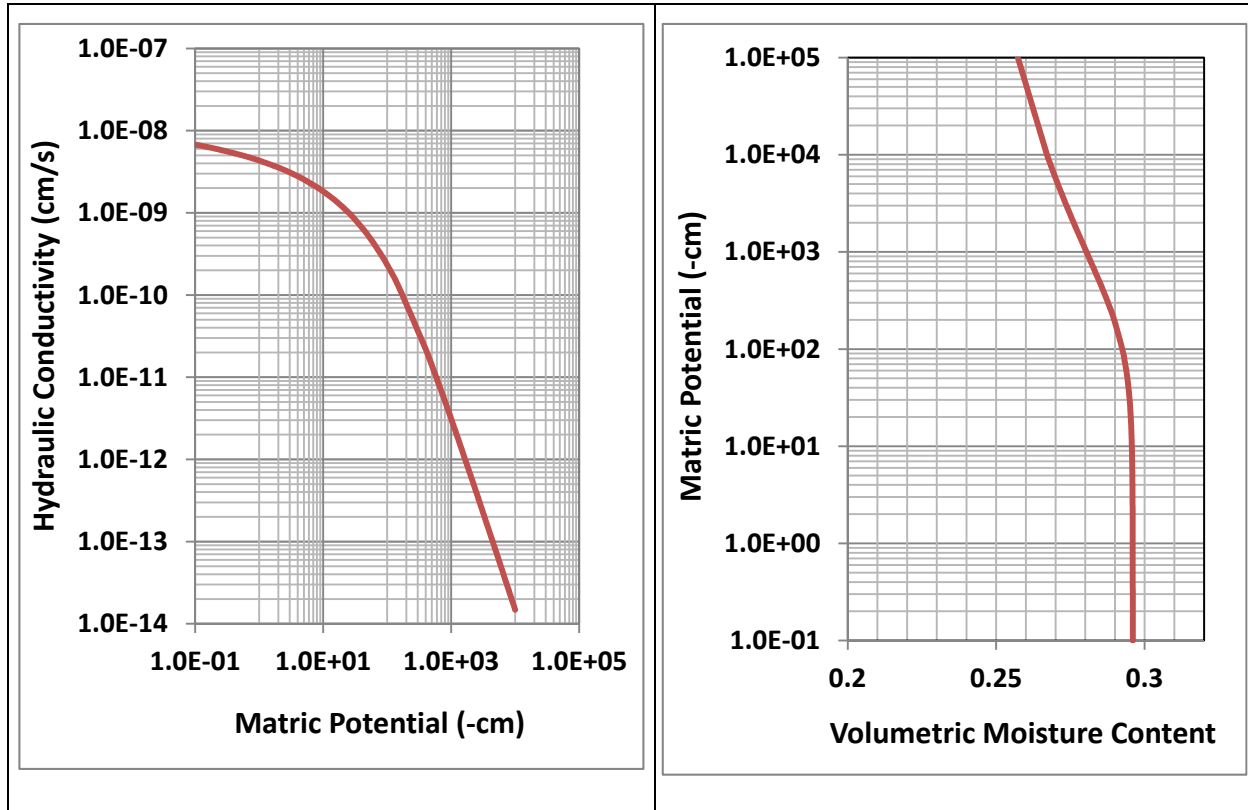
Reference: "Relationships between permeability and pore structure of hardened cement paste" (Nyame and Illston 1981).

A numerical simulation of flow around the grouted tank surrounded by backfill material was undertaken to evaluate the relative importance of advective flow. For this analysis, the tank was simplified by assuming that the concrete wall behaved identically to grout in hydraulic properties. The hydraulic properties assigned to the grout were chosen from WSRC-STI-2007-00369 that represented strong grout material. The corresponding characteristic curves are presented in Figure 6-33.

The numerical calculations were performed in a two-dimensional (2-D) vertical cross-section for a row of tanks under a 3.5 mm/yr (0.14 in./yr) constant recharge rate (same as the long-term post-closure recharge rate). The transient calculations were performed by setting the initial matric potential for the tank nodes to be -2,000 cm, representing conditions that are between fully saturated and near residual saturations. The 2-D cross-section, along with the long-term near steady-state flow field, is shown in Figure 6-34. The vertical Darcy flux in the backfill material is orders of magnitude higher than in the tank, consistent with the choice of parameters.

RPP-ENV-58782, Rev. 0

**Figure 6-33. Soil-Moisture Characteristics Curves
for the Grout Hydraulic Properties Evaluated.**



The transient conditions, showing the changing vertical Darcy flux and volumetric moisture content, are presented in Figure 6-35 for two selected nodes: one within the tank, and the other outside in the backfill. These results indicate that the vertical Darcy flux in the grout remains over three orders of magnitude lower than through the backfill. The Darcy flux in the grout is negligibly small for the first few thousand years, and gradually increases as the large capillary suction draws water in, eventually increasing the unsaturated hydraulic conductivity compared to the initial state.

To compare the relative importance of advection and diffusion, the dimensionless Peclet number (ratio of advective transport to diffusive transport rate) was calculated for the simulated results at 10,000 years. The characteristic length chosen was 1.25 m (4.1 ft), which is the vertical grid discretization over which the Darcy flux calculations are computed. The Peclet number for transport in the tank is approximately 0.1 while in the backfill it is about 2, indicating that transport through the tank is predominantly diffusion-controlled while transport through the backfill has a higher advective component. During the first 1,000 years, the Peclet number for the tank is close to zero due to negligibly small Darcy flux as shown in Figure 6-35, and increases gradually. Therefore, during the 10,000-year period, it is clear that diffusion dominates transport within the grouted tank; whereas in the backfill, both advection and diffusion play a role in transport.

Figure 6-34. Two-Dimensional Cross Section Model to Evaluate the Flow Through the Tanks along with the Flow-Field at Long Time Representing near Steady-State Conditions.

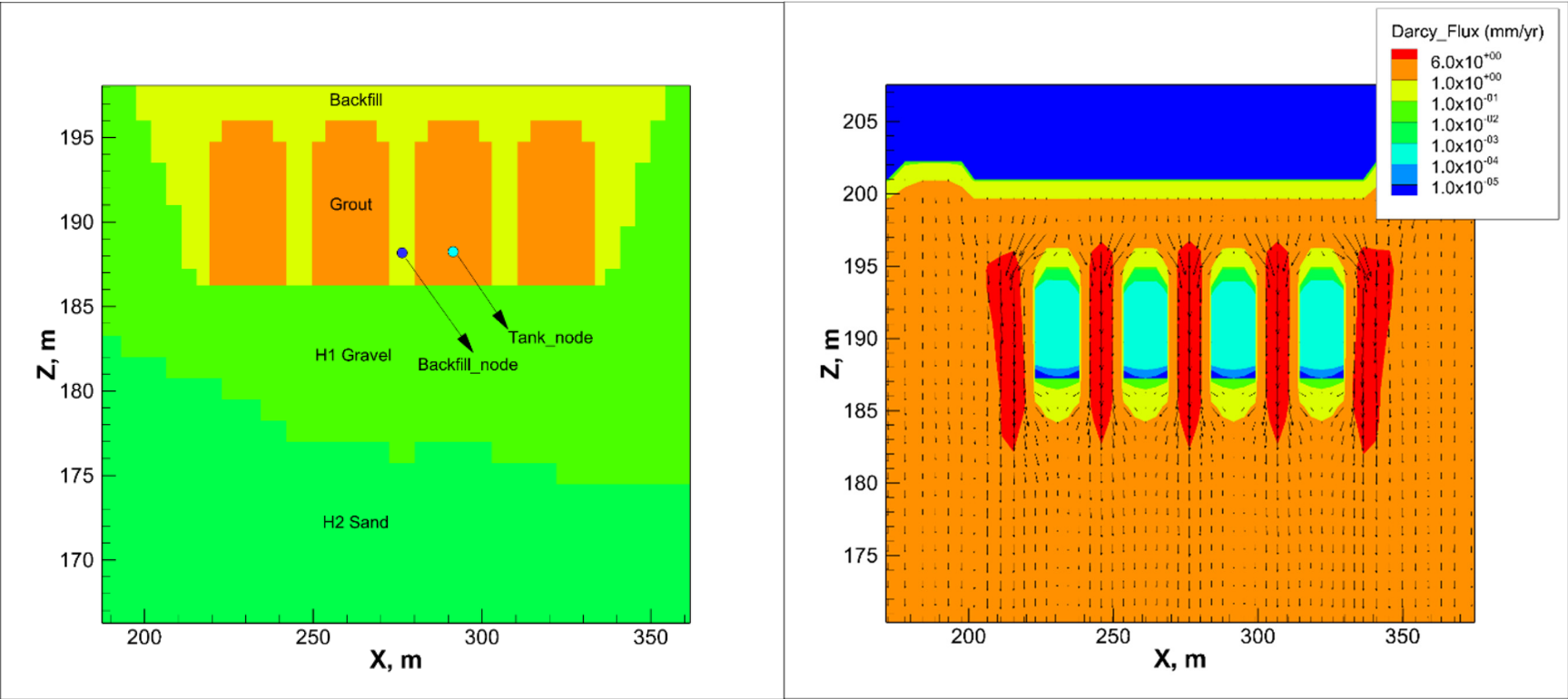
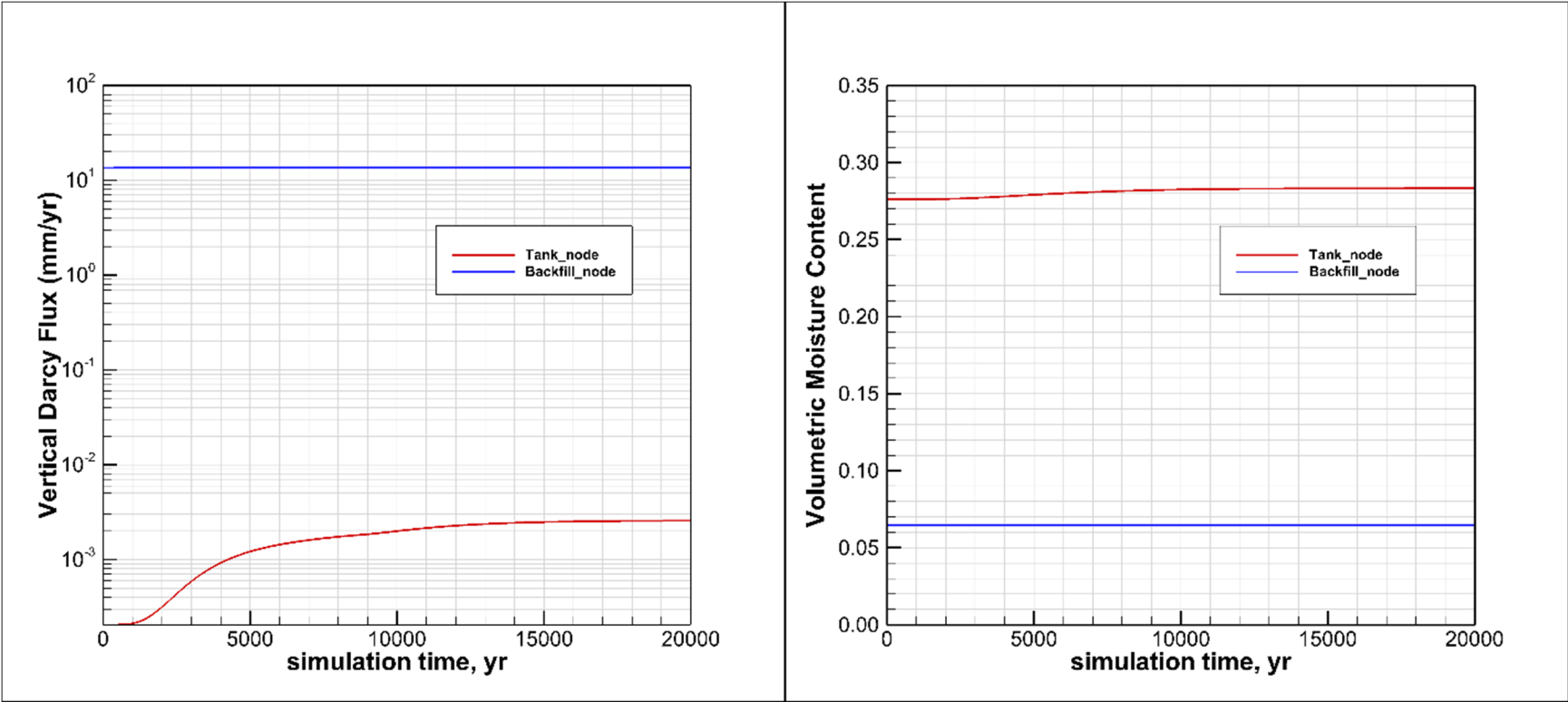


Figure 6-35. Simulated Vertical Darcy Flux and Volumetric Moisture Content for the Tank Node and Backfill Node over a Large Time Scale.



RPP-ENV-58782, Rev. 0

These analyses support the assumption of diffusion-dominated releases from an intact tank.

6.3.1.6 Parameters Used in Source Term Calculations. Following is the list of parameters used in developing source-term release calculations for the groundwater pathway.

Parameter	Value	Reference
Porosity of Residual Waste Layer	0.4	Assumed; based on evaluation of sludge waste phase from the retrieved tanks.
Saturation of Residual Waste Layer	1	Assumed fully saturated to maximize diffusive release
Residual Waste Volume	Variable by source	Section 3.1
Porosity of Concrete and Grout layer below the waste layer	0.11	SRNL-STI-2008-00421, Table 39
Porosity of in-fill Grout within the tank (at closure)	0.269	WSRC-STI-2007-00369, Table 29; Strong grout assumed.
Saturation of Concrete and Grout layer below the waste layer	1	Assumed to maximize diffusive release
Bulk Density of Concrete and Grout layer below the waste layer	2.41 g/cm ³ (151 lb/ft ³)	RPP-RPT-50934, p. C-3 (C-107 dome core density of 2.41 g/cm ³ [151 lb/ft ³])
Diffusive Length of Waste form layer	0 m (0 ft)	Assumed to maximize diffusive release
Diffusive Length of Concrete and Grout layer below the waste layer	0.203 m (8 in.)	Minimum diffusive thickness based on tank bottom geometry
Diffusive Area for source term release	410.4 m ² (4,417.5 ft ²) for 100-Series Tanks; 29.2 m ² (314.3 ft ²) for 200-Series Tanks and C-301 catch tank; 162.4 m ² (1748.1 ft ²) for CR-Vaults; 22,500 m ² (242,188.0 ft ²) for Pipelines	Base area for tanks based on circular geometry; area of CR-Vault is based on rectangular area with length of 28 m (92 ft) and average width of 5.8 m (19 ft); area of Pipeline assumed to be 150 m × 150 m (492 ft × 492 ft).
Effective Diffusion Coefficient through grout and concrete layer (incorporates effects of tortuosity)	3×10^{-8} cm ² /s (4.7×10^{-7} in. ² /s)	Section 6.3.1
Uranium solubility for intact tank conditions	1×10^{-4} M for 1,000 years; 1×10^{-6} M for time >1,000 years	Section 6.3.1

RPP-ENV-58782, Rev. 0

Parameter	Value	Reference
Uranium solubility for degraded tank conditions	1×10^{-4} M for 1,000 years; 2×10^{-5} M for time >1,000 years	Section 6.3.1
Technetium-99 release	6% of the waste inventory available for release instantaneously; remaining 94% waste form inventory made available based on first order fractional release rate of 6×10^{-4} day ⁻¹ .	Section 6.3.1
Contaminant K _d values for transport through the grout and concrete layer	Variable; See Table 6-5	Table 6-5
Release Type	Diffusive release from the tanks and CR-Vaults under intact conditions; Both advective and diffusive release for the Pipelines Both advective and diffusive release for tanks and CR-Vaults under degraded conditions	

References:

RPP-RPT-50934, "Inspection and Test Report for the Removed 241-C-107 Dome Concrete."

SRNL-STI-2008-00421, "Hydraulic and Physical Properties of Saltstone Grouts and Vault Concretes."

WSRC-STI-2007-00369, "Hydraulic and Physical Properties of Tank Grouts and Base Mat Surrogate Concrete for FTF Closure."

6.3.1.7 Source-Term Mathematical Model. The source-term model is implemented in GoldSim[®] using its Contaminant Transport Module. The Contaminant Transport Module allows the user to dynamically model mass transport using a compartment-based model of the system. The Contaminant Transport Module includes the following key features (GoldSim Technology Group 2014a).

- Radioactive decay chains can be simulated, taking account of ingrowth and decay.
- A large built-in database exists for radionuclide decay data (species, decay rates, and radioactive progeny) for over 1,300 radionuclides and their corresponding stable elements. The data is based on ICRP 2008.
- Specialized elements in GoldSim[®] called Source and Cells are available to model key release mechanisms from source term that include waste form degradation rate and solubility control.
- Both advective and diffusive transport mechanisms can be explicitly represented using the "Cell" pathway element, by specifying the flow rates for advective transport and the diffusion coefficient and geometric factors for diffusive transport. Media properties through which advection and diffusion occur also need to be specified.

RPP-ENV-58782, Rev. 0

- When multiple Cells are linked together via advective and diffusive mechanisms, the behavior of the Cell network is mathematically described using a coupled system of ordinary differential equations in time. A network of Cells is mathematically equivalent to a finite difference network of nodes. GoldSim[®] numerically solves the coupled system of equations to compute the contaminant mass present in each Cell and the mass fluxes between Cells as a function of time. The solution technique uses backwards-difference (fully implicit) algorithm for each cell-net and each species decay-chain family.

The basic mass balance equation for Cell i is as follows:

$$m'_{is} = -m_{is}\lambda_s + \sum_{p=1}^{NP_s} m_{ip}\lambda_p f_{ps} R_{sp} \left(\frac{A_s}{A_p} \right) + \sum_{c=1}^{NF_i} f_{cs} + S_{is} \quad (6-1)$$

Where:

- m'_{is} = rate of increase of mass of species s in Cell i (M/T)
- m_{is} = mass of species s in Cell i (M)
- λ_s = decay rate of species s (T⁻¹)
- NP_s = Number of direct parents for species s
- f_{ps} = fraction of parent p which decays into species s
- R_{sp} = stoichiometric ratio of moles of species s produced per mole of species p decayed
- A_s = molecular (or atomic) weight of species s (M/mol)
- A_p = molecular (or atomic) weight of species p (M/mol)
- NF_i = number of mass flux links from/to Cell i
- f_{cs} = influx rate of species s (into Cell i) through mass flux link c (M/T)
- S_{is} = rate of direct input of species s to Cell i from external source (M/T).

The first term on the right-hand side in Equation 6-1 represents decay (or chemical reaction), the second term represents ingrowth, the third term represents mass transfer in or out of the Cell via mass flux links, and the fourth term represents the rate of direct input to the Cell from other sources.

Equation 6-1 couples in two ways to other mass balance equations: 1) through the ingrowth terms, which couple all species in a decay chain; and 2) through the mass flux terms, which couple all Cells that are connected by mass flux links. Representation of the mass flux terms (f_{cs}) is the most complex part of the above equation, and is described in detail below in terms of advective mass flux and diffusive mass flux.

Advective mass flux from Cell i to Cell j for species s is computed as follows:

$$f_{s,i \rightarrow j} = c_{ims} q \quad (6-2)$$

Where:

- q = the rate of advection of water for the mass flux link i to j (L³/T)
- c_{ims} = the total dissolved concentration of species s in medium m within Cell i (M/L³).

RPP-ENV-58782, Rev. 0

Diffusive mass flux links are used to transport mass through a stagnant or slowly moving fluid via the process of molecular diffusion. Diffusive mass transport is proportional to a concentration difference, with mass diffusing from high concentration to low concentration. The constant of proportionality is referred to as the diffusive conductance:

$$\text{Diffusive Mass Rate} = (\text{Diffusive Conductance}) \times (\text{Concentration Difference})$$

In this equation, the Diffusive Mass Rate has dimensions of mass/time, the Diffusive Conductance has dimensions of volume/time, and the Concentration Difference has dimensions of mass/volume. Diffusive Conductance is a function of the properties of the species and fluids involved and the geometry of the diffusive process. For diffusion through a single fluid, the Diffusive Conductance for species s (D_s) is computed as:

$$D_s = \frac{(A d \tau \theta)}{L} \quad (6-3)$$

Where:

- A = mean cross-sectional area of the connection (L^2)
- d = free-water diffusivity of species s
- τ = tortuosity of continuous liquid film in the porous medium
- θ = moisture content (porosity times saturation)
- L = diffusive length.

The diffusive flux f_s from pathway i to pathway j is computed as follows:

$$f_{s,i \rightarrow j} = D_s(C_{ims} - C_{jms}) \quad (6-4)$$

Where C_{ims} and C_{jms} are the dissolved concentrations of species s for medium m in Cell i and j .

The diffusion can occur in either direction, so the flux can be positive or negative. When media properties are changing for diffusive release calculation, such as when diffusion occurs between tank wall concrete layer and the surrounding soil, the diffusive conductance is calculated using a harmonic average of the physical properties of the two cell pathways as follows:

$$D_s = \frac{A}{\frac{L_i}{d_{msi}\theta_i\tau_{Pi}} + \frac{L_j}{d_{msj}\theta_j\tau_{Pj}}} \quad (6-5)$$

Where:

- A = the area of the diffusive mass flux link (L^2)
- L_i = diffusive length for the diffusive mass flux link in Cell i (L)
- L_j = diffusive length for the diffusive mass flux link in Cell j (L)
- d_{msi} = free-water diffusivity of species s for fluid m in Cell i (L^2/T)
- d_{msj} = free-water diffusivity of species s for fluid m in Cell j (L^2/T)
- τ_{Pi} = tortuosity for the porous medium for Cell i

RPP-ENV-58782, Rev. 0

- 1 τ_{pj} = tortuosity for the porous medium for Cell j
 2 θ_i = moisture content of porous media in Cell i
 3 θ_j = moisture content of porous media in Cell j.
 4

5 When mass enters a Cell, it is instantaneously partitioned among the media present in the Cell.
 6 The partitioning is controlled by the partition coefficients defined for each species in each
 7 medium, and the quantity of each medium present. In the absence of solubility limits, the
 8 concentration of the species s in medium m in Cell i is computed by GoldSim[®] as follows:
 9

$$C_{ims} = \left(\frac{K_{mrs}}{\sum_{g=1}^{NM_i} K_{grs} \cdot VM_{ig}} \right) m_{is} \quad (6-6)$$

11
 12 Where:

- 13
 14 C_{ims} = concentration of species s in medium m in Cell i ([M/L³] for Fluids or [M/M] for
 15 Solids)
 16 m_{is} = mass of species s in Cell i (M)
 17 K_{mrs} = partition coefficient between medium m and Reference Fluid r for species s (L³/L³)
 18 for Fluids or (L³/M) for Solids
 19 K_{grs} = partition coefficient between medium g and Reference Fluid r for species s (L³/L³)
 20 for Fluids or (L³/M) for Solids
 21 VM_{ig} = quantity (volume or mass) of medium g in Cell i (L³ for Fluids or M for Solids)
 22 NM_i = the number of media in Cell i.
 23

24 When a solubility constraint is applied for a species in a Cell, the Cell has a saturation capacity
 25 with respect to that species, which represents the maximum amount of species mass the Cell can
 26 contain before the species will start to precipitate out of solution. It is calculated as:
 27

$$msat_{is} = sol_{sr} \sum_{g=1}^{NM_i} K_{grs} \cdot VM_{ig} \quad (6-7)$$

28
 29
 30 Where:

- 31
 32 $msat_{is}$ = saturation capacity for species s in Cell i (M)
 33 sol_{sr} = solubility of species s in the Reference Fluid r (M/L³)
 34 K_{grs} = partition coefficient between medium g and Reference Fluid r for species s
 35 ([L³/L³] for Fluids or [L³/M] for Solids)
 36 VM_{ig} = quantity (volume or mass) of medium g in Cell i (L³ for Fluids or M for Solids)
 37 NM_i = the number of media in Cell i.
 38

39 All or a portion of the mass within the Source can be specified to exist within the waste matrix,
 40 such that species that are bound in such a matrix are not released until the matrix itself degraded
 41 in some manner. Release of mass from the matrix is assumed to be congruent with the

RPP-ENV-58782, Rev. 0

degradation of the matrix. Degradation rates are specified by the user. The rate at which the waste is exposed for release is calculated as:

$$e_s(n, t) = M_s(t) \cdot k_s(t) \cdot I_s(n, t) \quad (6-8)$$

Where:

$e_s(n, t)$ = the exposure rate for species n in bound inventory s for the Source at time t (M/T)

$M_s(t)$ = fraction of unprotected but undegraded matrix (unitless)

$k_s(t)$ = fractional degradation rate of waste matrix for bound inventory s (1/T)

$I_s(n, t)$ = mass of species n in bound inventory s at time (M).

When applying a fractional degradation rate to the matrix (such as for release of ^{99}Tc), the fraction of undegraded matrix $M_s(t)$ can be determined by solving the following differential equation:

$$\frac{dM_s(t)}{dt} = h(t) - M_s(t) \cdot k_s(t) \quad (6-9)$$

Where:

$h(t)$ = rate at which matrix is being unprotected (T^{-1})

$k_s(t)$ = rate at which unprotected matrix is being degraded (T^{-1}).

If $h(t)$ and $k_s(t)$ are constant, the solution to the above equation is:

$$M_s(t) = \frac{h}{k_s} (1 - e^{-k_s t}) + M_s(0) e^{-k_s t} \quad (6-10)$$

6.3.2 Radionuclide Transport

This section provides the detailed methods of analysis for the transport of radionuclides for the hydrologic (groundwater), atmospheric, and biotic transport pathways. The process-based modeling involved the use of STOMP[®], and the system-level modeling involved the use of GoldSim[®] for the uncertainty analysis and certain sensitivity cases.

6.3.2.1 Process-Level Model Based on STOMP[®] Flow and Transport Simulator. The WMA C PA groundwater pathway modeling makes use of detailed process-level numerical models based on the STOMP[®] code, which was used to simulate 3-D flow and contaminant transport through the vadose zone and unconfined aquifer system. To calculate water flow, the STOMP[®]-based numerical model includes the assumption that the vadose zone and unconfined aquifer system can be represented and approximated by an equivalent porous continuum. The STOMP[®]-based numerical model solves a conservation of mass equation using a finite difference approximation to the matric potential form of the Richards' equation (Soil Physics,

RPP-ENV-58782, Rev. 0

6th edition [Jury and Horton 2004]) that calculates fluid flow entering, exiting, and accumulating within the finite numerical volumes as follows:

$$C(h) \frac{\partial h}{\partial t} = \frac{\partial}{\partial x} \left[K(h) \frac{\partial h}{\partial x} \right] + \frac{\partial}{\partial y} \left[K(h) \frac{\partial h}{\partial y} \right] + \frac{\partial}{\partial z} \left[K(h) \left(\frac{\partial h}{\partial z} + 1 \right) \right] \pm S \quad (6-11)$$

Where:

- h = matric potential $h = h(x, y, z, t)$, $t = \text{time}$
- $C(h) = d\theta/dh$ = specific moisture capacity, C for a given h , and is equal to $d\theta/dh$, i.e., the inverse slope of the matric potential-moisture content, θ , relation (cm)
- $K(h)$ = the hydraulic conductivity (cm/s), which may be anisotropic and is dependent on matric potential
- S = the amount of water added (source) or subtracted (sink) per unit volume through time (1/s).

Moisture content is a function of soil matric potential, and the soil matric potential-moisture retention relationship is described for each HSU using the following empirical relationship ("A Closed-form Equation for Predicting the Hydraulic Conductivity of Unsaturated Soils" [van Genuchten 1980]; EPA/600/2-91/065, The RETC Code for Quantifying the Hydraulic Functions of Unsaturated Soils):

$$\theta(h) = \theta_r + (\theta_s - \theta_r) \{1 + [\alpha h]^n\}^{-m} \quad (6-12)$$

Where $\theta(h)$ is the moisture content, here expressed explicitly as a function of the soil matric potential, and the other terms are defined as follows:

- θ_r = residual moisture content (dimensionless)
- θ_s = saturated moisture content (dimensionless)
- α = a fitting parameter (cm^{-1})
- n = a fitting parameter (dimensionless)
- $m = 1 - 1/n$.

Combining the van Genuchten model with Mualem's (1976) model ("A New Model for Predicting the Hydraulic Conductivity of Unsaturated Porous Media") for unsaturated conductivity produces the following relationship for hydraulic conductivity and soil matric potential:

$$K(h) = \frac{K_s \{1 - (\alpha h)^{mn} [1 + (\alpha h)^n]^{-m}\}^2}{[1 + (\alpha h)^n]^{ml}} \quad (6-13)$$

Where $K(h)$ is the hydraulic conductivity (cm/s), which is, as expressed, dependent on the soil matric potential; K_s is the saturated hydraulic conductivity (cm/s); and l is a pore-connectivity parameter (dimensionless) that Mualem (1976) estimates to be about 0.5 for many soils and is assumed to equal 0.5 in this analysis.

RPP-ENV-58782, Rev. 0

Within the STOMP[®] code, tension-dependent anisotropy provides a framework for upscaling small-scale measurements to the effective (upscaled) properties for the large-scale vadose zone (Section 6.4 and Appendix B). Each heterogeneous geologic unit is represented in the model by an EHM with macroscopic flow and transport properties. With each heterogeneous unit assigned its upscaled or effective hydraulic properties, the simulated flow fields predict the bulk or mean flow behavior at the field scale. Upscaling, in effect, accounts for the differences in scale between small, core-scale measurements and large, field-scale modeling. Tension-dependent anisotropy provides a framework for upscaling small-scale measurements to the effective (upscaled) properties for the large-scale, macroscopic vadose zone. The stochastic model developed in Polmann (1990) is used to evaluate and apply tension-dependent anisotropy for the HSUs at WMA C. Details about the development of the Polmann stochastic tension-dependent anisotropy model and its application to the HSUs at WMA C are presented in Appendix B, Section B.3.2. Figures B-19 through B-21 in Appendix B illustrate the relationship between the matric potential and the resulting anisotropy.

Contaminant transport within the STOMP[®] code is described by the conventional advective-dispersive transport solution to the conservation of mass equation described in Soil Physics (6th edition [Jury and Horton 2004]) and applied to finite difference volumes:

$$\frac{\partial}{\partial t} M_c = \frac{\partial}{\partial x} \left(D_e \frac{\partial C_l}{\partial x} \right) + \frac{\partial}{\partial y} \left(D_e \frac{\partial C_l}{\partial y} \right) + \frac{\partial}{\partial z} \left(D_e \frac{\partial C_l}{\partial z} \right) - \frac{\partial}{\partial x} (J_x C_l) - \frac{\partial}{\partial y} (J_y C_l) - \frac{\partial}{\partial z} (J_z C_l) - M_c \frac{\ln(2)}{t^{1/2}} \quad (6-14)$$

Where:

- $\frac{\partial}{\partial t} M_c$ = the change in contaminant mass or activity present in the finite volume (g or Ci) through time and the mass or activity is calculated according to the equation $(\rho_b C_a + \theta C_l)$
- ρ_b = soil bulk density (g/cm³)
- C_a = adsorbed solute concentration (g or Ci per g soil)
- θ = moisture content (dimensionless), and as discussed previously, dependent on the soil matric potential
- C_l = dissolved solute concentration (g or Ci per cm³ water)
- J_x, J_y, J_z = water or moisture flux (cm/s) along the x, y, and z directions, respectively
- D_e = effective dispersion/diffusion coefficient (cm²/s); note that the entire terms represent the flux of solutes that crosses the planes normal to the x, y, and z directions, respectively, because of diffusion and dispersion
- $\frac{\partial C_l}{\partial \{x,y,z\}}$ = the change in dissolved solute concentration through space in the x, y, and z directions, respectively; note that the entire terms represent the flux of solutes that crosses the planes normal to the x, y, and z directions, respectively, because of diffusion and dispersion
- $t^{1/2}$ = radioactive half-life(s), the entire term represents the mass of solute lost to radioactive decay.

In Equation 6-14, positive is used to indicate solute entering the finite volume, and negative is used to indicate what is exiting or lost to decay. The adsorbed and dissolved solute concentrations are related through an equilibrium linear sorption coefficient (K_d mL water per g

RPP-ENV-58782, Rev. 0

soil) formulation: $C_a = K_d C_l$. No temperature effects are considered for the vadose zone model (i.e., the model used is isothermal).

6.3.2.2 STOMP®-Based Process-Level Model Implementation of the Groundwater Pathway. This section describes the details of the implementation of the STOMP®-based process-level model used in the WMA C PA for evaluation of the groundwater pathway. The description presented in this section primarily addresses the development of the conceptual model components and base case parameters. The discussion includes the alternative geologic interpretations evaluated as part of the sensitivity analysis because those interpretations involve uncertainty in a conceptual model component. Parameter sensitivity and uncertainty are addressed in Section 8. DOE/RL-2011-50 contains the description of the generalized models, conditions, and parameters applicable to the Hanford Site vadose zone, which were refined and augmented for the WMA C PA evaluation.

The site-specific STOMP® model components for the WMA C PA evaluation are:

- Model domain and boundary conditions
- Hydrogeologic model
- Source term
- Recharge
- Vadose zone hydrogeology and fluid transport
- Groundwater domain and characteristics
- Geochemistry.

The model domain and boundary conditions are included in the list above to emphasize the fundamental nature of boundary conditions used in the modeling. The evaluation adopted modeling assumptions and parameter estimates for WMA C site-specific conditions to determine the impacts to groundwater resulting from post-retrieval residual waste remaining in tanks, ancillary equipment, and pipelines in accordance with DOE O 435.1 requirements.

The following subsections for the individual conceptual model components provide the basis, rationale, and references for the base case values. These parameters represent the values selected for use in the model from the ranges of plausible parameter values. These values may differ from parameter estimates for other Hanford Site modeling performed for different purposes or areas of the Hanford Site, or at different scales.

6.3.2.2.1 Model Domain and Boundary Conditions. The model domain and boundary conditions establish both a framework and limiting conditions for the numerical model. The model domain for flow and transport in the vadose zone is represented numerically in 3-D space, with one of the horizontal axes aligned in the general direction of groundwater flow. Aligning an axis with the general direction of groundwater flow allows concentrations to be calculated more easily downgradient of the waste sites. The numerical model adapts the physical elements of the conceptual model to a Cartesian grid, and also assigns numerical values to the parameters used in algorithms to represent the physical and geochemical systems and processes.

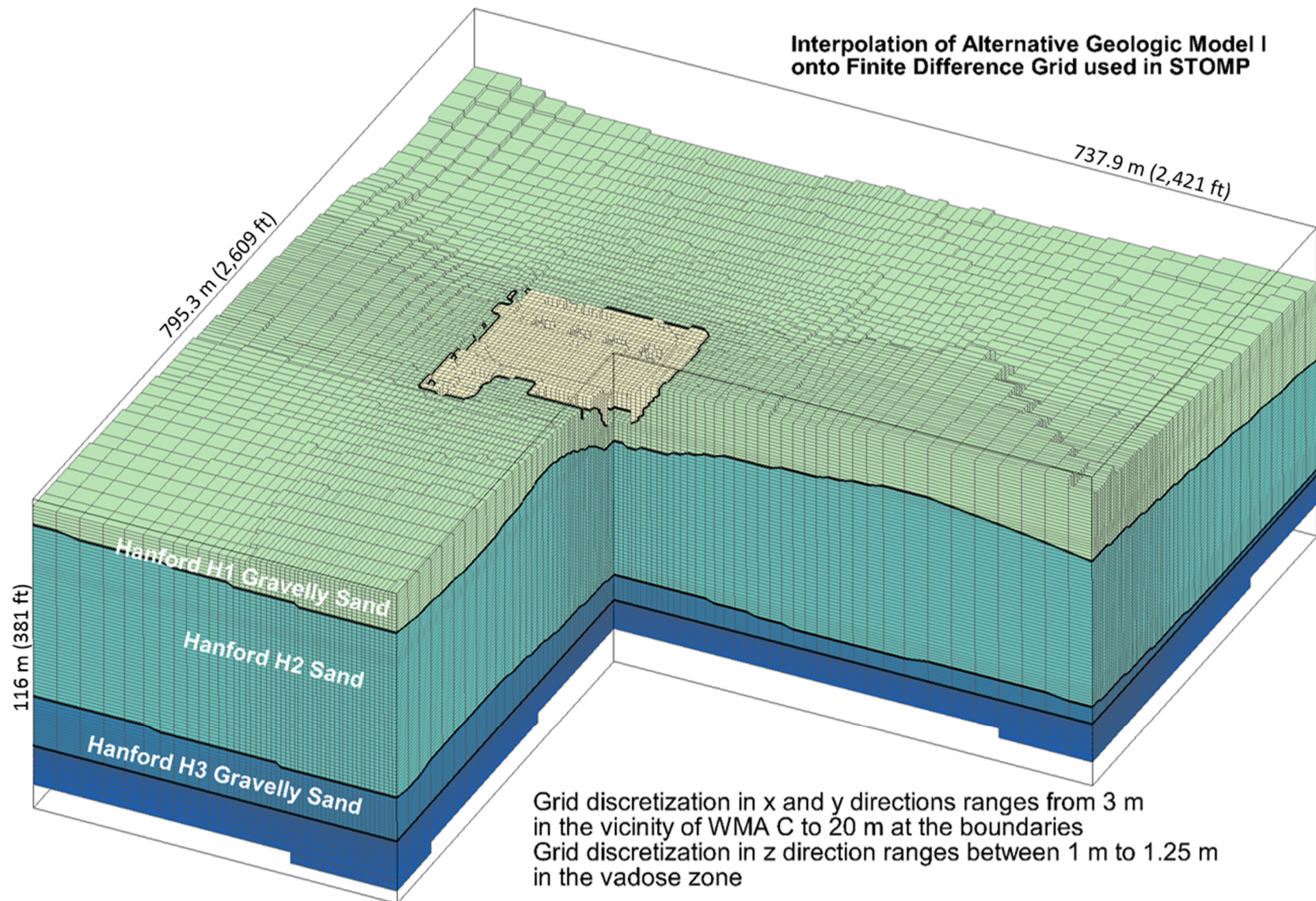
RPP-ENV-58782, Rev. 0

1 The WMA C model domain is 737.9 m (2,421 ft) northwest to southeast by 795.3 m (2,609 ft)
2 southwest to northeast by 116 m (381 ft), vertically, extending about 12 m (39 ft) below the
3 water table (Figure 6-36). The southwestern and northwestern boundaries of the model are
4 574656.09 m, 136454.41 m, and 575218.45 m, 137016.78 m, respectively (Lambert Coordinate
5 system easting, NOAA Manual NOS NGS 5, "State Plane Coordinate System of 1983"). The
6 southeastern and northeastern boundaries are 575177.86 m, 135932.64 m, and 575740.22 m,
7 136495.00 m, respectively. The vertical base elevation of the model is nominally 95 m (312 ft)
8 (North American Vertical Datum of 1988 [NAVD88]), although the bottom and top of the model
9 domain vary spatially according to the top of basalt elevation and surface relief, respectively
10 (RPP-RPT-56356).

11
12 The horizontal node spacing varies between 3.0 and 20 m (9.8 and 65.6 ft) to optimize the
13 discretization in the areas attempting to approximate the slopes associated with construction of
14 WMA C and the 100-series tanks without overwhelming the available computational resources.
15 Figure 6-37 shows the plan view distribution of the calculation nodes. The vertical spacing in
16 the vadose zone ranged between 1 and 1.25 m (3.28 and 4.10 ft) except around the water table,
17 where the spacing decreased to 0.5 m (1.6 ft) to capture the impact of the capillary fringe above
18 the water table. The total number of nodes in the modeled rectangular prism equals 736,653.
19 During the pre-operational phase, the number of active nodes equals 640,565 with
20 96,088 inactive. Inactive nodes represent space where no flow occurs, e.g., above ground
21 surface, within basalt, or within intact tanks. During the operational and post-closure phases, the
22 number of active nodes equals 637,543 with 99,110 inactive, the increase in inactive nodes
23 attributed to the inactivation of the tank and ancillary equipment nodes within the WMA C
24 excavation.

25
26 A specified-flux boundary condition was applied at the surface to simulate recharge. Recharge
27 rates varied spatially and temporally along the upper boundary, depending on surface conditions,
28 the presence of WMA C and other facilities, and the time of WMA C operations and surface
29 conditions simulated (RPP-RPT-44042). The bottom boundary of the unsaturated (vadose) zone
30 is the water table, and the bottom of the model (aquifer) was defined as a no-flow boundary
31 condition. Boundary conditions at the sides of the model domain were assumed to be no flow in
32 the vadose zone and prescribed flux and prescribed head in the aquifer on the upgradient and
33 downgradient boundaries, respectively. The boundary condition in the aquifer on the upgradient
34 boundary was assumed to be prescribed flux, calculated on the basis of the hydraulic
35 conductivity and gradient, and independent of recharge. The prescribed flux boundary condition
36 value includes a factor to account for the varying thickness of the unconfined aquifer and uneven
37 surface of the underlying basalt. To account for the non-uniform aquifer thickness from the
38 underlying basalt boundary, the nominal flux rate was calculated as the product of the hydraulic
39 conductivity and gradient (base case values of 11,000 m/day [6.8 mi/day] and 2×10^{-5} m/m
40 [6.6×10^{-5} ft/m], respectively; see the upcoming "Groundwater Domain and Characteristics"
41 discussion and Appendix C for the basis of these parameter estimates), and was proportioned
42 according to the ratio of the average aquifer cross-sectional area throughout the model domain
43 (9,440 m² [2.3 acres]) and the aquifer area along the upgradient boundary (6,151 m² [1.5 acres])
44 where the prescribed flux is applied. The aquifer cross-sectional area refers to the area
45 perpendicular to the direction of groundwater flow. The aquifer cross-sectional area varies from
46 the northwest to southeast boundaries because of the uneven top of the basalt.

1 **Figure 6-36. The Interpolated Numerical Three-Dimensional Post-Closure Alternative I Hydrogeologic Model.**



3 STOMP = Subsurface Transport Over Multiple Phases (computer code)

WMA = Waste Management Area

RPP-ENV-58782, Rev. 0

Hydrogeologic Model. The hydrogeologic conceptual model developed for the WMA C PA (RPP-RPT-46088 and RPP-RPT-56356) provides the information basis and data necessary to prepare the 3-D geologic inputs used in the 3-D numerical model. Each node in the numerical model represents a unique set of horizontal (x and y) coordinates and vertical (z) elevation. A node is assigned the hydrogeologic properties associated with the HSU identified in the RPP-RPT-56356 geologic models as existing in the space represented by the node coordinates and elevation.

Figure 6-38 shows the geologic interpretation prepared by Washington River Protection Solutions, LLC (WRPS) staff and identified as Alternative Geologic Model I as interpolated onto the numerical grid used in the fate and transport model. Figure 6-38 shows some internal cross-sections of the geology to illustrate the shape and layering of the hydrogeologic units. Figures 6-39 and 6-40 show the geologic interpretation prepared with input from technical staff of the Nez Perce and identified as Alternative Geologic Model II. Alternative Geologic Model II includes the separation of the Hanford H2 sand unit into three distinct subunits: the Hanford H2 sand, the Hanford H2 gravelly sand, and the Hanford H2 fine or silty sand. Explanation of the basis and the development of the two geologic interpretations is presented in RPP-RPT-56356. The sensitivity analysis includes evaluation of a third alternative geologic model that is identical to Alternative Geologic Model I, except that a clastic dike is assumed to exist under tanks C-102, C-105, C-108, and C-111, and another is assumed to exist under tanks C-110, C-111, and C-112. These clastic dikes extend the length and width, respectively, of WMA C, and extend from the bottom of the WMA C excavation to the capillary fringe of the aquifer.

6.3.2.2.2 Source Term. The results from the source term release model implemented using GoldSim[®] provide the time varying release functions of residual waste inventory for all sources (tanks and ancillary equipment) as input to the STOMP[®]-based model. The nodes in the STOMP[®]-based model that define the base of tanks and ancillary equipment uniformly distribute the mass release provided by the GoldSim[®]-based source term for simulating the fate and transport through the vadose zone and saturated zone. The source term model calculations are described in Section 6.3.1 and use residual inventory information presented in Tables 3-13, 3-14, and 3-15, where the radionuclide inventory has been decayed to January 1, 2020.

6.3.2.2.3 Recharge. The magnitude of recharge for soils at the Hanford Site varies as a function of the soil type, condition of the vegetation cover, and soil integrity (e.g., disturbed versus undisturbed). The range of recharge values reported in RPP-RPT-44042 represents distinct populations of data based on lysimetry and isotopic measurements, and interpretation—and, in some instances, extrapolation—by Hanford Site subject matter experts. The natural background recharge rates represent a population for natural vegetated conditions. The range of values for operational conditions represents a population of recharge rates for vegetation-free disturbed soil.

The final design for the surface barrier for WMA C at closure has not been developed. The surface barrier is expected to function comparably to a modified RCRA Subtitle C barrier (Section 3.2.1.2.2), which PNNL-16688 indicates should function similarly to the Prototype Hanford Barrier. Summary of data collected over 13 years at the Prototype Hanford Barrier (PNNL-17176, “200-BP-1 Prototype Hanford Barrier Annual Monitoring Report for Fiscal

RPP-ENV-58782, Rev. 0

Years 2005 Through 2007"; DOE/RL-93-33) indicates that infiltration through the prototype is much less than 0.1 mm/yr (0.004 in./yr), and evaluations of the design using lysimeter data indicate that the barrier is capable of limiting recharge to this amount even with a complete lack of vegetation (Fayer and Gee 2006). However, for base case simulations involving WMA C PA with a functioning surface barrier, a base case recharge rate of 0.5 mm/yr (0.02 in./yr) is assumed, which is consistent with the drainage design specification in DOE/RL-93-33.

At the end of 500 years, the surface barrier performance is assumed to degrade to permit an infiltration rate of 3.5 mm/yr (0.14 in./yr) and maintain that infiltration rate for the remainder of the simulation for the base case. No quantifying data are available for specifying the performance of the barrier top after its design life, but the performance of the surface barrier in limiting recharge is not expected to diminish appreciably (PNNL-16688). According to PNNL-13033, not even the erosion of the silt loam layer and deposition of dune sand on the barrier is likely to alter the barrier performance significantly. The value of 3.5 mm/yr (0.14 in./yr) corresponds to the recharge in an undisturbed area, which indicates that native vegetation is assumed to reclaim the land.

Although the side slopes and berm are likely to function and perform differently than the surface of the barrier, they are included as part of the barrier surface. The impact of the side slopes on the overall recharge rate is expected to be relatively negligible. The sandy gravel/gravelly sand barrier side slope and berm are assumed eventually to resemble a Burbank loamy sand, and if that assumption is valid, then PNNL-16688 indicates that the long-term recharge rate for that soil type is 1.9 mm/yr (0.07 in./yr), which is less than the 3.5 mm/yr (0.14 in./yr) used in the analysis for the degraded barrier surface. Table 6-6 presents a summary of the base case recharge rates applied to the different surface types present within the WMA C model domain.

6.3.2.2.4 Vadose Zone Hydrogeology and Transport. The vadose zone hydrogeology and transport information presented here is a brief summary of the information presented in Appendix B. Appendix B includes detailed discussion and description of the data available and the methods used to develop the base case parameters, and sensitivity and uncertainty distributions and percentile values.

The flow and transport pathway process used for the WMA C vadose zone modeling is porous media continuum flow. The porous media continuum assumption and the soil relative permeability/saturation/capillary pressure relations provide the basis for vadose zone flow and transport modeling (PNNL-11216, PNNL-12030). The vadose zone at the Hanford Site is composed of sediments ranging in particle size associated with gravels to silts or clays. In the model domain, the hydraulic properties describing fluid transport characteristics associated with each geologic layer (also referred to as hydrostratigraphic units) are approximated by average upscaled values, with each unit having different flow and transport parameter values (hydraulic conductivity, bulk density, and dispersivity). The model describes bulk (or mean) flow and radionuclide transport behavior in the vadose zone, limiting the evaluation to estimating overall and eventual radionuclide impacts to groundwater. Porous media continuum transport in unsaturated media of this type is regarded as the fundamental process and feature for modeling contaminant fate and transport behavior in the vadose zone at the Hanford Site (DOE/RL-2011-50).

RPP-ENV-58782, Rev. 0

Table 6-7 lists the upscaled composite-fitted van Genuchten-Mualem (van Genuchten 1980, Mualem 1976, EPA/600/2-91/065) base case parameters for the various strata at the WMA C site. A stochastic model of variable moisture or tension-dependent anisotropy provides the framework for upscaling small-scale measurements to the effective (upscaled) properties for the large-scale vadose zone (Polmann 1990). The upscaling processes factor the inherent spatial variability that occurs on different scales in heterogeneous media into the field-scale parameter estimates (“Stochastic analysis of moisture plume dynamics of a field injection experiment” [Ye et al. 2005], “Estimation of effective unsaturated hydraulic conductivity tensor using spatial moments of observed moisture plume” [Yeh et al. 2005]). Specific upscaled flow parameters include moisture retention, and saturated and unsaturated hydraulic conductivity. Upscaled transport parameters include bulk density, diffusivity, sorption coefficients, and macrodispersivity. Detailed discussion of the Polmann (1990) model and the derivation of the upscaled parameters are presented in Appendix B.

Estimated unsaturated conductivities, based on saturated conductivity and the van Genuchten retention model, can differ by up to several orders of magnitude with measured conductivities at the dry end (e.g., Khaleel et al. 1995). Therefore, unlike the conventional approach, the unsaturated conductivities are not based on predictions using the measured retention curve and the measured saturated conductivity. Rather, the soil hydraulic properties are based on a simultaneous fit of moisture retention and unsaturated conductivity data, and all five unknown parameters θ_r , θ_s , α , n , and K_s , with $m=1-1/n$ (van Genuchten 1980) were fitted to the data via a code named RETention Curve (RETC) (EPA/600/2-91/065). Thus, in order to obtain a better agreement with experimental data for the region of interest (i.e., relatively dry moisture regime), K_s is treated as a fitted parameter during the curve fitting process. This is considered appropriate because the WMA C PA predictions are needed for the relatively dry moisture regime observed in the field, rather than for the saturated or near-saturated regime. The pore size distribution factor, ℓ , was kept fixed at 0.5 during the simultaneous fitting.

For the Alternative Geologic Model II evaluation, the Hanford H2 gravel/coarse sand subunit was assumed to be more transmissive, and the Hanford H2 silty sand less transmissive, than the Hanford H2 sand. Therefore, as an initial estimate of these properties, the hydraulic properties associated with the 5th and 95th percentile realizations of unsaturated hydraulic conductivity curves developed for the Hanford H2 sand unit were considered representative of the Hanford H2 gravel/coarse sand and the Hanford H2 silty sand subunits, respectively.

The effective transport parameter (i.e., macrodispersivity, bulk density, and diffusivity) estimates used in the base case and sensitivity cases are presented. Because of natural variability, the transport parameters are all spatially variable. The purpose is similar to the upscaled flow parameters, to evaluate the effect of such variability on the large-scale transport process. Effective bulk density (ρ_b) estimates are needed to calculate retardation factors for different species. The average ρ_b , $E[\rho_b]$ estimates for various strata at WMA C are presented in Table 6-8. These estimates are derived from bulk density sample values listed in Appendix B. Appendix B also provides a summary of the numerical simulation, stochastic theory, and 200 Areas experimental data that provide the basis for the base case estimates of macrodispersivity (Table B-11). The estimated values of macrodispersivity applicable to the scale of the WMA C PA model for the base case evaluation are shown in Table 6-9.

RPP-ENV-58782, Rev. 0

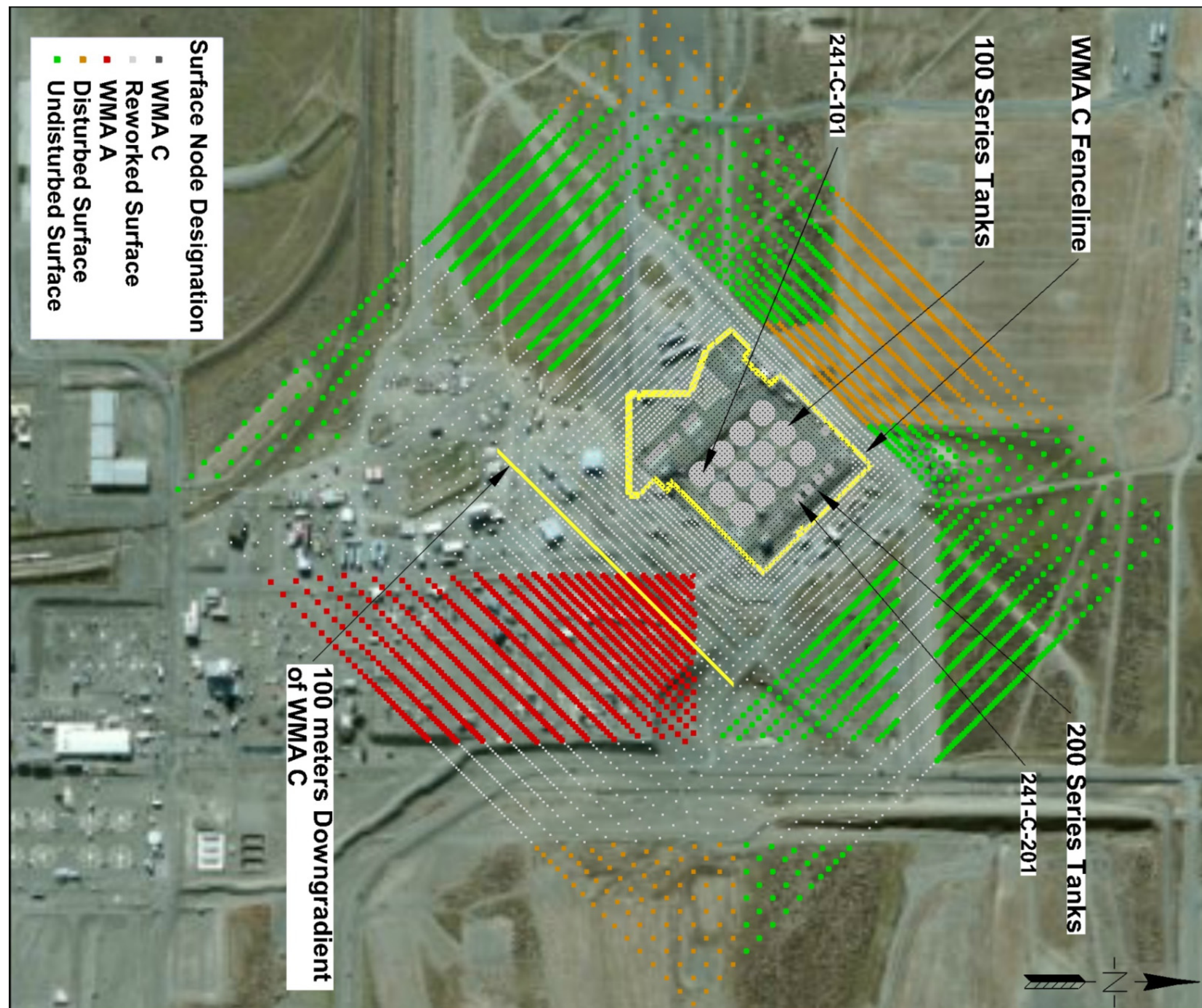


Figure 6-37. Plan View of Waste Management Area C Performance Assessment Model Domain Showing the Horizontal Distribution and Surface Type of the Irregularly-Spaced Calculation Nodes. The resolution increases in the area of Waste Management Area C.

WMA = Waste Management Area

Figure 6-38. Diagram of the Interpolated Numerical Three-Dimensional Post-Closure Alternative I Hydrogeologic Model.

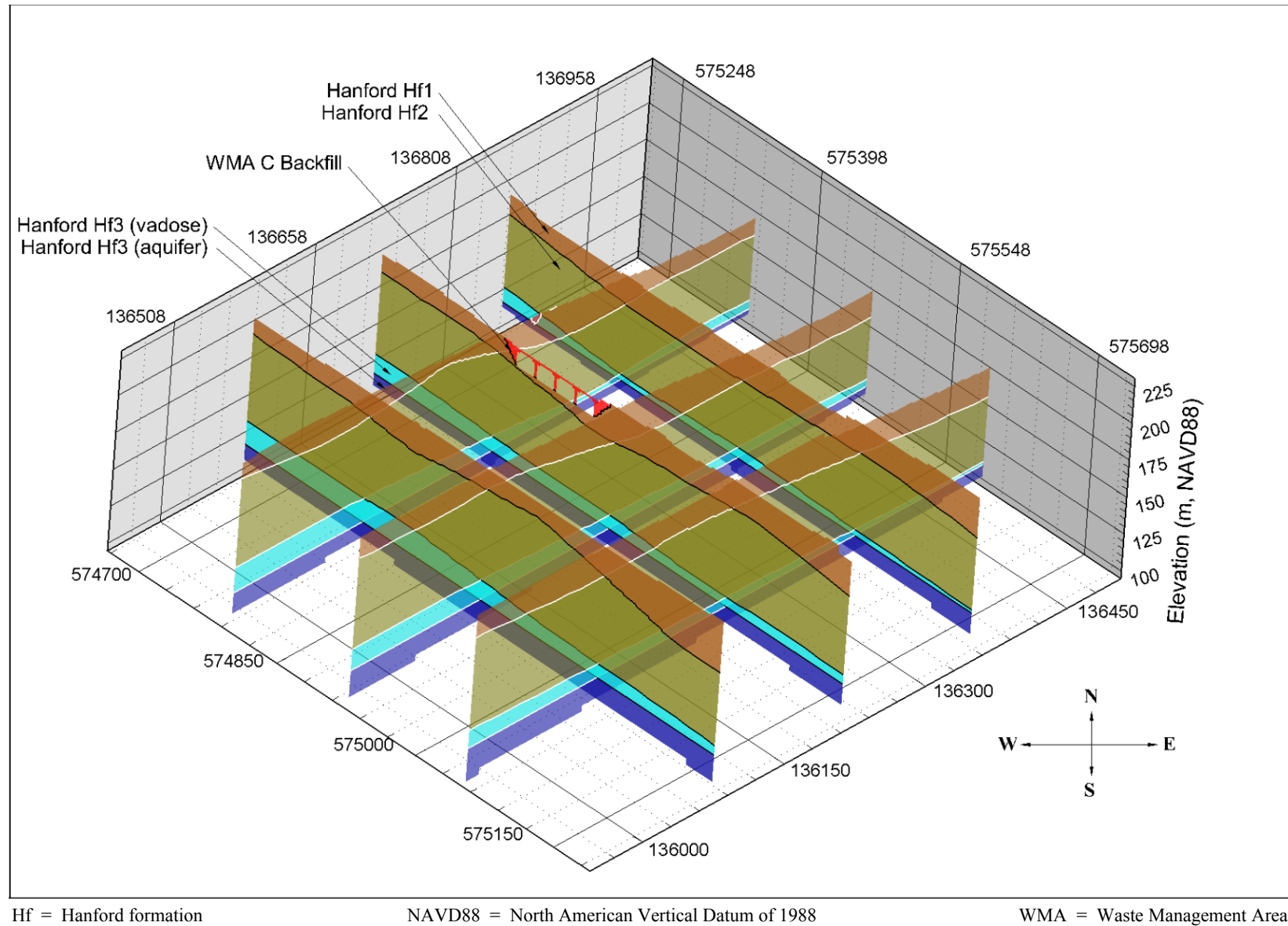
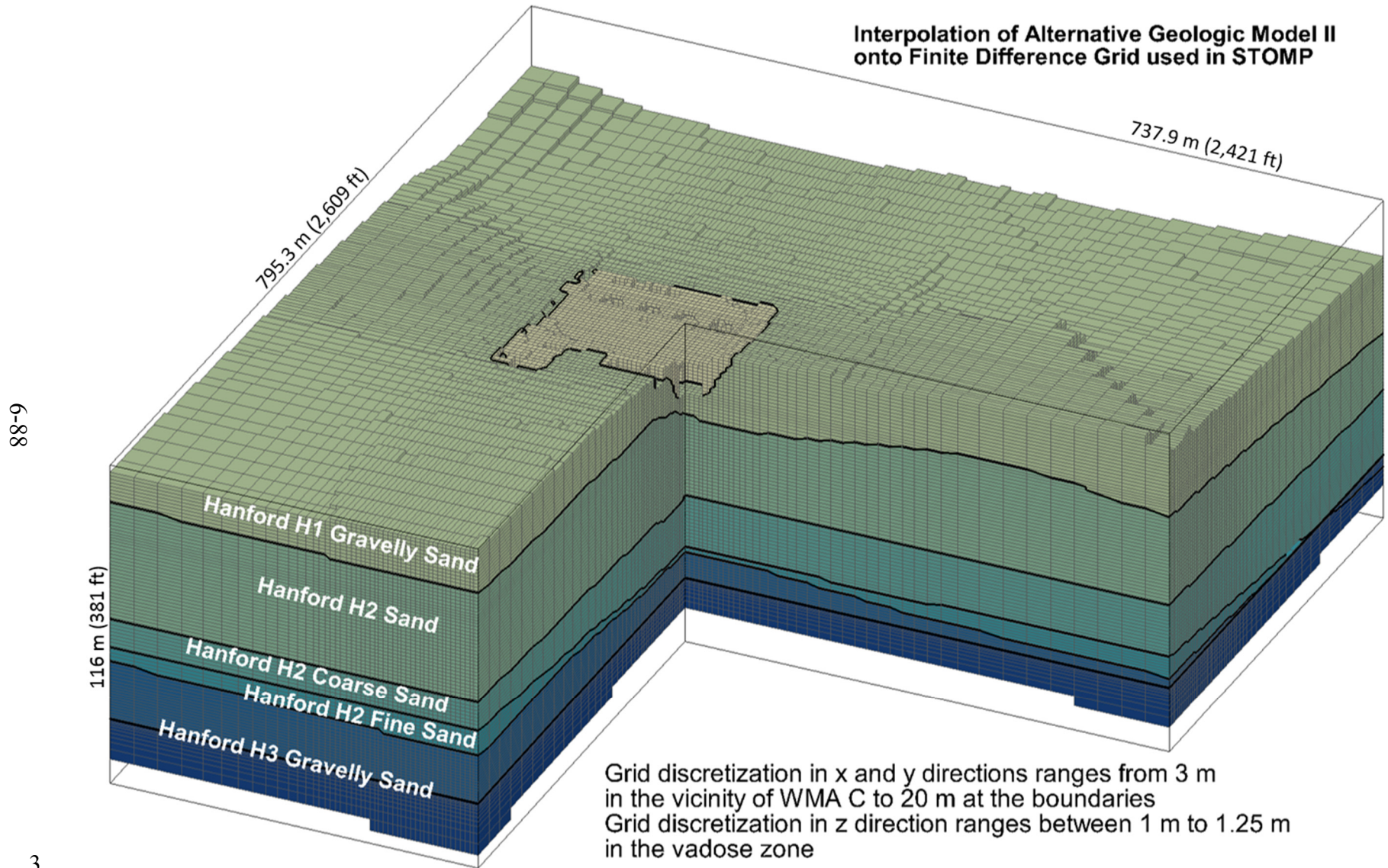


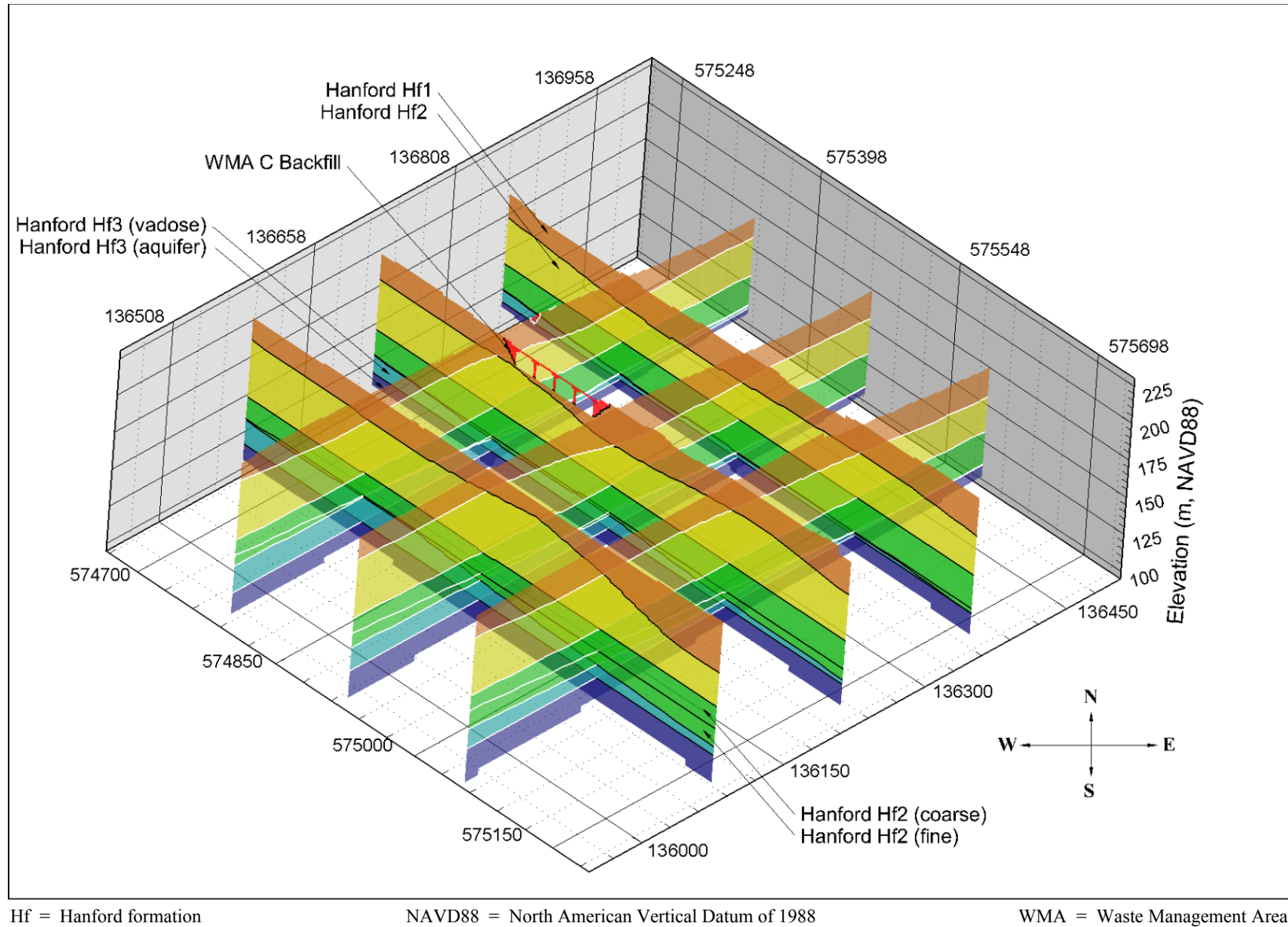
Figure 6-39. The Interpolated Numerical Three-Dimensional Post-Closure Alternative II Hydrogeologic Model.



RPP-ENV-58782, Rev. 0

WMA = Waste Management Area

Figure 6-40. Diagram of the Interpolated Numerical Three-Dimensional Post-Closure Alternative II Hydrogeologic Model.



RPP-ENV-58782, Rev. 0

Table 6-6. Base Case Recharge Rate (Net Infiltration) Estimates for Surface Conditions during the Pre-Construction, Operational, and Post-Closure Periods.

Period	Waste Management Area (WMA) C Region and Surface Condition	Base Case Value of Recharge Rate (mm/yr)
Pre-construction (before 1944)	Undisturbed region (Rupert sand with vegetation)	3.5
Operational period (1945 to 2020)	Undisturbed region (Rupert sand with vegetation)	3.5
	WMA C Surface region (Gravel without vegetation)	100
	WMA A Surface region (Gravel without vegetation)	100
	Disturbed revegetated region (Rupert sand with vegetation)	22
	Disturbed unvegetated region (Rupert sand with no vegetation)	63
Early post-closure (2020 to 2520)	Undisturbed region (Rupert sand with vegetation)	3.5
	WMA C Surface region (Surface barrier with vegetation)	0.5
	WMA A Surface region (Surface barrier with vegetation beginning in 2050)	0.5
	Disturbed revegetated region (Rupert sand with vegetation beginning in 2050 with vegetation recovery completed in 2080)	3.5
	Disturbed unvegetated region (Rupert sand with no vegetation until vegetation recovery begins in 2050 and completes in 2080)	3.5
Late post-closure (2520 to 3020 and beyond)	Undisturbed region (Rupert sand with vegetation)	3.5
	WMA C Surface region (Surface barrier with vegetation)	3.5
	WMA A Surface region (Degraded surface barrier with vegetation begins in 2550)	3.5
	Disturbed revegetated region (Rupert sand with vegetation recovery completed in 2080)	3.5
	Disturbed unvegetated region (Rupert sand with vegetation recovery completed in 2080)	3.5

It is assumed that the effective, large-scale diffusion coefficients for all strata in the vadose zone at the WMA C site are a function of volumetric moisture content, θ , and can be expressed using the Millington-Quirk ("Permeability of Porous Solids" [Millington and Quirk 1961]) empirical relation:

$$D_e(\theta) = D_0 \frac{\theta^{10/3}}{\theta_s^2} \quad (6-15)$$

Where:

$D_e(\theta)$ = the effective diffusion coefficient of an ionic species

RPP-ENV-58782, Rev. 0

- 1 D_0 = the effective diffusion coefficient for the same species in free water
 2 θ = the localized volumetric moisture content
 3 θ_s = the localized volumetric moisture content at saturation.
 4

Table 6-7. Composite van Genuchten-Mualem Parameters for Various Strata at the Waste Management Area C Site Used in the Base Case Evaluations of Alternative Geologic Models I and II.

Strata	Number of Samples	θ_s	θ_r	α (1/cm)	n	t^c	Fitted K_s (cm/s)
Backfill (Gravelly)	10	0.138	0.010	0.021	1.374	0.5	5.60E-04
Hanford H1/H3 (Gravel-dominated)	15	0.171	0.011	0.036	1.491	0.5	7.70E-04
Hanford H2 (Sand-dominated)	44	0.315	0.039	0.063	2.047	0.5	4.15E-03
Hanford H2 – Gravel/coarse sand subunit*	not applicable	0.265	0.002	0.108	1.724	0.5	1.68E-02
Hanford H2 – Silty-sand subunit*	not applicable	0.354	0.029	0.040	1.633	0.5	1.79E-03

*Hydraulic properties of these units are only used in numerical model simulation of Alternative Geologic Model II. As an initial estimate of these properties, the hydraulic properties associated with the 5th and 95th percentile realizations of unsaturated hydraulic conductivity curves developed in the Uncertainty and Sensitivity Analysis for the Hanford H2 sand unit were considered to be representative of the Hanford H2 silty sand and the Hanford H2 gravel/coarse sand subunits, respectively.

- 5 The tortuosity formulation in the Millington-Quirk model is based on theoretical considerations
 6 absent from other empirical models, and accounts for the ranges of moisture contents present in
 7 the vadose zone around WMA C. The molecular diffusion coefficient for all species in pore
 8 water is assumed to be 2.5×10^{-5} cm²/sec (6.98×10^{-4} in.²/sec) (WHC-SD-WM-EE-004), which
 9 is consistent with, and representative of, values used in other Hanford PAs (WHC-EP-0645,
 10 BHI-00169, WHC-SD-WM-TI-730, WHC-SD-WM-EE-004, and DOE/ORP-2000-24).

- 11 **6.3.2.2.5 Groundwater Domain and Characteristics.** The groundwater in the aquifer system
 12 in the vicinity of WMA C has been studied extensively as part of the site characterization that is
 13 discussed in RPP-RPT-46088. The groundwater conceptual model for WMA C includes the
 14 uppermost unconfined aquifer system that exists within a channel eroded by the cataclysmic
 15 floods of the Pleistocene age. The base of the aquifer is the underlying basalt surface. The
 16 undifferentiated lower sands and gravels associated with the Hanford formation, CCU, and the
 17 Ringold Formation (Unit A) that comprise the aquifer sediments are simply categorized as
 18 saturated Hanford H3 sediments in the model. The thickness of the uppermost aquifer beneath
 19 WMA C is ~12 m (39 ft). The model results provided represent concentrations in the upper 5 m
 20 (16.4 ft) of the aquifer. The 5 m (16.4 ft) vertical interval corresponds to the well screen length
 21 of a conceptual groundwater monitoring well, and the basis for that delimiter to the groundwater
 22 concentrations calculation is presented in upcoming discussion regarding “Point of Calculation,
 23 Protectiveness Metric, and Time Frame Considerations.”

RPP-ENV-58782, Rev. 0

Table 6-8. Effective Bulk Density ($E[\rho_b]$, g/cm³) Estimates for Various Strata at Waste Management Area C Used in the Base Case Evaluations of Alternative Geologic Models I and II.

Strata	$E[\rho_b]$
Backfill (Gravelly) ¹	2.13
Hanford H1/H3 (Gravel-dominated) ¹	2.05
Hanford H2 (Sand-dominated) ²	1.71
Hanford H2 – Gravel/coarse sand subunit ³	1.83
Hanford H2 – Silty-sand subunit ³	1.61

¹See Appendix B.

²From Table 7 of RPP-20621, “Far-Field Hydrology Data Package for the Integrated Disposal Facility Performance Assessment,” by taking the average of soil samples 7A through 35A.

³Effective bulk densities of these units are only used in numerical model simulation of Alternative Geologic Model II. The values are calculated based on particle density of 2.49 g/cm³ and porosity equal to saturated moisture content presented in Table 6-7. The particle density of 2.49 g/cm³ is derived from the bulk density of 1.71 g/cm³ for Hanford H2 sand with porosity of 0.315 (Table 6-7).

Table 6-9. Macrodispersivity Estimates for Various Strata at Waste Management Area C Used in the Base Case Evaluations of Alternative Geologic Models I and II.

Strata	A_L (cm)	A_T (cm)
Backfill (Gravelly)	~20	2.0
Hanford H1/H3 (Gravel-dominated)	~20	2.0
Hanford H2 (Sand-dominated)	~25	2.5
Hanford H2 – Gravel/coarse sand subunit*	~25	2.5
Hanford H2 – Silty-sand subunit*	~25	2.5

*Macrodispersivities of these units are only used in numerical model simulation of Alternative Geologic Model II.

See Appendix B.

Groundwater flow beneath WMA C has been historically difficult to measure because the hydraulic gradient is very small and the hydraulic conductivity is very high in this region of the Hanford Site. In addition, the water table continues to recover from the operational liquid discharges at 216-B-3 Pond system and other large discharge sites in 200 East Area. The projected equilibrium state is expected to be similar to its pre-Hanford behavior (see Section 3 and Appendix C). As a result, the post-closure position of the water table and associated hydraulic gradient can only be evaluated through modeling. Consequently, the groundwater flux

RPP-ENV-58782, Rev. 0

in the aquifer beneath WMA C is calculated on the basis of the aquifer hydraulic properties, and the hydraulic gradient projected to exist in the future.

The hydraulic heads around WMA C are expected to continue declining slowly until they stabilize around 119.5 m (392 ft) within 100 years in the future (CP-47631). The gradient is generally expected to slope from northwest to southeast with a value of about 0.00002 m/m, which is close to the one observed prior to start of Hanford operations (Figure 6-41). Appreciable changes in hydraulic gradient are not expected in the future once the hydraulic heads stabilize. Thus, the hydraulic gradient is assumed to remain stable for the base case analysis.

Appendix C discusses the scale dependence of aquifer properties and indicates that field-scale calibrated groundwater models are the most appropriate approach for parameterization of the WMA C saturated media hydraulic conductivity. To date, the Central Plateau Groundwater Model (CPGWM, CP-47631) appears to be the most appropriate and applicable calibrated model to provide that parameterization. The CPGWM provides calibrated hydraulic conductivity estimates for the model layers and HSUs present within the aquifer in the vicinity of WMA C. Within the WMA C flow domain, the weighted average of hydraulic conductivity derived from the CPGWM is approximately 11,000 m/day (33,000 ft/day). Thus, the base case horizontal saturated hydraulic conductivity for the aquifer is estimated to be 11,000 m/day (33,000 ft/day). The CPGWM estimate of vertical anisotropy ratio of 0.1 is also incorporated in the WMA C base case. Table 6-10 presents a summary of the aquifer base case hydraulic parameters for the Hanford H3 – aquifer. The aquifer, identified as Hanford H3 – aquifer, is separated from that portion of the Hanford H3 above the water table, reflecting the distinctly different saturation conditions.

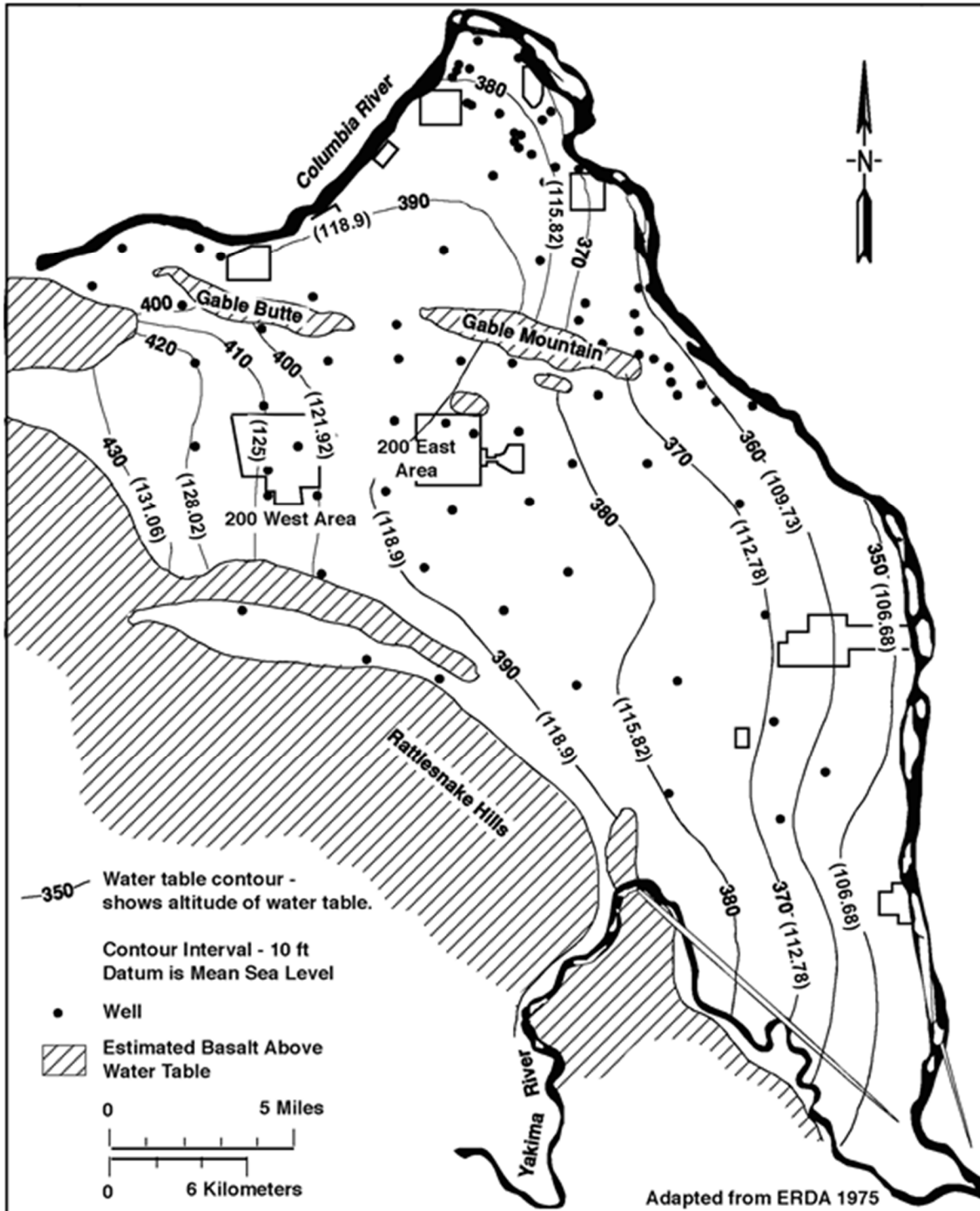
6.3.2.2.6 Sorption Characteristics. Linear K_d isotherm is a reasonable representation for modeling sorption of radionuclides on the sediments when released from tank residuals and ancillary equipment. The rationale for the use of a K_d -based approach for vadose zone units is presented in Section 6.2.2.1.5 and discussed in detail in DOE/RL-2011-50. The K_d values are chosen assuming low-salt, near-neutral waste chemistry in the vadose and saturated zone.

The basis for the K_d values used to approximate the transport of the contaminants and radionuclides are presented in Table 6-11, including the values lowered to account for the gravel content per the procedure described in PNNL-17154. PNNL-17154 indicates that K_d values are typically lower for materials that contain significant amounts of gravel (notably Backfill, Hanford H1, and Hanford H3) than those determined with <2-mm (0.08-in.)-size material. The gravel corrected values are not included in the table for the contaminants and radionuclides that the 3-D screening evaluation indicated would not arrive at the water table within 10,000 years.

6.3.2.2.7 Point of Calculation, Protectiveness Metric, and Time Frame Considerations. In accordance with risk assessment guidelines, the determination of soil contamination impacts to groundwater also requires the definition and rationale for (1) the PoCal, i.e., the place and points in the groundwater domain where modeled groundwater concentrations are to be assessed for potential impacts and protectiveness; (2) the protectiveness metric, i.e., the groundwater metric(s) to be used in the assessment of protectiveness at the PoCal, and; (3) the time frame considered applicable for the calculation of impacts to groundwater.

RPP-ENV-58782, Rev. 0

1 **Figure 6-41. Hindcast Water Table Map of the Hanford Site, January 1944.**
 2



G01010017.20
 S0012051.5.P:0

3 ERDA 1975 = ERDA-1538, "Final Environmental Statement, Waste Management Operations, Hanford Reservation,
 4 Richland, Washington."
 5

6 Source: WHC-SD-ER-TI-003, "Geology and Hydrology of the Hanford Site: A Standardized Text for Use in
 7 Westinghouse Hanford Company Documents and Reports."
 8

RPP-ENV-58782, Rev. 0

Table 6-10. Base Case Soil Hydraulic Properties for Aquifer Soil Type Used for Base Case at Waste Management Area C.

Aquifer Soil Type	Total Porosity	Saturated Moisture Content	Horizontal Saturated Hydraulic Conductivity ^a (m/day)	Longitudinal Dispersivity ^b (m)	Aquifer Hydraulic Gradient (m/m)	Average Aquifer Water Flux (m ³ /day/m ²)
Hanford H3 (aquifer)	0.20	0.20	11,000	10.5	0.00002	0.22

^a Vertical Saturated Hydraulic Conductivity assumed equal to 1/10 of the Horizontal Saturated Hydraulic Conductivity.

^b Transverse dispersivity assumed to be equal to 1/10 of the longitudinal dispersivity.

See Appendix C.

The PoCal for the groundwater impact analysis is 100 m (328 ft) downgradient from the WMA C fenceline. The PoCal is intended to effectively serve as the point where exposure point groundwater concentrations are evaluated in the model for the purpose of evaluating the achievement of the groundwater protection performance objectives. The PoCal for the protection of groundwater is related to “Point of Compliance” in Federal PA requirements (DOE M 435.1-1; DOE G 435.1-1, Chapter 4), which is described as follows:

“The point of compliance shall correspond to the point of highest projected dose or concentration beyond a 100 meter buffer zone surrounding the disposed waste.
A larger or smaller buffer zone may be used if adequate justification is provided.”

The aquifer mixing zone extends into the upper 5 m (16.4 ft) of the aquifer for the purpose of the evaluations. DOE M 435.1-1 does not specify the level of protection required for water resources, and there are no applicable parameterization requirements or guidelines indicated in DOE G 435.1-1, Chapter 4. The format and content guide (DOE G 435.1-2, Implementation Guide for use with DOE M 435.1-1, Format and Content Guide for U.S. Department of Energy Low-Level Waste Disposal Facility Performance Assessments and Composite Analyses) indicates that the aquifer mixing must be consistent with State or local laws, regulations, or agreements. The Washington Administrative Code does specify a 5-m (16.4-ft) mixing zone in groundwater that is consistent with a 5-m (16.4-ft) vertical interval corresponding to a conceptual groundwater monitoring well with the 4.6-m (15-ft) well screen length (and mixing zone dimension) associated with State monitoring well descriptions (e.g., see Equation 747-4 in WAC 173-340-747).

The compliance time frame is defined as 1,000 years following closure of the facility (DOE M 435.1-1; DOE G 435.1-1, Chapter 4). The sensitivity-uncertainty analysis along with NRC guidance (NUREG-1854) extends the evaluation to 10,000 years, which is sufficient to evaluate the peak dose from all of the radionuclides that the screening analysis indicates may not impact groundwater within the compliance period. DOE M 435.1-1 and DOE G 435.1-1, Chapter 4 state that the sensitivity-uncertainty analysis time frame should include calculation of the maximum dose regardless of the time at which the maximum occurs, as a means of increasing confidence in the outcome of the modeling and increasing the understanding of the

RPP-ENV-58782, Rev. 0

models used. However, EPA-SAB-RAC-ADV-99-006, An SAB Advisory: Modeling of Radionuclide Releases from Disposal of Low Activity Mixed Waste warns that extending the modeling time frame beyond 10,000 years could make the results irrelevant and hinder public acceptance of the results because of the inherent scientific and social uncertainties associated with such an extended time frame. The 10,000-year time frame is sufficient to address uncertainty associated with radionuclides that impact groundwater during the compliance period (NUREG-1573, A Performance Assessment Methodology for Low-Level Radioactive Waste Disposal Facilities: Recommendations of NRC's Performance Assessment Working Group).

DOE G 435.1-1, Chapter 4 states that DOE LLW disposal facilities must comply with legally-applicable requirements for water resource protection. The protectiveness metric determined to be most appropriate for the evaluation of impacts to groundwater during the compliance period from the radionuclide and contaminant inventory in WMA C are the maximum contaminant levels (MCLs). Maximum concentration limits represent the "allowable concentrations" and/or "acceptable limits" of a radionuclide for minimizing further degradation of groundwater in accordance with the conditions identified in State and Federal anti-degradation goals (e.g., EPA/540/R-92/003, Guidance for Data Useability in Risk Assessment (Part A) Final; OSWER Directive 9841.00-6C, Alternate Concentration Limit Guidance, Part I, ACL Policy and Information Requirements, Interim Final; DOE/RL-2002-59, Hanford Site Groundwater Strategy Protection, Monitoring, and Remediation).

Defining the protection of groundwater in the context of vadose zone fate and transport requires consideration of the soil and groundwater media as a hybrid or coupled pathway. This pathway involves the determination of future concentrations in the groundwater medium that result from the transport of the radionuclide and contaminant inventory existing in the WMA C tank residuals. Per this working definition, protection of groundwater pathway is considered achieved if the radionuclide and contaminant levels in the WMA C tank residuals do not cause groundwater concentrations to exceed MCLs at the PoCal within 1,000 years after closure, which is assumed to begin in 2020. Table 6-12 provides a summary of key site-specific model elements and parameters used for the model components.

6.3.2.3 Groundwater Pathway Screening Analysis Methodology. The screening phase streamlines the PA modeling effort and computation time by distinguishing those contaminants and radionuclides that may impact groundwater during the specified compliance, and sensitivity and uncertainty analysis, time frames. The screening phase uses the 3-D model to determine the maximum K_d value of contaminants contained within the WMA C tank residuals that reach the water table within 1,000 and 10,000 years. According to the facility performance requirements in DOE O 435.1, performance objectives must be met for 1,000 years, and post-closure evaluations must extend out to 10,000 years to clarify long-term impacts.

The K_d screening threshold values are based on any non-zero radionuclide impact to groundwater. This threshold represents the first indication of a groundwater impact, i.e., leading edge of a groundwater plume arriving at the water table, rather than peak concentration, which arrives later than the leading edge. The groundwater arrival time screening criteria are only focused on whether there was any non-zero impact to groundwater within the time frames considered and are applied regardless of subsequent peak concentrations. The screening analysis

RPP-ENV-58782, Rev. 0

includes vadose zone hydraulic property values and recharge rates developed for the uncertainty analysis, which are discussed in Appendix B. In particular, the screening analysis applies the maximum recharge rates associated with each period for each surface type, assigns the vadose zone hydraulic properties that produce the fastest pore water velocity for each HSU (as determined for the uncertainty analysis), and executes an advection release function for the radionuclides. Results from the groundwater pathway screening analysis are presented in Section 7.2.1.1.

Table 6-11. Distribution Coefficients (K_d) Values Used to Approximate the Transport of the Radionuclides in the Base Case. (2 sheets)

Element or Contaminant	Base Case K_d (mL/g)				
	< 2mm Material	Backfill	Hanford H1/H3	Hanford H2	Reference
Ac	350	NM	NM	NM	PNNL-16663
Al	1,500	NM	NM	NM	RPP-RPT-46088
Am	600	NM	NM	NM	PNNL-17154
B	3	NM	NM	NM	RPP-RPT-46088
C	1	0.46	0.58	0.8	PNNL-17154
Cm	350	NM	NM	NM	PNNL-16663
CN	0	NM	NM	NM	RPP-RPT-46088
Co	0	0	0	0	PNNL-17154
Cr	0	0	0	0	PNNL-17154
Cs	100	NM	NM	NM	PNNL-17154
Eu	10	NM	NM	NM	PNNL-17154
F	0	0	0	0	PNNL-17154
Fe	25	NM	NM	NM	RPP-RPT-46088
H	0	0	0	0	PNNL-17154
Hg	52	NM	NM	NM	RPP-RPT-46088
I	0.2	0.09	0.12	0.16	PNNL-17154
Mn	65	NM	NM	NM	RPP-RPT-46088
Nb	0	0	0	0	PNNL-16663
Ni	3	1.4	1.7	2.4	PNNL-17154
NO ₂	0	0	0	0	PNNL-17154
NO ₃	0	0	0	0	PNNL-17154
Np	10	NM	NM	NM	PNNL-17154
Pa	300	NM	NM	NM	PNNL-17154

RPP-ENV-58782, Rev. 0

Table 6-11. Distribution Coefficients (K_d) Values Used to Approximate the Transport of the Radionuclides in the Base Case. (2 sheets)

Element or Contaminant	Base Case K_d (mL/g)				
	< 2mm Material	Backfill	Hanford H1/H3	Hanford H2	Reference
Pb	10	NM	NM	NM	PNNL-17154
Pu	600	NM	NM	NM	PNNL-17154
Ra	10	NM	NM	NM	PNNL-17154
Rn	0	0	0	0	No relevant information available
Se	0.1	0.05	0.06	0.08	PNNL-17154
Sm	10	NM	NM	NM	PNNL-17154
Sn	0.5	0.23	0.29	0.4	PNNL-17154
Sr	10	NM	NM	NM	PNNL-17154
TBP	1.89	NM	NM	NM	RPP-RPT-46088
Tc	0	0	0	0	PNNL-16663
Th	300	NM	NM	NM	PNNL-16663
U	0.6	0.28	0.35	0.48	RPP-RPT-46088
Zr	300	NM	NM	NM	PNNL-16663

NM = not included in the three-dimensional modeling because the results of screening indicated the element or contaminant does not arrive at the water table within 10,000 years.

References:

PNNL-16663, "Geochemical Processes Data Package for the Vadose Zone in the Single-Shell Tank Waste Management Areas at the Hanford Site."

PNNL-17154, "Geochemical Characterization Data Package for the Vadose Zone in the Single-Shell Tank Waste Management Areas at the Hanford Site."

RPP-RPT-46088, "Flow and Transport in the Natural System at Waste Management Area C."

1
2 As part of the uncertainty evaluation (Section 8.1.3.1), parametric distributions of recharge
3 estimates were developed that identified maximum values for the different surface types and
4 simulation periods. The maximum net infiltration rate present during the different simulation
5 periods for each surface type (Table 6-13) is used for the screening evaluation. The maximum
6 net infiltration rate during the operations time frame is assumed to be sufficient to account for
7 any anthropogenic water sources and hypothetical leaks occurring during retrieval. Interim
8 measures enacted during fiscal year 2002 included constructing surface water controls to reduce
9 surface water run-on from major meteorological events and from breaks in waterlines; isolating,
10 cutting, and capping unnecessary waterlines; and testing operating waterlines and replacing any
11 lines found to be leaking (RPP-PLAN-39114). This provides almost 20 years of drainage before
12 the surface barrier is emplaced, and contaminant releases from tank residuals are assumed not to
13 occur. Long-term recharge after barrier failure is the only source of water expected to result in
14 any significant transport of contaminant from the facility to groundwater. WMA C tank

RPP-ENV-58782, Rev. 0

- 1 residuals are not expected to contain appreciable quantities of liquid, and the retrieval operations
 2 are conducted in a manner to minimize uncontrolled retrieval leachate from escaping the tanks.
 3

Table 6-12. Summary of Key Elements and Base Case Parameters Associated with Site-Specific Model Components for Waste Management Area C
(The basis for the elements and parameter selection provided in the individual model components sections). (2 sheets)

Model Domain and Boundary Conditions	<p>Rectangular Prism: 737.9 m (2,421 ft) × 795.3 m (2,609 ft) × 116 m (381 ft)</p> <p>Prescribed flux across the top (Recharge); no-flow along vertical side boundaries in the vadose zone; prescribed flux and head along the upgradient and downgradient vertical side boundaries in the aquifer, respectively; no-flow along the bottom of the model (aquifer). The prescribed volumetric water flux boundary condition is calculated to maintain mass conservation in the aquifer independent of recharge.</p>
Geologic Setting	<p>The Waste Management Area (WMA) C cross-section includes the following anthropogenic or natural units that occur from surface to groundwater (RPP-RPT-56356, “Development of Alternative Digital Geologic Models of Waste Management Area C”):</p> <ul style="list-style-type: none"> • WMA C Backfill • Hanford H1 (gravel-dominated, generally identified as gravel or very coarse sand) • Hanford H2 Sand (sand-dominated facies generally identified as fining upward sequences of gravel, sandy/gravel to sand to very fine sand) • Hanford H3 (coarse-grained open framework gravel to sandy gravel; in the vicinity of WMA C is variously referred to in different references as undifferentiated H3 gravels, Cold Creek, or Ringold) • In Alternative Geologic Model II, the Hanford H2 Sand includes following two additional subunits <ul style="list-style-type: none"> ○ Hanford H2 Coarse (gravel/coarse-grained facies that underlies the H2 fines) ○ Hanford H2 Silty Sand – (a silty sand unit that is only observed in deep groundwater wells and a mappable unit may not be readily identified)
Groundwater Domain and Characteristics	<p>WMA C post-closure water table elevation ~119.5 m NAVD88 and average hydraulic gradient ~0.00002 m/m</p> <p>Aquifer area along northwest cross-section boundary = 6,151 m² Aquifer area along southeast cross-section boundary = 13,998 m² Average aquifer area along all aquifer cross-sections = 9,440 m²</p> <p>Prescribed flux along northwest cross-section boundary (saturated K = 11,000 m/d); $11,000 \text{ m/d} \times 0.2000\text{E-}04 \times 365.25 \text{ d/yr} = 8.04\text{E+}01 \text{ m/yr}$; $8.04\text{E+}01 \text{ m/yr} \times 9,440 \text{ m}^2 / 6,151 \text{ m}^2 = 1.23\text{E+}02 \text{ m/yr}$</p> <p>Prescribed head along southeast cross-section boundary = 119.49 m</p> <p>Groundwater thickness is ~12 m (39 ft) in the aquifer; Groundwater concentrations evaluated for upper 5 m (16 ft) of the aquifer (rationale for aquifer depth presented in Section 6.3.2.2.9, Point of Calculation, Protectiveness Metric, and Time Frame Considerations)</p> <p>Aquifer Hydraulic Conductivity Horizontal to Vertical Anisotropy = 10:1 Aquifer Dispersivity Longitudinal to Transverse Anisotropy = 10:1</p> <p>Appendix C identifies and describes the methods used to derive the aquifer properties and parameter values.</p>

RPP-ENV-58782, Rev. 0

Table 6-12. Summary of Key Elements and Base Case Parameters Associated with Site-Specific Model Components for Waste Management Area C (The basis for the elements and parameter selection provided in the individual model components sections). (2 sheets)

Source Term/ Inventory	<p>Table 3-13 “241-C Tank Farm Residual Inventory Estimates for Retrieved Tanks with Post-Retrieval Sampling,” Table 3-14 “241-C Tank Farm Residual Inventory Estimates for Tanks Undergoing Retrieval,” and Table 3-15 “241-C Tank Farm Residual Inventory Estimates for Ancillary Equipment” include tank, ancillary equipment, and pipeline-specific WMA C Base Case inventory estimates for the contaminants evaluated in this performance assessment (PA).</p> <p>Diffusion-controlled release occurs from the grouted tanks, and advection-controlled release occurs from the pipelines along with equilibrium sorption-desorption processes (i.e., K_d control).</p>
Vadose Zone Hydrogeology and Fluid Transport	<p>Table 6-7 “Composite van Genuchten-Mualem Parameters for Various Strata at the Waste Management Area C Site Used in the Base Case Evaluations of Alternative Geologic Models I and II” includes the hydrogeologic property estimates for WMA C PA models.</p> <p>Vadose Zone Hydraulic Conductivity Anisotropy allowed to vary as a function of the moisture content in accordance with the Polmann model (“Application of Stochastic Methods to Transient Flow and Transport in Heterogeneous Unsaturated Soils” [Polmann 1990]).</p> <p>Vadose Zone Dispersivity Longitudinal to Transverse Anisotropy = 10:1</p> <p>Appendix B and Appendix D identify and describe the methods used to derive the properties and parameter values.</p>
Recharge	<p>Recharge varies spatially and temporally on the basis of surface conditions.</p> <p>Table 6-6 “Base Case Recharge Rate (Net Infiltration) Estimates for Surface Conditions during the Pre-Construction, Operational, and Post-Closure Periods” includes the base case recharge estimates applicable to the different surface conditions and periods evaluated in this PA.</p>
Sorption Characteristics	<p>K_d-control for radionuclide transport</p> <p>Table 6-11 “Distribution Coefficients (K_d) Values Used to Approximate the Transport of the Radionuclides in the Base Case” includes the base case distribution coefficient estimates applicable to the different radionuclides evaluated in this PA.</p>

*Applies to all subfacies of this unit.

NAVD88 = North American Vertical Datum of 1988, National Geodetic Survey, U.S. Department of Commerce.

NP = Not present

- 1
- 2 As discussed in Section 8.1.4, uncertainty in the vadose zone hydraulic properties was addressed
- 3 by randomly producing 200 combinations of van Genuchten-Mualem hydraulic parameter values
- 4 for each HSU from the parameter distributions identified in Section 8.1.4. From these
- 5 realizations, an empirical cumulative distribution function is calculated for the pore water
- 6 velocity estimates, and the hydraulic parameter set corresponding to the maximum pore water

RPP-ENV-58782, Rev. 0

velocity occurring with a steady flux of 3.5 mm/yr (0.14 in./yr) is selected for the screening evaluation (Table 6-14).

Table 6-13. Maximum Net Infiltration (Recharge) Estimates Developed for the Uncertainty Analysis for Pre-Construction Period, Operational Period, and Post-Closure of Waste Management Area C (Section 8.1.4.1).

Surface Status	Pre-Construction (mm/yr)	Operational Period (mm/yr)	Post Closure	
			Until End of Barrier Design Life (500 yr after closure) (mm/yr)	After End of Barrier Design Life (mm/yr)
Waste Management Area C	5.2	140	1.0	5.2
Undisturbed	5.2	5.2	5.2	5.2
Disturbed	5.2	22	5.2	5.2
Reworked	5.2	63	5.2	5.2
Waste Management Area A	5.2	140	1.0	5.2

Table 6-14. van Genuchten-Mualem Parameters Associated with the Maximum Pore Water Velocity Based on the Cumulative Distribution Functions in Section 8.1.4.

Strata	θ_s	θ_r	α (1/cm)	n	Fitted K_s (cm/s)
Hanford H1 (gravelly sand)	0.100	0.0006	0.0190	1.789	5.07E-04
Hanford H2 (sand-dominated)	0.239	0.0006	0.0743	2.042	8.84E-03
Hanford H3 (gravelly sand)	0.100	0.0006	0.0190	1.789	5.07E-04
Aquifer	0.20	0.0006	0.0190	1.789	1.27*
Backfill	0.100	0.0003	0.0116	1.464	9.42E-05

*Value listed is 1/10 of the aquifer horizontal hydraulic conductivity.

For the purpose of the screening evaluation, the screening-phase model considers only the advective release of contaminants from the sediments. All of the contamination in the source area is available for advective transport, and the release occurs during a one-year span at closure and according to the equilibrium K_d . Results from the groundwater pathway screening analysis are presented in Section 7.2.1.1.

To complement the results of the screening analysis, an additional evaluation case was run to evaluate the peak doses for all 43 radiological COPCs beyond the 10,000-year post-closure time frame. The primary focus of this analysis is to evaluate the time and magnitude of peak doses

RPP-ENV-58782, Rev. 0

1 resulting from some selected constituents, like the uranium isotopes, that were found to be rising
2 at the end of the 10,000-year period analysis, and other sorbed constituents that could potentially
3 reach groundwater beyond the 10,000-year post-closure time frame. The specific assumptions of
4 this evaluation case and its associated results are provided in Section 8.2.8 of this report.

5
6 **6.3.2.4 Abstraction Approach for System-Level Modeling.** The system model is
7 implemented to reduce the computational time needed to carry out sensitivity and uncertainty
8 analyses. The flow field for the vadose zone is derived from the 3-D STOMP[®]-based model
9 calculations, abstracted to provide a close approximation to the full STOMP[®]-based solution.
10 The objective of the system model is to evaluate the interaction of various submodels within the
11 overall system. This is carried out by conducting transport analyses in one dimension (1-D)
12 within the vadose zone and saturated zone for each source type (tank, ancillary equipment, and
13 pipeline). This flow-field abstraction methodology was considered reasonable because of the
14 EHM approach and upscaled flow parameters adopted in the STOMP[®]-based models. The
15 reasonableness of the abstraction approach is demonstrated by comparing the results of the
16 transport analysis conducted using the 1-D abstracted model to the full 3-D STOMP[®]-based
17 model.

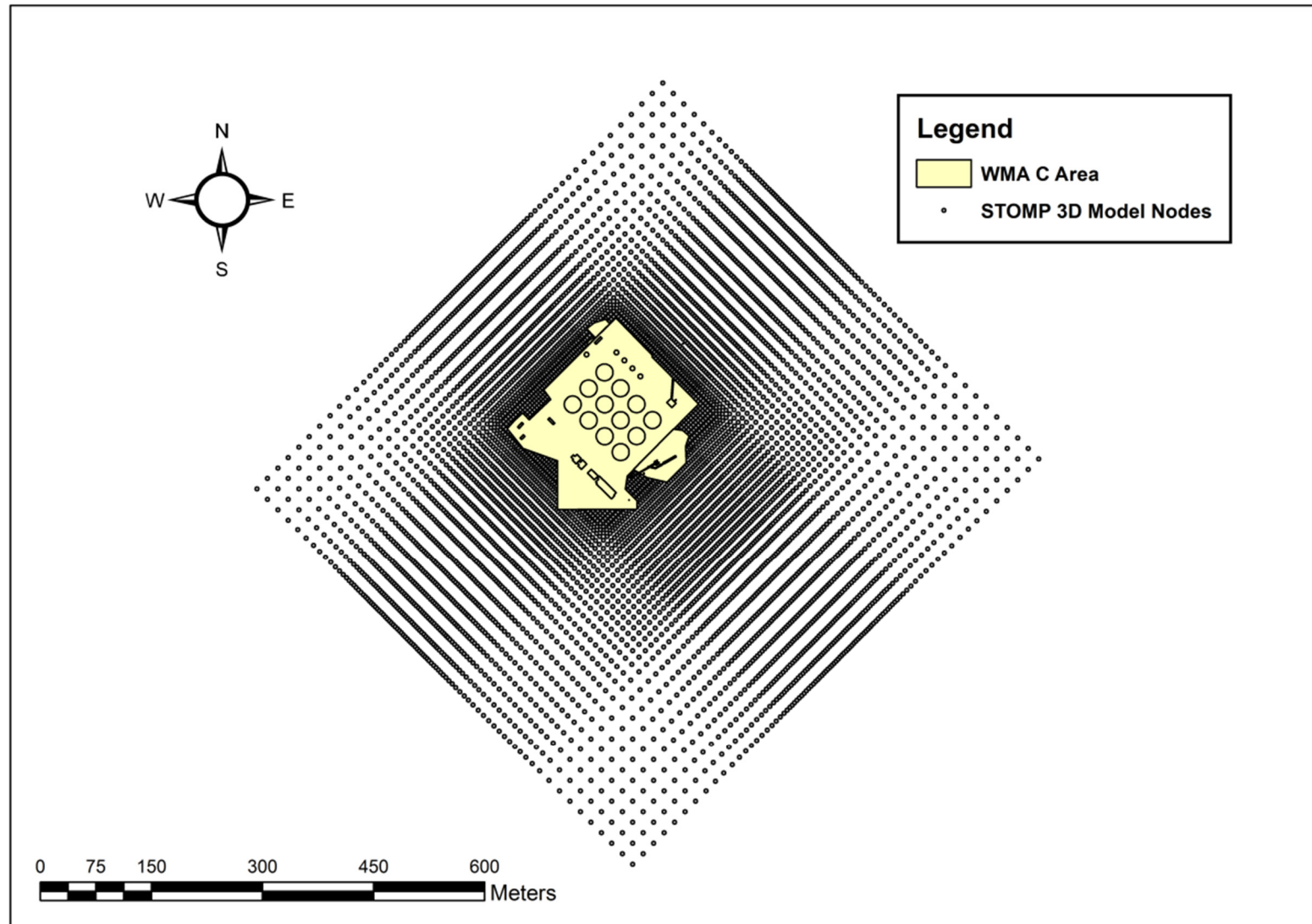
18
19 The flow field generated from the STOMP[®]-based model was evaluated by considering the
20 following aspects of the flow field abstraction:

- 21
22 1. Variable HSU thickness within the model domain and its impact on flow velocity
- 23
24 2. Spatial and temporal variability in imposed recharge rates
- 25
26 3. Spatial and temporal variability in flow underneath the tank
- 27
28 4. Variable distances of tanks from the compliance location boundary.
- 29

30 The GoldSim[®]-based system model relies on the user to provide the moisture content, saturation,
31 and Darcy flux as inputs; these flow-field related parameters were extracted from the
32 STOMP[®]-based model. Figure 6-42 shows the STOMP[®]-based model node locations along with
33 the extent of WMA C. For the abstraction of the flow field, the primary regions of interest were
34 the ones underneath the various source locations within WMA C.

35
36 First, the approximate thicknesses of the HSUs were extracted from the STOMP[®]-based model
37 under each of the twelve 100-series tank and four 200-series tank locations. Figure 6-43 shows
38 the location of the nodes, along with the cross-section lines used in extracting the HSU thickness.
39 Figure 6-44 shows the northwest-southeast trending geologic cross-sections through the tank
40 farm area, while Table 6-15 summarizes the thicknesses of the HSUs directly underneath the
41 tanks, along with the median values of the HSU thicknesses. The median value of the 100-series
42 tanks is very similar to the HSU thickness below tank C-105. Similarly, median value for
43 200-series tanks is close to the thickness below tank C-203. Therefore, tanks C-105 and C-203
44 were selected as representative columns for the flow-field abstraction for the 100-series tanks
45 and 200-series tanks, respectively.
46

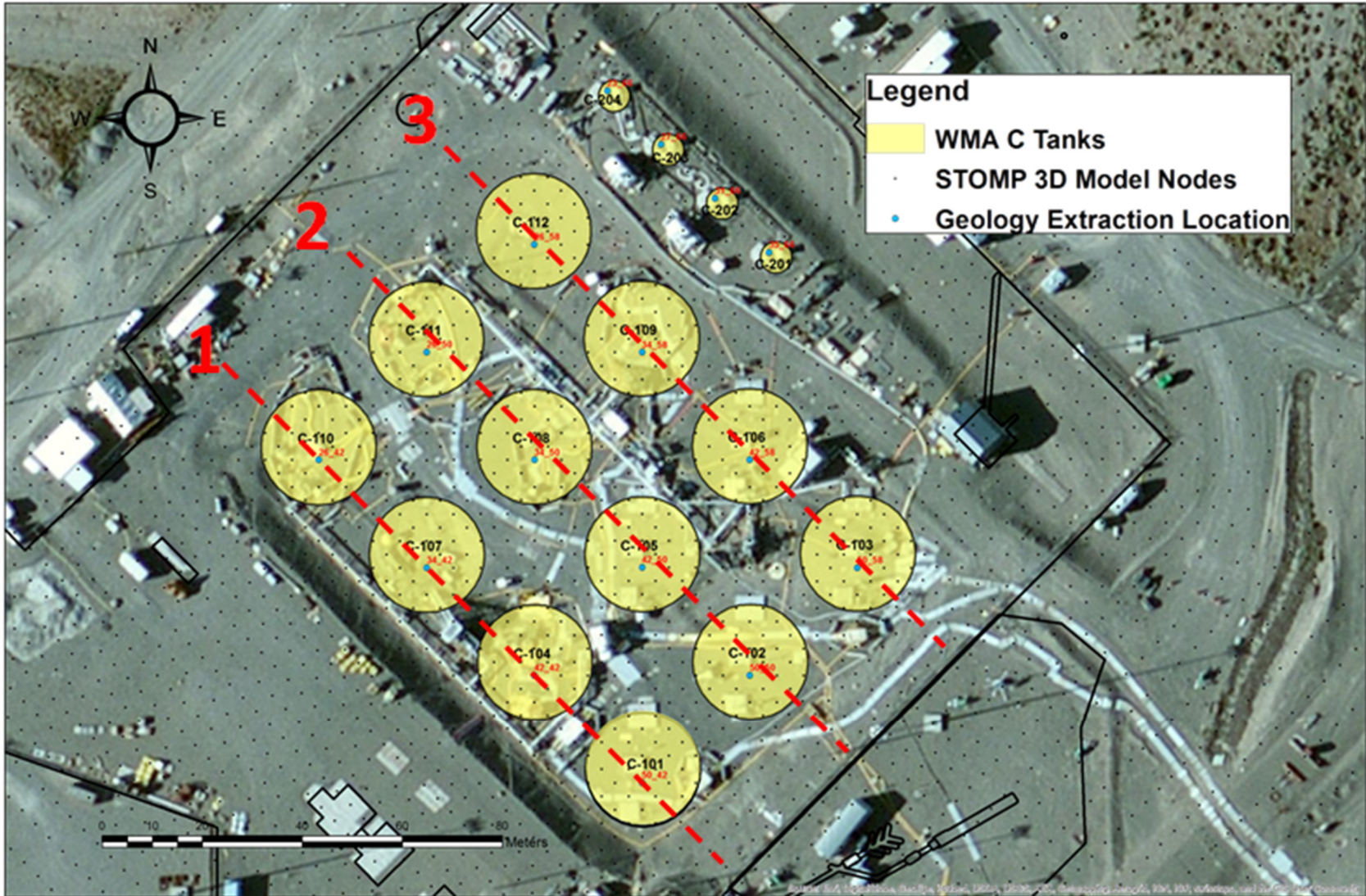
Figure 6-42. Waste Management Area C Three-Dimensional Model Subsurface Transport Over Multiple Phases (STOMP®)-Based Model Node Locations.



STOMP® 3D = Subsurface Transport Over Multiple Phases (code) three-dimensional

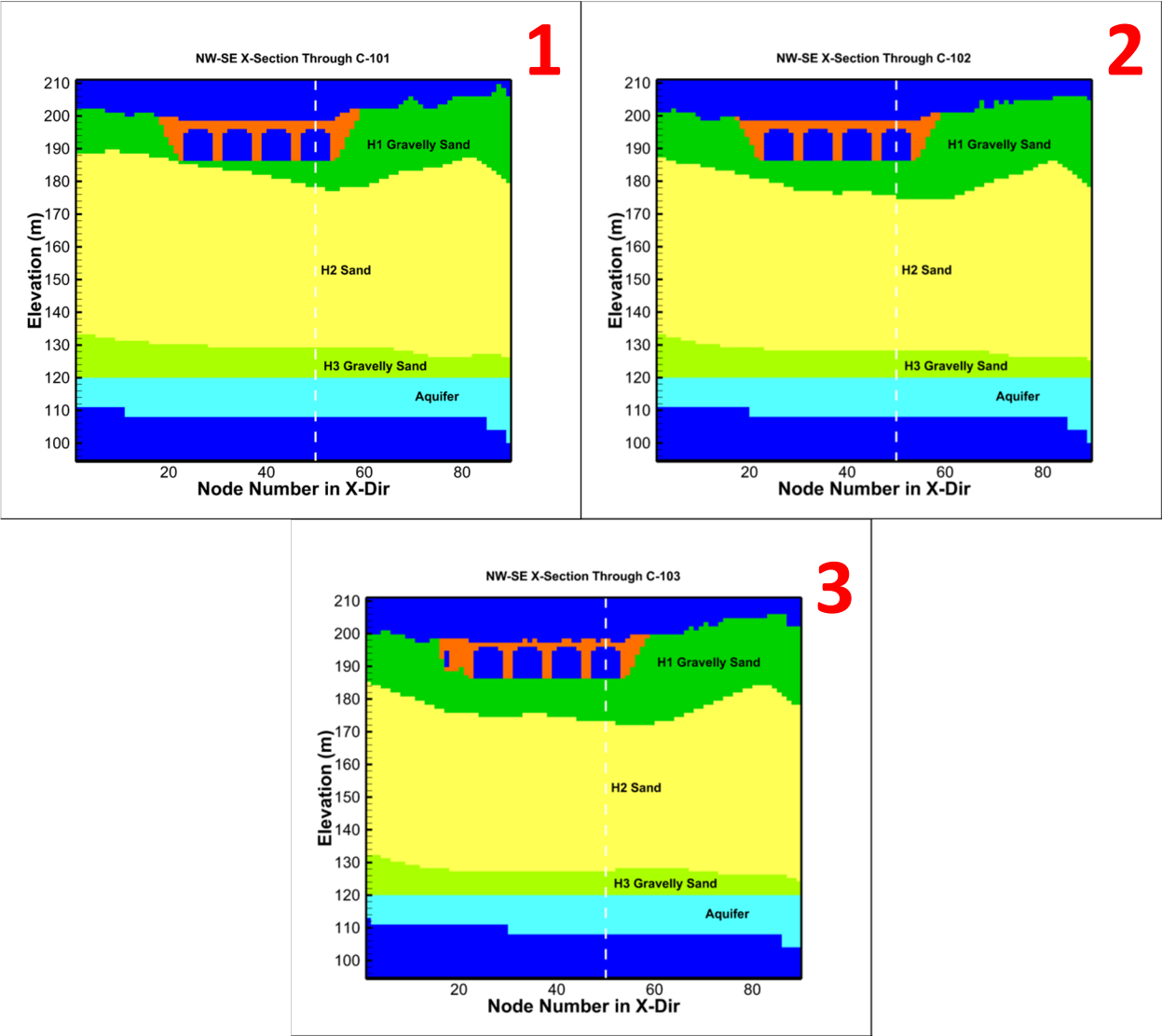
WMA = Waste Management Area

Figure 6-43. Three-Dimensional Subsurface Transport Over Multiple Phases (STOMP®)-Based Model Node Locations for Waste Management Area C along with Location of Cross-Section Lines.



STOMP® 3D = Subsurface Transport Over Multiple Phases (code) three-dimensional WMA = Waste Management Area

Figure 6-44. Northwest-Southeast Trending Geologic Cross-Sections Through the Tank Farm Using Information from Three-Dimensional Subsurface Transport Over Multiple Phases (STOMP®)-Based Model.



RPP-ENV-58782, Rev. 0

Table 6-15. Hydrostratigraphic Unit Thickness Under the Tanks Taken From the Three-Dimensional Subsurface Transport Over Multiple Phases (STOMP®)-Based Model.

Tank	STOMP_NODE (I_J)	H1 Gravelly Sand (m)	H2 Sand (m)	H3 Gravelly Sand (m)	Aquifer (m)
241-C-101	50_42	8.00	49.00	9.25	12.00
241-C-102	50_50	11.75	46.25	8.25	12.00
241-C-103	50_58	13.00	46.00	7.25	12.00
241-C-104	42_42	5.50	51.50	9.25	12.00
241-C-105	42_50	9.25	48.75	8.25	12.00
241-C-106	42_58	11.75	47.25	7.25	12.00
241-C-107	34_42	3.00	54.00	9.25	12.00
241-C-108	34_50	9.25	48.75	8.25	12.00
241-C-109	34_58	10.50	48.50	7.25	12.00
241-C-110	26_42	2.00	54.00	10.25	12.00
241-C-111	26_50	6.75	51.25	8.25	12.00
241-C-112	26_58	11.75	47.25	7.25	9.00
241-C-201	35_66	13.00	47.00	6.25	9.00
241-C-202	31_66	13.00	48.00	5.25	9.00
241-C-203	27_66	14.25	46.75	5.25	9.00
241-C-204	23_66	14.25	46.75	5.25	9.00
Median	100-Series Tank	9.2	48.7	8.2	12.0
Median	200-Series Tank	13.6	47.1	5.5	9.0

Subsurface Transport Over Multiple Phases (STOMP)® is copyrighted by Battelle Memorial Institute, 1996.

The flow-field abstractions were performed separately for the 100-series and 200-series tanks because (a) 100-series tanks are 22.9 m (75 ft) in diameter compared to 6.1 m (20 ft) in diameter for the 200-series tanks, which leads to different flow paths, and (b) the thickness of HSU below the 100-series tanks differs from the 200-series tanks.

Due to varying recharge conditions at the top boundary (see Section 6.3.2.2 for details), the moisture content and Darcy flux profiles within the soil column vary with depth and respond differently at different times as shown in Figures 6-45 and 6-46, respectively. While the surface barrier is effective (between years 2020 and 2520), moisture content and Darcy fluxes decrease with time as they respond to the change in the recharge rate from 100 mm/yr to 0.50 mm/yr (3.94 in./yr to 0.02 in./yr). After the barrier design period (year 2520 onwards), moisture content and Darcy fluxes equilibrate quickly to the change in recharge rate from 0.50 mm/yr to

RPP-ENV-58782, Rev. 0

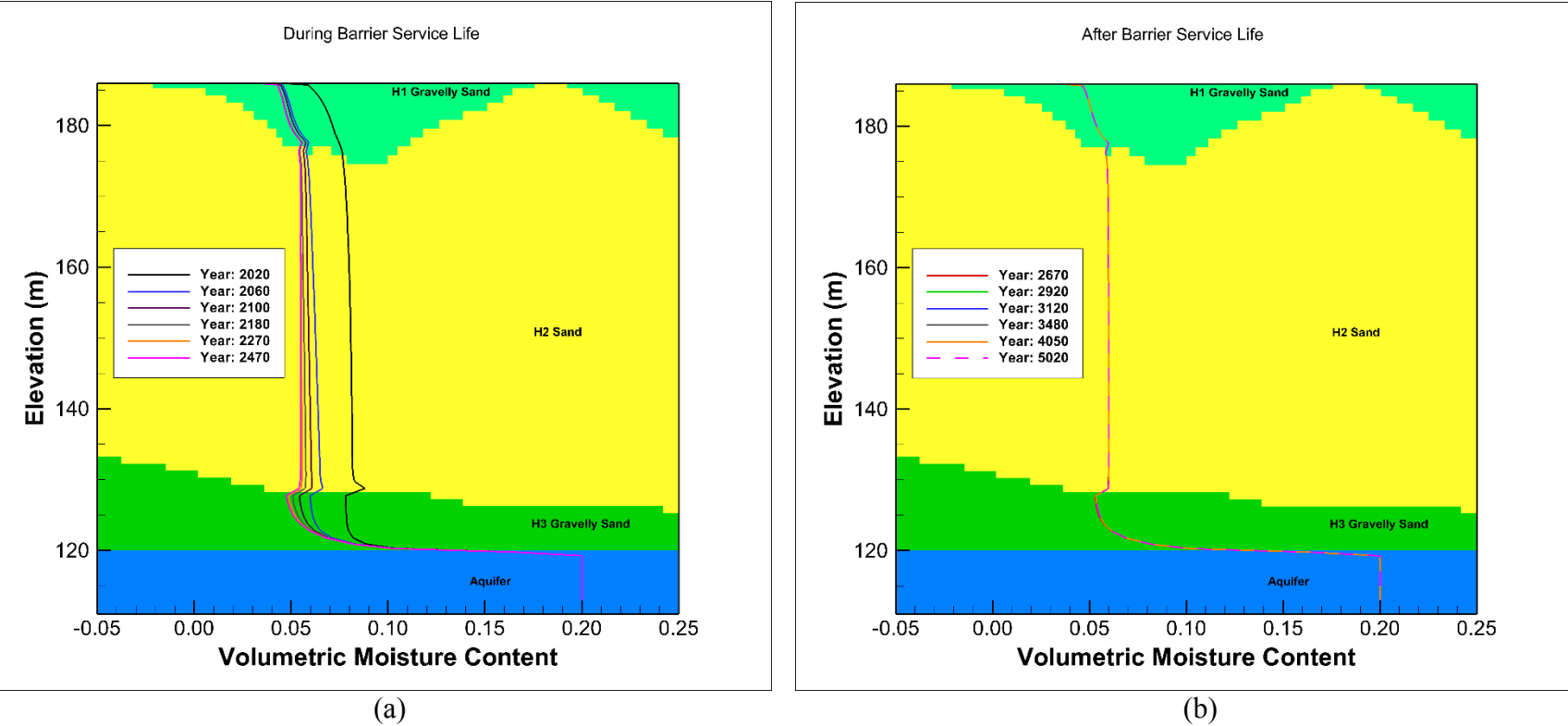
3.5 mm/yr (0.02 in./yr to 0.14 in./yr). The flow-field abstraction process was implemented to capture these trends.

The representative hydrostratigraphic columns for the 100-series tanks and 200-series tanks are compared against the vertical discretization chosen for the system-level model in Figure 6-47. Also presented is the vertical discretization implemented in the STOMP[®]-based model. For the system-level model, finer discretization was chosen at shallow depths with increasingly coarser discretization at deeper depths. However, near the HSU contacts, finer discretization was used to capture the flow field at the interface. Coarser discretization was allowable in the deeper portion of the vadose zone (e.g., H3 gravelly sand) because the flow field did not change appreciably with depth.

The STOMP[®]-based model nodes that were used to represent the moisture content and Darcy flux for the grid cells in the system model are highlighted in brown color in Figure 6-47. For example, the H1 Gravelly Sand unit in the representative column for the 100-series tank has a total thickness of 9.25 m (30.3 ft) and is divided into three grid cells of 2 m, 3.5 m and 3.75 m (6.6 ft, 11.5 ft and 12.3 ft) thickness. The flow field (moisture content and Darcy flux) extracted from STOMP[®] model node 69 is applied in the first cell of this unit in the system-level abstraction model. Similarly, the flow field from STOMP[®] model node 66 and node 63 is applied to the second and third cell of this unit in the system model. The H2 Sand unit is the thickest HSU in the vertical profile. It is discretized into a 3.75-m (12.3-ft) grid cell at the top and 5-m (16.4-ft) grid cell at the bottom. The middle 40 m (131 ft) is discretized into 80 grid cells, each being 0.5 m (1.6 ft) in length to match the 0.25-m (0.82-ft) longitudinal dispersivity applied within the H2 Sand unit (the numerical dispersivity in GoldSim[®] cell is calculated to be equal to half the cell length). The top and bottom grid cells for the H2 Sand unit are assigned the flow field extracted from STOMP[®] nodes 61 and 24, respectively, while the middle 40-m (131-ft) length (consisting of 20 grid cells) is represented by the flow field from STOMP[®] node 47. A single flow field over the 40-m (131-ft) length is used, since the flow field varies little for the corresponding STOMP[®] nodes at depth. A similar discretization scheme is adopted for the 200-series tanks as shown in Figure 6-47. The details of the grid discretization are presented in Table 6-16.

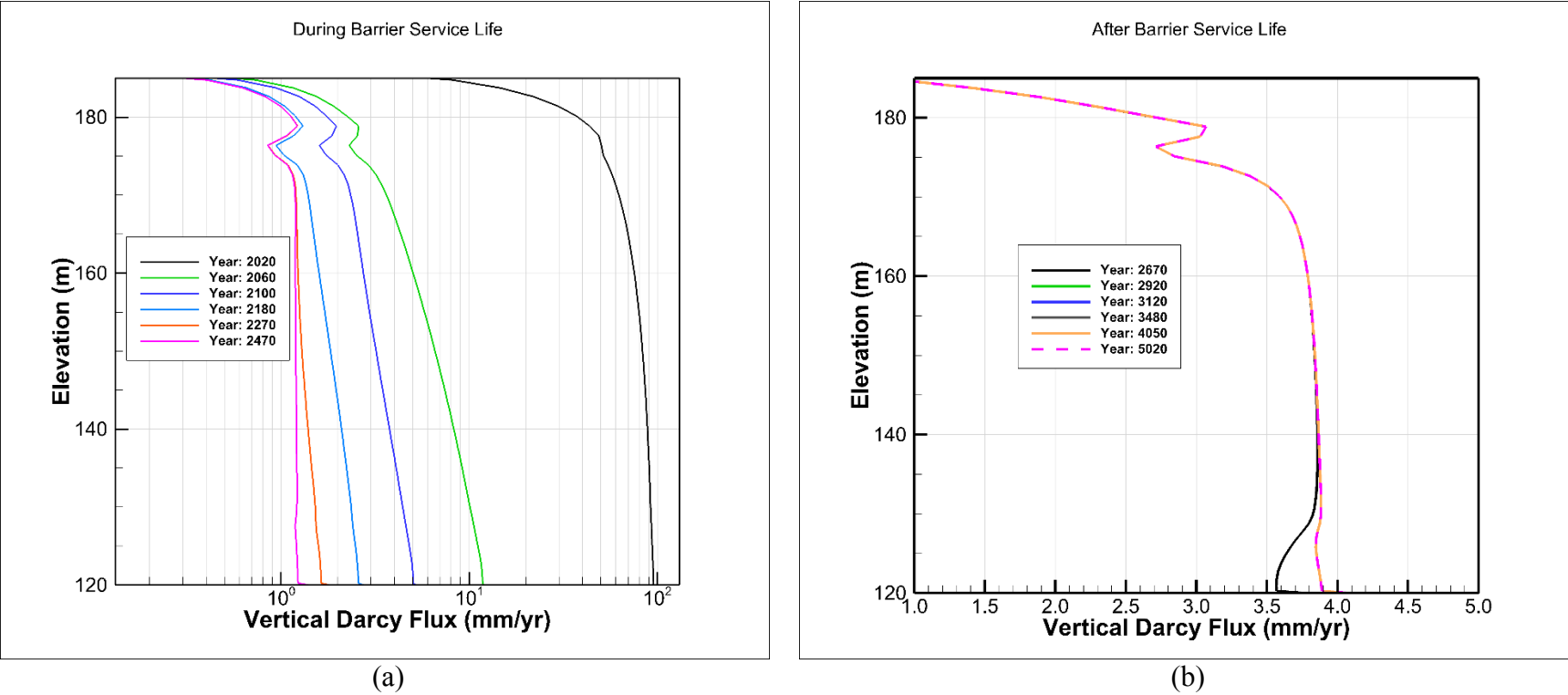
Figure 6-48 provides an overview of how the moisture content and Darcy flux vary over time for the selected STOMP[®] nodes in relation to the location in the vertical direction in the system model under an intact 100-series tank. This flow field is applied to model the transport underneath the 100-series tank. The representative flow field underneath an intact 200-series tank is presented in Figure 6-49. In the early time period, the moisture content and Darcy flux decrease due to the decrease in recharge rate from 100 mm/yr to 0.50 mm/yr (3.94 in./yr to 0.02 in./yr) associated with the emplacement of the surface barrier. As the surface barrier is assumed to be degraded 500 years after closure, the recharge rate transitions from a barrier rate of 0.5 mm/yr (0.02 in./yr) to a natural background rate of 3.5 mm/yr (0.14 in./yr), and reaches steady state by year 3000. The STOMP[®] node 14 used to set the flow field for the grid cell at the base of the H3 Gravelly Sand unit shows high moisture content because it is located in the capillary fringe just above the water table.

Figure 6-45. Moisture Content Distribution below Tank 241-C-105 at Various Times during (a) Surface Barrier Design Time Period of 500 years Following Closure and (b) Post-Surface Barrier Design Time Period.



Note: Barrier Service Life assumes intact surface cover leading to reduced net infiltration while Post-Barrier Service Life assumes degraded surface cover.

Figure 6-46. Vertical Darcy Flux Distribution below Tank 241-C-105 at Various Times.



RPP-ENV-58782, Rev. 0

**Figure 6-47. Representative Hydrostratigraphic Column for
(a) 100-Series and (b) 200-Series Tanks.**

Hydrostratigraphy Below C-105	STOMP Node Elevation (m)	STOMP Node Numbers	STOMP Vertical Discretization (m)	GoldSim Vertical Discretization (m)	Hydrostratigraphy Below C-203	STOMP Node Elevation (m)	STOMP Node Numbers	STOMP Vertical Discretization (m)	GoldSim Vertical Discretization (m)
H1 Gravelly Sand	185.75	69	1.00	2 m	H1 Gravelly Sand	185.75	69	1.00	2 m
	184.75	68	1.00			184.75	68	1.00	
	183.75	67	1.00	3.5 m		183.75	67	1.00	3.5 m
	182.625	66	1.25			182.625	66	1.25	
	181.375	65	1.25			181.375	65	1.25	
	180.125	64	1.25	3.75 m		180.125	64	1.25	3.75 m
	178.875	63	1.25			178.875	63	1.25	
	177.625	62	1.25			177.625	62	1.25	
	176.375	61	1.25	3.75 m		176.375	61	1.25	3.75 m
	175.125	60	1.25			175.125	60	1.25	
H2 Sand	173.875	59	1.25	2 m (over 40 m thickness)	H2 Sand	173.875	59	1.25	2 m (over 40 m thickness)
	172.625	58	1.25			172.625	58	1.25	
	171.375	57	1.25			171.375	57	1.25	
	170.125	56	1.25			170.125	56	1.25	
	168.875	55	1.25			168.875	55	1.25	
	167.625	54	1.25			167.625	54	1.25	
	166.375	53	1.25			166.375	53	1.25	
	165.125	52	1.25			165.125	52	1.25	
	163.875	51	1.25			163.875	51	1.25	
	162.625	50	1.25			162.625	50	1.25	
	161.375	49	1.25			161.375	49	1.25	
	160.125	48	1.25			160.125	48	1.25	
	158.875	47	1.25			158.875	47	1.25	
	157.625	46	1.25			157.625	46	1.25	
	156.375	45	1.25			156.375	45	1.25	
	155.125	44	1.25			155.125	44	1.25	
	153.875	43	1.25			153.875	43	1.25	
	152.625	42	1.25			152.625	42	1.25	
	151.375	41	1.25			151.375	41	1.25	
	150.125	40	1.25			150.125	40	1.25	
	148.875	39	1.25			148.875	39	1.25	
	147.625	38	1.25			147.625	38	1.25	
	146.375	37	1.25			146.375	37	1.25	
	145.125	36	1.25			145.125	36	1.25	
	143.875	35	1.25			143.875	35	1.25	
	142.625	34	1.25			142.625	34	1.25	
	141.375	33	1.25			141.375	33	1.25	
	140.125	32	1.25			140.125	32	1.25	
	138.875	31	1.25			138.875	31	1.25	
	137.625	30	1.25			137.625	30	1.25	
	136.375	29	1.25			136.375	29	1.25	
	135.125	28	1.25			135.125	28	1.25	
	133.875	27	1.25			133.875	27	1.25	
	132.75	26	1.00	5 m		132.75	26	1.00	3
	131.75	25	1.00			131.75	25	1.00	
	130.75	24	1.00			130.75	24	1.00	
	129.75	23	1.00			129.75	23	1.00	
H3 Gravelly Sand	128.75	22	1.00	7 m	H3 Gravelly Sand	128.75	22	1.00	4
	127.75	21	1.00			127.75	21	1.00	
	126.75	20	1.00			126.75	20	1.00	
	125.75	19	1.00			125.75	19	1.00	
	124.75	18	1.00	1.25 m		124.75	18	1.00	1.25
	123.75	17	1.00			123.75	17	1.00	
	122.75	16	1.00			122.75	16	1.00	
	121.75	15	1.00	12 m		121.75	15	1.00	9
	120.875	14	0.75			120.875	14	0.75	
	120.25	13	0.50			120.25	13	0.50	
Aquifer	119.75	12	0.50	12 m	Aquifer	119.75	12	0.50	9
	119.25	11	0.50			119.25	11	0.50	
	118.625	10	0.75			118.625	10	0.75	
	117.75	9	1.00			117.75	9	1.00	
	116.625	8	1.25			116.625	8	1.25	
	115.25	7	1.50			115.25	7	1.50	
	113.75	6	1.50			113.75	6	1.50	
	112	5	2.00			112	5	2.00	
	109.5	4	3.00			109.5	4	3.00	
	106	3	4.00			106	3	4.00	
Inactive	102	2	4.00		Inactive	102	2	4.00	
	97.5	1	5.00			97.5	1	5.00	
			Node used in Flow-Field abstraction					Node used in Flow-Field abstraction	

(a)

(a)

(b)

GoldSim® simulation software is copyrighted by GoldSim Technology Group LLC of Issaquah, Washington (see <http://www.goldsim.com>).

Subsurface Transport Over Multiple Phases (STOMP)® is copyrighted by Battelle Memorial Institute, 1996.

The above results are for the situation when the grout is structurally stable and provides a hydraulic barrier. However, a number of the sensitivity cases evaluate conditions where the effectiveness of grout as a hydraulic barrier is assumed to degrade at different times. Under degraded grout conditions, the grout is assumed to be highly fractured, and the infill material in the tank is assumed to behave like a porous material with hydraulic properties same as the

RPP-ENV-58782, Rev. 0

H2 Sand unit. The STOMP[®]-based model is run with the H2-sand hydraulic properties for the tank, and the flow field is calculated and abstracted in a manner similar to that described earlier for the intact tank. The flow field is calculated separately for the degraded tank conditions for the 100-series and 200-series tanks, as shown in Figure 6-50. One additional STOMP[®] node result (node 73) is extracted and added to the system model to represent the flow conditions inside the tank. In the sensitivity cases, when the tank degradation occurs, the flow field is switched from the intact tank flow field to the degraded tank flow field. As a result, the contaminants are released via advection at the time when the tank is degraded in addition to the ongoing diffusive release mechanism.

Table 6-16. Vertical Grid Discretization and Flow Field for the System-Level Model.

	Unit	Thickness (m)	Number of Grid Block Cells	Grid Discretization	Flow Field Discretization (Moisture Content and Vertical Darcy Flux)
100-Series Tanks	H1 Gravelly Sand	9.25	3	1 at 2 m, 1 at 3.5 m, 1 at 3.75 m	One flow field for each cell
	H2 Sand	48.75	22	1 at 3.75 m, 20 cells of 2 m thickness each for a total of 40 m 1 at 5 m	One flow field for the first cell. One flow field for the next 20 cells and One flow field for the remaining one cell
	H3 Gravelly Sand	8.25	2	1 at 7 m, 1 at 1.25 m.	One flow field for each cell
	Saturated Zone	12.00		Aquifer pathway	One flow field
200-Series Tanks	H1 Gravelly Sand	14.25	3	1 at 2 m, 1 at 3.5 m, 1 at 8.75 m	One flow field for each cell
	H2 Sand	46.75	22	1 at 3.75 m, 20 cells of 2 m thickness each for a total of 40 m 1 at 3 m	One flow field for the first cell. One flow field for the next 20 cells and One flow field for the remaining one cell
	H3 Gravelly Sand	5.50	2	1 at 4 m, 1 at 1.25 m.	One flow field per cell
	Saturated Zone	9.00		Aquifer pathway	One flow field

The flow field applied to pipeline releases is calculated separately. Vertical Darcy fluxes and volumetric moisture contents from the STOMP[®] nodes that fall within the pipeline source area (150 m by 150 m [492 ft by 492 ft]) but outside the tank footprint are averaged to calculate the pipeline flow-field. The representative hydrostratigraphic column for the 100-series tanks is applied to the pipeline source area. Advective flow occurs through the pipelines for all time periods. The hydraulic effect of the presence of buried pipelines in the vadose zone is not

RPP-ENV-58782, Rev. 0

1 modeled explicitly, and the areas occupied by the pipelines are modeled with hydraulic
2 properties of soil backfill material.

3
4 The saturated zone is modeled as a 1-D aquifer, oriented along the primary flow direction using
5 the aquifer pathway capability in GoldSim[®]. The volumetric flow rate through the aquifer is
6 calculated based on the hydraulic gradient under steady-state conditions and saturated hydraulic
7 conductivity consistent with the values used in the STOMP[®]-based model. The saturated zone
8 thickness for the 100-series tanks is chosen to be 12 m (39.4 ft), while that for the 200-series
9 tanks is chosen to be 9 m (29.5 ft) (Table 6-16).

10
11 The mass flux from the vadose zone for each source term (each of the 100- and 200-series tanks,
12 the C-301 catch tank, the 244-CR vault, and pipelines) is calculated separately. Each source
13 term is then transported to the aquifer, assuming that vertical mass transport in the vadose zone
14 stays within the footprint of the source area, ignoring any lateral dispersion as shown in
15 Figure 6-51. The aquifer pathway from each source area starts under its associated source in
16 WMA C and extends to the PoCal, 100 m (328 ft) downgradient from the WMA C fenceline
17 along the groundwater flow direction. The width of the aquifer pathway is taken to be the width
18 of the source area. The length of the aquifer pathway varies depending on the location of the
19 source area being modeled (tanks and ancillary equipment), relative to the PoCal 100 m (328 ft)
20 downgradient from the WMA C fenceline along the groundwater flow path. As an example, the
21 total length of the aquifer pathway from tank C-102 is ~144 m (472 ft), compared with ~174 m
22 (571 ft) for tank C-105, and ~235 m (771 ft) for tank C-111. For the pipeline source, the aquifer
23 pathway is assumed to begin at the center of the WMA C area leading to a total length of 175 m
24 (574 ft). This length represents an average distance from all of the pipeline sources to the PoCal.

25
26 The mass loading on the aquifer pathway from the vadose zone occurs over the length of the
27 source parallel to the flow path. For the tank sources, this is equivalent to the diameter of the
28 tank. For the pipeline source, the source loading from the vadose zone to the aquifer is
29 conservatively assumed to occur over the 75 m (246 ft) that represents the half-length of the
30 pipeline source area along the flow path.

31
32 The average aquifer pathway concentrations at the 100 m (328 ft) downgradient boundary are
33 calculated for each source separately, by assuming that the mass within the defined 1-D aquifer
34 stream tube configuration does not laterally disperse. This 1-D approach tends to maximize the
35 concentrations for a given source term, but it does not take account of overlapping plumes from
36 lateral dispersion from other sources that are on parallel flow paths (Figure 6-51). To determine
37 the maximum concentration, a separate calculation is performed. Since the highest
38 concentrations were expected to occur along the centerline of the WMA C width, extended to the
39 100 m (328 ft) boundary, due to location of highest residual inventory tanks along the centerline,
40 the calculated concentrations for the C-102, C-105, C-108 and C-111 tank sources at the 100 m
41 (328 ft) boundary were combined. These four tanks fall along a single flow path (stream tube),
42 since the flow direction is aligned with the orientation of these tanks. The amount of additional
43 contaminant mass from lateral dispersion along adjacent flow paths is included by using an
44 analytical solution (*Plume function* within GoldSim[®]) that calculates the concentration away
45 from the centerline of the plume. Using this approach, the concentrations from surrounding
46 aquifer pathways are calculated and added to the combined concentration for the aquifer pathway

RPP-ENV-58782, Rev. 0

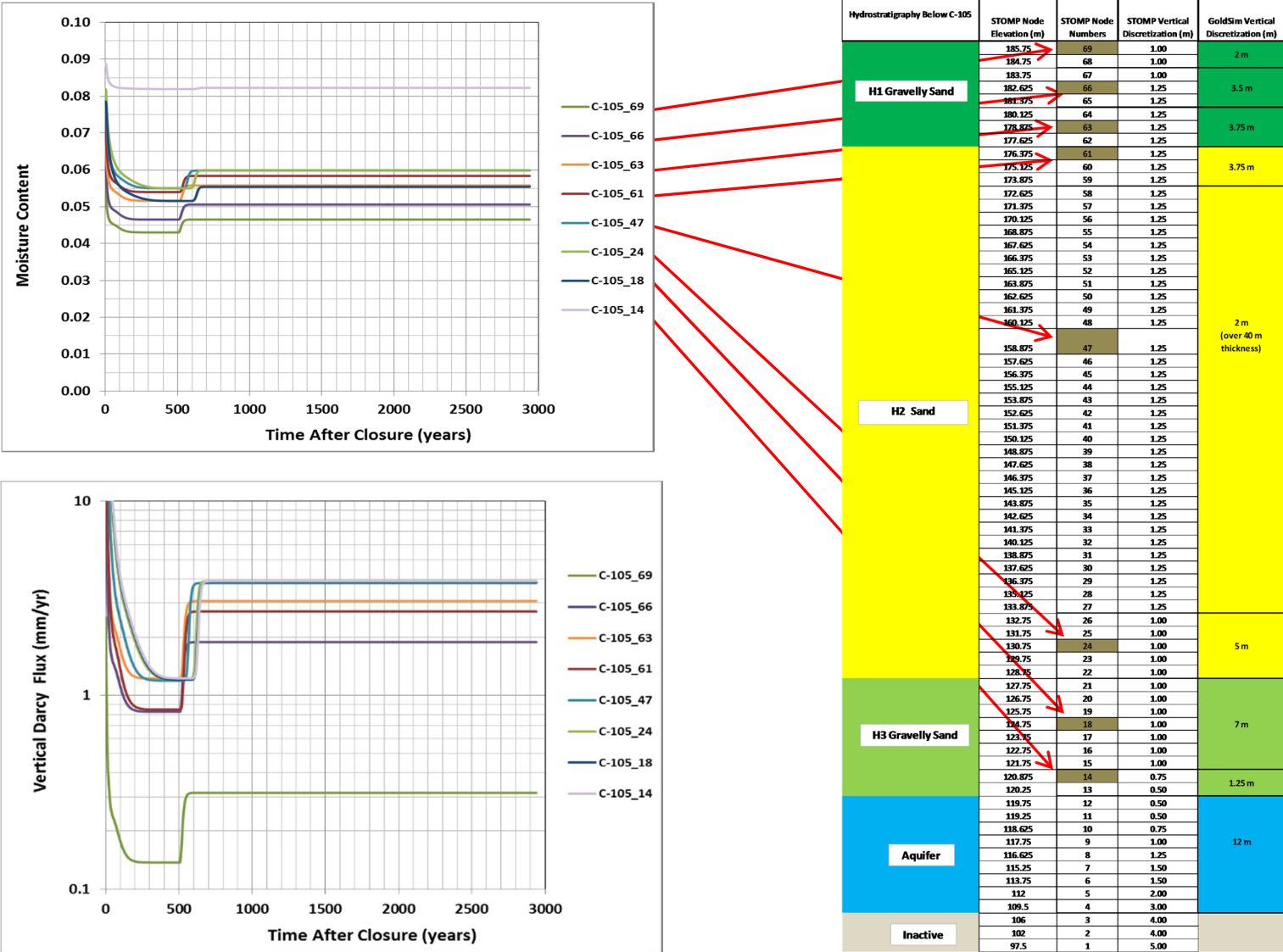
that includes C-102, C-105, C-108, and C-111 tank sources. The two laterally adjacent and parallel aquifer pathways are (a) along the orientation of tanks C-101, C-104, C-107, and C-110, and (b) along the orientation of tanks C-103, C-106, C-109, and C-112. The primary groundwater flow path on which the 200-series tanks occur is deemed too far to influence the concentrations along the centerline, and therefore is not considered based on evaluation of STOMP[®] 3-D model results.

A spatial-variability study was undertaken to evaluate the adequacy of using one representative flow field for all of the 100-series tanks. For this purpose, the vertical Darcy fluxes from STOMP[®]-based model nodes located underneath intact tanks were compared. The vertical Darcy flux underneath tank C-105 (located near the center of the tank farm) was compared to that of tank C-112 (located at the northern edge of the tank farm). The vertical Darcy flux under a 200-series tank (C-201) located near tank C-112 was also compared. The comparison results are presented in Figure 6-52 for two nodes. Node 69 is located ~0.5 m (1.6 ft) below the base of the tank, while node 63 is located ~3 m (9.8 ft) below node 69. The results indicate that for node 69 the vertical Darcy flux for tank C-105 matches closely with that of tank C-112, and is quite different from that of tank C-201. For node 63, which is deeper, the differences among the three tanks are minor. The large difference observed for node 63 is attributed to its location near the base of the tank, where the amount of flow diversion around the tank is influenced by its diameter. The smaller diameter of tank C-201 (6.1 m [20 ft]) exhibits small flow diversion, and the Darcy flux under the tank is relatively high compared to the larger flow diversion observed for the larger-diameter (23 m [75 ft]) C-105 and C-112 tanks. These observations support the use of one representative flow field for all 100-series tanks and another for all 200-series tanks.

Confirmation of the abstraction modeling approach for evaluating system performance was undertaken by comparing the contaminant transport results to the STOMP[®]-based model results for the base case. Due to coarser vertical discretization employed in the 1-D abstraction model, the results from those nodes that are closest to the STOMP[®]-based model grid nodes are compared. The time-varying diffusive mass flux of ⁹⁹Tc calculated using the source term parameters for tank C-105 was applied as boundary conditions in both models. A comparison between the dissolved concentration of ⁹⁹Tc in the vadose zone using a STOMP[®] 3-D model and a GoldSim[®] 1-D model is presented for selected locations in the vadose zone (Figure 6-53 and Figure 6-54). There is a good match between the 3-D process model and 1-D abstraction model throughout the full thickness of the vadose zone under the tank (~66 m [217 ft]).

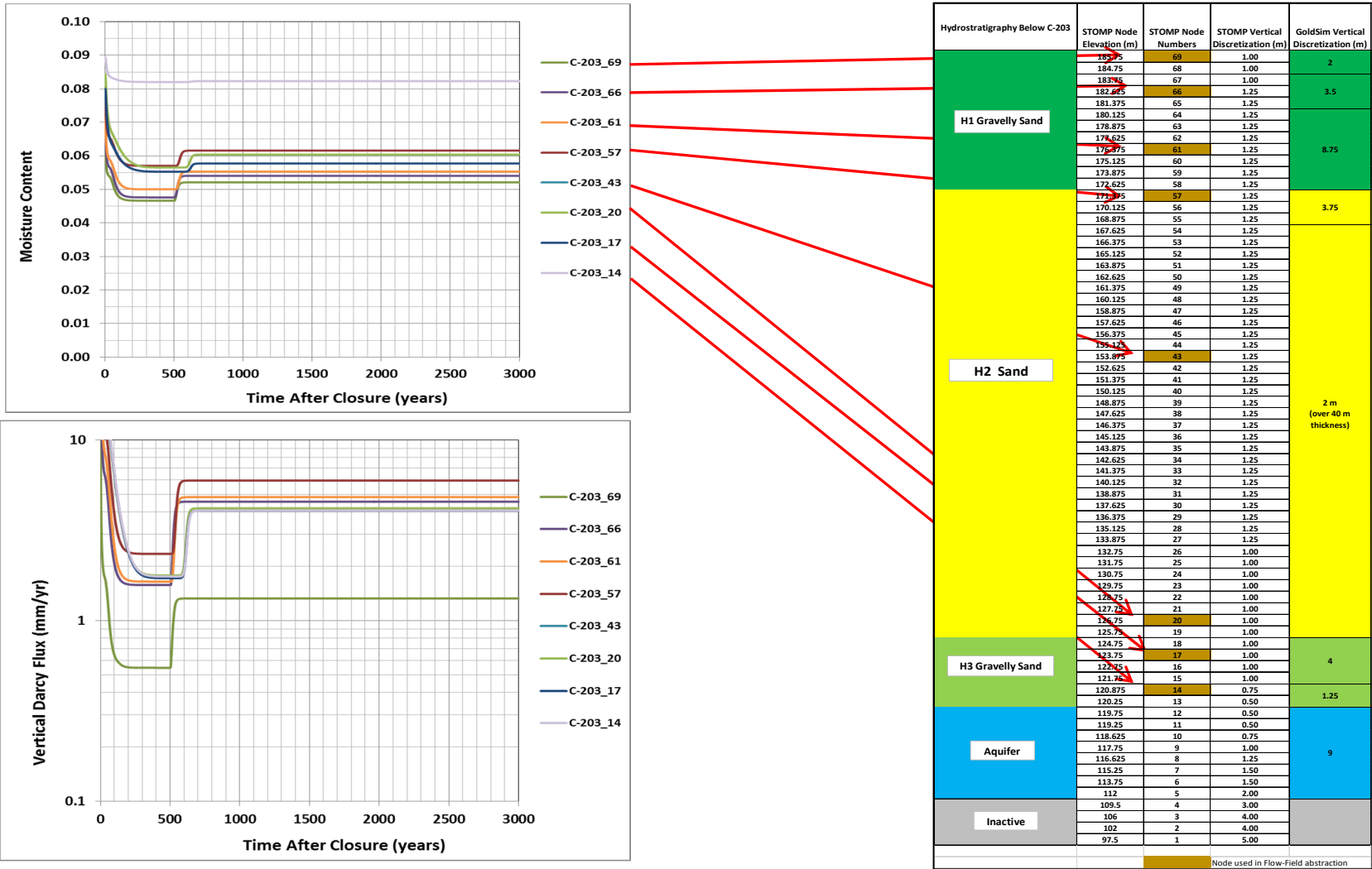
For the saturated zone, the groundwater concentration predicted by the STOMP[®]-based model (at the highest concentration PoCal) is compared to the GoldSim[®]-based abstraction model results at 100 m (328 ft) downgradient of the WMA C fenceline along the tank C-105 aquifer pathway (Figure 6-55). The first breakthrough times match well, but the 1-D model produces slightly higher concentrations following the peak. This result is expected, as the 1-D aquifer pathway does not allow lateral dispersion of the mass and assumes constant flow rate through the steam tube. Based on these results, the abstraction model was qualified as sufficiently accurate for its intended use in evaluating system performance.

Figure 6-48. Representative Flow Field Applied Under 100-Series Tank for the Base Case (Intact Tank Condition).



Subsurface Transport Over Multiple Phases (STOMP)® is copyrighted by Battelle Memorial Institute, 1996.
GoldSim® simulation software is copyrighted by GoldSim Technology Group LLC of Issaquah, Washington (see <http://www.goldsim.com>).

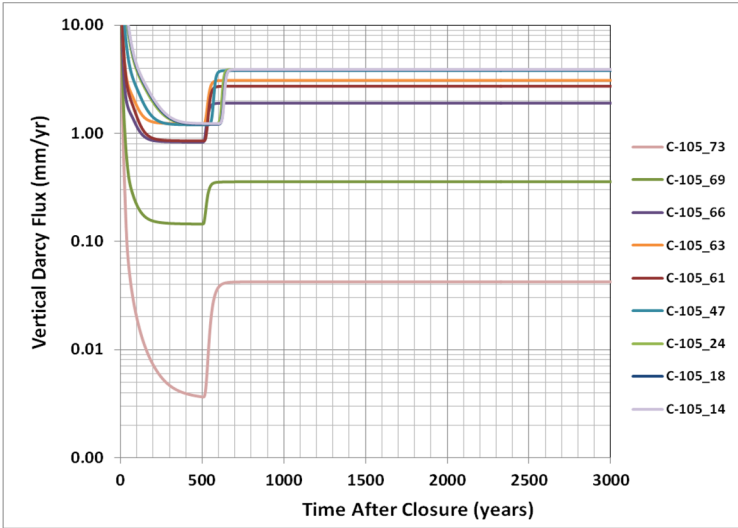
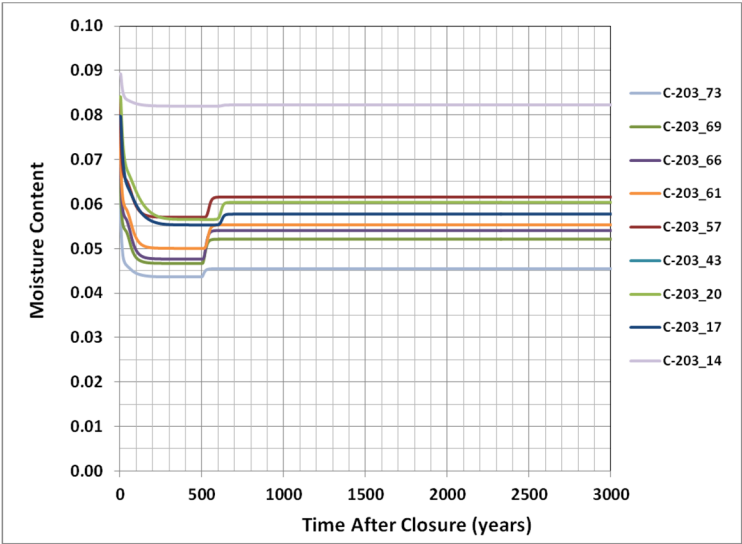
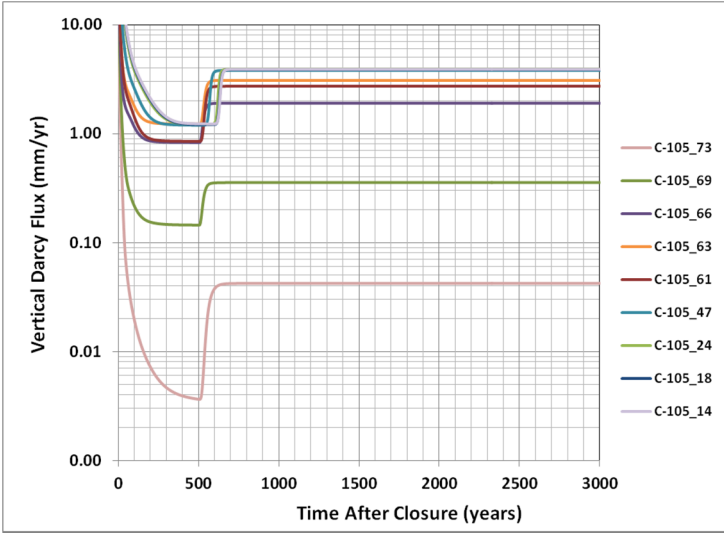
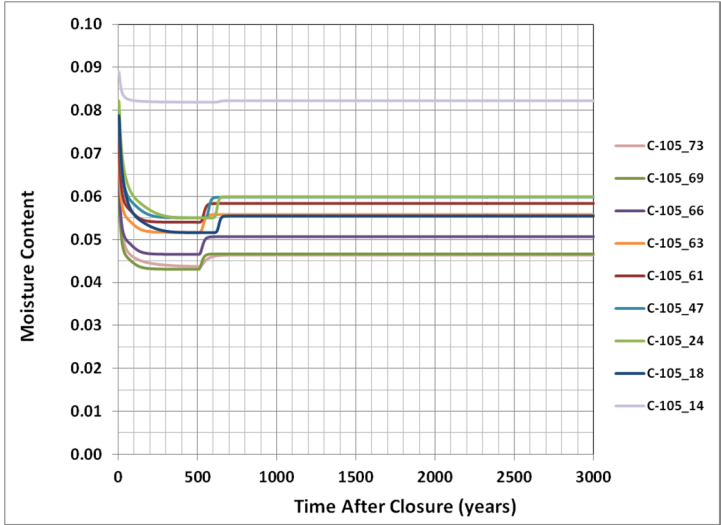
Figure 6-49. Representative Flow Field Applied Under 200-Series Tank for the Base Case (Intact Tank Condition).



RPP-ENV-58782, Rev. 0

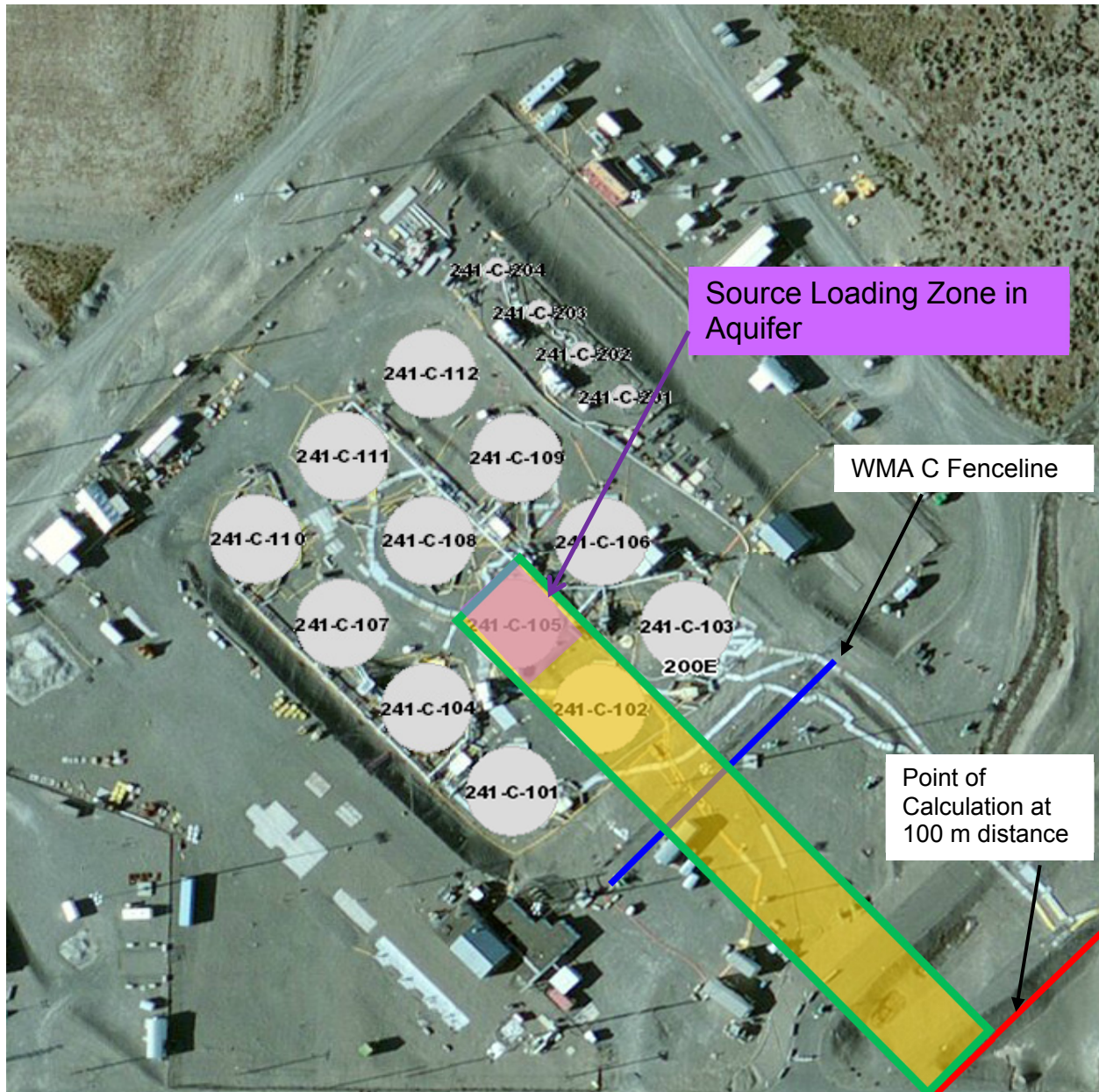
GoldSim® simulation software is copyrighted by GoldSim Technology Group LLC of Issaquah, Washington (see <http://www.goldsim.com>).
Subsurface Transport Over Multiple Phases (STOMP)® is copyrighted by Battelle Memorial Institute, 1996.

Figure 6-50. Representative Flow Field Applied For Degraded Tank Conditions for (a) 100-Series Tank and (b) 200-Series Tank.



RPP-ENV-58782, Rev. 0

Figure 6-51. Implementation of Aquifer Pathway for a Given Source Area along with Points of Evaluation of Concentrations.

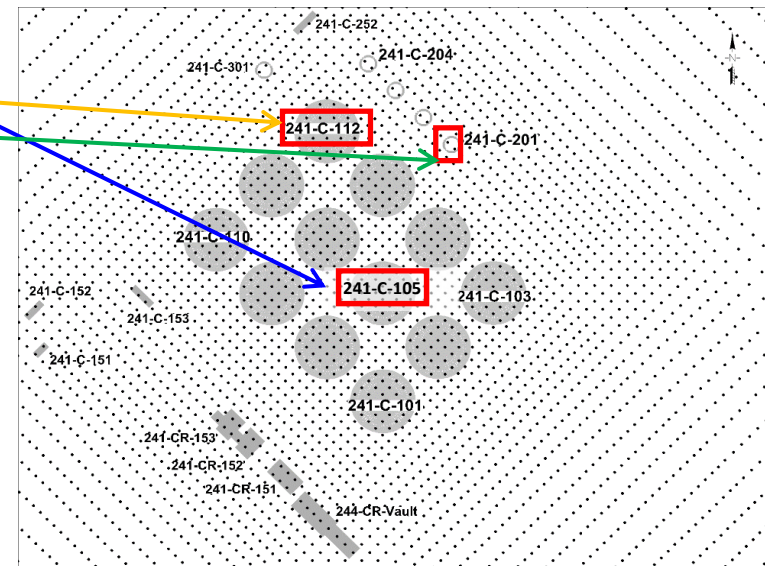
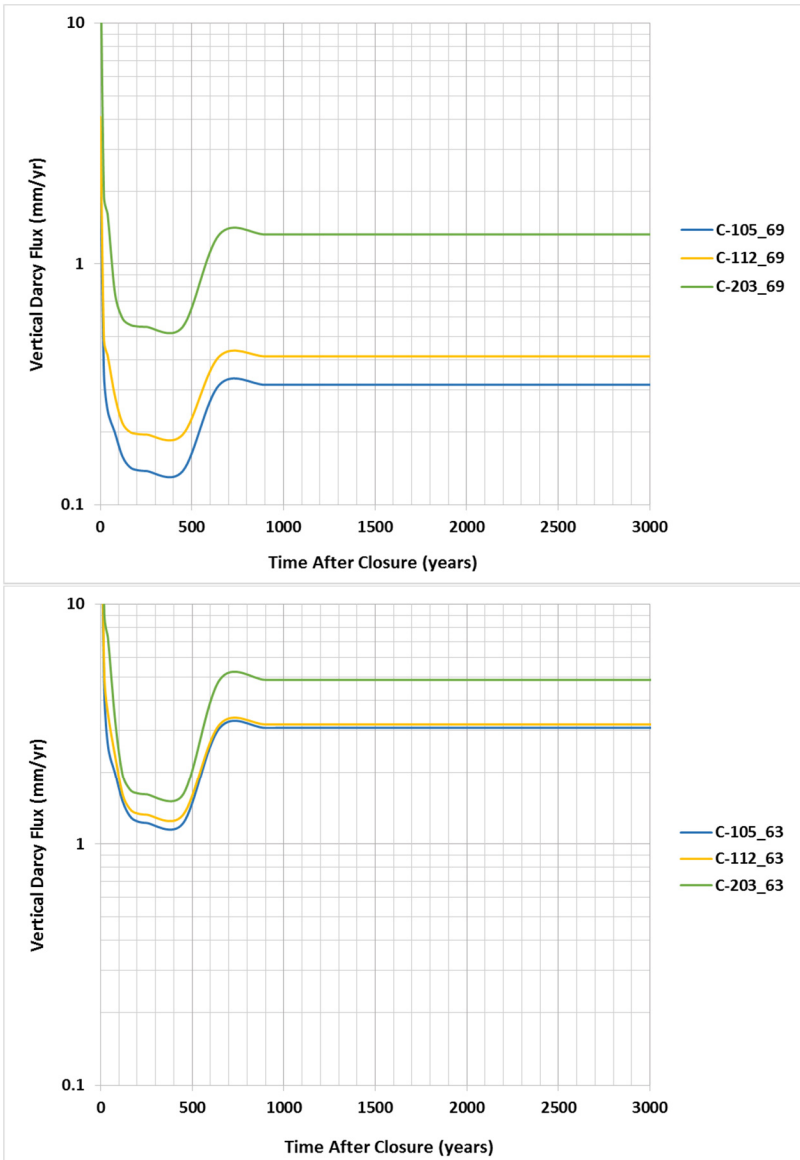


WMA = Waste Management Area

6.3.2.5 Atmospheric Transport Pathway. Gases and vapors could travel upward from the residual inventory within tanks and ancillary equipment through the surface barrier to the ground surface. The principal mechanism by which nuclides migrate from the waste to the ground surface is gaseous diffusion. For tanks, in which the residual waste is predominantly on the bottom of the tank, this means that the gases are transported through the tank infill grout, the tank dome, the soil overburden, and the surface barrier. For pipelines, the diffusion would occur through the soil overburden and the surface barrier.

Figure 6-52. Vertical Darcy Flux Extracted from Three-Dimensional Subsurface Transport Over Multiple Phases (STOMP®)-Based Model Nodes Located below Tanks 241-C-105, 241-C-112, and 241-C-201 along with Their Location in Waste Management Area C.

Node 69 is located 0.5 m below the tank bottom while node 63 is located about 3 m below node 69.



Subsurface Transport Over Multiple Phases (STOMP)® is copyrighted by Battelle Memorial Institute, 1996.

Figure 6-53. Comparison between Three-Dimensional Subsurface Transport Over Multiple Phases (STOMP®)-Based Model Prediction and GoldSim®-Based One-Dimensional Abstraction Model Prediction for Nodes Located in H1 Gravelly Sand Unit.

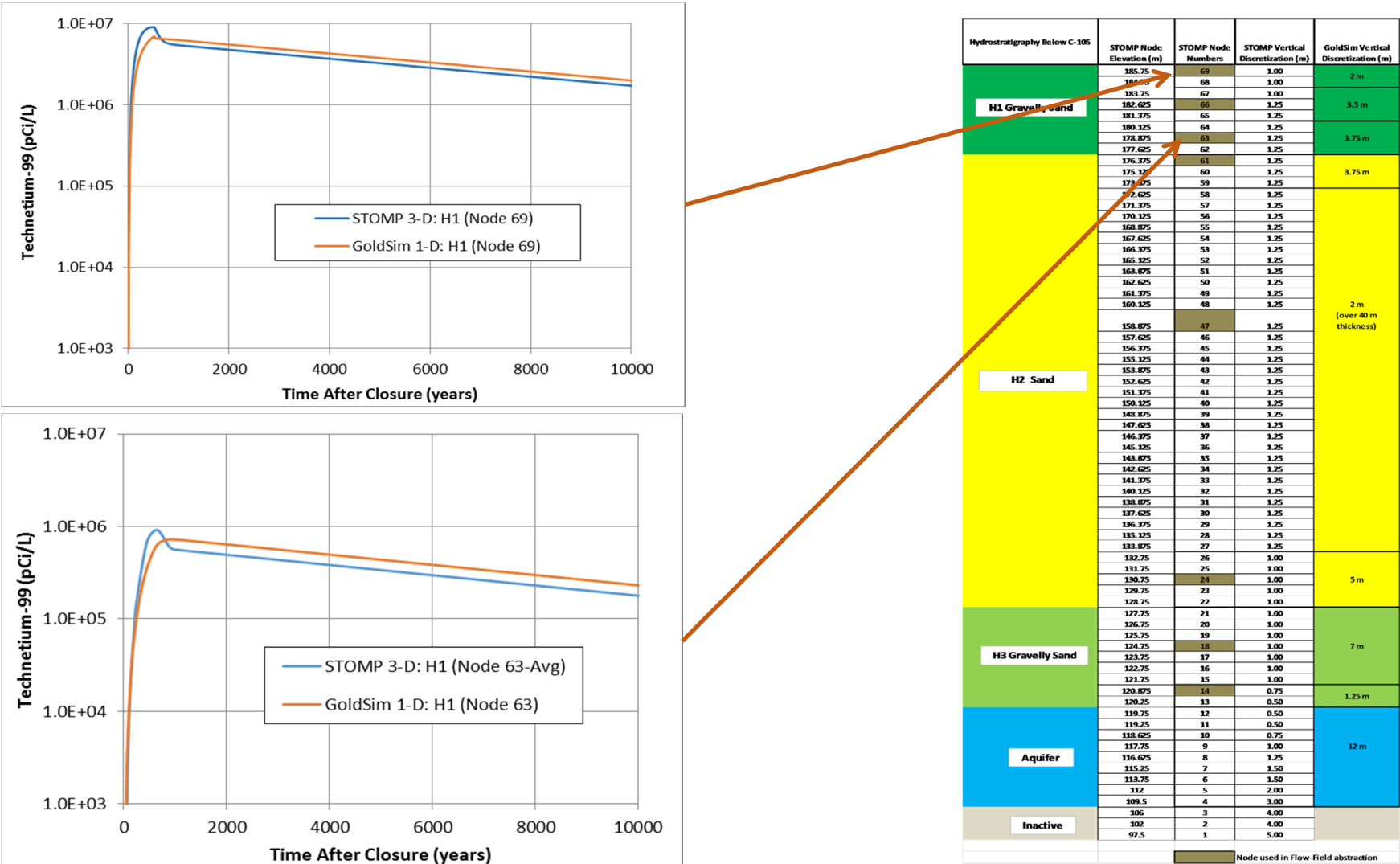
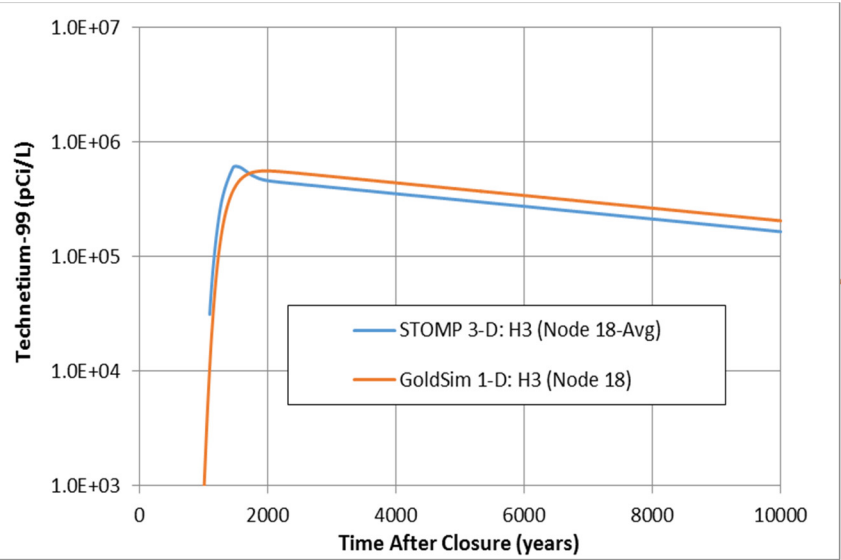
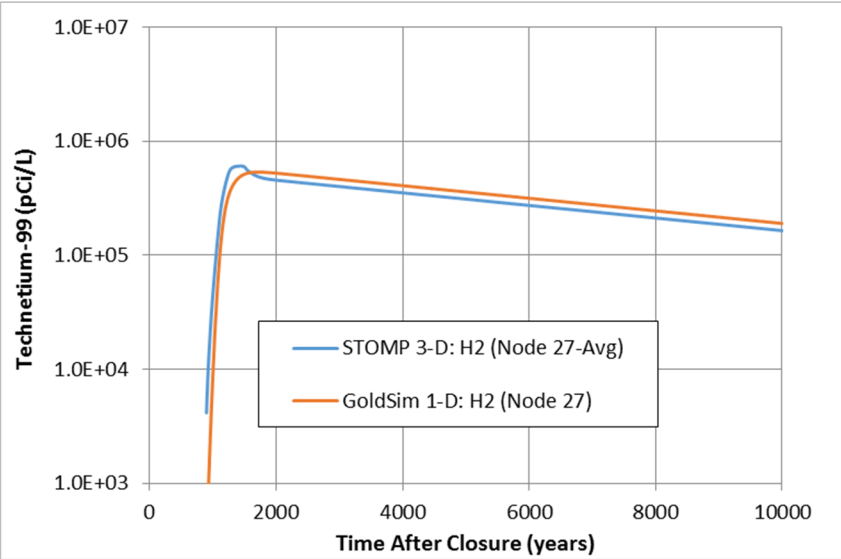


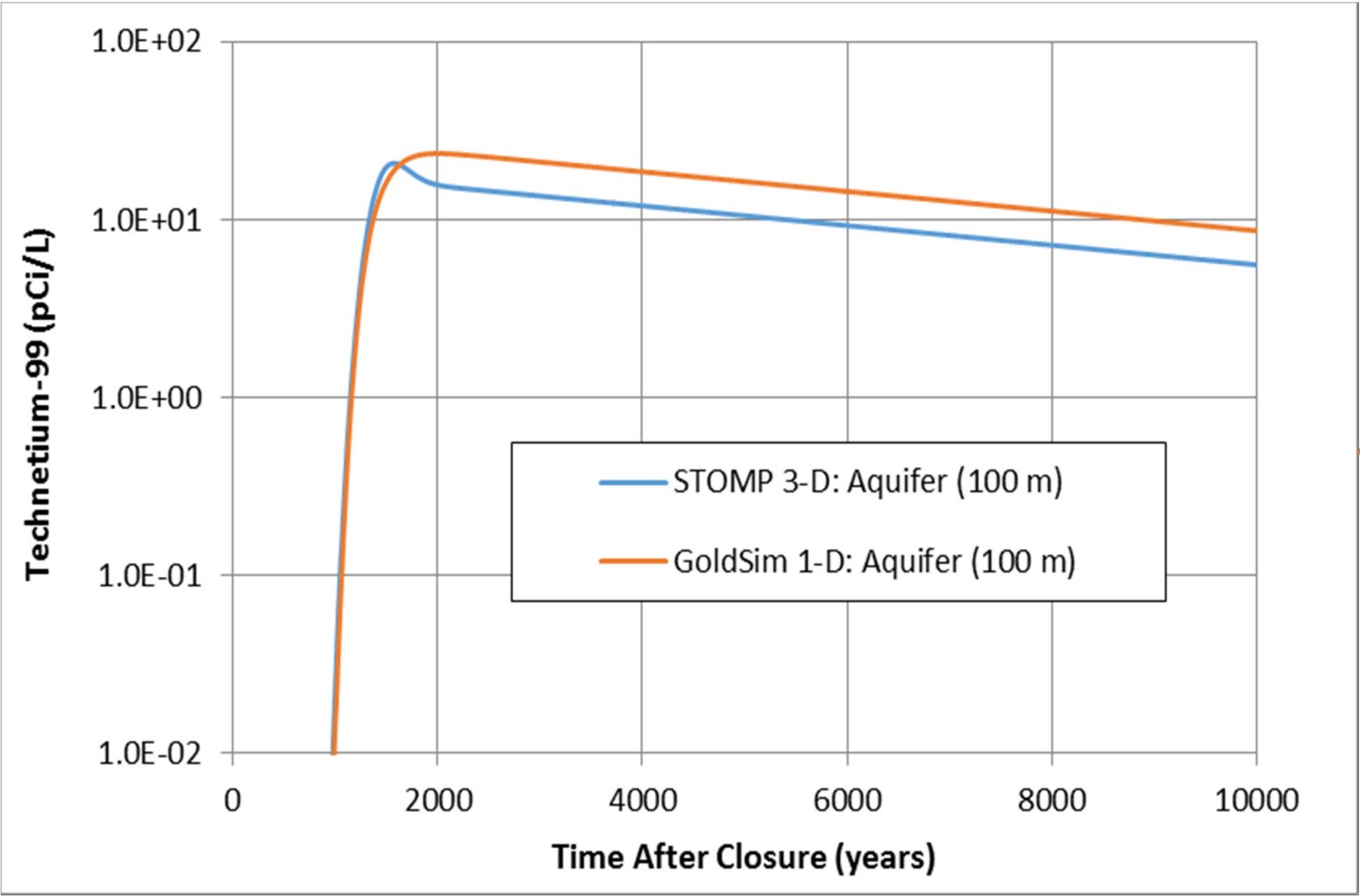
Figure 6-54. Comparison between Three-Dimensional Subsurface Transport Over Multiple Phases (STOMP®)-Based Model Prediction and GoldSim®-Based One-Dimensional Abstraction Model Prediction for Nodes Located in H2 Sand Unit and H3 Gravelly Sand Unit.



GoldSim® simulation software is copyrighted by GoldSim Technology Group LLC of Issaquah, Washington (see <http://www.goldsim.com>). Subsurface Transport Over Multiple Phases (STOMP)® is copyrighted by Battelle Memorial Institute, 1996.

Hydrostratigraphy Below C-105	STOMP Node Elevation (m)	STOMP Node Numbers	STOMP Vertical Discretization (m)	GoldSim Vertical Discretization (m)
H1 Gravelly Sand	185.75	69	1.00	2 m
	184.75	68	1.00	
	183.75	67	1.00	
	182.625	66	1.25	3.5 m
	181.375	65	1.25	
	180.125	64	1.25	
	178.875	63	1.25	3.75 m
	177.625	62	1.25	
	176.375	61	1.25	
	175.125	60	1.25	3.75 m
H2 Sand	173.875	59	1.25	
	172.625	58	1.25	
	171.375	57	1.25	
	170.125	56	1.25	
	168.875	55	1.25	
	167.625	54	1.25	
	166.375	53	1.25	
	165.125	52	1.25	
	163.875	51	1.25	
	162.625	50	1.25	
	161.375	49	1.25	
	160.125	48	1.25	
	158.875	47	1.25	2 m (over 40 m thickness)
	157.625	46	1.25	
	156.375	45	1.25	
	155.125	44	1.25	
	153.875	43	1.25	
	152.625	42	1.25	
	151.375	41	1.25	
	150.125	40	1.25	
	148.875	39	1.25	
	147.625	38	1.25	
	146.375	37	1.25	
	145.125	36	1.25	
	143.875	35	1.25	
	142.625	34	1.25	
	141.375	33	1.25	
	140.125	32	1.25	
	138.875	31	1.25	
	137.625	30	1.25	
	136.375	29	1.25	
	135.125	28	1.25	
	133.875	27	1.25	
H3 Gravelly Sand	132.75	26	1.00	
	131.75	25	1.00	
	130.75	24	1.00	5 m
	129.75	23	1.00	
	128.75	22	1.00	
	127.75	21	1.00	
	126.75	20	1.00	
	125.75	19	1.00	
	124.75	18	1.00	7 m
	123.75	17	1.00	
Aquifer	122.75	16	1.00	
	121.75	15	1.00	
	120.875	14	0.75	1.25 m
	120.25	13	0.50	
	119.75	12	0.50	
	119.25	11	0.50	
	118.625	10	0.75	
	117.75	9	1.00	
	116.625	8	1.25	
	115.25	7	1.50	
Inactive	113.75	6	1.50	
	112	5	2.00	
	109.5	4	3.00	
	106	3	4.00	
	102	2	4.00	
	97.5	1	5.00	
Node used in Flow-Field abstraction				

Figure 6-55. Comparison Between Three-Dimensional Subsurface Transport Over Multiple Phases (STOMP®)-Based Model Prediction and GoldSim®-Based One-Dimensional Abstraction Model Prediction in the Saturated Zone at 100 m Distance from the Waste Management Area C Fenceline.



1-D = one-dimensional
3-D = three-dimensional
GoldSim® simulation software is copyrighted by GoldSim Technology Group LLC of Issaquah, Washington (see <http://www.goldsim.com>).
Subsurface Transport Over Multiple Phases (STOMP)® is copyrighted by Battelle Memorial Institute, 1996.

RPP-ENV-58782, Rev. 0

Releases to the atmospheric pathway and groundwater pathway begin at the start of the simulation. The partitioning of inventory into the aqueous and gaseous phase occurs within the source-term model (in the residual waste layer). The mass partitioned into the aqueous phase is then available for transport to the underlying vadose zone, while the partitioned fraction in the gas phase is available for upward transport to the atmosphere. Although diffusive path length for the gas phase can vary based on lateral movement, in order to maximize the flux, only the shortest vertical upward path length is considered. In addition, to maximize the upward transport through the gas phase, the downward flow of water above the residual waste location is not modeled. Any physical effect of surface barrier on gaseous flux is also ignored.

Of the radionuclides contained in residual inventory at closure (Section 3), four could potentially originate as gas:

- Carbon-14 as CO₂ gas
- Hydrogen-3 (tritium) as H₂ gas
- Iodine-129 as I₂ gas
- Radon-222 as radon gas.

These releases are driven by the partitioning of the radionuclides among the solid fraction of the porous medium (sorbed fraction), aqueous dissolved fraction (grout/water partitioning), and the gaseous fraction (air/water partitioning) by considering the following equilibrium coefficients:

- K_d representing grout-to-water partitioning
- Henry's law constant (K_h) for representing air-to-water partitioning (see Table 6-17 for the constant used for the constituents above).

Table 6-17. Henry's Law Constants.

Radionuclide	Gas Form	Aqueous-to-Gas Henry's Constant	Reference	Calculated Gas-to-Aqueous Dimensionless Henry's Constant at 20 °C
¹⁴ C	CO ₂	4.5 (dimensionless)	Plummer et al. 2004	0.22
³ H	H ₂	7.80E-4 (mol atm ⁻¹ L ⁻¹)	Sander 1999	53.36
¹²⁹ I	I ₂	3.10E+0 (mol atm ⁻¹ L ⁻¹)	Sander 1999	0.013
²²² Rn	Rn	9.30E-3 (mol atm ⁻¹ L ⁻¹)	Sander 1999	4.47

References:

"Transport of Carbon-14 in a Large Unsaturated Soil Column" (Plummer et al. 2004).

"Compilation of Henry's Law Constants for Inorganic and Organic Species of Potential Importance in Environmental Chemistry," Version 3 (Sander 1999).

The atmospheric transport pathway calculations are conducted in three steps, as follows.

1. First, a calculation is performed to compute the upward diffusive flux from each source term to the surface. A zero-concentration boundary condition at the surface is imposed

RPP-ENV-58782, Rev. 0

for purpose of calculating the gaseous flux. This is conceptually equivalent to having a large enough wind speed above WMA C such that the air parcel is renewed constantly, thereby maximizing the diffusive gradient.

For all sources except pipelines, while the infill grout is intact, upward gaseous diffusion of volatile contaminants is modeled from the residual waste layer towards the atmosphere. Upward diffusive gas phase transport through the tanks (or 244-CR vault) is modeled to occur along a 10-m (32.8-ft)-long pathway towards the land surface (Figure 6-18). This pathway is split into a lower 5-m (16.4-ft) thickness composed of infill grout material, followed by another 5 m thickness of soil overburden. For the pipeline source area, the diffusive length chosen is the pipeline diameter (0.076 m [3 in.]) and the 5-m (16.4-ft) thickness of the soil overburden.

A surface barrier that will be emplaced at closure over the tank farm will provide additional depth to the waste and therefore greater diffusive length. For the purpose of performing the air pathway calculations, this additional thickness is ignored.

For all grouted facilities, the air content within the infill grout is assumed to be 6% based on characterization information for possible Hanford grout (WSRC-TR-2005-00195). The porosity and saturation of the infill grout for the purpose of diffusive release calculations are fixed over time. Studies have indicated that chemical transformation of initial grout minerals will likely cause porosity reduction over time due to increased molar volume of the newly formed mineral phases. Fixing porosity maximizes diffusion.

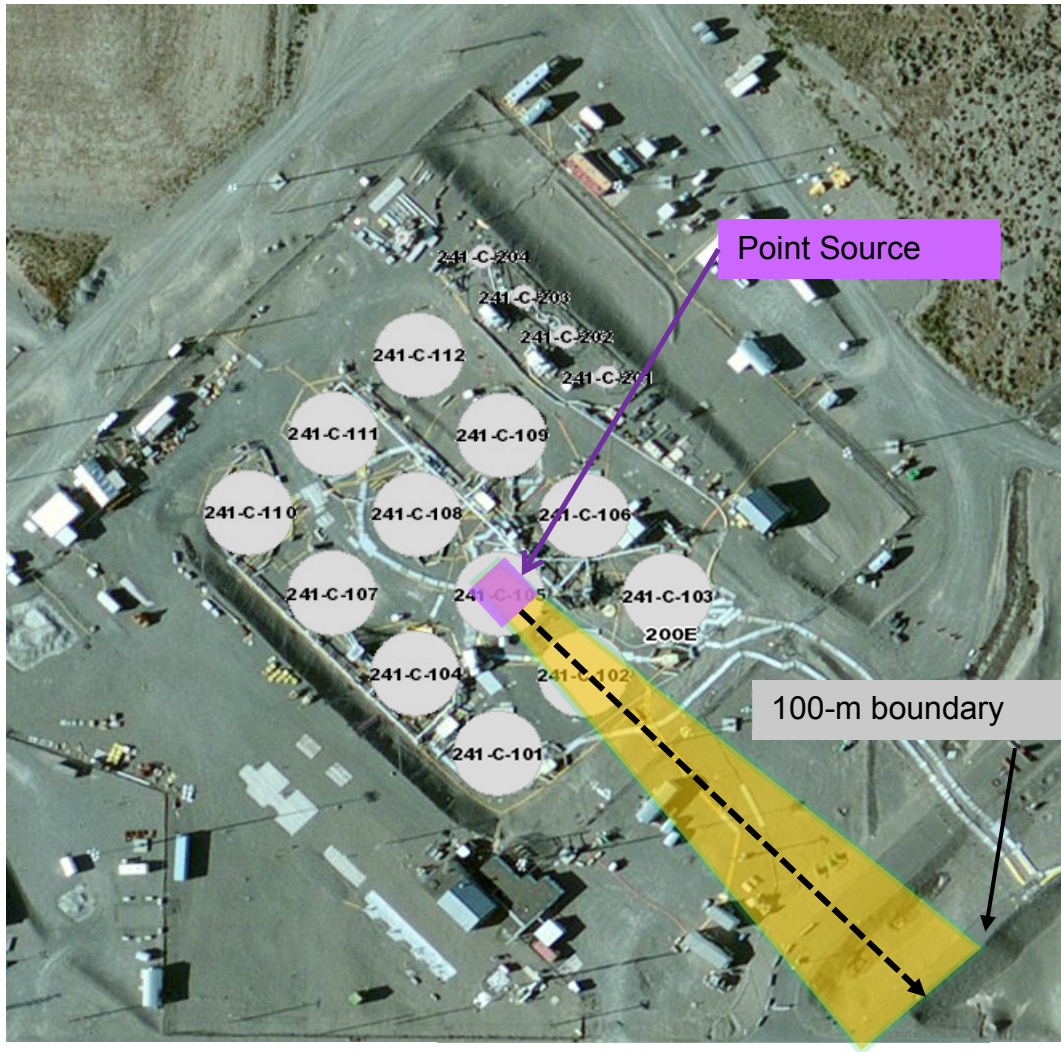
2. Second, for each source area, the radionuclide transport in air along the downwind direction is performed using Gaussian plume dispersion methodology, where advection and dispersion occur via wind movement to the receptor placed 100 m (328 ft) downwind at the PoCal as conceptualized in Figure 6-56. As a continuous stream of gas (pollutants) is released into the steady wind in open atmosphere, the gas plume will travel with the mean wind speed. The plume will also spread out or disperse in the horizontal and vertical directions along the centerline. A schematic is presented in Figure 6-57 for a single source based on effective stack height (includes plume rise).
3. In order to evaluate the effect of commingling of gas plumes from different sources that could lead to increased concentration at the receptor location located 100 m (328 ft) downwind, a separate calculation is performed, where the upward diffusive flux emanating from various sources (described in Step 1) are combined into a point source, with the location near the approximate center point of the WMA C area. This is conceptually equivalent to a point source (i.e., stack source), but with the release rate (emission rate) equal to all the sources within the WMA C area. This point location is chosen to be the center of the pipeline area, which is 75 m (246 ft) from the WMA C fenceline. The total distance to the receptor is therefore 175 m (574 ft).

The predominant wind direction in the 200 East Area is towards southeast as discussed in Section 3.1.2.4 (also see Figures 3-6 and 3-7), and therefore in the general direction of groundwater flow. The average annual wind speed of 3.4 m/s (11.2 ft/s) (average from

RPP-ENV-58782, Rev. 0

1944 to 2004) is applied to the pathway for transport. The air mixing height is assumed to be 2 m (6.6 ft). The calculated air concentrations at the receptor location are used for evaluating air-pathway dose.

Figure 6-56. Atmospheric Transport Pathway from a Source to the Receptor Located at the Point of Calculation Along the Centerline of the Gas Plume.



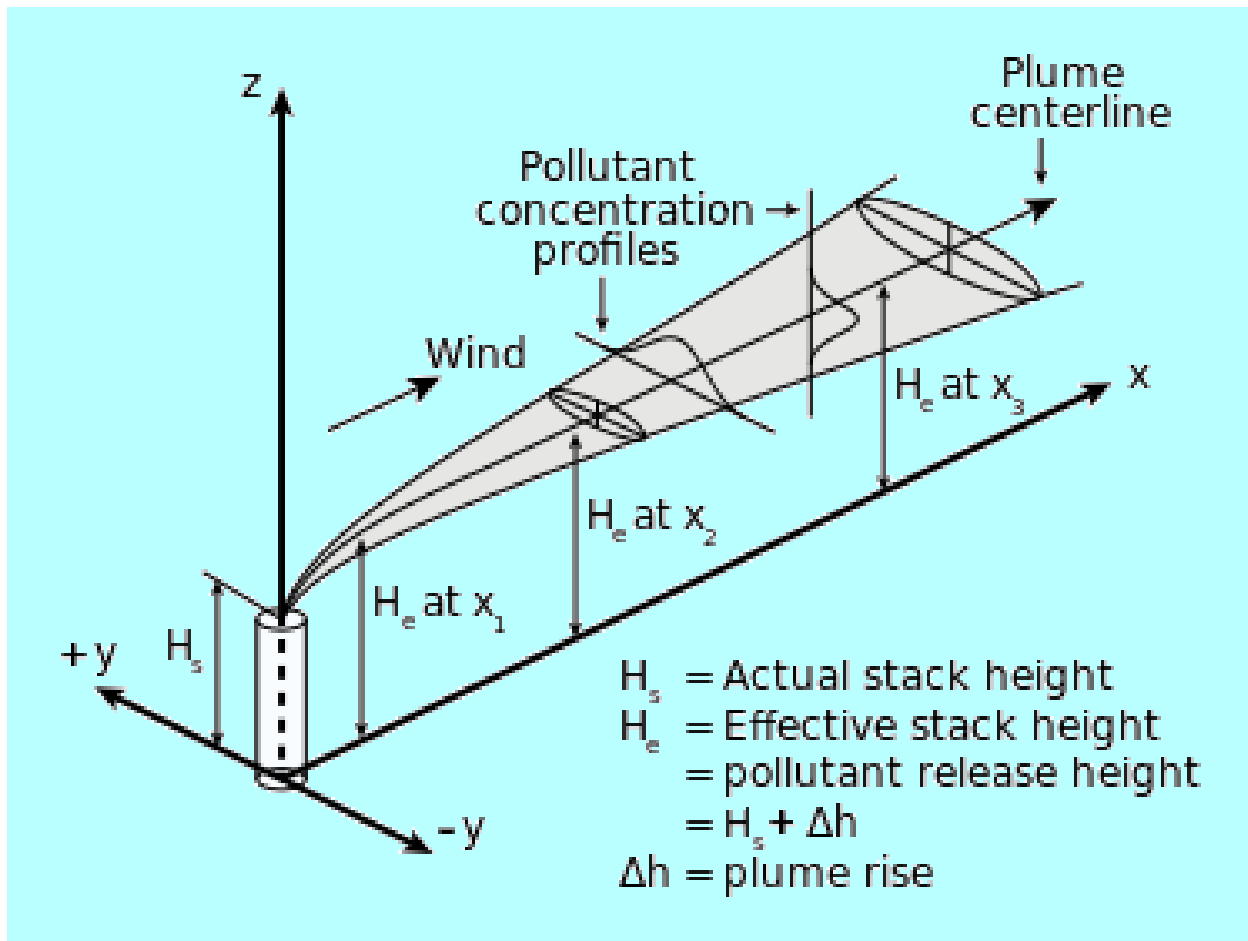
6.3.2.5.1 Mathematical Modeling of First Step. To calculate the diffusive flux emanating at the surface from a given source (buried tank or ancillary equipment), a 1-D model is developed using a finite-difference network of batch-reactor cells. The following transport equation (as per Fick's second law) is numerically solved using GoldSim[®] to compute the mass flux and concentration:

$$R_d \frac{\partial(\theta_a C)}{\partial t} = D_{ef} \frac{\partial^2 C}{\partial x^2} \quad (6-16)$$

Where:

$\theta_a (-)$ = the air content (or air-filled porosity) of the porous medium.

Figure 6-57. A Schematic of Gaseous Plume Movement Based on Gaussian Distribution in the Horizontal and Vertical Direction.



The diffusion coefficient for various gases of concern (CO₂, H₂, I₂, and radon) through the tortuous air pathway of the porous medium is calculated as follows:

$$D_{ef} = D_0 \tau \quad (6-17)$$

RPP-ENV-58782, Rev. 0

1 Where:

2 D_{ef} (m²/s) = the effective diffusion coefficient through the tortuous air pathway of the
3 porous medium for a given gas

4 D_0 (m²/s) = the binary diffusion coefficient of the gas of concern in the air

5 τ = the tortuosity of the porous medium for air pathway.

6 An effective zero concentration boundary condition is imposed above WMA C to maximize the
7 diffusive flux of gases. The diffusive area varies by the source geometry.

8 **6.3.2.5.2 Diffusion Coefficients and Tortuosity.** The binary diffusion coefficients of the
9 different gases of concern in air have been calculated using the EPA methodology (United States
10 Environmental Protection Agency, Queried 01/2012, [EPA On-line Tools for Site Assessment
11 Calculation], <https://www3.epa.gov/ceampubl/learn2model/part-two/onsite/estdiffusion.html>)
12 considering an atmospheric pressure of 1 atm and a temperature of 20 °C (68 °F). The calculated
13 diffusion coefficients are reported in Table 6-18, together with the gas boiling point estimates
14 used in the calculations. For radon, another reference has been considered (Radon and Its Decay
15 Products in Indoor Air [Nazaroff and Nero 1988]) as EPA (2012) did not consider diffusion
16 coefficient calculation for this gas.

Table 6-18. Diffusion Coefficients in Air at 20 °C and 1 Atm.

Radionuclide	Gas Form	Diffusion Coefficient in Air (cm ² s ⁻¹)	Reference	Boiling Point (°C) Used in EPA Calculations (Haynes and Lide 2011)
¹⁴ C	CO ₂	0.160	EPA 2012 (average method)	-78.55
³ H	H ₂	0.819	EPA 2012 (average method)	-252.76
¹²⁹ I	I ₂	0.0897	EPA 2012 (FSG/LaBas method)	184.45
²²² Rn	Rn	0.11	Nazaroff and Nero (1988) cited in ANL/EAD-4	(-)

EPA = U.S. Environmental Protection Agency

References:

ANL/EAD-4, "User's Manual for RESRAD Version 6."

CRC Handbook of Chemistry and Physics, 92nd Edition (Haynes and Lide 2011).

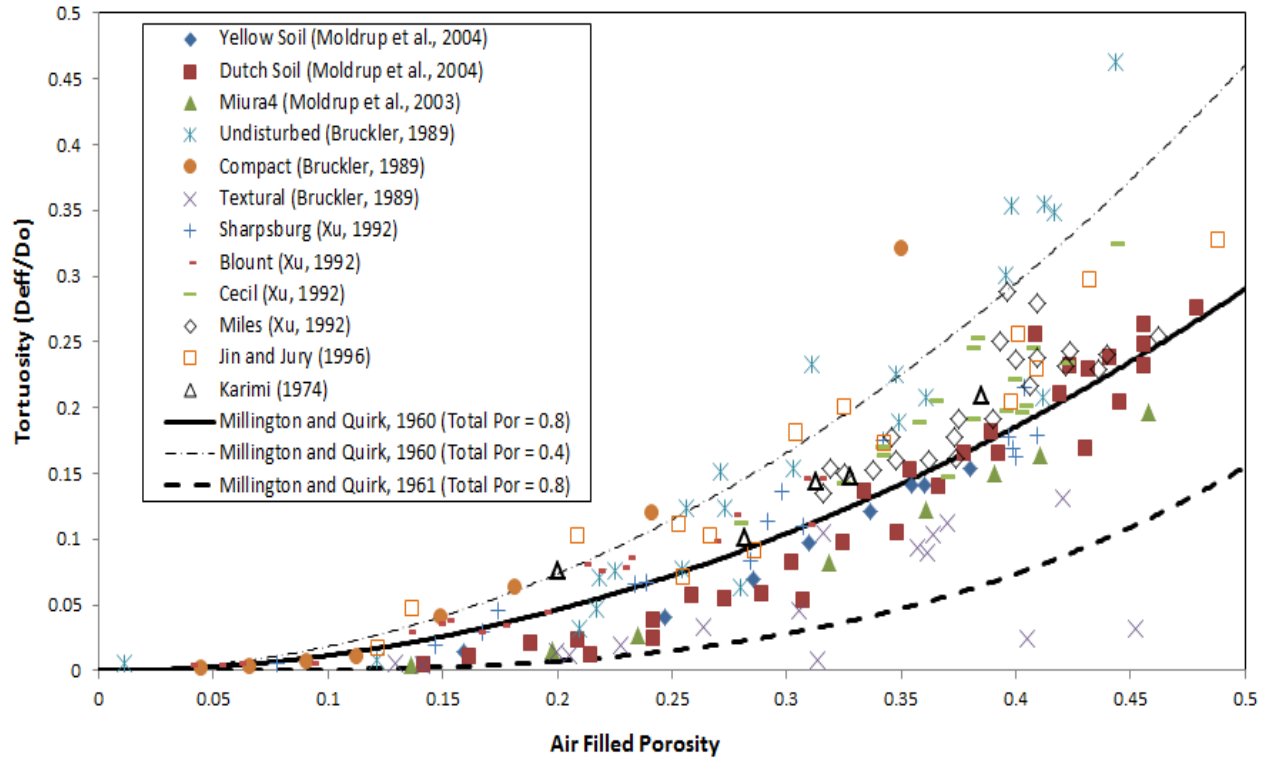
Radon and Its Decay Products in Indoor Air (Nazaroff and Nero 1988).

United States Environmental Protection Agency, Queried 01/2012, [EPA On-line Tools for Site Assessment Calculation], <https://www3.epa.gov/ceampubl/learn2model/part-two/onsite/estdiffusion.html>.

17 "Simulating the Gas Diffusion Coefficient in Macropore Network Images: Influence of Soil Pore
18 Morphology" (Liu et al. 2006) compiled data sets and presented the experimentally determined
19 gas tortuosity (ratio of the effective diffusion coefficient in soil [D_{ef}] to that in free air [D_0]) as a
20 function of the air-filled porosity (air content) for various soil types. They also provided the best
21 fit lines and bounding estimates based on models presented by "Transport in porous media"
22 (Millington and Quirk 1960) and Millington and Quirk (1961). The results from Liu et al. (2006)
23 are reproduced in Figure 6-58.

RPP-ENV-58782, Rev. 0

Figure 6-58. Comparison of Measured Tortuosity (i.e., Ratio of Diffusion Coefficient in Soil [D_{ef}] to that in Free Air [D_0]) with Fitted Tortuosity Models.



Source: "Simulating the Gas Diffusion Coefficient in Macropore Network Images: Influence of Soil Pore Morphology" (Liu et al. 2006).

References:

- "Characterizing the Dependence of Gas Diffusion Coefficient on Soil Properties" (Jin and Jury 1996).
- "Compaction Effect on the Gas Diffusion Coefficient in Soils" (Xu et al. 1992).
- "Gas Diffusivity in Undisturbed Volcanic Ash Soils: Test of Soil-Water-Characteristic-Based Prediction Models" (Moldrup et al. 2003).
- "Laboratory Estimation of Gas Diffusion Coefficient and Effective Porosity in Soils" (Bruckler et al. 1989).
- "Permeability of Porous Solids" (Millington and Quirk 1961).
- "Three-Porosity Model for Predicting the Gas Diffusion Coefficient in Undisturbed Soil" (Moldrup et al. 2004).
- "Transport in porous media" (Millington and Quirk 1960).
- "Vapor-phase Diffusion of Benzene in Soil" (Karimi et al. 1987).

Using the Millington and Quirk (1960) gas tortuosity equation below (Equation 6-18), Liu et al. (2006) found the best fit to the experimental data set by varying the value of the total porosity in the denominator and finally selecting a value of 0.8:

$$\tau = \frac{\theta_a^2}{\phi^{2/3}} = \frac{(\phi - \theta_w)^2}{\phi^{2/3}} \quad (6-18)$$

Where:

- τ = the tortuosity
- θ_a = the air content (or air-filled porosity) of the porous medium
- θ_w = the water content (or water-filled porosity) of the porous medium

RPP-ENV-58782, Rev. 0

ϕ = the total porosity (measured)

Φ = fitted total porosity; set equal to 0.8 for best fit (Liu et al. 2006).

The tortuosity in the infill grout material is calculated from first equality of Equation 6-18 using fixed value of θ_a (6%), while the second equality is used for calculating the tortuosity for the backfill material (soil overburden) where the θ_w (and hence tortuosity) varies as a function of time. Note that Liu et al. (2006) made an error in referencing the Millington and Quirk paper. They reversed a referenced paper's date ("1961" instead of correct date 1960) in the text and in the figure; the error is now corrected.

The solid surface within the tank and ancillary equipment (except for pipeline) is considered to be the infill grout. The grout-to-water partition coefficient (K_d) values applied are the same as those considered in Section 6.3.1.5 (and Table 6-5). These values are reported for conciseness in Table 6-19 for the relevant radionuclides. The K_d value for ^{222}Rn is set to zero because it is a noble gas, and unreactive with its surroundings.

Table 6-19. Best Estimate K_d (mL/g) for Grout Material.

Radionuclide	Best Estimated K_d for Grout (mL/g)
^{14}C	2.00E+02
^3H	1.00E-01
^{129}I	3.00E+00
^{222}Rn	0

Sorption on the backfill could be considered but is ignored since it is typically much smaller than on the grout and would lower the concentrations further.

6.3.2.5.3 Mathematical Modeling of Second Step. Once the gaseous diffusive flux from the source area is calculated, a plume dispersion model is applied using GoldSim[®] to evaluate the concentrations at the receptor (PoCal) using the double Gaussian plume equation of "The Estimation of the Dispersion of Windborne Material" (Pasquill 1961) as discussed in the CAP88-PC Version 4.0 User Guide (EPA 2014). This equation (which models the dispersion of a non-reactive gaseous pollutant from an emission point) is given below in a form that predicts the steady-state concentration as a point (x, y, z) located downwind from the source as shown in Figure 6-58:

$$C = \frac{Q}{2\pi u \sigma_y \sigma_z} \exp\left(-\frac{1}{2} \frac{y^2}{\sigma_y^2}\right) \left\{ \exp\left(-\frac{1}{2} \frac{(z-H)^2}{\sigma_z^2}\right) + \exp\left(-\frac{1}{2} \frac{(z+H)^2}{\sigma_z^2}\right) \right\} \quad (6-19)$$

Where:

C = steady-state concentration at x meters downwind, y meters crosswind, and z meters above ground (Ci/m^3)

Q = release rate (emission rate) from source (Ci/sec)

u = average wind speed at stack height (m/sec)

RPP-ENV-58782, Rev. 0

- 1 σ_y, σ_z = horizontal and vertical dispersion coefficient (spread parameters) (m)
 2 z = vertical distance from ground level (m)
 3 H = effective stack height (m) that includes physical stack height and plume rise.
 4

5 In this model, the highest concentration occurs along the centerline of the plume. For the
 6 purpose of estimating the concentration in air at exposure location, the receptor is assumed to be
 7 located at the centerline ($y = 0$ m [0 ft]) of the plume. The effective stack height (H), which
 8 includes the plume rise, and the vertical distance from ground level (z) are each taken to be 2 m
 9 (assumed approximate height of the adult person). The above equation simplifies to:
 10

$$11 \quad C = \frac{Q}{2 \pi u \sigma_y \sigma_z} \left\{ 1 + \exp \left(-\frac{1}{2} \frac{(z+H)^2}{\sigma_z^2} \right) \right\} \quad (6-20)$$

12
 13 Where $z + H = 4$ m, and u (the average wind speed) is chosen to be 3.4 m/s.
 14

15 **6.3.2.5.4 Horizontal and Vertical Plume Dispersivity in Air.** Horizontal and vertical
 16 dispersivities of the plume in air are required to calculate air concentrations downwind from
 17 WMA C, to simulate the effect of dispersion due to wind flow over a horizontal 1-D pathway.
 18

19 EPA (2014) provides equations to calculate horizontal dispersion coefficient (σ_y) and vertical
 20 dispersion coefficient (σ_z) for dispersion calculations using the Gaussian plume model. In these
 21 equations, the dispersion coefficient is a function of the downwind distance, x , from a point
 22 source for different atmospheric turbulence classes under open-country conditions. These
 23 atmospheric turbulence classes are categorized according to the Pasquill classification
 24 (Pasquill 1961). This classification defines six stability classes named A, B, C, D, E, and F, with
 25 class A being the most turbulent and class F the most stable or least turbulent class. According
 26 to the wind speeds observed on the Hanford Site (Table 6-20), which usually range from 2.7 m/s
 27 (8.9 ft/s) during winter to 4 m/s (13.1 ft/s) during summer (monthly average), the most
 28 conservative (lowest dispersivity) Pasquill class for a moderate solar radiation above WMA C is
 29 Class C (i.e., "slightly unstable class"). The following equations are used to calculate the
 30 horizontal and vertical dispersion coefficient for Class C (EPA 2014):
 31

$$32 \quad \sigma_y = 0.11 x (1 + 0.0001x)^{-1/2} \quad (6-21)$$

$$33 \quad \sigma_z = 0.08 x (1 + 0.0002x)^{-1/2} \quad (6-22)$$

34
 35 where σ_y and σ_z are the horizontal and vertical dispersion coefficients (m) for Pasquill class C,
 36 and x is the downwind distance (m) from the point source.
 37

38 The dispersion coefficient estimates for air transport to the fenceline vary by the distance of the
 39 source (tank and ancillary equipment) from the fenceline using the above equation. The air
 40 pathway calculations are performed for each source term (tank and ancillary equipment)
 41 separately, where the distance to the PoCal at 100 m (328 ft) boundary is calculated based on the
 42 location of the source.
 43

RPP-ENV-58782, Rev. 0

Table 6-20. Wind Speed Observed Above the Hanford Site and Corresponding Pasquill Class for a Moderate Solar Radiation.

Season	Wind Speed*	Pasquill Class for a Moderate Solar Radiation
Winter	2.7 to 3.1 m/s	B
Summer	3.6 to 4 m/s	B-C
Summertime drainage winds	13 m/s	D

*See Section 3.1.2.4 for additional details.

Source: "The Estimation of the Dispersion of Windborne Material" (Pasquill 1961).

6.3.2.5.5 Radon Analysis. The modeling approach for calculating radon flux at the surface is slightly different than the approach for the other contaminants, because there is a different mechanism for emanation of radon from the waste into air. Radon-222 is produced from the alpha decay of ^{226}Ra in the waste. During the decay, by alpha recoil the produced ^{222}Rn atom (initially in the solid phase) has the potential to end up in either solid, liquid, or gas phase, with the amount in gas available for further diffusion to the ground surface. The fraction of ^{222}Rn in the gas phase over the total ^{222}Rn produced at any time is called the emanation coefficient, which is typically determined empirically for a given material. The emanation coefficient is highly variable from one material to another, and depends on a variety of specific features of the contaminated material, including the distribution of radium within the material particles, grain size and pore size distributions, and moisture content of the contaminated material ("A comprehensive review of radon emanation measurements for mineral, rock, soil, mill tailing and fly ash" [Sakoda et al. 2011]). Emanation coefficients have not been measured for residual wastes. For the purposes of this assessment, the residual wastes are assumed to have emanation properties comparable to soils. NCRP Report No. 103, "Control of Radon in Houses" has recommended a nominal emanation coefficient of about 0.2 for soils, and this value is adopted for this PA. The target emanation coefficient is implemented in the GoldSim[®] model as the fractional mass of radon produced in the residual waste that enters the gas phase.

A 1-D transport model is used to calculate diffusive flux of radon along with other volatile radionuclides. However, the radon flux analysis is conducted assuming there is no downward migration of the parent radionuclide ^{226}Ra . This assumption was made to keep the ^{226}Ra fixed in the residual waste, with a constant diffusion path for the duration of the analysis. The ^{222}Rn release rate from the ground surface is estimated using the diffusion equation (using Equation 6-16).

Radium-226 (half-life of 1,600 years) produces ^{222}Rn (half-life of 3.82 days) by radioactive decay. Radium-226 is produced by the radioactive decay of: ^{238}U (half-life of 4.47×10^9 years), ^{234}U (half-life of 2.45×10^5 years), ^{238}Pu (half-life of 87.7 years), and ^{230}Th (half-life of 7.54×10^4 years). Once the initial inventory of ^{226}Ra is depleted, it will be generated slowly, primarily from decay of ^{238}U and ^{234}U .

RPP-ENV-58782, Rev. 0

1 **6.3.2.6 Biotic Pathway.** In this section, an evaluation is presented of the potential for
2 burrowing animals or deep-rooting plants to penetrate deeply enough to contact the residual
3 waste left in tanks and ancillary equipment in its final closed configuration.
4

5 At closure, a modified RCRA Subtitle C barrier (Section 3.2.1.2.2) will be placed over the waste.
6 The upper layer of this cover system is intended to mimic natural surface conditions to the extent
7 possible. That is, natural vegetation will be planted on a soil layer intended to support growth of
8 a stable ecology system that is the same as the surrounding conditions. The ambient ecological
9 system is not totally pristine because colonization and agricultural practices have introduced
10 additional nonnative species that will likely remain at the Hanford Site. Ecological conditions at
11 the Hanford Site have been studied extensively since the start of Hanford Site operations, and
12 numerous documents that describe and quantify local conditions have been completed. The most
13 recent compilation (DOE/RL-2007-50, Central Plateau Ecological Risk Assessment Data
14 Package Report) describes recent information and includes copies of significant previous
15 summaries (e.g., DOE/RL-2001-54). The descriptions provided below are based on these and
16 other documents.
17

18 The Hanford Site is a shrub-steppe ecosystem that is dominated by a shrub overstory with a grass
19 understory. Because the climate is semi-arid, the dominant large shrub is big sagebrush
20 (*Artemisia tridentate*) and the main grasses are Sandberg's bluegrass (*Poa Sandbergii*) and
21 bluebunch wheatgrass (*Pseudoregneria spicata*). A ubiquitous nonnative species at the Hanford
22 Site is cheatgrass, which often makes up a large fraction of the grasses. Less abundant plant
23 species on the Central Plateau include threetip sagebrush, bitterbrush, gray rabbitbrush, spiny
24 Hopsage, Indian ricegrass, and prairie June grass. Altogether, over 100 species of plants have
25 been observed in the 200 Area on the Central Plateau. A survey of the 200 Area made prior to
26 its construction showed the presence of big sagebrush and an understory of which approximately
27 90% was a mix of cheatgrass and Sandberg's bluegrass (PNNL-14233). The remaining 10% of
28 the understory was a mix of cheatgrass and needle-and-thread grass.
29

30 Range fires can be expected to occur every few years. Observation has shown that regrowth
31 vegetation is initially dominated by nonnative species, particularly cheatgrass and, to a lesser
32 extent, Russian thistle. Native grasses and shrubs take longer to reestablish, particularly the big
33 sagebrush, which must regenerate from seed. However, repopulation with sagebrush and other
34 smaller shrubs such as gray rabbitbrush, which reestablishes itself more easily than big
35 sagebrush, eventually happens because these species are abundant in undisturbed areas that have
36 been burned many times.
37

38 A wide variety of mammals (about 40 species), birds (about 100 species), reptiles (about
39 10 species), and insects (hundreds) have been observed on the Central Plateau. Large mammals
40 include elk (*Cervus elaphus*) and mule deer (*Odocoileus hemionus*). Smaller species include
41 badgers (*Taxidea taxus*), coyotes (*Canis latrans*), blacktail jackrabbits (*Lepus californicus*),
42 Townsend ground squirrels (*Spermophilus townsendii*), pocket mice (*Perognathus parvus*), and
43 deer mice (*Peromyscus maniculatus*). Of these, the Great Basin pocket mice are the most
44 abundant. The mammal most likely to burrow in the soil is the badger, which can dig several
45 feet down in search of food (e.g., mice and squirrels).
46

RPP-ENV-58782, Rev. 0

Birds commonly found on the Central Plateau include passerine varieties, raptors, game birds, and nesting birds. Common passerine birds are starlings (*Sturnus vulgaris*), meadowlarks (*Sturnella neglecta*), black-billed magpies (*Pica pica*), and ravens (*Corvus corax*). Common raptors are the American kestrels (*Falco sparverius*) and redtailed hawks (*Buteo jamaicensis*). Game birds include the mourning dove (*Zenaida macroura*), California quail (*Callipepla californica*), and Chukar partridge (*Alectoris chukar*). Nesting birds include burrowing owls (*Athene cunicularia*), sage sparrows (*Amphispiza belli*), loggerhead shrikes (*Lanius ludovicianus*), and long-billed curlews (*Numenius americanus*).

Abundant reptiles include gopher snakes (*Pituophis melanoleucus*) and sideblotched lizards (*Uta stansburiana*). Other less abundant species include sagebrush lizards (*Sceloporus graciosus*), horned toads (*Phrynosoma douglassii*), western spadefoot toads (*Scaphiopus intermontana*), yellow-bellied racers (*Coluber constrictor*), Pacific rattlesnakes (*Crotalus viridis*), and striped whipsnakes (*Masticophis taeniatus*). Amphibians are not expected at the WMA C location. Common groups of insects include several species of darkling beetles, grasshoppers, butterflies, bees, and ants. Of these, the harvester ants, darkling beetles, solitary bees, and pocket gophers burrow below ground surface (WMP-20570, “Central Plateau Terrestrial Ecological Risk Assessment Data Quality Objectives Summary Report - Phase I”).

The most likely means of plant and animal contact with buried waste is root penetration and burrowing habits. A summary of site-specific and generic data quantifying penetration depths for biota at the Hanford Site and similar semi-arid conditions is provided in WMP-20570. Most studies of biota at the Hanford Site catalog biota populations, record surface expression of biota, and measure contaminant uptake. However, a few studies have been completed to quantify penetration depths [PNL-5247, “Rooting Depth and Distributions of Deep-Rooted Plants in the 200 Area Control Zone of the Hanford Site”; RHO-SA-211, “Invasion of radioactive waste burial sites by the Great Basin Pocket Mouse (*Perognathus parvus*)”; DOE/RL-2001-54]. Measured maximum penetration depths at the Hanford Site are summarized in Table 6-21.

Two primary observations were made. First, the maximum likely depth is about 3 m (10 ft) bgs for both plant and animal behavior. Second, the frequency of roots and burrow depths are heavily skewed towards the surface (<1.5 m [5 ft] bgs), with only a few percent of penetration events reaching maximum depth. Soil sampling across Gable Mountain Pond and B Pond, two dried high-volume liquid discharge sites (DOE/RL-2001-54), yielded a large assortment of invertebrates that constructed burrows within a foot of the surface (several feet and 0.6 to 0.9 cm [2 to 3 ft], respectively). Deeper burrowing depths were associated with the harvester ants and solitary bees. Among mammals, badger burrows have been observed on a few occasions. One burrow in particular was found 1.2 m (4 ft) below a soil barrier (WHC-SA-1252-S, “Mammal Occurrence and Exclusion at the Hanford Site”). Offsite, badger burrows as deep as 3 m (10 ft) have been reported (The Mammals of North America [Hall 1981]).

Given the limited number of data collected at the Hanford Site, it is useful to compare these data with data collected at other semi-arid sites in the western United States. A collection of other site data is provided in INEEL/EXT-01-00273, “Biological Data to Support Operable Unit 7-13/14 Modeling of Plant and Animal Intrusion at Buried Waste Sites,” and WMP-20570 (Appendix F). Badgers, squirrels, and mice are found at several sites with burrow penetration

RPP-ENV-58782, Rev. 0

depths similar to the Hanford Site (Figure 6-59). Plant data from other northern desert sites in Idaho and Wyoming include a common set of species (e.g., sagebrush and various grasses) with similar penetration depth profiles (Figure 6-59).

Table 6-21. Maximum Penetration Depths for Biota at the Hanford Site.

Species	Maximum Depth		Reference
	(cm)	(ft)	
Plants			
Antelope bitterbrush	300	9.8	PNL-5247, “Rooting Depth and Distributions of Deep-Rooted Plants in the 200 Area Control Zone of the Hanford Site”
Big sagebrush	200	6.6	PNL-5247
Spiny hopsage	195	6.5	PNL-5247
Russian thistle	172	5.6	PNL-5247
Mammals			
Great Basin pocket mouse	200	6.6	RHO-SA-211, “Invasion of radioactive waste burial sites by the Great Basin Pocket Mouse (<i>Perognathus parvus</i>)”
Soil Biota			
Harvester ants	270	8.8	PNL-2774, “Characterization of the Hanford 300 Area Burial Grounds Task IV - Biological Transport”

Source: WMP-20570, "Central Plateau Terrestrial Ecological Risk Assessment Data Quality Objectives Summary Report - Phase I," Table 2-1.

A modified RCRA Subtitle C barrier will be placed above WMA C that will be about 4.5 m (14.8 ft) in thickness (Figure 3-51). This cover will be placed above the interim compacted soil cover of ~0.6 m (2 ft). Thus, the minimum depth of intrusion needed to access the waste will be more than 5 m, which is below the observations of the biologically active zone, described above. The upper 0.9 m (3.0 ft) of the soil cover system is composed of an admixture of silt and gravels. This layer is intended to both reduce infiltration through the cover and enhance the resistance of the cover to burrowing animals and long-term wind erosion. In addition, an asphaltic concrete layer and asphaltic base course layer will be present at depth, which will further enhance resistance to burrowing animals and plants. Given the features of the surface barrier above WMA C, the likelihood of a biotic pathway to access the radionuclides from the waste is extremely small. As a result, the dose impact from this pathway is not considered in further analyses.

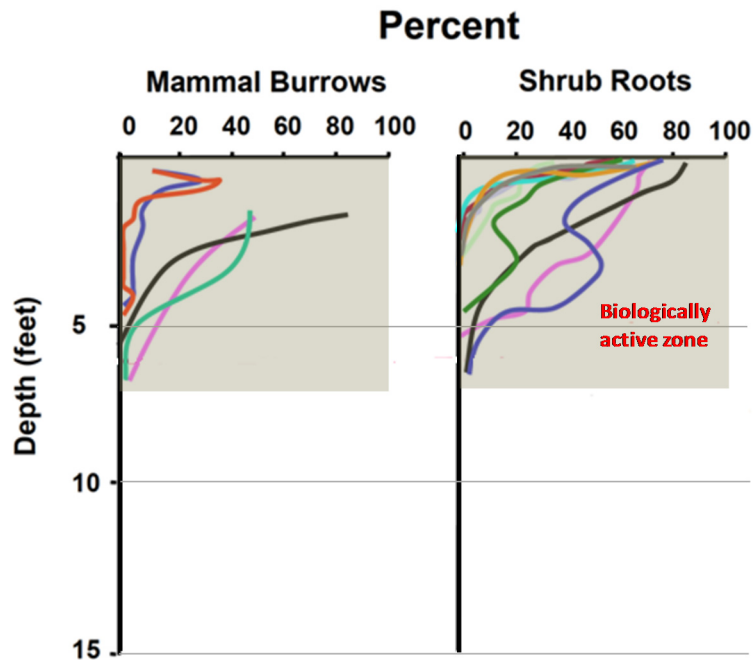
6.3.3 Exposure and Dose Analysis

The method for calculating doses from the radionuclide transport calculations discussed in previous sections is provided below. The dose calculation method for the all-pathway farmer scenario is discussed first, where contaminated groundwater is the pathway of contamination. This is followed by the air-pathway dose calculation methodology. Additional details are

RPP-ENV-58782, Rev. 0

presented in the supporting data package, RPP-ENV-58813, "Exposure Scenarios for Risk and Performance Assessments in Tank Farms at the Hanford Site, Washington."

Figure 6-59. Burrow and Root Density with Depth in Various Northwestern Semiarid Sites.



Adapted from Figure 2-3 of WMP-20570, "Central Plateau Terrestrial Ecological Risk Assessment Data Quality Objectives Summary Report – Phase I."

6.3.3.1 Groundwater Pathway Dose Analysis. For the all-pathways scenario, the individual who receives dose is a Representative Person who resides near the WMA C tank farm and draws contaminated water from a well downgradient of WMA C. The all-pathways Representative Person is assumed to use the water to drink, irrigate crops, and water livestock. The exposed Representative Person is assumed to receive dose by the exposure pathways shown in Figure 6-1.

Current DOE and ICRP guidance recommends the use of a Representative Person for describing the hypothetical member of the public for use in projecting future doses. The Representative Person is described as a person who is representative of the more highly exposed individuals in the population (see DOE O 458.1, ICRP 2006, and "ICRP Publication 103: The 2007 Recommendations of the International Commission on Radiological Protection" [ICRP 2007]). The concept of the Representative Person replaces the concept of an average member of the critical group used in older radiation protection guidance.

Internal doses to the Representative Person are calculated using the dose factors provided in DOE-STD-1196-2011, and external doses are calculated using dose factors in EPA-402-R-93-081. These dose factors represent effective dose coefficients calculated to a Reference Person in the manner of "ICRP Publication 72: Age-dependent Doses to the Members of the Public from Intake of Radionuclides - Part 5 Compilation of Ingestion and Inhalation Coefficients" (ICRP 1996). The Reference Person is a hypothetical aggregation of human (male

RPP-ENV-58782, Rev. 0

1 and female) physical and physiological characteristics arrived at by international consensus for
2 the purpose of standardizing radiation dose calculations (DOE-STD-1196-2011; “Environmental
3 Dosimetry” [Jannik 2014]).

4
5 The source of contamination for the all-pathways scenario is the portion of the inventory
6 transported by groundwater to the well location, and drawn through the well. As noted in
7 Section 1 (Table 1-2), dilution processes associated with drawing water through the well are not
8 taken into account in the PA, and the concentrations used for the all-pathways scenario
9 calculations are the maximum concentrations in groundwater at the PoCal. The contaminated
10 water is the only source of exposure. The exposed individual is assumed to use the water to
11 drink, shower, irrigate crops, and water livestock. Exposure occurs through the following
12 pathways:

- 13
- 14 • Ingestion of water
- 15 • Ingestion of fruits and vegetables grown on the farm
- 16 • Ingestion of beef raised on the farm
- 17 • Ingestion of milk from cows raised on fodder grown on the farm
- 18 • Ingestion of eggs from poultry fed with fodder grown on the farm
- 19 • Ingestion of poultry fed with fodder grown on the farm
- 20 • Ingestion of contaminated soil
- 21 • Inhalation of contaminated soil in the air
- 22 • Inhalation of water vapor
- 23 • External exposure to radiation.
- 24

25 Equations and calculation methodologies for each exposure pathway are summarized below.
26 They are described in detail in RPP-ENV-58813 and implemented in the system model using
27 GoldSim[®]. The scenario-dependent exposure parameters for the all-pathways Representative
28 Person scenario are summarized in Table 6-22. The element-specific factors (bioconcentration
29 factors [transfer coefficients]) are provided in Table 6-23, the radionuclide-specific shielding
30 factors are provided in Table 6-24, and the radionuclide-specific dose conversion factors are
31 provided in Table 6-25 (see RPP-ENV-58813 for additional details).

32
33 Age- and gender-weighted intake rates are generally developed for a Representative Person in
34 accordance with the recommendations described in DOE-STD-1196-2011. The 95th percentile
35 intake rates were obtained from EPA/600/R-090/052F, “Exposure Factors Handbook: 2011
36 Edition, National Center for Environmental Assessment,” based on available information. Even
37 though mean intake rates were available, the 95th percentile values from the underlying
38 distribution were chosen conservatively to maximize the likely exposure. Typically, the
39 95th percentile intake rates weighted by age and gender are calculated (Appendix P of
40 RPP-ENV-58813). The exceptions to this approach were the indoor inhalation rate (taken
41 directly from a reference source) and the soil ingestion rates (where simple age weighting is
42 performed for children and adults).

RPP-ENV-58782, Rev. 0

Table 6-22. Scenario-Dependent Exposure Parameters for the All-Pathways Reference Person Scenario. (2 sheets)

Parameter	Notation	Value	Unit	Reference
Soil ingestion rate	IR_s	108.6	mg/day	EPA/600/P-95/052F
Exposure frequency	EF	350	days/yr	OSWER Directive 9285.6-03
Water ingestion rate	IR_w	2.66	L/day	EPA/600/P-95/052F; EPA, 06/18/2015
Crop ingestion rate (includes homegrown fruits and vegetables)	IR_c	272.33	kg/yr	EPA/600/P-95/052F; EPA, 06/18/2015
Beef ingestion rate	IR_b	101.9	kg/yr	EPA/600/P-95/052F; EPA, 06/18/2015
Water ingestion rate for beef	$IR_{w,b}$	53	L/day	EPA, 06/18/2015
Soil ingestion rate for beef	$IR_{s,b}$	0.39	kg/day	EPA, 06/18/2015
Fodder ingestion rate for beef	$IR_{fodder,b}$	11.77	kg/day	EPA, 06/18/2015
Milk ingestion rate	IR_m	311.3	L/yr	DOE-STD-1196-2011; EPA/600/P-95/052F; EPA, 06/18/2015
Water ingestion rate for dairy cattle	$IR_{w,d}$	92	L/day	EPA, 06/18/2015
Soil ingestion rate for dairy cattle	$IR_{s,d}$	0.41	kg/day	EPA, 06/18/2015
Fodder ingestion rate for dairy cattle	$IR_{fodder,d}$	16.9	kg/day	EPA, 06/18/2015
Egg ingestion rate	IR_e	40.5	kg/yr	DOE-STD-1196-2011; EPA/600/P-95/052F; EPA, 06/18/2015
Poultry ingestion rate	IR_p	99.4	kg/yr	DOE-STD-1196-2011; EPA/600/P-95/052F; EPA, 06/18/2015
Water ingestion rate for poultry	$IR_{w,p}$	1	L/day	EPA, 06/18/2015
Soil ingestion rate for poultry	$IR_{s,p}$	0.022	kg/day	EPA, 06/18/2015
Fodder ingestion rate for poultry	$IR_{fodder,p}$	0.2	kg/day	EPA, 06/18/2015
Inhalation rate – water vapor	INH_w	20	m ³ /day	EPA/600/P-95/052F
Inhalation rate – indoors	INH_{in}	7,300	m ³ /yr	NCRP Report No. 129
Mass loading factor	M	6.66E-05	g/m ³	NCRP Report No. 129
Fraction of time spent indoors	t_{in}	0.4	unitless	EPA, 06/18/2015
Inhalation rate – outdoors	INH_{out}	12,775	m ³ /yr	NCRP Report No. 129
Fraction of time spent outdoors	t_{out}	0.486	unitless	EPA, 06/18/2015
Enrichment factor	E_f	0.7	unitless	NCRP Report No. 129
Transmission factor or shielding factor	ϵ	Isotope-specific 0.1 – 0.4	unitless	NCRP Report No. 129

RPP-ENV-58782, Rev. 0

Table 6-22. Scenario-Dependent Exposure Parameters for the All-Pathways Reference Person Scenario. (2 sheets)

Parameter	Notation	Value	Unit	Reference
Ratio of radionuclide concentrations in indoor versus outdoor air	I/O	0.3	unitless	NCRP Report No. 129
Andelman Volatilization Factor	K	0.5	L/m ³	EPA/540/R-92/003
Crop-soil bioconcentration factor through uptake	B _v	Element-specific	(pCi/kg fresh weight of crop)/ (pCi/kg dry weight of soil)	See Table 6-23 (for Vegetable, Fruit, and Grain)
Crop-soil bioconcentration factor from all resuspension/soil adhesion processes	B' _v	0.004	(pCi/kg fresh weight of crop)/ (pCi/kg dry weight of soil)	NCRP Report No. 129
Pasture-soil bioconcentration factor through uptake	B _p	Element-specific	(pCi/kg dry weight of fodder)/ (pCi/kg dry weight of soil)	See Table 6-23 (for Fodder and Grass)
Pasture-soil bioconcentration factor for all resuspension/soil adhesion processes	B' _p	0.1	(pCi/kg dry weight of fodder)/ (pCi/kg dry weight of soil)	NCRP Report No. 129
Fraction of locally-produced crops (fruits and vegetables) that is consumed	F _v	0.25	unitless	EPA/600/P-95/002Fa
Fraction of locally-produced animal products (beef, dairy, poultry, eggs) that is consumed	F _a	1	unitless	EPA/600/P-95/002Fa
Soil-water partition coefficient	K _d	Radionuclide-specific	mL/g	See Table 6-11
Soil volumetric water content – Theta W	θ _w	Soil-specific	mL water/cm ³ soil	—
Soil bulk density – Rho S	ρ _s	Soil-specific	g/cm ³	—
Unit conversion factor 1	CF	0.001	variable units	—
Unit conversion factor 2	CF ₁	1,000	g/kg	1,000 g = 1 kg

References:

DOE-STD-1196-2011, Derived Concentration Technical Standard.

EPA/540/R-92/003, Guidance for Data Useability in Risk Assessment (Part A) Final, Office of Research and Development.

EPA/600/P-95/002Fa, Exposure Factors Handbook Volume 1: General Factors.

NCRP Report No. 129, “Recommended Screening Limits for Contaminated Surface Soil and Review of Factors Relevant to Site-Specific Studies.”

OSWER Directive 9285.6-03, Risk Assessment Guidance for Superfund, Volume I: Human Health Evaluation Manual, Supplemental Guidance “Standard Default Exposure Factors.”

United States Environmental Protection Agency, Queried 06/18/2015, [Preliminary Remediation Goals for Radionuclides], <http://epa-prgs.ornl.gov/radionuclides/>.

Table 6-23. Bioconcentration Factors for the All-Pathways Reference Person Scenario. (2 sheets)

Element	Bioconcentration Factors					
	Vegetables, Fruit, and Grain (B _v)	Fodder and Grass (B _p)	Milk (BCF _{milk})	Beef (BCF _{beef})	Poultry (BCF _{poultry})	Egg (BCF _{egg})
	(pCi/kg fresh wgt of crop)/ (pCi/kg dry wgt of soil)	(pCi/kg dry wgt of fodder)/ (pCi/kg dry wgt of soil)	(day/L)	(day/kg)	(day/kg)	(day/kg)
Ac	1.00E-03 ^a	4.00E-03 ^a	2.00E-06 ^a	2.00E-05 ^a	4.00E-03 ^b	2.00E-03 ^b
Am	1.00E-03 ^a	4.00E-03 ^a	2.00E-06 ^a	5.00E-05 ^a	6.00E-03 ^b	9.00E-03 ^b
C	7.00E-01 ^b	7.00E-01 ^b	1.05E-02 ^c	4.89E-02 ^c	4.16E+00 ^c	3.12E+00 ^c
Cd	5.00E-01 ^a	1.00E+00 ^a	2.00E-03 ^a	1.00E-03 ^a	1.70E+00 ^d	1.00E-01 ^b
Cm	1.00E-03 ^a	4.00E-03 ^a	2.00E-06 ^a	2.00E-05 ^a	4.00E-03 ^b	2.00E-03 ^b
Co	8.00E-02 ^a	2.00E+00 ^a	2.00E-03 ^a	3.00E-02 ^a	9.70E-01 ^d	3.30E-02 ^d
Cs	4.00E-02 ^a	2.00E-01 ^a	1.00E-02 ^a	5.00E-02 ^a	2.70E+00 ^d	4.00E-01 ^d
Eu	2.00E-03 ^a	5.00E-02 ^a	6.00E-05 ^a	2.00E-03 ^a	4.00E-03 ^b	7.00E-03 ^b
H	2.86E+01 ^c	2.86E+01 ^c	3.36E+01 ^c	3.36E+01 ^c	3.36E+01 ^c	3.36E+01 ^c
I	2.00E-02 ^a	1.00E-01 ^a	1.00E-02 ^a	4.00E-02 ^a	8.70E-03 ^d	2.40E+00 ^d
Nb	1.00E-02 ^a	1.00E-01 ^a	2.00E-06 ^a	1.00E-06 ^a	3.00E-04 ^d	1.00E-03 ^d
Ni	5.00E-02 ^a	1.00E+00 ^a	2.00E-02 ^a	5.00E-03 ^a	1.00E-03 ^b	1.00E-01 ^b
Np	2.00E-02 ^a	1.00E-01 ^a	1.00E-05 ^a	1.00E-03 ^a	4.00E-03 ^b	2.00E-03 ^b
Pa	1.00E-02 ^a	5.00E-02 ^a	5.00E-06 ^a	5.00E-06 ^a	4.00E-03 ^b	2.00E-03 ^b
Pu	1.00E-03 ^a	1.00E-03 ^a	1.00E-06 ^a	1.00E-04 ^a	3.00E-03 ^b	8.00E-03 ^b
Ra	4.00E-02 ^a	2.00E-01 ^a	1.00E-03 ^a	1.00E-03 ^a	3.00E-02 ^b	2.00E-05 ^b
Rn	0.00E+00 ^e	0.00E+00 ^e	0.00E+00 ^e	0.00E+00 ^e	0.00E+00 ^e	0.00E+00 ^e
Se	1.00E-01 ^a	5.00E-01 ^a	1.00E-02 ^a	1.00E-01 ^a	9.70E+00 ^d	1.60E+01 ^d

Table 6-23. Bioconcentration Factors for the All-Pathways Reference Person Scenario. (2 sheets)

Element	Bioconcentration Factors					
	Vegetables, Fruit, and Grain (B _v)	Fodder and Grass (B _p)	Milk (BCF _{milk})	Beef (BCF _{beef})	Poultry (BCF _{poultry})	Egg (BCF _{egg})
	(pCi/kg fresh wgt of crop)/ (pCi/kg dry wgt of soil)	(pCi/kg dry wgt of fodder)/ (pCi/kg dry wgt of soil)	(day/L)	(day/kg)	(day/kg)	(day/kg)
Sm	2.00E-03 ^a	5.00E-02 ^a	6.00E-05 ^a	2.00E-03 ^a	4.00E-03 ^b	7.00E-03 ^b
Sn	3.00E-01 ^a	1.00E+00 ^a	1.00E-03 ^a	1.00E-02 ^a	2.00E-01 ^b	8.00E-01 ^b
Sr	3.00E-01 ^a	4.00E+00 ^a	2.00E-03 ^a	1.00E-02 ^a	2.00E-02 ^d	3.50E-01 ^d
Tc	5.00E+00 ^a	4.00E+01 ^a	1.00E-03 ^a	1.00E-04 ^a	3.00E-02 ^b	3.00E+00 ^b
Th	1.00E-03 ^a	1.00E-03 ^a	5.00E-06 ^a	1.00E-04 ^a	4.00E-03 ^b	2.00E-03 ^b
U	2.00E-03 ^a	1.00E-01 ^a	4.00E-04 ^a	8.00E-04 ^a	1.20E+00 ^b	9.90E-01 ^b
Zr	1.00E-03 ^a	5.00E-03 ^a	6.00E-07 ^a	1.00E-06 ^a	6.00E-05 ^d	2.00E-04 ^d

^aNCRP Report No. 129, "Recommended Screening Limits for Contaminated Surface Soil and Review of Factors Relevant to Site-Specific Studies," Appendix D.

^bNUREG/CR-5512, Residential Radioactive Contamination From Decommissioning, Vol. 1, Technical Basis for Translating Contamination Levels to Annual Total Effective Dose Equivalent, Final Report.

^cThe units are dimensionless. Hydrogen values are calculated from Equations 6-26b and 6-28b using equilibrium model for tritium. For carbon, the value is based on derivation of equilibrium model for ¹⁴C presented in Appendix O of RPP-ENV-58813, "Exposure Scenarios for Risk and Performance Assessments in Tank Farms at the Hanford Site, Washington."

^d"Technical Reports Series No. 472, Handbook of Parameter Values for the Prediction of Radionuclide Transfer in Terrestrial and Freshwater Environments" (IAEA 2010), Tables 34 and 35.

^eNot applicable (gas).

RPP-ENV-58782, Rev. 0

Table 6-24. Radionuclide-Specific Shielding Factors.

Radionuclide	Shielding Factor (ϵ) (unitless)	Radionuclide	Shielding Factor (ϵ) (unitless)
^{227}Ac	0.4	^{240}Pu	0.4
^{241}Am	0.2	^{241}Pu	0.4
^{243}Am	0.3	^{242}Pu	0.1
^{14}C	0.4	^{226}Ra	0.4
$^{113\text{m}}\text{Cd}$	0.3	^{228}Ra	0.4
^{243}Cm	0.4	^{222}Rn	0.4
^{244}Cm	0.1	^{79}Se	0.1
^{60}Co	0.4	^{151}Sm	0.1
^{137}Cs	0.3	^{126}Sn	0.3
^{152}Eu	0.4	^{90}Sr	0.3
^{154}Eu	0.4	^{99}Tc	0.2
^{155}Eu	0.3	^{229}Th	0.4
^3H	0.4	^{230}Th	0.3
^{129}I	0.1	^{232}Th	0.2
$^{93\text{m}}\text{Nb}$	0.1	^{232}U	0.3
^{59}Ni	0.4	^{233}U	0.4
^{63}Ni	0.4	^{234}U	0.2
^{237}Np	0.3	^{235}U	0.4
^{231}Pa	0.4	^{236}U	0.1
^{210}Pb	0.1	^{238}U	0.1
^{238}Pu	0.1	^{93}Zr	0.4
^{239}Pu	0.3	—	—

6.3.3.1.1 Equations to Calculate Soil Concentrations from Irrigation with Contaminated Water. When contaminated water is applied to soil, the contaminants are retained by the soil by two mechanisms: 1) sorption onto soil particles and 2) dissolved contaminants held in the water content in the soil. The following equation is used to calculate the concentration of contaminant sorbed on soil particles:

$$C_s = C_w \times K_d \times CF \quad (6-23)$$

RPP-ENV-58782, Rev. 0

Where:

- C_s = radionuclide concentration in soil (pCi/g)
- C_w = radionuclide concentration in irrigation water (pCi/L)
- K_d = soil-water partition coefficient (mL/g)
- CF = unit conversion factor of 0.001 (L/mL).

The following equation is used to calculate total radionuclide concentration in soil (i.e., sorbed plus dissolved plus vapor):

$$C_{stot} = C_w \times \left(K_d + \frac{\theta_w + \theta_a \times H'}{\rho_s} \right) \approx C_w \times \left(K_d + \frac{\theta_w}{\rho_s} \right) \times CF \quad (6-24)$$

Where:

- C_{stot} = total radionuclide concentration in surface soil layer (pCi/g)
- θ_w = soil volumetric water content ([mL water]/[cm³ soil])
- θ_a = air-filled soil porosity (unitless)
- H' = dimensionless Henry's Law constant (unitless)
- ρ_s = soil dry bulk density (g/cm³)
- CF = unit conversion factor of 0.001 (L/mL).

The volatile radionuclide inventory in contaminated water used for irrigation is likely to be negligibly small, so $\theta_a \times H'$ can be ignored. The above equations are used whenever C_s and C_{stot} are used in the remainder of this section.

6.3.3.1.2 Equations to Calculate Tritium Concentrations in Crops (Fruits, Vegetables and Livestock Fodder). The tritium concentration in home-grown crops (fruits and vegetables) and livestock fodder is calculated separately using an equilibrium model. The crop and livestock fodder become contaminated as a result of root uptake of radionuclides in the contaminated soil and groundwater. A summary of the parameters used to calculate tritium in crops is provided in Table 6-26. The following equation is used to calculate tritium concentrations ($C_{c,t}$; pCi/g fresh weight) in the crop using the equilibrium model:

$$C_{c,t} = \frac{C_w}{\rho_w} \times \frac{MW_{H2O}}{2 \times AW_H} \times F_{H,C} \times \frac{I}{I+P} \times F_{C,I} \times CF \quad (6-25)$$

The first term in the right-hand side of the equation expresses the water concentration in the unit of pCi/kg water. The second term is the ratio of the molecular weights of water and the atomic weight of hydrogen. This term is used to convert the hydrogen fractions ($F_{H,c}$) in the crop to water fractions. Since the hydrogen fractions include organically bound hydrogen as well as water, the crop concentration is a bounding value. The third term, which contains the total irrigation water amount (I) and total precipitation amount (P) during the irrigation period, adjusts the calculated concentration for the presence of uncontaminated water in the growing environment. The time-integration factor, $F_{C,I}$, is the factor that results from the time integral of the dose rate for tritium over the full year. For leafy vegetables, this factor value equals to 1. It is assumed that $F_{C,I} = 1$ for all crop types, as it would lead to a higher dose. The CF is the unit

RPP-ENV-58782, Rev. 0

conversion factor of 0.001 (kg/g). Using the parameter values given in Table 6-26, the tritium concentration in crops is calculated as:

$$C_{c,t} = 8.35 \times 10^{-4} \times C_w \quad (6-26a)$$

In the above equation the first term has units of liters of water per unit weight of crop. The above equation can be formulated in terms of C_{stot} instead of C_w by using the relationship presented in Equation 6-24. Considering soil K_d of 0 mL/g for tritium, soil dry bulk density of 2.05 g/cm³ (Hanford H1 unit; Table 6-8), and soil moisture content of 0.06 (typical value), Equation 6-26a can be written as:

$$C_{c,t} = 28.56 \left(\frac{g_{soil}}{g_{crop}} \right) \times C_{stot} \quad (6-26b)$$

6.3.3.1.3 Equations to Calculate Tritium Concentrations in Animal Products (Beef, Milk, Poultry and Eggs). The tritium concentration in animal products (C_a) is also calculated separately using an equilibrium model. A summary of the parameters used to calculate tritium in animal products is provided in Table 6-27. The following equation is used to calculate tritium concentrations in animal products (pCi/g) using the equilibrium model given as:

$$C_{a,t} = \frac{C_w}{\rho_w} \times \frac{MW_{H2O}}{2 \times AW_H} \times F_{H,A} \times \frac{M_{W,C}}{M_{W,T}} \times F_{A,I} \times CF \quad (6-27)$$

The first two terms in this equilibrium model have the same functions as that in the model for calculating the tritium concentration in crops. The ratio of contaminated water mass ingested per day to total mass of water ingested per day is closer to 1.0 in the irrigation cases because the drinking water for the animals in the irrigated areas is most likely to be contaminated. Therefore, it is assumed that all the water ingested by the animal is contaminated and, subsequently, the ratio of contaminated water mass ingested per day to total mass of water ingested per day is equal to 1. The time-integration factor is the same as shown above for tritium concentration in crops. The CF is the unit conversion factor of 0.001 (kg/g). Using the parameter values given in Table 6-27, the tritium concentration in animal products is calculated as

$$C_{a,t} = 9.83 \times 10^{-4} \times C_w \quad (6-28a)$$

In the above equation the first term has units of Liters of water per unit weight of animal products. The above equation can be formulated in terms of C_{stot} instead of C_w by using the relationship presented in Equation 6-24. Considering soil K_d of 0 mL/g for tritium, soil dry bulk density of 2.05 g/cm³ (Hanford H1 unit; Table 6-8), and soil moisture content of 0.06 (typical value), Equation 6-28a can be written as:

$$C_{c,t} = 33.62 \left(\frac{g_{soil}}{g_{animal\ product}} \right) \times C_{stot} \quad (6-28b)$$

Table 6-25. Radionuclide-Specific Dose Conversion Factors. (3 sheets)

Radionuclide	Inhalation (mrem/pCi)		Ingestion (mrem/pCi) (DCF _{ing}) ^b	External Exposure (Groundwater Pathway) (mrem/yr)/(pCi/g) (DCF _{ext}) ^c	External Exposure (Air Pathway) (mrem/yr)/(pCi/m ²) (DCF _{ext} for air pathway) ^d	Air Submersion (mrem/yr)/ (pCi/m ³) (DCF _{im}) ^e
	(DCF _{inh}) ^a	Lung Absorption Type ^a				
²²⁷ Ac	5.96E-01	F	1.45E-03	1.57E+00	4.52E-05	3.68E-03
²⁴¹ Am	1.56E-01	M	8.81E-04	3.41E-02	3.21E-06	7.85E-05
²⁴³ Am	1.54E-01	M	8.73E-04	6.98E-01	2.53E-05	1.08E-03
¹⁴ C	8.21E-06	M	2.34E-06	1.05E-05	1.88E-09	3.04E-07
^{113m} Cd	4.33E-04	F	9.51E-05	5.06E-04	3.07E-08	1.08E-05
²⁴³ Cm	1.20E-01	M	6.66E-04	4.55E-01	1.46E-05	6.22E-04
²⁴⁴ Cm	1.01E-01	M	5.59E-04	9.83E-05	1.03E-07	4.67E-07
⁶⁰ Co	4.14E-05	M	2.03E-05	1.27E+01	2.74E-04	1.39E-02
¹³⁷ Cs	1.70E-05	F	4.92E-05	2.66E+00	6.46E-05	2.98E-03
¹⁵² Eu	3.67E-04	F	6.44E-06	5.47E+00	1.28E-04	6.28E-03
¹⁵⁴ Eu	4.26E-04	F	9.66E-06	5.99E+00	1.39E-04	6.75E-03
¹⁵⁵ Eu	5.11E-05	F	1.67E-06	1.42E-01	6.89E-06	2.53E-04
³ H	1.97E-07	M	7.77E-08	0.00E+00	0.00E+00	0.00E+00
¹²⁹ I	1.50E-04	F	4.48E-04	1.01E-02	3.01E-06	3.34E-05
^{93m} Nb	2.26E-06	M	6.59E-07	8.12E-05	1.10E-07	3.55E-07
⁵⁹ Ni	5.48E-07	M	2.95E-07	0.00E+00	0.00E+00	8.08E-08
⁶³ Ni	2.01E-06	M	7.33E-07	0.00E+00	0.00E+00	0.00E+00
²³⁷ Np	8.51E-02	M	4.63E-04	8.57E-01	2.61E-05	1.18E-03
²³¹ Pa	8.77E-01	F	2.07E-03	1.49E-01	4.75E-06	1.69E-04
²¹⁰ Pb	4.48E-03	M	3.77E-03	4.76E-03	4.13E-07	3.57E-05

Table 6-25. Radionuclide-Specific Dose Conversion Factors. (3 sheets)

Radionuclide	Inhalation (mrem/pCi)		Ingestion (mrem/pCi) (DCF _{ing}) ^b	External Exposure (Groundwater Pathway) (mrem/yr)/(pCi/g) (DCF _{ext}) ^c	External Exposure (Air Pathway) (mrem/yr)/(pCi/m ²) (DCF _{ext} for air pathway) ^d	Air Submersion (mrem/yr)/ (pCi/m ³) (DCF _{im}) ^e
	(DCF _{inh}) ^a	Lung Absorption Type ^a				
²³⁸ Pu	1.72E-01	M	9.73E-04	1.18E-04	9.79E-08	3.92E-07
²³⁹ Pu	1.86E-01	M	1.07E-03	2.30E-04	4.29E-08	4.40E-07
²⁴⁰ Pu	1.86E-01	M	1.07E-03	1.14E-04	9.38E-08	3.84E-07
²⁴¹ Pu	3.31E-03	M	1.93E-05	4.61E-06	2.25E-10	7.18E-09
²⁴² Pu	1.77E-01	M	1.01E-03	9.99E-05	7.79E-08	7.51E-07
²²⁶ Ra	1.41E-02	M	1.68E-03	2.48E-02	1.94E-04	9.77E-03
²²⁸ Ra	1.14E-02	M	5.92E-03	1.26E+01	2.73E-04	1.47E-02
²²² Rn	0.00E+00		0.00E+00	8.70E+00	0.00E+00	0.00E+00
⁷⁹ Se	6.22E-06	F	1.73E-05	1.45E-05	2.42E-09	3.56E-07
¹⁵¹ Sm	3.64E-05	F	5.00E-07	7.68E-07	5.88E-10	3.09E-09
¹²⁶ Sn	6.14E-04	S	2.36E-05	9.25E+00	2.29E-04	1.05E-02
⁹⁰ Sr	1.45E-04	M	1.33E-04	1.92E-02	6.55E-07	1.04E-04
⁹⁹ Tc	1.64E-05	M	3.33E-06	9.80E-05	9.11E-09	3.36E-06
²²⁹ Th	2.79E-01	S	2.25E-03	1.24E+00	3.70E-05	1.58E-03
²³⁰ Th	5.44E-02	S	9.36E-04	9.43E-04	8.76E-08	1.77E-06
²³² Th	9.47E-02	S	1.03E-03	4.07E-04	6.44E-08	9.22E-07
²³² U	3.19E-02	M	1.49E-03	7.96E+00	1.64E-04	1.00E-02
²³³ U	1.44E-02	M	2.23E-04	1.09E-03	8.36E-08	1.24E-06
²³⁴ U	1.41E-02	M	2.15E-04	3.13E-04	8.74E-08	7.17E-07
²³⁵ U	1.25E-02	M	2.03E-04	5.91E-01	1.94E-05	8.56E-04

Table 6-25. Radionuclide-Specific Dose Conversion Factors. (3 sheets)

Radionuclide	Inhalation (mrem/pCi)		Ingestion (mrem/pCi) (DCF _{ing}) ^b	External Exposure (Groundwater Pathway) (mrem/yr)/(pCi/g) (DCF _{ext}) ^c	External Exposure (Air Pathway) (mrem/yr)/(pCi/m ²) (DCF _{ext} for air pathway) ^d	Air Submersion (mrem/yr)/ (pCi/m ³) (DCF _{im}) ^e
	(DCF _{inh}) ^a	Lung Absorption Type ^a				
²³⁶ U	1.29E-02	M	2.02E-04	1.68E-04	7.59E-08	4.41E-07
²³⁸ U	1.16E-02	M	1.94E-04	8.89E-02	2.82E-06	2.04E-04
⁹³ Zr	3.34E-05	M	3.70E-06	0.00E+00	0.00E+00	7.53E-11

^aDOE-STD-1196-2011, Derived Concentration Technical Standard, Table A-2: Effective Dose Coefficients from Inhaled Air. The lung absorption type for particulate aerosols is taken from Table 4: Classification of Absorption Types for Particulates, by using recommended default absorption type, where F is fast, M is moderate, and S is slow absorption as defined in “ICRP Publication 66: Human Respiratory Tract Model for Radiological Protection” (ICRP 1994). Where default values are not indicated, then the highest value is selected among the absorption types for a given radionuclide.

^bDOE-STD-1196-2011, Table A-1: Effective Dose Coefficients for Ingested Water.

^cEPA-402-R-93-081, Federal Guidance Report No. 12, External Exposure to Radionuclides in Air, Water, and Soil, Table III.7. Dose Coefficients for Exposure to Soil Contaminated to an Infinite Depth; modified to include effects of progeny.

^dEPA-402-R-93-081, Table III.3. Dose Coefficients for Exposure to Contaminated Ground Surface; modified to include effects of progeny.

^eDOE-STD-1196-2011, Table A-3: Effective Dose Rate Coefficients from Air Submersion; modified to include effects of progeny.

DCF = dose conversion factor

RPP-ENV-58782, Rev. 0

Table 6-26. Parameters Used to Calculate the Tritium Concentration in Crops.

Parameter	Definition	Units	Input Value	Reference
$C_{c,t}$	Tritium concentration in crop	pCi/g fresh weight	Calculated	—
C_w	Tritium concentration in the irrigation water	pCi/L	Calculated	—
ρ_w	Density of water	kg/L	1	EPA/540/R-96/018
MW_{H_2O}	Molecular weight of water	g	18.016	Calculated
AW_H	Atomic weight of hydrogen	g	1.008	Calculated
$F_{H,C}$	Mass fraction of hydrogen in crops (vegetable and fruit) that are locally produced	unitless	0.1	NUREG/CR-5512
$F_{C,I}$	Factor from time integral of tritium dose rate	unitless	1	NUREG/CR-5512
I	Total irrigation water applied during the irrigation period	cm	82.3	HNF-SD-WM-TI-707
P	Total precipitation during the irrigation period	cm	5.766	HNF-SD-WM-TI-707
CF	Unit conversion factor	kg/g	0.001	1 kg = 1,000 g

References:

EPA/540/R-96/018, Soil Screening Guidance: User's Guide, Second Edition, Publication 9355.4-23.

HNF-SD-WM-TI-707, "Exposure Scenarios and Unit Factors for the Hanford Tank Waste Performance Assessment."

NUREG/CR-5512, Residual Radioactive Contamination From Decommissioning, Vol. 1, Technical Basis for Translating Contamination Levels to Annual Total Effective Dose Equivalent, Final Report.

6.3.3.1.4 Dose Equations for the All-Pathways Representative Person. The dose equations that are presented in this section are for the all-pathways Representative Person. The equations are given for calculation of dose from a single radionuclide. To calculate total effective dose, it is necessary to sum the doses over all radionuclides at a particular time.

Age- and gender-weighted intake rates were developed for the all-pathways Representative Person in accordance with the recommendations described in DOE-STD-1196-2011 as described in RPP-ENV-58813. Table 6-28 presents a summary of the age- and gender-weighted intake rates used for the all-pathways Reference Person scenario.

6.3.3.1.5 Ingestion of Water. The following equation is used to calculate dose from ingestion of water (RPP-ENV-58813):

$$D_w = C_w \times IR_w \times EF \times DCF_{ing} \quad (6-29)$$

Where:

D_w = dose from drinking contaminated water (mrem/yr)
 C_w = radionuclide concentration in water (pCi/L)

RPP-ENV-58782, Rev. 0

- IR_w = water ingestion rate (L/day)
 EF = exposure frequency (days/yr)
 DCF_{ing} = ingestion dose conversion factor (mrem/pCi).

Table 6-27. Parameters for Tritium Concentration Calculation in Animal Products.

Parameter	Definition	Units	Input Value	Reference
$C_{a,t}$	Radionuclide concentration in animal products	pCi/g	Calculated	—
C_w	Radionuclide concentration in the irrigation water	pCi/L	Calculated	—
$F_{H,A}$	Mass fraction of hydrogen in animal products that are locally produced	unitless	0.11	NUREG/CR-5512
$F_{A,I}$	Factor from time integral of tritium dose rate	unitless	1	NUREG/CR-5512
$M_{W,C}$	Mass of contaminated water ingested daily by the animal	kg/day	$M_{W,C} = 1 M_{W,T}$	Assumption
$M_{W,T}$	Total mass of contaminated water ingested daily by the animal	kg/day		
CF	Unit conversion factor	kg/g	0.001	1 kg = 1,000 g

Reference: NUREG/CR-5512, Residual Radioactive Contamination From Decommissioning, Vol. 1, Technical Basis for Translating Contamination Levels to Annual Total Effective Dose Equivalent, Final Report.

6.3.3.1.6 Ingestion of Homegrown Crops (Fruits and Vegetables). The following equations are used to calculate the concentration of contaminant in the crop (homegrown fruits and vegetables) and the dose from consumption of the crop (NCRP Report No. 129, “Recommended Screening Limits for Contaminated Surface Soil and Review of Factors Relevant to Site-Specific Factors”). The following equation is used to calculate the concentration of contaminant in the crop:

$$C_c = C_{stot} \times (B_v + B'_v) \quad (6-30)$$

Where:

- C_c = radionuclide concentration in crop (pCi/g)
 C_{stot} = total radionuclide concentration in surface soil layer (pCi/g)
 B_v = crop-soil bioconcentration factor through uptake $\left(\frac{\left(\frac{pCi}{kg \text{ fresh weight of crop}} \right)}{\left(\frac{pCi}{kg \text{ dry weight of soil}} \right)} \right)$
 B'_v = crop-soil bioconcentration factor representing all resuspension-soil adhesion processes $\left(\frac{\left(\frac{pCi}{kg \text{ fresh weight of crop}} \right)}{\left(\frac{pCi}{kg \text{ dry weight of soil}} \right)} \right)$.

Table 6-28. Summary of Intake Rates for All-Pathways Reference Person.

Intake Parameter	Notation	Units	Value	Reference
Inhalation rate – indoor	INH _{in}	m ³ /yr	7,300	NCRP Report No. 129
Soil ingestion rate*	IR _s	mg/day	108.6	EPA/540/R-92/003
Drinking water ingestion rate*	IR _w	L/day	2.66	EPA/600/R-090/052F
Crop ingestion rate (includes fruits and vegetables)*	IR _c	kg/year	272.3	
Beef ingestion rate*	IR _b	kg/year	101.9	
Milk ingestion rate*	IR _m	L/year	311.3	
Egg ingestion rate*	IR _e	kg/year	40.5	
Poultry ingestion rate*	IR _p	kg/year	99.4	

*See Appendix P of RPP-ENV-58813 for more details regarding the derivation of intake rates for a Reference Person. The intake rates are generally calculated based on age- and gender-weighted fraction provided in DOE-STD-1196-2011, Derived Concentration Technical Standard. Where information regarding mean and 95th percentile intake rates is available, the 95th percentile value is chosen and then weighted by age and gender. For soil ingestion rate, the rate published for children and adults is used with simple age weighting.

References:
EPA/540/R-92/003, Risk Assessment Guidance for Superfund: Volume I – Human Health Evaluation Manual (Part B, Development of Risk-based Preliminary Remediation Goals) Interim, Publication 9285.7-01B.
EPA/600/R-090/052F, Exposure Factors Handbook: 2011 Edition, National Center for Environmental Assessment.
NCRP Report No. 129, “Recommended Screening Limits for Contaminated Surface Soil and Review of Factors Relevant to Site-Specific Studies.”
OSWER Directive 9200.1-120, “Human Health Evaluation Manual, Supplemental Guidance: Update of Standard Default Exposure Factors.”

The following equation is used to calculate dose from consumption of homegrown fruits and vegetables:

$$D_c = C_c \times IR_c \times F_v \times CF_1 \times DCF_{ing} \tag{6-31}$$

Where:

- D_c = dose from consumption of crop (homegrown fruits and vegetables) (mrem/yr)
- IR_c = crop ingestion rate (kg/yr)
- F_v = fraction of homegrown fruits and vegetables consumed (unitless)
- CF_1 = unit conversion factor of 1,000 (g/kg)
- DCF_{ing} = ingestion dose conversion factor (mrem/pCi).

6.3.3.1.7 Ingestion of Farm-Raised Beef. The following equations are used to calculate the concentration of contaminant in livestock fodder, the concentration of contaminant in beef, and the dose from consumption of the beef (NCRP Report No. 129).

RPP-ENV-58782, Rev. 0

The equation used to calculate the concentration of contaminant in livestock fodder is given by²

$$C_{fodder} = C_{stot} \times (B_p \times B'_p) \quad (6-32)$$

Where:

C_{fodder} = radionuclide concentration in livestock fodder (pCi/g)

C_{stot} = total radionuclide concentration in surface soil layer (pCi/g)

B_p = pasture-soil bioconcentration factor through uptake $\left(\frac{\left(\frac{pCi}{kg \text{ dry weight of fodder}} \right)}{\left(\frac{pCi}{kg \text{ dry weight of soil}} \right)} \right)$

B'_p = pasture-soil bioconcentration factor for all resuspension processes $\left(\frac{\left(\frac{pCi}{kg \text{ dry weight of fodder}} \right)}{\left(\frac{pCi}{kg \text{ dry weight of soil}} \right)} \right)$.

The following equation is used to calculate the concentration of contaminant in beef resulting from consumption of contaminated water, contaminated fodder, and contaminated soil:

$$C_b = (C_w \times IR_{w,b} + C_{fodder} \times IR_{fodder,b} \times CF_1 + C_{stot} \times IR_{s,b} \times CF_1) \times BCF_{beef} \quad (6-33)$$

Where:

C_b = radionuclide concentration in beef (pCi/kg)

C_w = radionuclide concentration in water (pCi/L)

$IR_{w,b}$ = ingestion rate of water for beef (L/day)

C_{fodder} = radionuclide concentration in livestock fodder (pCi/g)

$IR_{fodder,b}$ = ingestion rate of fodder for beef (kg/day)

CF_1 = unit conversion factor of 1,000 (g/kg)

C_{stot} = total radionuclide concentration in surface soil layer (pCi/g)

$IR_{s,b}$ = ingestion rate of soil for beef (kg/day)

BCF_{beef} = bioconcentration factor of radionuclides in beef (day/kg).

The equation used to calculate the dose from ingestion of farm-raised beef is given by

$$D_b = C_b \times IR_b \times F_a \times DCF_{ing} \quad (6-34)$$

Where:

D_b = dose from ingestion of beef (mrem/yr)

IR_b = beef ingestion rate (kg/yr)

F_a = fraction of farm-raised beef that is consumed (unitless)

DCF_{ing} = ingestion dose conversion factor (mrem/pCi).

² This equation is used for all food chain pathways that include consumption of livestock fodder.

RPP-ENV-58782, Rev. 0

6.3.3.1.8 Ingestion of Milk. This section describes the equations used to calculate the concentration of contaminant in milk and the dose from consumption of milk.

The following equation is used to calculate the concentration of contaminant in milk resulting from consumption of contaminated water, contaminated fodder, and contaminated soil by the dairy animal:

$$C_m = (C_w \times IR_{w,d} + C_{fodder} \times IR_{fodder,d} \times CF_1 + C_{stot} \times IR_{s,d} \times CF_1) \times BCF_{milk} \quad (6-35)$$

Where:

C_m	= radionuclide concentration in milk (pCi/L)
C_w	= radionuclide concentration in water (pCi/L)
$IR_{w,d}$	= ingestion rate of water by dairy cattle (L/day)
C_{fodder}	= radionuclide concentration in livestock fodder (pCi/g)
$IR_{fodder,d}$	= ingestion rate of fodder by dairy cattle (kg/day)
CF_1	= unit conversion factor of 1,000 (g/kg)
C_{stot}	= total radionuclide concentration in surface soil layer (pCi/g)
$IR_{s,d}$	= ingestion rate of soil by dairy cattle (kg/day)
BCF_{milk}	= bioconcentration factor of radionuclides in milk (day/L).

The equation used to calculate the dose from ingestion of milk is given by

$$D_m = C_m \times IR_m \times F_a \times DCF_{ing} \quad (6-36)$$

Where:

D_m	= dose from ingestion of milk (mrem/yr)
IR_m	= milk ingestion rate (L/yr)
F_a	= fraction of locally-produced milk that is consumed (unitless)
DCF_{ing}	= ingestion dose conversion factor (mrem/pCi).

6.3.3.1.9 Ingestion of Eggs. This section describes the equations used to calculate the concentration of contaminant in eggs and the dose from consumption of eggs.

The equation used to calculate the concentration of contaminant in eggs resulting from consumption of contaminated water, contaminated fodder, and contaminated soil by the poultry is given as

$$C_e = (C_w \times IR_{w,p} + C_{fodder} \times IR_{fodder,p} \times CF_1 + C_{stot} \times IR_{s,p} \times CF_1) \times BCF_{egg} \quad (6-37)$$

Where:

C_e	= radionuclide concentration in eggs (pCi/kg)
C_w	= radionuclide concentration in water (pCi/L)

RPP-ENV-58782, Rev. 0

1	$IR_{w,p}$	= ingestion rate of water by poultry (L/day)
2	C_{fodder}	= radionuclide concentration in livestock fodder (pCi/g)
3	$IR_{fodder,p}$	= ingestion rate of fodder by poultry (kg/day)
4	CF_1	= unit conversion factor of 1,000 (g/kg)
5	C_{stot}	= total radionuclide concentration in surface soil layer (pCi/g)
6	$IR_{s,p}$	= ingestion rate of soil by poultry (kg/day)
7	BCF_{egg}	= bioconcentration factor of radionuclides in eggs (day/kg).

8
9 The equation used to calculate the dose from ingestion of eggs:

$$D_e = C_e \times IR_e \times F_a \times DCF_{ing} \quad (6-38)$$

12
13 Where:

15	D_e	= dose from consumption of eggs (mrem/yr)
16	IR_e	= egg ingestion rate (kg/yr)
17	F_a	= fraction of locally-produced eggs that are consumed (unitless)
18	DCF_{ing}	= ingestion dose conversion factor (mrem/pCi).

19
20 **6.3.3.1.10 Ingestion of Farm-Raised Poultry.** This section describes the equations used to
21 calculate the concentration of contaminant in poultry and the dose from consumption of poultry.

22
23 The following equation is used to calculate the concentration of contaminant in poultry:

$$C_p = (C_w \times IR_{w,p} + C_{fodder} \times IR_{fodder,p} \times CF_1 + C_{stot} \times IR_{s,p} \times CF_1) \times BCF_{poultry} \quad (6-39)$$

26
27 Where:

29	C_p	= radionuclide concentration in poultry (pCi/kg)
30	C_w	= radionuclide concentration in water (pCi/L)
31	$IR_{w,p}$	= ingestion rate of water by poultry (L/day)
32	C_{fodder}	= radionuclide concentration in livestock fodder (pCi/g)
33	$IR_{fodder,p}$	= ingestion rate of fodder by poultry (kg/day)
34	CF_1	= unit conversion factor of 1,000 (g/kg)
35	C_{stot}	= total radionuclide concentration in surface soil layer (pCi/g)
36	$IR_{s,p}$	= ingestion rate of soil by poultry (kg/day)
37	$BCF_{poultry}$	= bioconcentration factor of radionuclides in poultry (day/kg).

38
39 The following equation is used to calculate dose from ingestion of poultry:

$$D_p = C_p \times IR_p \times F_a \times DCF_{ing} \quad (6-40)$$

42
43 Where:

45	D_p	= dose from ingestion of poultry (mrem/yr)
----	-------	--

RPP-ENV-58782, Rev. 0

- IR_p = ingestion rate of poultry (kg/yr)
 F_a = fraction of locally-produced poultry that is consumed (unitless)
 DCF_{ing} = dose conversion factor for ingestion (mrem/pCi).

6.3.3.1.11 Incidental Ingestion of Soil. The following equation is used to calculate the dose from incidental ingestion of soil:

$$D_s = C_s \times IR_s \times EF \times DCF_{ing} \times CF \quad (6-41)$$

Where:

- D_s = dose from incidental ingestion of soil (mrem/yr)
 IR_s = ingestion rate of soil (mg/day)
 EF = exposure frequency (days/yr)
 DCF_{ing} = ingestion dose conversion factor (mrem/pCi)
 CF = unit conversion factor of 0.001 (g/mg).

6.3.3.1.12 Inhalation of Soil Particulates. The following equation is used to calculate the dose from inhalation of soil particulates:

$$D_{inh} = C_s \times E_f \times M \times \left(INH_{in} \times t_{in} \times \left(\frac{I}{O} \right) + INH_{out} \times t_{out} \right) \times DCF_{inh} \quad (6-42)$$

This equation assumes the concentration and mass loading factor are the same indoors and outdoors.

Where:

- D_{inh} = dose from inhalation of soil (mrem/yr)
 E_f = enrichment factor (unitless)
 M = mass loading factor (g/m³)
 INH_{in} = indoor inhalation rate (m³/yr)
 t_{in} = fraction of time spent indoors (unitless)
 I/O = ratio of radionuclide concentrations in indoor and outdoor air (unitless)
 INH_{out} = outdoor inhalation rate (m³/yr)
 t_{out} = fraction of time spent outdoors (unitless)
 DCF_{inh} = inhalation dose conversion factor (mrem/pCi).

And:

$$E_f = \frac{C_p}{C_s} \quad (6-43)$$

- C_p = radionuclide concentration in airborne particles (pCi/g)
 C_s = radionuclide concentration in soil (pCi/g).

RPP-ENV-58782, Rev. 0

6.3.3.1.13 Inhalation of Water Vapor. The following equation is used to calculate dose resulting from the inhalation of water vapor from showering or other household activities:

$$D_{inh_w} = C_w \times INH_w \times EF \times K \times DCF_{inh} \quad (6-44)$$

Where:

- D_{inh_w} = dose resulting from inhalation of water vapor (mrem/yr)
- C_w = radionuclide concentration in water (pCi/L)
- INH_w = inhalation rate of water vapor (m³/day)
- EF = exposure frequency (days/yr)
- K = Andelman volatilization factor (L/m³)
- DCF_{inh} = inhalation dose conversion factor for inhalation (mrem/pCi).

6.3.3.1.14 External Exposure. The following equation is used to calculate the dose from external exposure:

$$D_{ext} = C_{stot} \times (t_{in} \times \epsilon + t_{out}) \times DCF_{ext} \quad (6-45)$$

Where:

- D_{ext} = dose from external exposure to soil (mrem/yr)
- C_{stot} = total radionuclide concentration in soil (pCi/g)
- t_{in} = fraction of time spent indoors (unitless)
- ϵ = transmission or shielding factor (unitless)
- t_{out} = fraction of time spent outdoors (unitless)
- DCF_{ext} = dose conversion factor for external exposure ([mrem/yr]/[pCi/g]).

6.3.3.1.15 Total Effective Dose for All-Pathways Reference Person. The following equation is used to calculate the total effective dose from all groundwater pathways:

$$D_{total} = \sum_i^N D_i \quad (6-46)$$

Where:

- D_{total} = total effective dose from all exposure pathways (mrem/yr)
- D_i = total dose for the ith exposure pathway (mrem/yr)
- N = number of exposure pathways.

6.3.3.2 Atmospheric-Pathway Dose Analysis. An atmospheric pathway scenario is considered in which an individual is exposed to radionuclides that are diffused to the surface from the wastes disposed at the WMA C tank farm and are transported 100 m downwind. Three exposure mechanisms are considered for the atmospheric pathway:

- Air immersion
- Inhalation

RPP-ENV-58782, Rev. 0

- External exposure to the contaminated ground surface.

External exposure results from a fraction of the waste in the air that settles on the ground via dry and wet depositions as they are transported by wind.

The exposed individual is assumed to encounter the same exposure conditions as the resident farmer (e.g., time spent indoors and outdoors). Inhalation of vapors from redeposition followed by resuspension and inhalation is considered. The dose-specific parameters for the atmospheric pathway are given in Table 6-29, and the dose conversion factors are summarized in Table 6-25.

Table 6-29. Dose-Specific Parameters for the Atmospheric Pathway.

Parameter	Notation	Value	Unit	Reference
Dry deposition rate for ^{129}I	V_d	0.035	m/s	EPA 2014
Dry deposition velocity for ^{14}C and ^3H	V_d	0	m/s	EPA 2014
Rainfall rate	RR	18.14*	cm/yr	Hanford.gov
Scavenging conversion factor	SCF	1.00E-07	yr/(cm s)	EPA 2014
Scavenging coefficient	SC	Calculated	s^{-1}	EPA 2014
Mixing layer height	H	2	m	Modeling assumption
Gamma shielding factor	GSF_o	1	(-)	PRGfR 2015
Inhalation rate when indoors	IR_{in}	7,300	m^3/yr	NCRP Report No. 129
Fraction of time spent indoors	t_{in}	0.4	(-)	PRGfR 2015; Based on 10 hr/day for 350 days/year
Inhalation rate when outdoors	IR_{out}	12,775	m^3/yr	NCRP Report No. 129
Fraction of time spent outdoors	t_{out}	0.4861	(-)	PRGfR 2015; Based on 12.167 hr/day for 350 days/year
Accumulation time	t_{accu}	3.15E+07	s	One-year time step

*Value given is 30-year average from 1981 to 2010.

References:

Hanford Site (Hanford.gov), Queried 07/2015, [Hanford Meteorological Station], <http://www.hanford.gov/page.cfm/HMS>.
NCRP Report No. 129, "Recommended Screening Limits for Contaminated Surface Soil and Review of Factors Relevant to Site-Specific Studies."

Preliminary Remediation Goals for Radionuclides (PRGfR), Queried 07/2015, [PRG User's Guide],

http://epa-prgs.ornl.gov/radionuclides/prg_guide.html.

Radiation Risk Assessment Software: CAP-88 and CAP-88 PC (EPA 2014), Queried 07/2015, [CAP88-PC Version 4.0 User Guide], <http://www.epa.gov/radiation/assessment/CAP88/index.html>.

RPP-ENV-58782, Rev. 0

6.3.3.2.1 Deposition of Airborne Contaminants on the Ground Surface. Contaminants in the air can be deposited on the ground surface under both dry and wet conditions (rain or mist). The following equation is used to calculate the dry deposition rate:

$$Dep_d = C_{air} \times V_d \quad (6-47)$$

Where:

Dep_d = deposition rate for radionuclides under dry conditions (pCi/[m² sec])
 C_{air} = radionuclide concentration in air (pCi/m³)
 V_d = velocity with which the dry deposition occurs (m/s).

The following equation is used to calculate wet deposition rate:

$$Dep_w = C_{air} \times SC \times H \quad (6-48)$$

And:

$$SC = RR \times SCF \quad (6-49)$$

Where:

Dep_w = deposition rate for radionuclides under wet conditions (pCi/[m² sec])
 C_{air} = radionuclide concentration in air (pCi/m³)
 SC = scavenging coefficient (sec⁻¹)
 H = mixing layer height (m)
 RR = rainfall rate (cm/yr)
 SCF = scavenging conversion factor (yr/cm-sec).

The following equation is used to calculate the total deposition rate (pCi/[m² sec]):

$$TDep = Dep_d + Dep_w \quad (6-50)$$

Where:

$TDep$ = total deposition rate for radionuclides (pCi/[m² sec]).

6.3.3.2.2 Air Immersion Dose. An individual in the contaminated volume of air will receive external radiation exposure, primarily from gamma photon emitters in the surrounding air. The following equation is used to calculate the air immersion dose:

$$D_{im} = C_{air} \times t_{out} \times GSF_o \times DCF_{im} \quad (6-51)$$

Where:

D_{im} = dose from air immersion (mrem/yr)

RPP-ENV-58782, Rev. 0

- C_{air} = radionuclide concentration in air (pCi/m³)
 t_{out} = fraction of time spent outdoors (unitless)
 GSF_o = outdoor gamma shielding factor (unitless)
 DCF_{im} = air immersion dose conversion factor $\left(\frac{(mrem/year)}{(pCi/m^3)}\right)$.

6.3.3.2.3 Inhalation Dose for Gaseous Radionuclides. In addition to the radiation dose received from air immersion, the exposed individual will receive a dose from inhalation of gaseous radionuclides in the air (tritium, ¹⁴C, and ¹²⁹I). The following equation is used to calculate inhalation dose:

$$D_{inh} = C_{air} \times (INH_{in} \times t_{in} + INH_{out} \times t_{out}) \times DCF_{inh} \quad (6-52)$$

Where:

- D_{inh} = dose from inhalation of gaseous radionuclides in air (mrem/yr)
 C_{air} = radionuclide concentration in air (pCi/m³)
 INH_{in} = inhalation rate while indoors (m³/yr)
 t_{in} = fraction of time spent indoors (unitless)
 INH_{out} = inhalation rate while outdoors (m³/yr)
 t_{out} = fraction of time spent outdoors (unitless)
 DCF_{inh} = dose conversion factor for inhalation for each radionuclide (mrem/pCi).

6.3.3.2.4 External Exposure to Contaminated Soil. The final exposure considered for the atmospheric pathway is external exposure to radionuclides that have been redeposited on the ground. The radionuclide dose coefficients assume radionuclides are uniformly distributed on the ground to a depth that approximates a plane that is infinitely thick and infinitely horizontal. The following equation is used to calculate the radionuclide concentration that has accumulated on the ground surface:

$$C_{grd} = TDep \times t_{accu} \quad (6-53)$$

Where:

- C_{grd} = radionuclide concentration on ground surface (pCi/m²)
 $TDep$ = total deposition rate (pCi/[m²·sec])
 t_{accu} = time interval over which the deposition has occurred (sec).

The following equation is used to calculate direct external exposure dose:

$$D_{ext} = C_{grd} \times (t_{in} \times \varepsilon + t_{out}) \times DCF_{ext} \quad (6-54)$$

Where:

- D_{ext} = dose from the external exposure to contaminated ground surface (mrem/yr)
 t_{in} = fraction of time spent indoors (unitless)

RPP-ENV-58782, Rev. 0

ϵ = transmission or shielding factor (unitless)
 t_{out} = fraction of time spent outdoors (unitless)
 DCF_{ext} = dose conversion factor for external exposure to contaminated ground surface
 ([mrem/yr]/[pCi/m²]).

6.3.3.2.5 Total Effective Dose for Atmospheric Pathway. The following equation is used to calculate the total effective dose from all atmospheric pathways:

$$D_{total} = \sum_i^N D_i \quad (6-55)$$

Where:

D_{total} = total effective dose from all exposure pathways (mrem/yr)
 N = number of exposure pathways
 D_i = total dose for the i^{th} exposure pathway (mrem/yr).

6.4 MODEL VALIDATION³

A substantial body of literature exists indicating the manner in which scientific validation of models is pursued (e.g., “Ground-Water Models: Validate or Invalidate” [Bredehoeft and Konikow 1993], “Validation of safety assessment models as a process of scientific and public confidence building” [Neuman 1992], “The Modeling Process and Model Validation” [Tsang 1991]). Because PA models cannot be tested over the spatial scales of interest and the long time periods for which the models make predictions, the customary definition of model validation (i.e., comparison of model estimates with actual data at the space-time scales of interest) is precluded (NUREG-1573; NUREG-1636, Regulatory Perspectives on Model Validation in High-Level Radioactive Waste Management Programs: A Joint NRC/SKI White Paper). Therefore, this section on model validation is viewed as a summary of the documented theoretical or scientific basis for each of the PA model components that have been developed and their suitability for supporting the PA decision-making. Below is presented a variety of topical discussions which serve as the basis of confidence building and model validation of WMA C PA process models and results.

6.4.1 Basis for Recharge Estimates Used for Land Surface Boundary Condition

Recharge rates have been estimated from studies conducted at the Hanford Site over the last 30 years. Recharge rates are available for natural and disturbed soils, for soils with and without vegetation, and for various plant communities. In addition, recharge has been estimated for surface covers with varying plant communities. These estimates are based on lysimeter records, tracer tests (chloride mass balance), and computer simulations to match field data. PNNL-16688 and PNNL-14702 provide primary sources of information on recharge estimates for the Hanford Site that are relevant to tank farms. The estimates used in the PA consider estimates of recharge

³ In this section and in the context of WMA C PA modeling, the terms “confidence,” “confidence building,” “confidence enhancement,” “validation,” and “validation process” are used interchangeably.

RPP-ENV-58782, Rev. 0

made for the 200 Areas and for conditions at WMA C inferred from measurements made at the Field Lysimeter Test Facility (Section 3.1.5.2.2).

An extensive set of data exists for estimates of recharge for engineered barriers. For example, almost two decades of field-scale recharge studies have been conducted on an engineered Prototype Hanford Barrier (PHB) (a 5-m [16.4-ft] thick multilayered capillary barrier with 2 m [6.6 ft] of silt loam) that was constructed in the 200 East Area (north of WMA C) in August 1994. The barrier performance was monitored almost continuously for 15 years to document structural stability, erosion, and components of the water balance including precipitation, surface runoff, water storage, percolation out of the root zone, and evapotranspiration. The barrier recharge estimates used in the PA are supported by the PHB data (PNNL-18845).

Section 8.1.3.1 provides additional details related to developing the uncertainty distributions for the recharge estimates.

6.4.2 Basis for Source-Term Model Development and Implementation

The basis for the source-term model development and implementation is rooted in results of laboratory studies conducted of the tank waste residuals collected in a number of tanks following cessation of retrieval. As part of the waste characterization efforts, analytical methods are used to measure the chemical and radiological constituents in the waste sludge and to understand their composition, solid-phase characteristics, and the leachability of primary contaminants of interest. Several detailed characterization reports are available for various tank residuals (see Section 5).

Both mineral phase solubility-limited and matrix degradation rate-limited processes are considered for release of contaminant from the waste. These conceptual models are based on observations made through multi-year leaching tests and identification of mineral phases as presented in Section 5. Results from the flow-through and batch leach tests were used to develop both thermodynamic equilibrium and reaction progress models. Both empirical and process model-based information were used to develop the waste form release models for the PA (Section 6.2.1 provides additional details).

The effective diffusion coefficient of mobile contaminants (such as ^{99}Tc and ^{129}I) through the combined grout and concrete base mat is considered a key parameter that controls the diffusive flux. Over the past decade, several experiments have been conducted to determine the effective diffusion coefficient through concrete for relatively mobile contaminants under unsaturated conditions. The results of various experiments are presented in PNNL-23841 and summarized in Section 6.3.1.4. Of particular interest are the sediment-concrete half-cell experiments conducted in Year 2008 (for a period of 351 days) with ^{99}Tc and stable iodine. Sediment half-cell specimens were spiked with ^{99}Tc (or stable iodine) to achieve a measurable diffusion profile in the concrete part of the half-cell. In these experiments, iron content was varied in the concrete specimens from 0% to 12%, sediment moisture content was varied (4%, 7%, or 15%), and half of the concrete monoliths were carbonated prior to preparing the half-cells. The characteristics of the concrete half-cells are listed in Table 6-4. Half-cell sampling was conducted at 351 days. The effective diffusion coefficient through grout and concrete is based on evaluation of such experiments.

RPP-ENV-58782, Rev. 0

A linear sorption isotherm (using a K_d approach) is considered for determining sorption within the grout and concrete layer for various contaminants as they undergo diffusive (and advective) transport through the tank. The K_d values are presented in Table 6-7 in terms of best estimate and the uncertainty range that are derived from relevant published literature for chemical conditions that are likely to exist within the grout/concrete layer within the tanks.

6.4.3 Basis for Vadose Zone Model Development

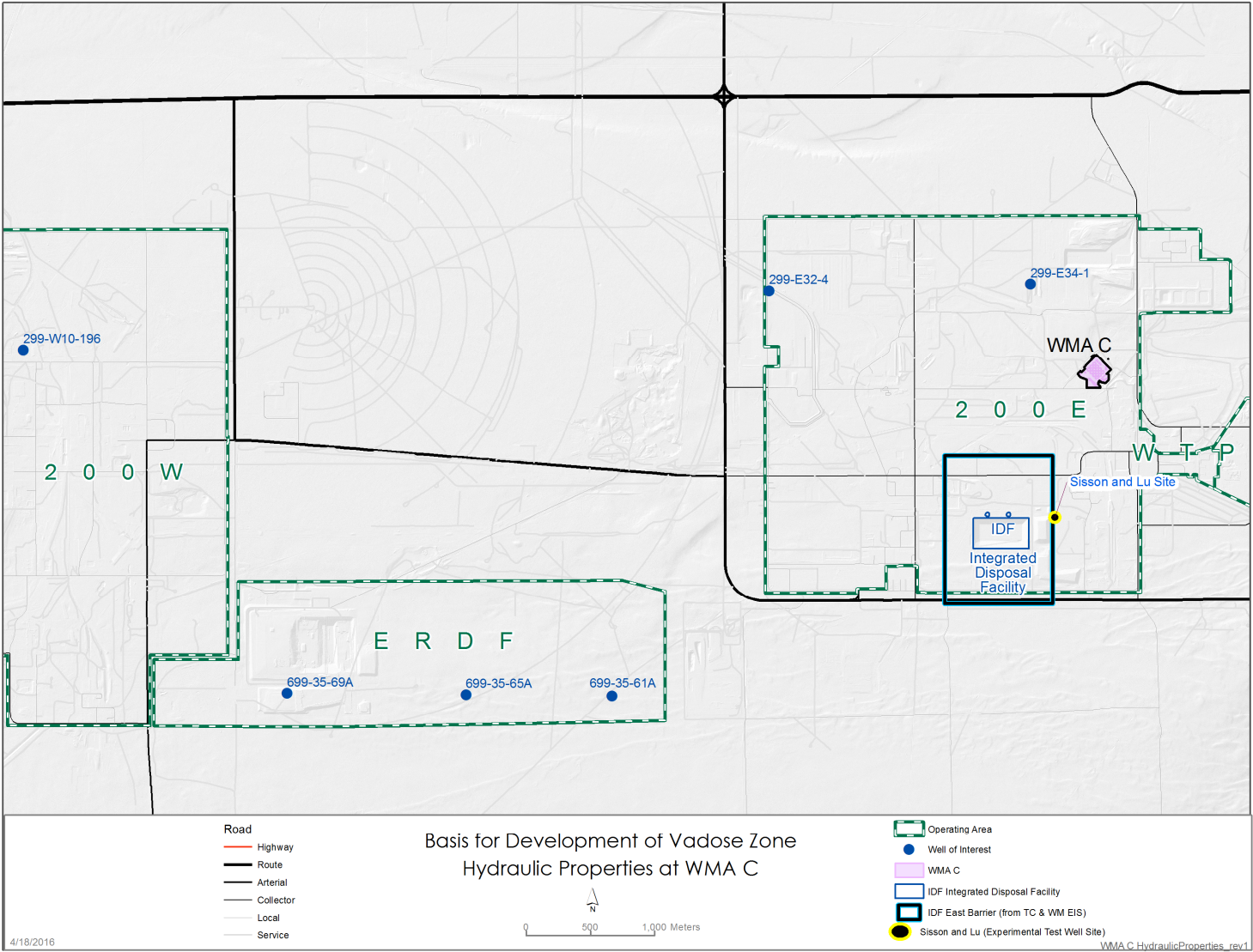
The spatial extent of various HSUs within the WMA C model domain are based on an extensive borehole dataset discussed in Section 3.2.1. The geologic framework model for WMA C is derived from the information provided in RPP-RPT-56356 (Section 3.2.1). It should be noted that at the Hanford Site more than 3,000 boreholes have been logged (PNNL-13653, "A Catalog of Geologic Data for the Hanford Site") and primary HSU designations and extents are well established.

The vadose zone hydraulic properties for WMA C are derived from a set of laboratory (core-scale) experiments conducted on samples representative of Hanford H1, H2, and H3 units and backfill material. The methodology is discussed in detail in Appendix B (Section B.2). For WMA C vadose zone modeling, each heterogeneous geologic unit is replaced by an EHM with macroscopic flow properties. With each heterogeneous unit assigned its upscaled or effective hydraulic properties, the simulated flow fields predict the bulk or mean flow behavior at the field scale. The method of upscaling is discussed in Appendix B (Section B.3).

An independent evaluation of the vadose zone conceptual model and the EHM approximation was performed using the 200 East Area Sisson and Lu injection test site (Figure 6-60) moisture content database. The database at the nearby Sisson and Lu site therefore serves as a proxy for WMA C, and is an important resource in understanding large-scale moisture movement in imperfectly stratified heterogeneous media and a relatively dry moisture regime such as those existing at WMA C. Details of the Sisson and Lu site, field injections and the spatio-temporal distribution of observed moisture plume are described elsewhere ("Simulating field-scale moisture flow using a combined power-averaging and tensorial connectivity-tortuosity approach" [Zhang and Khaleel 2010]; Ye et al. 2005).

Two variations of EHM model for the heterogeneous Hanford sediments were explored based on the Sisson and Lu experiments. In the first method, the small-scale core measurements for hydraulic properties were used to predict the large-scale flow behavior at the Sisson and Lu site (Zhang and Khaleel 2010). The second method is based on an inverse approach which inverts the large-scale unsaturated properties using the temporal evolution of the moisture content distribution (Yeh et al. 2005). For both approaches, a moment analysis (Ye et al. 2005) was used to quantify the center of mass and the spread of the injected water for the observed and simulated moisture plumes. The first moments represent the mass center of the moisture plume in different directions at a given time. The second moments measure the spread of the plume about its mass centers. For the forward as well as the inverse EHM-based methods, spatial moments (first and second) of the simulated plume based on the effective hydraulic conductivities were in good agreement with those for the observed plume (Zhang and Khaleel 2010; Yeh et al. 2005).

Figure 6-60. Location of Sisson and Lu Field Injection Site in 200 East Area.



ERDF = Environmental Restoration Disposal Facility
TC&WM EIS = Tank Closure and Waste Management Environmental Impact Statement

WMA = Waste Management Area
WTP = Waste Treatment Plant

6-161

RPP-ENV-58782, Rev. 0

RPP-ENV-58782, Rev. 0

The Sisson and Lu site database also provided a framework for testing two heterogeneous modeling approaches based on combining soft (initial moisture content, bulk density and particle-size distribution) and hard (soil hydraulic properties) data (“Simulation of field injection experiments in heterogeneous unsaturated media using cokriging and artificial neural network” [Ye et al. 2007]; “A Markov chain model for characterizing medium heterogeneity and sediment layering structure” [Ye and Khaleel 2008]). The heterogeneous models do not invoke the EHM approximation. The use of both soft and hard data was valuable in reproducing the detailed moisture plume for the two heterogeneous models (i.e., the splitting of the moisture plume sandwiched within the coarse media between two fine layers at the Sisson and Lu site). However, the observed and simulated spatial moments (first and second) were not significantly different from those using the EHM-based models. Hence, models using both hard and soft data, in addition to honoring the observed first and second moments, were able to reproduce the splitting of the observed plume. On the other hand, the EHM-based modeling does not capture the detailed plume behavior, but honors the first and second moments of the observed moisture plume. With the WMA C PA simulations being conducted over a large flow domain and over a long time frame, the fact that the calculated moments for both the EHM and heterogeneous models are of similar magnitude is an important finding, and provides justification for use of EHM approximation for vadose zone modeling.

6.4.4 Comparison of Vadose Zone Modeling Results with Measured Data in Vicinity of Waste Management Area C

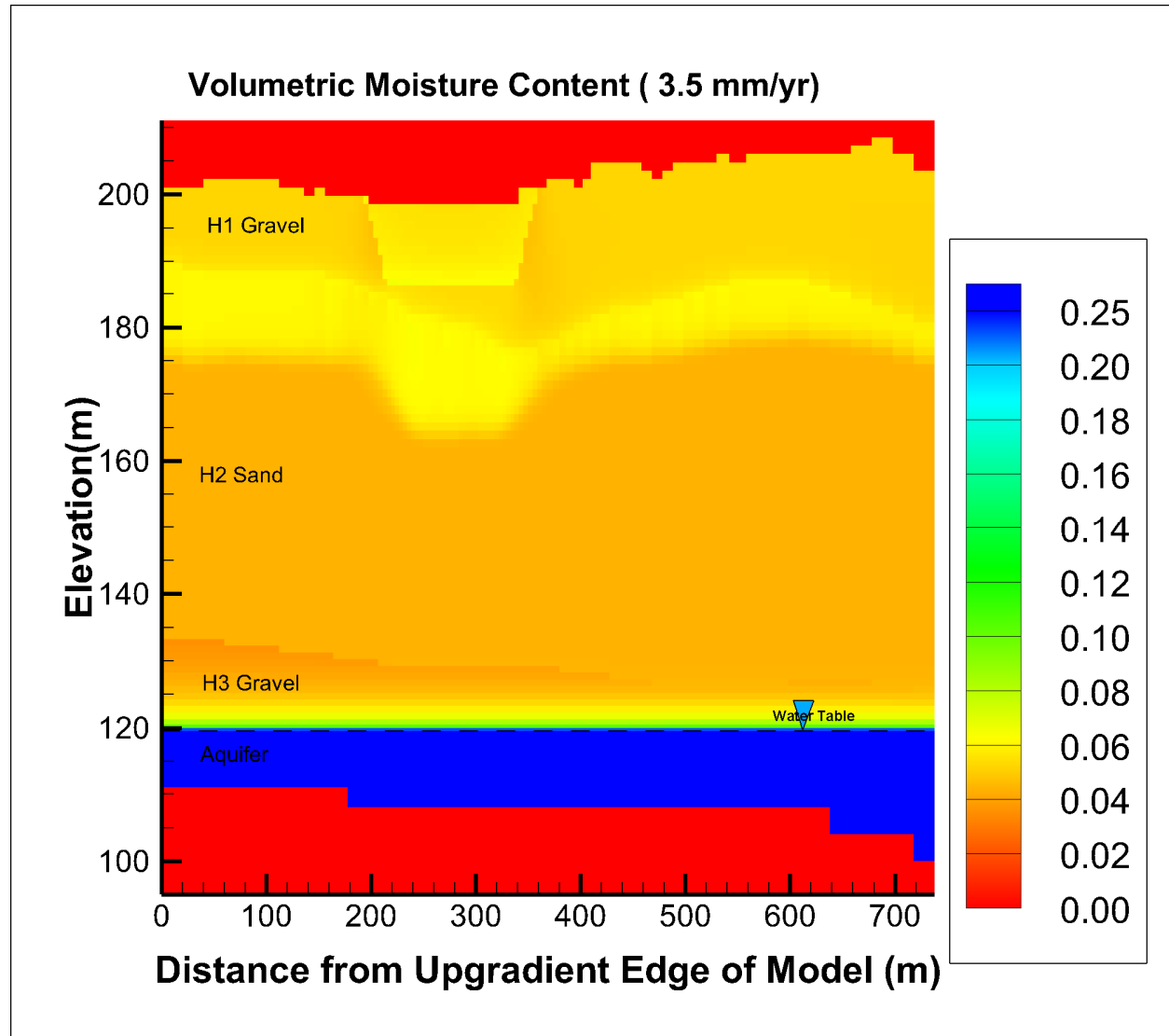
As part of WMA C site characterization, an extensive database of moisture content information is available for various HSUs. The moisture content database was developed as part of a direct push campaign conducted at WMA C in 2008, and understood as being long after the occurrence of past leaks and discharges at the farm. Figure 6-61 shows the simulated steady-state moisture profile for different stratigraphic units for the base case under long-term recharge conditions (3.5 mm/yr [0.14 in./yr]). The simulated volumetric moisture contents for different units vary within a narrow range of 4% and 7%. These values compare well with an extensive dataset of field observations where the average volumetric moisture content for the various HSUs vary from 5.1% to 6.2% (Appendix B, Table B-1). With moisture being the key driver for contaminant transport, the fact that the intermediate calculations for the simulated average moisture for different units is in overall agreement with field data enhances confidence in the PA modeling approach and calculations.

Figure 6-62 provides a comparison, for Hanford H2 unit, of the measured moisture profile (circles) for borehole C4297 that is located within WMA C and the simulated steady-state moisture profile (blue) from the base case. As indicated, for an expected long-term recharge estimate of 3.5 mm/yr (0.14 in./yr), the simulated H2 moisture profile, on the average, compares well with the measurements. As expected, the field-measured moisture contents are significantly impacted by small-scale heterogeneities and exhibit considerable variability (Figure 6-62). To the contrary, the PA simulations are based on upscaled or effective hydraulic properties; each heterogeneous formation is replaced by its homogeneous equivalent, and the upscaled or effective flow parameters are used to represent the EHM. This effectively results in a smoothing of the model estimates (Figure 6-3). Therefore, the variability of field-measured moisture contents, induced by media heterogeneities, is inherently larger in comparison to that based on

RPP-ENV-58782, Rev. 0

PA simulations using homogenized upscaled properties, and the ensemble average, embedded in EHM approximation, cannot capture the field-scale variability.

Figure 6-61. Simulated Average Moisture Contents for Different Stratigraphic Units Using Equivalent Homogeneous Medium Model.



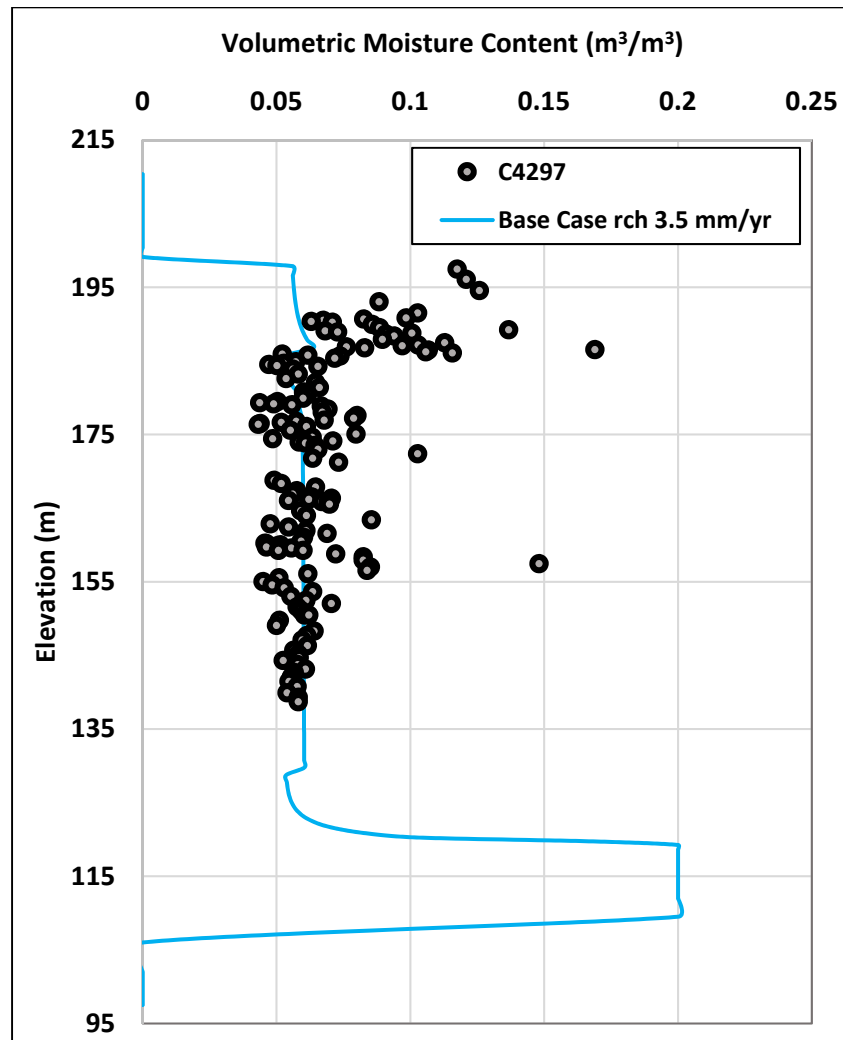
6.4.5 Comparison of Vadose Zone Model with Tank Closure and Waste Management Environmental Impact Statement Model for Alternative 2B

A comparison was performed to evaluate the vadose zone model developed for the WMA C PA against the TC&WM EIS model (DOE/EIS-0391) developed for WMA C. Due to varying inputs related to the residual waste inventory and waste release processes, direct comparison of results is not possible. Therefore, the residual waste inventory, waste release functions, and recharge rates were made consistent with the TC&WM EIS model by changing the inputs within the WMA C PA model (see Appendix G). The flux at the base of the vadose zone was compared

RPP-ENV-58782, Rev. 0

between the two models for ^{129}I . The time series releases of ^{129}I to the groundwater calculated in both models include two relative maxima and negligible difference between the two peak values are observed. The results of the comparison, provided in Appendix G, show that the two models are capable of producing consistent results indicating that the hydraulic properties used in the two models produce similar results.

Figure 6-62. Comparison of Simulated (Blue) and Observed (Circle) Moisture Content for Hanford H2 Sand-Dominated Unit.



6.4.6 Basis for Saturated Zone Model Development

For the WMA C PA modeling, the unconfined aquifer is treated as an EHM, where effective parameters and appropriate boundary conditions derived from a regional scale groundwater flow model are used. The development of the model parameters is discussed in Appendix C. A calibrated CPGWM (CP-47631, Revision 2) serves as the basis for developing macro-scale parameters for the unconfined aquifer at WMA C. The development of CPGWM incorporates over 30 years of experience on development and application of groundwater models for the

RPP-ENV-58782, Rev. 0

1 Central Plateau [PNL-10886, "Development of a Three-Dimensional Ground-Water Model of
2 the Hanford Site Unconfined Aquifer System: FY 1995 Status Report"; PNNL-13641;
3 PNNL-14398, "Transient Inverse Calibration of the Site-Wide Groundwater Flow Model
4 (ACM-2): FY 2003 Progress Report"; PNNL-14753, "Groundwater Data Package for Hanford
5 Assessments"; PNNL-12261].
6

7 The CPGWM incorporates the large-scale geologic and hydrogeologic features and provides
8 estimates of water levels, hydraulic gradients, and groundwater flows throughout the 200 West
9 and 200 East Areas, for current and expected future groundwater conditions. Simulated water
10 levels are compared to observed values for wells located upgradient (well 299-E27-15) and
11 downgradient (well 299-E27-14) of WMA C (Figure 6-63). The observed heads and
12 CPGWM-simulated heads, representing a time span of over 20 years, compare well, providing
13 confidence in the predictive capabilities of the CPGWM as well as how the WMA C saturated
14 media properties are parameterized and groundwater fluxes apportioned in the PA.
15

16 **6.4.7 Verification of Air Pathway Modeling Approach**

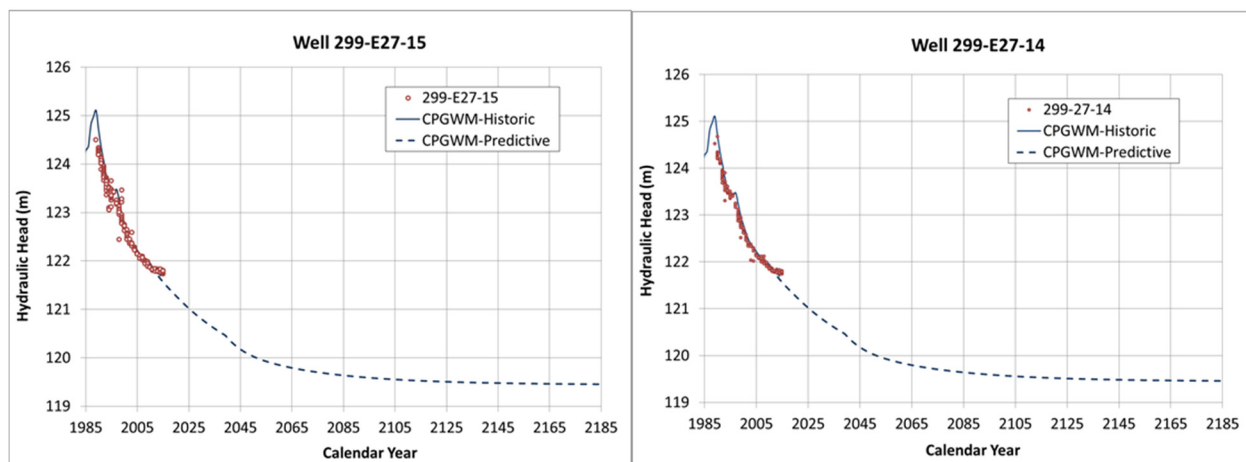
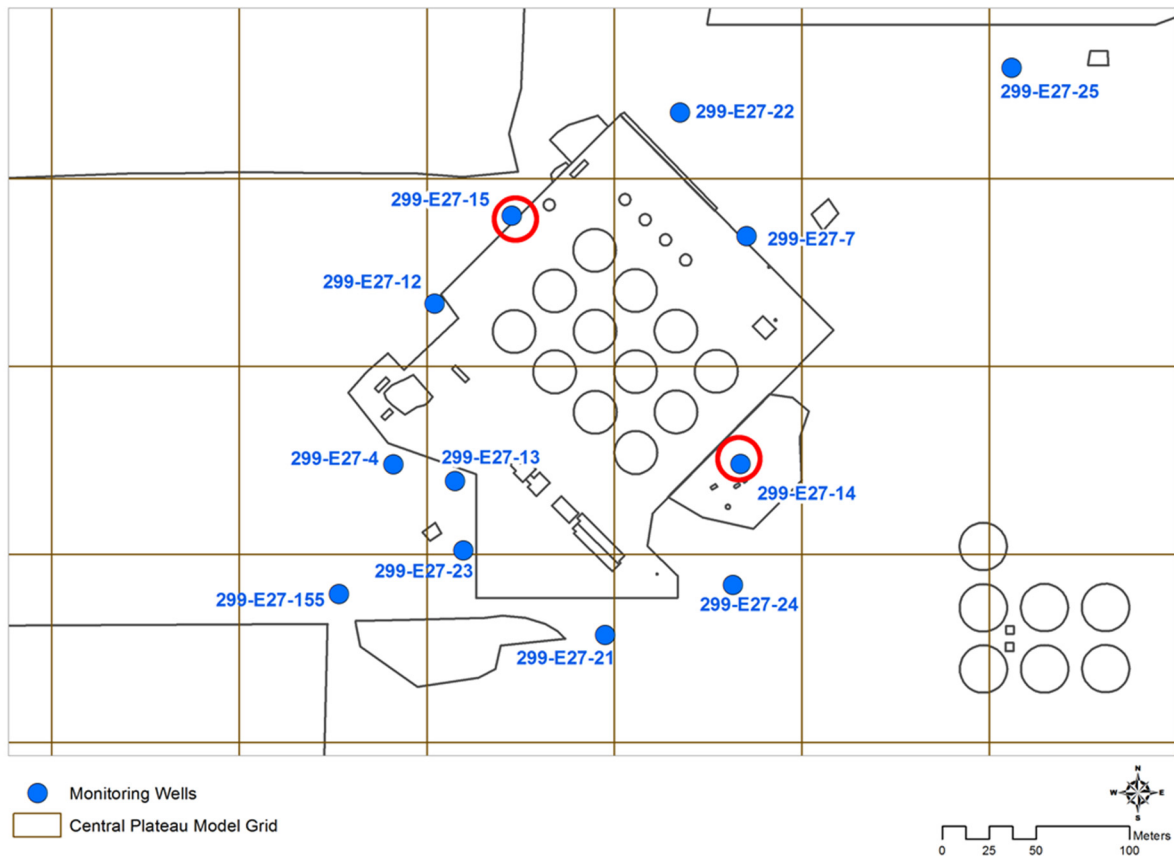
17

18 Among the radionuclides contained in the wastes in WMA C at closure, four of them can
19 potentially emanate in gaseous form. These radionuclides are ^{14}C (as CO_2), ^3H (as H_2), ^{129}I (as
20 I_2), and ^{222}Rn (as radon gas). However, radon is not included in the air pathway.
21

22 Appendix E provides verification of the air-pathway modeling approach by building confidence
23 that diffusive flux can be adequately modeled to meet the PA performance requirements. The
24 PA model methodology for air pathway calculations is compared to the modeling results
25 generated using EPA CAP88-PC model-based results and those calculated from the recent
26 Hanford Site NEPA Characterization Report (PNNL-6415) for a given receptor location and a
27 given set of inputs. The comparison of results indicates that the WMA C PA model built for the
28 air pathway calculation is valid for its intended purpose.
29
30

RPP-ENV-58782, Rev. 0

Figure 6-63. Central Plateau Groundwater Model Calibration Results in the Vicinity of Waste Management Area C.



CPGWM = Central Plateau Groundwater Model

Reference: CP-47631, "Model Package Report: Central Plateau Groundwater Model Version 6.3.3."

RPP-ENV-58782, Rev. 0

7.0 RESULTS OF ANALYSIS

This section presents the results of the analyses described in Section 6.0 and discusses the (1) release of radionuclides from the source term (Section 7.1), and (2) environmental transport of radionuclides via the groundwater pathway (Section 7.2.1) and the air pathway including the radon analysis (Section 7.2.2). The results of the analyses conducted for each part of the modeling effort are summarized independently, leading to separate discussions of the groundwater and all-pathways dose presented in Section 7.3. Intermediate results are presented to illustrate the influence of each analysis step on the overall result. Results are provided for two time periods: compliance period (1,000 years) (2020 to 3020), and post-compliance period (up to 10,000 years from closure). Results are provided for the receptor located 100 m (328 ft) downgradient from WMA C. Intermediate results and doses are also projected out 10,000 years to identify peaks for some radionuclides that migrate slowly through the environment. The results from 1,000 to 10,000 years are given for completeness, but these are not part of the DOE O 435.1 compliance determination.

7.1 SOURCE TERM

The source term is defined as the rate of release from the facility as a function of time (NCRP Report 152). Since it is defined as a release from the facility, it includes a number of processes associated with mobilization of contaminants from the waste form and migration of the contaminants to the boundary of the facility. The boundary of the facility for WMA C source term is considered the outer boundary of the engineered features (i.e., the bottom of the tank base mat, or the outer surface of catch tanks, pipelines, and other ancillary equipment).

For the groundwater pathway, a total of 19 different sources for releases to groundwater are evaluated in the PA, which contribute to the overall source term. These sources consist of the twelve 100-series tanks, four 200-series tanks, C-301 catch tank, 244-CR vaults, and pipelines. The residual inventory and waste volume associated with each source is treated separately, resulting in an analysis of transport through groundwater for each source. Sources are added together to calculate the total impact as part of the groundwater analysis because plumes from different sources overlap in the groundwater analysis. This allows the impacts from each individual source to be placed in context to other sources, as well as the calculation of an individual source to the total impact of WMA C on the groundwater pathway.

For the situation when the tank concrete and infill grout are intact, the conceptual model is as follows. The intact concrete and grout cause any water in contact with residual wastes to be stagnant. As a result, the only driving force for migration of contaminants in residual wastes to the boundary of the engineered barriers is the chemical potential gradient between the waste and the tank surroundings. Therefore, mass release calculations are controlled by diffusion through the engineered structures (for tanks, the base mat) for all the sources except for the pipelines, which are considered advection-dominated because it is uncertain how much reliance can be placed on the waste transfer pipelines being intact. It is noteworthy that the conditions that produce a diffusion-dominated transport condition are not primarily based on, and indeed are not reliant on, an assumption that the base mat is intact. Instead, the diffusional release is caused

RPP-ENV-58782, Rev. 0

1 mainly by the infill grout, which limits water flow rates through the base mat. As discussed in
2 Section 6.2.1.2 (Evaluation of Tank Stability), the infill grout is expected to be stable for long
3 periods of time based on samples taken from C-107 tank dome and the sidewall of
4 tank 241-A-106. As a result, this intact tank configuration with diffusional releases is the
5 primary situation modeled in this PA, and is included in the base case analysis. Other conceptual
6 models have been implemented in several of the sensitivity cases (see Section 8).

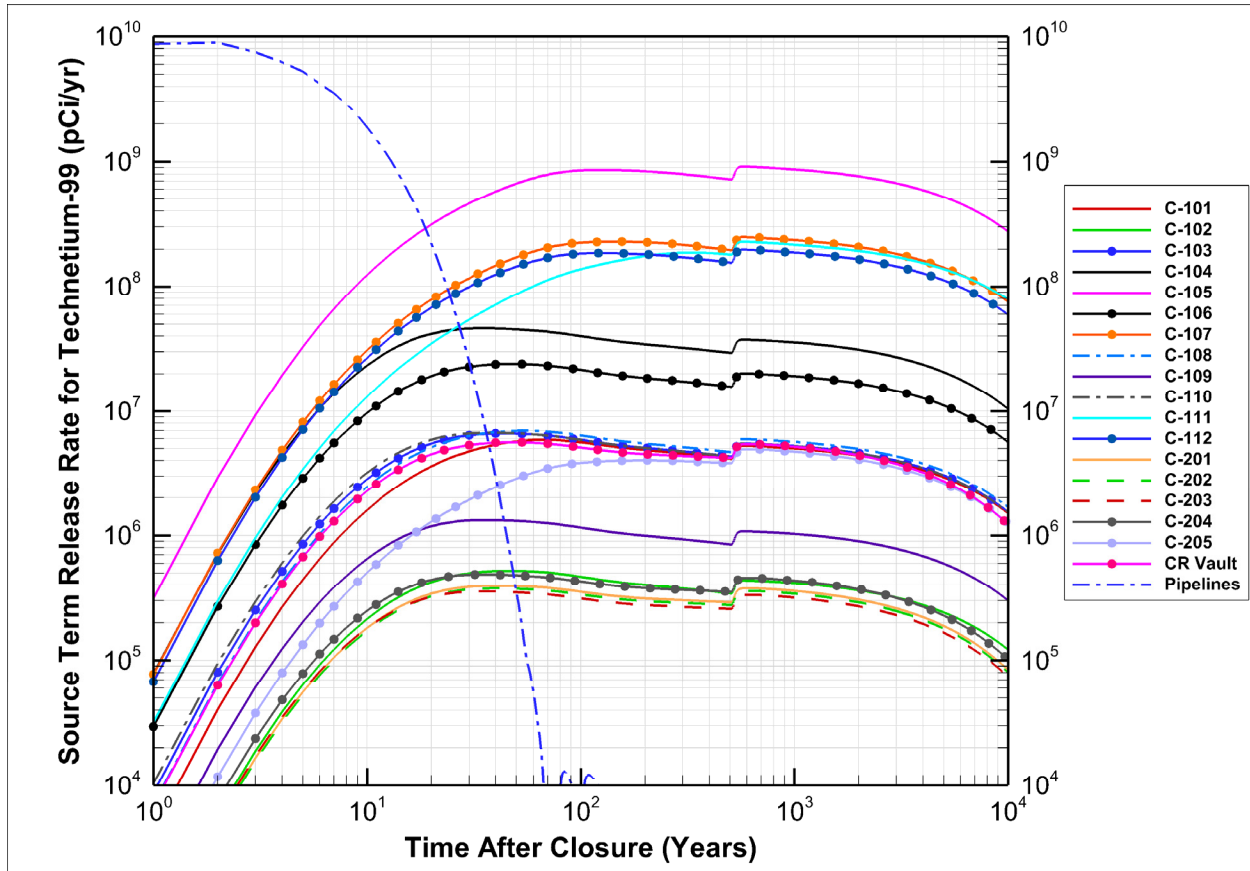
7
8 The base case release rate for ^{99}Tc from each of the sources in the source term is presented in
9 Figure 7-1. An initial large release rate occurs for the pipeline source, and is attributable to the
10 assumption that releases from the pipelines are dominated by advection. The sharp decline in the
11 release rate is a reflection of source inventory depletion, and to a lesser extent of declining flow
12 rate as the system responds to the placement of the cover. At closure (during emplacement of
13 surface cover), the recharge rate changes from 100 mm/yr (3.9 in./yr) (operations time period) to
14 the early Post-Closure recharge rate of 0.5 mm/yr (0.02 in./yr) (over 500 years). As a result, the
15 vertical flow rate through the vadose zone adjusts slowly to the imposed boundary conditions.
16 Nearly all of the ^{99}Tc inventory associated with the pipeline source term is released by
17 approximately 100 years after closure (see Figure 7-1). In contrast, the release rate from grouted
18 tanks increases gradually. This is partly attributable to an initial small release fraction (6%) of
19 the ^{99}Tc inventory that is available for instantaneous release, while the rest of the inventory is
20 made available gradually, reflecting waste form degradation process (see Section 6.3.1).
21 However, the gradual release occurs over a relatively short time, and the primary control for the
22 tank release rates is the diffusive transport through the tank base mat with associated sorption.

23
24 The magnitude of release rates for ^{99}Tc from each source is proportional to the chemical gradient
25 as determined by the amount of residual inventory of ^{99}Tc within each source. Therefore, the
26 release rate from tank C-105 is the highest since it has the highest residual inventory (7.83 Ci at
27 closure). Releases from tank C-107, tank C-111, and tank C-112 have similar releases rates, as
28 they have similar residual inventories of ^{99}Tc (~2 Ci each). The release rate from other sources
29 is much smaller, owing to their smaller inventories.

30
31 The small rise in release rate noticeable at about 500 years is due to an increase in Darcy flux,
32 when the surface barrier is assumed to transition to its degraded state and the recharge rate
33 changes from 0.5 mm/yr (0.02 in./yr) to 3.5 mm/yr (0.14 in./yr). The diffusive release rate
34 shows a slow gradual decline over the simulated time period, indicating that not all of the
35 inventory of ^{99}Tc has been released by 10,000 years.

36
37 Figure 7-2 compares the concentration resulting from release of ^{99}Tc from the waste to that from
38 the bottom of the tank base mat. There is a sharp initial spike in concentration due to the initial
39 release fraction, followed by a gradual decrease in concentration. However, the concentrations
40 exiting the tank base mat bottom show an initial increase reflecting the establishment of a steady
41 concentration gradient through the base mat. The concentration then slowly decreases as the
42 inventory is slowly depleted by diffusion.

RPP-ENV-58782, Rev. 0

Figure 7-1. Release Rate of Technetium-99 (pCi/yr) from Each Source.

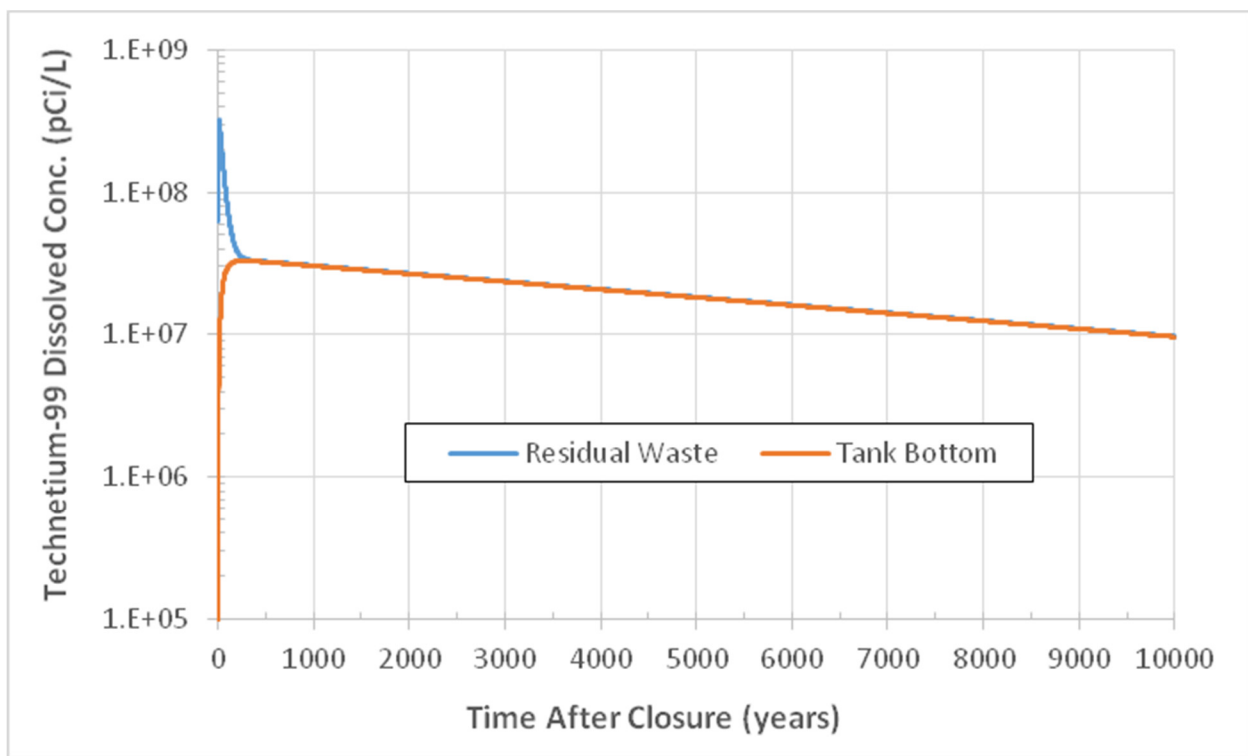
The release rate for ²³⁸U from selected sources is presented in Figure 7-3; these sources illustrate representative behavior of the other sources in WMA C. The uranium solubility limits in the source cause the ²³⁸U concentrations for several sources terms to be the same, and therefore only selected sources are presented in the figure. As discussed in Section 6.2.1, when the tank and infill grout are intact, the uranium solubility limit is set to 1 × 10⁻⁴ mol/L for the first 1,000 years and to 1 × 10⁻⁶ mol/L thereafter. Figure 7-4 presents two curves of the time-varying dissolved ²³⁸U concentrations; one exiting the residual waste, and the other exiting out the bottom of the tank base mat for tank C-105. The general trends of these curves for tank C-105 provide a good example of the general shape of the similar curves for dissolved ²³⁸U concentrations from other 100-series tanks. The concentrations released from the residual waste remain constant, consistent with the solubility limits, including the assumed step change at 1,000 years. This indicates that there is sufficient inventory of uranium retained in the tanks to maintain the solubility limit at the end of the simulation. The concentration leaving the tank remains at least an order of magnitude below the concentration leaving the residual waste, consistent with the sorption in the concrete and grout matrix.

The difference in release rates between tank C-105 and tank C-201 (Figure 7-3) are the result of different diffusive areas (tank bottom area). The release rate from the pipelines, as previously discussed, is primarily by advection, and therefore shows markedly different behavior. The pipeline release rate shows an initial decline, followed by increase at around 500 years and then

RPP-ENV-58782, Rev. 0

steep decline at around 700 years. The first 700 years reflect the transient effect of changing recharge as the system responds—first, to the addition of the closure cover, and second, to the assumed degradation of the cover function. The steep decline after 700 years is attributable to depletion of the pipeline inventory, such that dissolved concentrations drop below the solubility limit. The long-term gradual decline following the steep decline reflects the effect of near-field concentrations on advective and diffusive releases through the pipeline. As the released uranium mass moves slowly through the vadose zone, some backward diffusion occurs to the source inventory cell due to reversal of concentration gradient (for the pipeline). This mass then diffuses out of the inventory cell, resulting in a slowly declining release.

Figure 7-2. Comparison of Dissolved Concentration of Technetium-99 (pCi/L) in the Residual Waste and Tank Bottom for Tank 241-C-105.



The release rates for uranium (total) from representative sources are presented in Figure 7-5. These exhibit similar behavior to the release rates for ^{238}U , as expected.

For all other analytes modeled, the releases are simpler, as no solubility limits or waste form degradation mechanisms are considered. For pipelines, the release is primarily by advection. For the remaining sources, where intact grouted tank conditions are assumed, the release mechanism is diffusion through the tank base mat. The effective diffusion coefficient for all of the analytes through the concrete and grout layer is $3 \times 10^{-8} \text{ cm}^2/\text{s}$ ($4.7 \times 10^{-8} \text{ in.}^2/\text{s}$) (based on the half-cell diffusion experiments conducted on ^{99}Tc). Differences in diffusion behavior are the result of different partition coefficients (K_d), so that different apparent diffusion coefficients are applied to each analyte.

RPP-ENV-58782, Rev. 0

Figure 7-3. Release Rate of Uranium-238 (pCi/yr) from Representative Source Terms.

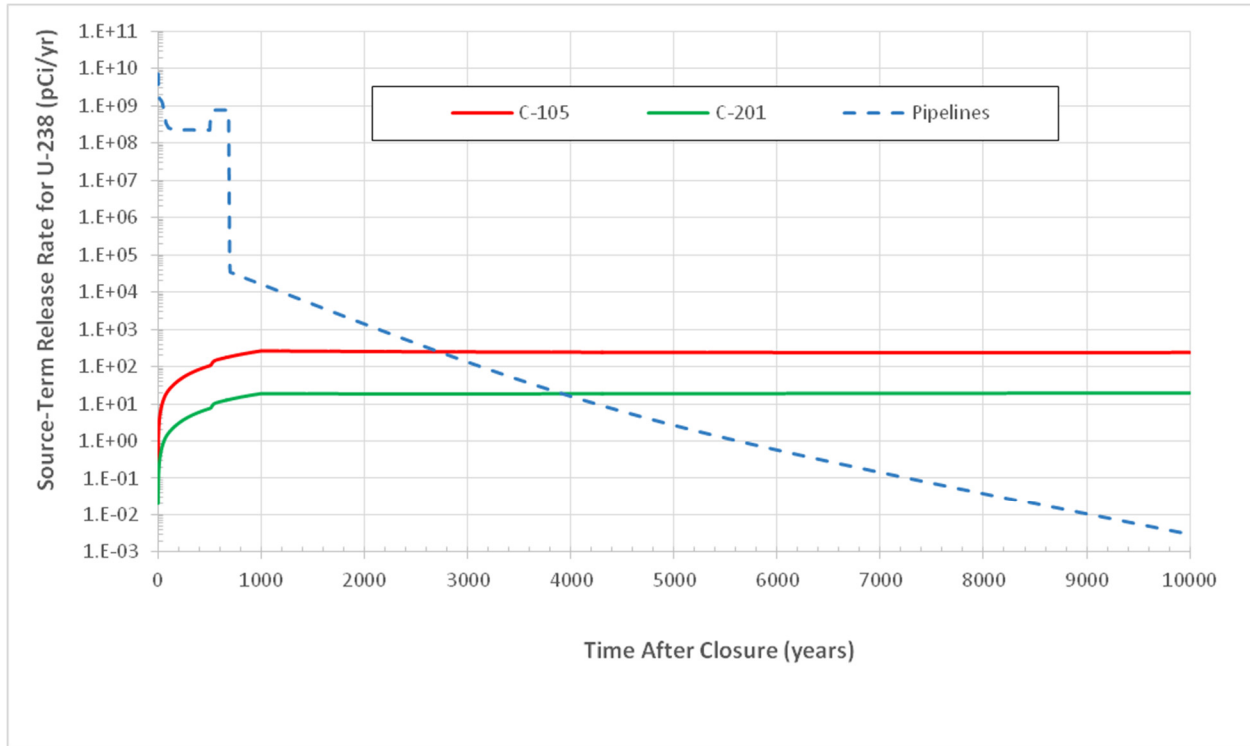
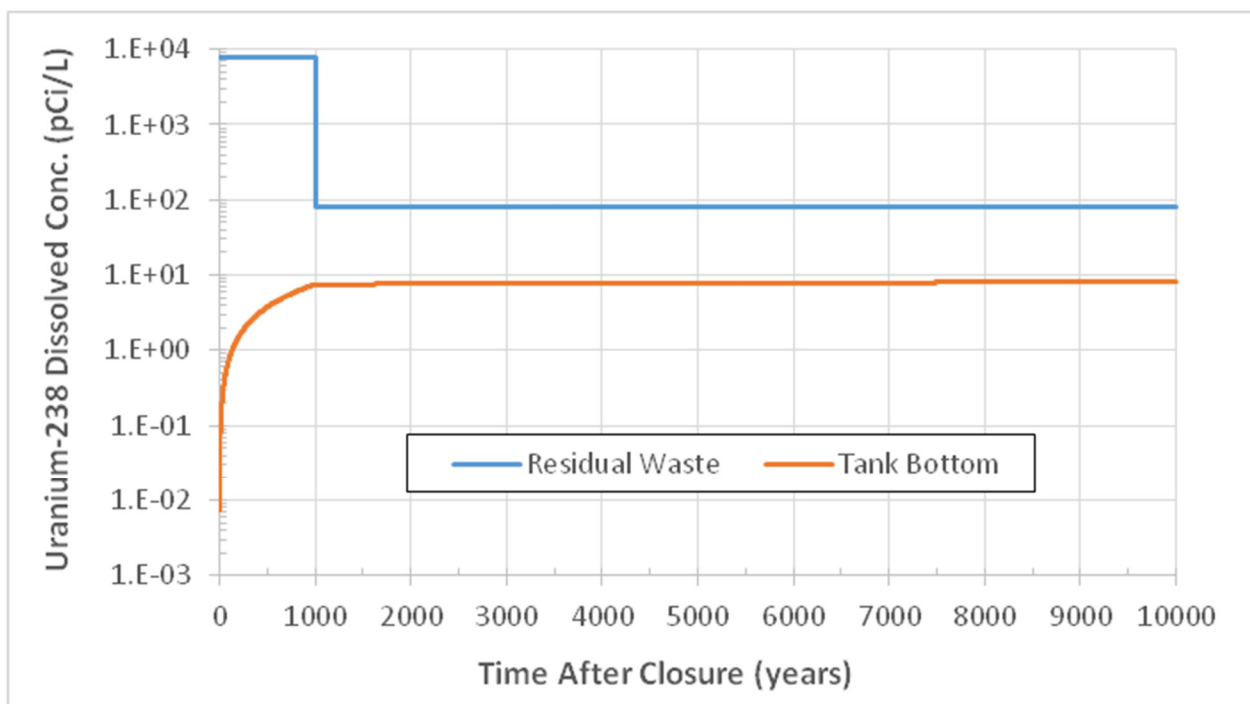
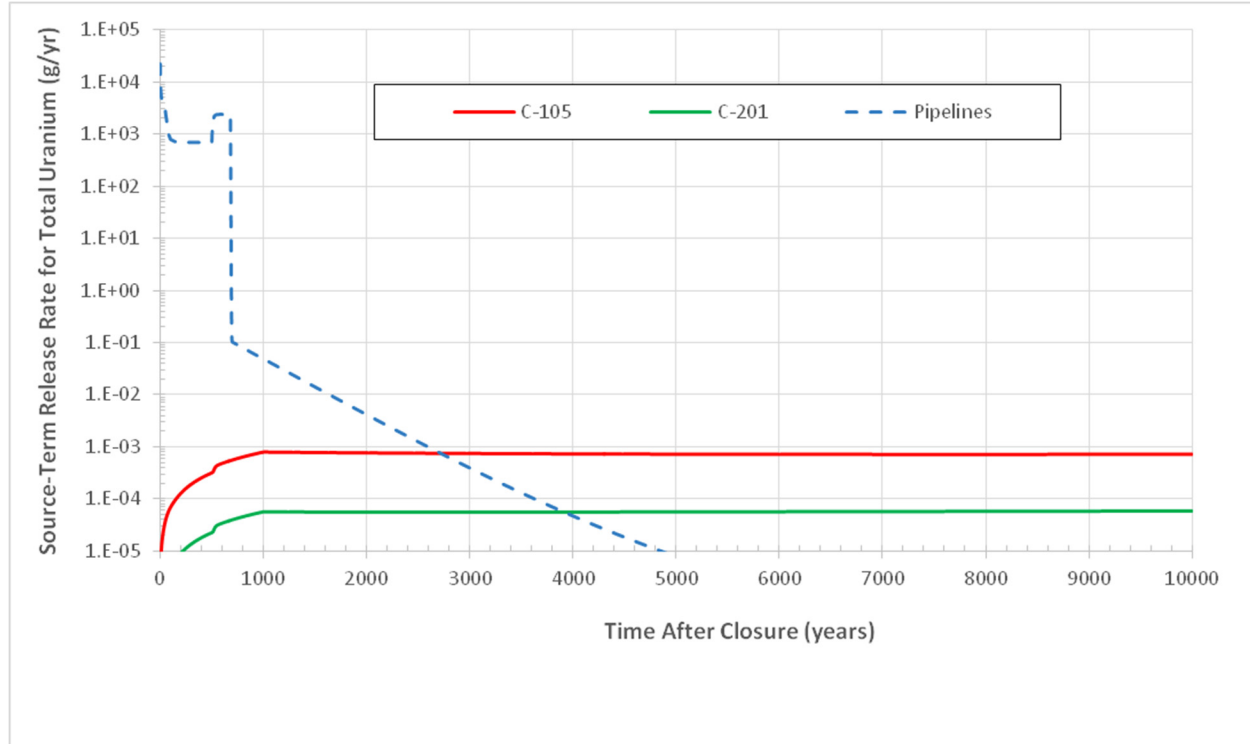


Figure 7-4. Comparison of Dissolved Concentration of Uranium-238 (pCi/L) in the Residual Waste and Tank Bottom for Tank 241-C-105.



RPP-ENV-58782, Rev. 0

Figure 7-5. Release Rate of Total Uranium (g/yr) from Representative Sources.

7.2 ENVIRONMENTAL TRANSPORT OF RADIONUCLIDES

This section presents the results of the analysis of the environmental transport of radionuclides for the groundwater pathway (Section 7.2.1) and the air pathway (Section 7.2.2). Tabular and graphical presentations of the summaries of the various transport calculations in water and air are presented. Discussions included in the air pathway results summarize the results of the transport of volatile radionuclides and transport analysis for radon.

7.2.1 Groundwater Transport of Radionuclides

This section presents the results of the analysis of the groundwater transport of radionuclides for the groundwater pathway, including its screening analysis. Tabular and graphical presentations of the summaries of the various transport calculations are presented. Discussions included in the air pathway results summarize the results of the volatile radionuclides and transport analysis for radon.

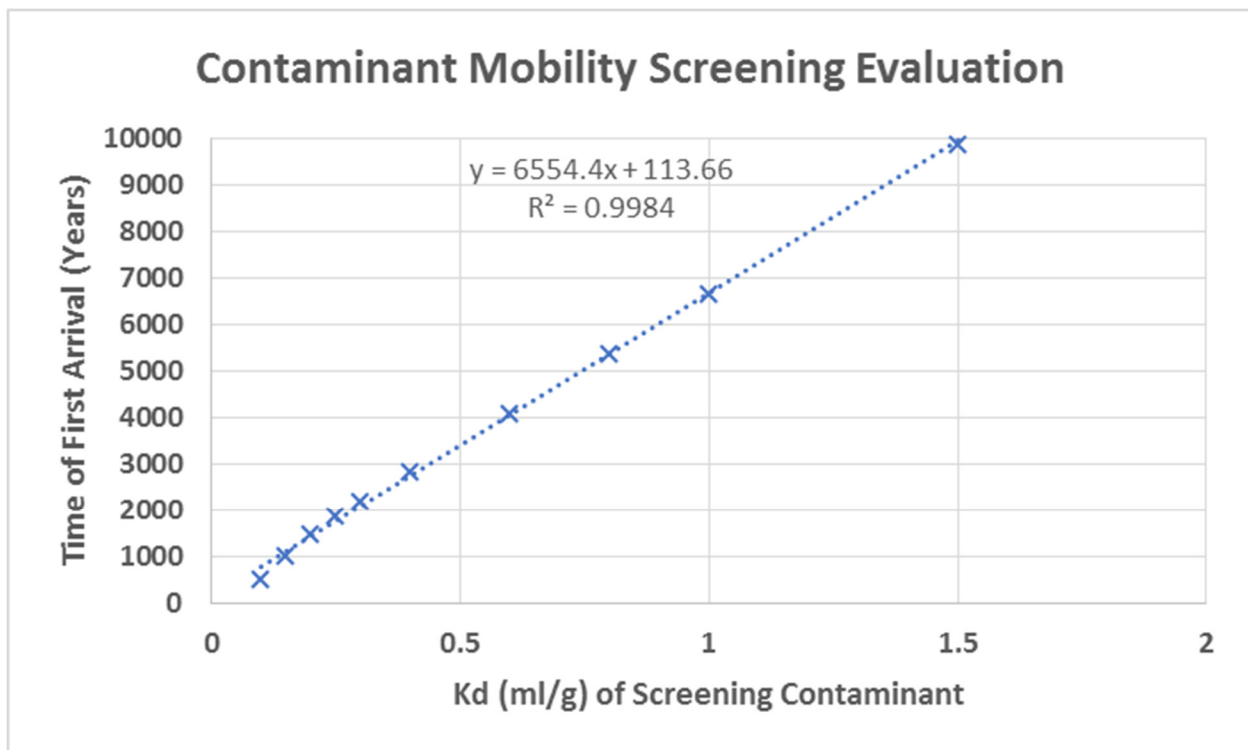
7.2.1.1 Result of Screening Analysis for Groundwater Pathway. The STOMP® 3-D groundwater flow and transport model was used to perform a screening analysis to identify those contaminants that are not sufficiently mobile to impact groundwater during the compliance and sensitivity/uncertainty analysis time frames. This screening step helps to streamline the PA, and to focus attention on the contaminants that affect performance.

RPP-ENV-58782, Rev. 0

The criterion chosen for screening is the first-arrival time of the contaminant. Hydraulic property selection was carried out to yield maximum transport rates. Maximum net infiltration rates were also assumed in the screening analysis. The screening evaluated an incremental range of K_d values between 0.1 mL/g and 2.5 mL/g (prior to gravel correction) to determine threshold values that reached the water table in 1,000 and 10,000 years. The use of screening methods is accepted by the EPA, and appropriate methods are outlined in EPA guidance (EPA/540/F-95/041, Soil Screening Guidance: Fact Sheet). This approach minimizes the number of contaminants eliminated from analysis. As a result, some contaminants may only arrive at the water table for particular sensitivity and uncertainty evaluations (i.e., evaluations that minimize the time of transport through the vadose zone). For the base case and many of the sensitivity cases, a number of the radionuclide contaminants not screened from further analysis may have no impact on the PA results because their transport to the water table requires more than 1,000 years (compliance time frame) or 10,000 years (the limit of the uncertainty/sensitivity analysis) for that particular case.

Results of the screening analysis are presented in Figure 7-6. The results show that the time of first arrival is a strong linear function of the K_d value. From this relationship, the first-arrival time for any radionuclide can be estimated accurately by using the trend equation shown on the figure. According to the screening model results, the minimum K_d value that produces an impact to groundwater within the 1,000-year compliance time frame is ~0.15 mL/g (without any gravel correction), and ~1.5 mL/g (without any gravel correction) within the 10,000-year compliance time frame.

Figure 7-6. First-Arrival Time (in Calendar Year) of Radionuclides for Various K_d Values Based on Screening Analysis Using Subsurface Transport Over Multiple Phases.



RPP-ENV-58782, Rev. 0

The first-arrival times for each of the representative K_d values used in the screening calculations using STOMP[®] are summarized in Table 7-1. The results of the screening analysis indicate that even when using parameter estimates biased to produce the greatest pore water velocity in the vadose zone: (1) contaminants with a $K_d > 0.15$ mL/g do not reach groundwater within the 1,000-year compliance time frame, and (2) radionuclides with a $K_d \geq 2.0$ mL/g do not reach groundwater within the 10,000-year post-compliance (i.e., uncertainty/sensitivity analysis) period (Table 7-1). While the actual K_d cutoff is likely only slightly greater than 1.5 mL/g, the screening evaluation did not include a representative contaminant with a K_d value between 1.5 mL/g and 2 mL/g (Table 6-11).

Table 7-1. First-Arrival Time (in Calendar Year) of Radionuclides for Various K_d Values Based on Screening Analysis Using Subsurface Transport Over Multiple Phases.

Contaminant K_d (material < 2 mm) (mL/g)	Calendar Year of First Arrival at Water Table	Time of Arrival, Post-Closure (Closure occurring in 2020) Years
0.10	2517.5	497.5
0.15	3022.5	1,002.5
0.20	3505	1,485
0.25	3900	1,880
0.30	4210	2,190
0.40	4840	2,820
0.60	6110	4,090
0.80	7390	5,370
1.0	8680	6,660
1.5	11900	9,880
2.0	>12020	>10,000
2.5	>12020	>10,000

Of the list of radionuclides in the WMA C residuals inventory and on the basis of the results of the screening phase, only seven (Table 7-2) are sufficiently mobile to arrive at groundwater during the compliance period, and three others (e.g., ¹²⁹I, ¹⁴C, and the uranium isotopes) are sufficiently mobile to arrive at groundwater during the sensitivity/uncertainty analysis time frame. The other radionuclides in the WMA C residual inventory are not included in further groundwater impact analysis because they do not reach the water table within the evaluation time frames.

To complement the results of this screening analysis, an additional evaluation case was run to evaluate the peak doses for all 43 radiological COPCs beyond the 10,000-year post-closure time frame. The primary focus of this analysis is to evaluate the time and magnitude of peak doses resulting from some selected constituents, like the uranium isotopes (that were found to be rising at the end of the 10,000-year period analysis) and other sorbed constituents that could potentially

RPP-ENV-58782, Rev. 0

reach groundwater beyond the 10,000-year post-closure time frame. The specific assumptions of this evaluation case and its associated results are provided in Section 8.2.8 of this report.

Table 7-2. Radionuclides that Arrive at the Water Table within the 1,000-Year Compliance and 10,000-Year Sensitivity and Uncertainty Time Frame Based on the Screening Analysis Conducted Using Subsurface Transport Over Multiple Phases.

Radionuclides	K _d (material < 2 mm) (mL/g)	K _d (Backfill) (mL/g)	K _d (Hanford H1 and H3) (mL/g)	K _d (Hanford H2) (mL/g)
Radionuclides that may arrive at the water table within 1,000 years				
Co Isotopes	0	0	0	0
H Isotopes	0	0	0	0
Nb Isotopes	0	0	0	0
Rn Isotopes	0	0	0	0
Tc Isotopes	0	0	0	0
Se Isotopes	0.1	0.05	0.06	0.08
I Isotopes	0.2	0.09	0.12	0.16
Radionuclides that may arrive at the water table within 10,000 years				
Sn Isotopes	0.5	0.23	0.29	0.4
U Isotopes	0.6	0.28	0.35	0.48
C Isotopes	1	0.46	0.58	0.8

7.2.1.2 Results of Base Case Evaluation for Groundwater Pathway.

7.2.1.2.1 Flow Analysis. The moisture content in the vadose zone underneath WMA C changes in response to changes in the recharge imposed by the surface conditions. This includes an increase in moisture content that occurs during the operations period, and an eventual decrease in moisture content caused by the performance of the surface barrier. The moisture content is also influenced by the presence of the tank structures, which divert the water around the low permeability structures. For the base case, the tank structures are assumed to remain intact for the duration of the analysis.

The calculated moisture content profile at tank C-105 is presented in Figure 7-7(a-d) for the base case inputs for flow, for four times in the evolution of the facility. The pre-Hanford profile is shown in Figure 7-7(a). This profile provides a reference point for the subsequent behavior of the system in response to changes in the net infiltration rates. The range for the Hanford H2 Sands is from 0.059 to 0.060 for the pre-Hanford time period. The moisture content profile at the time of closure, when the surface barrier has just been constructed, is shown in Figure 7-7(b). This moisture profile is higher relative to the pre-Hanford profile, ranging from 0.076 to 0.088 in the Hanford H2 Sands, owing to the elevated net infiltration during the operational period. The response after 100 years to the construction of the surface barrier is shown in Figure 7-7(c). The

RPP-ENV-58782, Rev. 0

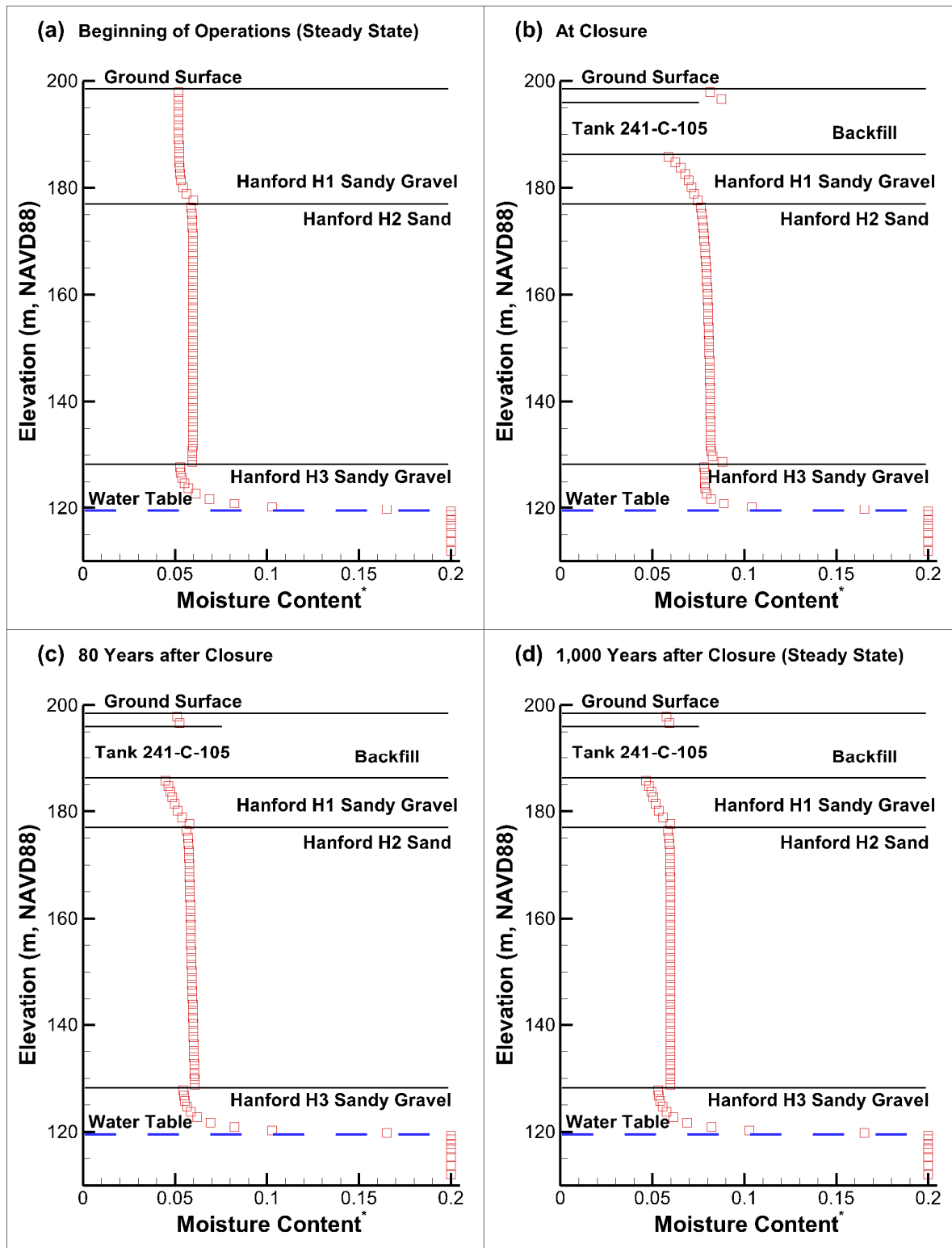
1 moisture content has decreased as the system responds to the lower recharge produced by the
2 surface barrier; the range for the Hanford H2 Sands is from 0.056 to 0.061. In the base case
3 analysis, the surface barrier is assumed to degrade after 500 years, leading to a return to a
4 pre-Hanford recharge rate. As shown in Figure 7-7(d), by 1,000 years after closure the system
5 has re-equilibrated to a steady-state moisture regime, with a moisture content profile similar to the
6 pre-Hanford moisture content distribution shown in Figure 7-7(a).

7
8 Throughout this evolution, the changes in the moisture content profile are relatively small, despite
9 the changes in net infiltration at the surface. These results are consistent with the hydraulic
10 conductivity-moisture content relationships presented for the HSUs in Appendix B. The
11 pre-Hanford and Hanford operations recharge rates, 3.5 mm/yr and 100 mm/yr (0.14 in./yr and
12 3.9 in./yr), respectively, translate to vertical unit gradient fluxes of 1.1×10^{-8} cm/s and
13 3.7×10^{-7} cm/s (4.3×10^{-9} in./s and 1.5×10^{-7} in./s), respectively. According to Figure B-13, the
14 equilibrium matric potential values of Hanford H2 Sand for unsaturated hydraulic conductivity
15 values of 1.1×10^{-8} cm/s and 3.7×10^{-7} cm/s (4.3×10^{-9} in./s and 1.5×10^{-7} in./s) are 190 cm and
16 90 cm (75 in. and 35 in.), respectively. According to Figure B-12, the equilibrium moisture
17 content values of Hanford H2 Sand for matric potential values of 190 cm and 90 cm (75 in. and
18 35 in.) are ~0.061 and 0.085, respectively, which is consistent with the range of values indicated
19 in Figure 7-7.

20
21 The calculated moisture content profile for a location between four 100-series tanks (C-105,
22 C-106, C-108, and C-109) is presented in Figure 7-8. The pre-Hanford profile and range in
23 Hanford H2 Sand moisture content shown in Figure 7-8(a) is almost identical to the profile
24 shown in Figure 7-7(a) because the two locations are so close and the geology is essentially the
25 same. Similar to Figure 7-7(a), Figure 7-8(a) provides a reference point for the subsequent
26 behavior of the system in response to changes in the net infiltration rates. The moisture content
27 profile at the time of closure shown in Figure 7-8(b) indicates that the moisture content, ranging
28 from 0.083 to 0.089 in the Hanford H2 Sands, is elevated compared to both the pre-Hanford
29 profile and the profile shown in Figure 7-7(b). The increase in moisture content compared to
30 Figure 7-7(b) results from the tank umbrella effect that diverts infiltrating water from the tank
31 domes to the area(s) surrounding the tanks. The response 100 years after closure is shown in
32 Figure 7-8(c). It is almost identical to the response below tank C-105 shown in Figure 7-7(c)
33 because with the surface barrier limiting net infiltration to 0.5 mm/yr (0.02 in./yr), the tank
34 umbrella effect becomes inconsequential. By 1,000 years after closure the system has
35 re-equilibrated to a steady-state moisture regime (Figure 7-8[d]). The moisture content profile
36 appears very similar to the pre-Hanford moisture content profile shown in Figure 7-8(a), and
37 Figure 7-7(a) and 7-7(d) below tank C-105.

RPP-ENV-58782, Rev. 0

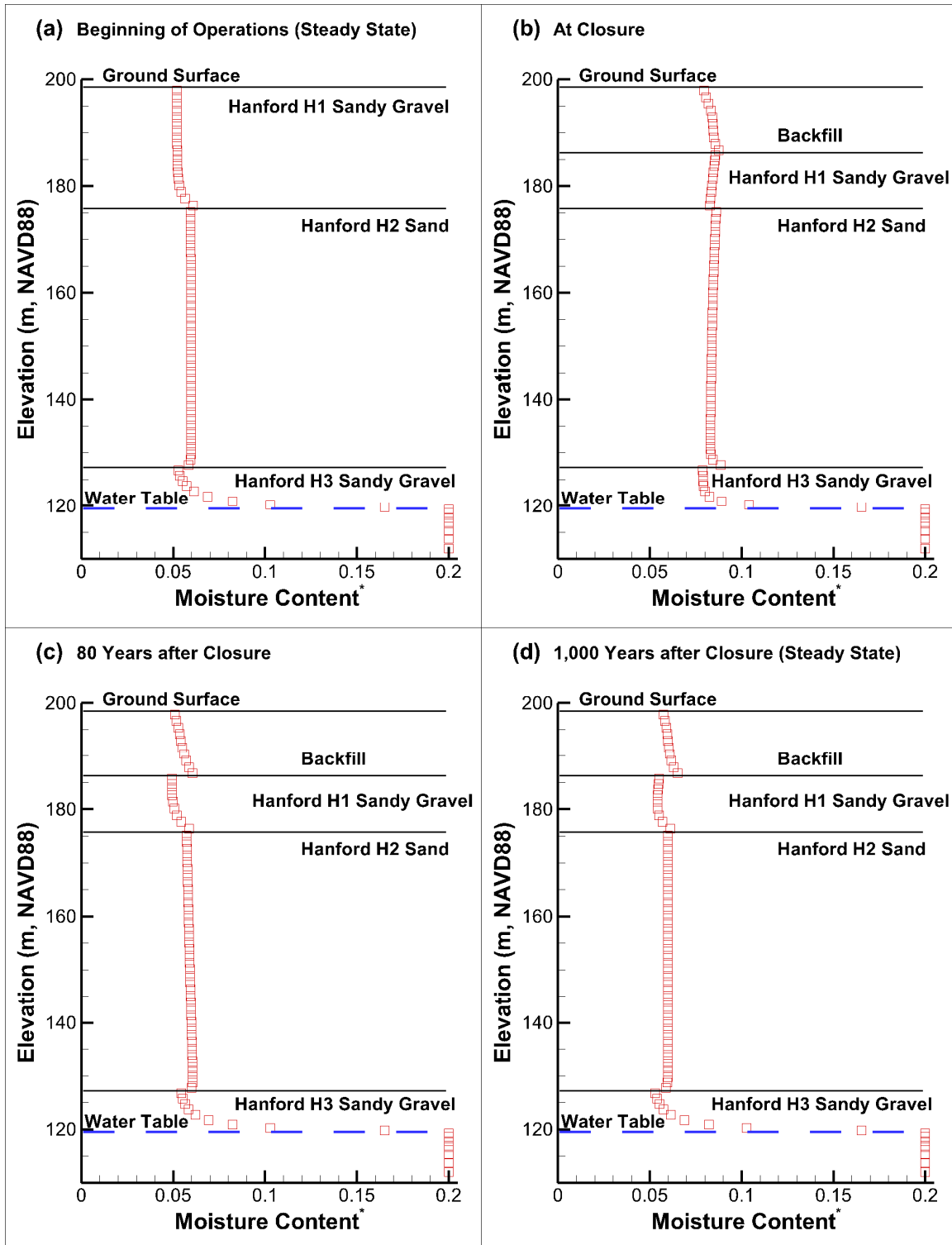
Figure 7-7. Moisture Content in the Vadose Zone at Tank 241-C-105 in Waste Management Area C for Four Times of Interest: (a) Pre-Hanford Steady State, (b) Waste Management Area C Closure, (c) 100 Years after Closure, and (d) At 1,000 Years.



*The moisture content below the water table is equal to the porosity.

RPP-ENV-58782, Rev. 0

Figure 7-8. Moisture Content in the Vadose Zone in Waste Management Area C between Tanks 241-C-105, 241-C-106, 241-C-108, and 241-C-109 for Four Times of Interest:
(a) Pre-Hanford Steady State, (b) Waste Management Area C Closure,
(c) 100 Years after Closure, and (d) At 1,000 Years.



*The moisture content below the water table is equal to the porosity.

RPP-ENV-58782, Rev. 0

1 By contrast, the changes in the vertical Darcy flow rate or flux are more apparent than the
2 changes in moisture content. Changes in the flux are going to be almost directly proportional to
3 the changes in net infiltration, except where and how the tank shadow and umbrella effects
4 influence the flow. The shadow effect of the tank appears most prominently immediately below
5 the base and diminishes throughout the depth. Prior to construction of the tanks, the vertical
6 velocity is essentially uniform, with only minor variations at the interfaces between soil units, as
7 shown in Figure 7-9(a). For the remaining times, immediately below the tanks a shadow effect is
8 observed, in which the velocity approaches zero, as shown in Figure 7-9(b-d). The shadow
9 effect is strongest in the H1 layer, and remains throughout the simulation. The depth and extent
10 of the shadow zone in the H2 layer is affected by the changing recharge on the system. The flux
11 approaches the recharge rate imposed at the surface at the greater depths, increasing toward the
12 value imposed at the surface (Figure 7-9[b] and [c]). The shape of the velocity profile shown in
13 Figure 7-9(c) reflects the drainage of antecedent moisture once the surface barrier is added,
14 indicating the velocity near the water table is the last to achieve steady state [compare
15 Figure 7-9(c) and (d)].
16

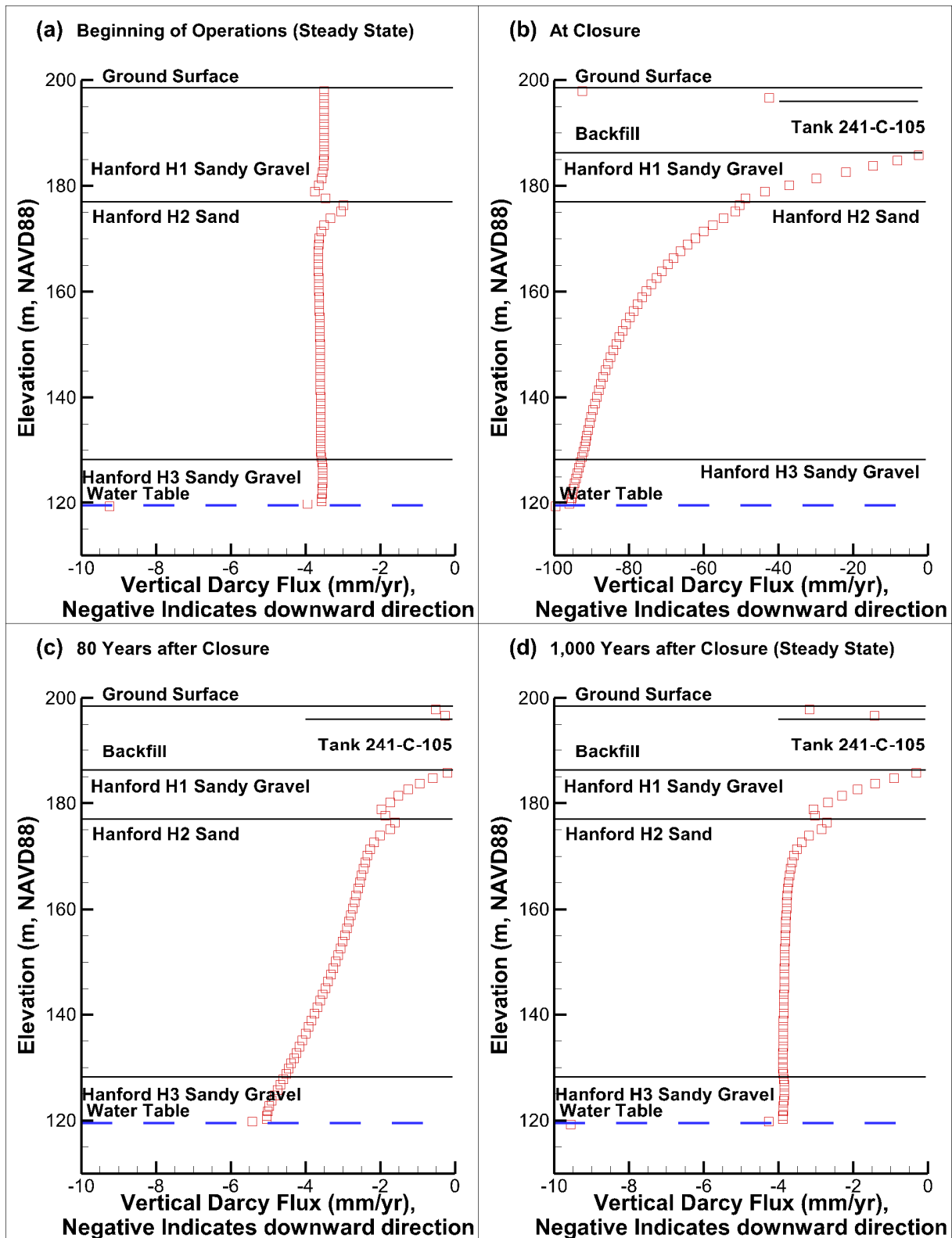
17 Figure 7-9(d) shows the response to the degradation of the surface barrier, and the velocity
18 profile in the H2 layer is similar to the pre-Hanford conditions shown in Figure 7-9(a). By
19 1,000 years post-closure, the moisture profile reaches a condition of nearly uniform downward
20 flow, particularly in the Hanford H2 Sand, reflective of the 3.5 mm/yr (0.14 in./yr) recharge
21 imposed in the modeling domain [see Figure 7-7(d)].
22

23 The consequences of the umbrella effect appear most prominently in the area between the tanks
24 (Figure 7-10). Figure 7-10(a) indicates that the flux prior to tank farm construction is fairly
25 uniform throughout the depth, similar to Figure 7-9(a). Once the tanks are present, the umbrella
26 effect diverts and concentrates infiltrating water between them, and the flux in the backfill
27 approaches almost twice the recharge rate imposed at the surface [Figure 7-10(b)]. At greater
28 depths, the umbrella effect dissipates and the flux approaches the recharge rate imposed at the
29 surface.
30

31 Figure 7-10(c) illustrates the transient conditions that occur after the surface barrier is emplaced.
32 Eighty years is not sufficient to reach steady state as indicated by the non-uniform flux profile.
33 The umbrella effect continues to concentrate water introduced during the operations period
34 between the tanks while it drains, but the flux in the shallower depths, both near the surface and
35 in the Hanford H1 Sandy Gravel, responds more quickly to changes in the recharge rate imposed
36 at the surface. Throughout the Hanford H2 Sand, the flux is decreasing compared to the
37 operation period [compare Figure 7-10(c) and (b)], but the flux has not achieved steady state, as
38 indicated by the non-uniform profile. After 1,000 years [Figure 7-10(d)], the profile below the
39 depths impacted by the umbrella effect appears fairly uniform, indicating that the system has
40 achieved steady state.
41

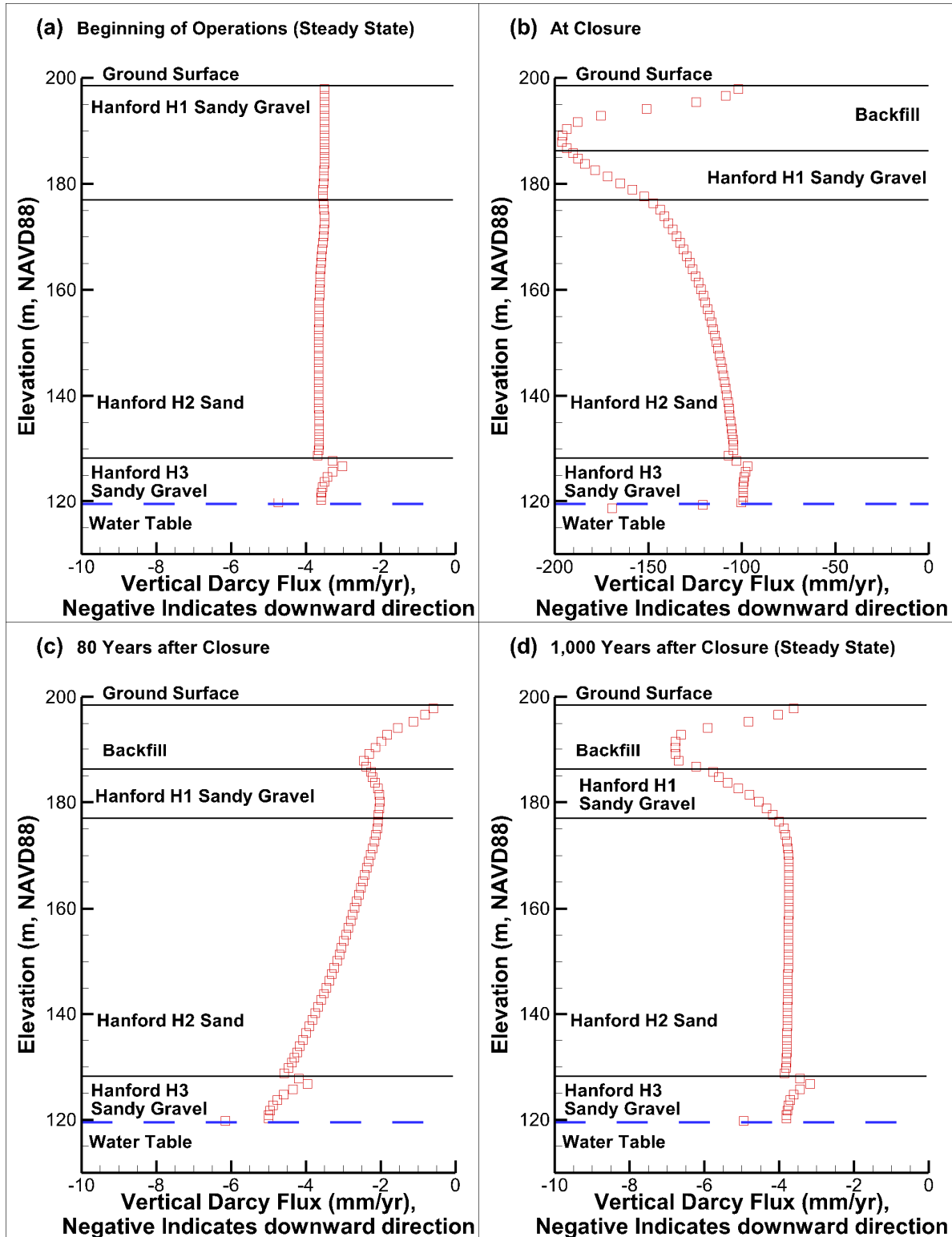
RPP-ENV-58782, Rev. 0

Figure 7-9. Darcy Flux in the Vadose Zone at Tank 241-C-105 in Waste Management Area C for Four Times of Interest: (a) Pre-Hanford Steady State, (b) Waste Management Area C at Closure, (c) 100 Years after Closure, and (d) At 1,000 Years after Closure.



RPP-ENV-58782, Rev. 0

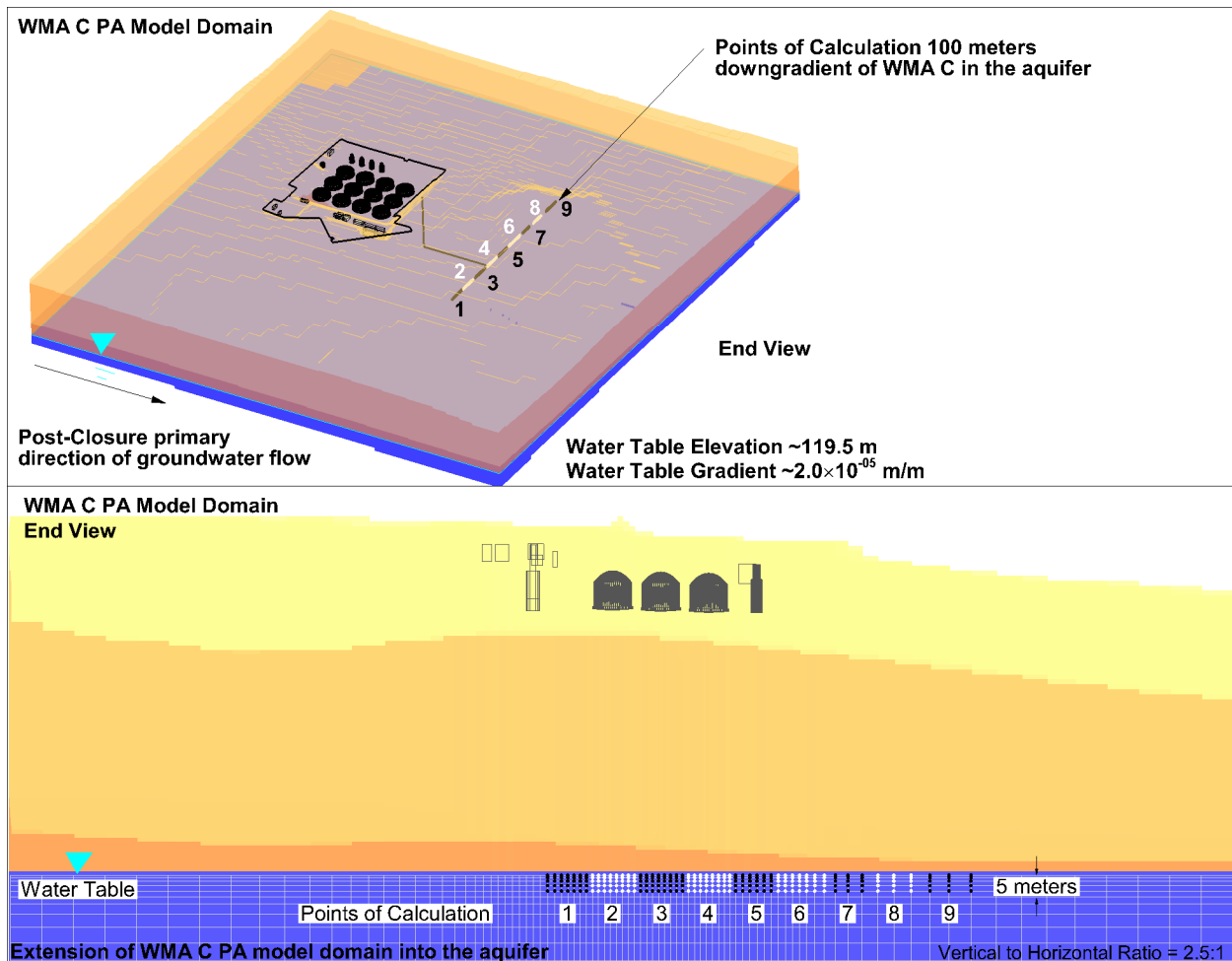
Figure 7-10. Darcy Flux in the Vadose Zone in Waste Management Area C between Tanks 241-C-105, 241-C-106, 241-C-108, and 241-C-109 for Four Times of Interest:
(a) Pre-Hanford Steady State, (b) Waste Management Area C at Closure,
(c) 100 Years after Closure, and (d) At 1,000 Years after Closure.



RPP-ENV-58782, Rev. 0

7.2.1.2.2 Transport Analysis. DOE M 435.1-1 requires that the WMA C PA includes calculations of the highest calculated concentration or dose, with an allowance for some volume averaging based on projected groundwater use, beyond a 100-m (328-ft) buffer zone surrounding WMA C. To determine the highest groundwater concentration, the modeling results indicate the average concentration in the aquifer within nine segments along the line perpendicular to, and 100 m (328 ft) beyond, the southeast edge of WMA C (Figure 7-11). The nine segments are ~30 m (98 ft) long (see Table D-11 in Appendix D), and aligned such that the centerlines of the plumes in the groundwater resulting from the residuals released from a single line of 100-series tanks parallel to the direction of groundwater flow (e.g., the centerline of the plumes resulting from the tank residuals in C-102, C-105, C-108, and C-111) intersect the perpendicular line within the same segment.

Figure 7-11. Points of Calculation 100 Meters Downgradient of Waste Management Area C.



PA = Performance Assessment

WMA = Waste Management Area

DOE M 435.1-1 does not specify the level of protection required for water resources and there are no applicable parameterization requirements or guidelines indicated in DOE G 435.1-1, Chapter 4. The DOE manual and guide state that the aquifer mixing must be consistent with

RPP-ENV-58782, Rev. 0

State or local laws, regulations, or agreements. EPA/540/R-95/128, Soil Screening Guidance: Technical Background Document and WAC 173-340-747 imply that the cross section width ought to equal the width of contamination entering the aquifer. Other PAs conducted at Hanford and other DOE facilities have used an aquifer mixing width equal to the width of the facility (e.g., WCH-520, “Performance Assessment for the Environmental Restoration Disposal Facility, Hanford Site, Washington”; WSRC-MS-2003-00582, “Performance Assessment/Composite Analysis Modeling to Support a Holistic Strategy for the Closure of F Area, a Large Nuclear Complex at the Savannah River Site”). As indicated previously, the width of the PoCal segments is sufficient to intercept the centerline of the plumes resulting from the tank residuals from a single line of 100-series tanks, which appears consistent with the intent of EPA/540/R-95/128 and WAC 173-340-747. The aquifer mixing zone extends into the upper 5 m (16.4 ft) of the aquifer on the basis of the 4.5 m (15 ft) well screen length (and mixing zone dimension) associated with state monitoring well descriptions (e.g., see Equation 747-4 in WAC 173-340-747).

Results of Base Case Evaluation for Groundwater Pathway for the Compliance Period

1,000 Years After Closure. The results of the base case modeling indicate that only contaminants with K_d values equal to zero reach the PoCals within the DOE O 435.1 compliance period of 1,000 years (Table 7-3). Among radionuclides, the only contaminant producing nonzero concentrations at 100 m from the WMA C fenceline in the compliance period is ^{99}Tc . Other mobile contaminants such as ^3H , ^{60}Co , and $^{93\text{m}}\text{Nb}$ decay to insignificant quantities before reaching the water table. The maximum concentration of ^{99}Tc in groundwater during this period is 0.1 pCi/L, which is a factor almost 4 orders of magnitude less than its MCL.

Concentration contours of ^{99}Tc in the vadose zone at 1,000 years are shown in Figure 7-12. Releases from the pipelines, vault, and tank residuals have reached the water table, but the center of the ^{99}Tc mass remains about halfway through the vadose zone above the water table. Immediately below WMA C, concentrations in groundwater are about 0.5 pCi/L.

Concentration contours of radionuclides with nonzero values of K_d are shown in Figure 7-13 (^{129}I , $K_d = 0.2 \text{ mL/g}$) and Figure 7-14 (^{238}U , $K_d = 0.6 \text{ mL/g}$) at 1,000 years. During the compliance period, both are contained within the Hanford H1 sandy gravel unit and upper H2 sandy unit, ~60 m (197 ft) above the water table (Figures 7-13 and 7-14). These contaminants do not reach the water table within 1,000 years.

Results of Base Case Evaluation for Groundwater Pathway for the Period Between 1,000 to

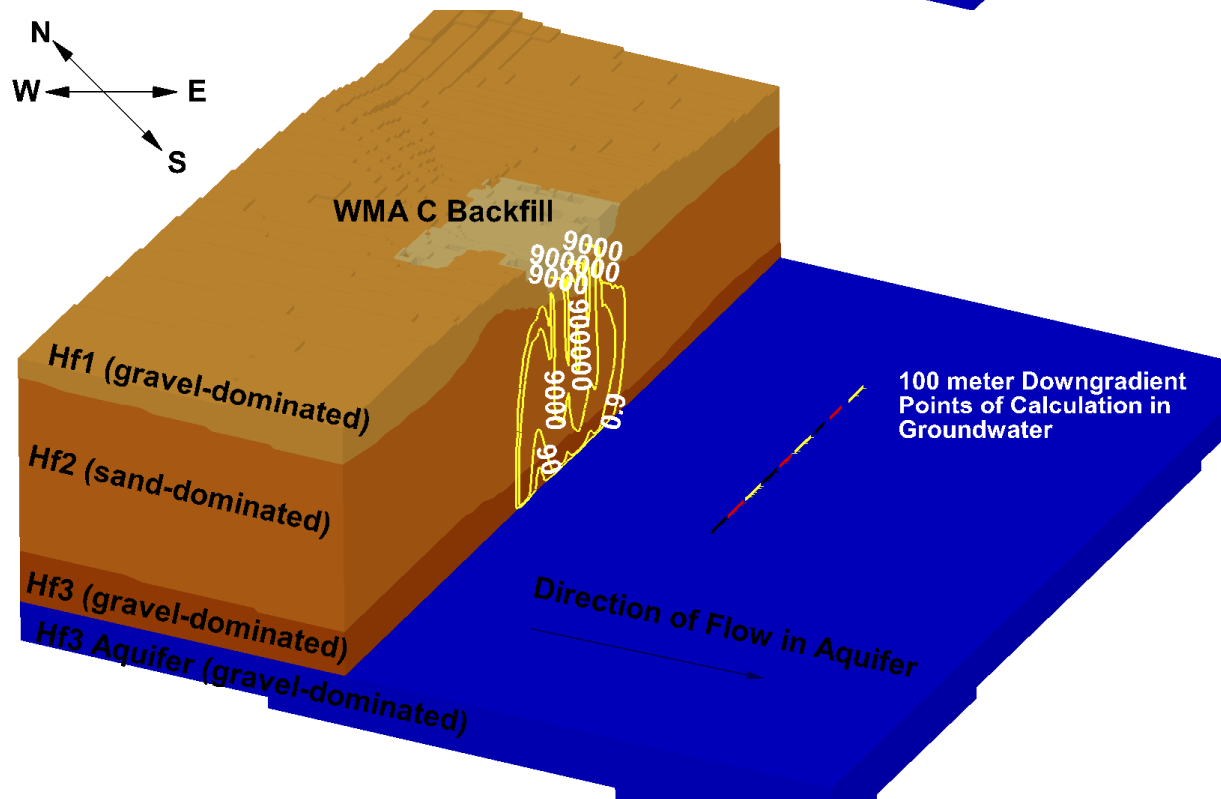
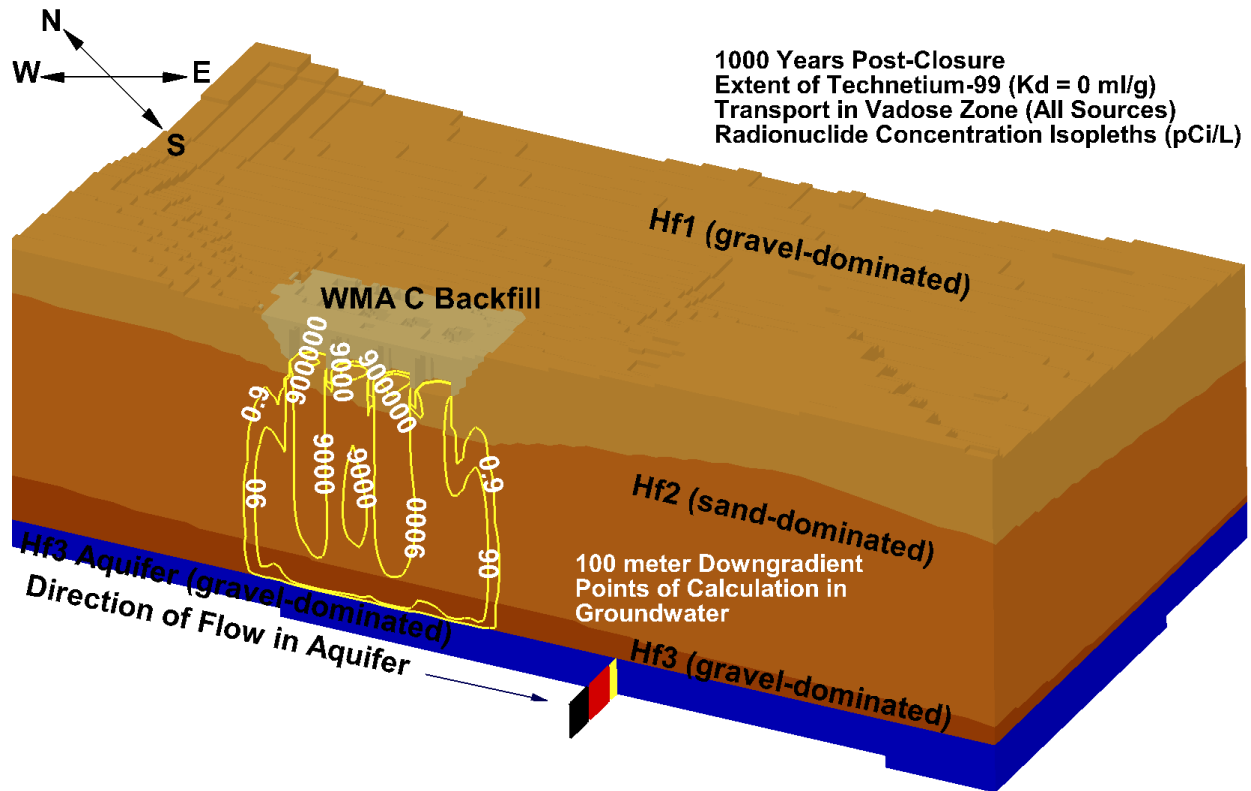
10,000 Years After Closure. As discussed in Section 6, the analysis approach evaluates the contribution of individual sources on the peak concentration in groundwater, and identifies at which PoCal that peak concentration occurs. The results are summarized in Table 7-3 and provide a comparison of simulation results with groundwater MCLs. Table 7-4 presents a summary of the results for the individual sources, identifying at which PoCal the peak concentration attributable to each source occurs.

Table 7-3. Summary of Base Case Peak Groundwater Concentrations and Arrival Times for Selected Radionuclides.

Radionuclide or Nonradiological Contaminant	Nominal K_d value (mL/g)	Maximum Concentration during Compliance Time Frame (pCi/L)	Point of Calculation where Maximum Concentration Occurs	Years after Closure of Maximum Concentration	Maximum Concentration during Sensitivity/Uncertainty Time Frame (pCi/L)	Point of Calculation where Maximum Concentration Occurs
Iodine-129	0.2	0	—	6,540	0.004	PoCal 4
Selenium-79	0.1	0	—	3,770	0.01	PoCal 5
Tin-126	0.5	0	—	10,000	0.05	PoCal 5
Technetium-99	0	0.1	PoCal 5	1,550	30	PoCal 4
Uranium-238	0.6	0	—	10,000	0.02	PoCal 3

RPP-ENV-58782, Rev. 0

Figure 7-12. Extent of Transport of Technetium-99 ($K_d = 0$ mL/g) in the Vadose Zone at the End of the 1,000-Year Compliance Period.

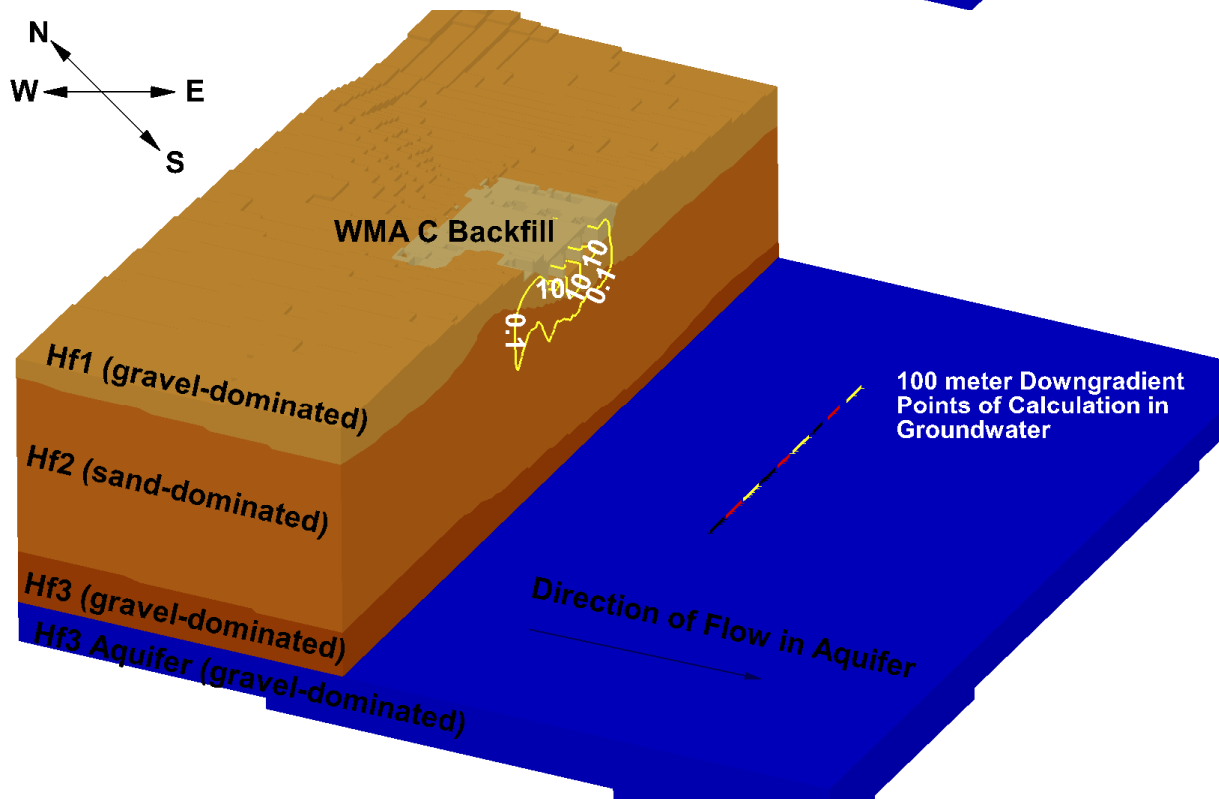
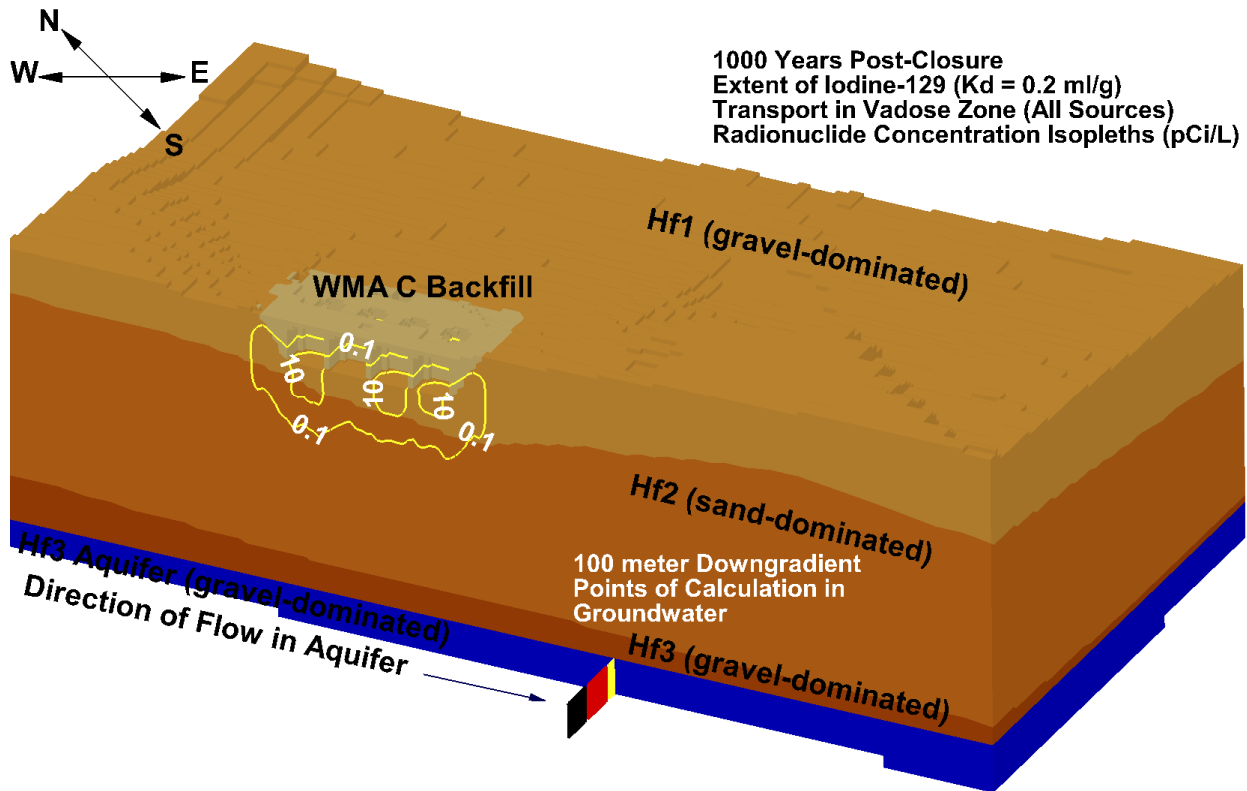


Hf = Hanford formation

WMA = Waste Management Area

RPP-ENV-58782, Rev. 0

Figure 7-13. Extent of Transport of Iodine-129 ($K_d = 0.2$ mL/g for Sand-Dominated Units) in the Vadose Zone at the End of the 1,000-Year Compliance Period.

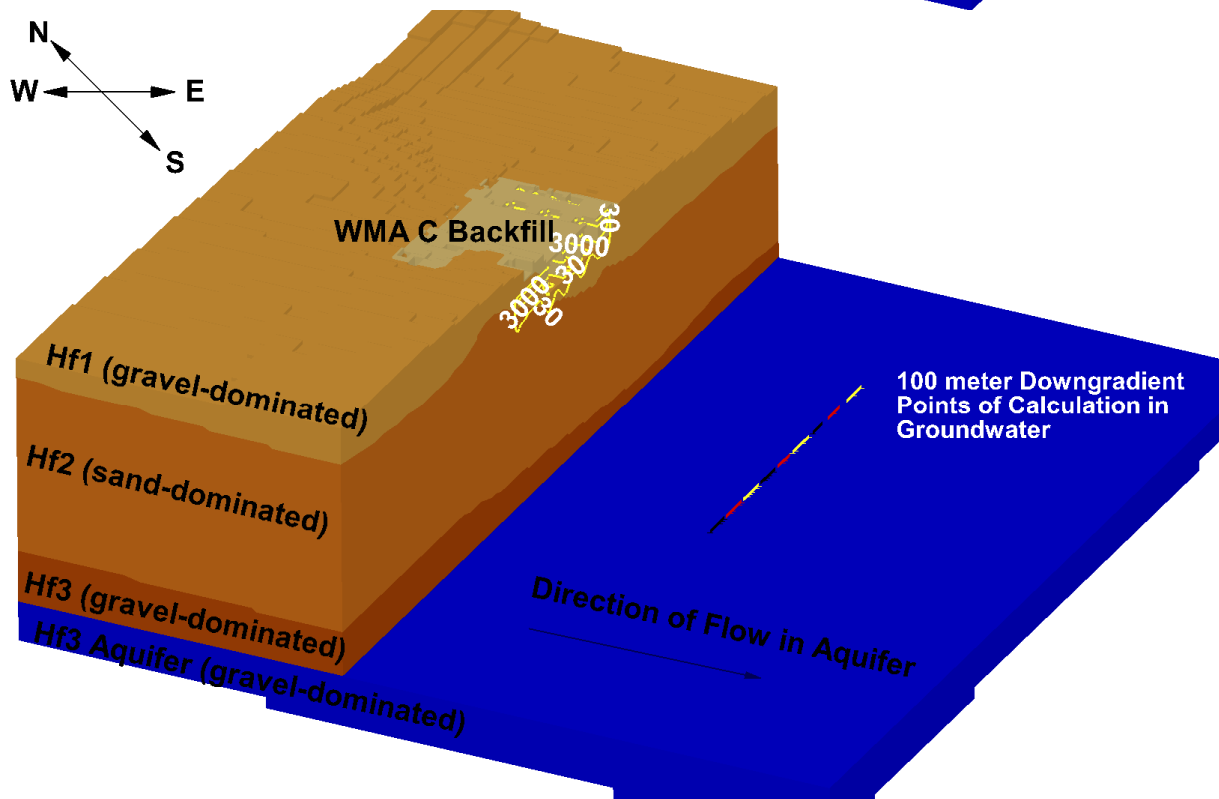
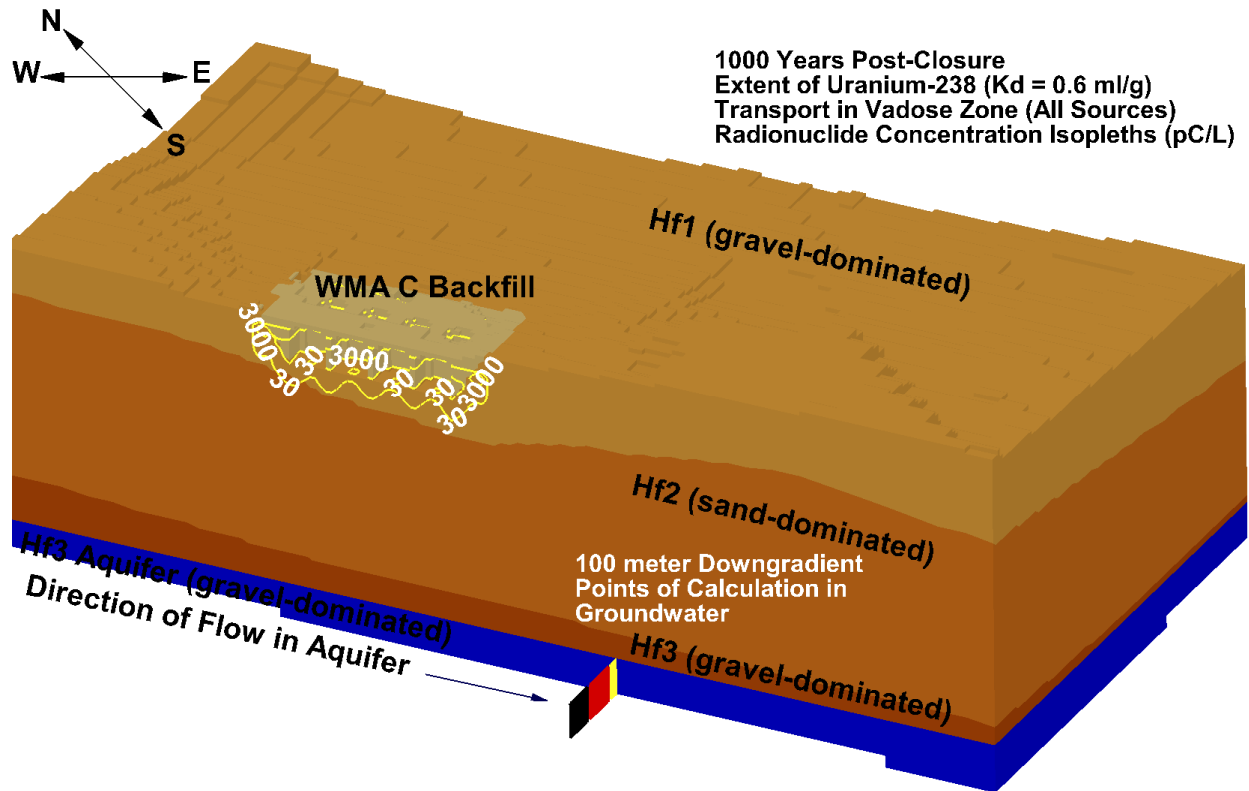


Hf = Hanford formation

WMA = Waste Management Area

RPP-ENV-58782, Rev. 0

Figure 7-14. Extent of Transport of Uranium-238 ($K_d = 0.6$ mL/g for Sand-Dominated Units) in the Vadose Zone at the End of the 1,000-Year Compliance Period.



Hf = Hanford formation

WMA = Waste Management Area

Table 7-4. Summary of Base Case Peak Groundwater Concentrations and Arrival Times for Selected Radionuclides.
(2 sheets)

Source	Selenium-79			Technetium-99			Iodine-129		
	Years after Closure of Arrival	Maximum Concentration (pCi/L)	PoCal	Years after Closure of Arrival	Maximum Concentration (pCi/L)	PoCal	Years after Closure of Arrival	Maximum Concentration (pCi/L)	PoCal
241-C-101	4,100	0.0001	3	1,395	0.1	3	6,230	4E-6	3
241-C-102	4,520	0.0000007	4	1,495	0.01	4	6,840	0.0002	4
241-C-103	4,540	0.00001	5	1,500	0.1	5	6,860	0.0002	5
241-C-104	4,540	0.004	3	1,500	0.9	3	6,890	0.00003	3
241-C-105	4,800	0.00006	4	1,575	20	4	7,190	0.0006	4
241-C-106	4,750	0.004	5	1,555	0.5	5	7,170	0.00004	5
241-C-107	4,510	0.0001	3	1,505	5	3	6,760	0.003	3
241-C-108	4,480	0.0006	4	1,485	0.1	4	6,770	2E-6	4
241-C-109	5,040	0.00005	5	1,620	0.02	5	7,580	2E-6	5
241-C-110	4,970	0.00001	3	1,595	0.1	3	7,280	0.00001	3
241-C-111	4,500	0.001	5	1,485	4	5	6,580	0.0008	5
241-C-112	4,390	0.00007	6	1,460	4	6	6,570	2E-6	6
241-C-201	4,120	0.00002	6	1,420	0.008	6	6,250	3E-8	6
241-C-202	4,110	0.00002	7	1,415	0.008	7	6,230	5E-7	7
241-C-203	3,910	0.00002	7	1,370	0.007	7	5,940	1.00E-6	7
241-C-204	3,940	0.00002	7	1,370	0.01	7	5,970	3E-8	7
241-C-301	5,000	0.0004	6	1,630	0.08	6	7,340	0.00001	6
244 CR Vault	5,440	0.0005	1	1,630	0.1	1	7,710	0.00002	1
Pipelines	3,590	0.008	5	1,345	1	5	5,810	0.001	5
All	3,770	0.01	5	1,550	30	4	6,540	0.004	4

**Table 7-4. Summary of Base Case Peak Groundwater Concentrations and Arrival Times for Selected Radionuclides.
(2 sheets)**

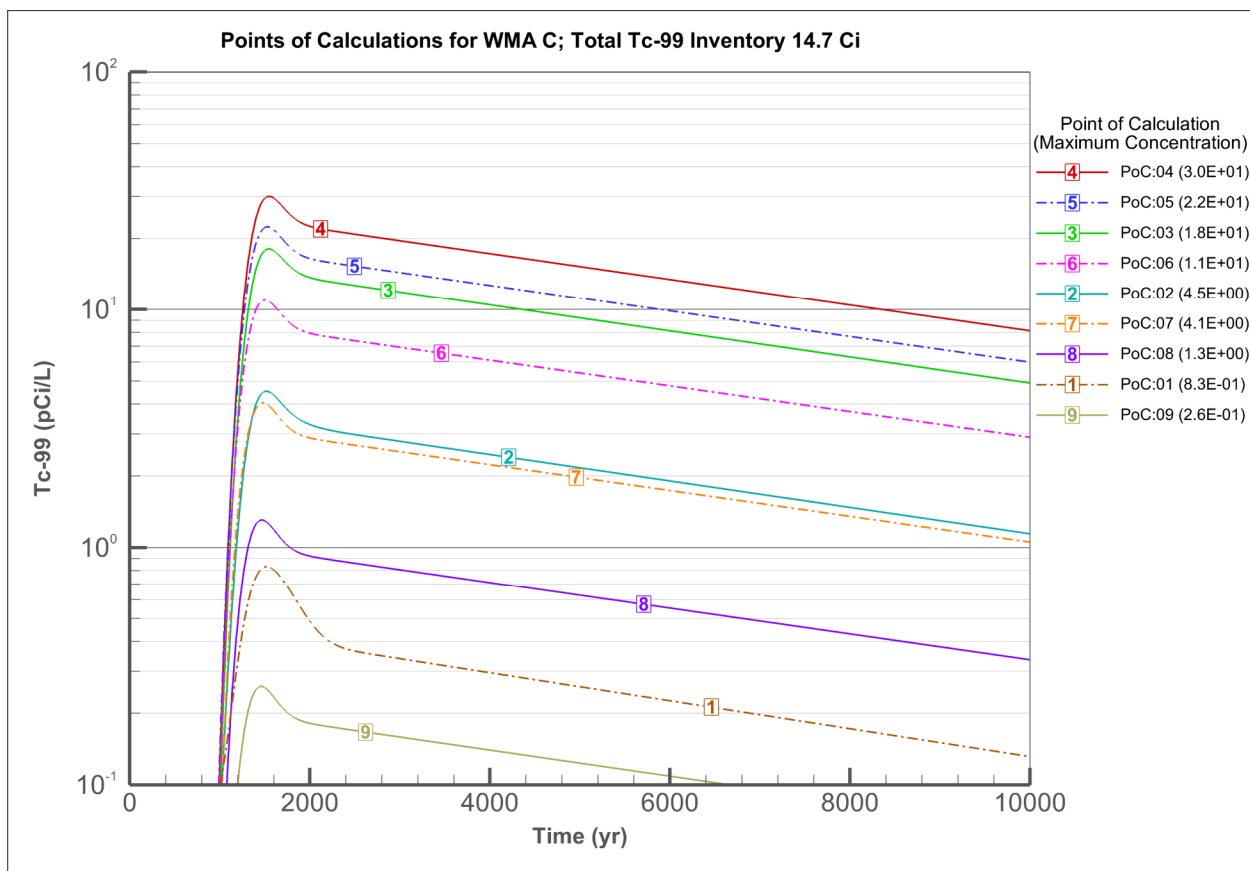
Source	Tin-126			Uranium-238					
	Years after Closure of Arrival	Maximum Concentration (pCi/L)	PoCal	Years after Closure of Arrival	Maximum Concentration (pCi/L)	PoCal			
241-C-101	10,000	5E-7	3	10,000	5E-8	3			
241-C-102	N/A	0	N/A	10,000	9E-9	4			
241-C-103	N/A	0	N/A	10,000	1E-8	5			
241-C-104	10,000	3E-6	3	10,000	1E-8	3			
241-C-105	N/A	0	N/A	10,000	3E-9	4			
241-C-106	10,000	0.0003	5	10,000	2E-9	5			
241-C-107	10,000	1E-7	3	10,000	1E-8	3			
241-C-108	N/A	0	N/A	10,000	1E-8	4			
241-C-109	N/A	0	N/A	10,000	1E-9	5			
241-C-110	10,000	7E-6	3	10,000	1E-8	4			
241-C-111	10,000	2E-6	5	10,000	2E-8	4			
241-C-112	N/A	0	N/A	10,000	2E-8	6			
241-C-201	N/A	0	N/A	10,000	2E-9	6			
241-C-202	N/A	0	N/A	10,000	2E-9	7			
241-C-203	N/A	0	N/A	10,000	6E-9	7			
241-C-204	N/A	0	N/A	10,000	6E-9	7			
241-C-301	10,000	4E-6	6	10,000	6E-11	6			
244 CR Vault	10,000	5E-6	1	10,000	4E-10	1			
Pipelines	10,000	0.04	3	10,000	0.02	3			
All	10,000	0.05	5	10,000	0.02	3			

N/A = not available

RPP-ENV-58782, Rev. 0

The evaluation of the peak PoCal for ^{99}Tc is shown in Figure 7-15; the peak concentration of ^{99}Tc is found to occur at PoCal 4. The contribution of individual sources within WMA C at PoCal 4 is shown in Figure 7-16. The peak contributor to the concentration of ^{99}Tc at all times is seen to be tank C-105. The peak concentration results predominantly from the combination of the tank C-105 releases and releases from the pipelines. Tank C-105 contains more than twice the amount of ^{99}Tc as any other WMA C source, and by itself the residual waste from tank C-105 produces a maximum concentration in groundwater of 21 pCi/L (note that the maximum concentration limit for ^{99}Tc is 900 pCi/L), which is more than five times the concentration that any other source contributes to the maximum.

Figure 7-15. Groundwater Concentration of Technetium-99 at All Points of Calculation 100 Meters Downgradient from Waste Management Area C.



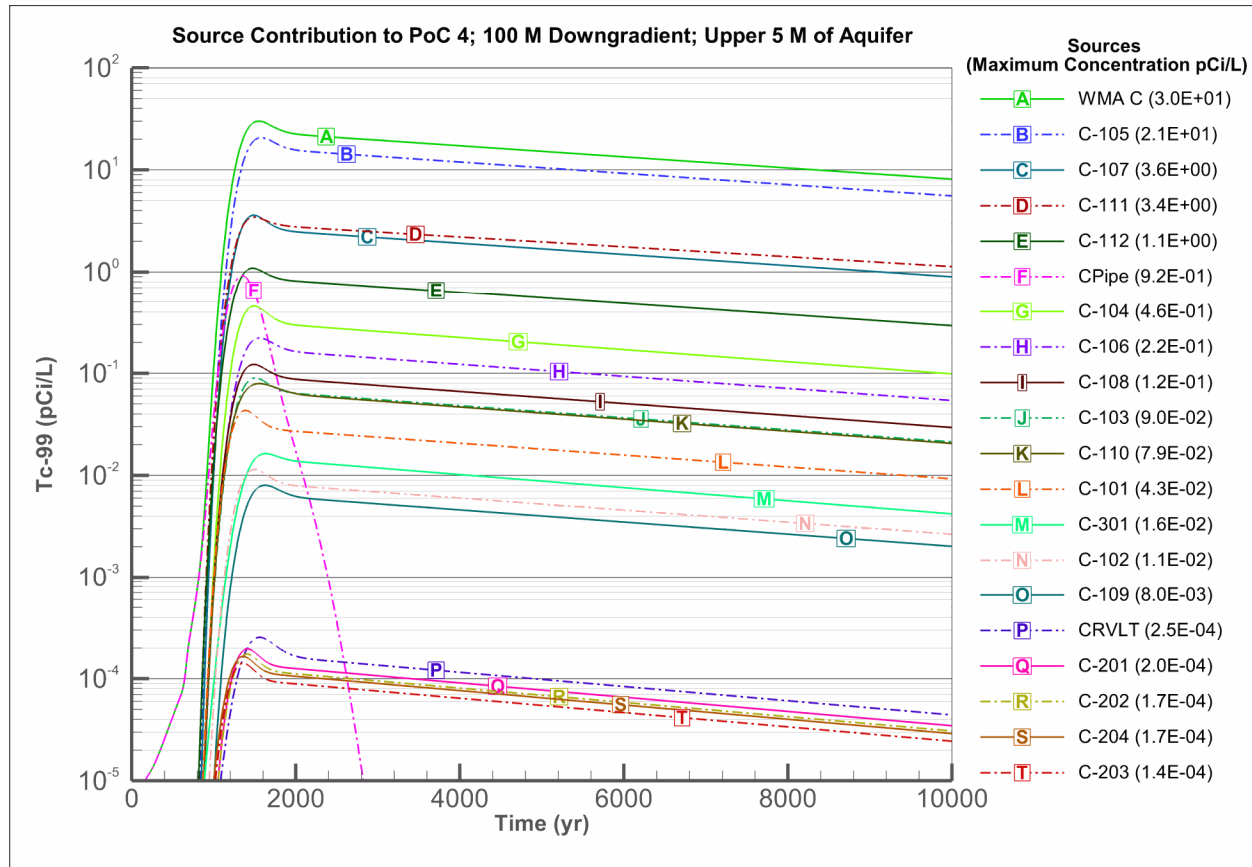
PoC = Point of Calculation

WMA = Waste Management Area

The evaluation of the peak PoCal for ^{129}I is shown in Figure 7-17; the peak concentration of ^{129}I is found to occur at PoCal 4, although the peak at PoCal 3 is almost as large. The contribution of individual sources within WMA C at PoCal 4 is shown in Figure 7-18. The breakthrough curves for ^{129}I show the effect of slight retardation on contaminant transport through the vadose zone. First arrival does not occur until after 2,600 years after closure, and the peak concentration (0.004 pCi/L) occurs approximately 6,500 years after closure. The residual waste from tank C-107 is responsible for providing the largest contribution to the overall concentration, followed by that from the pipelines and tanks C-111 and C-105.

RPP-ENV-58782, Rev. 0

Figure 7-16. Groundwater Concentration of Technetium-99 from Each Source at Point of Calculation 4.



PoC = Point of Calculation

WMA = Waste Management Area

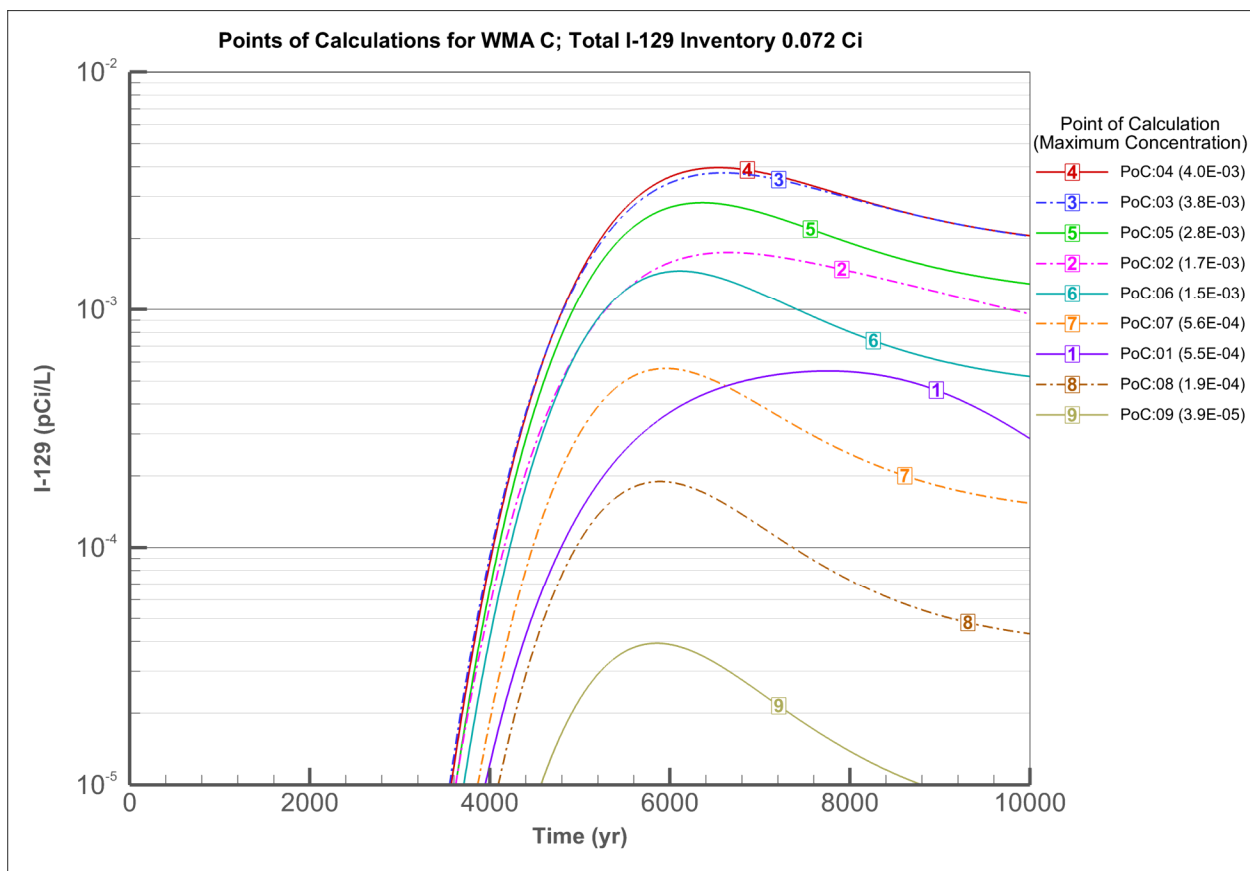
The evaluation of the peak PoCal for ^{238}U is shown in Figure 7-19; the peak concentration of ^{238}U is found to occur at PoCal 3, although the peaks at PoCals 2, 4, 5, and 6 are almost as large. The contribution of individual sources within WMA C at PoCal 3 is shown in Figure 7-20. The breakthrough curves for ^{238}U show the effect of moderate retardation on contaminant transport through the vadose zone. First arrival does not occur until after 5,600 years after closure, and the maximum concentration (note the regulatory standard for ^{238}U is 15 pCi/L) occurs at the end of the sensitivity/uncertainty analysis time frame (10,000 years after closure). The trend in concentration is increasing at the end of the analysis time frame, indicating that it has yet to reach a peak. The residual waste from the pipelines is responsible for releases within 10,000 years, with all other sources negligible. This occurs because the release from the pipelines occurs by advection and is not retarded by sorption on cementitious material. By contrast, releases from the tanks and vault are influenced by sorption on the grout and are released by diffusion.

A summary of the peak concentrations at their respective peak PoCals is presented in Figure 7-21. During the sensitivity/uncertainty analysis period (1,000 to 10,000 years after closure), the primary radionuclides that break through at the PoCals include ^{99}Tc , ^{79}Se , ^{126}Sn , ^{129}I , and the uranium isotopes and their progeny. Concentrations of the simply decaying isotopes

RPP-ENV-58782, Rev. 0

and ^{238}U are shown in Figure 7-21, on both linear (upper) and log (upper) scales. The semi-log plot is needed since there are so many orders of magnitude difference among the contaminants. Technetium-99 is by far the contaminant with the largest impact on groundwater; the maximum concentration of ^{99}Tc in groundwater is 30 pCi/L, which occurs approximately 1,500 years after closure. The concentrations of ^{79}Se and ^{129}I reach their peaks within 10,000 years after closure, and then decline. Concentrations of ^{127}Sn , uranium, and the uranium progeny are on the rise at the end of the 10,000-year analysis period. The remaining radionuclides in the analysis did not reach the PoCals during the 10,000-year period because of decay, sorption, or a combination of the two.

Figure 7-17. Groundwater Concentration of Iodine-129 at All Points of Calculation 100 Meters Downgradient from Waste Management Area C.



PoC = Point of Calculation

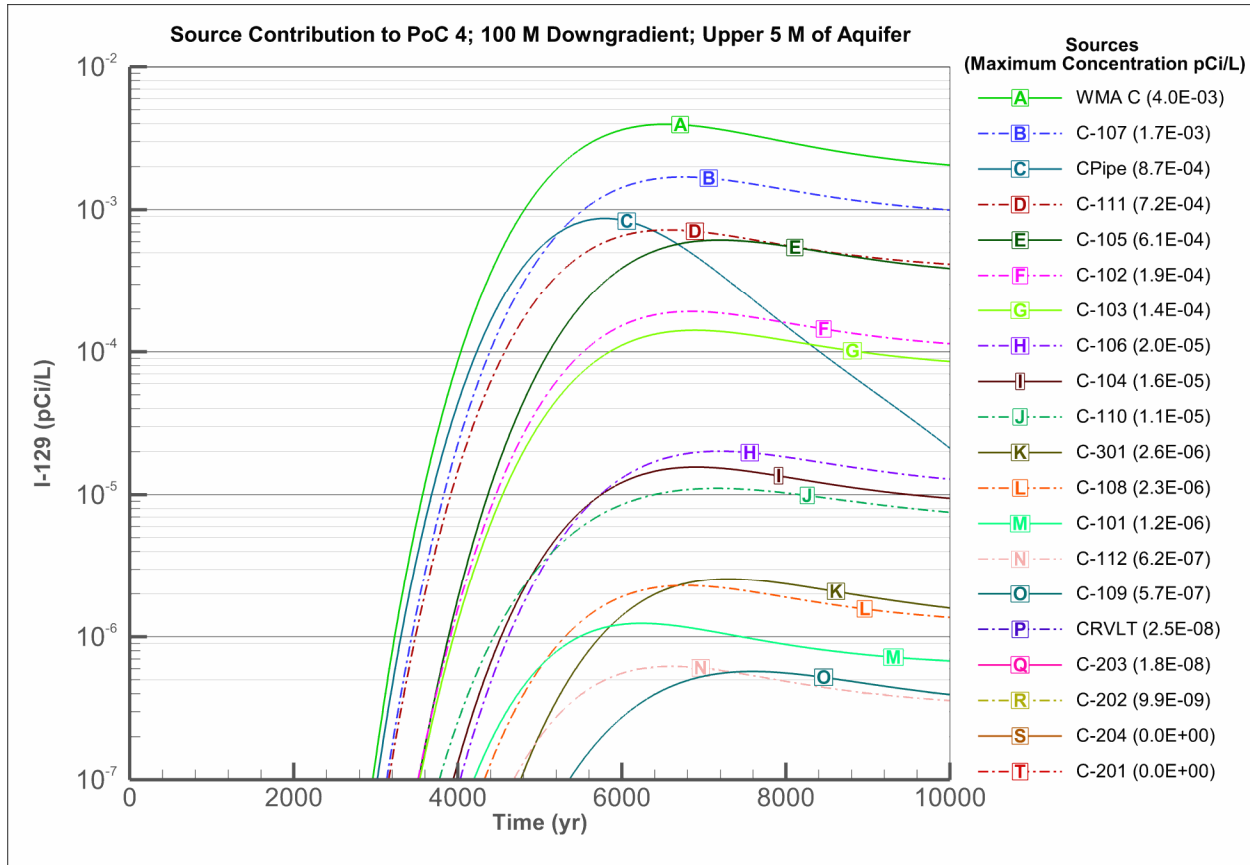
WMA = Waste Management Area

Figures 7-22 through 7-24 show the development of the ^{99}Tc plume in the groundwater at 500, 1,000, and 1,570 years post-closure. These times correspond to the surface barrier design life, the end of the compliance time period, and the approximate time of the peak concentration. At 500 years after closure, the first arrival approximately occurs near the south corner of the facility, in the vicinity of the 244-CR vault as shown in Figure 7-22. Technetium-99 from residuals in both the vault and the pipelines has reached the water table in this area. Although the plume increases in size from 500 to 1,000 years into the future, peak concentration in groundwater remains very low (less than 1 pCi/L) as shown in Figure 7-23. At the time of the maximum

RPP-ENV-58782, Rev. 0

concentration at the point of compliance, shown in Figure 7-24, the plume shows much higher concentrations from all sources, but the peak concentration becomes dominated by inventory released from tank C-105.

Figure 7-18. Groundwater Concentration of Iodine-129 from Each Source at Point of Calculation 4.



PoC = Point of Calculation

WMA = Waste Management Area

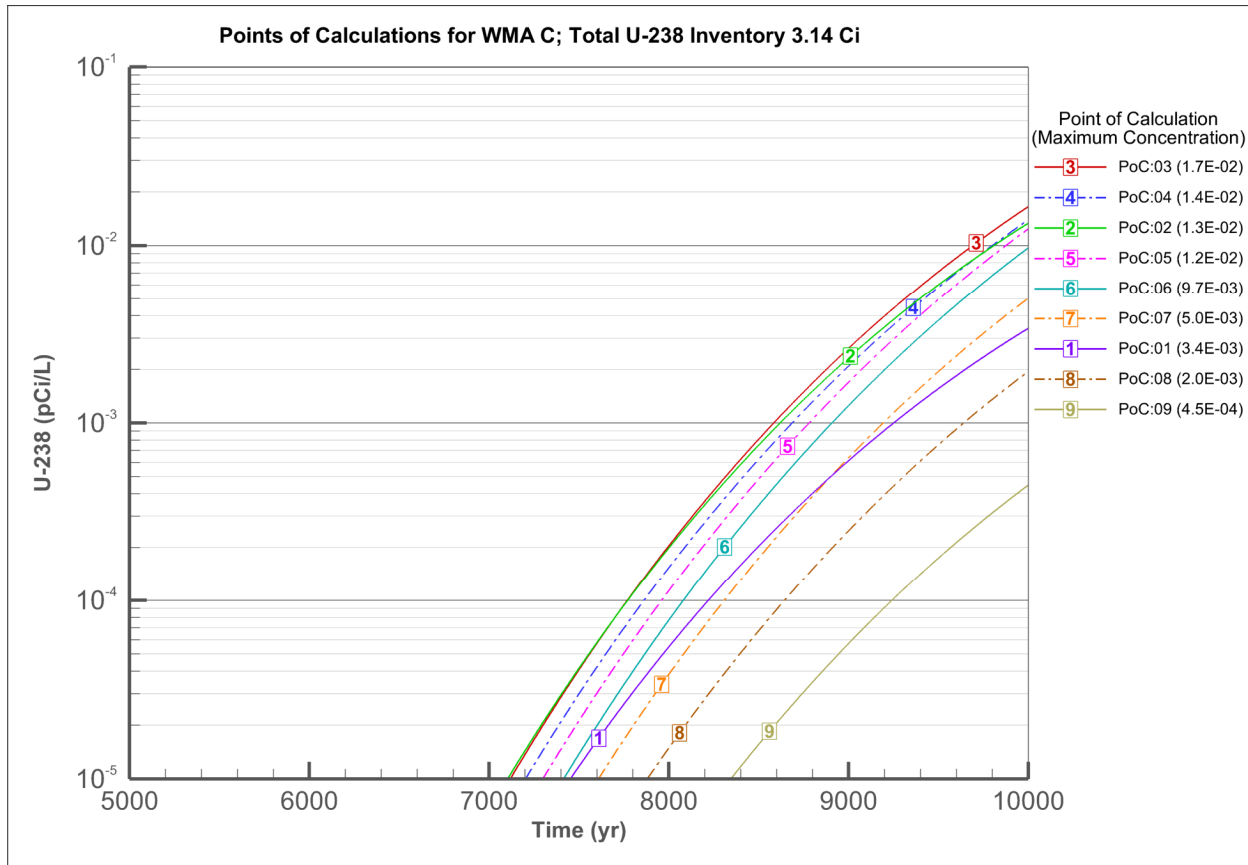
Plot of breakthrough curves for ^{99}Tc at different PoCals (PoCal 3, 4, 5, and 6) at different downgradient locations (e.g., fenceline, 100 m, and 200 m) illustrate small differences in ^{99}Tc concentrations in modeling results at different PoCals and downgradient locations from WMA C (see Figure 7-25).

7.2.1.2.3 Evaluation of Correlation between Leachate Flux to Water Table and Groundwater Concentration. There is a linear relationship between the concentration in the groundwater and the radionuclide flux entering the water table. Figure 7-26 shows the breakthrough curves of ^{99}Tc relative to the flux of ^{99}Tc (pCi/yr) entering the water table. As seen in the figures, the curves overlay one another fairly closely, indicating that the downgradient concentration in groundwater is likely correlated to the flux of ^{99}Tc and concentration of the leachate entering the aquifer. This relationship provides an indication of the extent to which the correlation is linear. As a result of this linearity, groundwater concentrations in this 3-D system may be evaluated more simply, using flux rates or leachate concentration entering the water table

RPP-ENV-58782, Rev. 0

and a simple linear convolution. This approach is referred to as a dilution-attenuation factor (EPA/540/R-95/128).

Figure 7-19. Predicted Groundwater Concentration of Uranium-238 at All Points of Calculation 100 Meters Downgradient from Waste Management Area C.



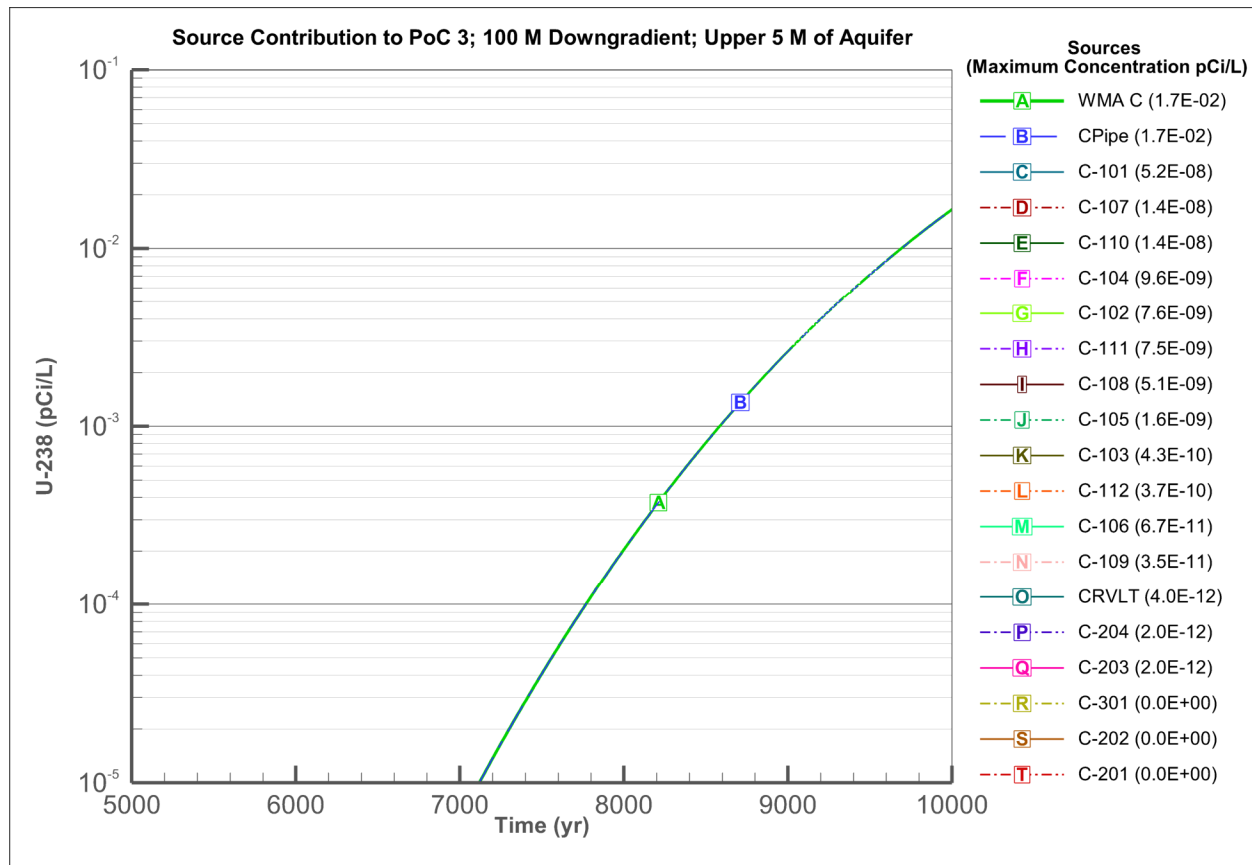
PoC = Point of Calculation

WMA = Waste Management Area

The coefficient of determination for the regression lines is very close to 1, which means the lines fit the values almost perfectly. Thus, the downgradient concentration in groundwater of ^{99}Tc can be estimated by either the flux or concentration of ^{99}Tc in the leachate entering the aquifer and a linear scalar particular to each source. In the case of the ^{99}Tc flux, the scalar needs only to account for the aquifer flow rate. For the base case evaluation at PoCal 4 for ^{99}Tc from the tank C-105 residuals, the inverse of the slope of the regression line between the groundwater and leachate concentration indicates that the leachate concentration is reduced by a factor of 305 in the aquifer, i.e., $1/0.003273$. For residuals from the pipelines, the scalar for PoCal 5 is $1/0.001504 = 665$. Because of differences in source and PoCal locations, the relationship will be different for each combination of source and PoCal, as indicated by the comparison of the tank C-105 and pipelines scalars. However, once the scalars are established, variability in the aquifer flow parameters may be estimated simply as a function of the scalars.

RPP-ENV-58782, Rev. 0

Figure 7-20. Groundwater Concentration of Uranium-238 According to Each Source at Point of Calculation 3 Where the Maximum Concentration Occurs 100 Meters Downgradient from Waste Management Area C.



PoC = Point of Calculation

WMA = Waste Management Area

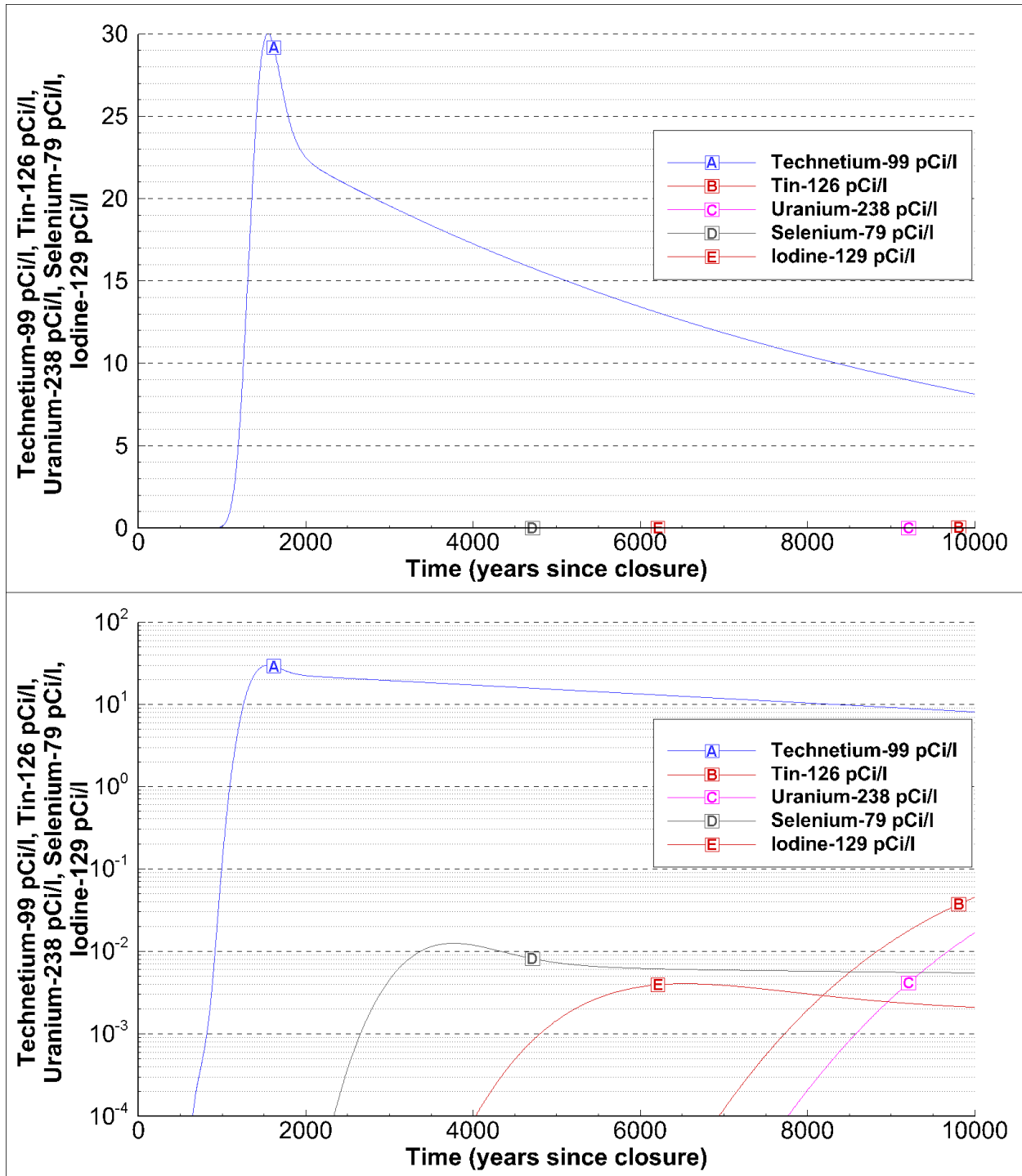
7.2.2 Air Transport of Radionuclides

The atmospheric release is modeled for only those radionuclides that can partition into the gas phase from the dissolved phase (in water). These radionuclides are ^{14}C , ^3H (tritium), ^{129}I , and ^{222}Rn . The atmospheric release calculation methodology is described in Section 6.3.2.3 (Atmospheric Pathway) for WMA C sources, where the diffusive flux from the residual waste to the surface of the facility is calculated first. For the radionuclides that are included in the air pathway performance objective (see Section 2.1), an air transport calculation is performed to calculate the concentration at a receptor located 100 m (328 ft) downwind from the WMA C fence line. The results of this calculation are presented in Figure 7-27 for ^{14}C , ^3H (tritium), and ^{129}I .¹

¹ As discussed in Section 2, ^{222}Rn is not included in the air pathway performance objective. Instead, it has a separate criterion for flux from the facility surface.

RPP-ENV-58782, Rev. 0

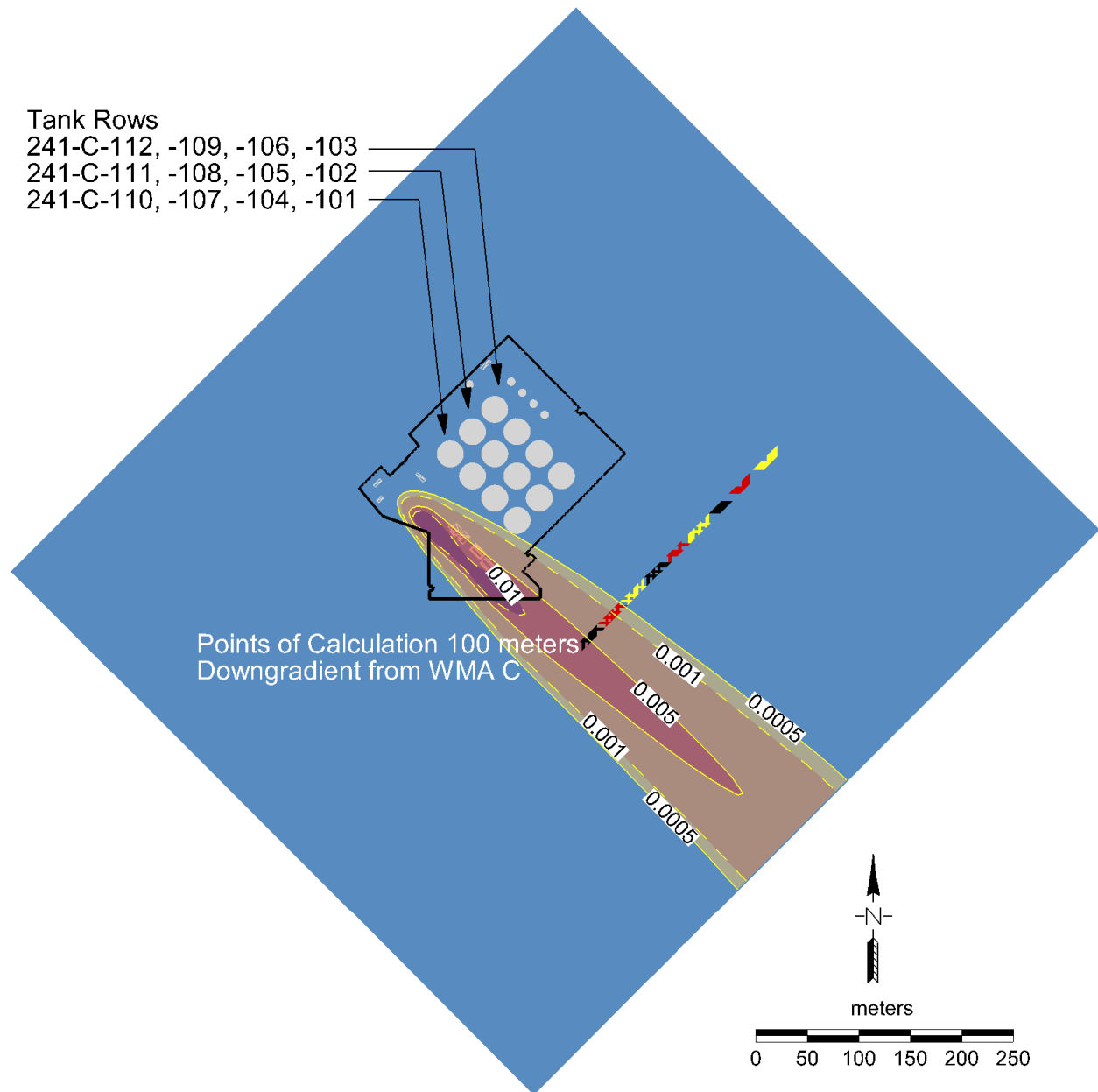
Figure 7-21. Maximum Calculated Groundwater Concentration at 100 Meters Downgradient from Waste Management Area C.



RPP-ENV-58782, Rev. 0

Figure 7-22. Extent of Technetium-99 Plume in Groundwater 500 Years after Closure at the End of the Surface Barrier Design Life.

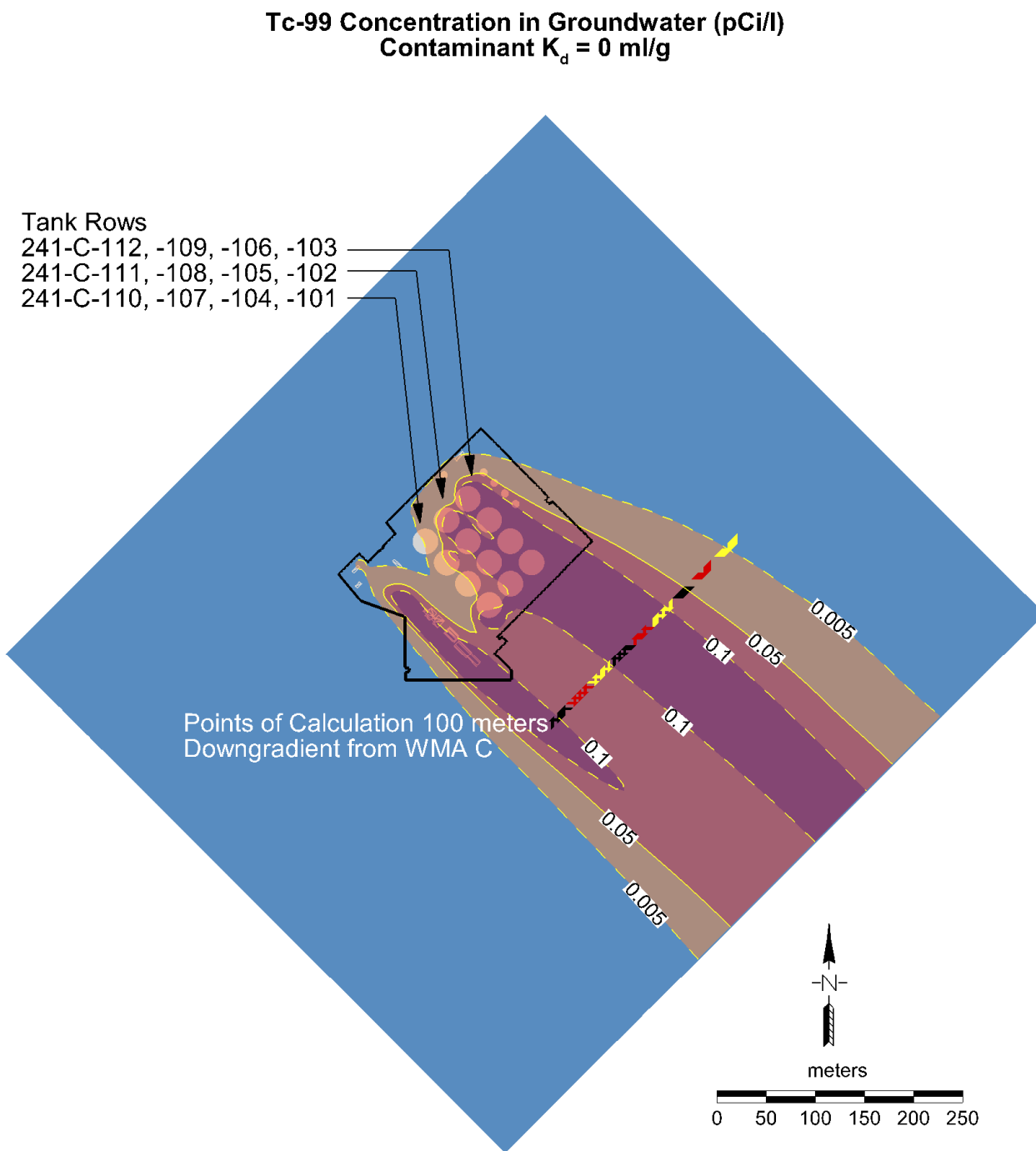
Tc-99 Concentration in Groundwater (pCi/l)
Contaminant $K_d = 0$ ml/g



500 Years after Closure
 End of barrier design life
 WMA = Waste Management Area

RPP-ENV-58782, Rev. 0

Figure 7-23. Extent of Technetium-99 Plume in Groundwater 1,000 Years after Closure at the End of the Compliance Time Frame.

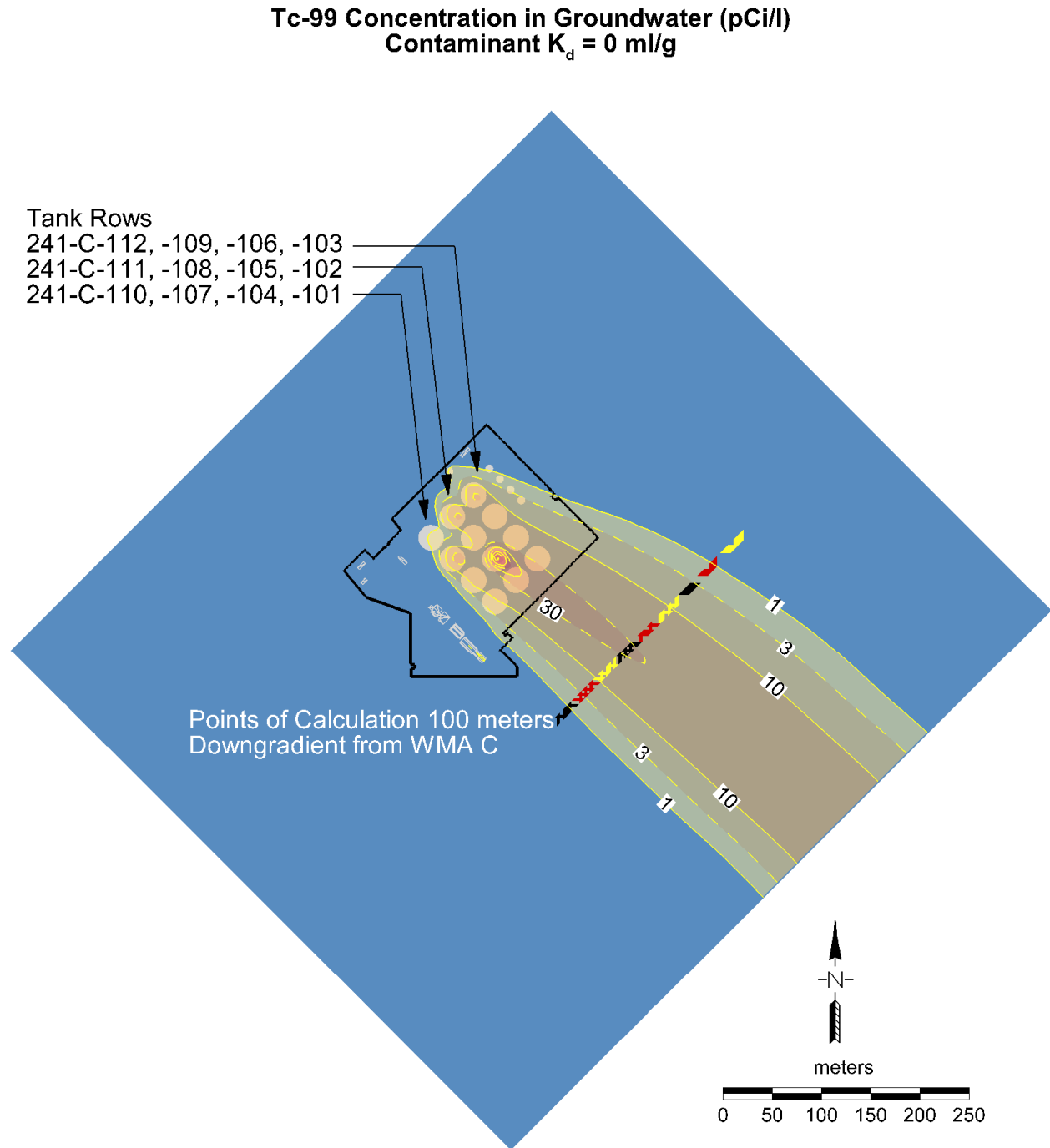


End of the 1,000 Year Compliance Period

WMA = Waste Management Area

RPP-ENV-58782, Rev. 0

Figure 7-24. Extent of Technetium-99 Plume in Groundwater 1,570 Years after Closure at the Time of the Maximum Concentration at the Point of Compliance.

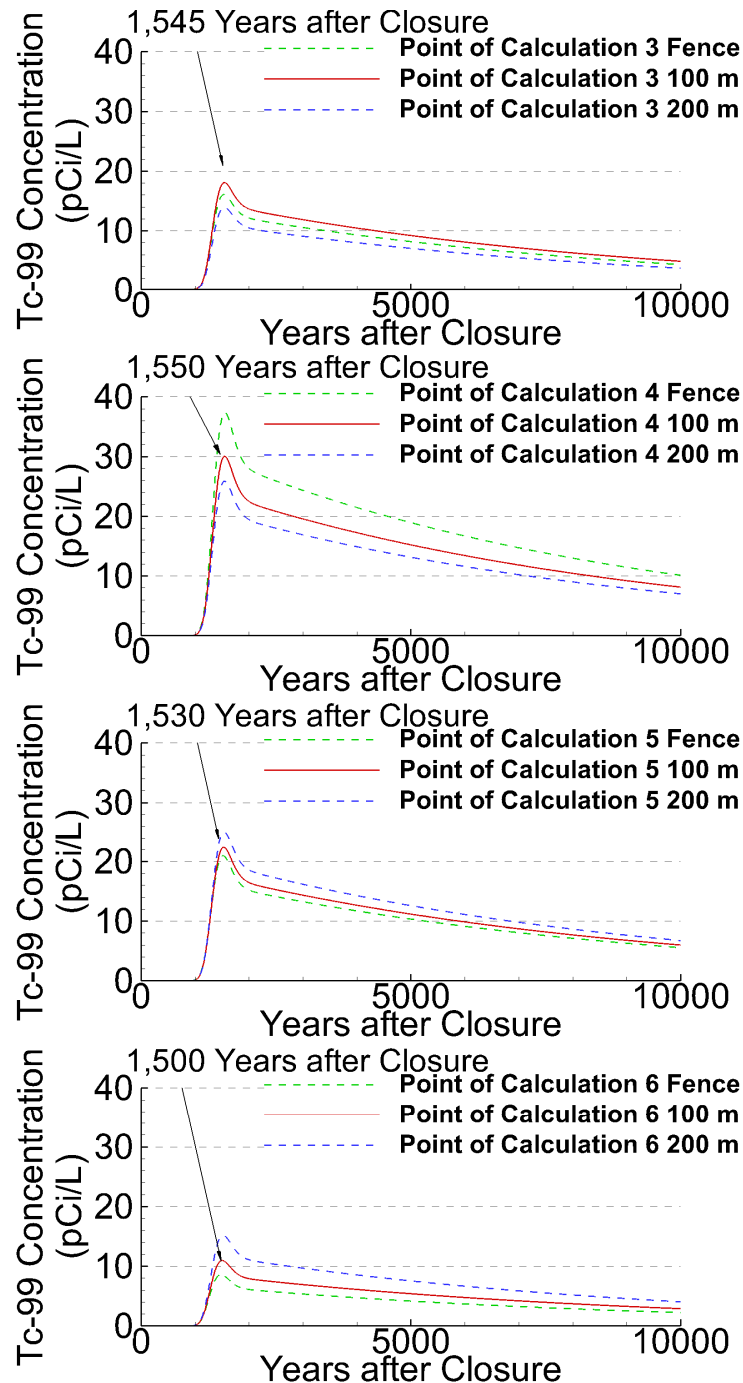


Approximate time of peak concentration at point of calculation

WMA = Waste Management Area

RPP-ENV-58782, Rev. 0

Figure 7-25. Technetium-99 Concentration Breakthrough Curves in Groundwater after Closure at Different Points of Calculation and Downgradient Locations.



The results in Figure 7-27 indicate that the atmospheric ^3H (tritium) release produces much higher concentrations than the other two at early times. The differences between the curves are attributable to differences in the K_d and Henry's Law behavior for the three contaminants. As discussed in Section 6, the release rate into the gas phase is dependent on both the K_d (which controls the partitioning between solid and liquid) and the Henry's Law constant (which controls

RPP-ENV-58782, Rev. 0

the partitioning between liquid and vapor). The ^3H concentration declines sharply, both because of its short half-life and because the entire inventory is immediately available for release, having a low K_d and relatively high Henry's Law constant. By contrast, ^{129}I has a low K_d and a low Henry's Law constant (and a low inventory), so while its aqueous phase concentration is relatively high, it does not readily partition into the gas phase. The high K_d of ^{14}C keeps the aqueous concentration of ^{14}C low, limiting its availability to partition into the gas phase. The three contaminants therefore exhibit qualitatively different behavior because of the differences in their properties.

The radon flux at the surface of the WMA C facility is calculated for each source separately. These sources are presented in Figure 7-28. The relative magnitude of the fluxes are the result of the initial residual inventory of ^{226}Ra and the amount of uranium inventory that decays to form ^{226}Ra and then to ^{222}Rn . The radon flux increases with time resulting from ingrowth due to decay of ^{234}U and ^{238}U inventory. The peak flux of 7×10^{-3} pCi/m²/sec results from tank C-203 at the end of the simulation. This value is much lower than the 20 pCi/m²/sec performance objective. The flux from other 200-series tanks and C-301 is also relatively high compared to the 100-series tanks. This is due to combination of high initial inventories of ^{234}U (and ^{238}U), smaller residual volume, and smaller cross-sectional area for the 200-series tanks and C-301 compared to the 100-series tanks and ancillary equipment resulting in higher concentration (and flux) of radon. As discussed in Section 6, for the analysis of radon flux, releases of contaminants from the residual waste are set to zero, so the inventory of ^{226}Ra is allowed to build up in the residual layer. This is a significant conservatism at long times, since uranium migrating downward through the groundwater pathway would decrease the later peaks. Despite this conservatism, even at 10,000 years the peak radon flux is several orders of magnitude below the performance objective. Tank C-106 contains little uranium and ^{230}Th , and as expected, ^{222}Rn flux decreases as the ^{226}Ra inventory is depleted through decay (Figure 7-28). The peak radon flux for the 1,000-year compliance period is about 2×10^{-4} pCi/m²/s.

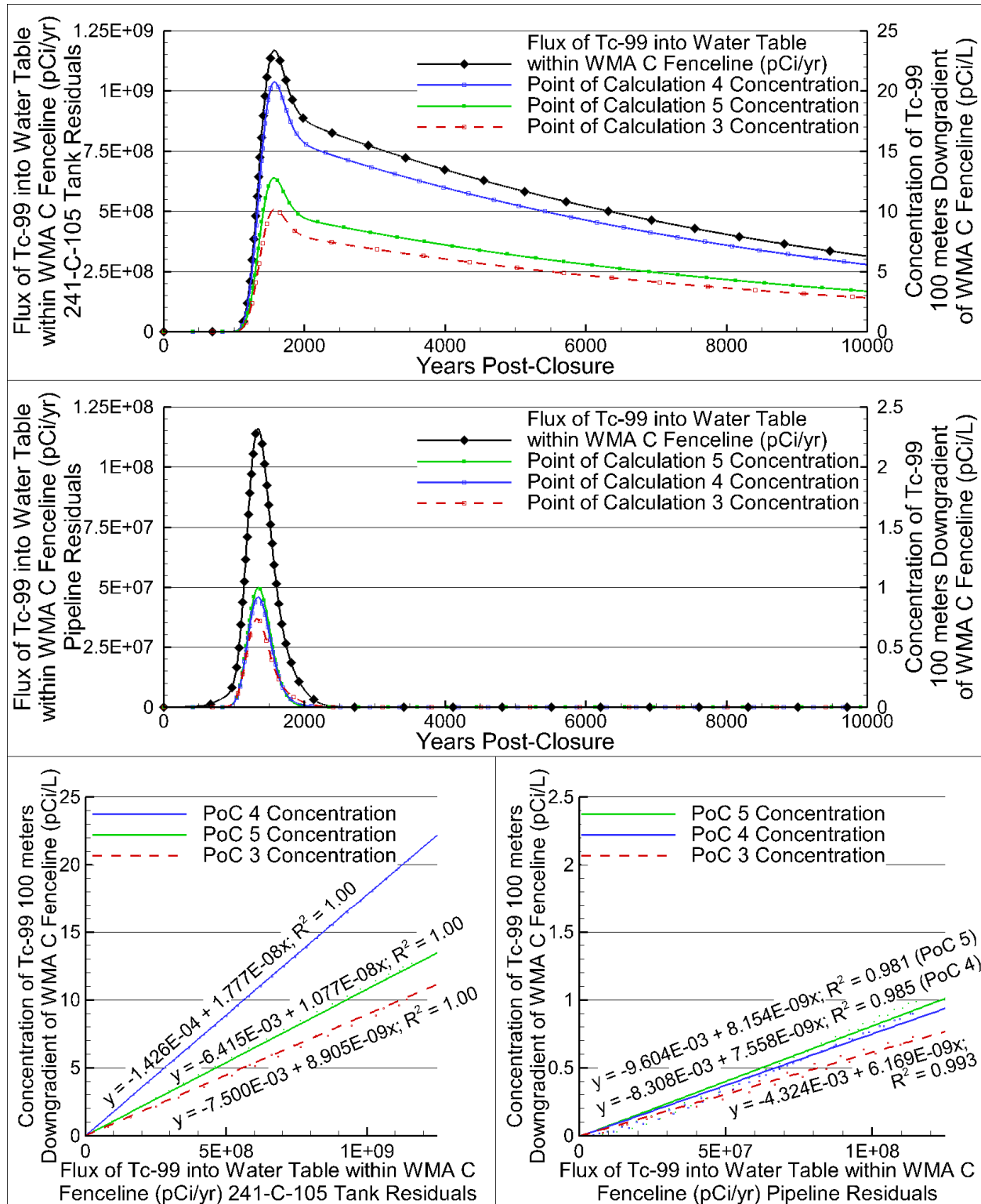
7.3 DOSE ANALYSIS

In this section, results are presented of the dose analyses conducted for the PA to demonstrate compliance with performance objectives outlined in DOE O 435.1, as discussed in Section 1. Results are presented as a set of deterministic "base case" results that represent reasonable best estimates for the input parameters, and for a situation in which all the safety functions discussed in Section 1 behave as expected. These results are supported by a suite of sensitivity cases (see Section 8.2), which have been selected to evaluate the importance of the safety functions on compliance. They are also supported by probabilistic analyses (see Section 8.1) that evaluate the importance of parameter uncertainty on the PA, and which demonstrate that the base case represents a central tendency of the range of outputs from the probabilistic analysis.

In this section, dose results are presented for the all-pathways performance objective and for the air pathway objective. Doses for the intruder performance objectives are presented in Section 9. As discussed in Section 2, the remaining performance objectives for the PA do not require dose calculations, and are presented in appropriate sections of the report.

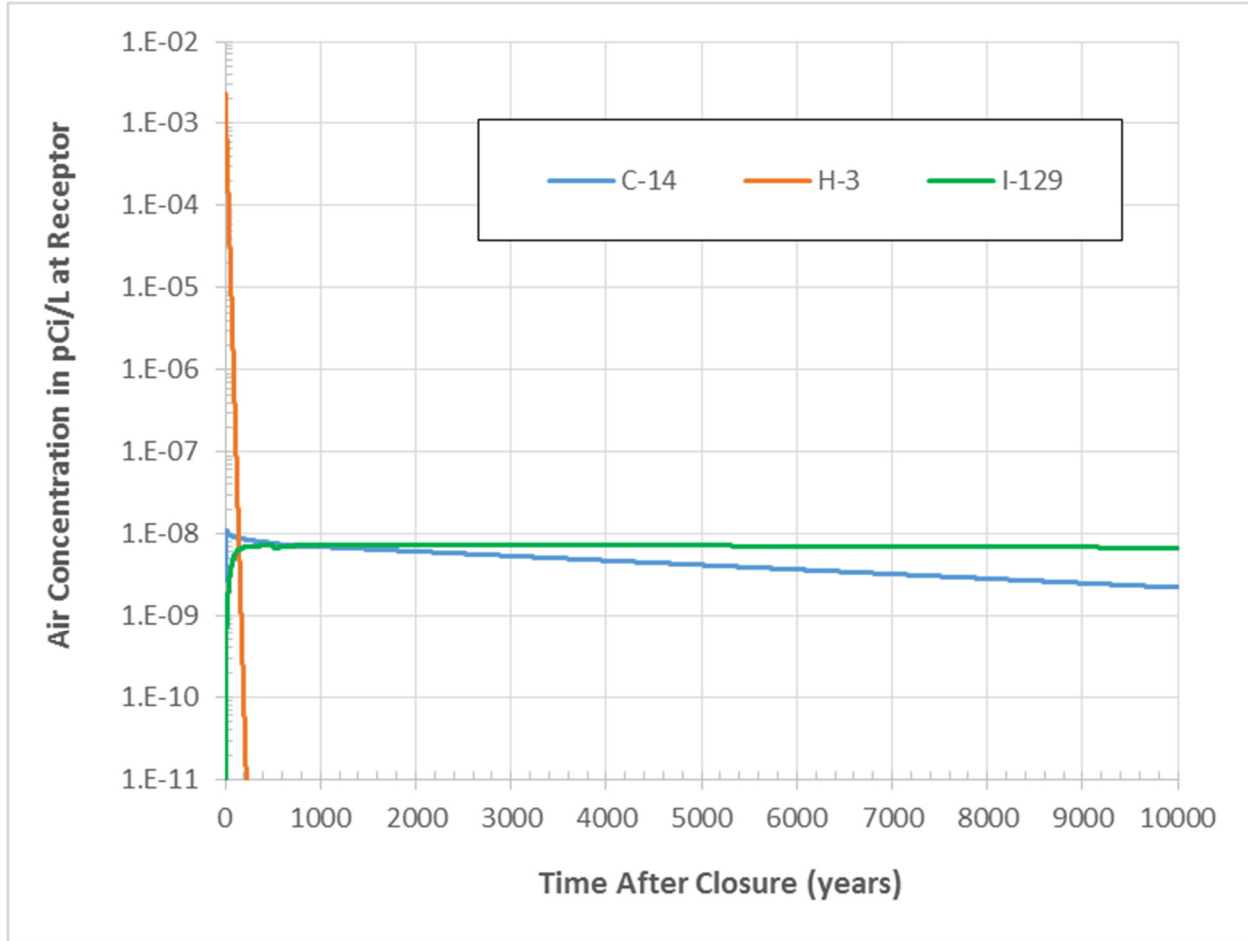
RPP-ENV-58782, Rev. 0

Figure 7-26. Results and Regression Lines Associated with the Vadose Leachate Flux to Groundwater for the Base Case Evaluation of Technetium-99.



WMA = Waste Management Area

RPP-ENV-58782, Rev. 0

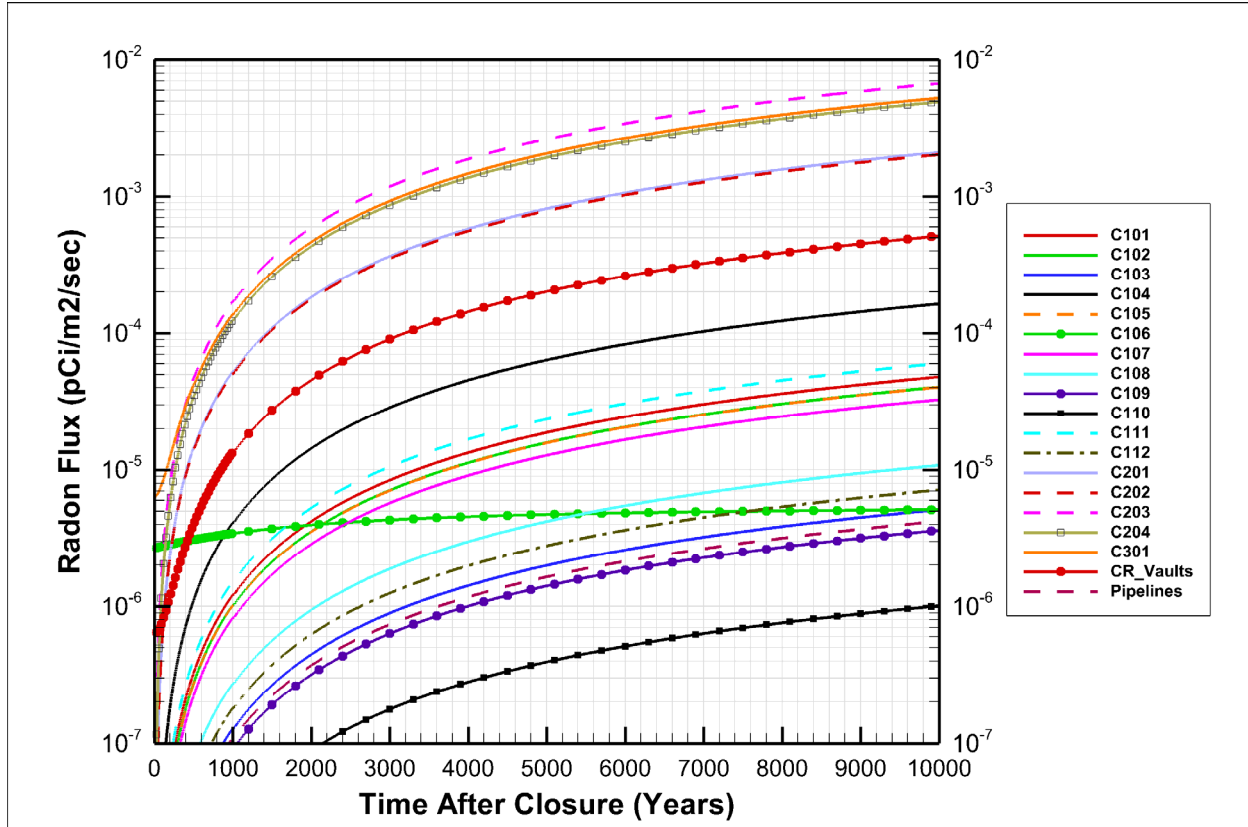
Figure 7-27. Air Concentration for Volatiles at Receptor Location in pCi/L.

7.3.1 All-Pathways Dose

The all-pathways dose is a combination of dose from the groundwater pathway and air pathway, with the concentrations calculated according to the methodology presented in Section 6. The receptor is considered to be a reasonably maximally-exposed individual and assumed to be located along the centerline of the air pathway plume and getting water from the well located at the highest concentration point in the aquifer at the 100 m (328 ft) boundary. The groundwater concentrations are used as the concentrations at the wellhead. This approach has been taken to maintain consistency between the groundwater protection performance objectives and the all-pathways dose performance objective, but does not take account of any dilution that may occur in the well as it is pumped.

Doses associated with the groundwater pathway are presented in Figure 7-29 for the 100 m (328 ft) compliance distance for each PoCal. Consistent with the groundwater protection concentration calculations, the peak dose in space is found at PoCal 4. Consequently, PoCal 4 is used as the compliance point for the PA all-pathways analysis.

RPP-ENV-58782, Rev. 0

Figure 7-28. Radon Flux at Surface of Waste Management Area C.

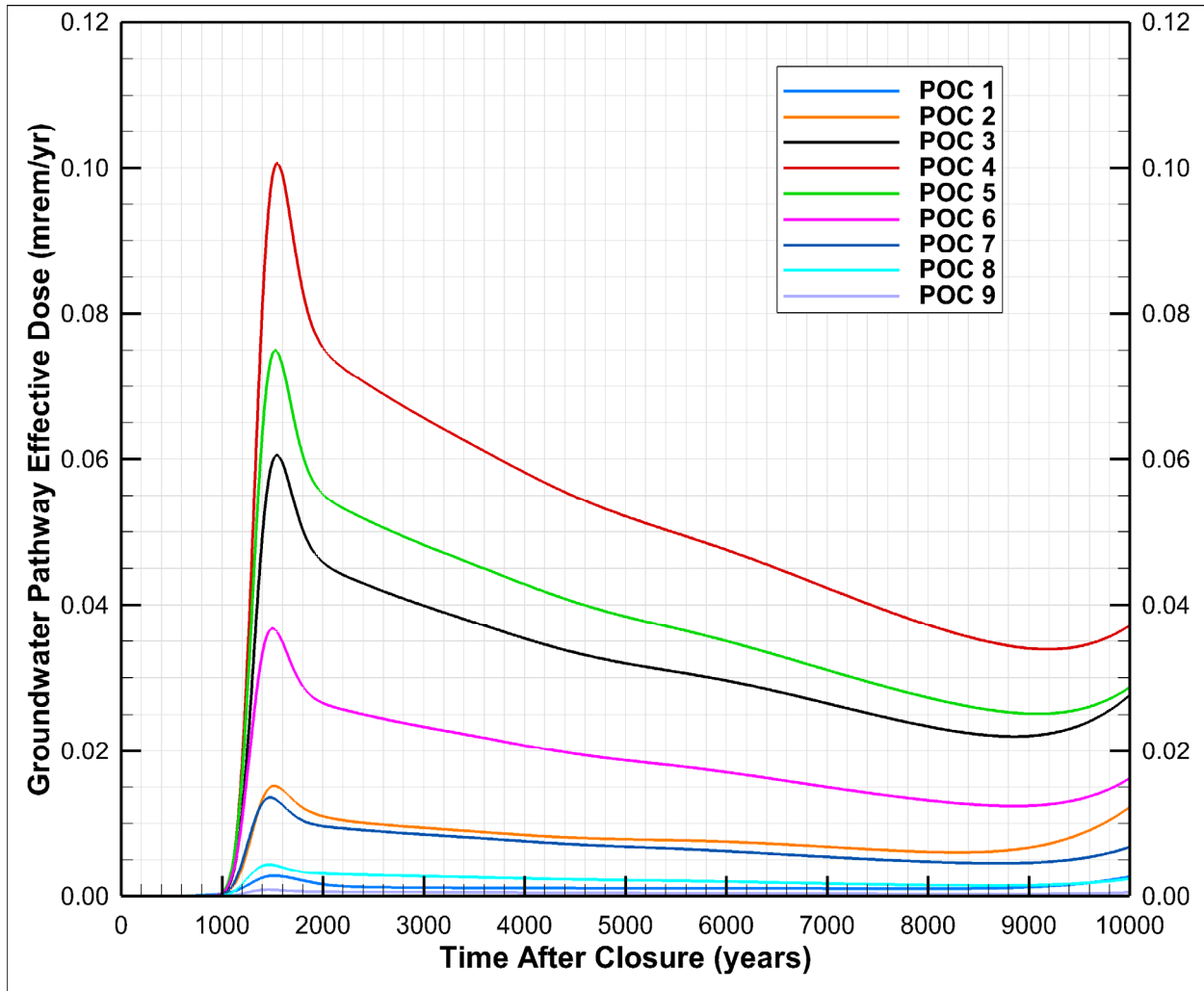
The all-pathway dose results for the groundwater (PoCal 4) and the air pathway are presented in Figure 7-30 for all radionuclides that produced a nonzero dose result within 10,000 years. Also shown on the figure are the DOE O 435.1 compliance time and compliance dose, for comparison. The peak dose summed over all radionuclides within the compliance time period is about 4×10^{-3} mrem/yr, primarily from ^3H release. Within the compliance time period, the early dose is due to contribution of ^3H and ^{129}I from the air pathway but after about 800 years the dose is dominated by ^{99}Tc contribution from the groundwater pathway. Within the sensitivity/uncertainty analysis time period (1,000 to 10,000 years), the peak dose summed over all radionuclides is 0.10 mrem/yr, which occurs about 1,500 years after closure.

The dose resulting from exposure along the groundwater pathway (PoCal 4) is by far the dominant dose in the sensitivity/uncertainty analysis time period (1,000 to 10,000 years) and is presented separately in Figure 7-31 along with the major dose-contributing radionuclides. The highest total dose from the groundwater pathway within the compliance time period is 4×10^{-4} mrem/yr and within the sensitivity/uncertainty analysis time period is 0.10 mrem/yr resulting from release of ^{99}Tc . Minor contributors to the total dose at long times are ^{79}Se , ^{129}I , ^{126}Sn , and uranium isotopes and their progeny.² A summary of the peak doses and time of peak occurrence is presented in Table 7-5.

² Radium-226+D includes doses associated with all its progeny, excluding inhalation doses from ^{222}Rn , as required in DOE O 435.1.

RPP-ENV-58782, Rev. 0

Figure 7-29. Groundwater Pathway Dose (mrem/yr) as a Function of Time for All Points of Calculation at the 100 Meters Compliance Distance.



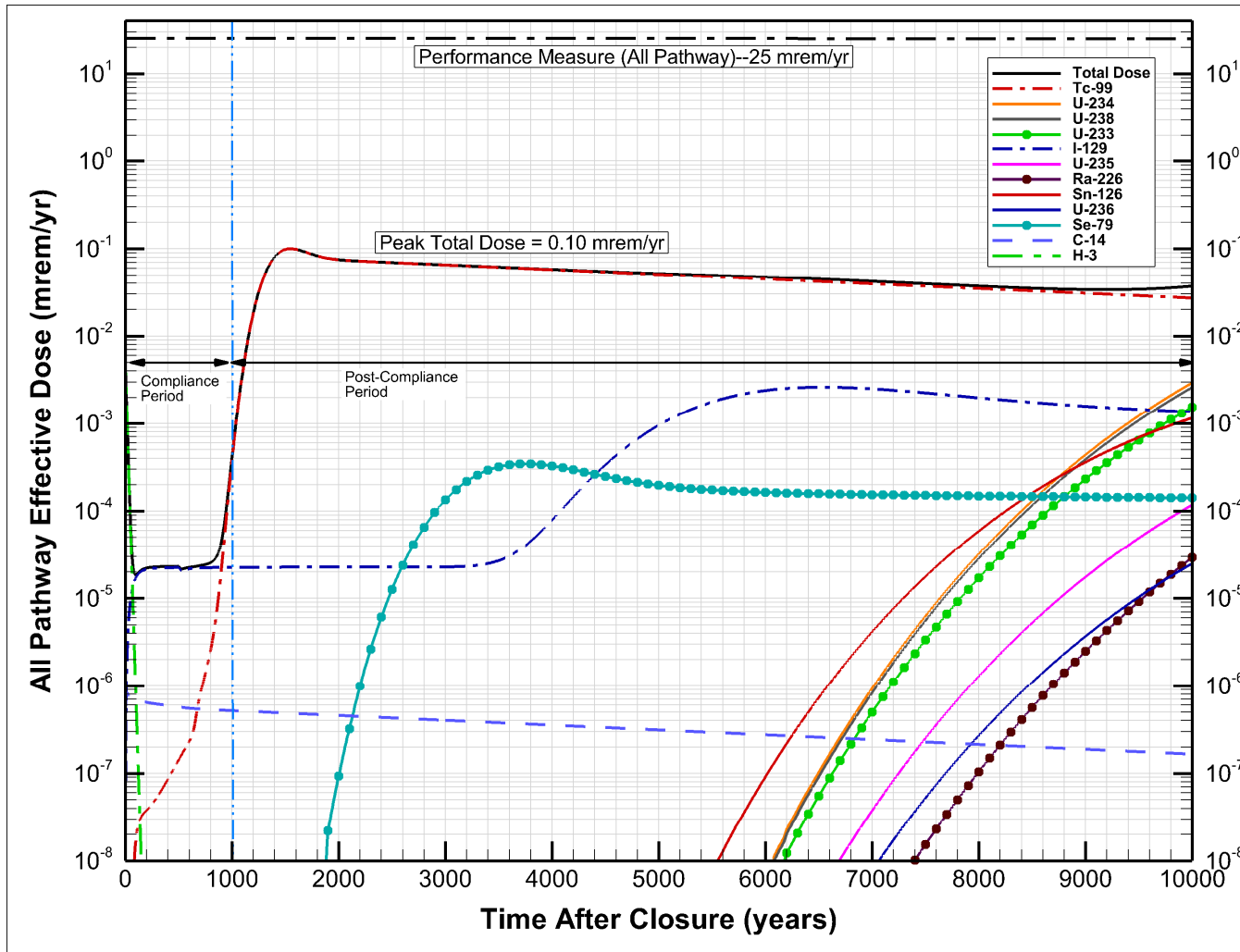
POC = Point of Calculation

7.3.2 Air Pathway Dose

Doses from radionuclides that may potentially be released in gaseous form are presented in Figure 7-32 along with the 10 mrem/yr air pathway dose performance objective from DOE O 435.1. Doses are very small, orders of magnitude below the dose performance objective, at all times. The peak dose of 4×10^{-3} mrem/yr occurs at very early time with ^3H being the primary dose contributor. Around 100 years, ^{129}I takes over as the primary dose contributor as ^3H dose declines due to its short half-life. Iodine-129 persists within the tank due to its long half-life and retention in the grout (from sorption), leading to a slow continuous diffusive flux. By about 300 years the ^{129}I dose reaches a steady value of 2×10^{-5} mrem/yr, indicating that the concentration gradient in the air phase from the tank to the surface has reached a steady state.

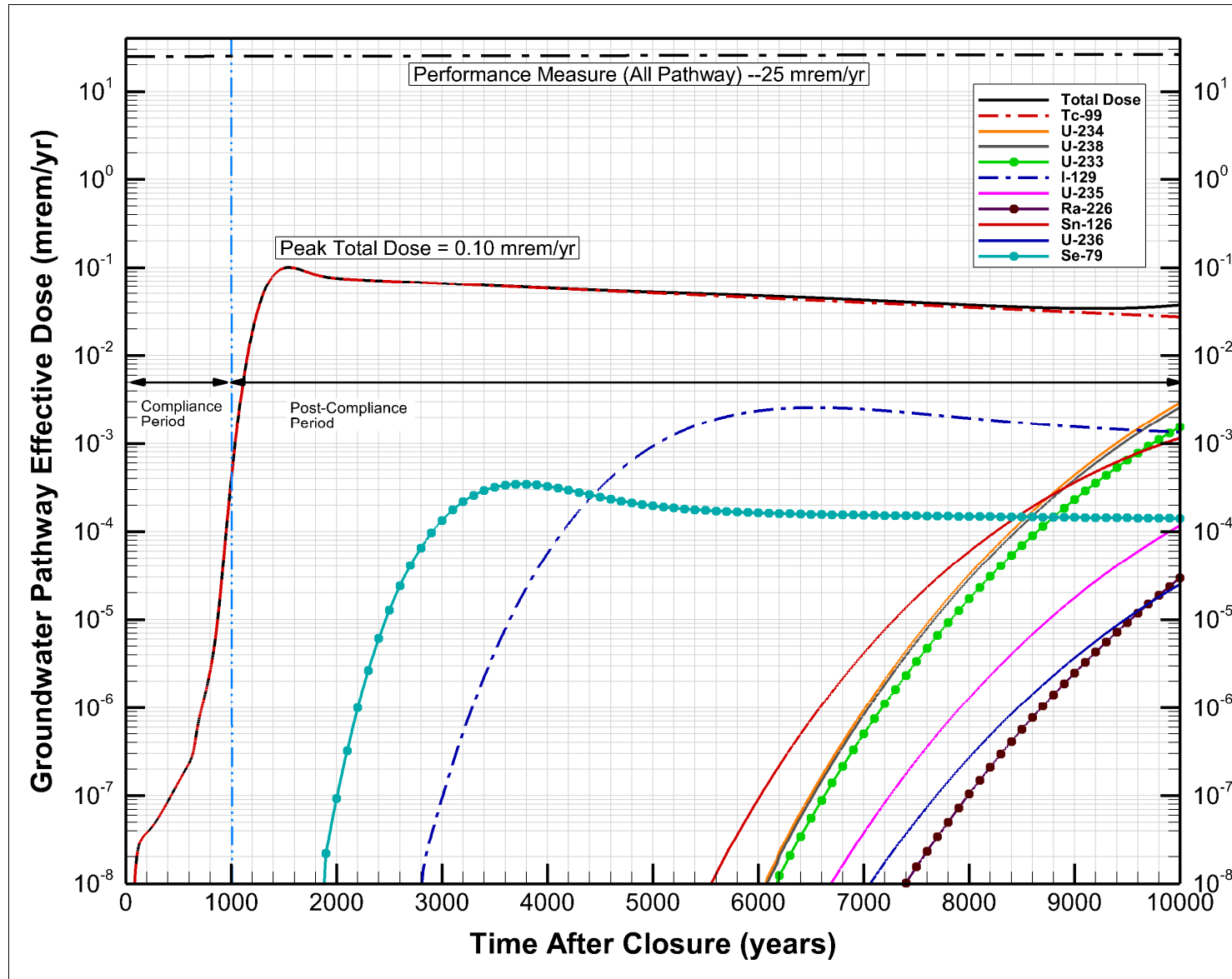
Figure 7-30. All-Pathways Dose Results that Includes Air and Groundwater Pathway Contributions at the Maximum Point of Concentration.

The DOE Order 435.1 compliance time (1,000 years) is shown as a vertical blue dashed line, and the compliance dose (25 mrem/yr) is shown as the black horizontal dashed line. Note the logarithmic vertical axis.



Reference: DOE O 435.1, Radioactive Waste Management.

Figure 7-31. Results of the Groundwater Pathway Dose Analysis at the Maximum Point of Concentration.



RPP-ENV-58782, Rev. 0

Table 7-5. Summary of Peak Doses (mrem/yr) for the Groundwater Pathway and the Time of Occurrence for All Radionuclides Giving Nonzero Doses in the Base Case Analysis.

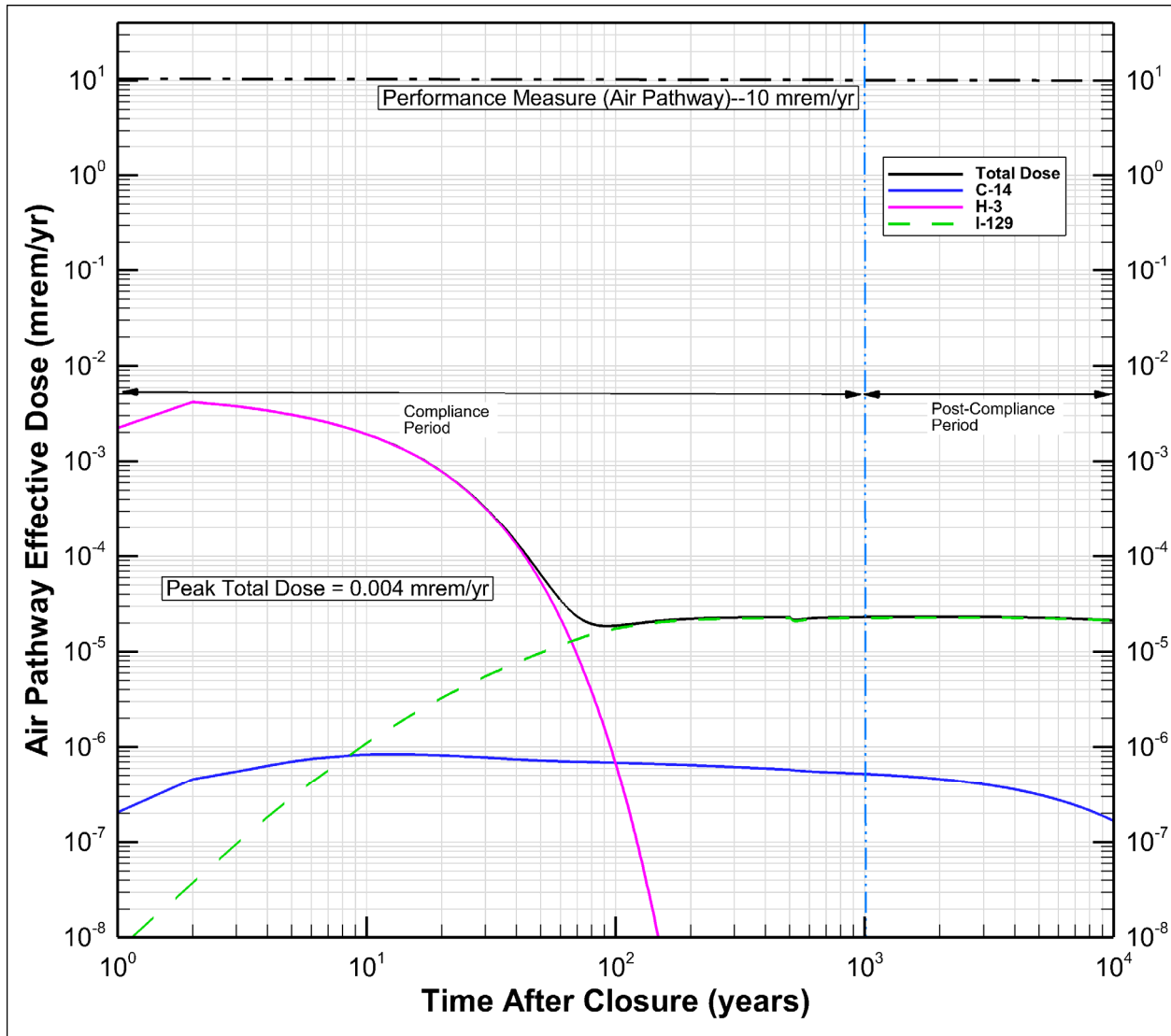
Radionuclide	Peak Dose (mrem/yr)	Post-Closure Time of Peak Dose (year)	Peak Dose within 1,000 years Post-Closure (mrem/yr)
⁹⁹ Tc	0.1	1,500	4E-4
⁷⁹ Se	3.4E-4	3,800	0
¹²⁹ I	2.6E-3	6,500	0
¹²⁶ Sn	1.2E-3	10,000	0
²³⁸ U	2.6E-3	10,000	0
²³⁶ U	2.5E-5	10,000	0
²³⁵ U	1.2E-4	10,000	0
²³⁴ U	3.0E-3	10,000	0
²³³ U	1.6E-3	10,000	0
²³⁰ Th	1.3E-7	10,000	0
^{226+D} Ra*	2.8E-5	10,000	0

*Radium-226+D includes doses associated with all its progeny, excluding inhalation doses from ²²²Rn, as required in DOE O 435.1, Radioactive Waste Management.

1
2

RPP-ENV-58782, Rev. 0

Figure 7-32. Results of the Air Pathway Dose Analysis.
Note the logarithmic vertical and horizontal axis.



RPP-ENV-58782, Rev. 0

- 1
- 2
- 3
- 4
- 5
- 6

This page intentionally left blank.

RPP-ENV-58782, Rev. 0

8.0 UNCERTAINTY AND SENSITIVITY ANALYSIS

The guidance for completing the uncertainty and sensitivity analyses (DOE G 435.1-1) states that the dose rates have associated uncertainties, and a discussion of uncertainties should be included in expressing the outcomes of any PA. The guidance further states that an estimate of the degree of uncertainty is needed for the analysis that includes the calculation of the maximum impact of the disposal facility beyond the 1,000-year compliance period.

The intent of the uncertainty and sensitivity analysis is to identify the assumptions and parameters that have the greatest impact on the projected doses, and evaluate the consequences of the associated uncertainties relative to the performance objectives. This is because exact or precise estimates of future impacts are not truly quantifiable, and even the sources of uncertainty remain unquantifiable because they must include elements of subjectivity (NCRP Report 152).

Uncertainty analysis evaluates how uncertainty in analysis inputs collectively affect uncertainty in the analysis outcomes (for example, estimate of dose). As part of the uncertainty analysis, all uncertain inputs are evaluated together within a system model to estimate plausible range of outcomes. It helps evaluate how combination of various parameters could lead to various outcomes (for example, high dose or low dose). The sensitivity analysis quantifies the cause-and-effect relationships due to single-parameter or limited number of multiple-parameter changes in the parameter estimates. The results of the sensitivity analysis identify those parameters for which the variability in their estimates, either because of lack of knowledge or foreknowledge, limited data, or inherent randomness, introduces the greatest uncertainty into the estimates of potential radionuclide contamination levels. The uncertainty and sensitivity analysis are complementary to each other.

8.1 UNCERTAINTY ANALYSIS

Projections of environmental processes are inherently uncertain. Assessment of uncertainty in model results arising from assumptions and parameter values is necessary to support the determination that there is reasonable expectation of meeting the performance objectives. The objective of the uncertainty analysis is to estimate the plausible range of radionuclide dose that results from selecting parameter values within their uncertainty ranges. When a sufficient number of parameter combinations is evaluated over their plausible range, the calculated range of potential radionuclide dose can be used to quantify the uncertainty in the dose estimates. This analysis supports the demonstration of meeting the requirements of DOE M 435.1-1.

The objectives of this section are to develop uncertainty ranges and probability distributions of input parameter values for use in the PA, and to perform a fully probabilistic uncertainty analysis. The methodology that will be applied to propagate uncertainty through these models is first presented, followed by a discussion of the rationale that guided the probability distribution functions of input parameters. Uncertainty in model parameters is subsequently examined, followed by an evaluation of uncertainty in the groundwater and air pathway.

RPP-ENV-58782, Rev. 0

8.1.1 Methodology for Propagation of Uncertainty

One of the primary expectations of the PA modeling is to provide sufficient explanation of the uncertainty in the dose estimates. A probabilistic uncertainty analysis as described is intended to quantify and capture, where possible, the uncertainty in the process-level models, input parameters, and assumptions about current or future events. The intent of these analyses is to improve understanding of what uncertain factors exert the greatest influence on the model results.

The uncertainty analysis is conducted using a model that is developed by abstracting the results of the process-level models. The process-level models are defined as those that are specifically developed to rigorously solve the governing equations of flow and transport with appropriate boundary conditions at the scale of the processes that can incorporate changes to physical, chemical, and hydrologic properties. The abstraction-based approach is adopted because exercising the process-level models to adequately cover all combinations of parameter values across their full ranges of uncertainty would be very time-consuming and challenging.

To streamline this process in order to examine the uncertainty in a timely manner, an abstraction-based approach has been adopted for performing uncertainty analyses. For this purpose, the GoldSim[®] software (GoldSim Technology Group 2009) is used. GoldSim[®] is specifically designed for performing PA analyses. It not only provides the platform for coupling all of the processes in the PA in a system-level model, but also provides tools for propagation of the uncertainty. Similar approaches have been used at other DOE sites for examining uncertainty, for example, SRR-CWDA-2009-00017, "Performance Assessment for the Saltstone Disposal Facility at the Savannah River Site"; LA-UR-08-06764, "Performance Assessment and Composite Analysis for Los Alamos National Laboratory Technical Area 54, Area G"; and DOE/NV/25946--107, "Probabilistic Performance Assessment of a Low-Level Radioactive Waste Disposal Site on the Nevada Test Site."

The vadose zone flow rates as a function of time were abstracted from the STOMP[®]-based process-level models. STOMP[®] results were then used to generate the flow field (spatially and temporally varying Darcy flux and moisture content), which were abstracted along with their uncertainty estimates for use in GoldSim[®]-based models. Because changes in hydraulic properties and recharge rates introduce uncertainty in the computed flow field in a non-linear manner, the abstraction was performed by first propagating the uncertainty in flow parameters using the STOMP[®]-based model and then evaluating the resulting flow field. Since running 3-D STOMP[®]-based models is numerically intensive, a selected combination of pre-determined hydraulic properties and recharge rates were used by assigning parameter values from select percentiles of their distribution. This approach led to development of a possible range of flow fields (vertical Darcy flux and moisture contents) that were abstracted as inputs to the transport calculations using the GoldSim[®]-based system model for uncertainty analysis.

8.1.2 Rationale for Assigning Probability Distributions

The lack of knowledge about the appropriate value to use in a model is generally called epistemic uncertainty. Epistemic uncertainty is distinct from variability, which arises from

RPP-ENV-58782, Rev. 0

heterogeneity or an inherent randomness in the behavior of the system. The knowledge of experts cannot be expected to reduce uncertainty due to variability, although their knowledge may be useful for quantifying it (“Uncertainty and sensitivity analysis techniques for use in performance assessment for radioactive waste disposal” [Helton 1993]). Both uncertainty and variability may be quantified using probability distributions. They can be tracked and evaluated separately during an analysis, or they can be analyzed within the same computational framework. However, EPA/630/R-97/001, Guiding Principles for Monte Carlo Analysis recommends that variability and uncertainty are tracked and evaluated separately to identify parameters where additional data are needed (i.e., to identify reducible uncertainty through further study).

Among the different uncertainty and sensitivity analysis approaches available, the Monte Carlo method has been widely used for PA of radioactive waste disposals. In this method, discrete sets of input parameter values are selected at random from probability distribution functions; each set is run through the model, and a probability distribution function of model output is constructed. That distribution represents the uncertainty in model output associated with uncertain input parameters. Among its main assets, this method is conceptually simple and able to cover the full range of parameter uncertainties. More importantly, the method allows for obtaining the predictive uncertainty results without using surrogate models to map relations between uncertain inputs and analysis results (Helton 1993).

The Monte Carlo approach involves the following steps (“Uncertainty and sensitivity analysis techniques for hydrologic modeling” [Mishra 2009]):

- Selecting model input parameters
- Assigning probability distributions to input parameters to quantify uncertainty
- Generating many sample sets (realizations) through sampling of probability distribution
- Propagating the uncertainty (via realizations) through the analysis
- Determining parametric and nonparametric estimates of the reliability in the model output once an appropriate sample size is reached that ensures stable estimates of the output distribution.

A Monte Carlo approach was implemented in the WMA C PA using the GoldSim[®] software, using stochastic variables that represent the range of uncertain parameters in the WMA C model.

Although an infinite number of theoretical distributions can be used to fit an empirical data set, only a handful of distributions are considered in practice (Technical Report TR-02-11, “Assigning probability distributions to input parameters of performance assessment models”). The key features of these distributions are described in Table 8-1.

Several studies have tried to assess the impact of a chosen distribution function on the sensitivity analysis results. For instance, the results obtained by “The Effect of Distribution Choice for Uncertain Parameters in a Monte Carlo Analysis” (Hoffman 1996) can be used as a rule of

RPP-ENV-58782, Rev. 0

thumb for focusing the attention on parameter distributions that will have a relevant impact.
Hoffman's conclusions are summarized in the following:

- As long as the uncertainty of a given parameter is small (coefficient of variation $\leq 30\%$), it makes very little difference which distribution is chosen
- As the coefficient of variation approaches and exceeds 30%, the use of distributions of log-transformed values is recommended
- The choice of distribution shape will be important if the analyst is interested in extreme values.

Table 8-1. Main Uses of Several Common Distribution Functions.

Distribution	Useful for Representing
Uniform (log-uniform) Triangular (log-triangular)	Low state of knowledge and/or subjective judgment
Normal	Errors due to additive processes
Log-normal	Errors due to multiplicative processes
Weibull	Component failure rates
Poisson	Frequency of rare events
Beta	Bounded, unimodal, random variables

Reference: Technical Report TR-02-11, "Assigning probability distributions to input parameters of performance assessment models."

Technical Report TR-02-11 recommends using, as a starting point, the guidelines given by EPA/630/R-97/001, the context of probabilistic health risk assessment. In selecting a distributional form, EPA/630/R-97/001 recommends that the analyst first considers the quality of the information in the database, and answers a series of questions including, but not limited to, the following:

- Is there any mechanistic basis for choosing a distribution family?
- Is the shape of the distribution likely to be dictated by physical or biological properties or other mechanisms?
- Is the variable discrete or continuous?
- What are the bounds of the variable?
- Is the distribution skewed or symmetric?

RPP-ENV-58782, Rev. 0

- If the distribution is thought to be skewed, in which direction?
- What other aspects of the shape of the distribution are known?
- How well do the tails of the distribution represent the observations?

For distributions representing the epistemic uncertainties common in PA analyses, Technical Report TR-02-11 recommends choosing a probability distribution function by considering the principle of maximum entropy. In this approach, a distribution is chosen that preserves the maximum uncertainty about the data, similar to the well-known concept of thermodynamic entropy related to the degree of disorder or randomness. The principle of maximum entropy seeks to choose a probability distribution function that maximizes the informational entropy, subject to known constraints. When developing the uncertainty distribution, the range was chosen carefully so as to be realistic and not to make the distribution excessively wide, which may have the potential of causing “risk dilution” (i.e., the peak dose using the peak-of-the-mean approach can be smaller for a wide parameter distribution than if a narrower distribution was used) (“History and Value of Uncertainty and Sensitivity Analyses at the Nuclear Regulatory Commission and Center for Nuclear Waste Regulatory Analyses” [CNWRA/NRC 2011]).

From a practical perspective, the use of the maximum entropy principle in assigning a distribution function implies the following considerations.

- If all the samples are equally likely because no constraint on the plausible parameter values is available, the maximum entropy is reached and corresponds to the uniform distribution.
- If some information is available, uncertainty is reduced as much as possible by using all information (i.e., by satisfying all constraints) but no further by unnecessary assumptions. This ensures that ignorance is acknowledged, and forces the analyst to retain maximum uncertainty in the distribution developed from the data. In that case, the distribution function will have a concentration of probability away from the extreme values, leading to a reduction of uncertainty and hence a reduction of entropy in comparison to the uniform distribution.

Based on these considerations, the maximum entropy principle implies that certain probability distribution functions are more appropriate for representing data with specific constraints, as summarized in Table 8-2. This approach has been used in this PA for assigning distribution functions.

8.1.3 Parameter Uncertainty Distributions

This section provides a description of the parameter uncertainty distributions evaluated in the uncertainty analysis for the WMA C PA.

8.1.3.1 Uncertainty in Recharge Rates. Recharge rates have been estimated from studies conducted at the Hanford Site over the last 30 years. Recharge rates are based on the estimate of

RPP-ENV-58782, Rev. 0

the downward water flux below the evapotranspiration zone representing deep drainage. Recharge rates are available for natural and disturbed soils, for soils with and without vegetation, and for various plant communities. In addition, recharge has been estimated for surface covers with varying plant communities. These estimates are based on lysimeter records, tracer tests (chloride mass balance), and computer simulations to match field data. PNNL-16688 and PNNL-14702 provide primary sources of information on recharge estimates for the Hanford Site that are relevant to tank farms. There is no site-specific information to WMA C on natural recharge. Natural recharge at WMA C is inferred from measurements made at the FLTF (Section 3.1.5.2.2).

Table 8-2. Guidance for Selection of Probability Distribution Function Considering the Data Constraints.

Constraint	Distribution
Upper bound, lower bound	Uniform
Minimum, maximum, mode	Triangular
Mean, standard deviation	Normal
Range, mean, standard deviation	Beta
Mean occurrence rate	Poisson

Reference: Reliability-Based Design in Civil Engineering (Harr 1987).

Spatial variability in recharge occurs at WMA C and surrounding areas due to variations in vegetative cover and disturbed surface conditions. Spatially, two zones have been identified with different disturbed surface conditions: one within the WMA C fenceline, designated as the WMA C Disturbed Surface, and the other outside the WMA C fenceline, designated as the Non-Tank Farm Disturbed Surface. After closure, it is expected that the disturbed areas will revegetate fully within 30 years.

The temporal uncertainty in recharge occurs due to time-varying changes resulting from construction and operations at WMA C and future changes after closure. These temporal recharge estimates have been grouped into a pre-operational phase, an operational phase, a post-closure phase with intact surface cover, and a post-closure phase with degraded surface. While both spatial and past temporal changes have influenced the recharge rates at WMA C and need to be considered, the focus of the PA is on developing uncertainty in long-term post-closure recharge rates, since that will influence the transport of contaminants from the residual waste in the future. In this regard, the temporal variability observed in the past climate records (50% to 128% of modern levels [Section 3.1.2.6]) is considered.

The area outside the WMA C fenceline, designated as the Non-Tank Farm Disturbed Surface, is not likely to influence the contaminant transport in the vadose zone, and, therefore, constant best-estimate values are used for those areas in the following manner.

- Disturbed areas observed during the operations phase using aerial photographs, where vegetation appears to have grown, are assigned a value of 22 mm/yr (0.87 in./yr) based

RPP-ENV-58782, Rev. 0

on estimates presented in PNNL-14702. These areas include surfaces where the existing shrub-steppe vegetation has been destroyed (e.g., by fire or Hanford operations), but shallow-rooted plants have been allowed, or were reintroduced, to re-vegetate the land.

- Disturbed areas observed during the operations phase using aerial photographs that appear to be reworked such that vegetation does not grow are assigned a value of 63 mm/yr (2.5 in./yr) based on estimates presented in PNNL-14702. These disturbed areas include construction and operations outside WMA C that removed the surface soil, broke up any near-surface layering, and exposed Hanford formation sands. These sediments tend to be coarser than the original soil, and, as indicated in photographs of the area around WMA C, plants have difficulty growing on them. The selected recharge rate is supported by drainage data collected from the 300 North Lysimeter, which contains coarse Hanford formation material screened to less than 1% gravel, where the long-term recharge rate averaged 62 mm/yr (2.4 in./yr) from 1981 to 2005 (PNNL-16688).
- Disturbed areas are allowed 30 years to revegetate fully after closure. Therefore, over time the disturbed area recharge changes to that assigned for the undisturbed natural vegetated land surface. Thirty years appears to be a reasonable estimate for the time required for the young shrub steppe to become mature and reclaim the land. Sagebrush and/or other native plant species at Hanford often reclaim the land within 5 years of planting or seeding (BHI-01745, "2004 Environmental Restoration Contractor Revegetation Monitoring Report"; WCH-223, "2007 River Corridor Closure Contractor Revegetation Monitoring Report"). The plant community at the Prototype Hanford Barrier began working almost immediately to transpire water and eliminate recharge (PNNL-17176), and 24 species of vegetation were identified on it one year after it burned (PNNL-18845). Data from other arid and semi-arid areas in the United States indicate that many stands of mountain big sagebrush achieve greater than 20% crown cover within 25 years of burning ("Trend of Mountain Big Sagebrush Crown Cover and Ground Cover on Burned Sites, Uinta Mountains and West Tavaputs Plateau, Utah" [Goodrich et al. 2008]). In a study conducted at 38 sites in southwest Montana, the average time to full recovery of basin sagebrush (ssp. *Tridentata*, the subspecies most prevalent at Hanford) required less than 32 years after burning ("Recovery of Big Sagebrush Following Fire in Southwest Montana" [Lesica et al. 2007]).

For the area within the WMA C fenceline, designated WMA C Disturbed Surface, the temporal evolution is presented below with the uncertainty estimates.

Pre-Operation Period: During the time prior to construction (before 1945), the area currently occupied by WMA C appears to have been covered by a mature shrub-steppe plant community growing in Rupert sand or Burbank loamy sand soil. It is difficult to distinguish between the two soil types because the divide between the Rupert sand and Burbank loamy sand soil appears to coincide with the northeastern boundary of WMA C.

For the vegetated Rupert sand, PNNL-14702 recommended using a value estimated using the Wye Barricade data (4 mm/yr [0.16 in./yr]) as the best-estimate value, although the surface is described as a stabilized dune area with low shrub cover. PNNL-16688 later

RPP-ENV-58782, Rev. 0

revised the estimate by considering an average of the three available tracer estimates (4, 0.26, and 0.9 mm/yr [0.16, 0.01 and 0.04 in./yr]). Moreover, they reported a good agreement between their suggested mean value (1.7 mm/yr) and their modeling results that considered a 50-year weather record (including the two wettest years: 1995 and 1996) and yielded a rate of 1.9 mm/yr (0.07 in./yr). Consequently, they recommended using an estimate of 1.7 mm/yr (0.07 in./yr) for vegetated Rupert sand soil.

For the vegetated Burbank loamy sand, PNNL-14702 recommended the average value of 3.0 mm/yr (0.12 in./yr) based on three chloride tracer-based estimates of recharge (0.66 mm/yr, 2.8 mm/yr, and 5.5 mm/yr [0.03 in./yr, 0.11 in./yr and 0.22 in./yr]). PNNL-16688 augmented these data with five additional tracer-based estimates that decreased the average to 1.9 mm/yr (0.07 in./yr), along with a simulation that suggested a rate of 5.2 mm/yr (0.2 in./yr), which is near the upper end of the range of tracer estimates.

Based on the available information, uncertainty in pre-operational (natural vegetation) recharge is developed through selection of a triangular distribution, with a minimum value of 0.5 mm/yr (0.02 in./yr), maximum value of 5.2 mm/yr (0.2 in./yr), and mode of 1.9 mm/yr (0.07 in./yr).

Operations Period: During the operations period, which started in 1945 and is assumed to last until 2020, two recharge zones have been defined within the WMA C fenceline: one that is disturbed, has no vegetation, and is covered with gravel; and the other that is largely undisturbed and characterized by a vegetative cover. For the latter, the same uncertainty distribution and range is considered that is developed for the pre-operations phase. For the former (the disturbed zone without vegetation [bare soil]), the range in recharge is based on the following discussion.

Disturbed zone recharge rates for the tank farms have been estimated to vary from 40 mm/yr to 140 mm/yr (1.57 in./yr to 5.51 in./yr). A reasonably conservative estimate of 100 mm/yr (3.94 in./yr) was recommended for disturbed Rupert sand zone without vegetation and with gravel cover (Gee et al. 1992). The upper bound value of 140 mm/year (5.51 in./yr) results from an enhanced precipitation experiment on the “sandy gravel side slope” of the Hanford Prototype Barrier installed at the 216-B-57 Crib. This treatment is referenced as being “useful for characterizing deep drainage at the high-level waste tank farms at Hanford” (PNNL-14744). Enhanced precipitation represented three times the average precipitation. Approximately 140 mm (5.51 in./yr) of the applied precipitation was observed to have infiltrated. For a lower bounding value, CP-14873, “200-BP-1 Prototype Hanford Barrier Annual Monitoring Report for Fiscal Year 2002” reported that 21.5% of precipitation (37.8 mm/yr [1.49 in./yr]) became recharge through sparsely vegetated sandy gravel representing the “sandy gravel side slope.” Such a percentage (i.e., 21.5%) represents a lower value of approximately 40 mm/yr (1.57 in./yr).

Based on the available information, uncertainty in operational period recharge for the disturbed zone within WMA C is developed through selection of a triangular distribution,

RPP-ENV-58782, Rev. 0

1 with a minimum value of 40 mm/yr (1.57 in./yr), maximum value of 140 mm/yr
2 (5.51 in./yr), and mode of 100 mm/yr (3.94 in./yr).

3
4 Post-Closure Period with Intact Surface Cover: For the area covered by the intact surface
5 barrier, the recharge rate is expected to decline to nearly zero, as the modified
6 RCRA-compliant surface cover is designed to prevent or significantly limit recharge.
7 The design criteria of such a barrier are identified in BHI-00007, "Prototype Hanford
8 Surface Barrier: Design Basis Document" and DOE/RL-93-33, and include limiting
9 recharge to 0.5 mm/yr (0.02 in./yr). The design life of surface cover as a recharge barrier
10 is assumed to be 500 years (DOE/RL-93-33).

11
12 Extensive laboratory and modeling work, and limited field testing of surface barriers,
13 have been performed with results summarized in PNNL-14744. Lysimeter testing has
14 been performed for different surface barrier concepts, including a Modified RCRA
15 Subtitle C Barrier with silt-loam layers having depths between 1 and 2 m (3.3 to 6.6 ft).
16 Lysimeter data from the prototype Hanford barrier (Wing and Gee 1994) have also been
17 collected and analyzed. Finally, modeling has been performed to address potential
18 climate change impacts and no vegetation impacts on surface barrier performance.

19
20 The lysimeter drainage data that have been collected since 1989 suggest that the recharge
21 rate beneath surface barriers having at least 1 m (3.3 ft) of silt loam is zero under ambient
22 precipitation conditions. Most of these lysimeters did not contain an asphalt layer.
23 Simulation results reported in PNNL-14744 investigated the sensitivity of the lysimeter
24 data to climate change, silt-loam hydraulic properties, vegetation changes, erosion, and
25 dune formation above the surface barrier. Results indicated that the performance of these
26 surface barriers was robust in that the estimated recharge rates remained below 0.1 mm/yr
27 (0.004 in./yr). For the cases investigated, only in the case of dune formation and no
28 vegetation on the surface barrier were the simulated recharge rates above 0.1 mm/yr
29 (0.004 in./yr). To account for such uncertainty (dune formation and no vegetation) within
30 the design life of the barrier, an upper-bound recharge of 0.9 mm/yr (0.04 in./yr) is
31 considered as suggested by PNNL-14744 for the post-barrier design life.

32
33 Based on the available information, uncertainty in recharge during post-closure period
34 with intact surface is developed through selection of a triangular distribution, with a
35 minimum value of 0.1 mm/yr (0.004 in./yr), a maximum value of 0.9 mm/yr (0.04 in./yr),
36 and mode of 0.5 mm/yr (0.02 in./yr).

37
38 Post-Closure Period with Degraded Surface Cover: In the post-closure period after
39 500 years, the recharge barrier capability of the surface cover is assumed to be degraded.
40 This recharge rate is applicable to the entire simulated duration (except for the first
41 500 years after closure) and influences the contaminant transport of residual tank waste
42 through the vadose zone. It is expected that once the surface cover is degraded, the
43 recharge will be similar to the recharge during the pre-operational phase, since the
44 surface will most likely be indistinguishable from the surrounding surface in terms of
45 vegetative cover. PNNL-14744 suggests that the performance of the barrier is not
46 expected to change after its design life. Conclusions in PNNL-14744 indicate that the

RPP-ENV-58782, Rev. 0

possibility of the most likely natural failure mechanisms (i.e., bioturbation of the silt loam layer, wind erosion, and accretion of windblown sand) of these natural systems is quite low with an appropriate design. The emplaced silt-loam soils should continue to perform as long as they remain in place.

To propagate uncertainty in post-closure recharge rate following degraded surface cover, a triangular distribution is chosen, with a minimum value of 0.5 mm/yr (0.02 in./yr), a mode value of 1.9 mm/yr (0.07 in./yr), and a maximum value of 5.2 mm/yr (0.2 in./yr). This uncertainty range is the same as that chosen for the pre-operational phase recharge rates and covers the natural variability observed in annual precipitation in the climate record for the last 100,000 years (Section 3.1.2.6).

The range in recharge rates selected for the various time periods are summarized in Table 8-3.

Table 8-3. Spatial and Temporal Uncertainty in Recharge Rates Considered for Waste Management Area C.

Spatially Distinct Zone	Uncertainty in Recharge Estimate (mm/yr)		
	Minimum	Maximum	Most Likely
Pre-operations Period (Prior to Year 1945)			
Undisturbed (Natural Vegetation) ^a	0.5	5.2	1.9
Operations Period (Years 1945 – 2020)			
Undisturbed (Natural Vegetation) ^a	0.5	5.2	1.9
Waste Management Area C Disturbed Surface	40	140	100
Non-Tank Farm Disturbed Surface ^b	22 / 63	22 / 63	—
Post-Closure Period with Intact Surface Cover (Years 2020 – 2520)			
Undisturbed (Natural Vegetation) ^a	0.5	5.2	1.9
Waste Management Area C Surface Barrier	0.1	0.9	0.5
Non-Tank Farm Disturbed Surface ^{a,c}	0.5	5.2	1.9
Late Post-Closure Period with Degraded Surface Cover (Years > 2520)			
Undisturbed (Natural Vegetation) ^a	0.5	5.2	1.9
Waste Management Area C Surface Barrier	0.5	5.2	1.9
Non-Tank Farm Disturbed Surface ^a	0.5	5.2	1.9

^aWaste Management Area C late post-closure surface barrier assumed to acquire natural vegetation recharge rate.

^bDisturbed areas that allow vegetation are assigned 22 mm/yr. Disturbed areas that are reworked such that vegetation does not grow are assigned 63 mm/yr.

^cDisturbed areas are allowed 30 years to revegetate fully.

RPP-ENV-58782, Rev. 0

8.1.3.2 Uncertainty in Residual Inventory Estimates. A best estimate of the residual inventory for tanks and ancillary equipment was developed and evaluated in the PA (Section 3.2.2). However, considerable uncertainty exists in estimating the residual inventory due to mixing of various waste types, differentiation between inventory associated with sludge and salt-cake, and the limited availability of direct measurements of contaminant concentrations. These uncertainties have been recognized in the BBI database, which is the official database for tank waste inventory. Uncertainties in concentration, waste volume, and waste density for each tank are accounted by developing standard deviation (SD) estimates in those parameters (assuming a normal distribution), which are then propagated to calculate the inventory uncertainty in 46 radionuclides and 25 chemicals that are tracked in the BBI. For the retrieved tanks, the uncertainty is based primarily on sample-based results. However, where information is lacking for a particular analyte, a template based on process knowledge is used to fill in the gaps.

For WMA C, the BBI database currently contains residual inventory information from 10 retrieved tanks: C-103, C-104, C-106, C-108, C-109, C-110, C-201, C-202, C-203, and C-204. These are the tanks from which post-retrieval samples were collected, and uncertainty in concentration (in solid phase), residual volume, and density is quantified in terms of relative standard deviations (RSD), which is SD divided by the mean value. All the relevant information related to 46 radionuclides and 25 chemicals from the BBI was obtained for these 10 tanks. The following steps were undertaken to reduce the dataset.

- Removal of the analytes that were below detection limits. This resulted in 25 radionuclides and 12 chemicals.
- Identification of mean solid-phase concentration, residual volume, and waste density for each analyte for the sludge waste form for each tank.
- Identification of RSD of concentration for each analyte, residual volume, and waste density for the sludge waste form for each tank.
- Calculation of SDs in concentration, residual volume, and waste density from the RSDs by multiplying by the mean values.

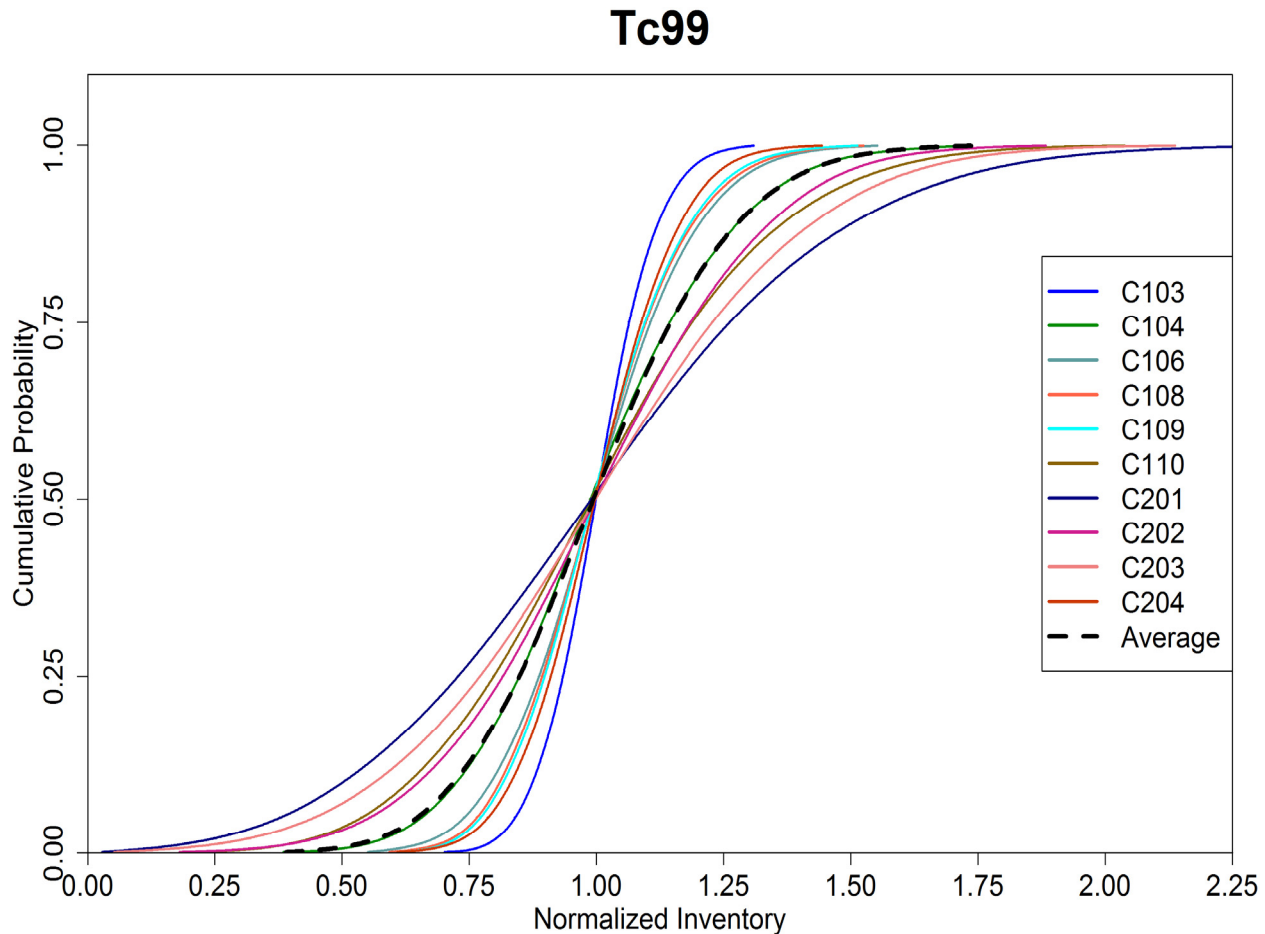
Since the residual inventory for a given analyte is calculated by multiplying the concentration in solid phase (sludge) with the residual waste volume and waste density, the mean inventory is calculated based on the mean values of these parameters.

Next, normal probability distributions were developed for the concentration of each analyte, residual volume, and density for each tank. This was done by defining the mean and SD for the parameter and implementing them in the GoldSim[®]-based system model. Following this, 10,000 realizations were run using Latin Hypercube Sampling (LHS), leading to 10,000 estimates of inventory for each analyte for each tank. The sampled inventory estimates were normalized by dividing by the mean inventory, leading to 10,000 normalized inventories for each analyte for each tank. These results can be expressed as a cumulative distribution function (CDF) of the normalized inventory. An example CDF for ⁹⁹Tc is presented in

RPP-ENV-58782, Rev. 0

Figure 8-1 for each tank. In addition, an average CDF was calculated by averaging the CDF values for all the tanks.

Figure 8-1. Cumulative Distribution Function of Normalized Inventory of Technetium-99 for Retrieved Tanks, and the Average Cumulative Distribution Function.



Development of normalized inventory CDF is attractive because the sampled value can be multiplied with the mean inventory to estimate inventory for a given realization. As shown in Figure 8-1, the average normalized inventory CDF for ^{99}Tc ranges from 0.4 to 1.75 and therefore indicates the factor by which the mean inventory can vary. Since the CDF of normalized inventory is calculated separately for each analyte for each tank, each CDF could be separately sampled for each tank to determine the multiplier factor for the inventory. However, this approach leads to a very large number of uncertain parameters related to inventory, due to the large number of analytes considered per source term. The analysis has therefore been simplified by sampling the analyte specific average CDF (averaged over the tanks) and then multiplying the sampled value by the mean inventory for a given analyte for each source term. This approach significantly simplifies the analysis while preserving the uncertainty in the analyte inventory.

The uncertainties in inventory for various analytes are presented in Figure 8-2. Not all the tanks have uncertainty in all the analytes quantified. This is because some analytes are below

RPP-ENV-58782, Rev. 0

detection limits in some of the tanks. In such cases, the average CDF is calculated based on the CDF of the tanks for which uncertainty estimates were available. For analytes for which uncertainty information is not available in the BBI, no uncertainty is propagated in the inventory. For the tanks where post-retrieval sampling-based inventory uncertainty estimates were not available in the BBI database, the uncertainty estimates based on average normalized CDF presented earlier are applied. This is a reasonable approximation, given that several tanks within WMA C have similar waste types (Table 3-12) and were operated in a similar manner.

In addition to developing uncertainty in the inventory, uncertainty is also propagated separately in the residual volume, as it is a key parameter in the source term release calculations. The methodology for deriving the uncertainty in residual volume is similar to that for the inventory derivation and is based on the same dataset. The normalized residual waste volume is derived from 10,000 LHS realizations of the same GoldSim[®] model file used for inventory uncertainty. The model file samples the underlying normal distribution for each tank and divides by the mean residual volume for that tank. The CDF of normalized residual waste volume uncertainty is presented in Figure 8-3 for each tank, along with the average CDF (average of all tanks). The average CDF of normalized waste volume is sampled to scale the mean residual volume for each source term. As shown in Figure 8-3, the normalized values in the average CDF vary from 0.75 to 1.25. Because some correlation is expected between residual waste volume and the residual inventory, the uncertainty distribution of residual waste volume is correlated to the uncertainty distribution of the residual uranium inventory, since it is the dominant radionuclide in terms of mass and forms mineral phases that contribute to the residual volume.

8.1.3.3 Uncertainty in Source Term Transport Parameters. The waste form degradation and release mechanisms from the source term are described in Section 6.3.1. Several interacting parameters determine the release rate from the base of the tanks and ancillary equipment into the underlying vadose zone. The uncertainty in these parameter estimates is described in Section 6.3.1 and summarized below.

- The initial release fraction of ⁹⁹Tc is observed to vary between 4.5% and 15%. Without additional information, a uniform distribution is applied.
- The remaining fraction of ⁹⁹Tc undergoes a slower release that is modeled using a first order reaction rate. The available information was used to identify a uniform distribution with a minimum of $5 \times 10^{-4} \text{ day}^{-1}$ and a maximum of $8 \times 10^{-4} \text{ day}^{-1}$.
- The solubility of uranium is also considered to be uncertain. The uncertainties arise from both the value of the solubility at any time and the mineral phases assumed to be controlling the solubility. The mean solubility is assumed to change from 10^{-4} M to 10^{-6} M at 1,000 years after closure, based on the assumption that solubility will be controlled by amorphous mineral phases early on, and later by a CaUO_4 mineral phase under $\text{Ca}(\text{OH})_2$ -saturated conditions. A factor of two uncertainty multiplier to solubility is imposed by assigning a log-uniform distribution varying from 0.5 to 2. This distribution is chosen because the median value of this distribution is 1 (and mean is about 1.1); therefore, the mean/median sampled multiplier will retain the base case solubility value.

RPP-ENV-58782, Rev. 0

- Uncertainty in the effective diffusion coefficient through the base mat is propagated through a log-uniform distribution with a minimum and maximum value of $6 \times 10^{-9} \text{ cm}^2/\text{s}$ and $2 \times 10^{-7} \text{ cm}^2/\text{s}$, based on the range of effective diffusion coefficients measured for ^{99}Tc as presented in Figure 6-32. This distribution leads to a median value of $3.5 \times 10^{-8} \text{ cm}^2/\text{s}$, which is close to the best-estimate value of $3 \times 10^{-8} \text{ cm}^2/\text{s}$.
- Uncertainty in sorption on cementitious material is represented using a triangular distribution of K_d values for each analyte (see Table 6-5). This distribution is appropriate for representing the mean values and ranges, which are the only values available in the literature. Where information is not available, a zero K_d value is used.

8.1.3.4 Uncertainties in Vadose Zone Hydraulic Properties. Uncertainties in vadose zone hydraulic properties are derived from a set of laboratory (core-scale) experiments conducted on samples representative of Hanford H1, H2, and H3 units and backfill material. The laboratory-measured soil-moisture retention and unsaturated hydraulic conductivity datasets were fit using van Genuchten-Mualem constitutive relationships to derive uncertainty in the following parameters¹:

- The saturated hydraulic conductivity K_s
- The van Genuchten fitting parameter α , which is proportional to inverse of air-entry matric potential (cm^{-1})
- The van Genuchten fitting parameter n , which is a dimensionless fitting parameter commonly taken to be the inverse of the pore-size SD
- The saturated and residual moisture contents (θ_s and θ_r).

A single, large, internally consistent soil-moisture retention and unsaturated hydraulic conductivity dataset consisting of 44 soil samples from the nearby IDF was analyzed for the H2 sand-dominated unit. The IDF is located southwest of WMA C within 200 East Area, and the dataset includes 44 samples to evaluate uncertainty and to derive probability distribution functions for K_s , α , n , θ_s , and θ_r for H2 sand-dominated unit.

The laboratory procedures used to analyze the IDF H2 borehole samples and to derive the van Genuchten-Mualem parameters are summarized in Appendix B (Section B.2) with additional details presented in RPP-20621, “Far-Field Hydrology Data Package for the Integrated Disposal Facility Performance Assessment.” The fitted van Genuchten-Mualem parameters for the IDF H2 sandy sequence (44 samples) are reproduced in Table B-3. The fitted moisture retention curves and unsaturated conductivity curves for H2 sandy sequence, as well as the WMA C H2 composite curves, are shown in Figures B-12 and B-13, respectively. A 20% gravel correction was applied to IDF H2 samples for use at WMA C based on empirical evidence of a greater gravel fraction being present at WMA C than IDF (Appendix B, Section B.2.1).

¹ The pore size distribution factor, ℓ (Mualem 1976) was kept fixed at 0.5 in this exercise.

Figure 8-2. Cumulative Distribution Function of Normalized Inventory of Various Analytes for the Retrieved Tanks along with the Average Cumulative Distribution Function. (sheet 1 of 10)

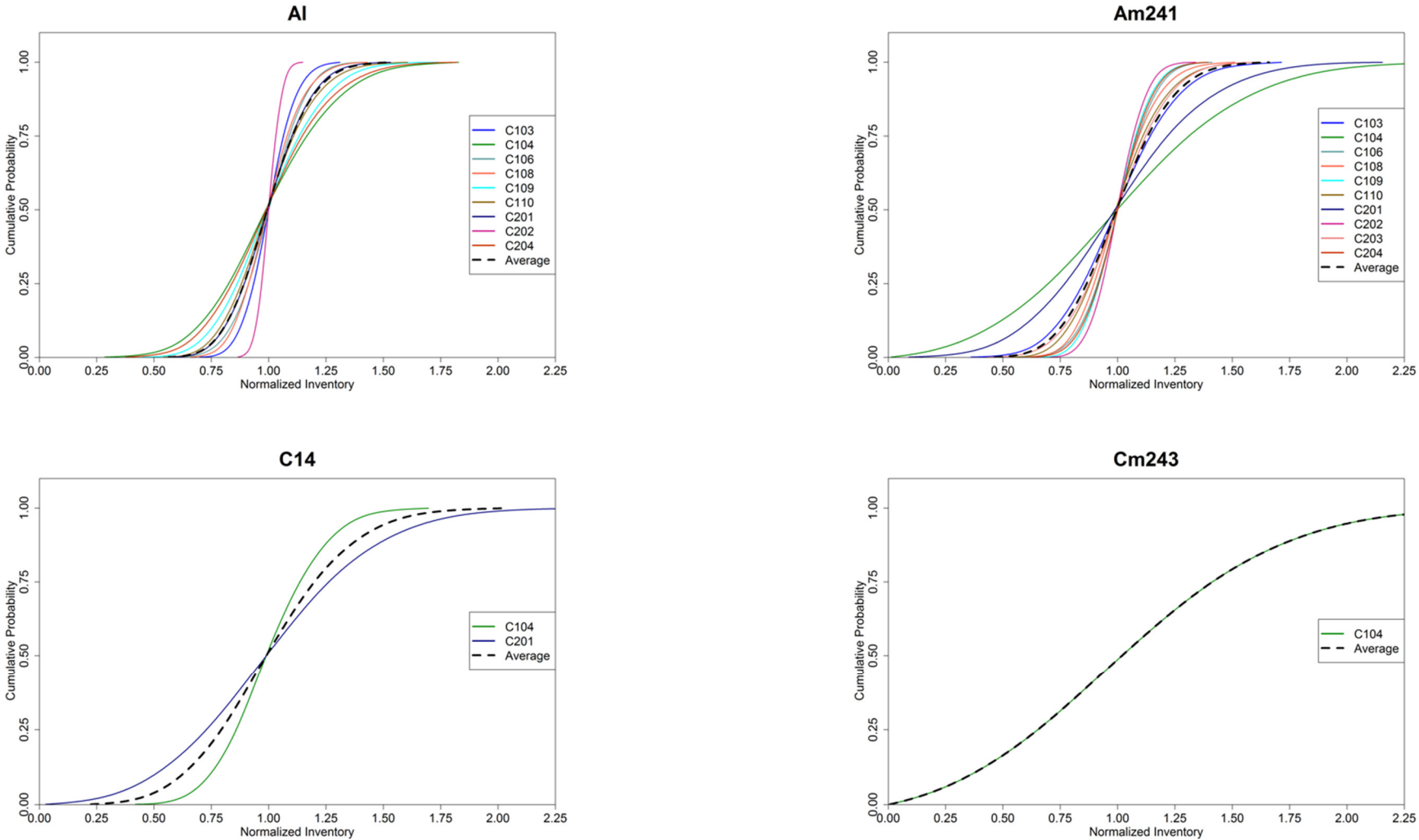


Figure 8-2. Cumulative Distribution Function of Normalized Inventory of Various Analytes for the Retrieved Tanks along with the Average Cumulative Distribution Function. (sheet 2 of 10)

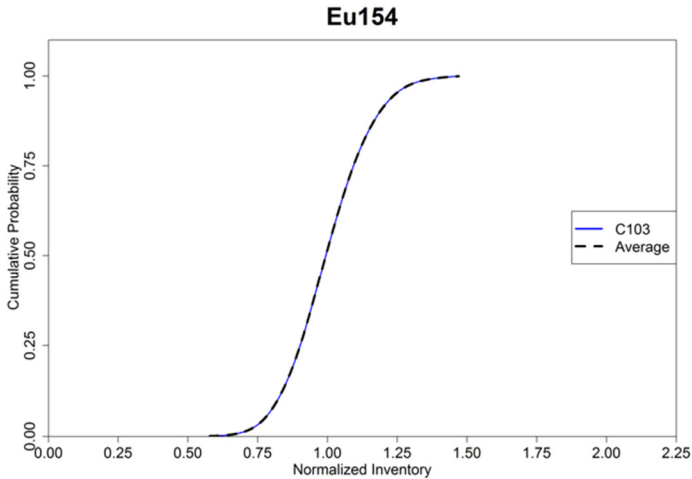
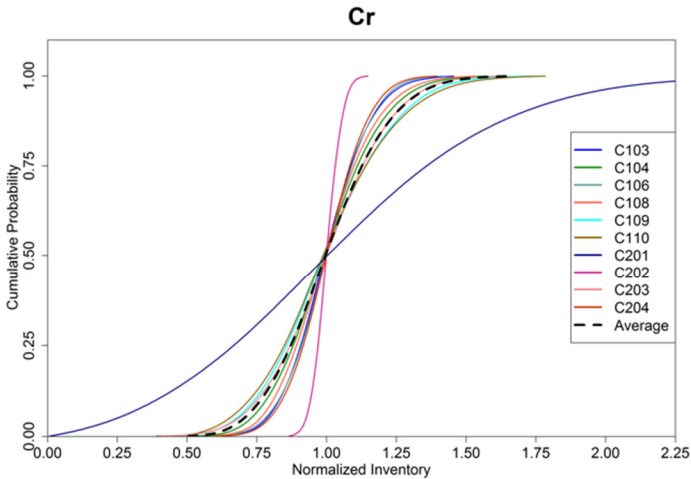
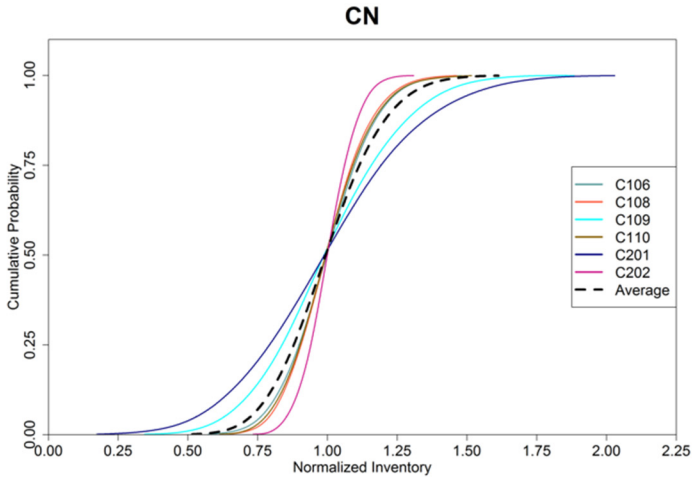
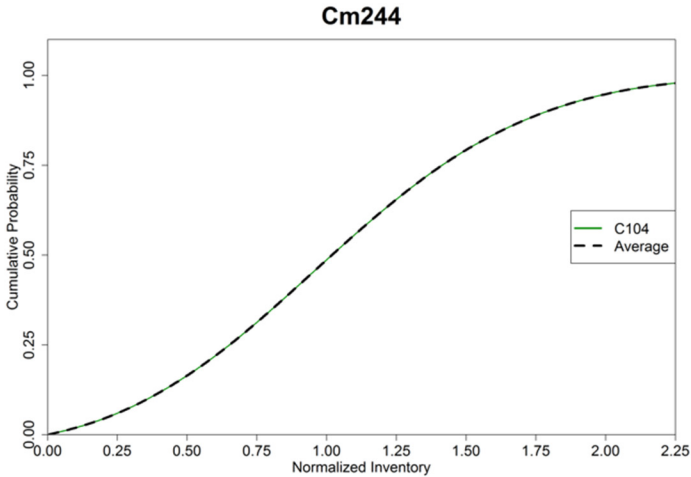


Figure 8-2. Cumulative Distribution Function of Normalized Inventory of Various Analytes for the Retrieved Tanks along with the Average Cumulative Distribution Function. (sheet 3 of 10)

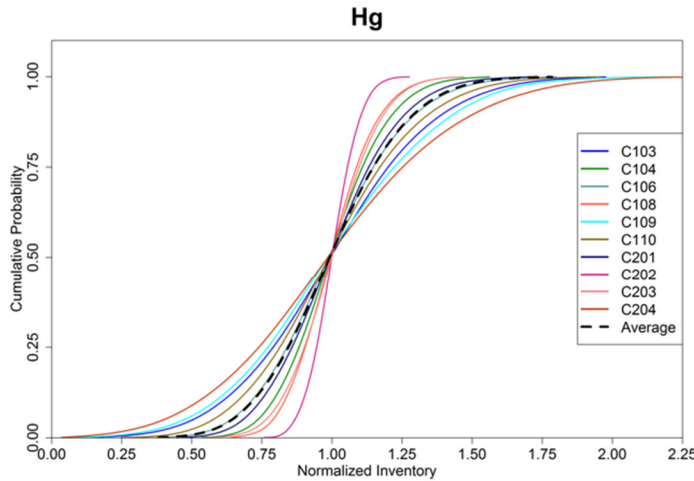
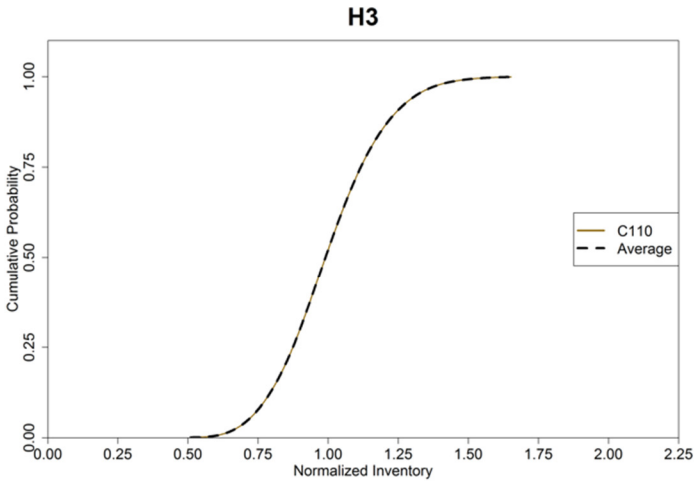
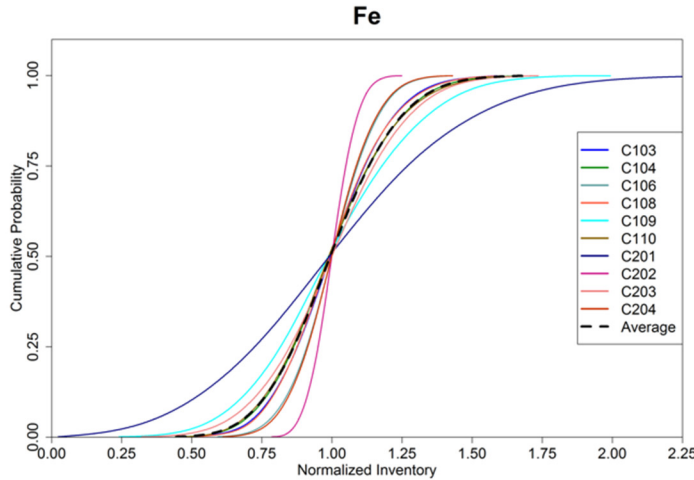
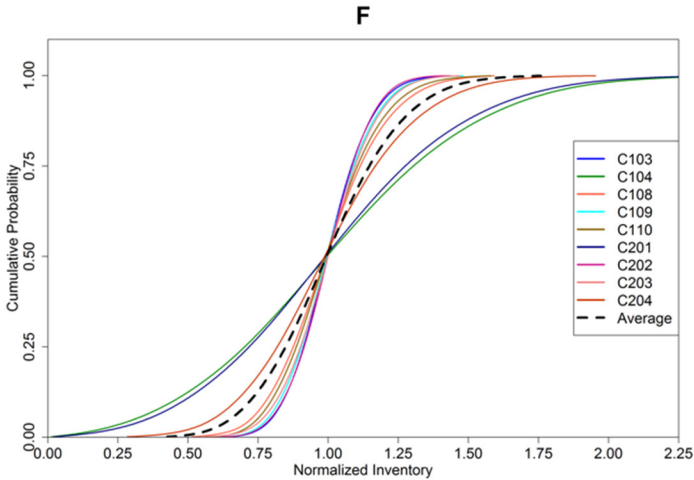


Figure 8-2. Cumulative Distribution Function of Normalized Inventory of Various Analytes for the Retrieved Tanks along with the Average Cumulative Distribution Function. (sheet 4 of 10)

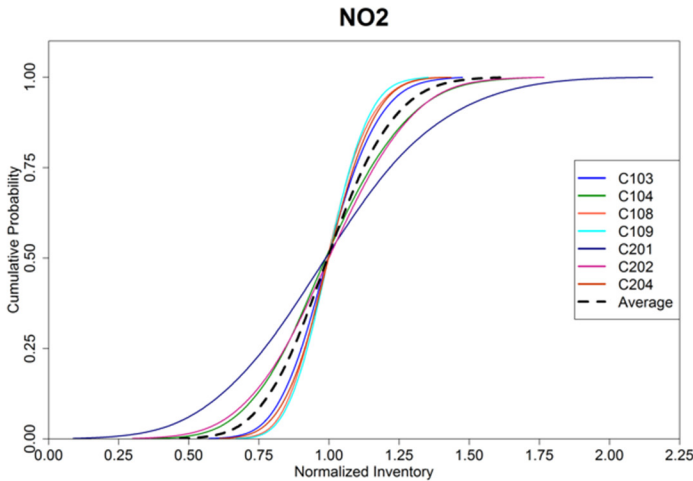
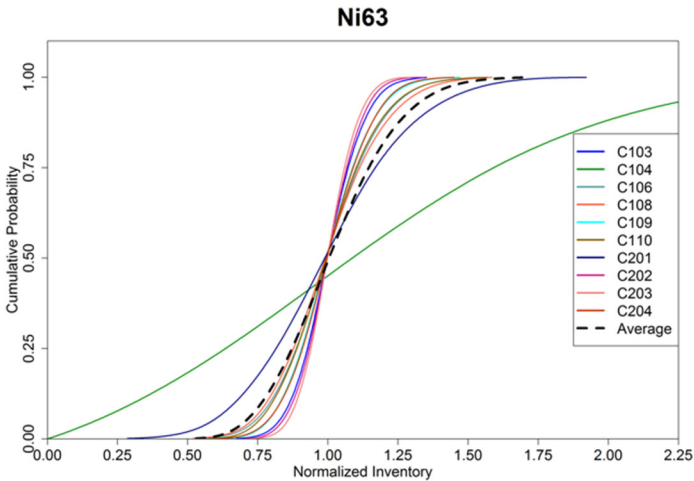
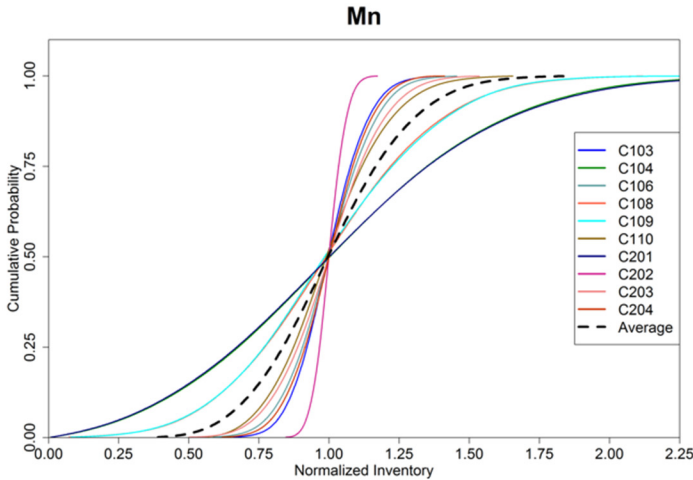
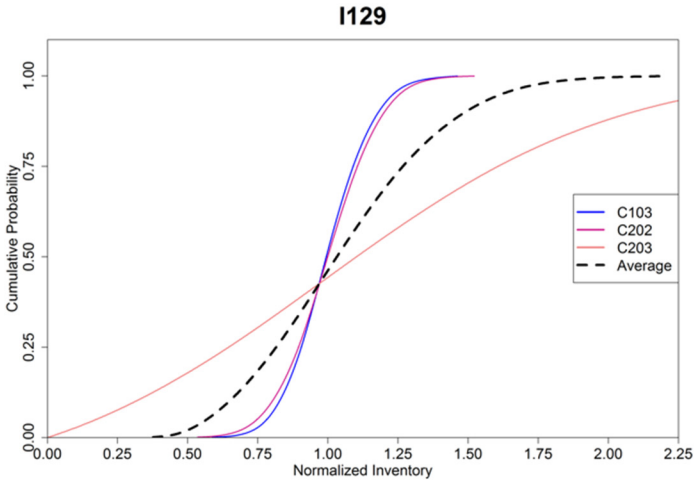


Figure 8-2. Cumulative Distribution Function of Normalized Inventory of Various Analytes for the Retrieved Tanks along with the Average Cumulative Distribution Function. (sheet 5 of 10)

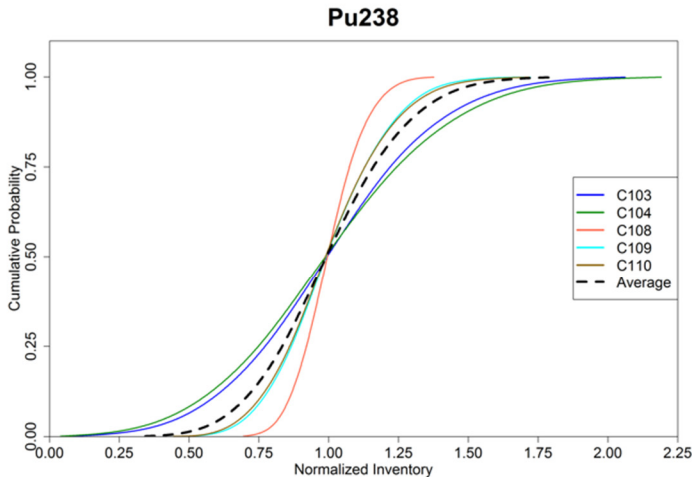
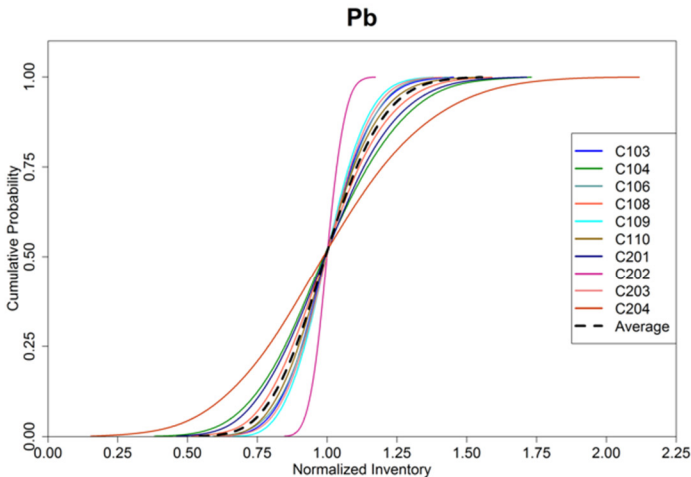
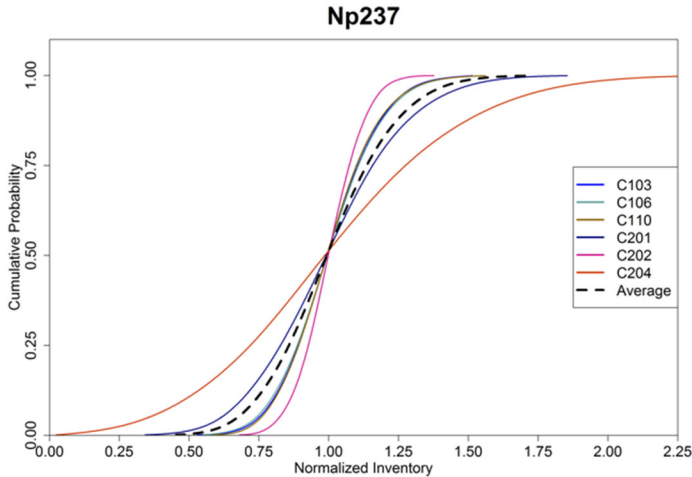
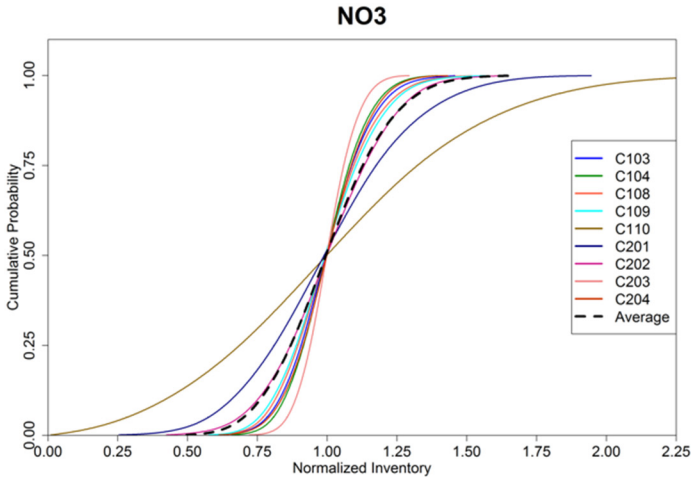


Figure 8-2. Cumulative Distribution Function of Normalized Inventory of Various Analytes for the Retrieved Tanks along with the Average Cumulative Distribution Function. (sheet 6 of 10)

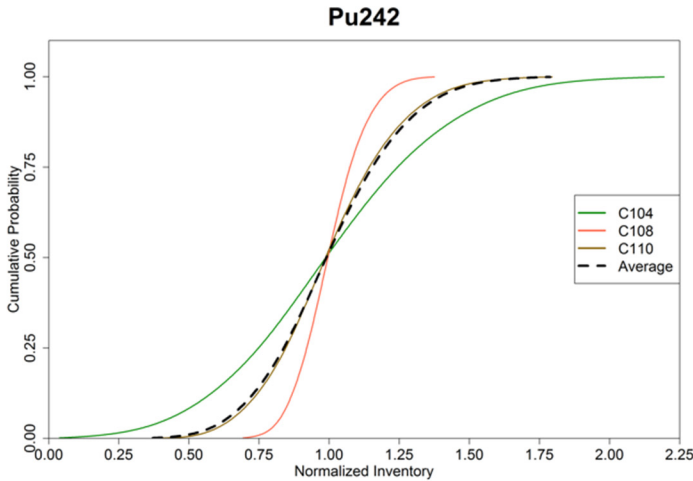
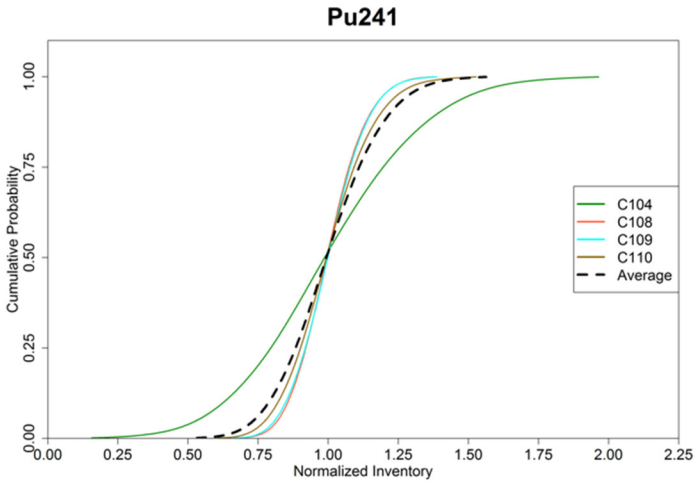
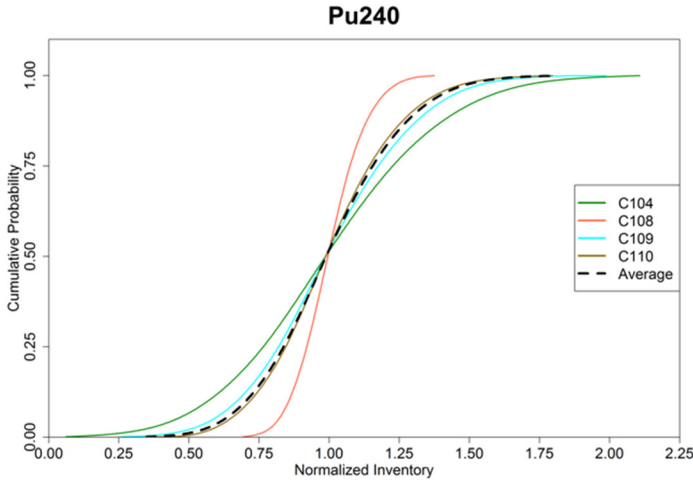
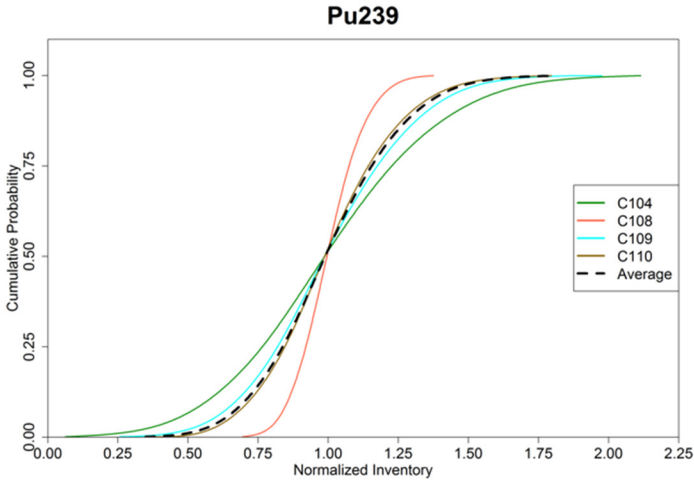


Figure 8-2. Cumulative Distribution Function of Normalized Inventory of Various Analytes for the Retrieved Tanks along with the Average Cumulative Distribution Function. (sheet 7 of 10)

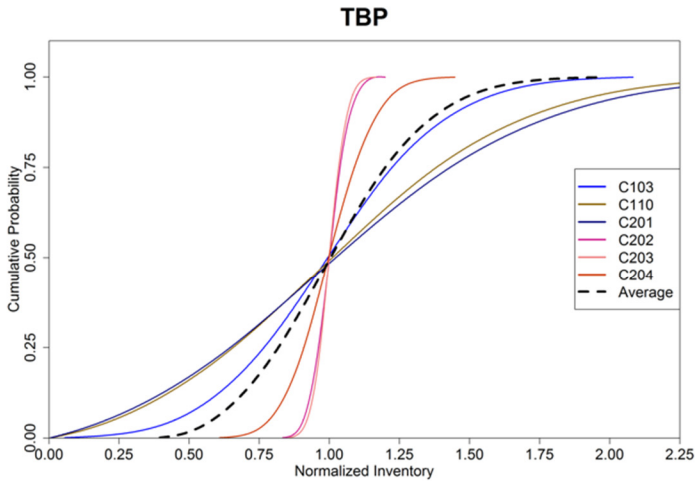
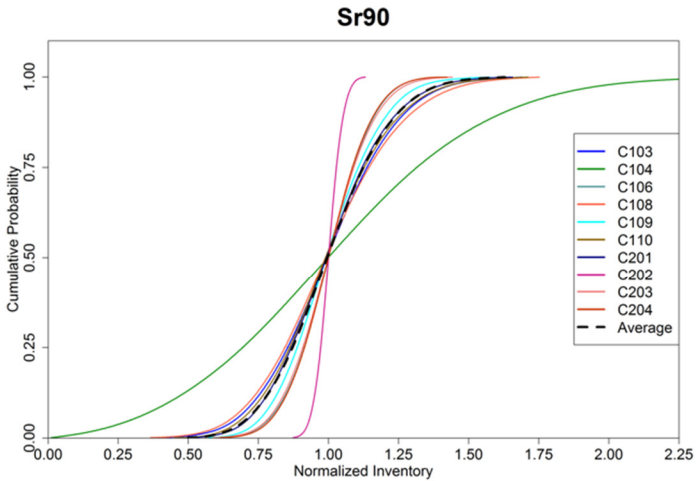
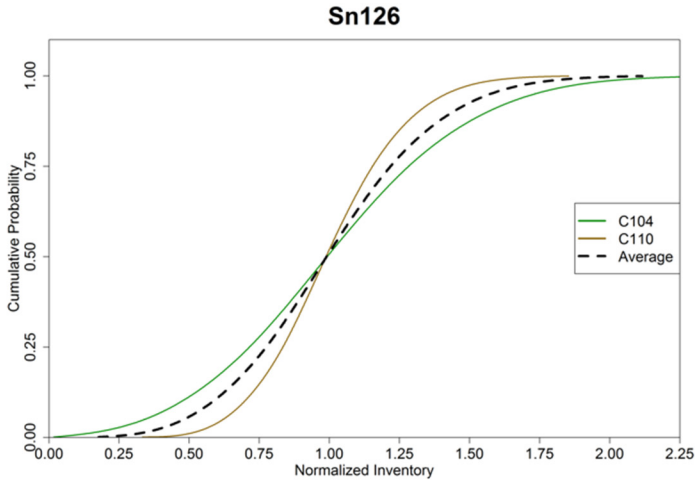
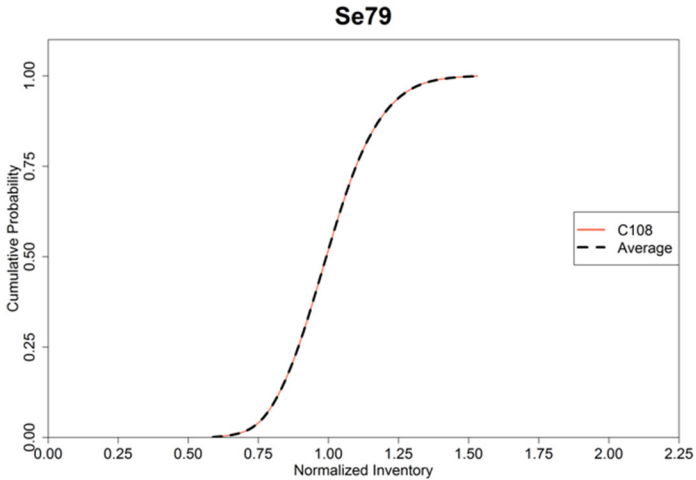


Figure 8-2. Cumulative Distribution Function of Normalized Inventory of Various Analytes for the Retrieved Tanks along with the Average Cumulative Distribution Function. (sheet 8 of 10)

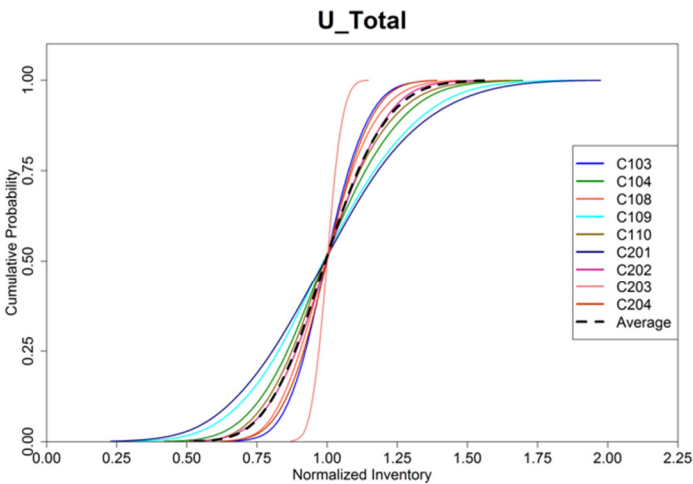
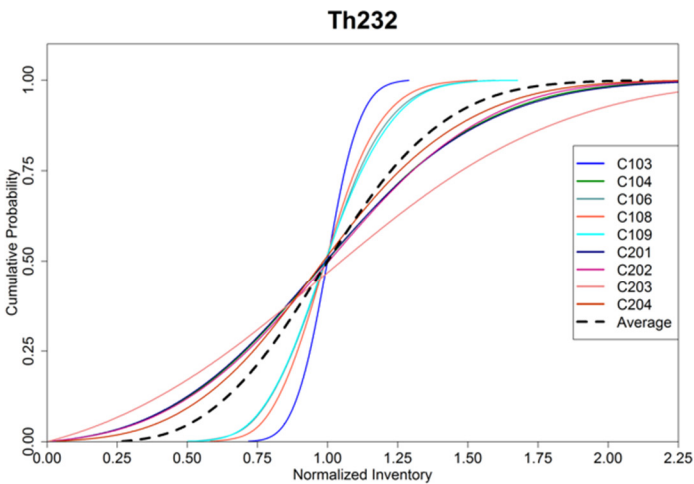
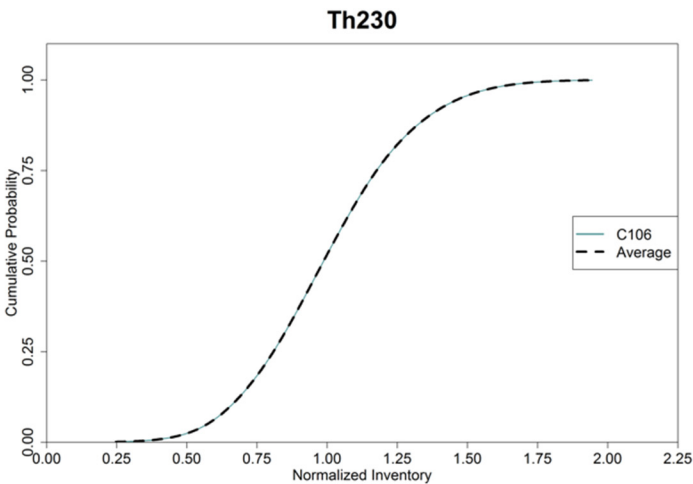
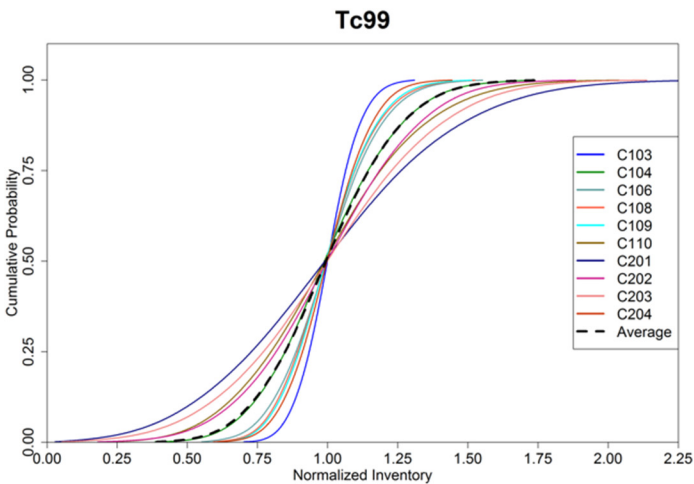
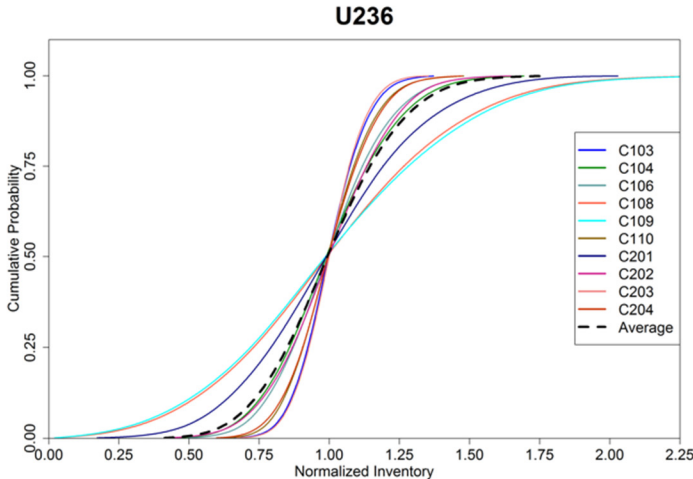
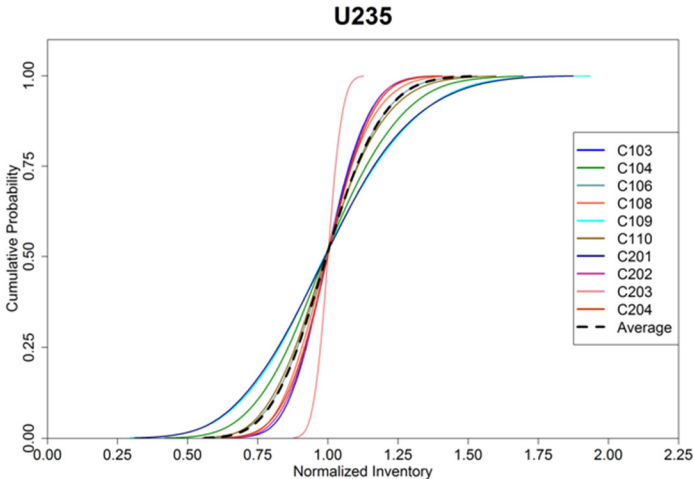
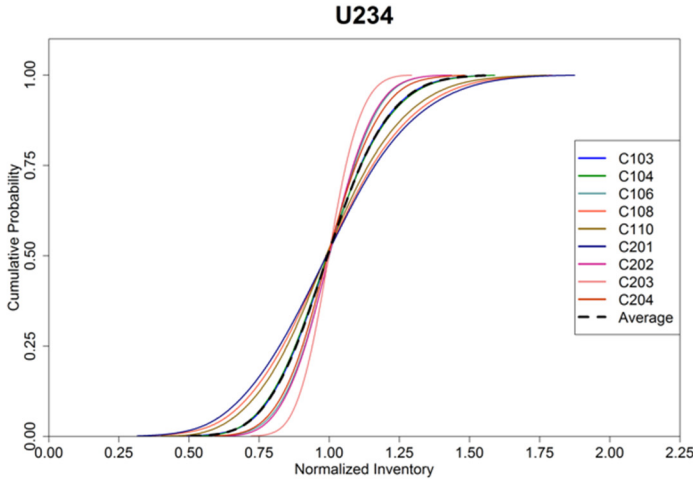
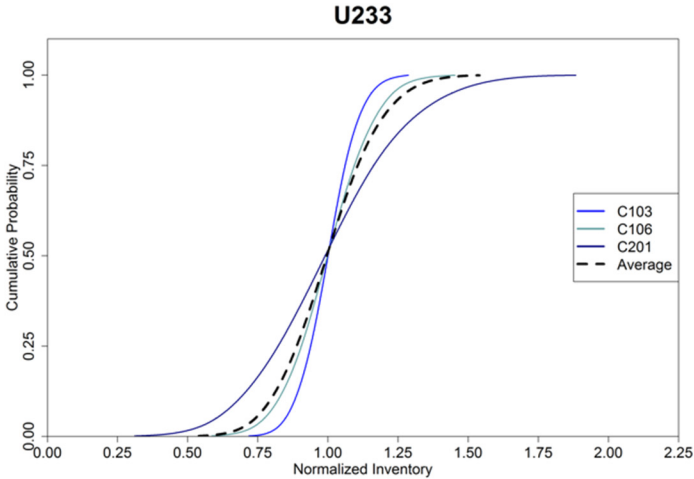
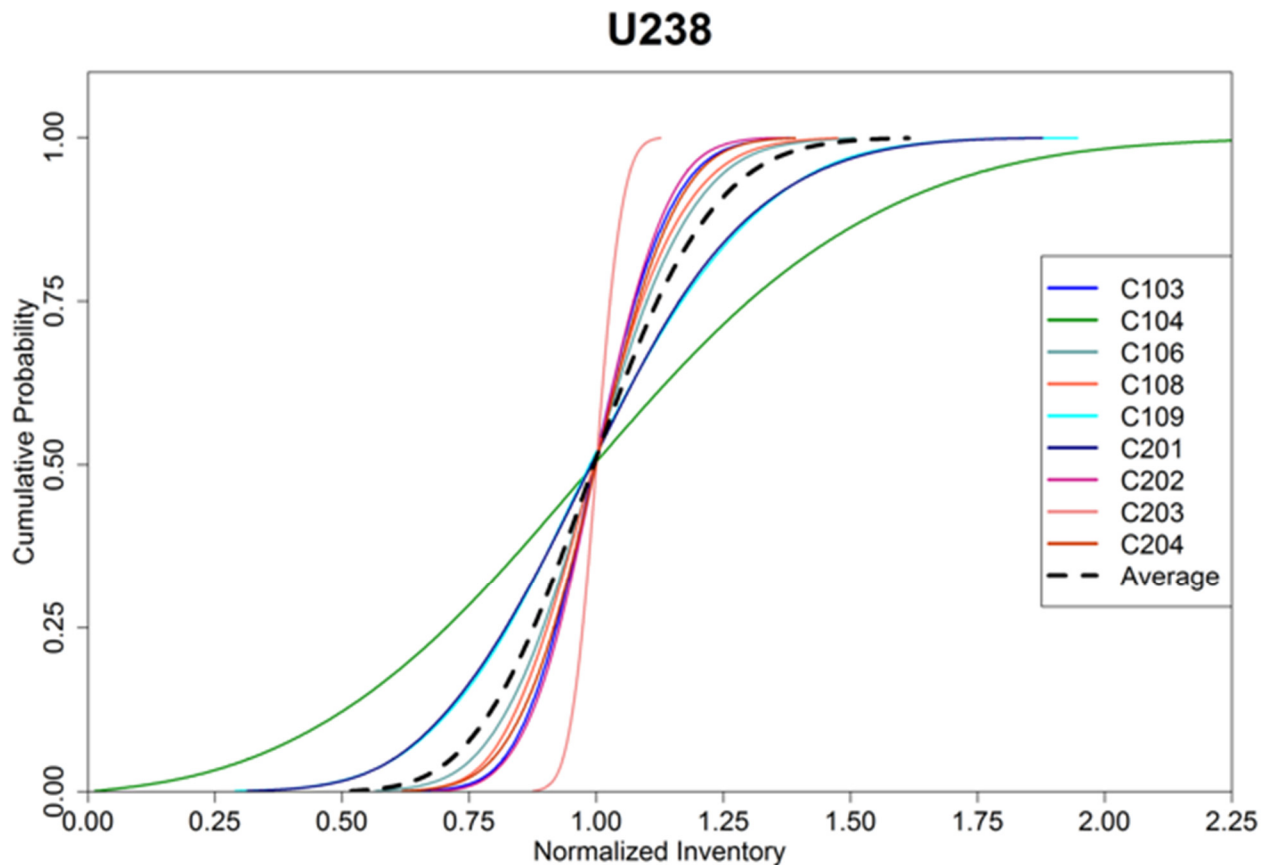


Figure 8-2. Cumulative Distribution Function of Normalized Inventory of Various Analytes for the Retrieved Tanks along with the Average Cumulative Distribution Function. (sheet 9 of 10)



RPP-ENV-58782, Rev. 0

Figure 8-2. Cumulative Distribution Function of Normalized Inventory of Various Analytes for the Retrieved Tanks along with the Average Cumulative Distribution Function. (sheet 10 of 10)



Similar uncertainty analyses were undertaken for the gravel-dominated Hanford H1 and H3 units and for the backfill sediments based on the soil-moisture dataset from other representative samples. Appendix B (Section B.2.2) discusses the methodology for measuring moisture retention data and unsaturated hydraulic conductivities for samples representative of gravel-dominated H1 and H3 units. A total of 17 sample measurements were used to represent the H1 and H3 gravelly units, and the fitted van Genuchten-Mualem parameters are reproduced in Table B-5 and displayed in Figures B-18 and B-19. For the backfill material (gravel-dominated), ten samples were used to derive van Genuchten-Mualem parameters. The results are presented in Table B-6 and shown in Figures B-20 and B-21.

8.1.3.4.1 Uncertainty in Saturated Hydraulic Conductivity (K_s) Parameter for H2 Unit.

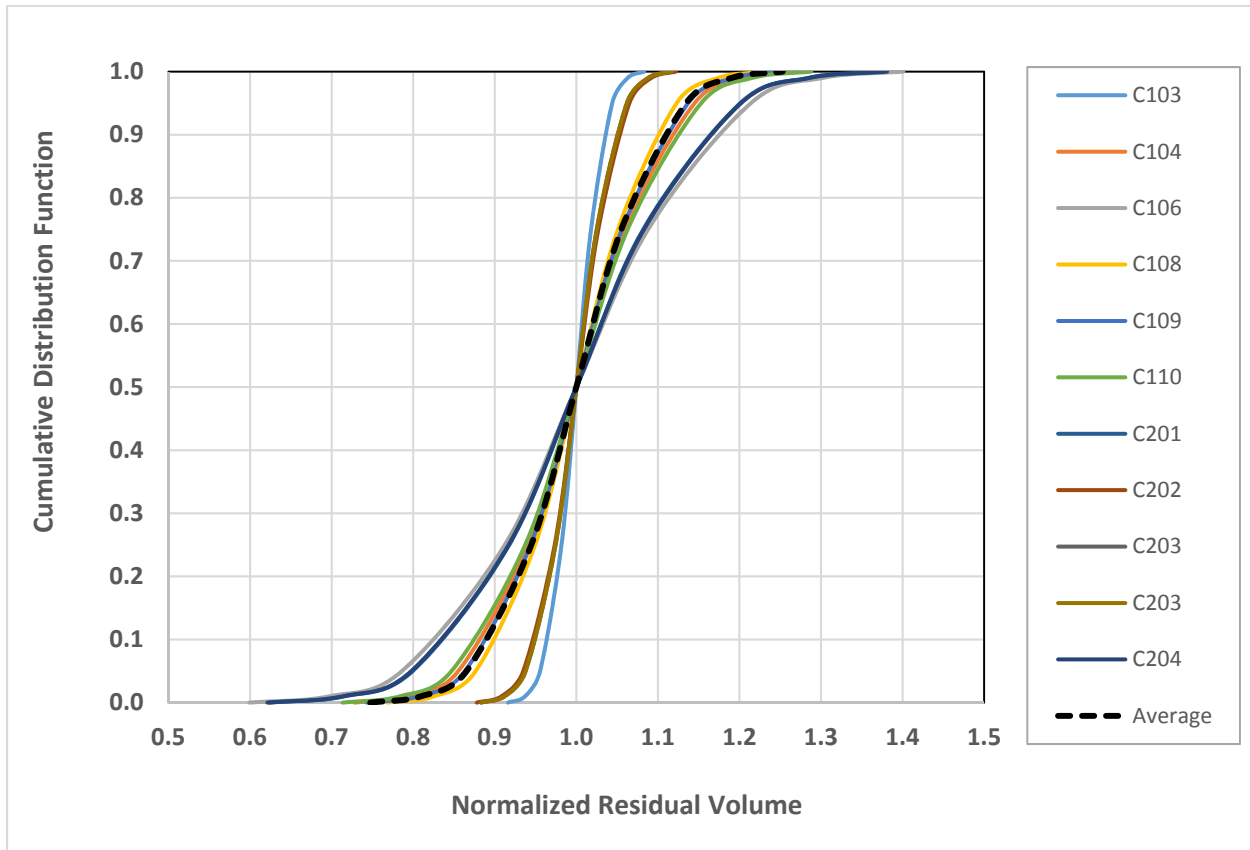
The derived K_s values from each of the 44 laboratory-measured, soil-moisture retention and unsaturated hydraulic conductivity datasets were fit to a log-normal distribution (Figure 8-4), as the number of samples allow an estimate of a mean and standard deviation. The distribution was

RPP-ENV-58782, Rev. 0

truncated at the minimum and maximum values of the data. The K_s distribution has the following characteristics:

- Geometric mean = 4.2×10^{-3} cm/s
- Geometric SD = 4.3
- Minimum = 2.5×10^{-4} cm/s and Maximum = 5×10^{-2} cm/s.

Figure 8-3. Cumulative Distribution Function of Normalized Residual Volume for the Retrieved Tanks along with the Average Cumulative Distribution Function.



8.1.3.4.2 Uncertainty in van Genuchten Alpha (α) Parameter for H2 Unit. The derived van Genuchten alpha (α) values from each of the 44 laboratory-measured, soil-moisture retention and unsaturated hydraulic conductivity datasets were fit to a log-normal distribution (Figure 8-5). The distribution was truncated at the minimum and maximum values of the data. The α distribution has the following characteristics:

- Geometric mean = 0.060 cm^{-1}
- Geometric SD = 1.85
- Minimum = 0.0058 cm^{-1} and Maximum = 0.201 cm^{-1} .

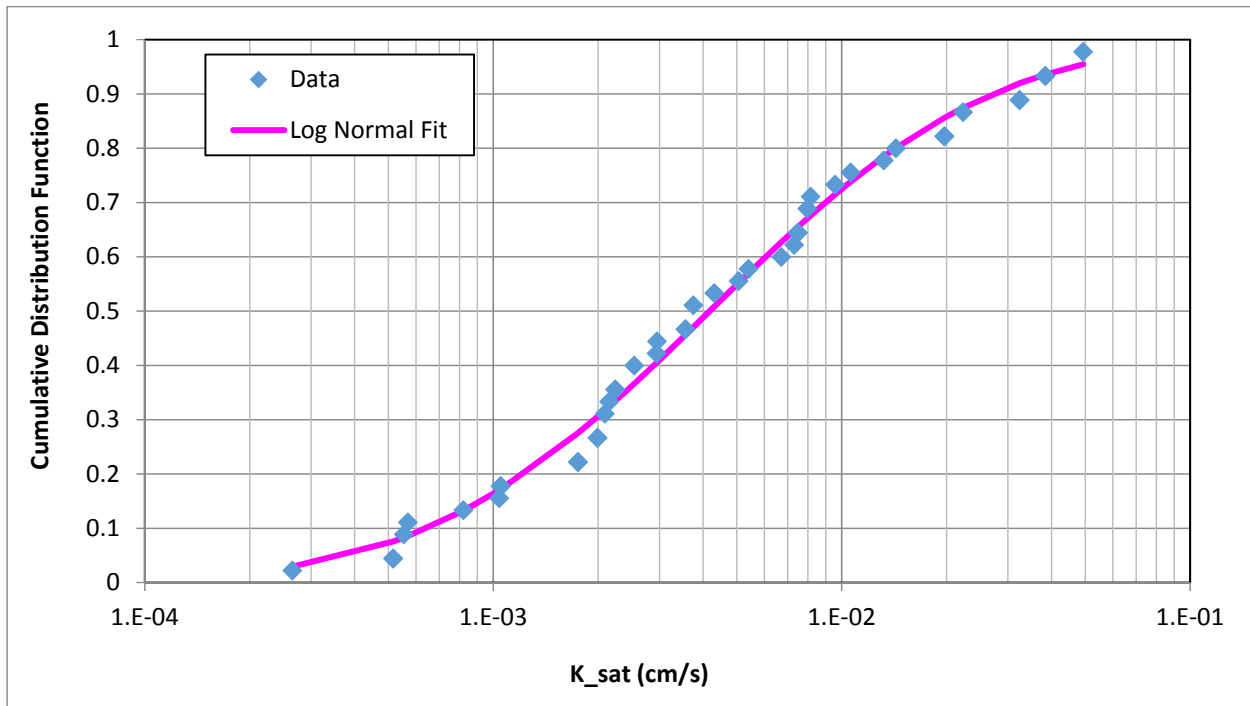
8.1.3.4.3 Uncertainty in van Genuchten n Parameter for H2 Unit. The derived van Genuchten n parameter values from each of the 44 laboratory-measured, soil-moisture

RPP-ENV-58782, Rev. 0

retention and unsaturated hydraulic conductivity datasets were fit to a log-normal distribution (Figure 8-6). The distribution is truncated at the minimum and maximum values of the data. The n distribution has the following characteristics:

- Geometric mean = 1.81
- Geometric SD = 1.15
- Minimum = 1.5 and Maximum = 3.18.

Figure 8-4. Fitted Log-Normal Distribution to the Saturated Hydraulic Conductivity Dataset Used for H2 Unit.



8.1.3.4.4 Uncertainty in Saturated and Residual Moisture Content (θ_s and θ_r) for H2 Unit.

The derived saturated and residual moisture content values (θ_s and θ_r) from each of the 44 laboratory-measured soil-moisture retention datasets were considered with a 20% gravel correction for WMA C. The fitted values have a small range, and as a result, a uniform distribution was assumed with the following minimum and maximum values:

- Saturated moisture content (θ_s): Minimum = 0.239 and Maximum = 0.355
- Residual moisture content (θ_r): Minimum = 0 and Maximum = 0.037.

8.1.3.4.5 Correlation between Parameters. The K_s , α , and n parameters were evaluated to see if any correlation exists that needs to be preserved. Based on rank correlation, it was found that α and K_s have a correlation coefficient of 0.77, while α and n have a correlation coefficient of -0.33. This correlation was implemented while sampling the above-defined log-normal distributions to preserve the relationships in the measured dataset.

RPP-ENV-58782, Rev. 0

Figure 8-5. Fitted Log-Normal Distribution to the van Genuchten “Alpha” Parameter Dataset Used for H2 Unit.

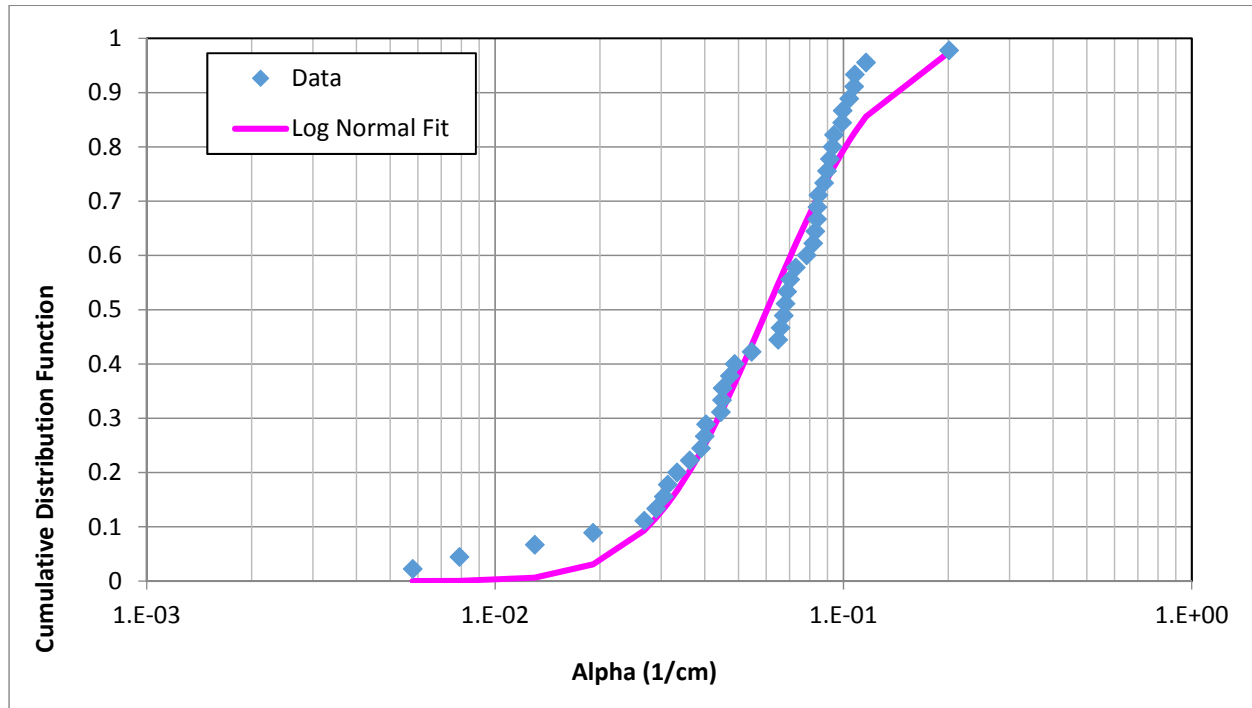
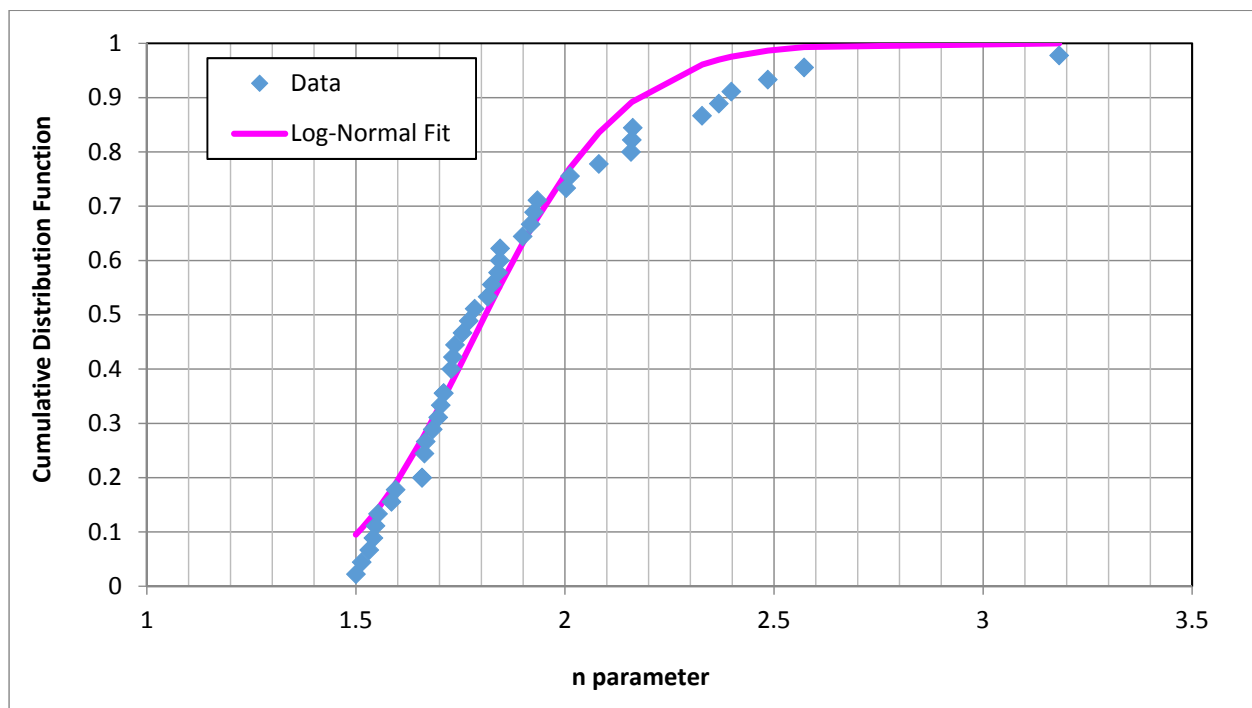


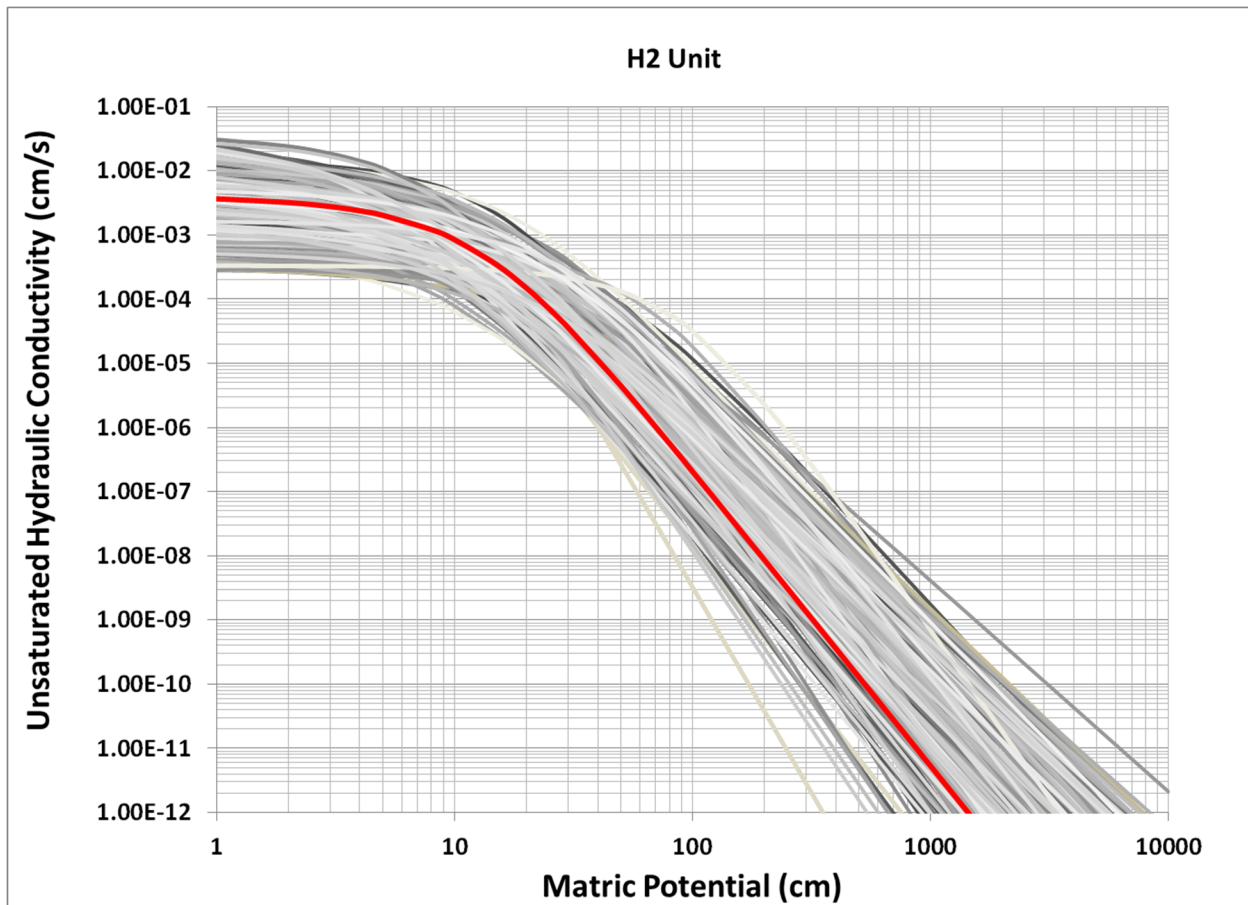
Figure 8-6. Fitted Log-Normal Distribution to the van Genuchten “n” Parameter Dataset Used for H2 Unit.



RPP-ENV-58782, Rev. 0

Using Monte Carlo analysis with LHS, functions of the van Genuchten parameters (including the correlation between parameters) were sampled 200 times. Using the van Genuchten-Mualem constitutive relationship functions, 200 realizations were generated of unsaturated hydraulic conductivity as a function of matric potential, and soil-moisture characteristic curves. These realizations are shown in Figure 8-7 and Figure 8-8 for the H2 unit. The 200 realizations were judged adequate based on the comparison of the distribution of moisture characteristic curves to the soil-moisture retention and unsaturated hydraulic conductivity datasets.

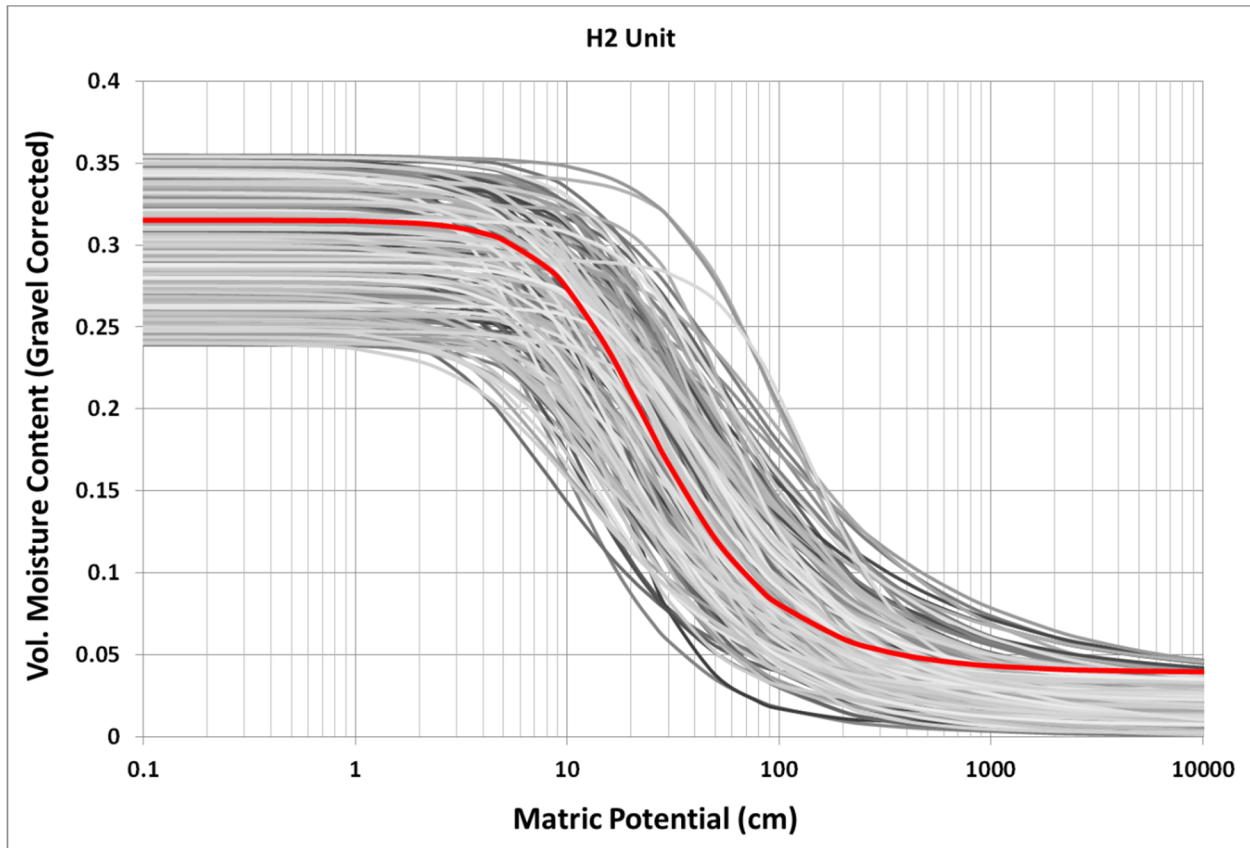
Figure 8-7. 200 Realizations of Unsaturated Hydraulic Conductivity as a Function of Matric Potential for H2 Unit. Red line indicates the Composite curve used in the Base Case.



Similar to the sand-dominated H2 unit, uncertainty in the hydraulic properties for the gravel-dominated H1 and H3 units (assumed to have the same properties) and the backfill material was developed. For the H1/H3 units, the derived uncertainty distributions are summarized in Table 8-4. The fitted log-normal distributions are presented in Figures 8-9 through 8-11. Using the van Genuchten-Mualem constitutive relationship functions, 200 realizations of unsaturated hydraulic conductivity as a function of matric potential and soil-moisture characteristic curves are generated, which are shown in Figure 8-12 and Figure 8-13.

RPP-ENV-58782, Rev. 0

Figure 8-8. 200 Realizations of Soil-Moisture as a Function of Matric Potential for H2 Unit. Red line indicates the Composite curve used in the Base Case.



For the backfill material, the uncertainty distributions are summarized in Table 8-5.

8.1.3.5 Uncertainty in Sorption Parameter for Natural System. A linear sorption isotherm (K_d) was implemented for evaluating the interaction of contaminants with soils, as discussed in Section 6.3.1.4. These values represent intermediate impact zones, which are defined as zones (or areas) in which the acidic or basic nature of the released waste was expected to have been largely neutralized by reaction with the natural sediment.

Uncertainties in K_d values were developed using a triangular distribution as shown in Table 8-6 for sand. The sampled K_d value is then corrected for gravel fraction based on the average gravel content as discussed in Section 6.3.1.4. To be consistent with the hydraulic properties, the average gravel content for H2 unit is 20% (Section B.2.1) and for H1 and H3 units is 42% (Table B-6).

8.1.3.6 Uncertainty in Darcy Flux in Saturated Zone. Uncertainty exists in determination of the saturated hydraulic conductivity and the future hydraulic gradient within the aquifer. As discussed in Appendix C, the base case effective hydraulic conductivity was derived from the current calibrated CPGWM. The CPGWM provides calibrated hydraulic conductivity estimates for the model layers and HSUs present within the aquifer in the vicinity of WMA C. The

RPP-ENV-58782, Rev. 0

weighted average hydraulic conductivity of the CPGWM HSUs mapped onto the WMA C flow domain provides the base case estimate of approximately 11,000 m/day (36,000 ft/day). However, estimates based on pumping tests and other modeling studies have indicated values both lower and higher than the CPGWM calibrated values. Hence, the uncertainty in saturated zone hydraulic conductivity was chosen to range from 1,000 m/day to 21,000 m/day (3,280 ft/day to 69,000 ft/day) based on evaluation of all available information presented in Appendix C (Section C.4).

Table 8-4. Uncertainty Distributions Developed for H1/H3 Hydraulic Properties.

Hydraulic Property	Selected Uncertainty Distribution	Parameters for Defining Uncertainty Distribution
Saturated hydraulic conductivity (K_s)	Log-Normal (truncated)	Geometric Mean = 1.95E-4 cm/s Geometric Standard Deviation = 8.37 Minimum = 1E-6 cm/s; Maximum = 7.77E-3 cm/s
van-Genuchten Alpha (α) parameter	Log-Normal (truncated)	Geometric Mean = 0.015 cm ⁻¹ Geometric Standard Deviation = 2.42 Minimum = 0.0043 cm ⁻¹ ; Maximum = 0.0438 cm ⁻¹
van-Genuchten n parameter	Log-Normal (truncated)	Geometric Mean = 1.58 Geometric Standard Deviation = 1.13 Minimum = 1.31; Maximum = 2.25
Saturated Moisture Content (θ_s)	Uniform	Minimum = 0.1; Maximum = 0.357
Residual Moisture Content (θ_r)	Uniform	Minimum = 0; Maximum = 0.033
Rank Correlation between hydraulic properties		Alpha and K_s = 0.92 Alpha and n = 0.38

Uncertainty also exists in the hydraulic gradient within 200 East Area. Even though the hydraulic gradients are likely to remain very small (around 10⁻⁵ m/m) as the water table declines in the future, current monitoring has indicated that gradients can vary by a factor of two, due to Columbia River stage fluctuations and interconnections to the aquifer in the Central Plateau.

While the uncertainties in hydraulic conductivity and hydraulic gradient can be defined independently, the parameters need to be considered together as they result in determination of Darcy flux, which is the parameter that is used in the system model. Consequently, the uncertainty in hydraulic conductivity and gradient is propagated by developing uncertainty in the Darcy flux relative to the base case value. This is implemented as a multiplicative factor to the base case Darcy flux at the upgradient boundary of the WMA C system model.

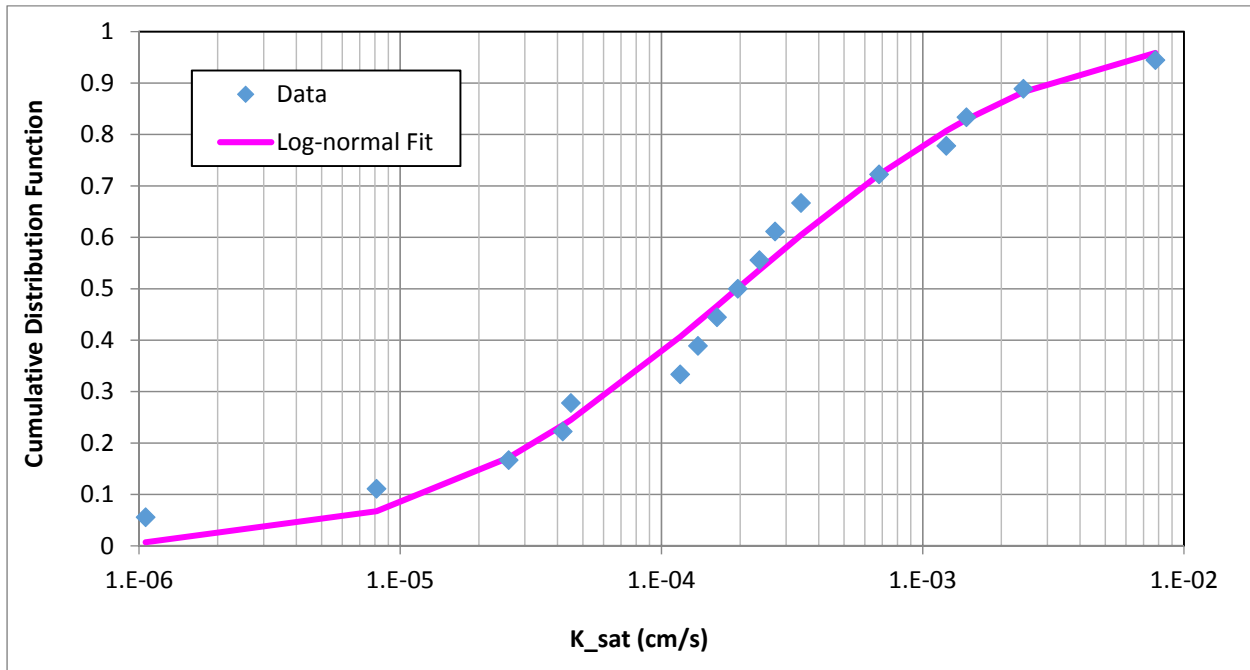
The uncertainty in the Darcy flux multiplier is dominated by uncertainty in the saturated zone hydraulic conductivity, which varies by an order of magnitude or more. To derive the Darcy flux multiplier, the saturated hydraulic conductivity range (1,000 to 21,000 m/day [3,280 ft/day to

RPP-ENV-58782, Rev. 0

69,000 ft/day]) was divided by the best-estimate value (11,000 m/day [36,000 ft/day]) and a triangular distribution was chosen with the following parameters:

- Minimum = 0.09
- Most Likely = 1
- Maximum = 1.91.

Figure 8-9. Fitted Log-Normal Distribution to the Saturated Hydraulic Conductivity Dataset Used for H1/H3 Units.



8.1.3.7 Uncertainty in Macrodispersivity in the Vadose Zone and the Saturated Zone. In unsaturated media, the longitudinal macrodispersivity is dependent on soil moisture content (or matric potential) and differs when the primary flow and transport is parallel to the bedding plane versus being primarily perpendicular to the bedding. A range of estimates are presented in Appendix B (Section B.4.3). These estimates are based on numerical simulations, stochastic theory, and experimental observations applicable to the relatively dry conditions observed in the vadose zone at WMA C. Table B-11 summarizes the various estimates for the H2 sand-dominated unit. A range from 25 cm to 100 cm (9.8 in. to 39.4 in.) is recommended for longitudinal macrodispersivity. Under the relatively dry conditions within the WMA C vadose zone, and because the primary flow and transport direction is vertical (perpendicular to the bedding plane in the H2 unit), the lower value of 25 cm (9.8 in.) is deemed as a best estimate. Consequently, a triangular distribution is used for the H2 unit with the following parameters:

- Minimum = 25 cm (9.8 in.)
- Most Likely = 25 cm (9.8 in.)
- Maximum = 100 cm (39.4 in.).

RPP-ENV-58782, Rev. 0

Figure 8-10. Fitted Log-Normal Distribution to the van Genuchten “Alpha” Parameter Dataset Used for H1/H3 Units.

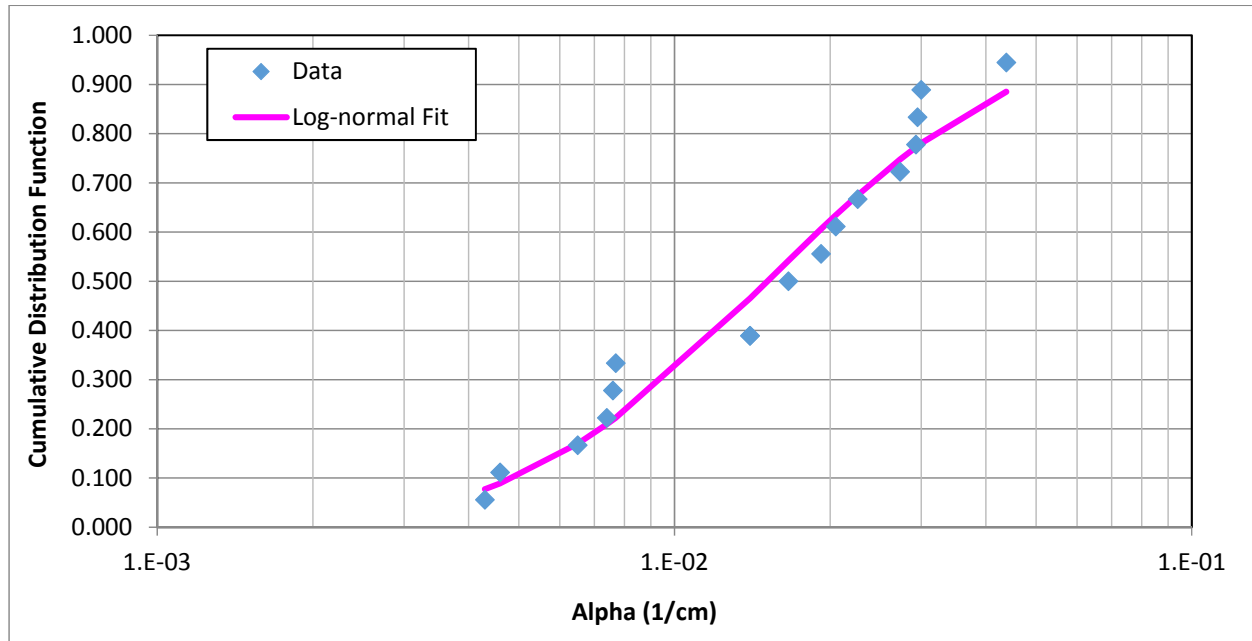
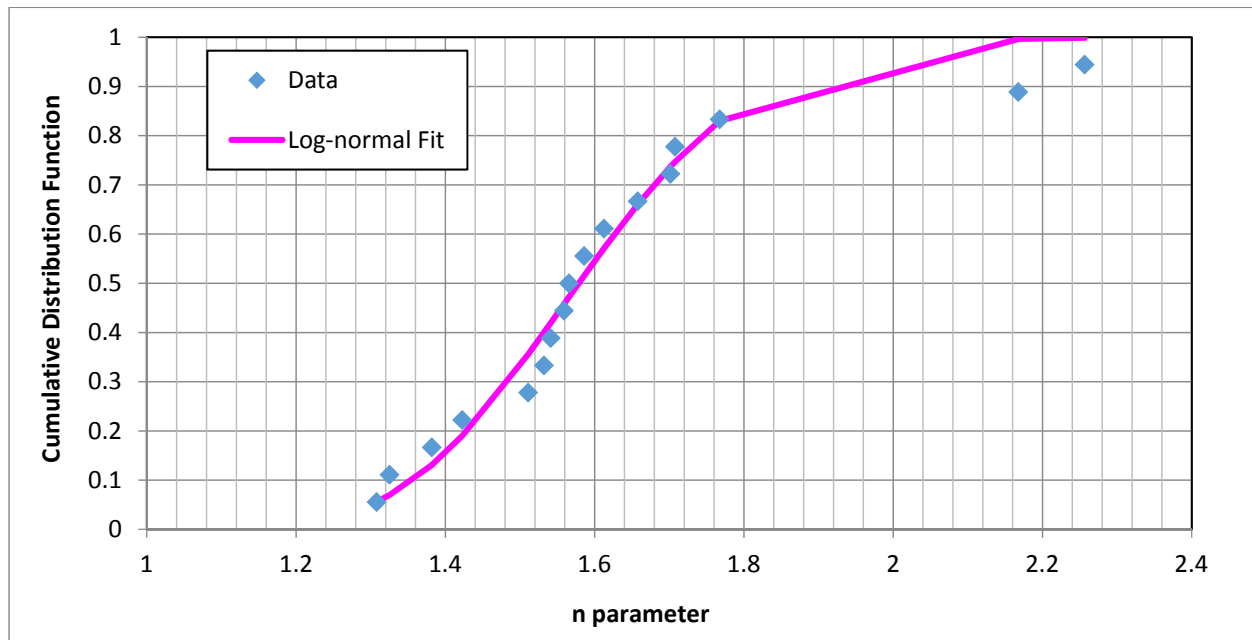


Figure 8-11. Fitted Log-Normal Distribution to the van Genuchten “n” Parameter Dataset Used for H1/H3 Units.



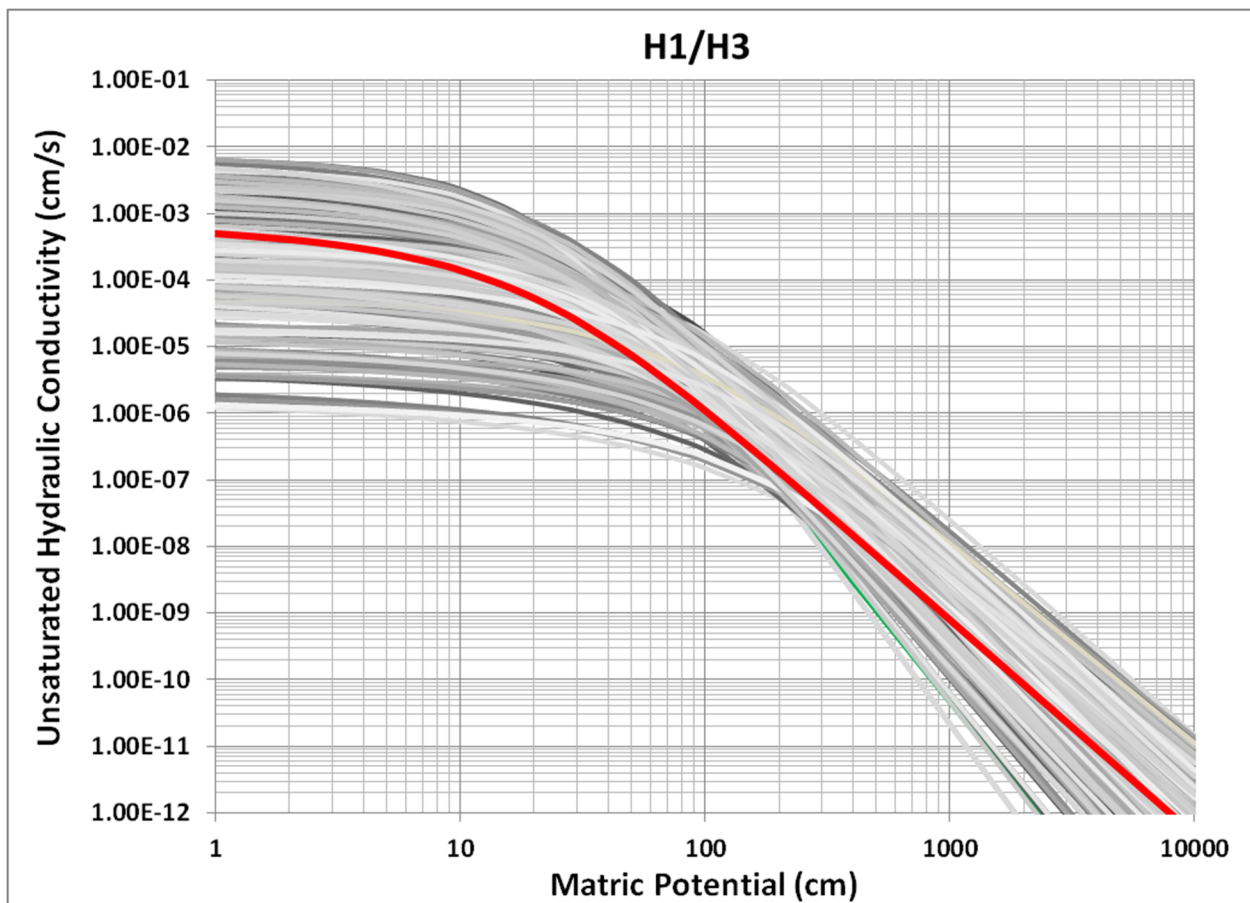
A range in the saturated zone macrodispersivity is discussed in Appendix C (Section C.4.2.2), based on a review of literature-based, scale-dependent relationships. The range in saturated zone macrodispersivity at the scale of the WMA C model is estimated to be from 1 m to 20 m (3.3 ft

RPP-ENV-58782, Rev. 0

to 65.6 ft). In the system model, it is necessary to use different macrodispersivity values for each source, as the transport distance in the saturated zone to the 100 m (328 ft) boundary varies by the location of the source (tank and ancillary equipment), and the appropriate macrodispersivity is dependent on the distance. It is therefore necessary to use different macrodispersivities for each source so that the results match with the STOMP[®] 3-D process-level model results for each source term. This is best accomplished by defining an uncertain parameter that multiplies (scales) the chosen macrodispersivity values for each source. To propagate uncertainty in macrodispersivity multiplier, a uniform distribution was chosen by taking the minimum and maximum values of the macrodispersivity range and dividing by the median value. This results in the following parameters that define the uniform distribution:

- Minimum = 0.095
- Maximum = 1.9.

Figure 8-12. 200 Realizations of Unsaturated Hydraulic Conductivity as a Function of Matric Potential for H1/H3 Units. Red line indicates the Composite curve used in the Base Case.



8.1.3.8 Uncertainty in Gas-Phase Tortuosity. Gas-phase tortuosity is considered to be a key parameter in the air-pathway transport calculation. Uncertainty in this parameter was implemented as a triangular distribution based on the fitted tortuosity models shown in

RPP-ENV-58782, Rev. 0

Figure 6-59 (and discussed in Section 6.3.2.5.2). The most likely value of the triangular distribution is based on the best fit line given by Equation 8-2. The minimum and maximum values are described below.

- The minimum envelope curve obtained with the model of Millington and Quirk (1961) with Φ , fitted total porosity = 0.8.

$$\tau = \frac{\theta_a^{10/3}}{\Phi^2} = \frac{(\phi - \theta_w)^{10/3}}{\Phi^2} \quad (8-1)$$

- The maximum envelope curve obtained with the model of Millington and Quirk (1960) with Φ , fitted total porosity = 0.4.

$$\tau = \frac{\theta_a^2}{\Phi^{2/3}} = \frac{(\phi - \theta_w)^2}{\Phi^{2/3}} \quad (8-2)$$

Where:

- τ = the tortuosity
- θ_a = the air content (or air-filled porosity) of the porous medium
- θ_w = the water content (or water-filled porosity) of the porous medium
- ϕ = the total porosity (measured)
- Φ = fitted total porosity.

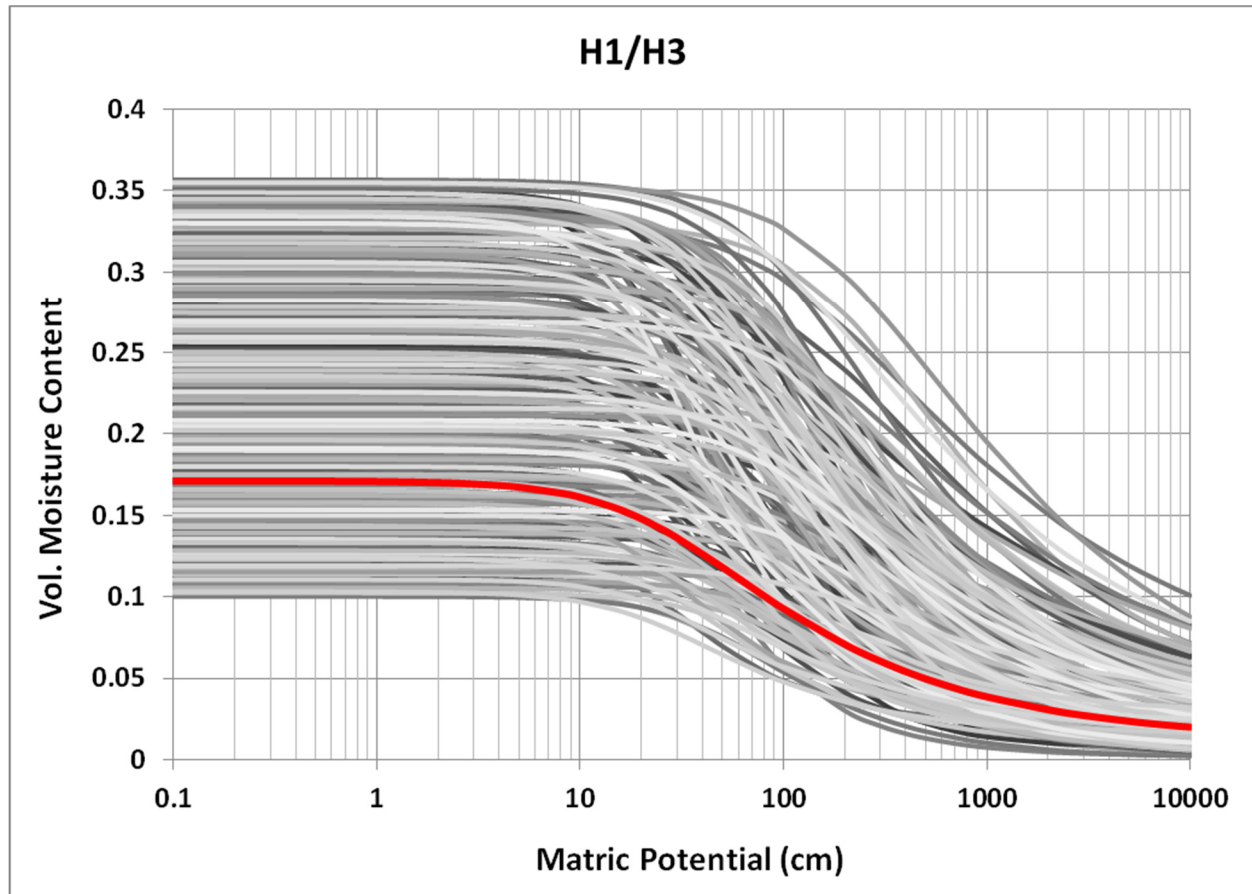
Two different triangular distributions were implemented related to gas-phase tortuosity, one for the gaseous transport through the tank grout and the other through the soil overburden due to different air contents.

8.1.3.9 Uncertainty in Annual Wind Speed. As discussed in Section 3.1.2.4, the wind speed at Hanford varies on a monthly basis, with speeds being higher in summer and lower during winter months. The monthly and annual average speeds from Years 1945 through 2004 are summarized in Tables 5.1 through 5.4 of PNNL-15160. The annual average wind speed for meteorological records kept from 1945 to 2004 is calculated to be ~3.4 m/s (7.6 mi/hr) at 15.2 m (50 ft) above the ground, with a maximum annual average value of 3.9 m/s (8.8 mi/hr) and a minimum annual average value of 2.8 m/s (6.2 mi/hr). Although seasonal variability in wind speed is observed, since the dose evaluations are performed on an annual basis, the annual averaged wind speeds are considered for evaluating the effect of uncertainty in this parameter. Based on the available information, a triangular distribution was implemented with the following parameters:

- Minimum = 2.8 m/s (6.2 mi/hr)
- Most Likely = 3.4 m/s (7.6 mi/hr)
- Maximum = 3.9 m/s (8.8 mi/hr).

RPP-ENV-58782, Rev. 0

Figure 8-13. 200 Realizations of Soil-Moisture as a Function of Matric Potential for H1/H3 Units. Red line indicates the Composite curve used in the Base Case.



8.1.4 Development of Vadose Zone Flow Fields and Propagation of Uncertainty

The flow field for the vadose zone was abstracted from the 3-D STOMP[®] results as a way to efficiently evaluate the effects of uncertainty in the vadose-zone flow using the GoldSim[®]-based system model. The 1-D transport model implemented in GoldSim[®] relies on the user to provide the time-varying vertical Darcy flux and volumetric moisture content as inputs. These flow field-related parameters were extracted from the 3-D STOMP[®]-based model. The flow-field abstractions were performed separately for the 100-series and 200-series tanks because of different tank dimensions and thickness of HSUs within the vadose zone. The details of the flow-field abstraction approach are discussed in Section 6.3.2.2. The reasonableness of the abstraction approach was demonstrated by comparisons of the results of the transport analysis conducted using the 1-D abstracted system model to the full 3-D STOMP[®]-based model (Section 6.3.2.2.1).

In this section, the methodology for propagating uncertainty in the flow field is discussed. The vadose zone flow field is a function of the imposed recharge rate and vadose zone hydraulic properties. The uncertainties in these two parameters are discussed in Section 8.1.4. The uncertainty in the flow field is propagated by jointly considering the uncertainty in vadose zone

RPP-ENV-58782, Rev. 0

hydraulic properties and the uncertainty in recharge rates. Because a comprehensive Monte Carlo analysis using the 3-D STOMP[®]-based model was too computationally intensive and impractical for propagating the uncertainty in the flow field, the STOMP[®]-based Monte Carlo analysis was approximated by a discrete number of analyses that span the range of behavior of the flow fields for a limited number of runs. This was accomplished by selecting 5 discrete hydraulic property sets along with 3 discrete recharge rates to cover the uncertainty range. Five sets of hydraulic properties were chosen because of the larger uncertainty range in the flow parameters relative to recharge rates. The combination of 5 hydraulic property sets with 3 recharge rates results in a matrix of 15 parameter sets. These 15 combinations of flow parameters were each run using the 3-D STOMP[®] model. For each STOMP[®] calculation, the resulting flow field was abstracted using the methodology discussed in Section 6.3.2.2.

Table 8-5. Uncertainty Distributions Developed for Backfill Hydraulic Properties.

Hydraulic Property	Selected Uncertainty Distribution	Parameters for Defining Uncertainty Distribution
Saturated hydraulic conductivity (K_s)	Log-Normal (truncated)	Geometric Mean = 5.52E-5 cm/s Geometric Standard Deviation = 5.48 Minimum = 1E-6 cm/s; Maximum = 3.42E-4 cm/s
van-Genuchten Alpha (α) parameter	Log-Normal (truncated)	Geometric Mean = 0.0086 cm ⁻¹ Geometric Standard Deviation = 2.63 Minimum = 0.0025 cm ⁻¹ ; Maximum = 0.030 cm ⁻¹
van-Genuchten n parameter	Log-Normal (truncated)	Geometric Mean = 1.53 Geometric Standard Deviation = 1.07 Minimum = 1.31; Maximum = 1.66
Saturated Moisture Content (θ_s)	Uniform	Minimum = 0.1; Maximum = 0.236
Residual Moisture Content (θ_r)	Uniform	Minimum = 0; Maximum = 0.018
Rank Correlation between hydraulic properties		Alpha and K_s = 0.71 Alpha and n = 0.47

A simplification of the flow-field sampling approach was identified by observing that variations in recharge could be reproduced using an appropriate scaling method using the base case recharge rate. Therefore, instead of implementing 15 flow fields, only 5 flow fields had to be implemented, defined by the combination of 5 hydraulic parameters with base case recharge rate. Therefore, the remaining 10 flow fields calculated by the 3-D STOMP[®]-based model were used to corroborate the scaling approach, but were not directly used in the GoldSim[®]-based system model.

The flow-field abstraction approach is described in following five steps.

Step 1 – Selection of Vadose Zone Hydraulic Properties:

The uncertainty in the vadose zone hydraulic properties is discussed in Section 8.1.3. For each HSU in the vadose zone, 200 realizations of unsaturated hydraulic conductivity (as a function of matric potential) and soil-moisture characteristic curves were generated. Although different

RPP-ENV-58782, Rev. 0

curves could be randomly selected from the 200 realizations, by using insights regarding the flow fields, the uncertainties relevant to the PA were more tightly defined. First is the recognition that under the post-closure conditions, the flow will closely approach a unit gradient flow field as the vertical Darcy flux equilibrates with the imposed recharge rate. Using the long-term base recharge rate of 3.5 mm/yr (0.14 in./yr) as an estimate of vertical Darcy flux, and with the unit hydraulic gradient assumption, the associated unsaturated hydraulic conductivity is $\sim 1 \times 10^{-8}$ cm/s. This allows the analysis to focus on a specific part of the characteristic curves at unsaturated hydraulic conductivity of $\sim 1 \times 10^{-8}$ cm/s (see Figure 8-7) in which the range of matric potential is smaller than the full range over all conditions.

Table 8-6. Uncertainty in K_d Values (mL/g) for Sand As a Triangular Distribution. (2 sheets)

Element	Most Likely	Minimum	Maximum	Reference
Ac	350	100	1,500	PNNL-16663
Al	1,500	1,500	1,500	RPP-RPT-46088
Am	600	200	2,000	PNNL-17154
B	3	3	3	RPP-RPT-46088
C	1	0	100	PNNL-17154
Cd	6.7	6.7	6.7	RPP-RPT-46088
Cm	350	100	1,500	PNNL-16663
CN	0	0	0	RPP-RPT-46088
Co	0	0	10	PNNL-17154
Cr	0	0	3	PNNL-17154
Cs	100	10	1,000	PNNL-17154
Eu	10	3	100	PNNL-17154
F	0	0	1	PNNL-17154
Fe	25	25	25	RPP-RPT-46088
H	0	0	0	PNNL-17154
Hg	52	52	100	RPP-RPT-46088
I	0.2	0	2	PNNL-17154
Mn	65	65	65	RPP-RPT-46088
Nb	0	0	0.1	PNNL-16663
Ni	3	1	20	PNNL-17154
NO ₂	0	0	0.1	PNNL-17154
NO ₃	0	0	0.1	PNNL-17154
Np	10	2	30	PNNL-17154

RPP-ENV-58782, Rev. 0

Table 8-6. Uncertainty in K_d Values (mL/g) for Sand As a Triangular Distribution. (2 sheets)

Element	Most Likely	Minimum	Maximum	Reference
Pa	300	40	500	PNNL-17154
Pb	10	3	100	PNNL-17154
Pu	600	200	2,000	PNNL-17154
Ra	10	5	20	PNNL-17154
Rn	0	0	0	No relevant information available
Se	0.1	0	3	PNNL-17154
Sm	10	3	100	PNNL-17154
Sn	0.5	0	20	PNNL-17154
Sr	10	5	100	PNNL-17154
TBP	1.89	1.89	1.89	RPP-RPT-46088
Tc	0	0	0.1	PNNL-16663
Th	300	40	500	PNNL-16663
U	0.6	0.2	2	RPP-RPT-46088
U_total	0.6	0.2	2	PNNL-17154
Zr	300	40	500	PNNL-16663

References:

PNNL-16663, "Geochemical Processes Data Package for the Vadose Zone in the Single-Shell Tank Waste Management Areas at the Hanford Site."

PNNL-17154, "Geochemical Characterization Data Package for the Vadose Zone in the Single-Shell Tank Waste Management Areas at the Hanford Site."

RPP-RPT-46088, "Flow and Transport in the Natural System at Waste Management Area C."

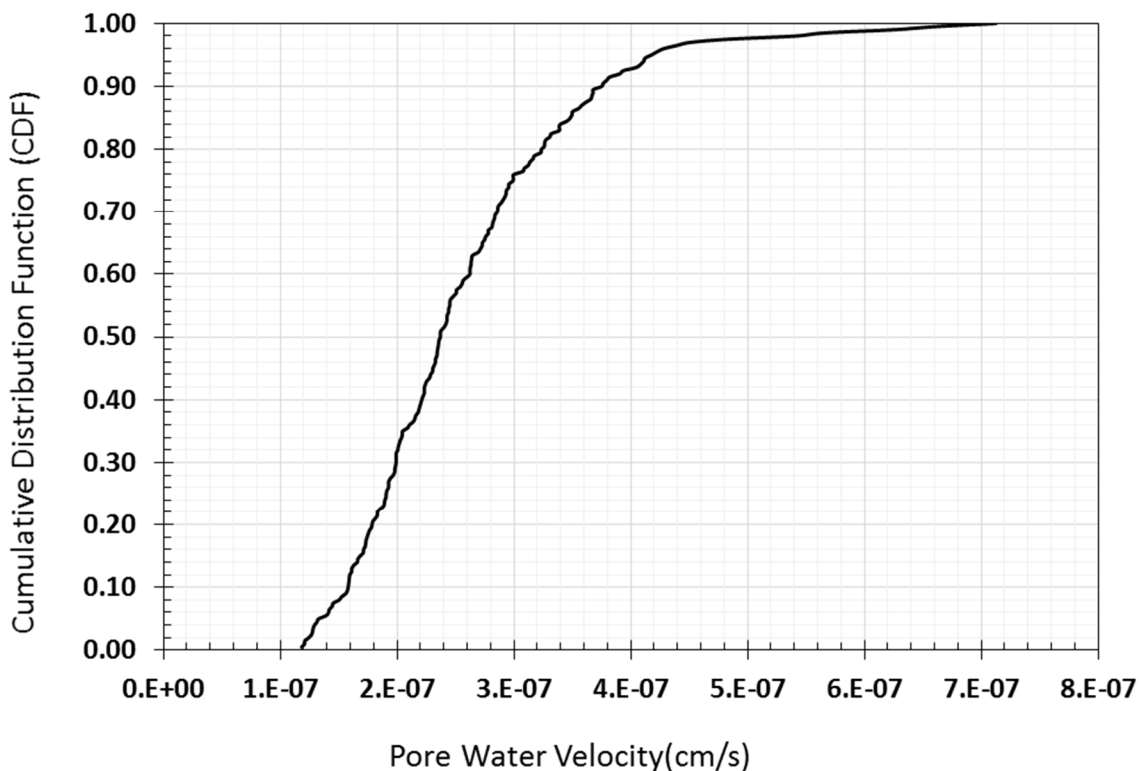
Fixing the unsaturated hydraulic conductivity, the following procedure was undertaken to derive uncertainty in hydraulic properties.

- The 200 realizations of the unsaturated hydraulic conductivity as a function of matric potential was first interrogated (for example, see Figure 8-7 for H2 unit and Figure 8-12 for H1/H3 units). For each realization, the matric potential corresponding to 1×10^{-8} cm/s unsaturated hydraulic conductivity was determined.
- Next, the 200 realizations of the soil-moisture characteristic curves (for example, see Figure 8-8 for H2 unit and Figure 8-13 for H1/H3 units) were interrogated based on the matric potential determined in the previous step, to determine the corresponding volumetric moisture content for that realization.

RPP-ENV-58782, Rev. 0

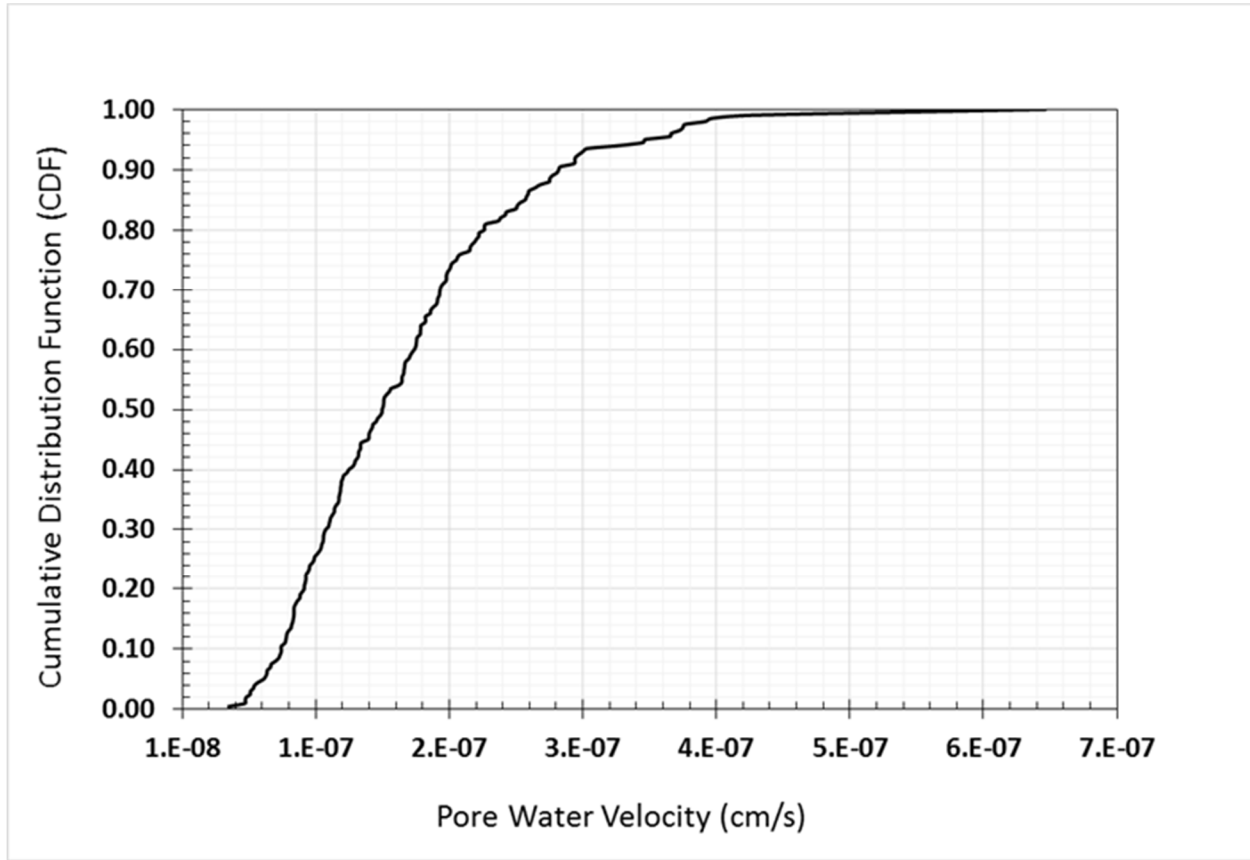
- The vertical pore water velocity was calculated for each realization by dividing the 1×10^{-8} cm/s unsaturated hydraulic conductivity by the corresponding volumetric moisture content.
- The resulting 200 vertical pore water velocity estimates were then sorted, and an empirical CDF was developed. For example, see the CDF shown in Figure 8-14 for the H2 unit.
- The above steps were repeated for each HSU, and the CDFs are presented in Figures 8-14 through 8-16.
- From the CDF, five pore water velocity values associated with the 5th, 25th, 50th, 75th, and 95th percentiles were chosen to represent the uncertainty in pore water velocity for a given HSU. The realizations associated with these percentiles were selected, and the hydraulic properties associated with the realization are noted for the HSU. Table 8-7 summarizes the sampled van Genuchten-Mualem parameters (K_s , α , n , θ_s , and θ_r) associated with the various percentiles. For the purpose of comparison, the parameters chosen for the base case are also presented.

Figure 8-14. Cumulative Distribution Function of Pore Water Velocity from 200 Realizations for the H2 Unit.



RPP-ENV-58782, Rev. 0

Figure 8-15. Cumulative Distribution Function of Pore Water Velocity from 200 Realizations for the H1/H3 Unit.



Step 2 – Selection of Recharge Rates:

Recharge rate varies both temporally and spatially as discussed in Section 8.1.3.1. Table 8-3 presents the uncertainty distribution in recharge rates for various time periods. For the purpose of abstracting the flow field, the time periods of interest are operational and post-closure periods, and the spatial area of interest is the one designated as WMA C since all of the contaminant sources are within this area. From the triangular distributions developed for each time period, the 5th percentile and the maximum (100th percentile) recharge rate values are selected along with the base case recharge rate values for the flow-field calculations. These values are representative of the uncertainty in recharge rates (the minimum value was not used due to very low probability of occurrence). The selected recharge rates are summarized in Table 8-8.

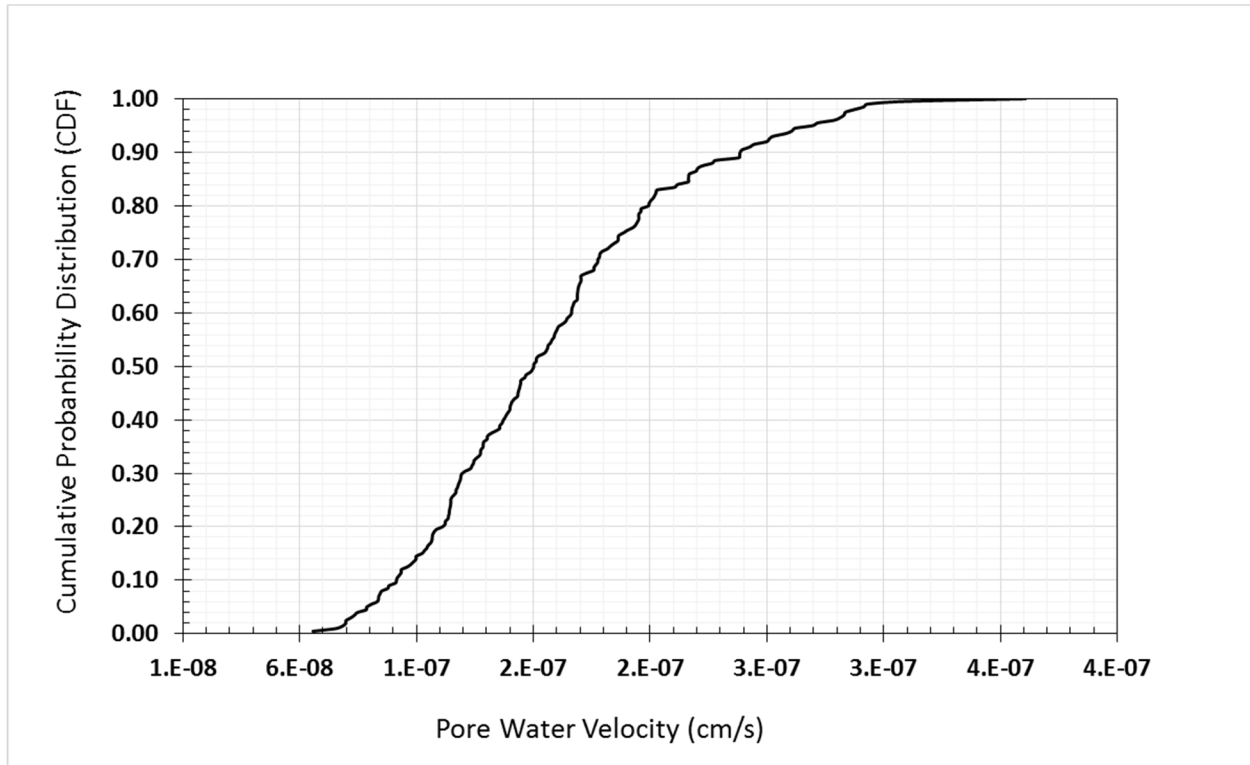
Step 3 – Flow-Field Abstraction:

The five hydraulic property sets corresponding to the vertical pore velocity percentiles (selected in Step 1 and presented in Table 8-7) and the three recharge rates (selected in Step 2 and presented in Table 8-8) were used to develop 15 combinations of flow-field inputs. The 3-D STOMP[®]-based model was used to calculate the flow field for each input combination. The results from the 3-D model were abstracted to generate separate flow fields for the 100-series

RPP-ENV-58782, Rev. 0

and 200-series tanks. Each flow field contains time-dependent vertical Darcy flux and volumetric moisture content that is applicable to the vertical grid discretization used in the GoldSim[®]-based system model (Table 6-16).

Figure 8-16. Cumulative Distribution Function of Pore Water Velocity from 200 Realizations for the Backfill Unit.



Step 4 – Scaling of Flow Field by Recharge Rate:

Upon evaluation of the 15 flow fields, it was found that a linear relationship exists between vertical Darcy flux and the recharge rate when hydraulic properties remain unchanged. Similarly, a linear relationship exists between volumetric moisture content and recharge rate. This information was used to reduce the number of flow fields being implemented in the system model to only five flow fields. The five flow fields were generated based on the combination of five hydraulic property sets with the *base case* recharge rate. These flow fields can be scaled based on sampled recharge rate using the regression equations. This approach allows to quickly and directly estimate the Darcy flux and volumetric moisture content for any sampled recharge rate without going through a demanding abstraction process.

The development of the regression equations was done as follows.

- For a selected hydraulic property percentile, the 3-D STOMP[®] model was used for three recharge rates presented in Table 8-8.

RPP-ENV-58782, Rev. 0

- 1 • Vertical Darcy flux and volumetric moisture content values were abstracted from
2 STOMP[®] model nodes that correspond to the GoldSim[®] 1-D discretization. This was
3 done for Calendar Year 2300 (to represent early the post-closure time period from
4 Calendar Year 2020 to 2520 while the surface cover is intact) and at Calendar Year 5020
5 (to represent the late post-closure period beyond Calendar Year 2520 following surface
6 barrier degradation).
7
- 8 • For the set of flow fields where the hydraulic property is held constant but recharge rate
9 varies, the extracted vertical Darcy flux and volumetric moisture content were normalized
10 by the base case recharge flow field. Table 8-9 provides an example of normalized Darcy
11 flux for Calendar Year 2300 below tank C-105 (a representative column) for the 3-D
12 STOMP[®] simulations with 5th percentile hydraulic properties at different recharge rates.
13 This analysis was done for each time period.
14
- 15 • Normalized Darcy flux was plotted against the normalized recharge rates, and a linear
16 regression analysis was performed to determine the relationships shown in Figures 8-17
17 and 8-18. These relationships are representative of the H1 unit and the deeper H2 and
18 H3 units. Results of the regression analysis shown in Figure 8-17 are based on a
19 STOMP[®] node located in H1 unit (node 66), and are used to scale the flow field for all
20 other nodes in H1 unit in the GoldSim[®]-based system model. For the deeper H2 and H3
21 units, the regression analysis shown in Figure 8-18 was performed after averaging the
22 results of several STOMP[®] nodes located in H2 and H3 units (nodes 63, 61, 55, 47, 39,
23 31, 24, 18, and 14). The averaging was performed because the vertical Darcy flux within
24 the deeper nodes does not vary appreciably. Results of the regression analysis were used
25 to scale the flow field for all nodes that define H2 and H3 in GoldSim[®]-based system
26 model.
27
- 28 • A regression equation was also developed between normalized volumetric moisture
29 content and normalized recharge rate in the same way. This is shown in Figures 8-19 and
30 8-20.
31
- 32 • These steps were repeated for each of the five hydraulic properties. This resulted in the
33 development of linear relationships between normalized Darcy flux and normalized
34 recharge rate, and between normalized volumetric moisture content and normalized
35 recharge rate.
36

37 This algorithm resulted in a total of 40 regression equations, which were implemented in the
38 GoldSim[®]-based system model for Darcy flux scaling calculations. The large number of
39 regression equations was the result of separate regression relationships for the early post-closure
40 time period (while the surface cover was intact) and the late post-closure time period (after
41 surface cover is degraded), and then calculated separately for H1 unit and H2/H3 units for the
42 100-series tanks and 200-series tanks. The regression equations are presented in Table 8-10 for
43 the 100-series tanks and in Table 8-11 for the 200-series tanks. Once a value is calculated from
44 the regression equation, then the Darcy flux derived from the base case recharge rate abstraction
45 process can be scaled to generate a new Darcy flux for the selected hydraulic property.
46

RPP-ENV-58782, Rev. 0

Table 8-7. van Genuchten-Mualem Parameters Corresponding to the Percentiles Selected from the Vertical Pore Water Velocity Cumulative Distribution Functions.

Strata (tension)	Percentile	K_s (cm/s)	θ_s	θ_r	α (1/cm)	n
Backfill	5th Percentile	7.91E-06	0.2217	1.23E-02	0.0026	1.441
	25th Percentile	1.08E-05	0.1319	1.57E-02	0.0031	1.310
	50th Percentile	7.31E-05	0.203	5.94E-03	0.0086	1.577
	75th Percentile	1.98E-04	0.1409	1.42E-02	0.0123	1.470
	95th Percentile	3.13E-04	0.1287	1.35E-02	0.0298	1.635
	Base Case	5.60E-04	0.138	1.10E-02	0.021	1.374
Hanford H1/H3	5th Percentile	7.78E-05	0.2887	3.24E-02	0.0121	1.335
	25th Percentile	5.14E-06	0.2118	2.08E-02	0.0062	1.733
	50th Percentile	1.49E-04	0.1735	3.06E-02	0.0124	1.603
	75th Percentile	1.58E-03	0.309	7.01E-03	0.0238	1.717
	95th Percentile	2.99E-04	0.102	1.45E-02	0.0152	1.760
	Base Case	7.70E-04	0.171	1.11E-02	0.036	1.491
Hanford H2	5th Percentile	1.79E-03	0.3541	2.89E-02	0.0402	1.633
	25th Percentile	1.15E-03	0.2893	2.99E-02	0.0266	1.971
	50th Percentile	2.20E-02	0.3304	2.72E-02	0.1253	1.889
	75th Percentile	3.79E-02	0.3474	2.05E-02	0.0966	1.966
	95th Percentile	1.68E-02	0.2652	2.11E-03	0.1076	1.724
	Base Case	4.15E-03	0.315	3.92E-02	0.063	2.047

Note: The connectivity parameter ℓ is assumed to be 0.5 for all strata and all percentile values.

During the regression analyses, it was observed that linear regression relationships between normalized volumetric moisture content and normalized recharge rate do not vary appreciably when different hydraulic properties were used, and between 100-series and 200-series tanks. As a result, only four regression equations are needed for scaling the volumetric moisture content. These are calculated separately for the H1 unit and the H2/H3 units for early post-closure and late post-closure time periods, and are summarized in Table 8-12. Once a value is calculated from the regression equation, then the volumetric moisture content derived from the base case recharge rate can be scaled by multiplying with this value to generate the new volumetric moisture content.

This scaling method was verified by comparing flow fields calculated using the regression equation with the flow field from 3-D STOMP[®] simulations for each of the hydraulic properties. An example of the comparison for the 5th percentile hydraulic property case is shown in Figure 8-21(a-d) for representative nodes from H1 and H2 units under 100-series and 200-series tanks. Very good agreement is observed between vertical Darcy flux calculated using the

RPP-ENV-58782, Rev. 0

1 regression equation and that obtained from STOMP[®] over the long simulated time period. Slight
 2 divergence that occurs just past Calendar Year 2500 results from switching from early
 3 post-closure period regression equation to late post-closure regression equation at Calendar
 4 Year 2520. This is because, although the step change in recharge rate occurs at Calendar
 5 Year 2520—reflecting degradation of surface cover (loss of hydraulic barrier capability)—the
 6 vertical Darcy flux in the STOMP[®] model slowly transitions to equilibrate to the new recharge
 7 rates. This transition period is not captured in the regression equations and leads to slight
 8 divergence in predicting the vertical Darcy flux.
 9

Table 8-8. Recharge Rate Used in Scaling Flow Field.

	Base Case Recharge Rate	5th Percentile Recharge Rate	Maximum Recharge Rate
Operational Period (Calendar Year 1945-2020)	100 mm/yr	57.30 mm/yr	140 mm/yr
Early Post-Closure (Calendar Year 2020-2520)	0.5 mm/yr	0.23 mm/yr	0.9 mm/yr
Late Post-Closure (Calendar Year >2520)	3.5 mm/yr	1.07 mm/yr	5.2 mm/yr

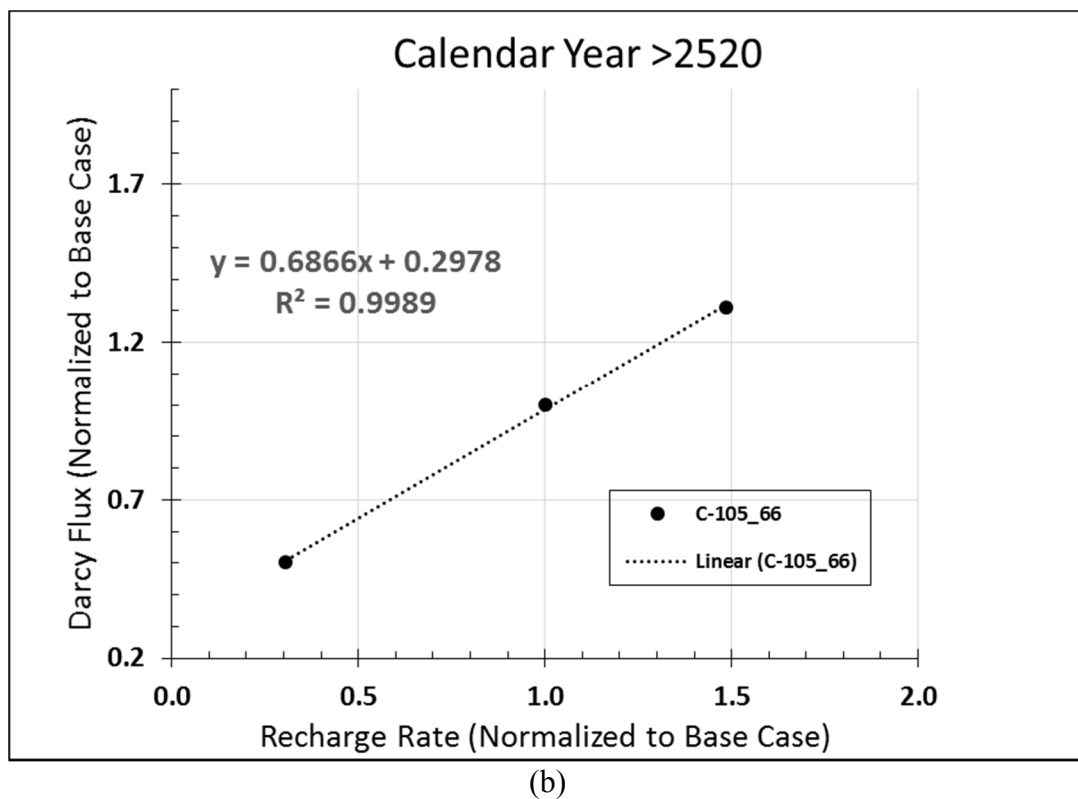
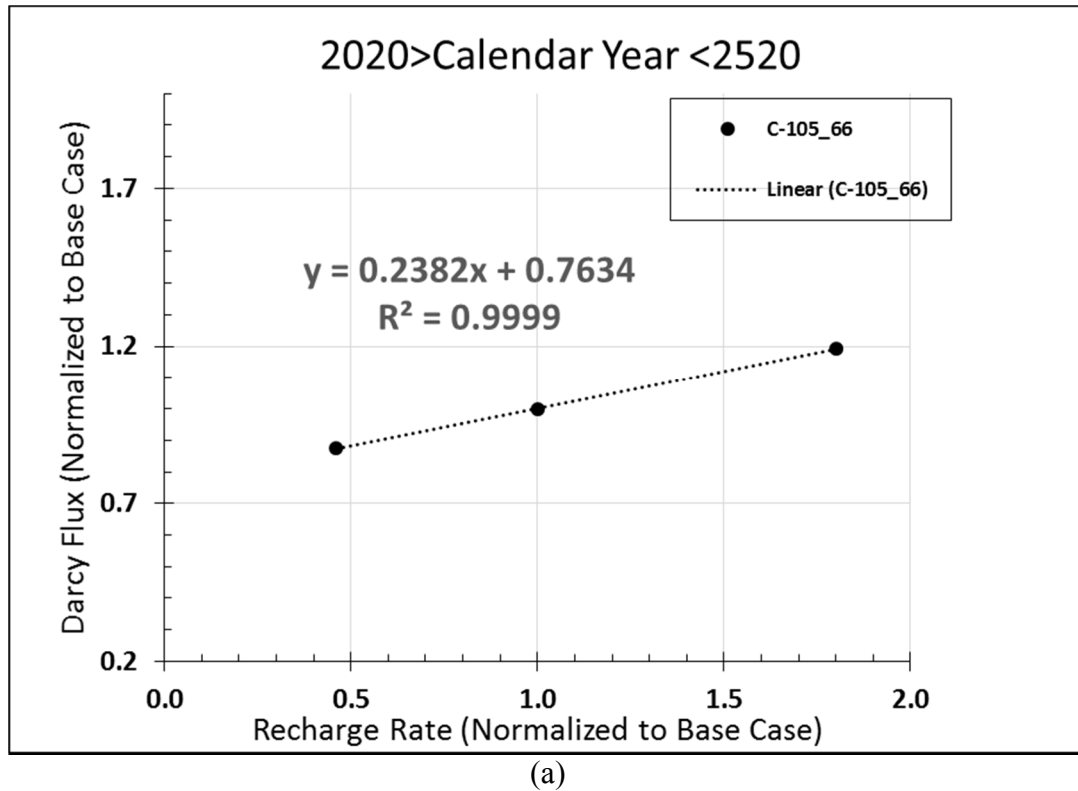
**Table 8-9. Example of Normalized Darcy Flux at Calendar Year 2300 from
 Selected Three-Dimensional STOMP[®]-Based Model Nodes under
 Tank 241-C-105 Using 5th Percentile Hydraulic Property.**

Node Location	Normalized Darcy Flux: Base Recharge Rate	Normalized Darcy Flux: 5th Percentile Recharge Rate	Normalized Darcy Flux: Maximum Recharge Rate
C-105_66	1	0.5012	1.3086
C-105_63	1	0.5079	1.2964
C-105_61	1	0.4588	1.3587
C-105_55	1	0.4936	1.3802
C-105_47	1	0.5427	1.3820
C-105_39	1	0.5947	1.3560
C-105_31	1	0.6407	1.3188
C-105_24	1	0.6765	1.2864
C-105_18	1	0.6759	1.2861
C-105_14	1	0.6832	1.2791

Subsurface Transport Over Multiple Phases (STOMP)[®] is copyrighted by Battelle Memorial Institute, 1996.

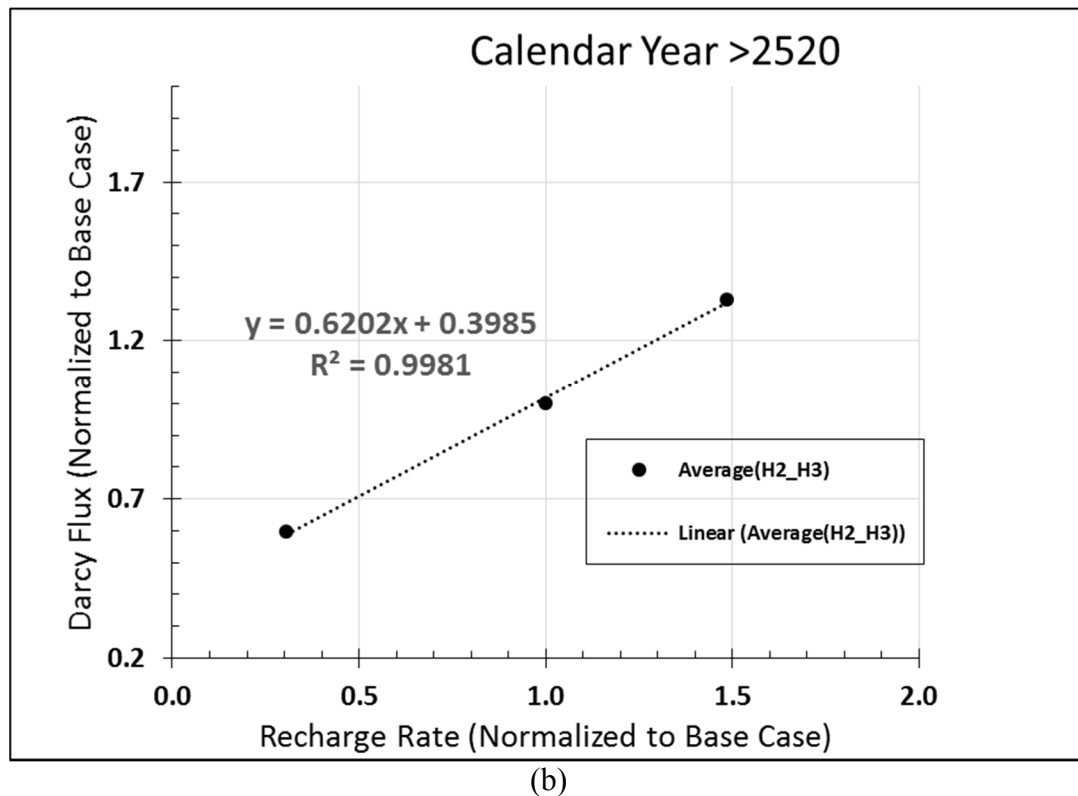
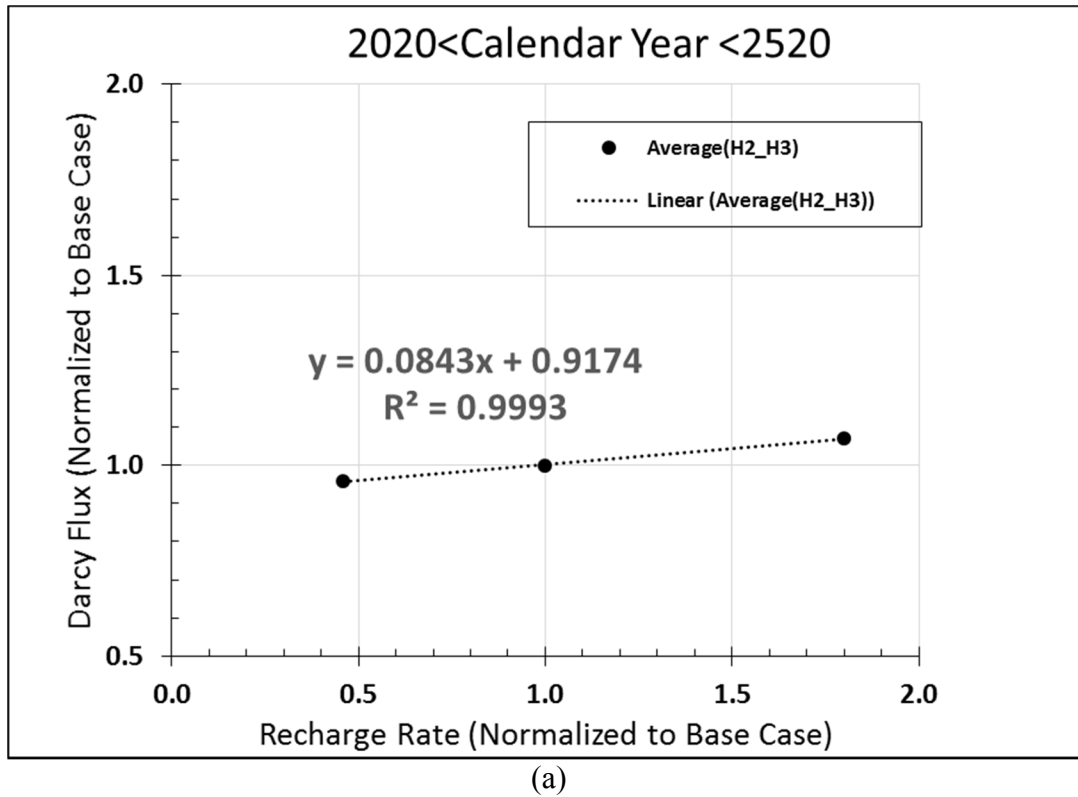
RPP-ENV-58782, Rev. 0

Figure 8-17. Normalized Darcy Flux for H1 Unit (Node 66) for 100-Series Representative Column during (a) Early Post-Closure Period (b) Late Post-Closure Period.



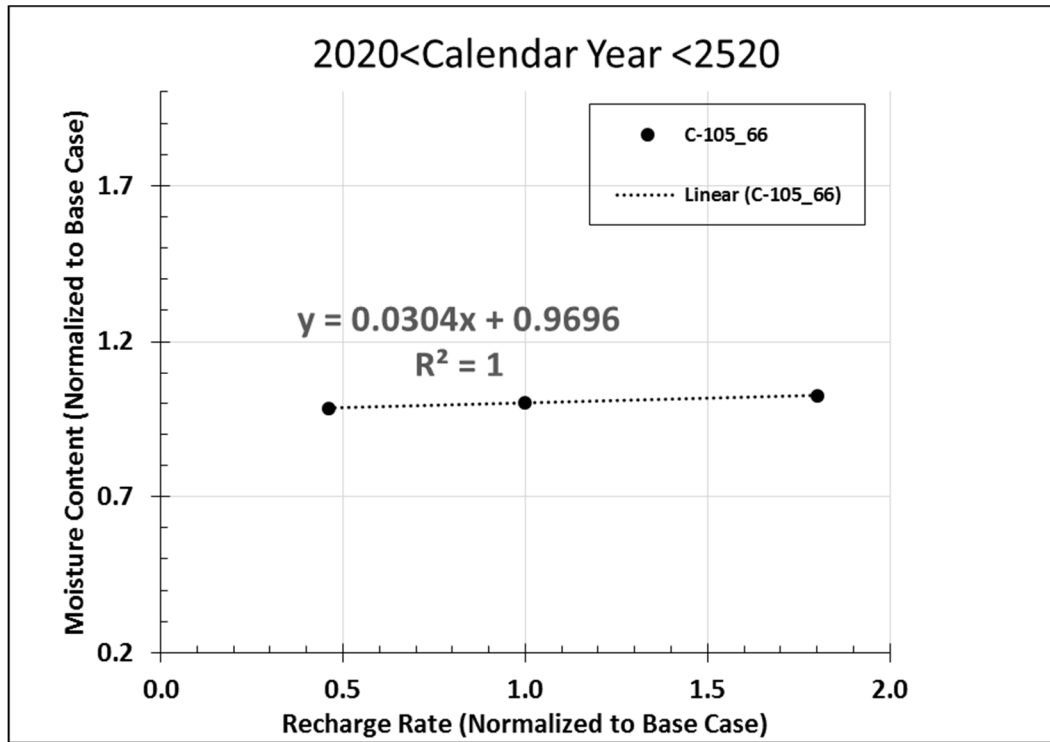
RPP-ENV-58782, Rev. 0

Figure 8-18. Normalized Darcy Flux for H2 and H3 Units for 100-Series Representative Column during (a) Early Post-Closure Period (b) Late Post-Closure Period.

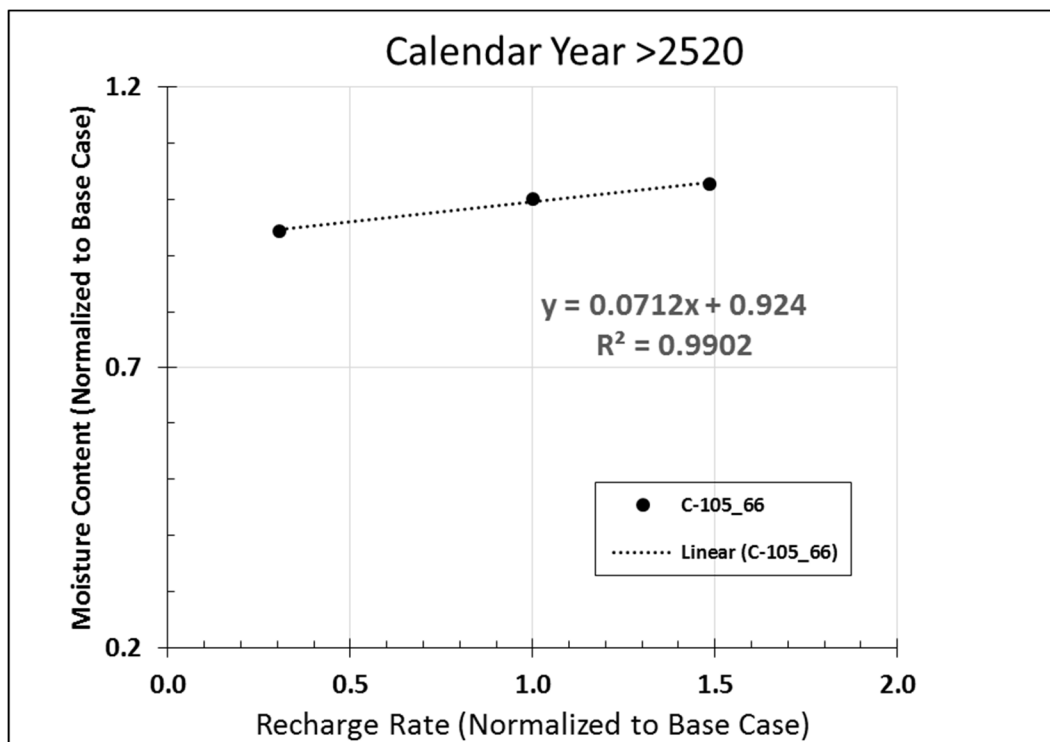


RPP-ENV-58782, Rev. 0

Figure 8-19. Normalized Moisture Content for H1 Unit (Node 66) for 100-Series Representative Column during (a) Early Post-Closure Period (b) Late Post-Closure Period.



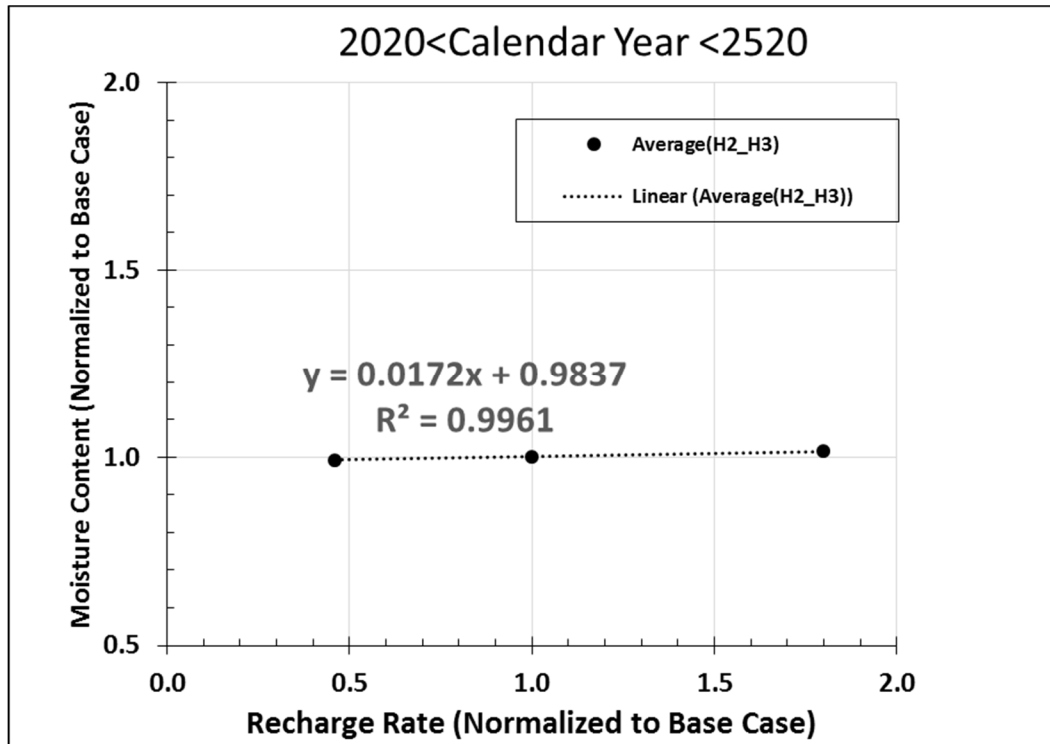
(a)



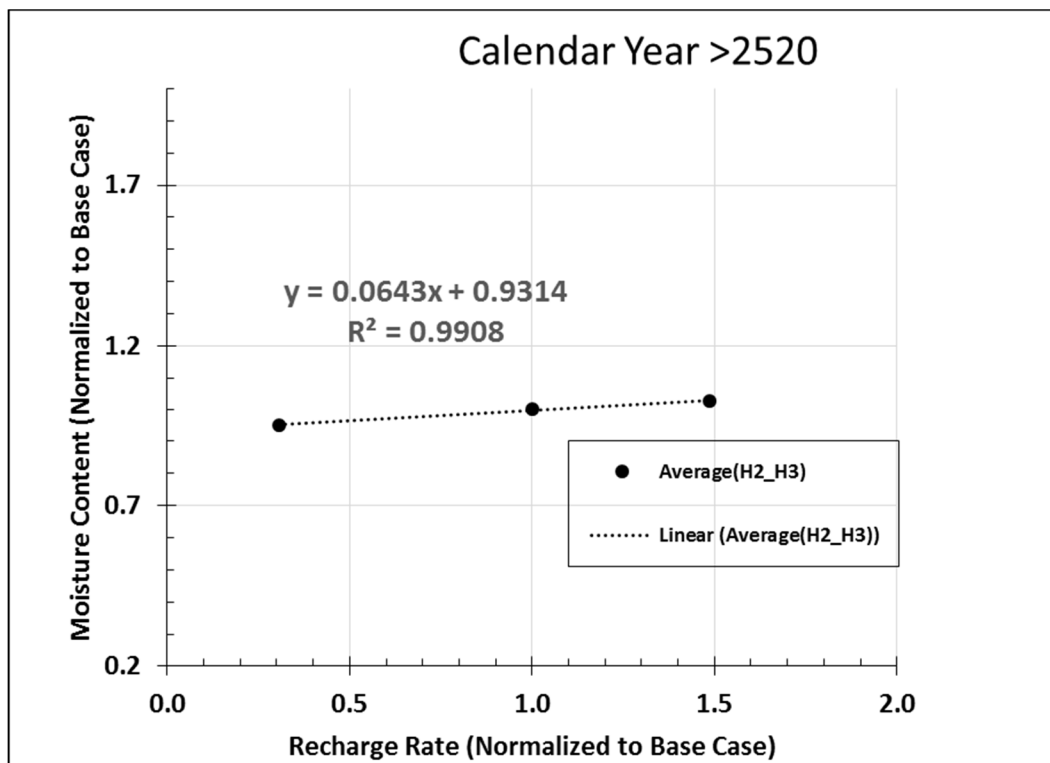
(b)

RPP-ENV-58782, Rev. 0

Figure 8-20. Normalized Moisture Content for H2 and H3 Units for 100-Series Representative Column during (a) Early Post-Closure Period (b) Late Post-Closure Period.



(a)



(b)

RPP-ENV-58782, Rev. 0

Table 8-10. Regression Equations for Scaling Darcy Flux for 100-Series Tank.

Vadose Zone Hydraulic Properties	Normalized Darcy Flux: 100 Series Tank			
	H1 Unit		H2/H3 Unit	
	2020<Calendar Year<2520	Calendar Year>2520	2020<Calendar Year<2520	Calendar Year>2520
5th Percentile Case Hydraulic Properties	$0.2382*x+0.7634$	$0.6866*x+0.2978$	$0.0843*x+0.9174$	$0.6202*x+0.3985$
25th Percentile Case Hydraulic Properties	$0.2562*x+0.7406$	$0.5083*x+0.4701$	$0.1261*x+0.8763$	$0.7149*x+0.3032$
50th Percentile Case Hydraulic Properties	$0.2652*x+0.7363$	$0.7305*x+0.2670$	$0.2243*x+0.7829$	$0.8141*x+0.1940$
75th Percentile Case Hydraulic Properties	$0.3265*x+0.6721$	$0.7233*x+0.2580$	$0.2602*x+0.7474$	$0.8109*x+0.1946$
95th Percentile Case Hydraulic Properties	$0.8006*x+0.2164$	$0.899*x+0.0660$	$0.2795*x+0.7409$	$0.9497*x+0.0775$

x = Sampled recharge rate / Base case recharge rate

Table 8-11. Regression Equations for Scaling Darcy Flux for 200-Series Tank.

Vadose Zone Hydraulic Properties	Normalized Darcy Flux: 200 Series Tank			
	H1 Unit		H2/H3 Unit	
	2020<Calendar Year<2520	Calendar Year>2520	2020<Calendar Year<2520	Calendar Year>2520
5th Percentile Case Hydraulic Properties	$0.2456*x+0.7566$	$0.7221*x+0.2714$	$0.0485*x+0.9523$	$0.4389*x+0.5651$
25th Percentile Case Hydraulic Properties	$0.2832*x+0.7155$	$0.7253*x+0.2754$	$0.0781*x+0.9237$	$0.5536*x+0.4573$
50th Percentile Case Hydraulic Properties	$0.2604*x+0.7415$	$0.7512*x+0.2540$	$0.1236*x+0.8783$	$0.5572*x+0.4463$
75th Percentile Case Hydraulic Properties	$0.3260*x+0.6735$	$0.7614*x+0.2361$	$0.1472*x+0.8554$	$0.6110*x+0.3950$
95th Percentile Case Hydraulic Properties	$0.3731*x+0.6336$	$0.8759*x+0.1345$	$0.1480*x+0.8567$	$0.6252*x+0.3798$

x = Sampled recharge rate / Base case recharge rate

Note that the scaling multipliers developed for vertical Darcy flux and volumetric moisture content are dimensionless and are applied to values calculated under base recharge conditions, as abstracted from the 3-D STOMP[®] model results for each of the five hydraulic properties. The results of using the regression equations over the minimum and maximum recharge rates are presented in Appendix I. The purpose of Appendix I is to illustrate the uncertainty range in

RPP-ENV-58782, Rev. 0

vertical average linear pore water velocities within the vadose zone for the post-closure time period. Based on the uncertainty ranges calculated for each hydraulic property under minimum and maximum recharge rates, it is found that the range in vertical linear pore water velocities is the largest for the 95th percentile hydraulic property (around a factor of 6.5) and minimum for the 25th percentile hydraulic property (factor of 2 to 2.5). For other hydraulic properties the range varies from factor of 3 to 4. These results indicate that for realizations where 95th percentile hydraulic property is selected during uncertainty analysis, greater variance in travel times can be expected compared to other hydraulic properties (under similar recharge rate range).

Table 8-12. Regression Equations for Scaling Volumetric Moisture Content.

Normalized Volumetric Moisture Content			
H1 Unit		H2/H3 Unit	
2020<Calendar Year<2520	Calendar Year>2520	2020<Calendar Year<2520	Calendar Year>2520
$0.0304*x+0.9696$	$0.0712*x+0.9240$	$0.0172*x+0.9837$	$0.0643*x+0.9314$

x = Sampled recharge rate / Base case recharge rate

Step 5 – Sampling of Flow Fields:

In the Monte Carlo analysis for the system model, a flow field is selected for each realization. Using the approach described in Steps 1 through 4, the flow fields are developed for five hydraulic property sets based on the selection of various percentiles from the vertical pore water velocity CDF (for example, see Figure 8-14 for the H2 unit). The percentiles selected were 5th, 25th, 50th, 75th, and 95th to discretely represent the uncertainty in the CDF (Table 8-7). A discrete probability distribution was developed for sampling the five hydraulic properties (flow fields). The 5th and 95th percentile hydraulic properties were given a probability of 0.1 each, the 25th and 75th percentile hydraulic properties were given a probability of 0.25 each, and the 50th percentile hydraulic property was given a probability of 0.3, leading to a discrete probability distribution with a median value being represented by the 50th percentile hydraulic property. The rationale for this probability weighting was based on the understanding that the 5th and 95th percentile hydraulic properties represent the extremes of the pore water velocity distribution, and should have a lower probability of being selected compared to the other percentile hydraulic properties, with the 50th percentile hydraulic property being the most probable. As a result, the 25th and 75th percentile hydraulic properties are given slightly lower weighting than the 50th percentile hydraulic property. The selected discrete probability distribution results in the median being the 50th percentile hydraulic property, which is also the most probable flow field.

8.1.5 Results of Uncertainty Analyses

A full uncertainty analysis is undertaken by performing multi-realization simulations in the probabilistic mode using the GoldSim[®]-based system model. The uncertainties are propagated using the Monte Carlo sampling methodology and the LHS scheme. In the Monte Carlo simulation, the entire system is simulated a large number of times. Each simulation is equally likely and is referred to as a *realization* of the system. For each realization, all of the uncertain

RPP-ENV-58782, Rev. 0

parameters are sampled, and the system is simulated through time (with the given set of input parameters) such that the performance of the system can be computed. At the start of each realization, each stochastic element generates a new random seed that forms the basis for sampling the element during the realization. The LHS scheme allows for efficient sampling of the probability space so that full uncertainty can be represented without a large number of realizations (GoldSim Technology Group 2014c). In this scheme, each stochastic element's probability distribution (0 to 1) is divided into equally likely strata or slices equal to the number of realizations. The strata are then "shuffled" into a random sequence, and a random value is picked from each stratum in turn. This approach ensures that uniform spanning sampling is achieved. Note that each element has an independent sequence of shuffled strata that are a function of the element's random number seed and the number of realizations in the simulation. The LHS appears to have a significant benefit for problems involving a few independent stochastic parameters, and with moderate number of realizations (GoldSim Technology Group 2014c).

The total mean annual dose, $\bar{D}(\tau)$, for a multi-realization case is estimated at time τ by numerically evaluating

$$\bar{D}(\tau) = \int_E D(\tau|\mathbf{e}) d_E(\mathbf{e})dE \quad (8-3)$$

where E is a probability space comprising the epistemic uncertain parameters, and $D(\tau|\mathbf{e})$ computes the annual dose at time τ for a given element \mathbf{e} (a vector of all uncertain parameters evaluated per realization) in E . The evaluation of the function $D(\tau|\mathbf{e})$ is performed by numerically solving a complex, coupled system of differential equations such as describing radionuclide decay, mass transport, flow, and other physical processes. The numerical integration is performed by the Monte Carlo technique and employing LHS of epistemic uncertain parameters.

The GoldSim[®]-based system model is exercised by running 300 realizations. The results are presented in Figure 8-22 in terms of mean of total dose (from all radionuclides from the groundwater and atmospheric transport pathways) along with the mean dose contribution of individual radionuclides. The early dose (from 100 to 600 years after closure) primarily results from the release of ³H (tritium) and ¹²⁹I to the air pathway, and the late dose (past 1,000 years after closure) results primarily from the ⁹⁹Tc release to the groundwater pathway. The mean dose reaches a peak value of about 0.17 mrem/yr around 3,400 years after closure and then declines gradually. Although the contribution of ⁹⁹Tc steadily declines, the mean total dose remains virtually unchanged beyond 7,000 years after closure until the end of the analysis time. This is because of increasing dose contributions from uranium isotopes (primarily ²³⁴U, ²³⁸U, and ²³³U) that have relatively long half-lives and are relatively mobile (low K_d value).

Besides ⁹⁹Tc and uranium isotopes, other radionuclides of interest are ¹²⁹I, ²²⁶Ra, ¹²⁶Sn, and ⁷⁹Se. The dose contribution of ¹²⁹I in the first 1,000 years after closure is primarily from the atmospheric pathway, and beyond that primarily from the groundwater pathway. Radium-226 dose results from it being in equilibrium with the uranium decay series, and therefore—although it has a high K_d by itself—it appears at the PoCal. Tin-126 and ⁷⁹Se are relatively mobile (low

RPP-ENV-58782, Rev. 0

K_d) and have relatively long half-lives (>200,000 years after closure), and therefore show breakthrough at PoCal within the simulated time period.

8.1.5.1 Evaluation of Uncertainty in Groundwater Pathway. Figure 8-23 shows the results of propagating parameter uncertainties in the groundwater pathway dose for 300 realizations, along with the mean, median, 5th, and 95th percentile values. The highest mean and median doses occur around 3,400 years after closure. For comparison purposes, the dose from base case is also presented. Comparing the base case dose with the mean dose from 300 realizations indicates that the peak occurs earlier in the base case, reflecting faster transport through the vadose zone and saturated zone. For all realizations, ⁹⁹Tc is the primary dose contributor, and thus the uncertainty in groundwater pathway dose is almost entirely due to uncertainty in ⁹⁹Tc dose. The mean of the total dose is higher than the median of the total dose and closer to the 75th percentile curve. This occurs because the values range over several orders of magnitude, so that an arithmetic mean will tend to be skewed to the higher values. The variance in dose, defined by the difference in 5th and 95th percentiles at a given time slice, is observed to decrease after 4,000 years following closure. This is due to occurrence of larger number of realizations having relatively similar breakthrough curves. Prior to this time, some realizations that have earlier ⁹⁹Tc breakthrough show a decline due to variable influence of flow fields, leading to increased variance. At late time also (>7,000 years after closure), the variance in dose increases marginally. This results from the increasing importance of uranium isotopes at late times.

To understand the relative influence of uncertain parameters on the peak dose resulting from the groundwater pathway, two realizations (Rlz# 142 and Rlz# 295) are shown in Figure 8-24, and demonstrate the highest dose values (Figure 8-24).

In Rlz# 142, the peak dose value is ~2.5 mrem/yr, and it occurs around 2,400 years after closure. This high dose value results from a combination of sampling the Darcy flux multiplier (0.33) near the low end of the uncertainty distribution and sampling the residual waste instantaneous ⁹⁹Tc release fraction (0.149) from the upper end of the distribution. In addition, the saturated zone dispersivity (2.3 m [7.5 ft]) is sampled at the lower end of the distribution. The high instantaneous release fraction leads to larger diffusive flux from the base of the tanks, and the lower Darcy flux multiplier leads to less dilution in the saturated zone leading to increased concentration in the aquifer. In addition, sampling lower dispersivity in the saturated zone leads to less dispersion and higher peak concentration that results in a high dose.

In Rlz# 295, the peak dose value is ~1.8 mrem/yr and it occurs around 5,000 years after closure. Unlike Rlz# 142, where the peak occurs quickly followed by steep decline, the dose curve in Rlz# 295 shows a gradual rise and a more gradual decline. This behavior results from a combination of sampling the Darcy flux multiplier (0.19) near the minimum value of the uncertainty distribution and sampling the ⁹⁹Tc inventory multiplier (1.36) from the upper end of the uncertainty distribution. This combination leads to increased residual inventory being available, along with lowest possible dilution in the saturated zone resulting in greater peak concentration. In this realization, the 25th percentile flow field is sampled that leads to lower pore water velocity in the vadose zone, and therefore the mass continues to arrive from the source term over a longer time period. This leads to a gradual rise and gradual decline in the dose curve.

Figure 8-21. Comparison between Darcy Flux Calculated Using Regression Equation and that Obtained from Three-Dimensional Subsurface Transport Over Multiple Phases-Based Model Simulation for the 5th Percentile Hydraulic Property Case for (a) H1 Unit under 100-Series Tank (Node 66); (b) H2 Unit under 100-Series Tank (Node 47); (c) H1 Unit under 200-Series Tank (Node 66); and (d) H2 Unit under 200-Series Tank (Node 43). (sheet 1 of 4)

(a)

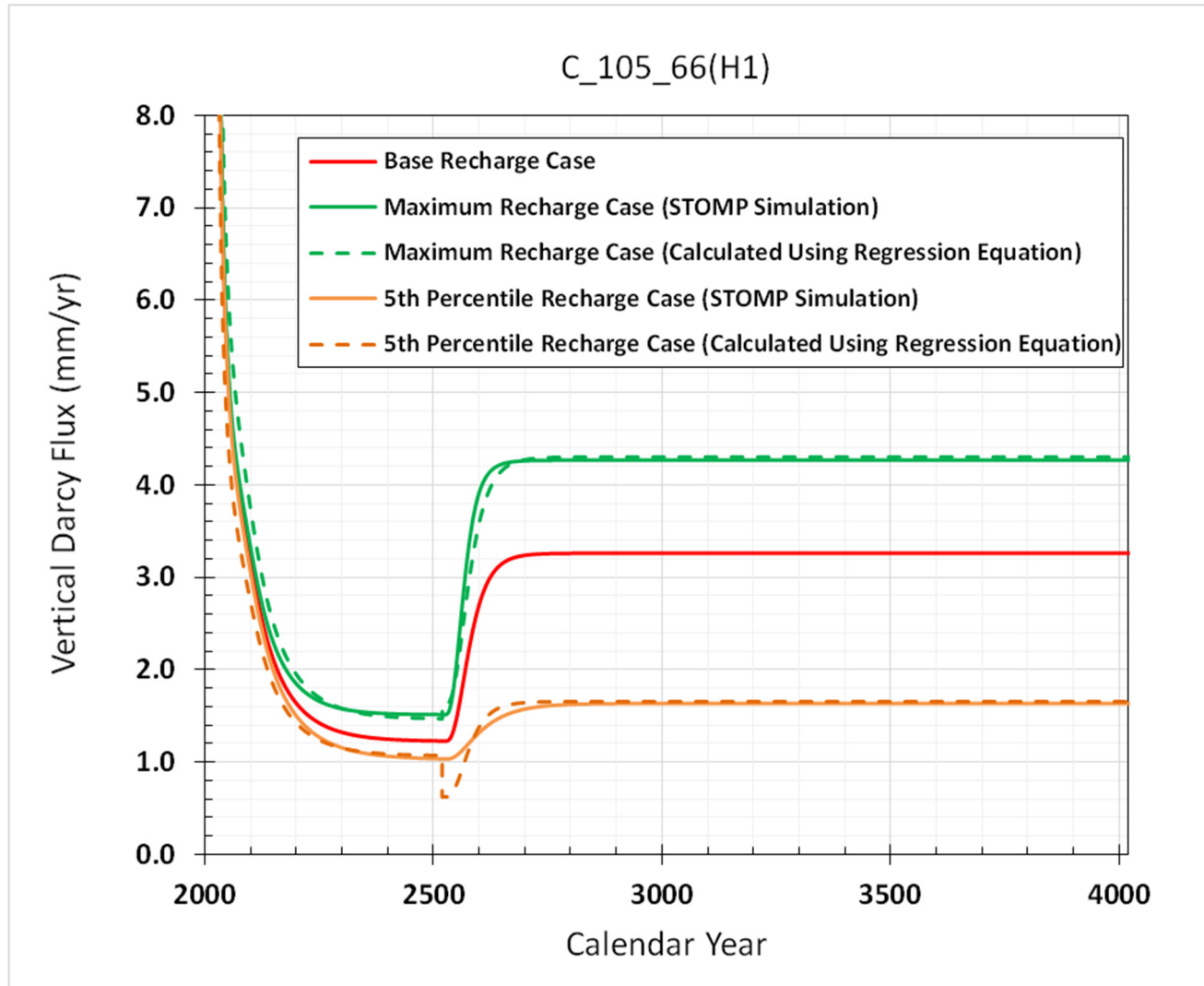


Figure 8-21. Comparison between Darcy Flux Calculated Using Regression Equation and that Obtained from Three-Dimensional Subsurface Transport Over Multiple Phases Based Model Simulation for the 5th Percentile Hydraulic Property Case for (a) H1 Unit under 100-Series Tank (Node 66); (b) H2 Unit under 100-Series Tank (Node 47); (c) H1 Unit under 200-Series Tank (Node 66); and (d) H2 Unit under 200-Series Tank (Node 43). (sheet 2 of 4)

(b)

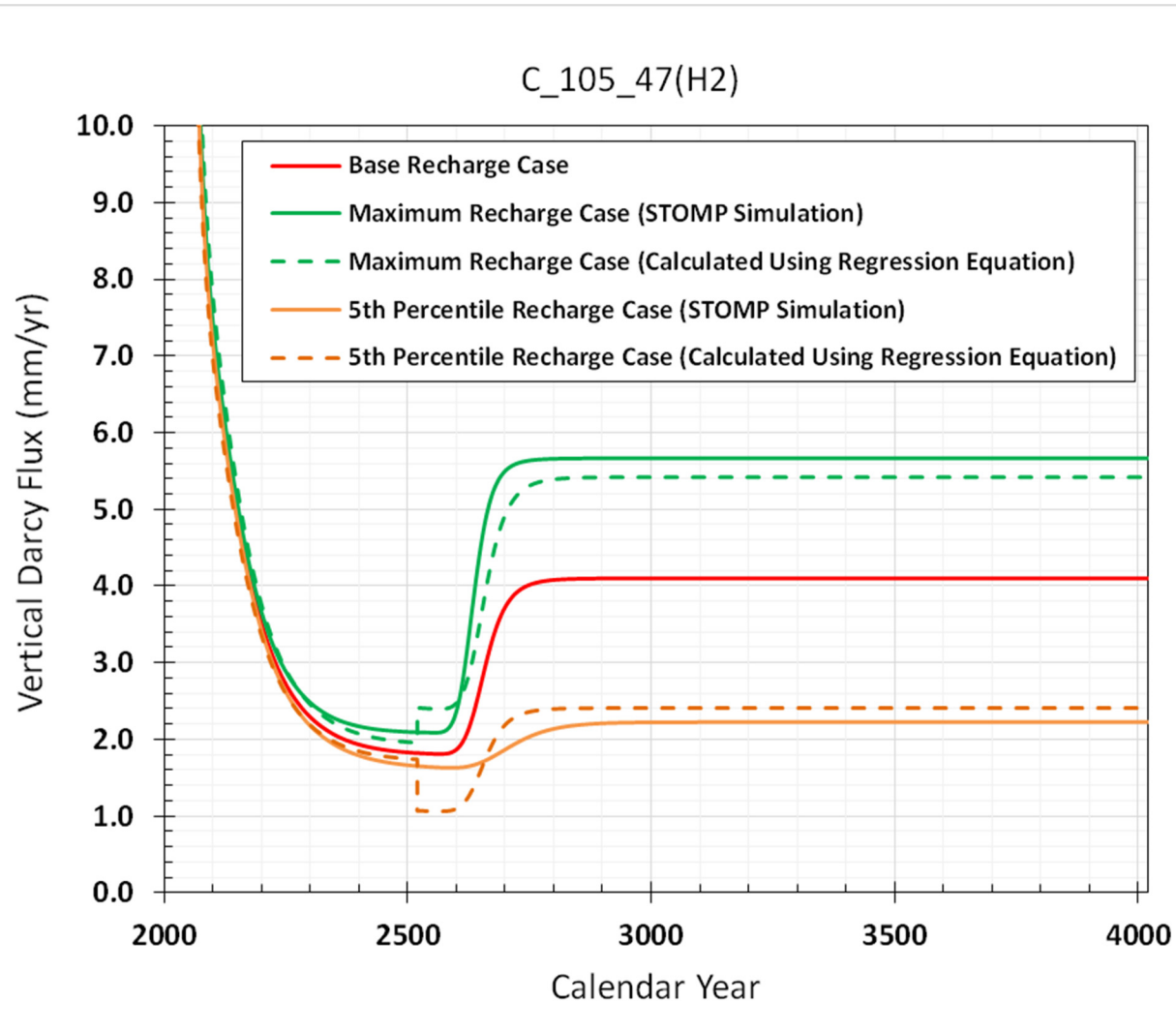


Figure 8-21. Comparison between Darcy Flux Calculated Using Regression Equation and that Obtained from Three-Dimensional Subsurface Transport Over Multiple Phases Based Model Simulation for the 5th Percentile Hydraulic Property Case for (a) H1 Unit under 100-Series Tank (Node 66); (b) H2 Unit under 100-Series Tank (Node 47); (c) H1 Unit under 200-Series Tank (Node 66); and (d) H2 Unit under 200-Series Tank (Node 43). (sheet 3 of 4)

(c)

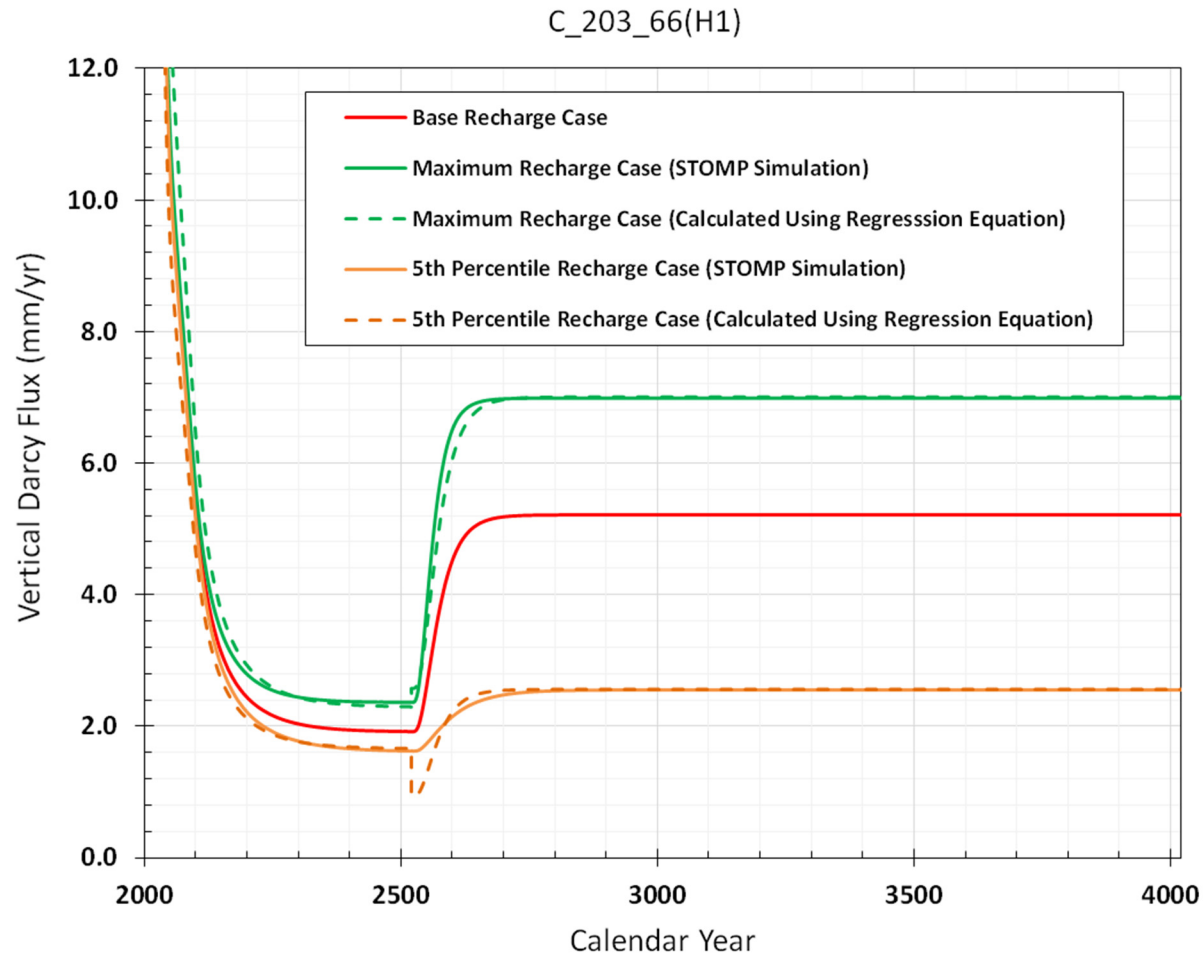
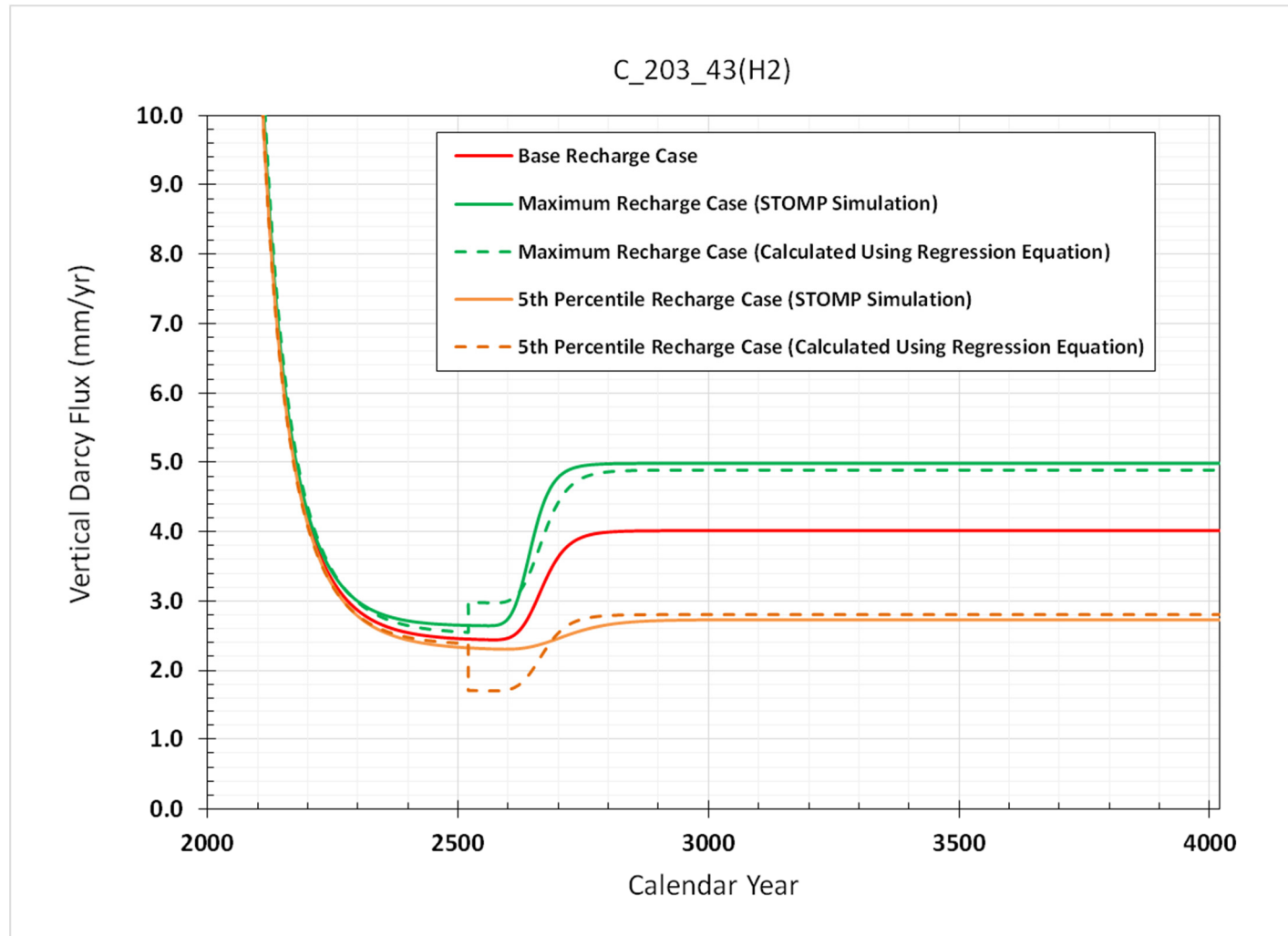


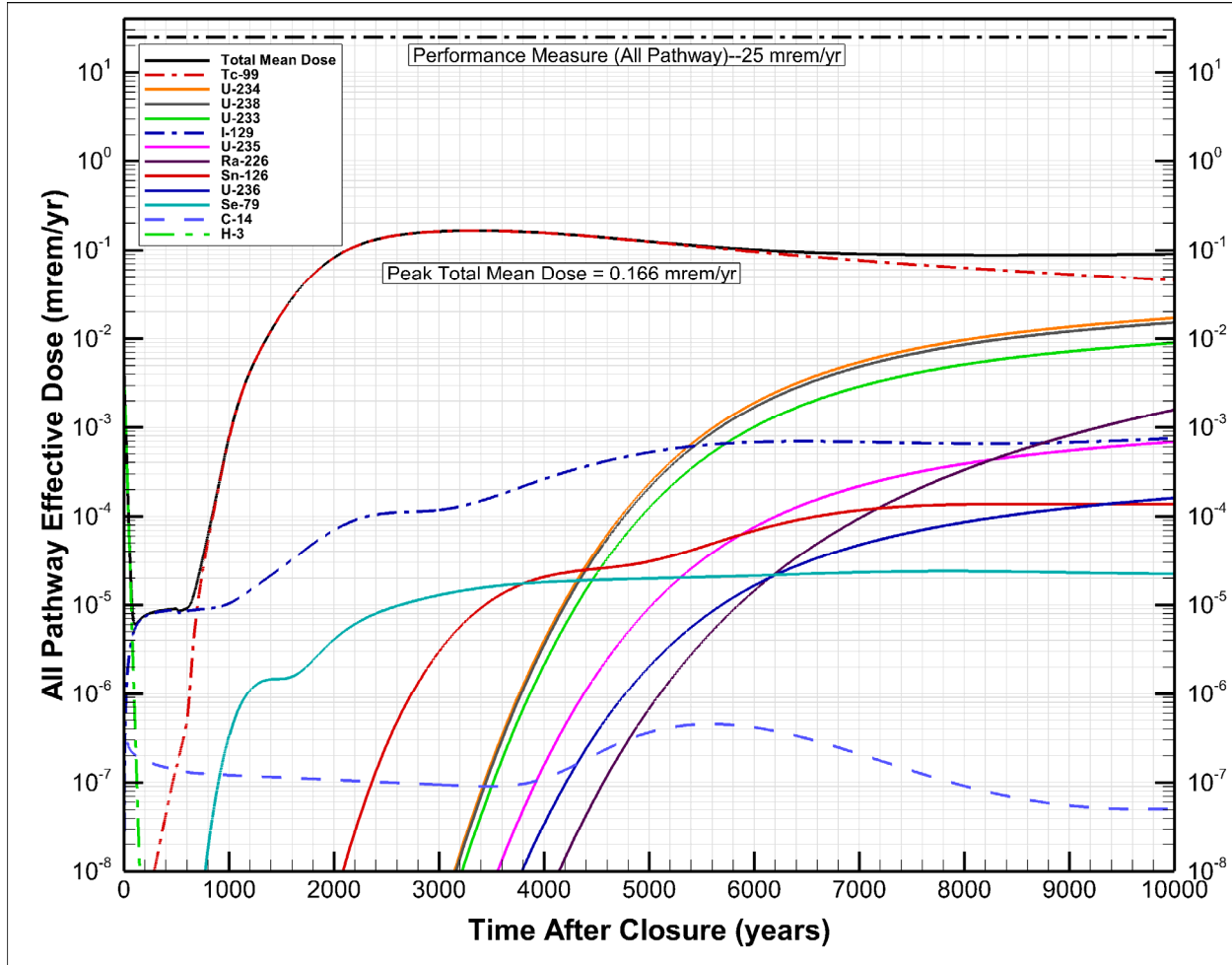
Figure 8-21. Comparison between Darcy Flux Calculated Using Regression Equation and that Obtained from Three-Dimensional Subsurface Transport Over Multiple Phases Based Model Simulation for the 5th Percentile Hydraulic Property Case for (a) H1 Unit under 100-Series Tank (Node 66); (b) H2 Unit under 100-Series Tank (Node 47); (c) H1 Unit under 200-Series Tank (Node 66); and (d) H2 Unit under 200-Series Tank (Node 43). (sheet 4 of 4)

(d)



Subsurface Transport Over Multiple Phases (STOMP)[®] is copyrighted by Battelle Memorial Institute, 1996.

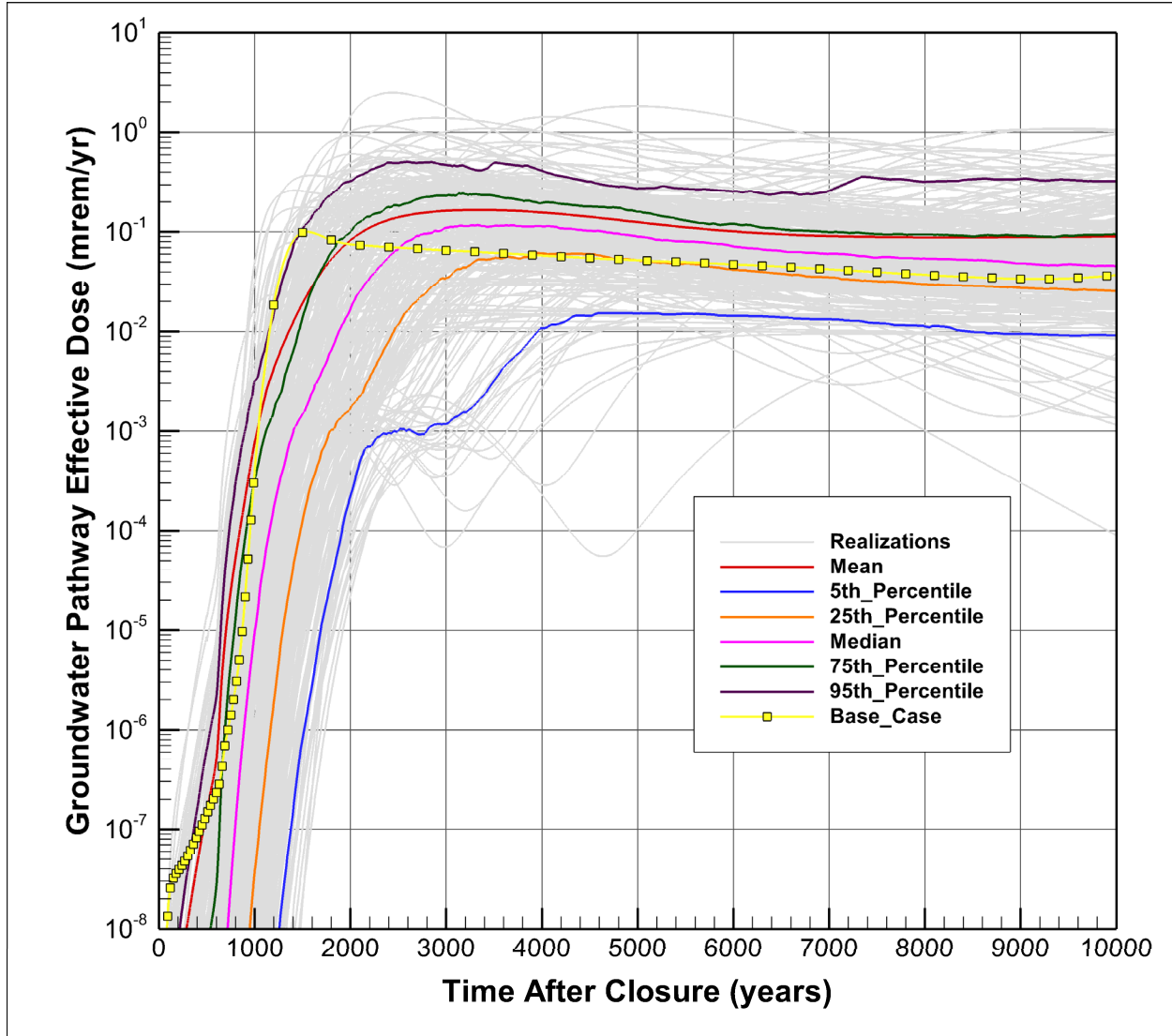
RPP-ENV-58782, Rev. 0

Figure 8-22. All-Pathway Mean Dose Calculation Results Based on 300 Realizations.

Some of the realizations presented in Figure 8-24 show a gradual rise late in time. This gradual increase is attributed to the increasing dose influence from uranium isotopes. Some of the realizations that show early peak dose result from sampling the 95th percentile flow field that leads to high pore-water velocity and earlier breakthrough.

Multivariate analyses were conducted to evaluate the importance of uncertain parameters on the groundwater pathway dose calculations. The analysis was conducted at the time of peak mean dose, which occurs about 3,400 years after closure. The analysis was based on the ranks (rather than values) of the uncertain parameters. Two types of analyses were conducted: (a) the rank (Spearman) correlation coefficient and (b) the Importance Measure. Standardized rank regression coefficients and partial rank correlation coefficients were also computed, but they do not provide additional insight and are not discussed further. The total number of uncertain parameters that are implemented in the system model is 130.

RPP-ENV-58782, Rev. 0

Figure 8-23. Uncertainty in Groundwater Pathway Dose Based on 300 Realizations.

The rank correlation coefficient expresses the extent to which there is a linear relationship between the selected result and an input variable. The coefficients range between -1 and 1 with extreme values indicating strong negative or positive correlations. The calculation is performed using the following equation (GoldSim Technology Group 2014c):

$$C_{rp,rank} = \frac{\sum_{i=1}^n (Rp_i - m_{Rp})(Rr_i - m_{Rr})}{\sqrt{\sum_{i=1}^n (Rp_i - m_{Rp})^2 \sum_{i=1}^n (Rr_i - m_{Rr})^2}} \quad (8-4)$$

Where:

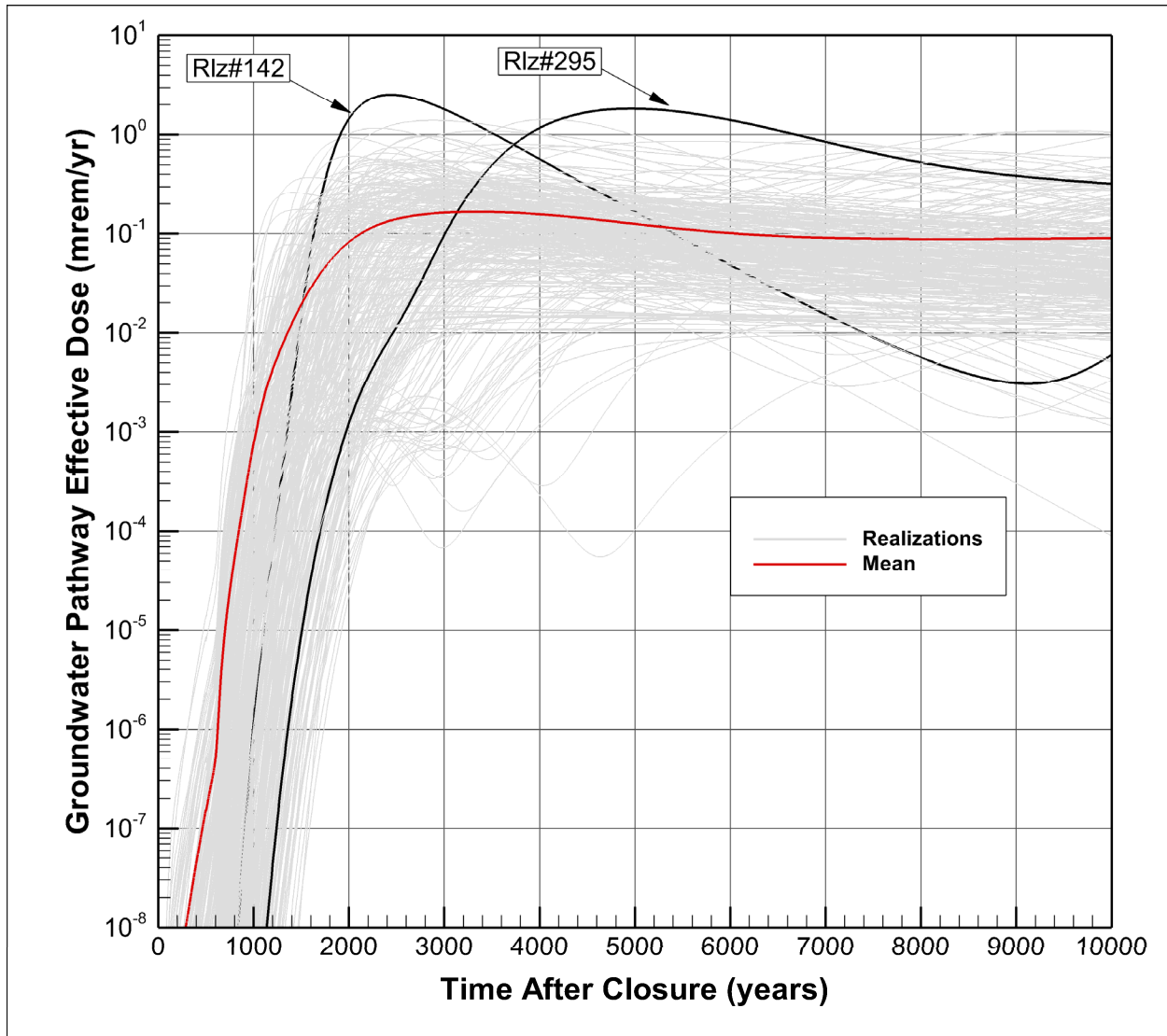
$C_{rp,rank}$ = the rank correlation coefficient

n = the number of selected data points (realizations)

RPP-ENV-58782, Rev. 0

- Rp_i = the rank (from 1 to n) of output p for realization I
 m_{Rp} = mean value of the rank of output p
 m_{Rr} = mean value of the rank of output r.

Figure 8-24. Selected Realizations for Groundwater Pathway Dose Analysis.



The standardized rank regression coefficients and partial rank correlation coefficients also vary between -1 and 1. These calculations are based on the variable ranks rather than on the actual values of the variables. The standardized rank regression coefficients provide a normalized measure of the linear relationship between variables and the result (dose). They are regression coefficients found when all of the variables and the results are transformed and expressed in terms of the number of standard deviations away from the mean. The partial correlation coefficients reflect the extent of the linear relationship between the selected result and an input variable, after removing the effects of any linear relationships between the other input variables and both the results and the input variable in question. Both formulations are based on

RPP-ENV-58782, Rev. 0

NUREG/CR-4122, A FORTRAN 77 Program and User's Guide for the Calculation of Partial Correlation and Standardized Regression Coefficients.

The importance measure (as calculated using GoldSim[®]) expresses the nonlinear, non-monotonic relationship between an input variable and the result, which the conventional correlation coefficient may not reveal. This measure varies between 0 and 1, and represents the fraction of the result's variance that is explained by the variable. The importance measure presented here is a normalized version of a measure discussed in "On the Relative Importance of Input Factors in Mathematical Models: Safety Assessment of Nuclear Waste Disposal" (Saltelli and Tarantola 2002), and is calculated as:

$$M_{y,i} = 1 - \frac{E[v_y(Y|X_i)]}{v_y} \quad (8-5)$$

Where:

$M_{y,i}$ = the importance measure for the sensitivity of the result (Y) to input variable X_i
 v_y = the current variance in the result Y
 $E[v_y(Y|X_i)]$ = the expected value of v_y if the input variable X_i was perfectly known.

Thus, the Importance Measure $M_{y,i}$ represents the fraction of the result variance that is explained by X_i . For additional computational details, refer to Appendix B of the GoldSim User's Guide (GoldSim Technology Group 2014b).

The uncertainty analysis results of the 300 realization case for the groundwater pathway are presented at the end of 1,000 years after closure (Table 8-13a) which is the end of compliance time period, and at 3,400 years after closure (Table 8-13b), the approximate time when the peak occurs in the mean dose. Only those parameters are presented that contribute significantly to the uncertainty in total dose for the groundwater pathway. The results are sorted by the uncertain parameters from highest to lowest in terms of their Importance Measures, for those parameters that have correlation coefficients equal to or greater than ~0.2. Other uncertainty analysis measures (e.g., partial correlation coefficients) generally follow the same trend. The uncertainty analysis for the groundwater pathway is conducted by evaluating the dose from all realizations at 1,000 years and 3,400 years after closure. The results of the multivariate analysis are only applicable to these times.

Based on the uncertainty analysis for the groundwater pathway conducted at 1,000 years after closure (end of compliance time period), the most important uncertain parameter is found to be the K_d of ^{99}Tc in the vadose zone sediments (Table 8-13a). It shows a high negative correlation with the dose at 1,000 years, which is primarily due to ^{99}Tc . Since the 1,000-year time is near the arrival time of ^{99}Tc at the water table (breakthrough time) and since the dose curves are rising steeply, the magnitude of the dose is being directly affected by the uncertainty in the K_d of ^{99}Tc in the vadose zone sediments. Due to steep rise in the dose curves, a small delay in arrival at the water table leads to a much lower magnitude of dose at the 1,000-year time plane compared to a realization where the arrival at the water table occurs marginally earlier. Therefore, even though

RPP-ENV-58782, Rev. 0

the uncertainty range in the K_d of ^{99}Tc in the vadose zone sediments is very small (0 to 0.1 mL/g), it leads to significant changes in the breakthrough time at the water table at 1,000 years. The coefficient of determination based on linear rank regression is ~ 0.96 and thus explains 96% of the variance in the dose at 1,000 years. All other uncertain parameters show much lower correlation to the dose at 1,000 years. The second and third most important parameters are related to uncertainty in dispersivity within the vadose zone and saturated zone. These parameters also affect the arrival times at the water table and receptor location.

Based on the uncertainty analysis for the groundwater pathway conducted at the time of peak dose (around 3,400 years after closure), the two most important uncertain parameters are found to be the vadose zone flow-field selector (hydraulic properties corresponding to the percentiles chosen from the vertical pore-water velocity CDF) and the saturated zone Darcy flux multiplier (scales the base case Darcy flux in the aquifer). Both uncertain parameters are negatively correlated to the groundwater pathway dose. The linear relationships in these parameters can be inferred from the scatter plots shown in Figure 8-25. Choosing higher flow field (higher percentile vadose zone hydraulic property set) leads to increased vertical pore water velocities, resulting in ^{99}Tc peak dose occurring earlier than 3,400 years after closure. In such realizations, dose from ^{99}Tc (which is approximately the total dose) shows a declining trend at 3,400 years after closure. On the other hand, realizations where lower flow field (lower percentile vadose zone hydraulic property set) is selected tend to have delayed peak dose from ^{99}Tc due to decreased vertical pore water velocities, resulting in an upwardly increasing dose trend at 3,400 years after closure. This combination results in a negative correlation between flow field and dose at 3,400 years after closure. The negative correlation observed for the saturated zone Darcy flux multiplier is more intuitive (Figure 8-25b), as the Darcy flux multiplier directly affects the volumetric flow rate in the aquifer, leading to dilution of the mass flux arriving from the vadose zone. Therefore, increasing the Darcy flux reduces the concentrations in the saturated zone for the simulated duration. The coefficient of determination based on linear rank regression for uncertain parameters shown in Table 8-13b is ~ 0.75 . This indicates that these six parameters represent about 75% of the total variance in the peak dose result (around 3,400 years after closure). The first two parameters alone account for more than half (59%) of the total variance in the dose.

The above uncertainty analyses are performed at fixed time planes and therefore provide information on important uncertain parameters that influence dose at that time. But since peak dose for each realization occurs at different times, a separate analysis is performed where correlation is performed between the input parameters and the peak dose regardless of the time. In this evaluation, the peak dose values from all 300 realizations are taken and a correlation is performed to identify uncertain parameters that influence the peak dose. The magnitude of peak dose for the groundwater pathway is shown in Figure 8-26 for all realizations. It shows that the peak dose values vary within about two orders of magnitude range (0.01 to 1 mrem/yr). The correlation coefficient analysis shows that the three most important uncertain parameters are saturated zone Darcy flux multiplier (correlation coefficient of -0.48), vadose zone flow-field selector (correlation coefficient of -0.45), and ^{99}Tc normalized inventory multiplier (correlation coefficient of 0.24). The scatter plots indicating the relationship between input parameters and peak dose are presented in Figure 8-27 (a,b,c). The parameters determined to be important are a subset of the parameters that were previously identified during uncertainty analysis performed at

RPP-ENV-58782, Rev. 0

3,400 years (Table 8-13b), which indicates that these parameters continue to affect the peak dose irrespective of time within the 10,000-year evaluation time period.

Figure 8-27(b) shows the relationship between the peak groundwater dose as a function of vadose zone hydraulic property (flow-field selector). The peak dose results from varying flow-field selectors mostly overlap except for flow-field #5 (corresponding to the 95th percentile hydraulic property), which shows somewhat lower peak dose and therefore causes an overall negative correlation. This result is likely due to greater variance in vertical pore water velocity estimated for the 95th percentile hydraulic property compared to other hydraulic properties (see Appendix I for illustration of the range). Since pore water velocity also affects the dispersion coefficient, larger variation in velocity also results in larger dispersion of solute mass within the vadose zone that affects the magnitude of the peak groundwater dose. Ignoring the results from 95th percentile hydraulic property results in lowering the negative correlation, which indicates that this parameter has lower influence on affecting peak dose than probably inferred based on simple correlation.

8.1.5.2 Evaluation of Uncertainty in the Atmospheric Pathway. Figure 8-28 presents the uncertainty in the atmospheric pathway dose for all 300 realizations, along with the mean, median, and other percentiles. In the first 100 years after closure, ³H (tritium) dose is the primary atmospheric pathway dose contributor, and after that it is ¹²⁹I (Figure 8-22). Hydrogen-3 dose declines sharply within the first 100 years after closure due to its short half-life and limited inventory. The ¹²⁹I dose, however, increases gradually and reaches a steady value after 500 years following closure. This is attributed to a relatively lower degree of partitioning into the air phase compared to ³H (and ¹⁴Co), and a relatively larger degree of sorption to the tank infill grout material compared to ³H. Due to these reasons, and in combination with long half-life, ¹²⁹I persists within the tank for a long time period. As shown in Figure 8-28, the dose resulting from atmospheric pathway remains negligibly small for all time periods.

The uncertainty analysis results of the 300 realization case for the atmospheric pathway are presented in Table 8-14 based on dose results at three different times: (a) early time period (at 2 years after closure) to represent the early peak followed by steep decline; (b) intermediate time period (at 100 years after closure) to represent the slowly increasing dose; and (c) long time period (at 1,000 years after closure) to represent the steady dose. Only the parameters are presented that contribute significantly to the uncertainty in total dose for the atmospheric pathway. The results are sorted by the uncertain parameters from highest to lowest numbers in terms of Importance Measure (that have correlation coefficient of greater than 0.2).

At early time period represented by sharp rise and fall, since ³H (tritium) dominates the dose, the most important uncertain parameter is found to be associated with the inventory. A strong positive correlation observed between dose and inventory uncertainty is not unexpected, indicating that increased inventory leads to larger concentration in the air pathway (see scatter plot presented in Figure 8-29). Uncertainty in wind speed shows a weak negative correlation, as it acts to dilute the concentration in air resulting from upward diffusive mass flux from the tanks.

Table 8-13. Uncertain Parameters Important to Groundwater Pathway at (a) End of Compliance Time Period (1,000 Years after Closure) and (b) Time of Peak Dose (about 3,400 Years after Closure).

Stochastic Parameter ID	Description	Correlation Coefficient Based on Ranks	Standardized Regression Coefficient Based on Ranks	Partial Correlation Coefficient Based on Ranks	Importance Measures Based on Ranks
Kd_Sand_Uncert[Tc]	Uncertainty in K_d of Tc-99 for sand	-0.98	-0.97	-0.99	0.92
SZ_Dispersivity	Dispersivity in the saturated zone; used to scale the 1-D transport model values	-0.16	-0.02	-0.14	0.06
VZ_H2_Dispersivity_Uncert	Dispersivity in the vadose zone for the H2 Unit	0.18	0.11	0.64	0.06

(a)

Stochastic Parameter ID	Description	Correlation Coefficient Based on Ranks	Standardized Regression Coefficient Based on Ranks	Partial Correlation Coefficient Based on Ranks	Importance Measures Based on Ranks
Hyd_Prop_Uncert	Vadose Zone Flow-Field selector based on pore-water velocity CDF	-0.63	-0.59	-0.78	0.40
Darcy_Flux_Mult_SZ	Darcy flux multiplier in the saturated zone	-0.44	-0.42	-0.67	0.22
Recharge_Late_PC_Uncert	Long-term recharge rate after degradation of surface cover; used in scaling the flow field	0.29	0.23	0.41	0.14
SZ_Dispersivity	Dispersivity in the saturated zone; used to scale the 1-D transport model values	-0.26	-0.23	-0.42	0.09
Kd_Sand_Uncert[Tc]	Uncertainty in K_d of Tc-99 for sand	-0.22	-0.18	-0.36	0.08
Tc99_Inv_Mult	Uncertainty in Tc-99 inventory; multiplies the base case value	0.22	0.19	0.36	0.06

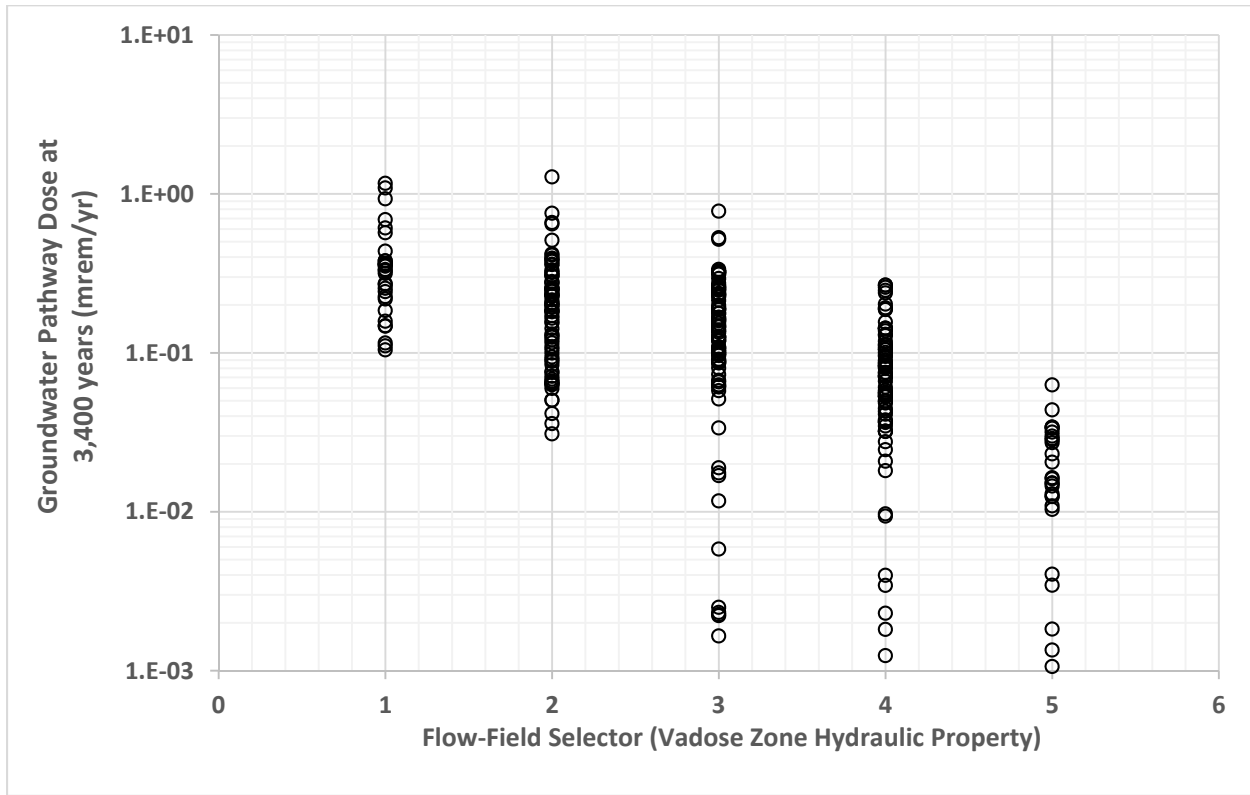
(b)

1-D = one-dimensional

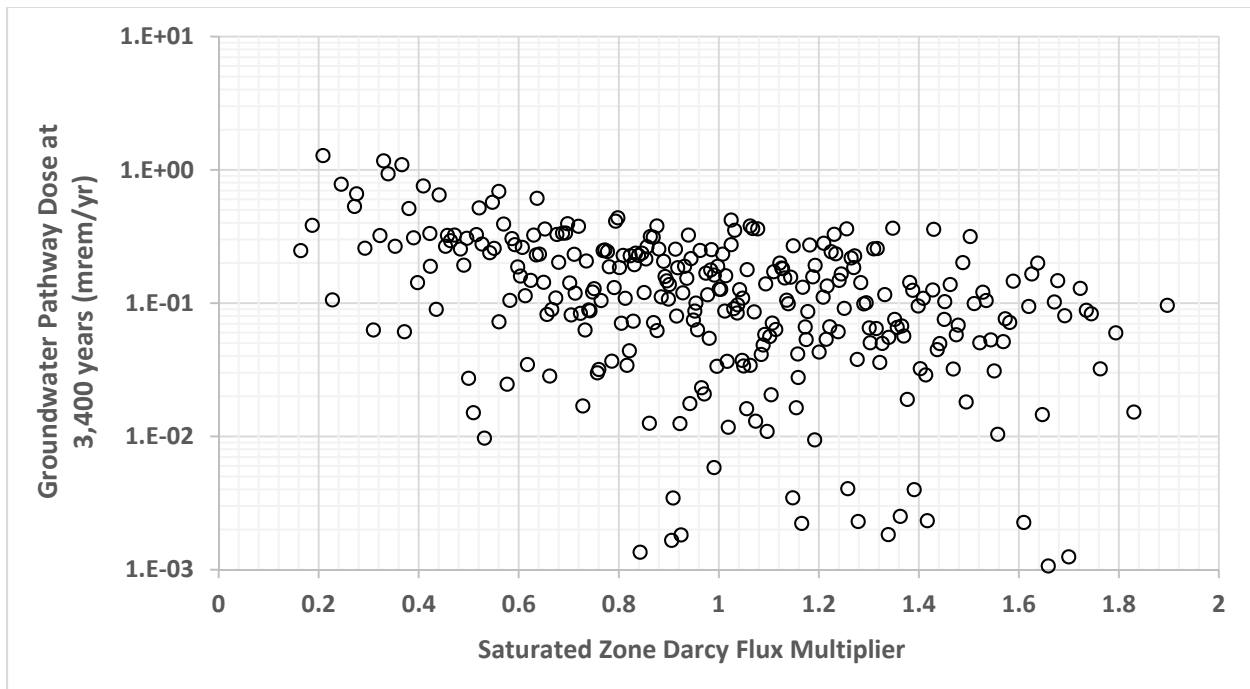
CDF = cumulative distribution function

RPP-ENV-58782, Rev. 0

Figure 8-25. Scatter Plots of Selected Uncertain Parameters Against Groundwater Pathway Dose at 3,400 Years after Closure.

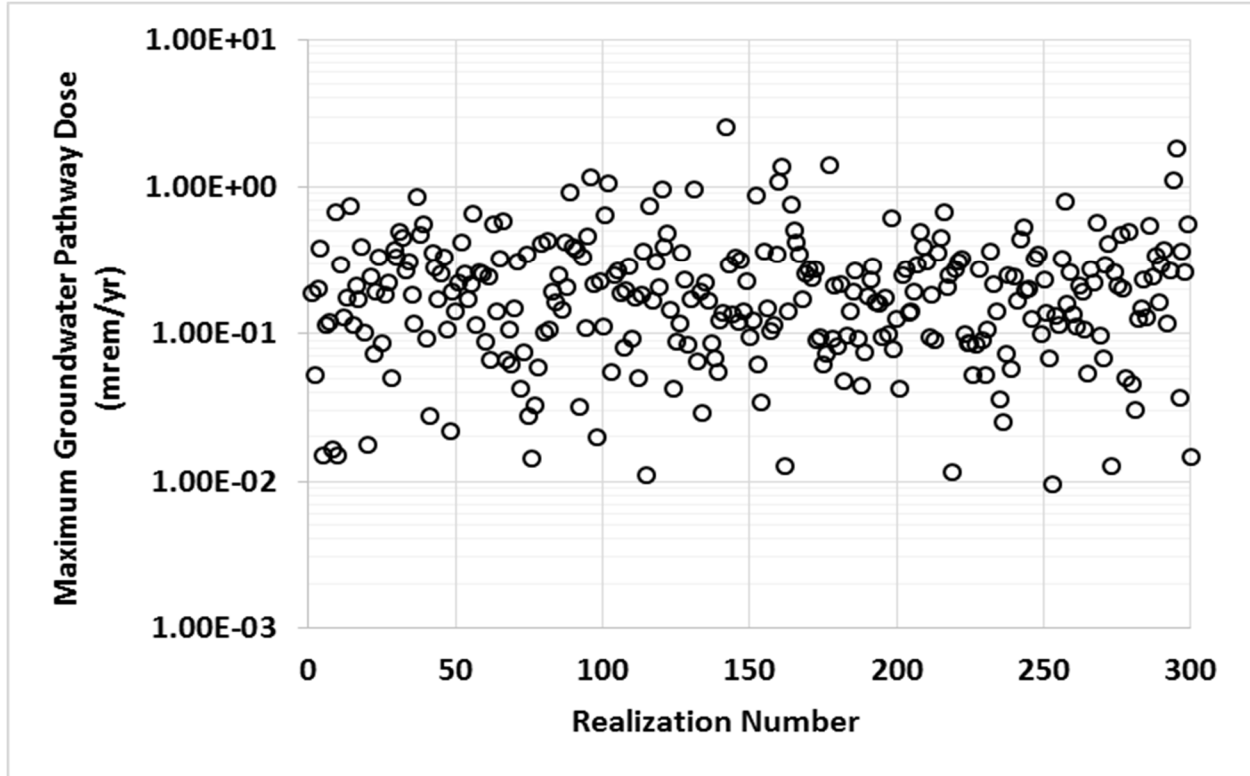


(a)



(b)

RPP-ENV-58782, Rev. 0

Figure 8-26. Peak Dose Values from Groundwater Pathway for 300 Realizations.

In the intermediate time period (around 100 years after closure), ^{129}I gradually becomes the dominant dose driver as ^3H dose continues to decline and ^{14}Co dose remains negligibly small. During this time, the total dose is seen to gradually increase with time. The most important uncertain parameter is associated with the K_d of ^{129}I for the grout tank infill material. A strong negative correlation is seen. This is expected as increased sorption of ^{129}I on the in-tank grout material will reduce the diffusive mass flux along the air pathway. Other important uncertain parameters in this time are related to tortuosity in the air pathway (used to calculate the effective diffusion coefficient) and residual inventory. See the scatter plots presented in Figure 8-30.

In the long time period (around 1,000 years after closure), the ^{129}I dose reaches a steady value, indicating that the concentration gradient in the air phase from the tank to the surface has reached a steady state. The most important uncertain parameter is associated with the K_d of ^{129}I for the grout tank infill material; a strong negative correlation is seen. The second most important uncertain parameter is associated with the residual inventory (see Figure 8-31).

8.1.6 Statistical Stability

A stability analysis was conducted to determine whether a sufficient number of realizations were used to ensure that the results of the calculations are statistically stable. The 1-D abstraction model is statistically stable if the mean annual dose computed by the model is stable.

Demonstrating stability of the mean annual dose requires evaluation of the sufficiency of sample size of uncertain parameters so that possible parameter combinations are adequately represented

RPP-ENV-58782, Rev. 0

1 in the system analyzed. Performing uncertainty analysis with an inadequate number of
2 realizations can result in erroneous interpretation of important uncertain parameters. Statistical
3 stability is generally determined by demonstrating that the estimate of the mean annual dose does
4 not depend on the sample size.

5
6 For stability analysis, the mean annual dose and uncertainty in underlying distribution is
7 evaluated by performing calculations with different number of realizations (i.e., by varying the
8 sample size). Since atmospheric pathway dose remains negligibly small over all time compared
9 to the groundwater dose, the stability analysis was performed with respect to the dose from
10 groundwater pathway. Three cases are performed with an increasing number of realizations:
11 (a) 100 realizations, (b) 300 realizations, and (c) 500 realizations. The dose statistics (mean,
12 median, and 95th percentile) derived from these cases are compared in Figure 8-32. The results
13 indicate that mean and median values among various cases are very similar. About
14 10% variance in the peak mean values between the three cases is seen, while the variance in the
15 median values is even smaller. The variance in the 95th percentile values among different cases
16 is slightly greater near the peak time, but still the peak mean dose is within a factor of two for all
17 cases. The larger variation noticed in the 95th percentile for the 100 realization case indicates
18 that only a few realizations have breakthrough at the 100 m (328 ft) downgradient location
19 around 3,000 years after closure, and as such the dose results are not stable due to small sample
20 size. However, the 95th percentile curves for the 300 realization and 500 realization case are
21 very similar, indicating adequate sample size has been reached. Based on these results, it can be
22 concluded that 300 realizations are adequate for the purpose of performing uncertainty analysis.

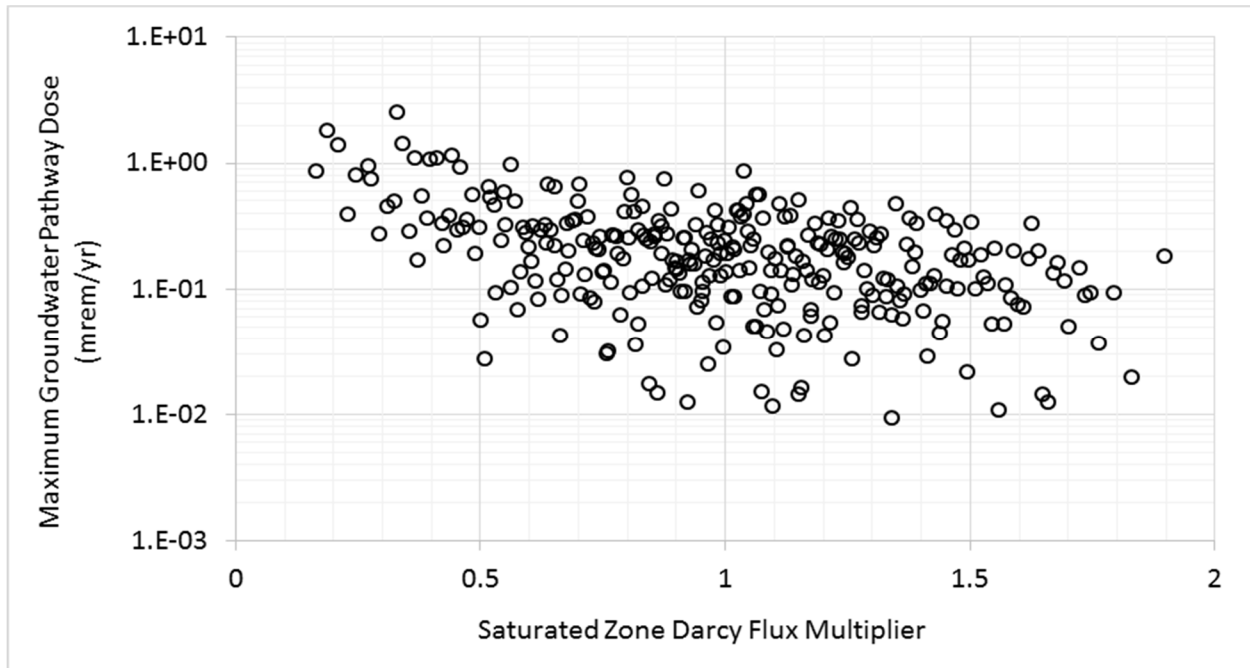
23
24 Figure 8-33 provides the upper and lower confidence limits on the grand mean (mean of the
25 means) based on the three different cases at a 95% confidence level (significance level,
26 $\alpha = 0.05$). The grand mean is shown in a thick black line and virtually overlaps the mean value
27 from the 300 realization case. The range between the confidence bounds encompasses the mean
28 from all three cases, indicating sufficiency of using 300 realizations for uncertainty analysis.

31 8.2 SENSITIVITY ANALYSIS FOR THE GROUNDWATER PATHWAY

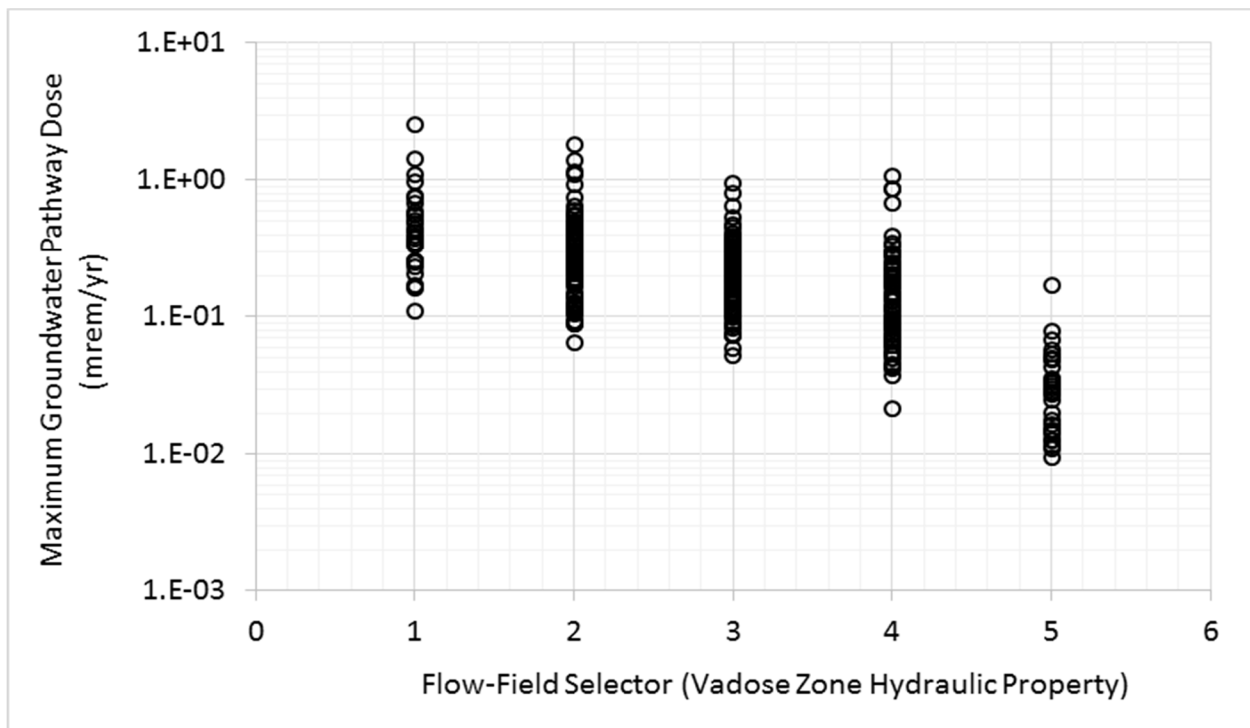
32
33 Sensitivity analyses evaluate changes in calculated groundwater impacts that result from changes
34 in input parameter estimates. Parameter value ranges used in these analyses were selected by
35 one of several methods. As discussed in Section 1, as part of the scoping process leading up to
36 the implementation of the PA, stakeholders expressed specific interest in seeing the results of
37 specific sets of input parameters. In addition to these agreed sets of sensitivity analyses,
38 additional sensitivity cases were identified during the implementation of the PA to evaluate the
39 importance of specific safety functions on the behavior of the disposal system. The result is a set
40 of sensitivity analyses intended to represent the effects of changing a broad set of input
41 assumptions. It is also emphasized that these sensitivity analyses have been augmented by
42 probabilistic uncertainty analyses (Section 8.1), which specifically evaluate parameter
43 uncertainties. By contrast, the sensitivity analyses are generally intended to evaluate changes in
44 parameters and modeling assumptions, to demonstrate the effect that alternatives have on the
45 groundwater concentrations at the PoCal.

RPP-ENV-58782, Rev. 0

Figure 8-27. Scatter Plots of Selected Uncertain Parameters Against Peak Dose for Groundwater Pathway for 300 Realizations. (sheet 1 of 2)



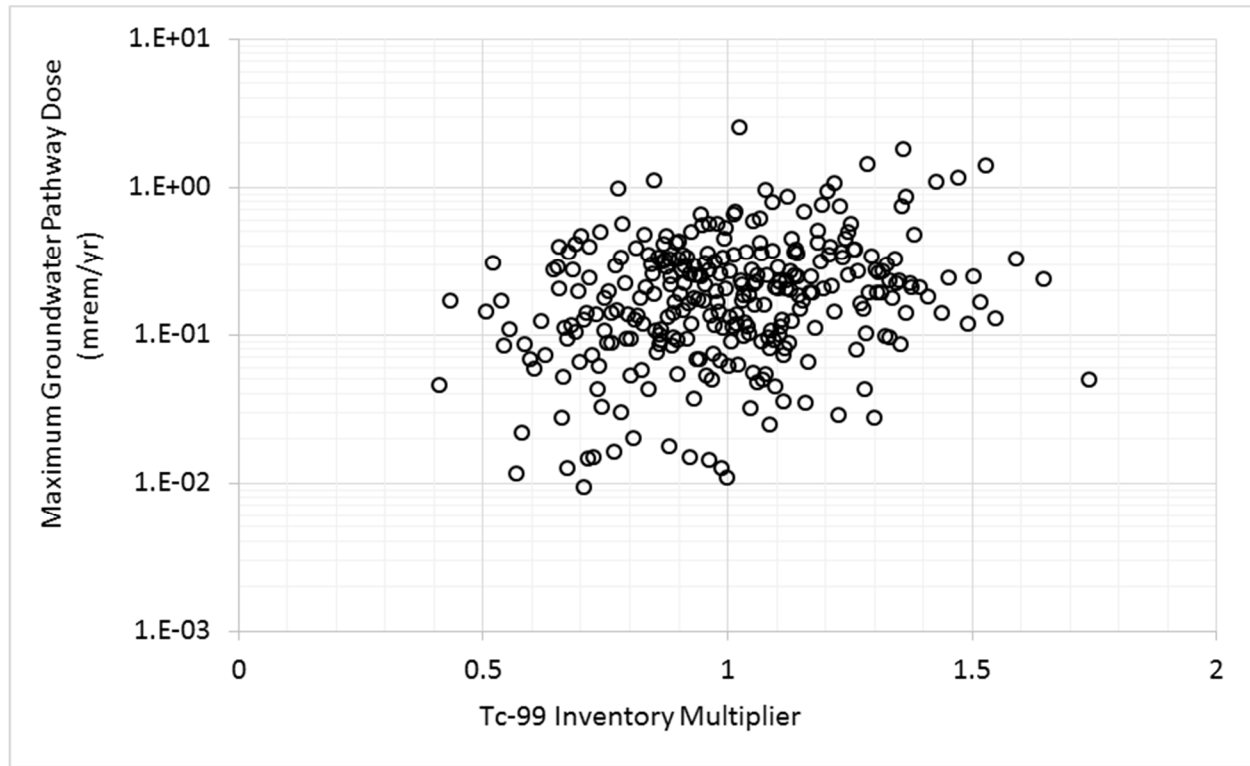
(a)



(b)

RPP-ENV-58782, Rev. 0

Figure 8-27. Scatter Plots of Selected Uncertain Parameters Against Peak Dose for Groundwater Pathway for 300 Realizations. (sheet 2 of 2)



(c)

Primary sources of alternative modeling assumptions are natural system heterogeneities, long-term engineered surface barrier performance, and human actions. Such assumptions can be categorized as scenario or model uncertainties, and as such are not readily amenable to the use of probabilistic methods (NCRP Report 152; “Decision Analysis for Low-Level Radioactive Waste Disposal Facilities” [Kozak 1994]). Consequently, these analyses are run as deterministic sensitivity analyses, without assigning a likelihood of occurrence to a particular result other than (in some cases) a qualitative evaluation of its likelihood.

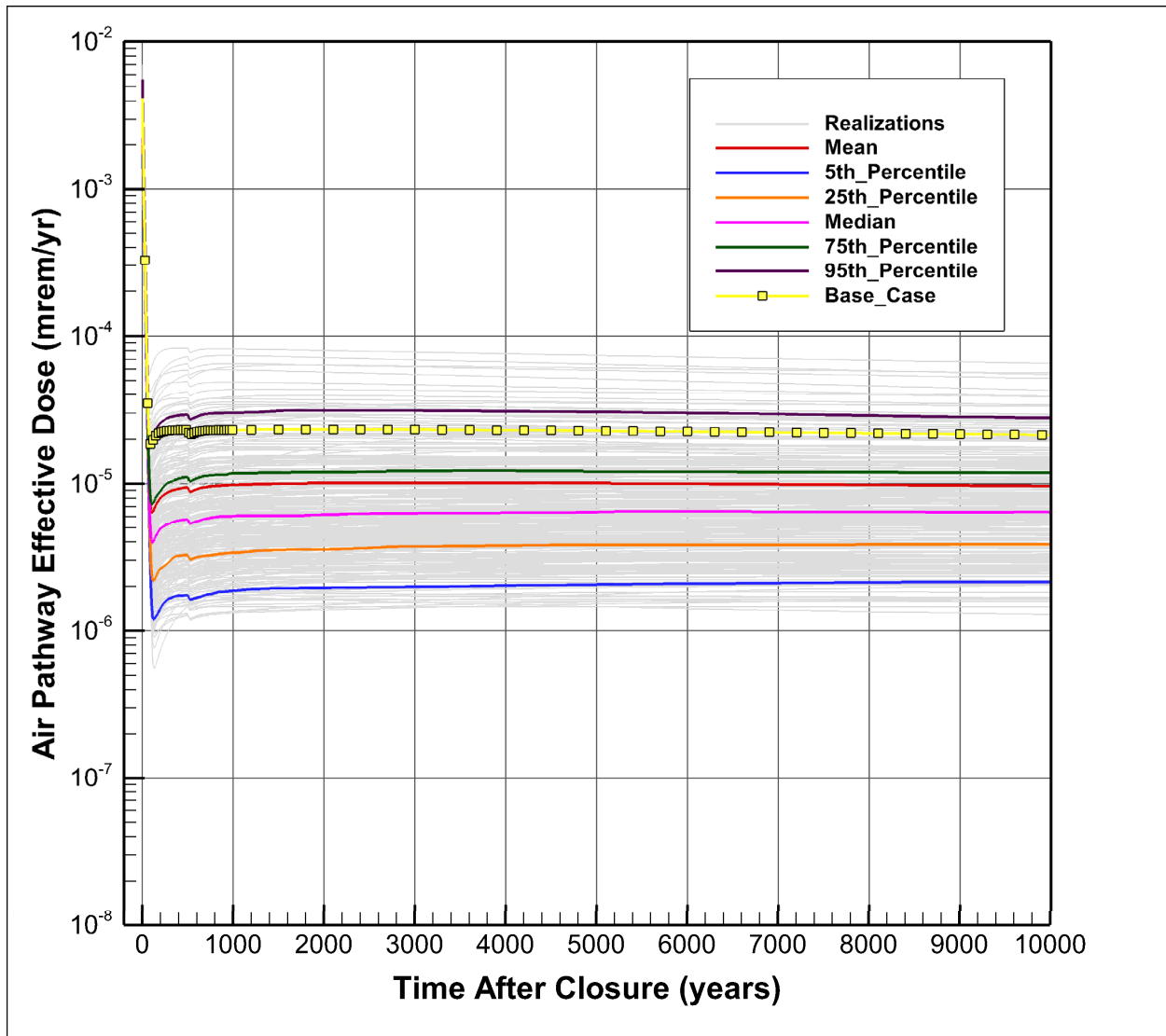
The sensitivity analyses quantify the ranges of calculated groundwater concentration outcomes due to single-parameter or multiple-parameter changes that represent an underlying shift in the conceptual model. With respect to the defense-in-depth concept, the analyses quantify the impacts that alternative views of the engineered barriers and natural attenuation may have on groundwater concentrations in the evaluation of total system performance. These analyses are an effective tool for supporting closure action decisions for WMA C, because they demonstrate the complementary and redundant nature of the safety functions evaluated in the PA.

The set of sensitivity analyses are presented in Table 8-15. Each sensitivity analysis is assigned a shorthand designator so it can be easily referenced. A brief explanation of each sensitivity analysis is also provided in the table, to provide insight into the alternative assumptions it is intended to evaluate. Depending on the nature of the sensitivity analysis, it was either run in STOMP[®] or using the GoldSim[®] abstraction of the STOMP[®] model; the selection of how to run

RPP-ENV-58782, Rev. 0

the analysis was made solely for pragmatic considerations. It is much faster to run the GoldSim[®] model, so when possible, that is the preferred approach. However, when the sensitivity case involved changes in the underlying flow field, by necessity, the analysis could only be done using STOMP[®]. Table 8-15 also identifies which numerical model was used in the sensitivity analyses.

Figure 8-28. Uncertainty in Atmospheric Pathway Dose Based on 300 Realizations.



In Table 8-15, the sensitivity analyses are subdivided into several categories corresponding to the categories of safety functions they are intended to evaluate. The sensitivity cases conducted using the 3-D STOMP[®] model can be grouped in three categories: (1) changes in aquifer properties, (2) changes in recharge, and (3) changes in vadose zone geology and hydrologic parameters. The sensitivity analysis for the aquifer parameters examines the impacts associated with radionuclide transport and mixing in the aquifer between WMA C and the PoCal 100 m (328 ft) downgradient of the facility. The recharge category of sensitivity simulations addresses

RPP-ENV-58782, Rev. 0

elements associated with the surface barrier function and the impacts of changes in recharge rate estimates during both pre- and post-design life performance periods of the surface barrier. The hydrologic cases examine the impacts of changes in the hydrologic parameters and address those elements of the natural attenuation within the vadose zone. This category includes the evaluation of Alternative Geologic Model II and the hypothesized presence of a clastic dike within the WMA C fenceline. Because the screening analysis and base case results indicate that only the most mobile radionuclides break through to a peak concentration in groundwater within the 10,000-year sensitivity-uncertainty evaluation time frame, comparative results are presented for radionuclides with K_d values equal to zero, in particular, ^{99}Tc . Technetium-99 was chosen for the sensitivity analyses because it accounts for the majority of the dose (Section 8.1.6 and Figure 8-22).

8.2.1 Surface Barrier Flow Sensitivity Analyses

In this evaluation, recharge-related parameters were varied to examine the impact of temporal and spatial variations in recharge at the 100 m (328 ft) PoCal. The recharge sensitivity evaluations address the safety function related to surface barrier flow. Because of the spatial component of this analysis, it was conducted using STOMP[®]. For this analysis, the vadose zone and aquifer hydraulic properties remain unchanged from their base case values.

Five recharge sensitivity cases were evaluated. Cases inf01 and inf02 address the minimum and maximum estimated values of net infiltration (recharge) after the design life of the surface barrier. Case inf03 represents significantly different conditions on the cover, with very high infiltration rate characteristic of infiltration rates for bare soil that existed during the operational period, and was specifically requested by Ecology during the scoping sessions. This case involves the assumption of present-day estimates of tank farm recharge resuming at WMA C after a 100-year period of institutional controls. Cases unc01 and unc02 address variability in recharge estimates outside WMA C. Case unc02 also applies to the evaluation of the impact of including additional water at the edge of the cover to represent runoff from the top surface and additional recharge occurring through the side-slopes and at the base of the barrier.

The peak groundwater concentration of ^{99}Tc ranges between 22 and 36 pCi/L for these cases (Table 8-16). This includes recharge rates applied to areas outside of WMA C ranging from 0.5 mm/yr to 100 mm/yr (0.02 in./yr to 3.94 in./yr) to evaluate the impact the outside recharge rates have on the results. The latter of these two cases also addresses the concern that increased recharge may occur through the side-slopes and around the base of the surface barrier.

Figures 8-34 and 8-35 show the overall results for ^{99}Tc at the nine PoCals for the minimum and maximum estimated values of post-design life barrier net infiltration, respectively, with a breakdown by source at the maximum PoCal. Figure 8-36 shows a comparison of the specific ^{99}Tc results for tank C-105 and the pipelines at the maximum PoCal. For the case with the post-design life recharge rate set to the minimum value, the maximum concentration of ^{99}Tc decreases from the base case value of 30 pCi/L to 22 pCi/L, a decrease of 27%. For the case with the maximum post-design life recharge rate, the peak groundwater concentration of ^{99}Tc increases from the base case value of 30 pCi/L to 36 pCi/L, an increase of 20% (Table 8-16).

RPP-ENV-58782, Rev. 0

Table 8-14. Uncertain Parameters Important to Atmospheric Pathway Dose at Various Times.

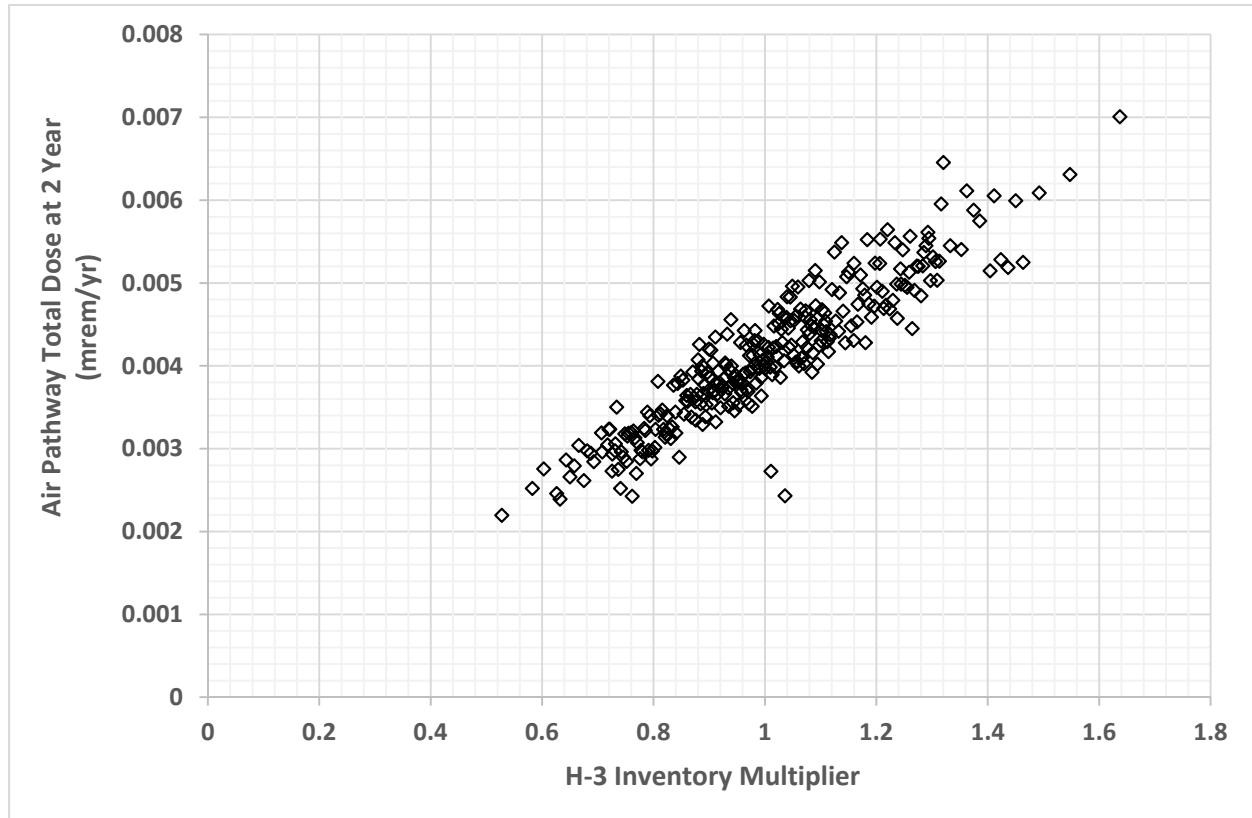
Stochastic Parameter ID	Description	Correlation Coefficient Based on Ranks	Standardized Regression Coefficient Based on Ranks	Partial Correlation Coefficient Based on Ranks	Importance Measures Based on Ranks
At Early Time (2 years after Closure)					
H3_Inv_Mult	Uncertainty in H-3 inventory; multiplies the base case value	0.92	0.94	0.98	0.82
Wind_Speed_Stoch	Uncertainty in wind speed	-0.25	-0.3	-0.82	0.07
At Intermediate Time (100 years after Closure)					
Grout_Kd_Uncert[I]	Uncertainty in K_d of Iodine for Grout	-0.78	-0.70	-0.85	0.59
Soil_Air_Tort_Stoch	Uncertainty in tortuosity term for diffusive transport along the air pathway in the backfill soil	0.38	0.22	0.46	0.16
Grout_Air_Tort_Stoch	Uncertainty in tortuosity term for diffusive transport along the air pathway in the Grout material within the tank	0.28	0.31	0.58	0.13
I129_Inv_Mult	Uncertainty in I-129 inventory; multiplies the base case value	0.34	0.28	0.54	0.11
At Late Time (1,000 years after Closure)					
Grout_Kd_Uncert[I]	Uncertainty in K_d of Iodine for Grout	-0.88	-0.83	-0.94	0.74
I129_Inv_Mult	Uncertainty in I-129 inventory; multiplies the base case value	0.42	0.33	0.73	0.16
Soil_Air_Tort_Stoch	Uncertainty in tortuosity term for diffusive transport along the air pathway in the backfill soil	0.26	0.08	0.25	0.08

1
2 Recharge in the areas outside WMA C has an inverse relationship with the results: peak ^{99}Tc
3 concentration in groundwater decreases as recharge in the areas outside WMA C increases. The
4 magnitude of the increase or decrease is within the range of values determined from the WMA C

RPP-ENV-58782, Rev. 0

surface barrier evaluation (Table 8-16). Therefore, for this range of recharge rates, the recharge outside of WMA C is encompassed in the uncertainty analysis. For very high infiltration, characteristic of alternative assumptions about future surface conditions leading to extreme infiltration, the peak groundwater concentration of ^{99}Tc increases by approximately 50% from the base case results and arrives at the PoCal approximately 50 years after the barrier ceases to exist (Table 8-16).

Figure 8-29. Scatter Plot of Selected Uncertain Parameters Against the Atmospheric Pathway Dose at Early Time Period (2 Years after Closure).



8.2.2 Aquifer Dilution Sensitivity Analyses

The aquifer property sensitivity evaluations address the safety function component related to dilution caused by the groundwater flux in the aquifer. The parameters that determine the groundwater flux and the amount of dilution that occurs in the aquifer are the hydraulic conductivity and hydraulic gradient. In a natural system, the two parameters offset one another. If the groundwater flux through an aquifer volume remains constant, then in areas with high hydraulic conductivity, the hydraulic gradient will be less, and vice versa. They are considered to be coupled parameters because changes to the flux term caused by changes made to one term are inseparable from changes made to the other term. These parameters act inversely proportional to one another, and the same change in the flux can be made by making the same proportional change to either parameter. Therefore, only one of the parameters, e.g., hydraulic

RPP-ENV-58782, Rev. 0

conductivity, needs to be varied to produce the variability in the flux necessary to conduct the sensitivity analysis. For this sensitivity evaluation, the hydraulic conductivity is varied.

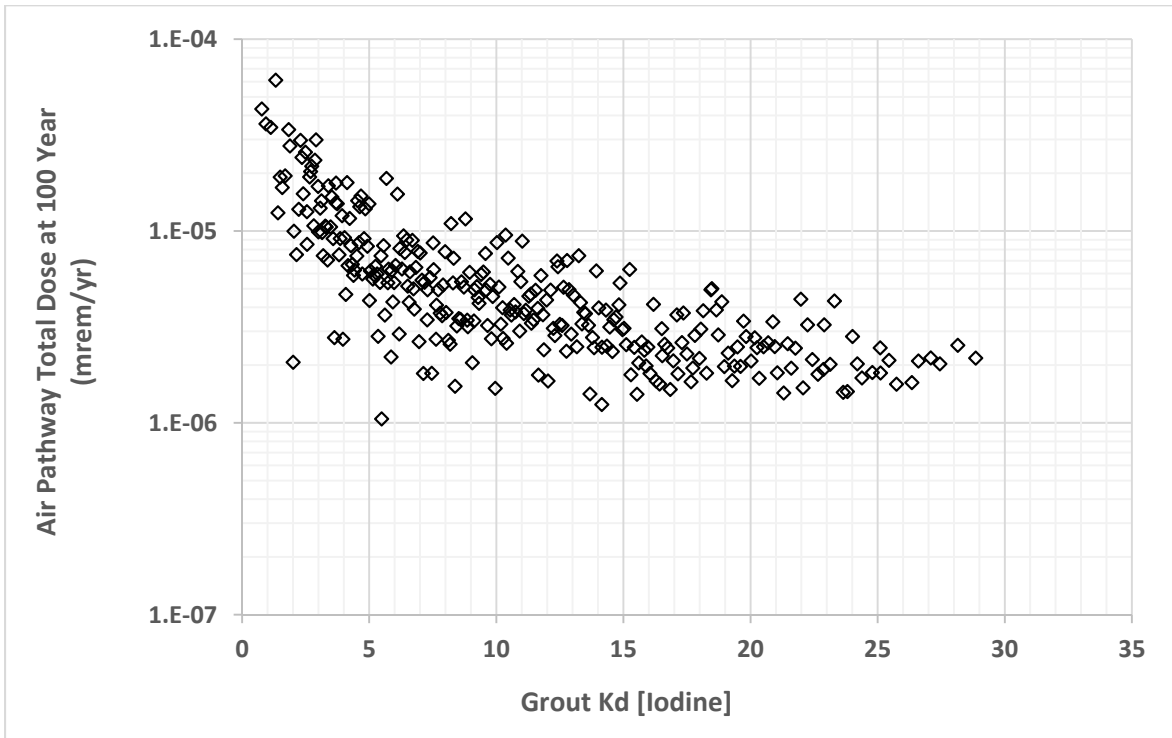
The sensitivity analysis includes two values of hydraulic conductivity, the 5th percentile value (4,200 m/day [13,800 ft/day] [gwp01]) and the 95th percentile value (17,800 m/day [58,400 ft/day] [gwp03]). The results provide some insight into the dilution mechanism of the aquifer (Table 8-17). Figures 8-37 and 8-38 show the overall results for WMA C at the nine PoCals for the 5th and 95th percentile values, respectively, with a breakdown by source at the maximum PoCal. Figure 8-39 shows a comparison of the specific results for tank C-105 and the pipelines at the maximum PoCal. Tank C-105 has the largest estimated residual inventory of ⁹⁹Tc, and the release from the pipelines is approximated as being advection-controlled instead of diffusion-controlled release used in the tanks. The results of the evaluation using the 5th percentile value are a factor of 2.6 greater than the base case; the hydraulic conductivity is a factor of 2.6 less than the base case value. Similarly, the results of the evaluation using the 95th percentile value are a factor of 1.6 less than the base case; the hydraulic conductivity is a factor of 1.6 greater than the base case value. The amount of dilution appears inversely proportional to the flux through an aquifer as determined from the hydraulic conductivity. The proportionality is observed in the tank C-105 and pipeline residuals evaluations. The results of the 5th percentile hydraulic conductivity evaluation indicate an approximate factor of 2.6 increase in the peak concentration compared to the base case, and the results of the 95th percentile hydraulic conductivity evaluation indicate an approximate factor of 1.6 decrease in the peak concentration compared to the base case. These results indicate that the aquifer flow parameters that affect the flux rate of water have an inversely proportional impact on the groundwater concentration. The timing of the peak arrival at the PoCals is essentially the same for all cases because the groundwater velocity for all three cases exceeds 100 m (328 ft) (the distance to the line of PoCals) per year.

8.2.3 Vadose Zone Flow and Dispersion Sensitivity Analyses

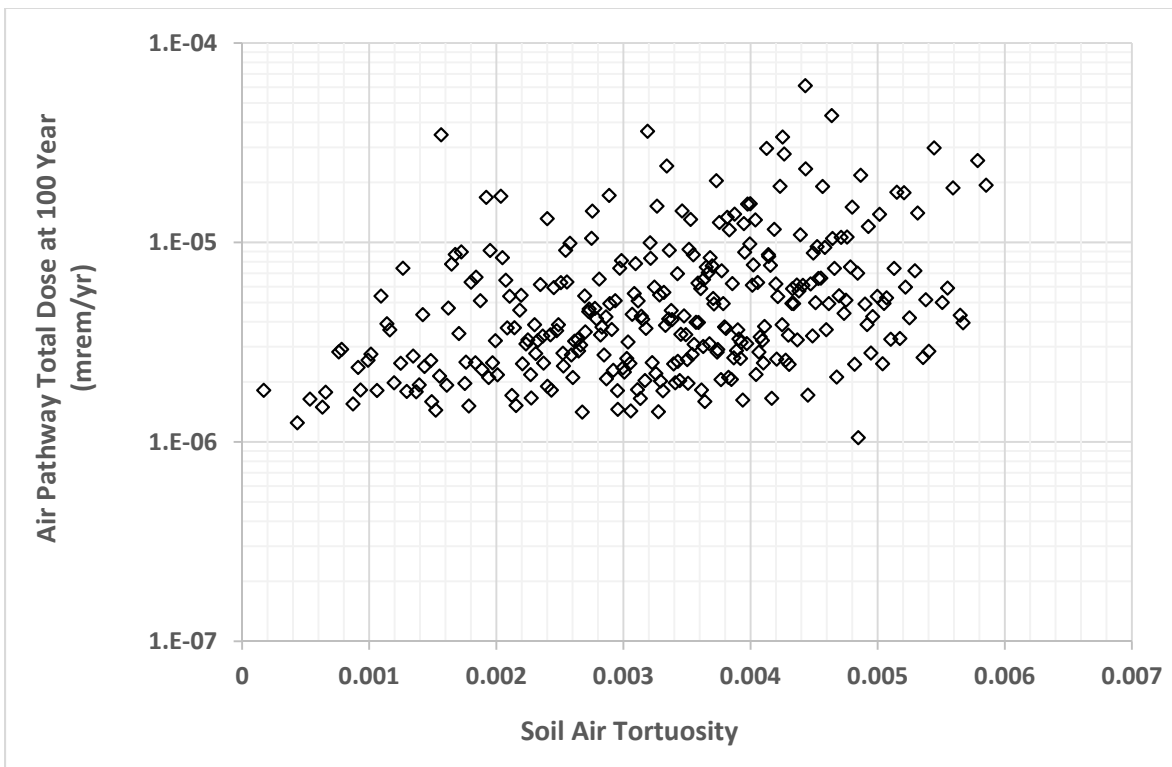
The vadose zone hydraulic properties were varied to determine the impact that the inherent variability in these parameters has on the groundwater results. This set of vadose zone hydraulic properties sensitivity evaluations addresses the safety functions associated with flow and dispersion in the vadose zone. Four vadose zone parameters were varied: van Genuchten α and n (coupled), saturated moisture content (θ_s), residual moisture content (θ_r), and fitted saturated hydraulic conductivity (K_s). The parameters were varied in accordance with the percentile relationships determined in the uncertainty analysis. Therefore, for the evaluations using the 5th percentile values, all of the geologic soil units were assigned their 5th percentile values. It is important to note that the percentiles refer to sets of parameter values and not to the properties individually (as discussed in Appendix B). Thus, the maximum van Genuchten residual saturation parameter does not necessarily represent the largest value of θ_r , but instead represents the value associated with the fitted unsaturated hydraulic conductivity curve that produces the highest flow velocity at the pre-Hanford operations recharge rate. The values of four vadose zone parameters, van Genuchten α and n (coupled), θ_s , θ_r , and fitted saturated hydraulic conductivity (K_s) varied for the three percentile cases (5th [vzp01], median [vzp02], and 95th [vzp03]) are presented in Section 8.1.4 (see Table 8-7). These evaluations used the base case recharge values and time sequence.

RPP-ENV-58782, Rev. 0

Figure 8-30. Scatter Plots of Selected Uncertain Parameters Against the Atmospheric Pathway Dose at Intermediate Time Period (100 Years after Closure).



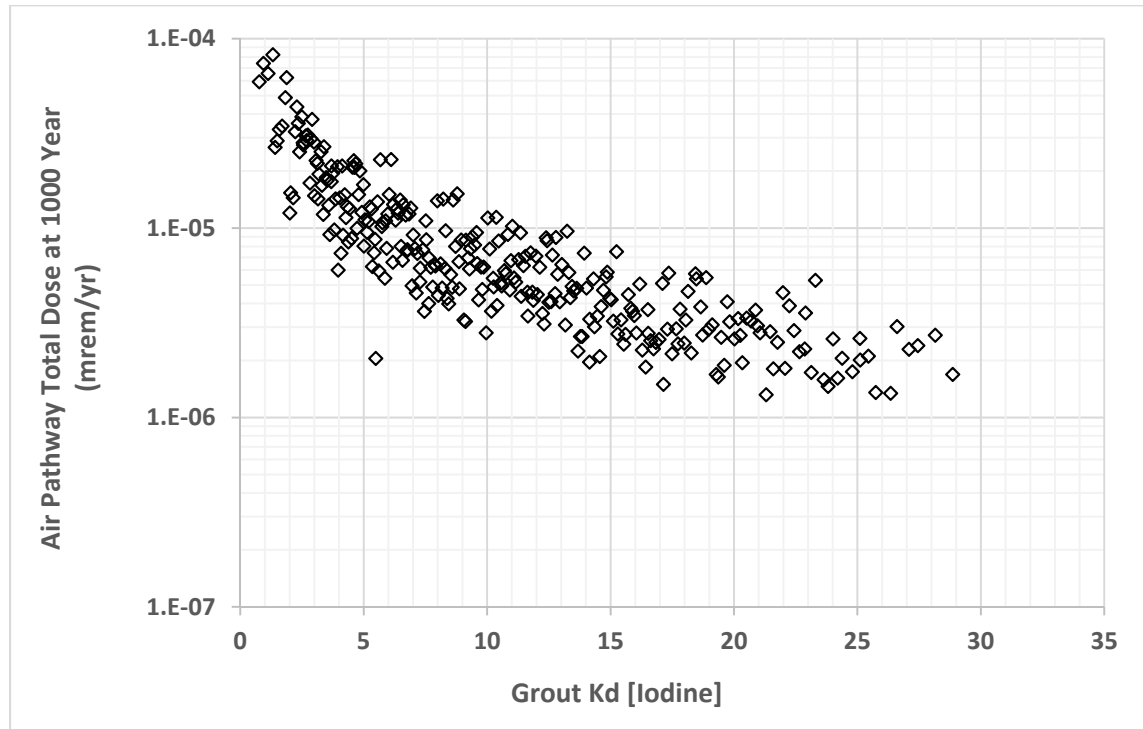
(a)



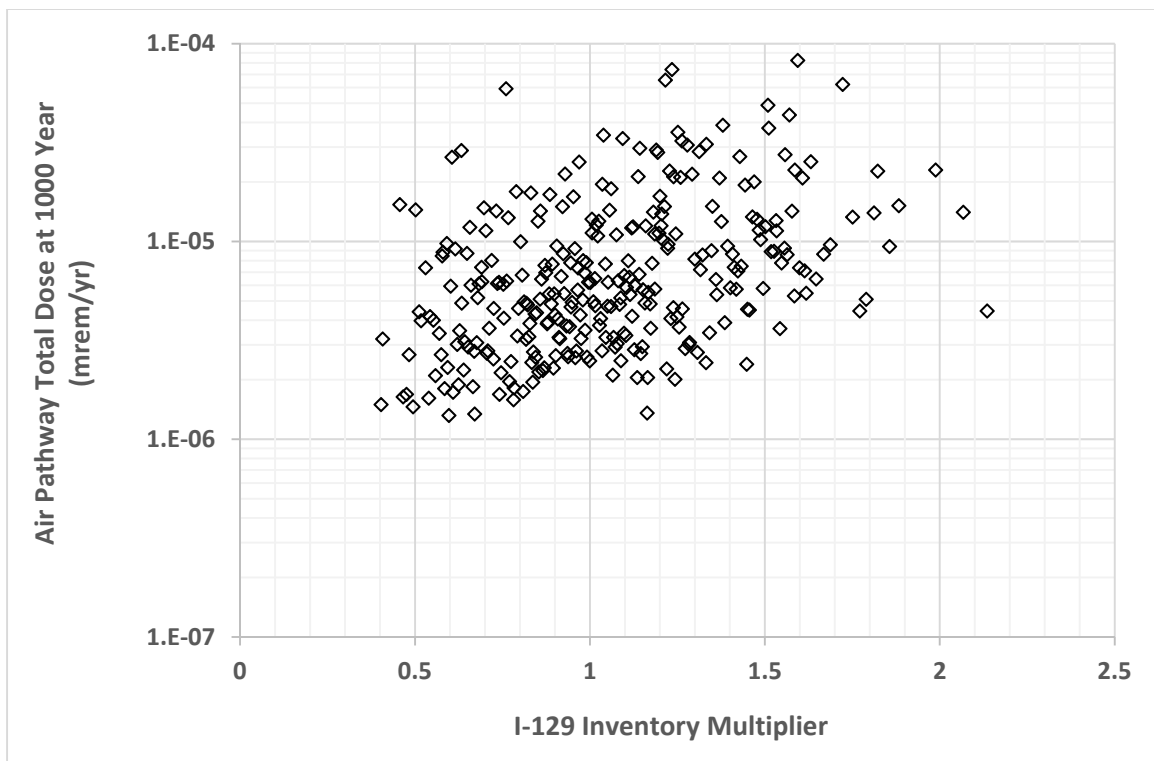
(b)

RPP-ENV-58782, Rev. 0

Figure 8-31. Scatter Plots of Selected Uncertain Parameters Against the Atmospheric Pathway Dose at Late Time Period (1,000 Years after Closure).



(a)



(b)

Figure 8-32. Statistical Stability Analysis with Different Number of Realizations, Comparing (a) Mean, (b) Median, and (c) 95th Percentile Values of the Groundwater Pathway Dose. (sheet 1 of 3)

(a)

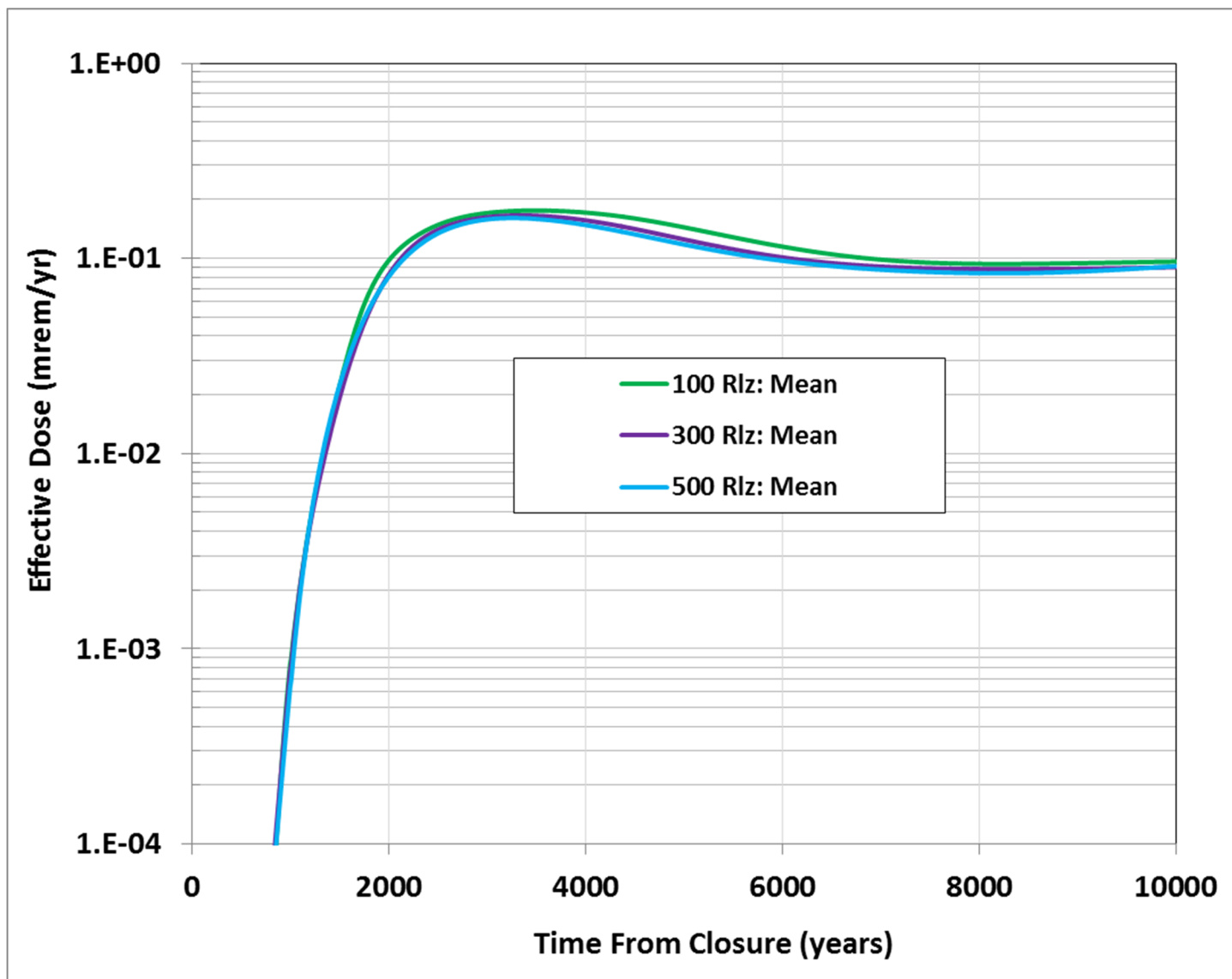


Figure 8-32. Statistical Stability Analysis with Different Number of Realizations, Comparing (a) Mean, (b) Median, and (c) 95th Percentile Values of the Groundwater Pathway Dose. (sheet 2 of 3)

(b)

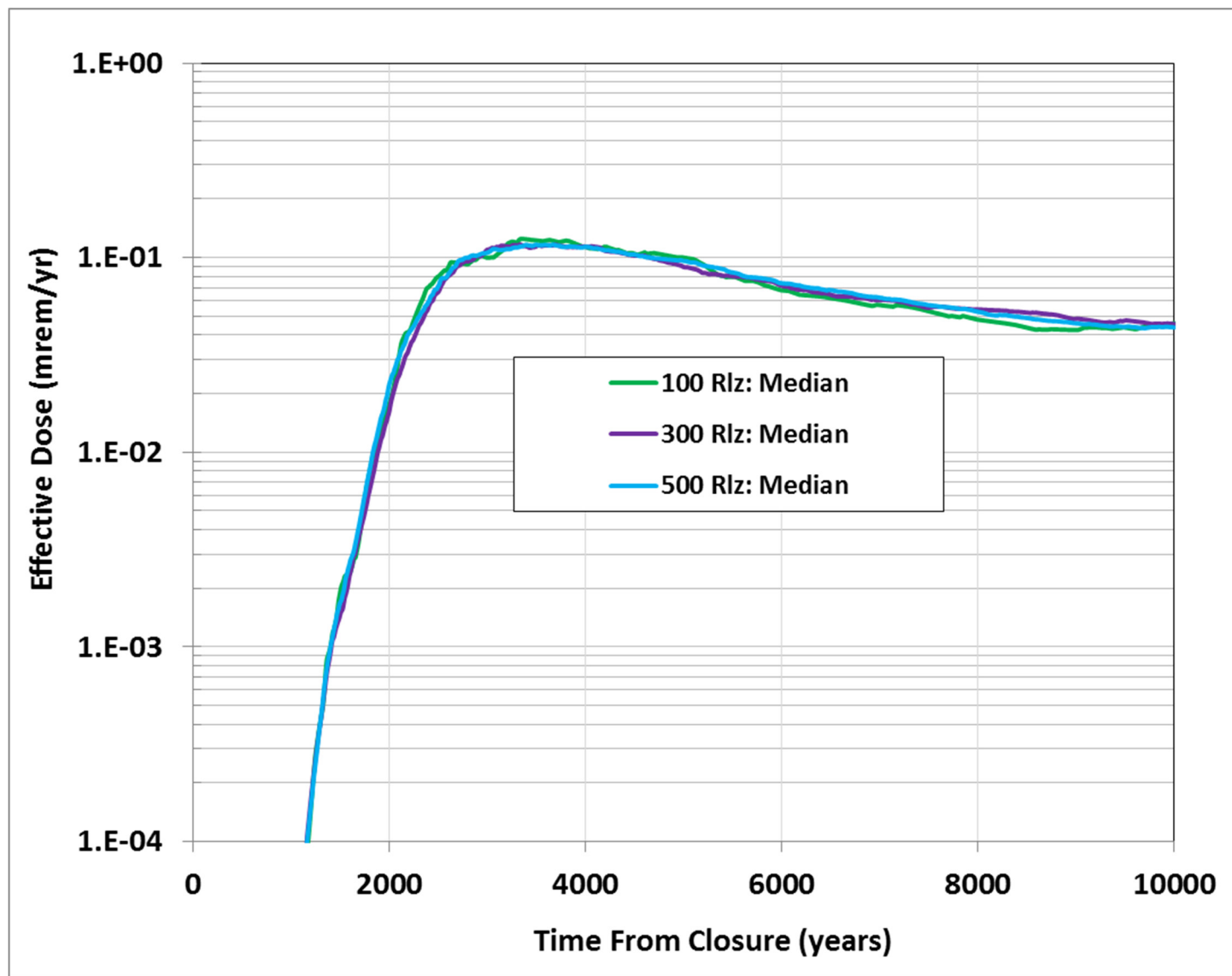
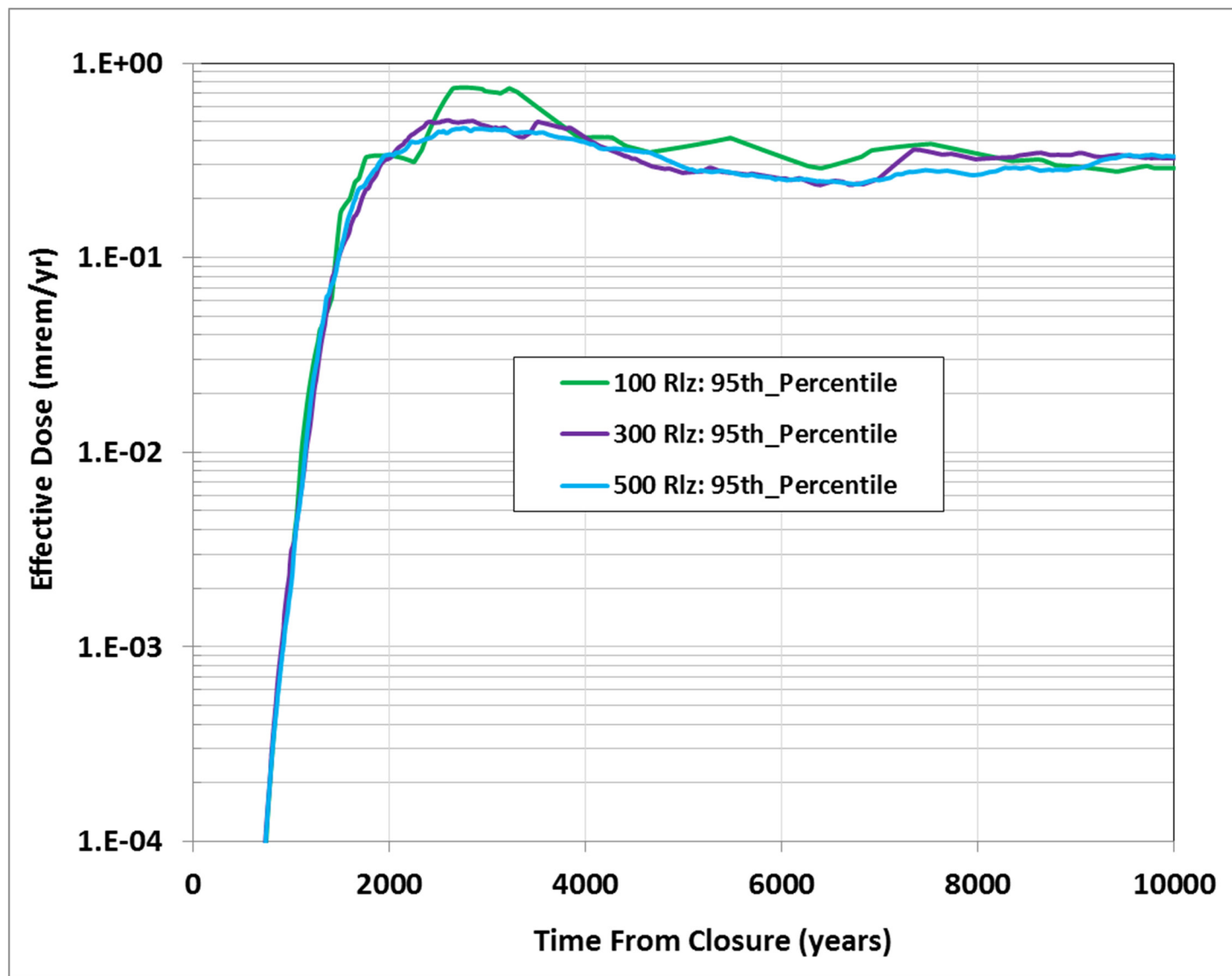
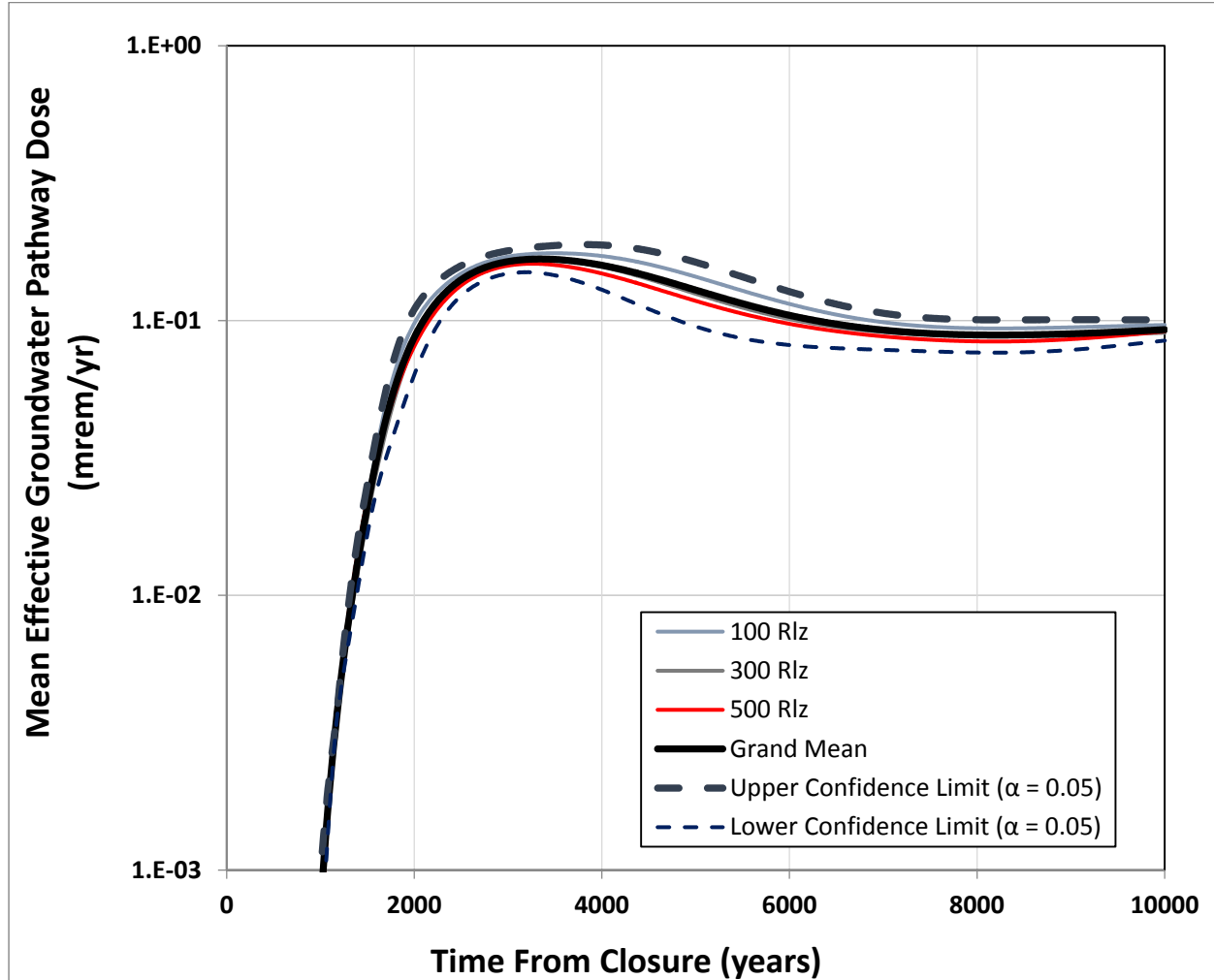


Figure 8-32. Statistical Stability Analysis with Different Number of Realizations, Comparing (a) Mean, (b) Median, and (c) 95th Percentile Values of the Groundwater Pathway Dose. (sheet 3 of 3)

(c)



RPP-ENV-58782, Rev. 0

Figure 8-33. Confidence Limits on the Mean Effective Groundwater Pathway Dose.

The vadose zone evaluation also included two alternate conceptual models of the geology. One alternative, referred to as Alternative II (vzp04), considers the Hanford H2 Sand unit to consist of three subunits that each possess different hydraulic characteristics (Figure D-7b). Most of the formation remains identified as H2 Sand and the hydraulic properties for it remain unchanged from the base case analysis. Near the base of the Hanford H2 Sand unit in Alternative II are fine and coarse sand subunits. For this sensitivity evaluation, these subunits are assigned the Hanford H2 Sand 5th and 95th percentile hydraulic property sets, respectively. The second alternative conceptual model of the geology includes the representation of a preferential pathway, such as a clastic dike or unsealed borehole, located underneath tank C-105 (vzp05). Clastic dikes are discrete polygonal (plan view) features, and typically range in width from 3 cm to 1 m (1.2 in. to 3.3 ft), from 1.5 m to 100 m (4.9 ft to 328 ft) in segment length, and from 2 m (6.6 ft) to greater than 20 m (65.6 ft) in depth (BHI-01103). An especially long clastic dike segment does not appear to exist within WMA C because, if one did, then the many neutron and drywell moisture measurements would likely have detected evidence of a continuous band of high moisture. For the sensitivity case, the length of the dike is assumed to extend for 7.6 m (25 ft), and 3-D model discretization imposes a minimum width of 3.8 m (12 ft) for the dike.

RPP-ENV-58782, Rev. 0

Although a width of 3.8 m (12 ft) is more representative of a planar feature than a dike, finer resolution of the model grid is not practicable with the available computational resources. The planar area of the dike is 29 m² (312 ft²), which is comparable to a 1-m (3.3-ft)-wide dike that extends the entire diameter of the tank (23 m² [246 ft²]). Clastic dikes of this size typically occur in sand, silt, and only occasionally in gravel (BHI-01103); therefore, the model representation of the dike extends throughout the depth of the Hanford H2 Sand (Figure D-7a shows the location of tank C-105; the clastic dike is centered beneath the tank in the Hanford H2 Sand shown in the figure). The hydraulic parameters assigned to the clastic dike material were selected to determine whether the flux conditions exist at WMA C such that the clastic dikes provide a preferential flow path for the residual waste. Thus, the set of clastic dike hydraulic parameters from among the samples listed in PNHL-23711, "Physical, Hydraulic, and Transport Properties of Sediments and Engineered Materials Associated with Hanford Immobilized Low-Activity Waste" that produced the highest pore water velocity at the undisturbed recharge rate of 3.5 mm/yr (0.14 in./yr) were assigned to the clastic dike material.

Table 8-15. Summary of Sensitivity Cases. (3 sheets)

Sensitivity Case Shorthand	Explanation	Model
Surface Barrier Flow Safety Function		
inf01	All parameters same as base case, except that post-design surface barrier net infiltration = 1.0 mm/yr. This is a case in which the surface barrier continues to provide limitation to flow beyond its design life.	STOMP [®]
inf02	All parameters same as base case, except that post-design surface barrier net infiltration = 5.2 mm/yr. This is a case in which the surface barrier behaves worse than expected after its design life, and allows more infiltration than the base case Hanford infiltration.	STOMP [®]
inf03	All parameters same as base case, except that operational period net infiltration = 140 mm/yr, and post-institutional control net infiltration = 100 mm/yr. This corresponds to future scenarios in which land use or vegetative cover are significantly different and disadvantageous compared to the base case. This may include vegetative progression, migration of sand dunes onto Waste Management Area (WMA) C, or agricultural irrigation on the site.	STOMP [®]
unc01	All parameters same as base case, except that net infiltration for all surfaces outside WMA C = 0.5 mm/yr for all times. This corresponds to future scenarios in which land use or vegetative cover are significantly different and advantageous compared to the base case, but the cover continues to have a nominal functionality.	STOMP [®]
unc02	All parameters same as base case, except that net infiltration for all surfaces outside WMA C = 100 mm/yr for all times. This corresponds to future scenarios in which land use or vegetative cover are significantly different and disadvantageous compared to the base case, but the cover continues to have a nominal functionality.	STOMP [®]
Aquifer Dilution Safety Function		
gwp01	All parameters same as base case, except that aquifer flow parameters are 5th percentile values. This corresponds to altered aquifer flow producing minimal aquifer dilution compared to the base case.	STOMP [®]

RPP-ENV-58782, Rev. 0

Table 8-15. Summary of Sensitivity Cases. (3 sheets)

Sensitivity Case Shorthand	Explanation	Model
gwp03	All parameters same as base case, except that aquifer flow parameters are 95th percentile values. This corresponds to altered aquifer flow producing a higher level of aquifer dilution compared to the base case.	STOMP®
Vadose Zone Flow and Dispersion Safety Functions		
vzp01	All parameters same as base case, except that vadose zone hydraulic properties are 5th percentile values. This is an exploration of the effect of vadose zone parameters.	STOMP®
vzp02	All parameters same as base case, except that vadose zone hydraulic properties are 50th percentile values (median). This is an exploration of the effect of vadose zone parameters.	STOMP®
vzp03	All parameters same as base case, except that vadose zone hydraulic properties are 95th percentile values. This is an exploration of the effect of vadose zone parameters.	STOMP®
vzp04	All parameters same as base case, except that the geologic model is Alternative II with 5th and 95th percentile values of H2 Sand applied to H2 Fine and H2 Coarse Sand, respectively. This is an exploration of the effect of vadose zone parameters.	STOMP®
vzp05	All parameters same as base case, except that the geologic conceptualization includes clastic dikes. This is an alternative conceptual model representing an unknown feature below the site.	STOMP®
Inventory Estimate		
inv1	All parameters same as base case, except that the estimated inventory is based on the TC&WM EIS (2012) values. This is an exploration of the effect of alternative inventory assumptions.	GoldSim®
inv2	All parameters same as base case, except that the estimated inventory is based on the upper bound values. This is an exploration of the effect of alternative inventory assumptions.	GoldSim®
Grout Flow Safety Function		
grt1	All parameters same as base case, except that after 5,000 years following closure, the grout degrades and the flow properties change to Hanford H2 sand values, with a step function change in the flow rate occurring at this time. This may represent an alternative in which the grout degradation is more rapid than the base case, either through weathering processes that are not included in the base case, or if failure occurs from unanticipated seismic activity.	GoldSim®
grt2	All parameters same as base case, except that after 1,000 years following closure, the grout degrades and the flow properties change to Hanford H2 sand values, with a step function change in the flow rate occurring at this time. This may represent an alternative in which the grout degradation is more rapid than the base case, either through weathering processes that are not included in the base case, or if failure occurs from unanticipated seismic activity.	GoldSim®

RPP-ENV-58782, Rev. 0

Table 8-15. Summary of Sensitivity Cases. (3 sheets)

Sensitivity Case Shorthand	Explanation	Model
grt3	All parameters same as base case, except that after 500 years following closure, the grout degrades and the flow properties change to Hanford H2 sand values, with a step function change in the flow rate occurring at this time. This may represent an alternative in which the grout degradation is more rapid than the base case, either through weathering processes that are not included in the base case, or if failure occurs from unanticipated seismic activity.	GoldSim®
grt4	All parameters same as base case, except that after 0 years following closure, the grout degrades and the flow properties change to Hanford H2 sand values, with a step function change in the flow rate occurring at this time.	GoldSim®
Residual Chemistry Safety Function		
rls1	All parameters same as base case, except that the release function is calculated assuming all waste is instantly available. This case evaluates a more conservative release function compared to the base case.	GoldSim®
Tank Flow Safety Function		
dif1	All parameters same as base case, except that the release function is based on diffusion coefficient 1E-7 cm ² /s. This case represents the tank and base mat in worse condition than the base case, but still limited by diffusion.	GoldSim®
dif2	All parameters same as base case, except that the release function is based on linearly changing diffusion coefficient over 500 years after closure from 1E-14 to 3E-8 cm ² /s. This case represents the tank and base mat degrading over 500 years after closure, but still limited by diffusion.	GoldSim®
dif4	All parameters same as base case, except that the tanks remain intact (no release) for 5,000 years after closure, followed by advective release beginning immediately. This case represents the steel shell remaining intact for longer than the base case, potentially allowing ingrowth of uranium progeny, followed by advective release with associated potential for higher releases of the progeny.	GoldSim®

GoldSim® simulation software is copyrighted by GoldSim Technology Group LLC of Issaquah, Washington (see <http://www.goldsim.com>).

Subsurface Transport Over Multiple Phases (STOMP)® is copyrighted by Battelle Memorial Institute, 1996.

TC&WM EIS = Tank Closure and Waste Management Environmental Impact Statement (DOE/EIS-0391, 2012, "Final Tank Closure and Waste Management Environmental Impact Statement for the Hanford Site, Richland, Washington," U.S. Department of Energy, Washington, D.C.)

- 1
- 2 Figures 8-40 through 8-42 show the overall results for ⁹⁹Tc at the nine PoCals for the 5th, median,
- 3 and 95th percentile values, respectively, with a breakdown by source at the maximum PoCal.
- 4 Figure 8-43 shows a comparison of the specific ⁹⁹Tc results for tank C-105 and the pipelines at
- 5 the maximum PoCal. The peak groundwater concentration ranges between 23 and 48 pCi/L for
- 6 these cases (Figure 8-39). The median hydraulic property values produce peak concentration
- 7 results very similar to the base case results (27 pCi/L arriving 1,465 years after closure compared
- 8 to 30 pCi/L arriving 1,550 years after closure for the base case; see Table 8-18). The range of

RPP-ENV-58782, Rev. 0

results for the vadose zone sensitivity analysis produced a similar range of results to that of the recharge estimates.

Table 8-16. Recharge Sensitivity Evaluation.

Sensitivity Case Shorthand	Pre-WMA C and Undisturbed Ground Recharge Rate Percentile (Value)	Recharge Rate of WMA C Ground During Operations Percentile (Value)	Design Life Surface Barrier and Degraded Liner Recharge Rate Percentile (Value)	Post-Design Life Surface Barrier Recharge Rate Percentile (Value)	Time of Arrival of Maximum Concentration at Downgradient Point of Calculation (Years after Closure)	Maximum Concentration at Downgradient Point of Calculation (pCi/L)
Base Case	3.5 mm/yr	100 mm/yr	0.5 mm/yr	3.5 mm/yr	1,555	30
inf01	3.5 mm/yr	100 mm/yr	0.5 mm/yr	1.0 mm/yr	3,150	22
inf02	5.2 mm/yr ^a	100 mm/yr	0.5 mm/yr	5.2 mm/yr	1,260	36
inf03	3.5 mm/yr	140 mm/yr	0.5 mm/yr	100 mm/yr ^b	174	47
unc01	3.5 mm/yr ^c	100 mm/yr ^c	0.5 mm/yr ^c	3.5 mm/yr ^c	1,630	32
unc02	3.5 mm/yr ^d	100 mm/yr ^d	0.5 mm/yr ^d	3.5 mm/yr ^d	1,230	26

^aOnly recharge in the area that will be occupied by Waste Management Area (WMA) C is 5.2 mm/yr. Recharge everywhere else remains the base case value of 3.5 mm/yr.

^bPost-design recharge begins 100 years after closure.

^cRecharge in the areas not occupied by WMA C is 0.5 mm/yr.

^dRecharge in the areas not occupied by WMA C is 100 mm/yr.

This evaluation of the alternative conceptual model of the geology indicates that these heterogeneous features do not strongly affect the results of the PA. Figures 8-44 and 8-45 show the overall results for WMA C at the nine PoCals for Alternative Model II and for the clastic dike analysis, respectively, with a breakdown by source at the maximum PoCal. Figure 8-46 shows a comparison of the specific results for tank C-105 and the pipelines at the maximum PoCal. The peak concentration values show little change from the base case value, although the clastic dike analysis shows a slightly reduced travel time (Table 8-18).

8.2.4 Inventory Sensitivity Analyses

An upper bound estimate of inventory is provided in Section 3.2.2.3 for both the retrieved tanks and for tanks undergoing retrieval (Tables 3-16 and 3-17). Since ⁹⁹Tc is the primary dose contributor for the groundwater pathway, a sensitivity case was performed by replacing the base case ⁹⁹Tc inventory with the upper bound value to evaluate the impact in terms of groundwater concentration at the PoCal. Additionally, the residual volume based on the upper bound estimate

RPP-ENV-58782, Rev. 0

1 was also updated to be consistent with the change in inventory. All other parameters were kept
2 the same as in the system model base case.

3
4 Upper bound residual inventory of 89.7 Ci was estimated for ^{99}Tc for all the sources in WMA C,
5 of which 81.40 Ci was estimated for tank C-105. In comparison, the estimated total ^{99}Tc
6 inventory for the base case was 14.70 Ci of which 7.83 Ci was for tank C-105. Results for these
7 analyses are summarized and compared with the base case in Table 8-19. Figure 8-47(a)
8 presents the results of the sensitivity case compared to the system-model base case. The peak
9 groundwater concentration increased by a factor of five (compared to the base case), which is
10 approximately the ratio of the inventories between the two cases (factor of six). Figure 8-47(b)
11 presents the source term release rate (pCi/yr) of ^{99}Tc from tank C-105 to the vadose zone
12 immediately below the tank. This release rate is proportional to the residual inventory change
13 and indicates that source term release provides the predominant control on the observed
14 differences in groundwater concentrations at the PoCal. In the base case, the source term release
15 rates show a decline after 500 years following closure as most of the ^{99}Tc inventory is depleted
16 by that time, while the upper bound case shows continued increase in the release rate until
17 1,000 years after closure because of the higher inventory and longer time to deplete. For this
18 reason, the peak groundwater concentration for the upper bound case occurs after 600 years
19 following closure compared to the base case.

21 8.2.5 Grout Flow Sensitivity Analyses

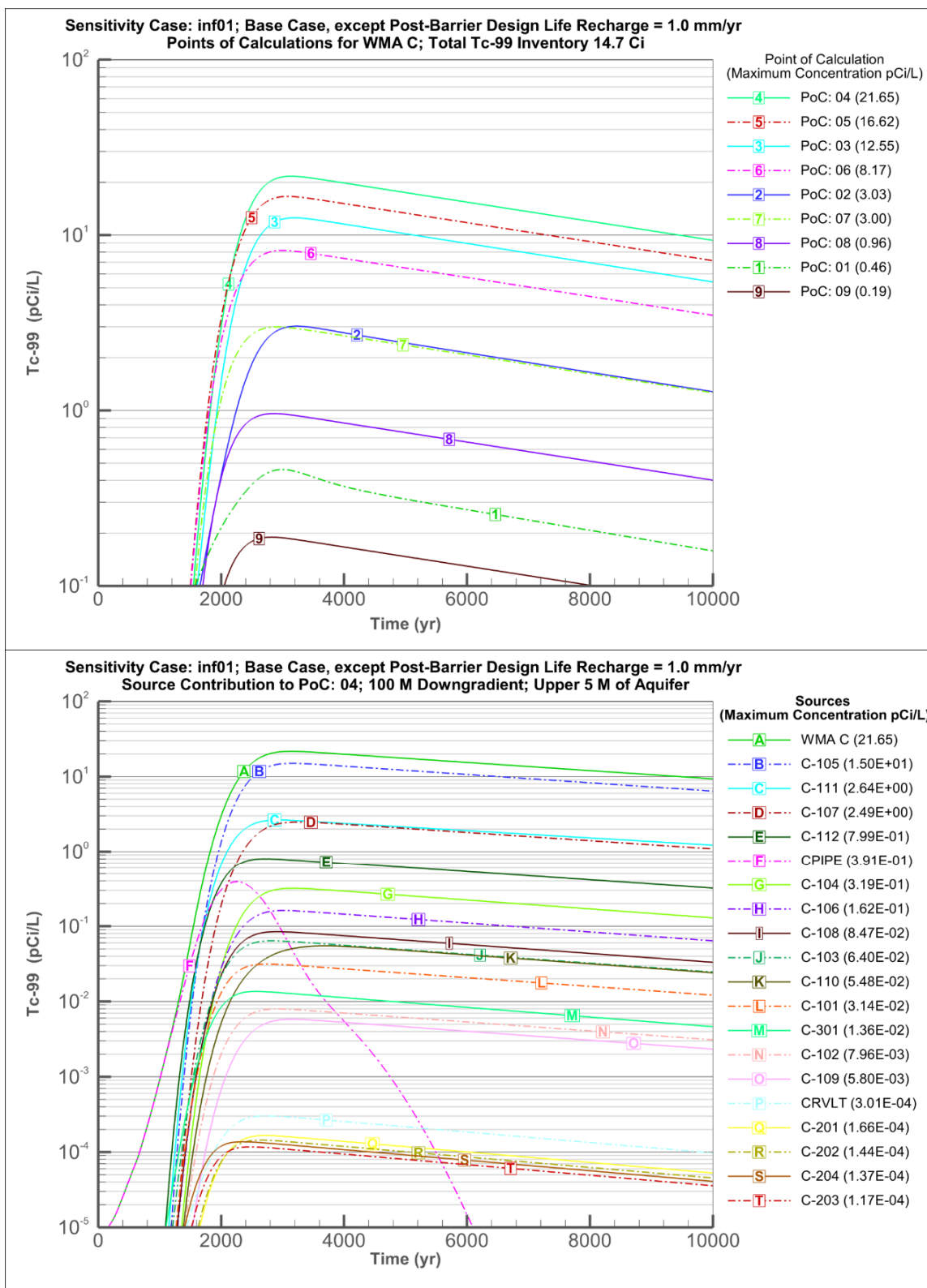
22
23 In the base case, the grouted tanks were assumed to remain intact throughout the 10,000-year
24 analysis time, based on the evaluation of grout durability presented in Section 6.2.12. To assess
25 the impact of early failure of the tank due to unforeseen events, sensitivity cases are performed
26 where the infill grout in the tank is assumed to provide no barrier to flow through the tank. For
27 this purpose, the grout properties are replaced by H2 sand properties and flow through the tank is
28 initiated at the following four degradation times:

- 29
30 1. Tank Degrades at 5,000 years after closure (GRT1)
- 31 2. Tank Degrades at 1,000 years after closure (GRT2)
- 32 3. Tank Degrades at 500 years after closure (GRT3)
- 33 4. Tank Degrades at 0 years after closure (GRT4)

34
35 Results for these analyses are summarized and compared with the base case in Table. Figure
36 8-48(a) presents the ^{99}Tc concentration in the saturated zone at the PoCal (cumulative for all the
37 sources) and Figure 8-48(b) presents the ^{99}Tc release rate (pCi/yr) from tank C-105 to the vadose
38 zone immediately below the tank for the four cases in comparison to the base case. Where the
39 tank grout is degraded at closure (0 years) the ^{99}Tc release rate from the tank at early times is
40 much higher, primarily due to advection, and drops sharply as the mass is depleted. This is in
41 contrast to the release rate for the tanks that are assumed to degrade later, where the release
42 occurs by diffusion (same as base case) until the tank degrades, and by both advection and
43 diffusion after the tank degradation. Until the degradation time, the tank release curves track the
44 base case results.

RPP-ENV-58782, Rev. 0

Figure 8-34. Recharge (Net Infiltration) Sensitivity Analysis Results of the Technetium-99 Concentration in Groundwater for the Minimum (inf01) Post-Design Life Value.

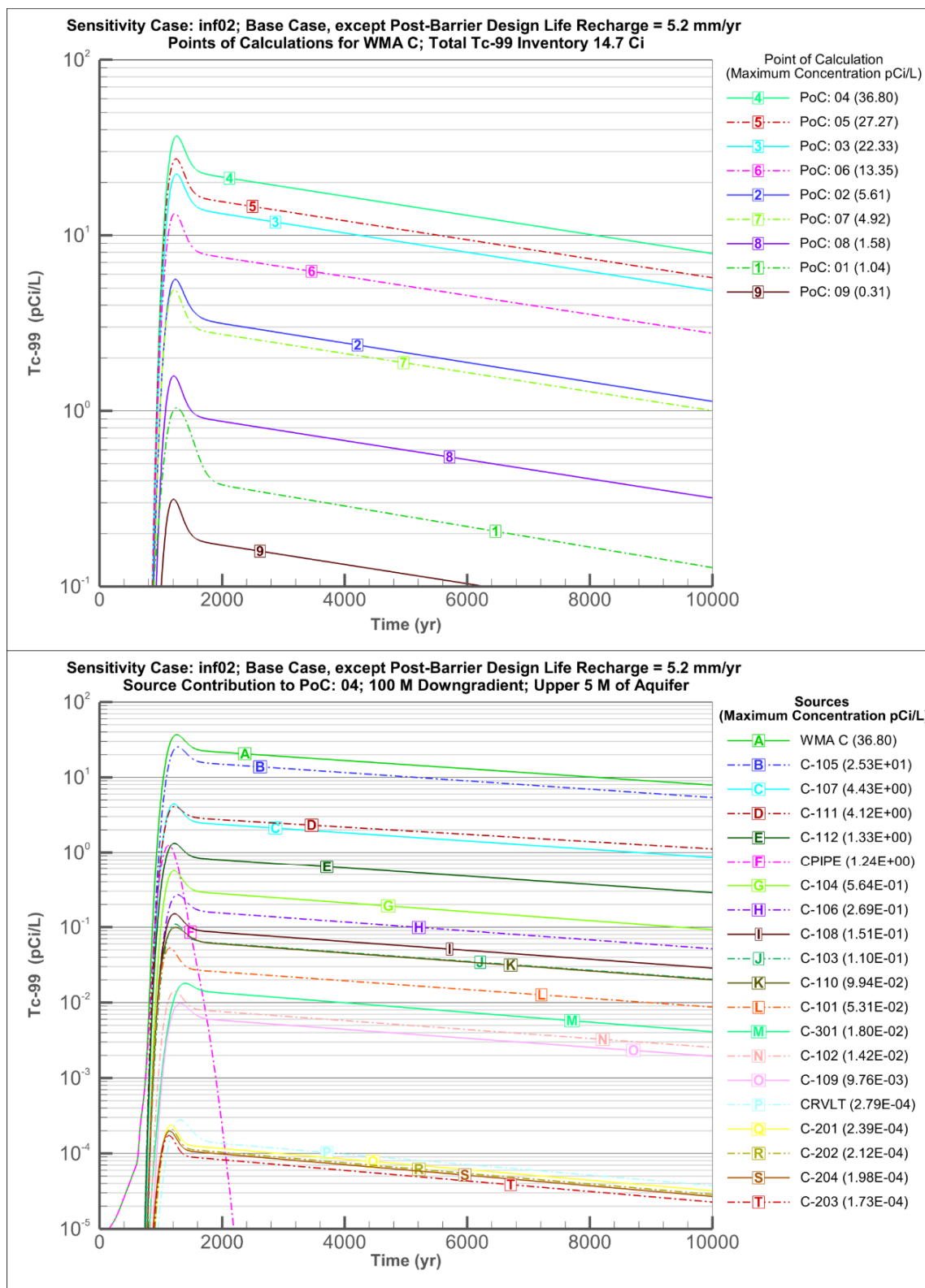


PoCal = Point of Calculation

WMA = Waste Management Area

RPP-ENV-58782, Rev. 0

Figure 8-35. Recharge (Net Infiltration) Sensitivity Analysis Results of the Technetium-99 Concentration in Groundwater for the Maximum (inf02) Post-Design Life Value.

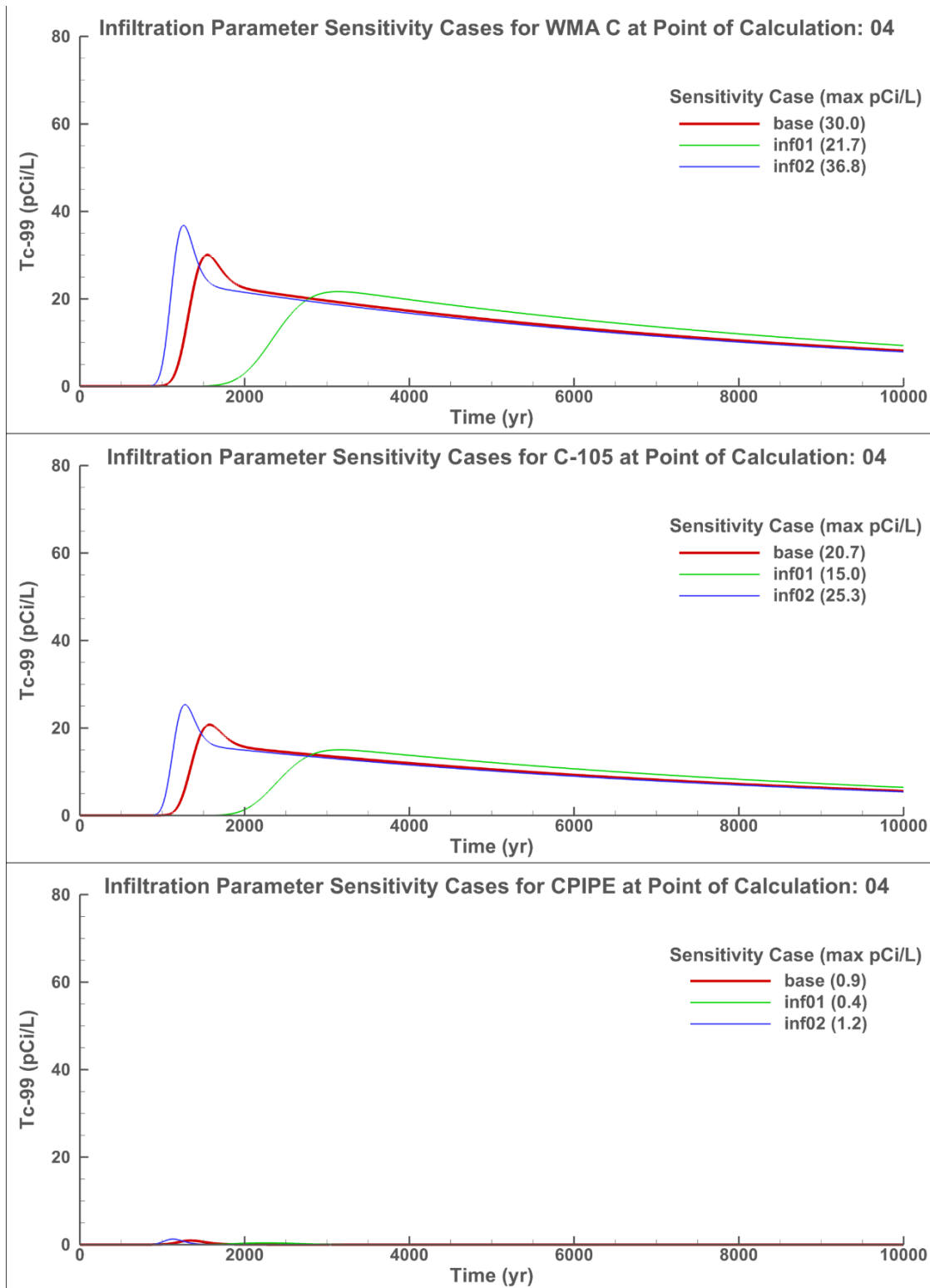


PoCal = Point of Calculation

WMA = Waste Management Area

RPP-ENV-58782, Rev. 0

Figure 8-36. Comparison of Recharge (Net Infiltration) Sensitivity Analysis Results of the Technetium-99 Concentration in Groundwater for the Base Case, Minimum (inf01), and Maximum (inf02) Post-Design Life Values.



CPIPE = WMA C Pipeline

WMA = Waste Management Area

RPP-ENV-58782, Rev. 0

Table 8-17. Aquifer Property Sensitivity Evaluation.

Aquifer Property	Sensitivity Case Shorthand	Aquifer Hydraulic Conductivity (m/day)	Time of Arrival of Maximum Concentration at Downgradient Point of Calculation (Years after Closure)	Maximum Concentration at Downgradient Point of Calculation (pCi/L)
5th Percentile Hydraulic Conductivity Value	gwp01	4,200	1,560	78
Median Hydraulic Conductivity Value	Base Case	11,000	1,555	30
95th Percentile Hydraulic Conductivity Value	gwp03	17,800	1,555	19

The magnitude in peak concentration (and peak release rate) in the saturated zone reduces with the delayed tank degradation time due to inventory depletion from diffusive release prior to the start of advection. For the case where the tank grout is degraded at closure (0 years) the peak concentration in the saturated zone is marginally higher than the case where the tank grout is degraded at 500 years after closure, and the peak concentration occurs after 1,500 years indicating delayed transport through the vadose zone.

8.2.6 Waste Form Sensitivity Analysis

In the base case, waste form degradation and dissolved concentration limits are applied in determining the source term release for some analytes, as discussed in Section 6.3.1. In this sensitivity analysis, such limits are removed to evaluate the impact on saturated zone concentration at the PoCal.

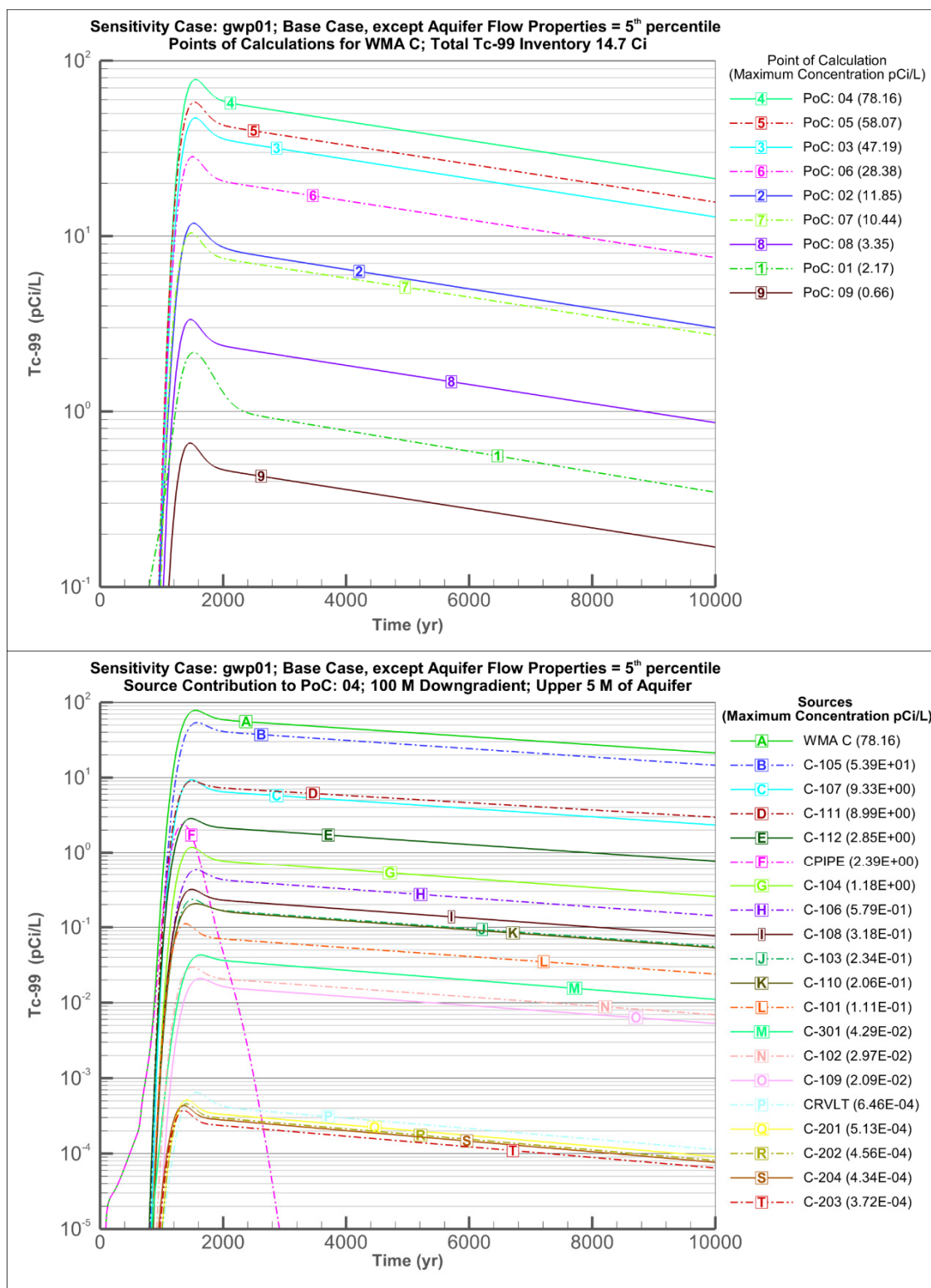
As described in Section 6.3.1, the following source term release models are applied for ^{99}Tc and uranium in the base case:

- For ^{99}Tc , 6% of the inventory is considered to be instantaneously available for release while the remaining 94% undergoes relatively slower release at the fractional rate of $6 \times 10^{-4} \text{ day}^{-1}$
- For uranium, a solubility limit of $1 \times 10^{-4} \text{ mol/L}$ is applied for 1,000 years after closure and $1 \times 10^{-6} \text{ mol/L}$ after 1,000 years after closure under intact tank conditions.

For the purpose of conducting the sensitivity analysis, all of the ^{99}Tc inventory was assumed to be instantaneously available for release and the solubility limit or dissolved concentration limits are not imposed for uranium.

RPP-ENV-58782, Rev. 0

Figure 8-37. Aquifer Property Sensitivity Analysis Results of the Technetium-99 Concentration in Groundwater for the 5th Percentile (gwp01) Hydraulic Conductivity Values.

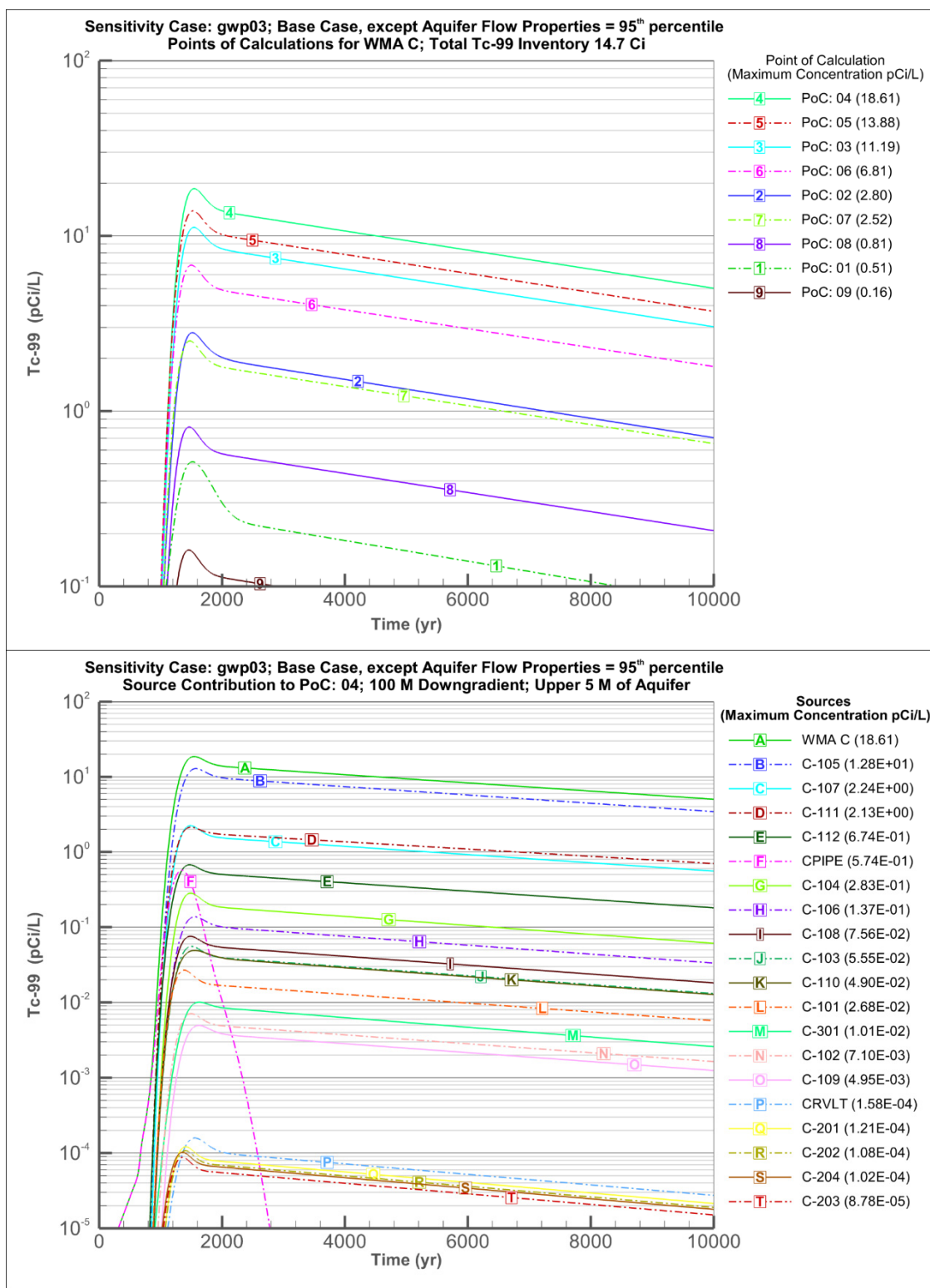


CPIPE = WMA C Pipeline

WMA = Waste Management Area

RPP-ENV-58782, Rev. 0

Figure 8-38. Aquifer Property Sensitivity Analysis Results of the Technetium-99 Concentration in Groundwater for the 95th Percentile (gwp03) Hydraulic Conductivity Values.

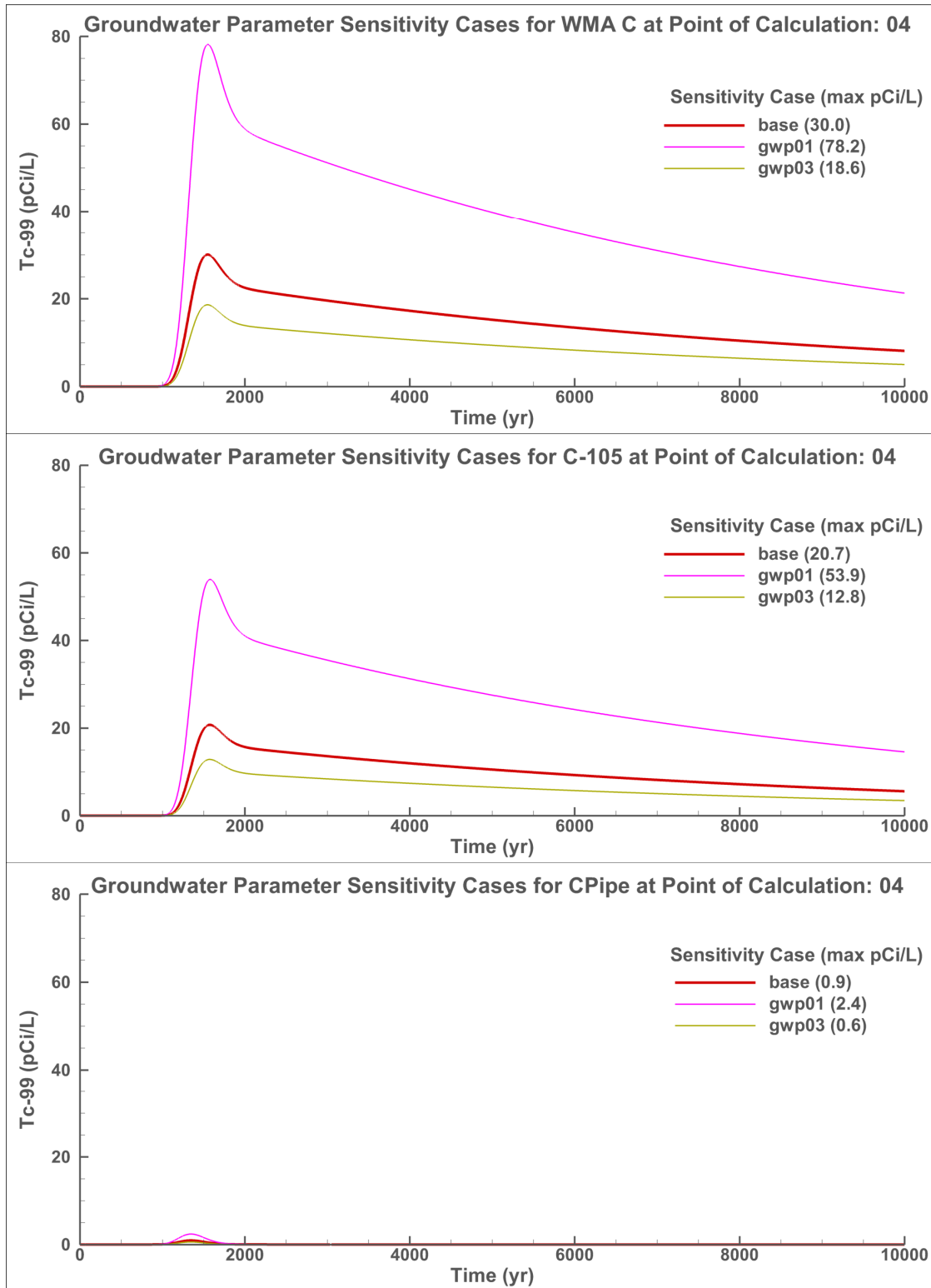


CPIPE = WMA C Pipeline

WMA = Waste Management Area

RPP-ENV-58782, Rev. 0

Figure 8-39. Comparison of the Aquifer Property Sensitivity Analysis Results of the Technetium-99 Concentration in Groundwater for the Base Case, 5th Percentile (gwp01), and 95th Percentile (gwp03) Hydraulic Conductivity Values at Point of Calculation 4.

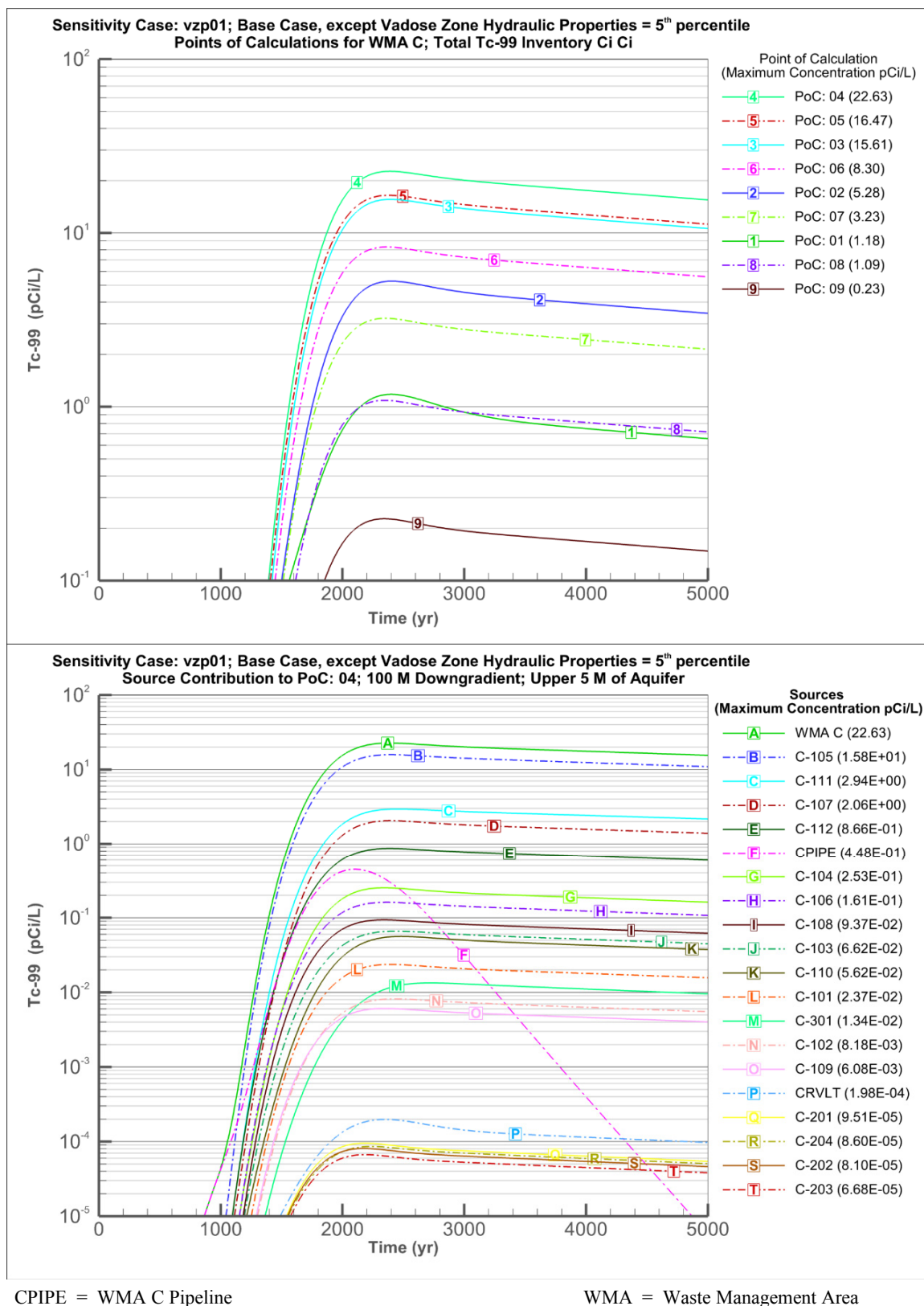


CPIPE = WMA C Pipeline

WMA = Waste Management Area

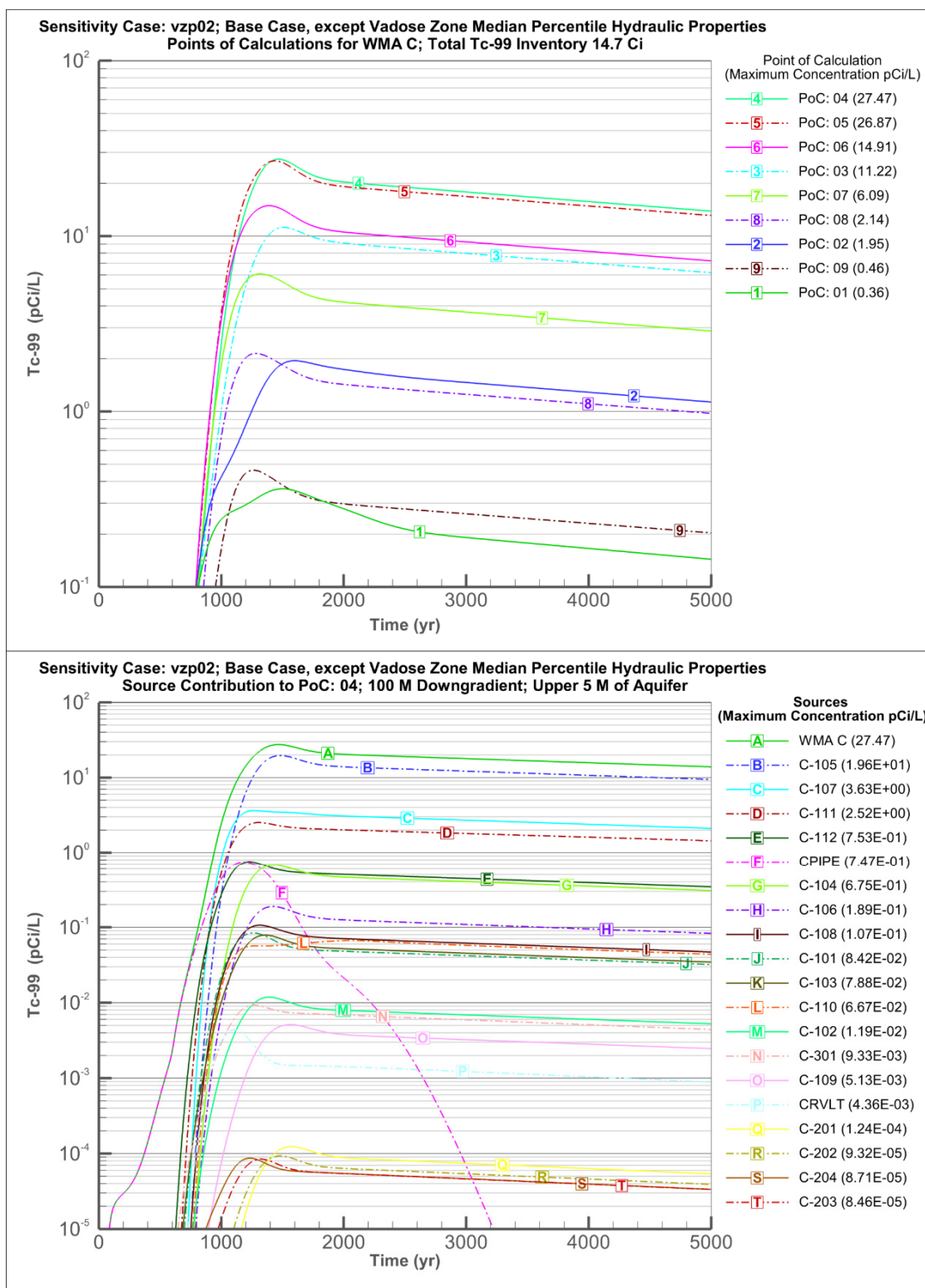
RPP-ENV-58782, Rev. 0

Figure 8-40. Vadose Zone Property Sensitivity Analysis Results of the Technetium-99 Concentration in Groundwater for the 5th (vzp01) Percentile Hydraulic Parameter Values.



RPP-ENV-58782, Rev. 0

Figure 8-41. Vadose Zone Property Sensitivity Analysis Results of the Technetium-99 Concentration in Groundwater for the Median (vzp02) Percentile Hydraulic Parameter Values.

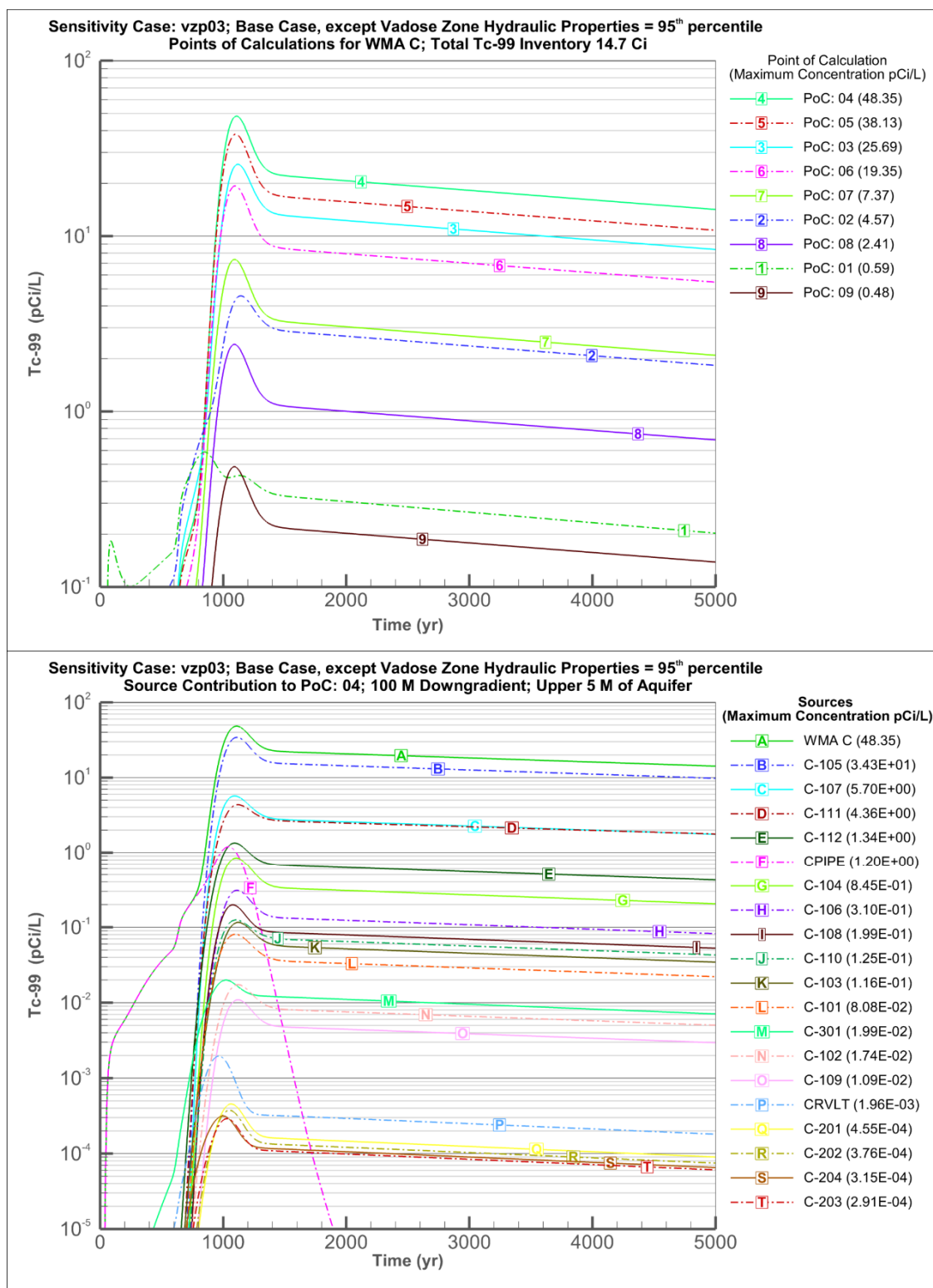


CPIPE = WMA C Pipeline

WMA = Waste Management Area

RPP-ENV-58782, Rev. 0

Figure 8-42. Vadose Zone Property Sensitivity Analysis Results of the Technetium-99 Concentration in Groundwater for the 95th (vzp03) Percentile Hydraulic Parameter Values.

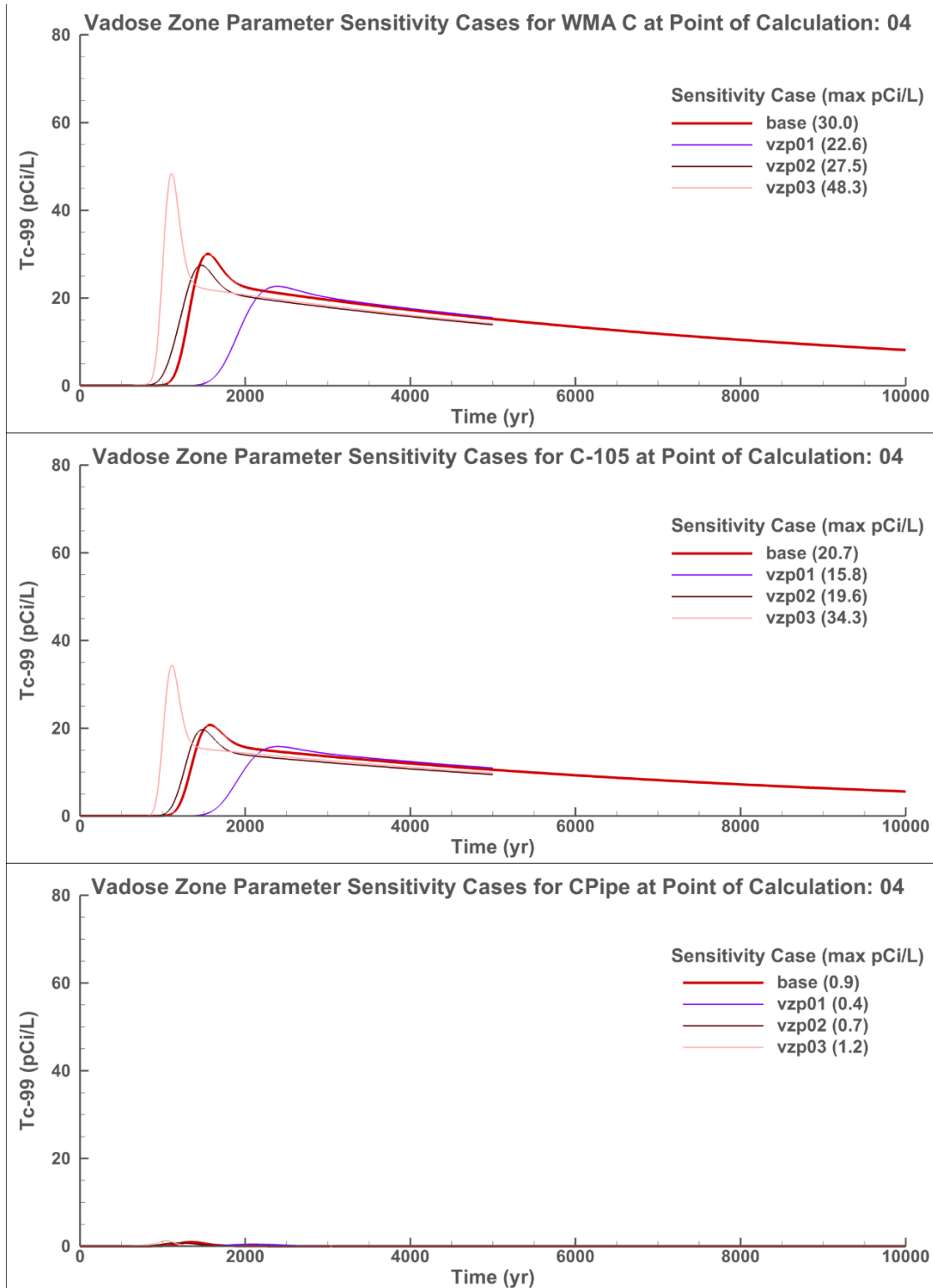


CPIPE = WMA C Pipeline

WMA = Waste Management Area

RPP-ENV-58782, Rev. 0

Figure 8-43. Comparison of Vadose Zone Property Sensitivity Analysis Results of the Technetium-99 Concentration in Groundwater for the Base Case, 5th (vzp01), Median (vzp02), and 95th Percentile (vzp03) Hydraulic Parameter Values.



CPIPE = WMA C Pipeline

WMA = Waste Management Area

RPP-ENV-58782, Rev. 0

Table 8-18. Vadose Zone Sensitivity Evaluation.

Vadose Zone Sensitivity	Sensitivity Case Shorthand	Time of Arrival of Maximum Concentration at Downgradient Point of Calculation (Years after Closure)	Maximum Concentration at Downgradient Point of Calculation (pCi/L)
Base Case	Base Case	1,555	30
5th Percentile Parameter Values	vzp01	2,390	23
Median Percentile Parameter Values	vzp02	1,465	27
95th Percentile Parameter Values	vzp03	1,110	48
Alternative Geologic Model II	vzp04	1,395	29
Presence of Clastic Dike	vzp05	1,460	26

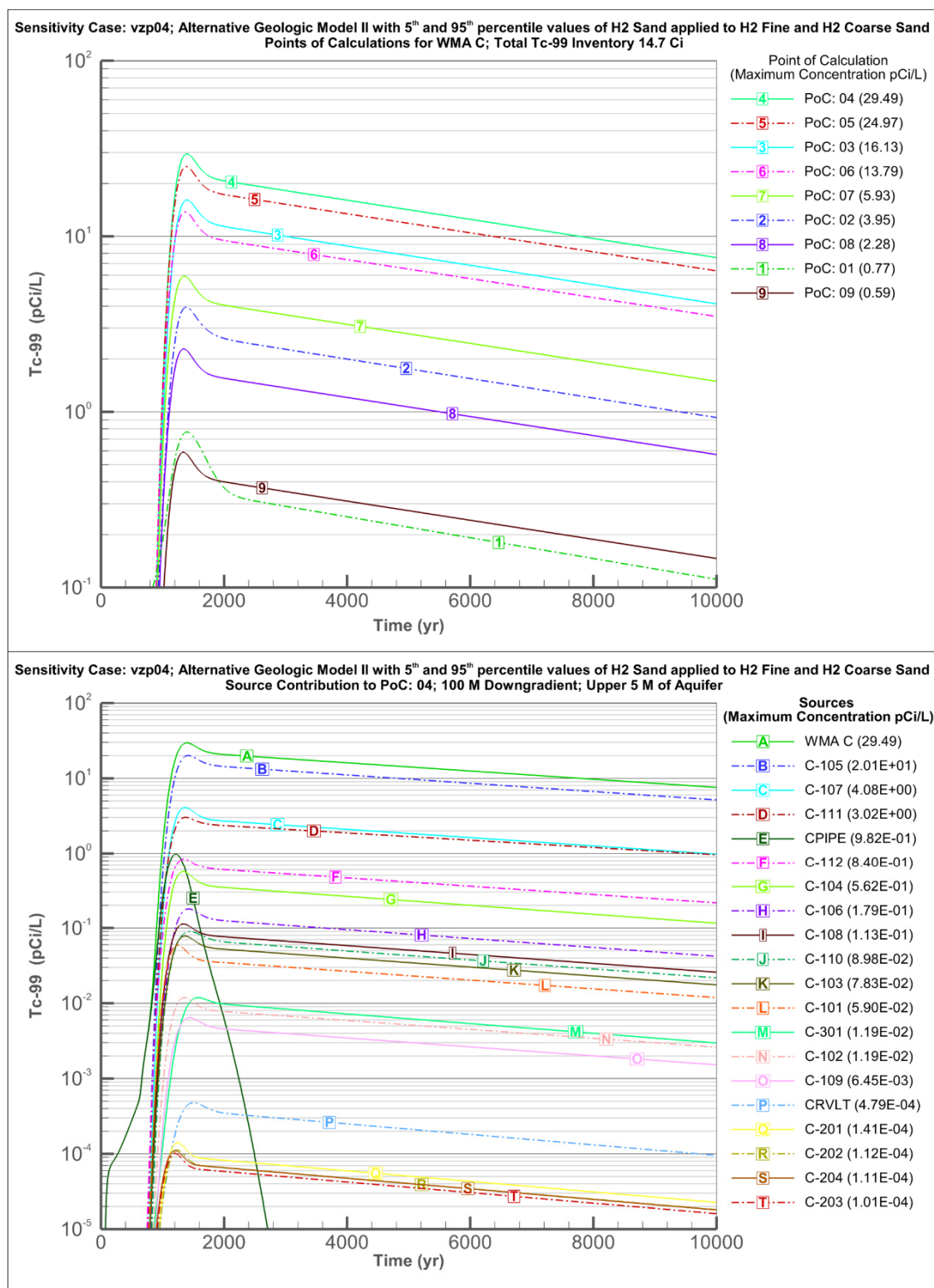
Figure 8-49(a) presents the ^{99}Tc concentration in the saturated zone at the PoCal (cumulative for all the sources) and Figure 8-49(b) presents the ^{99}Tc release rate from tank C-105 to the vadose zone immediately below the tank. Results for these analyses for ^{99}Tc are summarized and compared with the base case in Table 8-21. Figure 8-50 presents the ^{238}U concentration in the saturated zone.

For ^{99}Tc , very little difference is observed between the base case and sensitivity case (Table 8-21). This is because the degradation rate used in the base case itself results in almost all of the ^{99}Tc inventory being available for release within a few years after closure. The small difference in time in the waste form degradation results in negligible difference in the saturated zone concentrations due to larger dispersion caused by vadose zone and saturated zone processes.

For ^{238}U the increase in concentrations are appreciable, indicating the influence of the solubility/dissolved concentration limits. The effect on ^{238}U concentration is relatively small because the breakthrough curve for uranium is primarily from advective release from pipeline sources. Uranium is retarded within the tank due to sorption on the base mat (grout + concrete layer).

RPP-ENV-58782, Rev. 0

Figure 8-44. Alternative Geologic Model Evaluation Results of the Technetium-99 Concentration in Groundwater for the Alternative Geologic Model (vzp04) Geologic Conceptualization.

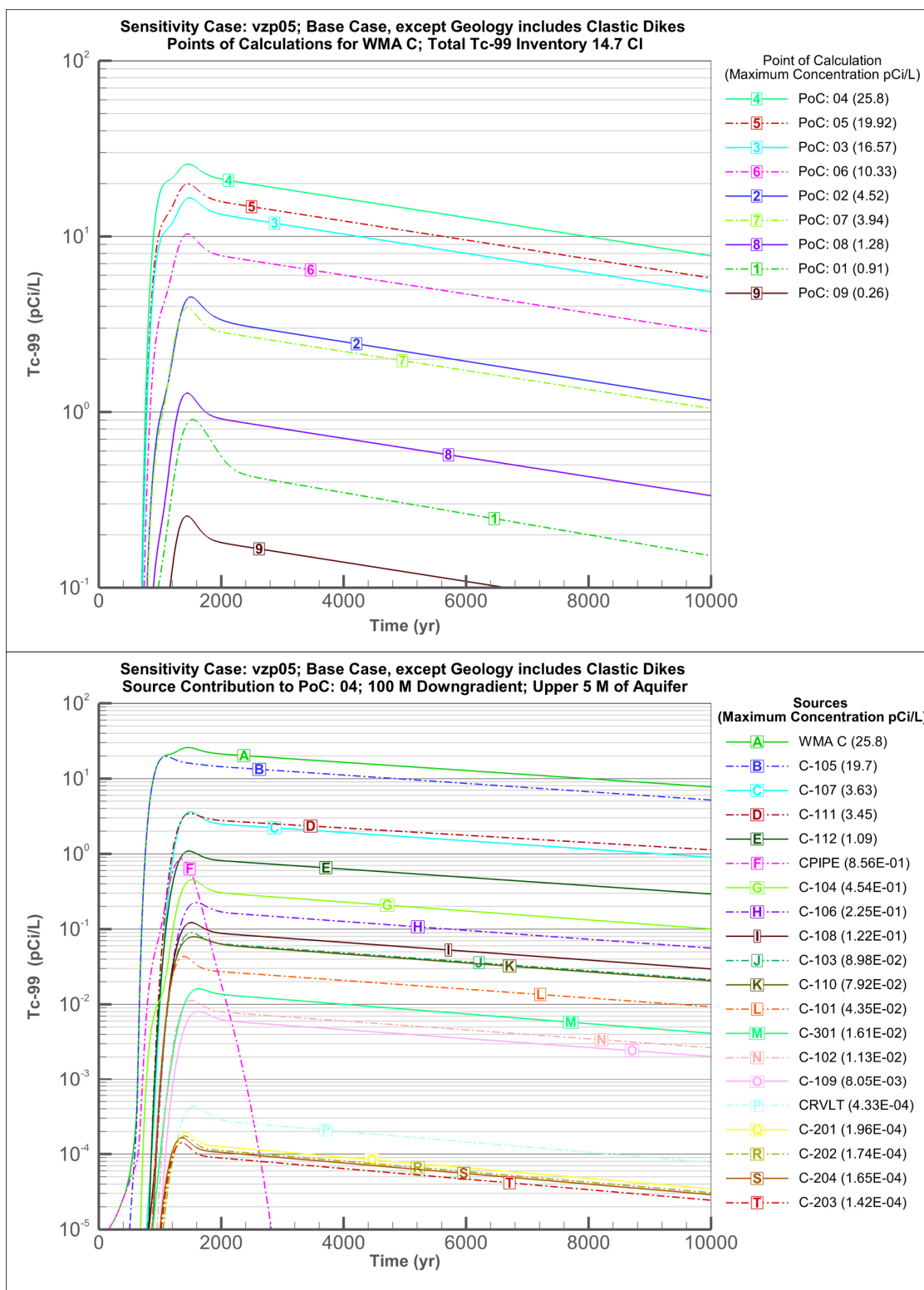


CPIPE = WMA C Pipeline

WMA = Waste Management Area

RPP-ENV-58782, Rev. 0

Figure 8-45. Alternative Geologic Model Evaluation Results of the Technetium-99 Concentration in Groundwater for the Hypothesized Clastic Dike (vzp05) Geologic Conceptualization.

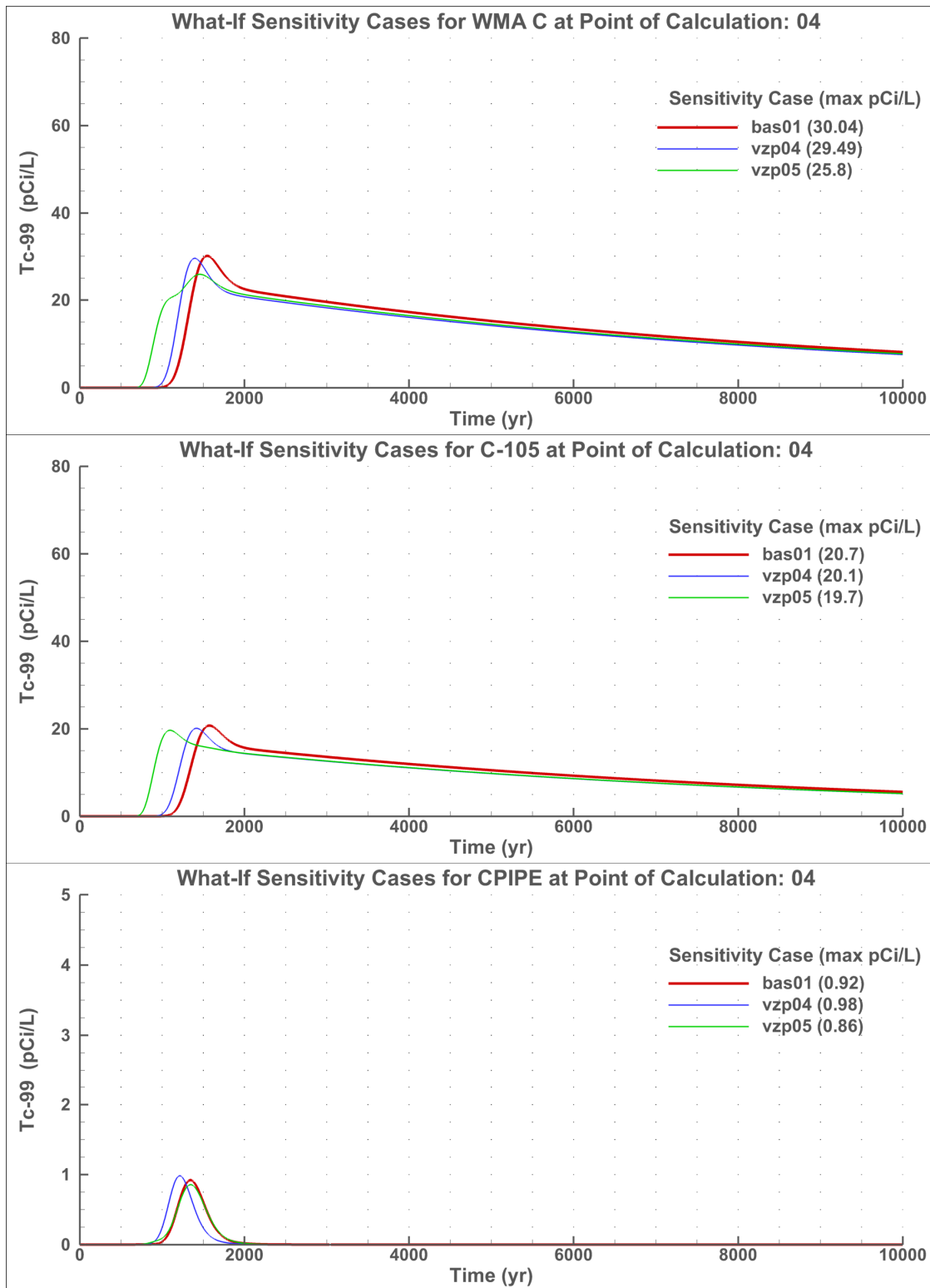


CPIPE = WMA C Pipeline

WMA = Waste Management Area

RPP-ENV-58782, Rev. 0

Figure 8-46. Comparison of the Results of the Technetium-99 Concentration in Groundwater for the Alternative Geologic Model (vzp04) and the Hypothesized Clastic Dike (vzp05) Geologic Conceptualizations.



CPIPE = WMA C Pipeline

WMA = Waste Management Area

RPP-ENV-58782, Rev. 0

Table 8-19. Inventory Estimate Sensitivity Evaluation.

Inventory	Sensitivity Case Shorthand	Time of Arrival of Maximum Concentration at Downgradient Point of Calculation (Years after Closure)	Maximum Concentration at Downgradient Point of Calculation (pCi/L)
Base case*	Base case	2,030	32
Upper bound Inventory for Technetium-99	inv2	2,480	144

*The base case analysis was run using the system model for this comparison. The results differ slightly from the base case analysis results from Subsurface Transport Over Multiple Phases (STOMP)[®] (copyrighted by Battelle Memorial Institute, 1996).

8.2.7 Tank Flow Sensitivity Analyses

Diffusive release through the base of the tank (made up of grout and concrete layer) is the primary release mechanism from the tanks in the base case. The effective diffusion coefficient through the concrete and grout layer is a key parameter in determining the diffusive flux. For the base case, an effective diffusion coefficient of $3 \times 10^{-8} \text{ cm}^2/\text{s}$ was considered (Section 6.3.1); the following three sensitivity cases were performed to evaluate the impact of changing the effective diffusion coefficient based on stakeholder inputs from the scoping process.

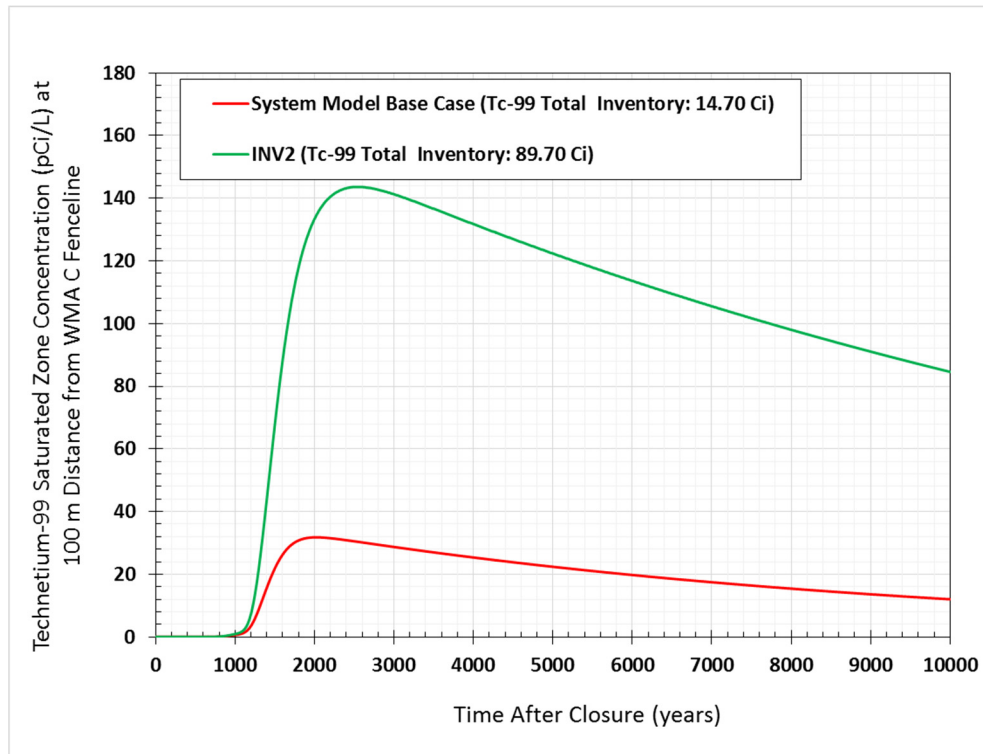
1. Effective diffusion coefficient for the grout is changed to $1 \times 10^{-7} \text{ cm}^2/\text{s}$ (DIF1).
2. Effective diffusion coefficient for the grout varies linearly from 1×10^{-14} to $3 \times 10^{-8} \text{ cm}^2/\text{s}$ in the first 500 years after closure and remains constant afterwards at $3 \times 10^{-8} \text{ cm}^2/\text{s}$ (DIF2).
3. Tanks (including 244-CR vault) remain fully intact with no advective release until 5,000 years after closure. The tank becomes fully degraded at 5,000 years after closure, resulting in both advective and diffusive releases. The effective diffusion coefficient remains the same as the base case (DIF3).

Results for these analyses are summarized and compared with the base case in Table 8-22. Figure 8-51(a) presents the ^{99}Tc concentration in the saturated zone at the PoCal and Figure 8-51(b) presents the ^{99}Tc release from tank C-105 to the vadose zone immediately below the tank for the three cases in comparison to the base case. For the DIF1 case, higher diffusion coefficient results in higher diffusive release and higher peak concentration. Once the source inventory depletes (following the peak value) the curves follow the same trend as the base case. For the DIF2 case, due to lower diffusion coefficient in the first 500 years after closure, the diffusive flux and therefore the concentration is lower than the base case early on. For the DIF3 case, since no release is allowed from the grouted tank sources in the first 5,000 years after closure, the only release prior to this time is from the pipeline source that results in a small increase in groundwater concentration around 1,000 years after closure [Figure 8-51(a)]. After 5,000 years after closure, both advective and diffusive release start resulting in higher peak concentration than the base case.

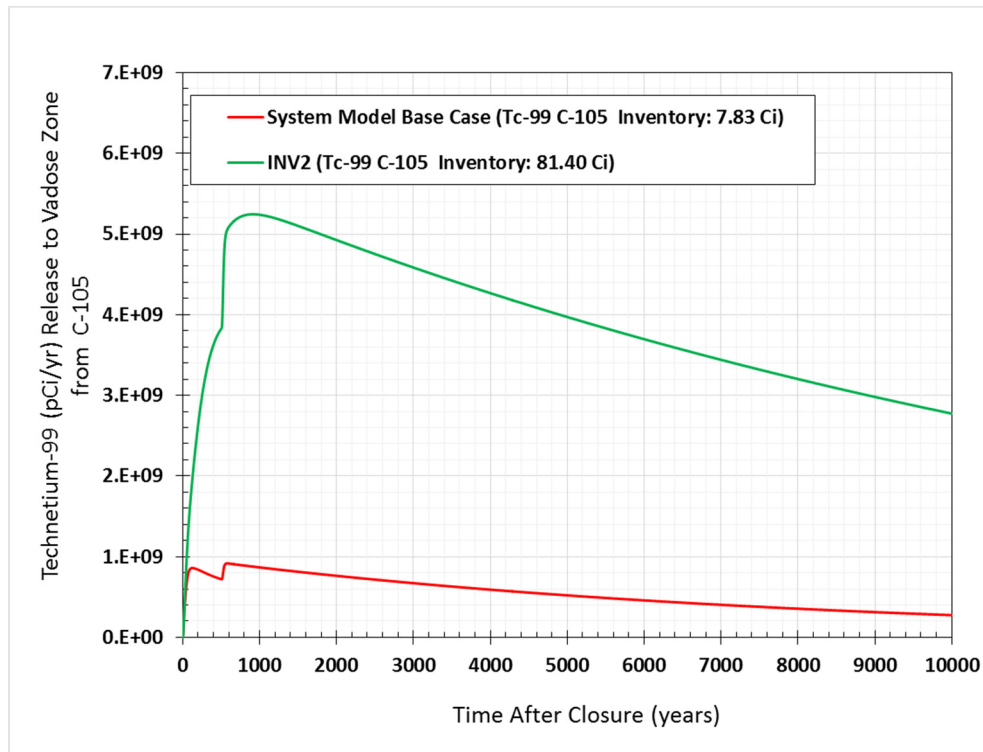
RPP-ENV-58782, Rev. 0

Figure 8-47. Comparison of Base Case and INV1 Case (a) Technetium-99 Concentration at 100 meter Boundary (b) Technetium-99 Release Rate to Vadose Zone from Tank 241-C-105.

(a)



(b)



WMA = Waste Management Area

RPP-ENV-58782, Rev. 0

Table 8-20. Grout Flow Safety Function Sensitivity Evaluation.

Tank Degradation Time	Sensitivity Case Shorthand	Time of Arrival of Maximum Concentration at Downgradient Point of Calculation (Years after Closure)	Maximum Concentration at Downgradient Point of Calculation (pCi/L)
Base case*	Base case	2,030	32
Tank Degrades at 5,000 yr	grt1	2,030	32
Tank Degrades at 1,000 yr	grt2	2,630	43
Tank Degrades at 500 yr	grt3	2,190	45
Tank Degrades at 0 yr	grt4	1,520	46

*The base case analysis was run using the system model for this comparison. The results differ slightly from the base case analysis results from Subsurface Transport Over Multiple Phases (STOMP)[®] (copyrighted by Battelle Memorial Institute, 1996).

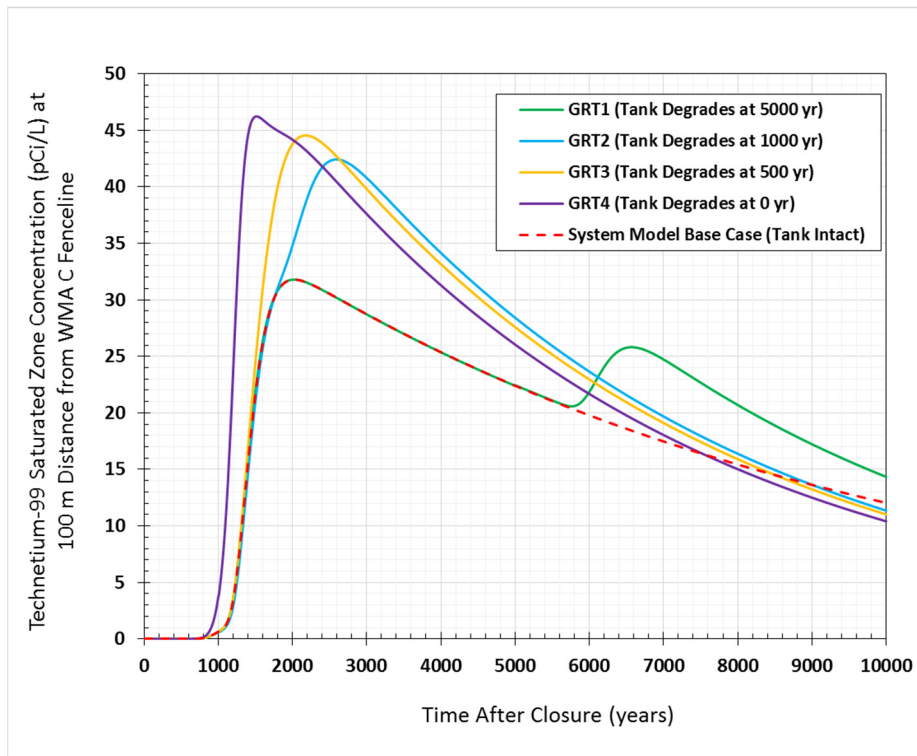
8.2.8 Evaluation of Long-Term Peak Dose

An additional evaluation case was run to evaluate the peak dose beyond the 10,000-year post-closure time frame. For this purpose, the base case flow-field that was developed for the 10,000-year post-closure time period was extended such that assumptions of constant recharge rate were maintained and all the processes that were applicable over the 10,000-year post-closure time frame were assumed to be applicable for the extended duration. The only change made to the base case is the one where the grouted tanks (including the 244-CR vault) are considered to be degraded at 30,000 years after closure. At this time, flow through the tank is applied based on the degraded tank flow field. The calculations were run for a period of 400,000 years after closure and the results are presented in Figure 8-52 in terms of effective dose from the groundwater pathway. The peak dose of 0.27 mrem/yr occurs around 15,000 years after closure. It is controlled by ⁹⁹Tc, uranium isotopes, and ²²⁶Ra. The peak dose from uranium isotopes results primarily from advective release from pipeline inventory that occurs at closure, indicating significant delay in the vadose and saturated zone. Following the peak, the dose from uranium isotopes declines sharply and then gradually increases over the simulated time period, indicating delayed arrival from tank sources that are diffusion controlled. The slower diffusive release from the tanks along with retardation in the natural system lead to very small dose from the long-lived uranium isotopes. The dose after 20,000 years following closure is dominated by ²²⁶Ra (including progeny) that results from ingrowth due to decay of parent uranium isotopes. After 30,000 years following closure, a small rise in the ⁹⁹Tc dose is noticeable, which results from an increased release when advection through the tank is assumed. At the end of 400,000 years of simulation, the dose contributions from ²²⁶Ra and ²¹⁰Pb are increasing. Both result from the decay of parent uranium isotopes, indicating establishment of secular equilibrium.

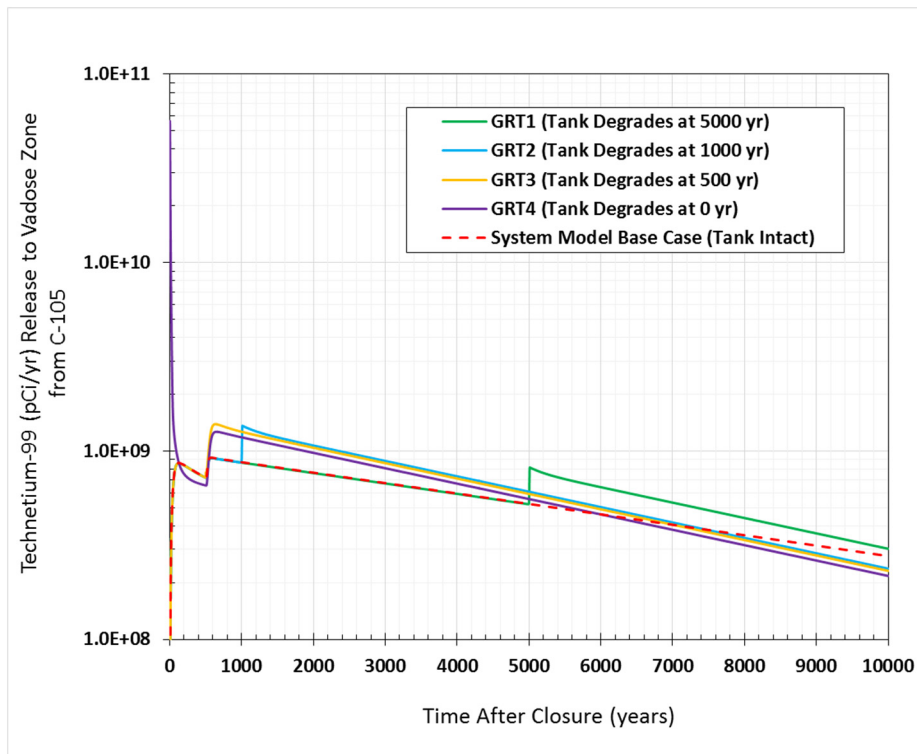
RPP-ENV-58782, Rev. 0

**Figure 8-48. Comparison of Base Case and GRT1, GRT2, GRT3, GRT4 Case
(a) Technetium-99 Concentration at 100 meter Boundary (b) Technetium-99
Release Rate to Vadose Zone from Tank 241-C-105.**

(a)



(b)

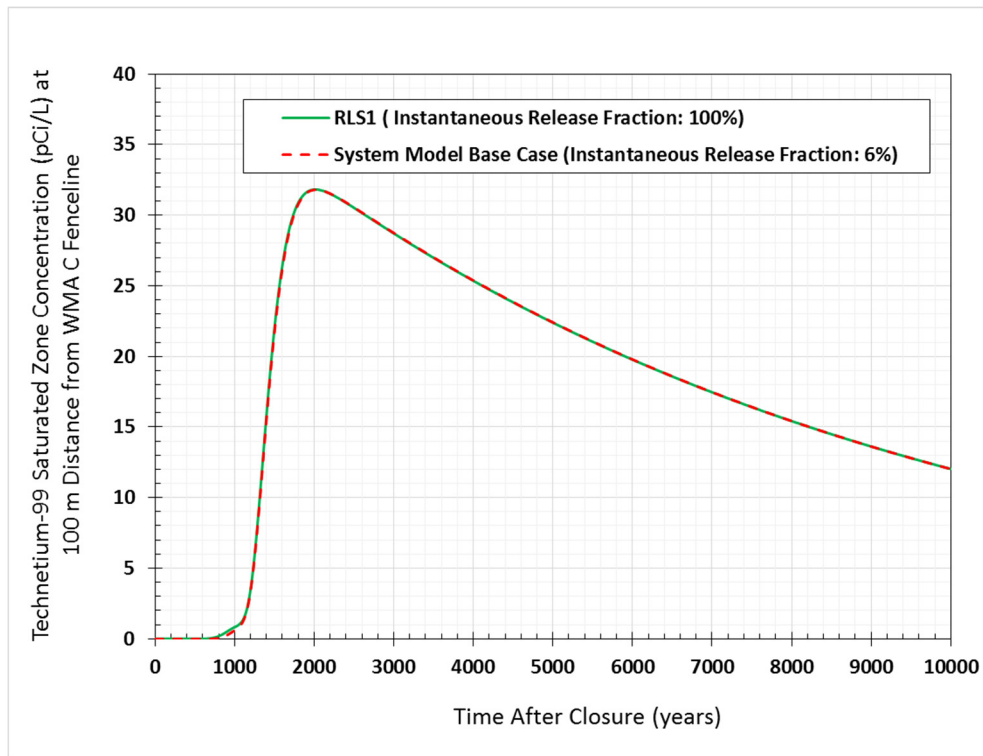


WMA = Waste Management Area

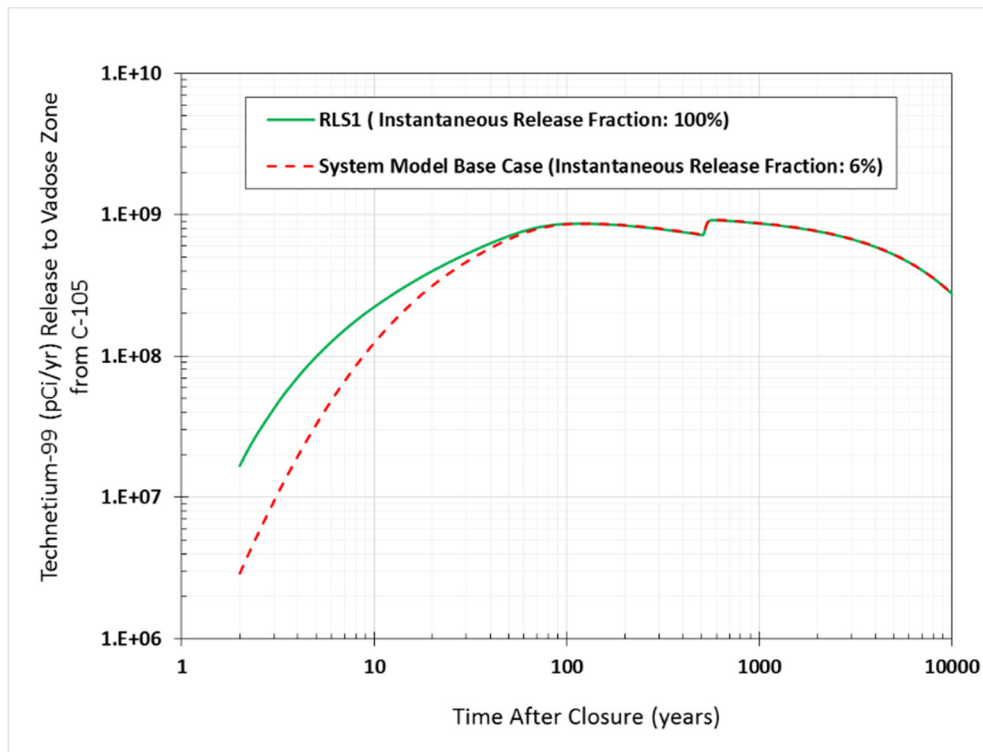
RPP-ENV-58782, Rev. 0

Figure 8-49. Comparison of Base Case and RLS1 Case (a) Technetium-99 Concentration at 100 meter Boundary (b) Technetium-99 Release to Vadose Zone from Tank 241-C-105.

(a)



(b)



WMA = Waste Management Area

RPP-ENV-58782, Rev. 0

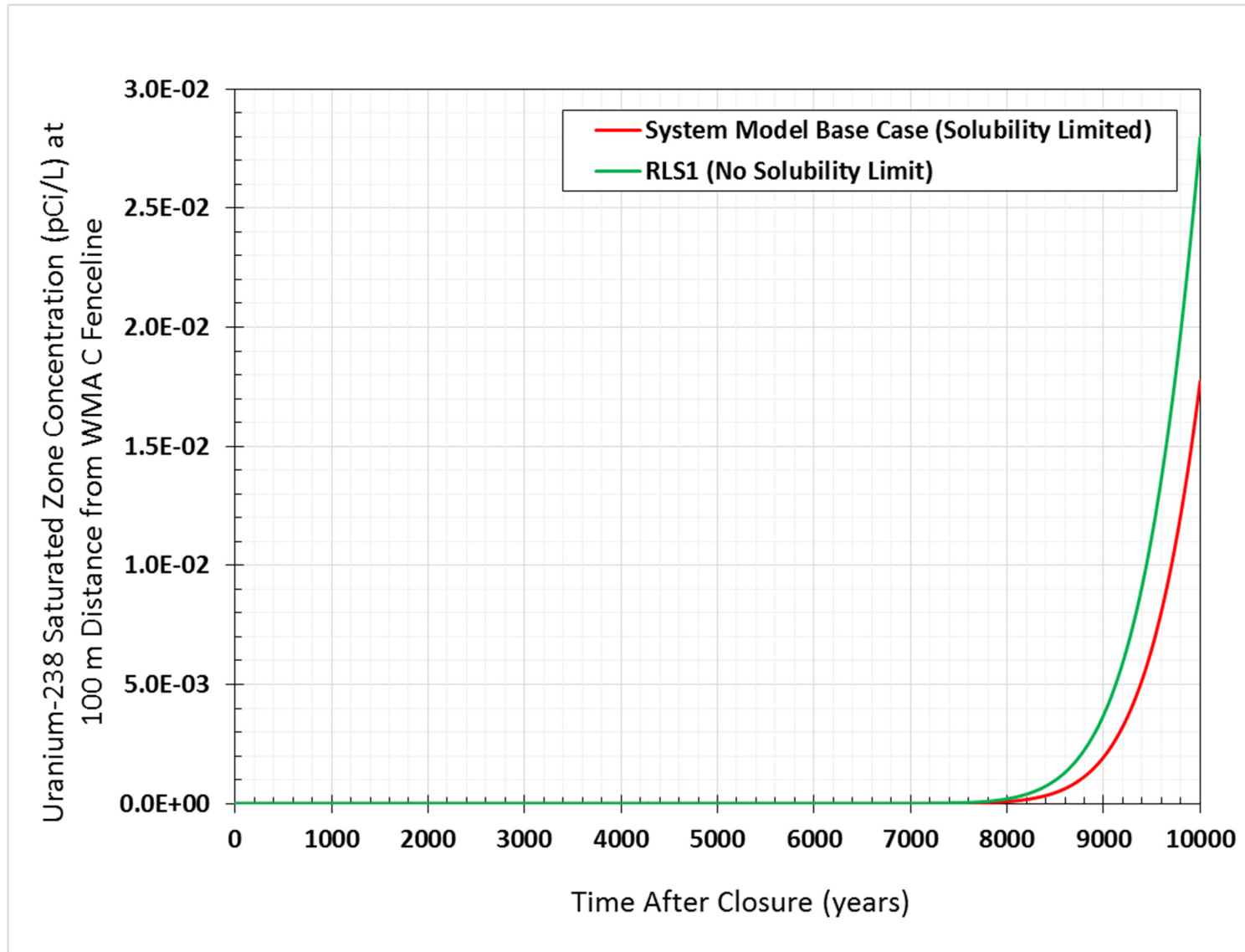
Table 8-21. Residual Chemistry Safety Function.

Residual Chemistry	Sensitivity Case Shorthand	Time of Arrival of Maximum Concentration at Downgradient Point of Calculation (Years after Closure)	Maximum Concentration at Downgradient Point of Calculation (pCi/L)
Base case for technetium-99*	Base case	2,030	32
100% Instantaneous release fraction for technetium-99	rls1(technetium-99)	2,030	32
Solubility Limited release for Uranium	rls1(Uranium-238)	Maximum concentration did not arrive within 10,000 years	Maximum concentration did not arrive within 10,000 years

*The base case analysis was run using the system model for this comparison. The results differ slightly from the base case analysis results from Subsurface Transport Over Multiple Phases (STOMP)[®] (copyrighted by Battelle Memorial Institute, 1996).

1
2

Figure 8-50. Comparison of Base Case and RLS1 Case for Uranium-238 Concentration at 100 meter Boundary.



WMA = Waste Management Area

RPP-ENV-58782, Rev. 0

Table 8-22. Tank Flow Safety Function Sensitivity Evaluation.

Tank Flow	Sensitivity Case Shorthand	Time of Arrival of Maximum Concentration at Downgradient Point of Calculation (Years after Closure)	Maximum Concentration at Downgradient Point of Calculation (pCi/L)
Base case*	Base case	2,030	32
Diffusion coefficient $1\text{E-}7\text{ cm}^2/\text{s}$	dif1	1,920	34
Linearly changing diffusion coefficient over 500 years from $1\text{E-}14$ to $3\text{E-}8\text{ cm}^2/\text{s}$	dif2	2,230	31
Tanks remain intact (no release) for 5,000 years, followed by advective release beginning immediately.	dif3	6,930	44

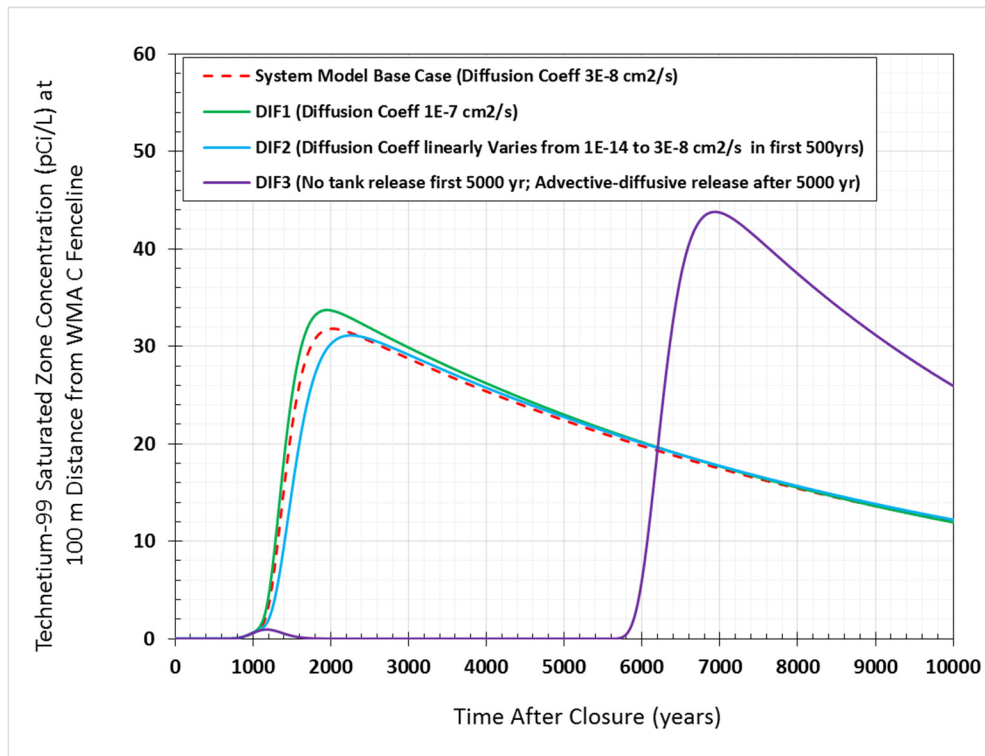
*The base case analysis was run using the system model for this comparison. The results differ slightly from the base case analysis results from Subsurface Transport Over Multiple Phases (STOMP)[®] (copyrighted by Battelle Memorial Institute, 1996).

1
2

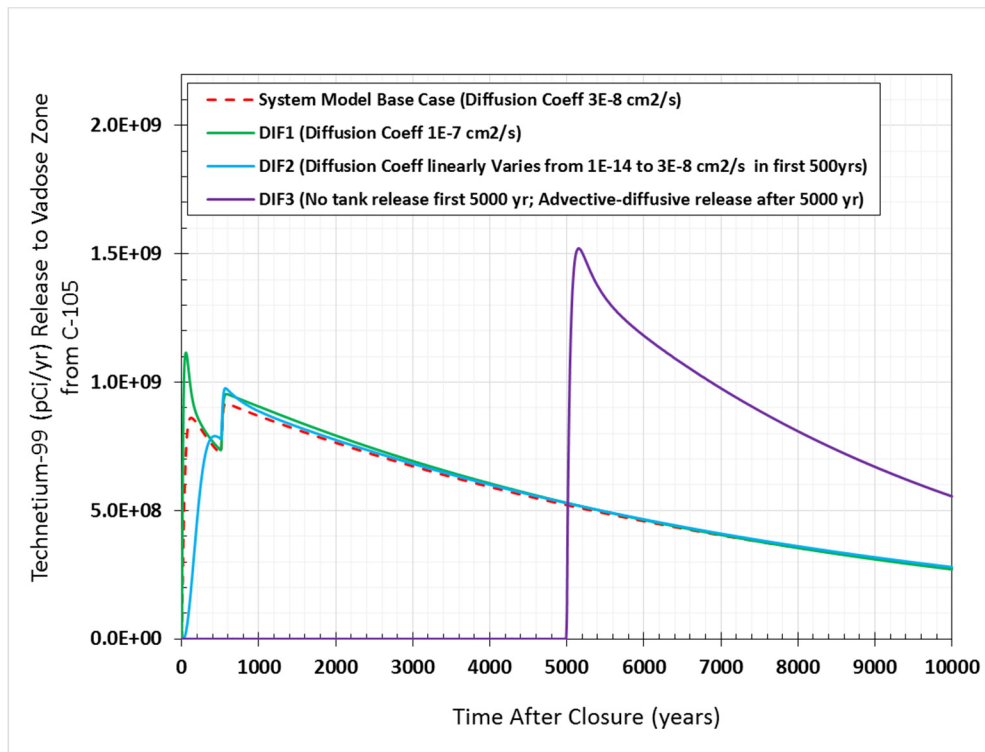
RPP-ENV-58782, Rev. 0

Figure 8-51. Comparison of Base Case and DIF1, DIF2, DIF3 Case (a) Technetium-99 Concentration at 100 meter Boundary (b) Technetium-99 Release to Vadose Zone from Tank 241-C-105.

(a)

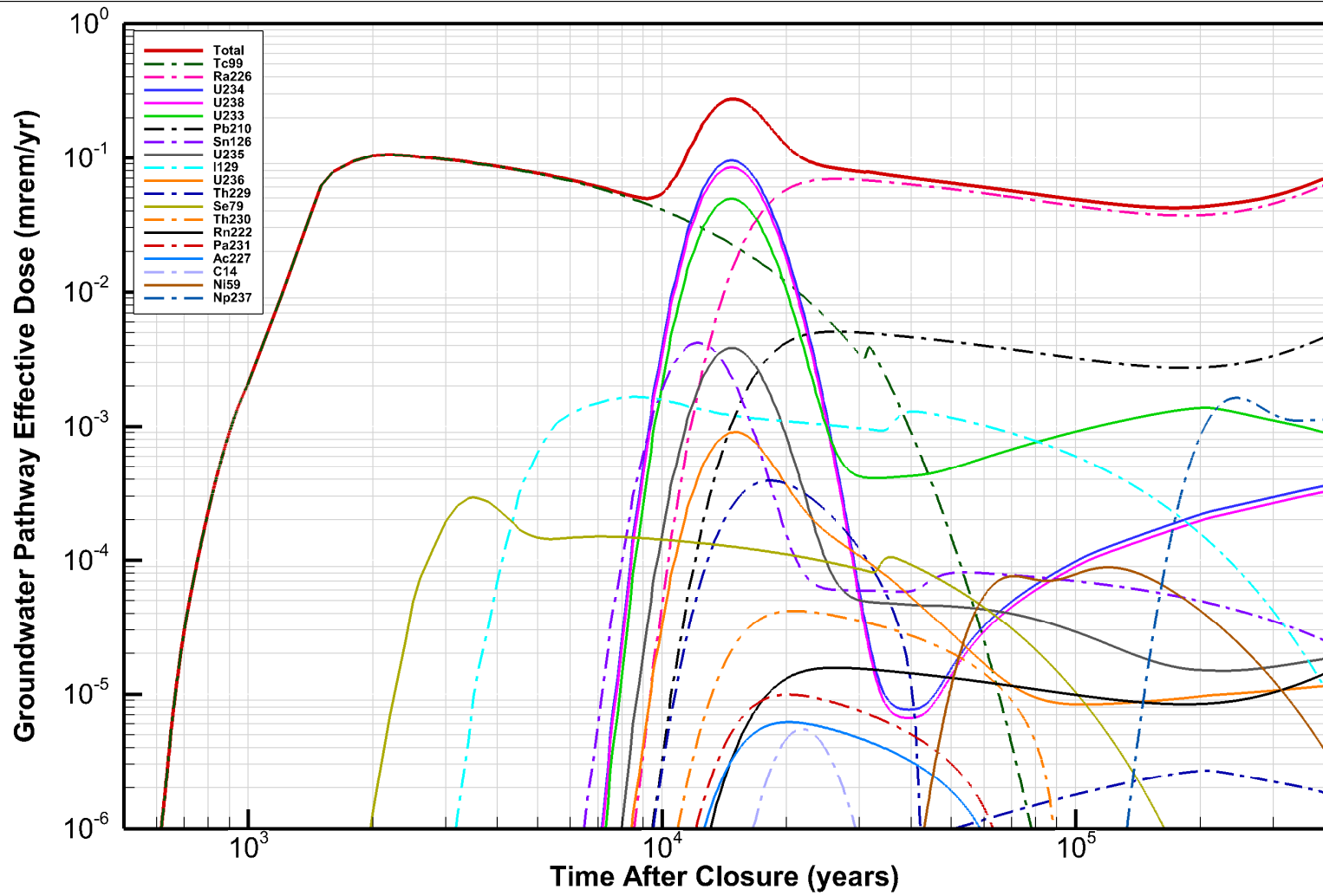


(b)



WMA = Waste Management Area

Figure 8-52. Sensitivity Case Showing the Results of Peak Groundwater Pathway Dose Calculations.



RPP-ENV-58782, Rev. 0

- 1
- 2
- 3
- 4
- 5
- 6

This page intentionally left blank.

RPP-ENV-58782, Rev. 0

9.0 INADVERTENT INTRUDER ANALYSIS

This section presents the analysis of the doses to a hypothetical individual who inadvertently intrudes into tanks or ancillary equipment at WMA C. The analyses were performed in accordance with DOE O 435.1 and DOE M 435.1-1 requirements. Guidance for the inadvertent intruder analysis comes from DOE G 435.1-1, which states the following:

“Although DOE is committed to retaining control of land containing residual radioactive material, such as disposed low-level waste, it is nonetheless appropriate to consider the impacts of potential inadvertent intrusion. Intrusion should be considered as an accident scenario which could occur during lapses of institutional controls. It is a hypothetical situation assumed simply to provide a basis for determining the acceptability of waste for near-surface disposal and may be used for establishing concentrations of radioactive material in a near-surface disposal facility.”

DOE G 435.1-1 states that the development of inadvertent intruder scenarios needs to be consistent with best management practices and other current industry standards, such as those issued by the NCRP and ICRP. In developing these scenarios, a supplemental document to DOE G 435.1-1 provides the following guidance on the groundwater pathway for use in the inadvertent intruder analysis (DOE G 435.1-2):

“The purpose of this [*the inadvertent intruder*] analysis is to provide a surrogate for the determination of LLW that is acceptable for near-surface disposal. The purpose of this analysis is not to protect future members of the public. As a result, the ingestion of contaminated water need not be considered as part of the inadvertent intruder analysis because protection of water resources is considered explicitly as one of the performance criteria for the performance assessment.”

Two types of exposure scenarios are considered to estimate dose to the hypothetical intruder: (1) acute scenarios and (2) chronic scenarios. Acute scenarios evaluate the dose received from well drilling and subsequent exposure to residual waste in the drill cuttings; exposure is evaluated over a short time period. Chronic scenarios evaluate the dose received from spreading the drill cuttings over a specific area while living and/or working on that area. One acute exposure scenario and three chronic exposure scenarios are evaluated in this PA, and brief descriptions of each scenario are provided in Table 9-1. The equations and input parameters are presented in the following sections, but additional details are provided in RPP-ENV-58813. Parameters common to all intruder scenarios are presented in Table 9-2.

Inadvertent intruder dose is calculated at times consistent with regulatory guidance contained in NUREG-1854. NUREG-1854 notes that it is inappropriate to strictly apply the waste classification system in 10 CFR 61.55 to tank farm residual wastes, because the underlying assumptions used in developing the generic waste classification system in 10 CFR 61.55 differ from the site-specific considerations at DOE tank farms. Nevertheless, NUREG-1854 further describes appropriate approaches for evaluating the conditions at DOE tank farms using the logic applied to the development of 10 CFR 61.55. They note that the depth to the waste and the use

RPP-ENV-58782, Rev. 0

of robust intruder barriers are the determining conditions for the type and timing of intruder scenarios. A robust intruder barrier is defined as one that will prevent intrusion into the waste for 500 years.

Table 9-1. Descriptions of the Inadvertent Intruder Scenarios Evaluated in the Waste Management Area C Performance Assessment.

Scenario	Description
Acute Exposure: Well Driller	Dose is the result of drilling through WMA C. Exposure pathways include external exposure, inhalation of soil particulates, and incidental soil ingestion. Exposure occurs during the drilling operation while in contact with the drill cuttings. Exposure does not depend on the borehole diameter.
Chronic Exposure: Rural Pasture	Dose is the result of drilling a well that serves a rural pasture. Contaminated drill cuttings are mixed with the soil over the pasture area. Exposure pathways include external exposure, inhalation of soil particulates, incidental soil ingestion, and milk consumption.
Chronic Exposure: Suburban Garden	Dose is the result of drilling a well that serves a suburban garden. Contaminated drill cuttings are mixed with the soil over the area where a residence and a garden are constructed. Exposure pathways include external exposure, inhalation of soil particulates, incidental soil ingestion, and fruit and vegetable consumption.
Chronic Exposure: Commercial Farm	Dose is the result of drilling a well that serves a commercial farm. Contaminated drill cuttings are mixed with the soil over the commercial farm area. Exposure pathways are external exposure, inhalation of soil particulates, and incidental soil ingestion.

Reference: RPP-ENV-58813, "Exposure Scenarios for Risk and Performance Assessments in Tank Farms at the Hanford Site, Washington."

NUREG-1854 concludes that for wastes at relatively shallow depths without robust intrusion barriers, it is appropriate to carry out the intrusion calculation at the end of institutional control: 100 years. For deeper wastes when robust intruder barriers exist, it is appropriate to assume that intrusion is prevented for at least 500 years, and therefore the intrusion calculation should be carried out at 500 years. For WMA C, these principles are applied by assuming that pipelines do not represent a significant intrusion barrier, and consequently the intrusion calculation is conducted beginning at 100 years after closure (end of institutional control period). By contrast, the tanks and infill grout represent very significant and robust barriers to intrusion, and therefore the intrusion calculation is conducted beginning at 500 years.

These principles are consistent with prior DOE and NRC approaches to evaluating inadvertent intrusion. DOE O 435.1 allows institutional controls to be effective in deterring intrusion for at least 100 years following closure.

Intruder scenarios are evaluated for each of the 19 waste sources (twelve 100-series tanks, four 200 series-tank, CR-vaults, C-301 catch tank and pipe line). The dose calculations are based on the emplaced radionuclide inventory in WMA C (considering radioactive decay and ingrowth), but ignoring any depletion due to transport of radionuclides from the waste site. The best-estimate inventory as mentioned in Tables 3-13a, 3-14a, and 3-15a is used for the intruder dose calculation. For all inadvertent intruder scenarios, the emplaced wastes are assumed to be distributed uniformly throughout the bottom area of the waste source.

RPP-ENV-58782, Rev. 0

Table 9-2. Parameters Common to the Inadvertent Intruder Scenarios.

Parameter	Notation	Value	Unit	Reference
Radionuclide concentration in residual waste	C_{ws}	Isotope-specific	pCi/g	Source term-specific
Soil dry bulk density for soil layers below WMA C	ρ_{sl}	2.05	g/cm ³	Site-specific
Bulk density of residual waste	ρ_{ws}	2.05	g/cm ³	Site-specific
Time of intrusion	t	100 years and 500 years after closure	year	DOE O 435.1
Radionuclide half-life	$t_{1/2}$	Isotope-specific	Year	ICRP 2008
Decay constant	λ	Isotope-specific	(year) ⁻¹	ICRP 2008
Depth to groundwater	Z_{gw}	7,900	cm	Site-specific
Thickness of wastes intercepted by the borehole	Z_{ws}	Calculated	cm	Source term-specific

DOE = U.S. Department of Energy

WMA = Waste Management Area

ICRP = International Commission on Radiological Protection

References:

DOE O 435.1, Radioactive Waste Management.

"ICRP Publication 107: Nuclear Decay Data for Dosimetric Calculations" (ICRP 2008).

According to RPP-PLAN-47559, there are ~11.2 km (7 mi) of pipelines at WMA C, with the majority of pipelines being pumped waste transfer pipelines (98% by length) and the remaining being gravity-fed cascade lines between the 100-series SSTs (including one known plugged pipeline, V122). The waste transfer pipelines are assumed to be 5% full, while the cascade lines (including pipeline V122) are assumed to be fully plugged and the residual inventory is estimated using average BBI concentration for retrieved tanks (Section 3.2.2.4.4). The waste transfer pipelines are more likely to be intruded as they cover 98% of the total pipeline length and correspondingly the area over which pipelines are distributed within WMA C. Based on assumptions and justifications in RPP-PLAN-47559, intrusion is considered through the 7.6-cm (3-in.)-diameter waste transfer pipeline (the most common pipe diameter) that is assumed to be 5% full of waste. Impact of improbable intrusion through a fully plugged cascade pipeline is evaluated as part of the sensitivity analysis to estimate the bounding dose.

9.1 CONSIDERATION OF THE PROBABILITY OF INTRUSION

As discussed in DOE G 435.1-1, NCRP Report No. 152, and NUREG-1854, the primary purpose of intrusion analyses is to establish waste classification identifying wastes appropriate for near-surface disposal. An intrusion calculation is not intended to represent a realistic calculation of doses to a future member of the public, but rather a stylized representation of hypothetical doses to people living in the future under extreme scenarios of uncertain but generally very low likelihood. The analyses are therefore usually carried out as deterministic calculations assuming

RPP-ENV-58782, Rev. 0

1 the occurrence of the intrusion event without regard to the likelihood of their occurrence, and the
2 deterministic results have the potential to be misinterpreted as representing a higher risk than
3 they actually do.

4
5 Therefore, in this section a qualitative discussion is presented on the likelihood of inadvertent
6 human intrusion at WMA C. This discussion is intended solely to help put intrusion results in a
7 risk-informed context; likelihoods of occurrence are not considered explicitly or included in any
8 further regulatory use of the intrusion analysis results.

9
10 The only credible potential intrusion event at WMA C is a drilling intrusion, owing to the depth
11 of the wastes (greater than 5 m after the modified RCRA Subtitle C barrier is put in place) in the
12 final closed facility. For a drilling event to intersect the waste, exhume contamination, and lead
13 to exposures to that contamination, a series of necessary events must occur, as shown in
14 Figure 9-1. These events can generally be regarded as independent, and each can only occur if
15 all of the previous necessary events have occurred. If at any stage of the sequence the necessary
16 event does not occur, the overall intrusion event will not occur. Also shown on the figure are a
17 set of precursor conditions that help to understand the likelihood of occurrence of each necessary
18 event. The precursor conditions relate to issues such as societal change, and motivations and
19 actions of the intruder. As such they are not readily amenable to rigorous probabilistic
20 calculation, but the evolution of each over the post-closure performance period can be
21 qualitatively assessed, supported by logical arguments.

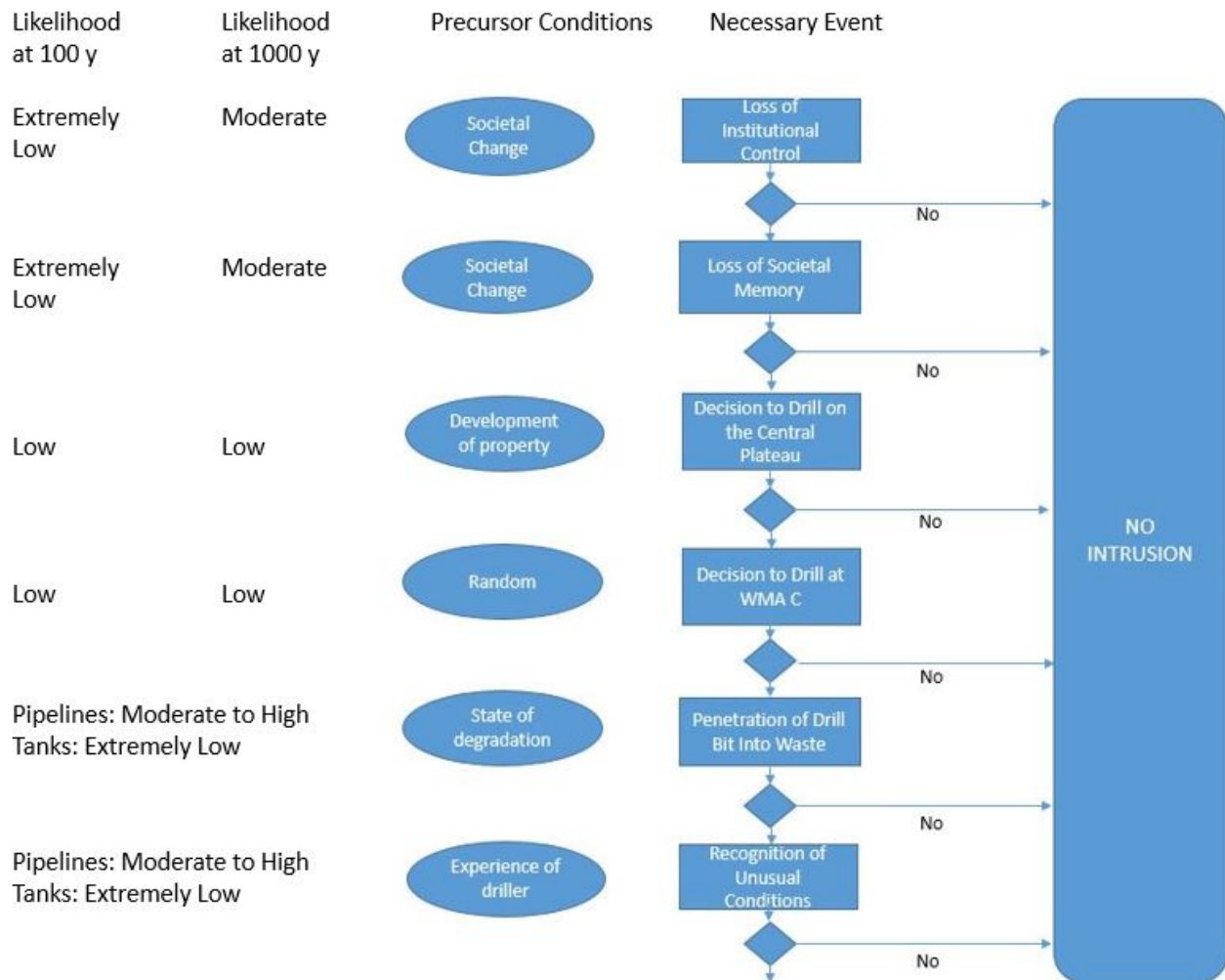
22
23 The initial necessary event leading to intrusion is the loss of institutional control. It is reasonable
24 to assume that as long as DOE and the U.S. Government exist, some form of governmental
25 control over the Central Plateau will be maintained as required under DOE P 454.1¹. Therefore,
26 a precursor condition to the loss of control would be an unforeseen major change in the
27 governance of the United States, to the extent that previously-established administrative controls
28 would be forgotten or deliberately disregarded. Such possibilities are regarded as extremely low
29 over the next 100 years, but moderate over 1,000 years. Such judgments are, of course, a
30 function of the optimism or pessimism with which one regards the future, but the general trend
31 should be for increasing likelihood of such changes over increasing longer time periods.

32
33 The second necessary event in the chain is the loss of societal memory of the existence of the
34 Hanford Site, and of waste disposal activities in the Central Plateau. This would involve both
35 loss of individuals' knowledge of the existence of Hanford as well as the loss of relevant records
36 and deed restrictions that would warn future inhabitants of the residual hazards existing under the
37 Central Plateau. The precursor condition for this event is similar to the loss of institutional
38 control: a profound societal change with disruption of the continuity of government. The loss of
39 memory is regarded as less likely than the loss of institutional control, since governmental
40 records of land ownership and deed restrictions are often maintained even when profound
41 changes in governments occur. Nevertheless, as time increases, there is an increasing likelihood
42 that such an event will occur.

¹ This policy specifically states the following: "DOE will maintain the institutional controls as long as necessary to perform their intended protective purposes and seek sufficient funds."

RPP-ENV-58782, Rev. 0

Figure 9-1. Sequence of Events Necessary for Inadvertent Human Intrusion at Waste Management Area C.



The third necessary event would be a decision to drill on the Central Plateau. The likelihood that this would occur is dependent on the motivation for drilling for water, so the precursor condition is a desire for some sort of property development on the Central Plateau that needs a source of water, such as a housing project or farm. It is also dependent on a desire to drill a local well rather than pump water from the Columbia River. This event is also conditional on the loss of institutional control and memory of Hanford; it is therefore reasonable to assume that in the absence of the Hanford worker base the population of the area would be substantially smaller than today, and would be concentrated closer to the river and focused on agriculture. Given these considerations, the likelihood that this event will occur is considered low; these motivational issues would not necessarily change in time, so it is regarded as low throughout the performance period.

The fourth necessary event would be a decision to drill at WMA C given the previous decision to drill on the Central Plateau, and furthermore to drill in a spot that would intersect residual contamination. In the absence of notable distinguishing features to modify the likelihood across

RPP-ENV-58782, Rev. 0

the Central Plateau, this can be regarded as a purely random decision. Therefore, in this case one could in principle evaluate the probability using the ratios of the area of WMA C to the area of the Central Plateau multiplied by the area of tanks or ancillary equipment over the area of WMA C. This event is the first in the chain of events that allows one to distinguish between the likelihood of intrusion into tanks as opposed to ancillary equipment. This likelihood depends on the definitions of these areas, but is low to extremely low for both tanks and ancillary equipment, and does not change in time.

The fifth necessary event is the penetration of the drill bit into waste. Here there is a clear distinction between drilling into tanks and drilling into ancillary equipment. The conditional likelihood, assuming all the previous events have occurred, of drilling into waste is reasonably high for pipelines, and would increase as the pipelines degrade in time. By contrast, it is extremely low for tanks, owing to the integrity and strength of the structure of the tank and infill grout. There are not expected to be significant changes in the structural integrity of the tanks and grout over the performance period (see Section 6.2.1.2 for estimates of the longevity of tank structures), and the likelihood of intrusion into a tank remains very small until much longer times in the future when the tank and infill grout may be considered degraded.

The sixth and final necessary event would be that the driller would not recognize that the drill had encountered unusual conditions as they drill to the depth of the waste. The conditional likelihood, assuming all the previous events have occurred, of not recognizing that one has hit a pipeline is reasonably high, and would increase as the pipelines degrade in time. By contrast, to reach residual material in a tank one must traverse an extended thickness of unusual material that would be obvious to the driller. The precursor condition for this necessary event to occur would be that the driller would have to be inexperienced or inattentive to not recognize the unusual nature of the tank and grout materials in the well bore. It is regarded as extremely unlikely that someone would not notice this, and would penetrate to the depth of the residual waste. Furthermore, the conditional likelihood of this event would not increase even at very long times when the tank materials may be structurally degraded, because the texture and color of the grout will continue to be easily distinguishable from the surrounding sands for the indefinite future.

Since these events are independent and sequential, one could in principle assign numerical conditional probabilities to each and calculate a joint probability of occurrence of the sequence as the product of the probabilities. Given the speculative and judgmental nature of any assessment of the precursor conditions, using such numerical probabilities is not recommended for this analysis. However, from a qualitative viewpoint, one can say that multiplying six low to extremely low numbers together would give a vanishingly small joint probability of the entire sequence occurring, regardless of the specific assignment of numerical values. It can therefore be concluded that the likelihood of occurrence into tanks at WMA C is vanishingly small, while the likelihood of intrusion into a pipeline is also very small, but somewhat larger than for tanks.

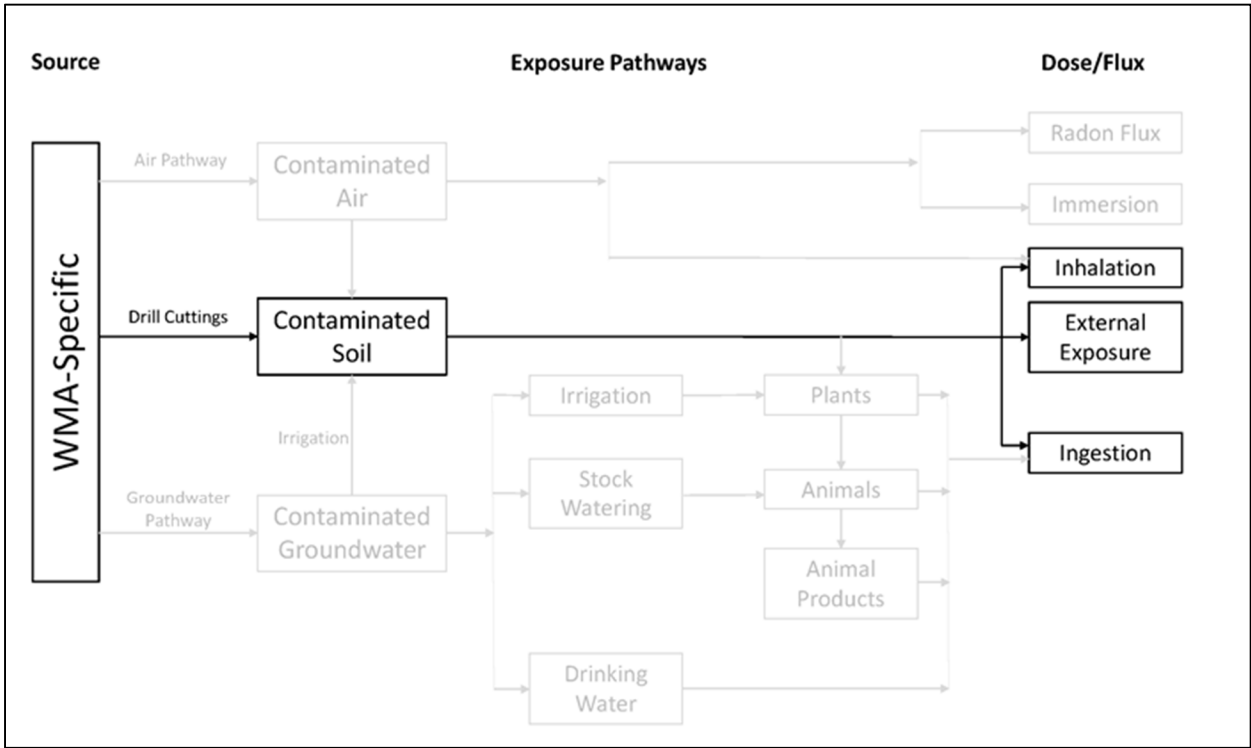
9.2 ACUTE EXPOSURE SCENARIOS

A single acute hypothetical inadvertent intruder exposure scenario is evaluated for the WMA C tank farm PA. This scenario evaluates the short-term exposure of a well driller to drill cuttings

that are exhumed from a well that is installed to the depth of the water table for the supply of water. As the well is drilled through the WMA C tank farm waste residuals, the driller will be exposed to the radiation dose from the drill cuttings. The well driller is assumed to be exposed to drill cuttings for a total of five days (8 hours per day for a total of 40 hours). The dose is calculated by assuming that the cuttings are uniformly spread across the drill pad and are not diluted by mixing with clean soil. As discussed above, the timing of the intrusion event is assumed to be 100 years for pipelines and 500 years for more highly stabilized wastes with robust intrusion barriers.

The borehole diameter is not a factor in determining dose for this scenario because the radionuclide concentrations in the drill cuttings are independent of the size of the borehole, and because the cuttings are assumed to be distributed over the drill pad with no mixing with clean soil. For the purpose of calculating dose from external exposure, the thickness and lateral extent of the contaminated layer is assumed to be infinite. Exposure pathways evaluated for the well driller scenario are incidental soil ingestion, inhalation of soil particulates, and direct external exposure as illustrated in Figure 9-2. Exposure parameters for the acute well driller scenario are provided in Table 9-3. Radionuclide-specific shielding factors and dose conversion factors are presented in Section 6.3.3, Tables 6-24 and 6-25, respectively.

Figure 9-2. Exposure Pathways Considered in the Inadvertent Intruder Acute Well Driller Scenario.



WMA = Waste Management Area

The intruder dose scenario is applied to an adult receptor but the dose conversion factors are derived for a Representative Person (Section 6.3.3.1). This is a conservative simplification

RPP-ENV-58782, Rev. 0

because these dose conversion factors represent effective dose coefficients calculated for a Reference Person and are generally marginally greater than that for the adult.

Table 9-3. Exposure Parameters for the Acute Well Driller Exposure Scenario.

Parameter	Notation	Value	Units	Reference
Radionuclide concentration in drill cuttings	C_{ds}	Calculated	pCi/g	—
Area of the well	A_{well}	1,379.51	cm ²	HNF-SD-WM-TI-707, Rev. 5
Diameter of the well	D_{well}	41.91	cm	HNF-SD-WM-TI-707, Rev. 5
Soil ingestion rate – well driller	$IR_{s,wd}$	100	mg/day	OSWER Directive 9285.6-03
Exposure frequency – well driller	EF_{wd}	5	days/yr	HNF-SD-WM-TI-707, Rev. 5
Enrichment factor	Ef	4	unitless	NCRP Report No. 129
Outdoor inhalation rate – well driller	$INH_{out,wd}$	12,775	m ³ /yr	NCRP Report No. 129
Mass loading factor	M	6.66E-05	g/m ³	ICRP 1994
Fraction of time spent outdoors	$t_{out,wd}$	0.0046	unitless	HNF-SD-WM-TI-707, Rev. 5 (40 hours in a year)
Unit conversion factor	UCF_1	0.001	g/mg	0.001 g = 1 mg

ICRP = International Commission on Radiological Protection

NCRP = National Council on Radiation Protection

References:

HNF-SD-WM-TI-707, “Exposure Scenarios and Unit Factors for the Hanford Tank Waste Performance Assessment.”

“ICRP Publication 66: Human Respiratory Tract Model for Radiological Protection” (ICRP 1994).

NCRP Report No. 129, “Recommended Screening Limits for Contaminated Surface Soil and Review of Factors Relevant to Site-Specific Studies.”

OSWER Directive 9285.6-03, Risk Assessment Guidance for Superfund, Volume I: Human Health Evaluation Manual, Supplemental Guidance “Standard Default Exposure Factors” Interim Final.

9.2.1 Radionuclide Concentration in Drill Cuttings

Radionuclide concentrations in the drill cuttings are calculated as shown in Equations 9-1 through 9-3 (RPP-ENV-58813).

$$A_{well} = \pi \times \left(\frac{d_{well}}{2} \right)^2 \quad (9-1)$$

$$C_{ds} = \frac{C_{ws} \times A_{well} \times Z_{ws} \times \rho_{ws}}{A_{well} \times Z_{ws} \times \rho_{ws} + A_{well} \times (Z_{gw} - Z_{ws}) \times \rho_{sl}} = \frac{C_{ws} \times Z_{ws} \times \rho_{ws}}{Z_{ws} \times \rho_{ws} + (Z_{gw} - Z_{ws}) \times \rho_{sl}} \quad (9-2)$$

Because bulk density of residual waste and the soil is very similar, to simplify the equations it is assumed that $\rho_{ws} = \rho_{sl}$. As a result, the above equation simplifies to:

$$C_{ds} = \frac{C_{ws} \times Z_{ws}}{Z_{gw}} \quad (9-3)$$

RPP-ENV-58782, Rev. 0

Where:

- A_{well} = area of well (cm²)
- d_{well} = diameter of well (cm)
- C_{ds} = radionuclide concentration in drill cuttings (pCi/g)
- C_{ws} = radionuclide concentration in the residual waste (pCi/g), varies as a function of time due to radioactive decay and ingrowth
- Z_{ws} = thickness of waste intercepted by borehole (cm)
- ρ_{ws} = residual waste bulk density (g/cm³)
- Z_{gw} = depth to groundwater (cm)
- ρ_{sl} = soil dry bulk density for soil layers below WMA C (g/cm³).

The following sections provide the equations used to calculate dose for this scenario.

9.2.2 Acute Well Driller Scenario – Incidental Soil Ingestion

The following equation is used to calculate dose to the well driller resulting from incidental ingestion of soil (RPP-ENV-58813):

$$D_s = C_{ds} \times IR_{s,wd} \times EF_{wd} \times UCF_1 \times DCF_{ing} \quad (9-4)$$

Where:

- D_s = dose resulting from incidental soil ingestion (mrem/yr)
- C_{ds} = radionuclide concentration in drill cuttings (pCi/g)
- $IR_{s,wd}$ = soil ingestion rate – well driller (mg/day)
- EF_{wd} = exposure frequency – well driller (days/yr)
- UCF_1 = unit conversion factor (g/mg)
- DCF_{ing} = ingestion dose conversion factor (mrem/pCi).

9.2.3 Acute Well Driller Scenario – Inhalation of Soil Particulates

The following equation is used to calculate dose to the well driller resulting from inhalation of soil particulates (RPP-ENV-58813):

$$D_{inh} = C_{ds} \times E_f \times INH_{out,wd} \times M \times t_{out,wd} \times DCF_{inh} \quad (9-5)$$

Where:

- D_{inh} = dose resulting from inhalation of soil (mrem/yr)
- C_{ds} = radionuclide concentration in drill cuttings (pCi/g)
- E_f = enrichment factor (unitless)
- $INH_{out,wd}$ = outdoor inhalation rate – well driller (m³/yr)
- M = mass loading factor (g/m³)

RPP-ENV-58782, Rev. 0

$t_{out,wd}$ = fraction of time spent outdoors – well driller (unitless)
 DCF_{inh} = inhalation dose conversion factor (mrem/pCi).

9.2.4 Acute Well Driller Scenario – External Exposure

The following equation is used to calculate dose to the well driller resulting from external exposure (RPP-ENV-58813):

$$D_{ext} = C_{ds} \times t_{out,wd} \times DCF_{ext} \quad (9-6)$$

Where:

D_{ext} = dose resulting from external exposure to drill cuttings (mrem/yr)
 C_{ds} = radionuclide concentration in drill cuttings (pCi/g)
 $t_{out,wd}$ = fraction of time spent outdoors by well driller (unitless)
 DCF_{ext} = external exposure dose conversion factor (mrem/yr)/(pCi/g).

9.3 CHRONIC SCENARIOS

Three chronic hypothetical inadvertent intruder exposure scenarios are evaluated for the WMA C tank farm PA which are representative of lifestyles in and around the Hanford Site. These scenarios evaluate the long-term exposure of three different receptors from previously exhumed drill cuttings that have been uniformly spread and tilled onto three different land areas or target fields. The three different target fields include the following: a rural pasture, a suburban garden, and a commercial farm. Radionuclide concentrations in the target field are dependent on the diameter of the well that is drilled to support the scenario, the area of the target field over which the drill cuttings are spread, and the depth to which the drill cuttings are tilled into the soil. In the chronic scenarios, the exposed individual does not drill or add the cuttings to the soil but simply lives or works on the land where the cuttings have been spread and tilled into the soil.

Based on well log data from the State of Washington from 1960 to 2003, the diameter of boreholes can range from 2.5 cm (1 in.) up to 76 cm (30 in.), with about 70% of the domestic water wells having about a 16.5-cm (6.5-in.) diameter (HNF-SD-WM-TI-707, “Exposure Scenarios and Unit Factors for the Hanford Tank Waste Performance Assessment”). Although a 16.5-cm (6.5-in.) well diameter may be common, it is not considered representative for the target fields in each scenario. Although irrigation of a rural pasture is a small-scale operation, it typically requires a larger diameter well because a larger pump is needed as compared to a normal well that is used for domestic purposes. Therefore, a well diameter of 26.67 cm (10.5 in.) was selected for the rural pasture scenario, and a 16.5-cm (6.5-in.) well diameter was selected for the suburban garden scenario. Similarly, a commercial farm using irrigation would require a larger diameter well than the rural pasture to extract water at a higher flow rate. As a result, a well diameter of 41.91 cm (16.5 in.) was selected for the commercial farm scenario. The size of target fields also varies over a broad range. The sizes of the target fields selected are 5,000 m² (1.24 acre) for the rural pasture scenario, 2,500 m² (0.62 acre) for the suburban garden scenario, and 64,750,000 m² (160 acre) for the commercial farm scenario (HNF-SD-WM-TI-707). In

RPP-ENV-58782, Rev. 0

selecting the well diameters and target field areas, characteristics specific to the Hanford Site and values selected from previous PAs were considered. Sensitivity analyses provide confidence that the calculated performance parameters are robust enough to support sound decisions.

The intruder dose scenario is applied to an adult receptor but the dose conversion factors are derived for a Representative Person (Section 6.3.3.1). This is a conservative simplification because these dose conversion factors represent effective dose coefficients calculated for a Reference Person and are generally marginally greater than that for the adult. The various exposure parameters used in the dose calculations were selected from DOE and EPA guidance documents, and from national and international standards such as the NCRP and ICRP, as appropriate for an adult. The exposure pathways are determined by the use of the target field.

9.3.1 Chronic Rural Pasture Scenario

The rural pasture scenario evaluates the long-term exposure to an individual who uses the target field as a residence, with a pasture used for milk production from dairy cows. In this scenario, a well diameter of 26.67 cm (10.5 in.) is assumed, the drill cuttings are spread over a pasture area of 5,000 m² (1.24 acre), and the cuttings are tilled to a depth of 15 cm (5.9 in.). This scenario represents an individual who resides and has a pasture on the target field area. The pasture is used to raise dairy cattle that eat fodder grown from the pasture, and the resident subsequently drinks the pasture cows' milk. In addition to exposure from milk consumption, the resident is exposed by incidental soil ingestion, inhalation of the soil particulates, and external exposure; these exposure pathways are illustrated in Figure 9-3. Exposure parameters for the chronic rural pasture scenario are provided in Table 9-4. Element-specific bioconcentration factors, radionuclide-specific shielding factors, and dose conversion factors are presented in Section 6.3.3, Tables 6-23, 6-24 and 6-25, respectively.

9.3.1.1 Radionuclide Activity in Drill Cuttings. The concentration of radionuclides in pasture soil resulting from the drill cuttings is determined by first calculating the activity of each radionuclide in the drill cuttings, and then calculating the radionuclide concentration in the pasture soil. Equation 9-7 and Equation 9-8 are used to calculate the radionuclide activities and radionuclide concentrations for all three of the chronic scenarios. The differences in radionuclide activities for each scenario are the well diameters and the depth that the drill cuttings are tilled into the soil of the target field (rural pasture, suburban garden, or commercial farm).

The following equation is used to calculate the total radionuclide activity in the drill cuttings (RPP-ENV-58813):

$$S_A = T_A \times \left(\frac{A_{well}}{A_{source_term}} \right) \quad (9-7)$$

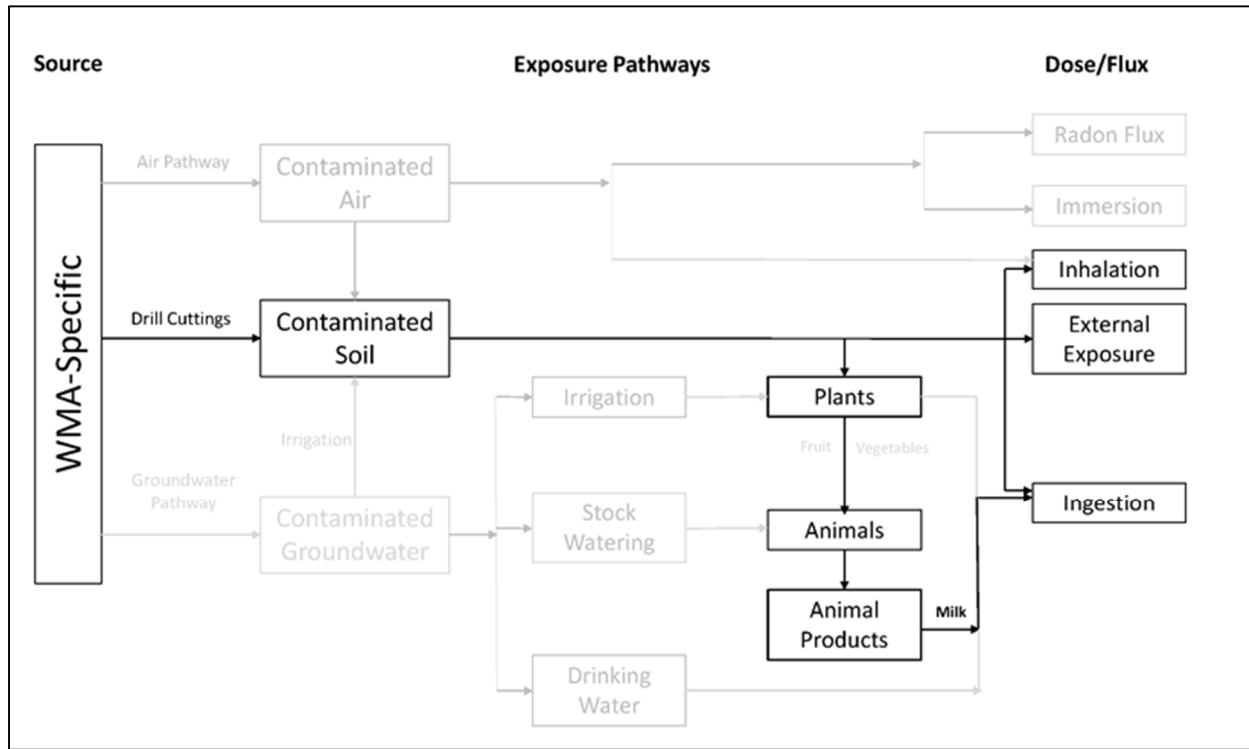
Where:

S_A = radionuclide activity in drill cuttings (pCi) at any given time
 T_A = residual radionuclide activity in the source term (pCi), varies with time due to radioactive decay and ingrowth

RPP-ENV-58782, Rev. 0

A_{well} = area of the well (cm²)
 A_{source_term} = area over which the residual waste is spread in the source term (cm²).

Figure 9-3. Exposure Pathways Considered for the Inadvertent Intruder Chronic Rural Pasture Exposure Scenario.



WMA = Waste Management Area

For the pipeline source term, the activity in the drill cuttings is based on the contaminated pipeline area that is interrogated by the borehole. If the borehole diameter is greater than the pipeline diameter, then the width of the contaminated zone is restricted to the pipeline diameter.

9.3.1.2 Radionuclide Concentrations in Pasture Soil. The following equation is used to calculate the radionuclide concentration in the pasture soil (RPP-ENV-58813):

$$C_{ps} = \frac{S_A}{A_p \times Z_p \times \rho_p + A_{well} \times Z_{gw} \times \rho_s} \quad (9-8)$$

Where:

C_{ps} = radionuclide concentration in pasture soil (pCi/g) at any given time
 S_A = radionuclide activity in soil from drill cuttings (pCi/g) at any given time
 A_p = area of the pasture (cm²)
 Z_p = depth the drill cuttings are tilled into the pasture (cm)
 ρ_p = soil dry bulk density in the pasture (g/cm³)
 A_{well} = area of the well (cm²)

RPP-ENV-58782, Rev. 0

Z_{gw} = depth to groundwater (cm)
 ρ_s = dry bulk density of the drill cuttings (g/cm³).

**Table 9-4. Exposure Parameters for the Chronic Rural Pasture Exposure Scenario.
(2 sheets)**

Parameter	Notation	Value	Units	Reference
Area over which residual waste is spread	$A_{\text{source_term}}$	Calculated	cm ²	Source term-specific
Area of the well	A_{well}	558.6	cm ²	HNF-SD-WM-TI-707, Rev. 5
Diameter of the well	D_{well}	26.67	cm	HNF-SD-WM-TI-707, Rev. 5
Area of rural pasture	A_p	5.00E+07	cm ²	HNF-SD-WM-TI-707, Rev. 5
Tilled depth of rural pasture	Z_p	15	cm	HNF-SD-WM-TI-707, Rev. 5
Soil ingestion rate – resident	$IR_{s,rp}$	100	mg/day	OSWER Directive 9285.6-03
Exposure frequency – resident	EF_{rp}	350	days/yr	OSWER Directive 9285.6-03
Milk ingestion rate	IR_m	155.96	L/yr	EPA/600/R-090/052F
Fraction of locally-produced dairy products that are consumed	F_a	1	unitless	PRGfR 2015
Water ingestion rate for dairy cattle	$IR_{w,d}$	92	L/day	PRGfR 2015
Radionuclide concentration in water consumed by dairy cattle	C_w	0	pCi/L	No groundwater contamination assumed
Soil ingestion rate for dairy cattle	$IR_{s,d}$	0.41	kg/day	PRGfR 2015
Radionuclide concentration in pasture soil consumed by dairy cattle	C_{ps}	Isotope-specific	pCi/g	Source term-specific
Fodder ingestion rate for dairy cattle	$IR_{\text{fodder},d}$	16.9	kg/day	PRGfR 2015
Pasture-soil bioconcentration factor through uptake	B_p	Isotope-specific	(pCi/kg dry weight of crop)/(pCi/kg dry weight of soil)	See Table 6-23
Pasture-soil bioconcentration factor from resuspension processes	B'_p	0.1	(pCi/kg dry weight of crop)/(pCi/kg dry weight of soil)	NCRP Report No. 129

RPP-ENV-58782, Rev. 0

**Table 9-4. Exposure Parameters for the Chronic Rural Pasture Exposure Scenario.
(2 sheets)**

Parameter	Notation	Value	Units	Reference
Enrichment factor	E_f	0.7	unitless	NCRP Report No. 129
Indoor inhalation rate – resident	$INH_{in,r}$	7,300	m ³ /yr	NCRP Report No. 129
Mass loading factor	M	6.66E-05	g/m ³	NCRP Report No. 129
Fraction of time spent indoors – rural pasture	$t_{in,rp}$	0.656	unitless	PRGfR 2015 (16.42 hours per day, 350 days per year)
Outdoor inhalation rate – rural pasture	$INH_{out,rp}$	9,125	m ³ /yr	NCRP Report No. 129
Fraction of time spent outdoors – rural pasture	t_{out}	0.16	unitless	HNF-SD-WM-TI-707, Rev. 5 (4 hours per day, 350 days per year)
Ratio of radionuclide concentrations in indoor versus outdoor air	I/O	0.3	unitless	NCRP Report No. 129
Unit conversion factor	UCF_1	0.001	g/mg	0.001 g = 1 mg
Unit conversion factor	UCF_2	1,000	g/kg	1,000 g = 1 kg

NCRP = National Council on Radiation Protection

References:

EPA/600/R-090/052F, Exposure Factors Handbook: 2011 Edition.

HNF-SD-WM-TI-707, "Exposure Scenarios and Unit Factors for the Hanford Tank Waste Performance Assessment."

NCRP Report No. 129, "Recommended Screening Limits for Contaminated Surface Soil and Review of Factors Relevant to Site-Specific Studies."

OSWER Directive 9285.6-03, Risk Assessment Guidance for Superfund, Volume I: Human Health Evaluation Manual, Supplemental Guidance "Standard Default Exposure Factors" Interim Final.

Preliminary Remediation Goals for Radionuclides (PRGfR), Queried 07/2015, [PRG User's Guide], http://epa-prgs.ornl.gov/radionuclides/prg_guide.html.

9.3.1.3 Chronic Rural Pasture Scenario – Incidental Soil Ingestion. The following equation is used to calculate dose to the rural pasture resident resulting from incidental ingestion of pasture soil (RPP-ENV-58813):

$$D_s = C_{ps} \times IR_{s,rp} \times EF_{rp} \times UCF_1 \times DCF_{ing} \quad (9-10)$$

Where:

 D_s = dose resulting from incidental soil ingestion (mrem/yr) C_{ps} = radionuclide concentration in pasture soil (pCi/g) at any given time $IR_{s,rp}$ = soil ingestion rate – rural pasture (mg/day) EF_{rp} = exposure frequency – rural pasture (days/yr)

RPP-ENV-58782, Rev. 0

UCF_1 = unit conversion factor (g/mg)

DCF_{ing} = ingestion dose conversion factor (mrem/pCi).

9.3.1.4 Chronic Rural Pasture Scenario – Consumption of Milk. The following equations are used to calculate the concentration of contaminant in livestock fodder, the concentration of contaminant in milk, and the dose from consumption of milk (RPP-ENV-58813).

The equation used to calculate the concentration of contaminant in livestock fodder is given by:

$$C_{fodder} = C_{ps} \times (B_p + B'_p) \quad (9-11)$$

Where:

C_{fodder} = radionuclide concentration in livestock fodder (pCi/g) at any given time

C_{ps} = radionuclide concentration in the pasture soil (pCi/g) at any given time

B_p = pasture-soil bioconcentration factor through uptake $\left(\frac{\left(\frac{pCi}{kg \text{ dry weight of fodder}} \right)}{\left(\frac{pCi}{kg \text{ dry weight of soil}} \right)} \right)$

B'_p = pasture-soil bioconcentration factor for resuspension effects

$$\left(\frac{\left(\frac{pCi}{kg \text{ dry weight of fodder}} \right)}{\left(\frac{pCi}{kg \text{ dry weight of soil}} \right)} \right).$$

The following equation is used to calculate the concentration of contaminant in milk resulting from consumption of contaminated water (if any), contaminated fodder, and contaminated soil by the dairy animal:

$$C_m = (C_w \times IR_{w,d} + C_{fodder} \times IR_{fodder,d} \times UCF_2 + C_{ps} \times IR_{s,d} \times UCF_2) \times BCF_{milk} \quad (9-12)$$

Where:

C_m = radionuclide concentration in milk (pCi/L) at any given time

C_w = radionuclide concentration in water (pCi/L) at any given time (assumed zero for the intruder scenario)

$IR_{w,d}$ = ingestion rate of water by dairy cattle (L/day)

$IR_{fodder,d}$ = ingestion rate of fodder by dairy cattle (kg/day)

UCF_2 = unit conversion factor (g/kg)

C_{ps} = radionuclide concentration in the pasture soil (pCi/g) at any given time

$IR_{s,d}$ = ingestion rate of soil by dairy cattle (kg/day)

BCF_{milk} = bioconcentration factor of radionuclides in milk (day/L).

The equation used to calculate the dose from ingestion of milk is given by:

$$D_m = C_m \times IR_m \times F_a \times DCF_{ing} \quad (9-13)$$

RPP-ENV-58782, Rev. 0

Where:

- D_m = dose resulting from ingestion of milk (mrem/yr)
- C_m = radionuclide concentration in milk (pCi/L) at any given time
- IR_m = milk ingestion rate (L/yr)
- F_a = fraction of locally-produced milk that is consumed (unitless)
- DCF_{ing} = ingestion dose conversion factor (mrem/pCi).

9.3.1.5 Chronic Rural Pasture Scenario – Inhalation of Soil Particulates. The following equation is used to calculate dose to the rural pasture resident resulting from inhalation of dust particulates (RPP-ENV-58813):

$$D_{inh} = C_{ps} \times E_f \times M \times \left(INH_{in,rp} \times t_{in,rp} \times \left(\frac{I}{O} \right) + INH_{out,rp} \times t_{out,rp} \right) \times DCF_{inh} \quad (9-14)$$

Where:

- D_{inh} = dose resulting from inhalation of soil
- C_{ps} = the radionuclide concentration in the pasture soil surface layer (pCi/g)
- E_f = enrichment factor (unitless)
- M = mass loading factor (g/m³)
- $INH_{in,rp}$ = indoor inhalation rate – rural pasture (m³/yr)
- $t_{in,rp}$ = fraction of time spent indoors – rural pasture (unitless)
- $\frac{I}{O}$ = ratio of radionuclide concentrations in indoor and outdoor air (unitless)
- $INH_{out,rp}$ = outdoor inhalation rate – rural pasture (m³/yr)
- $t_{out,rp}$ = fraction of time spent outdoors – rural pasture (unitless)
- DCF_{inh} = inhalation dose conversion factor (mrem/pCi).

9.3.1.6 Chronic Rural Pasture Scenario – External Exposure. The following equation is used to calculate dose to the rural pasture resident resulting from external exposure (RPP-ENV-58813):

$$D_{ext} = C_{ps} \times (t_{in,rp} \times \varepsilon + t_{out,rp}) \times DCF_{ext} \quad (9-15)$$

Where:

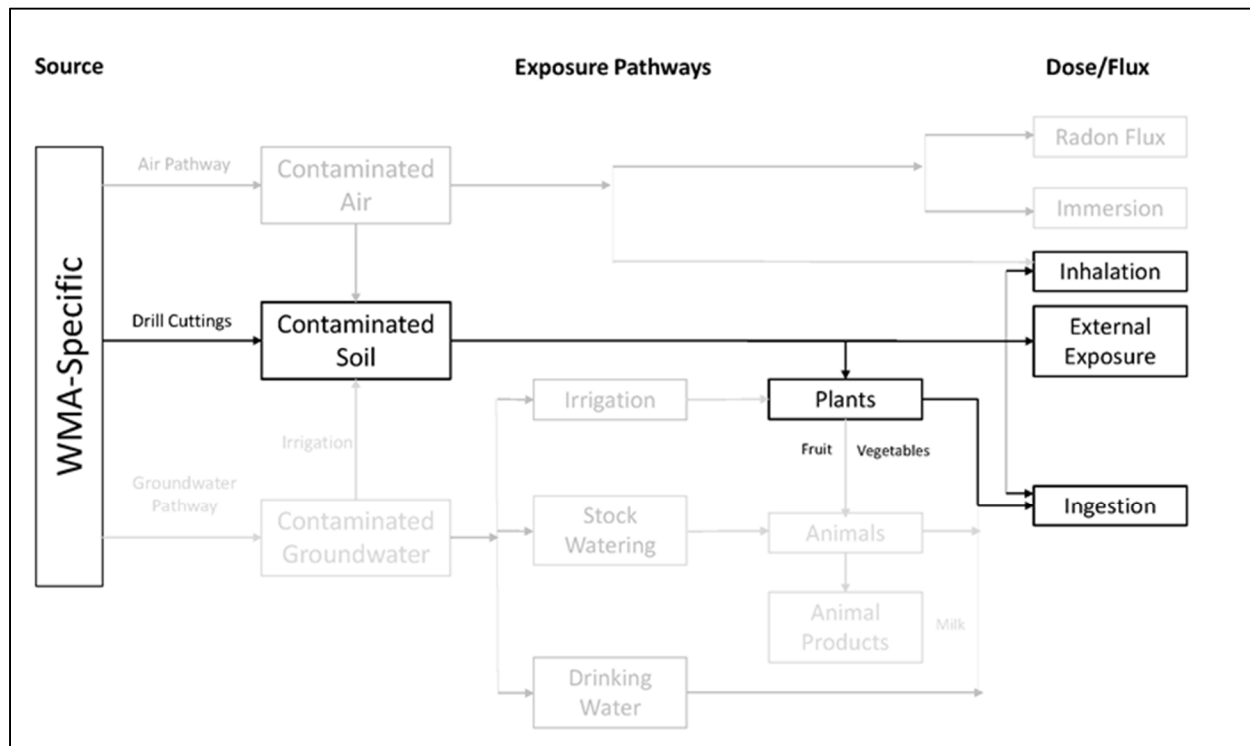
- D_{ext} = dose resulting from external exposure to pasture soil (mrem/yr)
- C_{ps} = radionuclide concentration in the pasture soil (pCi/g) at any given time
- $t_{in,rp}$ = fraction of time spent indoors – rural pasture (unitless)
- ε = transmission or shielding factor (unitless)
- $t_{out,rp}$ = fraction of time spent outdoors – rural pasture (unitless)
- DCF_{ext} = external exposure dose conversion factor (mrem/yr)/(pCi/g).

RPP-ENV-58782, Rev. 0

9.3.2 Chronic Suburban Garden Scenario

The suburban garden scenario evaluates the long-term exposure to an individual who uses the target field as a home construction lot with a garden. In this scenario, a well diameter of 16.51 cm (6.5 in.) is assumed that was drilled prior to the construction of the house and garden, and the drill cuttings are spread over the 2,500-m² (0.62-acre) lot and tilled to a depth of 15 cm (5.9 in.). The size of the home garden was chosen to be 100 m² (1,076 ft²) based on the discussions presented in Revision 5 of HNF-SD-WM-TI-707, where this garden size was deemed reasonable to provide 25% of the daily vegetable diet for a family of four living in the home. In addition to exposure from fruit and vegetable consumption, the resident is exposed by incidental soil ingestion, inhalation of the soil particulates, and external exposure; these exposure pathways are illustrated in Figure 9-4. Exposure parameters for the chronic suburban garden scenario are provided in Table 9-5.

Figure 9-4. Exposure Pathways Considered in the Inadvertent Intruder Chronic Suburban Garden Exposure Scenario.



WMA = Waste Management Area

As discussed in Section 9.3.1.1, Equation 9-7 is used to calculate the radionuclide activities, and Equation 9-8 is used to calculate the radionuclide concentrations for the suburban garden scenario (C_{gs}), with corresponding well area and target field area (home construction lot). Element-specific bioconcentration factors, radionuclide-specific shielding factors, and dose conversion factors are presented in Section 6.3.3, Tables 6-23, 6-24 and 6-25 respectively.

RPP-ENV-58782, Rev. 0

Table 9-5. Exposure Parameters for the Chronic Suburban Garden Exposure Scenario. (2 sheets)

Parameter	Notation	Value	Units	Reference
Radionuclide concentration in garden soil	C_{gs}	Calculated	pCi/g	Equation 9-8
Area over which residual waste is spread	A_{source_term}	Calculated	cm ²	Source term-specific
Diameter of the well	D_{well}	16.51	cm	HNF-SD-WM-TI-707, Rev. 5
Area of the well	A_{well}	214.08	cm ²	Calculated
Area of home construction lot (target field)	A_{tf}	25,000,000	cm ²	HNF-SD-WM-TI-707, Rev. 5
Tilled depth of garden	Z_g	15	cm	HNF-SD-WM-TI-707, Rev. 5
Soil ingestion rate – suburban garden	$IR_{s,sg}$	100	mg/day	OSWER Directive 9285.6-03
Exposure frequency – resident	EF_{sg}	350	day/yr	OSWER Directive 9285.6-03
Crop (fruit and vegetables) ingestion rate	IR_c	106.51	kg/yr	PRGfR 2015
Crop-soil bioconcentration factor from uptake	B_v	Element-specific	(pCi/kg fresh wt crop)/ (pCi/kg dry wt soil)	NCRP Report No. 129
Crop-soil bioconcentration factor from resuspension/soil adhesion	B'_v	0.004	(pCi/kg fresh wt crop)/ (pCi/kg dry wt soil)	NCRP Report No. 129
Fraction of locally-produced crop (fruit and vegetables) that are consumed	F_v	0.25	unitless	EPA/600/P-95/002Fa
Enrichment factor	E_f	0.7	unitless	NCRP Report No. 129
Indoor inhalation rate – suburban garden	$INH_{in,sg}$	7,300	m ³ /yr	NCRP Report No. 129
Mass loading factor	M	6.66E-05	g/m ³	ICRP 1994
Fraction of time spent indoors – suburban garden	$t_{in,sg}$	0.656	unitless	PRGfR 2015 (16.42 hours per day, 350 days per year)
Outdoor inhalation rate – suburban garden	$INH_{out,sg}$	9,125	m ³ /yr	NCRP Report No. 129
Fraction of time spent outdoors	$t_{out,sg}$	0.080	unitless	HNF-SD-WM-TI-707, Rev. 5 (2 hours per day, 350 days per year)

RPP-ENV-58782, Rev. 0

Table 9-5. Exposure Parameters for the Chronic Suburban Garden Exposure Scenario. (2 sheets)

Parameter	Notation	Value	Units	Reference
Ratio of radionuclide concentrations in indoor versus outdoor air	I/O	0.3	unitless	NCRP Report No. 129
Unit conversion factor	UCF ₁	0.001	g/mg	0.001 g = 1 mg
Unit conversion factor	UCF ₂	1,000	g/kg	1,000 g = 1 kg

ICRP = International Commission on Radiological Protection

NCRP = National Council on Radiation Protection

References:

EPA/600/P-95/002Fa, Exposure Factors Handbook Volume 1: General Factors.

EPA/600/R-090/052F, Exposure Factors Handbook: 2011 Edition.

HNF-SD-WM-TI-707, "Exposure Scenarios and Unit Factors for the Hanford Tank Waste Performance Assessment."

"ICRP Publication 66: Human Respiratory Tract Model for Radiological Protection" (ICRP 1994).

NCRP Report No. 129, "Recommended Screening Limits for Contaminated Surface Soil and Review of Factors Relevant to Site-Specific Studies."

OSWER Directive 9285.6-03, Risk Assessment Guidance for Superfund, Volume I: Human Health Evaluation Manual, Supplemental Guidance "Standard Default Exposure Factors" Interim Final.

Preliminary Remediation Goals for Radionuclides (PRGfR), Queried 07/2015, [PRG User's Guide],

http://epa-prgs.ornl.gov/radionuclides/prg_guide.html.

9.3.2.1 Chronic Suburban Garden Scenario – Incidental Soil Ingestion. The following equation is used to calculate dose to the suburban garden resident resulting from incidental ingestion of garden soil (RPP-ENV-58813):

$$D_s = C_{gs} \times IR_{s,sg} \times EF_{sg} \times UCF_1 \times DCF_{ing} \quad (9-16)$$

Where:

D_s = dose resulting from incidental soil ingestion (mrem/yr)

C_{gs} = radionuclide concentration in garden soil (pCi/g)

$IR_{s,sg}$ = soil ingestion rate – suburban garden (mg/day)

EF_{sg} = exposure frequency – resident (days/yr)

UCF_1 = unit conversion factor (g/mg)

DCF_{ing} = ingestion dose conversion factor (mrem/pCi).

9.3.2.2 Chronic Suburban Garden Scenario – Consumption of Homegrown Crops (Fruits and Vegetables). The following equations are used to calculate the concentration of contaminant in the crop (homegrown fruits and vegetables) and the dose from consumption of the crop. The following equation is used to calculate the concentration of contaminant in the crop (RPP-ENV-58813):

$$C_c = C_{gs} \times (B_v + B'_v) \quad (9-17)$$

RPP-ENV-58782, Rev. 0

Where:

C_c = radionuclide concentration in crop (pCi/g)

C_{gs} = radionuclide concentration in garden soil (pCi/g)

B_v = crop-soil bioconcentration factor through uptake $\left(\frac{\left(\frac{pCi}{kg \text{ fresh weight of crop}} \right)}{\left(\frac{pCi}{kg \text{ dry weight of soil}} \right)} \right)$

B'_v = crop-soil bioconcentration factor representing all resuspension-soil adhesion processes $\left(\frac{\left(\frac{pCi}{kg \text{ fresh weight of crop}} \right)}{\left(\frac{pCi}{kg \text{ dry weight of soil}} \right)} \right)$.

The following equation is used to calculate dose resulting from consumption of homegrown fruits and vegetables (RPP-ENV-58813):

$$D_c = C_c \times IR_c \times F_v \times UCF_1 \times DCF_{ing} \quad (9-18)$$

Where:

D_c = dose resulting from consumption of crops (homegrown fruits and vegetables) (mrem/yr)

C_c = radionuclide concentration in crop (pCi/g)

IR_c = crop ingestion rate (kg/yr)

F_v = fraction of homegrown fruits and vegetables consumed (unitless)

UCF_1 = unit conversion factor (1,000 g/kg)

DCF_{ing} = ingestion dose conversion factor (mrem/pCi).

9.3.2.3 Chronic Suburban Garden Scenario – Inhalation of Soil Particulates. The following equation is used to calculate dose to the suburban garden resident resulting from inhalation of dust particulates (RPP-ENV-58813):

$$D_{inh} = C_{gs} \times E_f \times M \times \left(INH_{in,sg} \times t_{in,sg} \times \frac{I}{O} + INH_{out,sg} \times t_{out,sg} \right) \times DCF_{inh} \quad (9-19)$$

Where:

D_{inh} = dose resulting from inhalation of soil (mrem/yr)

C_{gs} = radionuclide concentration in garden soil (pCi/g)

E_f = enrichment factor (unitless)

M = mass loading factor (g/m³)

$INH_{in,sg}$ = indoor inhalation rate – suburban garden (m³/yr)

$t_{in,sg}$ = fraction of time spent indoors – suburban garden (unitless)

I/O = ratio of radionuclide concentrations in indoor and outdoor air (unitless)

$INH_{out,sg}$ = outdoor inhalation rate – suburban garden (m³/yr)

$t_{out,sg}$ = fraction of time spent outdoors – suburban garden (unitless)

DCF_{inh} = inhalation dose conversion factor (mrem/pCi).

RPP-ENV-58782, Rev. 0

9.3.2.4 Chronic Suburban Garden Scenario – External Exposure. The following equation is used to calculate dose to the suburban garden resident resulting from external exposure (RPP-ENV-58813):

$$D_{ext} = C_{gs} \times (t_{in,sg} \times \varepsilon + t_{out,sg}) \times DCF_{ext} \quad (9-20)$$

Where:

- D_{ext} = dose resulting from external exposure (mrem/yr)
- C_{gs} = radionuclide concentration in garden soil (pCi/g)
- $t_{in,sg}$ = fraction of time spent indoors – suburban garden (unitless)
- ε = transmission or shielding factor
- $t_{out,sg}$ = fraction of time spent outdoors – suburban garden (unitless)
- DCF_{ext} = external exposure dose conversion factor (mrem/yr)/(pCi/g).

9.3.3 Chronic Commercial Farm Scenario

The commercial farm scenario evaluates the long-term exposure to an individual who uses the target field as a commercial farm. In this outdoor scenario, a well diameter of 41.91 cm (16.5 in.) is assumed and the drill cuttings are spread over a farm area of 647,000 m² (160 acres) for growing food crops. This scenario represents an individual who works on the commercial farm, and grows and tends to the crops but does not consume what is produced. The commercial farm worker is exposed by incidental soil ingestion, inhalation of soil particulates, and external exposure; these exposure pathways are illustrated in Figure 9-5. Exposure parameters for the chronic commercial farm scenario are provided in Table 9-6.

As discussed in Section 9.3.1.1, Equation 9-7 is used to calculate the radionuclide activities, and Equation 9-8 is used to calculate the radionuclide concentrations for the commercial farm scenario (C_{cf}) with corresponding well area and target field area. Radionuclide-specific shielding factors and dose conversion factors are presented in Section 6.3.3, Tables 6-24 and 6-25, respectively. Because the fraction of time spent indoors is assumed to be zero, the indoor shielding factor is not applicable in this scenario.

9.3.3.1 Chronic Commercial Farm Scenario – Incidental Soil Ingestion. The following equation is used to calculate dose to the commercial farmer resulting from incidental ingestion of soil (RPP-ENV-58813):

$$D_s = C_{cf} \times IR_{s,cf} \times EF_{cf} \times UCF_1 \times DCF_{ing} \quad (9-18)$$

Where:

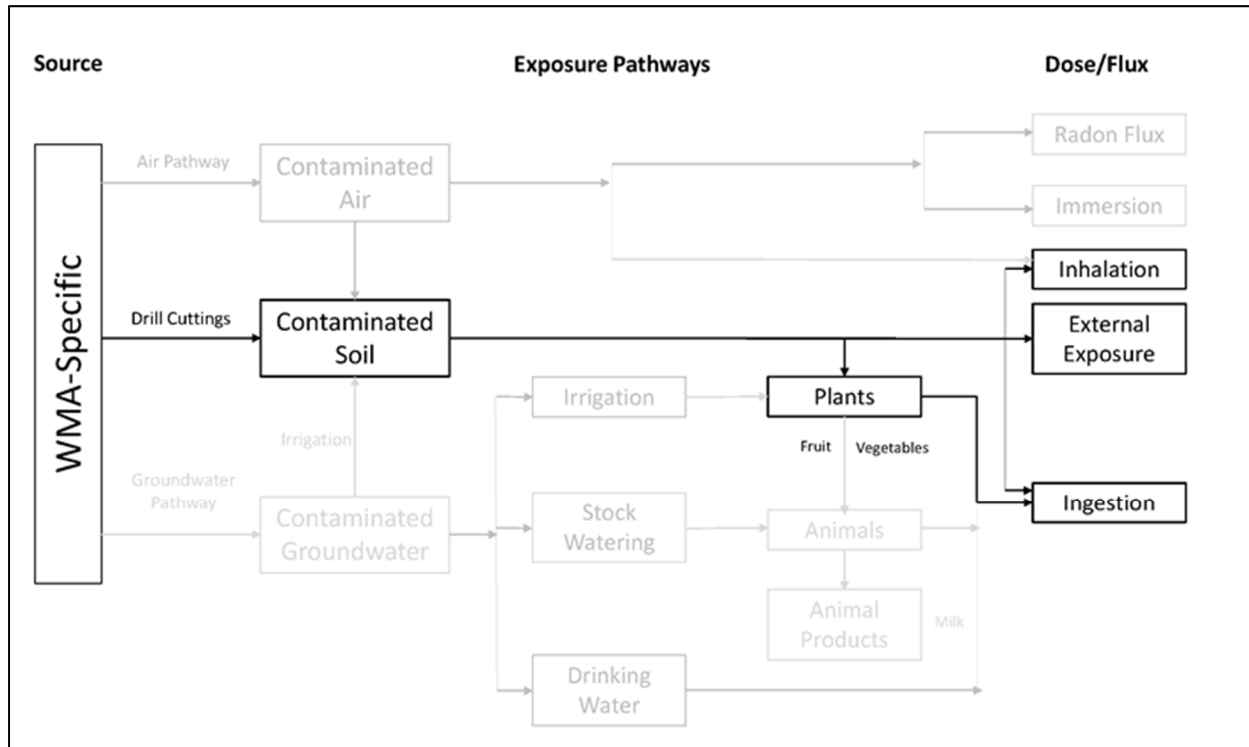
- D_s = dose resulting from incidental soil ingestion (mrem/yr)
- C_{cf} = radionuclide concentration in the commercial farm soil (pCi/g)
- $IR_{s,cf}$ = soil ingestion rate – commercial farmer (mg/day)
- EF_{cf} = exposure frequency – commercial farmer (days/yr)

RPP-ENV-58782, Rev. 0

UCF_1 = unit conversion factor (g/mg)

DCF_{ing} = ingestion dose conversion factor (mrem/pCi).

Figure 9-5. Exposure Pathways Considered for the Inadvertent Intruder Chronic Commercial Farm Exposure Scenario.



WMA = Waste Management Area

9.3.3.2 Chronic Commercial Farm Scenario – Inhalation of Soil Particulates. The following equation is used to calculate dose to the commercial farmer resulting from inhalation of dust particulates (RPP-ENV-58813):

$$D_{inh} = C_{cf} \times E_f \times M \times \left(INH_{in,cf} \times t_{in,cf} \times \frac{I}{O} + INH_{out,cf} \times t_{out,cf} \right) \times DCF_{inh} \quad (9-21)$$

Where:

D_{inh} = dose resulting from inhalation of soil (mrem/yr)

C_{cf} = radionuclide concentration in commercial farm soil (pCi/g)

E_f = enrichment factor (unitless)

M = mass loading factor (g/m³)

$INH_{in,cf}$ = indoor inhalation rate – commercial farmer (m³/yr)

$t_{in,cf}$ = fraction of time spent indoors – assumed to be zero for commercial farmer

I/O = ratio of radionuclide concentrations in indoor and outdoor air (unitless)

$INH_{out,cf}$ = outdoor inhalation rate – commercial farmer (m³/yr)

RPP-ENV-58782, Rev. 0

$t_{out,cf}$ = fraction of time spent outdoors – commercial farmer (unitless)
 DCF_{inh} = inhalation dose conversion factor (mrem/pCi).

Table 9-6. Exposure Parameters for the Chronic Commercial Farm Exposure Scenario.

Parameter	Notation	Value	Units	Reference
Area over which residual waste is spread	A_{source_term}	Calculated	cm ²	Source term-specific
Area of the well	A_{well}	1,379.51	cm ²	Calculated
Diameter of the well	D_{well}	41.91	cm	HNF-SD-WM-TI-707, Rev. 5
Area of commercial farm	A_{cf}	6.475E+09	cm ²	HNF-SD-WM-TI-707, Rev. 5
Tilled depth of commercial farm	Z_{cf}	15	cm	HNF-SD-WM-TI-707, Rev. 5
Soil ingestion rate – commercial farmer	$IR_{s,cf}$	100	mg/day	OSWER Directive 9285.6-03
Exposure frequency – commercial farmer	EF_{cf}	350	days/yr	OSWER Directive 9285.6-03
Enrichment factor	E_f	0.7	unitless	NCRP Report No. 129
Indoor inhalation rate – commercial farmer	$INH_{in,cf}$	7,300	m ³ /yr	NCRP Report No. 129
Mass loading factor	M	6.66E-05	g/m ³	NCRP Report No. 129
Fraction of time spent indoors – commercial farmer	$t_{in,cf}$	0	unitless	NCRP Report No. 129; Outdoor scenario
Outdoor inhalation rate – commercial farmer	$INH_{out,cf}$	10,950	m ³ /yr	HNF-SD-WM-TI-707, Rev. 5
Fraction of time spent outdoors – commercial farmer	$t_{out,cf}$	0.164	unitless	HNF-SD-WM-TI-707, Rev. 5
Ratio of radionuclide concentrations in indoor versus outdoor air	I/O	0.3	unitless	NCRP Report No. 129
Unit conversion factor	UCF ₁	0.001	g/mg	0.001 g = 1 mg

NCRP = National Council on Radiation Protection

References:

HNF-SD-WM-TI-707, "Exposure Scenarios and Unit Factors for the Hanford Tank Waste Performance Assessment."

NCRP Report No. 129, "Recommended Screening Limits for Contaminated Surface Soil and Review of Factors Relevant to Site-Specific Studies."

OSWER Directive 9285.6-03, Risk Assessment Guidance for Superfund, Volume I: Human Health Evaluation Manual, Supplemental Guidance "Standard Default Exposure Factors" Interim Final.

9.3.3.3 Chronic Commercial Farm Scenario – External Exposure. The following equation is used to calculate dose to the resident resulting from external exposure (RPP-ENV-58813):

$$D_{ext} = C_{cf} \times (t_{in,cf} \times \varepsilon + t_{out,cf}) \times DCF_{ext} \quad (9-22)$$

RPP-ENV-58782, Rev. 0

Where:

D_{ext}	= dose resulting from external exposure
C_{cf}	= radionuclide concentration in commercial farm soil (pCi/g)
$t_{in,cf}$	= fraction of time spent indoors – assumed to be zero for commercial farmer
ε	= transmission or shielding factor
$t_{out,cf}$	= fraction of time spent outdoors – commercial farmer (unitless)
DCF_{ext}	= external exposure dose conversion factor (mrem/yr)/(pCi/g).

9.4 INTRUDER ANALYSIS RESULTS

Sections 9.3.1 and 9.3.2 summarize the calculated effective dose for each of the four inadvertent intruder scenarios. Graphic displays show the effective dose starting 100 years after closure for intrusion into a pipeline source and 500 years after closure for the other sources that produce significant intruder dose. Over the compliance time period (1,000 years after closure), the relative contribution of radionuclides vary, but the total dose decreases, with highest dose being at 100 years after closure. Table 9-7 summarizes the calculated effective doses for each intruder scenario, assuming intrusion at 100 years for intrusion into a pipeline source and 500 years after closure for the other 18 waste sources. Although inadvertent intrusions into many of the tanks lead to potential doses, the likelihood of intrusion is considered to be very small due to the significant mechanical barrier to drilling from the large thickness of grout that will fill tanks at closure compared to drilling outside of grouted tank area. On the other hand, the inadvertent intrusion through pipelines is more likely as pipelines would not provide any appreciable mechanical barrier to drilling compared to drilling through the Hanford unit sediments.

For the purpose of analysis, the total intruder dose and doses from major radionuclide contributors from intrusion into tank C-301 (maximum intruder dose causing source term at 500-year intrusion time) and intrusion into a pipeline (most likely intruder source term) are presented separately for each intruder scenario. The relative importance of various pathways is presented for each intruder scenario in Table 9-8 for intruding through the pipeline.

9.4.1 Acute Exposure Dose

Figure 9-6 shows the calculated acute dose to the well driller assuming the intrusion takes place 100 years or beyond for pipelines and 500 years or beyond for sources with substantial intrusion barriers. Among the 19 residual waste sources, the sources with the top six intruder doses are displayed in the figure. For all sources, the dose remains below the 500 mrem performance measure. Figure 9-7(a) shows the total well driller dose produced by tank C-301 residual waste source along with major dose-contributing radionuclides, while Figure 9-7(b) shows the results for the intruded pipeline source. The major contributor to dose to the well driller is ^{239}Pu for both sources, although ^{137}Cs is an important contributor to intrusion into pipelines at early times. The major pathway for well driller dose is external exposure.

RPP-ENV-58782, Rev. 0

Table 9-7. Peak Effective Dose for the Inadvertent Intruder Scenarios for All Residual Waste Sources.

Source	Well Driller Acute Dose (mrem)	Commercial Farm Chronic Dose (mrem/yr)	Rural Pasture Chronic Dose (mrem/yr)	Suburban Garden Chronic Dose (mrem/yr)
241-C-101	1.24E+00	2.17E-03	1.44E-01	3.22E-01
241-C-102	4.59E+00	8.09E-03	5.37E-01	1.20E+00
241-C-103	4.09E-01	7.25E-04	6.14E-02	1.10E-01
241-C-104	5.77E-01	1.10E-03	1.21E-01	1.70E-01
241-C-105	3.80E+00	6.69E-03	7.18E-01	1.23E+00
241-C-106	3.47E+00	8.75E-03	8.93E-01	9.57E-01
241-C-107	1.49E+01	2.66E-02	1.82E+00	3.90E+00
241-C-108	5.80E-02	1.05E-04	1.09E-02	1.71E-02
241-C-109	3.10E-02	5.57E-05	7.63E-03	9.33E-03
241-C-110	8.24E-02	1.78E-04	1.99E-02	2.44E-02
241-C-111	7.47E+00	1.32E-02	1.40E+00	2.13E+00
241-C-112	3.48E-01	6.10E-04	9.17E-02	1.41E-01
241-C-201	1.45E+01	2.52E-02	1.58E+00	3.75E+00
241-C-202	1.28E+01	2.22E-02	1.39E+00	3.32E+00
241-C-203	4.61E-01	8.51E-04	7.25E-02	1.26E-01
241-C-204	5.60E-02	1.77E-04	2.97E-02	2.49E-02
241-C-301	2.12E+01	3.86E-02	2.69E+00	5.57E+00
CR-VAULT	3.91E+00	7.10E-03	4.96E-01	1.03E+00
Pipeline*	3.60E+01	1.13E-03	8.21E+00	3.92E+00

Note: Peak dose calculated at 500 years for all sources except for pipeline, which is reported at 100 years after closure.

*Maximum dose at 100 years after closure.

The peak dose for each scenario is shown in **bold**.

9.4.2 Chronic Exposure Dose

Figure 9-8 shows the calculated dose for the rural pasture scenario for the top six residual waste sources. All remain below the 100 mrem/yr performance measure throughout the simulated time period. Figure 9-9(a) shows the total rural pasture dose produced by intrusion into tank C-301 along with major dose-contributing radionuclides, while Figure 9-9(b) shows the results for intrusion into a pipeline. Strontium-90 is the major contributor to pipelines up until almost 500 years after closure, with major pathways being milk ingestion. Cesium-137 through the milk

RPP-ENV-58782, Rev. 0

ingestion pathway is also a major contributor to dose at early time period. Plutonium-239 becomes the major contributor for both pipelines and tank residuals after 500 years following closure.

Table 9-8. Relative Fraction of Pathway Contributions to the Inadvertent Intruder Dose for Pipeline at 100 Years After Closure.

Scenario	Pathways				
	External Exposure	Soil Inhalation	Soil Ingestion	Milk Ingestion	Vegetable Ingestion
Well Driller	0.59	0.30	0.11	x	x
Rural Pasture	0.01	<0.01	<0.01	0.98	x
Suburban Garden	0.03	<0.01	<0.01	x	0.96
Commercial Farm	0.69	0.05	0.26	x	x

x = pathway not considered

Pathway contributing the most is highlighted for each scenario.

Figure 9-10 shows the calculated dose for the suburban garden scenario for the top six residual waste sources. All doses remain below the 100 mrem/yr performance measure throughout the compliance time period. Figure 9-11(a) shows the total suburban garden dose produced by intrusion into tank C-301 along with major dose-contributing radionuclides, while Figure 9-11(b) shows the results for intruded pipeline source. Strontium-90 is the major contributor up until about 300 years after closure (for intrusion into a pipeline source), with major pathways being vegetable ingestion. Cesium-137 through the vegetable ingestion pathway is also a major contributor to dose at early times. Plutonium-239 becomes the major contributor after 500 years for both pipelines and tank residuals.

Figure 9-12 shows the calculated dose for the commercial farm scenario for the top six residual waste sources. The dose from all residual waste sources remains below the 100 mrem/yr performance measure throughout the simulated time period.

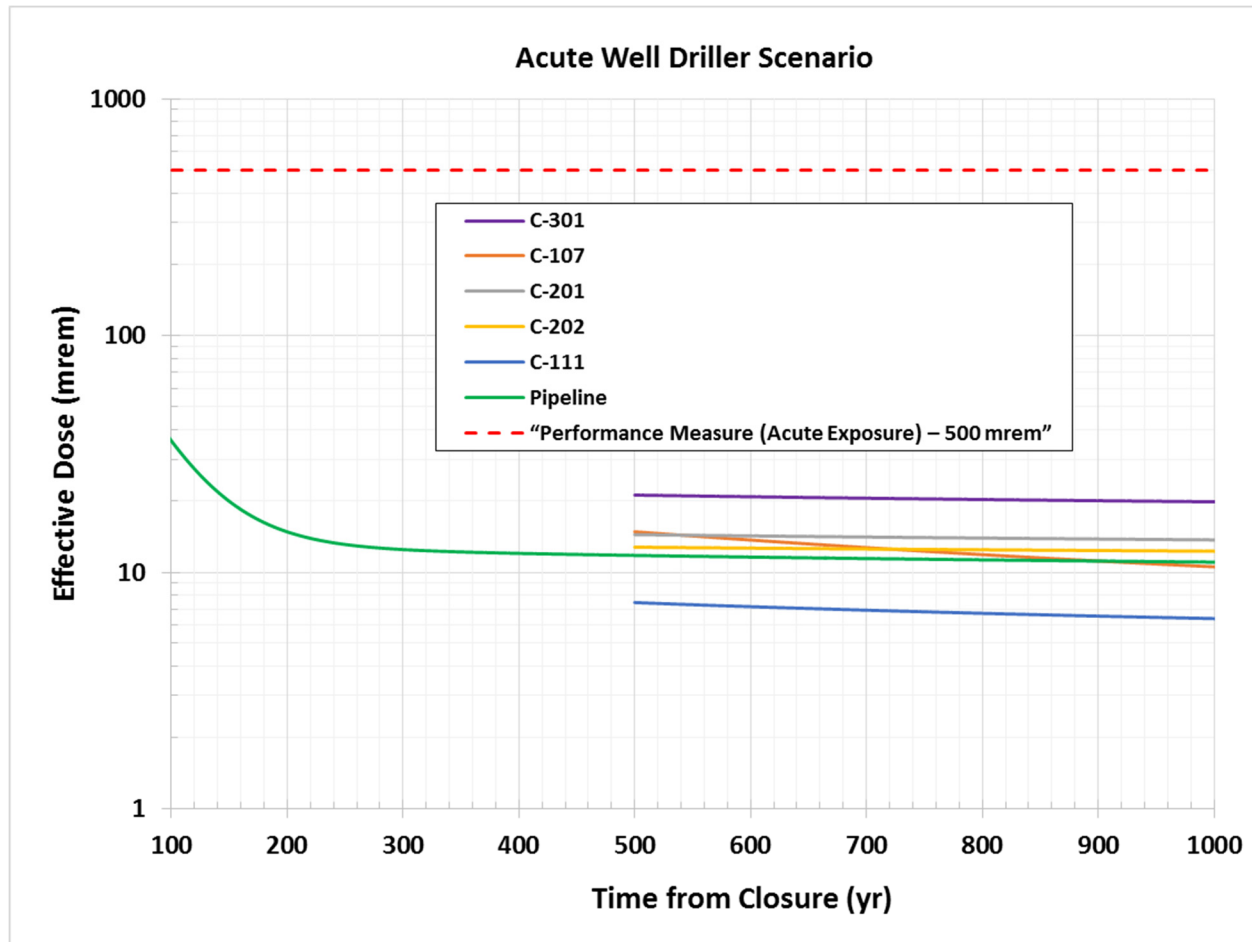
Figure 9-13(a) shows the total commercial farm dose produced by intrusion into tank C-301 along with major dose-contributing radionuclides, while Figure 9-13(b) shows the results for intrusion into a pipeline source. For intrusion into a pipeline source, ¹³⁷Cs and ⁹⁰Sr are the major contributor up until almost 300 years after, with major pathways being external exposure. Plutonium-239 and ²⁴¹Am become the major contributor to both pipelines and tank residuals after 500 years.

Figure 9-14(a-b) shows the total dose produced by intrusion into tank C-301 and a pipeline residual waste source for all three chronic scenarios. For about the first 300 years after closure (for intrusion into a pipeline source), the rural pasture scenario produces higher dose than the other chronic scenarios; after that time the suburban garden dose is highest among all of the chronic scenarios. Within the first 300 years for intrusion into a pipeline after closure, the milk

RPP-ENV-58782, Rev. 0

ingestion dose (dominant pathway in rural pasture scenario) from ^{90}Sr is higher than the vegetable ingestion dose (dominant pathway in suburban garden scenario). After that, the total vegetable ingestion dose from ^{90}Sr , ^{241}Am and ^{239}Pu exceeds the total milk ingestion dose from ^{90}Sr , ^{241}Am and ^{239}Pu . So, if intrusion occurs at 100 years after closure, the rural pasture scenario will produce the highest chronic dose.

Figure 9-6. Effective Dose for the Well Driller Acute Exposure Scenario.



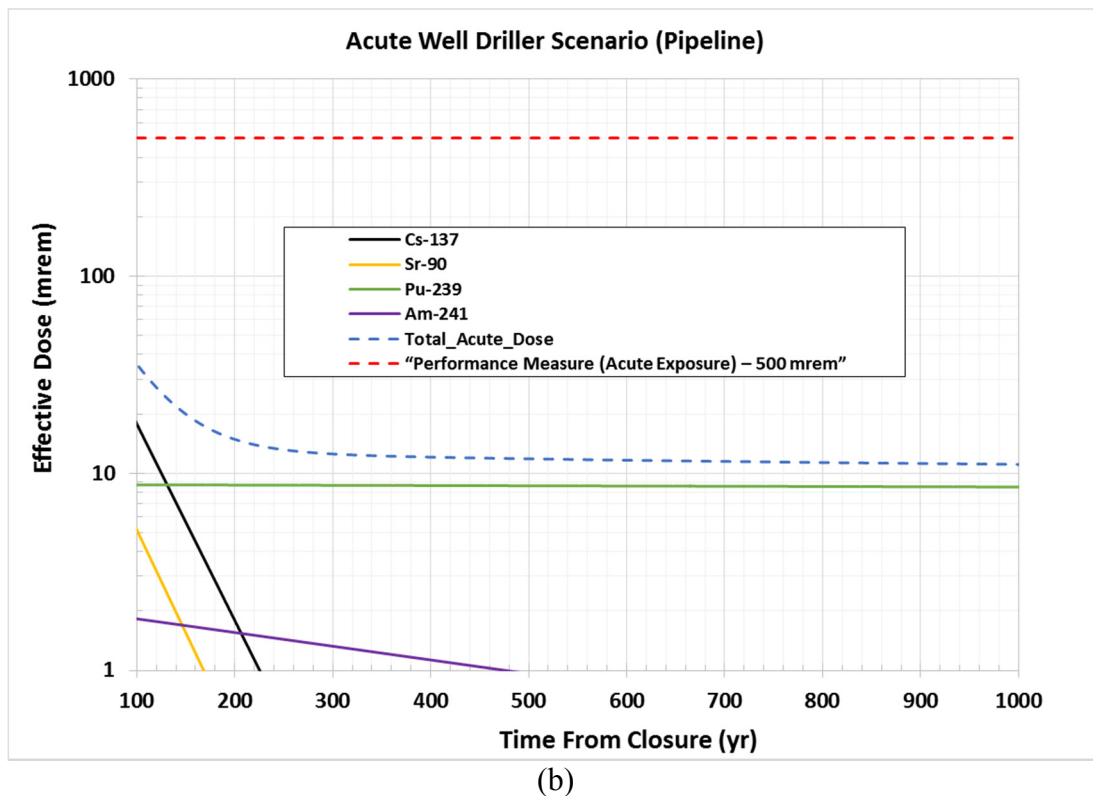
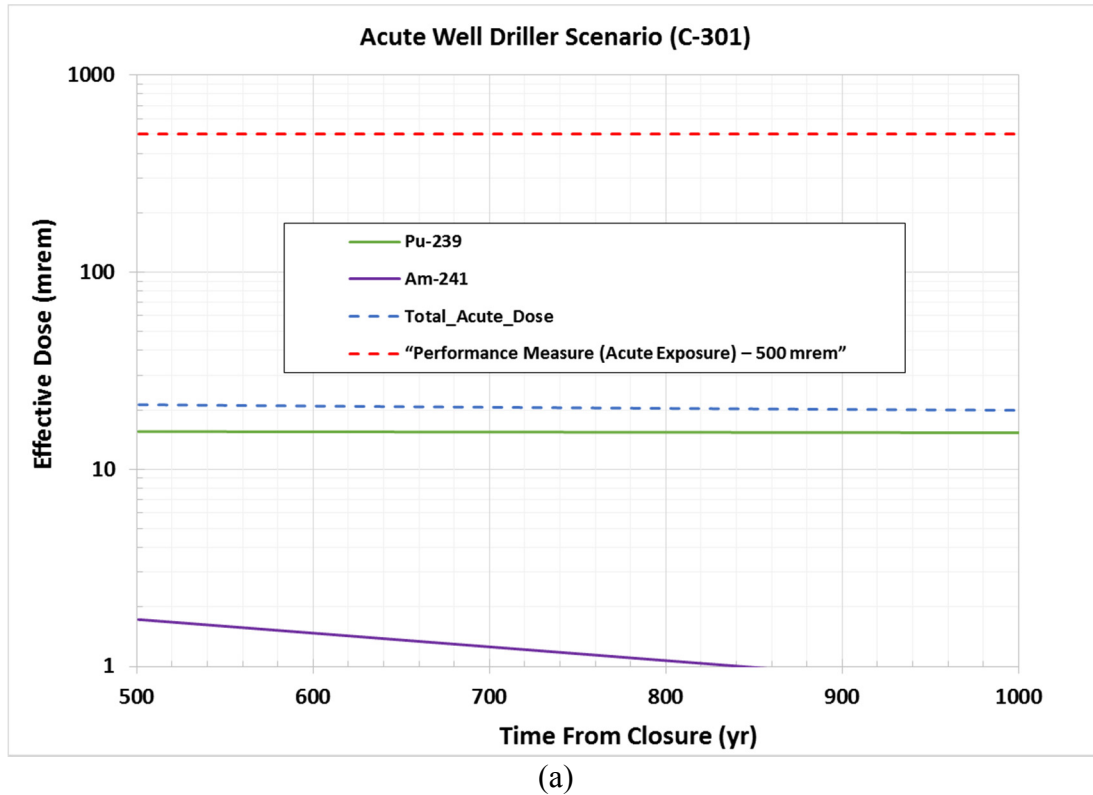
For intrusion into tank wastes, the suburban garden scenario produces the maximum chronic dose, with tank C-301 producing the highest dose. The commercial farm scenario is always lower than the other chronic scenarios.

9.5 INTRUDER SENSITIVITY/UNCERTAINTY ANALYSIS

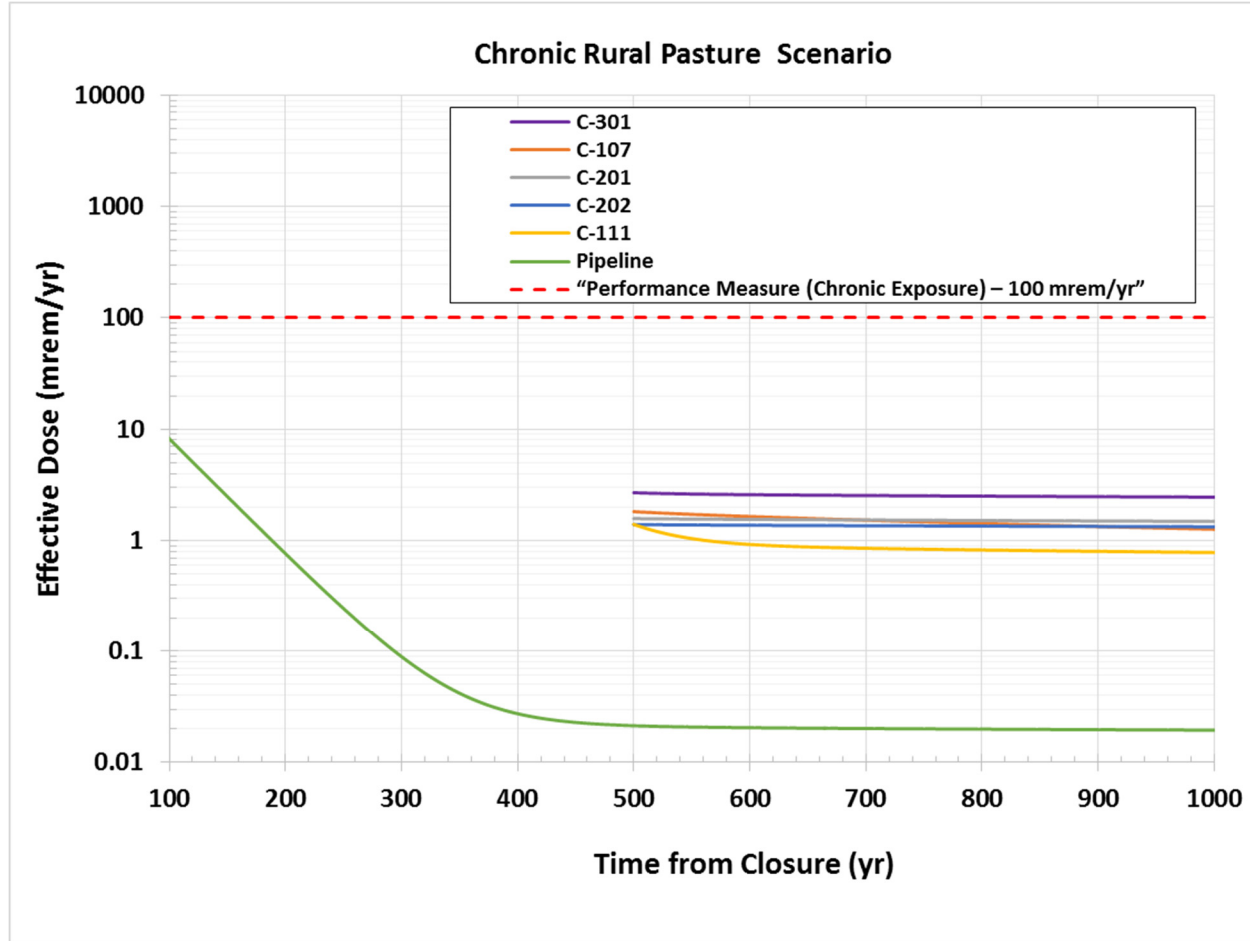
Sensitivity and uncertainty analyses for intruder analyses are somewhat limited, owing to the stylized and speculative nature of the scenarios. Consequently, for this PA only qualitative discussions are provided in this section.

RPP-ENV-58782, Rev. 0

Figure 9-7. Effective Dose for the Well Driller Acute Exposure Scenario for (a) Tank 241-C-301 and (b) Pipeline Residual Waste.



RPP-ENV-58782, Rev. 0

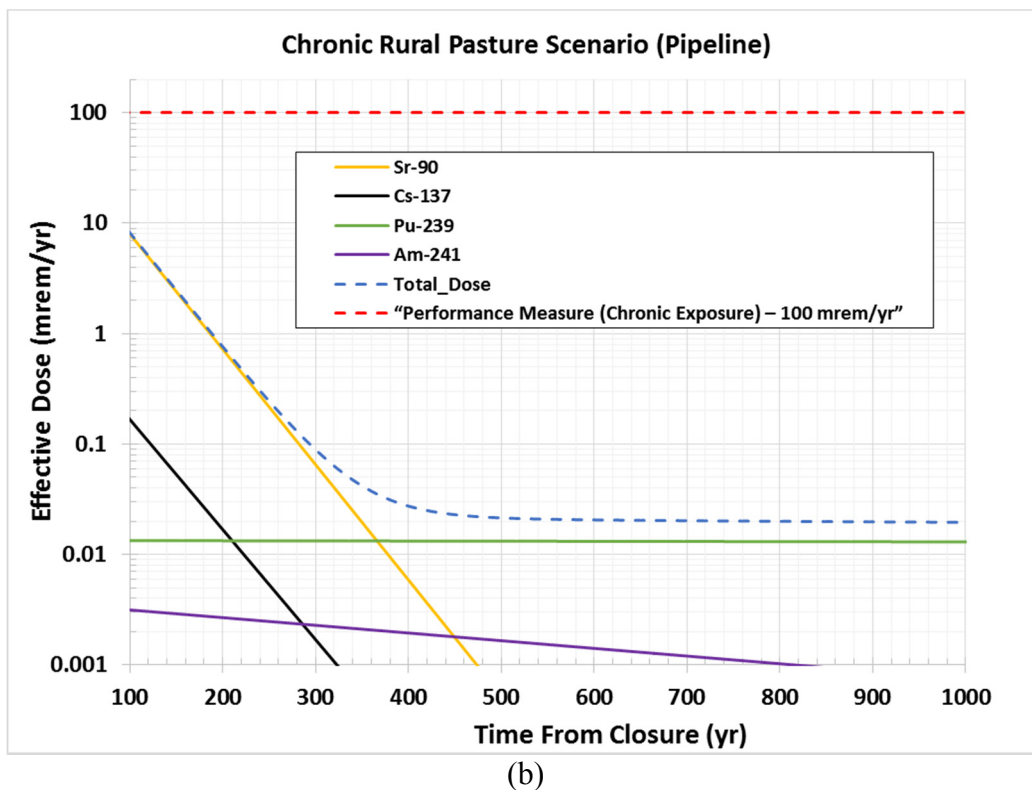
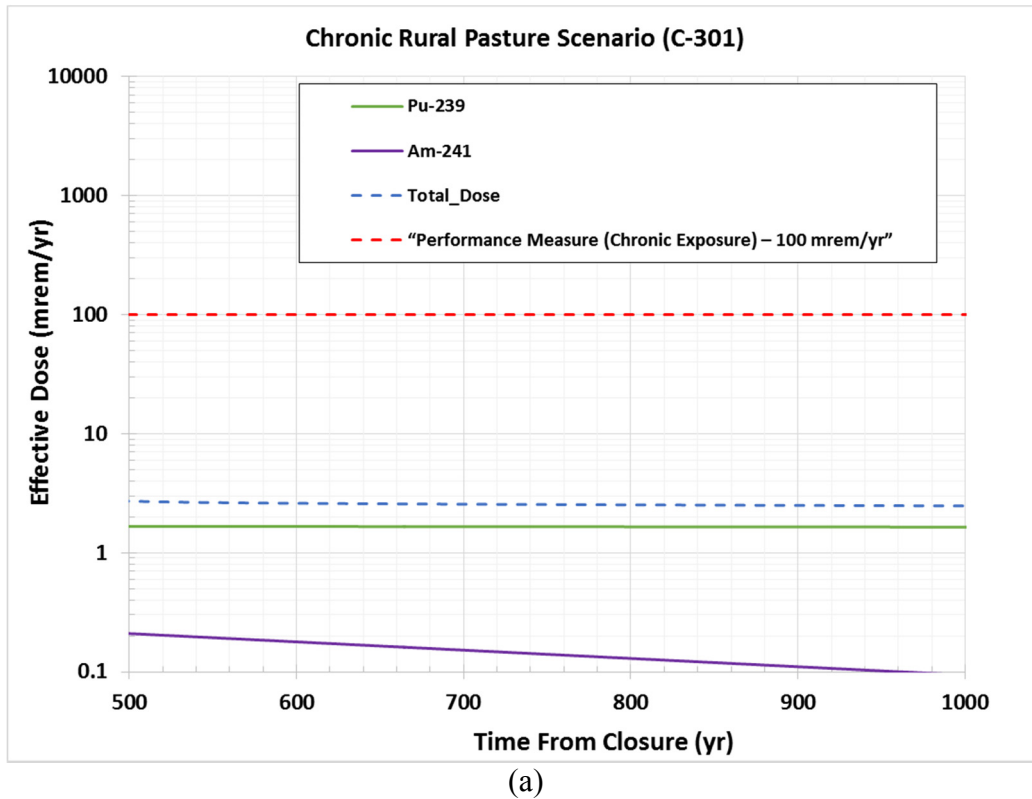
Figure 9-8. Effective Dose for the Rural Pasture Chronic Exposure Scenario.

The key parameter in the intruder analysis is concentration in the residual wastes. Calculated doses are linear with the activity of waste exhumed in the intrusion event. For example, the limiting inadvertent intruder scenario is the rural pasture scenario, as it leads to the highest dose at 100 years after closure. The major dose contributors in this scenario are ^{90}Sr and ^{137}Cs . Decreasing the closure inventory (or concentration) of those two nuclides would result in a proportional decrease in the rural pasture dose.

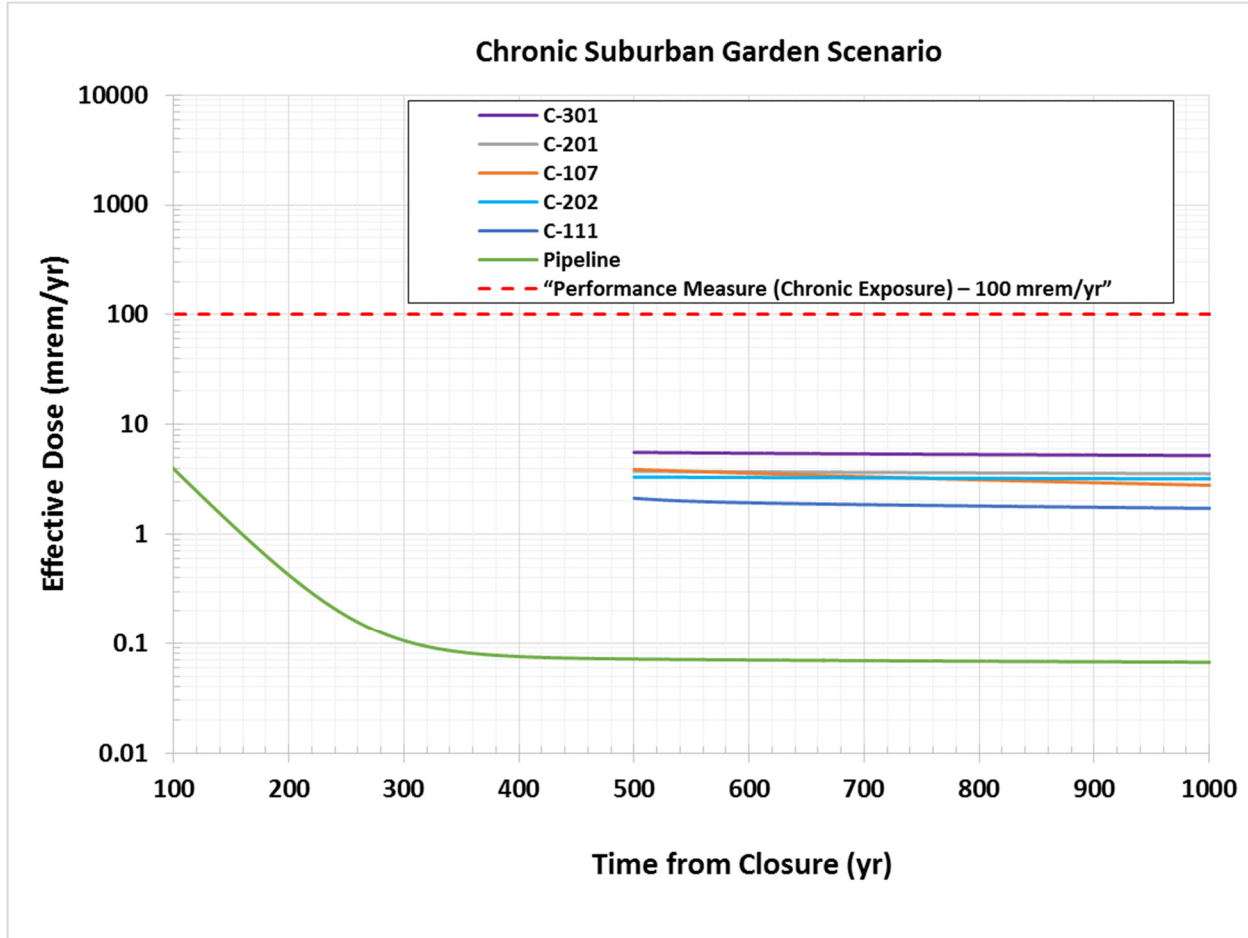
Sensitivities of other key parameters depend on which exposure pathways are the most important dose contributors. The relative importance of various pathways is presented for each scenario in Table 9-8 for pipeline (most likely source for intrusion) at 100 years after closure. It provides insight into the group of parameters that will have the greatest impact on the dose, and therefore the uncertainty in dose would be most impacted by the uncertainty in those parameter values. The relative contribution to the overall dose by a given pathway is provided. Based on the results presented in Table 9-8, the parameters associated with external exposure pathway are deemed to be most important for well driller and commercial farm scenarios, parameters associated with milk ingestion pathway are most important for rural pasture scenario, and for suburban garden scenario the parameters associated with vegetable ingestion pathway are most important.

RPP-ENV-58782, Rev. 0

Figure 9-9. Effective Dose for the Rural Pasture Chronic Exposure Scenario for (a) Tank 241-C-301 and (b) Pipeline Residual Waste.



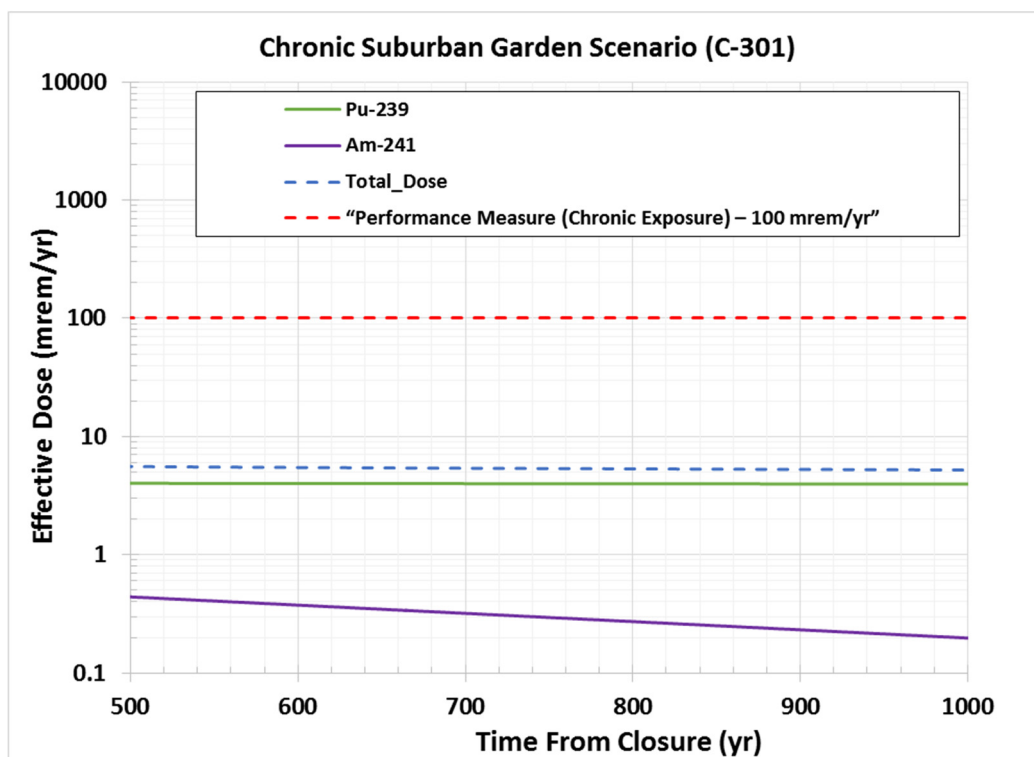
RPP-ENV-58782, Rev. 0

Figure 9-10. Effective Dose for the Suburban Garden Chronic Exposure Scenario.

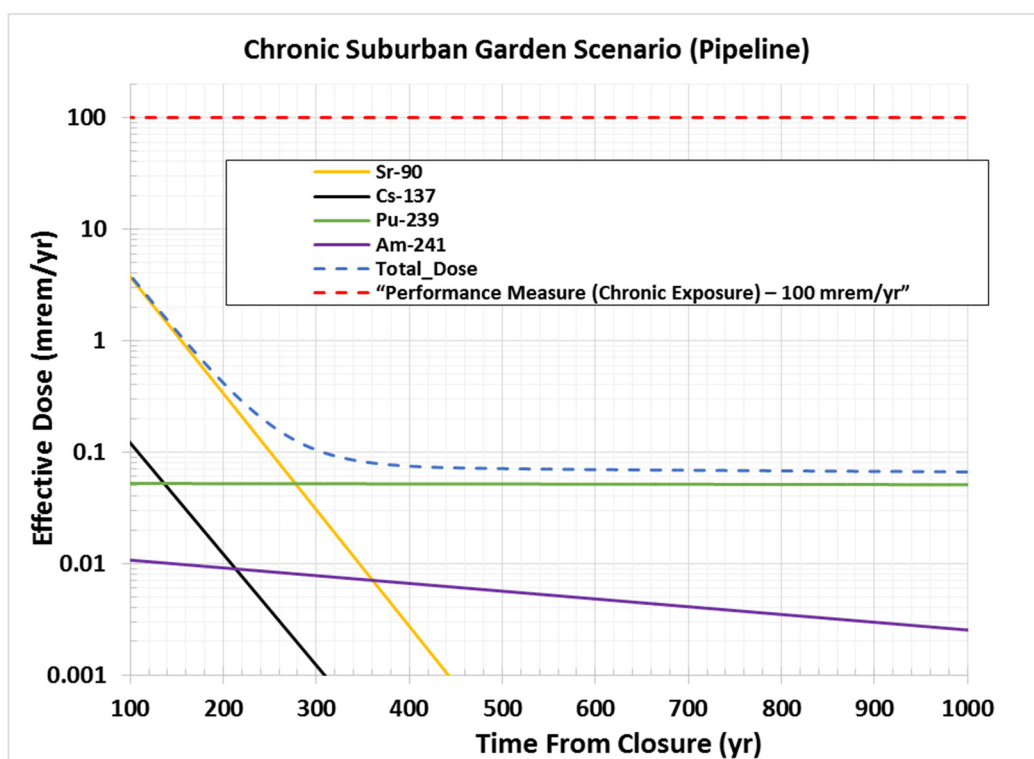
A sensitivity analysis was performed to evaluate the impact of intrusion through a fully plugged cascade pipeline. As discussed earlier, the plugged pipelines only occupy about 2% of the total pipeline length within WMA C. Performing intrusion calculation through the fully plugged cascade line will provide the bounding dose estimate for intrusion into a pipeline source. The calculations are performed in the same manner as discussed earlier for a pipeline source except that the cascade pipeline is assumed to be completely full (instead of 5% full for a waste transfer pipeline). The results of the three chronic scenarios are presented in Figure 9-15. Only the dose from the rural pasture scenario exceeds the performance measure at 100 years (about 160 mrem/yr) but quickly drops below within 20 years due to decay of ^{90}Sr . When compared to the dose estimates presented in Figure 9-14(b) for the transfer pipeline, the cascade pipeline dose values are a factor of 20 higher, indicating that the dose scales linearly with the waste volume assumption. The acute scenario dose for the cascade pipeline remains the same as that for the transfer pipeline [Figure 9-7(b)] as the calculation depends on the concentration of the residual waste, which is assumed to be the same.

RPP-ENV-58782, Rev. 0

Figure 9-11. Effective Dose for the Suburban Garden Chronic Exposure Scenario for (a) Tank 241-C-301 and (b) Pipeline Residual Waste.

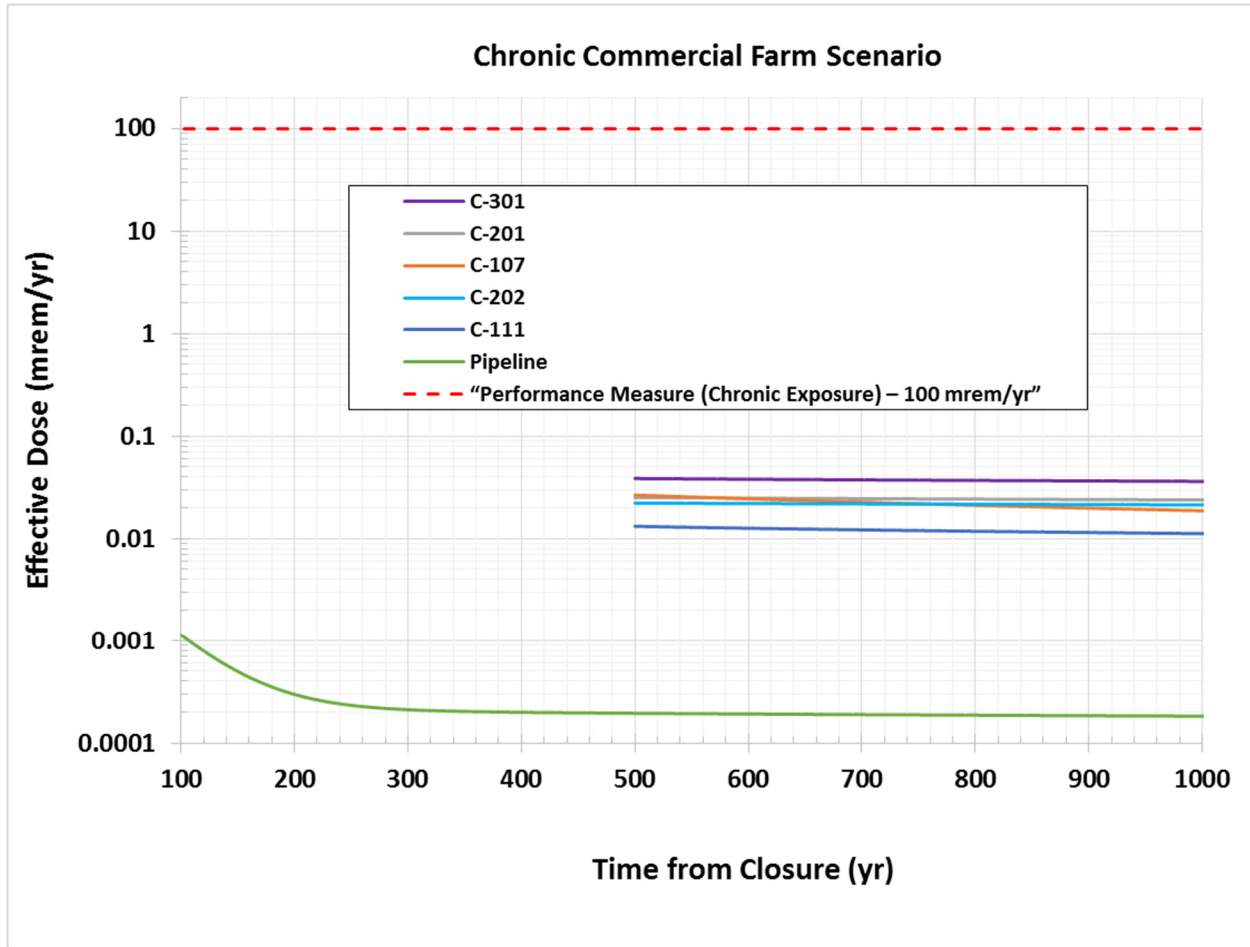


(a)



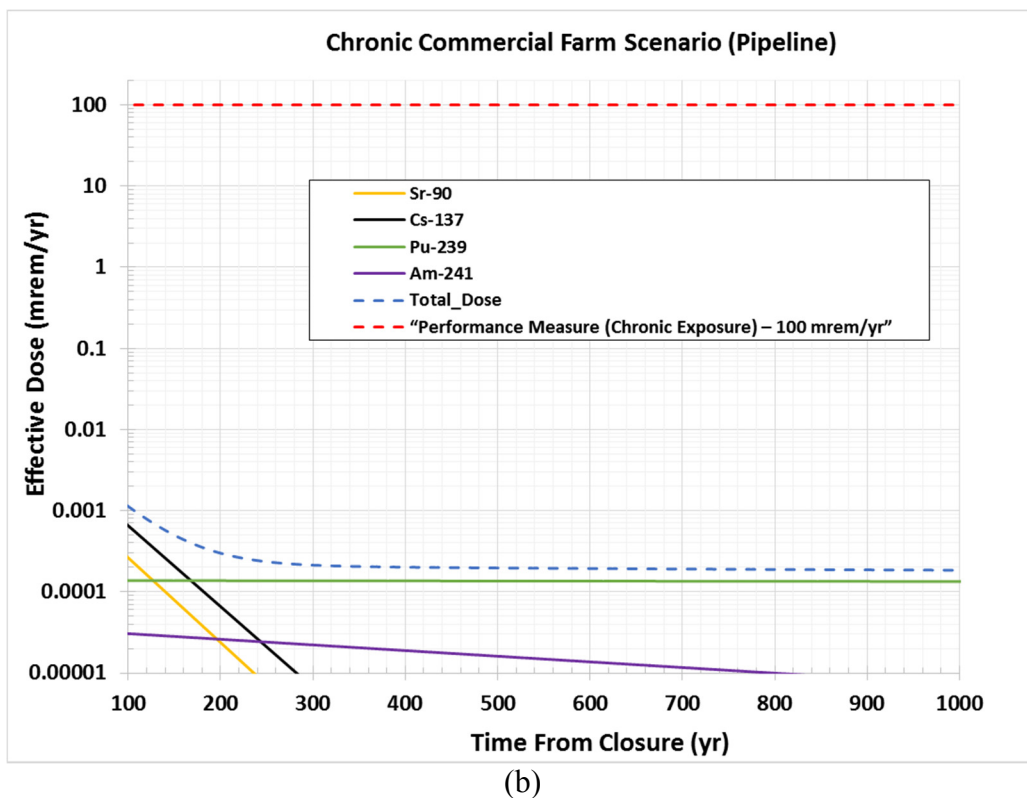
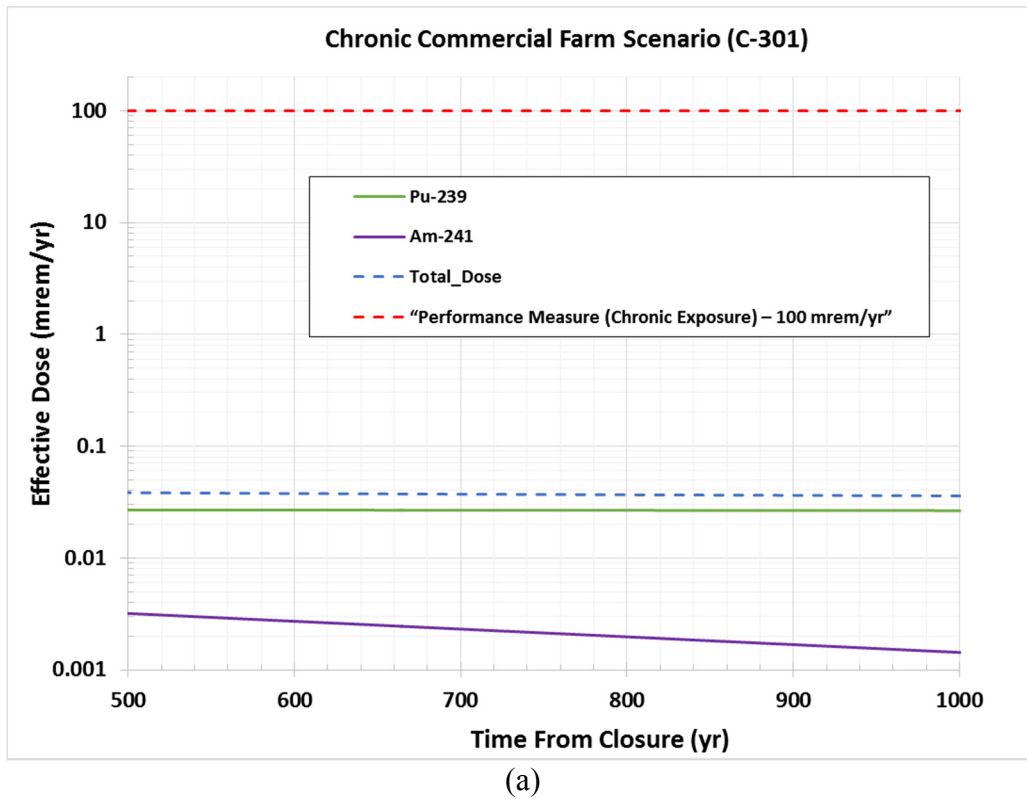
(b)

RPP-ENV-58782, Rev. 0

Figure 9-12. Effective Dose for the Commercial Farm Chronic Exposure Scenario.

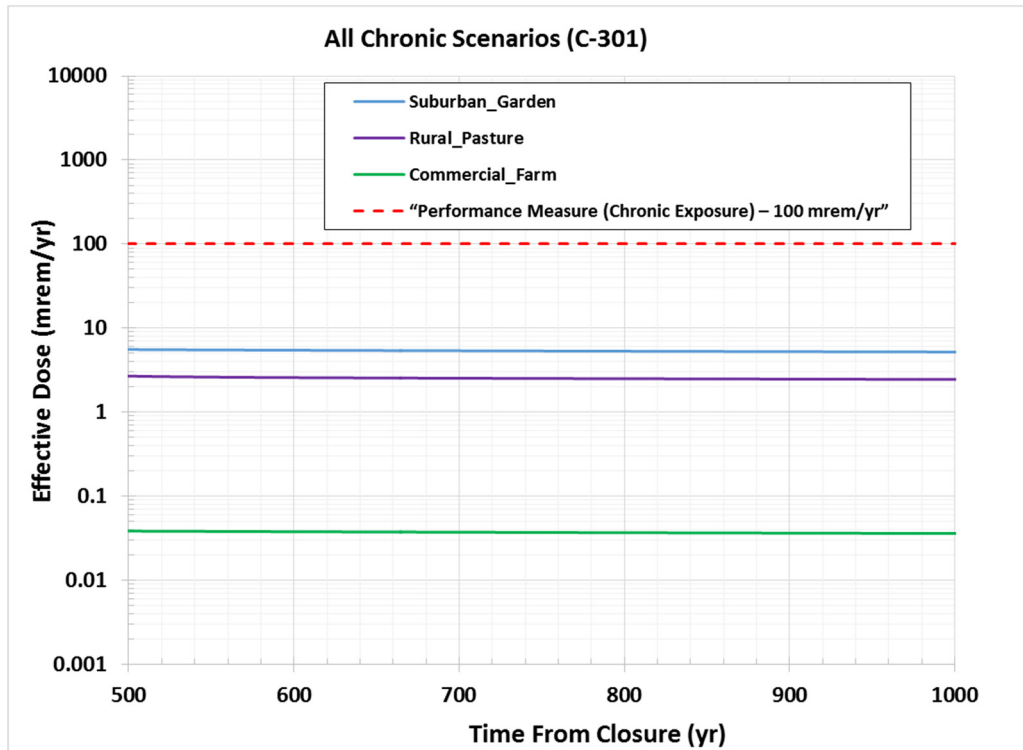
RPP-ENV-58782, Rev. 0

Figure 9-13. Effective Dose for the Commercial Farm Chronic Exposure Scenario for (a) Tank 241-C-301 and (b) Pipeline Residual Waste.

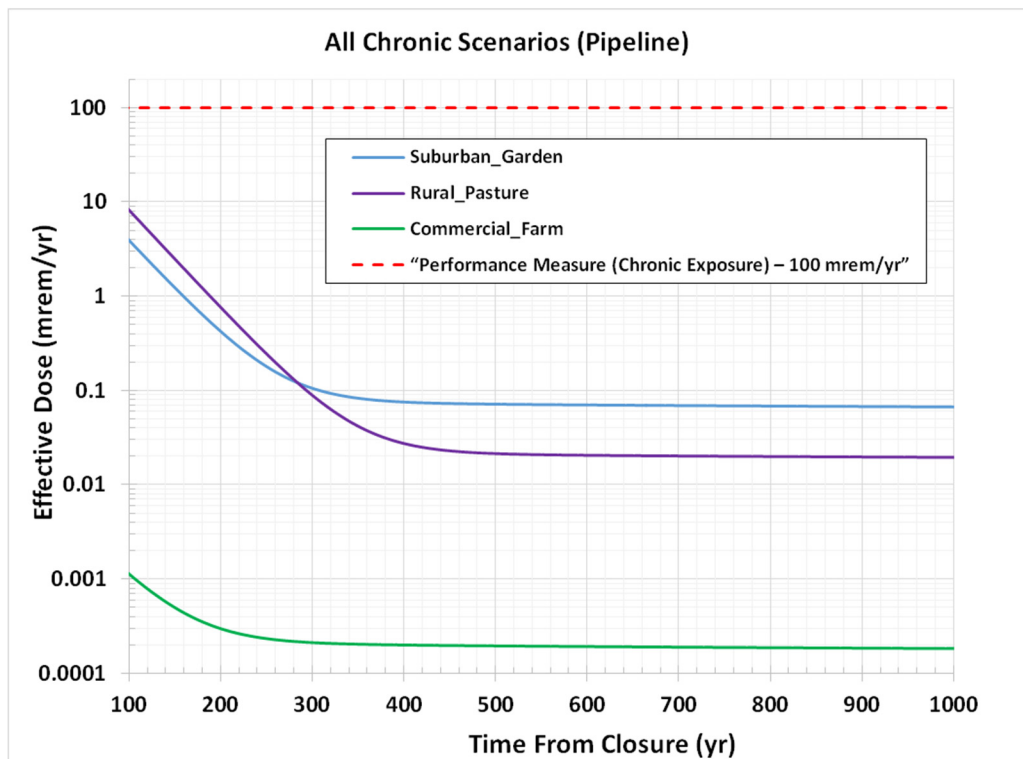


RPP-ENV-58782, Rev. 0

Figure 9-14. Effective Dose for All Three Chronic Exposure Scenarios for (a) Tank 241-C-301 and (b) Pipeline Residual Waste.



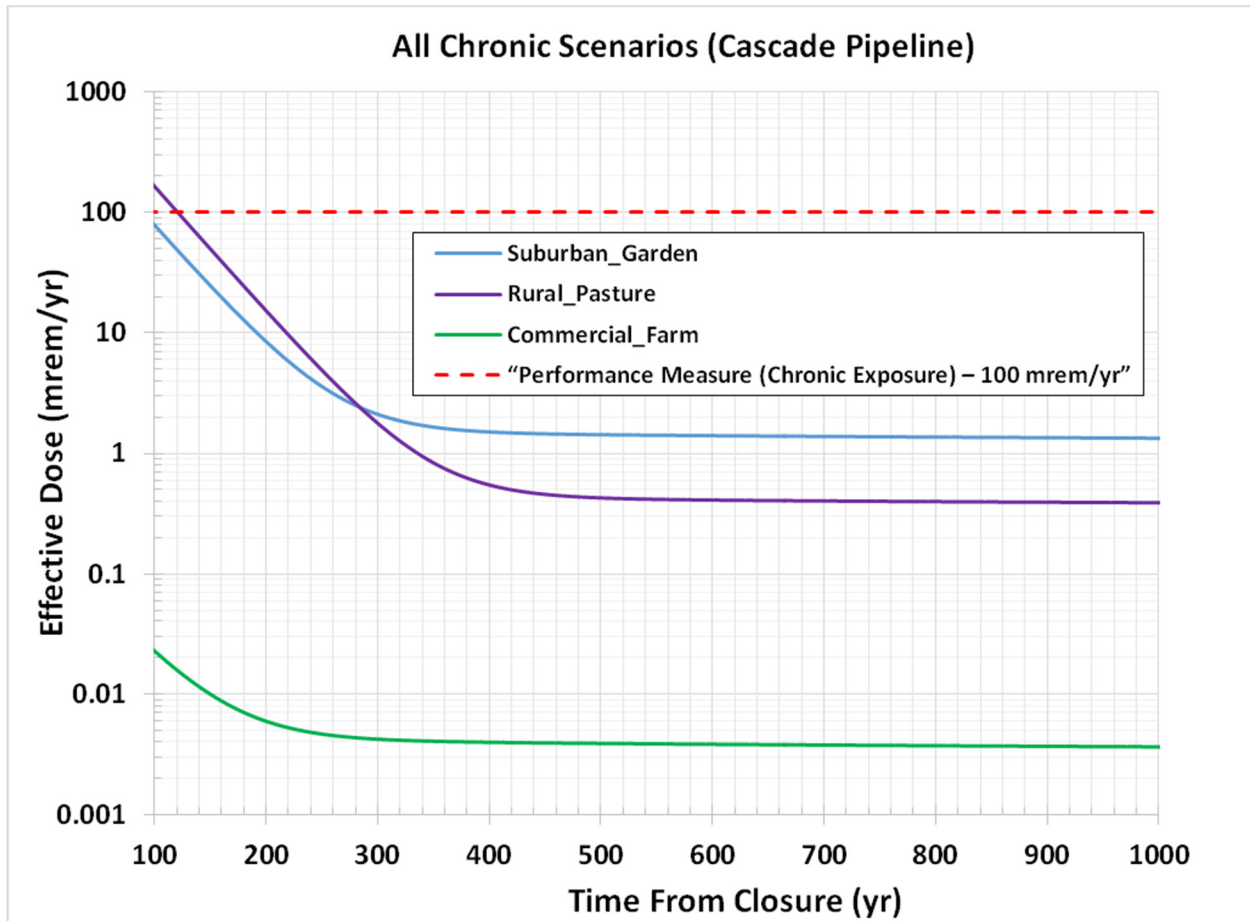
(a)



(b)

RPP-ENV-58782, Rev. 0

Figure 9-15. Effective Dose for All Three Chronic Exposure Scenarios for a Fully Plugged Cascade Pipeline.



RPP-ENV-58782, Rev. 0

10.0 PERFORMANCE EVALUATION AND INTERPRETATION OF RESULTS

In this section, the results of the PA are consolidated and compared against the performance objectives, to interpret their meaning and significance. The goals of this section are as follows:

- To compare the results of the PA against the applicable DOE O 435.1 performance objectives
- To provide a basis to conclude that the performance of waste residuals in tanks and ancillary equipment left at WMA C at closure has been adequately addressed, and that the results provide a sufficient basis for concluding that the closed facility meets the performance objectives in DOE O 435.1
- To provide context for the results of the sensitivity and uncertainty analyses, and the support they provide to the conclusion that release of radionuclides remaining in the tank and ancillary residuals at a closed WMA C meets the performance objectives
- To provide results and interpretation of human health and environmental impacts for the post-compliance sensitivity and uncertainty time period.

The results are presented and interpreted for the following performance objectives and measures:

- All-pathways analysis
- Radon flux analysis
- Biotic pathways
- Groundwater resource protection analysis
- Inadvertent intruder analysis
- Sensitivity analyses for the groundwater pathway.

10.1 ALL-PATHWAYS ANALYSIS

Doses from releases to the groundwater and the air pathways were combined and evaluated against performance objectives for the all-pathways analysis required by DOE O 435.1. The main analysis used to compare against these performance objectives has been called the “base case.” The base case is a deterministic analysis using a set of parameters that evaluates the condition when the safety functions provide their expected contribution to the performance of the facility¹. The all-pathways analysis combines the groundwater pathway analysis and the air pathway analysis for the base case, as discussed in Section 6. The all-pathways dose results are given in Section 7.3.1.

¹ The exceptions to this statement are the safety functions for institutional control and societal memory. As discussed in Section 1, under DOE O 435.1, performance assessment is predicated on the assumption that these safety functions are lost 100 years in the future, allowing exposures of members of the public to occur. If these safety functions were to remain intact, exposure of the kind evaluated in the performance assessment could not occur.

RPP-ENV-58782, Rev. 0

The peak dose from the all-pathways analysis during the 0- to 1,000-year compliance period is associated with the air pathway, with the peak dose of 4×10^{-3} mrem/yr dominated by tritium resulting from upward gaseous diffusive flux from the residual waste. This peak dose occurs in the institutional control period, between 10 and 20 years after closure. This peak dose does not consider the active monitoring measures that are anticipated during institutional control. The all-pathways dose remains substantially lower (approximately 4×10^{-5} mrem/yr) for about 800 years after closure, but shows a rapid increase near the end of the compliance time period due to breakthrough of ^{99}Tc at the PoCal along the groundwater pathway. The peak all-pathways dose during the post-compliance time period (1,000 to 10,000 years after closure) evaluated for the purpose of sensitivity and uncertainty analysis occurs at about 1,500 years after closure, and results primarily from peak in ^{99}Tc concentration at the PoCal in the groundwater pathway. The peak all-pathways' dose within the post-compliance time period is 0.1 mrem/yr.

The all-pathways' peak dose results are summarized in Table 10-1. This peak dose is over two orders of magnitude below the DOE O 435.1 performance objective of 25 mrem/yr during the 1,000-year compliance period, as well as in the sensitivity/uncertainty analysis period (1,000 to 10,000 years).

Table 10-1. Summary of All-Pathways Analysis Results for the Base Case.

Compliance Period (<1,000 yr)		Sensitivity/Uncertainty Period (1,000 – 10,000 yr)	
Peak Dose (mrem/yr)	Time of Peak (years after closure)	Peak Dose (mrem/yr)	Time of Peak (years after closure)
4E-3	10	0.1	1,500
Key radionuclide tritium dominates the peak dose		Key radionuclide ^{99}Tc is nearly 100% of this dose	

The results of the base case are supported by a number of sensitivity and uncertainty analyses, which are described below in Section 10.6.

10.2 AIR PATHWAY ANALYSIS

Potential releases into the gaseous pathway were evaluated and compared to the DOE O 435.1 performance objective of 10 mrem/yr for doses from airborne contamination. The number of contaminants that could potentially be released into the air is very limited, and the inventory of these radionuclides is not large. The results of the analyses (see Section 7.3.2) were orders of magnitude below the performance objective, as shown in Table 10-2. Additional sensitivity analyses were not considered necessary, owing to the negligible releases to the air.

10.3 RADON FLUX

Releases of radon from the facility were evaluated and compared to the 20 pCi/m²/s radon flux performance objective in DOE O 435.1. The inventory of ^{226}Ra (the parent of ^{222}Rn) in WMA C residual waste is small, and initial radon fluxes are very low compared to the performance objectives. Ingrowth of ^{226}Ra from decay of the ^{238}U decay chain leads to increasing radon

RPP-ENV-58782, Rev. 0

fluxes at longer times (Section 7.2.2). However, the fluxes remain many orders of magnitude below the performance objective at all times, as presented in Table 10-3.

Table 10-2. Summary of Results for the Air Pathway.

Compliance Period (<1,000 yr)		Sensitivity/Uncertainty Period (1,000 – 10,000 yr)	
Peak Dose (mrem/yr)	Time of Peak (years after closure)	Peak Dose (mrem/yr)	Time of Peak (years after closure)
4E-3	0	2E-5	1,000 – 10,000
Key radionuclide ^3H at early times, ^{129}I in the sensitivity/uncertainty period. The dose is approximately constant in the period 1,000 to 10,000 years.			

Table 10-3. Summary of Radon Flux Analyses.

Compliance Period (<1,000 yr)		Sensitivity/Uncertainty Period (1,000 – 10,000 yr)	
Peak Flux (pCi/m ² /yr)	Time of Peak (years after closure)	Peak Dose (pCi/m ² /s)	Time of Peak (years after closure)
2E-4	1,000	7E-3	10,000
Flux from Tank 301		Flux from Tank 201	

10.4 INADVERTENT HUMAN INTRUSION

Doses associated with hypothetical inadvertent human intrusion were calculated for all sources in WMA C (see Section 9.0), and compared to the acute and chronic performance measures in DOE O 435.1. However, the calculated doses do not take account of the likelihood of intrusion into the various sources, and there are significant differences between them.

As discussed in Section 3, the tank domes were constructed of reinforced concrete; they are still in good condition and will likely provide a very substantial barrier to a drilling intrusion. Furthermore, upon closure the tanks will be filled with grout, which will add a second, very significant barrier to drilling intrusion. As a result of these barriers, intrusion into grouted tanks is not regarded as a credible event, as the tank domes and infill grout form very substantial and long-lasting barriers to the intrusion. Consequently, while the potential doses that might arise from intrusion into a tank are the highest calculated, the likelihood of occurrence of intrusion into a tank is regarded as very small. As a result, the intrusion analyses for tanks should be regarded as informational, and should not be compared to the performance measures.

By contrast, barriers are much less robust or nonexistent for pipelines and other ancillary equipment, and as a result the primary potential for intrusion is considered to be into ancillary equipment. The likely event for ancillary equipment would be intrusion into a waste transfer pipeline, as discussed in Section 9. This event was used to represent intrusion into any ancillary equipment, and these results are used for comparison with performance measures.

RPP-ENV-58782, Rev. 0

The calculated doses associated with the acute and chronic exposure scenarios for intrusion into a waste transfer pipeline are summarized in Table 10-4 for the compliance time period and for the sensitivity/uncertainty analysis period. The calculated doses for acute and chronic exposure scenario from potential intrusion into a waste transfer pipeline remain below the DOE O 435.1 performance measure for the time period evaluated beyond 100 years after closure. The acute scenario dose is dominated by ^{137}Cs and ^{239}Pu , while chronic scenario doses are dominated by ^{90}Sr , ^{137}Cs and ^{239}Pu . The total dose generally shows a steep decline, compared to the timescales evaluated in the PA, due to short half-lives of ^{90}Sr and ^{137}Cs but becomes stable once long-lived ^{239}Pu becomes the dominant dose contributor. The dominant exposure condition for the assessment was the acute scenario, which had higher doses than the chronic exposure scenarios at 100 years after closure. At longer times (greater than about 500 years after closure), the acute scenario also produced higher calculated doses for the intrusion into waste transfer pipelines, mainly because long-lived ^{239}Pu plays a more important role in the dose calculation.

Table 10-4. Summary of Inadvertent Human Intrusion Analyses for Intrusion into Ancillary Equipment.

Exposure Scenario	Compliance Period ($<1,000$ yr)		Sensitivity/Uncertainty Period ($1,000 - 10,000$ yr)	
	Peak Dose (mrem/yr)	Time of Peak (years after closure)	Peak Dose (mrem/yr)	Time of Peak (years after closure)
Acute inadvertent intruder Performance measure – 500 mrem	36.0	100	11.1	1,000
Chronic inadvertent intruder Performance measure – 100 mrem/yr	8.2	100	0.07	1,000

10.5 GROUNDWATER RESOURCE PROTECTION

Groundwater protection was evaluated by comparing calculated concentrations in groundwater 100 m (328 ft) downgradient from the WMA C boundary during the compliance and sensitivity/uncertainty analysis time periods with the National Primary Drinking Water Regulations for MCLs for radionuclides listed in 40 CFR 141.66. The State of Washington has adopted the Federal drinking water regulations (revised as of July 1, 2009) for MCLs for radionuclides in WAC 246-290, “Group A Public Water Supplies” [WAC 246-290-025, “Adoption by Reference” and WAC 246-290-310, “Maximum Contaminant Levels (MCLs) and Maximum Residual Disinfectant Levels (MRDLs)”].

Peak calculated radionuclide groundwater concentrations are summarized and compared to applicable groundwater protection criteria in Table 10-4. For beta/gamma-emitting radionuclides (^{99}Tc , ^{129}I , ^{79}Se , and ^{126}Sn), an assessment of compliance with the radionuclides’ respective MCLs was conducted by computing the dose equivalent and comparing the sum of the dose over time to the 4-mrem/yr dose equivalent limit. For the man-made radionuclides other than tritium (^3H) and ^{90}Sr , 40 CFR 141.66 requires the maximum concentration limits to be calculated based on 4-mrem total body or organ dose equivalents from 2 L/day (0.5 gal/day) drinking water intake using the 168-hour data list in NBS 69 “Maximum Permissible Body

RPP-ENV-58782, Rev. 0

Burdens and Maximum Permissible Concentrations of Radionuclides in Air and in Water for Occupational Exposure” (National Bureau of Standards Handbook 69). Using this handbook, the MCLs for ^{99}Tc and ^{129}I are 900 pCi/L and 1 pCi/L, respectively. The maximum permissible concentrations in water for ^{79}Se and ^{126}Sn are not mentioned specifically in the handbook, and the MCL for these two radionuclides could not be established.

Table 10-5. Comparison of Peak Groundwater Pathway Results to Groundwater Protection Criteria.

Groundwater Performance Measure (Based on 40 CFR 141)	Compliance Period (100 m Downgradient) (Years 2035–3035)	Post-Compliance Period (100 m Downgradient) (Years 3035–12035)	Comments
Beta/gamma dose equivalent ≤ 4 mrem/yr	5E-4 mrem/yr ^a	0.13 mrem/yr ^a	Peak concentrations of ^{99}Tc within the compliance and post-compliance time periods are ~ 0.12 pCi/L and 30 pCi/L, respectively. ^{99}Tc accounts for almost all of the peak dose. Other minor contributors to dose are ^{129}I , ^{79}Se , and ^{126}Sn .
Gross alpha activity concentration (excluding radon and uranium) ≤ 15 pCi/L	0 pCi/L	1E-10 pCi/L ^b	No arrival at the water table due to high K_d of radionuclides such as ^{237}Np , ^{230}Th , and ^{226}Ra .
Combined ^{226}Ra and ^{228}Ra concentration ≤ 5 pCi/L	0 pCi/L	7E-7 pCi/L	Ingrowth from ^{238}U , ^{238}Pu , ^{234}U , and ^{232}Th .
Uranium concentration ≤ 30 $\mu\text{g/L}$ MCL	0 $\mu\text{g/L}$	0.05 $\mu\text{g/L}$	—
^{90}Sr concentration ≤ 8 pCi/L MCL	NA ^c	NA ^c	—
^3H concentration $\leq 20,000$ pCi/L	0 pCi/L	1E-10 pCi/L ^b	—

^a Calculated using the formula $(C_{\text{Peak}}/\text{MCL}) \times 4$ mrem/yr. For example, using C_{Peak} (peak concentration for ^{99}Tc) = 30 pCi/L and MCL = 900 pCi/L for ^{99}Tc , which is the most significant dose contributor, the equivalent dose is calculated to be 0.13 mrem/yr.

^b Concentrations less than 1E-10 pCi/L are essentially zero.

^c Not applicable; ^{90}Sr was not released to the groundwater pathway during the 10,000-year period due to its relatively short half-life and its low mobility in the subsurface.

MCL = maximum contaminant level

NA = not applicable

Reference: 40 CFR 141, “National Primary Drinking Water Regulations,” Code of Federal Regulations, as amended.

For beta/gamma-emitting radionuclides, the peak dose equivalent was 5×10^{-4} mrem/yr during the compliance time period and about 0.13 mrem/yr for the post-compliance time period, which was dominated by contribution of ^{99}Tc . This dose is below the 4-mrem/yr dose equivalent limit.

RPP-ENV-58782, Rev. 0

The peak gross alpha activity—combined ^{226}Ra and ^{228}Ra concentration, ^{90}Sr concentration, and tritium concentration in the groundwater—is zero during the compliance period, and is projected to be essentially zero during the post-compliance period. The peak uranium concentrations within the compliance and post-compliance time periods are 0 $\mu\text{g/L}$ and 0.05 $\mu\text{g/L}$, respectively.

All of the groundwater protection performance metrics are well below the performance measures, which provide confidence that there is a reasonable expectation that the facility will meet the requirements under the Safe Drinking Water Act of 1974 or 40 CFR 141.66.d.

10.6 SENSITIVITY AND UNCERTAINTY ANALYSES FOR THE GROUNDWATER PATHWAY

The interpretations and discussion in Sections 10.1 through 10.5 were based on the base case analysis. In Section 8, a series of sensitivity and uncertainty analyses were reported that evaluate changes in calculated groundwater impacts that result from changes in selected input parameter estimates.

A set of deterministic sensitivity analyses were conducted that show the effects when the safety functions are degraded compared to their expected behavior. The FEPs that may lead to this degraded behavior are identified in Appendix H. For the purposes of the PA, it is not necessary to quantify the likelihood that the FEPs will influence the system; if there is the potential for a safety function to be degraded, it is evaluated as a sensitivity analysis. The specific safety functions examined in this way relate to the various physical components of the disposal system that included model evaluations of groundwater impacts with the following:

- Higher than expected infiltrations rates; these may be the result of a number of potential effects, ranging from unexpectedly poor performance of the cover, through changes in land use with irrigation on top of the facility
- Changes in the effectiveness of the tanks and infill grout to act as barriers, by assuming that the hydraulic conductivity of the tanks increases at times earlier than expected
- Changes in the leachability of the residual wastes, by assuming that the material would dissolve instantly and completely upon contact with water
- Bounding inventories for unretrieved tanks
- Alternative conceptualizations of the stratigraphy of the vadose zone
- Alternative assumptions about dilution in the aquifer.

The maximum deviation from the base case was a factor of 4.8 higher than the base case, which occurred for sensitivity case INV01, which assumed the maximum ^{99}Tc inventory in the unretrieved tanks, as shown in Table 10-5. For this case, there is no change in the time dependence of the results compared to the base case; the peak occurs in the

RPP-ENV-58782, Rev. 0

sensitivity/uncertainty time period, and the concentration in the compliance time period is small. This case represents an assumption that no further retrieval of ^{99}Tc from tanks will be possible.

Of the sensitivity cases that evaluated safety functions, the maximum deviation from the base case was produced by cases that evaluated the aquifer safety function, as shown in Table 10-6. By setting the aquifer flow properties to their 5th percentile, the peak concentration increased by a factor of 2.6 compared to the base case. There is no change in the time dependence of the results compared to the base case; the peak occurs in the sensitivity/uncertainty time period, and the concentration in the compliance time period is small. This case represents an assumption of minimal dilution in the aquifer.

Table 10-6. Summary of Maximum Results from Sensitivity Cases.

Highest Calculated Peak Concentration of ^{99}Tc divided by the base case	Change in Time of Peak (years after closure) compared to base case
4.8	No change
Sensitivity case INV01, with maximum ^{99}Tc inventory in unretrieved tanks.	
Highest Calculated Peak Concentration of ^{99}Tc divided by the base case	Time of Peak (years after closure)
2.6	No change
Sensitivity case GWP01, with 5% aquifer properties leading to minimal dilution.	

For all of these sensitivity analyses, the disposal system met the performance objectives. This result demonstrates the robustness of the PA to alternative assumptions with respect to the behavior of the safety functions.

In addition to these deterministic analyses of the effect of the safety functions evaluated in Section 8, probabilistic analyses were conducted to show the effects of parameter uncertainty on the performance of the system. A number of parameters were assigned probability density functions, the PA was run probabilistically, and the results were evaluated as a probability density function of dose. The highest calculated groundwater dose in the compliance period was about 0.07 mrem/yr, and the highest calculated peak dose in the sensitivity/uncertainty analysis period was 2.5 mrem/yr, as shown in Table 10-7. The most important uncertain parameters that affect the peak dose in the groundwater pathway are the vadose zone hydraulic properties and Darcy flux in the saturated zone (see Section 8.1.4.4 for details).

For the entire range of input parameters, even including the extreme of the sampled inputs, the disposal system met the performance objectives. These results show the robustness of the PA to uncertainties in the input parameters used in the model.

RPP-ENV-58782, Rev. 0

Table 10-7. Summary of Relevant Results from the Probabilistic Uncertainty Analysis of Groundwater Pathway.

Compliance Period (<1,000 yr)		Sensitivity/Uncertainty Period (1,000 – 10,000 yr)	
Mean Peak Dose (mrem/yr)	Time of Peak (years after closure)	Mean Peak Dose (mrem/yr)	Time of Peak (years after closure)
7E-4	1,000	0.17	3,400
Key radionuclide ⁹⁹ Tc comprises nearly 100% of these doses			
Highest Calculated Peak Dose (mrem/yr)	Time of Peak (years after closure)	Highest Calculated Peak Dose (mrem/yr)	Time of Peak (years after closure)
0.07	1,000	2.5	2,400
Key radionuclide ⁹⁹ Tc comprises nearly 100% of these doses			

10.7 USE OF PERFORMANCE ASSESSMENT RESULTS

The PA has substantiated that landfill closure of residual wastes in WMA C can meet applicable performance objectives and measures. The result can be used to support decisions regarding further retrieval from tanks, in supporting determinations that sufficient retrieval has been accomplished. This will be done as part of a determination that the projected releases of radionuclides to the environment are maintained ALARA. DOE O 413.3B, Program and Project Management for the Acquisition of Capital Assets requires an analysis of ALARA analysis during the design and construction of DOE facilities. The purpose of an ALARA options analysis is to consider those actions that could be taken to reduce both costs and dose. For WMA C, the ALARA options analysis is in part addressed through the process associated with retrieval as documented in Retrieval Data Reports. Although ALARA is not specifically called out in the Retrieval Data Reports, these reports evaluate available waste retrieval technologies to identify (1) retrieval function requirements, (2) retrieval technologies, and (3) appropriate retrieval alternatives. The Retrieval Data Report is considered complete when “no retrieval” is identified as the preferred option, indicating that the amount of retrieval achieved is optimized.

The key result that supports these decisions is the sensitivity analysis case in which no further retrieval was assumed (see Section 10.6 sensitivity case INV01). This analysis case showed that the closed WMA C disposal system met the performance objectives without further retrieval.

In addition to these ALARA considerations that are embedded in the retrieval process, it is anticipated that the PA will be used to support optimization during final detailed design of the facility. This can be done using the PA to establish functional requirements for the design features, such as a functional requirement for infiltration through the surface cover barrier.

In addition, the PA will be used to support decisions related to WIR that will be left at closure within tanks and ancillary equipment. DOE M 435.1-1 Chapter IIB.(2)(a)2. is the second criteria for the WIR evaluation process. This criterion states that such wastes “(w)ill be managed to meet the safety requirements comparable to the performance objectives set out in 10 CFR 61

RPP-ENV-58782, Rev. 0

Subpart C, *Performance Objectives*.” This PA will be the primary tool used to demonstrate that 10 CFR 61.41 and 10 CFR 61.42 are met. Further, the PA will be used to develop the site-specific factors related to 10 CFR 61.55 Class C comparison.

10.8 FUTURE WORK

The current PA is based on partial retrieval of residual wastes from WMA C, and continued retrieval is ongoing. The PA will be updated to reflect updated inventory information when the tanks are considered to be fully retrieved and sample-based inventories are available. Additionally, detailed design of the closure system needs to be performed, including the specific grout formulation to be used in filling the tanks, and the detailed design of the final closure engineered surface cover system. These detailed designs may require updates of the PA.

Grout infill material and the tank concrete shell diverts any infiltrating water from flowing through the tank. Understanding the long-term degradation rates of these cementitious materials under Hanford shallow vadose zone conditions should be considered as an area of future research.

DOE M 435.1-1 Chg 1 [IV.P.(4)] includes a requirement for PA maintenance to evaluate the impact of design and operational changes and to incorporate any new information regarding waste forms, site characteristics, etc. In addition to a PA maintenance plan, required documentation in support of the Tier 1 Closure Authorization Statement (CAS) for WMA C includes a closure plan, monitoring plan, and annual reports documenting any recent changes to the plans for the facility or changes in the understanding of the environmental impacts from the facility. The path forward in the near term includes the following:

- Preparation of an updated PA that addresses key findings, secondary issues, and observations provided by the Low-Level Waste Disposal Facility Federal Review Group (LFRG) during its review of this document
- Development of an additional revision of the PA that resolves review comments by outside agencies (NRC, State Regulators, Public)
- Development and implementation of a change control process to address potential effects of changes in closure actions and decisions that could affect the validity of the analysis and conclusion of this PA.

RPP-ENV-58782, Rev. 0

- 1
- 2
- 3
- 4
- 5
- 6

This page intentionally left blank.

RPP-ENV-58782, Rev. 0

11.0 QUALITY ASSURANCE

Model development and application for the WMA C PA was performed under a general project plan for modeling for RCRA closure analyses and DOE O 435.1 PAs. This general project plan implements the requirements of Title 10, CFR, Part 830, "Nuclear Safety Management" (10 CFR 830) Subpart A, "Quality Assurance Requirements"; DOE O 414.1D, Quality Assurance; and State and Federal environmental regulations. Additionally, this general project plan follows EPA guidance provided in EPA/240/R-02/007, Guidance for Quality Assurance Project Plans for Modeling, EPA QA/G-5M. It addresses as relevant and important all nine "Group A" elements presented in EPA/240/B-01/003, EPA Requirements for Quality Assurance Project Plans, EPA QA/R-5. The nine elements include problem definition and background, quality objectives and criteria for measurements and data acquisition leading to model inputs and outputs, data validation and usability, references, documentation and records management, special training requirements and certifications for modelers, and assessments and reports to management. The model documentation requirements identified during project planning align with DOE management expectations for compliance listed in Revision 1 of EM-QA-001, EM Quality Assurance Program, Attachment H, "Model Development, Use, and Validation."

11.1 ENVIRONMENTAL MODEL LIFECYCLE QUALITY ASSURANCE PROCESS

The development, application, and preservation of environmental models used to support regulatory decision-making and analysis is conducted under a general project plan that implements the requirements of DOE O 414.1D and the direction related to modeling in EM-QA-001, as well as EPA guidance provided in EPA/240/R-02/007. This plan provides for modeling to be performed in a framework for quality assurance of the full lifecycle, with integrated control of models, implementing software, applications, and supporting information as depicted in Figure 11-1.

Highlights of the general plan requirements under which this PA was developed include the following.

- Training is stipulated in the general plan for modelers to complete that ensured the requirements and quality assurance process for model development and application are communicated.
- Software used to implement environmental models is controlled per the requirements of DOE O 414.1D (refer to Section 11.2, below, for further details on this with respect to this PA). Modeling software management is provided at the Hanford Site by CHPRC as part of that contractor's integration role for Hanford Site modeling activities. CHPRC's controlled software management procedure implements the DOE O 414.1D software requirements. This control includes configuration management of code; use of a central registry for software registration, grading and classification, approval tracking, and use logging; and software quality assurance documentation requirements. Software users are required to complete software-specific training assignments, obtain code from the

RPP-ENV-58782, Rev. 0

software owner (configuration management system), complete installation testing for specific computers per the test plan, and submit software installation and checkout documentation to record tested installations.

- A process for model documentation, control, and preservation is specified (refer to Section 11.3, below, for further details on this with respect to this PA). Features of this process include documentation of model development in model package reports (a quality configuration item); documentation of model applications in an Environmental Model Calculation File (EMCF, also a quality configuration item); and preservation of models, model applications, and model basis information (non-direct measurements) in an integrated archive. Full checking and senior review of model package reports and EMCFs is required as part of this process.

The general plan follows the EPA guidance in structure, and provides for flexibility to support with a specific plan for modeling projects that require additional quality assurance/quality control requirements. The WMA C PA modeling work was developed under the general plan and a complementary project-specific plan.

11.2 CONTROLLED SOFTWARE USE

Software used for model implementation was managed following a controlled software management procedure (PRC-PRO-IRM-309, "Controlled Software Management") that implements the requirements of 10 CFR 830 Subpart A, "Quality Assurance Requirements"; DOE O 414.1D; and State and Federal environmental regulations. This controlled software management procedure directs management of all software including configuration control, evaluation, implementation, acceptance and installation testing (verification and validation), and operation and maintenance. Software used to implement the models and perform calculations was approved for use under this controlled software management procedure that also implements the requirements of, and is compliant with, DOE management expectations for compliance listed in Revision 1 of EM-QA-001, Attachment G, "Software Quality Requirements."

The WMA C PA relies on two primary controlled-use software packages to simulate the flow and transport in the subsurface, simulate source term releases, conduct inadvertent intruder calculations, and simulate air-pathway transport in order to calculate doses resulting from the disposal of waste at the facility. These primary software packages are STOMP[®] and GoldSim[®] Pro, which are qualified for controlled use at the Hanford Site in accordance with their respective software management and testing plans. These software packages are registered in the Hanford Information Systems Inventory (HISI). HISI provides the platform for tracking all software in use at the Hanford Site. For safety software (which includes STOMP[®] and GoldSim[®] Pro), the HISI entry is used to record approval for use of software versions, to maintain a registry of authorized users, and to log all instances of the software's usage. Software is maintained using the established Hanford Site configuration management system, MKS Integrity^{TM1}, which is the Hanford Site standard for preserving and managing source code and executable versions of

¹ MKS Integrity, Integrity, and all other PTC product names and logos are trademarks or registered trademarks of Parametric Technology Corporation or its subsidiaries in the United States and in other countries.

RPP-ENV-58782, Rev. 0

software. MKS Integrity™ provides a “checkpoint” feature that locks files at particular points, such as when an executable has passed quality assurance testing, been documented in an acceptance test report, and been approved for use.

Software-specific descriptions, and associated quality assurance documentation for each software package used in the PA, are summarized below for the primary model implementation software packages used for the WMA C PA (STOMP® and GoldSim®).

11.2.1 Subsurface Transport Over Multiple Phases

The vadose zone fate and transport calculations are performed using “CHPRC Build 4” of the STOMP® simulator software (PNNL-12030; PNNL-15782, “STOMP Subsurface Transport Over Multiple Phases Version 4.0 User’s Guide”). STOMP® is registered in the HISI under identification number 2471. The STOMP® simulator was developed at PNNL, which maintains a program to test STOMP® code to meet ASME NQA-1-2008, “Quality Assurance Requirements for Nuclear Facility Applications” software requirements, as well as the requirements specified under DOE O 414.1D for Safety Software. The “Water” and “Water-Transport” operational modes of STOMP® were used for the WMA C PA, and all code elements of those modes that were used have been ASME NQA-1-2008 tested by PNNL. STOMP® use for the WMA C PA is managed and controlled such that the computational needs filled by use of STOMP® (and any associated utility codes) and the specific roles and responsibilities for management and the modeling staff and subcontractors have been identified and traced. These responsibilities include modeler training, source code installation and testing, preserving the software and verification test results, operation and maintenance of the original Fortran source code and executable files provided by PNNL, validation and verification that the PNNL quality assurance documentation demonstrate that STOMP® meets the CHPRC modeling needs and purposes, reporting and documenting any software errors (none were encountered during the development of the WMA C PA), management of the STOMP® input files, and contingency and disaster recovery (which was not encountered during development of the WMA C PA). Acceptance and installation tests of the STOMP® simulation software demonstrate that it is appropriate for its intended uses for the WMA C PA and that it has been successfully installed on computing systems used for STOMP® simulations to develop the WMA C PA.

STOMP® was executed on two independent computer systems. The first of these is the GREEN Linux^{®2} system that is owned and managed by INTERA, Incorporated, which is a subcontractor to WRPS. The GREEN system is physically located at INTERA’s Richland, Washington office, and is comprised of a Dell^{™3} PowerEdge[™] R510 with two 6-core Intel[®] Xeon^{®4} X5660 processors @ 2.80GHz and 48 GB of RAM. The second system used was the Tellus Subsurface Simulation Platform, a Linux[®] cluster system that is owned and managed by CHPRC to support Hanford Site integrated environmental modeling needs. The Tellus cluster system is comprised of a Dell[™] PowerEdge[™] M1000e blade enclosure with 16 Dell[™] PowerEdge[™] M610 and

² Linux[®] is a registered trademark of Linus Torvalds in the U.S. and other countries.

³ Dell and PowerEdge are trademarks of Dell Inc.

⁴ Intel and Xeon are trademarks of Intel Corporation in the U.S. and other countries.

RPP-ENV-58782, Rev. 0

1 1 Dell™ PowerEdge™ M710 blade servers. The M610 blade servers each have 6-core Intel®
2 Xeon X5670 processors @ 2.93 GHz (12MB cache) and 96 GB of RAM.

3
4 DOE/RL-2011-50 contains a summary of the main model attributes and code selection criteria
5 that serve as the basis for the demonstration of the adequacy of the STOMP® code for use in
6 vadose zone modeling at the Hanford Site. The results of the evaluation in DOE/RL-2011-50
7 show that the STOMP® code is capable of meeting or exceeding the identified attributes and
8 criteria.

10 **11.2.2 GoldSim®**

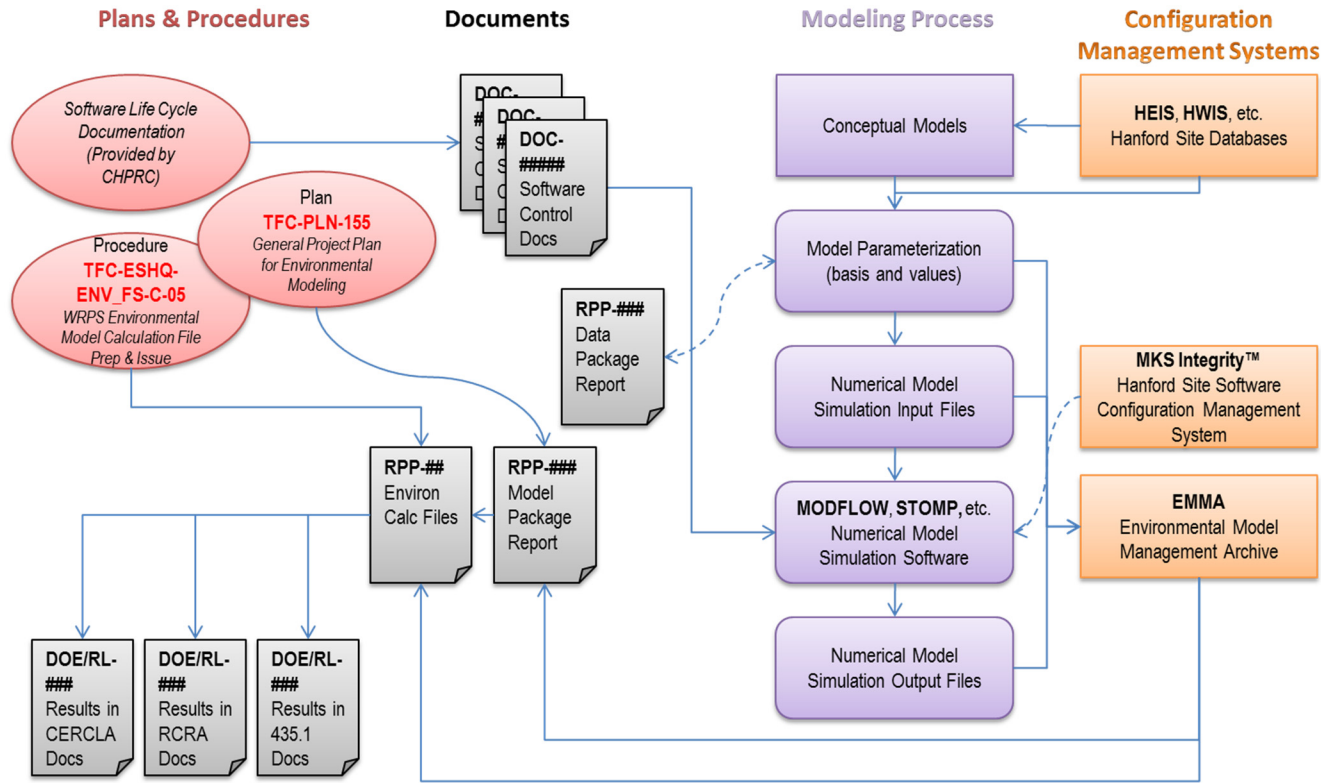
11
12 Software development of GoldSim® Pro meets ASME NQA-1-2008 software requirements, as
13 well as the requirements specified under DOE O 414.1D for Safety Software. GoldSim® Pro use
14 at the Hanford Site is managed and controlled such that the computational needs filled by use of
15 GoldSim® Pro (and any associated utility codes) and the specific roles and responsibilities for
16 management and the modeling staff and subcontractors have been identified and traced. These
17 responsibilities include modeler training, source code installation and testing, preserving the
18 software and verification test results, validation and verification that the GoldSim® Pro quality
19 assurance documentation demonstrate that GoldSim® Pro meets identified modeling needs and
20 purposes, reporting and documenting any software errors (none were encountered during the
21 development of the WMA C PA), management of the GoldSim® Pro input files, and contingency
22 and disaster recovery (which was not encountered during the development of the WMA C PA).
23 Acceptance and installation tests of the GoldSim® Pro simulation software demonstrate that it is
24 appropriate for its intended uses for the WMA C PA and that it has been successfully installed on
25 the computing systems used to conduct WMA C PA modeling.

27 **11.2.3 Other Hanford Site Tank Waste Management Software Tools**

28
29 The PA effort makes use of other tank waste management software tools available at the Hanford
30 Site in the preparation of model inputs.

31
32 **11.2.3.1 Tank Waste Information Network System/Best Basis Inventory.** TWINS is a
33 web-based database system providing access to Hanford tank waste data, documents, graphics,
34 photos and reports via the Hanford Local Area Network (HLAN) and to approved offsite users
35 via the Internet. This legacy software was developed over time and contains a number of
36 primary databases, reporting tools, and support tools. The database system consists of the Tank
37 Characterization Database, Tank Vapor Database, BBI Estimates and BBI Model tool, the
38 Automated Tank Characterization Report system, Data Source Access, Automated Statistics tool,
39 and Automated Vector creation tool. These systems were developed by various projects over a
40 number of years and have been consolidated within the TWINS architecture. A system
41 description can be found in RPP-RPT-39487, "TWINS Software Description." TWINS changes
42 are tracked in accordance with internal WRPS procedures used for TWINS software change
43 control.

Figure 11-1. Lifecycle Quality for Environmental Models.



435.1 = DOE O 435.1, 2001, Radioactive Waste Management, U.S. Department of Energy, Washington, D.C.

CERCLA = Comprehensive Environmental Response, Compensation, and Liability Act of 1980, 42 USC 9622, et seq.

CHPRC = CH2M HILL Plateau Remediation Company

HEIS = Hanford Environmental Information System

HWIS = Hanford Well Information System

RCRA = Resource Conservation and Recovery Act of 1976, 42 USC 6901, et seq.

References:

TFC-ESHQ-ENV_FS-C-05, "WRPS Environmental Model Calculation Preparation and Issuance," Washington River Protection Solutions LLC (WRPS) Tank Farms, Richland, Washington.

TFC-PLN-155, "General Project Plan for Environment Modeling," Washington River Protection Solutions LLC (WRPS) Tank Farms, Richland, Washington.

MKS Integrity, Integrity, and all other PTC product names and logos are trademarks or registered trademarks of Parametric Technology Corporation or its subsidiaries in the United States and in other countries.

MODFLOW software has been developed and distributed by the U.S. Geological Survey, Washington, D.C.

Battelle Memorial Institute (Battelle) retains copyright on all versions, revisions, and operational modes of the Subsurface Transport Over Multiple Phases (STOMP®) software simulator, as permitted by the U.S. Department of Energy. STOMP® is used here under a limited government use license.

RPP-ENV-58782, Rev. 0

Except as noted, BBI estimates with radionuclides decayed to January 1, 2020 were used as source terms for the PA. The BBI is developed using applicable output from the Tank Characterization Database, Automated Statistics tool, Automated Vector creation tool and BBI Model tool. The BBI values are based on sample- and/or model-based composition estimates multiplied by waste volume estimates. Best-Basis process outputs are described in Section 3.2.2. The BBI was developed in accordance with RPP-7625, "Guidelines for Updating Best-Basis Inventory" and TFC-ENG-CHEM-P-53, "Best-Basis Inventory Evaluations." BBI Model tool output was downloaded to a spreadsheet which was reviewed and checked in accordance with internal WRPS procedures used in the preparation and review of engineering calculations and incorporated into RPP-RPT-42323. Output from RPP-RPT-42323 is included in Tables 3-13 through 3-16 in this report.

11.2.3.2 Hanford Tank Waste Operations Simulator. The HTWOS model is a dynamic flowsheet mass balance model that tracks and predicts the movement of waste over the full River Protection Project mission (that is, from current tank contents through treatment to disposal). It establishes the timing of key process steps and the life-cycle system mass balance using a well-defined set of assumptions (the current set being described in Revision 6 of ORP-11242, "River Protection Project System Plan"). The various processes are modeled in sufficient detail to estimate the overall timing of each process and the quantities and composition of the primary and secondary waste streams, taking into account the interactions, including recycle, between the various processes and unit operations. The HTWOS model and validation of the model is described in RPP-RPT-39908, "Hanford Tank Waste Operations Simulator Model (HTWOS) Version 3.0 Verification and Validation Report." The HTWOS spreadsheet output for residual inventories is SVF-2109, Rev. 0, "Tank_Residuals_4MinTimestep(6Melters)-mmr-11-031-6.5-8.3r1-2011-03-18-at-01-31-58_M1.xlsm.

HTWOS residual inventories provided lower bound inventory estimates in the PA for tanks not yet retrieved as of September 1, 2014 (see Section 3.2.2.3.3). The HTWOS model is controlled in accordance with RPP-50816, "Software Management Plan for Grade D Custom Developed Hanford Tank Waste Operations Simulator (HTWOS)." The HTWOS output was downloaded to a spreadsheet to back decay values to January 1, 2020 and scale the values for a waste volume of 360 ft³. The spreadsheet was reviewed and checked in accordance with internal WRPS procedures used in the preparation and review of engineering calculations and incorporated into RPP-RPT-42323. HTWOS residual inventory estimates are included in Table 3-17 in this report.

11.2.3.3 Video Camera Computer-Aided Design Modeling System. The CCMS was used to estimate the volume of residual waste in retrieved tanks. The CCMS approach consists of obtaining in-tank videos showing the location of residual solids and liquid waste remaining in a tank after retrieval. The videos are reviewed and a 3-D CAD drawing of the residual waste is developed using a template of an empty tank. The volume of the residual waste is then calculated using CAD software. The CCMS approach and quality assurance/quality control requirements are described in RPP-52784, "Video camera/CAD Modeling System for Retrieval: HISI #3254 Software Management Plan." CCMS modelers are trained and qualified in accordance with internal WRPS procedures used for post-retrieval volume determinations. Uncertainty in CCMS estimates is described in RPP-23403. Actual and upper bound volumes

RPP-ENV-58782, Rev. 0

based on CCMS estimates are documented in applicable waste volume reports and incorporated into the BBI.

11.2.3.4 Other Legacy Software. This section provides information about legacy software tools, namely the HDW software and the ORIGEN2 software, that are cited in the PA but are not currently managed as controlled use software.

11.2.3.4.1 Hanford Defined Waste Model. The HDW model (RPP-19822) uses a spreadsheet format to combine tank waste transfer and process information with Hanford Site irradiated fuel and separation plant process records from the ORIGEN2 model (RPP-13489) to produce total chemical and radionuclide compositions by waste type. These estimates comprise 46 radionuclides (the standard radioisotopes in the BBI) and 33 nonradioactive species (24 of the 25 standard chemicals from the BBI plus citrate, N-[hydroxyethyl]-ethylenediaminetriacetic acid, ethylenediaminetetraacetic acid, glycolate, acetate, dibutyl phosphate, butanol, ammonia, and ferrocyanide) and four properties (density, water wt%, total organic carbon wt% and sludge void fraction [total organic carbon is a standard constituent in BBI]).

The HDW model concentration estimates are considered to have higher uncertainty compared to sample-based concentrations and are used in BBI to fill gaps where sample data do not exist for a waste type and/or constituent. RPP-19822 (HDW model, Revision 5) was checked in accordance with company procedures (see RPP-19822, Appendix G). Revision 5 uses the same software and formulas as Revision 4, but includes updated ORIGEN2 results and tank waste process inputs to estimate tank waste type compositions and does not include the supernatant mixing model, tank waste layering model, or tank-specific inventory estimates in Revision 4. Additional description of the waste type compositions model is provided in LA-UR-96-3860, "Hanford Tank Chemical and Radionuclide Inventories: HDW Model Rev. 4."

11.2.3.4.2 Oak Ridge Isotope Generation and Depletion Code 2. The primary radionuclide input to the HDW model consists of a file of "pre-decayed" isotopic inventories (Fuel Activity Records) generated using the ORIGEN2 and Radioactive Decay (DK) and Processing (PRO) (DKPRO) codes. The ORIGEN2 code is used to calculate initial radionuclide inventories as a function of fuel type, fuel burn-up, and reactor type, with subsequent decay and processing computed by the DKPRO code. Input to the DKPRO code includes an archive file of separations processing records by fuel batch, a file of processing directives, a file of summary directives, and a set of ORIGEN2 inventory files representing unprocessed radionuclide inventories. The ORIGEN2 and DKPRO software and outputs are described in RPP-13489. Review and checking ORIGEN2 results and verification and validation of DKPRO code are presented in Appendices A and F of RPP-13489.

11.3 MODEL DOCUMENTATION, CONTROL, AND PRESERVATION

The four basic model components necessary to provide traceable, reproducible models are (1) the basis for the model inputs, including data packages, (2) the models themselves, (3) the applications of the models, and (4) the implementing software.

RPP-ENV-58782, Rev. 0

1 As noted above regarding controlled software use, software used for the development of the
2 WMA C PA is maintained using the established Hanford Site configuration management system,
3 MKS Integrity™. However, models are comprised of more than just software. Control and
4 preservation of the other three identified model components (basis, models, and applications) are
5 necessary as well. Under the general project plan for modeling for RCRA closure analyses and
6 DOE O 435.1 PAs followed for development of the WMA C PA, these components are
7 maintained in the WRPS Environmental Model Management Archive (EMMA). The EMMA is
8 the approved means to maintain traceability and reproducibility for these model components by
9 providing for version documentation and preservation of the model basis, inputs, and output,
10 along with identification of the software packages and specific versions used. The EMMA is
11 fundamentally a highly disciplined file system, with defined structure, controls on staging and
12 uploading content, requirements for content preservation, and an active backup plan that ensures
13 the EMMA is frequently synchronized to a controlled, managed disk space inside HLAN.
14 EMMA's organization aligns to the three components mentioned: basis, models, and
15 applications.

- 16
17 • The EMMA "basis" bin includes Electronic Model Data Transmittal coversheets to
18 document preserved data and information that form the basis of model parameterization.
19
- 20 • The EMMA "model" bin includes model package reports that provide the description and
21 explanation of the modeling objectives, conceptualization, implementation, uncertainty
22 and sensitivity evaluations, version configuration control, and the limitations of the
23 models. Model input files that form the specific version of a configuration-controlled
24 model are preserved with the model package report that documents that specific model
25 and version.
26
- 27 • The EMMA "application" bin includes documentation of model applications. While the
28 model package reports include information regarding the complete configuration
29 managed version of the WMA C PA models, the EMCF documents information on
30 specific cases analyzed with the models. This includes the application of the STOMP®
31 and GoldSim® Pro models used to perform the calculations for the WMA C PA.
32
33

RPP-ENV-58782, Rev. 0

12.0 PREPARERS

Marcel P. Bergeron, Washington River Protection Solutions, LCC

M.A., Geology, Indiana University, Bloomington, Indiana
B.A., Geology, University of Vermont, Burlington, Vermont

Mr. Bergeron has more than 35 years of experience in a wide variety of subsurface investigations and studies at radioactive and hazardous waste facilities and contaminated sites. He is experienced in planning and implementation of environmental characterization and risk assessment investigations in a variety of roles including as a technical contributor, a project and task manager, and a line manager. He has performed quantitative analysis of subsurface systems using analytical and numerical models and visualization tools. He has significant technical project experience in managing technical teams, schedules, and budgets for multi-disciplinary projects and communication of project results with clients, regulators, and stakeholders.

For this document, Mr. Bergeron is the technical project lead for Washington River Protection Solutions, LLC and the document manager in the preparation for this performance assessment.

Michael P. Connelly, TecGeo, Inc.

M.S., Geology, University of Utah
B.S., Geology, University of Utah

Mr. Connelly provided technical support to the performance assessment team for the Tank Farm Vadose Zone Project and is a contributing author to this document. He has over 16 years of experience in environmental geohydrology including project management, groundwater modeling, and using computer techniques to analyze and interpret field data for remedial action and site characterization activities.

For this document, Mr. Connelly was the lead author for Section 3 (Site and Facility Characteristics) and provided technical support in the preparation of graphics and visualizations used in Sections 7 (Results of Analysis) and 8.2 (Sensitivity Analysis for the Groundwater Pathway).

James Field, Washington River Protection Solutions, LLC

Ph.D., Engineering Science, Washington State University, May 1989
M.S., Engineering Science, Washington State University, December 1986
B.S., Agricultural Engineering, University of Wyoming, August 1984

Dr. Field has 26 years of experience as engineer and manager in retrieval operations, RCRA/CERCLA waste site closure, technology testing and implementation, characterization, and data management. Dr. Field provides engineering support to the closure program. He was

RPP-ENV-58782, Rev. 0

1 lead for the inventory data package for the Hanford Closure and Waste Management EIS and
2 prepared inventory data packages for tank residuals and releases to the soil in WMA C and
3 WMA A-AX.

4
5 For this document, Dr. Field was the lead author for Section 3.2.2 (Tank Residual Waste
6 Inventory) and provided inventory support for the performance assessment.

7
8
9 **Nazmul Hasan**, INTERA, Inc.

10
11 M.S., Environmental Engineering, Washington State University
12 B.S., Civil Engineering, University of Engineering & Technology, Bangladesh

13
14 Mr. Hasan has over eight years of experience performing numerical modeling in the saturated
15 and unsaturated zones, including model calibration and sensitivity analysis, geostatistical
16 analysis, and programming.

17
18 For this document, Mr. Hasan provided technical assistance in checking flow and transport
19 models, developing the flow-fields for the abstraction model, and performing uncertainty
20 analyses. He also prepared Section 9 (Inadvertent Intruder Analysis) and technically supported
21 the overall document preparation and generation of figures and tables.

22
23
24 **Raziuddin Khaleel**, INTERA, Inc.

25
26 Ph.D., Soil and Water Engineering, Texas A&M University
27 M.S., Water Science and Engineering, Asian University of Technology
28 B.S., Civil Engineering, Bangladesh University of Engineering and Technology

29
30 Dr. Khaleel has over 25 years of experience in groundwater hydrology and numerical
31 simulations of subsurface flow and transport. He was a key contributor to the Hanford Site
32 Performance Assessment for the Disposal of Low-Level Waste in the 200 West Area Burial
33 Grounds, the Performance Assessment for the Disposal of Low-Level Waste in the 200 East
34 Area Burial Grounds, and the Hanford Immobilized Low-Activity Tank Waste Performance
35 Assessment, particularly in the area of conceptual model development, direction of modeling,
36 and in writing the document.

37
38 For this document, Dr. Khaleel developed the hydraulic parameter sets for the vadose zone,
39 technical basis for conceptual vadose zone flow and transport model discussed in Appendix A,
40 and document preparation.

RPP-ENV-58782, Rev. 0

Matthew W. Kozak, INTERA, Inc.

Ph.D., 1988, Chemical Engineering, University of Washington
B.S., 1981, Chemical Engineering, Cleveland State University

Dr. Kozak has more than 27 years of experience in the areas of performance assessment of near-surface and geological radioactive waste repositories, regulatory development, dose assessment for residual contamination of soils and buildings, toxic materials risk assessment, and mixed waste issues. He is the author of over 100 publications on these topics. He has supported national programs in the U.S. and countries in Europe, Asia, and Africa to site, develop, construct, and analyze facilities for disposal of radioactive waste.

He has participated in a number of international research programs, including the International Atomic Energy Agency's (IAEA) Coordinated Research Program on Improvement of Safety Assessment Methodologies (ISAM), and its successor programs: Application of Safety Assessment Methodologies (ASAM), Practical Illustration and Use of the Safety Case Concept in the Management of Near-Surface Disposal (PRISM), and most recently Modelling and Data for Radiological Impact Assessments (MODARIA).

For this document, Dr. Kozak has been one of the principal investigators, and was the lead author for Sections 1 (Introduction), 2 (Assessment Context), and 10 (Performance Evaluation and Interpretation of Results), and Appendix H (List of Features, Events, and Processes Applied to Waste Management Area C), with additional input on project coordination, reviews, and overall document preparation.

Sunil Mehta, INTERA, Inc.

Ph.D., Earth Sciences (Hydrogeology specialization), University of Kentucky
M.S., Geosciences, University of Louisiana at Monroe
M.Sc., Geology, University of Poona, India
B.Sc., Chemistry, Zoology, and Geology, University of Jodhpur, India

Dr. Mehta has more than 18 years of experience related to groundwater flow and transport modeling, reactive transport modeling, total system performance assessment, uncertainty analysis, geophysical logging, and well testing. He has worked on projects involving geologic isolation of radioactive wastes, environmental restoration activities, and water resources exploration and evaluation. Dr. Mehta has over 10 years of experience in designing, developing, and applying probabilistic tools to assess the long-term performance of radioactive waste storage and disposal facilities. He has performed reactive transport modeling and groundwater flow modeling to study behavior of contaminants such as uranium and hexavalent chromium in periodically rewetted zones influenced by aquifer-river interactions.

For this document, Dr. Mehta has been one of the principal investigators, performing the flow and transport abstraction modeling for uncertainty analysis and dose calculations, inadvertent

RPP-ENV-58782, Rev. 0

intruder analysis, and air-pathway analysis, focusing on project coordination, reviews, and overall document preparation.

William J. McMahon, CH2M HILL – Plateau Remediation Contractor

M.S., Agricultural Engineering, Texas A&M University

B.S., Agricultural Engineering, University of California, Davis

Mr. McMahon specializes in hydrologic data collection, analysis, and interpretation, and groundwater and vadose zone numerical modeling to support groundwater and vadose remedial projects. He has experience with a number of vadose zone and groundwater modeling packages. His other duties include directing hydrologic data collection efforts, analyzing and interpreting hydrologic data, assessing the effectiveness of groundwater remedial actions, developing work plans for data collection and interpretation, and performing numerical modeling to predict facility impacts to the aquifer to support remediation and construction decisions.

For this study, Mr. McMahon has been the one of the principal investigators, focusing on the flow and transport modeling using STOMP[®] code, groundwater pathway compliance calculations, sensitivity analysis, and document preparation.

Donna Morgans, INTERA, Inc.

M.S., Environmental Toxicology, Oregon State University

B.S., Microbiology, Oregon State University

Ms. Morgans has 27 years of experience in assessing the potential for adverse human health effects associated with exposure to radiological and chemical contaminants in air, soil, water, and plant and animal tissues. She has managed and performed complex risk assessment and data compilation efforts to address Federal and State regulations that include CERCLA and RCRA lifecycle decisions and DOE O 435.1 requirements. Her experience includes the development and review of elements within work plans, remedial investigations and RCRA facility investigations, and feasibility studies and corrective measure studies.

For this document, Ms. Morgans provided technical support in the development of exposure parameters and equations presented in Section 6.3.3 (Exposure and Dose Analysis). Exposure scenarios included in the performance assessment include the All-Pathways Representative Person Scenario, the Atmospheric Pathway, and the hypothetical Inadvertent Intruder scenarios. The exposure scenario included in the RCRA closure analysis includes the EPA tap water (resident) scenario used in the RCRA analysis.

RPP-ENV-58782, Rev. 0

1 **Benjing Sun**, Ramboll Environ, Inc.

2
3 Ph.D., Environmental Analytical/Atmospheric Chemistry, Brigham Young University

4 M.S., Environmental Sciences, Beijing Normal University

5 B.S., Physics, Beijing Normal University

6
7 Dr. Sun has expertise in managing and conducting projects in the areas of risk assessment,
8 performance assessment, environmental chemistry, and air quality modeling. He also has
9 experience in permitting, regulatory compliance and environmental forensic investigation. He
10 has in-depth knowledge in fate and transport modeling among multiple environmental media,
11 sensitivity and uncertainty analyses, and risk-based remediation goal setup following the
12 technical guidance under CERCLA and RCRA, and other Federal and State regulations. He has
13 managed and performed many risk assessment projects in support of remedial
14 investigation/feasibility study, permit application, regulatory compliance, and risk management.

15
16 For this document, Dr. Sun developed exposure scenarios and associated parameters, dose
17 calculation methodologies for various exposure pathways, and validation activities for the air
18 pathway.

19
20
21 **Kristin M. Singleton**, Washington River Protection Solutions, LLC

22
23 B.S., Cellular and Molecular Biology, University of Nevada, Reno

24
25 Mz. Singleton has six years of experience performing extensive risk assessments across the
26 Hanford Site Tank Farms and River Corridor. She has experience developing risk-based
27 remediation goals in compliance with Federal and State regulations and interpreting modeling
28 results for hazardous waste facilities and contaminated sites.

29
30 In this document, Mz. Singleton provided technical support in the development of waste
31 inventories and screening analysis and supported the preparation of Sections 3.2.2 (Tank
32 Residual Waste Inventory) and 4 (Screening Approaches).

RPP-ENV-58782, Rev. 0

- 1
- 2
- 3
- 4
- 5
- 6

This page intentionally left blank.

RPP-ENV-58782, Rev. 0

13.0 REFERENCES

- 04-TPD-083, 2004, “Agreement on Content of Tank Waste Retrieval Work Plans” (external letter from R. J. Schepens to M. A. Wilson, Nuclear Waste Program, State of Washington Department of Ecology, August 20), U.S. Department of Energy, Office of River Protection, Richland, Washington.
- 10 CFR 61, “Licensing Requirements for Land Disposal of Radioactive Waste,” Subpart C—Performance Objectives, Code of Federal Regulations, as amended.
- 10 CFR 61, “Licensing Requirements for Land Disposal of Radioactive Waste,” Subpart C—Performance Objectives, § 61.41, Protection of the General Population from Releases of Radioactivity, Code of Federal Regulations, as amended.
- 10 CFR 61, “Licensing Requirements for Land Disposal of Radioactive Waste,” Subpart C—Performance Objectives, § 61.42, Protection of individuals from inadvertent intrusion, Code of Federal Regulations, as amended.
- 10 CFR 61, “Licensing Requirements for Land Disposal of Radioactive Waste,” Subpart D—Technical Requirements for Land Disposal Facilities, § 61.52, Land disposal facility operation and disposal site closure, Code of Federal Regulations, as amended.
- 10 CFR 61, “Licensing Requirements for Land Disposal of Radioactive Waste,” Subpart D—Technical Requirements for Land Disposal Facilities, § 61.55, Waste classification, Code of Federal Regulations, as amended.
- 10 CFR 830, “Nuclear Safety Management,” Code of Federal Regulations, as amended.
- 10 CFR 830, “Nuclear Safety Management, Subpart A—Quality Assurance Requirements,” Code of Federal Regulations, as amended.
- 1301789, 2012, “Modeling to Support Regulatory Decisionmaking at Hanford” (internal memorandum from A. C. Williams to M. S. McCormick [Richland Operations Office] and S. L. Samuelson [Office Of River Protection], October 9), Associate Principal Deputy Assistant Secretary for Environmental Management, U.S. Department of Energy, Washington, D.C.
- 14-ECD-0030, 2014, “Transmittal of Clean Closure Practicability Demonstration for the Single-Shell Tanks DOE/ORP-2014-02” (letter from K. W. Smith to J. A. Hedges, Nuclear Waste Program, Washington State Department of Ecology, July 23), U.S. Department of Energy, Office of River Protection, Richland, Washington.
- 40 CFR 141, “National Primary Drinking Water Regulations,” Subpart G—National Primary Drinking Water Regulations: Maximum Contaminant Levels and Maximum Residual Disinfectant Levels, § 141.66 Maximum contaminant levels for radionuclides, Code of Federal Regulations, as amended.

RPP-ENV-58782, Rev. 0

- 1 62 FR 8693, 1997, “Record of Decision for the Tank Waste Remediation System, Hanford Site,
2 Richland, WA,” Federal Register, Vol. 62, pp. 8693–8704 (February 26).
- 3 64 FR 61615, 1999, “Record of Decision: Hanford Comprehensive Land-Use Plan
4 Environmental Impact Statement (HCP EIS),” Federal Register, Vol. 64,
5 pp. 61615–61625 (November 12).
- 6 65 FR 37253, 2000, “Establishment of the Hanford Reach National Monument,” Federal
7 Register, Vol. 65, pp. 37253–37257 (June 13).
- 8 73 FR 55824, 2008, “Amended Record of Decision for the Hanford Comprehensive Land-Use
9 Plan Environmental Impact Statement,” Federal Register, Vol. 73, pp. 55824–55826
10 (September 26).
- 11 78 FR 75913, 2013, “Record of Decision: Final Tank Closure and Waste Management
12 Environmental Impact Statement for the Hanford Site, Richland, Washington,” Federal
13 Register, Vol. 78, pp. 75913–75919 (December 13).
- 14 80 FR 16082, 2015, “Low-Level Radioactive Waste Disposal,” Federal Register, Vol. 80,
15 pp. 16082–16125 (March 26).
- 16 ANL/EAD-4, 2001, “User’s Manual for RESRAD Version 6,” Environmental Assessment
17 Division, Argonne National Laboratory, Argonne, Illinois.
- 18 ARH-CD-775, 1976, “Geohydrologic Study of the West Lake Basin,” Atlantic Richfield
19 Hanford Company, Richland, Washington.
- 20 ARH-LD-132, 1976, “Geology of the 241-C Tank Farm,” Atlantic Richfield Hanford Company,
21 Richland, Washington.
- 22 ASME NQA-1, 2000, “Quality Assurance Requirements for Nuclear Facility Applications,”
23 American National Standards Institute/American Society of Mechanical Engineers, New
24 York, New York.
- 25 ASTM A283/A283M-03, 2005, “Standard Specification for Low and Intermediate Tensile
26 Strength Carbon Steel Plates,” ASTM International, West Conshohocken, Pennsylvania.
- 27 Atomic Energy Act of 1954, 42 USC 2011, et seq., as amended.
- 28 Baker, V. R., B. N. Bjornstad, A. J. Busacca, K. R. Fecht, E. P. Kiver, U. L. Moddy, J. G. Rigby,
29 D. F. Stradling, and A. M. Tallman, 1991, “Quaternary Geology of the Columbia
30 Plateau,” The Geology of North America, Quaternary Nonglacial Geology:
31 Conterminous U.S., Vol. K-2, Chapter 8, pp. 215–250.
- 32 Bear, J. 1972, Dynamics of Fluids in Porous Media, American Elsevier Publishing
33 Company, Inc., New York, New York.

RPP-ENV-58782, Rev. 0

- 1 BHI-00007, 1994, "Prototype Hanford Surface Barrier: Design Basis Document," Rev. 00,
2 Bechtel Hanford, Inc., Richland, Washington.
- 3 BHI-00144, 1995, "Long-term Climate Change Effects Task for the Hanford Site Permanent
4 Isolation Barrier Development Program: Final Report," Bechtel Hanford Company,
5 Richland, Washington.
- 6 BHI-00169, 1995, "Environmental Restoration Disposal Facility Performance Assessment,"
7 Revision 00, Bechtel Hanford, Inc., Richland, Washington.
- 8 BHI-00184, 1995, "Miocene- to Pliocene-Aged Suprabasalt Sediments of the Hanford Site,
9 South-Central Washington," Rev. 00, Bechtel Hanford, Inc., Richland, Washington.
- 10 BHI-00230, 1996, "Geologic Field Inspection of the Sedimentary Sequence at the Environmental
11 Restoration Disposal Facility," Bechtel Hanford, Inc., Richland, Washington.
- 12 BHI-01103, 1999, "Clastic Injection Dikes of the Pasco Basin and Vicinity – Geologic Atlas
13 Series," Rev. 0, Bechtel Hanford, Inc., Richland, Washington.
- 14 BHI-01745, 2004, "2004 Environmental Restoration Contractor Revegetation Monitoring
15 Report," Bechtel Hanford Inc., Rev. 0, Richland, Washington.
- 16 Bjornstad, B. N., K. R. Fecht, and C. J. Pluhar, 2001, "Long History of Pre-Wisconsin, Ice Age
17 Cataclysmic Floods: Evidence from Southeastern Washington State," The Journal of
18 Geology, Vol. 109, pp. 695–713.
- 19 BNWL-243, 1966, "Soil Survey Hanford Project in Benton County Washington," Pacific
20 Northwest Laboratory, Richland, Washington.
- 21 BNWL-1709, 1973, "Collection and Analysis of Pump Test Data for Transmissivity Values,"
22 Pacific Northwest Laboratories, Richland, Washington.
- 23 BNWL-B-360, 1974, "Selected Water Table Contour Maps and Well Hydrographs for the
24 Hanford Reservation, 1944-1973," Pacific Northwest Laboratory, Richland, Washington.
- 25 BPF-73550, 1944, "Specifications For Construction of Composite Storage Tanks Bldg. No. 241
26 Hanford Engineer Works Project 9536," Rev. 2, Richland, Washington.
- 27 Bredehoeft, J. D., C. E. Neuzil, and P. C. D. Milly, 1983, "Regional Flow in the Dakota Aquifer:
28 A Study of the Role of Confining Layers," Water-Supply Paper 2237, U.S. Geological
29 Survey, Alexandria, Virginia.
- 30 Bredehoeft, J. D. and L. F. Konikow, 1993, "Ground-Water Models: Validate or Invalidate,"
31 Groundwater, Vol. 31, No. 2, pp. 178–179.

RPP-ENV-58782, Rev. 0

- 1 Brown, K. G., J. Arnold, S. Sarkar, G. Flach, H. van der Sloot, J.C.L. Meeussen and
2 D. S. Kosson, 2013, "Modeling Carbonation of High-Level Waste Tank Integrity and
3 Closure," EPJ Web of Conferences, Vol. 56, pp. 1–10.
- 4 Bruckler, L., B. C. Ball, and P. Renault, 1989, "Laboratory Estimation of Gas Diffusion
5 Coefficient and Effective Porosity in Soils," Soil Science, Vol. 147, pp. 1–10.
- 6 Cantrell, K. J., K. C. Carroll, E. C. Buck, D. Neiner, K. N. Geiszler, 2013, "Single-pass
7 flow-through test elucidation of weathering behavior and evaluation of contaminant
8 release models for Hanford tank residual radioactive waste," Applied Geochemistry,
9 Vol. 28, pp. 119–127.
- 10 Cantrell, K. J., W. J. Deutsch, and M. J. Lindberg, 2011, "Thermodynamic Model for Uranium
11 Release from Hanford Site Tank Residual Waste," Environmental Science &
12 Technology, Vol. 45, No. 4, pp. 1473–1480.
- 13 CHPRC-00269, 2013, "STOMP Requirements Traceability Matrix CHPRC Build 4," Rev. 3,
14 CH2M HILL Plateau Remediation Company, Richland, Washington.
- 15 CNWRA/NRC, 2011, "History and Value of Uncertainty and Sensitivity Analyses at the Nuclear
16 Regulatory Commission and Center for Nuclear Waste Regulatory Analyses," Center for
17 Nuclear Waste Regulatory Analyses, San Antonio, Texas/U.S. Nuclear Regulatory
18 Commission, Washington, D.C.
- 19 Comprehensive Environmental Response, Compensation, and Liability Act of 1980,
20 42 USC 9622, et seq.
- 21 Consent Decree, State of Washington v. Department of Energy, Case No. CV-08-5085-RMP,
22 United States District Court, Eastern District of Washington (October 25, 2010).
- 23 CP-14873, 2003, "200-BP-1 Prototype Hanford Barrier Annual Monitoring Report for Fiscal
24 Year 2002," Rev. 0, Fluor Hanford, Inc., Richland, Washington.
- 25 CP-47631, 2011, "Model Package Report: Central Plateau Groundwater Model Version 3.3,"
26 Rev. 0, CH2M HILL Plateau Remediation Company, Richland, Washington.
- 27 CP-47631, 2015, "Model Package Report: Central Plateau Groundwater Model Version 6.3.3,"
28 Rev. 2, INTERA, Inc., Richland, Washington.
- 29 D&D-25575, 2005, "Silt Borrow Source Field Investigation Report," Rev. 0, Fluor
30 Hanford, Inc., Richland Washington.
- 31 Deutsch, W. J., K. J. Cantrell, K. M. Krupka, M. L. Lindberg, and R. J. Serne, 2011, "Hanford
32 tank residual waste – Contaminant source terms and release models," Applied
33 Geochemistry, Vol. 26, pp. 1681–1693.

RPP-ENV-58782, Rev. 0

- 1 DOE/EIS-0222-F, 1999, "Final Hanford Comprehensive Land-Use Plan Environmental Impact
2 Statement," U.S. Department of Energy, Richland Operations Office, Richland,
3 Washington.
- 4 DOE/EIS-0222-SA-01, 2008, "Hanford Comprehensive Land-Use Plan Environmental Impact
5 Statement Supplement Analysis," Rev. 0, U.S. Department of Energy, Richland
6 Operations Office, Richland, Washington.
- 7 DOE/EIS-0222-SA-02, 2015, "Supplement Analysis of the Hanford Comprehensive Land-Use
8 Plan Environmental Impact Statement," Rev. 0, U.S. Department of Energy, Richland
9 Operations Office, Richland, Washington.
- 10 DOE/EIS-0310, 2000, "Final Programmatic Environmental Impact Statement for Accomplishing
11 Expanded Civilian Nuclear Energy Research and Development and Isotope Production
12 Missions in the United States, Including the Role of the Fast Flux Test Facility,"
13 U.S. Department of Energy, Office of Nuclear Energy, Science and Technology,
14 Washington, D.C.
- 15 DOE/EIS-0391, 2012, "Final Tank Closure and Waste Management Environmental Impact
16 Statement for the Hanford Site, Richland, Washington," U.S. Department of Energy,
17 Washington, D.C.
- 18 DOE G 435.1-1, 1999, Implementation Guide for Use with DOE M 435.1-1, Radioactive Waste
19 Management Manual, U.S. Department of Energy, Washington, D.C.
- 20 DOE G 435.1-2, DRAFT, Implementation Guide for use with DOE M 435.1-1, Format and
21 Content Guide for U.S. Department of Energy Low-Level Waste Disposal Facility
22 Performance Assessments and Composite Analyses, U.S. Department of Energy,
23 Washington, D.C.
- 24 DOE M 435.1-1, 2007, Radioactive Waste Management Manual, U.S. Department of Energy,
25 Washington, D.C.
- 26 DOE/NV/25946--107, 2008, "Probabilistic Performance Assessment of a Low-Level
27 Radioactive Waste Disposal Site on the Nevada Test Site," National Security
28 Technologies, LLC for the U.S. Department of Energy, National Nuclear Security
29 Administration Nevada Site Office.
- 30 DOE O 413.3B, 2010, Program and Project Management for the Acquisition of Capital Assets,
31 U.S. Department of Energy, Washington, D.C.
- 32 DOE O 414.1D, 2011, Quality Assurance, U.S. Department of Energy, Washington, D.C.
- 33 DOE O 430.1B, 2008, Real Property Asset Management, U.S. Department of Energy,
34 Washington, D.C.

RPP-ENV-58782, Rev. 0

- 1 DOE O 435.1, 2001, Radioactive Waste Management, U.S. Department of Energy,
2 Washington, D.C.
- 3 DOE O 458.1, 2013, Radiation Protection of the Public and the Environment, U.S. Department
4 of Energy, Office of Health, Safety and Security, Washington, D.C.
- 5 DOE/ORP-2000-24, 2001, Hanford Immobilized Low-Activity Waste Performance Assessment:
6 2001 Version, Rev. 0, U.S. Department of Energy, Office of River Protection, Richland,
7 Washington.
- 8 DOE/ORP-2003-11, 2003, Preliminary Performance Assessment for Waste Management Area C
9 at the Hanford Site, Washington, Rev. 0, U.S. Department of Energy, Office of River
10 Protection, Richland, Washington.
- 11 DOE/ORP-2005-01, 2006, Initial Single-Shell Tank System Performance Assessment for the
12 Hanford Site, Rev. 0, U.S. Department of Energy, Office of River Protection, Richland,
13 Washington.
- 14 DOE/ORP-2008-01, 2010, RCRA Facility Investigation Report for Hanford Single-Shell Tank
15 Waste Management Areas, Rev. 1, U.S. Department of Energy, Office of River
16 Protection, Richland, Washington.
- 17 DOE/ORP-2014-02, 2014, Clean Closure Practicability Demonstration for Single-Shell Tanks,
18 Rev. 1, U.S. Department of Energy, Office of River Protection, Richland, Washington.
- 19 DOE P 454.1, 2011, Use of Institutional Controls, U.S. Department of Energy, Washington, D.C.
- 20 DOE/RL-88-30, 2015, Hanford Site Waste Management Units Report, Rev. 24, U.S. Department
21 of Energy, Richland Operations Office, Richland, Washington.
- 22 DOE/RL-91-45, 1995, Hanford Site Risk Assessment Methodology, Rev. 3, U.S. Department of
23 Energy, Richland Operations Office, Richland, Washington.
- 24 DOE/RL-92-04, 1993, PUREX Source Aggregate Area Management Study Report, Rev. 0,
25 U.S. Department of Energy, Richland Operations Office, Richland, Washington.
- 26 DOE/RL-92-94, 2001, Hanford Site Background: Part 1, Soil Background for Nonradioactive
27 Analytes, Rev. 4, 2 vols., U.S. Department of Energy, Richland Operations Office,
28 Richland, Washington.
- 29 DOE/RL-93-33, 1996, Focused Feasibility Study of Engineered Barriers for Waste Management
30 Units in the 200 Areas, Rev. 1, U.S. Department of Energy, Richland Operations Office,
31 Richland, Washington.
- 32 DOE/RL-95-55, 1995, Hanford Site Background: Evaluation of Existing Soil Radionuclide
33 Data, Rev. 0, U.S. Department of Energy, Richland Operations Office, Richland,
34 Washington.

RPP-ENV-58782, Rev. 0

- 1 DOE/RL-96-12, 1996, Hanford Site Background: Part 2, Soil Background for Radionuclides,
2 Rev. 0, U.S. Department of Energy, Richland Operations Office, Richland, Washington.
- 3 DOE/RL-96-16, 1998, Screening Assessment and Requirements for a Comprehensive
4 Assessment: Columbia River Comprehensive Impact Assessment, Rev. 1,
5 U.S. Department of Energy, Richland Operations Office, Richland, Washington.
- 6 DOE/RL-96-81, 1997, Waste Site Grouping for 200 Areas Soil Investigations, Rev. 0,
7 U.S. Department of Energy, Richland Operations Office, Richland, Washington.
- 8 DOE/RL-97-02, 1997, National Register of Historic Places Multiple Property Documentation
9 Form - Historic, Archaeological and Traditional Cultural Properties of the Hanford Site,
10 Washington, Rev. 0, U.S. Department of Energy, Richland Operations Office, Richland,
11 Washington.
- 12 DOE/RL-99-11, 1999, 200-BP-1 Prototype Barrier Treatability Test Report, Rev. 0,
13 U.S. Department of Energy, Richland Operations Office, Richland, Washington.
- 14 DOE/RL-99-36, 2000, Phase 1 RCRA Facility Investigation/Corrective Measures Study Work
15 Plan for Single-Shell Tank Waste Management Areas, Rev. 1, U.S. Department of
16 Energy, Richland Operations Office, Richland, Washington.
- 17 DOE/RL-2001-41, 2009, Sitewide Institutional Controls Plan for Hanford CERCLA Response
18 Actions, Rev. 4, U.S. Department of Energy, Richland Operations Office, Richland,
19 Washington.
- 20 DOE/RL-2001-54, 2002, Ecological Evaluation of the Hanford 200 Areas-Phase 1: Compilation
21 of Existing 200 Areas Ecological Data, Draft A, U.S. Department of Energy, Richland
22 Operations Office, Richland, Washington.
- 23 DOE/RL-2001-54, 2005, Central Plateau Ecological Evaluation, Rev. 0, U.S. Department of
24 Energy, Richland Operations Office, Richland, Washington.
- 25 DOE/RL-2002-39, 2002, Standardized Stratigraphic Nomenclature for Post-Ringold-Formation
26 Sediments Within the Central Pasco Basin, Rev. 0, U.S. Department of Energy, Richland
27 Operations Office, Richland, Washington.
- 28 DOE/RL-2002-59, 2004, Hanford Site Groundwater Strategy Protection, Monitoring, and
29 Remediation, U.S. Department of Energy, Richland Operations Office, Richland,
30 Washington.
- 31 DOE/RL-2007-50, 2011, Central Plateau Ecological Risk Assessment Data Package Report,
32 Rev. 1, U.S. Department of Energy, Richland Operations Office, Richland, Washington.
- 33 DOE/RL-2009-10, 2013, Hanford Site Cleanup Completion Framework, Rev. 1,
34 U.S. Department of Energy, Richland Operations Office, Richland, Washington.

RPP-ENV-58782, Rev. 0

- 1 DOE/RL-2009-77, 2010, Groundwater Quality Assessment Plan for the Single-Shell Tank Waste
2 Management Area C, Rev. 0, U.S. Department of Energy, Richland Operations Office,
3 Richland, Washington.
- 4 DOE/RL-2009-85, 2012, Remedial Investigation Report for the 200-PO-1 Groundwater
5 Operable Unit, Rev. 1, U.S. Department of Energy, Richland Operations Office,
6 Richland, Washington.
- 7 DOE/RL-2010-97, 2011, Remedial Investigation/Feasibility Study for the 100-KR-1, 100-KR-2,
8 and 100-KR-4 Operable Units, Draft A, U.S. Department of Energy, Richland Operations
9 Office, Richland, Washington.
- 10 DOE/RL-2011-50, 2012, Regulatory Basis and Implementation of a Graded Approach to
11 Evaluation of Groundwater Protection, Rev. 1, U.S. Department of Energy, Richland
12 Operations Office, Richland, Washington.
- 13 DOE/RL-2013-22, 2013, Hanford Site Groundwater Monitoring Report for 2012, Rev. 0,
14 CH2M HILL Plateau Remediation Company, Richland, Washington.
- 15 DOE/RL-2014-32, 2014, Hanford Site Groundwater Monitoring Report for 2013, Rev. 0,
16 U.S. Department of Energy, Richland Operations Office, Richland, Washington.
- 17 DOE/RW-0070, 1986, Nuclear Waste Policy Act (Section 112), Environmental Assessment,
18 Reference Repository Location, Hanford Site, Washington, U.S. Department of Energy,
19 Office of Civilian Radioactive Waste Management, Washington, D.C.
- 20 DOE/RW-0164, 1988, Consultation Draft Site Characterization Plan Reference Repository
21 Location, Hanford Site, Washington, U.S. Department of Energy, Office of Civilian
22 Radioactive Waste Management, Washington, D.C.
- 23 DOE-STD-1196-2011, 2011, Derived Concentration Technical Standard, U.S. Department of
24 Energy, Washington, D.C.
- 25 DOE-STD-XXX, 2014 (Draft), Radioactive Waste Management Disposal Authorization
26 Statement Technical Basis Documentation Technical Standard, U.S. Department of
27 Energy, Washington, D.C.
- 28 Ecology, EPA, and DOE, 1989, Hanford Federal Facility Agreement and Consent Order –
29 Tri-Party Agreement, 2 vols., as amended, State of Washington Department of Ecology,
30 U.S. Environmental Protection Agency, and U.S. Department of Energy, Olympia,
31 Washington.
- 32 EM-QA-001, 2012, EM Quality Assurance Program (QAP), Rev. 1, Office of Environmental
33 Management, U.S. Department of Energy, Washington, D.C.
- 34 EPA, 2014, CAP88-PC Version 4.0 User Guide, U.S. Environmental Protection Agency,
35 Washington, D.C.

RPP-ENV-58782, Rev. 0

- 1 EPA/240/B-01/003, 2001, EPA Requirements for Quality Assurance Project Plans,
2 EPA QA/R-5, U.S. Environmental Protection Agency, Office of Environmental
3 Information, Washington, D.C.
- 4 EPA/240/R-02/007, 2002, Guidance for Quality Assurance Project Plans for Modeling,
5 EPA QA/G-5M, U.S. Environmental Protection Agency, Office of Environmental
6 Information, Washington, D.C.
- 7 EPA-402-R-93-081, 1993, Federal Guidance Report No. 12, External Exposure to Radionuclides
8 in Air, Water, and Soil, Office of Radiation and Indoor Air, U.S. Environmental
9 Protection Agency, Washington, D.C.
- 10 EPA/540/F-95/041, 1996, Soil Screening Guidance: Fact Sheet, Publication 9355.4-14FSA,
11 U.S. Environmental Protection Agency, Office of Solid Waste and Emergency Response,
12 Washington, D.C.
- 13 EPA/540/R-92/003, 1991, Guidance for Data Useability in Risk Assessment (Part A) Final,
14 Office of Research and Development, U.S. Environmental Protection Agency,
15 Washington, D.C.
- 16 EPA/540/R-92/003, 1991, Risk Assessment Guidance for Superfund: Volume I – Human Health
17 Evaluation Manual (Part B, Development of Risk-based Preliminary Remediation Goals)
18 Interim, Publication 9285.7-01B, Office of Research and Development,
19 U.S. Environmental Protection Agency, Washington, D.C.
- 20 EPA/540/R-95/128, 1996, Soil Screening Guidance: Technical Background Document,
21 Second Edition, U.S. Environmental Protection Agency, Washington, D.C.
- 22 EPA/540/R-96/018, 1996, Soil Screening Guidance: User's Guide, Second Edition,
23 Publication 9355.4-23, Office of Solid Waste and Emergency Response,
24 U.S. Environmental Protection Agency, Washington, D.C.
- 25 EPA/600/2-91/065, 1991, The RETC Code for Quantifying the Hydraulic Functions of
26 Unsaturated Soils, Office of Research and Development, U.S. Environmental Protection
27 Agency, Washington, D.C.
- 28 EPA/600/P-95/002Fa, 1997, Exposure Factors Handbook Volume 1: General Factors,
29 U.S. Environmental Protection Agency, National Center for Environmental Assessment,
30 Washington, D.C.
- 31 EPA/600/R-090/052F, 2011, Exposure Factors Handbook: 2011 Edition, National Center for
32 Environmental Assessment, Office of Research and Development, U.S. Environmental
33 Protection Agency, Washington, D.C.
- 34 EPA/630/R-97/001, 1997, Guiding Principles for Monte Carlo Analysis, Risk Assessment
35 Forum, U.S. Environmental Protection Agency, Washington, D.C.

RPP-ENV-58782, Rev. 0

- 1 EPA-SAB-RAC-ADV-99-006, 1999, An SAB Advisory: Modeling of Radionuclide Releases
2 from Disposal of Low Activity Mixed Waste, U.S. Environmental Protection Agency,
3 Science Advisory Board, Washington, D.C.
- 4 ERDA-1538, 1975, “Final Environmental Impact Statement, Waste Management Operations,
5 Hanford Reservation, Richland, Washington,” U.S. Energy Research and Development
6 Administration, Richland, Washington.
- 7 Fayer, M. J., and G. W. Gee, 2006, “Multiple-Year Water Balance of Soil Covers in a Semiarid
8 Setting,” *Journal of Environmental Quality*, Vol. 35, No. 2, pp. 366–377.
- 9 Fayer, M. J., G. W. Gee, M. L. Rockhold, M. D. Freshley, and T. B. Walters, 1996, “Estimating
10 Recharge Rates for a Groundwater Model Using a GIS,” *Journal of Environmental*
11 *Quality*, Vol. 25, pp. 510–518.
- 12 Fecht, K. R., S. P. Reidel, and A. M. Tallman, 1987, “Paleodrainage of the Columbia River
13 System on the Columbia Plateau of Washington State – A Summary,” *Selected Papers on*
14 *the Geology of Washington*, Washington Division of Geology and Earth Resources,
15 Washington State Department of Natural Resources, Bulletin 77, pp. 219–248.
- 16 Gee, G. W., M. J. Fayer, M. L. Rockhold, and M. D. Campbell, 1992, “Variations in Recharge at
17 the Hanford Site,” *Northwest Science*, Vol. 66, No. 4, pp. 237–250.
- 18 Gelhar, L. W., 1993, *Stochastic Subsurface Hydrology*, Prentice Hall, New York, New York.
- 19 Gelhar, L. W. and C. L. Axness, 1983, “Three-dimensional stochastic analysis of
20 macrodispersion in aquifers,” *Water Resources Research*, Vol. 19, pp. 161–180.
- 21 Gelhar, L. W., C. Welty, and K. R. Rehfeldt, 1992, “A Critical Review of Data on Field-Scale
22 Dispersion in Aquifers,” *Water Resources Research*, Vol. 28, pp. 1955–1974.
- 23 GJO-98-39-TAR/GJO-HAN-18, 1998, “Hanford Tank Farms Vadose Zone: C Tank Farm
24 Report,” U.S. Department of Energy, Grand Junction Office, Grand Junction, Colorado.
- 25 GJO-98-39-TARA/GJO-HAN-18, 2000, “Hanford Tank Farms Vadose Zone: Addendum to the
26 C Tank Farm Report,” U.S. Department of Energy, Grand Junction Office, Grand
27 Junction, Colorado.
- 28 GoldSim Technology Group, 2014a, “GoldSim Contaminant Transport Module User’s Guide,”
29 Version 6.4, GoldSim Technology Group, Issaquah, Washington.
- 30 GoldSim Technology Group, 2014b, “GoldSim Distributed Processing Module User’s Guide,”
31 Version 11.1, GoldSim Technology Group LLC, Issaquah, Washington.
- 32 GoldSim Technology Group, 2014c, “GoldSim Probabilistic Simulation Environment User’s
33 Guide,” Version 11.1, GoldSim Technology Group LLC, Issaquah, Washington.

RPP-ENV-58782, Rev. 0

- 1 Goodrich, S., A. Huber, and B. Monroe, 2008, "Trend of Mountain Big Sagebrush Crown Cover
2 and Ground Cover on Burned Sites, Uinta Mountains and West Tavaputs Plateau, Utah,"
3 in Proceedings—Shrublands Under Fire: Disturbance and Recovery in a Changing
4 World, Cedar City, Utah.
- 5 Hall, E. R., 1981, The Mammals of North America, John Wiley and Sons, Inc., New York,
6 New York.
- 7 Hanford Site (Hanford.gov), Queried 07/2015, [Hanford Meteorological Station],
8 <http://www.hanford.gov/page.cfm/HMS>.
- 9 Harr, M. E., 1987, Reliability-Based Design in Civil Engineering, McGraw-Hill, New York,
10 New York.
- 11 Haynes, W. M. and D. R. Lide, 2011, CRC Handbook of Chemistry and Physics, 92nd Edition,
12 CRC Press, Talyor & Francis Group, Boca Raton, Florida.
- 13 Helton, J. C., 1993, "Uncertainty and sensitivity analysis techniques for use in performance
14 assessment for radioactive waste disposal," Reliability Engineering & System Safety,
15 Vol. 42, Issues 2–3, pp. 327–367.
- 16 HFSUWG 1992a, "The Future for Hanford: Uses and Cleanup, Summary of the Final Report of
17 the Hanford Future Site Uses Working Group," Hanford Future Site Uses Working
18 Group, Westinghouse Hanford Company, Richland, Washington.
- 19 HFSUWG, 1992b, "The Future for Hanford: Uses and Cleanup, The Final Report of the
20 Hanford Future Site Uses Working Group," Hanford Future Site Uses Working Group,
21 Westinghouse Hanford Company, Richland, Washington.
- 22 HGLP-MBL-018, 2016, "241-C-102 Tank Waste Retrieval Project Final Report of Drywell
23 Monitoring Data," Rev. 0, Stoller Newport News Nuclear, Richland, Washington.
- 24 HNF-4769, 1999, "Far-Field Hydrology Data Package for Immobilized Low-Activity Tank
25 Waste Performance Assessment," Rev. 1, Fluor Daniel Northwest, Inc., Richland,
26 Washington.
- 27 HNF-EP-0182, 2005, "Waste Tank Summary Report for Month Ending August 31, 2005,"
28 Rev. 209, CH2M HILL Hanford Group, Inc., Richland, Washington.
- 29 HNF-EP-0182, 2014, "Waste Tank Summary Report for Month Ending September 30, 2013,"
30 Rev. 306, Washington River Protection Solutions, LLC, Richland, Washington.
- 31 HNF-EP-0182, 2014, "Waste Tank Summary Report for Month Ending May 31, 2014,"
32 Rev. 317, Washington River Protection Solutions, LLC, Richland, Washington.
- 33 HNF-EP-0182, 2014, "Waste Tank Summary Report for Month Ending July 31, 2014,"
34 Rev. 319, Washington River Protection Solutions, LLC, Richland, Washington.

RPP-ENV-58782, Rev. 0

- 1 HNF-EP-0182, 2015, "Waste Tank Summary Report for Month Ending February 28, 2015,"
2 Rev. 326, Washington River Protection Solutions, LLC, Richland, Washington.
- 3 HNF-EP-0182, 2016, "Waste Tank Summary Report for Month Ending February 29, 2016,"
4 Rev. 338, Washington River Protection Solutions, LLC, Richland, Washington.
- 5 HNF-SD-RE-TI-178, 2007, "Single-Shell Tank Interim Stabilization Record," Rev. 9a,
6 CH2M HILL Hanford Group, Inc., Richland, Washington.
- 7 HNF-SD-WM-SP-012, 2007, "Tank Farm Contractor Operation and Utilization Plan," Rev. 6,
8 CH2M HILL Hanford Group, Inc., Richland, Washington.
- 9 HNF-SD-WM-TI-707, 2007, "Exposure Scenarios and Unit Factors for the Hanford Tank Waste
10 Performance Assessment," Rev. 5, CH2M HILL Hanford Group, Inc., Richland,
11 Washington.
- 12 HNF-SD-WM-TI-740, 1999, "Standard Inventories of Chemicals and Radionuclides in Hanford
13 Site Tank Wastes," Rev. 0C, Lockheed Martin Hanford Corporation, Richland,
14 Washington.
- 15 Hoffman F. O., 1996, "The Effect of Distribution Choice for Uncertain Parameters in a Monte
16 Carlo Analysis," presented at Society of Risk Analysis Annual Meeting, Workshop on
17 Quantitative Techniques for Analysis of Variability and Uncertainty in Exposure and
18 Risk Assessment (December 8), New Orleans, Louisiana.
- 19 HW-7-1388-DEL, 1945, "Hanford Engineer Works Monthly Report February 1945,"
20 E. I. du Pont de Nemours and Company, Richland, Washington.
- 21 IAEA, 1994, "Technical Reports Series No. 364, Handbook of Parameter Values for the
22 Prediction of Radionuclide Transfer in Temperate Environments," International Atomic
23 Energy Agency, Vienna, Austria.
- 24 IAEA, 2010, "Technical Reports Series No. 472, Handbook of Parameter Values for the
25 Prediction of Radionuclide Transfer in Terrestrial and Freshwater Environments,"
26 International Atomic Energy Agency, Vienna, Austria.
- 27 ICRP, 1994, "ICRP Publication 66: Human Respiratory Tract Model for Radiological
28 Protection," Annals of the ICRP, International Commission on Radiation Protection,
29 Vol. 24, No. 1-3, pp. 1-482.
- 30 ICRP, 1996, "ICRP Publication 72: Age-dependent Doses to the Members of the Public from
31 Intake of Radionuclides - Part 5 Compilation of Ingestion and Inhalation Coefficients,"
32 Annals of the ICRP, International Commission on Radiation Protection, Vol. 26, No. 1.
- 33 ICRP, 2006, "ICRP Publication 101a: Assessing Dose of the Representative Person for the
34 Purpose of the Radiation Protection of the Public," Annals of the ICRP, International
35 Commission on Radiation Protection, Vol. 36, No. 3.

RPP-ENV-58782, Rev. 0

- 1 ICRP, 2007, "ICRP Publication 103: The 2007 Recommendations of the International
2 Commission on Radiological Protection," Annals of the ICRP, International Commission
3 on Radiation Protection, Vol. 37, No. 2–4, pp. 1–332.
- 4 ICRP, 2008, "ICRP Publication 107: Nuclear Decay Data for Dosimetric Calculations," Annals
5 of the ICRP, International Commission on Radiation Protection, Vol. 38, No. 3, pp. 7–96.
- 6 INDC-356-VOL3, 1945, "Construction Hanford Engineer Works U.S. Contract
7 Number W-7412-ENG-1 Du Pont Project 9536 History of the Project Volume III,"
8 E. I. du Pont de Nemours and Company, Wilmington, Delaware.
- 9 INEEL/EXT-01-00273, 2006, "Biological Data to Support Operable Unit 7-13/14 Modeling of
10 Plant and Animal Intrusion at Buried Waste Sites," Rev. 1, Idaho Cleanup Project, Idaho
11 Falls, Idaho.
- 12 Jannik, T., 2014, "Environmental Dosimetry," Savannah River Chapter of Health Physics
13 Society Seminar, Savannah River National Laboratory, Aiken, South Carolina.
- 14 Jin, Y. and W. A. Jury, 1996, "Characterizing the Dependence of Gas Diffusion Coefficient on
15 Soil Properties," Soil Science Society of America Journal, Vol. 60, No. 1, pp. 66–71.
- 16 Jones, V. C., 1985, United States Army in World War II, Special Studies -- Manhattan: The
17 Army and the Atomic Bomb, Center of Military History, United States Army,
18 Washington, D.C.
- 19 Jury, W. A., W. R. Gardner, and W. H. Gardner, 1991, Soil Physics, 5th edition, Wiley and Sons,
20 Inc., New York, New York.
- 21 Jury, W. A. and R. Horton, 2004, Soil Physics, 6th edition, Wiley and Sons, Inc., New York,
22 New York.
- 23 Karimi, A. A., W. J. Farmer, and M. M. Cliath, 1987, "Vapor-phase Diffusion of Benzene in
24 Soil," Journal of Environmental Quality, Vol. 16, No. 1, pp. 38–43.
- 25 Karl, T. R., J. M. Melillo, and T. C. Peterson, (eds.), 2009, Global Climate Change Impacts in
26 the United States: A State of Knowledge Report from the U.S. Global Change Research
27 Program, Cambridge University Press, New York, New York.
- 28 Khaleel, R., 1989, "Scale Dependence of Continuum Models for Fractured Basalts," Water
29 Resources Research, Vol. 25, No. 8, pp. 1847–1855.
- 30 Khaleel, R. and J. F. Relyea, 1997, "Correcting Laboratory-Measured Moisture Retention Data
31 for Gravels," Water Resources Research, Vol. 33, Issue 8, pp. 1875–1878.
- 32 Khaleel, R., J. F. Relyea, and J. L. Conca, 1995, "Evaluation of van Genuchten-Mualem
33 Relationships to Estimate Unsaturated Hydraulic Conductivity at Low Water Contents,"
34 Water Resources Research, Vol. 31, Issue 11, pp. 2659–2668.

RPP-ENV-58782, Rev. 0

- 1 Khaleel, R. and P. R. Heller, 2003, "On the Hydraulic Properties of Coarse-Textured Sediments
2 at Intermediate Water Contents," Water Resources Research, Vol. 39, Issue 9,
3 pp. 1233–1237.
- 4 Klute, A., 1986, Methods of Soil Analysis, Part 1—Physical and Mineralogical Methods,
5 Second Edition, American Society of Agronomy-Soil Science Society of America,
6 Madison, Wisconsin.
- 7 Kozak, M. W., 1994, "Decision analysis for low-level radioactive waste disposal facilities,"
8 Radioactive Waste Management and Environmental Restoration, Vol. 18, pp. 209–223.
- 9 Kozak, M. W., 2010, "Safety assessment for near-surface disposal of low- and intermediate-level
10 radioactive waste," in Geological repository systems for safe disposal of spent nuclear
11 fuels and radioactive waste, J. Ahn and M. J. Apted eds., Woodhead Publishing Limited,
12 Cambridge, UK and CRC Press LLC, Boca Raton, Florida.
- 13 LA-UR-08-06764, 2008, "Performance Assessment and Composite Analysis for Los Alamos
14 National Laboratory Technical Area 54, Area G," Rev. 4, Los Alamos National
15 Laboratory, Los Alamos, New Mexico.
- 16 LA-UR-96-3860, 1997, "Hanford Tank Chemical and Radionuclide Inventories: HDW Model
17 Rev. 4," Los Alamos National Laboratory, Los Alamos, New Mexico.
- 18 Leary, K. D., 1990, Analysis of Techniques for Estimating Potential Recharge and Shallow
19 Unsaturated Zone Water Balance near Yucca Mountain, Nevada, M.S. Thesis, University
20 of Nevada, Reno, Nevada.
- 21 Lesica, P., S. V. Cooper and G. Kudray, 2007, "Recovery of Big Sagebrush Following Fire in
22 Southwest Montana," Rangeland Ecology & Management, Vol. 60, Issue 3, pp. 261–269.
- 23 Liu, G., B. Li, K. Hu, and M. T. van Genuchten, 2006, "Simulating the Gas Diffusion
24 Coefficient in Macropore Network Images: Influence of Soil Pore Morphology," Soil
25 Science Society of America Journal, Vol. 70, pp. 1252–1261.
- 26 MASSFLUX-1, 2010, "Use and Measurement of Mass Flux and Mass Discharge," The Interstate
27 Technology & Regulatory Council, Integrated DNAPL Site Strategy Team,
28 Washington, D.C.
- 29 Millington, R. J., and J. P. Quirk, 1960, "Transport in porous media," in Transactions of the
30 7th International Congress of Soil Science, Madison, Wisconsin, Vol. 1, pp. 97–106.
- 31 Millington, R. J. and J. P. Quirk, 1961, "Permeability of Porous Solids," Transactions of the
32 Faraday Society, Vol. 57, pp. 1200–1207.
- 33 Mishra, S., 2009, "Uncertainty and sensitivity analysis techniques for hydrologic modeling,"
34 Journal of Hydroinformatics, Vol. 11, No. 3–4, pp. 282–296.

RPP-ENV-58782, Rev. 0

- 1 Moldrup, P., S. Yoshikawa, T. Olesen, T. Komatsu, and D. E. Rolston, 2003, "Gas Diffusivity in
2 Undisturbed Volcanic Ash Soils: Test of Soil-Water-Characteristic-Based Prediction
3 Models," Soil Science Society of America Journal, Vol. 67, No. 1, pp. 41–51.
- 4 Moldrup, P., T. Olesen, S. Yoshikawa, T. Komatsu, and D. E. Rolston, 2004, "Three-Porosity
5 Model for Predicting the Gas Diffusion Coefficient in Undisturbed Soil," Soil Science
6 Society of America Journal, Vol. 68, No. 3, pp. 750–759.
- 7 Mote, P. E., E. P. Salathé, V. Dulière, and E. Jump, 2008, Scenarios of future climate for the
8 Pacific Northwest, Climate Impacts Group, University of Washington, Seattle,
9 Washington.
- 10 Mualem, Y., 1976, "A New Model for Predicting the Hydraulic Conductivity of Unsaturated
11 Porous Media," Water Resources Research, Vol. 12, No. 3, pp. 513–522.
- 12 Murray, C. J., A. L. Ward, and J. L. Wilson, 2007, "Influence of Clastic Dikes on Vertical
13 Migration of Contaminants at the Hanford Site," Vadose Zone Journal, Vol. 6, No. 4,
14 pp. 959–970.
- 15 NAGRA NTB 02-20, 2002, "Cementitious Near-Field Sorption Data Base for Performance
16 Assessment of an ILW Repository in Opalinus Clay," Technical Report 02-20, National
17 Cooperative for the Disposal of Radioactive Waste, Hardstrasse, Zurich, Switzerland.
- 18 National Bureau of Standards Handbook 69, 1963, "Maximum Permissible Body Burdens and
19 Maximum Permissible Concentrations of Radionuclides in Air and in Water for
20 Occupational Exposure," as amended, U.S. Department of Commerce, Washington, D.C.
- 21 National Environmental Policy Act of 1969, 42 USC 4321-4347, et seq.
- 22 Nazaroff, W. W. and A. V. Nero, 1988, Radon and Its Decay Products in Indoor Air, John
23 Wiley & Sons, New York, New York.
- 24 NCRP Report No. 93, 1987, "Ionizing Radiation Exposure of the Population of the United
25 States," National Council on Radiation Protection, Bethesda, Maryland.
- 26 NCRP Report No. 103, 1989, "Control of Radon in Houses," National Council on Radiation
27 Protection, Bethesda, Maryland.
- 28 NCRP Report No. 129, 1999, "Recommended Screening Limits for Contaminated Surface Soil
29 and Review of Factors Relevant to Site-Specific Studies," National Council on Radiation
30 Protection, Bethesda, Maryland.
- 31 NCRP Report No. 152, 2005, "Performance Assessment of Near-Surface Facilities for Disposal
32 of Low-Level Radioactive Waste," National Council on Radiation Protection and
33 Measurements, Bethesda, Maryland.

RPP-ENV-58782, Rev. 0

- 1 NEA, 1987, “Shallow Land Disposal of Radioactive Waste: Reference Levels for Acceptance of
2 Long-Lived Radionuclides,” Nuclear Energy Agency, Organisation for Economic
3 Co-operation and Development, Paris, France.
- 4 Neuman, S. P., 1992, “Validation of safety assessment models as a process of scientific and
5 public confidence building,” in International High Level Radioactive Waste Management
6 (IHLRWM) Conference Proceedings, Las Vegas, Nevada.
- 7 Newcomb, R. C., 1958, “Ringold Formation of Pleistocene Age in Type Locality, the White
8 Bluffs, Washington,” American Journal of Science, Vol. 256, pp. 328–340.
- 9 Newcomb, R. C., J. R. Strand, and F. J. Frank, 1972, “Geology and Ground-Water
10 Characteristics of the Hanford Reservation of the U.S. Atomic Energy Commission,
11 Washington,” Professional Paper 717, U.S. Geological Survey, Washington, D.C.
- 12 NIROND-TR 2008-23 E, 2009, “Review of sorption values for the cementitious near field of a
13 near surface radioactive waste disposal facility, Project near surface disposal of category
14 A waste at Dessel,” Belgian Agency for Radioactive Waste and Enriched Fissile
15 Materials, Brussels, Belgium.
- 16 NOAA Manual NOS NGS 5, 1990, “State Plane Coordinate System of 1983,” National Geodetic
17 Survey, U.S. Department of Commerce, National Oceanic and Atmospheric
18 Administration, Rockville, Maryland.
- 19 Northern California Earthquake Data Center, Queried 09/2005, [Advanced National Seismic
20 System (ANSS) Catalog Search], <http://www.quake.geo.berkeley.edu/anss/catalog-search.html>.
21
- 22 NUREG-1573, 2000, A Performance Assessment Methodology for Low-Level Radioactive
23 Waste Disposal Facilities: Recommendations of NRC’s Performance Assessment
24 Working Group, U.S. Nuclear Regulatory Commission, Office of Nuclear Material
25 Safety and Safeguards, Washington, D.C.
- 26 NUREG-1636, 1999, Regulatory Perspectives on Model Validation in High-Level Radioactive
27 Waste Management Programs: A Joint NRC/SKI White Paper, U.S. Nuclear Regulatory
28 Commission, Office of Nuclear Material Safety and Safeguards, Washington, D.C.
- 29 NUREG-1854, 2007, NRC Staff Guidance for Activities Related to U.S. Department of Energy
30 Waste Determinations – Draft Final Report for Interim Use, U.S. Nuclear Regulatory
31 Commission, Office of Federal and State Materials and Environmental Management
32 Programs, Washington, D.C.
- 33 NUREG-2175, 2015, Guidance for Conducting Technical Analyses for 10 CFR Part 61 – Draft
34 Report for Comment, U.S. Nuclear Regulatory Commission, Office of Nuclear Material
35 Safety and Safeguards, Washington, D.C.

RPP-ENV-58782, Rev. 0

- 1 NUREG/CR-4122, 1985, A FORTRAN 77 Program and User's Guide for the Calculation of
2 Partial Correlation and Standardized Regression Coefficients, SAND85-0044,
3 U.S. Nuclear Regulatory Commission, Washington, D.C.
- 4 NUREG/CR-4370, 1986, Update of Part 61 Impacts Analysis Methodology, U.S. Nuclear
5 Regulatory Commission, Washington, D.C.
- 6 NUREG/CR-5512, 1992, Residual Radioactive Contamination From Decommissioning, Vol. 1,
7 Technical Basis for Translating Contamination Levels to Annual Total Effective Dose
8 Equivalent, Final Report, PNL-7994, U.S. Nuclear Regulatory Commission,
9 Washington, D.C.
- 10 Nyame, B. K. and J. M. Illston, 1981, "Relationships between permeability and pore structure of
11 hardened cement paste," Magazine of Concrete Research, Vol. 33, No. 116, p. 139–146.
- 12 O'Connor, J. E. and V. R. Baker, 1992, "Magnitudes and implications of peak discharges from
13 glacial Lake Missoula," Geological Society of America Bulletin, Vol. 104, No. 3,
14 pp. 267–279.
- 15 Olander, A. R. 2016-05-03, "RE: WMA C PA - Editing" (e-mail to J. G. Field), Washington
16 River Protection Solutions LLC (WRPS) Tank Farms, Richland, Washington.
- 17 Olander, A. R. 2016-08-18, "RE: WMA C PA - Editing" (e-mail to M. P. Bergeron), Washington
18 River Protection Solutions LLC (WRPS) Tank Farms, Richland, Washington.
- 19 Open File Report 87-222, 1987, "Subsurface Transport of Radionuclides in Shallow Deposits of
20 the Hanford Nuclear Reservation, Washington – Review of Selected Previous Work and
21 Suggestions for Further Study," U.S. Geological Survey, Tacoma, Washington.
- 22 Open File Report 94-8, 1994, "Geologic Map of the Richland 1:100,000 Quadrangle,
23 Washington," Washington Division of Geology and Earth Resources, Washington State
24 Department of Natural Resources, Olympia, Washington.
- 25 Open File Report 96-8, 1996, "The Miocene to Pliocene Ringold Formation and Associated
26 Deposits of the Ancestral Columbia River System, South-Central Washington and
27 North-Central Oregon," Washington Division of Geology and Earth Resources,
28 Washington State Department of Natural Resources, Olympia, Washington.
- 29 ORP-11242, 2011, "River Protection Project System Plan," Rev. 6, U.S. Department of Energy,
30 Office of River Protection, Richland, Washington.
- 31 OSWER Directive 9200.1-120, 2014, "Human Health Evaluation Manual, Supplemental
32 Guidance: Update of Standard Default Exposure Factors" (Memorandum from D. Stalcup
33 to Superfund National Policy Managers, Regions 1 – 10, February 6), Office of Solid
34 Waste and Emergency Response, U.S. Environmental Protection Agency,
35 Washington, D.C.

RPP-ENV-58782, Rev. 0

- 1 OSWER Directive 9285.6-03, 1991, Risk Assessment Guidance for Superfund, Volume I:
2 Human Health Evaluation Manual, Supplemental Guidance “Standard Default Exposure
3 Factors” Interim Final, Office of Emergency and Remedial Response, Toxics Integration
4 Branch, U.S. Environmental Protection Agency, Washington, D.C.
- 5 OSWER Directive 9841.00-6C, 1987, Alternate Concentration Limit Guidance, Part I, ACL
6 Policy and Information Requirements, Interim Final, EPA/530-SW-87-017, Office of
7 Solid Waste, Waste Management Division, U.S. Environmental Protection Agency,
8 Washington, D.C.
- 9 Pacific Northwest National Laboratory, Queried 12/18/2015, [STOMP User Guide],
10 http://stomp.pnnl.gov/user_guide/STOMP_guide.stm.
- 11 Pasquill, F., 1961, “The Estimation of the Dispersion of Windborne Material,” The
12 Meteorological Magazine, Vol. 90, No. 1063, pp. 33–49.
- 13 Plummer, M. A., L. C. Hull, and D. T. Fox, 2004, “Transport of Carbon-14 in a Large
14 Unsaturated Soil Column,” Vadose Zone Journal, Vol. 3, No. 1, pp. 109–121.
- 15 PNL-2774, 1979, “Characterization of the Hanford 300 Area Burial Grounds Task IV -
16 Biological Transport,” Pacific Northwest Laboratory, Richland, Washington.
- 17 PNL-5247, 1985, “Rooting Depth and Distributions of Deep-Rooted Plants in the 200 Area
18 Control Zone of the Hanford Site,” Pacific Northwest Laboratory, Richland, Washington.
- 19 PNL-5289, 1984, “Investigation of Ground-Water Seepage from the Hanford Shoreline of the
20 Columbia River,” Pacific Northwest Laboratory, Richland, Washington.
- 21 PNL-6328, 1988, “Estimation of Ground-Water Travel Time at the Hanford Site: Description,
22 Past Work, and Future Needs,” Pacific Northwest Laboratory, Richland, Washington.
- 23 PNL-6464, 1988, “Environmental Monitoring at Hanford for 1987,” Pacific Northwest
24 Laboratory, Richland, Washington.
- 25 PNL-7297, 1990, “Hanford Waste-Form Release and Sediment Interaction – A Status Report
26 with Rationale and Recommendations for Additional Studies,” Pacific Northwest
27 Laboratory, Richland, Washington.
- 28 PNL-7662, 1991, “An Evaluation of the Chemical, Radiological, and Ecological Conditions of
29 West Lake on the Hanford Site,” Pacific Northwest Laboratory, Richland, Washington.
- 30 PNL-8337, 1992, “Summary and Evaluation of Available Hydraulic Property Data for the
31 Hanford Site Unconfined Aquifer System,” Pacific Northwest Laboratory, Richland,
32 Washington.
- 33 PNL-8478, 1993, “Soil Erosion Rates Caused by Wind and Saltating Sand Stresses in a Wind
34 Tunnel,” Pacific Northwest Laboratory, Richland, Washington.

RPP-ENV-58782, Rev. 0

- 1 PNL-8889, 1993, "Solid-Waste Leach Characteristics and Contaminant-Sediment Interactions,
2 Volume 1: Batch Leach and Adsorption Tests and Sediment Characterization," Pacific
3 Northwest Laboratory, Richland, Washington.
- 4 PNL-10195, 1994, "Three-Dimensional Conceptual Model for the Hanford Site Unconfined
5 Aquifer System: FY 1994 Status Report," Pacific Northwest Laboratory,
6 Richland, Washington.
- 7 PNL-10817, 1995, "Hydrochemistry and Hydrogeologic Conditions within the Hanford Site
8 Upper Basalt Confined Aquifer System," Pacific Northwest Laboratory,
9 Richland, Washington.
- 10 PNL-10835, 1995, Comparison of Constant-Rate Pumping Test and Slug Interference Test
11 Results at the Hanford Site B Pond Multilevel Test Facility, Pacific Northwest
12 Laboratory, Richland, Washington.
- 13 PNL-10886, 1995, "Development of a Three-Dimensional Ground-Water Model of the Hanford
14 Site Unconfined Aquifer System: FY 1995 Status Report," Pacific Northwest National
15 Laboratory, Richland, Washington.
- 16 PNL-SA-23121 S, 1993, "Hanford Technical Exchange Program: Process Chemistry at Hanford
17 (Genesis of Hanford Wastes)," Pacific Northwest Laboratory, Richland, Washington.
- 18 PNNL-6415, 2005, "Hanford Site National Environmental Policy Act (NEPA) Characterization,"
19 Rev. 17, Pacific Northwest National Laboratory, Richland, Washington.
- 20 PNNL-6415, 2007, "Hanford Site National Environmental Policy Act (NEPA) Characterization,"
21 Rev. 18, Pacific Northwest National Laboratory, Richland, Washington.
- 22 PNNL-11216, 1997, "STOMP Subsurface Transport Over Multiple Phases Application Guide,"
23 Pacific Northwest National Laboratory, Richland, Washington.
- 24 PNNL-11485, 1996, "Radionuclide Adsorption Distribution Coefficients Measured in Hanford
25 Sediments for the Low Level Waste Performance Assessment Project," Pacific Northwest
26 National Laboratory, Richland, Washington.
- 27 PNNL-11800, 1998, "Composite Analysis for Low-Level Waste Disposal in the 200 Area
28 Plateau of the Hanford Site," Pacific Northwest National Laboratory, Richland,
29 Washington.
- 30 PNNL-11810, 1998, "Results of Phase I Groundwater Quality Assessment for Single-Shell Tank
31 Waste Management Areas S-SX at the Hanford Site," Pacific Northwest National
32 Laboratory, Richland, Washington.

RPP-ENV-58782, Rev. 0

- 1 PNNL-11965, 1998, "Effects of Aging Quartz Sand and Hanford Site Sediment with Sodium
2 Hydroxide on Radionuclide Sorption Coefficients and Sediment Physical and Hydrologic
3 Properties: Final Report for Subtask 2a," Pacific Northwest National Laboratory,
4 Richland, Washington.
- 5 PNNL-12030, 2000, "STOMP Subsurface Transport Over Multiple Phases Version 2.0 Theory
6 Guide," Pacific Northwest National Laboratory, Richland, Washington.
- 7 PNNL-12261, 2000, "Revised Hydrogeology for the Suprabasalt Aquifer System, 200-East Area
8 and Vicinity, Hanford Site, Washington," Pacific Northwest National Laboratory,
9 Richland, Washington.
- 10 PNNL-13024, 2001, "RCRA Groundwater Monitoring Plan for Single-Shell Tank Waste
11 Management Area C at the Hanford Site," as amended, Pacific Northwest National
12 Laboratory, Richland, Washington.
- 13 PNNL-13033, 1999, "Recharge Data Package for the Immobilized Low-Activity Waste
14 2001 Performance Assessment," Pacific Northwest National Laboratory, Richland,
15 Washington.
- 16 PNNL-13037, 2000, "Geochemical Data Package for the Hanford Immobilized Low-Activity
17 Tank Waste Performance Assessment (ILAW PA)," Rev. 1, Pacific Northwest National
18 Laboratory, Richland, Washington.
- 19 PNNL-13037, 2004, "Geochemical Data Package for the 2005 Hanford Integrated Disposal
20 Facility Performance Assessment," Rev. 2, Pacific Northwest National Laboratory,
21 Richland, Washington.
- 22 PNNL-13080, 2000, "Hanford Site Groundwater Monitoring: Setting, Sources, and Methods,"
23 Pacific Northwest National Laboratory, Richland, Washington.
- 24 PNNL-13342, 2000, "Analysis of the Hydrologic Response Associated with Shutdown and
25 Restart of the 200-ZP-1 Pump-and-Treat System," Pacific Northwest National
26 Laboratory, Richland, Washington.
- 27 PNNL-13378, 2001, "Results of Detailed Hydrologic Characterization Tests – Fiscal
28 Year 1999," Pacific Northwest National Laboratory, Richland, Washington.
- 29 PNNL-13514, 2001, "Results of Detailed Hydrologic Characterization Tests – Fiscal
30 Year 2000," Pacific Northwest National Laboratory, Richland, Washington.
- 31 PNNL-13641, 2001, "Uncertainty Analysis Framework – Hanford Site-Wide Groundwater Flow
32 and Transport Model," Pacific Northwest National Laboratory, Richland, Washington.
- 33 PNNL-13653, 2005, "A Catalog of Geologic Data for the Hanford Site," Rev. 2, Pacific
34 Northwest National Laboratory, Richland, Washington.

RPP-ENV-58782, Rev. 0

- 1 PNNL-13672, 2002, "A Catalog of Vadose Zone Hydraulic Properties for the Hanford Site,"
2 Rev. 1, Pacific Northwest National Laboratory, Richland, Washington.
- 3 PNNL-13674, 2001, "Zone of Interaction Between Hanford Site Groundwater and Adjacent
4 Columbia River: Progress Report for the Groundwater/River Interface Task Science and
5 Technology Groundwater/Vadose Zone Integration Project," Pacific Northwest National
6 Laboratory, Richland, Washington.
- 7 PNNL-13895, 2003, "Hanford Contaminant Distribution Coefficient Database and Users Guide,"
8 Rev. 1, Pacific Northwest National Laboratory, Richland, Washington.
- 9 PNNL-14058, 2002, "Prototype Database and User's Guide of Saturated Zone Hydraulic
10 Properties for the Hanford Site," Pacific Northwest National Laboratory, Richland,
11 Washington.
- 12 PNNL-14113, 2002, "Results of Detailed Hydrologic Characterization Tests – Fiscal
13 Year 2001," Pacific Northwest National Laboratory, Richland, Washington.
- 14 PNNL-14133, 2003, "Blanket Biological Review for General Maintenance Activities Within
15 Active Burial Grounds, 200 E and 200 W Areas, ECR #2002-200-034," Pacific
16 Northwest National Laboratory, Richland, Washington.
- 17 PNNL-14143, 2002, "The Hanford Site 1000-Year Cap Design Test," Pacific Northwest
18 National Laboratory, Richland, Washington.
- 19 PNNL-14202, 2003, "Mineralogical and Bulk-Rock Geochemical Signatures of Ringold and
20 Hanford Formation Sediments," Pacific Northwest National Laboratory, Richland,
21 Washington.
- 22 PNNL-14233, 2003, "Biological Review of the Hanford Solid Waste EIS – Borrow Area C
23 (600 Area), Stockpile and Conveyance Road Area (600 Area), Environmental Restoration
24 Disposal Facility (ERDF) (600 Area), Central Waste Complex (CWC) Expansion
25 (200 West), 218-W-5 Expansion Area (200 West), New Waste Processing Facility
26 (200 West), Undeveloped Portion of 218-W-4C (200 West), Western Half &
27 Northeastern Corner of 218-W-6 (200 West), Disposal Facility Near Plutonium-Uranium
28 Extraction (PUREX) Facility (200 East), ECR #2002-600-012b," Pacific Northwest
29 National Laboratory, Richland, Washington.
- 30 PNNL-14398, 2003, "Transient Inverse Calibration of the Site-Wide Groundwater Flow Model
31 (ACM-2): FY 2003 Progress Report," Pacific Northwest National Laboratory, Richland,
32 Washington.
- 33 PNNL-14548, 2004, "Hanford Site Groundwater Monitoring for Fiscal Year 2003," Pacific
34 Northwest National Laboratory, Richland, Washington.

RPP-ENV-58782, Rev. 0

- 1 PNNL-14586, 2004, "Geologic Data Package for 2005 Integrated Disposal Facility Waste
2 Performance Assessment," Rev. 1, Pacific Northwest National Laboratory, Richland,
3 Washington.
- 4 PNNL-14656, 2004, "Borehole Data Package for Four CY 2003 RCRA Wells 299-E27-4,
5 299-E27-21, 299-E27-22, and 299-E27-23 at Single-Shell Tank, Waste Management
6 Area C, Hanford Site, Washington," Pacific Northwest National Laboratory, Richland,
7 Washington.
- 8 PNNL-14702, 2006, "Vadose Zone Hydrogeology Data Package for Hanford Assessments,"
9 Rev. 1, Pacific Northwest Laboratory, Richland, Washington.
- 10 PNNL-14744, 2004, "Recharge Data Package for the 2005 Integrated Disposal Facility
11 Performance Assessment," Pacific Northwest National Laboratory, Richland,
12 Washington.
- 13 PNNL-14753, 2006, "Groundwater Data Package for Hanford Assessments," Rev. 1, Pacific
14 Northwest National Laboratory, Richland, Washington.
- 15 PNNL-14804, 2004, "Results of Detailed Hydrologic Characterization Tests – Fiscal
16 Year 2003," Pacific Northwest National Laboratory, Richland, Washington.
- 17 PNNL-14903, 2007, "Hanford Tanks 241-C-203 and 241-C-204: Residual Waste Contaminant
18 Release Model and Supporting Data," Rev. 1, Pacific Northwest National Laboratory,
19 Richland, Washington.
- 20 PNNL-14960, 2005, "200-BP-1 Prototype Hanford Barrier Annual Monitoring Report for Fiscal
21 Year 2004," Pacific Northwest National Laboratory, Richland, Washington.
- 22 PNNL-15160, 2005, "Hanford Site Climatological Summary 2004 with Historical Data," Pacific
23 Northwest National Laboratory, Richland, Washington.
- 24 PNNL-15187, 2007, "Hanford Tank 241-C-106: Residual Waste Contaminant Release Model
25 and Supporting Data," Rev. 1, Pacific Northwest National Laboratory, Richland,
26 Washington.
- 27 PNNL-15503, 2008, "Characterization of Vadose Zone Sediments Below the C Tank Farm:
28 Borehole C4297 and RCRA Borehole 299-E27-22," Rev. 1, Pacific Northwest National
29 Laboratory, Richland, Washington.
- 30 PNNL-15782, 2006, "STOMP Subsurface Transport Over Multiple Phases Version 4.0 User's
31 Guide," Pacific Northwest National Laboratory, Richland, Washington.
- 32 PNNL-15955, 2007, "Geology Data Package for the Single-Shell Tank Waste Management
33 Areas at the Hanford Site," Rev. 1, Pacific Northwest National Laboratory, Richland,
34 Washington.

RPP-ENV-58782, Rev. 0

- 1 PNNL-16229, 2007, "Hanford Tanks 241-C-202 and 241-C-203: Residual Waste Contaminant
2 Release Models and Supporting Data," Pacific Northwest National Laboratory, Richland,
3 Washington.
- 4 PNNL-16346, 2007, "Hanford Site Groundwater Monitoring for Fiscal Year 2006," Pacific
5 Northwest National Laboratory, Richland, Washington.
- 6 PNNL-16407, 2007, "Geology of the Waste Treatment Plant Seismic Boreholes," Rev. 1, Pacific
7 Northwest National Laboratory, Richland, Washington.
- 8 PNNL-16620, 2007, "Ecological Data in Support of the Tank Closure and Waste Management
9 Environmental Impact Statement Part 2: Results of Spring 2007 Field Surveys," Pacific
10 Northwest National Laboratory, Richland, Washington.
- 11 PNNL-16663, 2007, "Geochemical Processes Data Package for the Vadose Zone in the
12 Single-Shell Tank Waste Management Areas at the Hanford Site," Pacific Northwest
13 National Laboratory, Richland, Washington.
- 14 PNNL-16688, 2007, "Recharge Data Package for Hanford Single-Shell Tank Waste
15 Management Areas," Pacific Northwest National Laboratory, Richland, Washington.
- 16 PNNL-16738, 2008, "Hanford Tank 241-C-103 Residual Waste Contaminant Release Models
17 and Supporting Data," Pacific Northwest National Laboratory, Richland, Washington.
- 18 PNNL-17154, 2008, "Geochemical Characterization Data Package for the Vadose Zone in the
19 Single-Shell Tank Waste Management Areas at the Hanford Site," Pacific Northwest
20 National Laboratory, Richland, Washington.
- 21 PNNL-17176, 2007, "200-BP-1 Prototype Hanford Barrier Annual Monitoring Report for Fiscal
22 Years 2005 Through 2007," Pacific Northwest National Laboratory, Richland,
23 Washington.
- 24 PNNL-18845, 2011, "200-BP-1 Prototype Hanford Barrier – 15 Years of Performance
25 Monitoring," Rev. 1, Pacific Northwest National Laboratory, Richland, Washington.
- 26 PNNL-18934, 2009, "The Effects of Fire on the Function of the 200-BP-1 Engineered Surface
27 Barrier," Pacific Northwest National Laboratory, Richland, Washington.
- 28 PNNL-19425, 2010, "Hanford Site Tank 241-C-108 Residual Waste Contaminant Release
29 Models and Supporting Data," Pacific Northwest National Laboratory, Richland,
30 Washington.
- 31 PNNL-19702, 2010, "Hydrogeologic Model for the Gable Gap Area, Hanford Site," Pacific
32 Northwest National Laboratory, Richland, Washington.
- 33 PNNL-20302, 2011, "First Quarter Hanford Seismic Report for Fiscal Year 2011," Pacific
34 Northwest National Laboratory, Richland, Washington.

RPP-ENV-58782, Rev. 0

- 1 PNNL-20548, 2011, “Hanford Site Environmental Report for Calendar Year 2010 (Including
2 Some Early 2011 Information),” Pacific Northwest National Laboratory,
3 Richland, Washington.
- 4 PNNL-20616, 2011, “Contaminant Release from Hanford Tank Residual Waste – Results of
5 Single-Pass Flow-Through Tests,” Pacific Northwest National Laboratory, Richland,
6 Washington.
- 7 PNNL-20631, 2011, “Hanford Site Regional Population – 2010 Census,” Pacific Northwest
8 National Laboratory, Richland, Washington.
- 9 PNNL-23711, 2015, “Physical, Hydraulic, and Transport Properties of Sediments and
10 Engineered Materials Associated with Hanford Immobilized Low-Activity Waste,”
11 RPT-IGTP-004, Rev. 0, Pacific Northwest National Laboratory, Richland, Washington.
- 12 PNNL-23841, 2014, “Radionuclide Migration through Sediment and Concrete: 16 Years of
13 Investigations,” Pacific Northwest National Laboratory, Richland, Washington.
- 14 PNNL-SA-32152, 1999, “A Short History of Plutonium Production and Nuclear Waste
15 Generation, Storage, and Release at the Hanford Site,” Pacific Northwest National
16 Laboratory, Richland, Washington.
- 17 Polmann, D. J., 1990, “Application of Stochastic Methods to Transient Flow and Transport in
18 Heterogeneous Unsaturated Soils,” Ph.D. Thesis, Massachusetts Institute of Technology,
19 Cambridge, Massachusetts.
- 20 Portland State University College of Urban & Public Affairs: Population Research Center,
21 Queried 05/17/2015, [Population Estimates and Reports],
22 <http://www.pdx.edu/prc/population-reports-estimates>.
- 23 PRC-PRO-IRM-309, 2014, “Controlled Software Management,” Rev. 5, CH2M HILL Plateau
24 Remediation Company, Richland, Washington.
- 25 Preliminary Remediation Goals for Radionuclides (PRGfR), Queried 07/2015, [PRG User’s
26 Guide], http://epa-prgs.ornl.gov/radionuclides/prg_guide.html.
- 27 PSI Bericht Nr. 95-06, 1995, “Sorption Databases for the Cementitious Near-Field of a L/ILW
28 Repository for Performance Assessment,” Paul Scherrer Institute, Switzerland.
- 29 Radiation Risk Assessment Software: CAP-88 and CAP-88 PC (EPA 2014), Queried 07/2015,
30 [CAP88-PC Version 4.0 User Guide],
31 <http://www.epa.gov/radiation/assessment/CAP88/index.html>.
- 32 RCW 70.105, “Hazardous Waste Management,” Revised Code of Washington, as amended.
- 33 RCW 70.105D, “Hazardous Waste Cleanup — Model Toxics Control Act,” Revised Code of
34 Washington, as amended.

RPP-ENV-58782, Rev. 0

- 1 Reidel, S. P., N. P. Campbell, K. R. Fecht, and K. A. Lindsey, 1994, "Late Cenozoic Structure
2 and Stratigraphy of South-Central Washington," Regional Geology of Washington State,
3 Washington Division of Geology and Earth Resources, Washington State Department of
4 Natural Resources, Bulletin 80, pp. 159–180.
- 5 Reidel, S. P. and P. R. Hooper (editors), 1989, "Volcanism and Tectonism in the Columbia River
6 Flood-Basalt Province," Special Paper 239, The Geological Society of America, Inc.,
7 Boulder, Colorado.
- 8 Relander, C., 1956, *Drummers and Dreamers*, Caxton Printers, Caldwell, Idaho.
- 9 Resource Conservation and Recovery Act of 1976, 42 USC 6901, et seq.
- 10 RHO-BWI-C-64, 1979, "Clastic Dikes Of The Pasco Basin, Southeastern Washington, Final
11 Report," Rockwell Hanford Operations, Richland, Washington.
- 12 RHO-BWI-C-120/PNL-4219, 1981, "Flood Risk Analysis of Cold Creek near the Hanford Site,"
13 prepared by Pacific Northwest Laboratory for Rockwell Hanford Operations,
14 Richland, Washington.
- 15 RHO-BWI-ST-4, 1979, "Geologic Studies of the Columbia Plateau: A Status Report," Rockwell
16 Hanford Operations, Richland, Washington.
- 17 RHO-BWI-ST-14, 1981, "Subsurface Geology of the Cold Creek Syncline," "Chapter 2 –
18 Suprabasalt Sediments of the Cold Creek Syncline Area," Rockwell Hanford Operations,
19 Richland, Washington.
- 20 RHO-BWI-ST-14, 1981, "Subsurface Geology of the Cold Creek Syncline," "Chapter 3 –
21 Wanapum and Saddle Mountains Basalts of the Cold Creek Syncline Area," Rockwell
22 Hanford Operations, Richland, Washington.
- 23 RHO-RE-CR-2, 1982, "Strength and Elastic Properties Tests of Hanford Concrete Cores –
24 241-SX-115 Tank and 202-A Purex Canyon Building," Construction Technology
25 Laboratories, Skokie, Illinois.
- 26 RHO-SA-211, "Invasion of radioactive waste burial sites by the Great Basin Pocket Mouse
27 (*Perognathus parvus*)," Hanford Engineering Development Laboratory, Richland,
28 Washington.
- 29 RHO-ST-23, 1979, "Geology of the Separation Areas, Hanford Site, South-Central
30 Washington," Rockwell Hanford Operations, Richland, Washington.
- 31 RHO-ST-46 P, 1984, "Field Calibration of Computer Models for Application to Buried Liquid
32 Discharges: A Status Report," Rockwell International, Richland, Washington.

RPP-ENV-58782, Rev. 0

- 1 Rohay, A. C., 1989, "Earthquake Recurrence Rate Estimates for Eastern Washington and the
2 Hanford Site," CONF-8910192--18, in Proceedings, Second DOE Natural Phenomena
3 Hazards Mitigation Conference, Knoxville, Tennessee.
- 4 Ronald W. Reagan National Defense Authorization Act for Fiscal Year 2005, Public
5 Law 108-375.
- 6 RPP-7494, 2001, "Historical Vadose Zone Contamination from A, AX, and C Tank Farm
7 Operations," Rev. 0, Fluor Federal Services, Richland, Washington.
- 8 RPP-7625, 2015, "Guidelines for Updating Best-Basis Inventory," Rev. 12, Washington River
9 Protection Solutions, LLC, Richland, Washington.
- 10 RPP-8847, 2007, "Best-Basis Inventory Template Compositions of Common Tank Waste
11 Layers," Rev. 1B, CH2M HILL Hanford Group, Inc., Richland, Washington.
- 12 RPP-13033, 2014, "Tank Farms Documented Safety Analysis," Rev. 5-C, Washington River
13 Protection Solutions, LLC, Richland, Washington.
- 14 RPP-13489, 2002, "Activity of Fuel Batches Processed Through Hanford Separations Plants,
15 1944 Through 1989," Rev. 0, CH2M HILL Hanford Group, Inc., Richland, Washington.
- 16 RPP-13774, 2004, "Single-Shell Tank System Closure Plan," Rev. 2, CH2M HILL Hanford
17 Group, Inc., Richland, Washington.
- 18 RPP-13889, 2004, "Tank 241-C-106 Component Closure Action Data Quality Objectives,"
19 Rev. 1, CH2M HILL Hanford Group, Inc., Richland, Washington.
- 20 RPP-14430, 2003, "Subsurface Conditions Description of the C and A-AX Waste Management
21 Area," Rev. 0, CH2M HILL Hanford Group, Inc., Richland, Washington.
- 22 RPP-15043, 2003, "Single-Shell Tank System Description," Rev. 0, CH2M HILL Hanford
23 Group, Inc., Richland, Washington.
- 24 RPP-19822, 2005, "Hanford Defined Waste Model – Revision 5.0," Rev. 0-A, CH2M HILL
25 Hanford Group, Inc./Technical Resources International, Inc., Richland, Washington.
- 26 RPP-19866, 2004, "Calculation for the Post-Retrieval Waste Volume Determination for
27 Tank 241-C-106," Rev. 1, CH2M HILL Hanford Group, Inc., Richland, Washington.
- 28 RPP-20577, 2007, "Stage II Retrieval Data Report for Single-Shell Tank 241-C-106," Rev. 0,
29 CH2M HILL Hanford Group, Inc., Richland, Washington.
- 30 RPP-20621, 2004, "Far-Field Hydrology Data Package for the Integrated Disposal Facility
31 Performance Assessment," Rev. 0, CH2M HILL Hanford Group, Inc., Richland,
32 Washington.

RPP-ENV-58782, Rev. 0

- 1 RPP-20658, 2008, "Basis for Exception to the Hanford Federal Facility Agreement and Consent
2 Order Waste Retrieval Criteria for Single-Shell Tank 241-C-106," Rev. 3, CH2M HILL
3 Hanford Group, Inc., Richland, Washington.
- 4 RPP-23403, 2006, "Single-Shell Tank Component Closure Data Quality Objectives," Rev. 3,
5 CH2M HILL Hanford Group, Inc., Richland, Washington.
- 6 RPP-23403, 2013, "Single-Shell Tank Component Closure Data Quality Objectives," Rev. 5,
7 Washington River Protection Solutions, LLC, Richland, Washington.
- 8 RPP-26744, 2005, "Hanford Soil Inventory Model, Rev. 1," Rev. 0, CH2M HILL Hanford
9 Group, Inc., Richland, Washington.
- 10 RPP-29441, 2006, "Post-Retrieval Waste Volume Determination for Single Shell
11 Tank 241-C-201," Rev. 0, Freestone Environmental Services, Inc./CH2M HILL Hanford
12 Group, Inc., Richland, Washington.
- 13 RPP-32681, 2013, "Process to Assess Tank Farm Leaks in Support of Retrieval and Closure
14 Planning," Rev. 2, Washington River Protection Solutions, LLC, Richland, Washington.
- 15 RPP-35484, 2008, "Field Investigation Report for Waste Management Areas C and A-AX,"
16 Rev.1, CH2M HILL Hanford Group, Inc., Richland, Washington.
- 17 RPP-50233, 2011, "Waste Management Area C Closure Conceptual Design Support Report,"
18 Rev. 0, Washington River Protection Solutions, LLC, Richland, Washington.
- 19 RPP-50816, 2013, "Software Management Plan for Grade D Custom Developed Hanford Tank
20 Waste Operations Simulator (HTWOS)," Rev. 1, Washington River Protection
21 Solutions, LLC, Richland, Washington.
- 22 RPP-52784, 2012, "Video Camera/CAD Modeling System for Retrieval: HISI #3254 Software
23 Management Plan," Rev. 0, Washington River Protection Solutions, LLC, Richland,
24 Washington.
- 25 RPP-ASMT-46452, 2010, "Tank 241-C-105 Leak Assessment Completion Report," Rev. 0,
26 Washington River Protection Solutions, LLC, Richland, Washington.
- 27 RPP-CALC-54266, 2013, "Post-Hard Heel Retrieval Camera/CAD Modeling System Waste
28 Volume Estimate for Tank 241-C-108," Rev. 0, Washington River Protection
29 Solutions, LLC, Richland, Washington.
- 30 RPP-CALC-54284, 2013, "Post-Hard Heel Retrieval Camera/CAD Modeling System Waste
31 Volume Estimate for Tank 241-C-104," Rev. 0, Washington River Protection
32 Solutions, LLC, Richland, Washington.

RPP-ENV-58782, Rev. 0

- 1 RPP-CALC-54759, 2013, "Post-Hard Heel Retrieval Camera/CAD Modeling System Waste
2 Volume Estimate for Tank 241-C-109," Rev. 0, Washington River Protection
3 Solutions, LLC/Weirich Consulting Services Inc., Richland, Washington.
- 4 RPP-CALC-56399, 2013, "Post-Hard Heel Retrieval Camera/CAD Modeling System Waste
5 Volume Estimate for Tank 241-C-110," Rev. 0, Washington River Protection
6 Solutions, LLC, Richland, Washington.
- 7 RPP-CALC-56434, 2013, "Post-Retrieval Camera/CAD Modeling System Waste Volume
8 Estimate for Tank 241-C-101," Rev. 0, Washington River Protection Solutions, LLC/
9 Weirich Consulting Services Inc., Richland, Washington.
- 10 RPP-CALC-56856, 2014, "Estimated Waste Volume Remaining in Single Shell Tank 241-C-112
11 after Hard Heel Retrieval," Rev. 0, Washington River Protection Solutions, LLC,
12 Richland, Washington.
- 13 RPP-CALC-59985, 2014, "Post-Retrieval Camera/CAD Modeling System Waste Volume
14 Estimate for Tank 241-C-107," Rev. 0, Washington River Protection Solutions, LLC/
15 Weirich Consulting Services Inc., Richland, Washington.
- 16 RPP-CALC-60345, 2016, "Heterogeneous Media Model for Waste Management Area C
17 Performance Assessment," Rev. 0, Washington River Protection Solutions, LLC,
18 Richland, Washington.
- 19 RPP-ENV-33418, 2016, "Hanford C-Farm Leak Inventory Assessments Report," Rev. 4,
20 Washington River Protection Solutions, LLC, Richland, Washington.
- 21 RPP-ENV-58806, 2016, "RCRA Closure Analysis of Tank Waste Residuals Impacts at Waste
22 Management Area C, Hanford Site, Washington," Rev. 0, Washington River Protection
23 Solutions, LLC, Richland, Washington.
- 24 RPP-ENV-58813, 2016, "Exposure Scenarios for Risk and Performance Assessments in Tank
25 Farms at the Hanford Site, Washington," Rev. 0, Washington River Protection
26 Solutions, LLC, Richland, Washington.
- 27 RPP-PLAN-39114, 2012, "Phase 2 RCRA Facility Investigation/Corrective Measures Study
28 Work Plan for Waste Management Area C," Rev. 2, Washington River Protection
29 Solutions, LLC, Richland, Washington.
- 30 RPP-PLAN-47559, 2012, "Single-Shell Tank Waste Management Area C Pipeline Feasibility
31 Evaluation," Rev. 1, Washington River Protection Solutions, LLC/Cenibark
32 International, Inc., Richland, Washington.
- 33 RPP-RPT-24257, 2005, "244-CR Vault Liquid Level Assessment and Video Inspection
34 Completion Report," Rev. 0, CH2M HILL Hanford Group, Inc., Richland, Washington.

RPP-ENV-58782, Rev. 0

- 1 RPP-RPT-26475, 2008, "Retrieval Data Report for Single-Shell Tank 241-C-203," Rev. 1-A,
2 CH2M HILL Hanford Group, Inc., Richland, Washington.
- 3 RPP-RPT-29095, 2006, "Retrieval Data Report for Single-Shell Tank 241-C-202," Rev. 0,
4 CH2M HILL Hanford Group, Inc., Richland, Washington.
- 5 RPP-RPT-30181, 2006, "Retrieval Data Report for Single-Shell Tank 241-C-201," Rev. 0-B,
6 CH2M HILL Hanford Group, Inc., Richland, Washington.
- 7 RPP-RPT-33060, 2007, "Retrieval Data Report for Single-Shell Tank 241-C-103," Rev. 0,
8 CH2M HILL Hanford Group, Inc., Richland, Washington.
- 9 RPP-RPT-34062, 2007, "Retrieval Data Report for Single-Shell Tank 241-C-204," Rev. 0,
10 CH2M HILL Hanford Group, Inc., Richland, Washington.
- 11 RPP-RPT-39487, 2008, "TWINS Software Description," Rev. 0, Washington River Protection
12 Solutions, LLC, Richland, Washington.
- 13 RPP-RPT-39908, 2009, "Hanford Tank Waste Operations Simulator Model (HTWOS)
14 Version 3.0 Verification and Validation Report," Rev. 0, Washington River Protection
15 Solutions, LLC, Richland, Washington.
- 16 RPP-RPT-41918, 2010, "Assessment Context for Performance Assessment for Waste in C Tank
17 Farm Facilities after Closure," Rev. 0, Washington River Protection Solutions, LLC,
18 Richland, Washington.
- 19 RPP-RPT-42294, 2016, "Hanford Waste Management Area C Soil Contamination Inventory
20 Estimates," Rev. 2, Washington River Protection Solutions, LLC, Richland, Washington.
- 21 RPP-RPT-42323, 2015, "Hanford C-Farm Tank and Ancillary Equipment Residual Waste
22 Inventory Estimates," Rev. 3, Washington River Protection Solutions, LLC, Richland,
23 Washington.
- 24 RPP-RPT-44042, 2010, "Recharge and Waste Release within Engineered System in Waste
25 Management Area C," Rev. 0, Washington River Protection Solutions, LLC, Richland,
26 Washington.
- 27 RPP-RPT-45845, 2010, "Completion of Pumpable Liquid Removal from 244-CR Vault," Rev. 0,
28 Washington River Protection Solutions, LLC, Richland, Washington.
- 29 RPP-RPT-46088, 2016, "Flow and Transport in the Natural System at Waste Management
30 Area C," Rev. 2, Washington River Protection Solutions, LLC/GSI Water Solutions, Inc.,
31 Richland, Washington.
- 32 RPP-RPT-46879, 2016, "Corrosion and Structural Degradation within Engineered System in
33 Waste Management Area C," Rev. 3, Washington River Protection Solutions, LLC,
34 Richland, Washington.

RPP-ENV-58782, Rev. 0

- 1 RPP-RPT-47479, 2016, "Exposure Scenarios for the Waste Management Area C Performance
2 Assessment," Rev. 2, Washington River Protection Solutions, LLC, Richland,
3 Washington.
- 4 RPP-RPT-48490, 2011, "Technical Approach and Scope for Flow and Contaminant Transport
5 Analysis in the Initial Performance Assessment of Waste Management Area C,"
6 Washington River Protection Solutions, LLC, Richland, Washington.
- 7 RPP-RPT-49089, 2011, "Hanford B-Farm Leak Inventory Assessments Report," Rev. 0,
8 Washington River Protection Solutions, LLC, Richland, Washington.
- 9 RPP-RPT-49425, 2011, "Ecological Risk Assessment Approach for Hanford Waste Management
10 Area C," Rev. 1, Washington River Protection Solutions, LLC, Richland, Washington.
- 11 RPP-RPT-49701, 2011, "Waste Management Area C Closure – Conceptual Design Report,"
12 Rev. 0, Washington River Protection Solutions, LLC, Richland, Washington.
- 13 RPP-RPT-50097, 2011, "Hanford 241-U Farm Leak Inventory Assessment Report," Rev. 0,
14 Washington River Protection Solutions, LLC, Richland, Washington.
- 15 RPP-RPT-50870, 2013, "Hanford 241-TX Farm Leak Inventory Assessment Report," Rev. 0,
16 Washington River Protection Solutions, LLC, Richland, Washington.
- 17 RPP-RPT-50934, 2012, "Inspection and Test Report for the Removed 241-C-107 Dome
18 Concrete," Rev. 0, Washington River Protection Solutions, LLC, Richland, Washington.
- 19 RPP-RPT-54072, 2014, "Retrieval Data Report for Single-Shell Tank 241-C-104," Rev. 0,
20 Washington River Protection Solutions, LLC/YAHS GS, LLC, Richland, Washington.
- 21 RPP-RPT-55084, 2013, "Hanford 241-T Farm Leak Inventory Assessment Report," Rev. 0,
22 Washington River Protection Solutions LLC, Richland, Washington.
- 23 RPP-RPT-55284, 2014, "Retrieval Data Report for Single-Shell Tank 241-C-109," Rev. 0,
24 Washington River Protection Solutions, LLC/YAHS GS, LLC, Richland, Washington.
- 25 RPP-RPT-55896, 2013, "Retrieval Data Report for Single-Shell Tank 241-C-108," Rev. 1,
26 Washington River Protection Solutions, LLC/YAHS GS, LLC, Richland, Washington.
- 27 RPP-RPT-56356, 2014, "Development of Alternative Digital Geologic Models of Waste
28 Management Area C," Rev. 0, Freestone Environmental Services Inc./Washington River
29 Protection Solutions, LLC, Richland, Washington.
- 30 RPP-RPT-56796, 2014, "Retrieval Data Report for Single-Shell Tank 241-C-110," Rev. 0,
31 Washington River Protection Solutions, LLC, LLC, Richland, Washington.

RPP-ENV-58782, Rev. 0

- 1 RPP-RPT-58254, 2014, “Concrete Core Testing Report for the Single-Shell Tank 241-A-106
2 Sidewall Coring Project,” Rev. 0, Washington River Protection Solutions LLC, Richland,
3 Washington.
- 4 RPP-RPT-58295, 2015, “Retrieval Data Report for Single-Shell Tank 241-C-107,” Rev. 1,
5 Washington River Protection Solutions, LLC, LLC, Richland, Washington.
- 6 RPP-RPT-58329, 2016, “Baseline Risk Assessment for Waste Management Area C,” Rev. 1,
7 INTERA, Inc./Washington River Protection Solutions, LLC, Richland, Washington.
- 8 RPP-RPT-58339, 2014, “Phase 2 RCRA Facility Investigation Report for Waste Management
9 Area C,” Draft A, Washington River Protection Solutions, LLC, Richland, Washington.
- 10 RPP-RPT-58386, 2015, “Retrieval Data Report for Single-Shell Tank 241-C-101,” Rev. 2,
11 Washington River Protection Solutions, LLC, Richland, Washington.
- 12 RPP-RPT-58490, 2015, “Retrieval Data Report for Single-Shell Tank 241-C-112,” Rev. 2B,
13 Washington River Protection Solutions, LLC, Richland, Washington.
- 14 RPP-RPT-58676, 2015, “Practicability Evaluation Request to Forego a Third Retrieval
15 Technology for Tank 241-C-102,” Rev. 0, Washington River Protection Solutions, LLC,
16 Richland, Washington.
- 17 RPP-RPT-59197, 2016, “Analysis of Past Tank Waste Leaks and Losses in the Vicinity of Waste
18 Management Area C at the Hanford Site, Southeast Washington,” Rev. 0, Washington
19 River Protection Solutions LLC, Richland, Washington.
- 20 Safe Drinking Water Act of 1974, 42 USC 300, et seq.
- 21 Sakoda, A., Ishimori, Y., and Yamaoka, K., 2011, “A comprehensive review of radon emanation
22 measurements for mineral, rock, soil, mill tailing and fly ash,” Applied Radiation and
23 Isotopes, Vol. 69, Issue 10, pp. 1422–1435.
- 24 Saltelli, A. and S. Tarantola, 2002, “On the Relative Importance of Input Factors in
25 Mathematical Models: Safety Assessment of Nuclear Waste Disposal,” Journal of the
26 American Statistical Association, Vol. 97, No. 459, pp. 702–709.
- 27 Sander, R., 1999, “Compilation of Henry’s Law Constants for Inorganic and Organic Species of
28 Potential Importance in Environmental Chemistry,” Version 3, Max-Planck Institute of
29 Chemistry, Mainz, Germany.
- 30 Scanlon, B. R., K. E. Keese, A. L. Flint, L. E. Flint, C. B. Gaye, W. M. Edmunds, and
31 I. Simmers, 2006, “Global synthesis of groundwater recharge in semiarid and arid
32 regions,” Hydrological Processes, Vol. 20, Issue 15, pp. 3335–3370.

RPP-ENV-58782, Rev. 0

- 1 Scheibe, T. D., E. M. Murphy, X. Chen, A. K. Rice, K. C. Carroll, B. J. Palmer,
2 A. M. Tartakovsky, I. Battiato, and B. D. Wood, 2015, "An Analysis Platform for
3 Multiscale Hydrogeologic Modeling with Emphasis on Hybrid Multiscale Methods,"
4 Groundwater, Vol. 53, No. 1, pp. 38–56.
- 5 SD-BWI-TI-335, 1988, "Fresh-Water Potentiometric Map and Inferred Flow Direction of
6 Ground Water Within the Mabton Interbed, Hanford Site, Washington State –
7 January 1987," Rockwell Hanford Operations, Richland, Washington.
- 8 Seyfried, M. S., S. Schwinning, M. A. Walvoord, W. T. Pockman, B. D. Newman,
9 R. B. Jackson, and F. M. Phillips, 2005, "Ecohydrological Control of Deep Drainage in
10 Arid and Semiarid Regions," Ecology, Vol. 86, No. 2, pp. 277–287.
- 11 SGW-54165, 2014, "Evaluation of the Unconfined Aquifer Hydraulic Gradient Beneath the
12 200 East Area, Hanford Site," Rev. 0, CH2M HILL Plateau Remediation Company,
13 Richland, Washington.
- 14 SGW-58561, 2015, "WMA C Quarterly October through December 2014 Quarterly
15 Groundwater Monitoring Report," Rev. 0, CH2M HILL Plateau Remediation Company,
16 Richland, Washington.
- 17 Slate, J. L., 1996, "Buried carbonate paleosols developed in Pliocene-Pleistocene deposits of the
18 Pasco Basin, south-central Washington, U.S.A.," Quaternary International, Vol. 34–36,
19 pp. 191–196.
- 20 SKB Rapport R-05-75, 2005, "Assessment of uncertainty intervals for sorption coefficients,
21 SFR-1 uppföljning av SAFE," Swedish Nuclear Fuel and Waste Management Company,
22 Stockholm, Sweden.
- 23 SRNL-STI-2008-00421, 2008, "Hydraulic and Physical Properties of Saltstone Grouts and Vault
24 Concretes," Rev. 0, Savannah River National Laboratory, Savannah River Nuclear
25 Solutions, Aiken, South Carolina.
- 26 SRR-CWDA-2009-00017, 2009, "Performance Assessment for the Saltstone Disposal Facility at
27 the Savannah River Site," Rev. 0, SRR Closure & Waste Disposal Authority, Savannah
28 River Remediation, Aiken, South Carolina.
- 29 State of Washington Office of Financial Management, Queried 05/17/2015, [April 1 official
30 population estimates], <http://www.ofm.wa.gov/pop/april1/default.asp>.
- 31 SVF-2109, Rev. 0, "Tank_Residuals_4MinTimestep(6Melters)-mmr-11-031-6.5-8.3r1-2011-03-
32 18-at-01-31-58_M1.xlsm," Present residual waste inventory data for System Plan, Rev. 6,
33 Case 1 - Baseline Case, R. A. Kirkbride, Base Ops. Proc. Engrng./Modeling, B1-55,
34 372-2115, 4/5/2011
- 35 Tank Waste Information Network System [TWINS], Queried 02/10/2014, [WMA C Tanks, wt%
36 water in sludge/solid waste type], <http://twins.pnl.gov/twins.htm>.

RPP-ENV-58782, Rev. 0

- 1 Technical Report TR-02-11, 2002, "Assigning probability distributions to input parameters of
2 performance assessment models," INTERA Inc. for Swedish Nuclear Fuel and Waste
3 Management Company, Stockholm, Sweden.
- 4 TFC-ENG-CHEM-P-53, "Best-Basis Inventory Evaluations," Washington River Protection
5 Solutions LLC (WRPS) Tank Farms, Richland, Washington.
- 6 TFC-ESHQ-ENV_FS-C-05, "WRPS Environmental Model Calculation Preparation and
7 Issuance," Washington River Protection Solutions LLC (WRPS) Tank Farms, Richland,
8 Washington.
- 9 TFC-PLN-155, "General Project Plan for Environment Modeling," Washington River Protection
10 Solutions LLC (WRPS) Tank Farms, Richland, Washington.
- 11 Tsang, C.-F., 1991, "The Modeling Process and Model Validation," Ground Water, Vol. 29,
12 No. 6, pp. 825–831.
- 13 The Nature Conservancy, 1998, "Biodiversity Inventory and Analysis of the Hanford Site, 1997
14 Annual Report," The Nature Conservancy of Washington, Seattle, Washington.
- 15 UCRL-21069, 1988, "Probabilistic Flood Hazard Assessment for the N Reactor, Hanford,
16 Washington," Jack R. Benjamin and Associates, Inc., Mountain View, California.
- 17 United States Environmental Protection Agency, Queried 01/2012, [EPA On-line Tools for Site
18 Assessment Calculation], [https://www3.epa.gov/ceampubl/learn2model/part-](https://www3.epa.gov/ceampubl/learn2model/part-two/onsite/estdiffusion.html)
19 [two/onsite/estdiffusion.html](https://www3.epa.gov/ceampubl/learn2model/part-two/onsite/estdiffusion.html).
- 20 United States Environmental Protection Agency, Queried 06/18/2015, [Preliminary Remediation
21 Goals for Radionuclides], <http://epa-prgs.ornl.gov/radionuclides/>.
- 22 USACE, 1951, "Artificial Flood Possibilities on the Columbia River," U.S. Army Corps of
23 Engineers, 45 Washington District, Washington, D.C.
- 24 USACE, 1989, "Water Control Manual for McNary Lock and Dam, Columbia River, Oregon
25 and Washington," U.S. Army Corps of Engineers, Walla Walla District, Walla Walla,
26 Washington.
- 27 U.S. Department of Agriculture, Natural Resources Conservation Service, Queried 12/18/2015,
28 [Fact Sheets & Plant Guides/*Artemisia tridentata* ssp. *tridentata*],
29 http://plants.usda.gov/plantguide/pdf/pg_arttrt.pdf.
- 30 U.S. Geological Survey, Queried 09/2015, [USGS Water Data for the Nation],
31 <http://waterdata.usgs.gov/nwis/nwis>.
- 32 USGS Bulletin 1457-G, 1979, "Revisions in stratigraphic nomenclature of the Columbia River
33 Basalt Group," U.S. Geological Survey, Washington, D.C.

RPP-ENV-58782, Rev. 0

- 1 van Genuchten, M. Th., 1980, "A Closed-form Equation for Predicting the Hydraulic
2 Conductivity of Unsaturated Soils," Soil Science Society of America Journal, Vol. 44,
3 No. 5, pp. 892–898.
- 4 WA7 89000 8967, 2007, "Hanford Facility Resource Conservation and Recovery Act Permit,
5 Dangerous Waste Portion Revision 8C for the Treatment, Storage, and Disposal of
6 Dangerous Waste," State of Washington Department of Ecology, Richland, Washington.
- 7 WAC 173-160, "Minimum Standards for Construction and Maintenance of Wells," Washington
8 Administrative Code, as amended.
- 9 WAC 173-201A, "Water Quality Standards for Surface Waters of the State of Washington,"
10 Washington Administrative Code, as amended.
- 11 WAC 173-216, "State Waste Discharge Permit Program," Washington Administrative Code,
12 as amended.
- 13 WAC 173-303, "Dangerous Waste Regulations," Washington Administrative Code, as amended.
- 14 WAC 173-303-610, "Closure and Post-Closure," Washington Administrative Code, as amended.
- 15 WAC 173-303-640, "Tank Systems," Washington Administrative Code, as amended.
- 16 WAC 173-303-665, "Landfills," Washington Administrative Code, as amended.
- 17 WAC 173-340-745, "Soil Cleanup Standards for Industrial Properties," Washington
18 Administrative Code, as amended.
- 19 WAC 173-340-747, "Deriving Soil Concentrations for Groundwater Protection," Washington
20 Administrative Code, as amended.
- 21 WAC 246-290, "Group A Public Water Supplies," Washington Administrative Code, as
22 amended.
- 23 WAC 246-290-025, "Adoption by Reference," Washington Administrative Code, as amended.
- 24 WAC 246-290-310, "Maximum Contaminant Levels (MCLs) and Maximum Residual
25 Disinfectant Levels (MRDLs)," Washington Administrative Code, as amended.
- 26 Wang, J. S. Y. and T. N. Narasimhan, 1985, "Hydrologic Mechanisms Governing Fluid Flow in
27 a Partially Saturated, Fractured, Porous Medium," Water Resources Research, Vol. 21,
28 No. 12, pp. 1861–1874.
- 29 Waters, A. C., 1961, "Stratigraphic and Lithologic Variations in the Columbia River Basalt,"
30 American Journal of Science, Vol. 259, pp. 583–611.

RPP-ENV-58782, Rev. 0

- 1 WCH-223, 2007, "2007 River Corridor Closure Contractor Revegetation Monitoring Report,"
2 Rev. 0, Washington Closure Hanford, Richland, Washington.
- 3 WCH-520, 2013, "Performance Assessment for the Environmental Restoration Disposal Facility,
4 Hanford Site, Washington," Rev. 1, Washington Closure Hanford, Richland, Washington.
- 5 Webster, G. D. and J. W. Crosby, 1982, "Appendix 2R - Stratigraphic Investigation of the
6 Skagit/Hanford Nuclear Project," in Skagit/Hanford Nuclear Project, Preliminary Safety
7 Analysis Report, Volume 5, Pudget Power, Pudget Sound Power and Light Company,
8 Bellevue, Washington.
- 9 WHC-EP-0216, 1989, "Primary Operable Units Designation Project," Westinghouse Hanford
10 Company, Richland, Washington.
- 11 WHC-EP-0332, 1989, "Simulations of Infiltration of Meteoric Water and Contaminant Plume
12 Movement in the Vadose Zone at Single-Shell Tank 241-T-106 at the Hanford Site,"
13 Westinghouse Hanford Company, Richland, Washington.
- 14 WHC-EP-0595, 1993, "Westinghouse Hanford Company Operational Groundwater Status
15 Report, 1990-1992," Westinghouse Hanford Company, Richland, Washington.
- 16 WHC-EP-0645, 1995, "Performance Assessment for the Disposal of Low-Level Waste in the
17 200 West Area Burial Grounds," Westinghouse Hanford Company, Richland,
18 Washington.
- 19 WHC-EP-0673, 1994, "Permanent Isolation Surface Barrier Development Plan," Westinghouse
20 Hanford Company, Richland, Washington.
- 21 WHC-EP-0698, 1994, "Groundwater Impact Assessment Report for the 216-U-14 Ditch,"
22 Westinghouse Hanford Company, Richland, Washington.
- 23 WHC-EP-0707, 1994, "216-U-10 Pond and 216-Z-19 Ditch Characterization Studies," Rev. 0
24 (formerly RHO-ST-45), Westinghouse Hanford Company, Richland, Washington.
- 25 WHC-EP-0772, 1994, "Characterization of the Corrosion Behavior of the Carbon Steel Liner in
26 Hanford Site Single-Shell Tanks," Rev. 0, Westinghouse Hanford Company, Richland,
27 Washington.
- 28 WHC-EP-0815, 1995, "Groundwater Impact Assessment Report for the 216-T-4-2 Ditch,"
29 Westinghouse Hanford Company, Richland, Washington.
- 30 WHC-EP-0883, 1995, "Variability and Scaling of Hydraulic Properties for 200 Area Soils,
31 Hanford Site," Westinghouse Hanford Company, Richland, Washington.
- 32 WHC-MR-0293, 1992, "Legend and Legacy: Fifty Years of Defense Production at the Hanford
33 Site," Rev. 2, Westinghouse Hanford Company, Richland, Washington.

RPP-ENV-58782, Rev. 0

- 1 WHC-MR-0521, 1996, "The Plutonium Production Story at the Hanford Site: Processes and
2 Facilities History," Rev. 0, Westinghouse Hanford Company, Richland, Washington.
- 3 WHC-SA-1252-S, 1991, "Mammal Occurrence and Exclusion at the Hanford Site,"
4 Westinghouse Hanford Company, Richland, Washington.
- 5 WHC-SD-EN-AP-012, 1991, "Interim-Status Groundwater Monitoring Plan for the Single-Shell
6 Tanks," Rev. 1, Westinghouse Hanford Company, Richland, Washington.
- 7 WHC-SD-EN-EE-004, 1991, "Revised Stratigraphy for the Ringold Formation, Hanford Site,
8 South-Central Washington," Rev. 0, Westinghouse Hanford Company, Richland,
9 Washington.
- 10 WHC-SD-EN-TI-012, 1992, "Geologic Setting of the 200 East Area: An Update," Rev. 0,
11 Westinghouse Hanford Company, Richland, Washington.
- 12 WHC-SD-EN-TI-014, 1992, "Hydrogeologic Model for the 200 West Groundwater Aggregate
13 Area," Rev. 0, Westinghouse Hanford Company, Richland, Washington.
- 14 WHC-SD-EN-TI-019, 1992, "Hydrogeologic Model for the 200 East Groundwater Aggregate
15 Area," Rev. 0, Westinghouse Hanford Company, Richland, Washington.
- 16 WHC-SD-EN-TI-290, 1994, "Geologic Setting of the Low-Level Burial Grounds," Rev. 0,
17 Westinghouse Hanford Company, Richland, Washington.
- 18 WHC-SD-ER-TI-003, 1991, "Geology and Hydrology of the Hanford Site: A Standardized Text
19 for Use in Westinghouse Hanford Company Documents and Reports," Rev. 0,
20 Westinghouse Hanford Company, Richland, Washington.
- 21 WHC-SD-GN-ER-30009, 1992, "Bibliography and Summary of Geotechnical Studies at the
22 Hanford Site," Rev. 2, Westinghouse Hanford Company, Richland, Washington.
- 23 WHC-SD-GN-ER-30038, 2012, "Volcano Ashfall Loads for the Hanford Site," Rev. 2,
24 Washington River Protection Solutions LLC, Richland, Washington.
- 25 WHC-SD-W236A-TI-0002, 1993, "Probabilistic Seismic Hazard Analysis, DOE Hanford Site,
26 Washington," Rev. 0, prepared for Westinghouse Hanford Company by Geomatrix
27 Consultants, Richland, Washington.
- 28 WHC-SD-WM-EE-004, 1995, "Performance Assessment of Grouted Double-Shell Tank Waste
29 Disposal at Hanford," Rev. 1, Westinghouse Hanford Company, Richland, Washington.
- 30 WHC-SD-WM-TI-632, 1995, "Hanford Defined Wastes: Chemical and Radionuclide
31 Compositions," Rev. 0, Westinghouse Hanford Company, Richland, Washington.

RPP-ENV-58782, Rev. 0

- 1 WHC-SD-WM-TI-730, 1996, "Performance Assessment for the Disposal of Low-Level Waste in
2 the 200 East Area Burial Grounds," Rev. 0, Westinghouse Hanford Company, Richland,
3 Washington.
- 4 Whitlock, C. and P. J., Bartlein, 1997, "Vegetation and climate change in northwest America
5 during the past 125 kyr," *Nature*, Vol. 388, pp. 57–61.
- 6 Wing, N. R. and G. W. Gee, 1994, "Quest for the Perfect Cap," *Civil Engineering*, Vol. 64,
7 No. 10, pp. 38–41.
- 8 WMP-17524, 2003, "Vadose Zone Hydraulic Property Letter Reports," Rev. 0, Fluor Hanford,
9 Richland, Washington.
- 10 WMP-20570, 2006, "Central Plateau Terrestrial Ecological Risk Assessment Data Quality
11 Objectives Summary Report – Phase I," Rev. 0, Fluor Hanford, Richland, Washington.
- 12 WSRC-MS-2003-00582, 2004, "Performance Assessment/Composite Analysis Modeling to
13 Support a Holistic Strategy for the Closure of F Area, a Large Nuclear Complex at the
14 Savannah River Site," Rev. 1, Savannah River Technology Center, Aiken, South
15 Carolina.
- 16 WSRC-STI-2007-00369, 2007, "Hydraulic and Physical Properties of Tank Grouts and Base
17 Mat Surrogate Concrete for FTF Closure," Rev. 0, Savannah River National Laboratory,
18 Aiken, South Carolina.
- 19 WSRC-STI-2007-00607, 2007, "Chemical Degradation Assessment of Cementitious Materials
20 for the HLW Tank Closure Project (U)," Rev. 0, Washington Savannah River
21 Company/Savannah River National Laboratory, Aiken, South Carolina.
- 22 WSRC-TR-2005-00195, 2005, "Summary of Grout Development and Testing for Single Shell
23 Tank Closure at Hanford," Rev. 0, Savannah River National Laboratory, Aiken, South
24 Carolina.
- 25 Xu, X., J. L. Nieber, and S. C. Gupta, 1992, "Compaction Effect on the Gas Diffusion
26 Coefficient in Soils," *Soil Science Society of America Journal*, Vol. 56, No. 6,
27 pp. 1743–1750.
- 28 Ye, M. and R. Khaleel, 2008, "A Markov chain model for characterizing medium heterogeneity
29 and sediment layering structure," *Water Resources Research*, Vol. 44, Issue 9, W09427.
- 30 Ye, M., R. Khaleel, M. G. Schaap, and J. Zhu, 2007, "Simulation of field injection experiments
31 in heterogeneous unsaturated media using cokriging and artificial neural network," *Water
32 Resources Research*, Vol. 43, Issue 7, W07413.
- 33 Ye, M., R. Khaleel, T. J. Yeh, 2005, "Stochastic analysis of moisture plume dynamics of a field
34 injection experiment," *Water Resources Research*, Vol. 41, W03013.

RPP-ENV-58782, Rev. 0

- 1 Yeh, T.-C. J., M. Ye, R. Khaleel, 2005, "Estimation of effective unsaturated hydraulic
2 conductivity tensor using spatial moments of observed moisture plume," Water
3 Resources Research, Vol. 41, W03014.
- 4 Zhang, Z. F. and R. Khaleel, 2010, "Simulating field-scale moisture flow using a combined
5 power-averaging and tensorial connectivity-tortuosity approach," Water Resources
6 Research, Vol. 46, Issue 9, W09505.

RPP-ENV-58782, Rev. 0

1
2
3
4
5
6
7
8
9
10
11

APPENDIX A

KEY ASSUMPTIONS IN THE PERFORMANCE ASSESSMENT

RPP-ENV-58782, Rev. 0

1
2
3
4
5
6
7

This page intentionally left blank.

RPP-ENV-58782, Rev. 0

LIST OF TERMS

Abbreviations and Acronyms

DOE	U.S. Department of Energy
RCRA	Resource Conservation and Recovery Act of 1976
WMA	Waste Management Area

RPP-ENV-58782, Rev. 0

- 1
- 2
- 3
- 4
- 5
- 6
- 7

This page intentionally left blank.

RPP-ENV-58782, Rev. 0

APPENDIX A**KEY ASSUMPTIONS IN THE PERFORMANCE ASSESSMENT**

In this Appendix, a set of key assumptions used in the base case analysis of the Performance Assessment are listed. However, it is emphasized that the structure of the Performance Assessment is founded on the extensive use of sensitivity and uncertainty analyses that explore the consequences if alternative assumptions are used. The alternative analyses include sensitivity cases evaluating conditions well outside the range of the base case analysis. In all cases the calculations produced results that are below the performance measures. Therefore, it is not possible to identify key assumptions or design variables that must be met in order to meet the regulatory goals of DOE O 435.1, Radioactive Waste Management.

- It has been assumed that the landfill closure of Waste Management Area (WMA) C occurs in 2020, consistent with planning assumptions in the Tank Closure and Waste Management Environmental Impact Statement (DOE/EIS-0391). The results of the performance assessment are not significantly affected by alternative assumptions about closure timing.
- The Central Plateau has been designated Industrial-Exclusive for the indefinite future, based on several Records of Decision [64 FR 61615, "Record of Decision: Hanford Comprehensive Land-Use Plan Environmental Impact Statement (HCP EIS)"; 73 FR 55824, "Amended Record of Decision for the Hanford Comprehensive Land-Use Plan Environmental Impact Statement"]. This area, which includes the 200 East and 200 West Areas, includes WMA C. There is no stated intention to release the Central Plateau from this designation or from U.S. Department of Energy (DOE) control at any time in the future. Despite this designation, it is assumed in this analysis that institutional control and societal memory of the disposal activities are lost 100 years after site closure, for consistency with DOE O 435.1 requirements. This assumption is necessary to allow future hypothetical individuals to come onto the Central Plateau and engage in activities that might result in exposure.
- In the base case, the land use and land cover, including the barrier, remain shrub steppe indefinitely after closure. Alternative infiltration rates in the future are included in alternative analysis cases, which are intended to address a variety of potential future conditions, including progression to different land uses and land covers.
- The engineered cover for WMA C is not yet designed but is assumed to be similar to the Modified Resource Conservation and Recovery Act of 1976 (RCRA) Subtitle C Barrier that limits infiltration through the waste primarily by evapotranspiration processes (i.e., surface barrier) based on the work done for the Hanford Prototype barrier (DOE/ORP-2008-01, RCRA Facility Investigation Report for Hanford Single-Shell Tank Waste Management Areas, Appendix C). These processes are not modeled directly for this report, but those processes have been studied through field measurements, tracer studies, and numerical models to estimate net infiltration (PNNL-14744, "Recharge Data Package for the 2005 Integrated Disposal Facility Performance Assessment";

RPP-ENV-58782, Rev. 0

PNNL-14960, “200-BP-1 Prototype Hanford Barrier Annual Monitoring Report for Fiscal Year 2004”; “Multiple-Year Water Balance of Soil Covers in a Semiarid Setting” [Fayer and Gee 2006]). Instead, the recommended net infiltration rates from those reports are applied to the area under the engineered cover and are varied spatially and temporally as appropriate according to the estimated or assumed time-dependent performance of a surface barrier.

- The design life of the cover is assumed to be 500 years in the base case, following which the infiltration through the cover is assumed to return to the site-wide average infiltration rate for undisturbed soil. Alternative infiltration rates in the future are included in alternative analysis cases, which are intended to address a variety of potential future conditions, including progression to different land uses and land covers.
- It is assumed the tanks will be filled with grout according to the basic assumptions outlined for landfill closure in DOE/EIS-0391 (2012). The specific formulation of the grout has not yet been established, but consistent with DOE/EIS-0391 (2012), it is assumed the fill material for the tanks will be similar to the cold-cap grout formulation developed by the U.S. Army Corps of Engineers for the Hanford Grout Vault Program. This type of grout is assumed to behave chemically like ordinary cementitious material. It has been assumed that the grout formulation does not provide any specific or unusual chemical conditions, such as reducing conditions.
- Radionuclide and chemical release mechanisms from the sources are assumed to occur by one of two mechanisms: (a) the entire inventory of the residual waste is assumed to be instantly available for release and transport out of the tanks, or (b) a semi-empirical release function is applied based on leach tests performed on residual waste from WMA C.
- Transport of contamination from the tanks is assumed to be primarily controlled by diffusion from the grouted tanks through the base mat below the tank. Alternative assumptions are included as sensitivity cases that evaluate the consequences of hydraulic failure (i.e., fracturing) of the grouted tanks and base mat.
- The specific formulation of the grout has not yet been established, and site-specific measurements of the chemical influence of the grout have not been performed. The chemical effect of the grout is represented by contaminant-specific distributions of distribution coefficients (K_d), which have been developed from international literature on sorption of radionuclides on cementitious materials. These values are generally consistent with or more conservative than comparable values used for the facility-specific grout at the Savannah River F and H tank farm performance assessments [WSRC-STI-2007-00369, “Hydraulic and Physical Properties of Tank Grouts and Base Mat Surrogate Concrete for FTF Closure” and WSRC-STI-2007-00607, “Chemical Degradation Assessment of Cementitious Materials for the HLW Tank Closure Project (U)”].

RPP-ENV-58782, Rev. 0

- 1 • Release from one WMA C solute source and migration are independent of other solute
2 transport and source terms in the model.
3
- 4 • The post-retrieval inventory of contaminants in WMA C is assumed to be uniformly
5 distributed throughout the waste residual volume. The residual volume in the tanks is
6 assumed to be a uniform layer distributed at the bottom of the tanks. In pipelines and
7 ancillary equipment, the residual waste is assumed to be distributed in a homogeneous
8 layer across WMA C at the depth and area of the pipelines.
9
- 10 • Progeny radionuclides with a half-life of less than two years are assumed to be in secular
11 equilibrium with their parent, which allows a reduction in the number of species tracked
12 but still accounts for the radiological effects of the progeny.
13
- 14 • Inventories of contaminants in retrieved tanks are based on post-retrieval sampling and
15 measurements. It is assumed that the sampling results are representative of the entire
16 waste residual. Inventories for tanks that have not yet completed retrieval use the best
17 estimates of post-retrieval conditions available at this time. These data have been
18 estimated as of September 30, 2014. Additional sensitivity cases were executed based on
19 alternative inventories in the 2009 to 2011 working sessions.
20
- 21 • The vadose zone is modeled as an aqueous-gas porous media system where flow and
22 transport through the gas phase are assumed to be negligible.
23
- 24 • Hydraulic property heterogeneity is assumed to be insignificant within geologic units.
25 Hence, each geologic unit within the vadose zone is assigned upscaled, effective
26 hydraulic properties. These properties have been updated from the input parameters
27 presented in the 2009 and 2011 data packages based on consideration of field data for
28 moisture content, as discussed in Appendix B.
29
- 30 • Post-closure groundwater flow beneath WMA C is assumed to be northwest to southeast
31 and parallel to the four tank arrays of 100-series tanks in WMA C. The justification for
32 this assumption is found in RPP-RPT-46088, "Flow and Transport in the Natural System
33 at Waste Management Area C." Groundwater flow parameters have been derived from
34 the Central Plateau groundwater model (CP-47631, "Model Package Report: Central
35 Plateau Groundwater Model Version 6.3.3").
36
- 37 • Distribution coefficients (K_d) are used to represent sediment-contaminant chemical
38 interaction that best represent plausible levels of reactivity. The K_d values are chosen
39 assuming low-salt, near-neutral waste chemistry in the vadose and saturated zone.
40 Justification for the selected parameter values is found in RPP-RPT-46088;
41 PNNL-16663, "Geochemical Processes Data Package for the Vadose Zone in the
42 Single-Shell Tank Waste Management Areas at the Hanford Site"; and PNNL-17154,
43 "Geochemical Characterization Data Package for the Vadose Zone in the Single-Shell
44 Tank Waste Management Areas at the Hanford Site." In addition, uncertainties in K_d
45 values have been assessed as part of the uncertainty analysis.
46

RPP-ENV-58782, Rev. 0

- 1 • The point of calculation used in the calculation of the groundwater concentrations
2 corresponds to the location 100 m (328 ft) downgradient from the facility per
3 DOE O 435.1. For the purpose of calculating groundwater concentrations for comparison
4 with groundwater protection requirements, it is necessary to identify the peak location in
5 space at which the concentration occurs. The approach for identifying the location of
6 peak groundwater concentrations is described in Section 6.3.9.
7
- 8 • For volatiles released from the residual wastes, it is assumed that transport through the
9 tank infill grout material and the soil overburden is controlled by diffusion.
10
- 11 • Once volatile radionuclides reach the ground surface, a simplified Gaussian plume model
12 with uniform velocity and atmospheric conditions is assumed for the air transport
13 analysis.
14
- 15 • Assumptions used in the exposure scenarios to define input parameter values are based
16 on appropriate regulatory guidance as detailed in RPP-ENV-58813, "Exposure Scenarios
17 for Risk and Performance Assessments in Tank Farms at the Hanford Site, Washington."
18 These values represent conservative inputs to the exposure scenario calculations
19 characteristic of a highly exposed individual.
20
- 21 • Age- and gender-weighted intake rates are generally developed for a Representative
22 Person in accordance with the recommendations described in DOE-STD-1196-2011,
23 Derived Concentration Technical Standard. The 95th percentile intake rates were
24 obtained from EPA/600/R-090/052F, Exposure Factors Handbook: 2011 Edition,
25 National Center for Environmental Assessment, based on available information. Even
26 though mean intake rates were available, the 95th percentile values from the underlying
27 distribution were chosen conservatively to maximize the likely exposure. Typically, the
28 95th percentile intake rates weighted by age and gender are calculated (Appendix P of
29 RPP-ENV-58813). The exceptions to this approach were the indoor inhalation rate
30 (taken directly from a reference source) and the soil ingestion rates (where simple age
31 weighting is performed for children and adults).
32
- 33 • The following assumptions are specific to inadvertent human intrusion.
34
 - 35 ○ The only credible intrusion event is a drilling event. Both depth of disposal and the
36 existence of concrete and grout intrusion barriers limit credible intrusion scenarios.
37
 - 38 ○ Although results are provided for intrusion into individual single-shell tanks, the most
39 credible intrusion event is assumed to be into the ancillary equipment rather than a
40 tank. This type of event is more credible than a tank intrusion, since the tank dome
41 and grout form a substantial intruder protection barrier.
42
 - 43 ○ For the analysis of intrusion into the pipelines, the driller is assumed to penetrate a
44 transfer line at 100 years after closure. Sensitivity analyses have investigated
45 intrusion into a cascade line, which would release a larger inventory relative to other
46 pipeline locations in WMA C.

RPP-ENV-58782, Rev. 0

- For the intrusion analysis for the 100- and 200-series tanks, the C-301 catch tank, and the 244-CR Process Tank Vault, the intruder is assumed to penetrate the tank dome, tank shell, grout, and residual waste at 500 years after closure.
- The acute exposure to the driller is calculated using representative local assumptions about the duration of the drilling.
- Acute exposures are limited to a well driller that is exposed to waste exhumed by the drill bit during the drilling.
- Chronic post-intrusion exposures are calculated for several alternative exposure scenarios. In these scenarios, waste exhumed by the intrusion event is assumed to be mixed with a surface soil layer. In each scenario, the volume of soil in this layer represents the minimum area consistent with the assumed activities of the scenario. For instance, the residential garden scenario mixes the contamination in an area of a garden sufficient to grow vegetables, whereas the rural pasture scenario mixes the contamination in an area sufficient for cattle grazing. The effect of this assumption is that different post-intrusion chronic scenarios have different soil concentrations, and the relative importance of the scenarios is strongly dependent on the assumed area of contamination.

REFERENCES

- 64 FR 61615, 1999, "Record of Decision: Hanford Comprehensive Land-Use Plan Environmental Impact Statement (HCP EIS)," Federal Register, Vol. 64, pp. 61615–61625 (November 12).
- 73 FR 55824, 2008, "Amended Record of Decision for the Hanford Comprehensive Land-Use Plan Environmental Impact Statement," Federal Register, Vol. 73, pp. 55824–55826 (September 26).
- CP-47631, 2015, "Model Package Report: Central Plateau Groundwater Model Version 6.3.3," Rev. 2, INTERA, Inc., Richland, Washington.
- DOE/EIS-0391, 2012, "Final Tank Closure and Waste Management Environmental Impact Statement for the Hanford Site, Richland, Washington," U.S. Department of Energy, Washington, D.C.
- DOE O 435.1, 2001, Radioactive Waste Management, U.S. Department of Energy, Washington, D.C.
- DOE/ORP-2008-01, 2010, RCRA Facility Investigation Report for Hanford Single-Shell Tank Waste Management Areas, Rev. 1, U.S. Department of Energy, Office of River Protection, Richland, Washington.

RPP-ENV-58782, Rev. 0

- 1 DOE-STD-1196-2011, 2011, Derived Concentration Technical Standard, U.S. Department of
2 Energy, Washington, D.C.
- 3 EPA/600/R-090/052F, 2011, Exposure Factors Handbook: 2011 Edition, National Center for
4 Environmental Assessment, Office of Research and Development, U.S. Environmental
5 Protection Agency, Washington, D.C.
- 6 Fayer, M. J., and G. W. Gee, 2006, "Multiple-Year Water Balance of Soil Covers in a Semiarid
7 Setting," Journal of Environmental Quality, Vol. 35, No. 2, pp. 366–377.
- 8 PNNL-14744, 2004, "Recharge Data Package for the 2005 Integrated Disposal Facility
9 Performance Assessment," Pacific Northwest National Laboratory, Richland,
10 Washington.
- 11 PNNL-14960, 2005, "200-BP-1 Prototype Hanford Barrier Annual Monitoring Report for Fiscal
12 Year 2004," Pacific Northwest National Laboratory, Richland, Washington.
- 13 PNNL-16663, 2007, "Geochemical Processes Data Package for the Vadose Zone in the
14 Single-Shell Tank Waste Management Areas at the Hanford Site," Pacific Northwest
15 National Laboratory, Richland, Washington.
- 16 PNNL-17154, 2008, "Geochemical Characterization Data Package for the Vadose Zone in the
17 Single-Shell Tank Waste Management Areas at the Hanford Site," Pacific Northwest
18 National Laboratory, Richland, Washington.
- 19 Resource Conservation and Recovery Act of 1976, 42 USC 6901, et seq.
- 20 RPP-ENV-58813, 2016, "Exposure Scenarios for Risk and Performance Assessments in Tank
21 Farms at the Hanford Site, Washington," Rev. 0, Washington River Protection
22 Solutions, LLC, Richland, Washington.
- 23 RPP-RPT-46088, 2016, "Flow and Transport in the Natural System at Waste Management
24 Area C," Rev. 2, Washington River Protection Solutions, LLC/GSI Water Solutions, Inc.,
25 Richland, Washington.
- 26 WSRC-STI-2007-00369, 2007, "Hydraulic and Physical Properties of Tank Grouts and Base
27 Mat Surrogate Concrete for FTF Closure," Rev. 0, Savannah River National Laboratory,
28 Aiken, South Carolina.
- 29 WSRC-STI-2007-00607, 2007, "Chemical Degradation Assessment of Cementitious Materials
30 for the HLW Tank Closure Project (U)," Rev. 0, Washington Savannah River
31 Company/Savannah River National Laboratory, Aiken, South Carolina.
- 32

RPP-ENV-58782, Rev. 0

1
2
3
4
5
6
7
8
9
10
11

APPENDIX B

**BASIS FOR DEVELOPMENT OF VADOSE ZONE HYDRAULIC PROPERTIES AT
WASTE MANAGEMENT AREA C**

RPP-ENV-58782, Rev. 0

- 1
- 2
- 3
- 4
- 5
- 6
- 7

This page intentionally left blank.

RPP-ENV-58782, Rev. 0

TABLE OF CONTENTS

1			
2	APPENDIX B – BASIS FOR DEVELOPMENT OF VADOSE ZONE HYDRAULIC		
3	PROPERTIES AT WASTE MANAGEMENT AREA C	B-1	
4	B.1 MOISTURE CONTENT MEASUREMENTS AT WASTE		
5	MANAGEMENT AREA C	B-1	
6	B.1.1 Moisture Content Measurements for Hanford H2 Sand-Dominated		
7	Unit	B-2	
8	B.1.2 Moisture Content Measurements for Hanford H1, Hanford H3 and		
9	Backfill Gravelly Units	B-15	
10	B.2 LABORATORY-SCALE MEASUREMENTS FOR HYDRAULIC		
11	PROPERTIES	B-16	
12	B.2.1 Properties of the Hanford H2 Sand Unit.....	B-17	
13	B.2.2 Properties of the Hanford H1 and H3 Gravelly Units.....	B-27	
14	B.2.3 Properties for the Backfill Gravelly Unit.....	B-30	
15	B.3 EFFECTIVE (UPSCALED) FLOW PARAMETERS FOR VADOSE		
16	ZONE	B-31	
17	B.3.1 Composite Macroscopic Relationships and Effective Parameters.....	B-33	
18	B.3.2 Stochastic Model for Macroscopic Anisotropy	B-34	
19	B.3.3 Macroscopic Anisotropy Relations.....	B-36	
20	B.4 EFFECTIVE TRANSPORT PARAMETERS.....	B-36	
21	B.4.1 Bulk Density and K_d	B-38	
22	B.4.2 Diffusivity	B-39	
23	B.4.3 Vadose Zone Macrodispersivities.....	B-40	
24	B.5 REFERENCES	B-55	

RPP-ENV-58782, Rev. 0

LIST OF FIGURES

1		
2		
3	Figure B-1.	Distribution of Moisture Content Measurements Collected in and around
4		Waste Management Area C (a) Plan View with All Moisture Content Data,
5		(b) Plan View with All Moisture Content Data Inside the Single-Shell Tank
6		Footprint, (c) Plan View with All Moisture Content Data Outside the
7		Single-Shell Tank Footprint and (d) a Side View Looking Northwest. B-3
8	Figure B-2a.	Waste Management Area C Moisture Content Histogram for All H2 Data
9		(Includes the Data from Both Inside and Outside of the Single-Shell Tank
10		Footprint). B-4
11	Figure B-2b.	Waste Management Area C Moisture Content Histogram for H2 Data Within
12		the Single-Shell Tank Footprint. B-5
13	Figure B-2c.	Waste Management Area C Moisture Content Histogram for H2 Data
14		Outside of the Single-Shell Tank Footprint. B-6
15	Figure B-3.	Location of Sisson and Lu Site, Integrated Disposal Facility and Selected
16		Boreholes in 200 Area. B-7
17	Figure B-4.	(a) Pre- and (b) Post-Injection Moisture Plumes for the Field Injection
18		Experiment in the 200 East Area. B-8
19	Figure B-5.	Borehole Location Map for Waste Management Area C. B-9
20	Figure B-6a.	Borehole C4297 Lithology and Gravimetric Moisture Content Measurements
21		(the shaded areas in light blue and gray are regions of increased moisture). B-10
22	Figure B-6b.	Borehole 299-E27-22 Lithology and Gravimetric Moisture Content
23		Measurements (the shaded areas in light blue and gray are regions of
24		increased moisture). B-11
25	Figure B-7a.	Matric Potentials Measured by Filter Paper Technique on Core Samples from
26		Borehole C4297. B-13
27	Figure B-7b.	Matric Potentials Measured by Filter Paper Technique on Core Samples
28		from Borehole 299-E27-22. B-14
29	Figure B-8a.	Comparison of Gravimetric Moisture Content Measurements for
30		Boreholes C4297 and 299-E27-22. B-18
31	Figure B-8b.	Comparison of Soil Moisture Tension Measurements for Boreholes C4297
32		and 299-E27-22. B-19

RPP-ENV-58782, Rev. 0

1	Figure B-9a. Waste Management Area C Moisture Content Histogram for All H1 Data	
2	(Includes the Data from Both Inside and Outside of the Single-Shell Tank	
3	Footprint).	B-20
4	Figure B-9b. Waste Management Area C Moisture Content Histogram for H1 Data Within	
5	the Single-Shell Tank Footprint.	B-20
6	Figure B-9c. Waste Management Area C Moisture Content Histogram for H1 Data	
7	Outside of the Single-Shell Tank Footprint.....	B-21
8	Figure B-10a. Waste Management Area C Moisture Content Histogram for All Backfill	
9	Data (Includes the Data from Both Inside and Outside of the Single-Shell	
10	Tank Footprint).	B-21
11	Figure B-10b. Waste Management Area C Moisture Content Histogram for Backfill Data	
12	Inside of the Single-Shell Tank Footprint.	B-22
13	Figure B-10c. Waste Management Area C Moisture Content Histogram for Backfill Data	
14	Outside the Single-Shell Tank Footprint.	B-23
15	Figure B-11. Waste Management Area C Hanford H2 Sand-Dominated Core.....	B-24
16	Figure B-12. Moisture Retention Data for H2 Unit (44 Samples).....	B-28
17	Figure B-13. Unsaturated Hydraulic Conductivity Data for H2 Unit (44 Samples).	B-29
18	Figure B-14. Comparison of Simulated (Blue) and Observed (Circle) Moisture Content for	
19	Hanford H2 Sand-Dominated Unit.....	B-30
20	Figure B-15. Moisture Retention Curves for Various Hydrostratigraphic Units and	
21	Selected Properties for Alternative Geologic Model II.	B-32
22	Figure B-16. Unsaturated Hydraulic Conductivity Curves for Various Hydrostratigraphic	
23	Units and Selected Properties for Alternative Geologic Model II.....	B-33
24	Figure B-17. Unsaturated Hydraulic Conductivity Measurements for Sand-Dominated and	
25	Gravel-Dominated Samples.....	B-34
26	Figure B-18. Moisture Retention Data for H1 and H3 Units (17 Samples).	B-38
27	Figure B-19. Unsaturated Hydraulic Conductivity Data for H1 and H3 Units (17 Samples). B-39	
28	Figure B-20. Moisture Retention Data for Backfill Unit (10 Samples).....	B-42
29	Figure B-21. Unsaturated Hydraulic Conductivity Data for Backfill Units (10 Samples).	B-43

RPP-ENV-58782, Rev. 0

1	Figure B-22. Experimental (Triangles) and Fitted Theoretical (Squares) Variogram for	
2	Saturated Hydraulic Conductivity ($\text{Ln}K_s$).	B-44
3	Figure B-23. Calculated Macroscopic Anisotropy as a Function of Mean Matric Potential	
4	for the H2 Sand-Dominated Unit.....	B-45
5	Figure B-24. Calculated Macroscopic Anisotropy as a Function of Mean Matric Potential	
6	for the H1 and H3 Gravelly Units.	B-45
7	Figure B-25. Calculated Macroscopic Anisotropy as a Function of Mean Matric Potential	
8	for Backfill Gravelly Unit.....	B-46
9	Figure B-26. (a) K_s , (b) α , and (c) n Random Distribution for a Single Realization.	B-47
10	Figure B-27. Simulated Concentration Distribution for a Single Realization at	
11	(a) 400 days, (b) 700 days, and (c) 1,000 days and (d) the Averaged	
12	Concentration Profile at Those Times for Flow Perpendicular to Bedding for	
13	a Mean Pressure Head (H) of -1 m.	B-48
14	Figure B-28. Simulated Concentration Distribution for a Single Realization at	
15	(a) 400 days, (b) 700 days, and (c) 1,000 days and (d) the Averaged	
16	Concentration Profile at Those Times for Flow Parallel to Bedding for a	
17	Mean Pressure Head (H) of -1 m.....	B-50
18	Figure B-29. Longitudinal Laboratory- and Field-Scale Dispersivities in Unsaturated	
19	Media as a Function of Overall Problem Scale.	B-54
20		
21		

RPP-ENV-58782, Rev. 0

LIST OF TABLES

1		
2		
3	Table B-1. Summary Statistics for Waste Management Area C Moisture Content	
4	(% Volume) Database.....	B-4
5	Table B-2. Mean Moisture and Matric Potentials for Borehole Samples Inside and Outside	
6	of Waste Management Area C.....	B-15
7	Table B-3. van Genuchten Parameters (Based on the Multistep Method) and Saturated	
8	Hydraulic Conductivity Data for 44 Integrated Disposal Facility Borehole	
9	Samples from the H2 Sandy Sequence.....	B-25
10	Table B-4. Wet Sieve Particle Size Distribution for Borehole 299-E27-22 Sediments.	B-27
11	Table B-5. van Genuchten Parameters, Fitted Saturated Hydraulic Conductivity, and	
12	Measured Bulk Density Data for H1/H3 Units (17 Samples).	B-37
13	Table B-6. van Genuchten Parameters, Fitted Saturated Hydraulic Conductivity, and	
14	Measured Bulk Density Data for Backfill Unit (10 Samples).....	B-41
15	Table B-7. Composite van Genuchten-Mualem Parameters for Waste Management Area C	
16	Hydrostratigraphic Units.	B-43
17	Table B-8. Simulated Average Tension Ranges for Polmann Anisotropy Model.....	B-44
18	Table B-9. Variable, Macroscopic Anisotropy Parameter Estimates for Various Waste	
19	Management Area C Units.	B-44
20	Table B-10. Effective Bulk Density (g/cm^3) Estimates for Waste Management Area C	
21	Hydrostratigraphic Units.	B-46
22	Table B-11. Longitudinal Macrodispersivity Estimates (cm).....	B-55

23

24

RPP-ENV-58782, Rev. 0

LIST OF TERMS**Abbreviations and Acronyms**

ACM-I/ACM1	Alternative Geologic Model I
ACM-II/ACM2	Alternative Geologic Model II
EHM	equivalent homogeneous medium
ERDF	Environmental Restoration Disposal Facility
HSU	hydrostratigraphic unit
IDF	Integrated Disposal Facility
MC	Monte Carlo
MPa	megapascal
PA	performance assessment
RCRA	Resource Conservation and Recovery Act of 1976
RETC	REtention Curve
S&L	Sisson and Lu
SST	single-shell tank
WMA	Waste Management Area

RPP-ENV-58782, Rev. 0

APPENDIX B**BASIS FOR DEVELOPMENT OF VADOSE ZONE HYDRAULIC PROPERTIES AT
WASTE MANAGEMENT AREA C**

This appendix provides a description of the basis for the selection of hydraulic properties for hydrostratigraphic units (HSUs) identified at Waste Management Area (WMA) C. No WMA C site-specific data are available that can be used to directly develop estimates of hydraulic properties needed for the performance assessment (PA). As a result, a process has been developed for identifying surrogate hydraulic properties based on samples collected at other sites within the 200 Areas that are considered to be representative of sediments characteristic of the major HSUs identified at WMA C. The selected properties were then used to simulate a WMA C vadose zone flow field and the simulation results were cross-checked against field moisture contents for different WMA C units. This step allowed an updating of the properties by incorporating data sets developed from data collected at other nearby sites within the 200 Areas that are consistent with WMA C field data.

The following information is included in this Appendix:

- WMA C moisture content database, its consistency with nearby field data, and a summary of available data on 241-C Tank Farm (C Farm) soil-water matric potential and their impact on the selection of moisture characteristic data for PA modeling (see Section B.1)
- Evaluation of laboratory measurements for vadose zone soil moisture retention, saturated and unsaturated hydraulic conductivity for samples in the vicinity of C Farm and 200 Areas (see Section B.2 below) as the basis for the selection of hydraulic properties for the major HSUs identified at WMA C (see Section B.2)
- Comparison of observed and simulated moisture content using selected hydraulic properties (see Section B.2.1.1)
- Moisture characteristic curves for major HSUs identified for Alternative Geologic Models I and II (see Section B.2.1.2)
- Effective (upscaled) moisture retention, saturated and unsaturated hydraulic conductivity, bulk density, diffusivity, and macrodispersivity estimates for various strata (see Sections B.3 and B.4).

**B.1 MOISTURE CONTENT MEASUREMENTS AT WASTE MANAGEMENT
AREA C**

As part of WMA C site characterization, an extensive database of moisture content information is available for various HSUs. The moisture content database was developed as part of a direct push campaign conducted at WMA C in 2008, and understood as being long after the occurrence

RPP-ENV-58782, Rev. 0

of past leaks and discharges at the farm. A summary of these measurements for the WMA C area and associated statistics presented in this Appendix is provided in RPP-CALC-60450, “Process for Determining the Volumetric Moisture Content for the Vadose Zone Geologic Units Underlying Waste Management Area.”

The spatial distribution of all moisture measurements collected in and around WMA C is shown in Figure B-1(a); the database includes moisture content data collected both within the footprint of the single-shell tanks (SSTs) (i.e., where the backfill is thickest) [Figure B-1(b)] and outside this area (where the backfill is thin or non-existent) [Figure B-1(c)]. The green line on Figure B-1(b) and (c) reflects the approximate demarcation of areas inside and outside of the SST footprint. In each of the four plots on Figure B-1, the size of the circles depicted at each borehole is indicative of the magnitude of moisture content. The larger-diameter circles (higher moisture content) are more prevalent in the shallower units and outside the farm. Figure B-1(d) is a perspective view looking north-northwest, showing both the vertical direct pushes, dry wells, groundwater well, characterization borehole, and slant direct pushes.

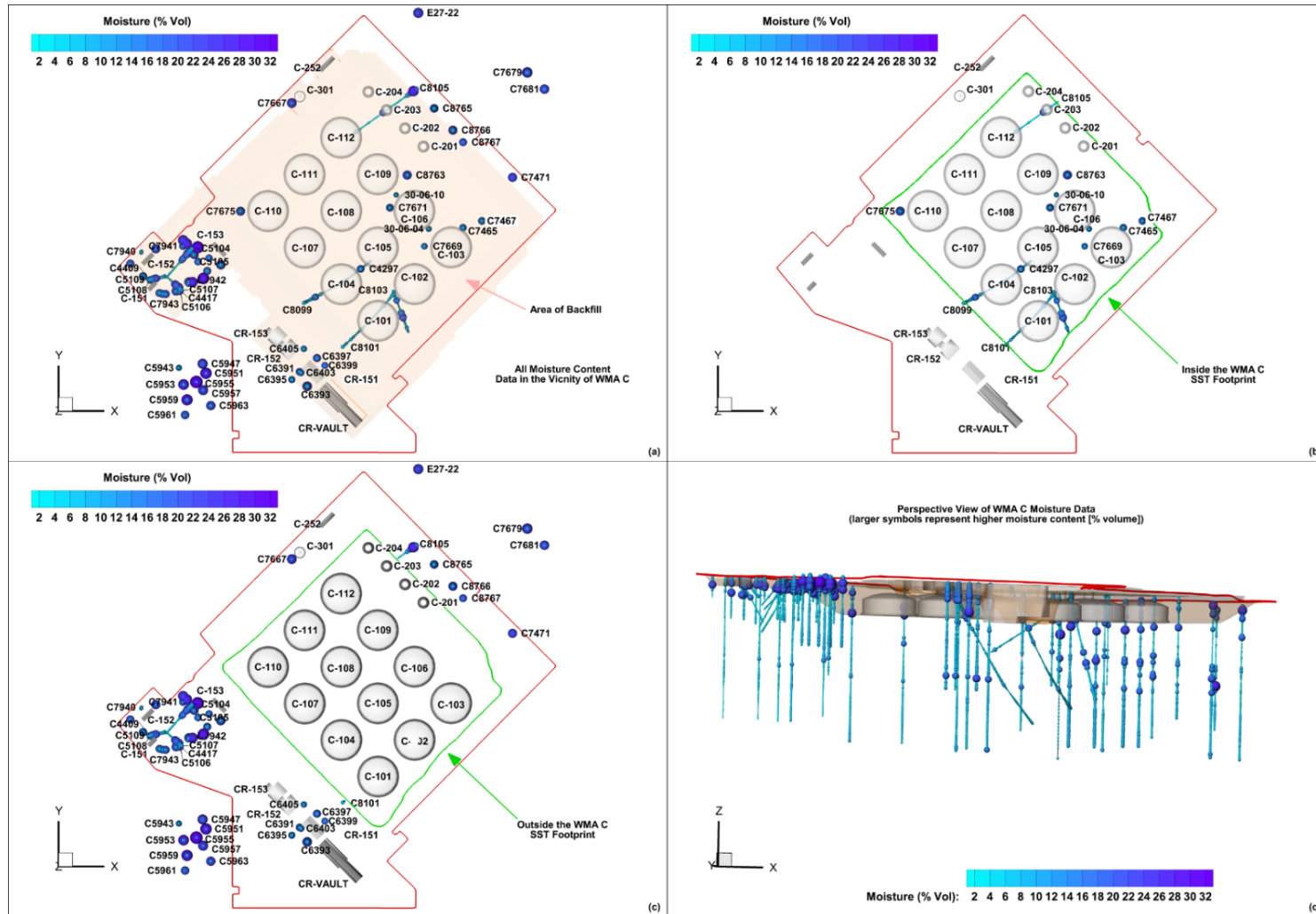
A summary of the statistics of the moisture content measurements by major HSUs is provided in Table B-1. Overall, the moisture content data show considerable variability: the range varies from a low of 0.11 (% volume) for backfill to as high as 30.64 (% volume) for H1 unit (Table B-1).

B.1.1 Moisture Content Measurements for Hanford H2 Sand-Dominated Unit

The Hanford H2 (sand-dominated) unit is the dominant unit at WMA C in terms of vadose zone thickness. The largest number of the moisture content measurements is associated with the Hanford H2 unit (Table B-1).

Figure B-1(a) and (b) show the location of where moisture content measurements were made in the Hanford H2 unit relative to the green line that marks the boundary of where the backfill is thickest (i.e., within the footprint of the SSTs). Figure B-2a shows the histogram for H2 moisture data for all measurements inside and outside of the SST footprint. Figure B-2b shows the histogram for measurements inside the SST footprint, whereas Figure B-2c shows the histogram for measurements outside the SST footprint. While the average for all H2 measurements (inside as well as outside of SST footprint) is ~5.15 (% volume) (Figure B-2a), inside the tank farm, the average is 5.09 (% volume), with the range varying from ~1.86% to 19.9% and a variance of 3.03% (Figure B-2b). Outside the SST footprint, the average is 5.17 (% volume), with the range varying from ~1.06% to 26.32% and a variance of 3.39% (Figure B-2c). The statistics suggest that the averages for moisture content measurements inside and outside the SST footprint are not significantly different. The variance for measurements inside the SST footprint is lower, compared to variance for measurements outside the SST footprint. This may simply be a reflection of a smaller sample size (a count of 5,143 inside of the SST footprint versus a count of 15,733 outside of the SST footprint), or may reflect differences in media heterogeneities within the H2 unit.

Figure B-1. Distribution of Moisture Content Measurements Collected in and around Waste Management Area C
(a) Plan View with All Moisture Content Data, (b) Plan View with All Moisture Content Data Inside the
Single-Shell Tank Footprint, (c) Plan View with All Moisture Content Data Outside the
Single-Shell Tank Footprint and (d) a Side View Looking Northwest.



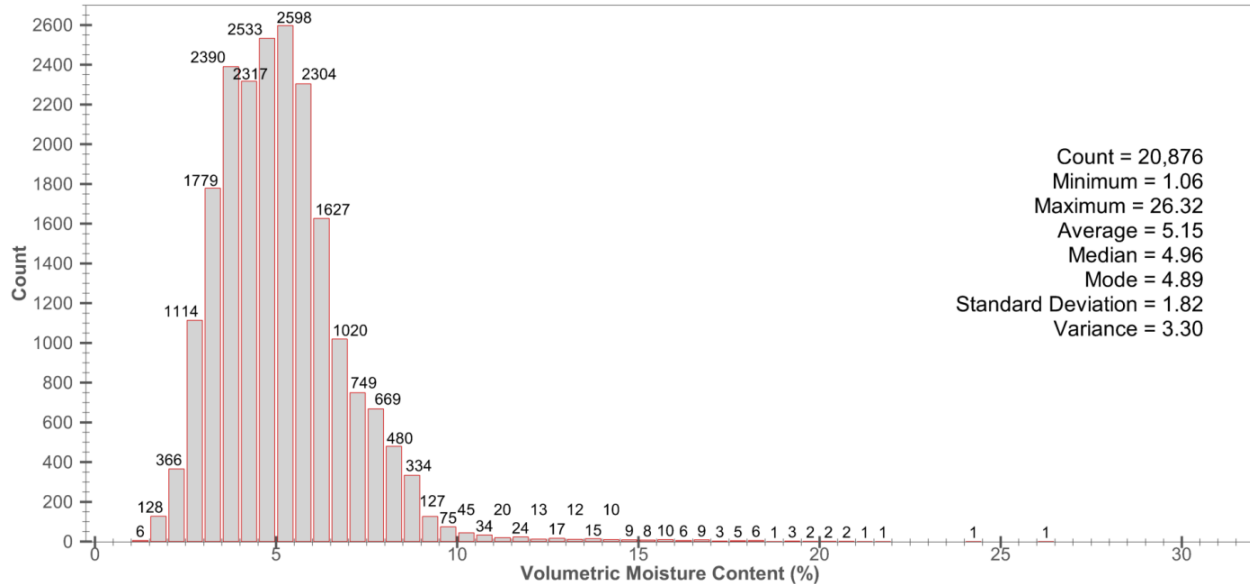
SST = single-shell tank

WMA = waste management area

RPP-ENV-58782, Rev. 0

Table B-1. Summary Statistics for Waste Management Area C Moisture Content (% Volume) Database.

Unit	Count	Minimum	Maximum	Average
Backfill	4,052	0.11	30.61	8.09
H1	7,977	0.13	30.64	5.88
H2	20,876	1.06	26.32	5.15
H3	7	5.54	7.09	6.18
All Units	32,912	0.11	30.64	5.69

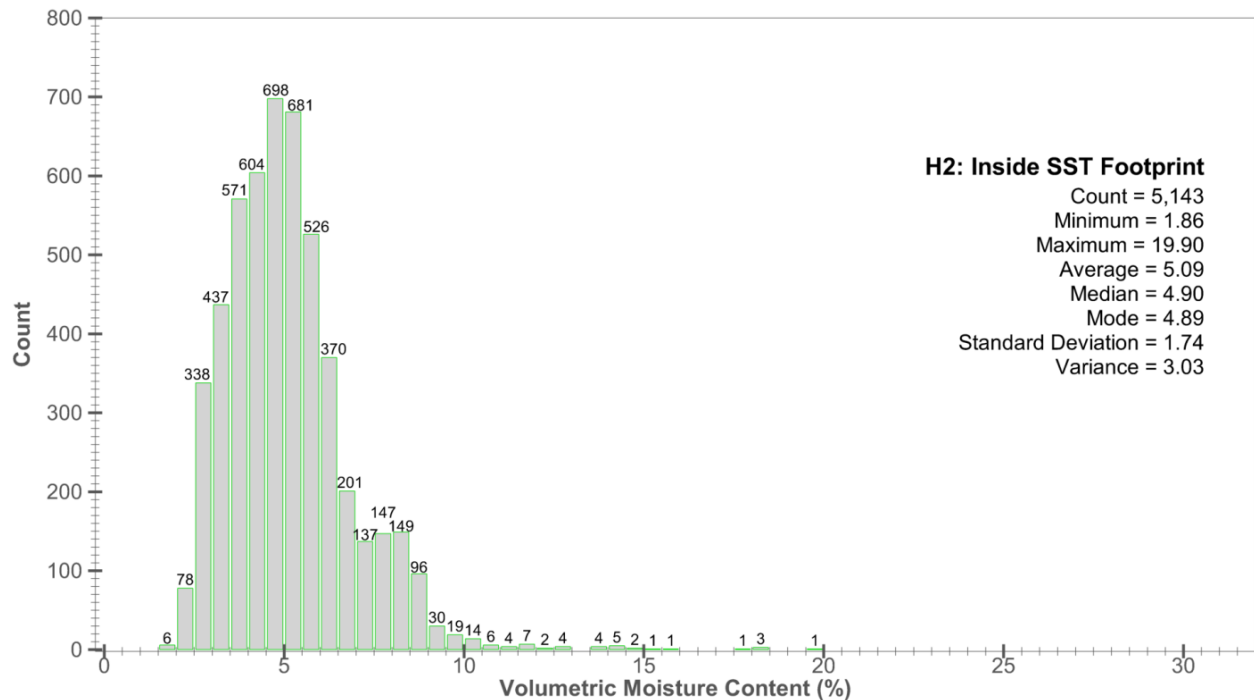
Figure B-2a. Waste Management Area C Moisture Content Histogram for All H2 Data (Includes the Data from Both Inside and Outside of the Single-Shell Tank Footprint).

B.1.1.1 Comparison with Sisson and Lu Site Moisture Content Measurements. In this section of the Appendix, the moisture content measurements for the Hanford H2 unit at WMA C are compared to, and checked for consistency against, another extensive set of moisture content measurements collected at the nearby Sisson and Lu (S&L) field injection site in 200 East Area (Figure B-3). Unlike WMA C, soil hydraulic properties data are available for the S&L site (PNNL-14284, “Laboratory Measurements of the Unsaturated Hydraulic Properties at the Vadose Zone Transport Field Study Site”; “Evaluation of van Genuchten-Mualem relationships to estimate unsaturated hydraulic conductivity at low water contents” [Khaleel et al. 1995]). Furthermore, unlike WMA C, moisture content measurements are available before and after application of anthropogenic recharge at the S&L site. Thus, the S&L site serves as a backdrop for WMA C moisture measurements for Hanford H2 unit. Details of the S&L site, field injections and the spatio-temporal distribution of observed moisture plume are described elsewhere (“Stochastic analysis of moisture plume dynamics of a field injection experiment”

RPP-ENV-58782, Rev. 0

[Ye et al. 2005]; PNNL-13795, “Vadose Zone Transport Field Study: Soil Water Content Distributions by Neutron Moderation”).

Figure B-2b. Waste Management Area C Moisture Content Histogram for H2 Data Within the Single-Shell Tank Footprint.



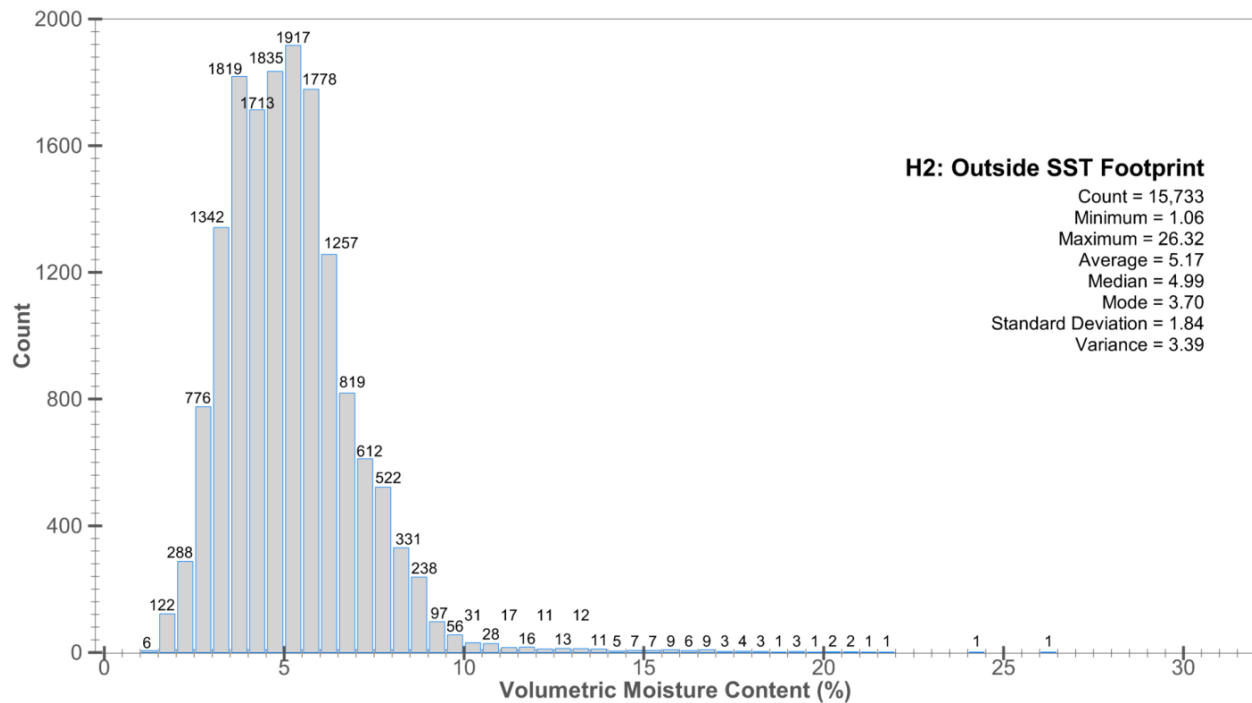
SST = single-shell tank

Figure B-4 shows the composite set of all moisture content measurements collected before and after injection at the S&L site. The S&L site initial moisture content data were collected on May 5, 2000 [Figure B-4 (a)] and post-injection and post-redistribution data were collected about two months later [Figure B-4(b)]. These measurements are all within an HSU that would correlate with the Hanford H2 sand unit identified at WMA C. The S&L moisture content profiles are in general agreement with the known stratigraphic cross-section (Ye et al. 2005), with larger moisture content values being associated with the fine-textured sediments and smaller values being associated with the coarse-textured sediments. In addition to the 2000 S&L field experiment, data also exist on the 1980 field experiment conducted at the same site (RHO-ST-46P, “Field Calibration of Computer Models for Application to Buried Liquid Discharges: A Status Report”). Although not shown here, the 1980 moisture content measurements are nearly identical to the 2000 moisture content measurements. The consistency in the moisture content profiles over the 20-year time interval suggests that, in the absence of anthropogenic recharge, the moisture content distribution is under a state of natural equilibrium with meteoric recharge. The S&L moisture content profiles (Figure B-4) clearly illustrate the impact of media heterogeneities and natural capillary breaks (“Simulating field-scale moisture flow using a combined power-averaging and tensorial connectivity-tortuosity approach” [Zhang and Khaleel 2010]; Ye et al. 2005). During and following field injections, the capillary breaks created due to textural discontinuities allow flow to occur laterally until the pressure head in the fine layer is sufficient to overcome the entry pressure head of the underlying coarse layer.

RPP-ENV-58782, Rev. 0

Nonetheless, as indicated in Figure B-4, the pre- and post-injection moisture plumes are essentially confined within three layers (i.e., two fine-textured layers and a coarse-textured layer that is sandwiched in between the two fine-textured layers).

Figure B-2c. Waste Management Area C Moisture Content Histogram for H2 Data Outside of the Single-Shell Tank Footprint.

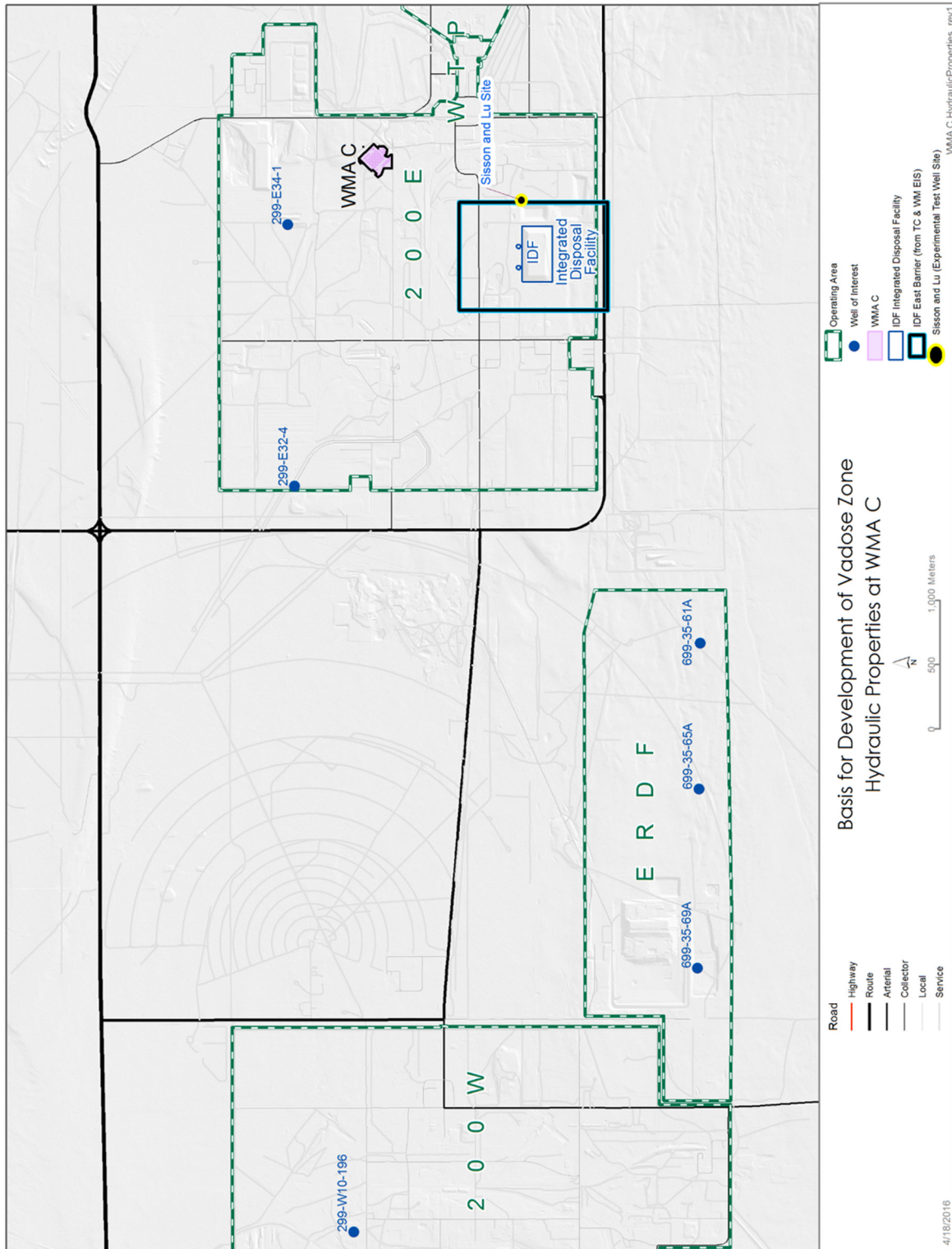


SST = single-shell tank

At WMA C, the volumetric moisture content for the Hanford H2 unit inside the tank farm (see Figure B-2c) ranges from 1.86 to 19.90 with a mean of 5.09 (% volume), whereas at the S&L site the volumetric moisture content ranges from 4.60 to 24.50 with a mean of 8.92 (% volume) (Ye at al. 2005). Even though the natural recharge at the two sites are not identical and the sediment textural data are different, the WMA C H2 unit moisture contents compare well and show similar trends relative to variability with field-measured H2 moisture contents at the nearby S&L site (i.e., higher moisture contents for fine-textured units and lower moisture contents for coarse-textured units as illustrated in Figure B-4). However, the S&L mean moisture content is much higher than the WMA C (inside the tank farm) mean value. This is consistent with the ubiquitous occurrence of fine-textured units at the S&L site (Ye at al. 2005), and the apparent non-occurrence of such units at WMA C. These data show that the field measurements at both WMA C and S&L sites are significantly impacted by small-scale heterogeneities. However, if the moisture content data is used as a surrogate for characterizing media heterogeneities, the higher mean (~8.92 [% volume]) moisture values at the S&L site suggest that the Hanford H2 unit is much coarser at WMA C than at the nearby S&L site. Therefore, while the comparison with the S&L site generally corroborates the understanding of the WMA C H2 unit, the S&L site is not a useful surrogate for development of hydraulic properties for the Hanford H2 sand unit at WMA C. Furthermore, the comparison demonstrates that substantial variability can occur in the H2 unit over fairly short spatial distances.

RPP-ENV-58782, Rev. 0

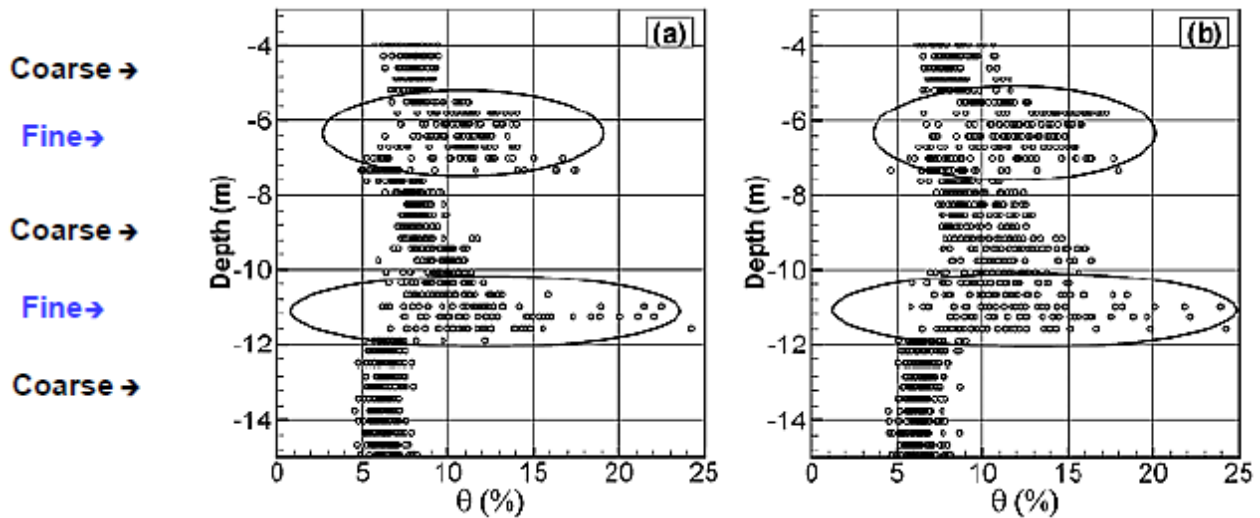
Figure B-3. Location of Sisson and Lu Site, Integrated Disposal Facility and Selected Boreholes in 200 Area.



ERDF = Environmental Restoration Disposal Facility WMA = Waste Management Area
 TC & WM EIS = Tank Closure and Waste Management Environmental Impact Statement
 WTP = Waste Treatment Plant

RPP-ENV-58782, Rev. 0

Figure B-4. (a) Pre- and (b) Post-Injection Moisture Plumes for the Field Injection Experiment in the 200 East Area.



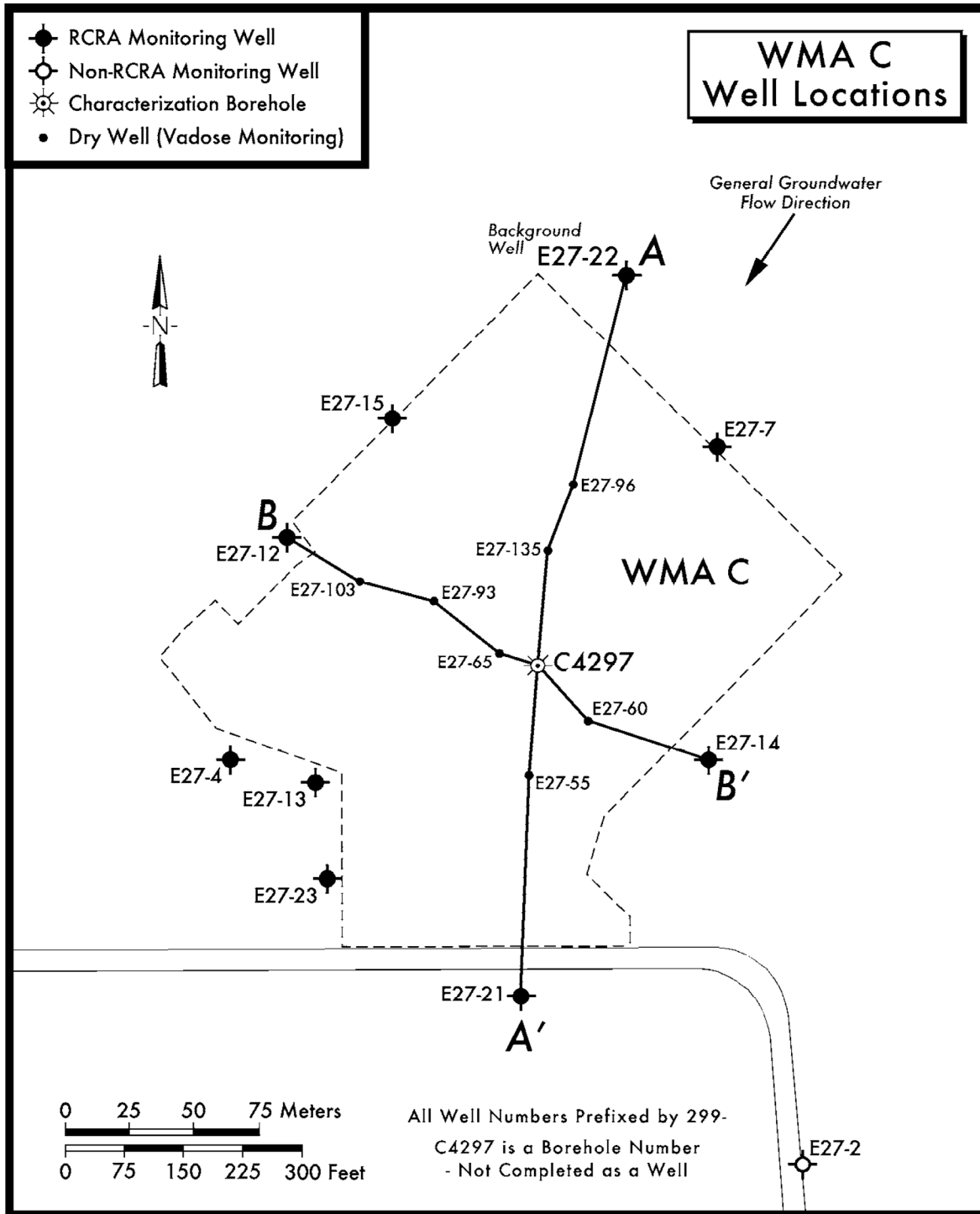
Profiles of volumetric moisture content (%) measured on (a) May 5, 2000, and (b) July 31, 2000. The figures illustrate the fact that, in the absence of anthropogenic recharge, moisture contents at the field site are in equilibrium with natural recharge at the site.

Reference: "Stochastic analysis of moisture plume dynamics of a field injection experiment" (Ye et al. 2005).

B.1.1.2 Soil-Moisture and Matric Potential Data for Borehole Samples Inside and Outside the Tank Farm. In addition to the moisture content measurements developed from neutron logging of direct push boreholes presented in Section B.1, additional moisture content data as well as matric potential information are available for two individual boreholes. Boreholes C4297 (inside the tank farm near tank C-105) and 299-E27-22 (Resource Conservation and Recovery Act of 1976 [RCRA] borehole just outside the tank farm) (Figure B-5) provide moisture content (gravimetric) measurements as well as matric potential (using filter paper) data (PNNL-15503, "Characterization of Vadose Zone Sediments Below the C Tank Farm: Borehole C4297 and RCRA Borehole 299-E27-22"). The two sets of data on moisture content and matric potential were collected to evaluate differences between one being outside the farm (a lower expected average moisture content and a more negative matric potential) and the other inside the farm (a higher expected average moisture content and a less negative matric potential indicative of a draining soil profile). However, as stated earlier (Section B.1.1), the averages for moisture content measurements inside and outside the SST footprint were not significantly different.

The moisture content profiles for the two boreholes are shown in Figures B-6a and B-6b, respectively. Zones with relatively high moisture are illustrated via a light blue bar immediately to the right of the lithologic log in these diagrams. The moisture content and lithological data are generally consistent; the elevated levels of moisture in the vadose zone at C Farm are associated with fine-grained lenses of fine sand and/or silt. Most of these occur within the Hanford formation H2 unit, although there is also one at the base of the backfill in borehole C4297, and within the H1 unit in RCRA borehole 299-E27-22, which is consistent with the concentration of moisture at an abrupt, large contrast in grain size. This is illustrated at the 82-ft depth in RCRA borehole 299-E27-22 (Figure B-6b), where there is a sharp contact between gravelly sand overlying fine to coarse sand (PNNL-15503).

RPP-ENV-58782, Rev. 0

Figure B-5. Borehole Location Map for Waste Management Area C.

2005/DCL/C/003 (08/30)

RCRA = Resource Conservation and Recovery Act of 1976

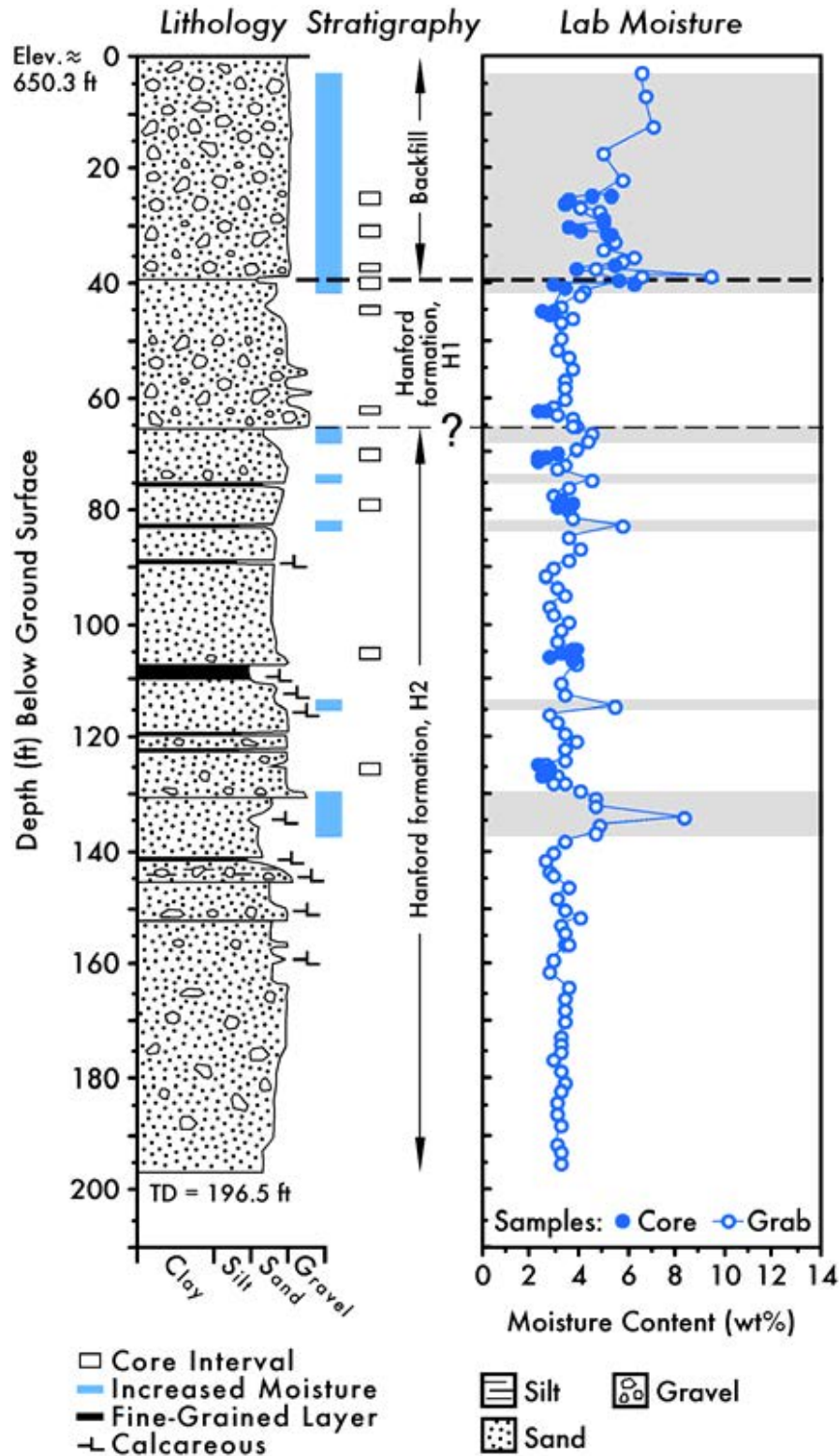
WMA = Waste Management Area

Source: PNNL-15503, "Characterization of Vadose Zone Sediments Below the C Tank Farm: Borehole C4297 and RCRA Borehole 299-E27-22."

Note: Cross-sections AA' and BB' are Figures 2.4 and 2.5, respectively, in PNNL-15503.

RPP-ENV-58782, Rev. 0

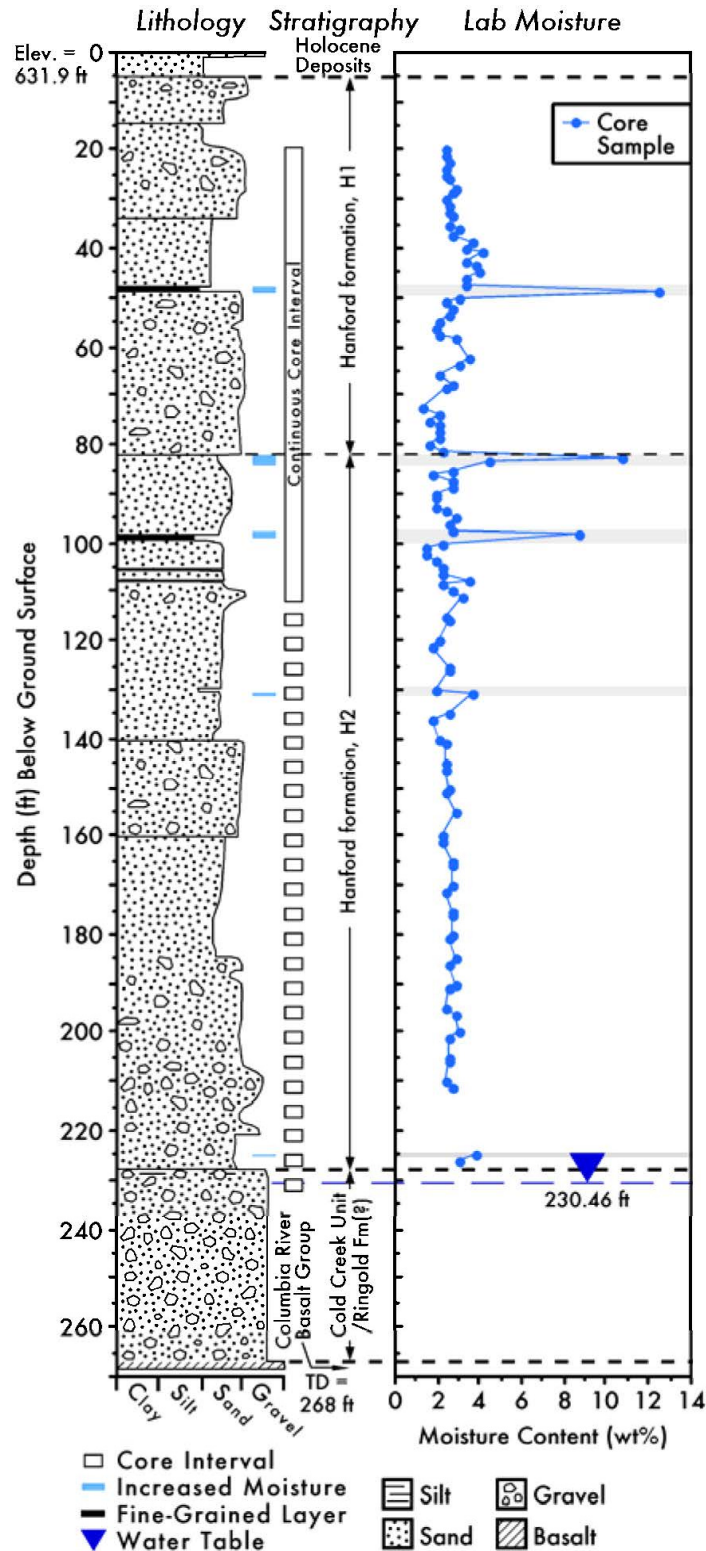
1 **Figure B-6a. Borehole C4297 Lithology and Gravimetric Moisture Content Measurements**
 2 **(the shaded areas in light blue and gray are regions of increased moisture).**
 3



Reference: PNNL-15503, "Characterization of Vadose Zone Sediments Below the C Tank
 Farm: Borehole C4297 and RCRA Borehole 299-E27-22."

RPP-ENV-58782, Rev. 0

Figure B-6b. Borehole 299-E27-22 Lithology and Gravimetric Moisture Content Measurements (the shaded areas in light blue and gray are regions of increased moisture).



Reference: PNNL-15503, "Characterization of Vadose Zone Sediments Below the C Tank Farm: Borehole C4297 and RCRA Borehole 299-E27-22."

RPP-ENV-58782, Rev. 0

The distribution of moisture in the vadose zone at these two borehole locations was developed by gravimetric moisture measured directly from core samples in the laboratory (Figures B-6a and B-6b). Moisture data based on grab sampling is only available for one of the two boreholes (C4297), and these data generally corroborate the laboratory-measured moisture content measurements (Figure B-6a). However, several pronounced spikes that appear on the laboratory-moisture plot do not appear in the moisture log. This is likely the result of a number of thin (a few inches or less) fine-grained layers that were preferentially sampled during core processing. These thin layers are not visible on the geophysical log because the neutron flux is averaged over a larger area beyond the limits of the fine-grained layer, including adjacent relatively dry layers. Thus, the resulting field logging signal is dampened. In general, the neutron-moisture log appears to accurately reflect the relative bulk moisture content, and can confidently be used as a substitute to estimate bulk moisture conditions when core samples are unavailable. However, most thin (<6 in.) moist zones go undetected on neutron-moisture logs (PNNL-15503).

While the moisture content profiles provide useful information, the moisture profiles, by themselves, cannot be used to describe the soil-water energy status and the vadose zone flow dynamics. Data on soil-moisture matric potentials are needed to establish the energy level and the subsequent flow status. A simple measure of direction of flow can be approximated by plotting field-measured matric potentials versus the height above the water table. The hydraulic potential at any given elevation is given by the sum of matric potential and gravitational potential and the flux is calculated from the Darcy-Buckingham law (Soil Physics [Jury and Horton 2004]).

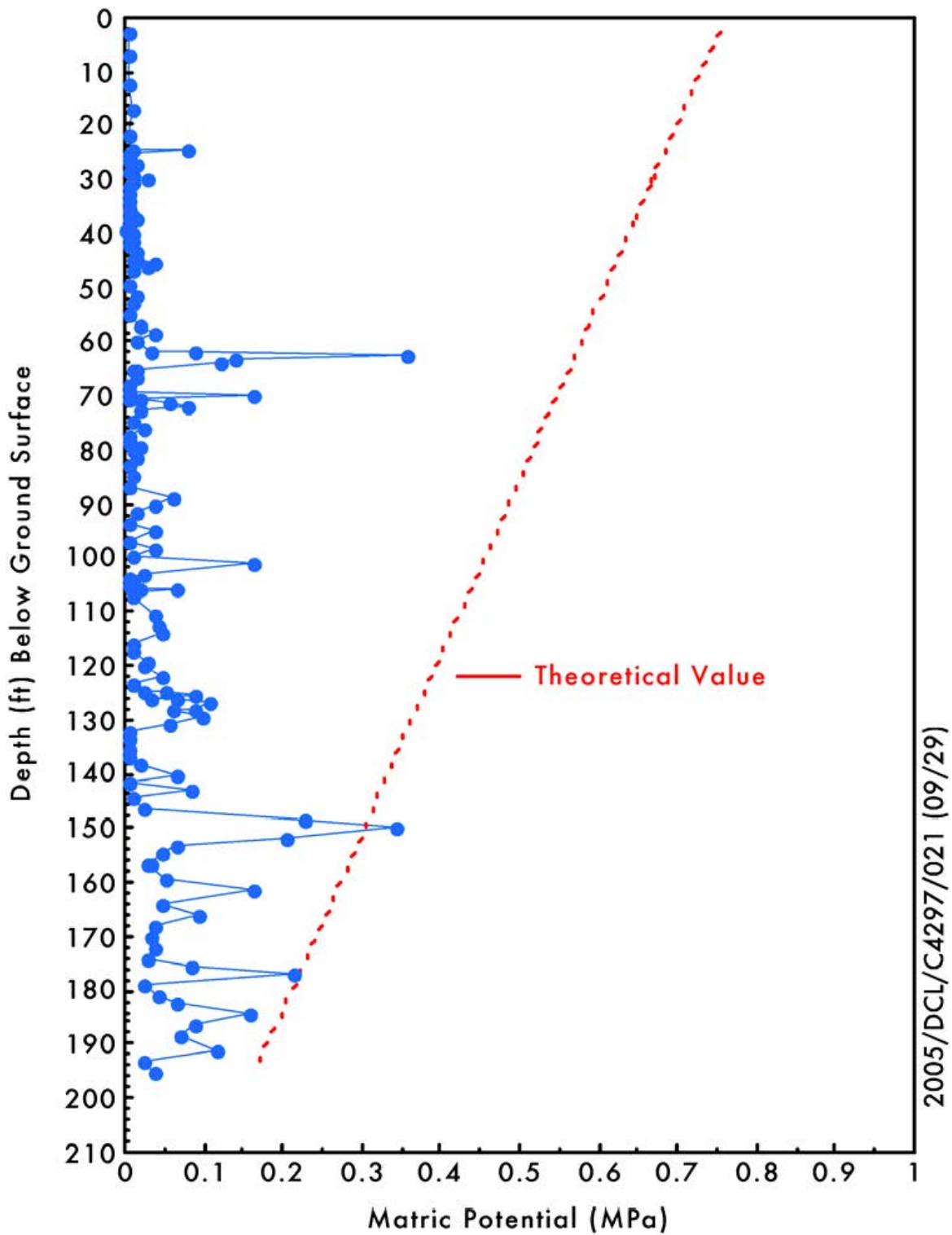
Figures B-7a and B-7b illustrate the respective filter paper-based matric potential measurements, as a function of depth for sediment samples from the two boreholes: C4297 (inside the farm) and 299-E27-22 (outside the farm), with the potentials (MPa) shown as absolute values (PNNL-15503). With the filter paper technique, the moisture in a filter material reaches equilibrium with the surrounding environment. In both figures, the red line, labeled “theoretical value” is the theoretical line that represents the steady-state equilibrium condition. Matric potential values to the left of the theoretical line suggest a draining profile. The general trend for the data is that the measured potentials for both boreholes are consistent with those of a draining profile.

For borehole 299-E27-22 (Figure B-7b), matric potentials for three of the samples (27.0, 72.0, and 74.5 ft below ground surface) suggest very dry conditions; these appear to be erroneous because of inadvertent drying of the samples or weighing errors (PNNL-15503). The matric suction values are generally below 0.5 MPa (~5,000 cm) for the sediment profile in borehole 299-E27-22 as well as borehole C4297.

Filter paper-based soil matric potentials are point measurements, and are not consistent with the use of averaged upscaled (effective) properties (Section 6) for the large blocks used in the PA simulations. In addition, the error bar for filter paper measurements is rather large (0.1 to 0.2 MPa). Soil moisture measurements are typically more accurate than matric potential measurements, and the matric potential variability is typically larger than the soil moisture variability (PNNL-15503). Overall, however, the WMA C moisture and tension data appear to be internally consistent and represent a relatively dry moisture regime.

RPP-ENV-58782, Rev. 0

**Figure B-7a. Matric Potentials Measured by Filter Paper Technique
on Core Samples from Borehole C4297.
Matric potentials are presented as absolute values.**

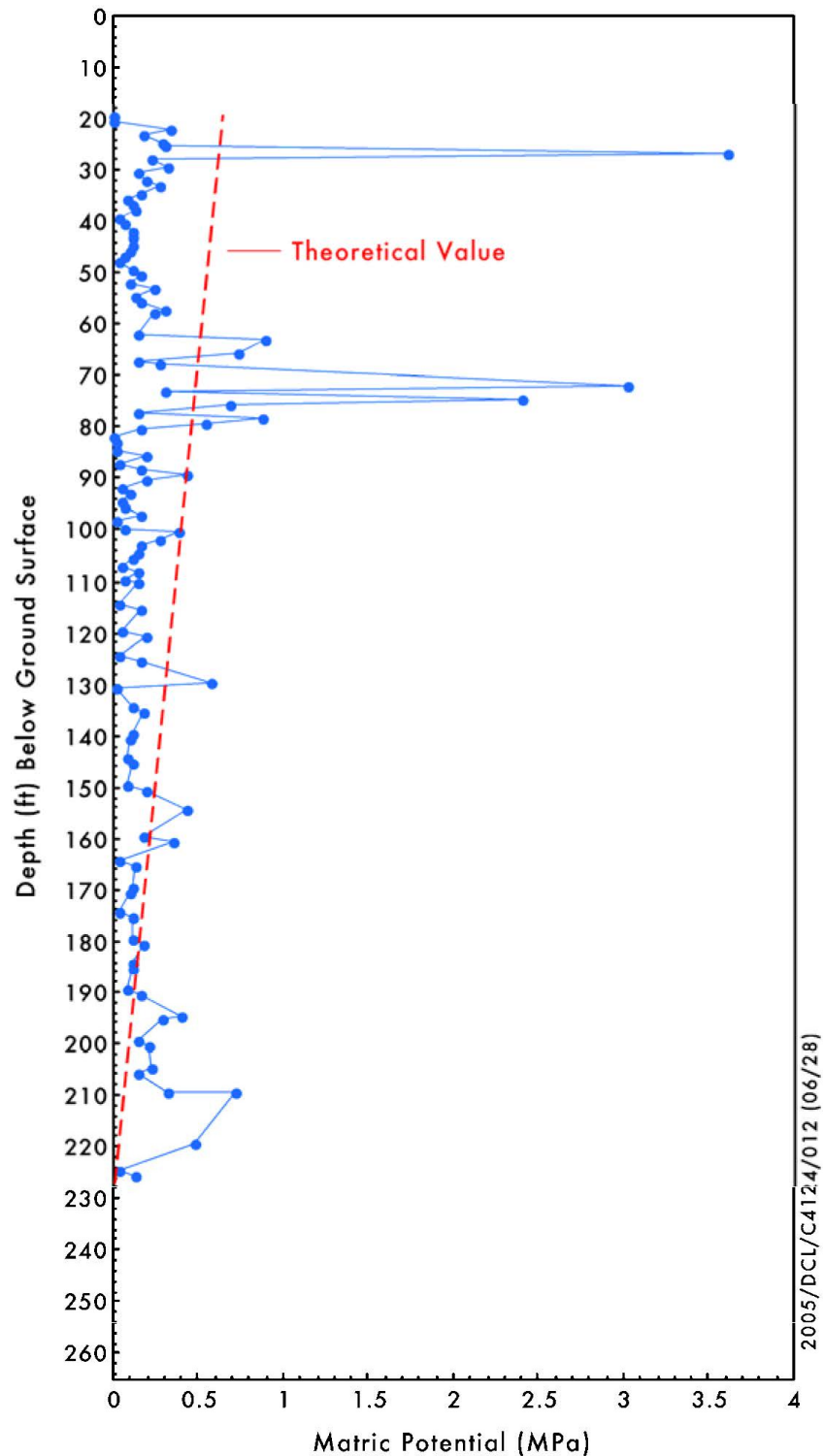


Reference: PNNL-15503, "Characterization of Vadose Zone Sediments Below the C Tank Farm: Borehole C4297 and RCRA Borehole 299-E27-22."

RPP-ENV-58782, Rev. 0

Figure B-7b. Matric Potentials Measured by Filter Paper Technique on Core Samples from Borehole 299-E27-22.

Matric potentials are presented as absolute values.



Reference: PNNL-15503, "Characterization of Vadose Zone Sediments Below the C Tank Farm: Borehole C4297 and RCRA Borehole 299-E27-22."

RPP-ENV-58782, Rev. 0

Table B-2 summarizes the mean moisture content and mean filter paper-based matric potential measurements for the two borehole samples. The data show a drier moisture content for measurements outside the farm compared to those inside the farm. A comparison of the moisture and matric potential profiles for the two boreholes is shown in Figures B-8a and B-8b, respectively.

Table B-2. Mean Moisture and Matric Potentials for Borehole Samples Inside and Outside of Waste Management Area C.

Borehole	C4297 (inside tank farm)	299-E27-22 (outside tank farm)
Mean moisture content (% volume)*	6.00	4.60
Mean matric potential (-cm)	498.45	1,616.43

*Gravimetric data were converted to volumetric moisture content using an assumed sediment bulk density of 1.7 g cm⁻³.

Reference: PNNL-15503, "Characterization of Vadose Zone Sediments Below the C Tank Farm: Borehole C4297 and RCRA Borehole 299-E27-22."

As stated earlier, matric potential measurements for both boreholes suggest a draining soil profile (PNNL-15503). Intuitively, it might be postulated that the higher mean observed moisture and a less negative mean matric potential inside the farm is due to the combined effects of both natural recharge and the operational use of water during the period of past tank farm operations. However, whereas the mean moisture contents for the two borehole samples suggest a slightly higher moisture content from measurements inside the tank farm, the much more negative mean matric potential for outside borehole samples (Table B-2) could simply be a reflection of differences in moisture retention characteristics for the two datasets, albeit being of similar lithology. A comparison of the field-measured and simulated moisture contents for the sand-dominated H2 unit is provided in Section B.2.1.1.

B.1.2 Moisture Content Measurements for Hanford H1, Hanford H3 and Backfill Gravelly Units

The statistics of moisture content measurement for Hanford H1 and H3 gravelly units and backfill gravelly unit are summarized in Table B-1. As indicated in Table B-1, unlike moisture content measurements made in the H1 gravelly unit, the sample size of moisture content measurements made in the H3 gravelly unit is too small to generate any meaningful statistics.

B.1.2.1 Hanford H1 Gravelly Unit. Figure B-9a shows the histogram for all moisture content measurements made in the H1 gravelly unit inside and outside the tank farm (Figure B-2c). Figure B-9b shows the histogram for measurements inside the SST footprint, whereas Figure B-9c shows the histogram for measurements outside the SST footprint. While the average for all H1 measurements is about 5.88% on a volume basis (Figure B-9a), inside the tank farm the average is 4.24 (% volume), with the range varying from ~1.47% to 23.11% and a variance of 3.76% (Figure B-9b). Outside of the SST footprint the average is 6.41 (% volume), with the range varying from ~0.13% to 30.64% and a large variance of 15.42% (Figure B-9c). Once again, similar to H2 data and contrary to expectation, the statistics suggest a considerably higher H1 average moisture content for measurements outside the SST footprint, compared with

RPP-ENV-58782, Rev. 0

the average for measurements inside the SST footprint. The variance for H1 measurements outside the SST footprint is higher, compared to variance for measurements inside the SST footprint. This might simply be a reflection of a smaller sample size (a count of 1,921 inside versus a count of 6,056 outside), and/or media heterogeneities that are prevalent within the H1 unit.

It is questionable as to whether the observed high moisture contents (e.g., 30.64 [% volume] for the gravel-dominated H1 unit) are reflective of the natural moisture regime. As discussed earlier, other moisture data in the nearby S&L test site suggest that, in the absence of anthropogenic recharge, the moisture profiles are typically in equilibrium with meteoric recharge. Furthermore, in the absence of anthropogenic recharge, moisture contents correlate with sediment texture (i.e., coarse-textured sediments have a lower moisture content and fine-textured sediments have a higher moisture content) (Figure B-4). Nonetheless, none of the S&L moisture content measurements for the fine-textured horizons approach as high as 30.64% (% volume); such an unusually high value for the gravel-dominated H1 unit is considered an outlier.

B.1.2.2 Backfill Gravelly Unit. In general, tank farm backfill materials consist of unstructured, poorly-sorted mixtures of gravel, sand, and silt removed during tank excavation, and then later used as fill around the tanks. Backfill materials extend to depths of ~50 ft (~15.24 m) within the tank farms. Most or all of the recent deposits of eolian sand and silt material found elsewhere across the Hanford Site have been removed and replaced with backfill in the immediate vicinity of the tank farms.

For the backfill unit, the average moisture content is 8.08 (% volume) (Table B-1), and is the highest among averages for all the units. The backfill unit also has the lowest measured moisture content of 0.11 (% volume) among all units. The maximum measured moisture content for backfill is 30.61 (% volume).

Figure B-10a shows the histogram for all moisture content measurements made in the backfill gravelly unit inside and outside the tank farm (Figure B-2c). Figure B-10b shows the histogram for measurements inside the SST footprint, whereas Figure B-10c shows the histogram for measurements outside the SST footprint. While the average for all backfill measurements is ~8.09% (% volume) (Figure B-10a), inside the tank farm, the average is 6.61 (% volume), with the range varying from ~0.31% to 23.05% and a variance of 7.69% (Figure B-10b). Outside of the SST footprint, the average is considerably higher (9.30 [% volume]), with the range varying from ~0.11% to 30.61% and a large variance of 15.47% (Figure B-10c).

B.2 LABORATORY-SCALE MEASUREMENTS FOR HYDRAULIC PROPERTIES

The purpose of this section is to summarize data sources and laboratory measurements of core-scale sample properties for different HSUs; these are later upscaled for use in WMA C PA modeling (Section B.3 below). Core-scale measurements and their parameterization are described below for the following HSUs:

- Hanford H2 Sand Unit

RPP-ENV-58782, Rev. 0

- Hanford H1 and H3 Gravelly Units
- Backfill Gravelly Unit.

B.2.1 Properties of the Hanford H2 Sand Unit

Figure B-11 shows a representative sample of sediments associated with the Hanford H2 sand-dominated unit identified at WMA C. Because site-specific hydraulic properties data are unavailable, the available hydraulic properties database for coarse sands as well as the WMA C moisture content distribution were used to identify and characterize hydraulic properties for the Hanford H2 sand unit identified at WMA C. Soils used to characterize the WMA C Hanford H2 unit properties were similar to those shown in Figure B-11. Using moisture as a proxy, the nearby 200 East Area Integrated Disposal Facility (IDF) site (Figure B-3) coarse sand unit correlates well with the Hanford H2 sand unit identified at WMA C; the IDF coarse sands were thus used as surrogate for the WMA C H2 sands. The primary mission of RCRA-permitted IDF (Figure B-3) is disposal of low-level wastes, mixed low-level wastes, and Immobilized Low-Activity Waste (i.e., the Hanford tank waste that has undergone separations treatment to remove the bulk of the radionuclides and then solidified at the Hanford Waste Treatment and Immobilization Plant).

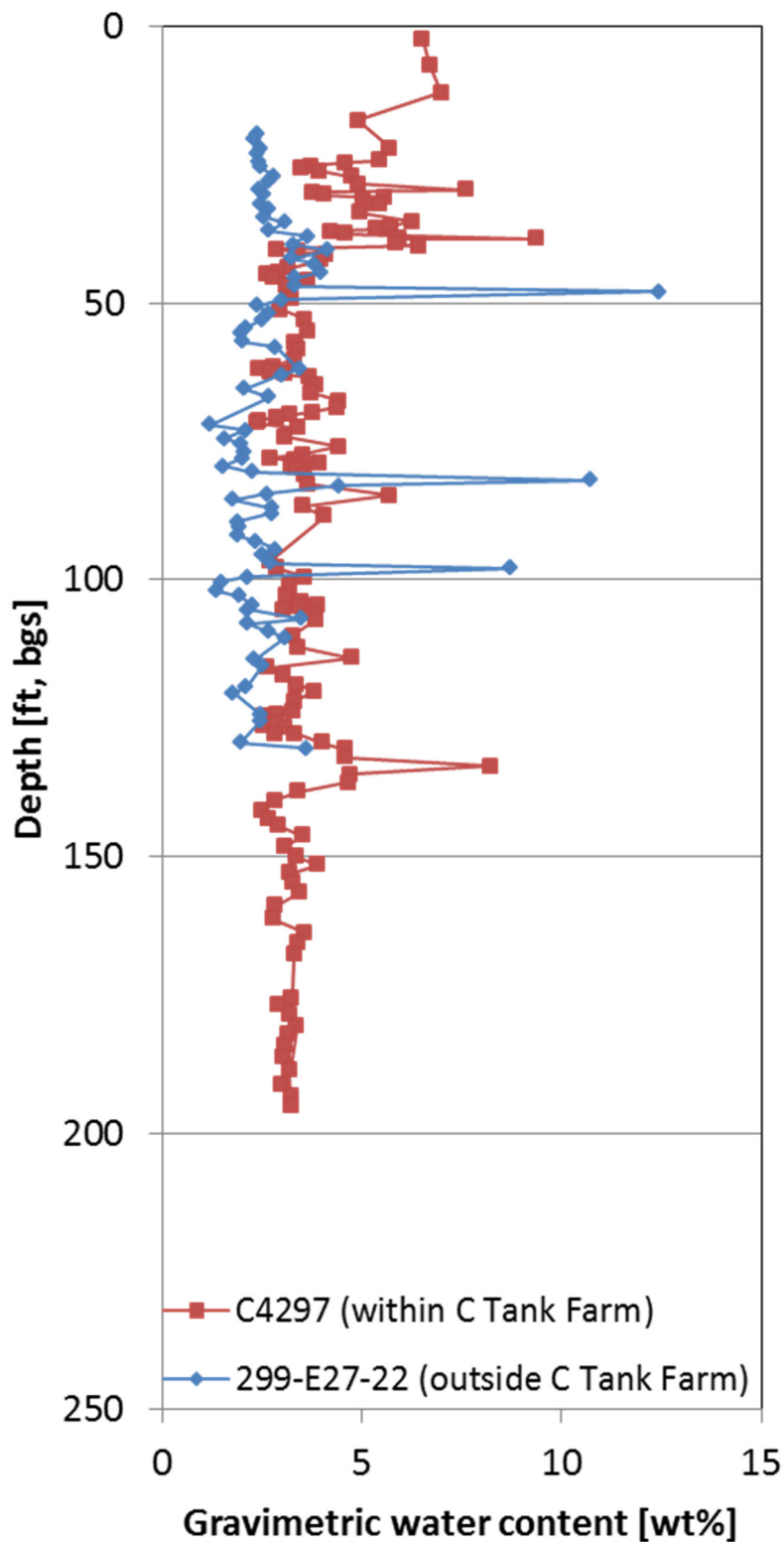
As part of site characterization for IDF, sediment samples were obtained in fiscal years 1998, 2001 and 2002 via a borehole drilling and sampling program. The Hanford formation sandy H2 sequence identified at the IDF site is ~200 ft (~61 m) thick and, like WMA C, is the dominant facies at the site.

The laboratory procedures used to analyze the IDF H2 borehole samples and analysis of samples from the three boreholes are described in appendices found in RPP-20621, “Far-Field Hydrology Data Package for the Integrated Disposal Facility Performance Assessment.” Briefly, the multistep and steady-state methods were used to obtain moisture retention and unsaturated conductivity data. The specific details for the two methods are described in RPP-20621 appendices. Both methods were performed on the same core using the same sensor locations. In addition to cumulative outflow, the multistep method provides water content-matric potential (θ - ψ) pairs. These data were used in conjunction with a numerical inversion procedure (“Optimization of Hydraulic Functions from Transient Outflow and Soil Water Pressure Data” [Eching and Hopmans 1993]) to determine the optimal set of van Genuchten model (“A Closed-form Equation for Predicting the Hydraulic Conductivity of Unsaturated Soils” [van Genuchten 1980]) parameters (RPP-20621). The steady-state method, described in “Hydraulic Conductivity and Diffusivity: Laboratory Methods” (Klute and Dirksen 1986), provides water content-matric potential-unsaturated conductivity (θ - ψ - K) triplets; the method was primarily used as a check on the multistep method.

RPP-20621 (Tables 1 through 3) provides the van Genuchten model parameters determined using the numerical inversion procedure and data from the multistep test. The pore-size distribution parameter ℓ (“A New Model for Predicting the Hydraulic Conductivity of Unsaturated Porous Media” [Mualem 1976]) was kept fixed at 0.5. The fitted van Genuchten-Mualem parameters for the IDF H2 sandy sequence (44 samples) are reproduced in Table B-1.

RPP-ENV-58782, Rev. 0

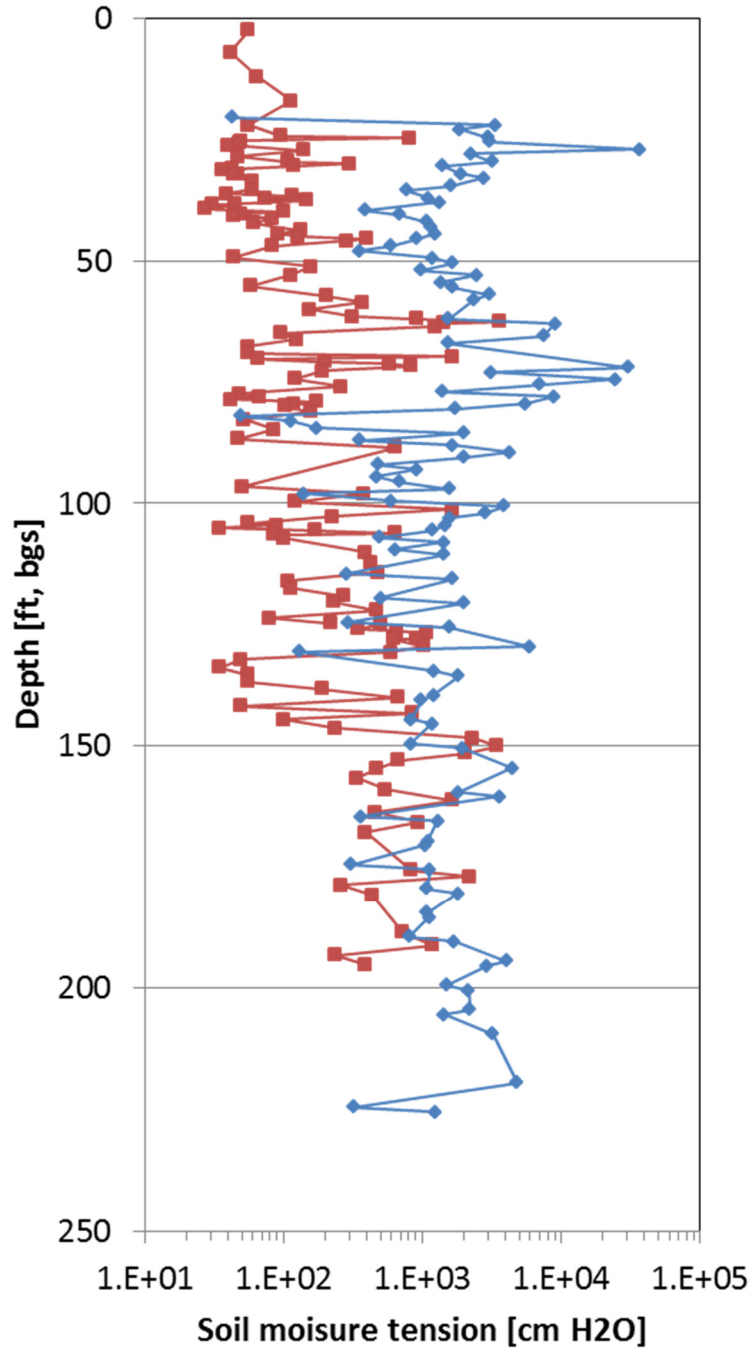
Figure B-8a. Comparison of Gravimetric Moisture Content Measurements for Boreholes C4297 and 299-E27-22.



Reference: PNNL-15503, "Characterization of Vadose Zone Sediments Below the C Tank Farm: Borehole C4297 and RCRA Borehole 299-E27-22."

RPP-ENV-58782, Rev. 0

Figure B-8b. Comparison of Soil Moisture Tension Measurements for Boreholes C4297 and 299-E27-22.



—■— C4297 (within C Tank Farm)

—◆— 299-E27-22 (outside C Tank Farm)

Reference: PNNL-15503, "Characterization of Vadose Zone Sediments
Below the C Tank Farm: Borehole C4297 and RCRA Borehole 299-E27-22."

RPP-ENV-58782, Rev. 0

Figure B-9a. Waste Management Area C Moisture Content Histogram for All H1 Data (Includes the Data from Both Inside and Outside of the Single-Shell Tank Footprint).

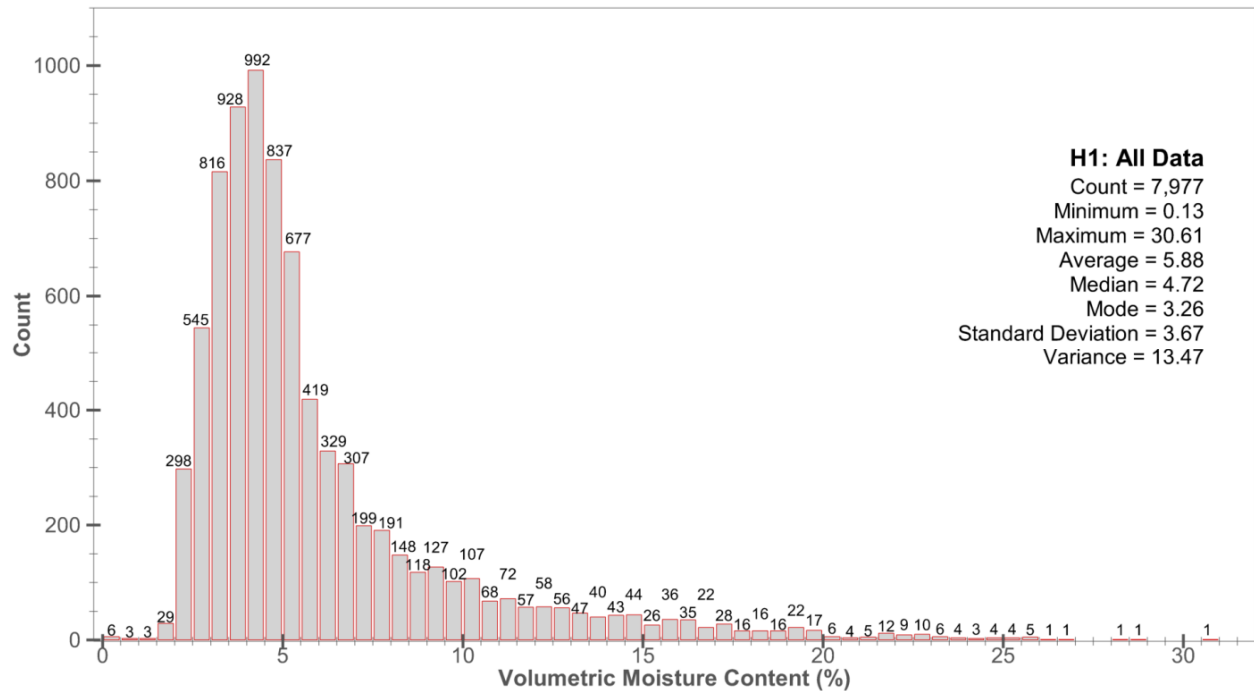
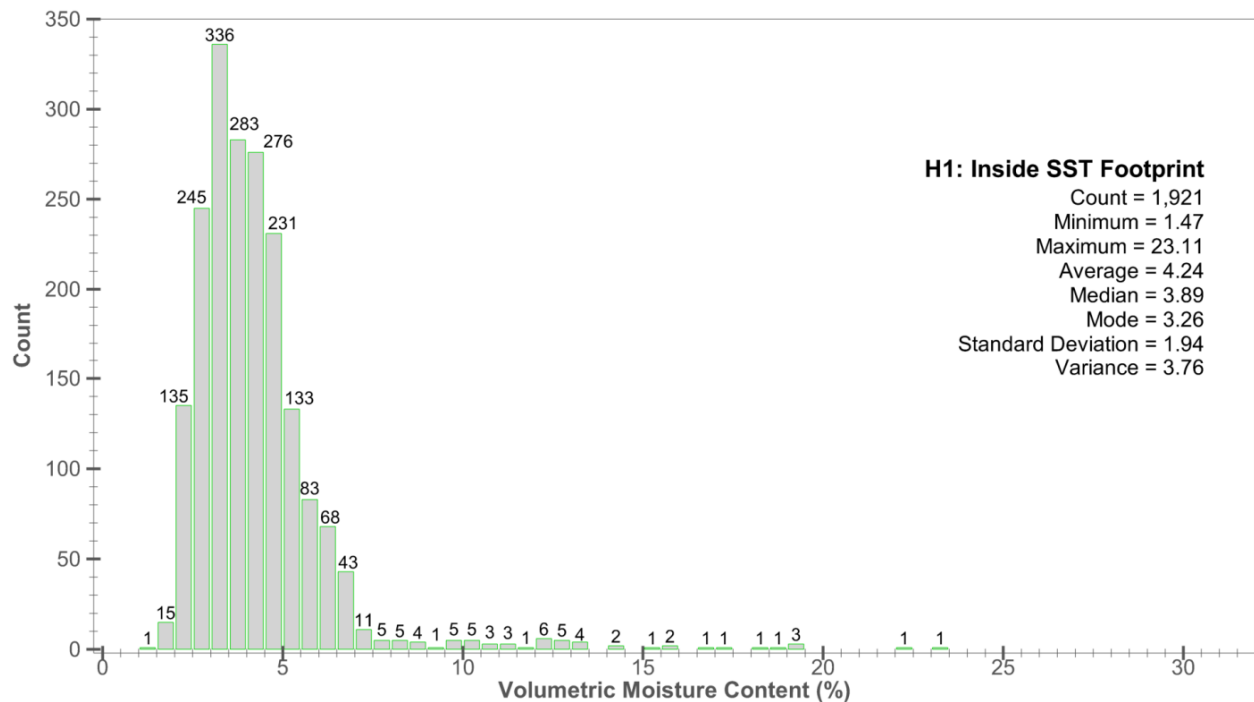


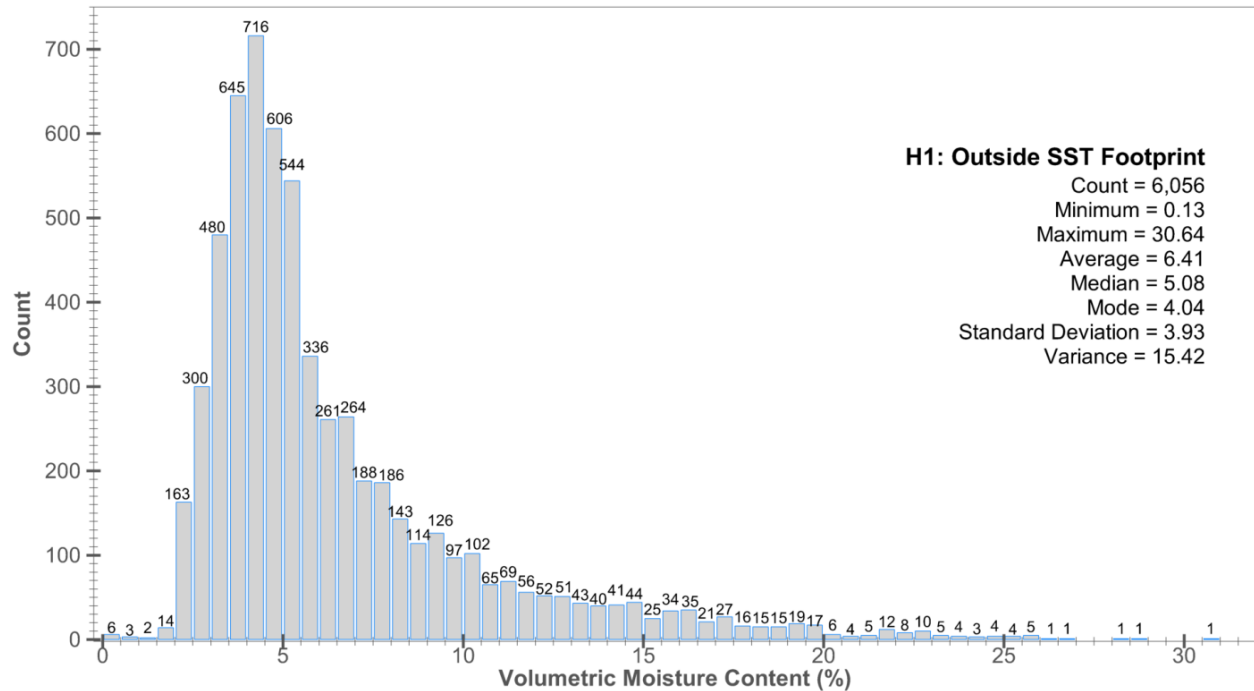
Figure B-9b. Waste Management Area C Moisture Content Histogram for H1 Data Within the Single-Shell Tank Footprint.



SST = single-shell tank

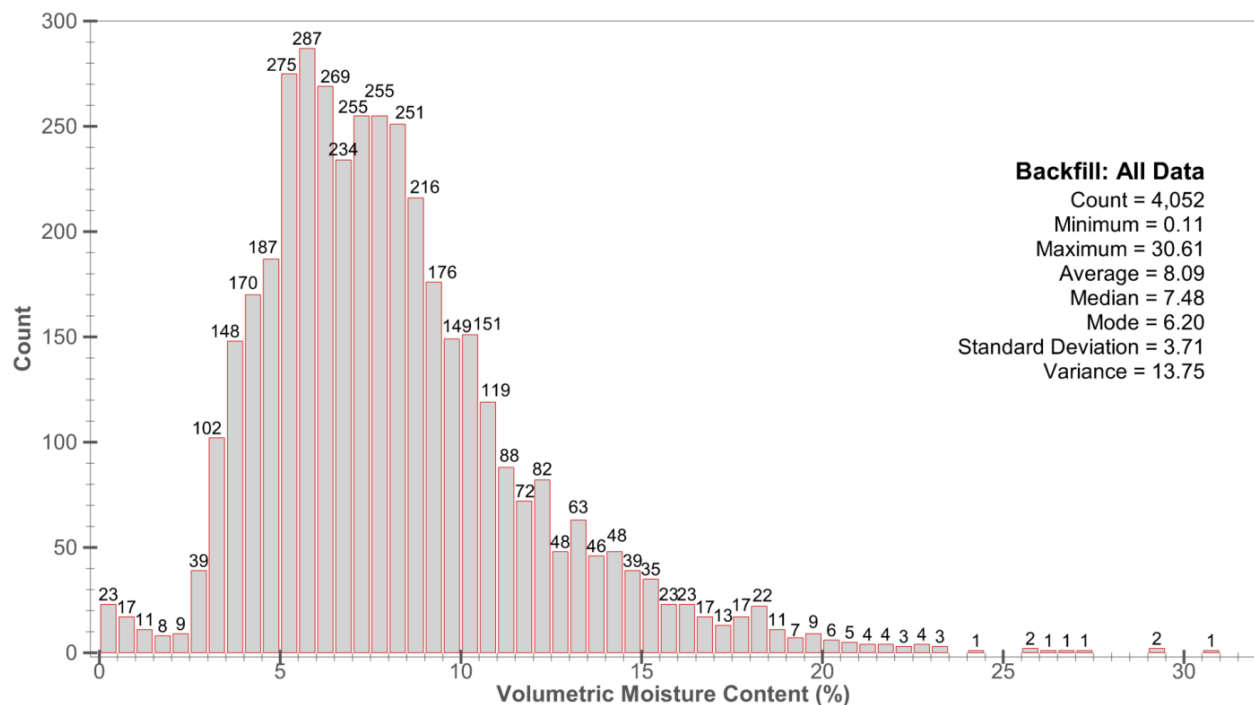
RPP-ENV-58782, Rev. 0

Figure B-9c. Waste Management Area C Moisture Content Histogram for H1 Data Outside of the Single-Shell Tank Footprint.



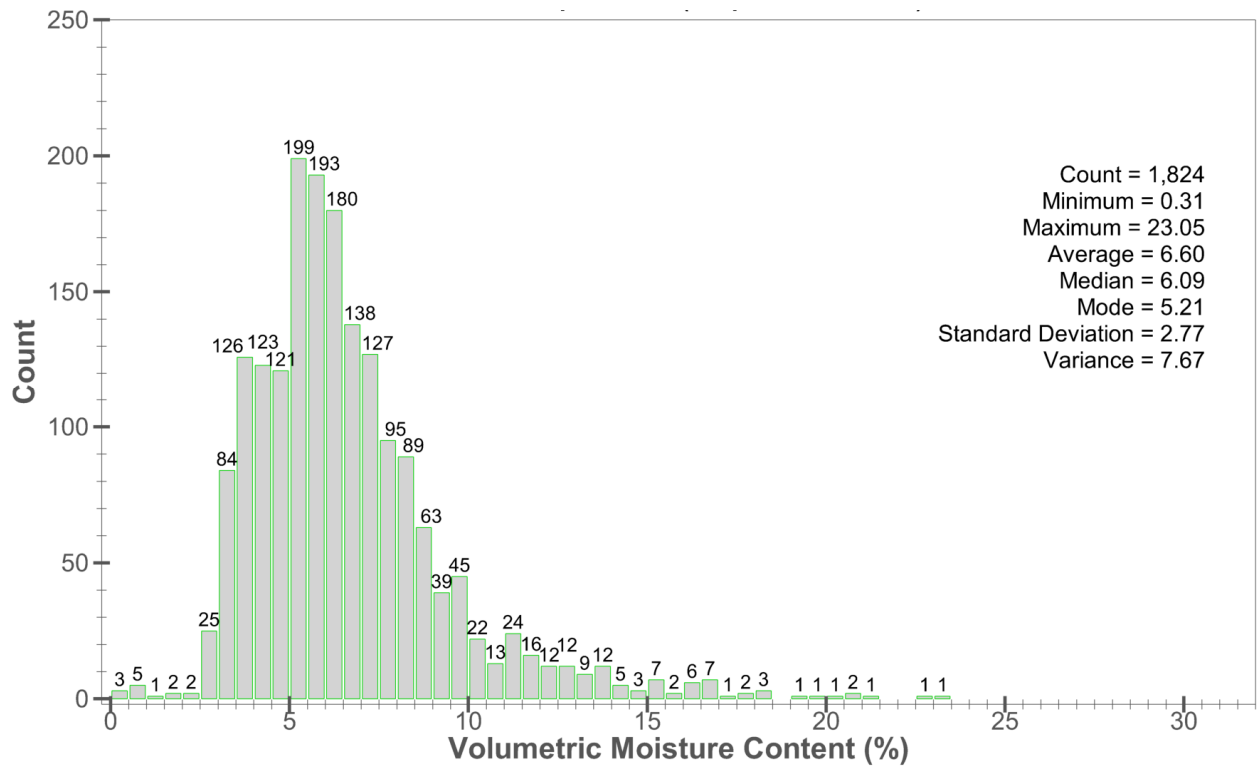
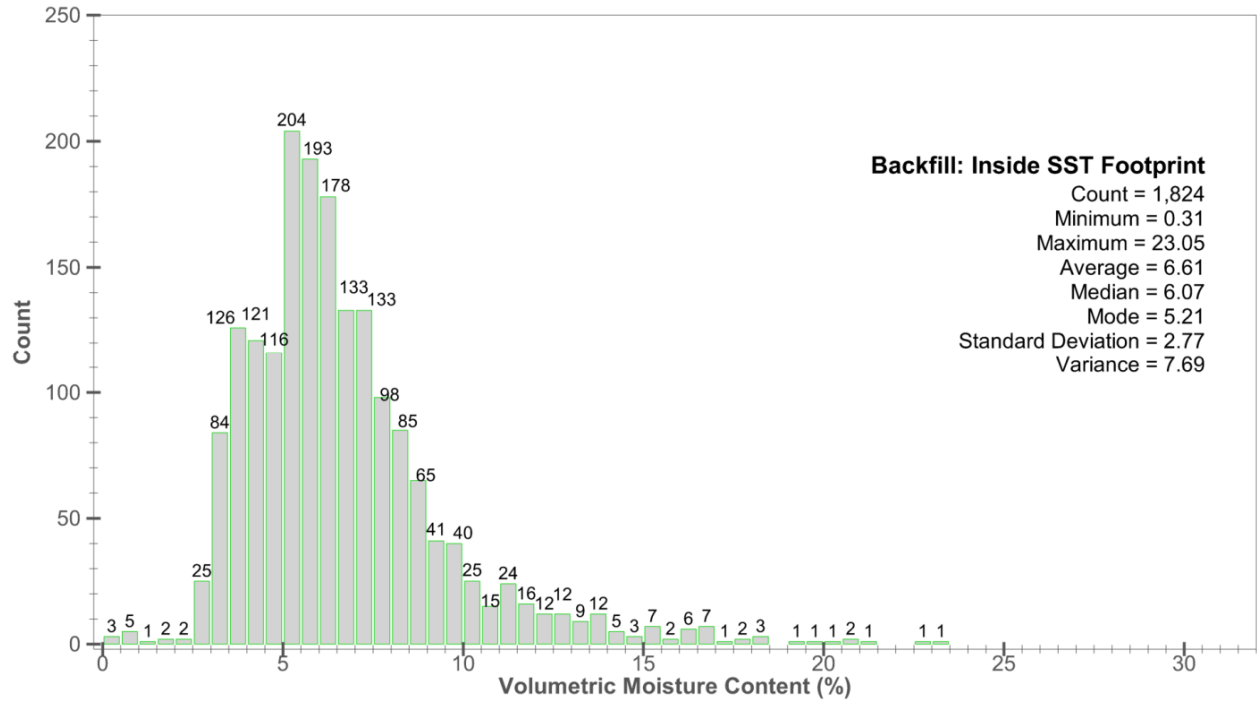
SST = single-shell tank

Figure B-10a. Waste Management Area C Moisture Content Histogram for All Backfill Data (Includes the Data from Both Inside and Outside of the Single-Shell Tank Footprint).



RPP-ENV-58782, Rev. 0

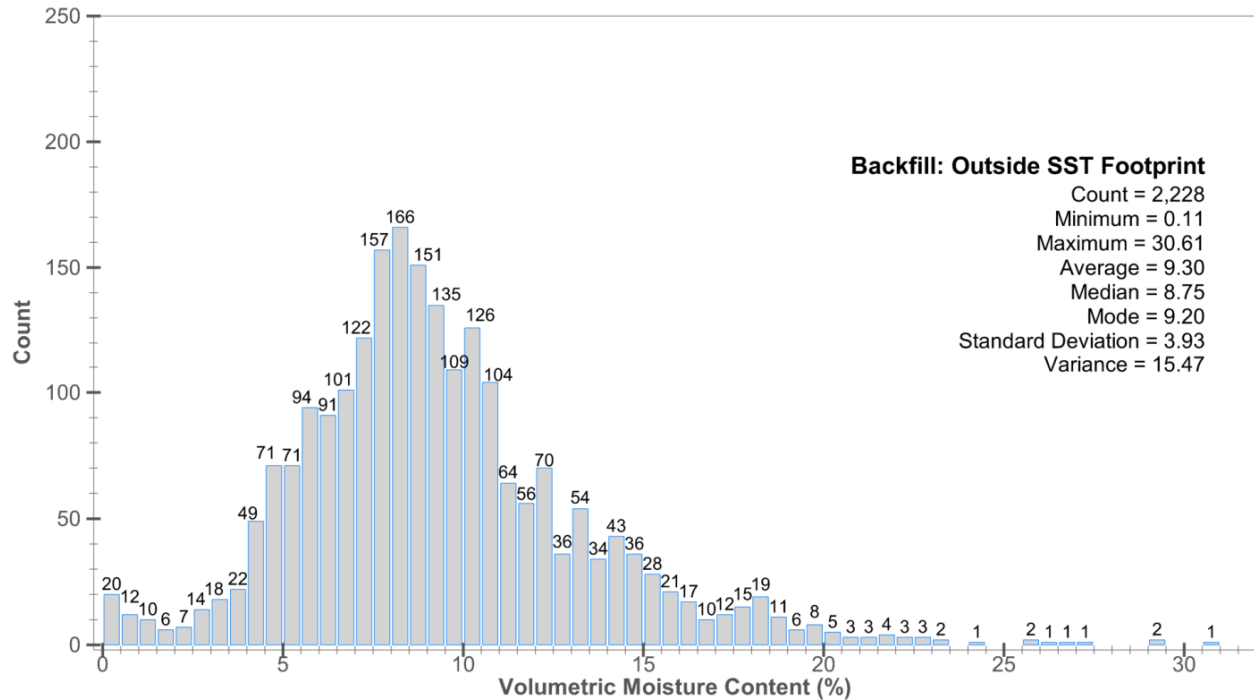
Figure B-10b. Waste Management Area C Moisture Content Histogram for Backfill Data Inside of the Single-Shell Tank Footprint.



SST = single-shell tank

RPP-ENV-58782, Rev. 0

Figure B-10c. Waste Management Area C Moisture Content Histogram for Backfill Data Outside the Single-Shell Tank Footprint.



SST = single-shell tank

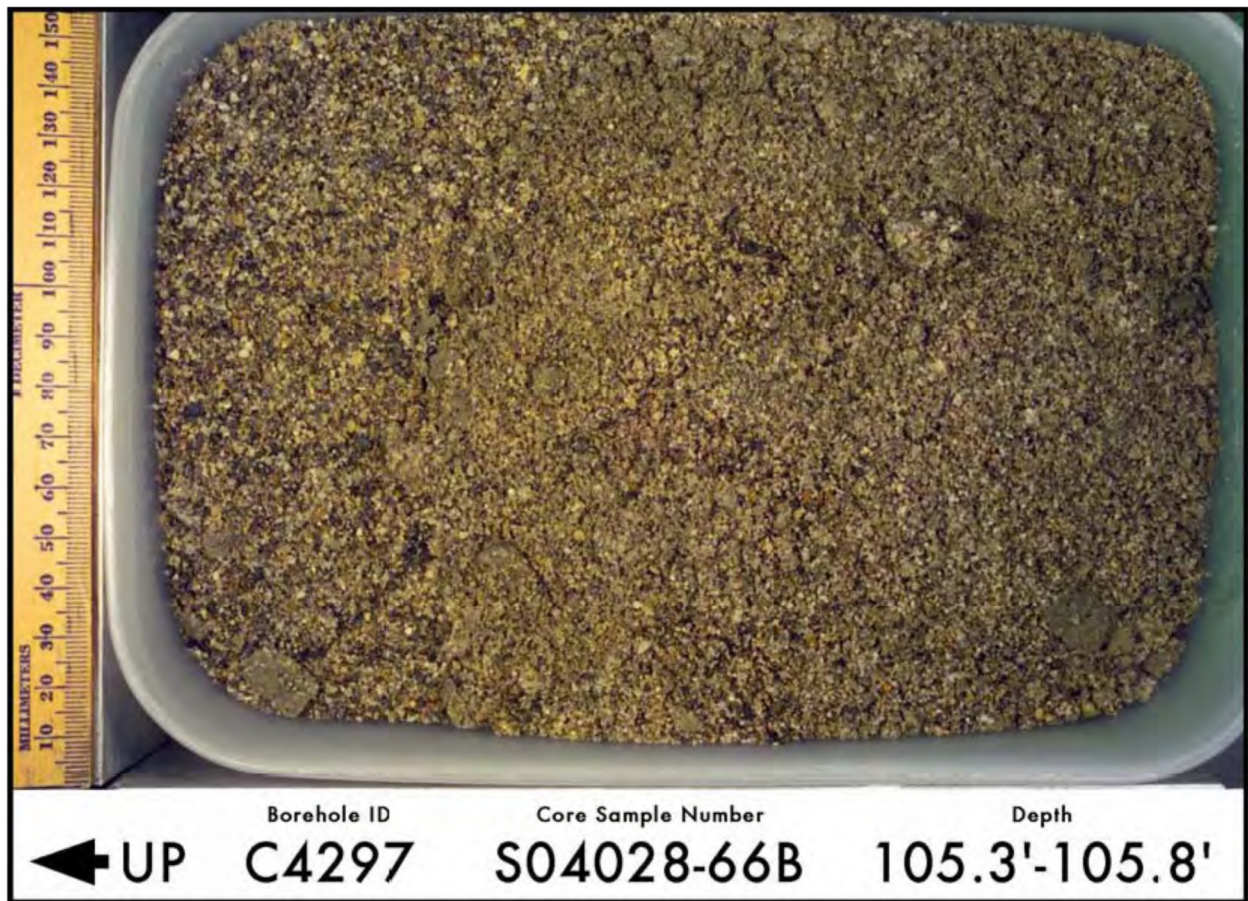
The IDF H2 samples contain very little gravel (>2-mm size) (RPP-20621). To account for the presence of gravel fraction for WMA C samples, the IDF H2 moisture retention data (Table B-3) were corrected (“Correcting laboratory-measured moisture retention data for gravels” [Khaleel and Relyea 1997]). Table B-4 data suggest that the gravel fraction for the H2 unit can range from less than 1% to about 25%. Also, borehole logs (PNNL-15503) suggest the presence of a high gravel fraction, and many WMA C H2 samples are characterized as “sandy pebble gravel” and “pebbly sand.” A gravel fraction of 20% was assumed and applied to correct the IDF retention data. The fitted moisture retention curves and unsaturated conductivity curves for H2 sandy sequence as well as the WMA C H2 composite curves are shown in Figures B-12 and B-13, respectively. To obtain the composite curves, all measurements for an equivalent homogeneous medium (EHM) were pooled and the composite van Genuchten parameters were obtained via RETC (REtention Curve) code (EPA/600/2-91/065, The RETC Code for Quantifying the Hydraulic Functions of Unsaturated Soils) and a simultaneous fit of both moisture retention and unsaturated conductivity data. The composite curves account for gravel correction (Khaleel and Relyea 1997).

B.2.1.1 Comparison of Simulated and Observed Moisture Content. As stated earlier, the selected properties were used to simulate a vadose zone flow field and the simulation results were cross-checked against WMA C field-measured moisture contents. Figure B-14 shows a comparison of measured moisture profile for borehole C4297 (Figure B-5) and the simulated steady-state moisture profile for WMA C. As indicated, for an expected long-term recharge estimate of 3.5 mm/yr, the simulated H2 moisture profile compares well with the measurements. Overall, the simulated H2 moisture content of ~6 (% volume) is in agreement with the average

RPP-ENV-58782, Rev. 0

WMA C H2 moisture of ~5.15 (% volume) (Table B-1). As stated in Section B.1.1, the averages for moisture content measurements for H2 inside and outside the SST footprint were not significantly different even though the recharge conditions outside the farm are different (lower infiltration) from those inside the farm (higher infiltration). As expected, the field-measured moisture contents are significantly impacted by small-scale heterogeneities and exhibit considerable variability (Figure B-14). To the contrary, the PA simulations are based on upscaled or effective hydraulic properties; each heterogeneous formation is replaced by its homogeneous equivalent, and the upscaled or effective flow parameters are used to represent the EHM. This effectively results in a smoothing of the model estimates (Figure 6-3). Therefore, the variability of field-measured moisture contents, induced by media heterogeneities, is inherently larger in comparison to that based on PA simulations using homogenized upscaled properties, and the ensemble average, embedded in EHM approximation, cannot capture the field-scale variability.

Figure B-11. Waste Management Area C Hanford H2 Sand-Dominated Core.



Reference: PNNL-15503, "Characterization of Vadose Zone Sediments Below the C Tank Farm: Borehole C4297 and RCRA Borehole 299-E27-22."

Similar comparison was also made for other units using their selected properties (presented below); for a recharge estimate of 3.5 mm/yr, the steady-state simulated moisture contents and the field-measured average moisture contents (Table B-1) compared well.

RPP-ENV-58782, Rev. 0

Table B-3. van Genuchten Parameters (Based on the Multistep Method) and Saturated Hydraulic Conductivity Data for 44 Integrated Disposal Facility Borehole Samples from the H2 Sandy Sequence. (2 sheets)

Sample	θ_s (cm ³ /cm ³)	θ_r (cm ³ /cm ³)	α (1/cm)	n (-)	Saturated Hydraulic Conductivity (cm/s)
7A ¹	0.377	0.0404	0.0290	1.825	1.04E-03
10A ¹	0.413	0.0279	0.1161	1.784	2.95E-03
12A ¹	0.363	0.0309	0.0650	1.755	2.15E-03
14A ¹	0.416	0.0324	0.0445	1.728	1.99E-03
15A ¹	0.380	0.0254	0.0487	1.844	2.09E-03
16A ¹	0.420	0.0228	0.0682	1.710	9.57E-03
17A ¹	0.423	0.0382	0.0689	1.899	1.99E-03
19A ¹	0.444	0.0279	0.2010	1.542	4.31E-03
20A ¹	0.419	0.0321	0.0305	2.081	2.54E-03
21A ¹	0.403	0.0276	0.0545	1.926	2.94E-03
22A ¹	0.352	0.0252	0.1078	1.585	5.06E-03
23A ¹	0.371	0.0411	0.0079	1.553	2.65E-04
24A ¹	0.321	0.0413	0.0130	1.684	5.69E-04
25A ¹	0.345	0.0267	0.0842	2.158	5.40E-03
27A ¹	0.377	0.0354	0.0830	1.532	8.14E-03
29A ¹	0.359	0.0317	0.0784	1.732	3.75E-03
31A ¹	0.418	0.0444	0.0058	2.012	8.21E-04
32A ¹	0.359	0.0401	0.0931	1.703	6.71E-03
34A ¹	0.316	0.0324	0.0819	2.398	1.32E-02
35A ¹	0.299	0.0428	0.0897	2.160	1.06E-02
45L ²	0.385	0.008	0.1039	1.737	3.24E-2
45U ²	0.385	0.005	0.088	1.664	3.24E-2
50L ²	0.420	0.025	0.073	1.710	1.75E-3
50U ²	0.420	0.013	0.045	1.667	1.75E-3
80L ²	0.359	0.031	0.0403	2.368	1.05E-3
80U ²	0.359	0.033	0.0313	2.572	1.05E-3

RPP-ENV-58782, Rev. 0

Table B-3. van Genuchten Parameters (Based on the Multistep Method) and Saturated Hydraulic Conductivity Data for 44 Integrated Disposal Facility Borehole Samples from the H2 Sandy Sequence. (2 sheets)

Sample	θ_s (cm ³ /cm ³)	θ_r (cm ³ /cm ³)	α (1/cm)	n (-)	Saturated Hydraulic Conductivity (cm/s)
85L ²	0.406	0.023	0.1074	1.697	3.84E-2
85U ²	0.406	0.027	0.0847	1.595	3.84E-2
110L ²	0.412	0.039	0.0362	2.328	5.16E-4
110U ²	0.412	0.046	0.0268	3.182	5.16E-4
130L ²	0.358	0.032	0.0940	2.003	1.97E-2
130U ²	0.358	0.036	0.0674	1.934	1.97E-2
150L ²	0.431	0.015	0.0992	1.547	7.48E-3
150U ²	0.431	0.024	0.0703	1.514	7.48E-3
200L ²	0.410	0.002	0.0995	2.162	4.93E-2
215L ²	0.370	0.028	0.0448	1.918	2.24E-3
215U ²	0.370	0.023	0.0333	1.815	2.24E-3
230L ²	0.309	0.040	0.0472	1.658	3.56E-3
230U ²	0.309	0.038	0.0400	1.658	3.56E-3
251L ²	0.427	0.032	0.084	1.845	1.43E-2
261L ²	0.390	0.045	0.0191	2.485	5.54E-4
C3826-171 ³	0.382	0.0226	0.0390	1.840	7.96E-3
C3827-63.5 ³	0.444	0.0	0.0914	1.500	2.23E-2
C3827-221 ³	0.361	0.0220	0.0660	1.770	7.30E-3

¹Fiscal year 1998 borehole.

²Fiscal year 2001 borehole.

³Fiscal year 2002 borehole.

Reference: RPP-20621, "Far-Field Hydrology Data Package for the Integrated Disposal Facility Performance Assessment."

B.2.1.2 Alternative Geologic Model Properties. The preceding sections have identified parameters for the soils in Alternative Geologic Model I (ACM-I). Alternative Geologic Model II (ACM-II) is a slight variation (see Section 6) of ACM-I. The primary difference between the two alternative models concerns whether or not a sandy gravel facies followed by a silty sandy layer exist at the bottom of the H2 unit in the vicinity of WMA C. Figure B-15 illustrates the moisture retention curves for ACM-II, whereas Figure B-16 illustrates the unsaturated conductivity curves for ACM-II.

RPP-ENV-58782, Rev. 0

Table B-4. Wet Sieve Particle Size Distribution for Borehole 299-E27-22 Sediments.

Depth (ft bgs)	Stratigraphic Unit (Hanford formation)	Weight Percent		
		Gravel	Sand	Silt/Clay
28.0	H1	28.2	62.9	8.78
40.5	H1	0.104	85.1	14.3
45.5	H1	0.136	88.9	10.5
48.0	H1	0	61.6	36.3
50.5	H1	22.1	72.3	5.58
78.0	H1	11.0	77.6	11.2
82.0	H2	0.165	87.5	11.9
85.5	H2	1.74	89.6	8.61
95.5	H2	1.10	88.4	10.4
100.5	H2	0.424	90.8	8.62
139.5	H2	0.112	88.4	11.0
145.5	H2	24.7	66.1	9.09
160.5	H2	15.9	68.8	15.2
164.5	H2	3.21	89.1	7.53
185.5	H2	18.9	60.9	20.0
200.5	H2	17.3	73.5	9.12
210.5	H2	17.1	68.5	14.2
225.5	H2	11.7	76.2	11.9

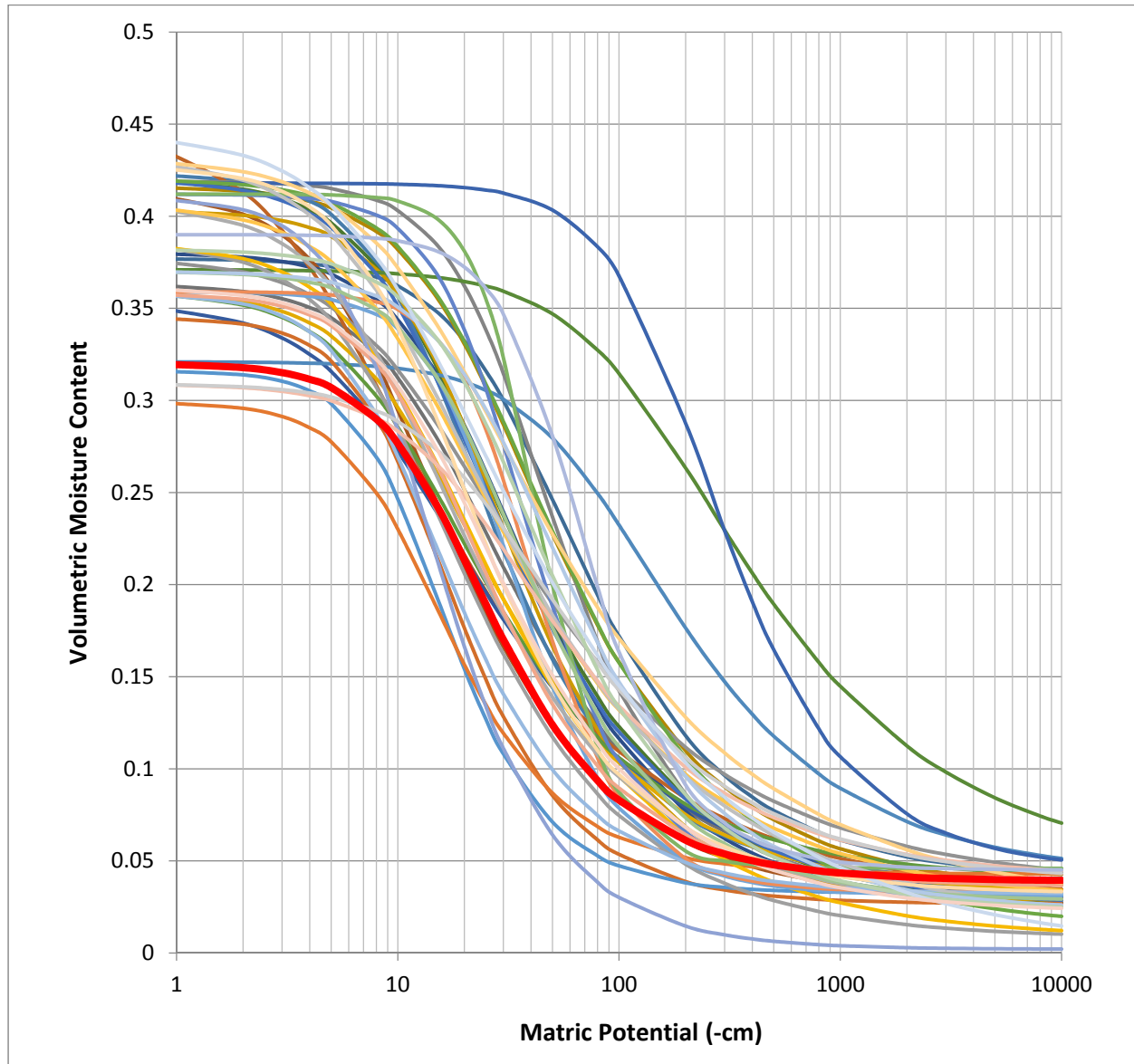
Reference: PNNL-15503, "Characterization of Vadose Zone Sediments
Below the C Tank Farm: Borehole C4297 and RCRA Borehole 299-E27-22."

B.2.2 Properties of the Hanford H1 and H3 Gravelly Units

Similar to the Hanford H2 sand-dominated unit, no site-specific data are available for the WMA C Hanford H1 and H3 gravelly units. However, as part of other Hanford Site projects, particle-size distribution, bulk density, saturated hydraulic conductivity, moisture retention, and unsaturated conductivity data have been collected for several borehole samples (Figure B-3) at other sites in the vicinity of C Farm and within 200 Areas. These sites include the 218-E-12B and 218-E-10 low-level solid waste burial grounds in 200 East Area, the Environmental Restoration Disposal Facility site located in between the 200 West and 200 East Areas, and the 241-T-106 tank site located in 200 West Area. Borehole sediment samples from these sites were used as surrogates to represent the hydraulic properties for WMA C H1 and H3 gravel-dominated units.

RPP-ENV-58782, Rev. 0

**Figure B-12. Moisture Retention Data for H2 Unit (44 Samples).
The Waste Management Area C H2 composite curve is shown in red.**



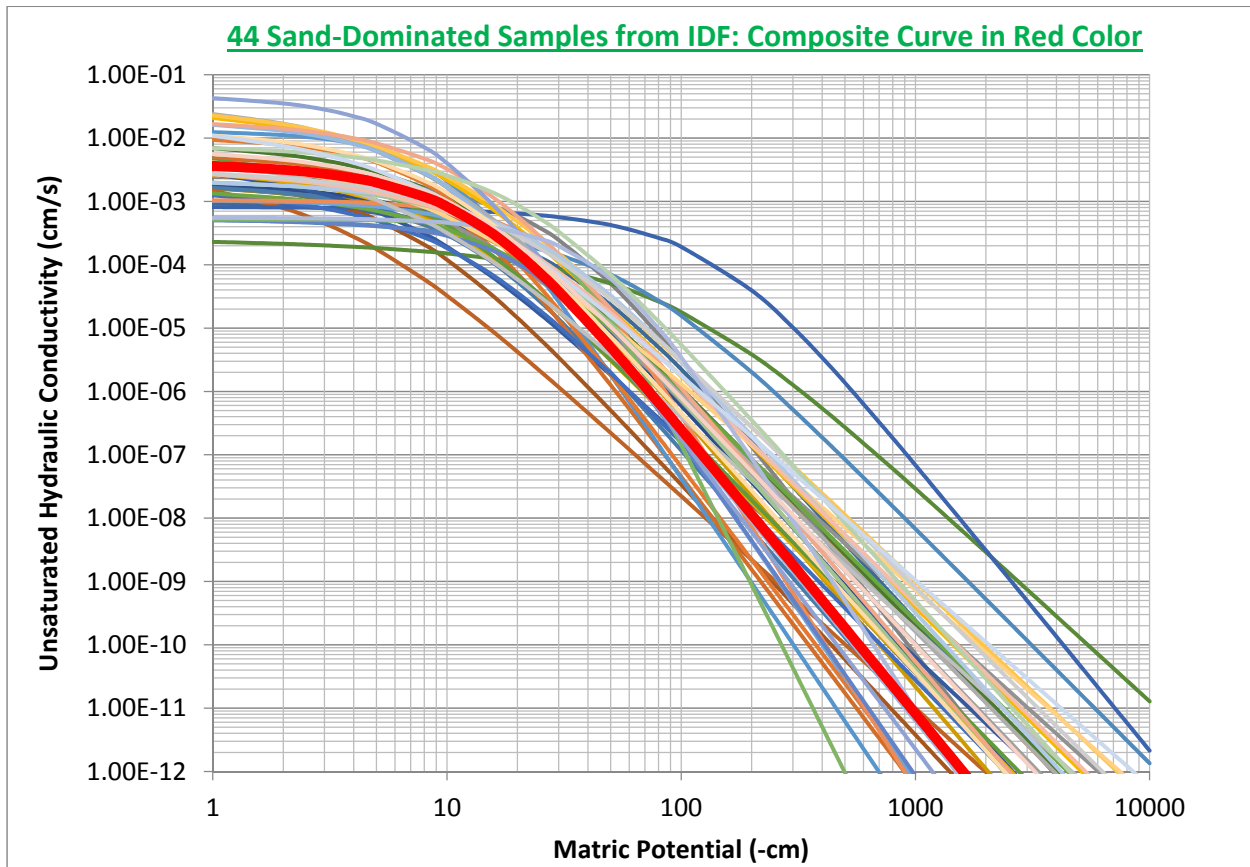
Reference: RPP-20621, "Far-Field Hydrology Data Package for the Integrated Disposal Facility Performance Assessment."

Unlike H2 sediments, both H1 and H3 sediments are comprised of a significant gravel (>2-mm size) fraction. To explore the impact of gravelly sediments for the drier moisture regime, a separate study was conducted ("Variability of Gardner's α for coarse-textured sediments" [Khaleel and Relyea 2001]); a total of 79 gravelly and sandy samples were analyzed in the laboratory. The gravel fraction for 41 samples ranged from 20 to 71% (by weight); the remaining 38 samples were sandy with very little gravel fraction (Figure B-17). A noteworthy feature of Figure B-17 is the fact that the variability in saturated conductivity is much greater than the variability in unsaturated conductivity near saturation. Furthermore, the measured unsaturated conductivities for the gravelly samples showed less variability for the drier moisture

RPP-ENV-58782, Rev. 0

regime, fell within a narrower range, and were well within the range of measured unsaturated conductivities for the sandy samples (see Figure B-17). Such a generic behavior for the gravelly sediments for the drier moisture regime prompted assigning similar properties for both H1 and H3 units.

**Figure B-13. Unsaturated Hydraulic Conductivity Data for H2 Unit (44 Samples).
The Waste Management Area C H2 composite curve is shown in red.**

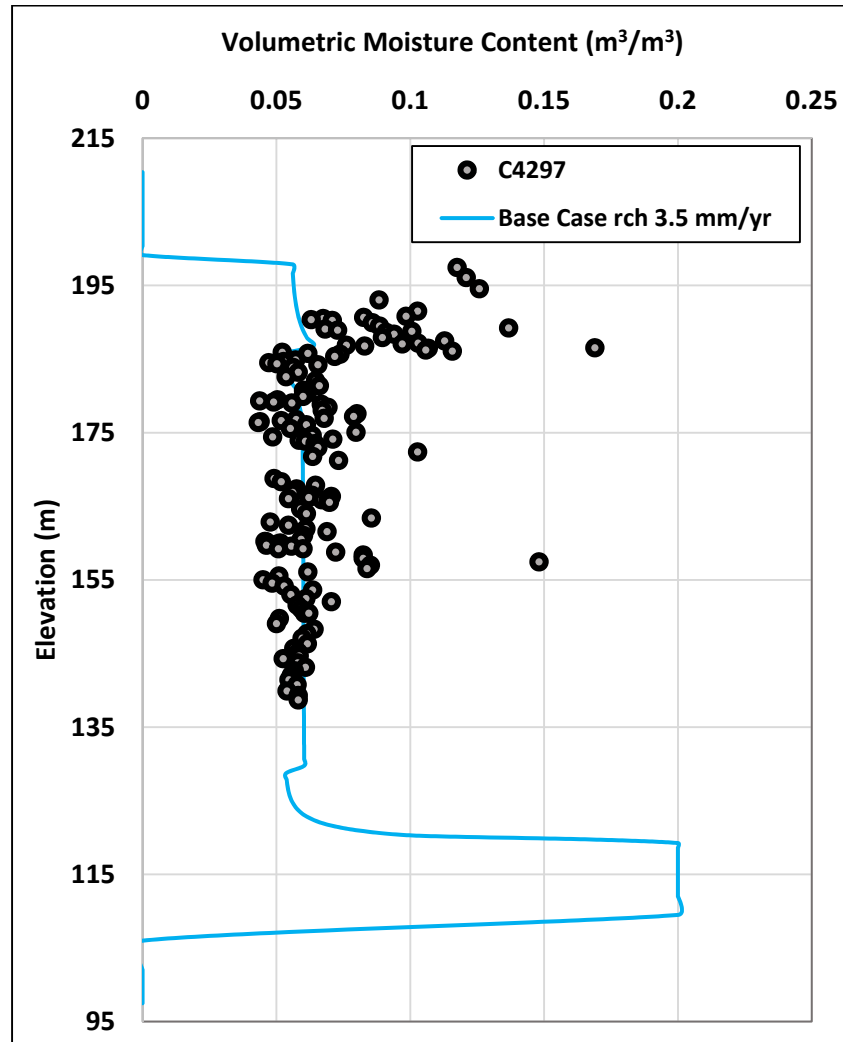


Reference: RPP-20621, "Far-Field Hydrology Data Package for the Integrated Disposal Facility Performance Assessment."

Standard laboratory and Westinghouse Hanford Company quality assurance procedures (WHC-IP-0635, "Geotechnical Engineering Procedure Manual") were used to analyze the H1 and H3 sediment samples. The moisture retention data for the fine fraction (<2 mm) and the drainage cycle of up to -1,000 cm of pressure head were measured using "Tempe" pressure cells; the rest of the drainage data up to -15,000 cm was measured using the pressure plate extraction method ("Water Retention: Laboratory Methods" [Klute 1986]). A variation of the unit gradient method (Klute and Dirksen 1986, Khaleel et al. 1995) was used to measure unsaturated hydraulic conductivities for the bulk samples. The laboratory measured data on <2 mm size fraction were corrected for the gravel fraction ("Water Content" in Methods of Soils Analysis, Part 1—Physical and Mineralogical Methods [Gardner 1986; Khaleel and Relyea 1997]). No correction was needed for the saturated and unsaturated conductivities, since these were measured on the bulk sample.

RPP-ENV-58782, Rev. 0

Figure B-14. Comparison of Simulated (Blue) and Observed (Circle) Moisture Content for Hanford H2 Sand-Dominated Unit.



As was done for the Hanford H2 sandy unit, a simultaneous fit of both laboratory-measured moisture retention and unsaturated conductivity data was used; and all five unknown parameters (i.e., θ_r , θ_s , α , n , and K_s), with $m=1-1/n$ (van Genuchten 1980), were fitted to the data via RETC (EPA/600/2-91/065). The pore size distribution factor, ℓ (Mualem 1976), was kept fixed at 0.5 during the simultaneous fitting. The fitted parameters, based on moisture retention and unsaturated conductivity measurements for H1 and H3 units, are shown in Table B-5. The fitted retention and conductivity curves for H1 and H3 units are shown in Figure B-18 and Figure B-19, respectively.

B.2.3 Properties for the Backfill Gravelly Unit

Because of high gravel content, the backfill hydraulic properties are expected to be similar to H1 and H3 gravelly media properties. Table B-6 catalogs the van Genuchten-Mualem parameters for samples that were selected from the 200 Areas database to represent the WMA C tank farm

RPP-ENV-58782, Rev. 0

backfill sediments. Because the backfill includes a significant gravel fraction, most of the samples (Table B-6) are the same as the 17 samples used to represent the H1 and H3 gravelly units. The fitted retention and conductivity curves for the backfill unit are shown in Figure B-20 and Figure B-21, respectively.

B.3 EFFECTIVE (UPSCALED) FLOW PARAMETERS FOR VADOSE ZONE

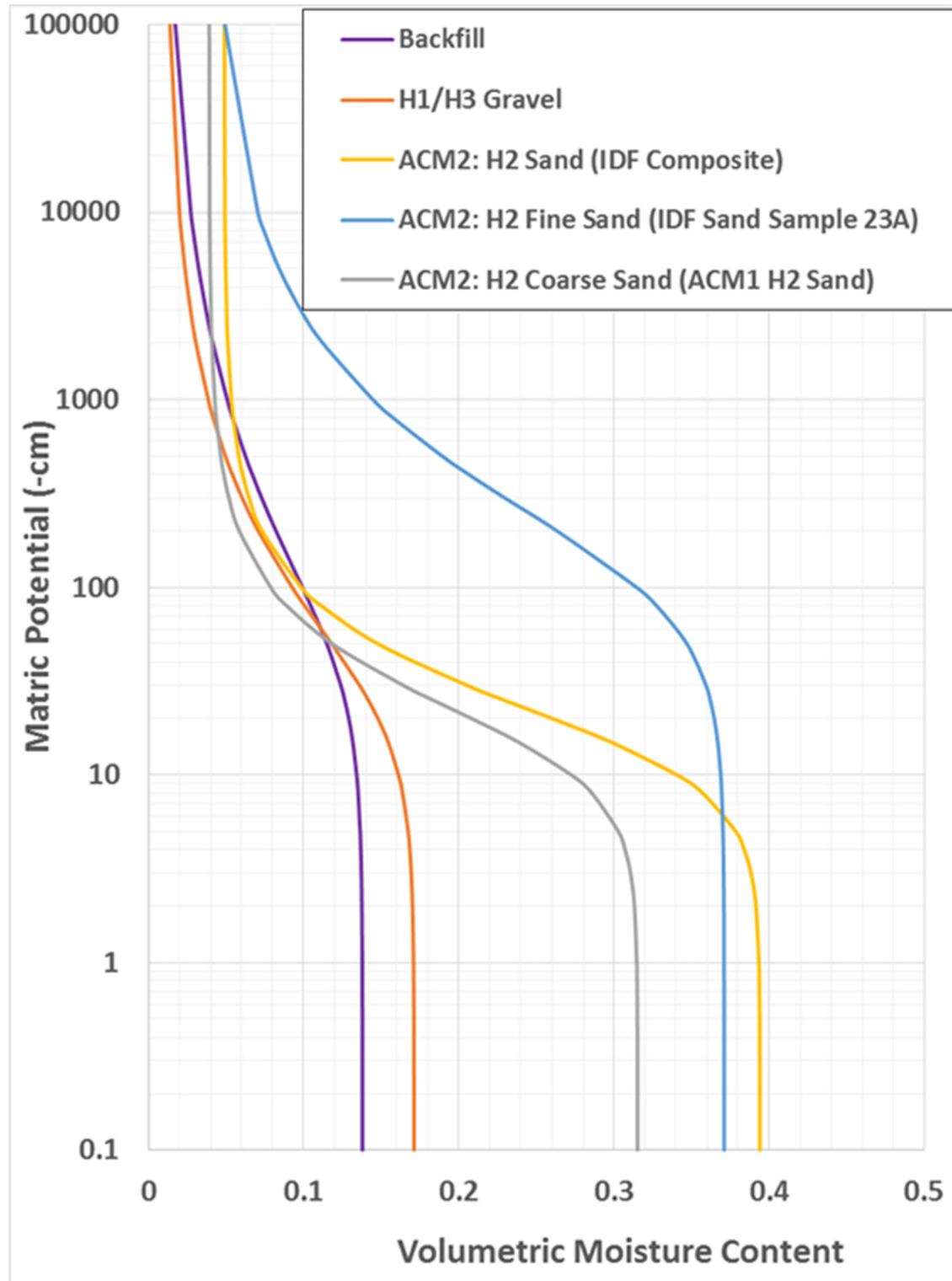
Data on hydraulic properties, described in the preceding sections, were obtained via laboratory tests on core samples (scales of the order of a few centimeters). However, numerical models of fluid flow and contaminant transport in the unsaturated zone require specifying hydraulic properties for each discretized grid block (scales of the order of meters), which are much larger than the core scale at which the unsaturated properties are measured. The process of defining large-scale properties for the numerical grid blocks based on small, core-scale measurements is called upscaling (“Upscaled Flow and Transport Properties for Heterogeneous Unsaturated Media” [Khaleel et al. 2002]).

For stratified sediments such as those existing in the 200 Areas, the effective hydraulic conductivity tensor is anisotropic with a moisture-dependent (or tension-dependent) degree of anisotropy. The anisotropy ratio of horizontal hydraulic conductivity to vertical hydraulic conductivity increases with decreasing moisture content. Theoretical work on variable anisotropy includes, for example, “Stochastic Analysis of Unsaturated Flow in Heterogeneous Soils, 2. Statistically Anisotropic Media with Variable α ” (Yeh et al. 1985), “Stochastic Modeling of Large-Scale Transient Unsaturated Flow Systems” (Mantoglou and Gelhar 1987), and “Estimation of effective unsaturated hydraulic conductivity tensor using spatial moments of observed moisture plume” (Yeh et al. 2005). Experimental studies supporting variable anisotropy include, for example, “Dependence of Anisotropy on Saturation in a Stratified Sand” (Stephens and Heermann 1988), “Effective Unsaturated Hydraulic Conductivity of Layered Sands” (Yeh and Harvey 1990), and “Hysteresis and State-Dependent Anisotropy in Modeling Unsaturated Hillslope Hydrologic Processes” (McCord et al. 1991). Variable, moisture-dependent anisotropy in unsaturated soils, in effect, is an effective, large-scale (macroscopic) flow property which results from media heterogeneities at a smaller scale, and provides a framework for upscaling laboratory-scale measurements to delineate the effective or upscaled properties for the large-scale vadose zone. A stochastic model (i.e., “Application of Stochastic Methods to Transient Flow and Transport in Heterogeneous Unsaturated Soils” [Polmann 1990]) is used to describe moisture- or tension-dependent anisotropy for WMA C sediments. Such an upscaling process recognizes the spatial variability inherent in heterogeneous media such as those existing at WMA C.

Effective or upscaled values of flow parameters for the WMA C vadose zone are presented in Section B.3.1. Specific upscaled flow parameters include moisture retention, saturated, and unsaturated hydraulic conductivity. Transport parameters (e.g., bulk density, diffusivity, sorption coefficients, and macrodispersivity) are discussed later in Section B.4.

RPP-ENV-58782, Rev. 0

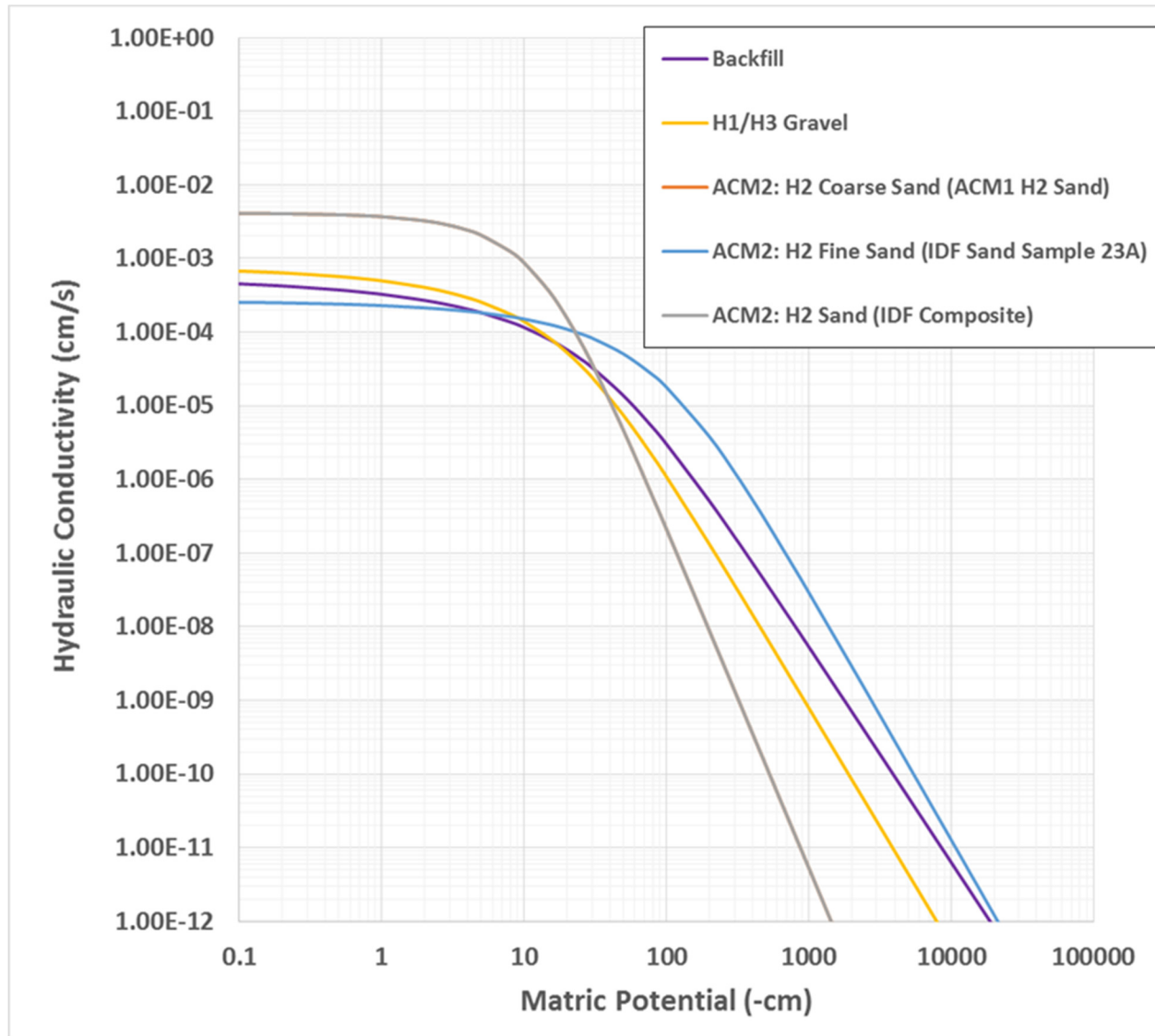
Figure B-15. Moisture Retention Curves for Various Hydrostratigraphic Units and Selected Properties for Alternative Geologic Model II.



ACM1 = Alternative Geologic Model I
 ACM2 = Alternative Geologic Model II
 IDF = Integrated Disposal Facility

RPP-ENV-58782, Rev. 0

Figure B-16. Unsaturated Hydraulic Conductivity Curves for Various Hydrostratigraphic Units and Selected Properties for Alternative Geologic Model II.



ACM1 = Alternative Geologic Model I
 ACM2 = Alternative Geologic Model II
 IDF = Integrated Disposal Facility

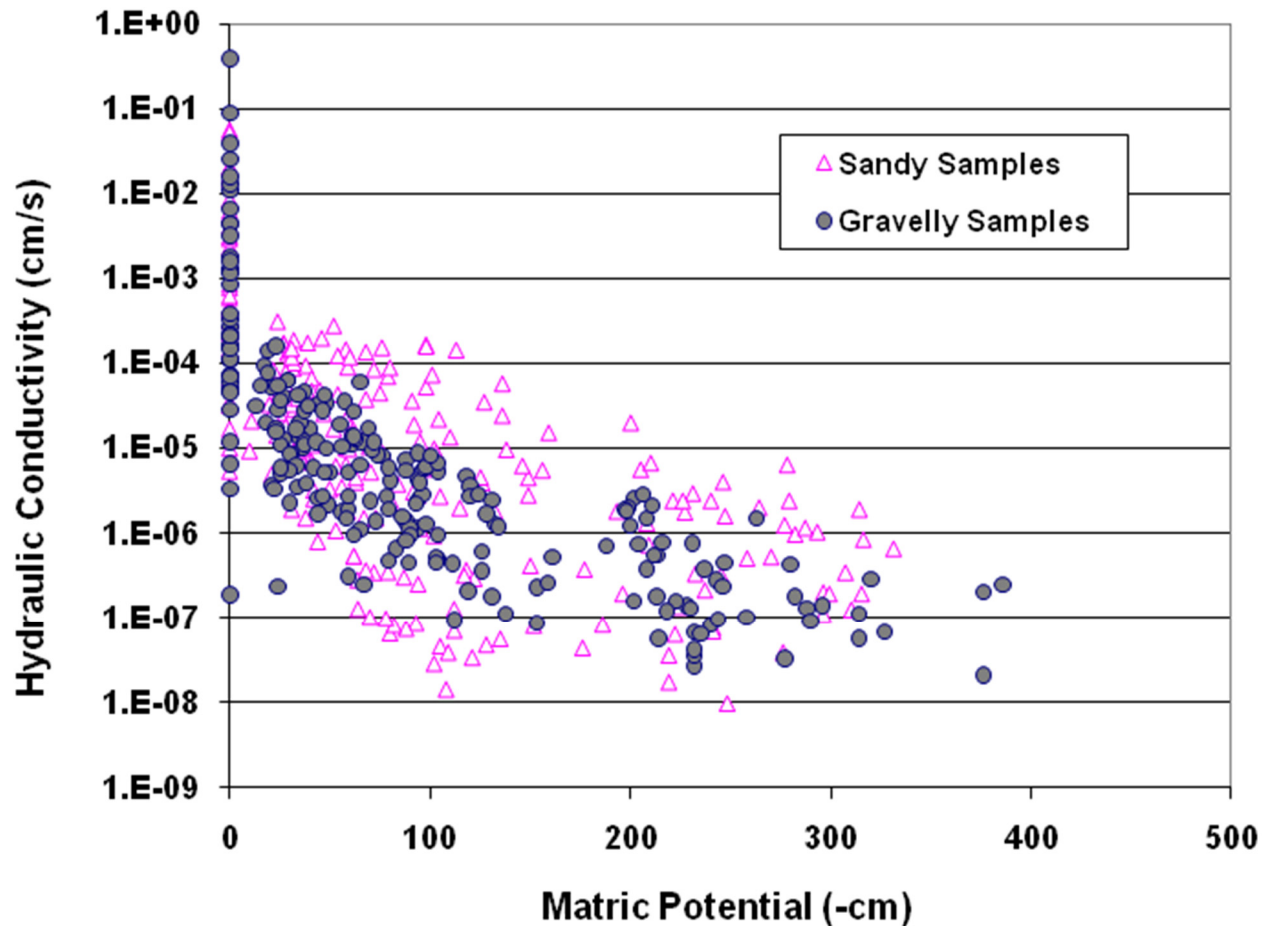
B.3.1 Composite Macroscopic Relationships and Effective Parameters

The WMA C composite parameters for moisture characteristics are derived based on laboratory measurements presented in preceding sections. The fitted moisture retention curves (e.g., Figure B-12 for H2 unit) show spatial variability, albeit the degree of variation at a given tension is more modest than that of hydraulic conductivity (e.g., Figure B-13 for H2 unit). For both sandy (e.g., H2 unit) and gravelly (e.g., H1, H3, and backfill units) sediments, the composite van Genuchten parameters were obtained via RETC (EPA/600/2-91/065) and a simultaneous fit of both moisture retention and unsaturated conductivity data. The pore size

RPP-ENV-58782, Rev. 0

distribution factor ℓ (van Genuchten 1980) was kept constant at 0.5 during the simultaneous fitting.

Figure B-17. Unsaturated Hydraulic Conductivity Measurements for Sand-Dominated and Gravel-Dominated Samples.



Reference: "Variability of Gardner's α for coarse-textured sediments" (Khaleel and Relyea 2001).

The fitted composite van Genuchten-Mualem parameters for different HSUs are shown in Table B-7. Estimates for the equivalent horizontal and vertical hydraulic conductivities are discussed in Section B.3.2.

B.3.2 Stochastic Model for Macroscopic Anisotropy

As discussed earlier, variable, tension-dependent anisotropy provides a framework for upscaling small-scale measurements to the effective or upscaled properties for the large-scale vadose zone. A stochastic model is used to describe tension-dependent anisotropy for sediments at the C Farm.

Yeh et al. (1985) analyzed steady unsaturated flow through heterogeneous porous media using a stochastic model. Parameters such as hydraulic conductivity are treated as random variables rather than as deterministic quantities. The Gardner relationship ("Some Steady-State Solutions

RPP-ENV-58782, Rev. 0

of the Unsaturated Moisture Flow Equation with Application to Evaporation from a Water Table” [Gardner 1958]) was used by Yeh et al. (1985) to describe unsaturated hydraulic conductivity (K) as a function of saturated hydraulic conductivity (K_s) and tension (h), as shown in Equations B-1 and B-2.

$$K(h) = K_s \exp(-\beta h) \quad (\text{B-1})$$

Where β is a fitting parameter.

Equation B-1 can be written as

$$\ln(K(h)) = \ln(K_s) - \beta h \quad (\text{B-2})$$

Equation B-2 is referred to as the log-linear model, since $\ln(K(h))$ is linearly related to h through the constant slope β . However, such a constant slope is often inadequate in describing $\ln(K(h))$ over ranges of tension of practical interest for field applications. As an alternative, the slope β can be approximated locally by straight lines over a fixed range of tension. The pseudo “ $\ln(K_s)$ ” term in Equation B-2 can then be derived by extrapolating the local slopes back to zero tension.

Using a linear correlation model between the log-conductivity zero-tension intercept and β , Polmann (1990) presents a generalized model that accounts for the cross-correlation of the local soil property [i.e., $\ln(K_s)$ and β] residual fluctuations. When compared with the uncorrelated $\ln(K_s) - \beta$ model, a partial correlation of the properties is shown to have a significant impact on the magnitude of the effective parameters derived from the stochastic theory. The Polmann (1990) equations for deriving the effective parameters are shown in Equation B-3.

$$\begin{aligned} \langle \ln K \rangle &= \langle \ln K_s \rangle - A \langle h \rangle - \sigma_{\ln K_s}^2 \lambda [p - p^2 \langle h \rangle - \zeta^2 \langle h \rangle] / (1 + A\lambda) \\ \sigma_{\ln K}^2 &= \sigma_{\ln K_s}^2 [(1 - p \langle h \rangle)^2 + \zeta^2 \langle h \rangle^2] / (1 + A\lambda) \\ K_h^{eq} &= \exp[\langle \ln K \rangle + (\sigma_{\ln K}^2 / 2)] \\ K_v^{eq} &= \exp[\langle \ln K \rangle - (\sigma_{\ln K}^2 / 2)] \end{aligned} \quad (\text{B-3})$$

Where:

- $\sigma_{\ln K}^2$ = variance of log unsaturated conductivity (which depends on mean tension)
- $\langle h \rangle$ = mean tension (positive) = $|\psi|$
- ψ = matric potential (negative)
- $\sigma_{\ln K_s}^2$ = variance of pseudo “log saturated conductivity”
- $\langle \ln K_s \rangle$ = mean of $\ln(K_s)$
- p = slope of the β versus $\ln(K_s)$ regression line, where β is the slope of the unsaturated conductivity curve and approximated locally based on Gardner’s (1958) exponential model
- ζ = $\sigma_\delta / \sigma_{\ln(K_s)}$

RPP-ENV-58782, Rev. 0

- 1 σ_δ = standard deviation of the residuals in the β versus $\ln(K_s)$ regression
 2 A = mean slope, β , for $\ln(K)$ vs. h
 3 λ = vertical correlation lengths for $\ln(K_s)$ (assumed to be same as that of β)
 4 K_h^{eq} = equivalent unsaturated horizontal conductivity
 5 K_v^{eq} = equivalent unsaturated vertical conductivity.

6 **B.3.3 Macroscopic Anisotropy Relations**

7
 8 Results of application of Equation B-3 for variable anisotropy are presented below. The data for
 9 individual HSUs (Tables B-3, B-5 and B-6) are used to obtain the Polmann parameters
 10 $\langle \ln(K_s) \rangle$, $\sigma_{\ln K_s}^2$, p , ζ , and A (Equation B-3). The slope and pseudo $\ln(K_s)$ estimates, discussed
 11 in the preceding section, are evaluated for the expected moisture regime of interest
 12 (i.e., relatively high tension range) (Table B-8). However, it should be noted that often no
 13 experimental data are available for unsaturated conductivities in the tension range of interest; β
 14 and $\ln(K_s)$ estimates are then based on the fitted van Genuchten-Mualem curves.

15
 16 An estimate of correlation length λ is needed for anisotropy calculations. Most of the
 17 measurements in the 200 Areas have been obtained at sampling intervals that are too coarse to
 18 yield a reasonable estimate for the correlation length. However, one data set is available that
 19 provides saturated conductivity estimates at about 30-cm intervals for a depth of 18 m within the
 20 Hanford formation; the site is located about 0.5 mi east of the IDF site (Figure B-3) in the
 21 200 East Area. Figure B-22 shows the experimental variogram and the fitted theoretical
 22 variogram for saturated conductivities. The fitted variogram suggests a correlation length λ of
 23 about 50 cm (i.e., the distance at which the variogram drops to $[1-(1/e)]$ times the sill)
 24 (Figure B-22). Correlation length λ for both $\ln(K_s)$ and β were assumed to be equal.

25
 26 Table B-9 lists the variable, macroscopic anisotropy parameter estimates for various WMA C
 27 units. The calculated macroscopic variable anisotropy relations for various HSUs are shown in
 28 Figures B-23, B-24, and B-25. A supporting document presents the anisotropy calculations
 29 (RPP-CALC-60452, "Moisture Dependent Anisotropy Calculations Supporting WMA C PA").

30
 31 Note that values listed in Table B-7 are the composite van Genuchten-Mualem parameters for
 32 different units. Equation B-3 is used to assign the variable Polmann anisotropy (i.e., the ratio of
 33 equivalent unsaturated horizontal conductivity to equivalent unsaturated vertical conductivity) as
 34 a function of saturation. The van Genuchten-Mualem parameters in Table B-7 are then used to
 35 assign the actual unsaturated hydraulic conductivity estimates. The fitted K_s values in Table B-7
 36 represent the vertical components.

37 **B.4 EFFECTIVE TRANSPORT PARAMETERS**

38
 39 Base case effective transport parameter (bulk density, diffusivity, and dispersivity) estimates are
 40 presented in this section. Because of natural variability, the transport parameters are all spatially
 41 variable. The purpose is again, similar to the flow parameters, to evaluate the effect of such
 42 variability on the large-scale transport process.

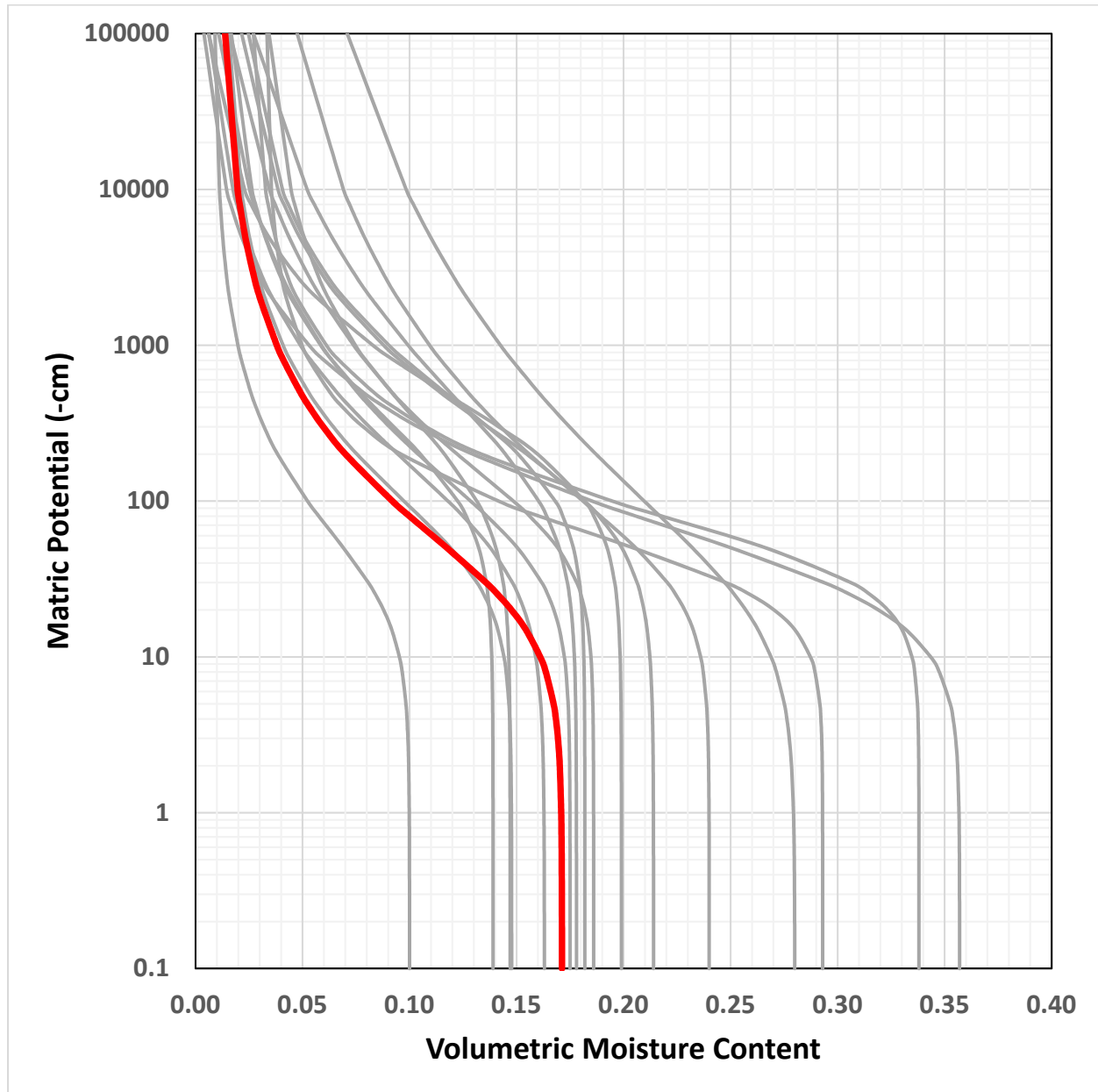
Table B-5. van Genuchten Parameters, Fitted Saturated Hydraulic Conductivity, and Measured Bulk Density Data for H1/H3 Units (17 Samples).

Sample	Site/Operable Unit	Borehole Number	Depth m	Percent Gravel	Θ_s cm ³ /cm ³	Θ_r cm ³ /cm ³	α 1/cm	n	Fitted Ks cm/s	Bulk Density g/cm ³
5-0150	218-E-12B	299-E34-1	24.84	17	0.240	0.023	0.030	1.7077	1.47E-03	1.95
5-0157	218-E-10	299-E32-4	3.50	13	0.293	0.033	0.027	2.1675	7.77E-03	1.88
5-0152	218-E-12B	299-E34-1	65.50	26	0.280	0.025	0.044	1.3253	2.43E-03	1.85
5-0158	218-E-10	299-E32-4	71.50	44	0.214	0.013	0.008	1.4226	1.38E-04	2.15
5-0148	218-E-12B	299-E34-1	15.25	54	0.148	0.013	0.021	1.5589	2.72E-04	2.16
4-1080	ERDF	699-35-61A	93.50	43	0.178	0.000	0.007	1.3819	8.11E-06	2.00
4-0791	ERDF	699-35-65A	63.20	0	0.338	0.026	0.023	2.2565	6.81E-04	1.60
4-0792	ERDF	699-35-65A	75.40	71	0.100	0.008	0.030	1.5858	3.42E-04	2.32
4-1076	ERDF	699-35-61A	76.40	0	0.357	0.000	0.029	1.7015	1.23E-03	1.74
4-1079	ERDF	699-35-61A	90.90	61	0.163	0.000	0.014	1.3079	1.18E-04	2.06
4-1013	ERDF	699-35-69A	77.90	65	0.139	0.013	0.007	1.5656	1.06E-06	2.20
4-1012	ERDF	699-35-69A	73.90	55	0.147	0.000	0.008	1.5109	4.50E-05	2.19
3-0668	241-T-106	299-W10-196	38.90	62	0.175	0.000	0.019	1.6124	1.63E-04	2.13
3-0682	241-T-106	299-W10-196	46.10	51	0.224	0.000	0.017	1.6577	2.37E-04	2.14
3-0210	241-T-106	299-W10-196	3.10	48	0.186	0.029	0.014	1.7674	1.96E-04	2.11
3-0688	241-T-106	299-W10-196	48.50	49	0.199	0.000	0.004	1.5321	2.60E-05	2.17
3-0690	241-T-106	299-W10-196	53.7	53	0.182	0.018	0.005	1.5410	4.19E-05	2.19

ERDF = Environmental Restoration Disposal Facility

RPP-ENV-58782, Rev. 0

Figure B-18. Moisture Retention Data for H1 and H3 Units (17 Samples).
The composite curve is shown in red.



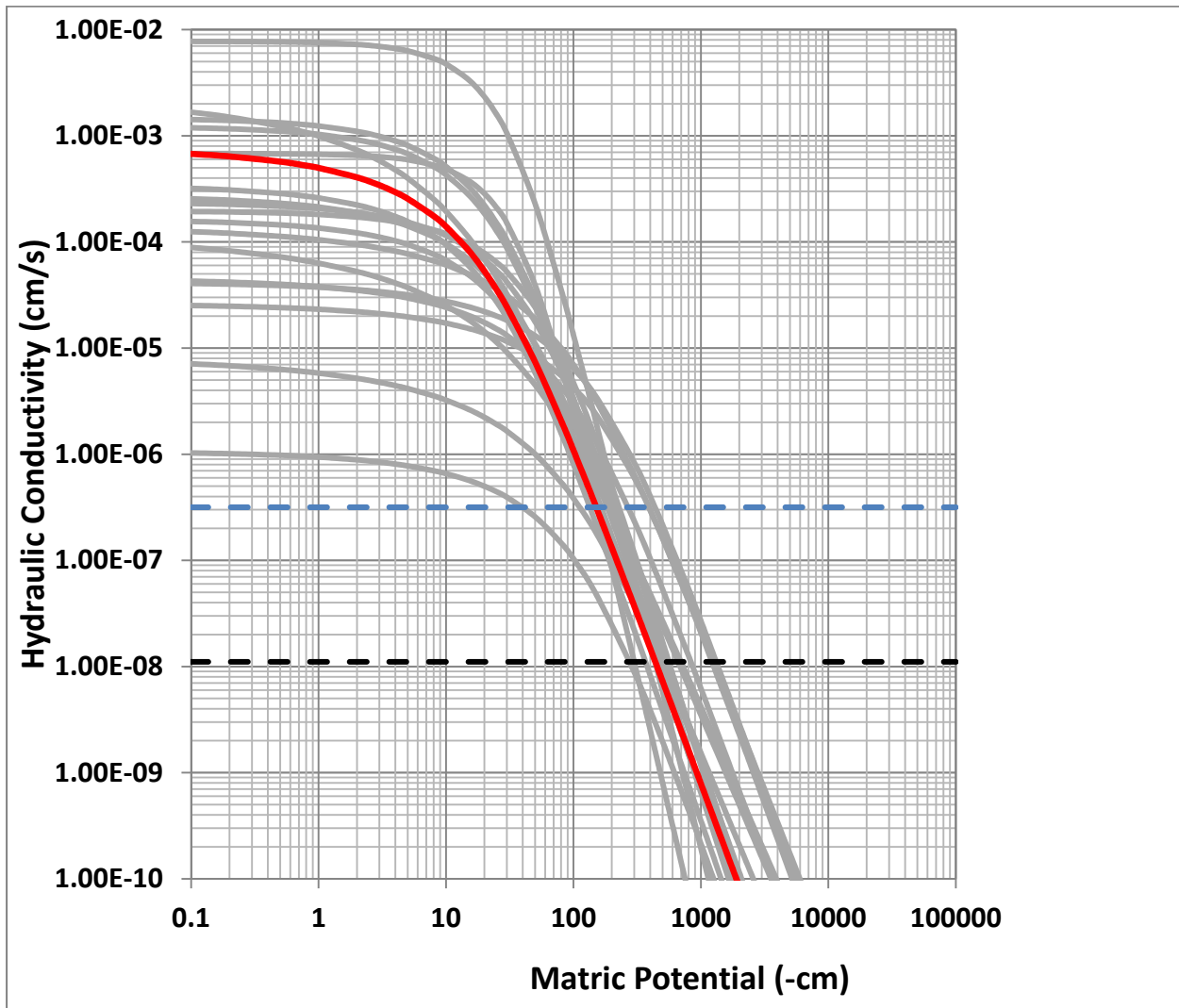
B.4.1 Bulk Density and K_d

Both bulk density (ρ_b) and K_d estimates are needed to calculate retardation factors for different species. The effective, large-scale estimate for bulk density is the average of the small-scale laboratory measurements for bulk density (Stochastic Subsurface Hydrology [Gelhar 1993]). Table B-10 provides the effective, large-scale bulk density estimates for WMA C HSUs. The K_d values, presented in Section 6, were corrected for the gravel (>2-mm size) fraction, and are not repeated here. The correction procedure followed is described in PNNL-17154, "Geochemical Characterization Data Package for the Vadose Zone in the Single-Shell Tank Waste Management

RPP-ENV-58782, Rev. 0

Areas at the Hanford Site.” For materials that contain significant amounts of gravel (notably H1 and H3), K_d values are typically lower than those determined with <2-mm size material because the surface area and the corresponding quantity of adsorption sites is lower (PNNL-17154).

Figure B-19. Unsaturated Hydraulic Conductivity Data for H1 and H3 Units (17 Samples). The composite curve is shown in red.



B.4.2 Diffusivity

It is assumed that the effective, large-scale diffusion coefficients for all HSUs are a function of volumetric moisture content, θ , and can be estimated based on an empirical relation (“Permeability of Porous Solids” [Millington and Quirk 1961]):

$$D_e(\theta) = D_0 \frac{\theta^{10/3}}{\theta_s^2} \quad (\text{B-4})$$

RPP-ENV-58782, Rev. 0

1 where $D_e(\theta)$ is the effective diffusion coefficient of an ionic species, and D_0 is the effective
2 diffusion coefficient for the same species in free water. The molecular diffusion coefficient for
3 all species in pore water is assumed to be 2.5×10^{-5} cm²/sec (WHC-SD-WM-EE-004,
4 “Performance Assessment of Grouted Double-Shell Tank Waste Disposal at Hanford”).

5 6 **B.4.3 Vadose Zone Macrodispersivities**

7
8 Field-scale dispersivities are referred to as macrodispersivities. The terms macrodispersivity and
9 dispersivity are used interchangeably in this section. Readers can go directly to Section B.4.3.4
10 for the macrodispersivity values recommended for WMA C PA calculations. Details on how the
11 selections are made using different methods are provided in Section B.4.3.1 (Numerical
12 Simulations), Section B.4.3.2 (Stochastic Theory) and Section B.4.3.3 (Experimental
13 Observations).

14
15 Field observations indicate that the dispersion coefficients required to describe the large-scale
16 transport processes, at field scales of tens or hundreds of meters, are much different from those
17 observed in small-scale laboratory experiments (Gelhar 1993). In fact, field-scale dispersivities
18 may often be orders of magnitude larger than those observed in the laboratory. Consequently,
19 laboratory-scale dispersivities, which are typically ~1 cm or less, are of little use in estimating
20 field-scale dispersivities.

21
22 There is general agreement in hydrology literature that hydraulic conductivity variations induced
23 by field-scale heterogeneities play an important role in field-scale transport processes. However,
24 there does not appear to be a clear consensus about how best to describe such processes
25 quantitatively (Gelhar 1993). While well-designed, large-scale tracer experiments would provide
26 useful information, limited field data are available at this time to quantify macrodispersivities in
27 unsaturated media.

28
29 Dispersivities are a function of matric potential (or soil moisture content) in unsaturated media
30 (Mantoglou and Gelhar 1987). As with saturated media, heterogeneities that exist at various
31 length scales result also in a scale dependence of macrodispersivities in unsaturated media
32 (“A Critical Review of Data on Field-Scale Dispersion in Aquifers” [Gelhar et al. 1992]).
33 Dispersivities increase with time, or equivalently with distance, until they tend to converge on
34 their unique asymptotic (large-time) values. However, it can take a long time (e.g., years or
35 decades) for the asymptotic Fickian approximation to take hold. Nonetheless, the
36 second-moment evolution or the time-dependent, preasymptotic dispersivities are of marginal
37 interest in simulations involving long-times or large-mean travel distances such as those in the
38 WMA C PA modeling. This well-known behavior is usually attributed to heterogeneity-induced
39 spreading and mixing until the point at which all of the heterogeneity has effectively been
40 “sampled” by the contaminant plume such that dispersion becomes constant. The use of a
41 constant (asymptotic) macrodispersivity is thus considered appropriate in PA simulations
42 (NUREG/CR-6114, Auxiliary Analyses in Support of Performance Assessment of a
43 Hypothetical Low-Level Waste Facility: Groundwater Flow and Transport Simulation, Vol. 3;
44 NUREG/CR-5965, Modeling Field Scale Unsaturated Flow and Transport Processes).

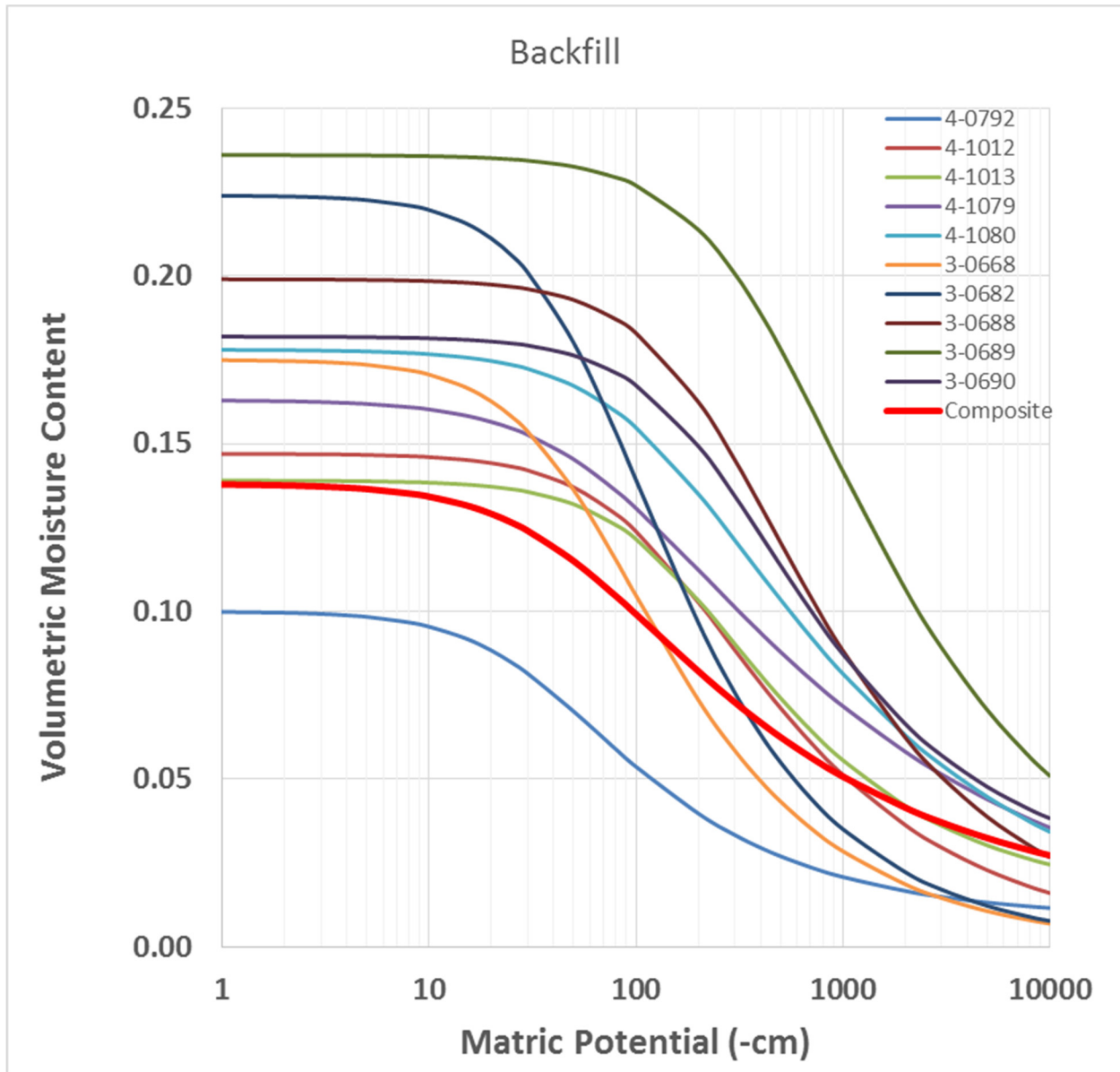
Table B-6. van Genuchten Parameters, Fitted Saturated Hydraulic Conductivity, and Measured Bulk Density Data for Backfill Unit (10 Samples).

Sample	Site	Borehole Number	Depth (m)	Percent Gravel	θ_s (cm ³ /cm ³)	θ_r (cm ³ /cm ³)	α (1/cm)	n (-)	Fitted K _s (cm/s)	Bulk Density (g/cm ³)
4-0792	ERDF	699-35-65A	75.4	71	0.100	0.0084	0.03	1.5858	3.42E-04	2.32
4-1012	ERDF	699-35-69A	73.9	55	0.147	0	0.0076	1.5109	4.50E-05	2.19
4-1013	ERDF	699-35-69A	77.9	65	0.139	0.0127	0.0065	1.5656	1.06E-06	2.20
4-1079	ERDF	699-35-61A	90.9	61	0.163	0	0.014	1.3079	1.18E-04	2.06
4-1080	ERDF	699-35-61A	93.5	43	0.178	0	0.0074	1.3819	8.11E-06	2.00
3-0668	241-T-106	299-W10-196	38.9	62	0.175	0	0.0192	1.6124	1.63E-04	2.13
3-0682	241-T-106	299-W10-196	46.1	51	0.224	0	0.0166	1.6577	2.37E-04	2.14
3-0688	241-T-106	299-W10-196	48.5	49	0.199	0	0.0043	1.5321	2.60E-05	2.17
3-0689	241-T-106	299-W10-196	52.2	28	0.236	0	0.0025	1.4747	4.58E-05	1.93
3-0690	241-T-106	299-W10-196	53.7	53	0.1819	0.0177	0.0046	1.541	4.19E-05	2.19

ERDF = Environmental Restoration Disposal Facility

RPP-ENV-58782, Rev. 0

Figure B-20. Moisture Retention Data for Backfill Unit (10 Samples).
The composite curve is shown in red.



Note that, because of the relatively dry moisture regime, unsaturated media macrodispersivity estimates are expected to be smaller, compared to saturated media estimates. Below, a range of estimates on the basis of numerical simulations (Section B.4.3.1), stochastic theory (Section B.4.3.2) and experimental observations (Section B.4.3.3) is provided. To obtain macrodispersivity, the local pore-scale dispersivities, which are typically small (<1 cm), are not included either in numerical simulations or stochastic solutions. This is consistent with the approach used by other investigators ("Stochastic analysis of adsorbing solute transport in three-dimensional, heterogeneous, unsaturated soils" [Yang et al. 1997]; Gelhar 1993; "Three-Dimensional Stochastic Analysis of Macrodispersion in Aquifers" [Gelhar and Axness 1983]).

Figure B-21. Unsaturated Hydraulic Conductivity Data for Backfill Units (10 Samples).
The composite curve is shown in red.

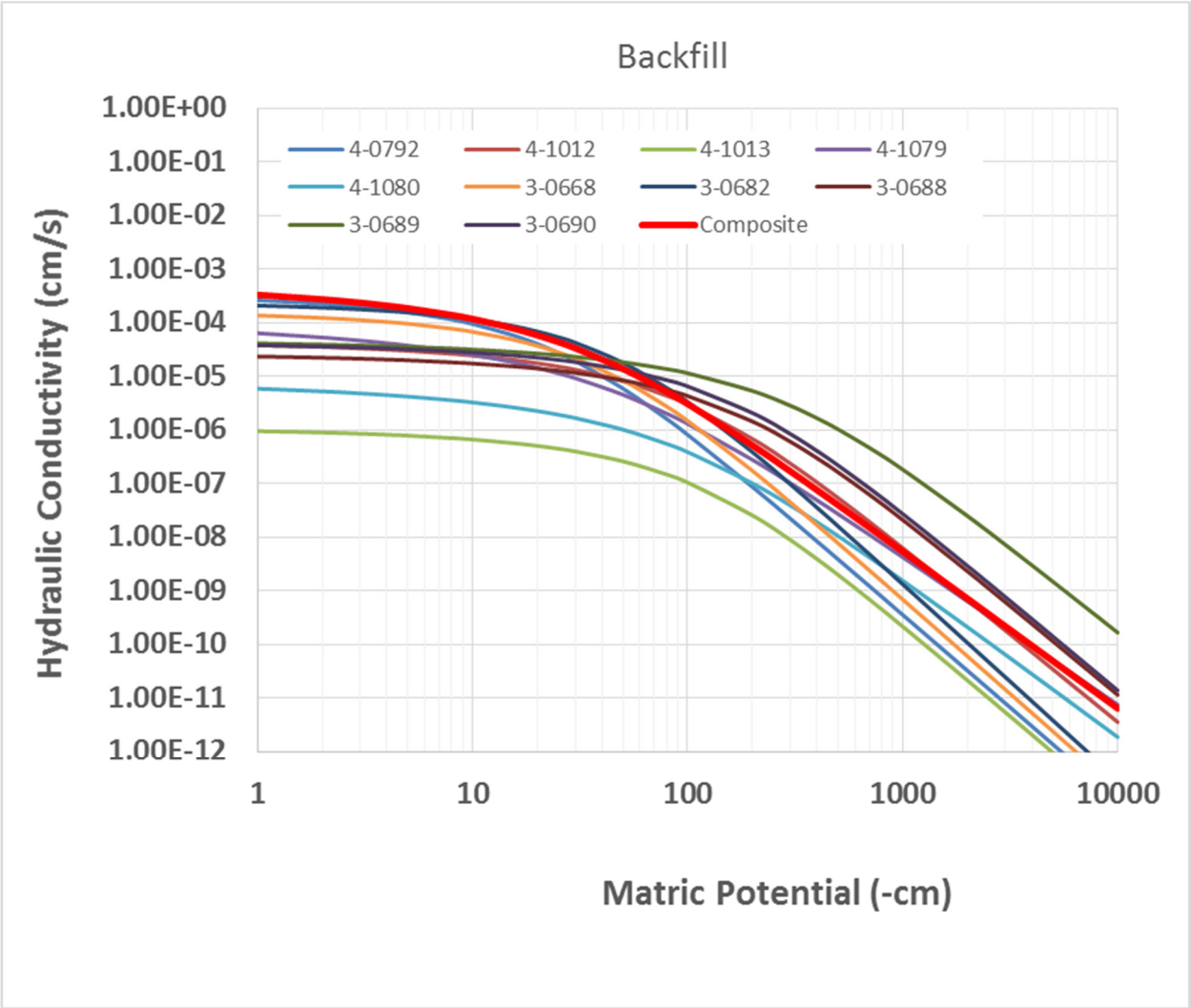


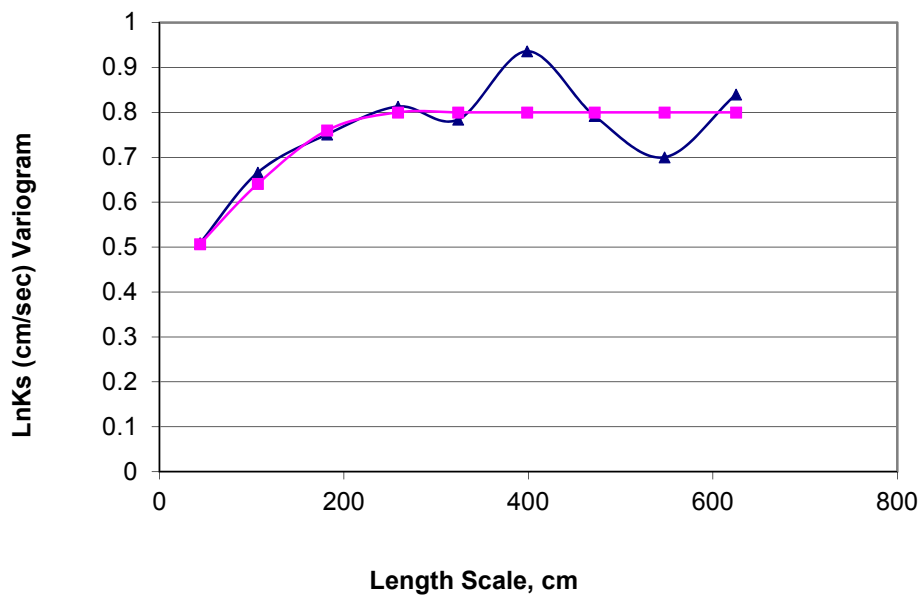
Table B-7. Composite van Genuchten-Mualem Parameters for Waste Management Area C Hydrostratigraphic Units.

Hydrostratigraphic Unit	Number of samples	θ_s	θ_r	α (1/cm)	n	ℓ	Fitted K_s (cm/s)
Backfill Gravelly Unit	10	0.138	0.010	0.021	1.374	0.5	5.60E-04
H1 and H3 Gravelly Units	15	0.171	0.011	0.036	1.491	0.5	7.70E-04
H2 Sand-Dominated Unit	44	0.315	0.0392	0.0631	2.047	0.5	4.15E-03

RPP-ENV-58782, Rev. 0

Table B-8. Simulated Average Tension Ranges for Polmann Anisotropy Model.

Hydrostratigraphic Unit	Simulated Average Tension (cm)
Backfill Gravelly Unit	400 – 750
H1 and H3 Gravelly Units	150 – 400
H2 Sand-Dominated Unit	80 – 300

Figure B-22. Experimental (Triangles) and Fitted Theoretical (Squares) Variogram for Saturated Hydraulic Conductivity ($\ln K_s$).

Reference: RPP-20621, "Far-Field Hydrology Data Package for the Integrated Disposal Facility Performance Assessment."

Table B-9. Variable, Macroscopic Anisotropy Parameter Estimates for Various Waste Management Area C Units.

Hydrostratigraphic Unit	Number of samples	$\langle \ln K_s \rangle$	$\sigma_{\ln K_s}^2$	p	ζ	λ (cm)	A
Backfill Gravelly Unit	10	-14.60	2.98	-2.28E-04	3.53E-04	30	0.00534
H1 and H3 Gravelly Units	17	-12.34	1.41	1.04E-03	2.68E-03	30	0.01249
H2 Sand-Dominated Unit	44	-11.79	2.50	-7.45E-04	3.33E-03	50	0.02415

RPP-ENV-58782, Rev. 0

Figure B-23. Calculated Macroscopic Anisotropy as a Function of Mean Matric Potential for the H2 Sand-Dominated Unit.

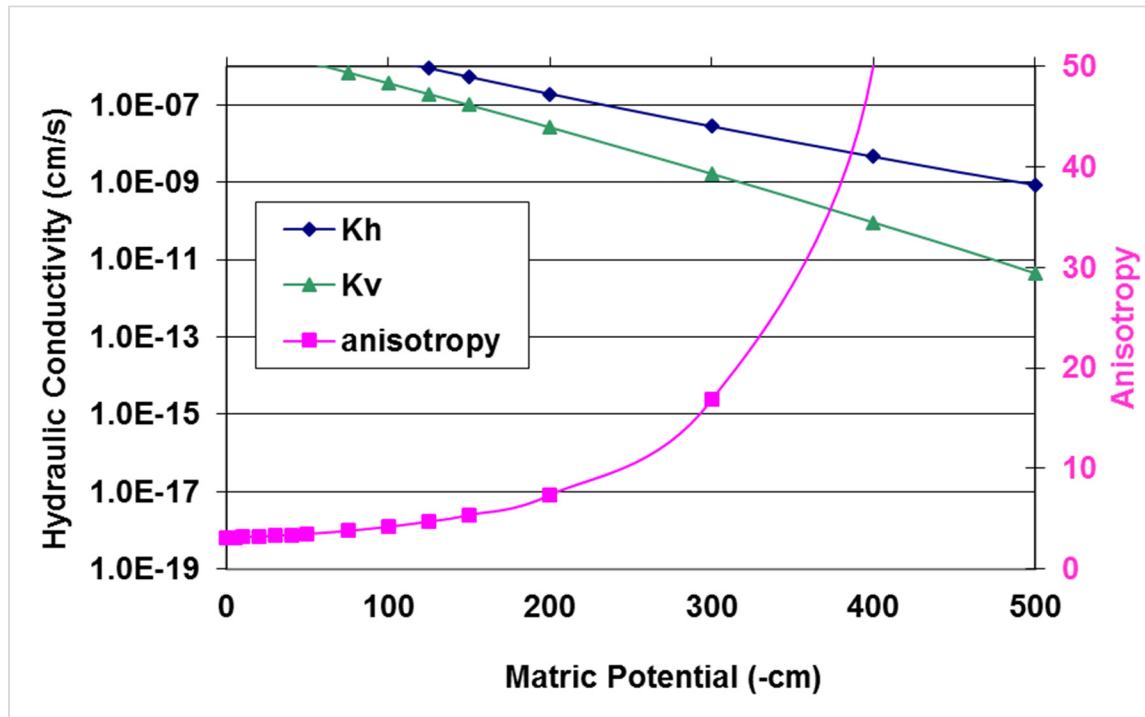
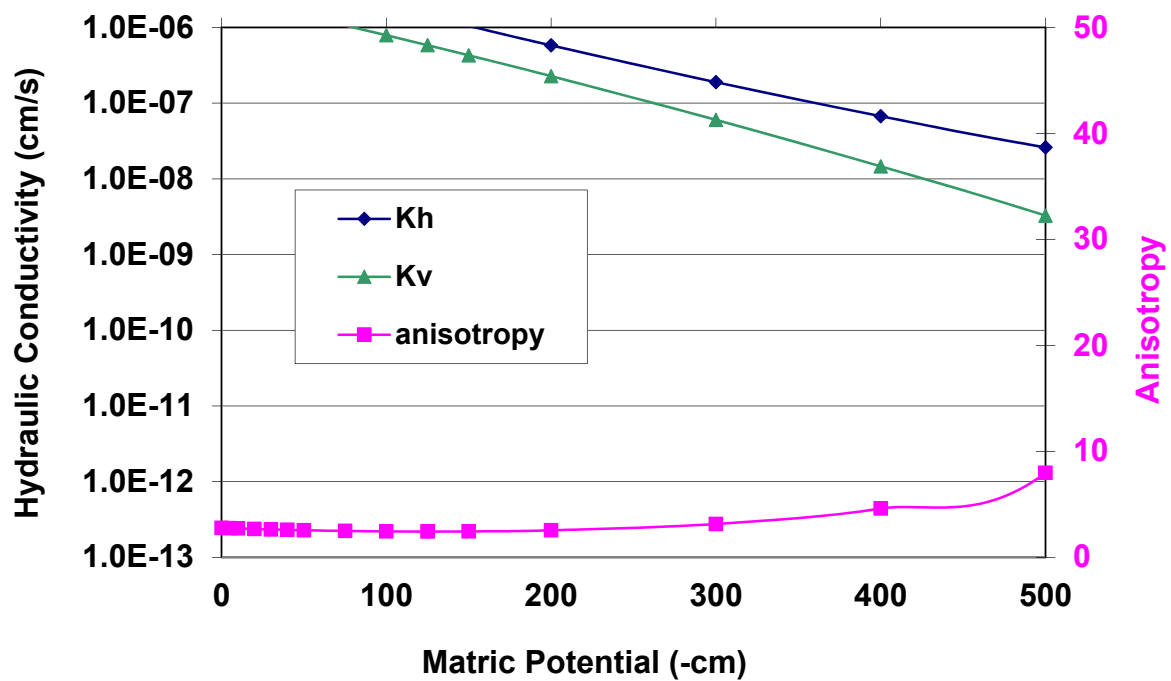


Figure B-24. Calculated Macroscopic Anisotropy as a Function of Mean Matric Potential for the H1 and H3 Gravelly Units.



RPP-ENV-58782, Rev. 0

Figure B-25. Calculated Macroscopic Anisotropy as a Function of Mean Matric Potential for Backfill Gravelly Unit.

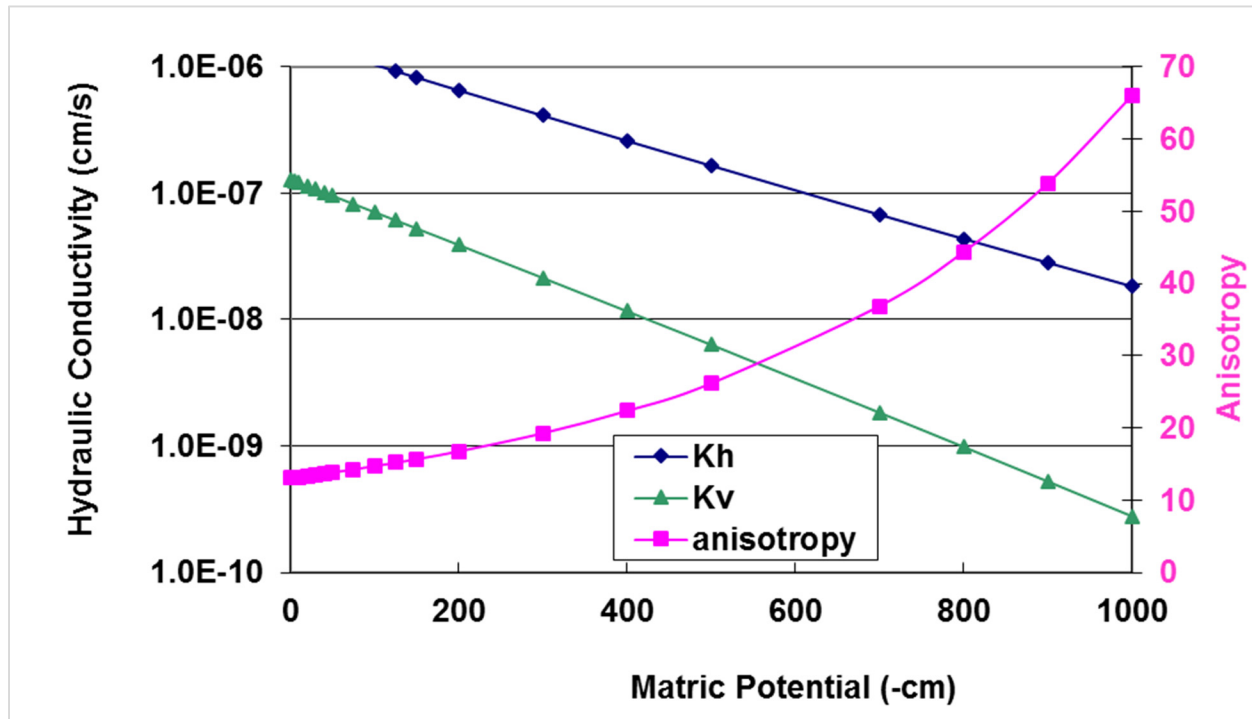


Table B-10. Effective Bulk Density (g/cm³) Estimates for Waste Management Area C Hydrostratigraphic Units.

Hydrostratigraphic Unit	E[ρ_b]*
Backfill Gravelly Unit	2.13
Hanford H2 Sand-dominated Unit	1.71
Hanford H1 and H3 Gravelly Units	2.05

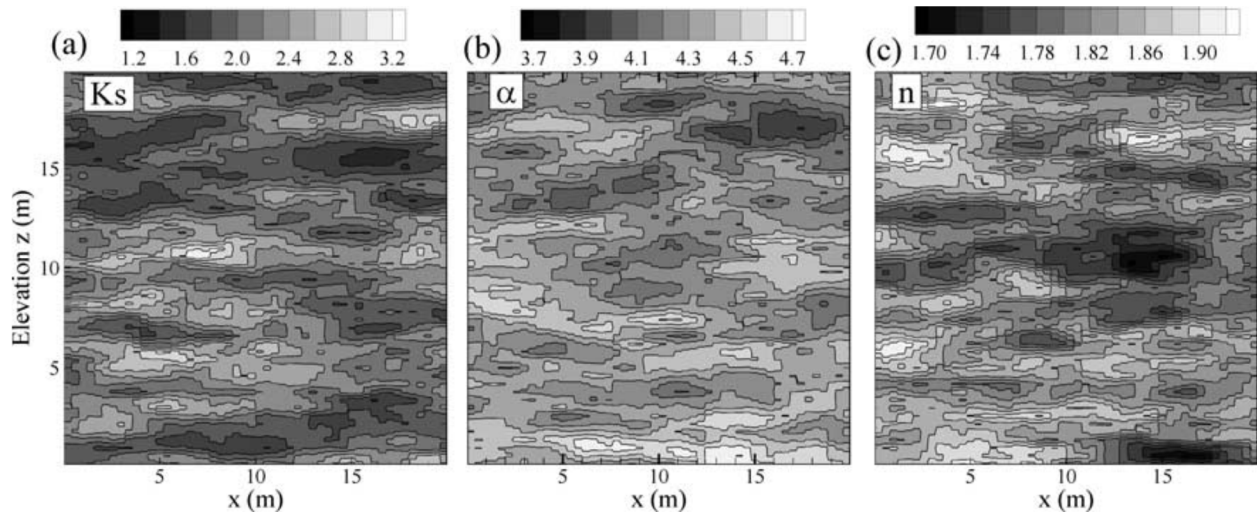
*E = Expectation.

B.4.3.1 Numerical Simulations. Details of the numerical simulation approach are described in Khaleel et al. (2002). Briefly, Monte Carlo (MC) simulations are used to obtain upscaled (effective) properties. The simulations mimic steady state, gravity infiltration for 50 realizations in two-dimensional (20 m \times 20 m) heterogeneous flow regions. Constitutive relations for unsaturated media at the mesh-size scale are based on the van Genuchten-Mualem relationships. A realization of the flow field is shown in Figure B-26. The sediment properties are based on laboratory measurements of moisture retention and unsaturated K for coarse-textured sandy samples from the upper Hanford formation (HNF-4769, “Far-Field Hydrology Data Package for Immobilized Low-Activity Tank Waste Performance Assessment”); these data show somewhat less variability when compared to the 44 Hanford formation H2 samples discussed earlier. A unit-mean-gradient approach is used to derive upscaled properties for flow perpendicular to

RPP-ENV-58782, Rev. 0

bedding. For a specified infiltration rate, the simulated pressure head distributions for 50 realizations are averaged to yield a mean pressure head, H . Because the simulated flow field is under a unit mean gradient condition, the infiltration rate is equal to the effective conductivity at the calculated H .

Figure B-26. (a) K_s , (b) α , and (c) n Random Distribution for a Single Realization.



Reference: "Upscaled Flow and Transport Properties for Heterogeneous Unsaturated Media" (Khaleel et al. 2002).

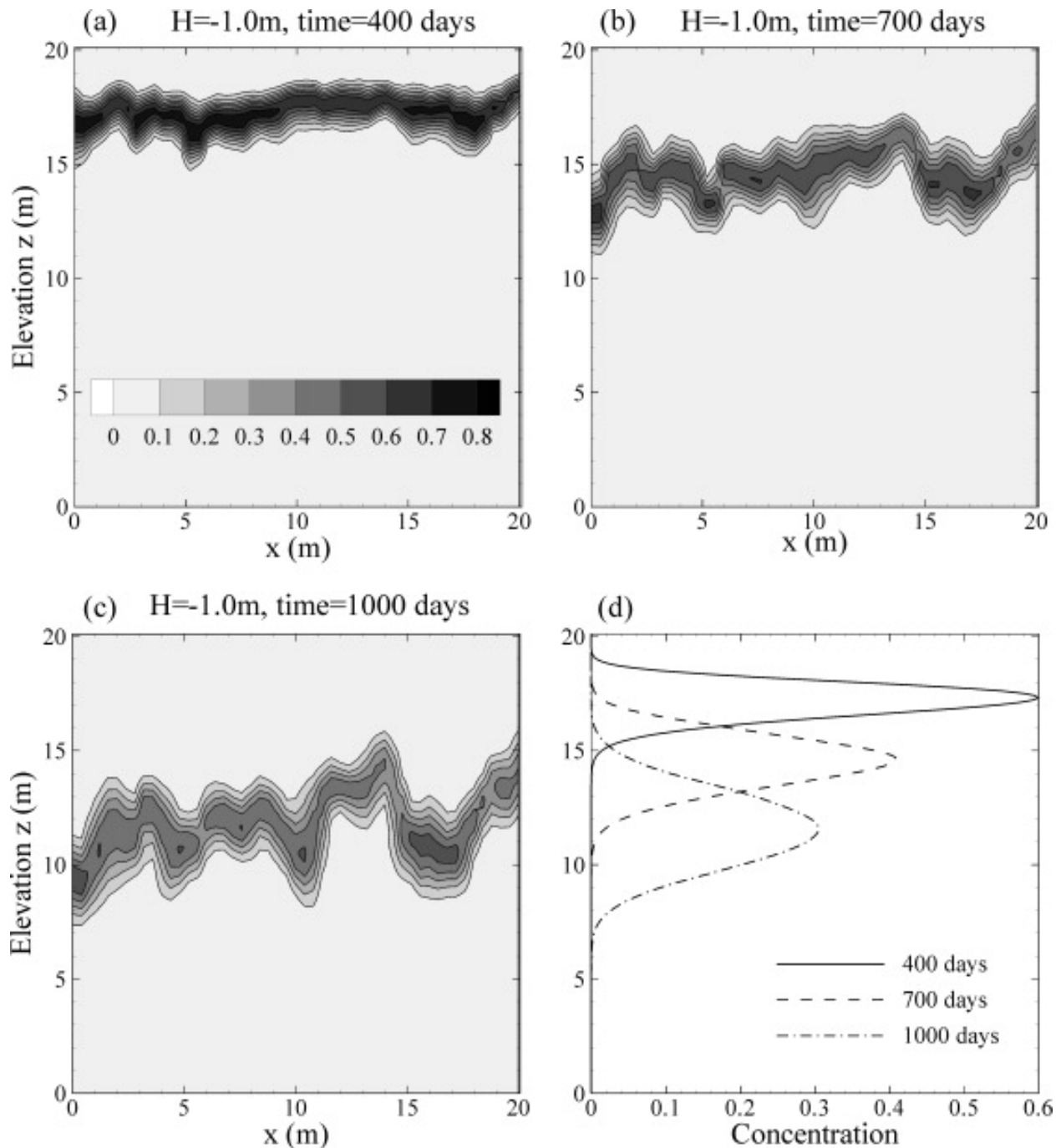
Following flow simulations, macrodispersivities are calculated on the basis of spatial moments of the ensemble-mean plume (Khaleel et al. 2002). For a given steady flow and a prescribed flux, the migration and spread of a slug of simulated tracer is simulated. Snapshots are taken of the two-dimensional plume distribution at different times. The snapshot at each sampling time is then averaged over the length across the flow domain to obtain the solute concentration profiles as a function of depth. The concentration profiles for all realizations are averaged to obtain the ensemble mean profile; these profiles are then used to evaluate their spatial moments. The calculated second spatial moment of the plume about the center of mass (i.e., spatial variance) over time allows estimation of the longitudinal macrodispersivity.

Figures B-27a, B-27b and B-27c are snapshots, for a mean pressure head of -1.0 m, of the simulated plume for a single realization and for flow perpendicular to bedding at 400, 700, and 1,000 days after simulating the release of a conservative tracer across the top boundary of a mildly heterogeneous media (Figure B-26). The averaged concentration profiles for the flow regime and for the corresponding sampling times are illustrated in Figure B-27d. Bedding perpendicular to flow direction enhances lateral mixing and prevents growth of irregular flow paths. Consequently, the averaged concentration profiles for flow perpendicular to bedding (Figure B-27d) exhibit the typical bell-shaped distribution as described by the classical Fickian advection-dispersion equation. The computed longitudinal macrodispersivity for a mean pressure head (H) of -2 m was ~25 cm, ranging from ~15 cm to ~40 cm for the 50 realizations. On the other hand, for a mean H of -20 m, the macrodispersivity was ~100 cm, ranging from ~70 cm to ~130 cm for the 50 realizations. As the MC simulations indicate, considerable variability in longitudinal macrodispersivity estimates is expected depending on the mean matric potential. Nonetheless, results show a clear dependence of longitudinal macrodispersivity on the

RPP-ENV-58782, Rev. 0

1 moisture regime; longitudinal macrodispersivity estimates are higher for the drier moisture
 2 regime.

3
 4 **Figure B-27. Simulated Concentration Distribution for a Single Realization at (a) 400 days,**
 5 **(b) 700 days, and (c) 1,000 days and (d) the Averaged Concentration Profile at Those Times**
 6 **for Flow Perpendicular to Bedding for a Mean Pressure Head (H) of -1 m.**
 7



8
 9 Reference: "Upscaled Flow and Transport Properties for Heterogeneous Unsaturated Media" (Khaleel et al. 2002).
 10

RPP-ENV-58782, Rev. 0

To evaluate directional dependence, simulations were also run for flow parallel to geologic bedding for the same flow domain. Figures B-28a, B-28b, and B-28c are snapshots of the plume at identical times for flow parallel to bedding for the same realization and for $H=-1$ m; Figure B-28d shows the averaged profile. A comparison of Figures B-27 and B-28 shows that the two-dimensional concentration distribution is more irregular in case of flow parallel to bedding than for flow perpendicular to bedding (Figures B-28a, B-28b, and B-28c versus Figures B-27a, B-27b, and B-27c). Compared with flow perpendicular to bedding, the concentration profiles for flow parallel to bedding are highly skewed and characterized by multiple peaks, and spread out over greater distances, characteristics of a non-Fickian behavior. Thus, while the averaged concentration profiles for flow perpendicular to bedding show “textbook like” Fickian behavior, the averaged profiles for flow parallel to bedding are highly skewed and non-Fickian. At $H=-2$ m, the computed longitudinal macrodispersivity for flow parallel to bedding is considerably higher (~ 120 cm) than for flow perpendicular to bedding (~ 25 cm). For a mean H of -20 m, the macrodispersivity is ~ 180 cm for flow parallel to bedding versus ~ 100 cm for flow perpendicular to bedding.

In summary, the numerical results for Hanford H2 sands having mild heterogeneity (HNF-4769) show that the longitudinal dispersivities for flow parallel to bedding are higher than those for flow perpendicular to bedding (Khaleel et al. 2002). For both perpendicular and parallel to bedding, macrodispersivities increase as the mean matric potential becomes more negative. However, the Fickian regime is reached much earlier for cases with flow perpendicular to bedding than parallel to bedding (Khaleel et al. 2002). For WMA C PA modeling, the flow is mostly perpendicular to geologic bedding; nonetheless, the preceding analysis provides estimates in situations where the flow is not necessarily perpendicular to bedding.

B.4.3.2 Stochastic Models. For unsaturated media, in addition to the size of flow domain and media heterogeneities, macrodispersivities are expected to be a function of soil moisture content (or matric potential). Furthermore, as demonstrated via preceding MC simulations, macrodispersivities are larger for flow parallel to bedding than for flow perpendicular to bedding. The following describes two stochastic models to estimate WMA C longitudinal macrodispersivities for flow perpendicular to the geologic bedding.

B.4.3.2.1 Mantoglou Model. Using spectral perturbation techniques (Gelhar and Axness 1983; Gelhar 1993), an approximate equation was derived for macrodispersivities in unsaturated media for flow perpendicular to bedding (“Large-Scale Models of Transient Unsaturated Flow and Contaminant Transport Using Stochastic Methods” [Mantoglou 1984]). Mantoglou showed that the asymptotic value of tension-dependent longitudinal macrodispersivity, A_{\perp} under unit mean gradient condition, for flow perpendicular to bedding, is

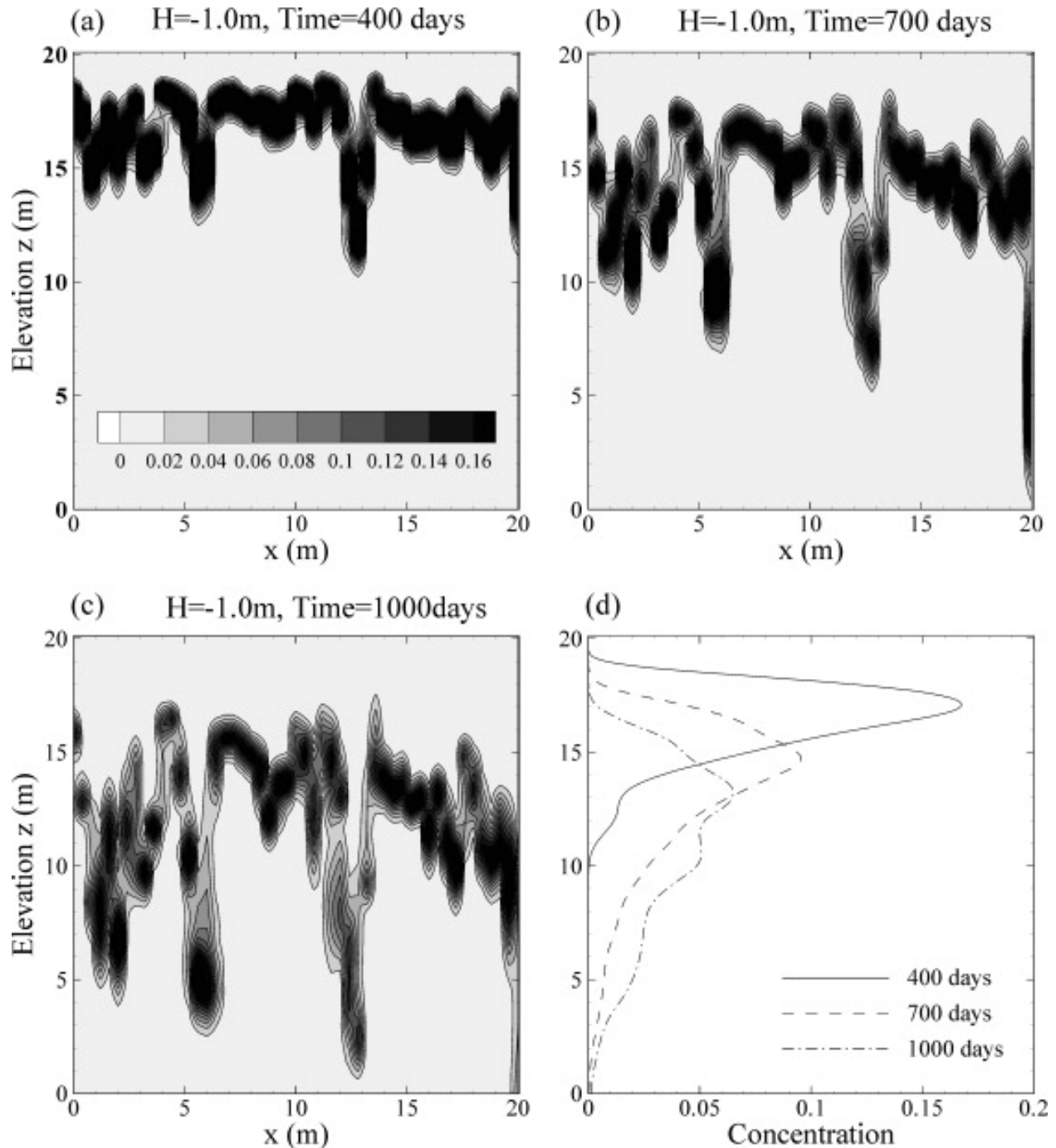
$$A_{\perp}(H) = \frac{\sigma_{\ln K_u}^2 \lambda_u}{\gamma^2} \quad (\text{B-5})$$

where A_{\perp} depends on the mean pressure head H , $\sigma_{\ln K_u}^2$ is the variance in log unsaturated K , λ_u is the correlation length scale for unsaturated hydraulic conductivity, and γ is a flow factor that

RPP-ENV-58782, Rev. 0

depends on the direction of mean flow and the orientation of heterogeneity (Gelhar and Axness 1983).

Figure B-28. Simulated Concentration Distribution for a Single Realization at (a) 400 days, (b) 700 days, and (c) 1,000 days and (d) the Averaged Concentration Profile at Those Times for Flow Parallel to Bedding for a Mean Pressure Head (H) of -1 m.



Reference: "Upscaled Flow and Transport Properties for Heterogeneous Unsaturated Media" (after Khaleel et al. 2002).

RPP-ENV-58782, Rev. 0

Equation B-5 represents the asymptotic macrodispersivity estimate for steady-state uniform flow with uniform mean tension. Because macrodispersivity modeled by Equation B-5 is an asymptotic parameter, it applies only when the concentration plume has traveled a large distance in a geologic unit and has encountered numerous heterogeneities in the formation. Furthermore, it is important to note that similar to other stochastic perturbation approaches (Gelhar 1993), the validity of Equation B-5 relies on the variance of hydraulic properties being relatively small (i.e., $\sigma_{LnK_u}^2 < 1$).

Mantoglou (1985; Figure 5.9) presents longitudinal macrodispersivity estimates, based on Equation B-5, for Maddock sandy loam ("Spatial Variability of in Situ Unsaturated Hydraulic Conductivity of Maddock Sandy Loam" [Carvallo et al. 1976]) and Panoche silty clay loam ("Spatial Variability of Field-Measured Soil-Water Properties" [Nielsen et al. 1973]) soil types. Mantoglou results show considerable variability even for mild tensions. Based on the Mantoglou model (Equation B-5), for Maddock soil type, the asymptotic longitudinal macrodispersivity was 2.4 m at a mean tension of 50 cm. For Panoche soil type, the estimate was 0.8 m at a mean tension of 300 cm.

B.4.3.2.2 Russo Model. Using the Lagrangian framework in conjunction with the Yeh et al (1985) velocity covariance, theoretical expressions were developed for evolution of contaminant plume spatial moments in unsaturated heterogeneous media under steady-state conditions ("Stochastic Analysis of Simulated Vadose Zone Solute Transport in a Vertical Cross Section of Heterogeneous Soil During Nonsteady Water Flow" [Russo 1991]). The spatial moments were then used to assess the preasymptotic evolution of macrodispersivity.

$$A_{zz}(t) = \sigma_{LnK_u}^2 \lambda_u \{1 - 3(2\tau)^{-1} - 3(\tau)^{-2} \exp(-\tau) + 3(\tau)^{-3} [1 - \exp(-\tau)]\} \quad (B-6)$$

where A_{zz} is the longitudinal macrodispersivity (i.e., similar to A_{\perp}), z denotes vertical direction, t is time, λ_u is vertical correlation length, and $\tau = z_c(t) / \lambda_u$. The unsaturated conductivity variance $\sigma_{LnK_u}^2$ was derived by Russo (1991) using the Gardner (1958) exponential model for unsaturated conductivity. At large times, $\tau \rightarrow \infty$; the longitudinal asymptotic macrodispersivity is therefore

$$A_{zz}(\infty) = \sigma_{LnK_u}^2 \lambda_u. \quad (B-7)$$

Note that this is the same as Mantoglou Equation B-5 without the flow factor γ in the denominator. For hypothetical vadose zone flow domains having $\sigma_{LnK_u}^2 = 0.29$ and extending 15 m and 10 m in the horizontal and vertical directions, respectively, and a correlation length of 0.12 m in the vertical direction, Russo (1991) computed an asymptotic longitudinal macrodispersivity (Equation B-7) of 3.48 cm. As discussed later, the conductivity variance of 0.29 is, however, much smaller compared to variance for Hanford H2 unsaturated conductivity data.

RPP-ENV-58782, Rev. 0

B.4.3.2.3 Stochastic Theory-Based Macrodispersivity Estimates for Waste Management

Area C. To apply stochastic Equations B-5 and B-7, an estimate of λ_u for unsaturated K is needed. As discussed earlier, a correlation length of the order of 50 cm was used for saturated conductivity. However, as saturation decreases, an increase in the variance of log unsaturated conductivity is accompanied by a decrease in the correlation scale of log unsaturated K (“Stochastic Modeling of Macrodispersion for Solute Transport in a Heterogeneous Unsaturated Porous Formation” [Russo 1993]). Also, the Equation B-5 flow factor γ (Mantoglou 1984) in a predominantly vertical unsaturated flow through a layered system would be less than 1; it is approximately the ratio of the harmonic and geometric means of unsaturated K (Gelhar 1993; Gelhar and Axness 1983). Assuming a correlation length of 10 cm (approximate measurement scale for small-scale unsaturated K measurements), and γ estimates based on the ratio of the harmonic and geometric means (Khaleel et al. 2002), for H2 sands, Mantoglou’s model yields asymptotic macrodispersivity estimates, for flow perpendicular to bedding, that are ~360 cm at relatively low tensions of ~2 m. For the Russo (1991) model (Equation B-7), at ~2 m tension, the asymptotic longitudinal macrodispersivity for H2 sands is ~32 cm. Note that the MC simulations (Khaleel et al. 2002) yielded a longitudinal macrodispersivity of ~25 cm for flow perpendicular to bedding and for H=-2m. However, the favorable comparison with Russo’s

model is coincidental since σ_{LnK}^2 and mean tension values are different.

Reported values have a relatively low tension of 2 m because of the limitation of low perturbation for stochastic models. The variance σ_{LnKu}^2 in Equation B-5 becomes rather large for H2 sands; at a mean tension of 1 m, σ_{LnKu}^2 is about 1.96, whereas at a tension of 2 m, σ_{LnKu}^2 is about 4.73. Compared to H2 sands, σ_{LnKu}^2 for the H1/H3/Backfill gravelly units is significantly lower; at a mean tension of 150 cm, σ_{LnKu}^2 is about 1.22, whereas at a mean tension of 400 cm, σ_{LnK}^2 is about 2.02. Such variance results are consistent with the unsaturated K data reported earlier for sandy and gravelly samples (Figure B-17). Unsaturated K for gravelly samples fall within a narrow range, and well within the range of measured K for sandy samples. At a matric potential of -1 m, the unsaturated K for sandy samples ranges over four orders of magnitude, whereas the unsaturated K for gravelly samples ranges over two orders of magnitude (Figure B-17).

B.4.3.3 Experimental Data from 200 Areas and Other Sites. Field experiments were conducted at a location in 200 East Area, using potassium chloride as a tracer (RPP-20621 Appendix E, “Hanford Low-Activity Tank Waste Performance Assessment Activity: Determination of in Situ Hydraulic Parameters of the Upper Hanford Formation”). Analysis of the data, using moment analysis, provided dispersivities that ranged from 1.3 cm to 7.8 cm for travel distances ranging from 25 cm to 125 cm. Although these estimates are for the Hanford formation, the transport distance within the vadose zone is indeed of limited extent. Nonetheless, results based on the limited data are consistent with the concept of a scale-dependent dispersivity; it is expected that the asymptotic value will be larger than those based on the small-scale tracer experiment. In fact, extrapolation of the trend line for the data (RPP-20621 Appendix E) suggests that an asymptotic dispersivity estimate of ~1 m is not

RPP-ENV-58782, Rev. 0

unlikely if the heterogeneity at the field site is similar to that of the sandy sediments underlying C Farm, and if the entire sandy sequence of the Hanford formation is treated as EHM.

In addition to the preceding data, results of artificial tracer experiments are available from several arid/semi-arid regions. Two massively instrumented solute transport experiments were performed in desert soils near Las Cruces, New Mexico ("The Las Cruces Trench Site: Characterization, Experimental Results, and One-Dimensional Flow Predictions" [Wierenga et al. 1991]; "The Second Las Cruces Trench Experiment: Experimental Results and Two-Dimensional Flow Predictions" [Hills et al. 1991]). Drip emitters were used to irrigate a plot adjoining a deep trench in heterogeneous media, with well in excess of one order of magnitude standard deviation in saturated hydraulic conductivity. Monitoring of the trench face showed a spatially uniform progression of the wetting front and did not reveal indications of preferential flow (Wierenga et al. 1991). Hills et al. (1991) found that a dispersivity of 5 cm provided reasonably realistic simulations of tritium and bromine tracer distributions.

One additional study ("Chlorine 36 and Tritium From Nuclear Weapons Fallout as Tracers for Long-Term Liquid and Vapor Movement in Desert Soils" [Phillips et al. 1988]) assessed the degree of mixing in desert soils using the conventional advection-dispersion modeling, yielding a dispersion coefficient of 50 cm²/yr. This compares with the calculated effective diffusion coefficient of 25 cm²/yr. A similar study ("Evaluation of Liquid and Vapor Water Flow in Desert Soils Based on Chlorine 36 and Tritium Tracers and Nonisothermal Flow Simulations" [Scanlon 1992]) at another southwestern arid site obtained a dispersion coefficient of about 14 cm²/yr. These, then, lead to effective dispersivities of about 7 cm and 4 cm at the two arid sites, and Peclet numbers (displacement divided by dispersivity) of 23 and 17. In summary, long-term environmental tracer studies at several arid southwestern sites indicate vadose zone dispersivities being less than 10 cm.

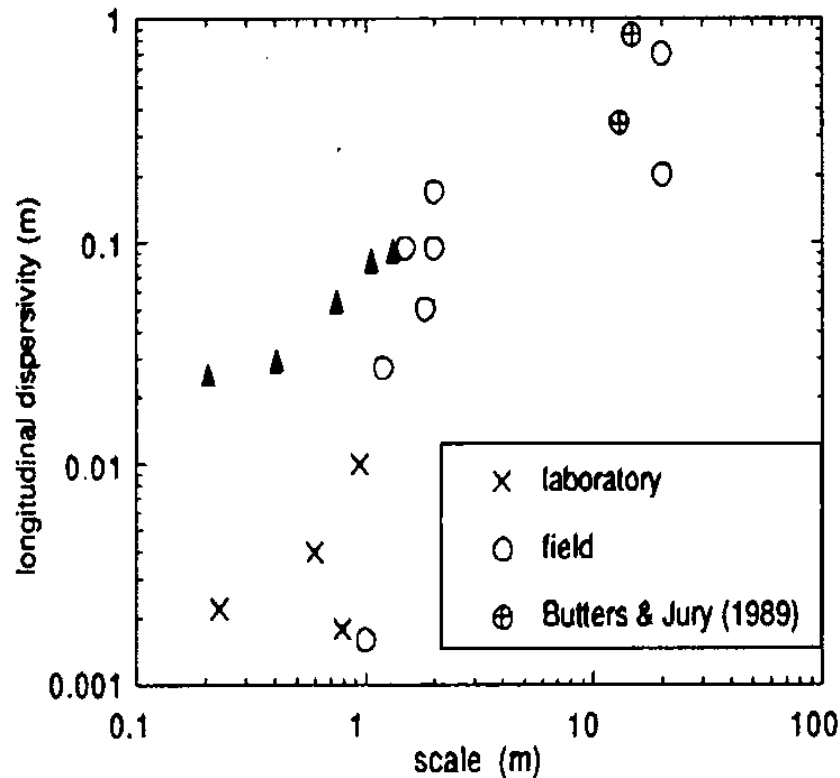
Based on a different survey of literature, Gelhar (1993) presented the longitudinal vadose zone dispersivities as a function of the scale of the experiment (Figure B-29). The figure shows sparse data for scales larger than 2 m. Nonetheless, similar to saturated flow (Gelhar et al. 1992), Figure B-29 shows an increase of dispersivity with an increase in scale. Also, shown in Figure B-29 are results of the 200 East Area field experiment (RPP-20621 Appendix E); the trend line dispersivity estimate at a field scale of ~10 m is in close agreement with "Field Scale Transport of Bromide in an Unsaturated Soil, 2. Dispersion Modeling" (Butters and Jury 1989) field data.

B.4.3.4 Recommended Macrodispersivities for Waste Management Area C Performance Assessment. Table B-11 summarizes the macrodispersivity estimates based on results of numerical simulation, stochastic theory, and 200 Areas experimental data. Table B-11 shows that, for H2 sands, estimates are available by all three methods. For the H2 sand unit, for the PA modeling, the recommendation is to use longitudinal macrodispersivity values ranging from 25 cm (based on numerical simulations) to 100 cm (based on field experiments). For H1/H3/Backfill sediments, the recommendation is to use, based on stochastic theory, longitudinal macrodispersivity values ranging from 20 cm to 100 cm. The transverse macrodispersivity is typically much lower; in saturated media, it may range from 1 to 10% of the longitudinal macrodispersivity (Gelhar and Axness 1983). In the absence of unsaturated media

RPP-ENV-58782, Rev. 0

experimental data, the recommendation is to use a transverse macrodispersivity 1/10th of the longitudinal macrodispersivity.

Figure B-29. Longitudinal Laboratory- and Field-Scale Dispersivities in Unsaturated Media as a Function of Overall Problem Scale.



Note: The triangles are data from RPP-20621, "Far-Field Hydrology Data Package for the Integrated Disposal Facility Performance Assessment," Appendix E, "Hanford Low-Activity Tank Waste Performance Assessment Activity: Determination of In Situ Hydraulic Parameters of the Upper Hanford Formation."

References:

"Field Scale Transport of Bromide in an Unsaturated Soil, 2. Dispersion Modeling" (Butters and Jury 1989).
Stochastic Subsurface Hydrology (Gelhar 1993).

RPP-ENV-58782, Rev. 0

Table B-11. Longitudinal Macrodispersivity Estimates (cm).

Hydrostratigraphic Unit	Numerical Simulation	Stochastic Theory (Russo and Mantoglou Equations 5 and 7)	200 Area Field Experiments
H2 Sand-Dominated Unit	25	$\sim 32^a - 360^a$	$\sim 100^c$
H1, H3, and Backfill Gravelly Units	NA	$\sim 20^b - 100^b$	NA

^aEvaluated at a mean tension of 2 m.^bEvaluated at a mean tension of 4 m.^cExtrapolated experimental data (RPP-20621, “Far-Field Hydrology Data Package for the Integrated Disposal Facility Performance Assessment,” Appendix E, “Hanford Low-Activity Tank Waste Performance Assessment Activity: Determination of In Situ Hydraulic Parameters of the Upper Hanford Formation”).

NA = Not Available

References:

“Large-Scale Models of Transient Unsaturated Flow and Contaminant Transport Using Stochastic Methods” (Mantoglou 1984).

“Stochastic Analysis of Simulated Vadose Zone Solute Transport in a Vertical Cross Section of Heterogeneous Soil During Nonsteady Water Flow” (Russo 1991).

B.5 REFERENCES

Butters, G. L., and W. A. Jury, 1989, “Field Scale Transport of Bromide in an Unsaturated Soil, 2. Dispersion Modeling,” *Water Resources Research*, Vol. 25, No. 7, pp. 1583–1589.

Carvallo, H. O., D. K. Cassel, J. Hammond, and A. Bauer, 1976, “Spatial Variability of in Situ Unsaturated Hydraulic Conductivity of Maddock Sandy Loam,” *Soil Science*, Vol. 121, pp. 1–8.

Eching, S. O. and J. W. Hopmans, 1993, “Optimization of Hydraulic Functions from Transient Outflow and Soil Water Pressure Data,” *Soil Science Society of America Journal*, Vol. 57, No. 5, pp. 1167–1175.

EPA/600/2-91/065, 1991, The RETC Code for Quantifying the Hydraulic Functions of Unsaturated Soils, Office of Research and Development, U.S. Environmental Protection Agency, Washington, D.C.

Gardner, W. H., 1986, “Water Content,” in *Methods of Soils Analysis, Part 1—Physical and Mineralogical Methods*, pp. 493–544, American Society of Agronomy-Soil Science Society of America, Madison, Wisconsin.

Gardner, W. R., 1958, “Some Steady-State Solutions of the Unsaturated Moisture Flow Equation with Application to Evaporation from a Water Table,” *Soil Science*, Vol. 85, No. 4, pp. 228–232.

Gelhar, L. W., 1993, *Stochastic Subsurface Hydrology*, Prentice Hall, New York, New York.

RPP-ENV-58782, Rev. 0

- 1 Gelhar, L. W. and C. L. Axness, 1983, "Three-Dimensional Stochastic Analysis of
2 Macrodispersion in Aquifers," Water Resources Research, Vol. 19, No. 1, pp. 161–180.
- 3 Gelhar, L. W., C. Welty, and K. R. Rehfeldt, 1992, "A Critical Review of Data on Field-Scale
4 Dispersion in Aquifers," Water Resources Research, Vol. 28, No. 7, pp. 1955–1974.
- 5 HNF-4769, 1999, "Far-Field Hydrology Data Package for Immobilized Low-Activity Tank
6 Waste Performance Assessment," Rev. 1, Fluor Daniel Northwest, Richland,
7 Washington.
- 8 Hills, R. G., P. J. Wierenga, D. B. Hudson, and M. R. Kirkland, 1991, "The Second Las Cruces
9 Trench Experiment: Experimental Results and Two-Dimensional Flow Predictions,"
10 Water Resources Research, Vol. 27, No. 10, pp. 2707–2718.
- 11 Jury, W. A. and R. Horton, 2004, Soil Physics, 6th edition, Wiley and Sons, Inc., New York,
12 New York.
- 13 Khaleel, R. and J. F. Relyea, 1997, "Correcting laboratory-measured moisture retention data for
14 gravels," Water Resources Research, Vol. 33, No. 8, pp. 1875–1878.
- 15 Khaleel, R. and J. F. Relyea, 2001, "Variability of Gardner's α for coarse-textured sediments,"
16 Water Resources Research, Vol. 37, No. 6, pp. 1567–1575.
- 17 Khaleel, R., J. F. Relyea and J. L. Conca, 1995, "Evaluation of van Genuchten-Mualem
18 relationships to estimate unsaturated hydraulic conductivity at low water contents,"
19 Water Resources Research, Vol. 31, No. 11, pp. 2659–2668.
- 20 Khaleel, R., T.-C. J. Yeh, and Z. Lu, 2002, "Upscaled Flow and Transport Properties for
21 Heterogeneous Unsaturated Media," Water Resources Research, Vol. 38, No. 5,
22 pp. 11.1–11.12.
- 23 Klute, A., 1986, "Water Retention: Laboratory Methods," in Methods of Soil Analysis, Part 1—
24 Physical and Mineralogical Methods, pp. 635–660, American Society of Agronomy-Soil
25 Science Society of America, Madison, Wisconsin.
- 26 Klute, A. and C. Dirksen, 1986, "Hydraulic Conductivity and Diffusivity: Laboratory Methods,"
27 in Methods of Soil Analysis, Part 1—Physical and Mineralogical Methods, pp. 687–734,
28 American Society of Agronomy-Soil Science Society of America, Madison, Wisconsin.
- 29 Mantoglou, A., 1984, "Large-Scale Models of Transient Unsaturated Flow and Contaminant
30 Transport Using Stochastic Methods," Ph.D. Thesis, Massachusetts Institute of
31 Technology, Department of Civil Engineering, Cambridge, Massachusetts.
- 32 Mantoglou, A. and L. W. Gelhar, 1987, "Stochastic Modeling of Large-Scale Transient
33 Unsaturated Flow Systems," Water Resources Research, Vol. 23, No. 1, pp. 37–46.

RPP-ENV-58782, Rev. 0

- 1 McCord, J. T., D. B. Stephens, and J. L. Wilson, 1991, "Hysteresis and State-Dependent
2 Anisotropy in Modeling Unsaturated Hillslope Hydrologic Processes," Water Resources
3 Research, Vol. 27, No. 7, pp. 1501–1518.
- 4 Millington, R. J. and J. P. Quirk, 1961, "Permeability of Porous Solids," Transactions of the
5 Faraday Society, Vol. 57, pp. 1200–1207.
- 6 Mualem, Y., 1976, "A New Model for Predicting the Hydraulic Conductivity of Unsaturated
7 Porous Media," Water Resources Research, Vol. 12, No. 3, pp. 513–522.
- 8 Nielsen, D. R., J. M. Biggar, and K. T. Erh, 1973, "Spatial Variability of Field-Measured
9 Soil-Water Properties," Hilgardia, Vol. 42, No. 7, pp. 215–260.
- 10 NUREG/CR-5965, 1994, Modeling Field Scale Unsaturated Flow and Transport Processes,
11 Nuclear Regulatory Commission, Washington, D.C.
- 12 NUREG/CR-6114, 1994, Auxiliary Analyses in Support of Performance Assessment of a
13 Hypothetical Low-Level Waste Facility: Groundwater Flow and Transport Simulation,
14 Vol. 3, U.S. Nuclear Regulatory Commission, Washington, D.C.
- 15 Phillips, F. M., J. L. Mattick, T. A. Duval, D. Elmore, and P. W. Kubik, 1988, "Chlorine 36 and
16 Tritium From Nuclear Weapons Fallout as Tracers for Long-Term Liquid and Vapor
17 Movement in Desert Soils," Water Resources Research, Vol. 24, No. 11, pp. 1877–1891.
- 18 PNNL-13795, 2000, "Vadose Zone Transport Field Study: Soil Water Content Distributions by
19 Neutron Moderation," Pacific Northwest National Laboratory, Richland, Washington.
- 20 PNNL-14284, 2003, "Laboratory Measurements of the Unsaturated Hydraulic Properties at the
21 Vadose Zone Transport Field Site," Pacific Northwest National Laboratory, Richland,
22 Washington.
- 23 PNNL-15503, 2008, "Characterization of Vadose Zone Sediments Below the C Tank Farm:
24 Borehole C4297 and RCRA Borehole 299-E27-22," Rev. 1, Pacific Northwest National
25 Laboratory, Richland, Washington.
- 26 PNNL-17154, 2008, "Geochemical Characterization Data Package for the Vadose Zone in the
27 Single-Shell Tank Waste Management Areas at the Hanford Site," Pacific Northwest
28 National Laboratory, Richland, Washington.
- 29 Polmann, D. J., 1990, "Application of Stochastic Methods to Transient Flow and Transport in
30 Heterogeneous Unsaturated Soils," Ph.D. Thesis, Massachusetts Institute of Technology,
31 Department of Civil Engineering, Cambridge, Massachusetts.
- 32 Resource Conservation and Recovery Act of 1976, 42 USC 6901, et seq.
- 33 RHO-ST-46P, 1984, "Field Calibration of Computer Models for Application to Buried Liquid
34 Discharges: A Status Report," Rockwell Hanford Operations, Richland, Washington.

RPP-ENV-58782, Rev. 0

- 1 RPP-20621, 2004, "Far-Field Hydrology Data Package for the Integrated Disposal Facility
2 Performance Assessment," Rev. 0, CH2M HILL Hanford Group, Inc., Richland,
3 Washington.
- 4 RPP-20621, 2004, "Far-Field Hydrology Data Package for the Integrated Disposal Facility
5 Performance Assessment," Appendix E, "Hanford Low-Activity Tank Waste
6 Performance Assessment Activity: Determination of In Situ Hydraulic Parameters of the
7 Upper Hanford Formation," Rev. 0, CH2M HILL Hanford Group, Inc., Richland,
8 Washington.
- 9 RPP-CALC-60450, 2016, "Process for Determining the Volumetric Moisture Content for the
10 Vadose Zone Geologic Units Underlying Waste Management Area," Rev. 0, Washington
11 River Protection Solutions, LLC, Richland, Washington.
- 12 RPP-CALC-60452, 2016, "Moisture Dependent Anisotropy Calculations Supporting WMA C
13 PA," Rev. 0, Washington River Protection Solutions, LLC, Richland, Washington.
- 14 Russo, D., 1991, "Stochastic Analysis of Simulated Vadose Zone Solute Transport in a Vertical
15 Cross Section of Heterogeneous Soil During Nonsteady Water Flow," Water Resources
16 Research, Vol. 27, No. 3, pp. 267–283.
- 17 Russo, D., 1993, "Stochastic Modeling of Macrodispersion for Solute Transport in a
18 Heterogeneous Unsaturated Porous Formation," Water Resources Research, Vol. 29,
19 No. 2, pp. 383–397.
- 20 Scanlon, B. R., 1992, "Evaluation of Liquid and Vapor Water Flow in Desert Soils Based on
21 Chlorine 36 and Tritium Tracers and Nonisothermal Flow Simulations," Water Resources
22 Research, Vol. 28, No. 1, pp. 285–297.
- 23 Stephens, D. B., and S. Heermann, 1988, "Dependence of Anisotropy on Saturation in a
24 Stratified Sand," Water Resources Research, Vol. 24, No. 5, pp. 770–778.
- 25 van Genuchten, M. Th., 1980, "A Closed-form Equation for Predicting the Hydraulic
26 Conductivity of Unsaturated Soils," Soil Science Society of America Journal, Vol. 44,
27 No. 5, pp. 892–898.
- 28 WHC-IP-0635, 1991, "Geotechnical Engineering Procedure Manual," Vols. 1 and 2,
29 Westinghouse Hanford Company, Richland, Washington.
- 30 WHC-SD-WM-EE-004, 1995, "Performance Assessment of Grouted Double-Shell Tank Waste
31 Disposal at Hanford," Rev. 1, Westinghouse Hanford Company, Richland, Washington.
- 32 Wierenga, P. J., R. G. Hills, and D. B. Hudson, 1991, "The Las Cruces Trench Site:
33 Characterization, Experimental Results, and One-Dimensional Flow Predictions," Water
34 Resources Research, Vol. 27, No. 10, pp. 2695–2705.

RPP-ENV-58782, Rev. 0

- 1 Yang, J., R. Zhang, J. Wu, and M. B. Allen, 1997, "Stochastic analysis of adsorbing solute
2 transport in three-dimensional, heterogeneous, unsaturated soils," Water Resources
3 Research, Vol. 33, No. 3, pp. 1947–1956.
- 4 Ye, M., R. Khaleel, and T.-C. J. Yeh, 2005, "Stochastic analysis of moisture plume dynamics of
5 a field injection experiment," Water Resources Research, Vol. 41, W03013, pp. 1–13.
- 6 Yeh, T.-C. J., and D. J. Harvey, 1990, "Effective Unsaturated Hydraulic Conductivity of Layered
7 Sands," Water Resources Research, Vol. 26, No. 6, pp. 1271–1279.
- 8 Yeh, T.-C. J., L. W. Gelhar and A. L. Gutjahr, 1985, "Stochastic Analysis of Unsaturated Flow
9 in Heterogeneous Soils, 2. Statistically Anisotropic Media with Variable α ," Water
10 Resources Research, Vol. 21, No. 4, pp. 457–464.
- 11 Yeh, T.-C. J., M. Ye, and R. Khaleel, 2005, "Estimation of effective unsaturated hydraulic
12 conductivity tensor using spatial moments of observed moisture plume," Water
13 Resources Research, Vol. 41, W03014, pp. 1–12.
- 14 Zhang, Z. F. and R. Khaleel, 2010, "Simulating field-scale moisture flow using a combined
15 power-averaging and tensorial connectivity-tortuosity approach," Water Resources
16 Research, Vol. 46, W09505, pp. 1–14.

17

18

RPP-ENV-58782, Rev. 0

- 1
- 2
- 3
- 4
- 5
- 6

This page intentionally left blank.

RPP-ENV-58782, Rev. 0

1
2
3
4
5
6
7
8
9
10
11

APPENDIX C

TECHNICAL BASIS FOR WASTE MANAGEMENT AREA C UNCONFINED AQUIFER CONCEPTUAL MODEL: FIELD DATA AND RELATED INVESTIGATIONS

RPP-ENV-58782, Rev. 0

- 1
- 2
- 3
- 4
- 5
- 6
- 7

This page intentionally left blank.

RPP-ENV-58782, Rev. 0

TABLE OF CONTENTS

1			
2			
3	APPENDIX C – TECHNICAL BASIS FOR WASTE MANAGEMENT AREA C		
4	UNCONFINED AQUIFER CONCEPTUAL MODEL: FIELD DATA AND		
5	RELATED INVESTIGATIONS	C-1	
6	C.1 HIERARCHY OF LENGTH SCALES AND SCALE DEPENDENCE OF		
7	MEDIA PROPERTIES	C-2	
8	C.2 HYDROGEOLOGIC CONDITIONS AND STRUCTURE	C-3	
9	C.2.1 Paleochannel Configuration and Flow Paths	C-4	
10	C.2.2 Theoretical Basis for Hydraulic Conductivity Estimates of		
11	Paleochannel Sediments.....	C-6	
12	C.3 ESTIMATES OF UNCONFINED AQUIFER FLOW AND TRANSPORT		
13	PROPERTIES	C-7	
14	C.3.1 Groundwater Flow Velocities and Fluxes	C-7	
15	C.3.2 Hydraulic Conductivity of Unconfined Aquifer Sediments	C-8	
16	C.3.3 Groundwater Flow Directions and Hydraulic Gradients	C-12	
17	C.3.4 Anisotropy.....	C-16	
18	C.3.5 Properties for Contaminant Transport	C-16	
19	C.4 UNCONFINED AQUIFER FLOW AND TRANSPORT PROPERTIES		
20	USED IN THE WASTE MANAGEMENT AREA C PERFORMANCE		
21	ASSESSMENT	C-21	
22	C.4.1 Flow Properties	C-21	
23	C.4.2 Contaminant Transport Properties	C-23	
24	C.5 DEVELOPMENT OF UNCERTAINTY IN GROUNDWATER FLUX		
25	AND MACRODISPERSIVITY FOR SATURATED ZONE	C-23	
26	C.6 REFERENCES	C-25	

RPP-ENV-58782, Rev. 0

LIST OF FIGURES

1		
2		
3	Figure C-1. Schematic Illustrating Scale in a Heterogeneous Media and Scale Dependence	
4	of Saturated Hydraulic Conductivity.....	C-2
5	Figure C-2. Interpreted Extent of a Paleochannel Associated with the Ancestral Columbia	
6	River in 200 East Area in the Vicinity of Waste Management Area C.....	C-5
7	Figure C-3. Digital Photo Log for Borehole 299-E27-4 with an Expansion Showing the	
8	Open Framework Gravel below the Water Table.....	C-9
9	Figure C-4. (a) An Idealized Hexagonal Model Approximation of Open-Framework	
10	Gravelly Media, and (b) Representative Flow Regions used to Determine	
11	Equivalent Hydraulic Conductivity.....	C-10
12	Figure C-5. Plan View of the Central Plateau Groundwater Model Representing the	
13	Aquifer and the Volumetric Flux Calculation Window in the Vicinity of Waste	
14	Management Area C.....	C-13
15	Figure C-6. Hanford Formation Saturated Hydraulic Conductivity Estimates Based on	
16	Slug Tests, Pump Tests, and Model Calibration.	C-14
17	Figure C-7. Borehole Log of Well 299-E27-22.....	C-15
18	Figure C-8. Pacific Northwest National Laboratory Site-Wide Model Calibration of	
19	Hydraulic Conductivity of the Unconfined Aquifer with the Location of Waste	
20	Management Area C and Magnitude of Hydraulic Conductivity Indicated.....	C-16
21	Figure C-9. Central Plateau Groundwater Model Layer Discretization In the Saturated	
22	Zone and Extent of Various Hydrostratigraphic Units within the Model Layer	
23	in the Vicinity of Waste Management Area C (shown by the Rectangle).	C-17
24	Figure C-10. Longitudinal Macrodispersivity in Saturated Media as a Function of Overall	
25	Problem Scale with Data Classified by Reliability.	C-19
26	Figure C-11. Central Plateau Groundwater Model Calibration Results in the Vicinity of	
27	Waste Management Area C.....	C-22
28	Figure C-12. Low-Gradient Low-Level Waste Management Area 1 Monitoring Network	
29	Results.	C-24
30		
31		

RPP-ENV-58782, Rev. 0

LIST OF TABLES

Table C-1. Calculation of Weighted Average Hydraulic Conductivity Value and Volumetric Water Flux from the Central Plateau Groundwater Model.	C-18
Table C-2. Relationship Between Saturated Longitudinal Macrodispersivity (α_L) and Scale of Measurement (L_s).	C-20
Table C-3. Triangular Distribution of Aquifer Flux and Proportional Hydraulic Conductivity Values Applicable to the Uncertainty Analysis.	C-25

RPP-ENV-58782, Rev. 0

LIST OF TERMS

1		
2		
3	CCu	Cold Creek unit
4		
5	CPGWM	Central Plateau Groundwater Model
6		
7	EHM	equivalent homogeneous medium
8		
9	FY	fiscal year
10		
11	HSU	hydrostratigraphic unit
12		
13	LLWMA	Low-Level Waste Management Area
14		
15	PA	Performance Assessment
16		
17	RCRA	Resource Conservation and Recovery Act of 1976
18		
19	STOMP	Subsurface Transport Over Multiple Phases
20		
21	TC&WM EIS	Tank Closure and Waste Management Environmental Impact Statement
22		
23	WMA	Waste Management Area
24		

RPP-ENV-58782, Rev. 0

APPENDIX C**TECHNICAL BASIS FOR WASTE MANAGEMENT AREA C UNCONFINED
AQUIFER CONCEPTUAL MODEL: FIELD DATA AND RELATED
INVESTIGATIONS**

The groundwater pathway analysis is an important aspect of the Waste Management Area C (WMA C) Performance Assessment (PA). As the contaminant mass flux arriving from the vadose zone enters the aquifer, it mixes with the groundwater and undergoes dilution, dispersion, and retardation while traveling along the flow path. The amount of dilution is strongly dependent on the ratio of volumetric groundwater flux to contaminant mass flux within the mixing zone. However, groundwater flux is not ordinarily a measurable quantity. Instead, it is inferred from hydraulic head measurements and from hydraulic properties of the aquifer (i.e., estimates of the hydraulic gradients and hydraulic conductivities), which are deduced from a variety of measurement methods, such as pump and slug tests, or derived from inverse modeling of the aquifer to estimate conductivity from measured head values.

Past and present measured field data (hydraulic heads) in observation boreholes in the vicinity of WMA C must be used carefully as the region is recovering from the effects of both surface (ponds, cribs, trenches, and ditches) and subsurface (leaking pipelines, leaking tanks, and injection wells) liquid discharges from Hanford operations for many years. Groundwater mounding continues to dissipate to an equilibrium condition that is likely to be similar to the pre-Hanford operations condition (see Section 3.1.5.4.2 and Figure 3-35). As a result, the post-closure position of the water table, and its hydraulic gradient, can only be estimated through evaluating the current water table and forecasting the anticipated changes. Modeling is a critical tool in this evaluation, as it can be used to estimate both the hydraulic gradient and the recovery of hydraulic heads from the operational liquid discharges. Consequently, this analysis uses modeling tools to calculate the future groundwater flux, based on aquifer hydraulic properties and the projected hydraulic gradient.

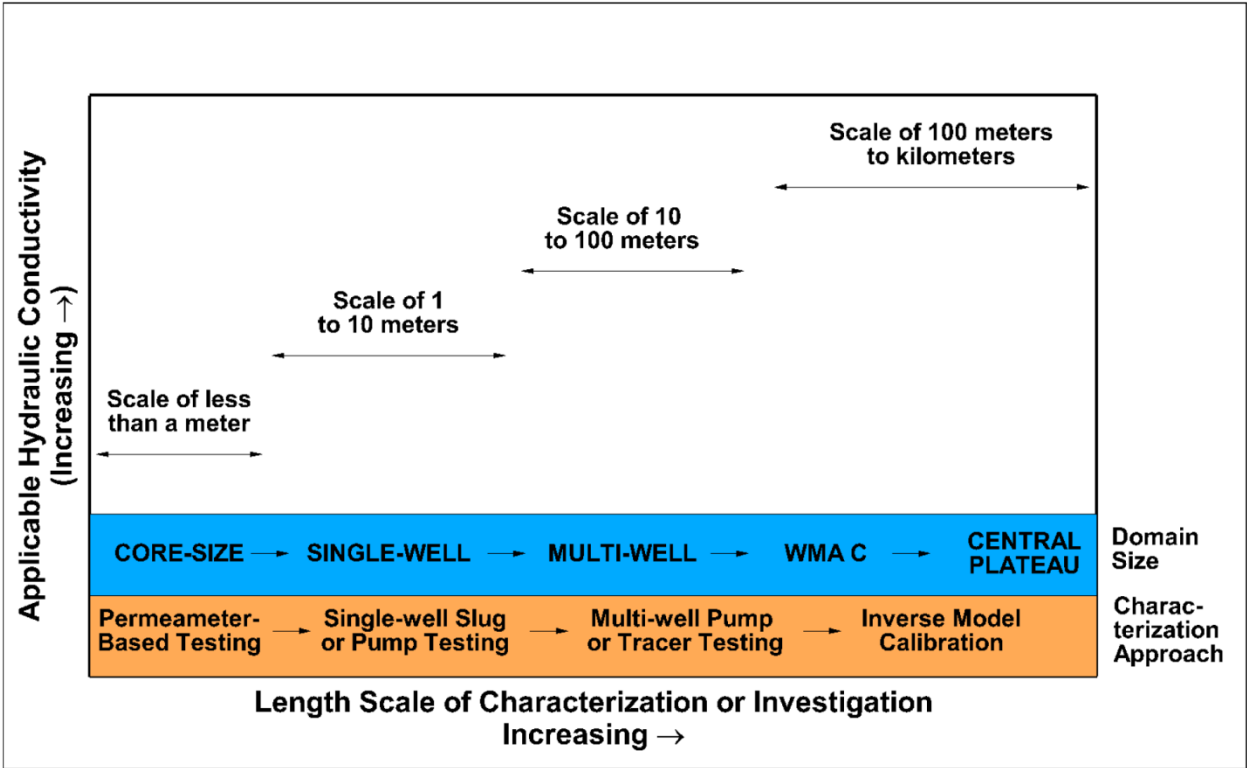
This appendix provides a detailed assessment and evaluation of saturated media field data used to estimate the aquifer hydraulic properties, including saturated hydraulic conductivity, groundwater fluxes, and hydraulic gradients, and specifies the technical basis for parameter selection and use in the WMA C PA modeling. Included in this assessment/evaluation is the following:

- A brief review of scale dependence of saturated media parameters (Section C.1)
- A brief overview of the hydrogeologic conditions pertinent to WMA C (Section C.2)
- A summary of measured and theoretically-estimated aquifer hydraulic parameter estimates available for the areas near WMA C (Section C.3)
- A summary of how this information is used for the PA (Section C.4), including a discussion of the sensitivity and uncertainties of groundwater flux and flow parameters used in the PA (Section C.5).

C.1 HIERARCHY OF LENGTH SCALES AND SCALE DEPENDENCE OF MEDIA PROPERTIES

A variety of methods exist which can be used to estimate hydraulic conductivity, including permeameter cells, slug tests, pump tests, and model calibration. In general, estimates of saturated hydraulic conductivity, either inferred by aquifer testing or determined from calibrated models, tend to increase as the scale of the flow domain increases (e.g., U.S. Geological Survey Water-Supply Paper 2237, “Regional Flow in the Dakota Aquifer: A Study of the Role of Confining Layers”). The evolving heterogeneities at various length scales result in a scale dependence of effective parameters such as saturated hydraulic conductivity (“An Analysis Platform for Multiscale Hydrogeologic Modeling with Emphasis on Hybrid Multiscale Methods” [Scheibe et al. 2015]). For WMA C PA saturated media modeling, the flow domain size of interest is shown on the right side of Figure C-1, with the characteristic length scale for flow and transport on the order of hundred meters. As the length scale of observation increases, the effective properties increase in discretely hierarchical stages or evolve continuously (Scheibe et al. 2015). The effects of large-scale heterogeneity on flow and determination of media properties can therefore be inferred most effectively by using regional scale groundwater models.

Figure C-1. Schematic Illustrating Scale in a Heterogeneous Media and Scale Dependence of Saturated Hydraulic Conductivity.



WMA = Waste Management Area

Determining effective hydraulic conductivities applicable to the field scale appears to be best evaluated using inverse modeling conditioned by available data, using appropriate boundary

RPP-ENV-58782, Rev. 0

conditions. Measurements of hydraulic conductivity appear to be dependent on the test scale, and increase as the scale increases, particularly in heterogeneous media (“Scale Dependency of Hydraulic Conductivity Measurements” [Rovey and Cherkauer 1995]; “Scale Dependency of Hydraulic Conductivity in Heterogeneous Media” [Schulze-Makuch et al. 1999]). In-situ measures of aquifer flow and hydraulic properties inferred from hydraulic testing represent relatively small areas (Figure C-1) compared to the overall scale and dimensions of the model domain, and therefore do not provide representative results appropriate for the field scale (“Use and Measurement of Mass Flux and Mass Discharge” [ITRC 2010]). Similarly, individual well-based slug and pump tests provide information at a relatively small scale, albeit larger than core-scale permeameter tests. Permeameter, slug, and pump tests are also limited in their ability to quantify spatial averages or trends, and are less likely to produce central measures of flow magnitudes than a regional model (ITRC 2010). Field estimates for saturated hydraulic conductivity based on slug tests, for example, provide estimates of hydraulic representation at a scale of meters and are not considered generally appropriate to be used directly in the modeling, even though slug and pumping test data are important input for model calibration (ITRC 2010).

Consequently, in evaluating available information for the aquifer at WMA C, hydraulic conductivities derived from a calibrated model are regarded as more reliable than direct measurements by permeameter, slug, or pump tests. This distinction is important because, as Section C.2 will show, substantially different values for hydraulic conductivity have been estimated by various investigators using different methods.

C.2 HYDROGEOLOGIC CONDITIONS AND STRUCTURE

To understand the groundwater flow conditions in the vicinity of WMA C, and in particular the large-scale saturated hydraulic conductivity and hydraulic gradient, it is important to note the regional geology and the hydrogeologic conditions and geologic structure in the 200 Areas. Groundwater in the unconfined aquifer at Hanford generally flows from recharge areas in the elevated region near the western boundary of the Hanford Site, toward the Columbia River on the eastern and northern boundaries. The Columbia River is the primary discharge area for the unconfined aquifer.

The unconsolidated sediments of the present-day Central Plateau reflect deposits of the ancient Columbia River, and the Pleistocene cataclysmic flooding (Section 3.1.4 and 3.1.9 provide a detailed discussion of the regional and local geology that is not repeated here). Briefly, WMA C lies on the northern flank of the Cold Creek bar, a large compound flood bar formed during Pleistocene cataclysmic flooding, which last occurred about 15,000 years ago (On the Trail of the Ice Age Floods: A Geological Field Guide to the Mid-Columbia Basin [Bjornstad 2006]). The cataclysmic floods caused repeated large erosional and depositional events, which have significantly shaped the Central Plateau and the present WMA C geology. Erosion by Ice-Age flooding and the ancestral Columbia River are believed to have removed much of the Ringold Formation from the area and created a highly transmissive paleochannel. The cataclysmic floods deposited into the channel the gravel-dominated facies of the Hanford formation that consist of coarse-grained basaltic sand and granule- to boulder-size gravel displaying an open framework. These large-scale features significantly influence groundwater flow and plume migration because

RPP-ENV-58782, Rev. 0

the deposits in the channel are much more transmissive than those outside of the channel. The groundwater flow direction in the unconfined aquifer in the vicinity of WMA C trends toward the southeast. This conclusion is based on the following: 1) slightly higher hydraulic heads to the northwest, 2) the orientation of the southeast trending paleochannel in the area, and 3) the configuration of the major contamination plumes.

C.2.1 Paleochannel Configuration and Flow Paths

As discussed above, the paleochannel has a significant influence on flow and contaminant transport under WMA C. The open-framework gravels of the paleochannel are highly conductive, and as such constitute a potential fast pathway for migration of contaminants. It is therefore important to characterize the spatial extent of the paleochannel in the vicinity of WMA C, and to appropriately estimate its permeability.

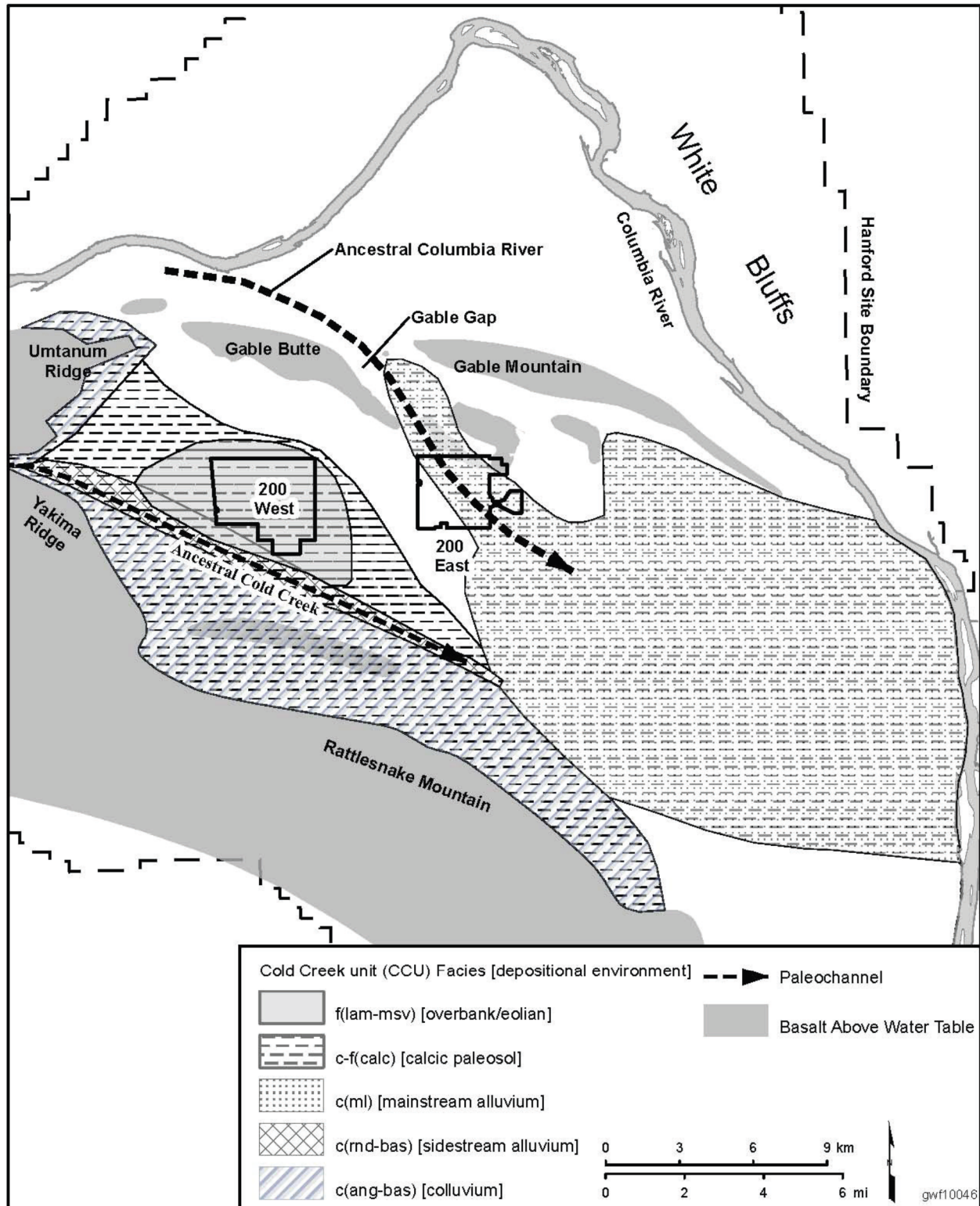
Based on current understanding of the ancestral Columbia River deposits, a large paleochannel is interpreted extending southeast through Gable Gap (Figure C-2) that bifurcates just south of the gap. One sub-channel trends easterly following along the direction of strike of the Gable Mountain anticline while the other sub-channel trends in a more southerly direction through the eastern portion of the 200 Area Inner Boundary (the paleochannel identified in Figure C-2). The southerly trending paleochannel configuration, flow path, and dimensions have been the subject of numerous studies, owing to their importance to site-wide contaminant transport.

Recent reports providing information supporting the current interpretation of the extent of the paleochannel include the following.

- PNNL-12261, "Revised Hydrogeology for the Suprabasalt Aquifer System, 200-East Area and Vicinity, Hanford Site, Washington." The report includes detailed interpretations on the paleo and flood channels, and has several cross sections and figures displaying their configuration and flow paths.
- Aero-Metric LiDAR, "RCCC-Hanford Battelle/PNNL/DOE, Digital Orthophotography & LiDAR Surveys Photogrammetric Report," prepared by Aero-Metric, Seattle, Washington. The report includes LiDAR data; surficial expression of paleochannel outlines are apparent from ground-processed Aero-Metric LiDAR data collected in 2008.
- Fiscal year (FY) 2013 and 2014 Annual Groundwater Monitoring Reports, CHPRC. Interpretation of tritium and ¹²⁹I plume extents follow the highly conductive flow paleochannel flow path.
- ECF-Hanford-13-0029, "Development of the Hanford South Geologic Framework Model, Hanford Site, Washington." The report shows areas where interpolated sediment volumes are not present, suggesting scouring along the paleochannel flow paths. All but two of the wells used in ECF-Hanford-13-0029 in the immediate vicinity of WMA C lie within the paleochannel. Geologic and geophysical logging data from the wells were also used in estimating paleochannel location.

RPP-ENV-58782, Rev. 0

Figure C-2. Interpreted Extent of a Paleochannel Associated with the Ancestral Columbia River in 200 East Area in the Vicinity of Waste Management Area C.



Source: DOE/RL-2011-118, Hanford Site Groundwater Monitoring for 2011, Appendix E.

RPP-ENV-58782, Rev. 0

Scouring of suprabasalt sediments in the paleochannels is evident in that, along much of its path, only the Hanford formation overlies the top of the basalt. Hanford formation material makes up almost entirely the material within the paleochannels in general, as well as all of the material within the paleochannel at the WMA C water table. Removal of pre-Hanford formation suprabasalt sediments, with the possible exception of a thin layer of Cold Creek unit (CCu) beneath the eastern half of WMA C, is apparent suggesting a paleochannel width of over 500 m beneath WMA C. Wells 299-E27-14 and 299-E27-15 penetrate the Hanford formation within the paleochannel beneath WMA C. The Hanford formation is ~86 m thick and the saturated thickness from the water table to the top of the basalt is ~13 m.

C.2.2 Theoretical Basis for Hydraulic Conductivity Estimates of Paleochannel Sediments

As discussed above, the paleochannel comprises an open-framework gravelly medium below WMA C. Figure C-3 is a digital photo log for borehole 299-E27-4 showing its proximity to WMA C and the open-framework gravelly media below the water table (the broken blue line is the water table location). The importance of the paleochannel to groundwater transport in the central plateau has led to a number of efforts to characterize its permeability, which can be applied to the WMA C PA.

Permeability measurements in open-framework gravelly media present special challenges, as the permeabilities are so high that they are above the measurement range of most laboratory constant-head permeameters—the head difference is too small to be measured. “Measuring the permeability of open-framework gravel” (Ferreira et al. 2010) addresses the challenge of measuring the high permeability by using a 3-m long permeameter. The head difference over this length was of the order of 10^{-2} to 10^{-3} m, which could be measured to the nearest 10^{-5} m. Measured permeability values varied between 3,456 m/day (for uniform pebbles) to 86,400 m/day (for open-framework gravels).

Figure C-4 illustrates an idealized unit cell model of an open-framework gravelly medium. “Scale Dependence of Continuum Models for Fractured Basalts” (Khaleel 1989) derived an expression (Equation C-1) for the isotropic saturated hydraulic conductivity (K) for such idealized media.

$$K_1 = K_2 = \frac{b^3 g}{12\sqrt{3}\ell\nu} \quad (\text{C-1})$$

where g is the acceleration (LT^{-2}) due to gravity, b is the open space aperture (L), ℓ is the coordinate length (L) along the opening of the unit cell, and ν is the kinematic viscosity (L^2T^{-1}) of the fluid. By inspection of equation (C-1) for equivalent isotropic K , the aperture size or width b is the most sensitive parameter in influencing conductivity estimates. For different aperture widths, and for a hexagon side length of 0.005 m (i.e., representative of 0.01-m [10-mm]-diameter pebbles), the calculated equivalent K estimates range from a low of 8 m/day to 65,000 m/day for aperture widths (b) ranging from a rather modest spacing of 0.1 mm to as high as 2 mm. In regard to WMA C, according to sieve results of sandy gravel samples collected from near the water table and below at well 299-E27-4, the grain size of approximately 35% to 40% of the material exceeds 10 mm (PNNL-14656, “Borehole Data Package for Four CY 2003

RPP-ENV-58782, Rev. 0

RCRA Wells 299-E27-4, 299-E27-21, 299-E27-22, and 299-E27-23 at Single-Shell Tank, Waste Management Area C, Hanford Site, Washington”).

A theoretical estimate of the permeability of a uniform pebble network can also be obtained using the Kozeny-Carman equation (Dynamics of Fluids in Porous Media [Bear 1972]):

$$k = \frac{d}{180} \frac{\phi^3}{(1-\phi)^2} \quad (\text{C-2})$$

The 10-mm diameter (d) uniform pebble model having a measured porosity $\phi=40\%$ yields a permeability of about 86,000 m/day. Therefore, the two theoretical approaches are the same order of magnitude, and both provide very high estimates of saturated conductivity that are comparable to those based on the large-scale permeameter experiments (Ferreira et al. 2010).

C.3 ESTIMATES OF UNCONFINED AQUIFER FLOW AND TRANSPORT PROPERTIES

Estimation of aquifer flow and transport parameters at WMA C are necessary for evaluating the rate and extent of migration of contaminants arriving from the vadose zone and to assess the groundwater quality as required under the Resource Conservation and Recovery Act of 1976 (RCRA). The RCRA groundwater quality assessment program requires determination of whether past releases from WMA C are affecting groundwater quality and estimation of the rate and extent of migration of dangerous waste or dangerous waste constituents in the groundwater (DOE/RL-2009-77, Groundwater Quality Assessment Plan for the Single-Shell Tank Waste Management Area C; SGW-54508, “WMA C September 2012 Quarterly Groundwater Monitoring Report”).

C.3.1 Groundwater Flow Velocities and Fluxes

Estimates of groundwater flow velocity or Darcy flux can provide valuable information about the hydraulic properties of the aquifer. These estimates can be made by measuring the flow within a borehole (using downhole flowmeters) or by interrogating the local or regional scale flow models.

Few direct measurements of groundwater flow exist in the 200 East Area, and none are particularly relevant to the groundwater flow conditions forecast for the unconfined aquifer in the immediate vicinity of WMA C. Measurements of groundwater flow velocity (groundwater flux divided by porosity) in the vicinity of WMA B-BX-BY, collected using a colloidal borescope circa 2001, reflected the impact of the large mound caused by the discharges at 216-B-3 Pond diverting flow from the east or southeast. The results did indicate that the flow velocities appeared to be greater in magnitude in the southern half of WMA B-BX-BY than in the northern half (“Application of the Colloidal Borescope to Determine a Complex Groundwater Flow Pattern” [Narbutovskih et al. 2002]). WHC-SD-EN-WP-012, “Groundwater Screening Evaluation/Monitoring Plan -- 200 Area Treated Effluent Disposal Facility (Project W-049H)” documents the results of an evaluation conducted using a heat pulse

RPP-ENV-58782, Rev. 0

flowmeter used to measure the magnitude and direction of groundwater flow velocity in three wells located east of the 216-B-3 Pond complex. However, during January and February 1994 when the evaluation occurred, the 216-B-3 Pond complex still received effluent and sustained the prominent groundwater mound, and the results of the testing were influenced by the mound created by the 216-B-3 pond discharges.

Groundwater flux information for particular subareas of regional models is often difficult to obtain from previous studies, and often must be inferred from whatever information is available. DOE/EIS-0391, "Final Tank Closure and Waste Management Environmental Impact Statement for the Hanford Site, Richland, Washington" estimated the future steady-state flow velocity in the highly conductive Hanford formation sediments at the 216-BY Cribs to be approximately 2 to 3 m/day toward the southeast, according to figures in Appendix L (i.e., Figures L-55, L-56, and L-57). According to the range of specific yield values presented in Table L-12 of Appendix L of DOE/EIS-0391, the flux in the aquifer is between 0.3 and 0.9 m/day.

Groundwater flux in the aquifer is estimated using the Central Plateau Groundwater Model (CPGWM) (CP-47631, "Model Package Report: Central Plateau Groundwater Model Version 6.3.3") by evaluating the water budget through a planar rectangular window (300 m × 200 m that encompasses most of WMA C flow domain) over the unconfined aquifer thickness (Figure C-5). The results of the CPGWM include two times of interest, present day and post-closure steady state:

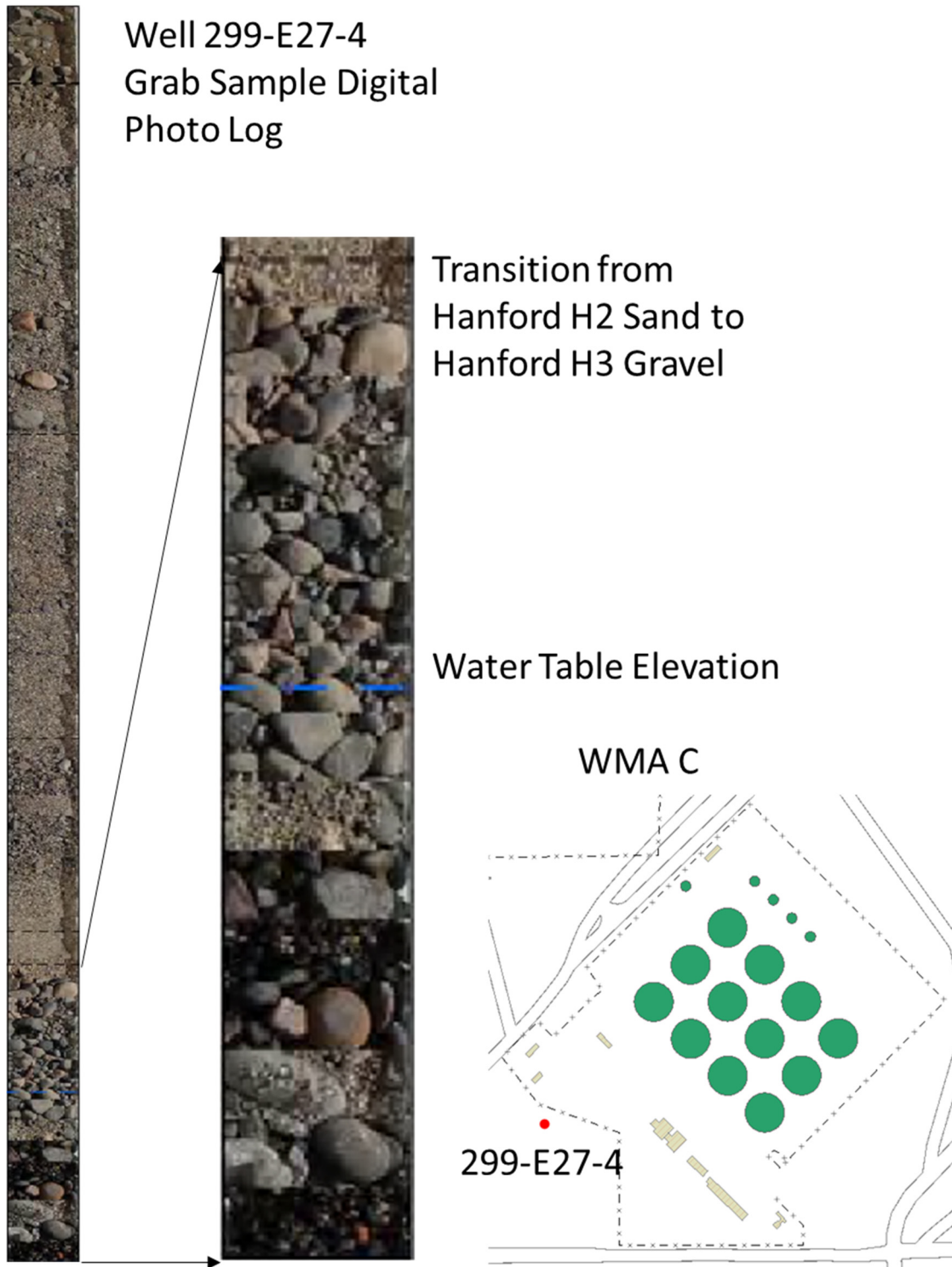
- For Year 2014 (approximating present day conditions), the CPGWM-calculated flow through the window volume is 1,100 m³/day, which divided by the cross-sectional area of 3,300 m² translates to a Darcy flux of 0.33 m/day
- For Year 2100 (approximating post-closure steady state conditions), the CPGWM-calculated flow through the window volume is 580 m³/day, which divided by the cross-sectional area of 3,300 m² translates to a Darcy flux of 0.18 m/day.

C.3.2 Hydraulic Conductivity of Unconfined Aquifer Sediments

The basis for the hydraulic conductivity of the unconfined aquifer used in the PA takes account of the accumulated knowledge and experience of many years of study of the aquifer beneath the Central Plateau, undertaken for a variety of purposes by different investigators, using a variety of measurement and modeling approaches. The hydraulic conductivity estimates from various investigations, with focus on the aquifer within the 200 East Area, are presented in Figure C-6 in such a manner that the length scale of observation increases from left to right. The results presented on the left-hand side are from slug tests (small spatial scale measurements), while the pumping test-based measurements are in the middle and the regional scale model-based estimates are on the right-hand side. Where multiple results are provided within a single report that cover slug and pump test data, the range of hydraulic conductivity is shown with a vertical line (Figure C-6). The generally increasing estimates of effective hydraulic conductivity moving from the left to the right are consistent with Figure C-1 and the description in Section C.1. The results of most hydrologic tests indicate the presence of highly permeable conditions in the unconfined aquifer within the Central Plateau, and measured hydraulic conductivity estimates range as high as 51,500 m/day.

RPP-ENV-58782, Rev. 0

Figure C-3. Digital Photo Log for Borehole 299-E27-4 with an Expansion Showing the Open Framework Gravel below the Water Table.

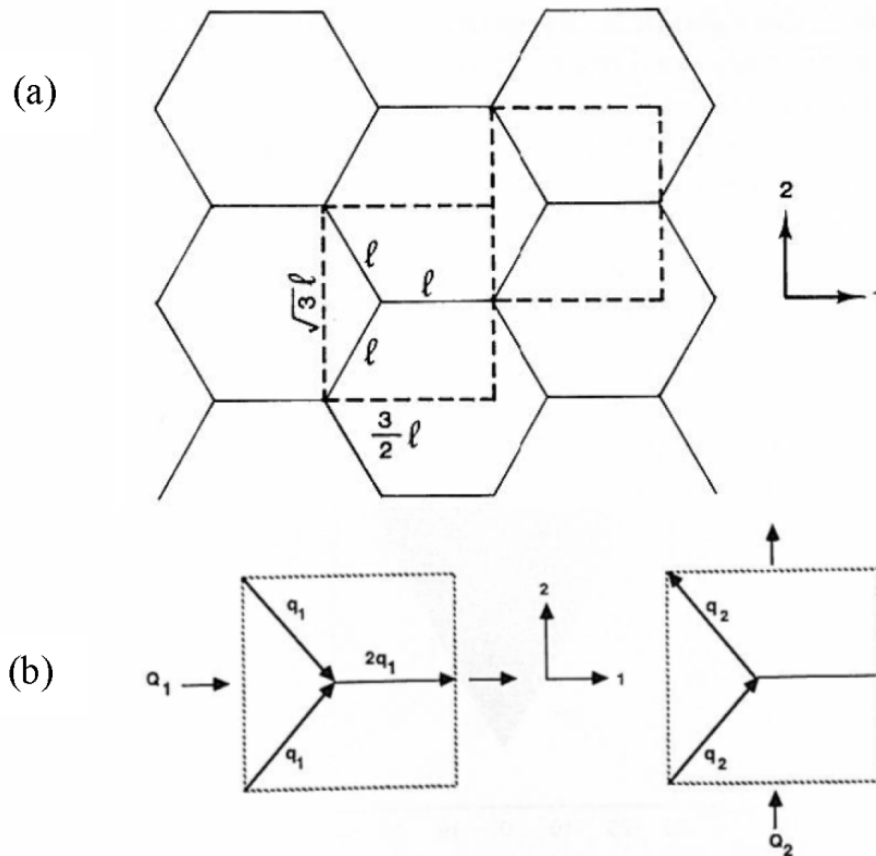


Adapted from PNNL-14656, "Borehole Data Package for Four CY 2003 RCRA Wells 299-E27-4, 299-E27-21, 299-E27-22, and 299-E27-23 at Single-Shell Tank, Waste Management Area C, Hanford Site, Washington."

WMA = Waste Management Area

RPP-ENV-58782, Rev. 0

Figure C-4. (a) An Idealized Hexagonal Model Approximation of Open-Framework Gravelly Media, and (b) Representative Flow Regions used to Determine Equivalent Hydraulic Conductivity.



SGW-54508 considers hydraulic conductivity of the Hanford gravel at WMA C to range from 100 to 2,100 m/day on the basis of the results of slug and pumping tests conducted in the immediate vicinity of WMA C. Excluded from this range are unpublished slug test results from well 299-E27-24 that produced hydraulic conductivity estimates ranging from 3,650 to 51,500 m/day, and slug test results from well 299-E27-22 that range from 1,888 to 6,888 m/day (shown in Figure C-6). SGW-54508 discounts the results from well 299-E27-24 because the open interval and well radius were not controlled and sloughing conditions existed before testing. SGW-54508 also discounts the results from well 299-E27-22 because the sediment borehole log description at well 299-E27-22 indicates a more dominant silt matrix with less gravel content than at well 299-E27-23, where slug test results indicated that the hydraulic conductivity measures 100 to 108 m/day. However, the borehole log of well 299-E27-22 (Figure C-7) does indicate the presence of the open-framework gravel in the aquifer, and SGW-54508 does not explain why sloughing would cause hydraulic conductivity estimates derived from a slug test to be overestimated. In addition, the slug test data presented in SGW-48722, "Borehole Summary Report for the ARRA Installation of Five RCRA Groundwater Monitoring Wells in the 200 Areas, FY 2010" collected from wells 299-E27-24 and 299-E27-25 exhibit the oscillatory response indicative of highly permeable conditions. While the summary of data presented in SGW-54508 is appropriate for the purposes of the RCRA groundwater quality assessment

RPP-ENV-58782, Rev. 0

1 program, which include collecting and analyzing the available data, the data represent
2 measurements made at a much smaller observation scale than is appropriate for developing an
3 effective hydraulic conductivity estimate for WMA C (Figure C-1).

4
5 PNNL-14656 indicates that the high values measured at the wells are indicative of, and
6 consistent with, the geologic interpretation of the open, highly permeable lower Hanford H3
7 gravels. The slug test and well screen development drawdown data also indicate comparable
8 highly permeable conditions in the aquifer at wells 299-E27-21 and 299-E27-22 (PNNL-14656).
9 Lastly, the results of an aquifer test with multiple observation wells conducted at well 699-55-50
10 indicate an aquifer hydraulic conductivity of 2,700 m/day (HW-60601, "Aquifer Characteristics
11 and Ground-Water Movement at Hanford"). HW-60601 describes the aquifer as consisting of
12 "Glaciofluvial sands and gravels," which are described as unconsolidated sands and gravels
13 occurring chiefly as glacial outwash. This description matches that given to the highly
14 permeable gravel contained in the paleochannel.

15
16 Past calibration efforts (e.g., PNL-10886, "Development of a Three-Dimensional Ground-Water
17 Model of the Hanford Site Unconfined Aquifer System: FY 1995 Status Report"; PNNL-11801,
18 "Three-Dimensional Analysis of Future Groundwater Flow Conditions and Contaminant Plume
19 Transport in the Hanford Site Unconfined Aquifer System: FY 1996 and 1997 Status Report")
20 estimated that an upper limit of hydraulic conductivity for coarse-gravel flood deposits found in
21 the central part of the Hanford Site is on the order of several tens of thousands of meters per day
22 (Figure C-8). Figure C-8 shows the influence of the high hydraulic conductivity paleochannel in
23 the aquifer beneath WMA C, as denoted by the swath of red. This swath indicates hydraulic
24 conductivity exceeding 7,000 m/day, extending from the Gable Gap through the southeast corner
25 of the 200 East Area. In one calibration effort, the hydraulic conductivity ranged from
26 271 m/day to 8,840 m/day within the WMA C PA model domain, and a value of 7,020 m/day in
27 the immediate vicinity of WMA C (PNNL-14753, "Groundwater Data Package for Hanford
28 Assessments"). In another effort, the hydraulic conductivity of the Hanford formation sediments
29 ranged up to about 1,000,000 m/day for the Hanford flood deposits (PNNL-13641, "Uncertainty
30 Analysis Framework – Hanford Site-Wide Groundwater Flow and Transport Model"). The Tank
31 Closure and Waste Management Environmental Impact Statement (TC&WM EIS) model
32 estimates the hydraulic conductivity of the highly conductive Hanford gravel present at WMA C
33 to be ~4,000 m/day (DOE/EIS-0391). In a more recent modeling effort, CP-57037, "Model
34 Package Report: Plateau to River Groundwater Transport Model Version 7.1" developed a
35 calibrated estimate of 17,000 m/day for the Hanford formation associated with the paleochannel.

36
37 The CPGWM provides calibrated hydraulic conductivity estimates for the hydrostratigraphic
38 units (HSUs) present within the aquifer. The CPGWM represents the most recent culmination of
39 understanding of the unconfined aquifer under the Central Plateau and, given the rigorous nature
40 of the development effort, is deemed to be the most suitable for predicting flow. The thicknesses
41 and extent of the different HSUs within the selected model layers in the vicinity of WMA C for
42 the saturated zone are shown in Figure C-9. The equivalent hydraulic conductivity for a given
43 layer within the rectangular area (approximate extent of WMA C) ranges between 5,802 m/day
44 and 17,000 m/day (Table C-1). Using a layer thickness weighted averaging scheme, the
45 effective hydraulic conductivity for an equivalent homogeneous medium (EHM) is estimated to
46 be 11,000 m/day for the entire aquifer (Table C-1). The EHM approach is used for representing

RPP-ENV-58782, Rev. 0

the saturated zone in the three-dimensional WMA C PA model using Subsurface Transport Over Multiple Phases (STOMP)¹, as discussed in Appendix D, and therefore the value of 11,000 m/day is used for the aquifer.

C.3.3 Groundwater Flow Directions and Hydraulic Gradients

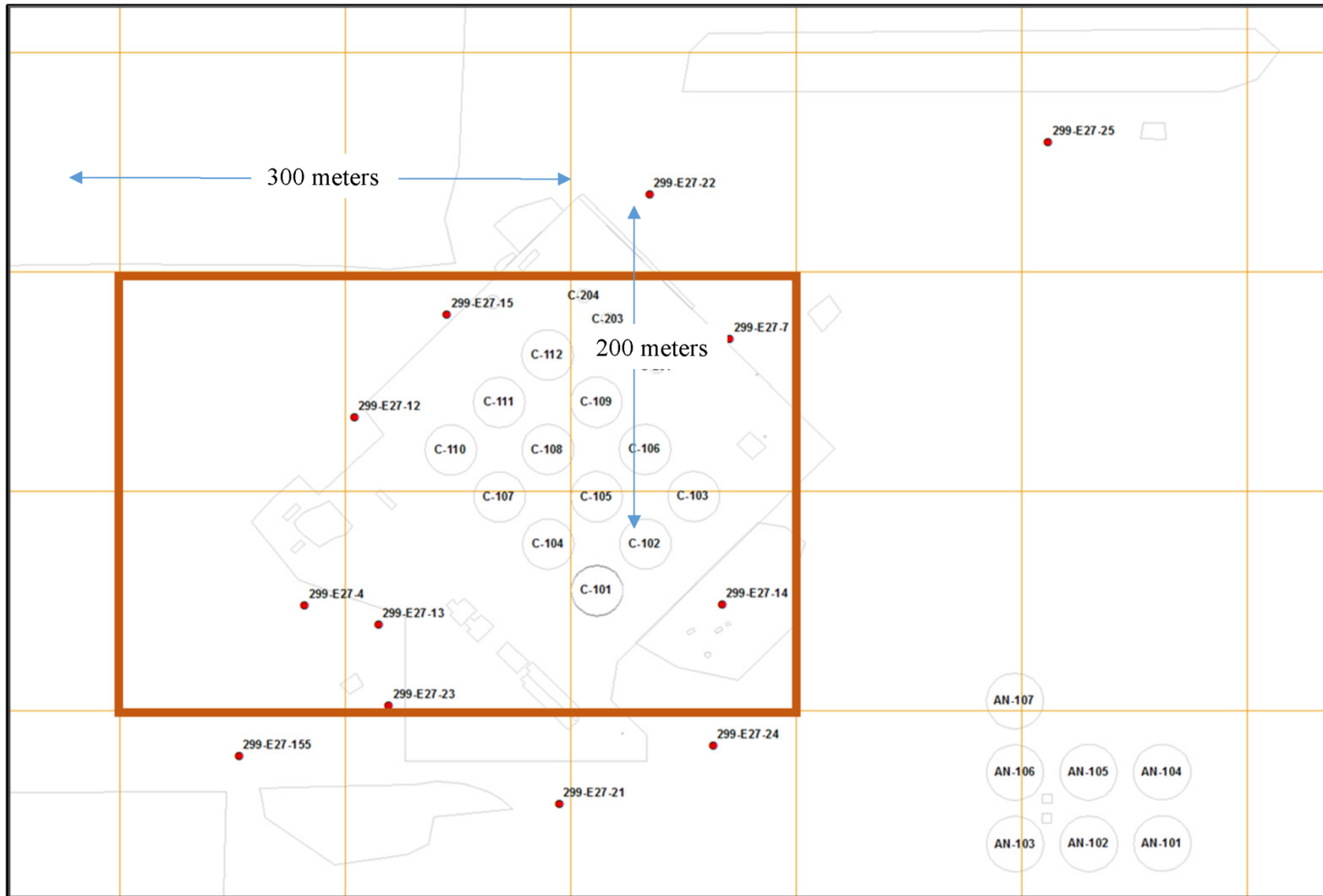
In the vicinity of WMA C, directions of groundwater flow and hydraulic gradients are inferred from water-level measurements in another part of the 200 East Area, around Low-Level Waste Management Area (LLWMA)-1 (DOE/RL-2013-22, Hanford Site Groundwater Monitoring Report for 2012), which is located northwest of WMA C. According to DOE/RL-2014-32, Hanford Site Groundwater Monitoring Report for 2013, the hydraulic gradient ranges between 2.2×10^{-5} m/m and 2.9×10^{-5} m/m, with flow moving in a southeastern direction. The average hydraulic gradient estimated from July 2011 through September 2012 was 2.5×10^{-5} ($\pm 0.4 \times 10^{-5}$) m/m toward the south (SGW-54165, "Evaluation of the Unconfined Aquifer Hydraulic Gradient Beneath the 200 East Area, Hanford Site"). SGW-54165 indicates that while the hydraulic gradient determination represents a spatial average across the entire Low-gradient Monitoring Network in the vicinity of LLWMA-1, mapping of water levels from August 2011 indicates that the flow direction directly beneath LLWMA-1 is more toward the southeast rather than toward the south.

Hydraulic gradient estimates in groundwater based on the CPGWM estimates of future conditions within the Central Plateau are summarized in Table C-1. Although water levels in the 200 East Area continue to decline, an evaluation of current groundwater flow directions and rates at WMA C is difficult due to the very low hydraulic gradient (on the order of 10^{-5} m/m). The hydraulic gradient according to the CPGWM is calculated from the volumetric flux through the window described in Section C.3.1.2 and the hydraulic conductivity value described in Section C.3.1.2. As indicated previously, the results of the CPGWM include two times of interest, present day and post-closure steady state (Table C-1), as follows.

- For Year 2014 (approximating present day conditions), the CPGWM-calculated flow through the window volume is 1,000 m³/day, which divided by the cross-sectional area of 3,300 m² and equivalent hydraulic conductivity of 11,000 m/day translates to a hydraulic gradient of 3×10^{-5} . The direction of flow inferred from the modeling and consistent with plume movements is in a south-to-southeasterly direction.
- For Year 2100 (approximating post-closure steady state conditions), the CPGWM-calculated flow through the window volume is 730 m³/day, which divided by the cross-sectional area of 3,300 m² and equivalent hydraulic conductivity of 11,000 m/day translates to a hydraulic gradient of 2×10^{-5} . The direction of flow inferred from the model is in a southeasterly direction.

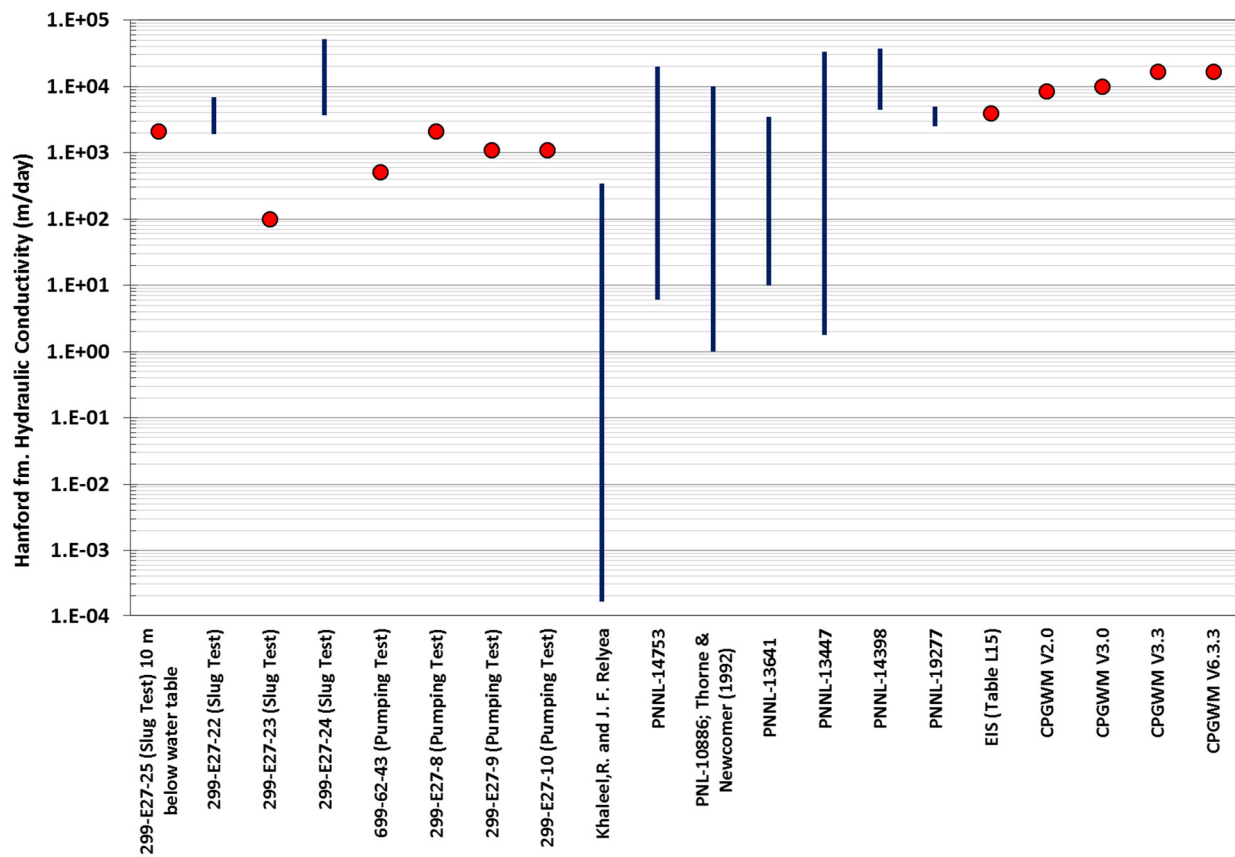
¹ Subsurface Transport Over Multiple Phases (STOMP)[®] is copyrighted by Battelle Memorial Institute, 1996.

Figure C-5. Plan View of the Central Plateau Groundwater Model Representing the Aquifer and the Volumetric Flux Calculation Window in the Vicinity of Waste Management Area C.



RPP-ENV-58782, Rev. 0

Figure C-6. Hanford Formation Saturated Hydraulic Conductivity Estimates Based on Slug Tests, Pump Tests, and Model Calibration.



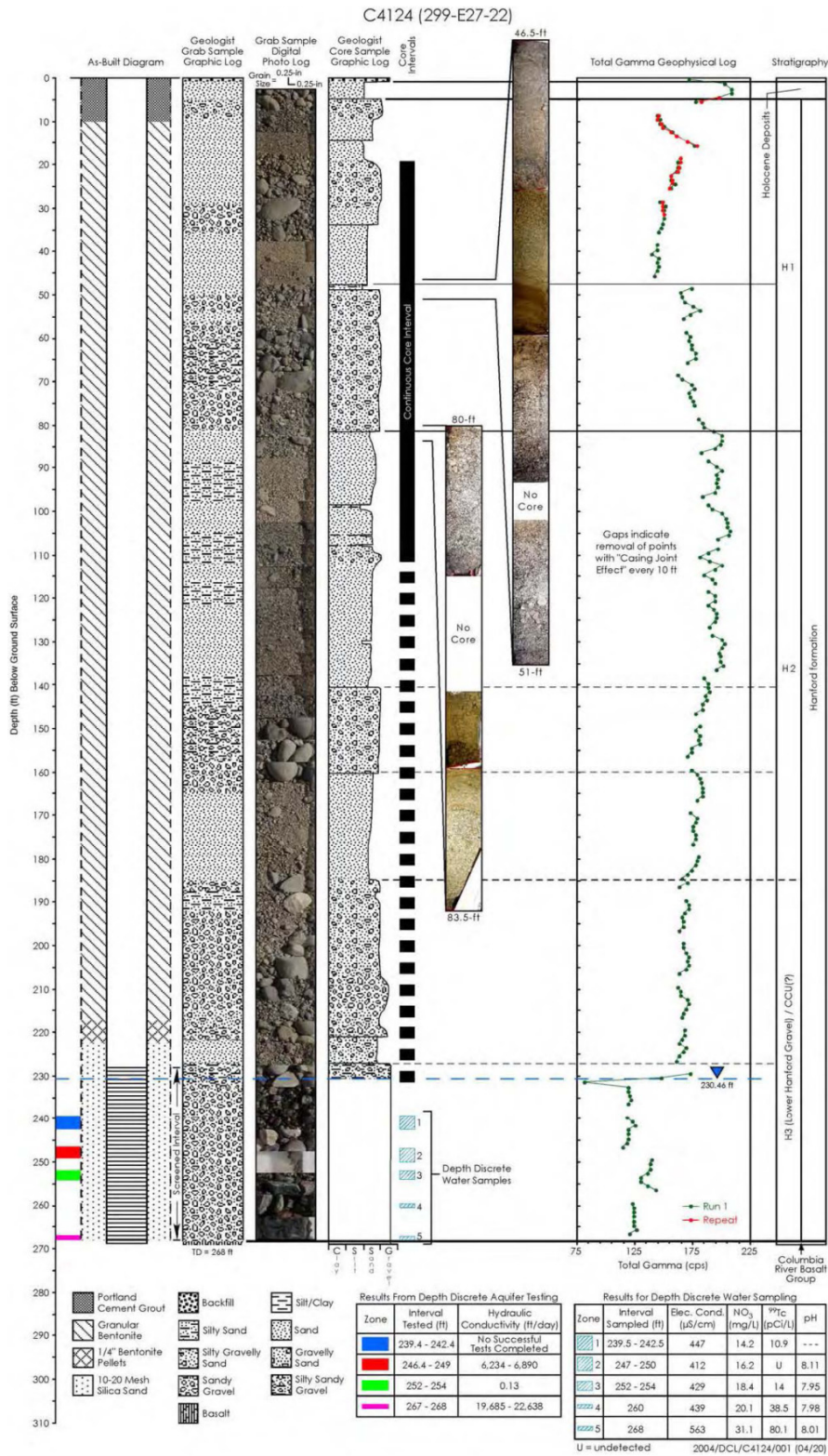
References:

- “Correcting Laboratory-Measured Moisture Retention Data for Gravels” (Khaleel and Relyea 1997).
- CP-47631, “Model Package Report: Central Plateau Groundwater Model Version [as amended].”
- DOE/EIS-0391, “Final Tank Closure and Waste Management Environmental Impact Statement for the Hanford Site, Richland, Washington.”
- PNL-10886, “Development of a Three-Dimensional Ground-Water Model of the Hanford Site Unconfined Aquifer System: FY 1995 Status Report.”
- PNNL-13447, “Transient Inverse Calibration of Hanford Site-Wide Groundwater Model to Hanford Operational Impact – 1943 to 1996.”
- PNNL-13641, “Uncertainty Analysis Framework – Hanford Site-Wide Groundwater Flow and Transport Model.”
- PNNL-14753, “Groundwater Data Package for Hanford Assessments.”
- PNNL-14398, “Transient Inverse Calibration of the Site-Wide Groundwater Flow Model (ACM-2): FY 2003 Progress Report.”
- PNNL-19277, “Conceptual Models for Migration of Key Groundwater Contaminants Through the Vadose Zone and Into the Unconfined Aquifer Below the B-Complex.”
- Thorne & Newcomer (1992) = PNL-8337, “Summary and Evaluation of Available Hydraulic Property Data for the Hanford Site Unconfined Aquifer System.”

The CPGWM model estimate of 3×10^{-5} m/m for year 2014 is consistent with the average gradient measured during 2013 (2.6×10^{-5} m/m) (DOE/RL-2014-32), and within the range of what is reported in SGW-54508 and SGW-58561, “WMA C Quarterly October through December 2014 Quarterly Groundwater Monitoring Report” (5.9×10^{-6} to 4.5×10^{-5} m/m).

RPP-ENV-58782, Rev. 0

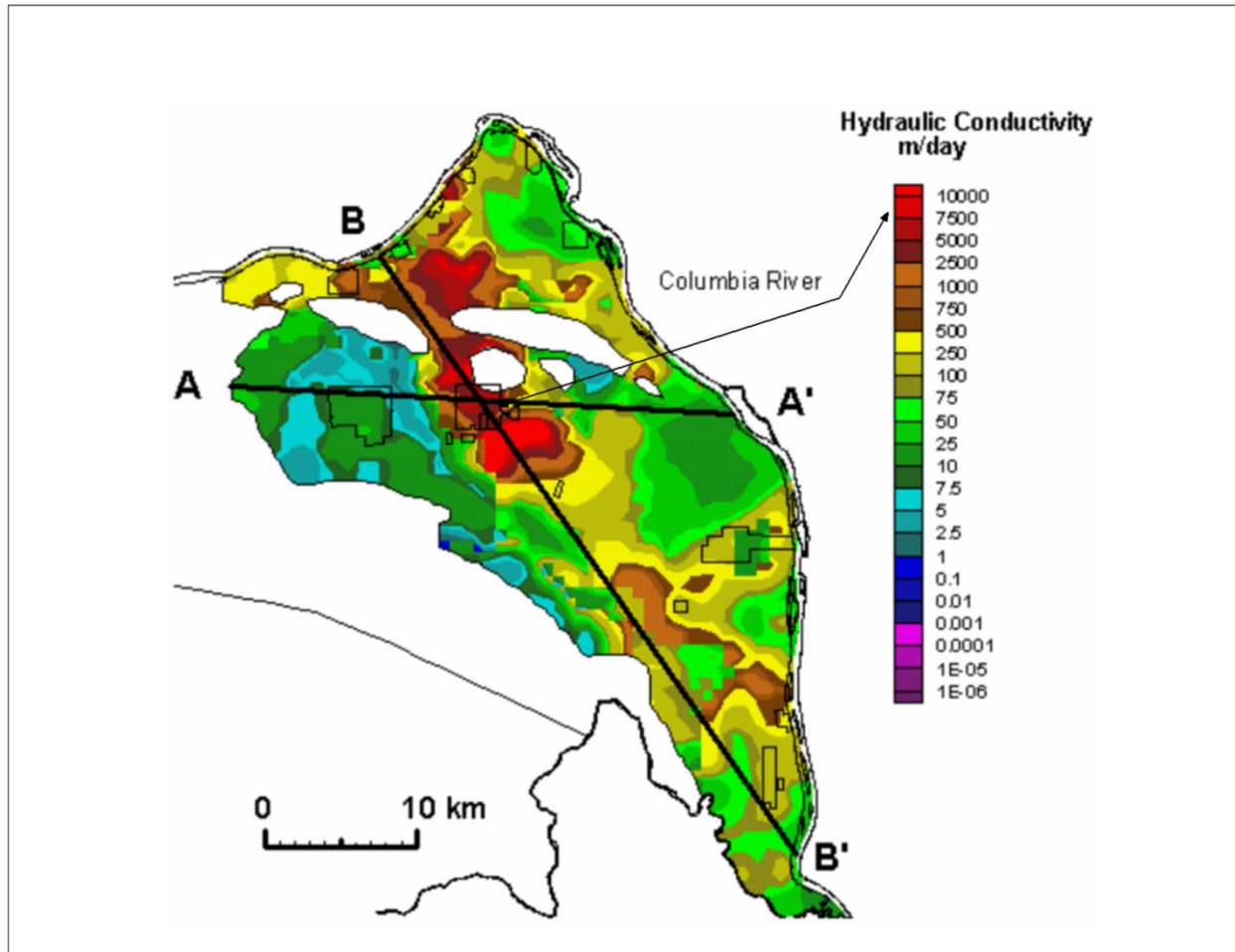
Figure C-7. Borehole Log of Well 299-E27-22.



Source: PNNL-14656, "Borehole Data Package for Four CY 2003 RCRA Wells 299-E27-4, 299-E27-21, 299-E27-22, and 299-E27-23 at Single-Shell Tank, Waste Management Area C, Hanford Site, Washington."

RPP-ENV-58782, Rev. 0

Figure C-8. Pacific Northwest National Laboratory Site-Wide Model Calibration of Hydraulic Conductivity of the Unconfined Aquifer with the Location of Waste Management Area C and Magnitude of Hydraulic Conductivity Indicated.



Excerpted and adapted from PNNL-13447, "Transient Inverse Calibration of Hanford Site-Wide Groundwater Model to Hanford Operational Impact – 1943 to 1996."

C.3.4 Anisotropy

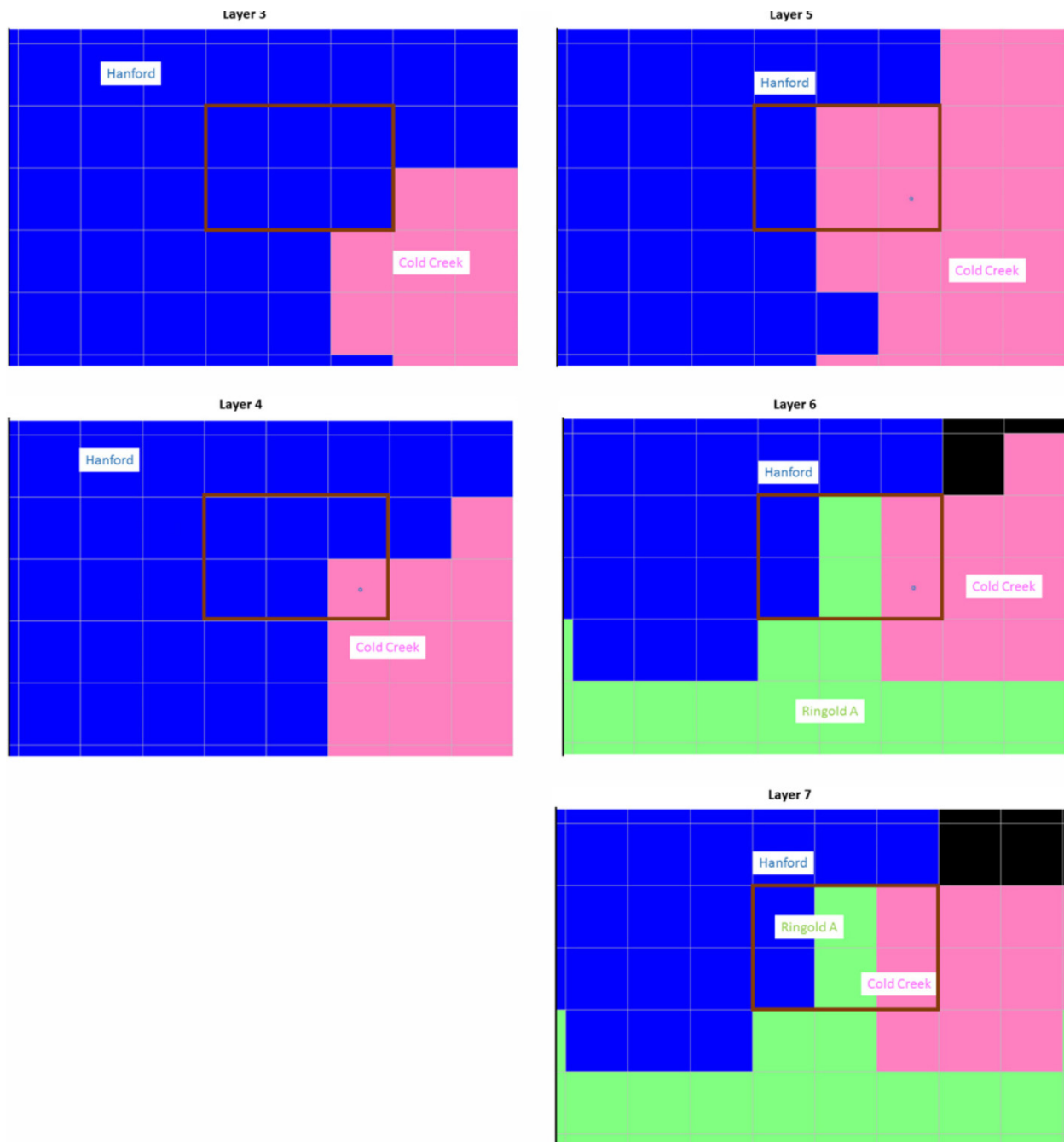
Anisotropy in saturated hydraulic conductivity for Hanford H3 gravels has been estimated from pumping tests, which indicate values ranging from 0.01 to 0.1 (PNL-10886) and 0.015 to 0.5 (DOE/RL-2007-28, Feasibility Study Report for the 200-ZP-1 Groundwater Operable Unit) for post-year 2000 testing. Previous modeling analyses (e.g., PNNL-14398, "Transient Inverse Calibration of the Site-Wide Groundwater Flow Model [ACM-2]: FY 2003 Progress Report"; PNNL-14753; DOE/EIS-0391; and CPGWM [CP-47631]) estimate anisotropy to be 0.1.

C.3.5 Properties for Contaminant Transport

The transport of contaminants also requires estimates of the porosity, the volume of pore space in the aquifer, and the macrodispersivity, which accounts for the mixing that occurs because of variations in the flow and velocity caused by heterogeneities.

RPP-ENV-58782, Rev. 0

Figure C-9. Central Plateau Groundwater Model Layer Discretization In the Saturated Zone and Extent of Various Hydrostratigraphic Units within the Model Layer in the Vicinity of Waste Management Area C (shown by the Rectangle).



C.3.5.1 Porosity. According to RPP-14430, "Subsurface Conditions Description of the C and A-AX Waste Management Area," porosity is generally estimated to be about 30% for unconsolidated coarse-grained sediments, but a value closer to 20% may be more appropriate where boulders and cobbles are present and mixed with sand and gravels, such as at WMA C. Other estimated values include 0.06 determined from an aquifer pumping test at a well

RPP-ENV-58782, Rev. 0

(699-62-43) screened within the Hanford gravel sequence similar to that at WMA C (HW-60601); 0.1 derived from laboratory tests of Hanford gravels discussed in PNNL-19277, “Conceptual Models for Migration of Key Groundwater Contaminants Through the Vadose Zone and Into the Unconfined Aquifer Below the B-Complex”; and 0.25 in RPP-RPT-46088, “Flow and Transport in the Natural System at Waste Management Area C.” DOE/EIS-0391 identified 0.15 to 0.30 as a reasonable range for the storage property value (expressed as specific yield values) of the highly conductive Hanford formation present in the paleochannel. CP-57037 estimated porosity of the Hanford formation associated with the paleochannel to be 0.2.

Table C-1. Calculation of Weighted Average Hydraulic Conductivity Value and Volumetric Water Flux from the Central Plateau Groundwater Model.

Year	Model Layer	Predicted Volumetric Water Flux (m ³ /day)	Length of Window (m)	Layer Thickness (m)	Hanford Unit Calibrated Horizontal Hydraulic Conductivity (m/day)	Calculated Gradient (m/m)
2014	3	277.1	300	3	17,000	1.81E-05
2014	4	319.1	300	3	14,233	2.49E-05
2014	5	253.4	300	3	5,933	4.75E-05
2014	6	143.1	300	1	5,802	8.22E-05
2014	7	52.5	300	1	5,802	3.02E-05
2100	3	161.3	300	3	17,000	1.05E-05
2100	4	238.4	300	3	14,233	1.86E-05
2100	5	188.7	300	3	5,933	3.53E-05
2100	6	104.6	300	1	5,802	6.01E-05
2100	7	38.5	300	1	5,802	2.21E-05
Layer Thickness Weighted Hydraulic Conductivity (m/day, rounded):						11,000
Hydraulic Gradient 2014 (m/m, rounded):						3E-05
Hydraulic Gradient 2200 (m/m, rounded):						2E-05

C.3.5.2 Macrodispersivity Estimates. Field-scale dispersivities are referred to as macrodispersivities. Field observations indicate that the dispersion coefficients required to describe the large-scale transport processes, at field scales of tens or hundreds of meters, are much different from those observed in small-scale laboratory experiments (Stochastic Subsurface Hydrology [Gelhar 1993]). In fact, macrodispersivities may often be orders of magnitude larger than those observed in the laboratory. Consequently, laboratory-scale dispersivities, which are typically ~1 cm or less, are of little use in estimating field-scale dispersivities.

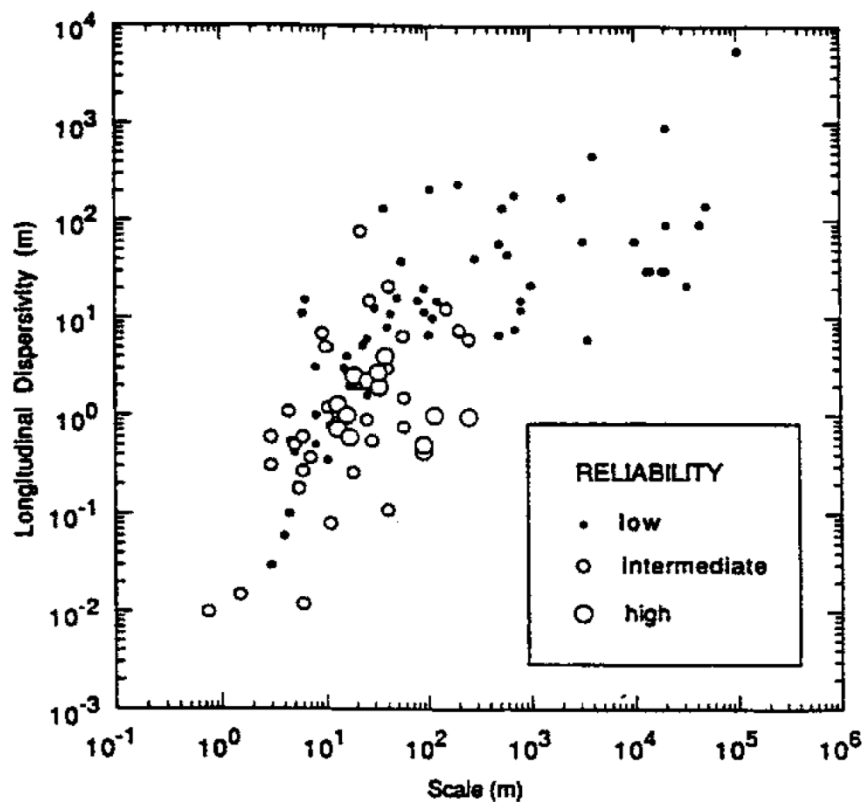
There is general agreement in hydrology literature that hydraulic conductivity variations induced by field-scale heterogeneities play an important role in field-scale transport processes. However, there does not appear to be a clear consensus about how best to describe such processes quantitatively (Gelhar 1993). While well-designed, large-scale tracer experiments would provide

RPP-ENV-58782, Rev. 0

1 useful information, limited field data are available at this time to quantify macrodispersivities in
 2 unsaturated media.

3
 4 Heterogeneities that exist at various length scales result in a scale dependence of
 5 macrodispersivities (Figure C-10; “A Critical Review of Data on Field-Scale Dispersion in
 6 Aquifers” [Gelhar et al. 1992]). Dispersivities increase with time, or equivalently with distance,
 7 until they tend to converge on their unique asymptotic (large-time) values. However, it can take
 8 a long time (e.g., years or decades) for the asymptotic Fickian approximation to take hold.
 9 Nonetheless, the second-moment evolution or the time-dependent, preasymptotic dispersivities
 10 are of marginal interest in simulations involving long-times or large-mean travel distances such
 11 as those in PA modeling. The use of a constant (asymptotic) macrodispersivity is thus
 12 considered appropriate in PA simulations (NUREG/CR-6114, Auxiliary Analyses in Support of
 13 Performance Assessment of a Hypothetical Low-Level Waste Facility: Groundwater Flow and
 14 Transport Simulation).

15
 16 **Figure C-10. Longitudinal Macrodispersivity in Saturated Media as a Function of Overall**
 17 **Problem Scale with Data Classified by Reliability.**
 18



19
 20 Reference: “A Critical Review of Data on Field-Scale Dispersion in Aquifers” (Gelhar et al. 1992).
 21

22 The longitudinal and transverse macrodispersivity estimates in the saturated zone are based on a
 23 review of three general relationships (“Universal Scaling of Hydraulic Conductivities and
 24 Dispersivities in Geologic Media” [Neuman 1990]; “Longitudinal Dispersivity Data and
 25 Implications for Scaling Behavior” [Schulze-Makuch 2005]; and “Use of Weighted
 26 Least-Squares Method in Evaluation of the Relationship Between Dispersivity and Field Scale”

RPP-ENV-58782, Rev. 0

[Xu and Eckstein 1995]) that quantify the dependence of this parameter on measurement scale (L_s). For the 100 m scale of transport calculations considered in the PA effort, which is the approximate distance of transport from source areas to a compliance well located in the saturated zone, the calculated values fall within the range of 3.5 to 17 m (Table C-2).

Table C-2. Relationship Between Saturated Longitudinal Macrodispersivity (α_L) and Scale of Measurement (L_s).

Reference	Relationship	Origin	Saturated Longitudinal Macrodispersivity Estimate (m) for a Scale ≈ 100 m
Neuman (1990)	$\alpha_L \approx 0.017 L_s^{1.5}$	“Universal relationship” established considering both field and laboratory data (excluding modeling results)	17
Schulze-Makuch (2005)	$\alpha_L \approx 0.085 L_s^{0.81}$	Established considering field and modeling results (all reliabilities) and excluding laboratory data	3.5
Xu and Eckstein (1995)	$\alpha_L \approx 0.94 (\log_{10} L_s)^{2.693}$	Established considering the same data set as Neuman (1990) including numerical model results	6

References:

“Universal Scaling of Hydraulic Conductivities and Dispersivities in Geologic Media” (Neuman 1990).

“Longitudinal Dispersivity Data and Implications for Scaling Behavior” (Schulze-Makuch 2005).

“Use of Weighted Least-Squares Method in Evaluation of the Relationship Between Dispersivity and Field Scale” (Xu and Eckstein 1995).

RPP-17209, “Modeling Data Package for an Initial Assessment of Closure of the S and SX Tank Farms,” and “Field Study of a Long and Very Narrow Contaminant Plume” (van der Kamp et al. 1994) indicate that a value of 10 represents a reasonable estimate of the ratio of longitudinal to transverse macrodispersivity, and the aquifer lateral and vertical dispersivity values used in the model appear to be consistent with the distribution of the ^{99}Tc in the aquifer observed around WMA C. The elevated ^{99}Tc concentrations around WMA C appear to extend throughout the depth of the aquifer, indicating that the plume is well mixed. The peak ^{99}Tc activity (20,800 pCi/L) was determined at a depth of ~ 9 m below the water table in well 299-E27-23 during depth discrete sampling, although the activity was relatively constant at each depth measured in the well (i.e., 19,900 pCi/L and 20,500 pCi/L at depths of 3 m and 6 m, respectively) (DOE/RL-2011-01, Hanford Site Groundwater Monitoring Report for 2010). Depth discrete samples collected at wells 299-E27-4, 299-E27-7, and 299-E27-21 further indicate that ^{99}Tc activity increases with depth and that the ^{99}Tc is not contained in the upper part of the aquifer. For example, well 299-E27-4 had activity measurements of 727 and 761 pCi/L in the first two intervals but 7,260 pCi/L in the lowest sample interval (DOE/RL-2011-01). Thus, the aquifer dispersivity values appear to be consistent with the distribution indicated by the measured data.

RPP-ENV-58782, Rev. 0

C.4 UNCONFINED AQUIFER FLOW AND TRANSPORT PROPERTIES USED IN THE WASTE MANAGEMENT AREA C PERFORMANCE ASSESSMENT

The WMA C PA mostly adopted flow and transport properties derived from results developed from the calibrated CPGWM. The CPGWM takes into account the accumulated knowledge and experience of many years of study of the aquifer beneath the Central Plateau. One of the objectives for the CPGWM is to create a common modeling platform that can be used for investigations that support remedial activities and decisions in the four groundwater operable units that exist in the Central Plateau region (CP-47631). As discussed in Section C.1, the scale of the WMA C PA requires aquifer flow property estimates consistent with large area model calibration studies that are on the appropriate spatial scale.

The CPGWM incorporates the large-scale geologic and hydrogeologic features, and provides estimates of water levels, hydraulic gradients, and groundwater flows throughout the 200 West and 200 East Areas for current and expected future groundwater conditions. The model domain includes six suprabasalt HSUs with hydraulic properties established primarily through a transient calibration of the model to historical water level measurements. The CPGWM calibration places emphasis on matching water level data from the 1940s, early 1950s, and first decade of the 21st century to estimate hydraulic properties using flow conditions relatively unperturbed by site operations. Simulated water levels are compared to observed values for wells located upgradient and downgradient of WMA C (Figure C-11). The observed heads and CPGWM-simulated heads, representing a time span of over 20 years, compare well as indicated in Figure C-11, providing confidence in the predictive capabilities of the CPGWM.

The CPGWM is not a single-time-use tool, but represents the product of ongoing development and continued improvement that began in FY 2009 (CP-47631). The CPGWM represents the most recent culmination of understanding of the unconfined aquifer under the Central Plateau. CP-47631 provides information pertaining to the CPGWM objectives; conceptualization; model implementation; sensitivity, calibration, and uncertainty analyses; configuration control; and limitations of the groundwater flow component of the CPGWM.

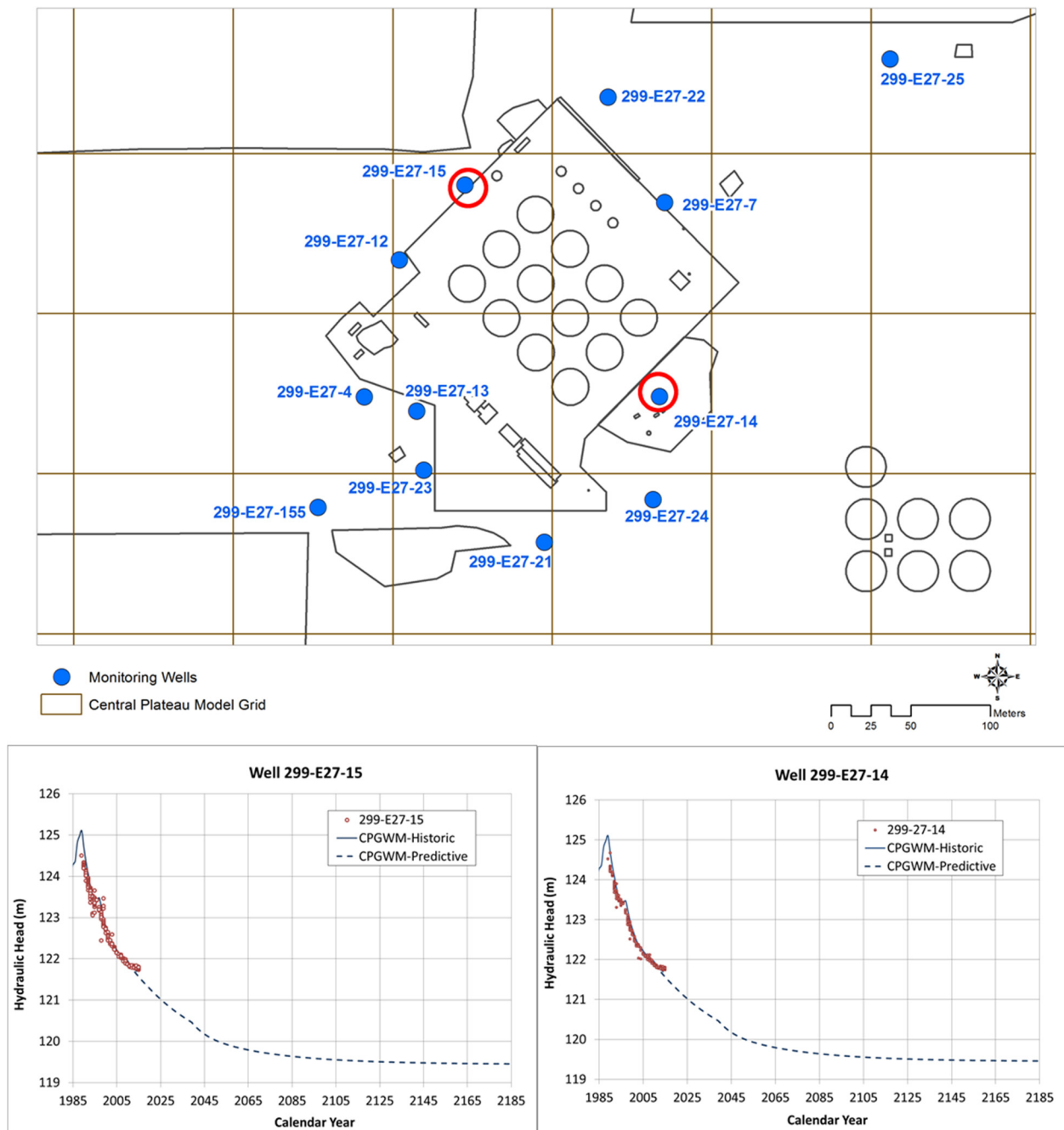
The CPGWM has undergone several revisions (currently at Revision 6.3.3) to improve its performance with respect to calibration. CPGWM 6.3.3 takes account of the historical development of understanding the unconfined aquifer, along with current interpretations of the geology (including the extent of the paleochannel), and up-to-date measurements of the recovery of the water table from operational discharges. Hence, it represents the best current understanding of flow under the Central Plateau.

C.4.1 Flow Properties

C.4.1.1 Hydraulic Conductivity. As discussed in Section C.3.2, the effective hydraulic conductivity for the entire aquifer at WMA C using an EHM approach is estimated to be 11,000 m/day (Table C-1). This is based on the layer thickness weighted averaging scheme of calibrated hydraulic conductivity of the HSUs in the CPGWM in the vicinity of WMA C flow domain.

RPP-ENV-58782, Rev. 0

Figure C-11. Central Plateau Groundwater Model Calibration Results in the Vicinity of Waste Management Area C.



CPGWM = Central Plateau Groundwater Model

C.4.1.2 Hydraulic Gradient. The hydraulic gradient estimate (2×10^{-5} m/m, Table C-1) is based on the CPGWM estimates of future conditions within the Central Plateau. Water levels in the 200 East Area continue to decline, and evaluation of current flow direction and rate of groundwater flow at WMA C is difficult due to the very low hydraulic gradient. However, no appreciable change in hydraulic gradient is expected to occur after about 100 years after closure of WMA C, once the remedial actions in the nearby operable units are completed and the water

RPP-ENV-58782, Rev. 0

1 table is at or near steady state. It is expected that by the time the contaminants are released from
2 WMA C and reach the water table, several hundred years would have passed and the water table
3 would be at a steady-state condition. These conditions justify the use of a single value of
4 hydraulic gradient for the water table, even though it is known to have changed substantially in
5 the past owing to operational releases.

6
7 **C.4.1.3 Anisotropy.** The CPGWM estimate of 0.1 (CP-47631) for the anisotropy, which is
8 defined here as the ratio of vertical to horizontal hydraulic conductivity, is consistent with
9 previous modeling analyses (e.g., PNNL-14398, PNNL-14753, and DOE/EIS-0391).

10 11 **C.4.2 Contaminant Transport Properties**

12
13 **C.4.2.1 Porosity.** The CPGWM value of 0.20 is consistent with the conclusion in RPP-14430,
14 the vadose zone value of 0.17 for the Hanford H1 and H3 sediments discussed in Section 6.3.2.2,
15 and with the aquifer test results presented in HW-60601. The porosity value is within the range
16 of other estimated values (e.g., PNNL-19277 and RPP-RPT-46088).

17
18 **C.4.2.2 Macrodispersivity Estimates.** A value of 10.5 m is considered representative and the
19 midpoint of the range of values presented in Section C.3.5.2. The ratio of longitudinal to
20 transverse macrodispersivity is chosen to be 10. The reasonableness of these selected
21 macrodispersivity values for the PA effort is discussed in Section C.3.5.2.

22 23 24 **C.5 DEVELOPMENT OF UNCERTAINTY IN GROUNDWATER FLUX AND** 25 **MACRODISPERSIVITY FOR SATURATED ZONE**

26
27 In the WMA C PA, the contaminant concentrations in the aquifer largely depend on the
28 groundwater flux through the aquifer. While the groundwater flux can vary spatially due to local
29 changes in hydraulic properties, the peak concentration at a particular location appears to
30 correlate strongly to the mean groundwater flux, even in a heterogeneous aquifer (ITRC 2010;
31 NUREG/CR-6767, Evaluation of Hydrologic Uncertainty Assessments for Decommissioning
32 Sites Using Complex and Simplified Models).

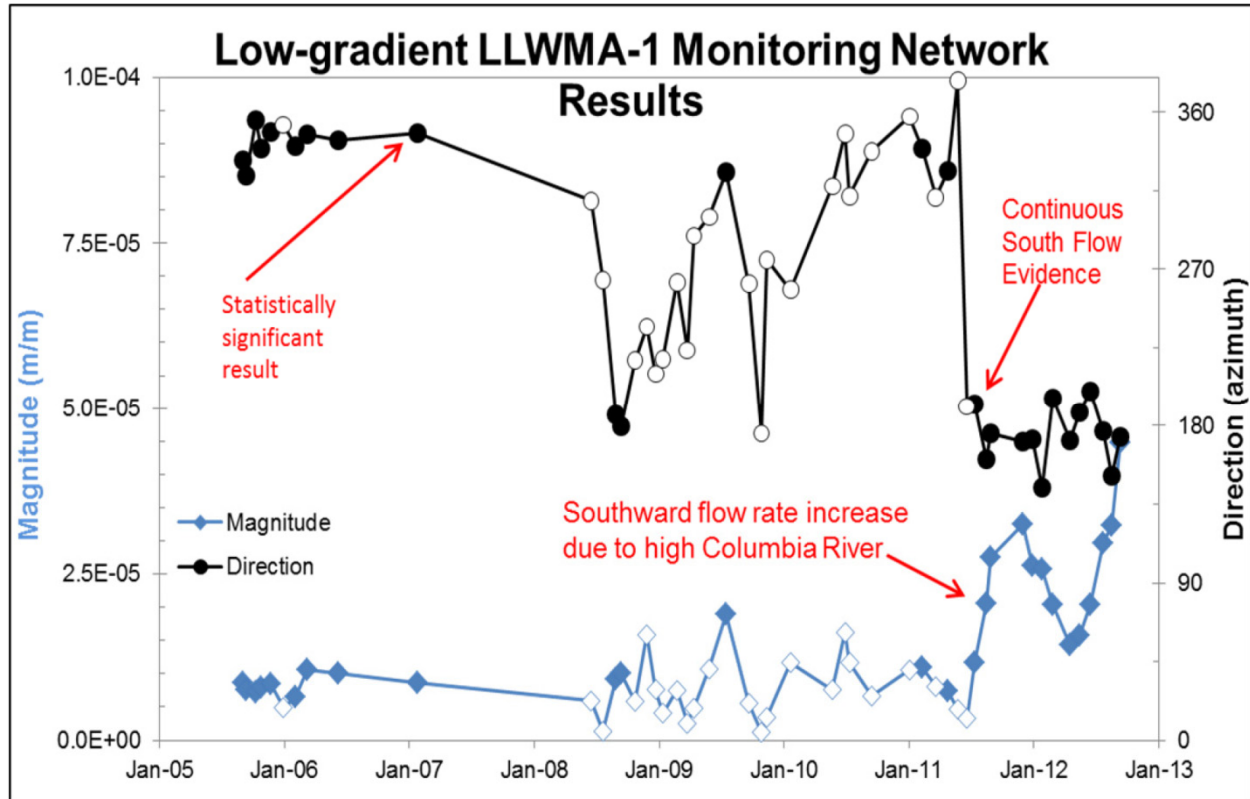
33 Groundwater flux is linearly proportional to the hydraulic conductivity and hydraulic gradient.
34 In the vicinity of WMA C, estimates of hydraulic gradient appear to include much less variability
35 than estimates of hydraulic conductivity, as indicated by the results of detailed studies of the
36 hydraulic gradient in the 200 East Area (Figure C-12). Because changes in one of the parameters
37 can be negated by reciprocal changes to the other, for the purpose of evaluating uncertainty range
38 in the groundwater flux, only the uncertainty in effective hydraulic conductivity is considered.

39
40 The general understanding of the groundwater flux in the aquifer around WMA C was used to
41 evaluate the uncertainty in that parameter. The groundwater flux estimate from the calibrated
42 CPGWM is considered to be the best estimate. The uncertainty in groundwater flux is
43 represented by propagation of uncertainty in hydraulic conductivity (K_s) and by holding the
44 long-term hydraulic gradient constant (2×10^{-5} m/m). A lower bound estimate of K_s is chosen to
45 be 1,000 m/day and the upper bound estimate is chosen to be 21,000 m/day with the best
46 estimate of 11,000 m/day. The lower bound estimate of 1,000 m/day is in the middle of the

RPP-ENV-58782, Rev. 0

range of test results presented in DOE/RL-2013-22, but appears to substantially underestimate the regional-scale value estimated using the CPGWM. The upper bound estimate of 21,000 m/day is chosen as a reasonable upper bound given that the hydraulic gradient is kept fixed. Based on this information, the uncertainty distribution for K_s is represented by a triangular distribution with minimum of 1,000 m/day, maximum of 21,000 m/day, and mode of 11,000 m/day.

Figure C-12. Low-Gradient Low-Level Waste Management Area 1 Monitoring Network Results.



Excerpted from SGW-54165, "Evaluation of the Unconfined Aquifer Hydraulic Gradient Beneath the 200 East Area, Hanford Site."

LLWMA-1 = Low-Level Waste Management Area 1

The base case groundwater flux (Darcy flux) value of 0.22 m/day is calculated from best-estimate hydraulic gradient and hydraulic conductivity. This represents the mode of the triangular distribution with the minimum and maximum values estimated to be 0.02 m/day and 0.42 m/day, respectively. The minimum and maximum values are chosen in the same proportion (relative to the best estimate) as for the K_s , as discussed above. The uncertainty distributions are summarized in Table C-3.

The uncertainty in macrodispersivity within the unconfined aquifer was based on a review of literature-based, scale-dependent relationships for this parameter as discussed in Section C.3.5.2.

RPP-ENV-58782, Rev. 0

The range in saturated zone macrodispersivity at the scale of the WMA C model is estimated to be from 1 m to 20 m.

Table C-3. Triangular Distribution of Aquifer Flux and Proportional Hydraulic Conductivity Values Applicable to the Uncertainty Analysis.

Triangular Distribution	Minimum	Mode/Median	Maximum
Aquifer Flux (m/day)	0.02	0.22	0.42
Resultant Hydraulic Conductivity (m/day)	1,000	11,000	21,000

Uncertainty in the anisotropy and porosity in the aquifer are not considered as they have small range and are not likely to appreciably impact the contaminant concentrations (WCH-520, “Performance Assessment for the Environmental Restoration Disposal Facility, Hanford Site, Washington”). Furthermore, the uncertainty associated with these effects is considered to be minor and included within the uncertainty in the concentration results associated with the uncertainty in the groundwater flux.

C.6 REFERENCES

- Aero-Metric LiDAR, 2008, “RCCC-Hanford Battelle/PNNL/DOE, Digital Orthophotography & LiDAR Surveys Photogrammetric Report,” Aero-Metric, Inc., Seattle, Washington.
- Bear, J. 1972, Dynamics of Fluids in Porous Media, American Elsevier Publishing Company, Inc., New York, New York.
- Bjornstad, B., 2006, On the Trail of the Ice Age Floods: A Geological Field Guide to the Mid-Columbia Basin, Keokee Co. Publishing, Inc., Sandpoint, Idaho.
- CP-47631, 2015, “Model Package Report: Central Plateau Groundwater Model Version 6.3.3,” Rev. 2, INTERA, Inc., Richland, Washington.
- CP-57037, 2015, “Model Package Report: Plateau to River Groundwater Transport Model Version 7.1,” Rev. 0, CH2M HILL Plateau Remediation Company, Richland, Washington.
- DOE/EIS-0391, 2012, “Final Tank Closure and Waste Management Environmental Impact Statement for the Hanford Site, Richland, Washington,” U.S. Department of Energy, Washington, D.C.
- DOE/RL-2007-28, 2008, Feasibility Study Report for the 200-ZP-1 Groundwater Operable Unit, Rev. 0, U.S. Department of Energy, Richland Operations Office, Richland, Washington.
- DOE/RL-2009-77, 2010, Groundwater Quality Assessment Plan for the Single-Shell Tank Waste Management Area C, Rev. 0, U.S. Department of Energy, Richland Operations Office, Richland, Washington.

RPP-ENV-58782, Rev. 0

- 1 DOE/RL-2011-01, 2011, Hanford Site Groundwater Monitoring Report for 2010, Rev. 0,
2 U.S. Department of Energy, Richland Operations Office, Richland, Washington.
- 3 DOE/RL-2011-118, 2012, Hanford Site Groundwater Monitoring for 2011, Rev. 0,
4 U.S. Department of Energy, Richland Operations Office, Richland, Washington.
- 5 DOE/RL-2013-22, 2013, Hanford Site Groundwater Monitoring Report for 2012, Rev. 0,
6 CH2M HILL Plateau Remediation Company, Richland, Washington.
- 7 DOE/RL-2014-32, 2014, Hanford Site Groundwater Monitoring Report for 2013, Rev. 0,
8 U.S. Department of Energy, Richland Operations Office, Richland, Washington.
- 9 ECF-Hanford-13-0029, 2015, “Development of the Hanford South Geologic Framework Model,
10 Hanford Site, Washington,” Rev. 1, CH2M HILL Plateau Remediation Company,
11 Richland, Washington.
- 12 Ferreira, J. T., R. W. Ritzi, and D. F. Dominic, 2010, “Measuring the permeability of
13 open-framework gravel,” *Ground Water*, Vol. 48, pp. 593–597.
- 14 Gelhar, L. W., 1993, *Stochastic Subsurface Hydrology*, Prentice Hall, New York, New York.
- 15 Gelhar, L. W., C. Welty, and K. R. Rehfeldt, 1992, “A Critical Review of Data on Field-Scale
16 Dispersion in Aquifers,” *Water Resources Research*, Vol. 28, pp. 1955–1974.
- 17 HW-60601, 1959, “Aquifer Characteristics and Ground-Water Movement at Hanford,” General
18 Electric Company, Hanford Atomic Products Operation, Richland, Washington.
- 19 ITRC, 2010, “Use and Measurement of Mass Flux and Mass Discharge,” The Interstate
20 Technology & Regulatory Council, Integrated DNAPL Site Strategy Team,
21 Washington, D.C.
- 22 Khaleel, R., 1989, “Scale Dependence of Continuum Models for Fractured Basalts,” *Water*
23 *Resources Research*, Vol. 25, No. 8, pp. 1847–1855.
- 24 Khaleel, R. and J. F. Relyea, 1997, “Correcting Laboratory-Measured Moisture Retention Data
25 for Gravels,” *Water Resources Research*, Vol. 33, Issue 8, pp. 1875–1878.
- 26 Narbutovskih, S. M., J. P. McDonald, R. Schalla, M. D. Sweeney, 2002, “Application of the
27 Colloidal Borescope to Determine a Complex Groundwater Flow Pattern,” in *Evaluation*
28 *and Remediation of Low Permeability and Dual Porosity Environments*, pp. 176–190,
29 *Symposium on Evaluation and Remediation of Low Permeability and Dual Porosity*
30 *Environments*, Reno, Nevada.
- 31 Neuman, S. P., 1990, “Universal Scaling of Hydraulic Conductivities and Dispersivities in
32 Geologic Media,” *Water Resources Research*, Vol. 26, No. 8, pp. 1749–1758.

RPP-ENV-58782, Rev. 0

- 1 NUREG/CR-6114, 1994, Auxiliary Analyses in Support of Performance Assessment of a
2 Hypothetical Low-Level Waste Facility: Groundwater Flow and Transport Simulation,
3 Vol. 3, U.S. Nuclear Regulatory Commission, Washington, D.C.
- 4 NUREG/CR-6767, 2002, Evaluation of Hydrologic Uncertainty Assessments for
5 Decommissioning Sites Using Complex and Simplified Models, PNNL-13832, Pacific
6 Northwest National Laboratory prepared for Division of Systems Analysis and
7 Regulatory Effectiveness, Office of Nuclear Regulatory Research, U.S. Nuclear
8 Regulatory Commission, Washington, D.C.
- 9 PNL-8337, 1992, "Summary and Evaluation of Available Hydraulic Property Data for the
10 Hanford Site Unconfined Aquifer System," Pacific Northwest Laboratory, Richland,
11 Washington.
- 12 PNL-10886, 1995, "Development of a Three-Dimensional Ground-Water Model of the Hanford
13 Site Unconfined Aquifer System: FY 1995 Status Report," Pacific Northwest
14 Laboratory, Richland, Washington.
- 15 PNNL-11801, 1997, "Three-Dimensional Analysis of Future Groundwater Flow Conditions and
16 Contaminant Plume Transport in the Hanford Site Unconfined Aquifer System: FY 1996
17 and 1997 Status Report," Pacific Northwest National Laboratory, Richland, Washington.
- 18 PNNL-12261, 2000, "Revised Hydrogeology for the Suprabasalt Aquifer System, 200-East Area
19 and Vicinity," Hanford Site, Washington, Pacific Northwest National Laboratory,
20 Richland, Washington.
- 21 PNNL-13447, 2001, "Transient Inverse Calibration of Hanford Site-Wide Groundwater Model to
22 Hanford Operational Impact – 1943 to 1996," Pacific Northwest National Laboratory,
23 Richland, Washington.
- 24 PNNL-13641, 2001, "Uncertainty Analysis Framework – Hanford Site-Wide Groundwater Flow
25 and Transport Model," Pacific Northwest National Laboratory, Richland, Washington.
- 26 PNNL-14398, 2003, "Transient Inverse Calibration of the Site-Wide Groundwater Flow Model
27 (ACM-2): FY 2003 Progress Report," Rev. 0, Pacific Northwest National Laboratory,
28 Richland, Washington.
- 29 PNNL-14656, 2004, "Borehole Data Package for Four CY 2003 RCRA Wells 299-E27-4,
30 299-E27-21, 299-E27-22, and 299-E27-23 at Single-Shell Tank, Waste Management
31 Area C, Hanford Site, Washington," Pacific Northwest National Laboratory, Richland,
32 Washington.
- 33 PNNL-14753, 2006, "Groundwater Data Package for Hanford Assessments," Rev. 1, Pacific
34 Northwest National Laboratory, Richland, Washington.

RPP-ENV-58782, Rev. 0

- 1 PNNL-19277, 2010, “Conceptual Models for Migration of Key Groundwater Contaminants
2 Through the Vadose Zone and Into the Unconfined Aquifer Below the B-Complex,”
3 Rev. 0, Pacific Northwest National Laboratory, Richland, Washington.
- 4 Resource Conservation and Recovery Act of 1976, 42 USC 6901, et seq.
- 5 Rovey, C. W. II and D. S. Cherkauer, 1995, “Scale Dependency of Hydraulic Conductivity
6 Measurements,” Ground Water Vol. 33, No. 5, pp. 769–780.
- 7 RPP-14430, 2003, “Subsurface Conditions Description of the C and A-AX Waste Management
8 Area,” Rev. 0, CH2M HILL Hanford Group, Inc., Richland, Washington.
- 9 RPP-17209, 2006, “Modeling Data Package for an Initial Assessment of Closure of the S and
10 SX Tank Farms,” Rev. 1, CH2M HILL Hanford Group, Inc., Richland, Washington.
- 11 RPP-RPT-46088, 2016, “Flow and Transport in the Natural System at Waste Management
12 Area C,” Rev. 2, Washington River Protection Solutions, LLC/GSI Water Solutions, Inc.,
13 Richland, Washington.
- 14 Scheibe, T. D., E. M. Murphy, X. Chen, A. K. Rice, K. C. Carroll, B. J. Palmer,
15 A. M. Tartakovsky, I. Battiato, and B. D. Wood, 2015, “An Analysis Platform for
16 Multiscale Hydrogeologic Modeling with Emphasis on Hybrid Multiscale Methods,”
17 Ground Water, Vol. 53, No. 1, pp. 38–56.
- 18 Schulze-Makuch, D., 2005, “Longitudinal Dispersivity Data and Implications for Scaling
19 Behavior,” Ground Water, Vol. 43, No. 3, pp. 443–456.
- 20 Schulze-Makuch, D., D. A. Carlson, D. S. Cherkauer, P. Malik, 1999, “Scale Dependency of
21 Hydraulic Conductivity in Heterogeneous Media,” Ground Water, Vol. 37, No. 6,
22 pp. 904–919.
- 23 SGW-48722, 2011, “Borehole Summary Report for the ARRA Installation of Five RCRA
24 Groundwater Monitoring Wells in the 200 Areas, FY 2010,” Rev. 0, Freestone
25 Environmental Services, Inc., Richland, Washington.
- 26 SGW-54165, 2014, “Evaluation of the Unconfined Aquifer Hydraulic Gradient Beneath the
27 200 East Area, Hanford Site,” Rev. 0, CH2M HILL Plateau Remediation Company,
28 Richland, Washington.
- 29 SGW-54508, 2013, “WMA C September 2012 Quarterly Groundwater Monitoring Report,”
30 Rev. 0, CH2M HILL Plateau Remediation Company, Richland, Washington.
- 31 SGW-58561, 2015, “WMA C Quarterly October through December 2014 Quarterly
32 Groundwater Monitoring Report,” Rev. 0, CH2M HILL Plateau Remediation Company,
33 Richland, Washington.

RPP-ENV-58782, Rev. 0

- 1 U.S. Geological Survey Water-Supply Paper 2237, 1983, "Regional Flow in the Dakota Aquifer:
2 A Study of the Role of Confining Layers," U.S. Government Printing Office, Alexandria,
3 Virginia.
- 4 van der Kamp, G., L. D. Luba, J. A. Cherry, and H. Maathuis, 1994, "Field Study of a Long and
5 Very Narrow Contaminant Plume," Ground Water, Vol. 32, No. 6, pp. 1008–1016.
- 6 WCH-520, 2013, "Performance Assessment for the Environmental Restoration Disposal Facility,
7 Hanford Site, Washington," Rev. 1, Washington Closure Hanford, Richland, Washington.
- 8 WHC-SD-EN-WP-012, 1996, "Groundwater Screening Evaluation/Monitoring Plan -- 200 Area
9 Treated Effluent Disposal Facility, Project W-049H," Rev. 1, Westinghouse Hanford
10 Company, Richland, Washington.
- 11 Xu, M. and Y. Eckstein, 1995, "Use of Weighted Least-Squares Method in Evaluation of the
12 Relationship Between Dispersivity and Field Scale," Ground Water, Vol. 33, No. 6,
13 pp. 905–908.

14
15

RPP-ENV-58782, Rev. 0

1
2
3
4
5
6

This page intentionally left blank.

RPP-ENV-58782, Rev. 0

1
2
3
4
5
6
7
8
9
10
11

APPENDIX D**FLOW AND CONTAMINANT TRANSPORT NUMERICAL MODEL FOR THE
WASTE MANAGEMENT AREA C PERFORMANCE ASSESSMENT**

RPP-ENV-58782, Rev. 0

1
2
3
4
5
6
7
8

This page intentionally left blank.

RPP-ENV-58782, Rev. 0

TABLE OF CONTENTS

1			
2	D1.0	INTRODUCTION	D-1
3	D2.0	PURPOSE	D-2
4	D3.0	MODELING OBJECTIVES.....	D-3
5	D4.0	MODEL CONCEPTUALIZATION.....	D-4
6	D4.1	FEATURES, EVENTS, AND PROCESSES	D-4
7	D4.1.1	Model Domain and Boundary Conditions	D-6
8	D4.1.2	Geologic Setting.....	D-7
9	D4.1.3	Source Term.....	D-8
10	D4.1.4	Vadose Zone Hydrogeology and Contaminant Transport	D-14
11	D4.1.5	Infiltration and Recharge	D-19
12	D4.1.6	Geochemistry and Sorption.....	D-22
13	D4.1.7	Groundwater Domain.....	D-24
14	D4.1.8	Point of Calculation, Protectiveness Metric, and Time Frame	
15		Considerations	D-26
16	D4.2	NATURE AND EXTENT OF CONTAMINATION.....	D-30
17	D5.0	STOMP [®] SOFTWARE.....	D-32
18	D5.1	STOMP [®] CONTROLLED CALCULATION SOFTWARE	D-33
19	D5.2	SOFTWARE INSTALLATION AND CHECKOUT	D-33
20	D5.3	STATEMENT OF VALID SOFTWARE APPLICATION	D-34
21	D6.0	MODEL IMPLEMENTATION.....	D-34
22	D6.1	DISCRETIZATION.....	D-34
23	D6.2	PARAMETERIZATION	D-40
24	D6.3	MODELING STAGES	D-41
25	D6.4	CALIBRATION	D-42
26	D6.5	SCREENING	D-42
27	D7.0	MODEL LIMITATIONS.....	D-46
28	D8.0	MODEL CONFIGURATION MANAGEMENT.....	D-48
29	D9.0	MODEL APPLICATION.....	D-50
30	D10.0	REFERENCES	D-50

RPP-ENV-58782, Rev. 0

LIST OF FIGURES

1		
2		
3	Figure D-1. Waste Management Area C Tanks and Associated Infrastructure and	
4	Unplanned Releases.	D-3
5	Figure D-2. Plan View of Waste Management Area C Performance Assessment Model	
6	Domain Showing the Horizontal Distribution and Surface Type of the	
7	Irregularly-Spaced Calculation Nodes. The resolution increases in	
8	the area of Waste Management Area C.....	D-9
9	Figure D-3. Fence Diagram of Alternative Geologic Models Used in the Performance	
10	Assessment for Waste Management Area C.	D-11
11	Figure D-4. Central Plateau Groundwater Model Calibration Results in the Vicinity of	
12	Waste Management Area C.....	D-28
13	Figure D-5. Points of Calculation 100 Meters Downgradient of Waste Management	
14	Area C.	D-31
15	Figure D-6. Horizontal Alignment of Three-Dimensional Model Computational Nodes	
16	with Waste Management Area C Single-Shell Tanks, 241-C-301 Catch Tank,	
17	244-CR-Vault, and Other Waste Management Area C Ancillary Equipment.	D-35
18	Figure D-7. Horizontal and Vertical Alignment and Distribution of Waste Management	
19	Area C Performance Assessment Three-Dimensional Model	
20	Computational Nodes.....	D-37
21	Figure D-8. Relative Change in Moisture Content from the Pre-Hanford Steady State	
22	Condition at the Four Vertical Boundaries of the Model at Three Times	
23	of Interest: Year 2020, Year 2520, and Year 3020.	D-38
24	Figure D-9. Comparison of the Technetium-99 Concentration at the Nine Points of	
25	Calculation Located 100 Meters Downgradient between the	
26	Base Case Dispersivity Values and the Numerical	
27	Dispersion Test Case Dispersivity Values.	D-39

28

29

30

RPP-ENV-58782, Rev. 0

LIST OF TABLES

1		
2		
3	Table D-1. Post-Retrieval Residual Waste Inventory for Waste Management Area C	
4	Tanks, Ancillary Equipment, and Pipelines.	D-15
5	Table D-2. Summary Explanation and List of Parameters Used to Develop the	
6	Source-Term Release Calculations and Functions.	D-17
7	Table D-3. Partition Coefficient Values for Grout/Concrete Used for Waste Management	
8	Area C Performance Assessment Source Release Functions.	D-20
9	Table D-4. Composite van Genuchten-Mualem Parameters for Various Strata at the Waste	
10	Management Area C Site Used in the Base Case Evaluations of Alternative	
11	Geologic Models I and II.	D-21
12	Table D-5. Effective Bulk Density ($E[\rho_b]$, g/cm ³) Estimates for Various Strata at Waste	
13	Management Area C Used in the Base Case Evaluations of Alternative	
14	Geologic Models I and II.	D-21
15	Table D-6. Macrodispersity Estimates for Various Strata at Waste Management Area C	
16	Used in the Base Case Evaluations of Alternative Geologic Models I and II.	D-22
17	Table D-7. Base Case Recharge Rate (Net Infiltration) Estimates for Surface Conditions	
18	during the Pre-Construction, Operational, and Post-Closure Periods.	D-23
19	Table D-8. Summary of the Waste Management Area C Performance Assessment Base	
20	Case K_d (mL/g) Values.	D-24
21	Table D-9. Relationship Between Saturated Longitudinal Macrodispersivity (α_L) and	
22	Scale of Measurement (L_s).	D-29
23	Table D-10. Waste Management Area C Performance Assessment Unconfined Aquifer	
24	Flow and Transport Properties.	D-30
25	Table D-11. Width of Point of Calculation Segments 100 Meters Downgradient of Waste	
26	Management Area C.	D-32
27	Table D-12. Horizontal and Vertical Spacing of the Finite Difference Cells in the	
28	Three-Dimensional Waste Management Area C Flow and Transport	
29	Model Domain.	D-36
30	Table D-13. Waste Management Area C Performance Assessment Vadose Zone	
31	Dispersivity Values and Numerical Dispersion Evaluation.	D-40
32	Table D-14. Waste Management Area C Performance Assessment Vadose Zone Courant	
33	Criteria and Numerical Dispersion Evaluation.	D-41

RPP-ENV-58782, Rev. 0

1	Table D-15. Summary of Key Elements and Base Case Parameters Associated with	
2	Site-Specific Model Components for Waste Management Area C	
3	(The basis for the elements and parameter selection provided in	
4	the individual model components sections).....	D-43
5	Table D-16. van Genuchten-Mualem Parameters Associated with the Maximum Pore	
6	Water Velocity at Specific Tension Ranges Based on Cumulative	
7	Distribution Functions.	D-45
8	Table D-17. Maximum Net Infiltration (Recharge) Estimates Used in the Screening	
9	Analysis for Pre-Construction Period, Operational Period, and	
10	Post-Closure of Waste Management Area C (Section 8.1.4).	D-45
11	Table D-18. First-Arrival Time (in Calendar Year) of Radionuclides for Various K_d Values	
12	Based on Screening Analysis Using Subsurface Transport Over Multiple	
13	Phases.	D-46
14	Table D-19. Radionuclides that Arrive at the Water Table within the 1,000-Year	
15	Compliance and 10,000-Year Sensitivity and Uncertainty	
16	Time Frame Based on the Screening Analysis Conducted	
17	Using Subsurface Transport Over Multiple Phases.....	D-49
18		
19		

RPP-ENV-58782, Rev. 0

LIST OF TERMS

1		
2	3-D	three-dimensional
3	CERCLA	Comprehensive Environmental Response, Compensation, and Liability Act of
4		1982
5	CHPRC	CH2M HILL Plateau Remediation Company
6	Ci	curie(s)
7	cm	centimeter(s)
8	cm/s	centimeters per second
9	CPGWM	Central Plateau Groundwater Model
10	Cr	chromium
11	DOE	U.S. Department of Energy
12	EHM	equivalent homogeneous medium
13	EMMA	Environmental Model Management Archive
14	EPA	U.S. Environmental Protection Agency
15	FEPs	Features, Events, and Processes
16	ft	feet
17	g	gram(s)
18	h	hour(s)
19	HSU	hydrostratigraphic unit
20	in.	inch
21	kg	kilogram(s)
22	K-U-T	potassium, uranium, and thorium
23	m	meter(s)
24	µg/L	micrograms per liter
25	mg/kg	milligrams per kilogram

RPP-ENV-58782, Rev. 0

1	mi	mile(s)
2	mL/g	microliters per gram
3	mm/yr	millimeters per year
4	NAVD88	North American Vertical Datum of 1988, National Geodetic Survey, U.S. Department of Commerce.
5		
6	PA	Performance Assessment
7	PNNL	Pacific Northwest National Laboratory
8	RCRA	Resource Conservation and Recovery Act of 1976
9	RETC	RETention Curve (software)
10	STOMP	Subsurface Transport Over Multiple Phases
11	UPR	unplanned release
12	WMA	Waste Management Area
13	WRPS	Washington River Protection Solutions
14	yr	year
15		

RPP-ENV-58782, Rev. 0

D1.0 INTRODUCTION

This appendix documents the development of the vadose zone flow and transport model for the Waste Management Area (WMA) C performance assessment (PA). The results of the flow and transport model are intended to assist in evaluating the potential long-term impact on groundwater of post-retrieval single-shell tank waste residuals, and waste left in ancillary equipment, including pipelines. Impacts related to historical unplanned releases (UPRs) are outside the scope of this modeling effort. The objectives are to address the requirements outlined in Appendix I of the Hanford Federal Facility Agreement and Consent Order (Ecology et al. 1989) for assessment of radiological impacts of waste residuals in a closed WMA C under U.S. Department of Energy (DOE) Order 435.1, Radioactive Waste Management, and evaluation of hazardous chemical impacts for the same wastes under the Resource Conservation and Recovery Act of 1976 (RCRA). The modeling results are used to estimate the possible future concentration in groundwater of various radionuclides and non-radiological contaminants to support WMA C closure decisions associated with the PA. The overall objective of the modeling effort is to provide a basis for making informed closure decisions pertinent to WMA C.

This appendix discusses the development and translation of the conceptual model for flow and contaminant transport into the WMA C three-dimensional (3-D) numerical flow and transport model evaluated using the Subsurface Transport Over Multiple Phases (STOMP)¹ simulator. The development of the geologic conceptual model is described, along with the implementation of waste release models used to represent contaminant releases from waste residuals remaining in tanks and ancillary equipment. The technical basis for specific model parameters and boundary conditions, along with description of modeling assumptions, is provided. The methodology used in estimating the peak concentrations in the groundwater from residual contamination in the tank residuals and ancillary equipment is described in detail. The modeling includes a screening process used to identify and narrow the list of contaminants of potential concern that require specific evaluation in the 3-D numerical flow and transport model of the post-retrieval closed WMA C. Control of all software used to implement the model is directed by the requirements of PRC-PRO-IRM-309, "Controlled Software Management."

This appendix documents the 3-D numerical flow and transport model itself and its applicability, along with certain calculations that are necessary to demonstrate the soundness of the model. This appendix does not discuss base case results, or the uncertainty and sensitivity analyses. Those results are presented in Sections 7 and 8. Parameters, values, and ranges identified for evaluation in the uncertainty and sensitivity analyses are presented in Sections 5, 7, and 8.

¹ Subsurface Transport Over Multiple Phases (STOMP)[®] is copyrighted by Battelle Memorial Institute, 1996.

RPP-ENV-58782, Rev. 0

D2.0 PURPOSE

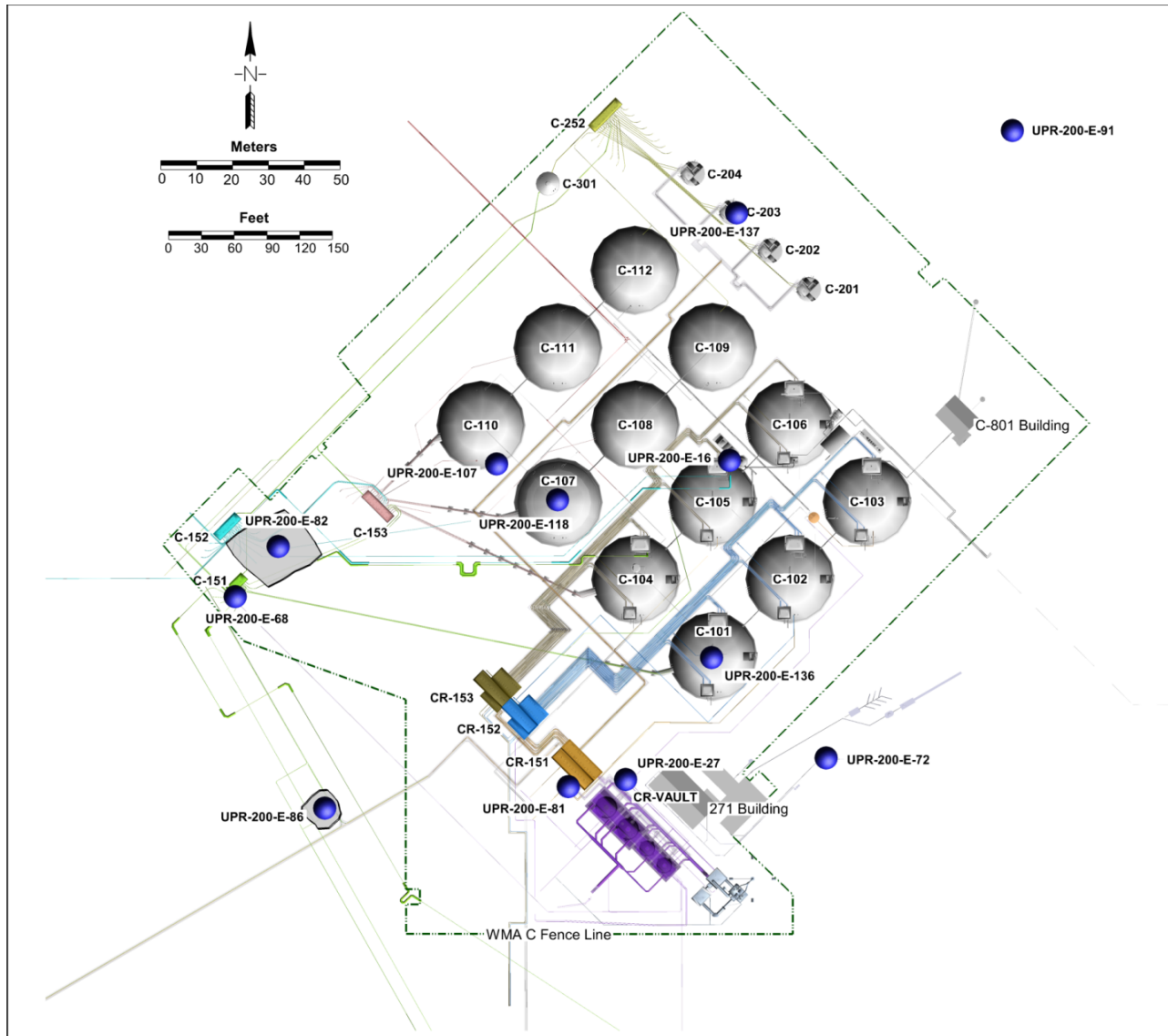
The 3-D WMA C PA flow and transport model evaluates quantitatively foreseeable or plausible future radiological and non-radiological contaminant concentrations in groundwater to determine the extent of protection to human health and the environment that the planned WMA C retrieval and closure activities provide. The purpose of the WMA C PA flow and transport modeling is to evaluate the impacts to groundwater associated with waste remaining in tank residuals after closure of WMA C. While there are no Federal requirements for protection of water resources for a radioactive waste disposal facility, the impacts from the WMA C tank residuals must comply with any applicable State or local law, regulation, or other legally-applicable requirement for water resource protection (DOE M 435.1-1, Radioactive Waste Management Manual). Therefore, water resources protection impacts are assessed on the basis of comparison to Washington State (Washington Administrative Code [WAC] 173-340, “Model Toxics Control Act – Cleanup”) or Federal Drinking Water Standards (Title 40, Code of Federal Regulations, Part 141, “National Primary Drinking Water Regulations”), whichever are more restrictive.

The modeling is conducted in accordance with the DOE G 435.1-1, Implementation Guide for Use with DOE M 435.1-1, Radioactive Waste Management Manual PA guidelines. The modeling includes both a screening phase and detailed evaluation of the groundwater concentrations and radionuclide arrival times during the 1,000-year compliance and 10,000-year sensitivity-uncertainty periods per DOE O 435.1, Radioactive Waste Management. This analysis does not consider contaminant release during WMA C operations, only the post-closure impacts of the radionuclides and non-radiological contaminants to the environment. The intent of the screening phase is to limit the model analysis to those radionuclides sufficiently mobile to impact groundwater within the compliance and sensitivity-uncertainty periods. The screening phase follows Federal soil screening guidance and DOE PA guidelines (EPA/540/F-95/041, Soil Screening Guidance: Fact Sheet; DOE G 435.1-1, Chapter 4) that approve of the use of simple site-specific models for risk assessment screening purposes. For the WMA C PA reference case evaluation, the flow and transport model is 3-D to account for the lateral movement of water and radionuclides and to maintain comparability with other vadose zone transport analyses conducted at the Hanford Site.

Details of the site and facilities (Figure D-1) are provided in Sections 2 and 3 that describe to date the conditions, geologic and hydrologic interpretations, subsurface contamination approximations, and source term estimates. During its operational history, a number of confirmed or suspected waste release events have occurred at WMA C. These included suspected tank leaks and known UPRs from waste transfer lines and systems. Although these suspected tank leaks and UPRs are believed to have impacted groundwater, the evaluation of their impacts to groundwater is outside the scope of this WMA C PA model.

RPP-ENV-58782, Rev. 0

Figure D-1. Waste Management Area C Tanks and Associated Infrastructure and Unplanned Releases.



WMA = Waste Management Area

D3.0 MODELING OBJECTIVES

The objectives of the vadose zone fate and transport modeling include the capability to provide results that support the water resource impact evaluation and the estimation of dose at the point of assessment for the “all-pathways” exposure scenario described in DOE M 435.1-1. The analysis needs to include time history results of the transport of radionuclides and non-radiological contaminants individually and collectively, and be suitable for estimating the maximum concentration in the environment. DOE M 435.1-1 requires that the WMA C PA

RPP-ENV-58782, Rev. 0

1 includes calculations of potential doses to representative future members of the public and
2 environmental impacts from potential releases from the tank residuals for a 1,000-year period
3 after closure. The point of compliance for this performance objective is at the point of highest
4 calculated concentration or dose, with an allowance for some volume averaging based on
5 projected groundwater use, beyond a 100-m buffer zone around WMA C.

6
7 The modeling objectives also include conducting sensitivity and uncertainty analyses with the
8 goal of defining bounding estimates for modeling predictions. The sensitivity-uncertainty
9 analyses extend to 10,000 years to calculate the maximum dose and the time of that dose. These
10 analyses take account of parameter values, initial conditions, boundary conditions, and changes
11 in properties with time that are appropriate for the longer time frame. These
12 sensitivity-uncertainty analyses are used to evaluate the significance of the assumptions used in
13 the development of the transport modeling and their relevance to the controlling pathways or
14 scenarios analyzed in DOE M 435.1-1. Assumptions necessary to develop inputs to the transport
15 models, or to address uncertainties, data gaps, or linkages to other models used in the analysis
16 are identified, justified, and shown to be consistent with the conceptual model.

21 **D4.0 MODEL CONCEPTUALIZATION**

22
23 This section describes the modeling methodology and approach for the determination of the
24 WMA C residual waste impacts to groundwater. A synopsis of vadose zone conceptual model,
25 conceptual model components, and the technical basis and rationale for the selection of
26 parameters is provided here, along with supporting information and rationale. This section
27 includes a description of the WMA C vadose zone geology and the pertinent vadose zone
28 physical and chemical features, events, and processes (FEPs). A summary of the rationale and
29 basis for selection of the Point of Calculation, a protectiveness metric, and the time frame for
30 compliance is also presented.

33 **D4.1 FEATURES, EVENTS, AND PROCESSES**

34
35 The development of conceptual models and exposure scenarios for the WMA C PA builds upon
36 work that began in 1999 with the intent to promote consistency and completeness in the
37 development of conceptual models to support ongoing long-term assessments at Hanford through
38 implementation of the FEPs methodology developed by the Nuclear Energy Agency for the
39 Organization for Economic Co-operation and Development (RPP-RPT-41918, "Assessment
40 Context for Performance Assessment for Waste in C Tank Farm Facilities after Closure"). The
41 FEPs methodology, as adopted by the Hanford Site, identifies a list of FEPs that are relevant to
42 the assessment of long-term safety or risks associated with solid radioactive waste repositories
43 and other waste disposal sites (RPP-RPT-41918). DOE/RL-2011-50, Regulatory Basis and
44 Implementation of a Graded Approach to Evaluation of Groundwater Protection identifies and
45 describes the FEPs applicable to most vadose zone modeling applications in the 200 Areas, and
46 concludes with the development of a "basic" Hanford Site-specific vadose zone conceptual

RPP-ENV-58782, Rev. 0

1 model. This conceptual model provides a basis for identifying the model attributes and criteria
2 that lead to the selection of the appropriate model type and computer code applicable for most
3 Hanford Site vadose zone modeling needs (DOE/RL-2011-50).

4
5 The following list of key conceptual model components derives from the basic Hanford Site
6 vadose zone conceptual model identified in DOE/RL-2011-50 and includes:

- 7
8
 - Model domain and boundary conditions
 - 9 • Geologic setting
 - 10 • Source term
 - 11 • Vadose zone hydrogeology and contaminant transport
 - 12 • Infiltration and recharge
 - 13 • Geochemistry and sorption
 - 14 • Groundwater domain.

15
16 These conceptual model components are consistent with those identified in EPA guidelines for
17 the evaluation of the protection of groundwater pathway [EPA 402-R-94-012, A Technical
18 Guide to Ground-Water Model Selection at Sites Contaminated with Radioactive Substances;
19 OSWER No. 9200.4-18, “Establishment of Cleanup Levels for CERCLA Sites with Radioactive
20 Contamination”; and HNF-5294, “Computer Code Selection Criteria for Flow and Transport
21 Code(s) To Be Used in Vadose Zone Calculations for Environmental Analyses in the Hanford
22 Site’s Central Plateau”]. The principal FEPs associated with these conceptual model
23 components include the following:

- 24
25
 - Relatively thick vadose zone composed of predominantly similar sediments (geologic
26 setting conceptual model component)
 - 27
 - 28 • Semi-arid region (infiltration recharge conceptual model component)
 - 29
 - 30 • Underlying unconfined aquifer (groundwater domain conceptual model component)
 - 31
 - 32 • Relatively few contaminants of concern in the vadose zone soils (source term) that have
33 potential impacts to groundwater.

34
35 To apply the general or basic FEPs to the WMA C PA, conceptual model components must
36 account for the source release of radionuclides and non-radiological contaminants from the
37 grouted tanks, contaminant transport through engineered barriers, and contaminant transport
38 through the natural environment, while accounting for decay and ingrowth of daughter isotopes
39 (RPP-RPT-48490, “Technical Approach and Scope for Flow and Contaminant Transport
40 Analysis in the Initial Performance Assessment of Waste Management Area C”). Transport
41 through engineered barriers must take into account the degradation of the tank structures, as well
42 as flow of water through the waste in the tanks and contaminant releases into the vadose zone
43 (RPP-RPT-41918). These processes include details of physical and chemical mechanisms on a
44 refined local scale.

RPP-ENV-58782, Rev. 0

The key conceptual model components listed above and their associated FEPs are discussed in the following subsections. The discussion includes the rationale and basis for each of the conceptual model components, and describes the function each conceptual model component and corresponding FEPs serve in the model, the assumptions associated with them, a description of the FEPs included in each component, and a qualitative assessment of the impact the component has on the model results.

D4.1.1 Model Domain and Boundary Conditions

The model domain and boundary conditions establish both a framework and limiting conditions for the numerical model. The model domain for flow and transport in the vadose zone is represented in 3-D space, with one of the horizontal axes aligned in the general direction of groundwater flow. Aligning an axis with the general direction of groundwater flow allows concentrations to be calculated more easily downgradient of the waste sites. The numerical model adapts the physical elements of the conceptual model to a Cartesian grid, and also assigns numerical values to the parameters used in algorithms to represent the physical and geochemical systems and processes.

The WMA C model domain is 737.9 m (2,421 ft) northwest to southeast by 795.3 m (2,609 ft) southwest to northeast by 116 m (381 ft) vertically, extending about 12 m (49 ft) below the water table. The southwestern and northwestern boundaries of the model are 574656.09 m, 136454.41 m, and 575218.45 m, 137016.78 m, respectively (Lambert Coordinate system easting, NOAA Manual NOS NGS 5, "State Plane Coordinate System of 1983"). The southeastern and northeastern boundaries are 575177.86 m, 135932.64 m, and 575740.22 m, 136495.00 m, respectively. The vertical base elevation of the model is nominally 95 m (North American Vertical Datum of 1988 [NAVD88]), although the bottom and top of the model domain vary spatially according to the top of basalt elevation and surface relief, respectively (RPP-RPT-56356, "Development of Alternative Digital Geologic Models of Waste Management Area C").

A specified-flux boundary condition is applied at the surface, and net infiltration rates representing recharge vary spatially and temporally along the upper boundary depending on site and surface conditions simulated, the location and physical dimensions of WMA C (recharge parameterization is discussed in Section 3.1.5), and the time of WMA C operations (RPP-RPT-44042, "Recharge and Waste Release within Engineered System in Waste Management Area C") (Figure D-2). The bottom boundary of the unsaturated (vadose) zone is the water table, and the bottom of the model (aquifer) is defined as a vertical no flow boundary condition. Boundary conditions at the sides of the model domain are assumed to be no flow in the vadose zone and prescribed flux and prescribed head in the aquifer on the upgradient and downgradient boundaries, respectively.

The boundary condition in the aquifer on the upgradient boundary applies a prescribed flux calculated on the basis of the aquifer hydraulic conductivity and gradient, independent of recharge. The prescribed flux boundary condition value includes a factor to account for the fact that the thickness of the unconfined aquifer varies because of the uneven surface of the underlying basalt. To account for the non-uniform aquifer thickness from the underlying basalt

RPP-ENV-58782, Rev. 0

boundary, the nominal flux rate calculated as the product of the hydraulic conductivity and gradient (base case values of 11,000 m/day and 2.0×10^{-5} m/m, respectively; see Section D4.1.7) is proportioned according to the ratio of the average aquifer area throughout the model domain (9,440 m²) and the aquifer area along the southwest-northwest boundary (6,151 m²) where the prescribed flux is applied. The aquifer area refers to the area perpendicular to the direction of groundwater flow.

D4.1.2 Geologic Setting

The geological setting information presented here is a summary of the information presented in RPP-RPT-46088, “Flow and Transport in the Natural System at Waste Management Area C” and RPP-RPT-56356. Waste Management Area C is located near the eastern edge of the 200 East Area on the Hanford Site on what is known as the Central Plateau. The vadose zone is ~80 to 100 m (262.4 to 328.1 ft) thick, and there are ~68 m between the base of WMA C and the present-day water table. Waste Management Area C lies within the gravel-dominated H1 unit in the vadose zone. The stratigraphic units recognized in the WMA C area include:

- Recent (Holocene) backfill material (Hdb) (~10 m thick)
- Hanford formation unit H1 – Gravel-dominated sequence (~10 m to 30 m thick)
- Hanford formation unit H2 –
 - Hanford H2 Sand-dominated sequence (~45 m to 70 m thick)
 - Hanford H2 Coarse subunit (gravel/coarse-grained facies that underlies the H2 sands)
 - Hanford H2 Silty sand subunit (silty sand lower permeability laminations/lenses)
- Hanford formation unit H3 – gravel-dominated sequence (~0 m to 20 m thick)
- Columbia River Basalt Group.

As part of the RCRA facility investigations (DOE/ORP-2008-01, RCRA Facility Investigation Report for Hanford Single-Shell Tank Waste Management Areas and RPP-PLAN-39114, “Phase 2 RCRA Facility Investigation/Corrective Measures Study Work Plan for Waste Management Area C”), the geologic strata underlying WMA C have been characterized in conjunction with soil sampling and borehole logging for radionuclides and hazardous waste constituents. The geophysical and geologic logging from the boreholes has been used to identify the elevations of tops of the geologic units in the vicinity of WMA C. Specifically, potassium, uranium, and thorium (K-U-T) data from geophysical logs were used to map the tops of the different geologic units at WMA C (RPP-RPT-56356).

In discussions associated with the 2009 to 2011 working sessions and additional discussions with regulators in 2013 and 2014, two alternative geological models were proposed and developed on

RPP-ENV-58782, Rev. 0

1 the basis of the data discussed in the preceding paragraph. Both of these models have been
2 incorporated into the PA as a means to explore the performance implications of the alternative
3 conceptualizations. This section provides a brief summary of important differences between
4 these alternative models. Details on the basis for their development are provided in
5 RPP-RPT-56356 and only briefly summarized here.

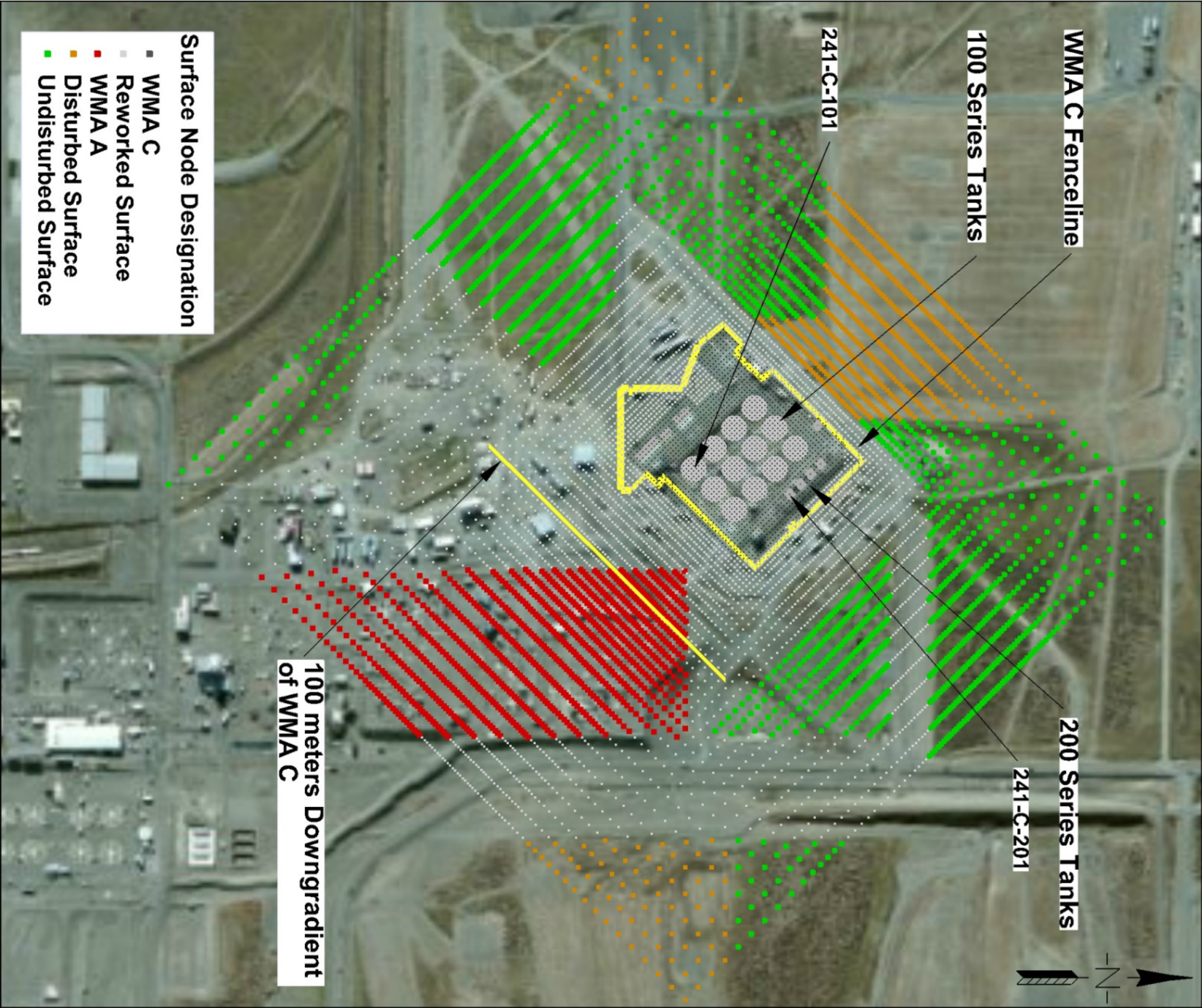
6
7 The primary difference between the two alternative models concerns whether or not a sandy
8 gravel facies followed by a silty sand layer exist at the bottom of the H2 subunit in the vicinity of
9 WMA C. The K-U-T data (i.e., a lower gross gamma and potassium count) indicates that there
10 is a coarsening of the sand at the bottom of the H2 that turns more into a sandy gravel.
11 Underlying this sandy gravel facies is a silty sand unit that presents a strong potassium peak and
12 an occasional but strong natural uranium peak. The difficulty in making the determination
13 between the two alternative models is that there are few direct pushes or drywells that go deep
14 enough in which there are both good geophysical logs and geologic logs (with drill cuttings).
15 For the most part, only the nearby groundwater wells extend to a sufficient depth. The drill
16 cuttings from nearby ground wells indicate that there is a definite fining of the sands, along with
17 some silty sands found at the vertical location as indicated by the K-U-T data in the geophysical
18 logs, but a competent silt layer was not observed. Alternative Model I does not distinguish the
19 sandy gravel and underlying silty sand unit distinctly from Hanford H2, while Alternative
20 Model II does distinguish them. The significance of distinguishing these layers is that their
21 differing characteristics, as expressed by different soil hydraulic property values, could cause
22 increased lateral movement in the vadose zone. A series of fence diagrams showing the
23 differences between the two models within WMA C is given in RPP-RPT-56356. The fence
24 diagram for both these models running southwest to northeast through the center of WMA C is
25 given in Figure D-3.

26
27 The WMA C PA includes the evaluation of Alternative Model II in its sensitivity analysis. This
28 appendix includes the discussion of Alternative Model II because Alternative Model II represents
29 an alternative conceptualization of the entire geologic model, and not a parametric variation.

31 **D4.1.3 Source Term**

32
33 The radionuclide inventory information presented here is a summary of the information
34 presented in RPP-RPT-42323, "Hanford C-Farm Tank and Ancillary Equipment Residual Waste
35 Inventory Estimates" and the WMA C PA. The source term conceptual model component
36 defines the characteristics of the inventory and the release of residual waste from the tanks,
37 ancillary equipment, and pipelines. RPP-RPT-42323 presents the basis for chemical and
38 radiological inventory estimates for residual waste remaining in 241-C Tank Farm single-shell
39 tanks and associated transfer equipment after tank waste is retrieved. As discussed in
40 RPP-RPT-42323, a conservative or bounding bias is built into the inventory estimating process,
41 generally resulting in larger than likely inventory estimates. Inventory estimates applicable to
42 the vadose zone fate and transport evaluation presented in Table D-1 are derived from the values
43 presented in RPP-RPT-42323 (Appendix B-1, C-3 and C-5), with the radionuclides decayed to
44 January 1, 2020.

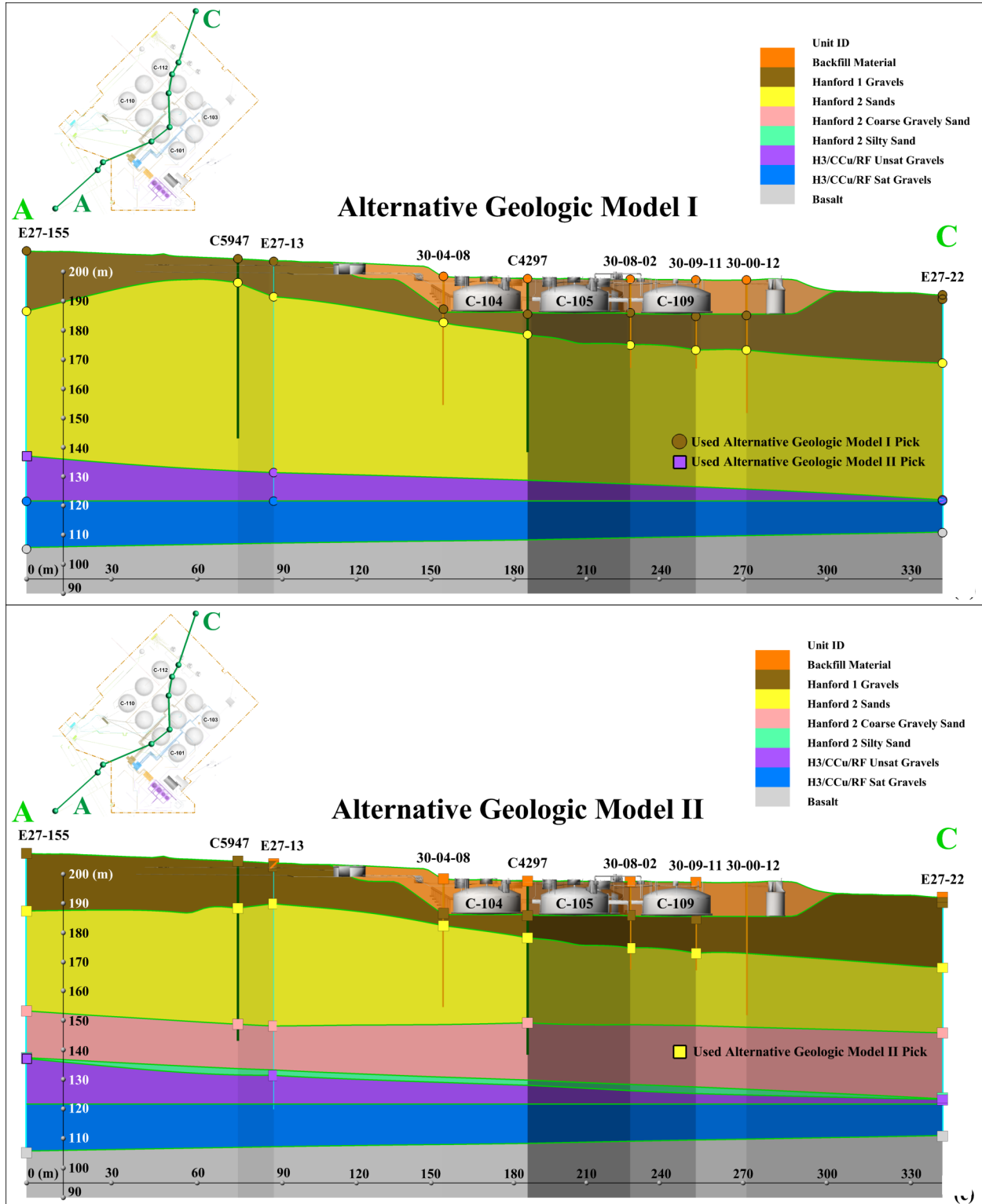
Figure D-2. Plan View of Waste Management Area C Performance Assessment Model Domain Showing the Horizontal Distribution and Surface Type of the Irregularly-Spaced Calculation Nodes. The resolution increases in the area of Waste Management Area C.



WMA = Waste Management Area

RPP-ENV-58782, Rev. 0

Figure D-3. Fence Diagram of Alternative Geologic Models Used in the Performance Assessment for Waste Management Area C.



H3/CCu/RF = undifferentiated H3, Cold Creek unit and Ringold Formation

RPP-ENV-58782, Rev. 0

Both mineral phase solubility-limited and matrix degradation rate-limited processes are considered for the key radionuclides and non-radiological contaminants ^{99}Tc , chromium, and uranium. Release processes associated with these three contaminants have been studied in detail in the laboratory, and the laboratory results have been incorporated in the source term analysis. In particular, the following release models are used, which are based on empirical evidence (Section 6.3.1):

- Matrix-degradation-rate-based release of ^{99}Tc that considers an initial 6% fraction of the ^{99}Tc inventory to be instantaneously available for release while the remaining 94% fraction undergoes relatively slower release at the fractional rate of $6 \times 10^{-4} \text{ day}^{-1}$
- Solubility-controlled releases of uranium that impose a solubility limit of $1 \times 10^{-4} \text{ M}$ for 1,000 years followed by solubility limit of $1 \times 10^{-6} \text{ M}$
- Dissolved concentration limited release for chromium that imposes a dissolved concentration upper limit of 2,000 $\mu\text{g/L}$.

For the other analytes evaluated in the WMA C PA, conservative source-term calculations are performed whereby all the analytes are assumed to be instantly and completely available in solution within the residual waste volume, and available for an immediate diffusive release.

While the tank (and ancillary equipment) infill material remains intact, it is assumed that releases occur by a diffusion process through the base of the tank base mat, consisting of grout and concrete layers. The diffusive thickness being considered is the 8-in. combined thickness of concrete and grout layer located at the base of the tank (ignoring the steel plate) because the shortest diffusive pathway for release to the near-field environment is through the base of the tank. The aqueous phase diffusive transport occurs along the thin water films within the pore spaces of the grout and concrete layer. The effective diffusion coefficient of contaminant (which includes effects of tortuosity), and sorption behavior within the grout and concrete layer, control the diffusive mass flux, in addition to the concentration gradient.

Section 6.3.1 of the WMA C PA presents detailed discussion about the theoretical and empirical development and applicability of the equations and the parameters incorporated into the release functions for the individual radionuclides and non-radiological contaminants. That discussion and all of those equations are not repeated here. The discussion and equations presented here only intend to provide context for the relationship between the equations and parameters used to develop the release functions, and an indication of the magnitude of the parameter values associated with the different radionuclides and non-radiological contaminants.

Conceptually, the diffusive release occurs in response to the solute concentration gradient that develops through the interstitial fluid contained in the tank grout and the surrounding soil. Diffusive mass transport is proportional to the concentration gradient. Solute mass diffuses from fluid volumes containing the higher concentration to volumes containing the lower concentration in proportion to the diffusive conductance. Diffusive conductance is a function of the properties

RPP-ENV-58782, Rev. 0

of the contaminant, the fluid media, and the geometry of the diffusive process. For the diffusion release model, the diffusive conductance for a contaminant solute (D_s) is computed as:

$$D_s = \frac{(A d \tau)}{L} \quad (D-1)$$

Where:

- D_s = diffusive conductance of the solute in the fluid (L^3/T)
- A = mean cross-sectional area of the connection (L^2)
- d = free-water diffusivity of the contaminant solute (L^2/T)
- τ = tortuosity of the porous medium that implicitly includes the effect of porosity and saturation (dimensionless)
- L = diffusive length, i.e., the length through which diffusion occurs (L).

The diffusive flux f_s (M/T) through the fluid is computed as follows:

$$f_s = D_s(C_{high} - C_{low}) \quad (D-2)$$

where C_{high} and C_{low} (M/L^3) are the high concentration to low concentration values of the dissolved solute. The parameters used to populate the diffusion equations in Section 6.3.1 of the WMA C PA are presented in Table D-2.

As the solute mass diffuses through the fluid in the grout, it instantaneously partitions between the solid (grout and/or soil) and fluid (water and/or air) media. The partitioning is controlled by the partition coefficients defined for each solute in each media, and the quantities of fluid and solid media present. Thus, there becomes a concentration in each medium. In the absence of solubility limits, the concentration of the solute in a particular medium (referred to as medium “m” in Equation 3) is calculated as follows:

$$C_{ims} = \left(\frac{K_{dm}}{\sum_{g=1}^{NM} K_{grs} V M_g} \right) m_s \quad (D-3)$$

Where:

- C_{ims} = concentration of solute in a particular medium (medium “m”), either fluid or solid ($[M/L^3]$ for fluid media or $[M/M]$ for solid media)
- m_s = total mass of solute present (M)
- K_{dm} = partition coefficient of the solute between medium “m” and a reference fluid ($[L^3/L^3]$ for fluid media or $[L^3/M]$ for solids)
- g = media identifying index
- K_{grs} = partition coefficient between the other media present, as identified by the index, and a reference fluid for the solute ($[L^3/L^3]$ for fluid media or $[L^3/M]$ for solids)
- $V M_g$ = quantity (volume or mass) of a particular medium present (L^3 for fluids or M for solids)
- NM = the number of media present.

RPP-ENV-58782, Rev. 0

1 The partition coefficients for the radionuclides and non-radiological contaminants evaluated in
2 the vadose zone flow and transport model are listed in Table D-3.

4 **D4.1.4 Vadose Zone Hydrogeology and Contaminant Transport**

5
6 The vadose zone hydrogeology and transport information presented here is a summary of the
7 information presented in Section 6.3.2.2. Detailed discussion and description of the data
8 available and the methods used to develop the parameters, distributions, and percentile values are
9 not repeated here.

10
11 The flow and transport pathway process used for the WMA C vadose zone modeling is porous
12 media continuum flow. The porous media continuum assumption and the soil relative
13 permeability/saturation/capillary pressure relations provide the basis for vadose zone flow and
14 transport modeling (PNNL-11216, “STOMP Subsurface Transport Over Multiple Phases
15 Application Guide”; PNNL-12030, “STOMP Subsurface Transport Over Multiple Phases
16 Version 2.0 Theory Guide”). The vadose zone at the Hanford Site is composed of sediments
17 ranging in particle size associated with gravels to silts or clays. In the model domain, the
18 hydraulic properties describing fluid transport characteristics associated with each geologic layer
19 are approximated by average upscaled values, with each unit having different flow and transport
20 parameter values (hydraulic conductivity, bulk density, and dispersivity). The model describes
21 bulk (or mean) flow and radionuclide transport behavior in the vadose zone, limiting the
22 applicability of the evaluation to estimating overall and eventual radionuclide impacts to
23 groundwater. Porous media continuum transport in unsaturated media of this type is regarded as
24 the fundamental process and feature for modeling contaminant fate and transport behavior in the
25 vadose zone at the Hanford Site (DOE/RL-2011-50).

26
27 Table D-4 lists the upscaled composite-fitted van Genuchten-Mualem parameters for the various
28 strata at the WMA C site (“A Closed-form Equation for Predicting the Hydraulic Conductivity of
29 Unsaturated Soils” [van Genuchten 1980]; “A New Model for Predicting the Hydraulic
30 Conductivity of Unsaturated Porous Media” [Mualem 1976]; EPA/600/2-91/065, The RETC
31 Code for Quantifying the Hydraulic Functions of Unsaturated Soils). A simultaneous fit of both
32 laboratory-measured moisture retention and unsaturated conductivity data was used in this work,
33 and all five unknown parameters θ_r , θ_s , α , n , and K_s , with $m=1-1/n$ (van Genuchten 1980) were
34 fitted to the data via a code named RETention Curve (RETC) (EPA/600/2-91/065). K_s is treated
35 as a fitted parameter during the curve fitting process in order to obtain a better agreement with
36 experimental data for the region of interest (i.e., relatively dry moisture regime). Estimated
37 unsaturated conductivities, based on saturated conductivity (K_s) and the van Genuchten retention
38 model parameters, have been shown to differ by up to several orders of magnitude with
39 measured conductivities at the dry end (e.g., “Evaluation of van Genuchten-Mualem
40 Relationships to Estimate Unsaturated Hydraulic Conductivity at Low Water Contents”
41 [Khaleel et al. 1995]). The pore size distribution factor ℓ (Mualem 1976) was kept fixed at 0.5
42 during the simultaneous fitting.
43

Table D-1. Post-Retrieval Residual Waste Inventory for Waste Management Area C Tanks, Ancillary Equipment, and Pipelines.

Source	241-C-101	241-C-102	241-C-103	241-C-104	241-C-105	241-C-106	241-C-107	241-C-108	241-C-109	241-C-110	241-C-111	241-C-112	241-C-201	241-C-202	241-C-203	241-C-204	241-C-301	244-CR-Vault	Pipelines
Carbon-14 (Ci)	0.003	0.001	0.007	0.003	0.05	0.008	0.02	0.008	0.0008	0.002	0.1	0.02	0.0008	0.0002	0.0002	0.0002	0.002	0.002	0.003
Cobalt-60 (Ci)	0.0002	0.21	0.02	0.47	0.68	2.2	0.0009	0.0007	0.0005	0.0001	0.1	0.0007	0.002	0.002	0.002	0.002	0.12	0.12	0.19
Tritium (Ci)	0.02	2E-5	0.004	0.009	4.1	0.004	0.01	0.02	0.004	0.002	2.6	0.01	0.0002	0.0002	0.0001	0.0001	0.002	0.002	0.003
Iodine-129 (Ci)	6E-5	0.003	0.003	0.0005	0.009	0.0006	0.04	4E-5	3E-5	0.0003	0.01	4E-5	5E-7	7E-6	1E-5	4E-7	0.0002	0.0002	0.0003
Niobium-93m (Ci)	2E-5	0.01	0.0004	0.03	0.001	5.9	0.08	0.05	0.05	0.01	0.1	0.06	0.0007	0.0008	0.0006	0.0006	0.23	0.24	0.38
Radium-226 + Daughters (Ci)	6E-7	3E-7	2E-8	3E-7	2E-7	0.0005	6E-7	5E-7	3E-7	9E-8	5E-6	4E-7	1E-9	1E-9	8E-10	8E-10	2E-5	2E-5	3E-5
Selenium-79 (Ci)	0.0003	2E-6	3E-5	0.009	0.0002	0.01	0.0003	0.002	0.0001	4E-5	0.004	0.0002	5E-5	6E-5	5E-5	4E-5	0.001	0.001	0.002
Tin-126 + Daughters (Ci)	0.0005	0.0002	5E-5	0.009	0.0003	1.8	0.0005	0.0004	0.0003	0.02	0.007	0.0004	0.0001	0.0001	9E-5	9E-5	0.07	0.07	0.11
Technetium-99 (Ci)	0.04	0.004	0.04	0.3	7.8	0.16	2.1	0.05	0.009	0.04	2.2	1.7	0.003	0.002	0.002	0.003	0.04	0.04	0.06
Uranium-232* (Ci)	2E-6	0.03	4E-6	0.04	9E-6	0.0005	2E-6	5E-7	1E-7	2E-8	2E-5	5E-7	2E-6	2E-6	7E-6	5E-6	0.002	0.002	0.003
Uranium-233* (Ci)	2E-7	2.2	0.006	2.2	5E-7	0.002	2E-7	4E-8	1E-8	2E-9	5E-5	4E-8	1E-5	1E-5	3E-5	3E-5	0.12	0.12	0.19
Uranium-234* (Ci)	0.17	0.11	0.01	0.42	0.24	0.0009	0.21	0.03	0.009	0.003	0.77	0.04	0.04	0.04	0.11	0.08	0.23	0.24	0.37
Uranium-235* (Ci)	0.008	0.004	0.0007	0.02	0.01	4E-5	0.009	0.002	0.0004	0.0001	0.03	0.002	0.001	0.001	0.005	0.003	0.01	0.01	0.02
Uranium-236* (Ci)	0.002	0.001	0.0004	0.005	0.005	2E-5	0.002	0.0003	1E-4	3E-5	0.01	0.0005	0.0005	0.0004	0.0008	0.0005	0.002	0.002	0.003
Uranium-238 +Daughters (Ci)	0.17	0.1	0.02	0.44	0.24	0.0009	0.21	0.04	0.01	0.003	0.79	0.04	0.04	0.03	0.11	0.08	0.23	0.23	0.36
Chromium (VI) (dissolved) (Kg)	7.2	11.3	2.4	3.1	37	3.8	55.4	0.63	0.18	1.1	73.3	57.8	12.2	9.1	2.6	1.4	17.9	18.3	28.6
Fluoride (Kg)	34.6	0.006	0.16	15.4	79.2	0.54	605	121	96.8	138	807	709	2.7	2.3	1.6	0.008	21.2	21.8	34.1
Nitrite (Kg)	564	0.03	0.48	5.1	647	41.4	2,148	5.8	3.8	2.7	5,500	675	0.53	0.45	0.99	0.03	3.9	4	6.2
Nitrate (Kg)	8,200	0.1	0.87	9.4	783	34.8	3,588	9.2	4.5	6.7	14,700	8,760	1.4	1.3	3.8	0.02	7.5	7.7	12
Total Uranium (soluble salts) (Kg)	516	293	49.1	1320	734	2.7	632	121	28.6	5.5	2,360	129	111	98.8	326	243	676	693	1,084
Cobalt (Kg)	0	0	0.09	0.04	0	0.38	0	0.05	0.01	0.02	0	0	0.08	0.08	0.02	0.04	0	0	0
Cyanide (Kg)	0	0	0.01	0.02	0	0.08	0	0.16	0.39	0.008	0	0	0.002	0.004	0.004	0.0007	0	0	0
Selenium and compounds (Kg)	0	0	0.69	0.14	0	2.9	0	0.31	0.08	0.04	0	0	0.11	0.09	0.18	0.4	0	0	0
Tin (Kg)	0	0	1.1	0.37	0	2.4	0	0.15	0.04	0.85	0	0	0.13	0.38	0.15	0.2	0	0	0
Tributyl Phosphate (Kg)	0	0	1	0.02	0	0	0	0.05	0.009	0.1	0	0	19.9	5.3	8.7	65.5	0	0	0

*The base case analysis also includes Uranium-232, Uranium-233, Uranium-234, Uranium-235, and Uranium-236, but these isotopes were not evaluated directly using the STOMP® model.

Subsurface Transport Over Multiple Phases (STOMP)® is copyrighted by Battelle Memorial Institute, 1996.

RPP-ENV-58782, Rev. 0

Table D-2. Summary Explanation and List of Parameters Used to Develop the Source-Term Release Calculations and Functions. (2 sheets)

Parameter	Value	Reference
Release Type	Diffusive release from the tanks and CR-Vaults under intact conditions; Both advective and diffusive release for the Pipelines; Both advective and diffusive release for tanks and CR-Vaults under degraded conditions.	
Technetium-99 release	6% of the waste inventory available for release instantaneously; remaining 94% waste form inventory made available based on first order fractional release rate of $6\text{E-}4 \text{ day}^{-1}$.	Waste Management Area (WMA) C Performance Assessment (PA) Section 6.3.1
Chromium dissolved concentration limit	2,000 $\mu\text{g/L}$ dissolved concentration limit imposed	WMA C PA Section 6.3.1
Uranium solubility for intact tank conditions	$1\text{E-}4 \text{ M}$ for 1,000 years; $1\text{E-}6 \text{ M}$ for time $>1,000$ years	WMA C PA Section 6.3.1
Uranium solubility for degraded tank conditions	$1\text{E-}4 \text{ M}$ for 1,000 years; $2\text{E-}5 \text{ M}$ for time $>1,000$ years	WMA C PA Section 6.3.1
Contaminant K_d values for transport through the grout and concrete layer	Variable; See Table D-3	WMA C PA Table 6-5
Porosity of Residual Waste Layer	0.4	Assumed
Saturation of Residual Waste Layer	1	Assumed fully saturated to maximize diffusive release
Residual Waste Volume	Variable by source	WMA C PA Section 3.1
Porosity of Concrete and Grout layer below the waste layer	0.11	SRNL-STI-2008-00421, Table 39
Saturation of Concrete and Grout layer below the waste layer	1	Assumed to maximize diffusive release
Bulk Density of Concrete and Grout layer below the waste layer	2.41 g/cm^3	RPP-RPT-50934, pp. C-3 (C-107 dome core density of 151 lb/ft^3)
Diffusive Length of Waste form layer	0 m	Assumed to maximize diffusive release
Diffusive Length of Concrete and Grout layer below the waste layer	0.203 m (8 in.)	Minimum diffusive thickness based on tank bottom geometry

RPP-ENV-58782, Rev. 0

Table D-2. Summary Explanation and List of Parameters Used to Develop the Source-Term Release Calculations and Functions. (2 sheets)

Parameter	Value	Reference
Diffusive Area for source term release	410.4 m ² for 100-Series Tanks; 29.2 m ² for 200-Series Tanks and C-301 catch tank; 162.4 m ² for CR_Vaults; 22,500 m ² for Pipelines	Base area for tanks based on circular geometry; area of CR-Vault is based on rectangular area with length of 92 ft and average width of 19 ft; area of Pipeline assumed to be 150 m × 150 m.
Effective Diffusion Coefficient through grout and concrete layer (incorporates effects of tortuosity)	3E-8 cm ² /s	WMA C PA Section 6.3.1

References:

RPP-RPT-50934, "Inspection and Test Report for the Removed 241-C-107 Dome Concrete."

SRNL-STI-2008-00421, "Hydraulic and Physical Properties of Saltstone Grouts and Vault Concretes."

A stochastic model of variable moisture or tension-dependent anisotropy provides the framework for upscaling small-scale measurements to the effective (upscaled) properties for the large-scale vadose zone ("Application of Stochastic Methods to Transient Flow and Transport in Heterogeneous Unsaturated Soils" [Polmann 1990]). The upscaling processes factor the inherent spatial variability that occurs on different scales in heterogeneous media into the field scale parameter estimates ("Stochastic analysis of moisture plume dynamics of a field injection experiment" [Ye et al. 2005]; "Estimation of effective unsaturated hydraulic conductivity tensor using spatial moments of observed moisture plume" [Yeh et al. 2005]). Specific upscaled flow parameters include moisture retention, and saturated and unsaturated hydraulic conductivity. Upscaled transport parameters include bulk density, diffusivity, sorption coefficients, and macrodispersivity. Detailed discussion of the Polmann (1990) model and the derivation of the upscaled parameters are presented in Section 6.3.2.2.

For the Alternative Geologic Model II evaluation, the Hanford H2 gravel/coarse sand subunit was assumed to be more transmissive, and the Hanford H2 silty sand less transmissive, than the Hanford H2 sand. Therefore, as an initial estimate of these properties, the hydraulic properties associated with the 5th and 95th percentile realizations of unsaturated hydraulic conductivity curves developed for the Hanford H2 sand unit were considered representative of the Hanford H2 gravel/coarse sand and the Hanford H2 silty sand subunits, respectively.

The effective transport parameter (i.e., macrodispersivity, bulk density, and diffusivity) estimates used in the base case and sensitivity cases are presented. Because of natural variability, the transport parameters are all spatially variable. The purpose is similar to the upscaled flow parameters, to evaluate the effect of such variability on the large-scale transport process. Effective bulk density (ρ_b) estimates are needed to calculate retardation factors for different species. The average ρ_b ($E[\rho_b]$) estimates for various strata at WMA C are presented in Table D-5. These estimates are derived from bulk density values listed in Section 3.2.2. According to "Solute transport in heterogeneous porous formations" (Dagan 1984),

RPP-ENV-58782, Rev. 0

macrodispersivity reaches a constant, asymptotic value after the solute travels a few tens of correlation scales (~50 cm) of the hydraulic conductivity field; therefore, the use of a constant (asymptotic) macrodispersivity value is considered appropriate in PA simulations (Section 3.2.2). On the basis of results of numerical simulation, stochastic theory, and 200 Areas experimental data, the recommendation is to use a longitudinal macrodispersivity value of 25 cm for the H2 sand unit in the WMA C PA base case. For H1/H3/Backfill sediments, the recommendation is to use a longitudinal macrodispersivity value of 20 cm. The transverse macrodispersivity is typically much lower; in saturated media, it may range from 1 to 10% of the longitudinal macrodispersivity ("Three-dimensional stochastic analysis of macrodispersion in aquifers" [Gelhar and Axness 1983]). In the absence of unsaturated media experimental data, the recommendation is to use a transverse macrodispersivity 1/10th of the longitudinal macrodispersivity. The estimated values of macrodispersivity applicable to the scale of the WMA C PA model for the base case are shown in Table D-6. It is assumed that the effective, large-scale diffusion coefficients for all strata in the vadose zone at the WMA C site are a function of volumetric moisture content, θ , and can be expressed using the Millington-Quirk ("Permeability of Porous Solids" [Millington and Quirk 1961]) empirical relation:

$$D_e(\theta) = D_0 \frac{\theta^{10/3}}{\theta_s^2} \quad (4-1)$$

Where:

- $D_e(\theta)$ = the effective diffusion coefficient of an ionic species
- D_0 = the effective diffusion coefficient for the same species in free water
- θ = the localized volumetric moisture content.

The tortuosity formulation in the Millington-Quirk model is based on theoretical considerations absent from other empirical models, and accounts for the ranges of moisture contents present in the vadose zone around WMA C. The molecular diffusion coefficient for all species in pore water is assumed to be 2.5×10^{-5} cm²/sec (WHC-SD-WM-EE-004, "Performance Assessment of Grouted Double-Shell Tank Waste Disposal at Hanford") which is consistent with, and representative of, values used in other Hanford PAs.

D4.1.5 Infiltration and Recharge

The magnitude of recharge for soils at the Hanford Site varies as a function of the soil type, condition of the vegetation cover, and soil integrity (e.g., disturbed versus undisturbed). The range of recharge values reported in RPP-RPT-44042 represents distinct populations of data based on lysimetry and isotopic measurements, and based on interpretation and, in some instances, extrapolation by Hanford Site subject matter experts. The natural background recharge rates represent a population for natural vegetated conditions. The range of values for operational conditions represents a population of recharge rates for vegetation-free disturbed soil. Table D-7 presents a summary of the base case recharge rates applied to the different surface types.

RPP-ENV-58782, Rev. 0

Table D-3. Partition Coefficient Values for Grout/Concrete Used for Waste Management Area C Performance Assessment Source Release Functions.

Radionuclide or Non-radiological Contaminant	Best Estimate K _d Value (mL/g)	Reference
C	2.53E+03	PSI Bericht Nr. 95-06
CN	0.00E+00	No relevant information
Co	4.00E+01	SKB R-05-75
Cr	0.00E+00	No relevant information
F	0.00E+00	No relevant information
H	1.00E-01	NAGRA NTB 02-20
I	3.00E+00	SKB R-05-75
Nb	5.00E+02	SKB R-05-75
NO ₂	0.00E+00	No relevant information
NO ₃	0.00E+00	No relevant information
Ra	5.00E+01	SKB R-05-75
Rn	0.00E+00	No relevant information
Se	6.00E+00	SKB R-05-75
Sn	5.00E+02	SKB R-05-75
Tri-butyl Phosphate	0.00E+00	No relevant information
Tc	1.00E+00	NAGRA NTB 02-20
U isotopes	2.00E+03	NAGRA NTB 02-20
U _{total}	2.00E+03	NAGRA NTB 02-20

References:

NAGRA NTB 02-20, "Cementitious Near-Field Sorption Data Base for Performance Assessment of an ILW Repository in Opalinus Clay."

PSI Bericht Nr. 95-06, "Sorption Databases for the Cementitious Near-Field of a L/ILW Repository for Performance Assessment."

SKB Rapport R-05-75, "Assessment of uncertainty intervals for sorption coefficients, SFR-1 uppföljning av SAFE."

1
2 The design for the WMA C surface barrier at closure has not been finalized, but it is expected to
3 function comparably to a Modified RCRA Subtitle C Barrier. Summary of data collected over
4 13 years at the Prototype Hanford Barrier (PNNL-17176, "200-BP-1 Prototype Hanford Barrier
5 Annual Monitoring Report for Fiscal Years 2005 Through 2007"; DOE/RL-93-33, Focused
6 Feasibility Study of Engineered Barriers for Waste Management Units in the 200 Areas)
7 indicates that infiltration through the prototype is much less than 0.1 mm/yr, and evaluations of
8 the design using lysimeter data indicate that the barrier is capable of limiting recharge to this
9 amount even with a complete lack of vegetation ("Multiple-Year Water Balance of Soil Covers
10 in a Semiarid Setting" [Fayer and Gee 2006]). However, for PA simulations involving WMA C

RPP-ENV-58782, Rev. 0

with a functioning surface barrier, a base case recharge rate of 0.5 mm/yr is assumed, which is consistent with the drainage design specification in DOE/RL-93-33.

Table D-4. Composite van Genuchten-Mualem Parameters for Various Strata at the Waste Management Area C Site Used in the Base Case Evaluations of Alternative Geologic Models I and II.

Strata	Number of Samples	θ_s	θ_r	α (1/cm)	n	t^c	Fitted K_s (cm/s)
Backfill (Gravelly)	10	0.138	1.11E-02	0.021	1.374	0.5	5.60E-04
Hanford H1/H3 (Gravel-dominated)	15	0.171	1.11E-02	0.036	1.491	0.5	7.70E-04
Hanford H2 (Sand-dominated)	44	0.315	3.92E-02	0.063	2.047	0.5	4.15E-03
Hydrostratigraphic Units only applicable to Alternative Geologic Model II							
Hanford H2 – Gravel/coarse sand subunit*	not applicable (75th Percentile)	0.265	2.11E-03	0.108	1.724	0.5	1.68E-02
Hanford H2 – Silty sand subunit*	not applicable (5th Percentile)	0.354	2.89E-02	0.040	1.633	0.5	1.79E-03

* Hydraulic properties of these units are only used in numerical model simulation of Alternative Geologic Model II. As an initial estimate of these properties, the hydraulic properties associated with the 5th and 95th percentile realizations of unsaturated hydraulic conductivity curves developed in the Uncertainty and Sensitivity Analysis for the Hanford H2 sand unit were considered to be representative of the Hanford H2 gravel/coarse sand and the Hanford H2 silty sand subunits.

Table D-5. Effective Bulk Density ($E[\rho_b]$, g/cm³) Estimates for Various Strata at Waste Management Area C Used in the Base Case Evaluations of Alternative Geologic Models I and II.

Strata	$E[\rho_b]$
Backfill (Gravelly)	2.13
Hanford H1/H3 (Gravel-dominated)	2.05
Hanford H2 (Sand-dominated)	1.71
Hydrostratigraphic Units only applicable to Alternative Geologic Model II	
Hanford H2 – Gravel/coarse sand subunit*	1.83
Hanford H2 – Silty sand subunit*	1.61

* Effective bulk densities of these units are only used in numerical model simulation of Alternative Geologic Model II.

At the end of 500 years, the surface barrier performance is assumed to degrade to permit an infiltration rate of 3.5 mm/yr and maintain that infiltration rate for the remainder of the sensitivity and uncertainty analysis time frame. No quantifying data are available for specifying the performance of the barrier top after its design life. According to PNNL-13033, "Recharge

RPP-ENV-58782, Rev. 0

Data Package for the Immobilized Low-Activity Waste 2001 Performance Assessment,” the erosion of the silt loam layer and deposition of dune sand on the barrier is not likely to alter the barrier performance significantly. The value of 3.5 mm/yr (0.14 in./yr) corresponds to the recharge in an undisturbed area, which indicates that native vegetation is assumed to reclaim the land.

Table D-6. Macrodispersivity Estimates for Various Strata at Waste Management Area C Used in the Base Case Evaluations of Alternative Geologic Models I and II.

Strata	A _L (cm)	A _T (cm)
Backfill (Gravelly)	~20	2
Hanford H1/H3 (Gravel-dominated)	~20	2
Hanford H2 (Sand-dominated)	~25	2.5
Hydrostratigraphic Units only applicable to Alternative Geologic Model II		
Hanford H2 –Gravel/coarse sand subunit*	~25	2.5
Hanford H2 – Silty sand subunit*	~25	2.5

* Macrodispersivities of these units are only used in numerical model simulation of Alternative Geologic Model II.

Although the side slopes and berm are likely to function and perform differently than the surface of the barrier, they are included as part of the barrier surface. The impact of the side slopes on the overall recharge rate is expected to be relatively minor. The sandy gravel/gravelly sand barrier side slope and berm are assumed eventually to resemble a Burbank loamy sand, and PNNL-16688, “Recharge Data Package for Hanford Single-Shell Tank Waste Management Areas” indicates that the long-term recharge rate for that soil type is 1.9 mm/yr, which is less than the value of 3.5 mm/yr used in the analysis for the degraded barrier surface.

D4.1.6 Geochemistry and Sorption

The geochemistry conceptual model component involves the partitioning behavior or sorption characteristics regarding release, retardation, and attenuation mechanisms, and any simplifying assumptions for specific radionuclides and non-radiological contaminants. The key aspects of this geochemistry conceptual model and its applicability to the Hanford Site 200 Areas include the following, and are discussed in detail in DOE/RL-2011-50:

- The use of a linear K_d isotherm is a reasonable description for the release and attenuation of radionuclides in the context of providing an upper-bounding condition
- The source(s) of the data used in the selection of radionuclide K_d values
- The use of a single K_d in the individual vadose zone hydrostratigraphic units (HSUs).

RPP-ENV-58782, Rev. 0

Table D-7. Base Case Recharge Rate (Net Infiltration) Estimates for Surface Conditions during the Pre-Construction, Operational, and Post-Closure Periods.

Period	Waste Management Area (WMA) C Region and Surface Condition	Base Case Value of Recharge Rate (mm/yr)
Pre-construction (before 1944)	Undisturbed region (Rupert sand with vegetation)	3.5
Operational period (1945 to 2020)	Undisturbed region (Rupert sand with vegetation)	3.5
	WMA C Surface region (Gravel without vegetation)	100
	WMA A Surface region (Gravel without vegetation)	100
	Disturbed revegetated region (Rupert sand with vegetation)	22
	Disturbed unvegetated region (Rupert sand with no vegetation)	63
Early post-closure (2020 to 2520)	Undisturbed region (Rupert sand with vegetation)	3.5
	WMA C Surface region (Surface barrier with vegetation)	0.5
	WMA A Surface region (Surface barrier with vegetation beginning in 2050)	0.5
	Disturbed revegetated region (Rupert sand with vegetation beginning in 2050 with vegetation recovery completed in 2080)	3.5
	Disturbed unvegetated region (Rupert sand with no vegetation until vegetation recovery begins in 2050 and completes in 2080)	3.5
Late post-closure (2520 to 3020 and beyond)	Undisturbed region (Rupert sand with vegetation)	3.5
	WMA C Surface region (Surface barrier with vegetation)	3.5
	WMA A Surface region (Degraded surface barrier with vegetation begins in 2550)	3.5
	Disturbed revegetated region (Rupert sand with vegetation recovery completed in 2080)	3.5
	Disturbed unvegetated region (Rupert sand with vegetation recovery completed in 2080)	3.5

The geochemistry conceptual models for the Hanford Site are based on extensive laboratory studies, testing, and measurements of adsorption and desorption coefficients under saturated and unsaturated conditions involving Hanford Site-specific sediments, contaminants, and conditions (DOE/RL-2011-50; RPP-RPT-46088; PNNL-13895, “Hanford Contaminant Distribution Coefficient Database and Users Guide”). The basis and rationale for the K_d values used to approximate the transport of the radionuclides is presented in RPP-RPT-46088, and the base case values are presented in Table D-8. The differing values for the different geologic units represent the adjustment of values resulting from the approximate gravel content of each unit.

The radionuclides and non-radiological contaminants listed in Table D-8 are limited to those with K_d values less than 2 mL/g (prior to any adjustments because of gravel content) because the

RPP-ENV-58782, Rev. 0

results of the screening analysis indicated that radionuclides with K_d values greater than 2 mL/g did not impact groundwater within the 10,000-year sensitivity-uncertainty time frame (see Section 7.2.1.1 Result of Screening Analysis for Groundwater Pathway regarding this determination).

Table D-8. Summary of the Waste Management Area C Performance Assessment Base Case K_d (mL/g) Values.

Radionuclide or Non-radiological Contaminant	K_d (mL/g)			
	Backfill	H1	H2	H3
Carbon-14 (C-14)	0.46	0.58	0.8	0.58
Cobalt/Cobalt-60 (Co/Co-60)	0	0	0	0
Chromium (Cr)	0	0	0	0
Fluoride (F)	0	0	0	0
Tritium (H-3)	0	0	0	0
Iodine-129 (I-129)	0.09	0.12	0.16	0.12
Niobium-93m (Nb-93m)	0	0	0	0
Nitrite (NO ₂)	0	0	0	0
Nitrate (NO ₃)	0	0	0	0
Radon-222 (Rn-222)	0	0	0	0
Selenium/Selenium-79 (Se/Se-79)	0.05	0.06	0.08	0.06
Tin/Tin-126 (Sn/Sn-126)	0.23	0.29	0.4	0.29
Technetium-99 (Tc-99)	0	0	0	0
Total Uranium/Uranium-238 (U Total/U-238*)	0.28	0.35	0.48	0.35
Tri-butyl Phosphate (TBP)	1.89	0.87	1.1	1.5

* The base case analysis also includes Uranium-232, Uranium-233, Uranium-234, Uranium-235, Uranium-236, and the Uranium-238 daughter products, but these isotopes were not evaluated directly using the STOMP® model.

Subsurface Transport Over Multiple Phases (STOMP)® is copyrighted by Battelle Memorial Institute, 1996.

D4.1.7 Groundwater Domain

The integrated, saturated-unsaturated, 3-D WMA C model calculates groundwater concentrations of contaminants approximately 100 m downgradient of the WMA C fenceline that are estimated to occur several hundred to several thousand years into the future. The unconfined aquifer flow and transport parameters play a critical role in WMA C PA modeling because of the dilution that occurs as recharge containing contaminants enters the aquifer. Additional dilution and concentration attenuating dispersion occurs as the contaminants travel through the aquifer. The dilution and dispersion are strongly dependent on the groundwater flux, which is a rate measure defined as the flow through a defined area. Groundwater flow beneath WMA C has been

RPP-ENV-58782, Rev. 0

difficult to measure historically because the hydraulic gradient is very small and the hydraulic conductivity is very large in this region of the Hanford Site.

The groundwater in the aquifer system in the vicinity of WMA C has been studied extensively as part of the site characterization as discussed in RPP-RPT-46088 and Appendix C. The groundwater conceptual model for WMA C includes the uppermost unconfined aquifer system that exists within a channel eroded by the cataclysmic floods of the Pleistocene. The base of the aquifer is the underlying basalt surface. The undifferentiated lower sands and gravels associated with the Hanford formation, Cold Creek unit, and the Ringold Formation (Unit A) that comprise the aquifer sediments are simply categorized as saturated Hanford H3 sediments in the model. The thickness of the uppermost aquifer beneath WMA C is approximately 12 m (39 ft). The model results provided represent concentrations in the upper 5 m (16.4 ft) of the aquifer. The 5-m vertical interval corresponds to the well screen length of a conceptual groundwater monitoring well, and the basis for that delimiter to the groundwater concentrations calculation is presented in Section D4.1.8 Point of Calculation, Protectiveness Metric, and Time Frame Considerations. The aquifer, identified as Hanford H3 – aquifer, is separated from that portion of the Hanford H3 above the water table, reflecting the distinctly different saturation conditions.

For the WMA C PA modeling, the unconfined aquifer is treated as an equivalent homogeneous medium (EHM) that requires parameterization for the appropriate scale. Effective parameterization for WMA C saturated media hydraulic conductivity appears to be best achieved via a field-scale calibrated regional groundwater model that accounts for appropriate local-scale boundary conditions, flow configuration, and history matching of well head data (WMA C PA Appendix C). The Central Plateau Groundwater Model (CPGWM) provides calibrated hydraulic conductivity estimates for the model layers and HSUs present within the aquifer in the vicinity of WMA C. The thicknesses of the different aquifer HSUs are mapped from the CPGWM onto the WMA C PA STOMP[®] model flow domain, and an averaging scheme weighted according to HSU thickness provides estimates of the EHM effective saturated hydraulic conductivity and the hydraulic gradient.

The weighted average of hydraulic conductivity of the CPGWM HSUs mapped onto the WMA C flow domain indicates that the effective STOMP[®] EHM saturated hydraulic conductivity is approximately 11,000 m/day. As discussed previously, field-scale calibrated groundwater models provide an effective parameterization for WMA C saturated media hydraulic conductivity for the overall dimensions of the WMA C PA model domain. The hydraulic gradient is calculated from a planar rectangular window (300 m × 200 m) in the CPGWM having an unconfined aquifer depth that encompasses most of the WMA C flow domain (Figure D-4, adapted from CP-47631, “Model Package Report: Central Plateau Groundwater Model Version 3.4”) by taking into account the net volumetric flux through the domain. Volumetric flux through the window is divided by the vertical cross-sectional area of the aquifer and the STOMP[®] EHM hydraulic conductivity to calculate the hydraulic gradient.

In the future, the gradient is generally expected to be from northwest to southeast. The water table in the unconfined aquifer is expected to continue declining because the large discharges of operational liquid to the ground at 216-B-3 Pond system and other large discharge sites in 200 East Area have ceased. The hydraulic heads around WMA C are expected to continue

RPP-ENV-58782, Rev. 0

declining slowly until they stabilize around year 2030 at 119.5 m (392 ft) (Figure D-4). For Year 2100 (approximating post-closure steady state conditions), the CPGWM-calculated flow through the window volume is 580 m³/day, which divided by the cross-sectional area of 3,300 m² translates to a Darcy flux of 0.18 m/day with a hydraulic gradient of 2×10^{-5} , which is close to the one observed prior to start of Hanford operations, as estimated from Figure 6-42 (adapted from Figure 2-8 in WHC-EP-0645, “Performance Assessment for the Disposal of Low-Level Waste in the 200 West Area Burial Grounds”). Changes in hydraulic gradient are only expected to occur within the first 10 to 50 years of the post-closure simulation period, which, according to the screening analysis (see Sections 6.3.2.3 Groundwater Pathway Screening Analysis Methodology and 7.2.1.1 Result of Screening Analysis for Groundwater Pathway), is before the mobile radionuclides reach the water table. Thus, the hydraulic gradient is assumed to be stable for this analysis.

According to RPP-14430, “Subsurface Conditions Description for C and A-AX Waste Management Area,” porosity is generally estimated to be about 30% for unconsolidated coarse-grained sediments, but a value closer to 20% may be more appropriate where boulders and cobbles are present and mixed with sand and gravels, such as at WMA C. The STOMP[®] EHM porosity value of 0.20 is consistent with the vadose zone value of 0.17 for the Hanford H1 and H3 sediments, and with the aquifer test results from well 699-55-50 presented in HW-60601, “Aquifer Characteristics and Ground-Water Movement at Hanford.” The STOMP[®] EHM includes the CPGWM estimate of 0.1 (CP-47631) for the anisotropy, which is defined here as the ratio of vertical to horizontal hydraulic conductivity. The longitudinal and transverse macrodispersivity estimates in the saturated zone are based on a review of three general relationships (“Universal Scaling of Hydraulic Conductivities and Dispersivities in Geologic Media” [Neuman 1990]; “Longitudinal Dispersivity Data and Implications for Scaling Behavior” [Schulze-Makuch 2005]; and “Use of Weighted Least-Squares Method in Evaluation of the Relationship Between Dispersivity and Field Scale” [Xu and Eckstein 1995]) that quantify the dependence of this parameter on measurement scale (L_s). For 100 m, which is the approximate distance of travel to the compliance well located in the saturated zone, the calculated values fall within the range of 1 to 20 m (Table D-9). Thus, a value of 10.5 m is chosen for the base calculation. The ratio of longitudinal to transverse macrodispersivity is chosen to be 10 based on RPP-17209, “Modeling Data Package for an Initial Assessment of Closure of the S and SX Tank Farms” and “Field Study of a Long and Very Narrow Contaminant Plume” (van der Kamp et al. 1994). Table D-10 presents a summary of the aquifer hydraulic parameters for the Hanford H3 – aquifer used for the base case.

D4.1.8 Point of Calculation, Protectiveness Metric, and Time Frame Considerations

In accordance with risk and performance assessment guidelines, the determination of soil contamination impacts to groundwater also requires the definition and rationale for (1) the point of calculation, i.e., the place and points in the groundwater domain where modeled groundwater concentrations are to be assessed for potential impacts and protectiveness; (2) the protectiveness metric, i.e., the groundwater metric(s) to be used in the assessment of protectiveness at the point of calculation; and (3) the time frame considered applicable for the calculation of impacts to groundwater. The point of calculation is intended to effectively serve as the point where exposure point groundwater concentrations are evaluated in the model for the purpose of

RPP-ENV-58782, Rev. 0

1 evaluating the achievement of the groundwater protection performance objectives. The point of
2 calculation for the protection of groundwater is related to “Point of Compliance” in Federal PA
3 requirements (DOE M 435.1-1; DOE G 435.1-1, Chapter 4) and described as follows:

4
5 “The point of compliance shall correspond to the point of highest projected dose or
6 concentration beyond a 100 meter buffer zone surrounding the disposed waste.
7 A larger or smaller buffer zone may be used if adequate justification is provided.”
8

9 Thus, the point of calculation for the groundwater impact analysis is 100 m downgradient from
10 the WMA C fenceline. While the DOE manual and guide state that point of compliance is the
11 point of highest calculated dose (groundwater concentration), neither indicates how that
12 groundwater concentration should be calculated—i.e., within what volume the concentration is to
13 be calculated, apart from indicating that the aquifer mixing must be consistent with State or local
14 laws, regulations, or agreements.
15

16 The approach identified in EPA/540/R-95/128, Soil Screening Guidance: Technical Background
17 Document and WAC 173-340-747, “Deriving Soil Concentrations for Groundwater Protection”
18 indicates that the cross section of the aquifer volume is usually prescribed to be a unit width of
19 1 m (3.3 ft), because the equations are developed on the basis of a unit width. This implies that
20 the cross section width is equal to the width of contamination entering the aquifer. Consistent
21 with this reasoning, other performance assessments conducted at Hanford and other DOE
22 facilities have used an aquifer mixing width equal to the width of the facility (e.g., WCH-520,
23 “Performance Assessment for the Environmental Restoration Disposal Facility, Hanford Site,
24 Washington”; WSRC-MS-2003-00582, “Performance Assessment/Composite Analysis
25 Modeling to Support a Holistic Strategy for the Closure of F Area, a Large Nuclear Complex at
26 The Savannah River Site”).
27

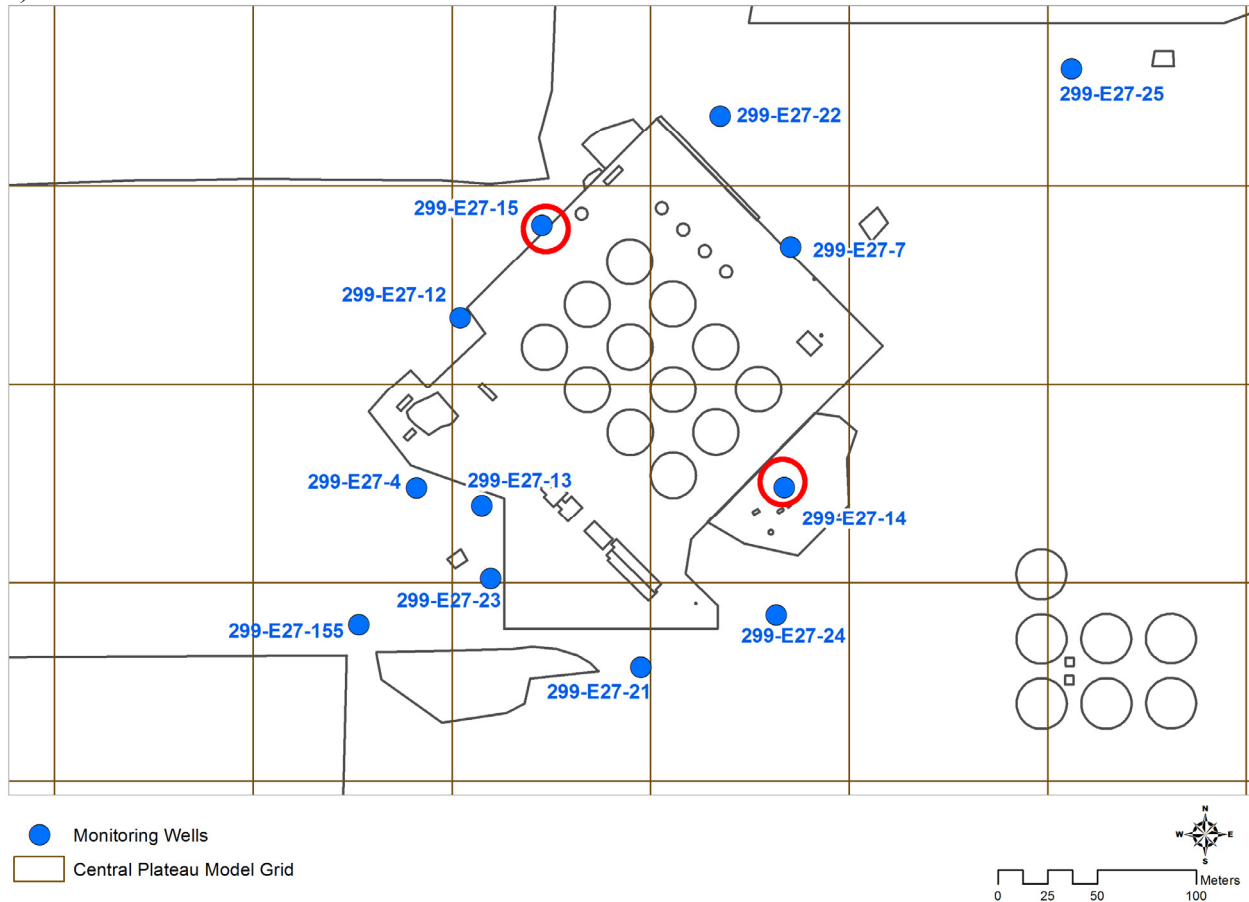
28 To calculate the highest groundwater concentration, the base case evaluated the average
29 concentration in the aquifer within nine segments along the line perpendicular to, and 100 m
30 beyond, the southeast edge of WMA C (Figure D-5). Concentrations calculated in the
31 nine segments of the aquifer are assumed to be comparable to concentrations that would be
32 measured by sampling a monitoring well at that location. The nine segments are approximately
33 30 m long (Table D-11), and aligned such that the centerlines of the plumes in the groundwater
34 resulting from the residuals released from a single line of 100-series tanks parallel to the
35 direction of groundwater flow (e.g., the centerline of the plumes resulting from the tank residuals
36 in 241-C-102, 241-C-105, 241-C-108, and 241-C-111) intersect the perpendicular line within the
37 same segment.
38

39 The WAC specifies a 5-m mixing zone in groundwater that is consistent with a 5-m vertical
40 interval corresponding to a conceptual groundwater monitoring well with the 15-ft well screen
41 length (and mixing zone dimension) associated with State monitoring well descriptions (e.g., see
42 Equation 747-4 in WAC 173-340-747). The aquifer mixing zone extends into the upper 5 m of
43 the aquifer for the purpose of the evaluations. DOE M 435.1-1 does not specify the level of
44 protection required for water resources, and there are no applicable parameterization
45 requirements or guidelines indicated in DOE G 435.1-1, Chapter 4.
46

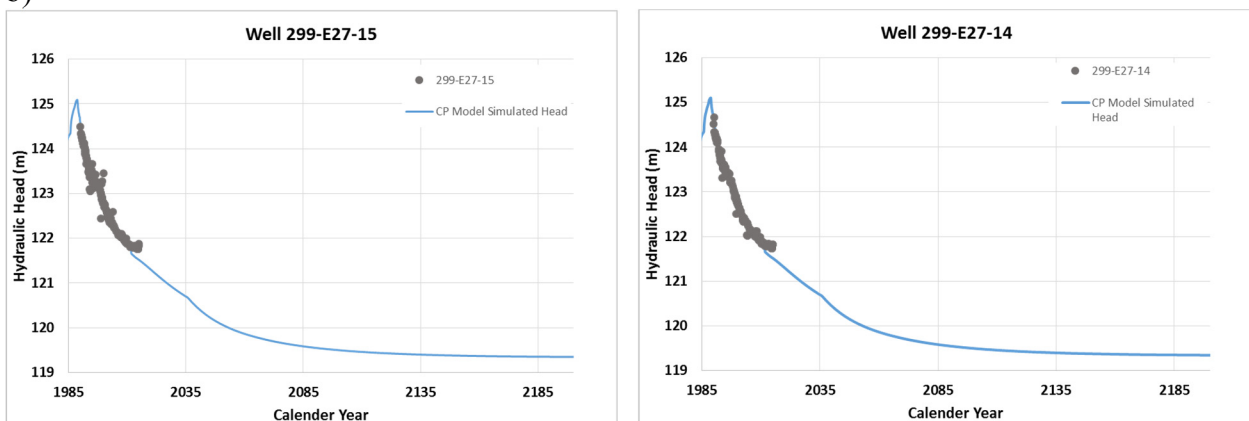
RPP-ENV-58782, Rev. 0

Figure D-4. Central Plateau Groundwater Model Calibration Results in the Vicinity of Waste Management Area C.

a)



b)



The compliance time frame is defined as 1,000 years following closure of the facility (DOE M 435.1-1; DOE G 435.1-1, Chapter 4). The sensitivity-uncertainty analysis along with the Nuclear Regulatory Commission's guidance (NUREG-1854, NRC Staff Guidance for Activities Related to U.S. Department of Energy Waste Determinations – Draft Final Report for

RPP-ENV-58782, Rev. 0

Interim Use) extends the evaluation to 10,000 years, which is sufficient to evaluate the peak dose from all of the radionuclides that the screening analysis indicates may not impact groundwater within the compliance period. DOE M 435.1-1 and DOE G 435.1-1, Chapter 4 state that the sensitivity-uncertainty analysis time frame should include calculation of the maximum dose regardless of the time at which the maximum occurs, as a means of increasing confidence in the outcome of the modeling and increasing the understanding of the models used. However, EPA-SAB-RAC-ADV-99-006, An SAB Advisory: Modeling of Radionuclide Releases from Disposal of Low Activity Mixed Waste warns that extending the modeling time frame beyond 10,000 years could make the results irrelevant, and hinder public acceptance of the results because of the inherent scientific and social uncertainties associated with such an extended time frame. The 10,000-year time frame is sufficient to address uncertainty associated with radionuclides that impact groundwater during the compliance period (NUREG-1573, A Performance Assessment Methodology for Low-Level Radioactive Waste Disposal Facilities: Recommendations of NRC's Performance Assessment Working Group).

Table D-9. Relationship Between Saturated Longitudinal Macrodispersivity (α_L) and Scale of Measurement (L_s).

Reference	Relationship	Origin	Saturated Longitudinal Macrodispersivity Estimate (m) for a Scale ≈ 100 m
Neuman (1990)	$\alpha_L \approx 0.017 L_s^{1.5}$	"Universal relationship" established considering both field and laboratory data (excluding modeling results)	17
Schulze-Makuch (2005)	$\alpha_L \approx 0.085 L_s^{0.81}$	Established considering field and modeling results (all reliabilities) and excluding laboratory data	3.5
Xu and Eckstein (1995)	$\alpha_L \approx 0.94 (\log_{10} L_s)^{2.693}$	Established considering the same data set as Neuman (1990) including numerical model results	6

References:

"Longitudinal Dispersivity Data and Implications for Scaling Behavior" (Schulze-Makuch 2005).

"Universal Scaling of Hydraulic Conductivities and Dispersivities in Geologic Media" (Neuman 1990).

"Use of Weighted Least-Squares Method in Evaluation of the Relationship Between Dispersivity and Field Scale" (Xu and Eckstein 1995).

DOE G 435.1-1, Chapter 4 states that DOE low-level waste disposal facilities must comply with legally applicable requirements for water resource protection. The protectiveness metrics determined to be most appropriate for the evaluation of impacts to groundwater during the compliance period from the radionuclide and contaminant inventory in WMA C are the maximum concentration limits. Maximum concentration limits represent the "allowable concentrations" and/or "acceptable limits" of a radionuclide for minimizing further degradation of groundwater in accordance with the conditions identified in State and Federal anti-degradation goals (e.g., EPA/540/R-92/003, Guidance for Data Useability in Risk Assessment (Part A) Final; EPA/530-SW-87-017, Alternate Concentration Limit Guidance; DOE/RL-2002-59, Hanford Site Groundwater Strategy Protection, Monitoring, and Remediation).

RPP-ENV-58782, Rev. 0

Table D-10. Waste Management Area C Performance Assessment Unconfined Aquifer Flow and Transport Properties.

Property	Waste Management Area C
Horizontal saturated hydraulic conductivity (m/day) ^a	11,000
Ratio of vertical to horizontal saturated hydraulic conductivity	0.1
Specific storage (1/m) ^b	1.1E-3
Effective porosity (dimensionless)	0.20 (Hanford Gravel)
Hydraulic gradient (m/m) ^c	2.0E-5
Depth to water table (m)	80
Longitudinal macrodispersivity (m)	10.5
Longitudinal to transverse macrodispersivity ratio	10

^a Thickness weighted average conductivity estimate derived from Central Plateau Groundwater Model based on Equivalent Homogeneous Media approach adopted for representing the aquifer in the model.

^b Using the assumed values of an aquifer compressibility of 1.0E-7 1/Pa (STOMP default), a water compressibility of 0.0046 1/atm (CRC Handbook of Chemistry and Physics [Haynes and Lide 2011]), and a water density of 1,000 kg/m³ (Haynes and Lide 2011).

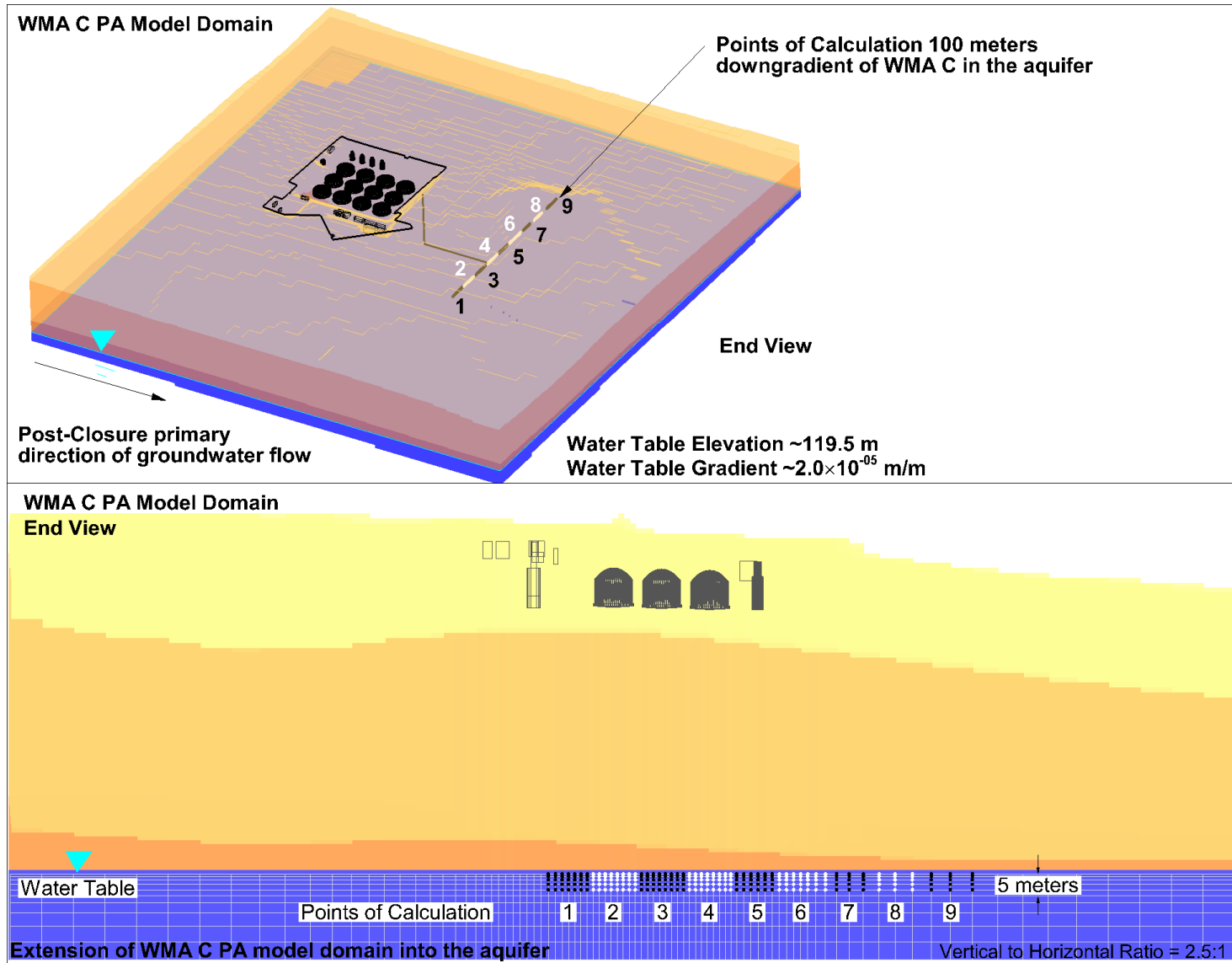
^c Thickness weighted gradient estimate derived from Central Plateau Groundwater Model based on Equivalent Homogeneous Media approach adopted for representing the aquifer in the model.

Defining the protection of groundwater in the context of vadose zone fate and transport requires consideration of the soil and groundwater media as a hybrid or coupled pathway. This pathway involves the determination of future concentrations in the groundwater medium that result from the transport of the radionuclide and contaminant inventory existing in the WMA C tank residuals. The working definition of protectiveness for the protection of groundwater pathway is considered achieved if the radionuclide and contaminant levels in the WMA C tank residuals do not cause groundwater concentrations to exceed maximum concentration limits at the point of calculation within 1,000 years after closure, which is assumed to begin in 2020.

D4.2 NATURE AND EXTENT OF CONTAMINATION

The WMA C PA addresses the radionuclide and non-radiological contaminant inventory contained in waste residuals in tanks and ancillary equipment in WMA C at the assumed time of closure. Tank waste can be grouped into three types based on physical properties: supernate, salt, and sludge (RPP-RPT-42323). The 241-C Tank Farm contains little salt types, and with the supernate having been pumped out as part of interim stabilization, the tanks now mainly contain sludge (RPP-RPT-42323). As of the summer of 2015, all retrieval has been completed in all but three tanks.

Figure D-5. Points of Calculation 100 Meters Downgradient of Waste Management Area C.



PA = Performance Assessment

WMA = Waste Management Area

RPP-ENV-58782, Rev. 0

**Table D-11. Width of Point of Calculation Segments 100 Meters
Downgradient of Waste Management Area C.**

Point of Calculation Segment	1	2	3	4	5	6	7	8	9
Width (m)	28.8	30.5	30.4	29.6	27	34.5	36	34	28

The residual waste volume for tanks not yet retrieved is unknown; therefore, assumptions about the inventory have been made based on current threshold requirements. Most constituents' inventory uncertainties vary by a factor of 5 or less, but may vary by as much as a factor of 10 for certain constituents in tanks not yet retrieved. For tanks already retrieved, uncertainty in residual waste estimates is on the order of 20 to 30% for most constituents, assuming no additional retrieval is required.

Specific information about the residual inventory and the release of the radionuclide and non-radiological contaminant inventory from the tanks, ancillary equipment, and pipelines is presented in Section D4.1.3.

D5.0 STOMP® SOFTWARE

STOMP® is used to solve the Richards equation (the water mass conservation equation in PNNL-12030) and the Advection-Dispersion equation (the solute mass conservation equation in PNNL-12030) that govern water flow and solute transport, respectively, under variably-saturated conditions in the vadose zone and groundwater in and around WMA C. STOMP® (PNNL-11216; PNNL-12030; PNNL-15782, "STOMP Subsurface Transport Over Multiple Phases Version 4.0 User's Guide") was selected to simulate the transport of contaminants in the vadose zone of the 100 Area because it fulfills the following specifications.

- The STOMP® simulator operational modes needed for implementation of this model are available free for government use under a limited government-use agreement.
- The STOMP® simulator solves the necessary governing equations, e.g., the Richards equation, the van Genuchten soil water retention equation, the Mualem unsaturated hydraulic conductivity equation, and the Advection-Dispersion equation.
- It is capable of directly simulating the principal FEPs that are relevant (see Section D4.1).
- The STOMP® simulator is well documented (PNNL-11216; PNNL-12030; PNNL-15782).
- The STOMP® simulator development is compliant with DOE O 414.1C, Quality Assurance requirements [PNNL-SA-54024, "Project Management Plan for Subsurface Transport Over Multiple Phases (STOMP) Software Maintenance and Development";

RPP-ENV-58782, Rev. 0

PNNL-SA-54022, “STOMP Software Test Plan Rev. 1.0”; PNNL-SA-54023, “STOMP Software Configuration Management Plan Rev. 1.3”; PNNL-SA-54079, “Requirements for STOMP Subsurface Transport Over Multiple Phases”].

- The STOMP[®] simulator is distributed with source code, enhancing transparency.
- The modeling team implementing this model has expertise in use of this simulator.
- There is an extensive history of application of STOMP[®] at Hanford and elsewhere including verification, validation, and benchmarking (DOE/RL-2011-50).
- Use of STOMP[®] is in keeping with DOE direction for simulation of vadose zone flow and transport at the Hanford Site (Letter 06-AMCP-0133, “Hanford Groundwater Modeling Integration”).

The software used to implement this model and perform calculations was approved under the requirements of, and use was compliant with, PRC-PRO-IRM-309. This software is managed under the following software quality assurance documents consistent with PRC-PRO-IRM-309 that address all aspects of STOMP[®] usage and management: functional requirements, software management, software installation and acceptance testing and reporting, and the preparation of a requirements traceability matrix.

D5.1 STOMP[®] CONTROLLED CALCULATION SOFTWARE

The following describes the STOMP[®] controlled calculation software.

- Software Title: STOMP-W (a scientific tool for analyzing single- and multiple-phase subsurface flow and transport using the integrated finite volume discretization technique with Newton-Raphson iteration).
- Software Version: STOMP-W was provided by Pacific Northwest National Laboratory on January 30, 2013, and was tested and approved for use by CH2M HILL Plateau Remediation Company (CHPRC) as “CHPRC Build 4.”
- Hanford Information System Inventory Identification Number: 2471 (Safety Software S3, graded Level C).

D5.2 SOFTWARE INSTALLATION AND CHECKOUT

Safety Software (CHPRC Build 4 of STOMP[®]) is checked out in accordance with procedures specified in the software management plan. Source or executable files are obtained from the CHPRC software owner, who maintains the configuration-managed copies in MKS Integrity^{TM2}.

² MKS Integrity is a trademark of MKS, Incorporated.

RPP-ENV-58782, Rev. 0

1 Installation tests identified in the test plan are performed. Upon confirmation of successful
2 installation, software installation and checkout forms are required and must be approved for
3 installations used to perform model runs. Approved users are registered in the Hanford
4 Information System Inventory for safety software.
5
6

7 **D5.3 STATEMENT OF VALID SOFTWARE APPLICATION**

8

9 Use of the STOMP[®] software for implementing the model described in this report is consistent
10 with its intended use for CHPRC (DOE/RL-2011-50), as identified in the functional
11 requirements document.
12
13
14
15

16 **D6.0 MODEL IMPLEMENTATION**

17

18 The 3-D model incorporates spatial heterogeneity and temporal changes of geologic and recharge
19 conditions, with the ability to include lateral spreading, commingling of plumes, and preferential
20 flow. The gridding scheme and extent of the domain intend to minimize the numerical error and
21 impact that the boundary conditions have on the model calculations in the areas of interest,
22 i.e., the points of calculation. The discretization scheme allows the distinct representation of the
23 different sources within WMA C such that no sources, with the exception of the pipelines,
24 overlap one another.
25
26

27 **D6.1 DISCRETIZATION**

28

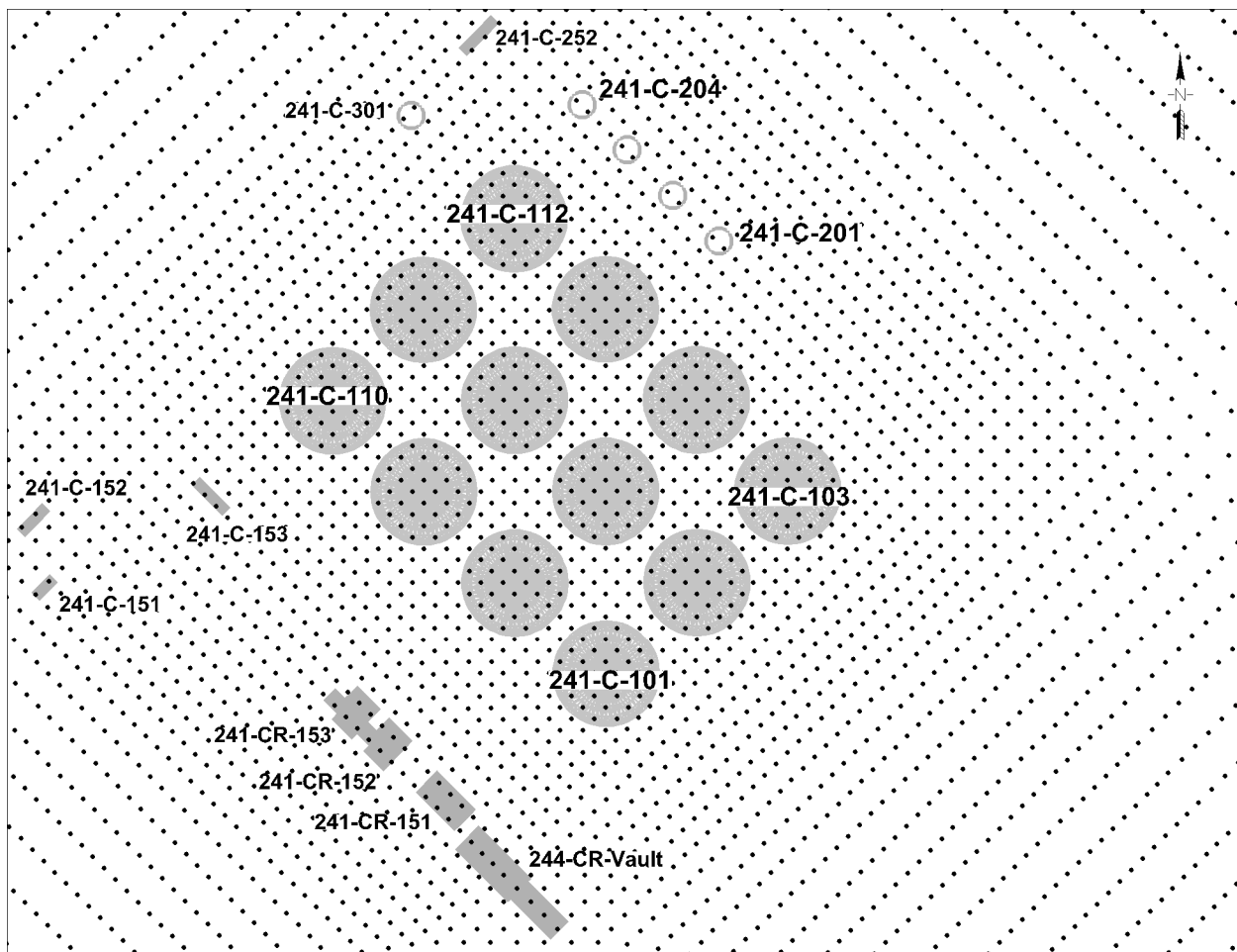
29 The horizontal node spacing varies between 3.0 and 20 m to optimize the discretization in the
30 areas attempting to approximate the slopes associated with construction of WMA C and the
31 100-series tanks without overwhelming the available computational resources. Within the
32 confines of WMA C, the horizontal grid cell dimensions ranged between 3 and 4 m to align the
33 nodes with the tanks, vault, and other ancillary equipment (Figure D-6). Outside of WMA C, the
34 grid cells expanded in size such that no adjoining grids differed in length by more than a factor
35 of 1.5. Table D-12 presents the pattern of the spacing of the finite difference cells. Vertical
36 spacing in the vadose zone ranged between 1 and 1.25 m, except around the water table where
37 the spacing decreased to 0.5 m to capture the impact of the capillary fringe above the water table
38 (Figure D-7).
39

40 The total number of nodes in the modeled rectangular prism equaled 736,653. During the
41 pre-operational phase, the engineered structures were non-existent. Hence, the number of active
42 nodes equaled 640,565 with 96,088 inactive. During the operational and post-closure phases,
43 WMA C backfill replaced Hanford H1 Gravel, and the number of active nodes equaled 637,543
44 with 99,110 inactive. The increase in inactive nodes is attributed to the inactivation of the tank
45 and ancillary equipment nodes within the WMA C excavation. Figure D-8 shows the relative
46 change in moisture content from the pre-Hanford steady-state condition at the four vertical
47 boundaries of the model at three times of interest: at Year 2020, at the end of the WMA C

RPP-ENV-58782, Rev. 0

operational period; at Year 2520, at the end of the design life of the WMA C surface barrier; and at Year 3020, which is the end of the compliance time frame and when the system has reacquired or nearly reacquired steady-state conditions. In general, the effects are contained within a relatively small segment along the boundaries near the water table and appear to be minor (less than 1.0×10^{-5}). The changes in moisture content are negligibly small in magnitude, which indicates that the boundaries are far enough removed from the area of interest to avoid unintentional impacts to the model solution. Consequently, they are not considered to affect adversely the evaluation of radionuclide transport and groundwater impacts associated with the radionuclide and non-radiological contaminant inventory in WMA C.

Figure D-6. Horizontal Alignment of Three-Dimensional Model Computational Nodes with Waste Management Area C Single-Shell Tanks, 241-C-301 Catch Tank, 244-CR-Vault, and Other Waste Management Area C Ancillary Equipment.



For the base case, the vadose Peclet number equaled approximately 6 (1.25 m / 0.20 m), with an imposed Courant (number) restriction of 10. While the value of 1 for these numbers is often considered ideal, it has been demonstrated that acceptably small numerical oscillations may be obtained with local Peclet numbers as high as 10 (Computational Methods in Subsurface Flow [Huyakorn and Pinder 1983]). It is difficult to assess numerical impacts on the solution caused

RPP-ENV-58782, Rev. 0

by the grid spacing, apart from consideration of the Peclet criteria. The total number of nodes in the model is close to the maximum that the computer hardware and solver can accommodate, so evaluating solution stability through grid refinement is not feasible. Other comparably-scaled models indicate that the WMA C PA grid size and spacing is sufficient. DOE/EIS-0391, "Final Tank Closure and Waste Management Environmental Impact Statement for the Hanford Site, Richland, Washington," Appendix N indicates that the horizontal grid size and spacing of 5 m within WMA C, and vertical spacing of 2 m, are small enough in that 3-D model to provide accurate simulation of flow and transport.

Table D-12. Horizontal and Vertical Spacing of the Finite Difference Cells in the Three-Dimensional Waste Management Area C Flow and Transport Model Domain.

West to East Spacing; Southeastern Boundary Coordinate = 574656 m (Lambert Coordinate System ¹ Easting)						
4@ 20.00 m	2@ 16.00 m	2@ 12.00 m	2@ 10.00 m	2@ 8.00 m	2@ 6.00 m	7@ 4.50 m
1@ 3.70 m	6@ 3.80 m	2@ 3.85 m	14@ 3.80 m	2@ 3.85 m	6@ 3.80 m	1@ 3.00 m
7@ 4.50 m	3@ 6.00 m	4@ 8.00 m	10@ 10.00 m	2@ 12.00 m	1@ 16.00 m	9@ 20.00 m
South to North Spacing; Southwestern Boundary Coordinate = 136454 m (Lambert Coordinate System ¹ Northing)						
8@ 20.00 m	3@ 16.00 m	2@ 12.00 m	4@ 10.00 m	3@ 8.00 m	2@ 6.00 m	11@ 4.50 m
4@ 4.00 m	8@ 3.80 m	1@ 3.90 m	15@ 3.80 m	1@ 3.00 m	11@ 4.50 m	2@ 6.00 m
2@ 8.00 m	3@ 10.00 m	3@ 12.00 m	4@ 16.00 m	6@ 20.00 m		
Vertical Spacing; Bottom Elevation = 95 m (NAVD88 ²)						
1@ 5.00 m	2@ 4.00 m	1@ 3.00 m	1@ 2.00 m	2@ 1.50 m	1@ 1.25 m	1@ 1.00 m
1@ 0.75 m	3@ 0.50 m	1@ 0.75 m	12@ 1.00 m	40@ 1.25 m	4@ 1.00 m	19@ 1.25 m

¹ NOAA Manual NOS NGS 5, State Plane Coordinate System of 1983.

² North American Vertical Datum of 1988, National Geodetic Survey, U.S. Department of Commerce.

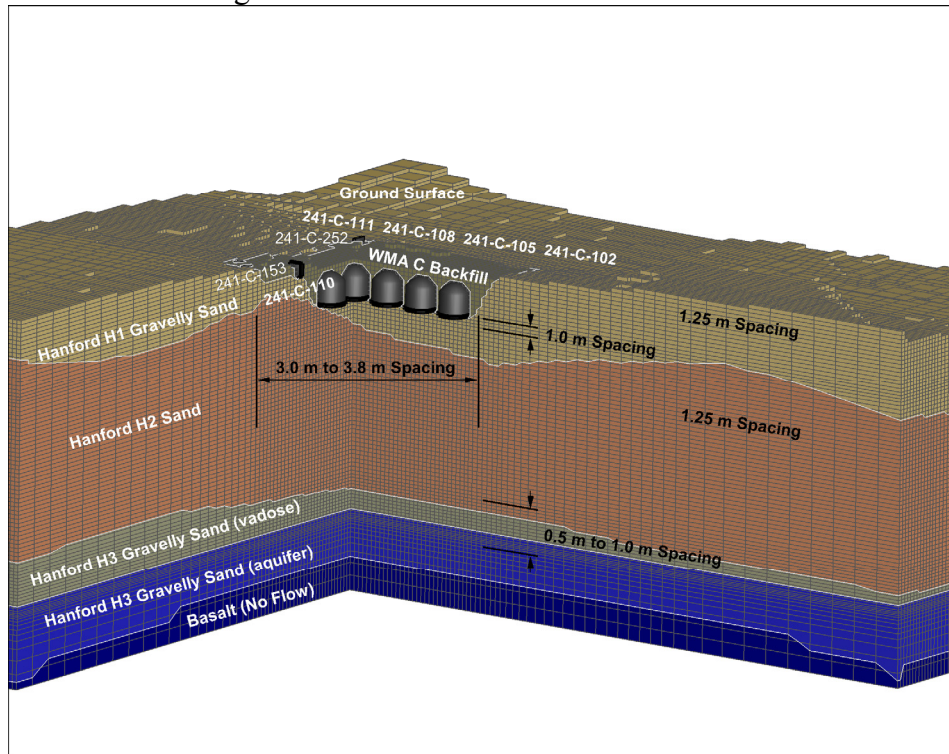
Note: The sequences read left to right. The number preceding the "@" symbol indicates the number of columns (west to east), rows (south to north), or vertical layers (bottom to top) that have the length indicated by the distance following it.

Figure D-9 shows a comparison of the ⁹⁹Tc concentration at the nine points of calculation located 100 m downgradient between the base case dispersivity values and dispersivity values intended to test numerical dispersion (Table D-13). These values represent the approximate maximum values associated with the different HSUs. The perceptible increase in maximum concentration observed in the base case results, compared to the numerical dispersion test case results, indicates that the grid is sized adequately such that numerical dispersion is not unduly affecting or obscuring the model computations.

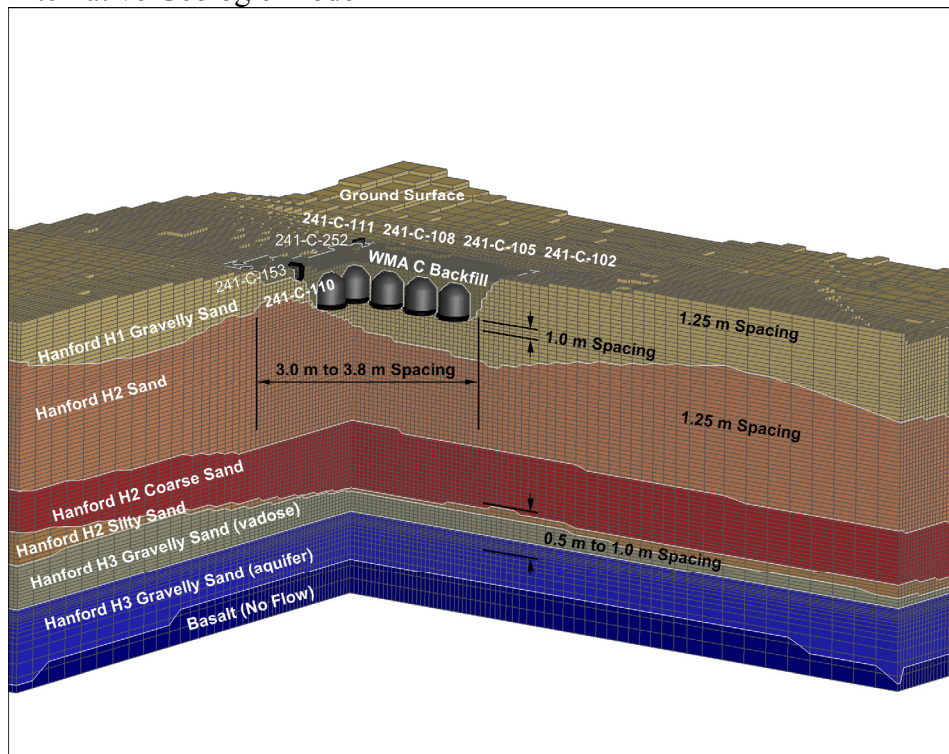
RPP-ENV-58782, Rev. 0

Figure D-7. Horizontal and Vertical Alignment and Distribution of Waste Management Area C Performance Assessment Three-Dimensional Model Computational Nodes.

a) Alternative Geologic Model I



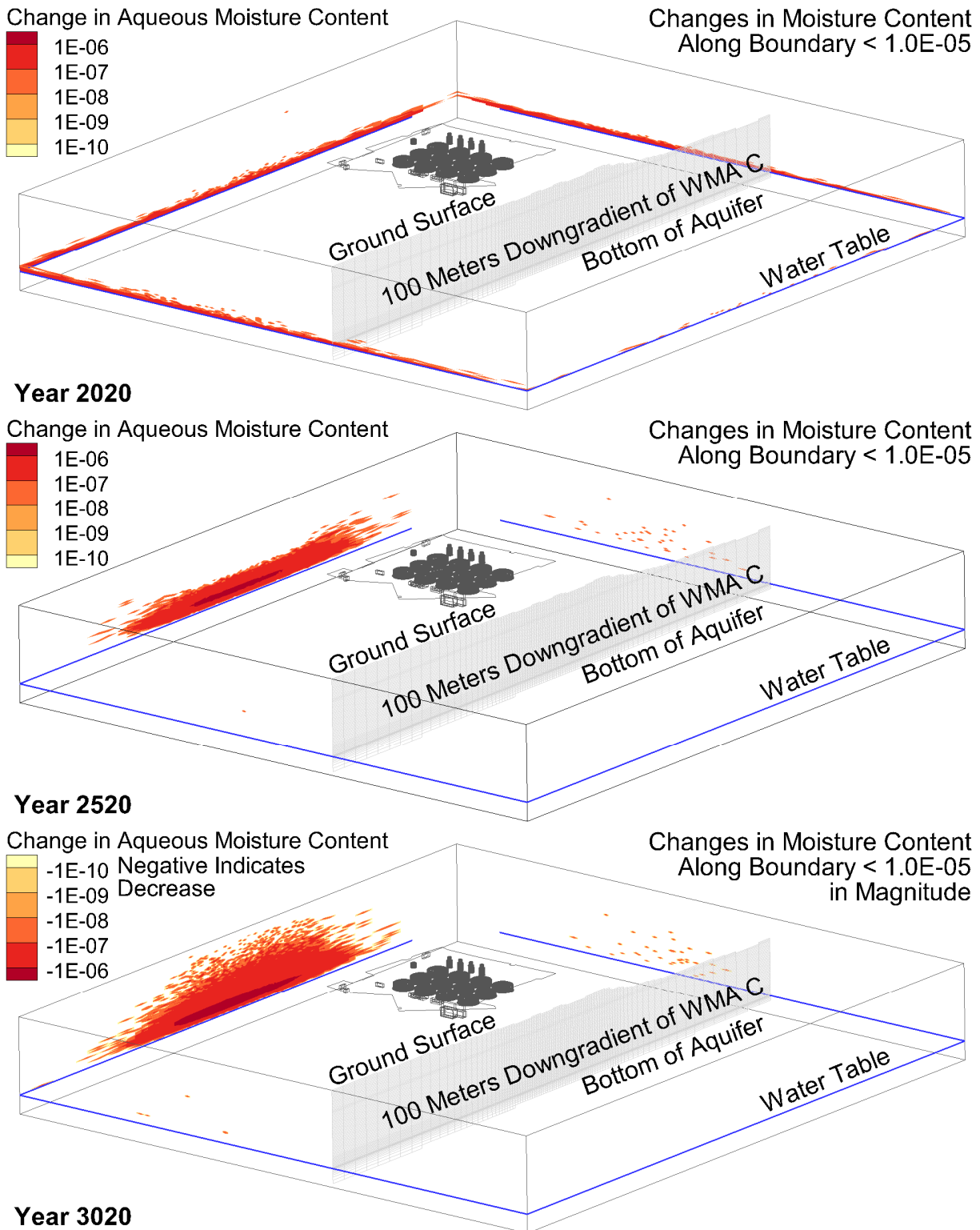
b) Alternative Geologic Model II



WMA = Waste Management Area

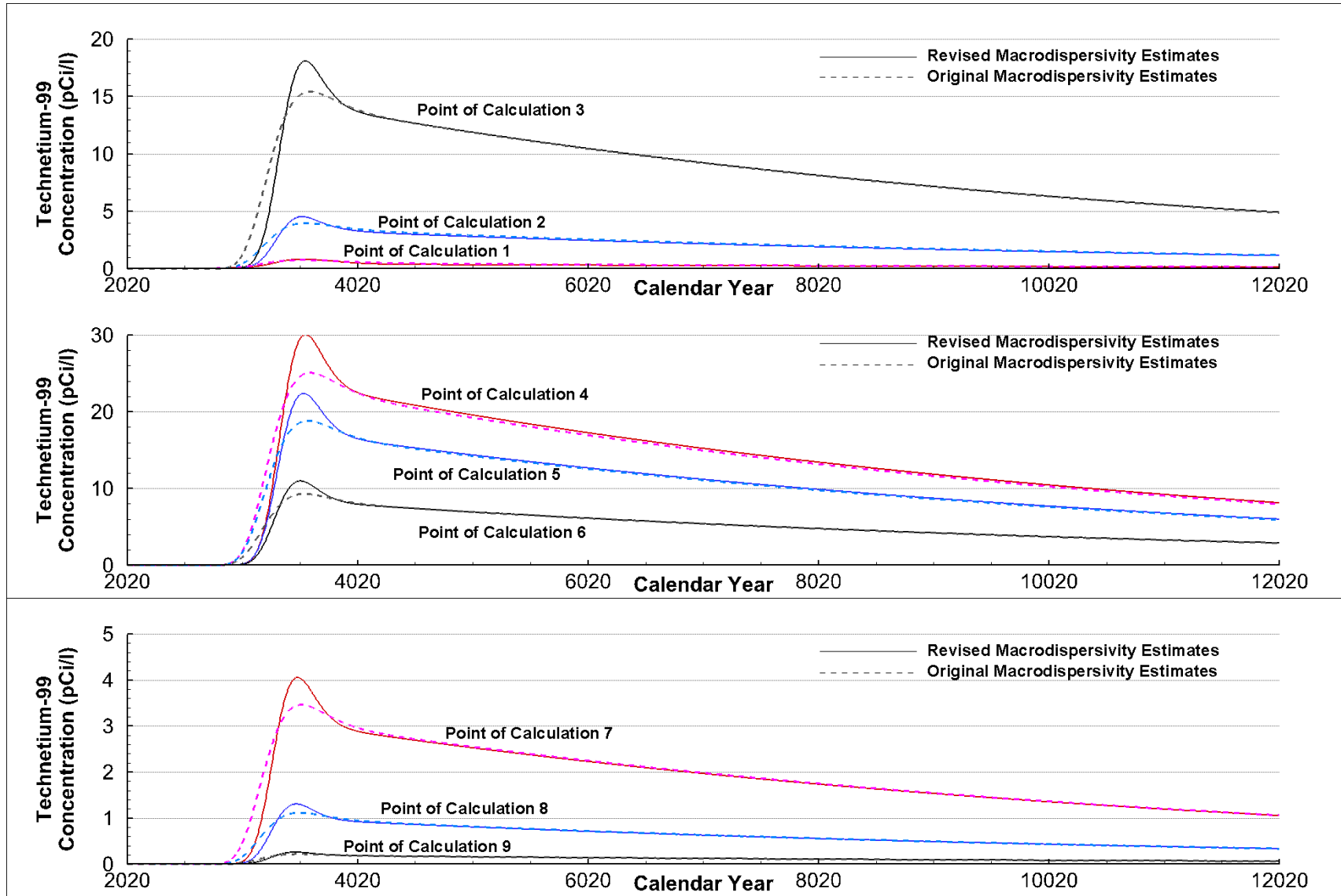
RPP-ENV-58782, Rev. 0

Figure D-8. Relative Change in Moisture Content from the Pre-Hanford Steady State Condition at the Four Vertical Boundaries of the Model at Three Times of Interest: Year 2020, Year 2520, and Year 3020.



WMA = Waste Management Area

Figure D-9. Comparison of the Technetium-99 Concentration at the Nine Points of Calculation Located 100 Meters Downgradient between the Base Case Dispersivity Values and the Numerical Dispersion Test Case Dispersivity Values.



RPP-ENV-58782, Rev. 0

Table D-13. Waste Management Area C Performance Assessment Vadose Zone Dispersivity Values and Numerical Dispersion Evaluation.

Hydrostratigraphic Unit	Numerical Dispersion Test Case Longitudinal Macrodispersivity (cm)	Base Case Longitudinal Macrodispersivity (cm)
Backfill	150	20
Hanford H1	100	20
Hanford H2	200	25
Hanford H3	100	20
Point of Calculation 100 meters downgradient of Waste Management Area C	Maximum Concentration (pCi/L)	Maximum Concentration (pCi/L)
1	0.80	0.83
2	4.0	4.5
3	15	18
4	25	30
5	19	22
6	9.2	11
7	3.4	4.1
8	1.1	1.3
9	0.22	0.26

The vertical Courant numbers in the vadose zone tend to be small (e.g., $10 \text{ yr} \times 0.0035 \text{ m/yr recharge} / 0.05 \text{ moisture content} / 1 \text{ m grid spacing} = 0.7$), but the horizontal Courant numbers become large near the water table and capillary fringe where the velocity approaches 400 m/yr. These few places impose an impractical limit on the time step while the Courant number remains small elsewhere. Table D-14 presents the results of a Courant criteria evaluation, which evaluated the maximum concentration of ^{99}Tc at the points of calculation associated with a subset of the WMA C sources: tank 241-C-105, tank 241-C-203, and the pipelines contained in a single STOMP[®] input file. The negligible differences in the results indicate that an overly strict Courant restriction does not affect the solution and appears to be unwarranted, especially considering the improved efficiency in solution time when the Courant restriction is relaxed to 10. These evaluations indicate that the grid is adequately discretized.

D6.2 PARAMETERIZATION

Table D-15 presents a summary of the model parameters and values assigned, including boundary and initial conditions, and identifies the section where the data sources and data quality are discussed. Parameters and values that are already tabularized in the subsections of Section D4.1 are simply referenced by the applicable table number.

RPP-ENV-58782, Rev. 0

Table D-14. Waste Management Area C Performance Assessment Vadose Zone Courant Criteria and Numerical Dispersion Evaluation.

	Numerical Dispersion Test Case Courant Number = 1 (pCi/L)			Base Case Courant Number = 10 (pCi/L)		
Simulation Duration and Time to Complete	4,000 years completed in 112.51 hours			10,000 years completed in 32.08 hours		
Point of Calculation 100 meters downgradient of Waste Management Area C	Maximum Concentration (pCi/L)			Maximum Concentration (pCi/L)		
	Source			Source		
	241-C-105	241-C-203	Pipelines	241-C-105	241-C-203	Pipelines
1	0.02	0	0.36	0.02	0	0.36
2	0.86	0	0.53	0.86	0	0.53
3	10	0.000003	0.74	10	0.000003	0.73
4	21	0.0001	0.94	21	0.0001	0.92
5	13	0.002	1.0	13	0.002	1.0
6	4.1	0.006	0.74	4.1	0.006	0.73
7	0.92	0.007	0.34	0.91	0.007	0.34
8	0.22	0.004	0.12	0.22	0.004	0.12
9	0.03	0.001	0.03	0.03	0.001	0.03

D6.3 MODELING STAGES

The WMA C tank residual simulations using STOMP[®] require running three separate stages of the model in sequence. The first stage is a long-term transient simulation of only water flow resulting from historic recharge conditions. This stage is needed to obtain near steady-state soil moisture conditions throughout the model domain at the start time for the second stage. The second stage begins with the initial moisture distribution provided from the first stage, and simulates only water flow during the operational period of WMA C, which is the time between the construction of WMA C in 1945 and its assumed closure in 2020. The use of a previously simulated condition as a starting point for another simulation is referred to as a “restart” condition in STOMP[®]. The contaminant transport stage (stage 3) begins with the moisture distribution provided from the second stage, and simulates flow and transport for 10,000 years, from 2020 to 12020. Each tank, ancillary equipment, and pipeline residual source is simulated individually. The groundwater concentrations resulting from each source are summed according to the principle of superposition to produce time series concentration breakthrough curves at the points of calculation identified in Section D4.1.8. The principle of superposition also applies to the spatial distribution of the pore water concentrations in the vadose zone resulting from each

RPP-ENV-58782, Rev. 0

source. The superposition and summing of the concentration results occurs outside of STOMP[®], and is not addressed in this appendix.

D6.4 CALIBRATION

DOE G 435.1-1 and Federal risk assessment guidelines [e.g., EPA/540/1-89/002, Risk Assessment Guidance for Superfund Volume I Human Health Evaluation Manual (Part A) Interim Final] acknowledge that the assessment of uncertainties associated with how well models approximate actual relationships and conditions in the field (i.e., field validation) is desirable, but that field data for model calibration is generally not available and/or attainable for vadose zone models. No specific effort to calibrate the WMA C PA flow and transport model has been made; however, a comparison of measured and simulated water contents was carried out for this analysis, and parameters were adjusted accordingly (Appendix B).

D6.5 SCREENING

The screening analysis uses the 3-D model to determine the maximum K_d value of contaminants in the WMA C tank residuals that reach the water table in 1,000 and 10,000 years. The purpose of this screening phase was to streamline the PA modeling by identifying those contaminants sufficiently mobile to impact groundwater during the compliance, sensitivity and uncertainty analysis time frames. This analysis was performed to considerably reduce the computation time required to conduct the PA modeling by limiting the number of radionuclides evaluated in the model. According to the facility performance requirements in DOE O 435.1, performance objectives must be met for 1,000 years, and post-closure evaluations must extend out to 10,000 years to clarify long-term impacts. Given the combination of low infiltration rates and a deep vadose zone below the facility, it is evident that contaminants that are highly sorptive on the soils may not reach the water table within 10,000 years,³ even for combinations of input parameters that are highly conservative. If the travel time exceeds 10,000 years, even for conservative combinations of input parameters, the contaminant will not affect any of the calculated results in the PA, and can reasonably be screened from the analysis.

The specific methodology, basis for the parameters selected, and key assumptions used in the screening phase analysis are described in detail in Section 6.3.2.3 Groundwater Pathway Screening Analysis Methodology. The screening analysis includes vadose zone hydraulic property values and recharge rates developed for the uncertainty analysis, which are discussed in Section 8.1.4. In particular, the screening analysis applies the maximum recharge rates associated with each period for each surface type (Table D-16), assigns the vadose zone hydraulic properties that produce the fastest pore water velocity for each HSU as determined for the uncertainty analysis (Table D-17), and implements an advection release function for the radionuclides. Other parameters (e.g., dispersivity, distribution coefficient gravel correction, and aquifer hydraulic properties) remain the same as the base case parameters. The use of these

³ In this analysis, the travel time to the aquifer is defined as the time to first arrival of the contaminant at the aquifer, taking into account advection, diffusion, and dispersion. This metric will tend to screen fewer contaminants than using the arrival of the peak concentration.

RPP-ENV-58782, Rev. 0

parameter values prevents the occurrence of a false negative, i.e., that a radionuclide or non-radioactive contaminant that could impact groundwater within the 1,000- or 10,000-year simulation time frames is screened from the fate and transport evaluations. Model results indicating the time of first arrival at the water table for contaminants with distribution coefficients ranging between 0.1 and 2.0 mL/g are summarized in Table D-18 and presented in graphical form in Figure 7-6.

Table D-15. Summary of Key Elements and Base Case Parameters Associated with Site-Specific Model Components for Waste Management Area C (The basis for the elements and parameter selection provided in the individual model components sections). (2 sheets)

Model Domain and Boundary Conditions	<p>Rectangular Prism: 737.9 m (2,421 ft) × 795.3 m (2,609 ft) × 116 m (381 ft)</p> <p>Prescribed flux across the top (Recharge); no-flow along vertical side boundaries in the vadose zone; prescribed flux and head along the upgradient and downgradient vertical side boundaries in the aquifer, respectively; no-flow along the bottom of the model (aquifer).</p> <p>The prescribed volumetric water flux boundary condition is calculated to maintain mass conservation in the aquifer independent of recharge.</p>
Geologic Setting	<p>The Waste Management Area (WMA) C cross section includes the following anthropogenic or natural units that occur from surface to groundwater (RPP-RPT-56356, "Development of Alternative Digital Geologic Models of Waste Management Area C," Rev. 0):</p> <ul style="list-style-type: none"> • WMA C Backfill • Hanford H1 (gravel-dominated, generally identified as gravel or very coarse sand) • Hanford H2 Sand (sand-dominated facies generally identified as fining upward sequences of gravel, sandy/gravel to sand to very fine sand) • Hanford H3 (coarse-grained open framework gravel to sandy gravel; in the vicinity of WMA C is often referred to as undifferentiated H3 gravels, Cold Creek, and Ringold) • In Alternative Geologic Model II, the Hanford H2 Sand includes following two additional subunits <ul style="list-style-type: none"> ○ Hanford H2 Coarse (gravel/coarse-grained facies that underlies the H2 fines) ○ Hanford H2 Silty Sand – (a silty sand unit that is only observed in deep groundwater wells and a mappable unit may not be readily identified)
Groundwater Domain and Characteristics	<p>WMA C post-closure water table elevation ~119.5 m NAVD88 and average hydraulic gradient ~0.00001 m/m</p> <p>Aquifer area along northwest cross section boundary = 6,151.04 m²</p> <p>Aquifer area along southeast cross section boundary = 13,997.55 m²</p> <p>Average aquifer area along all aquifer cross sections = 9,439.56 m²</p> <p>Prescribed flux along northwest cross section boundary (saturated K = 11,000 m/d); 11,000 m/d × 0.2000E-04 × 365.25 d/yr = 0.80355E+02 m/yr; 0.80355E+02 m/yr × 9,439.56 m² / 6,151.04 m² = 0.12331E+03 m/yr</p> <p>Prescribed head along southeast cross section boundary = 119.49 m</p> <p>Groundwater thickness is ~12 m (39 ft) in the aquifer; Groundwater concentrations evaluated for upper 5 m (16 ft) of the aquifer (rationale for aquifer depth presented in section D4.1.8 Point of Calculation, Protectiveness Metric, and Time Frame Considerations)</p>
Source Term/ Inventory	<p>WMA C Base Case inventory presented in Table D-3.</p> <p>Diffusion controlled release from the grouted tanks and advection controlled release from the pipelines along with equilibrium sorption-desorption processes (i.e., K_d control).</p>

RPP-ENV-58782, Rev. 0

Table D-15. Summary of Key Elements and Base Case Parameters Associated with Site-Specific Model Components for Waste Management Area C (The basis for the elements and parameter selection provided in the individual model components sections). (2 sheets)

Vadose Zone Hydrogeology and Fluid Transport	WMA C Base Case hydrogeologic properties presented in Table D-4.				
	Aquifer Hydraulic Conductivity Horizontal to Vertical Anisotropy 10:1 ; Vadose Zone Hydraulic Conductivity Anisotropy allowed to vary as a function of the moisture content in accordance with the Polmann model (“Application of Stochastic Methods to Transient Flow and Transport in Heterogeneous Unsaturated Soils” [Polmann 1990]).				
	Aquifer and Vadose Zone Dispersion Horizontal to Vertical Anisotropy 10:1 .				
	K_d -control for radionuclide transport in the vadose zone and groundwater.				
Recharge	Phase	Recharge on Surface (mm/yr [in./yr])			
		Natural Vegetation	Tank Farm Disturbed Surface	Non-Tank Farm Disturbed Surface*	Surface Barrier
	Pre-operations	3.5 [0.14]	NP	NP	NP
	Operations	3.5 [0.14]	100 [3.9]	22 [0.87]/63 [2.5]	NP
	First 100 years Post-Closure	3.5 [0.14]	NP	3.5 [0.14]	0.5 [0.02]
	Early Post-Closure (100 to 500 years)	3.5 [0.14]	NP	3.5 [0.14]	0.5 [0.02]
	Late Post-Closure (after 500 years)	3.5 [0.14]	NP	3.5 [0.14]	3.5 [0.14]
	* Disturbed areas that allow vegetation are assigned 22 mm/yr [0.87 in./yr]. Disturbed areas that are reworked such that vegetation does not grow are assigned 63 mm/yr [2.5 in./yr].				
Sorption Characteristics	WMA C Base Case K_d values (partition coefficients) presented in Table 6-11.				

*Applies to all subfacies of this unit.

NAVD88 = North American Vertical Datum of 1988, National Geodetic Survey, U.S. Department of Commerce.

NP = Not present

- 1
- 2 The results of the screening analysis indicate that, even when using parameter estimates biased to
- 3 produce the greatest pore water velocity in the vadose zone, contaminants with a K_d in the fine
- 4 fraction > 0.15 mL/g do not reach groundwater within the 1,000-year compliance time frame,
- 5 and radionuclides with a K_d > 1.5 mL/g do not reach groundwater within the 10,000-year

RPP-ENV-58782, Rev. 0

post-compliance period (Table D-18). The screening evaluation helps in reducing the number of radionuclides to be evaluated using 3-D modeling analysis.

Table D-16. van Genuchten-Mualem Parameters Associated with the Maximum Pore Water Velocity at Specific Tension Ranges Based on Cumulative Distribution Functions.

Strata	θ_s	θ_r	α (1/cm)	n	Fitted K_s (cm/s)
Hanford H1 (gravelly sand)	0.100	0.0006	0.0190	1.789	5.07E-04
Hanford H2 (sand-dominated)	0.239	0.0006	0.0743	2.042	8.84E-04
Hanford H3 (gravelly sand)	0.100	0.0006	0.0190	1.789	5.07E-04
Backfill	0.100	0.0003	0.0116	1.601	9.42E-05
Aquifer	0.20	0.016	0.0190	1.789	3.49E-03*

* The vertical aquifer hydraulic conductivity value is determined from the horizontal hydraulic conductivity value and the aquifer anisotropy.

Table D-17. Maximum Net Infiltration (Recharge) Estimates Used in the Screening Analysis for Pre-Construction Period, Operational Period, and Post-Closure of Waste Management Area C (Section 8.1.4).

Surface Status	Pre-Construction (mm/yr)	Operational Period (mm/yr)	Post Closure	
			Until End of Barrier Design Life (500 yr after closure) (mm/yr)	After End of Barrier Design Life (mm/yr)
Waste Management Area C	5.2	140	1.0	5.2
Undisturbed	5.2	5.2	5.2	5.2
Disturbed	5.2	22	5.2	5.2
Reworked	5.2	63	5.2	5.2
Waste Management Area A	5.2	140	1.0	5.2

Of the list of radionuclides in the WMA C residuals inventory and on the basis of the results of the screening phase, only 12 (Table D-19) appear to be sufficiently mobile to arrive at groundwater during the compliance period, with 6 others sufficiently mobile to arrive at groundwater during the sensitivity and uncertainty analysis time frame. During the sensitivity and uncertainty analysis time frame, even some contaminants that undergo appreciable retardation in the vadose zone, e.g., ^{129}I , ^{14}C , and ^{238}U , are sufficiently mobile to arrive at groundwater within the sensitivity and uncertainty analysis time frame. The other contaminants in the WMA C residual inventory are not included in further groundwater impact analysis because they do not reach the water table within the evaluation time frames.

RPP-ENV-58782, Rev. 0

Table D-18. First-Arrival Time (in Calendar Year) of Radionuclides for Various K_d Values Based on Screening Analysis Using Subsurface Transport Over Multiple Phases.

Contaminant K_d (mL/g)				Calendar Year of First Arrival at the Water Table	Time of Arrival, Post-Closure (Closure occurring in 2020) Years
Fine Fraction	Backfill	Hanford H1 and H3	Hanford H2		
0.10	0.05	0.06	0.08	2517.5	497.5
0.15	0.07	0.09	0.12	3022.5	1,002.5
0.20	0.09	0.12	0.16	3505	1,485
0.25	0.12	0.15	0.20	3900	1,880
0.30	0.14	0.17	0.24	4210	2,190
0.40	0.18	0.23	0.32	4840	2,820
0.60	0.28	0.35	0.48	6110	4,090
0.80	0.37	0.46	0.64	7390	5,370
1.0	0.46	0.58	0.80	8680	6,660
1.5	0.69	0.87	1.2	11900	9,880
2.0	0.92	1.2	1.6	>12020	>10,000

D7.0 MODEL LIMITATIONS

The evaluation of WMA C PA tank residuals model limitations must consider two types of limitations: (1) the limitations associated with the model that affect the results, and (2) the limitations associated with the applicability of the model results outside the model's intended purpose. Model limitations primarily depend on the inherent capabilities of the model; the scale and boundary conditions of the model domain; assumptions used in the model design; the extent to which the model input parameters represent actual, bounding, or limiting conditions; and the ability of the model and code to represent individual and combinations of dynamic FEPs. Limitations associated with the applicability of the model results concern the extent to which the model results are relevant and applicable to model conditions, parameters, or assumptions that differ from those of the specific modeling purpose and objectives (e.g., attempting to apply the tank residuals model to the evaluation of past UPRs).

DOE/RL-2011-50 identifies generalized model and code limitations associated with the relevant FEPs for the 200 Areas vadose zone. Other limitations specific to WMA C were considered during FEPs process working sessions conducted from 2009 to 2011, and additional discussions with regulators in 2013 and 2014. The description of the limitations involves a summary of those FEPs considered and not considered in the model, along with possible consequences of their omission on the model results. The limitations also address or involve uncertainties in the

RPP-ENV-58782, Rev. 0

1 model results. Some specific examples of limitations in the applicability of the WMA C PA tank
2 residuals vadose zone model results include the following.

3
4 • Domain and scale limitations:

- 5
6 – Results represent incremental groundwater contamination from WMA C residuals and
7 do not include interaction with earlier WMA C waste releases or contamination from
8 other sources
9
10 – Applicability of model results limited to releases containing no accompanying water
11 discharges within the model domain.
12

13 • Geologic setting limitations:

- 14
15 – Applicability of model results limited to evaluations with a comparable stratigraphy to
16 WMA C.
17

18 • Source-term limitations:

- 19
20 – Applicability of model results limited to source-term components of finite or estimable
21 volume within the model domain
22
23 – Applicability of model results limited to contaminant release and retardation
24 mechanisms based on the assumption of diffusion control or reversible equilibrium
25 conditions.
26

27 • Groundwater domain limitations:

- 28
29 – Applicability of model results limited to sites with dilution effects comparable to
30 WMA C aquifer hydrologic properties.
31

32 • Hydrogeologic parameter limitations:

- 33
34 – Applicability of WMA C model results limited to evaluations where flow and transport
35 are dominated by unsaturated porous media continuum flow, with comparable or
36 acceptably bounding moisture content profiles
37
38 – Applicability of WMA C model results limited to evaluations where hydrogeologic
39 parameter values remain constant (unchanging) over time
40
41 – Applicability of model results limited to sites where preferential pathways
42 (e.g., discordant voids such as well seals/casing, clastic dikes, and sills) are not
43 considered important.
44

RPP-ENV-58782, Rev. 0

- 1 • Recharge limitations:
 - 2
 - 3 – Applicability of model results limited to conditions similar to or bounded by the values
 - 4 of recharge rates evaluated in the WMA C PA.
 - 5
- 6 • Geochemical limitations:
 - 7
 - 8 – Applicability of model results limited to radionuclides and non-radiological
 - 9 contaminants exhibiting linear isotherm behavior for contaminant release and
 - 10 attenuation, which neglect surface complexation and precipitation
 - 11
 - 12 – Applicability of model results limited to the radionuclides and non-radiological
 - 13 contaminants for which the assumption applies that the adsorption K_d and desorption
 - 14 K_d values are equivalent
 - 15
 - 16 – Applicability of model results limited to radionuclides and non-radiological
 - 17 contaminants with transport characteristics similar to, or within the range of, evaluated
 - 18 K_d values.
 - 19

20 For the purposes of establishing that the requirements of DOE O 435.1 to protect the public and
21 environment from exposure to radiation from radioactive materials are being met, these
22 limitations appear to be acceptable because the results represent reasonable (upper) bounding or
23 limiting conditions, or the risk implications of the results are not sensitive to the limitations apart
24 from those identified through the sensitivity analysis (DOE/RL-2011-50; Section 8).

25 26 27 28 29 **D8.0 MODEL CONFIGURATION MANAGEMENT**

30
31 Consistent with the requirements of CHPRC-00189, “CH2M Hill Plateau Remediation Company
32 Environmental Quality Assurance Program Plan,” Revision 9, all inputs and outputs for the
33 development of WMA C PA models are committed to the Environmental Model Management
34 Archive (EMMA) to maintain and preserve configuration managed models. Basis information
35 (that information collected to form the basis for model input parameterization) is also stored in
36 the EMMA for traceability purposes.

37
38 The STOMP[®] software is used to implement the models collectively described in this report.
39 These models are managed as discussed in Section 11.2.1. Safety Software (CHPRC Build 4 of
40 STOMP[®]) is checked out in accordance with procedures specified in CHPRC-00176, “STOMP
41 Software Management Plan.” Source or executable files are obtained from the CHPRC software
42 owner, who maintains the configuration-managed copies in MKS Integrity[™]. Installation tests
43 identified in CHPRC-00211, “STOMP Software Test Plan” are performed and successful
44 installation confirmed, and software installation and checkout forms (see Appendix A) are
45 required and must be approved for installations used to perform model runs. Approved users are
46 registered in the Hanford Information System Inventory for Safety Software.

RPP-ENV-58782, Rev. 0

Table D-19. Radionuclides that Arrive at the Water Table within the 1,000-Year Compliance and 10,000-Year Sensitivity and Uncertainty Time Frame Based on the Screening Analysis Conducted Using Subsurface Transport Over Multiple Phases.

Contaminant	K _d [Fine Fraction] (mL/g)	K _d [Backfill] (mL/g)	K _d [Hanford H1 and H3] (mL/g)	K _d [Hanford H2] (mL/g)
Radionuclides and non-radiological contaminants that may arrive at the water table within 1,000 years				
CN	0	0	0	0
Co/Co-60	0	0	0	0
Cr	0	0	0	0
F	0	0	0	0
H-3	0	0	0	0
Hg	0	0	0	0
Nb-93m	0	0	0	0
NO ₂	0	0	0	0
NO ₃	0	0	0	0
Rn-222	0	0	0	0
Tc-99	0	0	0	0
Se/Se-79	0.1	0.05	0.06	0.08
Radionuclides and non-radiological contaminants that may arrive at the water table within 10,000 years				
I-129	0.2	0.09	0.12	0.16
Sn/Sn-126	0.5	0.23	0.29	0.40
U-238	0.6	0.28	0.35	0.48
U Total	0.6	0.28	0.35	0.48
C-14	1.0	0.46	0.58	0.80
Tri-butyl Phosphate	1.89	0.87	1.1	1.5

Use of the STOMP[®] software for implementing the model described in this report is consistent with its intended use for CHPRC, as identified in CHPRC-00222, “STOMP Functional Requirement Document.”

RPP-ENV-58782, Rev. 0

D9.0 MODEL APPLICATION

The STOMP® simulation results developed from this modeling effort are recommended for use in the WMA C PA residual waste evaluation. These results provide adequate confidence that the radioactive waste management requirements of DOE O 435.1 are being met. The activities associated with the disposition of the tank, ancillary equipment, and pipeline residual waste of WMA C are being systematically planned, documented, executed, and evaluated. These activities appear sufficient to protect the environment and the public from exposure to radiation from radioactive materials per the requirements contained in DOE O 5400.1, General Environmental Protection Program and DOE O 5400.5, Radiation Protection of the Public and the Environment. The results also indicate that any eventual groundwater impacts will comply with applicable Federal, State, and local laws and regulations.

The WMA C PA tank residuals model represents a closure condition, and would therefore need to be evaluated for applying this model to other conditions, such as in the evaluation of past releases. In addition, the effects of preferential pathways or other phenomena that direct or deflect transport may become important considerations because of the enhanced net infiltration of precipitation through the gravel surface and the planned and unplanned anthropogenic releases of water.

D10.0 REFERENCES

- 06-AMCP-0133, 2006, "Hanford Groundwater Modeling Integration" (external letter from K. A. Klein to P. L. Pettiette, Washington Closure Hanford, March 9) U.S. Department of Energy, Richland Operations Office, Richland, Washington.
- 40 CFR 141, "National Primary Drinking Water Regulations," Code of Federal Regulations, as amended.
- CHPRC-00176, 2011, "STOMP Software Management Plan," Rev. 2, CH2M HILL Plateau Remediation Company, Richland, Washington.
- CHPRC-00189, 2012, "CH2M Hill Plateau Remediation Company Environmental Quality Assurance Program Plan," Rev. 9, CH2M HILL Plateau Remediation Company, Richland, Washington.
- CHPRC-00211, 2014, "STOMP Software Test Plan," Rev. 2, CH2M HILL Plateau Remediation Company, Richland, Washington.
- CHPRC-00222, 2011, "STOMP Functional Requirement Document," Rev. 1, CH2M HILL Plateau Remediation Company, Richland, Washington.
- CP-47631, 2013, "Model Package Report: Central Plateau Groundwater Model Version 3.4," Rev. 1, CH2M HILL Plateau Remediation Company, Richland, Washington.

RPP-ENV-58782, Rev. 0

- 1 Dagan, G., 1984, "Solute transport in heterogeneous porous formations," Journal of Fluid
2 Mechanics, Vol. 145, pp. 151–177.
- 3 DOE/EIS-0391, 2012, "Final Tank Closure and Waste Management Environmental Impact
4 Statement for the Hanford Site, Richland, Washington," U.S. Department of Energy,
5 Washington, D.C.
- 6 DOE G 435.1-1, 1999, Implementation Guide for Use with DOE M 435.1-1, Radioactive Waste
7 Management Manual, U.S. Department of Energy, Washington, D.C.
- 8 DOE M 435.1-1, 2007, Radioactive Waste Management Manual, U.S. Department of Energy,
9 Washington, D.C.
- 10 DOE O 414.1C, 2005, Quality Assurance, U.S. Department of Energy, Washington, D.C.
- 11 DOE O 435.1, 2001, Radioactive Waste Management, U.S. Department of Energy,
12 Washington, D.C.
- 13 DOE O 5400.1, 1990, General Environmental Protection Program, Change 1, U.S. Department
14 of Energy, Washington, D.C.
- 15 DOE O 5400.5, 1993, Radiation Protection of the Public and the Environment, U.S. Department
16 of Energy, Washington, D.C.
- 17 DOE/ORP-2008-01, 2010, RCRA Facility Investigation Report for Hanford Single-Shell Tank
18 Waste Management Areas, Rev. 1, U.S. Department of Energy, Office of River
19 Protection, Richland, Washington.
- 20 DOE/RL-93-33, 1996, Focused Feasibility Study of Engineered Barriers for Waste Management
21 Units in the 200 Areas, Rev. 1, U.S. Department of Energy, Richland Operations Office,
22 Richland, Washington.
- 23 DOE/RL-2002-59, 2004, Hanford Site Groundwater Strategy Protection, Monitoring, and
24 Remediation, U.S. Department of Energy, Richland Operations Office, Richland,
25 Washington.
- 26 DOE/RL-2011-50, 2012, Regulatory Basis and Implementation of a Graded Approach to
27 Evaluation of Groundwater Protection, Rev. 1, U.S. Department of Energy, Richland
28 Operations Office, Richland, Washington.
- 29 Ecology, EPA, and DOE, 1989, Hanford Federal Facility Agreement and Consent Order –
30 Tri-Party Agreement, 2 vols., as amended, State of Washington Department of Ecology,
31 U.S. Environmental Protection Agency, and U.S. Department of Energy, Olympia,
32 Washington.

RPP-ENV-58782, Rev. 0

- 1 EPA 402-R-94-012, 1994, A Technical Guide to Ground-Water Model Selection at Sites
2 Contaminated with Radioactive Substances, U.S. Environmental Protection Agency,
3 Washington, D.C.
- 4 EPA/530-SW-87-017, 1987, Alternate Concentration Limit Guidance, Interim Final, OSWER
5 Directive 9841.00-6C, U.S. Environmental Protection Agency, Office of Emergency
6 Response, Washington, D.C.
- 7 EPA/540/1-89/002, 1989, Risk Assessment Guidance for Superfund Volume I Human Health
8 Evaluation Manual (Part A) Interim Final, U.S. Environmental Protection Agency,
9 Washington, D.C.
- 10 EPA/540/F-95/041, 1996, Soil Screening Guidance: Fact Sheet, Publication 9355.4-14FSA,
11 U.S. Environmental Protection Agency, Office of Solid Waste and Emergency Response,
12 Washington, D.C.
- 13 EPA/540/R-92/003, 1991, Guidance for Data Useability in Risk Assessment (Part A) Final,
14 U.S. Environmental Protection Agency, Office of Research and Development,
15 Washington, D.C.
- 16 EPA/540/R-95/128, 1996, Soil Screening Guidance: Technical Background Document,
17 Second Edition, U.S. Environmental Protection Agency, Office of Solid Waste and
18 Emergency Response, Washington, D.C.
- 19 EPA/600/2-91/065, 1991, The RETC Code for Quantifying the Hydraulic Functions of
20 Unsaturated Soils, Office of Research and Development, U.S. Environmental Protection
21 Agency, Washington, D.C.
- 22 EPA-SAB-RAC-ADV-99-006, 1999, An SAB Advisory: Modeling of Radionuclide Releases
23 from Disposal of Low Activity Mixed Waste, U.S. Environmental Protection Agency,
24 Science Advisory Board, Washington, D.C.
- 25 Fayer, M. J., and G. W. Gee, 2006, "Multiple-Year Water Balance of Soil Covers in a Semiarid
26 Setting," Journal of Environmental Quality, Vol. 35, No. 2, pp. 366–377.
- 27 Gelhar, L. W. and C. L. Axness, 1983, "Three-dimensional stochastic analysis of
28 macrodispersion in aquifers," Water Resources Research, Vol. 19, pp. 161–180.
- 29 Haynes, W. M. and D. R. Lide, 2011, CRC Handbook of Chemistry and Physics, 92nd Edition,
30 CRC Press, Talyor & Francis Group, Boca Raton, Florida.
- 31 HNF-5294, 1999, "Computer Code Selection Criteria for Flow and Transport Code(s) To Be
32 Used in Vadose Zone Calculations for Environmental Analyses in the Hanford Site's
33 Central Plateau," Rev. 0, CH2M HILL Hanford Group, Inc. Richland, Washington.
- 34 Huyakorn, P. S. and G. F. Pinder, 1983, Computational Methods in Subsurface Flow, Academic
35 Press, Salt Lake City, Utah.

RPP-ENV-58782, Rev. 0

- 1 HW-60601, 1959, "Aquifer Characteristics and Ground-Water Movement at Hanford," General
2 Electric Company, Richland, Washington.
- 3 Khaleel, R., J. F. Relyea, and J. L. Conca, 1995, "Evaluation of van Genuchten-Mualem
4 Relationships to Estimate Unsaturated Hydraulic Conductivity at Low Water Contents,"
5 Water Resources Research, Vol. 31, Issue 11, pp. 2659–2668.
- 6 Millington, R. J. and J. P. Quirk, 1961, "Permeability of Porous Solids," Transactions of the
7 Faraday Society, Vol. 57, pp. 1200–1207.
- 8 Mualem, Y., 1976, "A New Model for Predicting the Hydraulic Conductivity of Unsaturated
9 Porous Media," Water Resources Research, Vol. 12, No. 3, pp. 513–522.
- 10 NAGRA NTB 02-20, 2002, "Cementitious Near-Field Sorption Data Base for Performance
11 Assessment of an ILW Repository in Opalinus Clay," Technical Report 02-20, National
12 Cooperative for the Disposal of Radioactive Waste, Hardstrasse, Zurich, Switzerland.
- 13 Neuman, S. P., 1990, "Universal Scaling of Hydraulic Conductivities and Dispersivities in
14 Geologic Media," Water Resources Research, Vol. 26, No. 8, pp. 1749–1758.
- 15 NOAA Manual NOS NGS 5, 1989, "State Plane Coordinate System of 1983," National Geodetic
16 Survey, Rockville, Maryland.
- 17 NUREG-1573, 2000, A Performance Assessment Methodology for Low-Level Radioactive
18 Waste Disposal Facilities: Recommendations of NRC's Performance Assessment
19 Working Group, U.S. Nuclear Regulatory Commission, Office of Nuclear Material
20 Safety and Safeguards, Washington, D.C.
- 21 NUREG-1854, 2007, NRC Staff Guidance for Activities Related to U.S. Department of Energy
22 Waste Determinations – Draft Final Report for Interim Use, U.S. Nuclear Regulatory
23 Commission, Office of Federal and State Materials and Environmental Management
24 Programs, Washington, D.C.
- 25 OSWER No. 9200.4-18, 1997, "Establishment of Cleanup Levels for CERCLA Sites with
26 Radioactive Contamination" (memorandum from S. D. Luftig and L. Weinstock to
27 Addressees, August 22), U.S. Environmental Protection Agency, Washington, D.C.
- 28 PNNL-11216, 1997, "STOMP Subsurface Transport Over Multiple Phases Application Guide,"
29 Pacific Northwest National Laboratory, Richland, Washington.
- 30 PNNL-12030, 2000, "STOMP Subsurface Transport Over Multiple Phases Version 2.0 Theory
31 Guide," Pacific Northwest National Laboratory, Richland, Washington.
- 32 PNNL-13033, 1999, "Recharge Data Package for the Immobilized Low-Activity Waste 2001
33 Performance Assessment," Pacific Northwest National Laboratory, Richland,
34 Washington.

RPP-ENV-58782, Rev. 0

- 1 PNNL-13895, 2003, "Hanford Contaminant Distribution Coefficient Database and Users Guide,"
2 Rev. 1, Pacific Northwest National Laboratory, Richland, Washington.
- 3 PNNL-15782, 2006, "STOMP Subsurface Transport Over Multiple Phases Version 4.0 User's
4 Guide," Pacific Northwest National Laboratory, Richland, Washington.
- 5 PNNL-16688, 2007, "Recharge Data Package for Hanford Single-Shell Tank Waste
6 Management Areas," Pacific Northwest National Laboratory, Richland, Washington.
- 7 PNNL-17176, 2007, "200-BP-1 Prototype Hanford Barrier Annual Monitoring Report for Fiscal
8 Years 2005 Through 2007," Pacific Northwest National Laboratory, Richland,
9 Washington.
- 10 PNNL-SA-54022, 2007, "STOMP Software Test Plan Rev. 1.0," Pacific Northwest National
11 Laboratory, Richland, Washington.
- 12 PNNL-SA-54023, 2007, "STOMP Software Configuration Management Plan Rev. 1.3," Pacific
13 Northwest National Laboratory, Richland, Washington.
- 14 PNNL-SA-54024, 2007, "Project Management Plan for Subsurface Transport Over Multiple
15 Phases (STOMP) Software Maintenance and Development," Rev. 1, Pacific Northwest
16 National Laboratory, Richland, Washington.
- 17 PNNL-SA-54079, 2007, "Requirements for STOMP Subsurface Transport Over Multiple
18 Phases," Pacific Northwest National Laboratory, Richland, Washington.
- 19 Polmann, D. J., 1990, "Application of Stochastic Methods to Transient Flow and Transport in
20 Heterogeneous Unsaturated Soils," Ph.D. Thesis, Massachusetts Institute of Technology,
21 Cambridge, Massachusetts.
- 22 PRC-PRO-IRM-309, 2014, "Controlled Software Management," Rev. 5, CH2M HILL Plateau
23 Remediation Company, Richland, Washington.
- 24 PSI Bericht Nr. 95-06, 1995, "Sorption Databases for the Cementitious Near-Field of a L/ILW
25 Repository for Performance Assessment," Paul Scherrer Institute, Switzerland.
- 26 Resource Conservation and Recovery Act of 1976, 42 USC 6901, et seq.
- 27 RPP-14430, 2003, "Subsurface Conditions Description of the C and A-AX Waste Management
28 Area," Rev. 0, CH2M HILL Hanford Group, Inc., Richland, Washington.
- 29 RPP-17209, 2006, "Modeling Data Package for an Initial Assessment of Closure of the S and
30 SX Tank Farms," Rev. 1, CH2M HILL Hanford Group, Inc., Richland, Washington.
- 31 RPP-PLAN-39114, 2012, "Phase 2 RCRA Facility Investigation/Corrective Measures Study
32 Work Plan for Waste Management Area C," Rev. 2, Washington River Protection
33 Solutions, LLC, Richland, Washington.

RPP-ENV-58782, Rev. 0

- 1 RPP-RPT-41918, 2010, "Assessment Context for Performance Assessment for Waste in C Tank
2 Farm Facilities after Closure," Rev. 0, Washington River Protection Solutions, LLC,
3 Richland, Washington.
- 4 RPP-RPT-42323, 2015, "Hanford C-Farm Tank and Ancillary Equipment Residual Waste
5 Inventory Estimates," Rev. 3, Washington River Protection Solutions, LLC, Richland,
6 Washington.
- 7 RPP-RPT-44042, 2016, "Recharge and Waste Release within Engineered System in Waste
8 Management Area C," Rev. 1, Washington River Protection Solutions, LLC, Richland,
9 Washington.
- 10 RPP-RPT-46088, 2016, "Flow and Transport in the Natural System at Waste Management
11 Area C," Rev. 2, Washington River Protection Solutions, LLC/GSI Water Solutions, Inc.,
12 Richland, Washington.
- 13 RPP-RPT-48490, 2011, "Technical Approach and Scope for Flow and Contaminant Transport
14 Analysis in the Initial Performance Assessment of Waste Management Area C,"
15 Washington River Protection Solutions, LLC, Richland, Washington.
- 16 RPP-RPT-50934, 2012, "Inspection and Test Report for the Removed 241-C-107 Dome
17 Concrete," Rev. 0, Washington River Protection Solutions, LLC, Richland, Washington.
- 18 RPP-RPT-56356, 2014, "Development of Alternative Digital Geologic Models of Waste
19 Management Area C," Rev. 0, Freestone Environmental Services Inc./Washington River
20 Protection Solutions, LLC, Richland, Washington.
- 21 Schulze-Makuch, D., 2005, "Longitudinal Dispersivity Data and Implications for Scaling
22 Behavior," Groundwater, Vol. 43, No. 3, pp. 443–456.
- 23 SKB Rapport R-05-75, 2005, "Assessment of uncertainty intervals for sorption coefficients,
24 SFR-1 uppföljning av SAFE," Swedish Nuclear Fuel and Waste Management Company,
25 Stockholm, Sweden.
- 26 SRNL-STI-2008-00421, 2008, "Hydraulic and Physical Properties of Saltstone Grouts and Vault
27 Concretes," Rev. 0, Savannah River National Laboratory, Savannah River Nuclear
28 Solutions, Aiken, South Carolina.
- 29 van der Kamp, G., L. D. Luba, J. A. Cherry, and H. Maathuis, 1994, "Field Study of a Long and
30 Very Narrow Contaminant Plume," Groundwater, Vol. 32, No. 6, pp. 1008–1016.
- 31 van Genuchten, M. Th., 1980, "A Closed-form Equation for Predicting the Hydraulic
32 Conductivity of Unsaturated Soils," Soil Science Society of America Journal, Vol. 44,
33 No. 5, pp. 892–898.
- 34 WAC 173-340, "Model Toxics Control Act – Cleanup," Washington Administrative Code, as
35 amended.

RPP-ENV-58782, Rev. 0

- 1 WAC 173-340-747, “Deriving Soil Concentrations for Groundwater Protection,” Washington
2 Administrative Code, as amended.
- 3 WCH-520, 2013, “Performance Assessment for the Environmental Restoration Disposal Facility,
4 Hanford Site, Washington,” Rev. 1, Washington Closure Hanford, Richland, Washington.
- 5 WHC-EP-0645, 1995, “Performance Assessment for the Disposal of Low-Level Waste in the
6 200 West Area Burial Grounds,” Westinghouse Hanford Company, Richland,
7 Washington.
- 8 WHC-SD-WM-EE-004, 1995, “Performance Assessment of Grouted Double-Shell Tank Waste
9 Disposal at Hanford,” Rev. 1, Westinghouse Hanford Company, Richland, Washington.
- 10 WSRC-MS-2003-00582, 2003, “Performance Assessment/Composite Analysis Modeling to
11 Support a Holistic Strategy for the Closure of F Area, a Large Nuclear Complex at The
12 Savannah River Site,” Rev. 1, Savannah River Technology Center, Aiken, South
13 Carolina.
- 14 Xu, M. and Y. Eckstein, 1995, “Use of Weighted Least-Squares Method in Evaluation of the
15 Relationship Between Dispersivity and Field Scale,” Groundwater, Vol. 33, No. 6,
16 pp. 905–908.
- 17 Ye, M., R. Khaleel, T. J. Yeh, 2005, “Stochastic analysis of moisture plume dynamics of a field
18 injection experiment,” Water Resources Research, Vol. 41, W03013.
- 19 Yeh, T.-C. J., M. Ye, R. Khaleel, 2005, “Estimation of effective unsaturated hydraulic
20 conductivity tensor using spatial moments of observed moisture plume,” Water
21 Resources Research, Vol. 41, W03014.

22

RPP-ENV-58782, Rev. 0

1
2
3
4
5
6
7
8
9
10

APPENDIX E

VALIDATION OF THE AIR-PATHWAY MODELING APPROACH

RPP-ENV-58782, Rev. 0

1
2
3
4
5
6
7

This page intentionally left blank.

RPP-ENV-58782, Rev. 0

TABLE OF CONTENTS

APPENDIX E – VALIDATION OF THE AIR-PATHWAY MODELING APPROACH.....	E-1
E.1 AIR CONCENTRATIONS USING WASTE MANAGEMENT AREA C PERFORMANCE ASSESSMENT MODEL	E-1
E.2 MODELED AIR CONCENTRATIONS USING EPA CAP88-PC SOFTWARE	E-2
E.2.1 Receptor Location and Population.....	E-2
E.2.2 Meteorological Data.....	E-2
E.2.3 Source and Radionuclide Data.....	E-4
E.2.4 CAP88 Modeling Results	E-4
E.3 COMPARISON OF MODELED AIR CONCENTRATIONS	E-4
E.4 COMPARISON AGAINST HANFORD SITE NATIONAL ENVIRONMENTAL POLICY ACT CHARACTERIZATION REPORT.....	E-5
E.5 REFERENCES	E-6

LIST OF FIGURES

Figure E-1. 2011 Wind Rose for Hanford Meteorological Station Showing the Incoming Wind Direction.	E-3
--	-----

LIST OF TABLES

Table E-1. Predicted Maximum Air Concentration Using Waste Management Area C Performance Assessment Model.....	E-1
Table E-2. Source Terms for CAP88 Run.	E-4
Table E-3. Maximum Air Concentrations Based on CAP88 Model.	E-4
Table E-4. Estimated Air Concentrations at the Receptor Location.....	E-5

RPP-ENV-58782, Rev. 0

LIST OF TERMS

1		
2		
3	EPA	U.S. Environmental Protection Agency
4		
5	HMS	Hanford Meteorological Station
6		
7	NEPA	National Environmental Policy Act
8		
9	PA	performance assessment
10		
11	WMA C	Waste Management Area C
12		
13		

RPP-ENV-58782, Rev. 0

APPENDIX E

VALIDATION OF THE AIR-PATHWAY MODELING APPROACH

As a part of the performance assessment (PA) requirements, potential gas emissions and the resulting air concentrations of radionuclides originating from Waste Management Area C (WMA C) need to be modeled for calculating potential doses by the atmospheric pathway. Among the radionuclides contained in the wastes in WMA C at closure, three of them can potentially emanate in gaseous form. These radionuclides are ^{14}C (as CO_2), ^3H (as H_2), and ^{129}I (as I_2). Using the WMA C PA model, the release rates and concentrations for the three radionuclides over WMA C are calculated. The PA model conceptualization for air-pathway modeling is discussed in Section 6.3.2.5 (Atmospheric Transport Pathway).

This section provides evidence that the air-pathway modeling approach has been adequately modeled to meet the performance requirements of the PA. This is done by comparing the PA model for air-pathway calculations to modeling results generated using the U.S. Environmental Protection Agency's (EPA) CAP88-PC code, and to those reported in the recent Hanford Site National Environmental Policy Act (NEPA) Characterization Report [PNNL-6415, "Hanford Site National Environmental Policy Act (NEPA) Characterization"]. The comparison of results indicates that the GoldSim^{®1}-based WMA C PA model built for the air-pathway calculation is appropriate for its intended purpose.

E.1 AIR CONCENTRATIONS USING WASTE MANAGEMENT AREA C PERFORMANCE ASSESSMENT MODEL

The WMA C PA air pathway model was used to calculate the release rates and concentrations for three radionuclides— ^{14}C (as CO_2), ^3H (as H_2), and ^{129}I (as I_2)—at the receptor location (see Sections 6.3.2.5 and 7.2.2). The PA model calculates the diffusive flux of volatiles to the surface of WMA C and then transports them through the air to the receptor location. The air concentrations for the volatiles (^{14}C [as CO_2], ^3H [as H_2], ^{129}I) from all residual waste sources in WMA C are calculated out to 10,000 years. The maximum calculated air concentration is presented in Table E-1. These values were used for comparison.

Table E-1. Predicted Maximum Air Concentration Using Waste Management Area C Performance Assessment Model.

Nuclides	Unit	Maximum Air Concentration
^{14}C	pCi/m ³	2.4E-6
^3H		1.1
^{129}I		3.5E-6

¹ GoldSim[®] Pro is a registered trademark of GoldSim Technologies, Issaquah, Washington, in the United States and other countries.

RPP-ENV-58782, Rev. 0

E.2 MODELED AIR CONCENTRATIONS USING EPA CAP88-PC SOFTWARE

To verify the modeled radionuclide concentrations by the WMA C PA model, a comparative modeling study was performed using the CAP88-PC Version 4 computer program (EPA 2014). The CAP88 (which stands for Clean Air Act Assessment Package – 1988) computer model is a set of computer programs, databases, and associated utility programs for estimation of concentrations, dose, and risk from radionuclide emissions to the air.

CAP88-PC uses a modified Gaussian plume equation to estimate the average dispersion of radionuclides released from up to six emitting sources. The sources may be either elevated stacks (such as a smoke stack) or uniform area sources (such as a landfill or a pile of uranium mill tailings). Plume rise can be calculated assuming either a momentum or buoyant-driven plume. Assessments are done for a circular grid of distances and directions for a radius of up to 80 km (50 mi) around the facility. The Gaussian plume model produces results that agree with experimental data, and with other similar regulatory models.

The CAP88-PC model requires the following inputs:

- Facility data
- Receptor location and population
- Meteorological data
- Source data
- Radionuclide data
- Agriculture data (for dose estimation and risk calculation).

For this comparative study, the CAP88-PC modeling was conducted using the options and input parameters described in the following sections.

E.2.1 Receptor Location and Population

The CAP88 modeling was set up for “individual assessment” (rather than for “population assessment”) to be consistent with modeled results in the PA effort. The modeled receptor distance was calculated as the distance from the center of the tank farm within WMA C to 100 m downwind from the fenceline. As a result, a total receptor distance for the CAP88 modeling was set to be 175 m.

E.2.2 Meteorological Data

The following site-specific meteorological input parameters for the comparative modeling were determined based on the averages of 30-year meteorological data collected at the Hanford Meteorological Station (HMS). The HMS is located near the center of the Hanford Site, just outside the northeast corner of the 200 West Area:

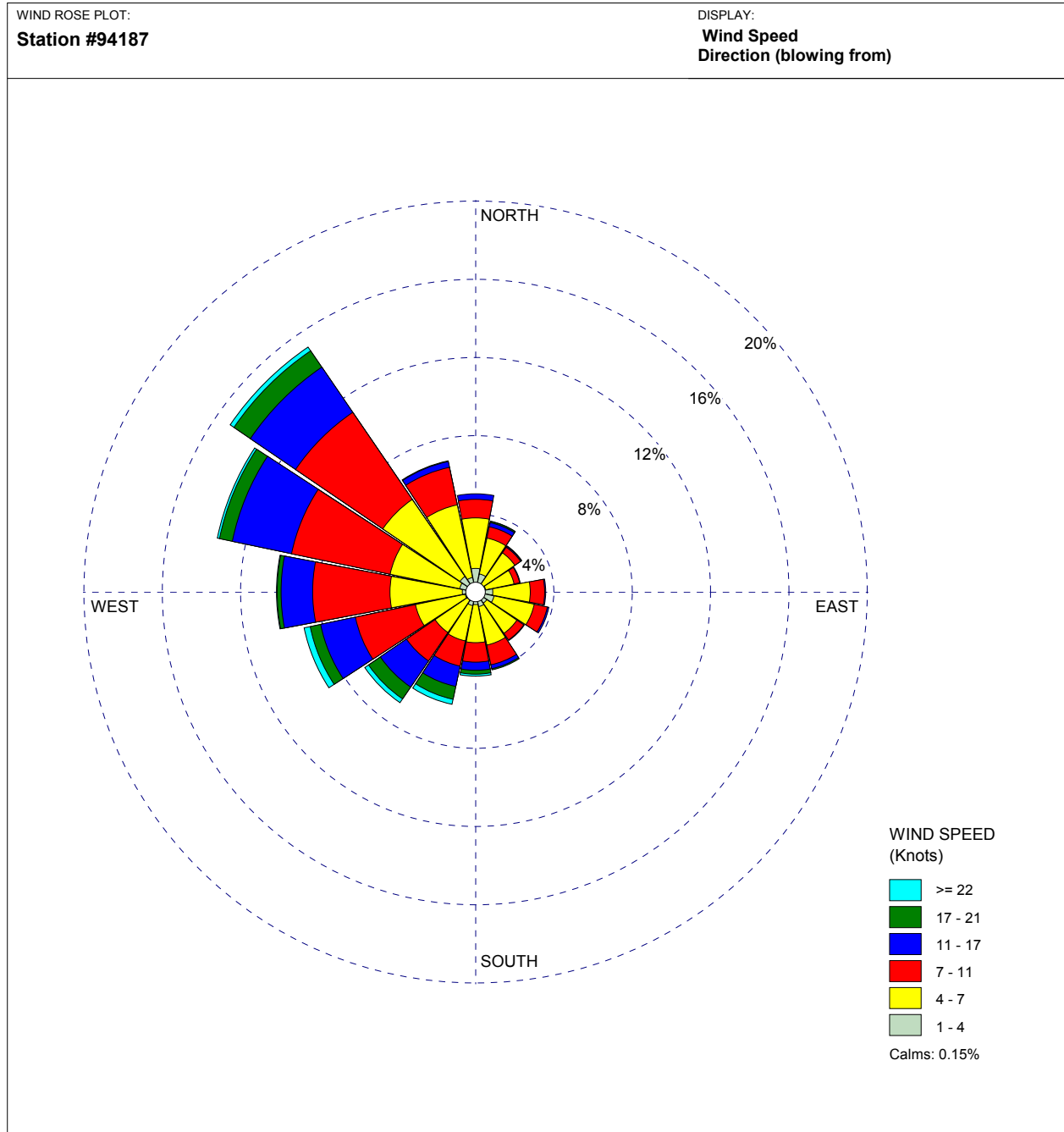
- Annual ambient temperature: 10°C
- Annual precipitation: 17 cm/year

RPP-ENV-58782, Rev. 0

- Height of the mixing layer: 1,000 m (default)
- Absolute humidity: 8.00 g/m³ (default, similar to the HMS value).

The wind rose for HMS for 2011 is presented in Figure E-1. The figure showed that the prevailing wind direction is from west-northwest towards the east-southeast.

Figure E-1. 2011 Wind Rose for Hanford Meteorological Station Showing the Incoming Wind Direction.



RPP-ENV-58782, Rev. 0

E.2.3 Source and Radionuclide Data

The emissions from the tank farm within WMA C were modeled as a point source (stack emission) at a height of 2 m above the ground level. The point source is conceptualized to be conservative and located at the center of the tank farm. The effective diameter for the stack was set to be the 100-series tank diameter (75 ft).

The combined diffusive flux for the volatiles (^{14}C [as CO_2], ^3H [as H_2], ^{129}I) from all sources was used as the source term for stack emission for CAP88 calculation. For the purpose of verification, the maximum emission rate for each radionuclide at the surface of WMA C calculated by the WMA C PA model was selected. The maximum emission rates are presented in Table E-2.

Table E-2. Source Terms for CAP88 Run.

Nuclides	Unit	Emission Rate
^{14}C	Ci/yr	4.35E-7
^3H		2.06E-1
^{129}I		6.54E-7

E.2.4 CAP88 Modeling Results

Using the wind file from HMS (200 Area), the CAP88 modeling determined the maximum concentration for each radionuclide at the receptor location; those concentrations are presented in Table E-3. The maximum concentration occurred along the 175 m distance in the southeast direction from the center of the tank farm, consistent with the predominant wind direction.

Table E-3. Maximum Air Concentrations Based on CAP88 Model.

Nuclides	Unit	Maximum Air Concentration
^{14}C	pCi/m ³	1.57E-6
^3H		0.744E-1
^{129}I		2.37E-6

E.3 COMPARISON OF MODELED AIR CONCENTRATIONS

Tables E-1 and E-3 present maximum air concentration results for three radionuclides— ^{14}C (as CO_2), ^3H (as H_2), and ^{129}I (as I_2)—at the receptor location using the WMA C PA model and CAP88 model. The results showed that the maximum concentrations for both models are in reasonable agreement, with the PA model producing results about 50% higher than CAP88. The difference between the two models lies in an approximation used in the PA model where

RPP-ENV-58782, Rev. 0

concentration along the center of the plume is calculated at the same height as the stack without accounting for horizontal and vertical dispersion.

E.4 COMPARISON AGAINST HANFORD SITE NATIONAL ENVIRONMENTAL POLICY ACT CHARACTERIZATION REPORT

As part of the annual Hanford Site NEPA Characterization Report, an atmospheric dispersion analysis is performed to characterize the distribution of the identified radionuclides in the ambient air and to estimate the potential exposure. These are presented in Revision 18 of PNNL-6415. The annual sector-averaged dispersion coefficients for the major Hanford Site areas are presented, taking into account the wind-related data from 1983 through 2006 from various meteorological stations on the Hanford Site. These dispersion factors are presented as a function of direction and distance from the release point.

The atmospheric dispersion analysis in the PNNL-6415 report was conducted using simple dispersion models and the joint frequency distribution of atmospheric stability, wind speed, and wind direction to compute diffusion factors for both chronic and acute releases. Joint frequency distributions for atmospheric stability, wind speed, and transport direction have been estimated and presented for the meteorological data collected from the 100-N, 200, 300, and 400 Areas at two release heights (9.1 m [30 ft] and 60 m [197 ft]).

To verify the WMA C PA air-pathway modeling results, an evaluation was performed by comparing the WMA C PA modeled concentrations at a selected distance with the derived air concentrations for the same distance. This evaluation used the reported annual sector average dispersion coefficients (X/Q' , where X is the air concentration [Ci/m^3] and Q' is the emission rate) in PNNL-6415 for a given WMA C gas emission rate.

For this comparison analysis, joint frequency distributions presented for the 200 Area were used (PNNL-6415). The atmospheric dispersion coefficient (X/Q') of $1.1 \times 10^{-4} \text{ s} \cdot \text{m}^{-3}$ for the ground level release was selected based on a distance of 175 m (approximate effective distance of receptor from the center of WMA C) in the southeast direction (the predominant direction of flow) from Table A11 of PNNL-6415. The emission rates for three radionuclides are presented in Table E-2. The atmospheric dispersion coefficient (X/Q') was multiplied with the emission rates for three radionuclides to calculate their estimated ground level air concentrations at 175 m downgradient from the source. The results are presented in Table E-4.

Table E-4. Estimated Air Concentrations at the Receptor Location.

Nuclides	X/Q (s/m ³)	Emission Rate		Estimated Air Concentrations at 175 m Downgradient (pCi/m ³) = X/Q (s/m ³) × Emission Rate (pCi/s)
		(Ci/yr)	(pCi/s) = (Ci/yr) × (10 ¹² pCi/Ci) × (1 yr/3.15E7 s)	
¹⁴ C	1.1E-4	4.35E-7	1.38E-02	1.52E-06
³ H		2.06E-1	6.54E+03	7.20E-01
¹²⁹ I		6.54E-7	2.07E-02	2.28E-06

RPP-ENV-58782, Rev. 0

1 Comparison with the WMA C concentrations (Table E-1) shows that, like the CAP88
2 comparison, the WMA C results are about 50% higher. As in that comparison, the difference is
3 attributable to the centerline approximation used in the WMA C PA model, which tends to
4 overestimate concentrations relative to other models.
5
6

7 **E.5 REFERENCES**
8

9 EPA, 2014, CAP88-PC Version 4.0 User Guide, U.S. Environmental Protection Agency,
10 Washington, D.C.
11

12 National Environmental Policy Act of 1969, 42 USC 4321-4347, et seq.
13

14 PNNL-6415, 2007, “Hanford Site National Environmental Policy Act (NEPA) Characterization,”
15 Rev. 18, Pacific Northwest National Laboratory, Richland, Washington.
16

RPP-ENV-58782, Rev. 0

1
2
3
4
5
6
7
8
9
10
11
12

APPENDIX F**DEVELOPMENT OF HETEROGENEOUS MEDIA MODEL AND COMPARISON TO
BASE CASE MODEL RESULTS FOR WASTE MANAGEMENT AREA C
PERFORMANCE ASSESSMENT**

RPP-ENV-58782, Rev. 0

- 1
- 2
- 3
- 4
- 5
- 6
- 7

This page intentionally left blank.

RPP-ENV-58782, Rev. 0

TABLE OF CONTENTS

1			
2			
3		APPENDIX F – DEVELOPMENT OF HETEROGENEOUS MEDIA MODEL AND	
4		COMPARISON TO BASE CASE MODEL RESULTS FOR WASTE	
5		MANAGEMENT AREA C PERFORMANCE ASSESSMENT	F-1
6	F.1	INTRODUCTION	F-1
7	F.2	METHODOLOGY FOR DEVELOPING TWO-DIMENSIONAL	
8		CROSS-SECTION MODELS FROM THE THREE-DIMENSIONAL MODEL	F-2
9	F.2.1	Waste Management Area C Performance Assessment Three-Dimensional	
10		STOMP [®] Model	F-2
11	F.2.2	Development of Three-Dimensional Distributions of Moisture Content	F-2
12	F.2.3	Development of Two-Dimensional STOMP [®] -Based Models from Three-	
13		Dimensional Models	F-2
14	F.3	RESULTS	F-14
15	F.3.1	Moisture Content Prediction	F-14
16	F.3.2	Matric Potential Measurements	F-14
17	F.3.3	Calculation of Technetium-99 Concentration	F-15
18	F.4	CONCLUSIONS	F-15
19	F.5	REFERENCES	F-25

RPP-ENV-58782, Rev. 0

LIST OF FIGURES

1		
2		
3	Figure F-1. Geologic Layers in the Three-Dimensional Waste Management Area C	
4	Performance Assessment Model.....	F-5
5	Figure F-2. Plan View of Waste Management Area C Performance Assessment Model and	
6	Moisture Content-Based Model.....	F-6
7	Figure F-3. Waste Management Area C Basemap with Moisture Content (vol %) Data	
8	Locations.....	F-7
9	Figure F-4. Cross Section B-B' with Continuous Contours for Moisture Content (vol %)	
10	Interpolation.....	F-8
11	Figure F-5. Cross Section C-C' with Continuous Contours for Moisture Content (vol %)	
12	Interpolation.....	F-9
13	Figure F-6. Location of Selected Cross Sections for the Two-Dimensional Models.	F-10
14	Figure F-7. View along Cross Section 1 (North to South) Shown in Figure F-6.	F-11
15	Figure F-8. View along Cross Section 2 (North to South) Shown in Figure F-6.	F-12
16	Figure F-9. View along Cross Section 3 (West to East) Shown in Figure F-6.....	F-13
17	Figure F-10. Moisture Retention Curves and Unsaturated Hydraulic Conductivity Curves	
18	for the 44 Integrated Disposal Facility Samples.	F-16
19	Figure F-11. Moisture Retention Curves and Unsaturated Hydraulic Conductivity Curves	
20	for the Four New Units.	F-17
21	Figure F-12. Location of Contaminant Source and Point of Calculation.	F-18
22	Figure F-13. Location of Well C4297 and 299-E27-22 Relative to Cross Section 1.	F-19
23	Figure F-14. Comparison of Measured (C4297) and Simulated Moisture Contents for	
24	(a) Base Case (Equivalent Homogeneous Medium) Model, and	
25	(b) Heterogeneous Model for Cross Section 1.....	F-20
26	Figure F-15. Comparison of Measured (299-E27-22) and Simulated Moisture Contents for	
27	(a) Base Case (Equivalent Homogeneous Medium) Model, and	
28	(b) Heterogeneous Model for Cross Section 1.....	F-21
29	Figure F-16. Technetium-99 Breakthrough Curves for Cross Section 1.	F-22
30	Figure F-17. Technetium-99 Breakthrough Curves for Cross Section 2.	F-23
31	Figure F-18. Technetium-99 Breakthrough Curves for Cross Section 3.	F-24

RPP-ENV-58782, Rev. 0

LIST OF TABLES

Table F-1.	Vadose Zone Hydraulic Properties for Waste Management Area C Hydrostratigraphic Units (Appendix B).....	F-14
Table F-2.	Summary of Vadose Zone Hydraulic Properties for the New Units (Appendix B).....	F-18
Table F-3.	Average Moisture and Matric Potentials for Borehole Samples Inside and Outside of Waste Management Area C.....	F-21
Table F-4.	Summary of Technetium-99 Transport Model Results.....	F-24

RPP-ENV-58782, Rev. 0

LIST OF TERMS**Abbreviations and Acronyms**

2D	two-dimensional
3D	three-dimensional
cm	centimeter
EHM	equivalent homogeneous medium
HSU	hydrostratigraphic unit
L	Liter
m	meter
MPa	megapascal
NAVD88	North American Vertical Datum of 1988
pCi	picocurie
PA	performance assessment
RCRA	Resource Conservation and Recovery Act of 1976
s	second
S&L	Sisson and Lu
STOMP	Subsurface Transport Over Multiple Phases
WMA	Waste Management Area

RPP-ENV-58782, Rev. 0

APPENDIX F**DEVELOPMENT OF HETEROGENEOUS MEDIA MODEL AND COMPARISON TO
BASE CASE MODEL RESULTS FOR WASTE MANAGEMENT AREA C
PERFORMANCE ASSESSMENT****F.1 INTRODUCTION**

Small-scale laboratory measurements were used to estimate field-scale parameters for the Waste Management Area (WMA) C model (Section 6). Each heterogeneous geologic unit was replaced by an equivalent homogeneous medium (EHM) with macroscopic flow properties. Each heterogeneous unit was assigned its upscaled or effective hydraulic properties; the simulated flow fields calculated the bulk or mean flow behavior at the field scale. Upscaling, in effect, accounts for differences in scale between small, core-scale measurements and large, field-scale modeling.

While the EHM model is the base case for performance assessment (PA) modeling, an alternative case is considered here based on the natural moisture content distribution. For heterogeneous media, the natural moisture content distribution, in the absence of anthropogenic recharge, can be used as an indicator of sediment texture (Appendix B). Field-measured moisture contents can then be used as indirect evidence from which estimates of soil hydraulic properties can be inferred.

In the absence of anthropogenic recharge, moisture content data correlate well with sediment texture ("Stochastic analysis of moisture plume dynamics of a field injection experiment" [Ye et al. 2005]). Higher moisture contents are associated with fine-textured sediments and lower moisture contents are associated with coarse-textured sediments. In the absence of anthropogenic recharge, field-measured moisture contents are assumed to be in equilibrium with natural recharge. These inferences, as well as the results of geostatistical analysis of the moisture content database, are used to identify and select hydraulic properties for input into a vadose zone model for WMA C.

An extensive set of moisture content data exists at WMA C for neutron moisture logging of direct push borehole and drywell locations. Using a geostatistical interpretation of the moisture data, an alternative vadose zone conceptual model has been developed, which is denoted as the "Heterogeneous Case" (RPP-CALC-60345, "Heterogeneous Media Model for Waste Management Area C Performance Assessment"). From the three-dimensional (3D) WMA C base case model, three cross sections have been selected to develop two-dimensional (2D) Subsurface Transport Over Multiple Phases (STOMP)¹ models for both the EHM base case model and heterogeneous case model. The results are compared to identify the impact of heterogeneity for predicting concentrations in the water table.

¹ Subsurface Transport Over Multiple Phases (STOMP)[®] is copyrighted by Battelle Memorial Institute, 1996.

RPP-ENV-58782, Rev. 0

F.2 METHODOLOGY FOR DEVELOPING TWO-DIMENSIONAL CROSS-SECTION MODELS FROM THE THREE-DIMENSIONAL MODEL

Two-dimensional cross sections are developed from a 3D moisture content distribution model by interpolating on the grid discretization developed for the 3D STOMP[®] WMA C PA model. These selected cross sections form the basis for developing alternative heterogeneous case models based on moisture content data. The details of the approach for developing the 2D cross-sectional model are described in Sections F.2.1 through F.2.3.

F.2.1 Waste Management Area C Performance Assessment Three-Dimensional STOMP[®] Model

Figure F-1 (Section 6.3.2.2) presents a cutaway section of geologic units in the 3D STOMP[®] WMA C PA model domain. The WMA C PA 3D STOMP[®]-based model domain is 737.9 m (2,421 ft) northwest to southeast by 795.3 m (2,609 ft) southwest to northeast by 116 m (381 ft), vertically, extending about 12 m (49 ft) below the water table.

For the purpose of developing the heterogeneous geologic models, the moisture content distribution was interpolated on the 3D STOMP[®] WMA C PA model domain and then cross sections were developed.

F.2.2 Development of Three-Dimensional Distributions of Moisture Content

A 3D model of the distribution of moisture content has been developed based on a geostatistical evaluation of soil moisture data collected at WMA C. An extensive set of moisture content data and information exists at WMA C from neutron moisture logging of direct push borehole and drywell locations. These moisture content data have been collected long after the occurrence of past leaks and discharges at the farm (RPP-CALC-60345), and therefore are regarded as representing the vadose zone at equilibrium with natural recharge. A geostatistical analysis of the moisture content data yielded vertical as well as horizontal correlation length scales for moisture content. The experimental variograms for moisture content used in the geostatistical analysis were fit with an exponential model having a vertical correlation length of ~15 m and a horizontal correlation length of ~85 m. Subsequent krigging yielded a heterogeneous moisture distribution, which, unlike the EHM approximation, captures a higher level of spatial variability of moisture content and associated variability in hydraulic properties (RPP-CALC-60345). Figure F-2 represents the plan view of 3D WMA C PA model domain and krigged moisture content based on the level of discretization of the model domain. Figure F-3 (RPP-CALC-60345) presents the location of the different cross sections of the model; Figure F-4 and Figure F-5 show the 2D cross sections of the model.

F.2.3 Development of Two-Dimensional STOMP[®]-Based Models from Three-Dimensional Models

F.2.3.1 Base Case Two-Dimensional Model. From the 3D base case model, 2D models were extracted for three different cross sections for comparison to the heterogeneous case model-based cross sections. Figure F-6 shows the location of the selected cross sections. These cross sections

RPP-ENV-58782, Rev. 0

were selected to be in the same locations as the cross section B-B' and cross section C-C' shown in Figure F-3. Two orthogonal directions were chosen to represent behavior in different directions. Only cross section 1 slices through the tanks. Heterogeneity was only considered for the H1 and H2 units because of lack of moisture data for the deeper units.

F.2.3.1.1 Interpretation of the Three-Dimensional Moisture Model. The following steps were followed to develop the geology of the heterogeneous model from the moisture content model.

1. Four different moisture content bands were used to define the heterogeneous layers in the H1 and H2 units based on the histogram of the observed moisture content data reported in RPP-CALC-60345. These moisture content bands qualitatively correlate with the sand/silt content of the sediments as inferred from the characterization of vadose zone sediments within WMA C (PNNL-15503, "Characterization of Vadose Zone Sediments Below the C Tank Farm: Borehole C4297 and RCRA Borehole 299-E27-22"). Typically, increasing volumetric moisture content from 6% to >10% reflects increasing silt content in the sediments. Based on the characterization of vadose zone sediments in WMA C (PNNL-15503), it is observed that <6% moisture content is associated with sediments with no, or negligible, silt content (primarily sand or gravelly sand), while sediment with >10% volumetric moisture content is silt-dominated. For volumetric moisture contents within 6% and 10%, the increasing moisture content is understood to reflect increasing silt content. To define the moisture content bands for the purpose of model parameterization, two additional classes are introduced, one with 6% to 8% and the other with 8% to 10% volumetric moisture content. The four moisture content bands are summarized below:
 - 2%-6% – correlates to sand with some gravel fraction
 - 6%-8% – correlates to sandy units with minor silt fraction
 - 8%-10% – correlates to sandy-silty sand units
 - >10% – correlates to predominantly silty units.
2. The moisture content values from the moisture model were interpolated on the 3D STOMP[®] model grid.
3. The STOMP[®] model zonation number for each of the model grid blocks was printed out along with the moisture content values.
4. The base case 3D STOMP[®] model has five different hydrostratigraphic units (HSUs) defined as implemented in STOMP[®] as rock/soil zones:
 - Backfill: gravel-dominated
 - H1: gravel-dominated unit
 - H2: sand-dominated unit
 - H3: gravel-dominated unit
 - Aquifer.

RPP-ENV-58782, Rev. 0

5. Four additional rock/soil zones are introduced corresponding to the four moisture content bands by altering the original zones. These four zones are added within the WMA C model domain defined by the krigged area in Figure F-6 (red rectangular box). For areas outside this box, the original five rock/soil zones are retained, thus leading to total of nine different rock/zones.
6. Generate 2D models for the heterogeneous case and the base case along three selected cross sections. Figure F-7, Figure F-8, and Figure F-9 contrast the geologic representation of the PA base case model and the heterogeneous model for the selected cross sections.

F.2.3.2 Vadose Zone Hydraulic Properties for Different Units. Table F-1 shows the vadose zone hydraulic properties for the HSUs defined in the base case model. For the heterogeneous case, hydraulic properties for four additional zones/layers have been selected that compare favorably with the moisture content data under current recharge conditions.

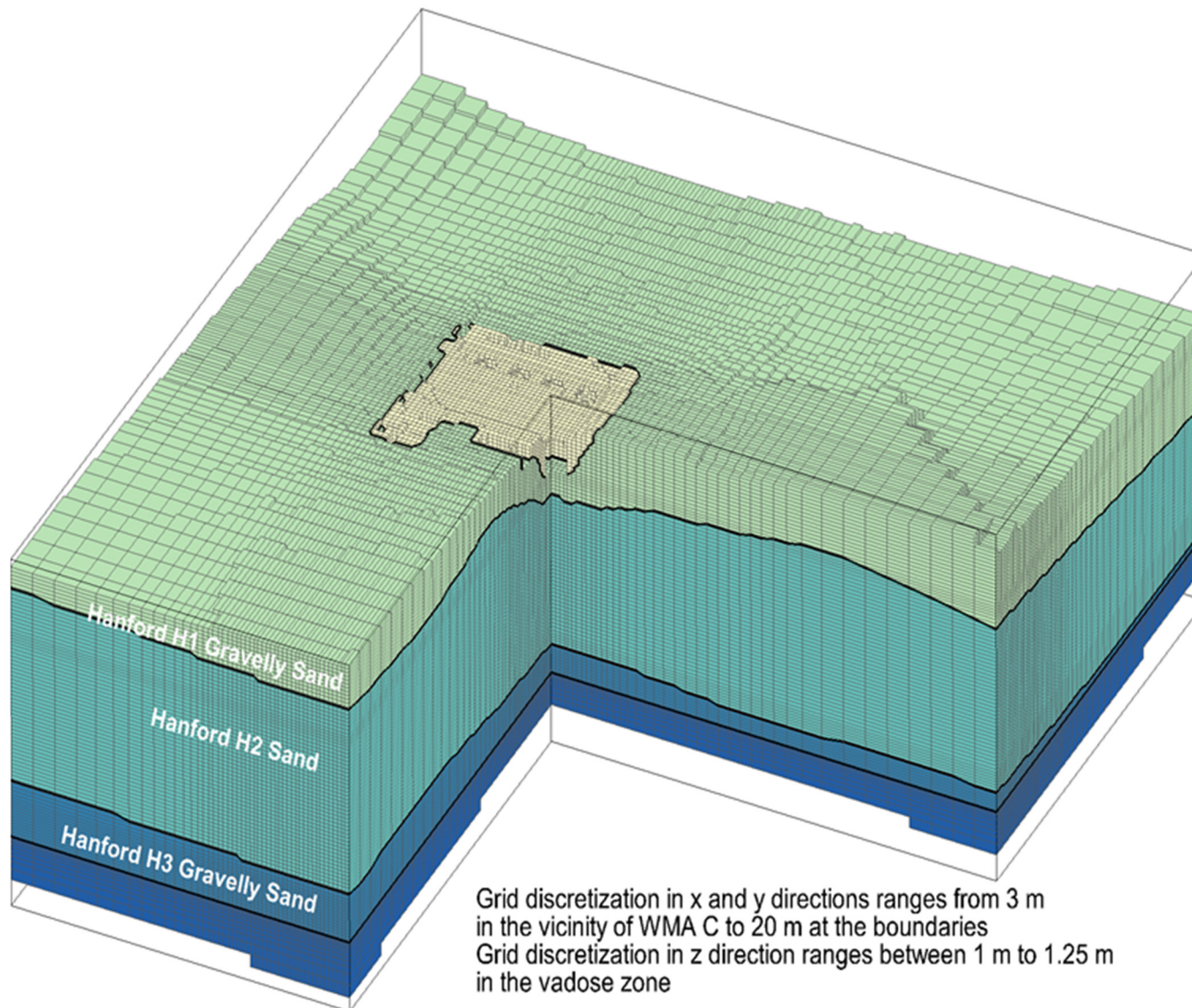
The hydraulic properties for the new zones/layers have been selected by analyzing 44 Integrated Disposal Facility sandy samples as presented in Appendix B, Basis for Development of Vadose Zone Hydraulic Properties at Waste Management Area C. Figure F-10 shows the moisture retention curves and unsaturated hydraulic conductivity curves for the 44 Integrated Disposal Facility samples. Four samples out of the 44 samples were selected to represent the new moisture content-based units. The four samples were chosen such that the resulting moisture content distribution at unit gradient condition corresponds to the moisture content bands represented by the samples. Figure F-11 shows the moisture retention curves and unsaturated hydraulic conductivity curves for the four new units that correlate with the four zones based on moisture content. Table F-2 summarizes the properties for all the new units.

Moisture-dependent anisotropy was applied to the 2D cross-section model derived from the 3D base case model to be consistent with the upscaling methodology used for EHM-based models. However, the impact of anisotropy was assumed to be represented by the heterogeneous distribution of sediments and was therefore not applied for the 2D heterogeneous models.

F.2.3.2.1 Contaminant Source and Model Output. For each cross-sectional model, an arbitrary source concentration of 1,000 pCi/m³ of ⁹⁹Tc (in bulk volume) was injected into the subsurface at the base of the backfill material beginning in the calendar year 2020. Here the objective was to compare the transport behavior of the contaminant between the EHM and heterogeneous model. Figure F-12 shows the location of the source and the point of calculation for all the cases. The vertical location of the contaminant mass is positioned 68 m above the water table. The output concentrations were observed at a point of calculation 100 m downgradient from the source location.

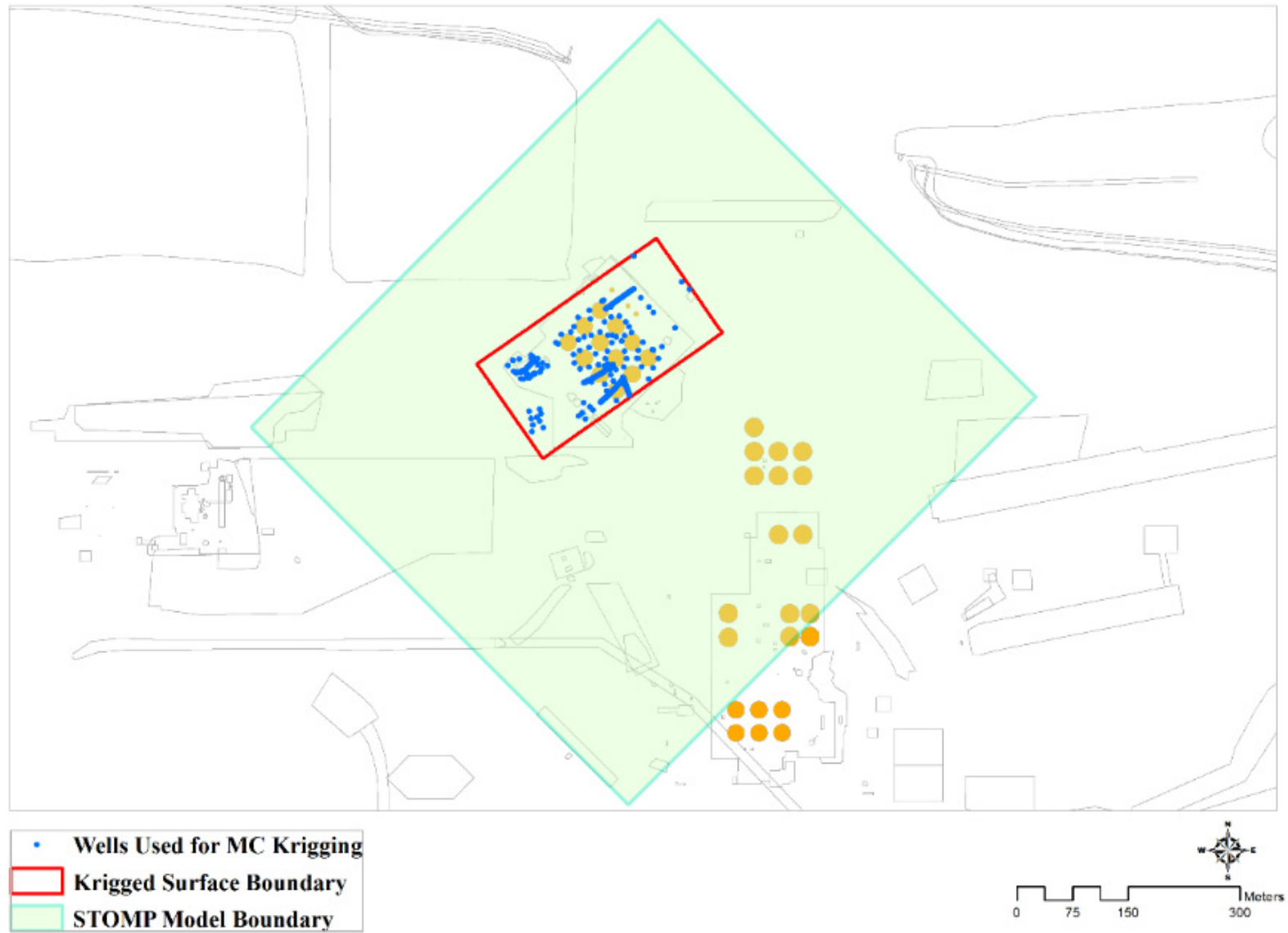
F.2.3.2.2 Recharge Rate. A 3.5 mm/yr recharge rate corresponding to long-term recharge rate for the WMA C base model domain was applied throughout the simulation duration.

Figure F-1. Geologic Layers in the Three-Dimensional Waste Management Area C Performance Assessment Model.



WMA = Waste Management Area

Figure F-2. Plan View of Waste Management Area C Performance Assessment Model and Moisture Content-Based Model.

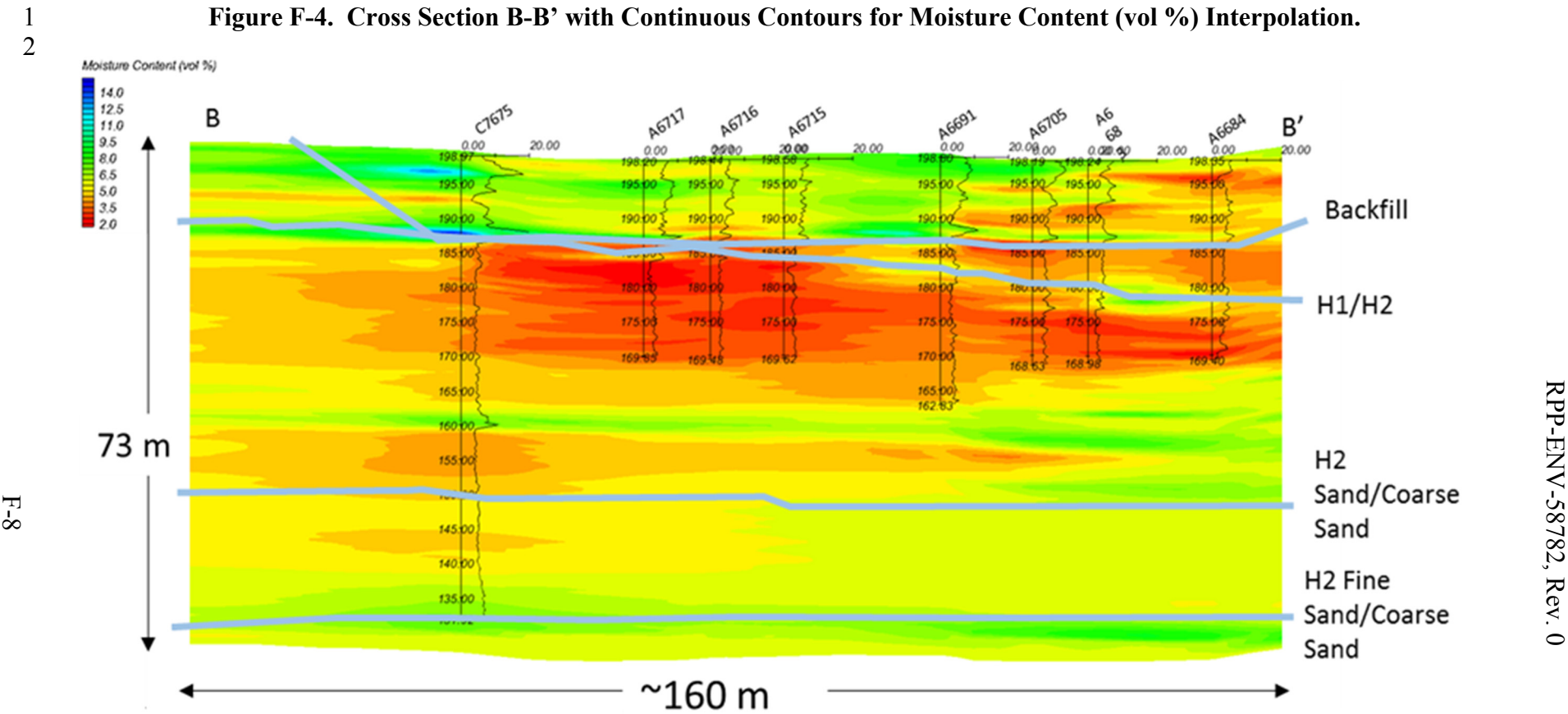


Subsurface Transport Over Multiple Phases (STOMP)® is copyrighted by Battelle Memorial Institute, 1996.

1
2

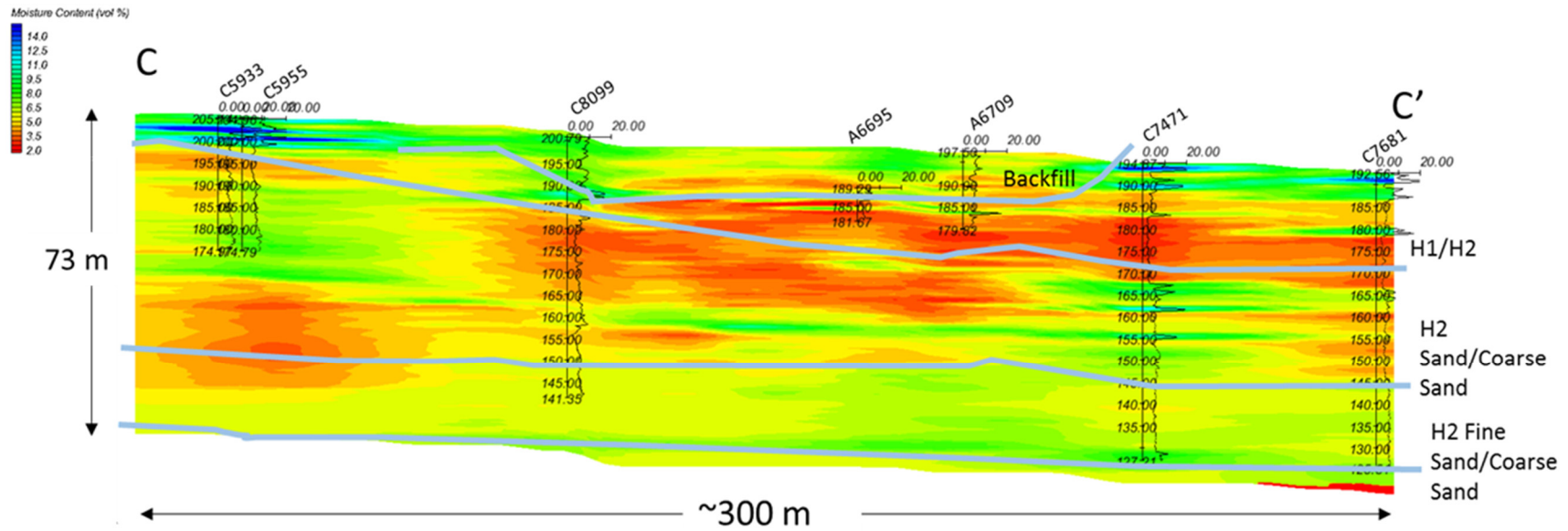
34

Figure F-4. Cross Section B-B' with Continuous Contours for Moisture Content (vol %) Interpolation.



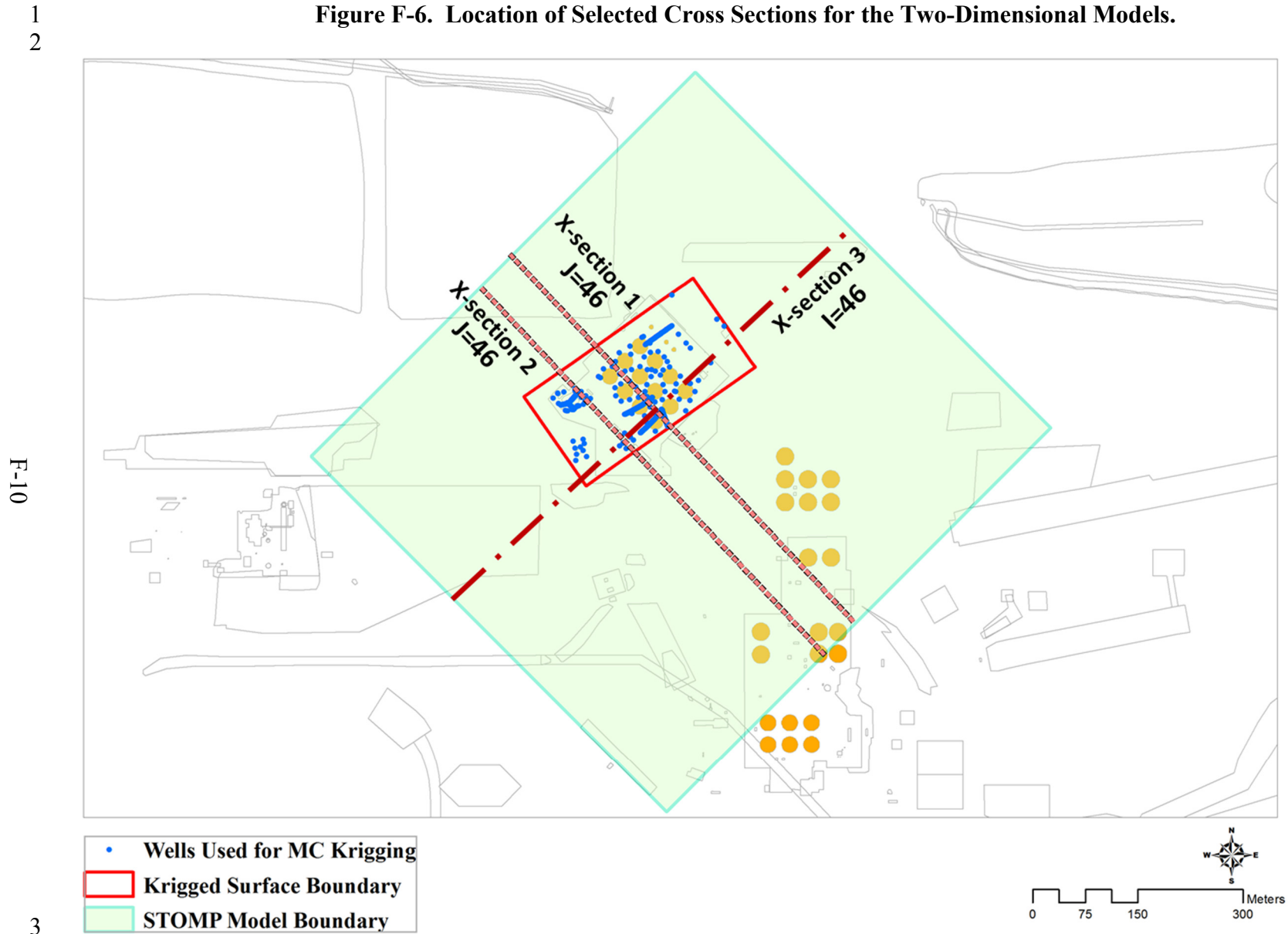
Reference: RPP-CALC-60345, "Heterogeneous Media Model for Waste Management Area C Performance Assessment."

Figure F-5. Cross Section C-C' with Continuous Contours for Moisture Content (vol %) Interpolation.



Reference: RPP-CALC-60345, "Heterogeneous Media Model for Waste Management Area C Performance Assessment."

Figure F-6. Location of Selected Cross Sections for the Two-Dimensional Models.



3
4 Subsurface Transport Over Multiple Phases (STOMP)[®] is copyrighted by Battelle Memorial Institute, 1996.

Figure F-7. View along Cross Section 1 (North to South) Shown in Figure F-6.

The left hand figure has the original 5 rock/soil zones (hydrostratigraphic units) while the right hand figure has 4 additional rock/soil zones to incorporate the moisture content bands-based heterogeneity within the krigged area shown in Figure F-6.

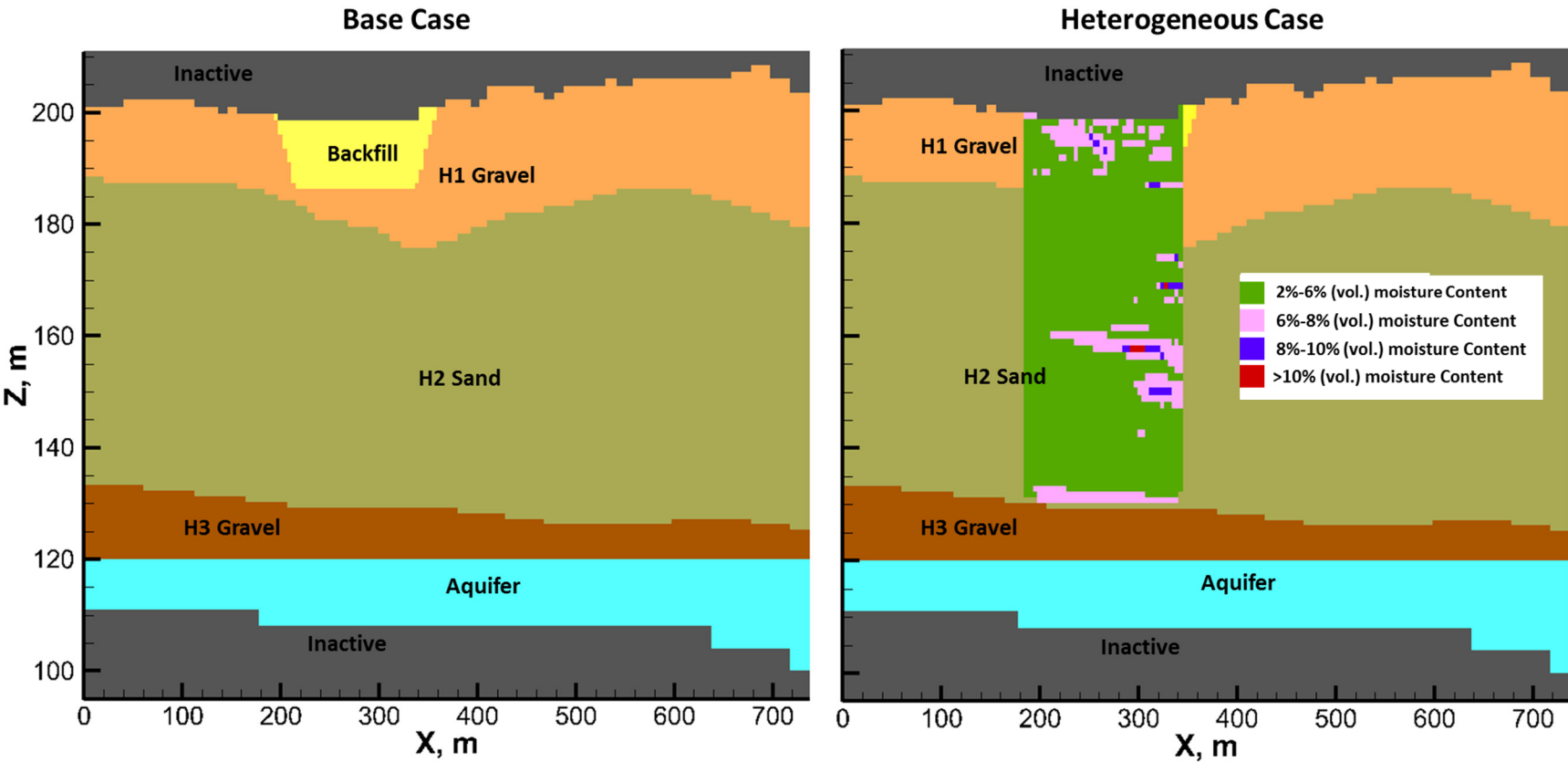


Figure F-8. View along Cross Section 2 (North to South) Shown in Figure F-6.

The left hand figure has the original 5 rock/soil zones (hydrostratigraphic units) while the right hand figure has 4 additional rock/soil zones to incorporate the moisture content bands-based heterogeneity within the kriggered area shown in Figure F-6.

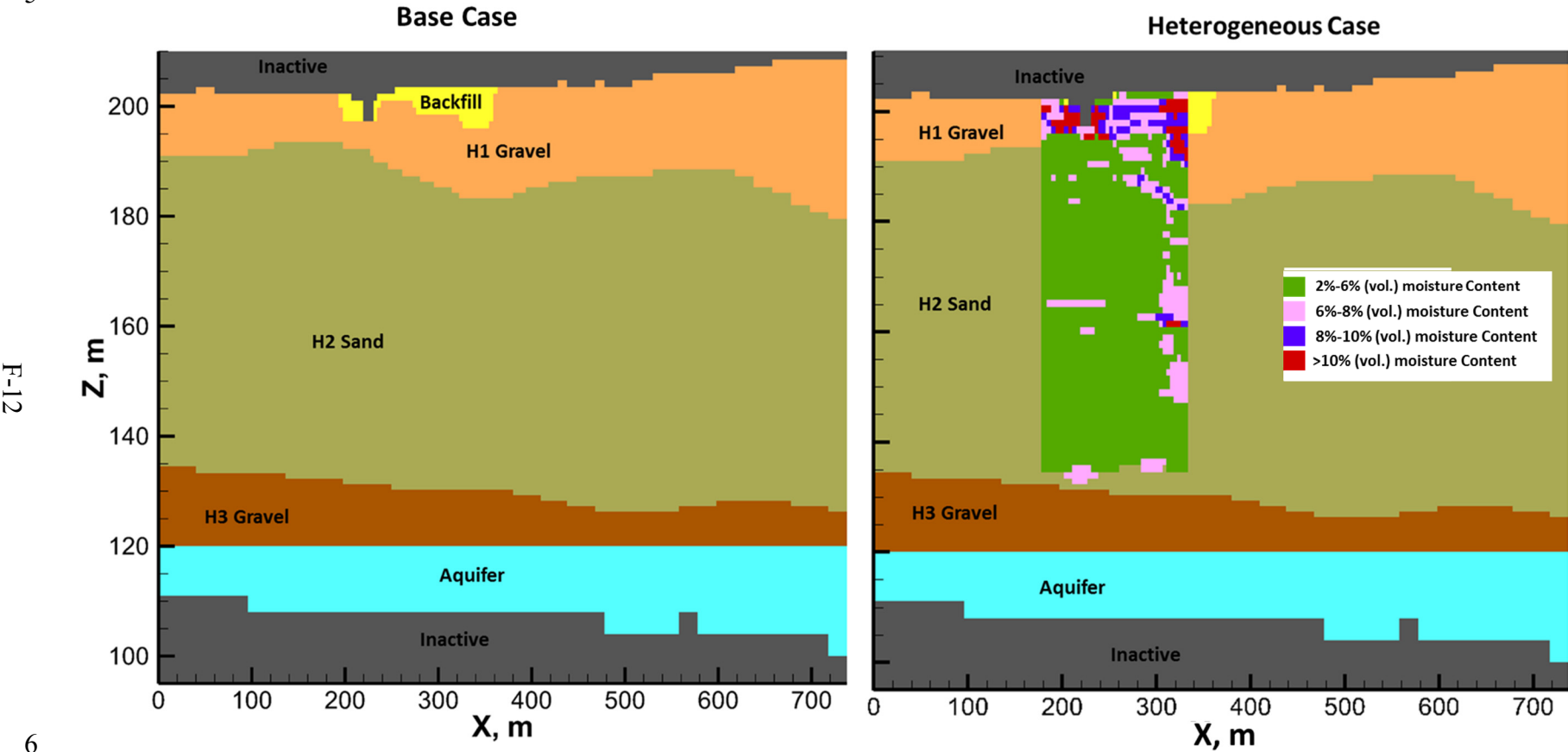
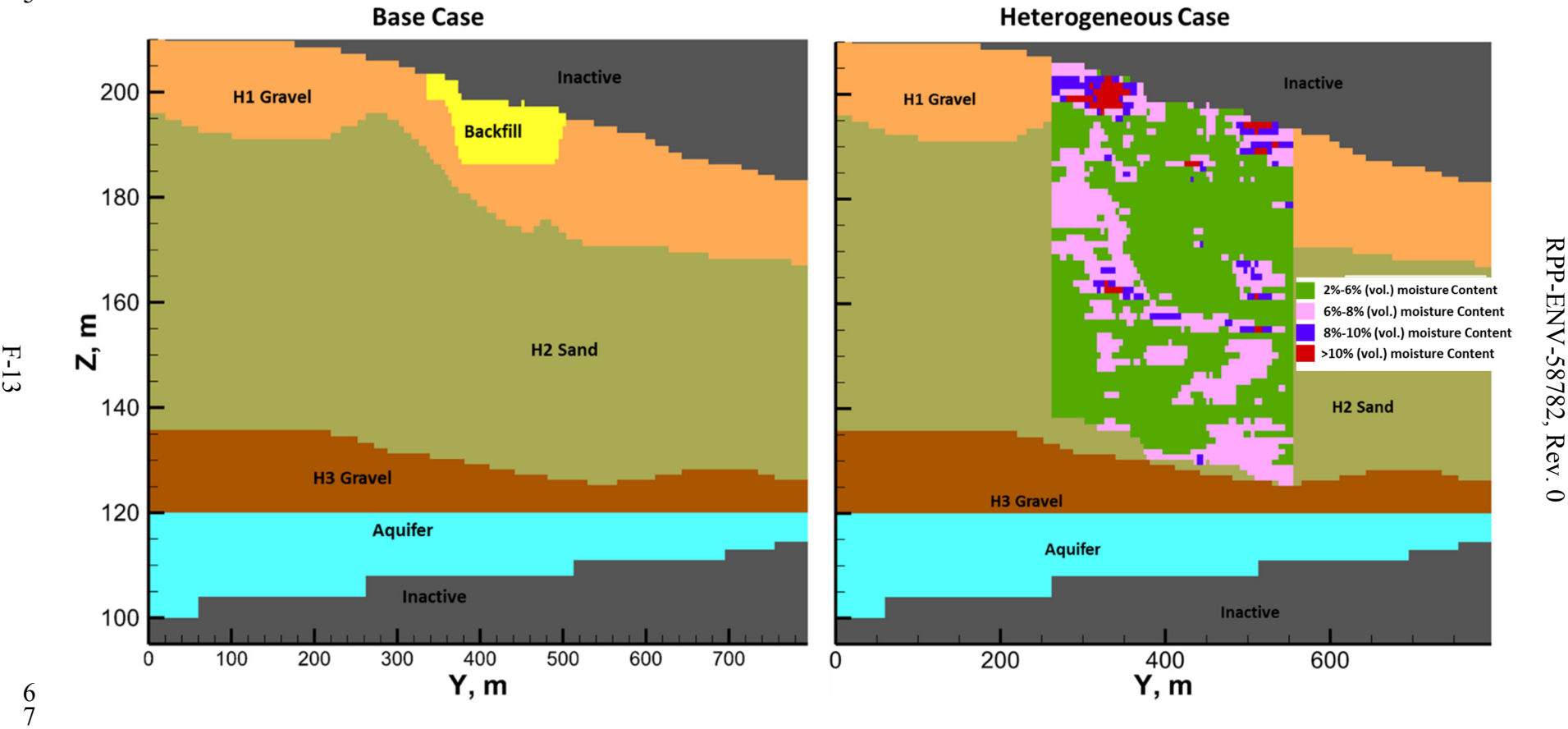


Figure F-9. View along Cross Section 3 (West to East) Shown in Figure F-6.

The left hand figure has the original 5 rock/soil zones (hydrostratigraphic units) while the right hand figure has 4 additional rock/soil zones to incorporate the moisture content bands-based heterogeneity within the krigged area shown in Figure F-6.



RPP-ENV-58782, Rev. 0

Table F-1. Vadose Zone Hydraulic Properties for Waste Management Area C Hydrostratigraphic Units (Appendix B).

Hydrostratigraphic Unit	θ_s	θ_r	α (1/cm)	n	ℓ	Fitted K_s (cm/s)
Backfill Gravelly Unit	0.138	0.010	0.021	1.374	0.5	5.60E-04
H1 and H3 Gravelly Units	0.171	0.011	0.036	1.491	0.5	7.70E-04
H2 Sand-Dominated Unit	0.315	0.039	0.063	2.047	0.5	4.15E-03

 θ_s = Saturated water content θ_r = Residual water content α = van Genuchten alpha

n = van Genuchten n

 ℓ = Pore size connectivity factor K_s = Saturated Conductivity

F.3 RESULTS

The STOMP[®] modeling results are presented in this section for the base case and the heterogeneous case. Comparisons are made for simulated moisture contents and contaminant breakthrough curves.

F.3.1 Moisture Content Prediction

The simulated moisture content values from the STOMP[®] models were compared to the observed moisture profiles from two wells (C4297 and 299-E27-22). Moisture content data at boreholes C4297 (located near tank 241-C-105) and 299-E27-22 (outside the tank) were obtained from PNNL-15503. The borehole C4297 is in close proximity to cross section 1 (Figure F-13). Figure F-14 shows a comparison of simulated steady-state moisture contents from the cross section 1 model and measured moisture profile for borehole C4297, and Figure F-15 does the same for well 299-E27-22. As indicated, for a recharge of 3.5 mm/yr, the simulated moisture content profile (blue line) for cross section 1 compares well with the measurements (black circles) for both the base case (EHM approximation) and the heterogeneous case. In the heterogeneous case, the model simulation also shows higher moisture contents observed at depth.

F.3.2 Matric Potential Measurements

Table F-3 summarizes the average moisture content and the average filter paper-based matric potential measurements for the two borehole samples C4297 (near tank 241-C-105) and 299-E27-22 (Figure F-13), and the model-predicted average moisture content and matric potential values for both cases. As indicated, the simulated steady-state moisture contents (0.06) for the Hanford H2 unit compare well with field-measured moisture contents for both the cases (Table F-3). However, when compared to the model results, the simulated matric potentials for the Hanford H2 unit were much smaller in magnitude (~ -150 cm) for both cases. The base case results in a smoothing of the model estimates. By contrast, the filter paper-based soil matric potentials are point measurements, and are not consistent with the smoothing resulting from the use of averaged upscaled or effective properties for the large grid blocks used in PA simulations. Therefore, the variability of filter paper-based point measurements is inherently larger compared to that based on PA simulations using homogenized upscaled properties. In addition, the error

RPP-ENV-58782, Rev. 0

bar for filter paper measurements is rather large (0.1 to 0.2 MPa or ~1,000 to ~2,000 cm). Similar arguments are applicable to the heterogeneous case. Soil moisture measurements are typically more accurate than matric potential measurements, and the matric potential variability is typically larger than the soil moisture variability. Nonetheless, the overall characterization data are consistent with the relatively dry moisture regime predicted by the PA simulations. The deviation in soil matric potential values is due to a mismatch between the modeling scale and the measurement scale.

F.3.3 Calculation of Technetium-99 Concentration

The breakthrough curves of ^{99}Tc for both cases for three different cross-section models are presented in Figure F-16, Figure F-17, and Figure F-18.

Table F-4 summarizes all the ^{99}Tc transport model results for all the cases. In all three cross-sectional models, the base case shows a higher peak concentration than the heterogeneous model. In cross section 3, the heterogeneous case shows a much lower concentration than the base case because the contrast is greater: there is more heterogeneity than in the other cross sections.

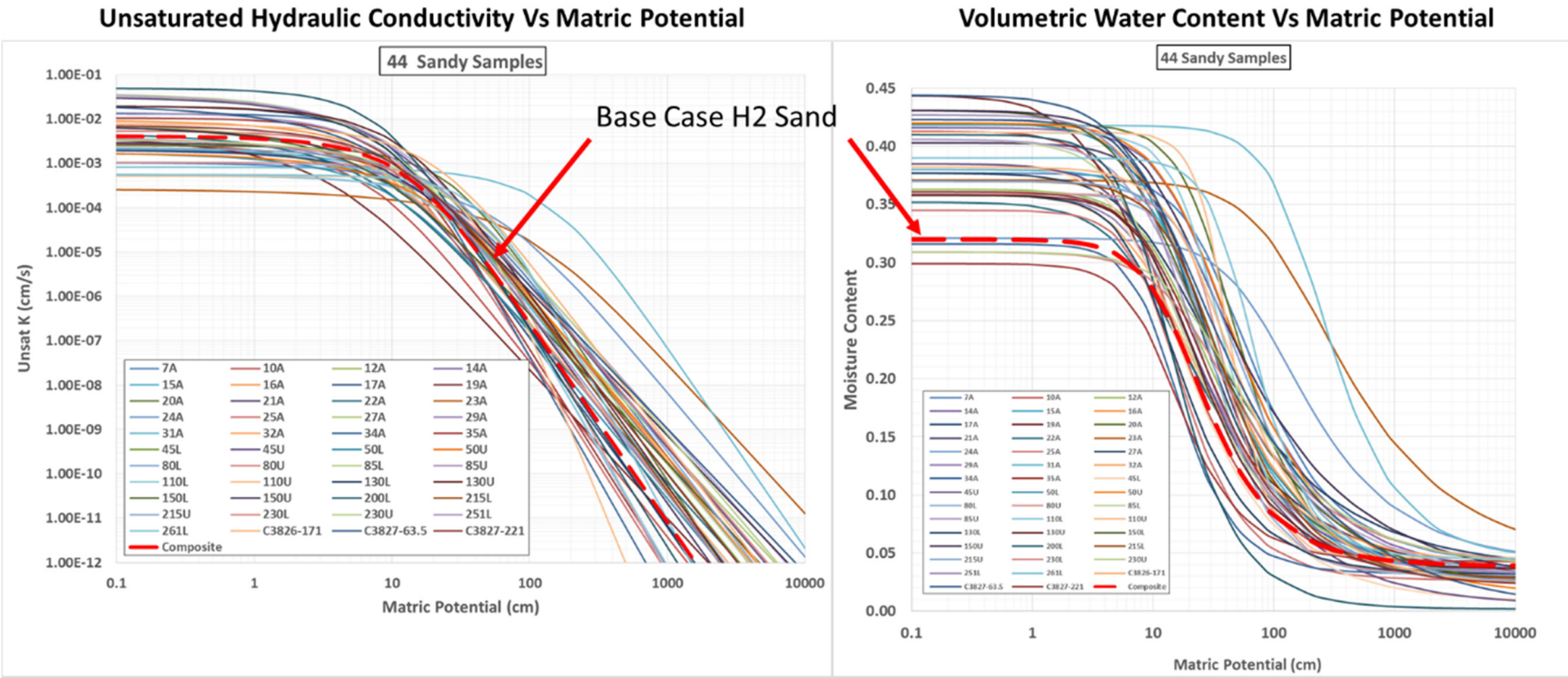
Peak concentrations for the heterogeneous model and the base case are very similar, with the heterogeneities leading to a smearing of the contaminant plume, resulting in a slightly lower peak concentration than the base case. The good agreement between the two models supports the use of the base case model for the post-closure evaluation of releases of residuals.

F.4 CONCLUSIONS

The following summarizes the conclusions of the alternative heterogeneous conceptual model:

- Calculated moisture contents are in very good agreement with field measurements for both the base case and the heterogeneous case.
- The peak concentrations are in good agreement between the two models, with the peak for the heterogeneous cases slightly lower than the base cases. These results support the use of the EHM modeling approach for the post-closure period when the flow is in equilibrium with natural recharge.

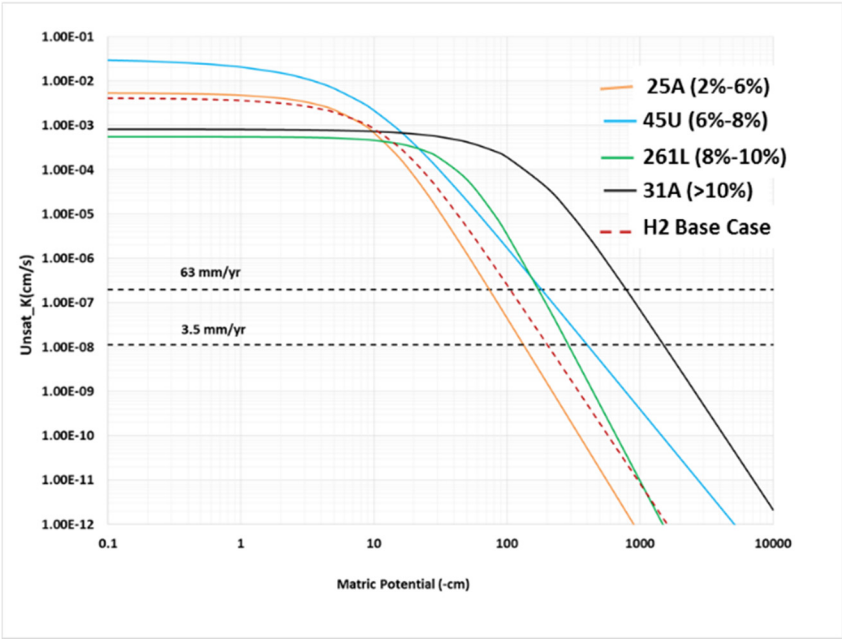
Figure F-10. Moisture Retention Curves and Unsaturated Hydraulic Conductivity Curves for the 44 Integrated Disposal Facility Samples.



F-16

Figure F-11. Moisture Retention Curves and Unsaturated Hydraulic Conductivity Curves for the Four New Units.

Unsaturated Hydraulic Conductivity Vs Matric Potential



Volumetric Water Content Vs Matric Potential

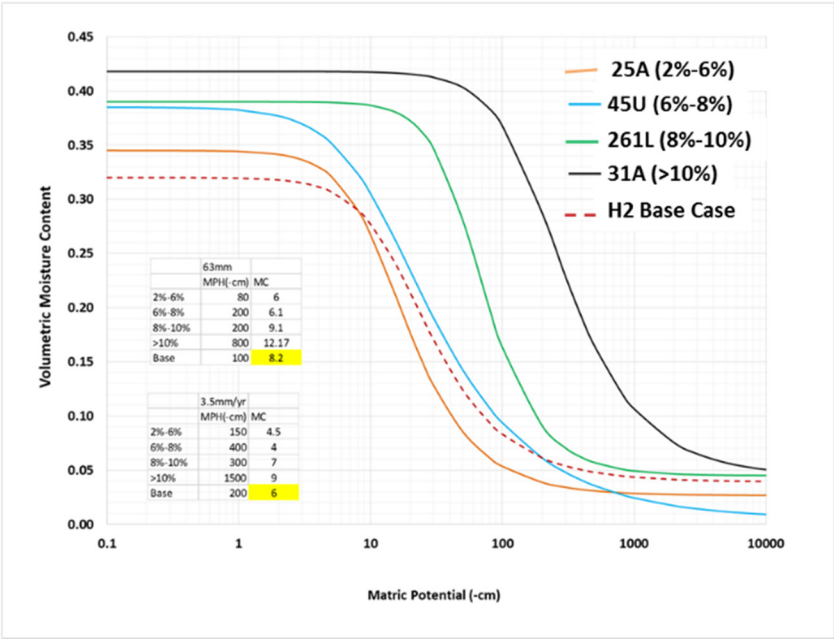
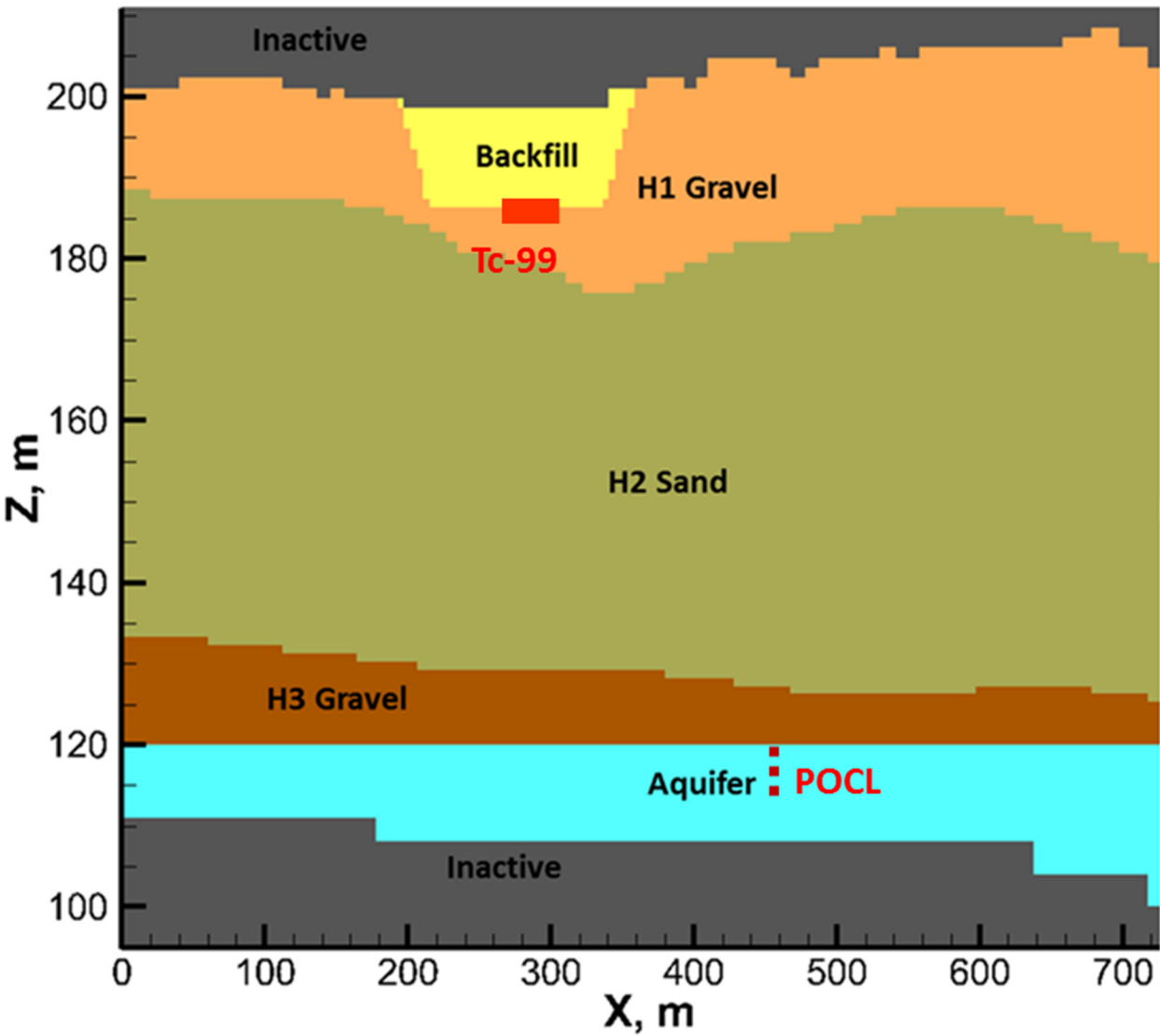


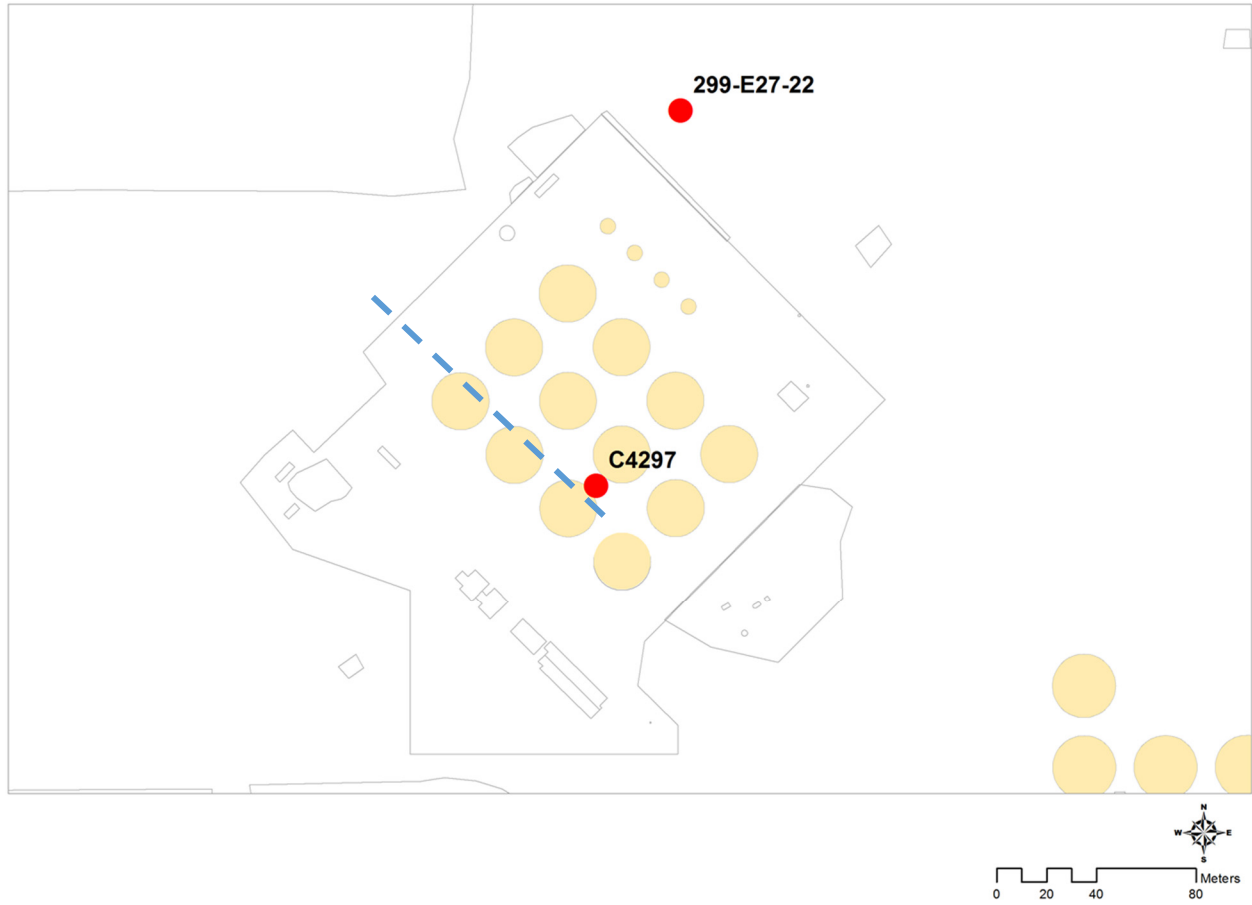
Table F-2. Summary of Vadose Zone Hydraulic Properties for the New Units (Appendix B).

Samples (Moisture Content zones)	θ_s	θ_r	α (1/cm)	n	ℓ	Fitted K_s (cm/s)
25A (2%-6%)	0.345	0.0267	0.0842	2.158	0.5	5.40E-03
45U (6%-8%)	0.385	0.0050	0.0880	1.664	0.5	3.24E-02
261L (8%-10%)	0.390	0.0450	0.0191	2.485	0.5	5.54E-04
31A (>10%)	0.418	0.0444	0.0058	2.012	0.5	8.21E-04

Figure F-12. Location of Contaminant Source and Point of Calculation.

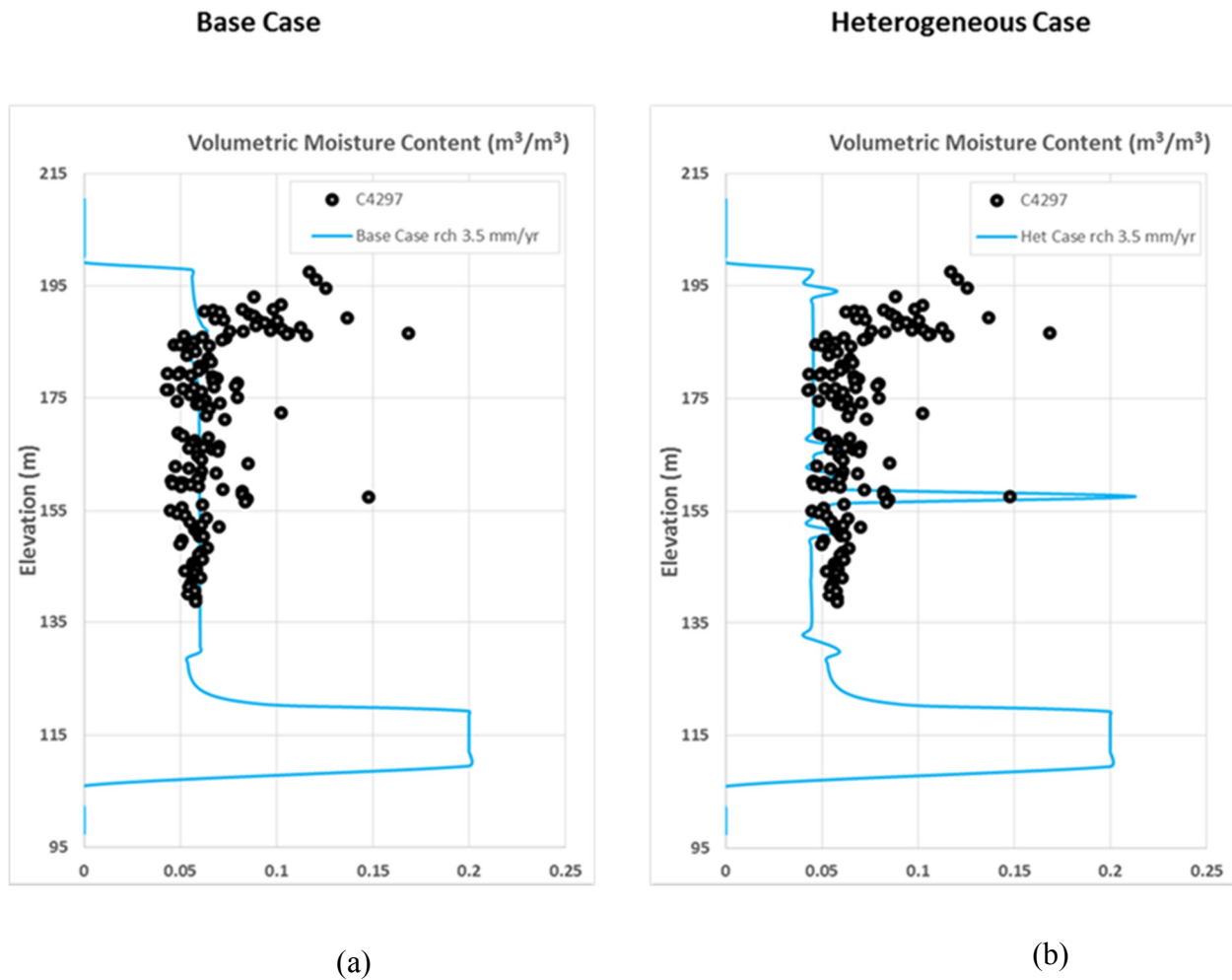


RPP-ENV-58782, Rev. 0

Figure F-13. Location of Well C4297 and 299-E27-22 Relative to Cross Section 1.

RPP-ENV-58782, Rev. 0

Figure F-14. Comparison of Measured (C4297) and Simulated Moisture Contents for (a) Base Case (Equivalent Homogeneous Medium) Model, and (b) Heterogeneous Model for Cross Section 1.



RPP-ENV-58782, Rev. 0

Figure F-15. Comparison of Measured (299-E27-22) and Simulated Moisture Contents for (a) Base Case (Equivalent Homogeneous Medium) Model, and (b) Heterogeneous Model for Cross Section 1.

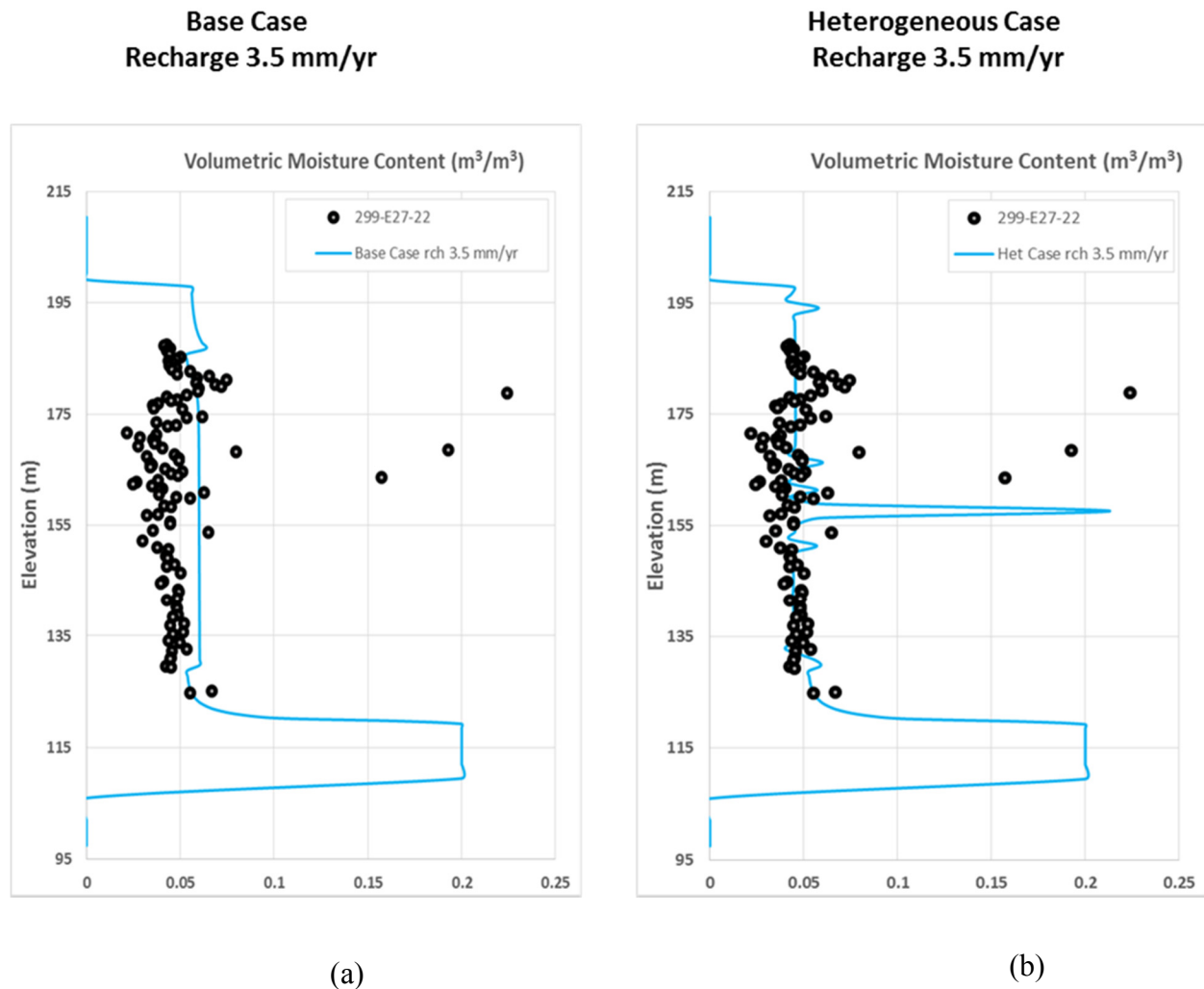


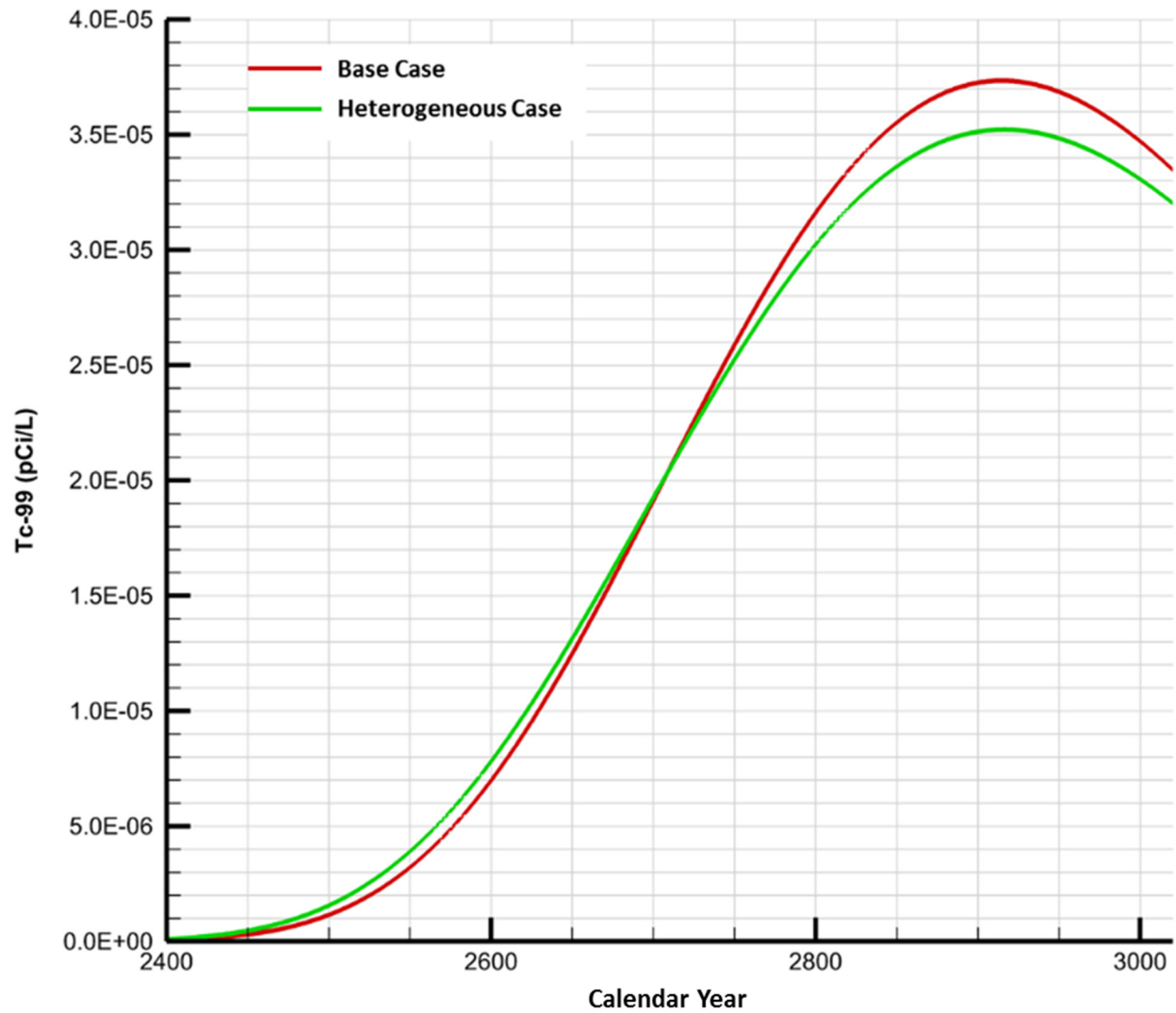
Table F-3. Average Moisture and Matric Potentials for Borehole Samples Inside and Outside of Waste Management Area C.

Borehole	C4297 (inside tank farm)	299-E27-22 (outside tank farm)
Mean moisture content *	0.060	0.046
Mean matric potential (-cm)	498.45	1,616.43

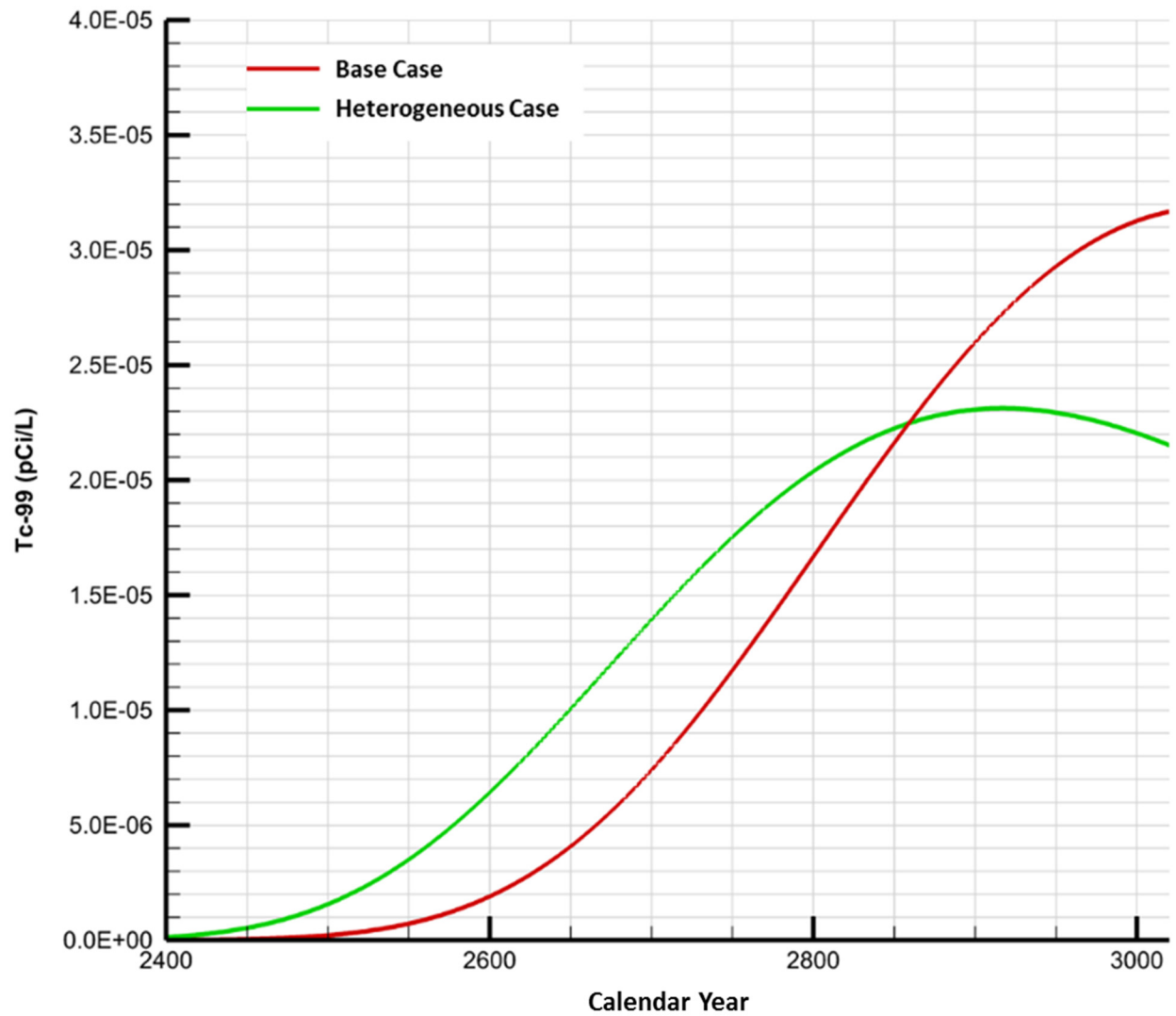
*Gravimetric data were converted to volumetric moisture content using an assumed sediment bulk density of 1.7 g cm^{-3} .

Source: PNNL-15503, "Characterization of Vadose Zone Sediments Below the C Tank Farm: Borehole C4297 and RCRA Borehole 299-E27-22."

RPP-ENV-58782, Rev. 0

Figure F-16. Technetium-99 Breakthrough Curves for Cross Section 1.

RPP-ENV-58782, Rev. 0

Figure F-17. Technetium-99 Breakthrough Curves for Cross Section 2.

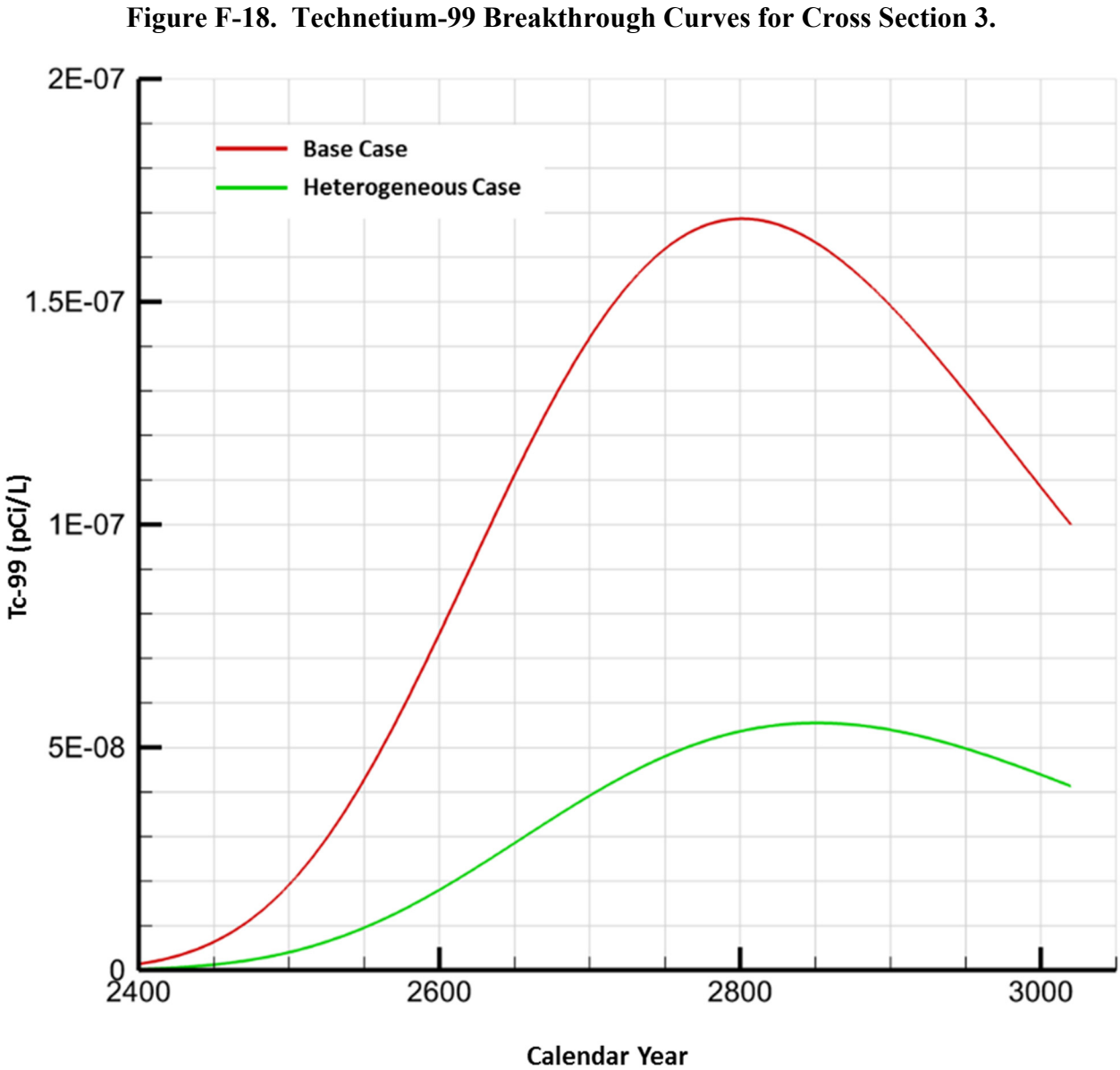


Table F-4. Summary of Technetium-99 Transport Model Results.

Cross Section	Time of Breakthrough (Calendar Year)		Time of Peak (Calendar Year)		Peak Concentration (pCi/L)	
	Base Case	Heterogeneous Case	Base Case	Heterogeneous Case	Base Case	Heterogeneous Case
1	2226	2210	2916	2916	3.73E-05	3.52E-5
2	2253	2205	>3000	2918	>3.16E-5	2.31E-5
3	2212	2232	2798	2843	1.69E-7	5.44E-8

RPP-ENV-58782, Rev. 0

F.5 REFERENCES

- NOAA Manual NOS NGS 5, 1990, "State Plane Coordinate System of 1983," National Geodetic Survey, U.S. Department of Commerce, National Oceanic and Atmospheric Administration, Rockville, Maryland.
- PNNL-15503, 2008, "Characterization of Vadose Zone Sediments Below the C Tank Farm: Borehole C4297 and RCRA Borehole 299-E27-22," Rev. 1, Pacific Northwest National Laboratory, Richland, Washington.
- Resource Conservation and Recovery Act of 1976, 42 USC 6901, et seq.
- RPP-CALC-60345, 2016, "Heterogeneous Media Model for Waste Management Area C Performance Assessment," Rev. 0, Washington River Protection Solutions, LLC, Richland, Washington.
- RPP-CALC-60448, 2016, "WMA C Performance Assessment Contaminant Fate and Transport Model to Evaluate Impacts to Groundwater," Rev. 0, Washington River Protection Solutions, LLC, Richland, Washington.
- Ye, M., R. Khaleel, T. J. Yeh, 2005, "Stochastic analysis of moisture plume dynamics of a field injection experiment," Water Resources Research, Vol. 41, W03013.

RPP-ENV-58782, Rev. 0

1
2
3
4
5
6

This page intentionally left blank.

RPP-ENV-58782, Rev. 0

APPENDIX G**COMPARISON OF SELECTED MODEL RESULTS FOR ALTERNATIVE 2B FROM
THE TANK CLOSURE AND WASTE MANAGEMENT ENVIRONMENTAL IMPACT
STATEMENT FOR WASTE MANAGEMENT AREA C WITH EQUIVALENT
RESULTS USING THE WASTE MANAGEMENT AREA C PERFORMANCE
ASSESSMENT BASE CASE MODEL**

RPP-ENV-58782, Rev. 0

1
2
3
4
5
6
7

This page intentionally left blank.

RPP-ENV-58782, Rev. 0

TABLE OF CONTENTS

1			
2			
3	APPENDIX G – COMPARISON OF SELECTED MODEL RESULTS FOR		
4	ALTERNATIVE 2B FROM THE TANK CLOSURE AND WASTE		
5	MANAGEMENT ENVIRONMENTAL IMPACT STATEMENT FOR WASTE		
6	MANAGEMENT AREA C WITH EQUIVALENT RESULTS USING THE		
7	WASTE MANAGEMENT AREA C PERFORMANCE ASSESSMENT BASE		
8	CASE MODEL	G-1	
9	G.1 GENERAL DESCRIPTION OF ALTERNATIVE 2B RESULTS USING THE		
10	2012 TANK CLOSURE AND WASTE MANAGEMENT ENVIRONMENTAL		
11	IMPACT STATEMENT MODEL FOR WASTE MANAGEMENT AREA C	G-1	
12	G.2 GENERAL APPROACH FOR COMPARISON OF THE ALTERNATIVE 2B		
13	RESULTS USING PERFORMANCE ASSESSMENT AND THE 2012 TANK		
14	CLOSURE AND WASTE MANAGEMENT ENVIRONMENTAL IMPACT		
15	STATEMENT MODELS OF WASTE MANAGEMENT AREA C	G-2	
16	G.3 COMPARISONS OF MODEL INPUTS FOR 2012 TANK CLOSURE AND		
17	WASTE MANAGEMENT ENVIRONMENTAL IMPACT STATEMENT AND		
18	PERFORMANCE ASSESSMENT MODELS OF WASTE MANAGEMENT		
19	AREA C	G-5	
20	G3.1 Inventory Estimates	G-5	
21	G3.2 Inventory Release Rates.....	G-5	
22	G3.3 Recharge	G-6	
23	G3.4 Hydrogeologic Framework and Hydrologic Properties.....	G-7	
24	G3.5 Partitioning Coefficients and Dispersivity.....	G-9	
25	G.4 COMPARISON OF SELECTED RESULTS FOR ALTERNATIVE 2B USING		
26	THE PERFORMANCE ASSESSMENT AND TANK CLOSURE AND WASTE		
27	MANAGEMENT ENVIRONMENTAL IMPACT STATEMENT MODELS OF		
28	WASTE MANAGEMENT AREA C	9	
29	G.5 REFERENCES	12	
30			
31			
32			
33			

RPP-ENV-58782, Rev. 0

LIST OF FIGURES

1		
2		
3	Figure G-1. Lines of Analysis in the Tank Closure and Waste Management Environmental	
4	Impact Statement.....	G-3
5	Figure-G-2. STOMP [®] Model Horizontal Grid Distribution Showing the Source Area for	
6	the Waste Management Area C Tank Residual Component of the Tank	
7	Closure and Waste Management Environmental Impact Statement.....	G-6
8	Figure G-3. Time Series of Net Infiltration Tank Closure and Waste Management	
9	Environmental Impact Statement.....	G-8
10	Figure G-4. Waste Management Area C Vadose Zone Stratigraphy as Depicted in the	
11	Tank Closure and Waste Management Environmental Impact Statement.....	G-8
12	Figure G-5. Tank Closure and Waste Management Environmental Impact Statement	
13	Analysis of Iodine-129 Flux from the Vadose Zone into the Aquifer for	
14	Alternative 2b (Baseline) and Three Flux Reduction Sensitivity Cases.....	G-10
15	Figure G-6. Waste Management Area C Performance Assessment Analysis of Tank	
16	Closure and Waste Management Environmental Impact Statement	
17	Alternative 2b Model of Iodine-129 Flux from the Vadose Zone into the	
18	Aquifer.....	G-11

LIST OF TABLES

19		
20		
21		
22		
23	Table G-1. Peak Constituent of Potential Concern Concentrations (pCi/L) and Time of	
24	Occurrence (Calendar Year) at the A Barrier Calculated in the Environmental	
25	Impact Statement Associated with All Tank Residuals and Ancillary	
26	Equipment.....	G-4
27	Table G-2. Summary of Rates of Release for Iodine-129.....	G-7

LIST OF TERMS

30		
31		
32	PA	performance assessment
33	STOMP	Subsurface Transport Over Multiple Phases (computer code)
34	TC&WM EIS	Tank Closure and Waste Management Environmental Impact Statement
35	WMA	Waste Management Area

RPP-ENV-58782, Rev. 0

APPENDIX G**COMPARISON OF SELECTED MODEL RESULTS FOR ALTERNATIVE 2B FROM THE TANK CLOSURE AND WASTE MANAGEMENT ENVIRONMENTAL IMPACT STATEMENT FOR WASTE MANAGEMENT AREA C WITH EQUIVALENT RESULTS USING THE WASTE MANAGEMENT AREA C PERFORMANCE ASSESSMENT BASE CASE MODEL**

The purpose of this appendix is to compare, to the extent possible, the model developed for the Waste Management Area (WMA) C performance assessment (PA) to results from DOE/EIS-0391, "Final Tank Closure and Waste Management Environmental Impact Statement for the Hanford Site, Richland, Washington" (TC&WM EIS). The intent is to show the similarities and differences between the models, and to demonstrate that both models are appropriate for their intended purposes. The extent to which the two models can be directly compared is limited, given the different modeling objectives, spatial scales and levels of detail in the treatment of the engineered barrier system. However, a comparison provides perspectives on interpreting modeling results within the context of the modeling objectives.

G.1 GENERAL DESCRIPTION OF ALTERNATIVE 2B RESULTS USING THE 2012 TANK CLOSURE AND WASTE MANAGEMENT ENVIRONMENTAL IMPACT STATEMENT MODEL FOR WASTE MANAGEMENT AREA C

The analysis in the TC&WM EIS supports U.S. Department of Energy decisions regarding proposed actions to retrieve, treat, and dispose of tank waste; decommission the Fast Flux Test Facility; and expand waste disposal capacity at Hanford. The TC&WM EIS evaluates the potential sitewide cumulative environmental impacts and cost consequences associated with 11 proposed alternatives for tank closure, including the preferred alternative to retrieve at least 99% of the tank waste and institute landfill closure of the single-shell tank farms. The TC&WM EIS describes groundwater impacts in terms of the concentrations of ^{129}I , ^{99}Tc , chromium, nitrate, ^3H (tritium), ^{238}U , and total uranium at prescribed polygonal "lines of interest" or "barriers," including one that surrounds WMA C and WMA A-AX. The results at a line of interest or barrier represent the outcome of vadose zone model results evaluated using Subsurface Transport Over Multiple Phases (STOMP)¹ (Appendix N of DOE/EIS-0391) input to a groundwater flow field developed in MODFLOW² (Appendix L of DOE/EIS-0391), with concentration calculated using a proprietary particle-tracking code (Appendix O of DOE/EIS-0391).

The TC&WM EIS evaluated a local-scale vadose zone-only model representing WMA C, and used the vadose zone releases from this model as a source to a regional groundwater model to estimate the impacts of residual wastes and past releases originating in WMA C at specific points for analysis. However, the groundwater impact results reported in Appendix O of DOE/EIS-0391 do not distinguish between the impacts caused by the residual wastes, past leaks, and releases in WMA C from those originating in other tank farms in the A Complex of the

¹ Subsurface Transport Over Multiple Phases (STOMP)[®] is copyrighted by Battelle Memorial Institute, 1996.

² MODFLOW software has been developed and distributed by the U.S. Geological Survey, Washington, D.C.

RPP-ENV-58782, Rev. 0

200 East Area. In addition, the point of analyses in the TC&WM EIS groundwater impact analysis are not coincident with the 100 meter point of calculation prescribed by DOE M 435.1-1, Radioactive Waste Management Manual. Instead, the TC&WM EIS reported cumulative results from facilities at a number of polygonal “lines of analysis” that are shown in Figure G-1. The line of analysis most relevant to WMA C is the “A Barrier,” at which the cumulative contributions and impacts from tank farm residual waste and past leaks from WMAs C, A, and AX, and other nearby double-shell tank farm facilities are evaluated in groundwater. The WMA C PA provides concentration-based results along a hypothetical line of analysis located 100 m downgradient of the WMA C fenceline. The line of analysis is divided into nine segments to account for the spatial distribution of the impacts along the line of analysis resulting from the spatial distribution of sources within WMA C. The results for each segment distinguish between the impacts caused by residuals from the different tanks and ancillary equipment, including pipelines within WMA C, and integrate the individual results into a composite concentration.

Therefore, while the “A Barrier” results are not directly comparable to the PA model results, they still provide the best available comparison point between the analyses, and are summarized here (Table G-1). According to the groundwater transport analysis results of Preferred Alternative 2B at A Barrier (found in Table O-26 in Appendix O of DOE/EIS-0391), the peak concentrations of radionuclides ^{99}Tc and ^{129}I at A Barrier related to tank residuals are 160 pCi/L and 0.1 pCi/L, respectively, with the years of peak arrival being 3685 and 3896, respectively. The peak concentrations of chromium and nitrate are 5 $\mu\text{g/L}$ and 536 $\mu\text{g/L}$, respectively, with the years of peak arrival being 3451 and 3614, respectively. The peak concentrations of radionuclides ^{99}Tc and ^{129}I related to ancillary equipment at A Barrier are 31 pCi/L and 0.1 pCi/L, respectively, with the years of peak arrival being 3610 and 3694, respectively. The peak concentrations of chromium and nitrate are 1 $\mu\text{g/L}$ and 183 $\mu\text{g/L}$, respectively, with the years of peak arrival being 3647 and 3606, respectively (Table O-22 in Appendix O of DOE/EIS-0391).

G.2 GENERAL APPROACH FOR COMPARISON OF THE ALTERNATIVE 2B RESULTS USING PERFORMANCE ASSESSMENT AND THE 2012 TANK CLOSURE AND WASTE MANAGEMENT ENVIRONMENTAL IMPACT STATEMENT MODELS OF WASTE MANAGEMENT AREA C

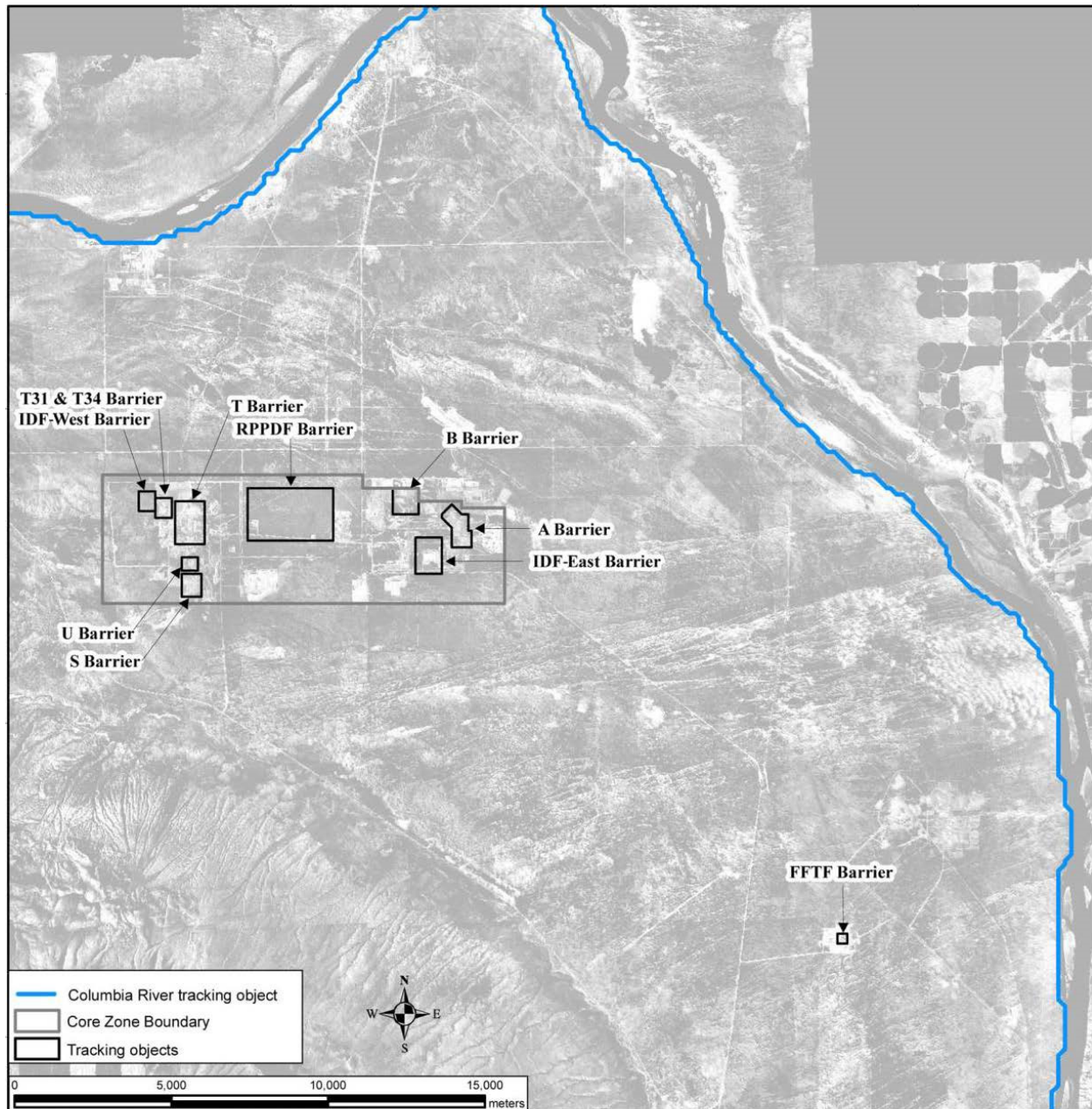
To compare the WMA C PA and TC&WM EIS models for consistency, it was necessary to modify the base case results to provide a common technical basis between the two models. The tank residual waste inventory, residual waste release functions, and spatial and temporal recharge from the small-scale TC&WM EIS WMA C vadose zone-only model were introduced into the WMA C PA vadose zone-groundwater model.

As a metric for comparisons, Appendix U of DOE/EIS-0391 includes a figure that shows the modeling results for Alternative 2B for the ^{129}I radionuclide fluxes exiting the vadose zone. The results from this plot are compared against similar results using similar source term and assumption for Alternative 2B using the PA model of WMA C. To facilitate this comparison, the tank residual waste inventory, residual waste release functions, and spatial and temporal

RPP-ENV-58782, Rev. 0

recharge from the small-scale TC&WM EIS WMA C vadose zone-only model were introduced into the WMA C PA vadose zone-groundwater model.

Figure G-1. Lines of Analysis in the Tank Closure and Waste Management Environmental Impact Statement.



Note: To convert meters to feet, multiply by 3.281.

Key: FFTF=Fast Flux Test Facility; IDF-East=200-East Area Integrated Disposal Facility; IDF-West=200-West Area Integrated Disposal Facility; RPPDF=River Protection Project Disposal Facility; T31 & T34=trenches 31 and 34.

Excerpted from DOE/EIS-0391, "Final Tank Closure and Waste Management Environmental Impact Statement for the Hanford Site, Richland, Washington," Appendix O, pp. O-16.

RPP-ENV-58782, Rev. 0

Table G-1. Peak Constituent of Potential Concern Concentrations and Time of Occurrence (Calendar Year) at the A Barrier Calculated in the Environmental Impact Statement Associated with All Tank Residuals and Ancillary Equipment.

Radionuclide	Tank Residuals (Calendar Year Time of Peak)	Ancillary Equipment (Calendar Year Time of Peak)
Tc-99	160 pCi/L (3685)	31 pCi/L (3610)
I-129	0.1 pCi/L (3896)	0.1 pCi/L (3694)
Contaminant		
Cr	5 µg/L (3451)	1 µg/L (3647)
Nitrate	536 µg/L (3614)	183 µg/L (3606)

Values excerpted from DOE/EIS-0391, "Final Tank Closure and Waste Management Environmental Impact Statement for the Hanford Site, Richland, Washington" Tables O-22 and O-26.

Other elements of the models are similar. As in the WMA C PA, the assumed end state of the tanks evaluated in DOE/EIS-0391 was that the single-shell tank waste system would be filled with grout to immobilize residual waste, prevent long-term degradation of the tanks, and discourage intruder access. The closed tank system would be covered with an engineered modified Resource Conservation and Recovery Act of 1976 Subtitle C barrier with a design life of 500 years. The TC&WM EIS STOMP[®]-based vadose zone model incorporates a number of elements that are similar in approach to the WMA C PA model:

- Residual waste inventory in tanks and ancillary equipment
- Three-dimensional representation of geology, hydraulic properties, and grid geometry
- Temporal and spatial variability of net infiltration at the ground surface
- Temporal variability of radionuclide and non-radiological contaminant introduction (i.e., source term) at specific horizontal locations and vertical depths
- Water and radionuclide and non-radiological contaminant output fluxes at specified locations (referred to in STOMP[®] as surfaces)
- Radionuclide and non-radiological contaminant movement through, and exit from the vadose zone.

Unlike the WMA C PA, the TC&WM EIS modeling methodology calculates the following outside of STOMP[®]:

- Contaminant movement in the groundwater to various calculation points
- Concentrations calculated at a contiguous polygon surrounding WMA C and WMA A-AX in the saturated-zone model (referred to in DOE/EIS-0391 as "A Barrier").

RPP-ENV-58782, Rev. 0

G.3 COMPARISONS OF MODEL INPUTS FOR 2012 TANK CLOSURE AND WASTE MANAGEMENT ENVIRONMENTAL IMPACT STATEMENT AND PERFORMANCE ASSESSMENT MODELS OF WASTE MANAGEMENT AREA C

The primary areas where the models differ internally involve inventory estimates, waste release rates, geological description and hydrological properties, the partitioning coefficients and dispersivity applied to certain radionuclides, and the spatial distribution of recharge rates. The following discussion describes these differences and any adjustments made to the WMA C PA model so that the two model predictions could be compared.

G3.1 Inventory Estimates

DOE/ORP-2003-02, Environmental Impact Statement for Retrieval, Treatment, and Disposal of Tank Waste and Closure of Single-Shell Tanks at the Hanford Site, Richland, WA: Inventory and Source Term Data Package provides the estimated radionuclide inventory present at each tank farm as of December 1, 2002. According to Table M-24 in Appendix M of DOE/EIS-0391, the estimated quantities of ^{129}I under tank closure Alternative 2B are 0.00993 of ^{129}I . The alternatives analysis evaluated impacts from the tank farms as entities, not individual tanks; thus, the tank residual wastes are composited into a single source for the entire tank farm. The TC&WM EIS model represents the residual wastes in the tanks as a uniform concentration distributed across an area that approximately encompasses the 100- and 200-series tanks of the tank farm (Figure G-2). The residual waste inventory estimates have been revised since the issuance of DOE/EIS-0391 because more waste has been retrieved from the tanks, and the new inventory is based on direct measurement of the end state of the retrieval. The WMA C PA includes the updated information.

For the purpose of comparing the two model results for Alternative 2B, the WMA C PA model was modified to run with the TC&WM EIS inventory estimates and an approximation of the TC&WM EIS release area in its evaluation.

G3.2 Inventory Release Rates

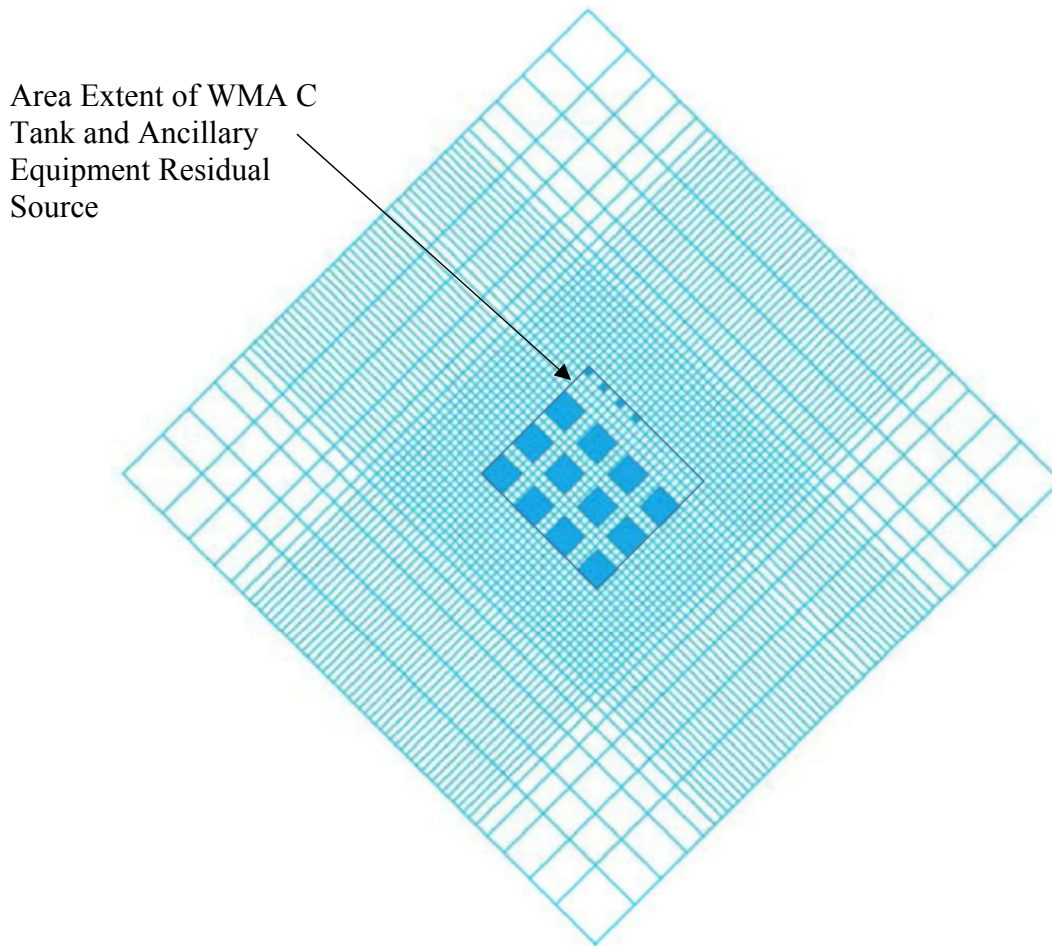
DOE/EIS-0391 calculated the release of contaminants from stabilized tank grout using a partitioning-limited, advective-flow release model (Table M-2 of Appendix M of DOE/EIS-0391). In this model, only the rate of water movement through the waste volume, and the partitioning of the contaminant between the solid and liquid phases of the waste volume, control the release of contaminants from the waste form to the vadose zone (Appendix M of DOE/EIS-0391). Contaminant concentrations are assumed to maintain equilibrium between the liquid and solid phases within the pore space of the waste form according to the contaminant's partitioning coefficient in the waste form material. The amount of contaminant mass exiting the waste form is therefore equal to the quantity of liquid exiting from the waste form and the concentration of the contaminant in that liquid.

For the purpose of comparing the two model results of Alternative 2B, the WMA C PA model was run using the TC&WM EIS (2012) release function for ^{129}I in its evaluation. Equations M-1

RPP-ENV-58782, Rev. 0

through M-8 in Appendix M of DOE/EIS-0391 provide the basis for the release models used to develop the release functions for the solid sources. Summarized rates of release for ¹²⁹I developed according to this model are presented in Table G-2.

Figure-G-2. STOMP® Model Horizontal Grid Distribution Showing the Source Area for the Waste Management Area C Tank Residual Component of the Tank Closure and Waste Management Environmental Impact Statement.



Excerpted and adapted from Figure N-4, Appendix N of DOE/EIS-0391, "Final Tank Closure and Waste Management Environmental Impact Statement for the Hanford Site, Richland, Washington."

Subsurface Transport Over Multiple Phases (STOMP)® is copyrighted by Battelle Memorial Institute, 1996.

WMA = Waste Management Area

G3.3 Recharge

In the TC&WM EIS release model calculations, the quantity of liquid exiting from the waste form is assumed to equal the water infiltrating into it. The water infiltrating into the waste form is assumed to be equal to the net infiltration at the surface, which is subject to change according to the conditions at the surface such as natural vegetation or the presence of an engineered barrier. Figure M-2 in Appendix M of DOE/EIS-0391 displays the time series of net infiltration

RPP-ENV-58782, Rev. 0

rates applicable to tank farms (Figure G-3). For WMA C, the background conditions represent a steady state net infiltration rate of 3.5 mm/yr. The disturbed conditions (100 mm/yr) coincide with the beginning of tank farm operations and the assumed closure of the farm in 2050. The cap conditions follow closure, and last 500 years until the cap becomes degraded and the net infiltration reverts to the background value. The net infiltration applied to surfaces outside the WMA C source area does not change from the background conditions throughout the simulation period.

Table G-2. Summary of Rates of Release for Iodine-129.

Year	I-129 Release Rate (Ci/yr)
2050	4.57E-06
2267	4.09E-06
2510	3.81E-06
2550	2.64E-05
2551	2.46E-05
2592	2.12E-05
2639	1.78E-05
2695	1.44E-05
2764	1.10E-05
2854	7.62E-06
2984	4.15E-06
3223	6.07E-07
4515	0

Values based on Equations M-1 through M-8 in Appendix M of DOE/EIS-0391, "Final Tank Closure and Waste Management Environmental Impact Statement for the Hanford Site, Richland, Washington."

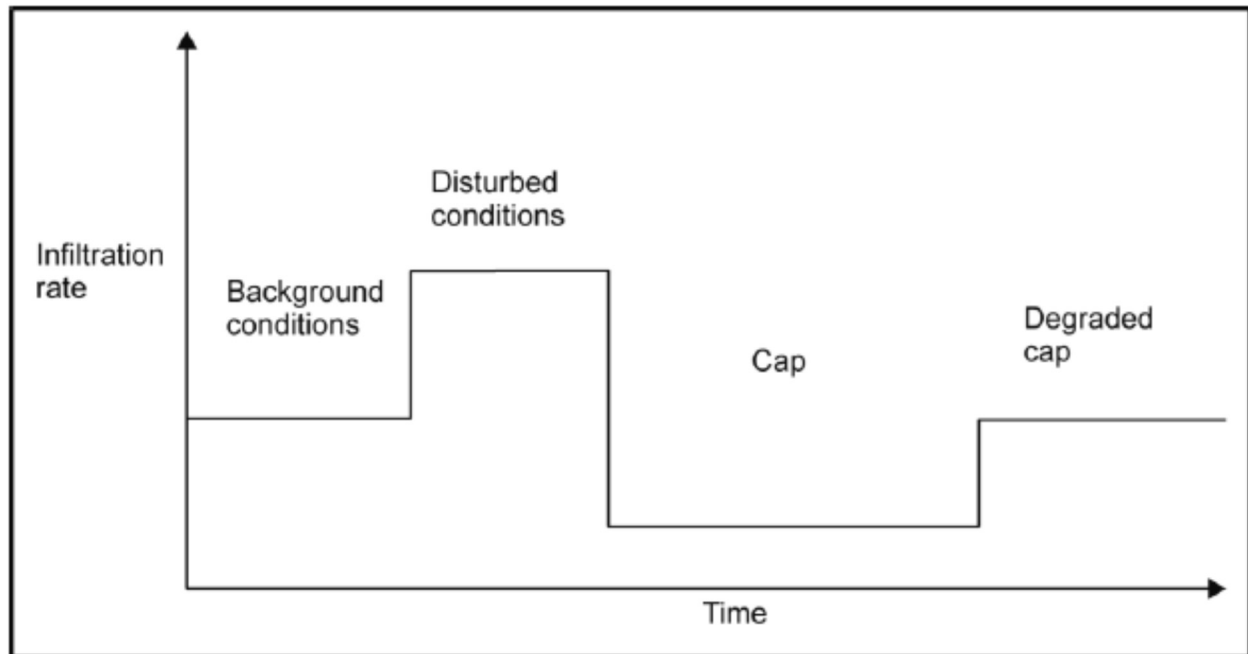
For the purpose of comparing the two models of Alternative 2, the WMA C PA model was run using the TC&WM EIS recharge sequence in its evaluation.

G3.4 Hydrogeologic Framework and Hydrologic Properties

In the TC&WM EIS geologic model, most of the vadose zone consists of units identified as Hanford sand with a layer of Hanford gravel at the bottom and another layer of Hanford gravel existing about two-thirds the depth from the surface to groundwater. Both gravel units vary in thickness, and the shallower sand is not continuous and is not present in the southeastern corner of the model (Figure G-4). The TC&WM EIS geologic model does not account for the presence of the WMA C tanks and ancillary equipment. The volumes associated with those features remain active in the model and unchanged from the natural system. The TC&WM EIS developed hydraulic properties for the Hanford sand and gravel units according to the procedure described in Section N.3.6.1 in Appendix N of DOE/EIS-0391.

RPP-ENV-58782, Rev. 0

Figure G-3. Time Series of Net Infiltration Tank Closure and Waste Management Environmental Impact Statement.



Excerpted from Figure M-1, Appendix M of DOE/EIS-0391, "Final Tank Closure and Waste Management Environmental Impact Statement for the Hanford Site, Richland, Washington."

Figure G-4. Waste Management Area C Vadose Zone Stratigraphy as Depicted in the Tank Closure and Waste Management Environmental Impact Statement.

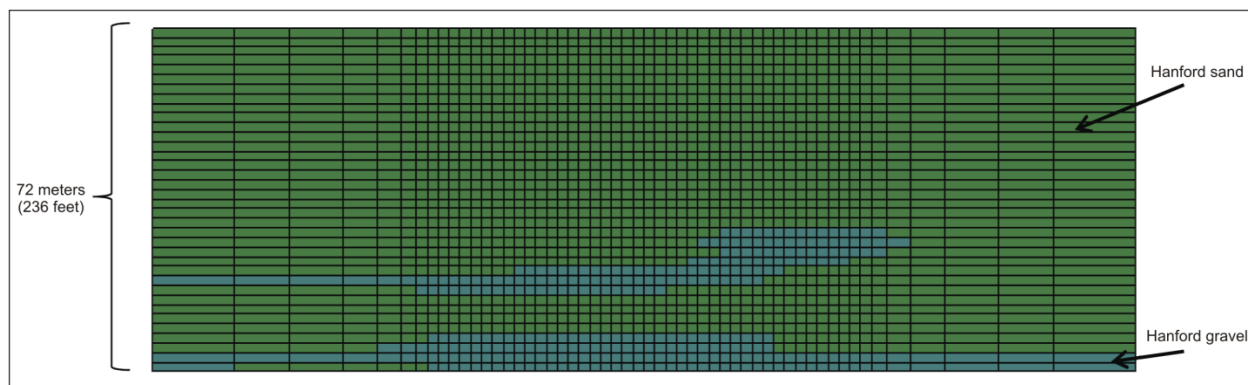


Figure U-58. West-to-East Cross Section of Vadose Zone Lithology for C Tank Farm

Excerpted from Figure U-58, Appendix U of DOE/EIS-0391, "Final Tank Closure and Waste Management Environmental Impact Statement for the Hanford Site, Richland, Washington"; green is Hanford Sand and blue is Hanford Gravel).

For the purpose of comparing the two model results for Alternative 2B, the WMA C PA model was not modified, and includes the geology and hydraulic properties developed for the PA using local scale information on the hydrogeologic conditions at WMA C. In the PA model of WMA C, the inactive nodal areas representing the tanks and selective ancillary equipment

RPP-ENV-58782, Rev. 0

volumes were treated as active using hydraulic properties being used to represent properties of Hanford H2 Sand hydrostratigraphic unit.

G3.5 Partitioning Coefficients and Dispersivity

The TC&WM EIS model applied a constant partitioning coefficient value of 0 mL/g to ^{129}I . The WMA C PA base case analysis partitioning coefficient value for ^{129}I is 0.2 mL/g in fine-grained material. This value is then adjusted downward for the different hydrogeologic units in the WMA C PA model according to the estimated gravel content associated with those hydrogeologic units.

The TC&WM EIS model applied the same longitudinal and transverse dispersivity values of 1 m and 0.1 m, respectively, to all hydrogeologic units. The WMA C PA base case analysis vadose zone longitudinal and transverse dispersivity values vary according to the hydrogeologic unit. For Hanford H2 Sand, the longitudinal and transverse dispersivity values are 25 cm and 2.5 cm, respectively. For backfill and both Hanford H1 and H3 Sandy Gravel/Gravelly Sand, the longitudinal and transverse dispersivity values are 20 cm and 2.0 cm, respectively.

For the purpose of comparing the two model results for Alternative 2B, the PA model of WMA C was run with constant partitioning coefficient values of 0 mL/g to ^{129}I , respectively for all hydrogeologic units. The longitudinal and transverse dispersivity values for the hydrogeologic units remained the same as in the WMA C PA base case.

G.4 COMPARISON OF SELECTED RESULTS FOR ALTERNATIVE 2B USING THE PERFORMANCE ASSESSMENT AND TANK CLOSURE AND WASTE MANAGEMENT ENVIRONMENTAL IMPACT STATEMENT MODELS OF WASTE MANAGEMENT AREA C

The WMA C base case was run with the adaptations described in Sections G.2 and G.3. The flux of ^{129}I into the water table generated by this analysis was compared to the results presented in Figure U-122 in Appendix U of DOE/EIS-0391, which is replicated as Figure G-5. Comparable results of the WMA C PA model are shown in Figure G-6.

The time series releases of ^{129}I to the groundwater calculated in both models include two relative maxima, and there is negligible difference between the two peak values calculated by the different models. The primary difference between the model results is that the WMA C model shows the release of ^{129}I to the groundwater continuing throughout the simulation period. This tail of the release rate curve is a consequence of the inclusion of the aquifer in the WMA C PA model, which introduces some persistence of transport between the capillary fringe and water table.

The results of the comparison show that the two models are capable of producing consistent results. To make the comparison meaningful, several differences in inputs had to be reconciled, e.g., the radionuclide inventory and release functions associated with the release of the radionuclides from the grout. When these differences are reconciled, the two models agree well.

Figure G-5. Tank Closure and Waste Management Environmental Impact Statement Analysis of Iodine-129 Flux from the Vadose Zone into the Aquifer for Alternative 2b (Baseline) and Three Flux Reduction Sensitivity Cases.

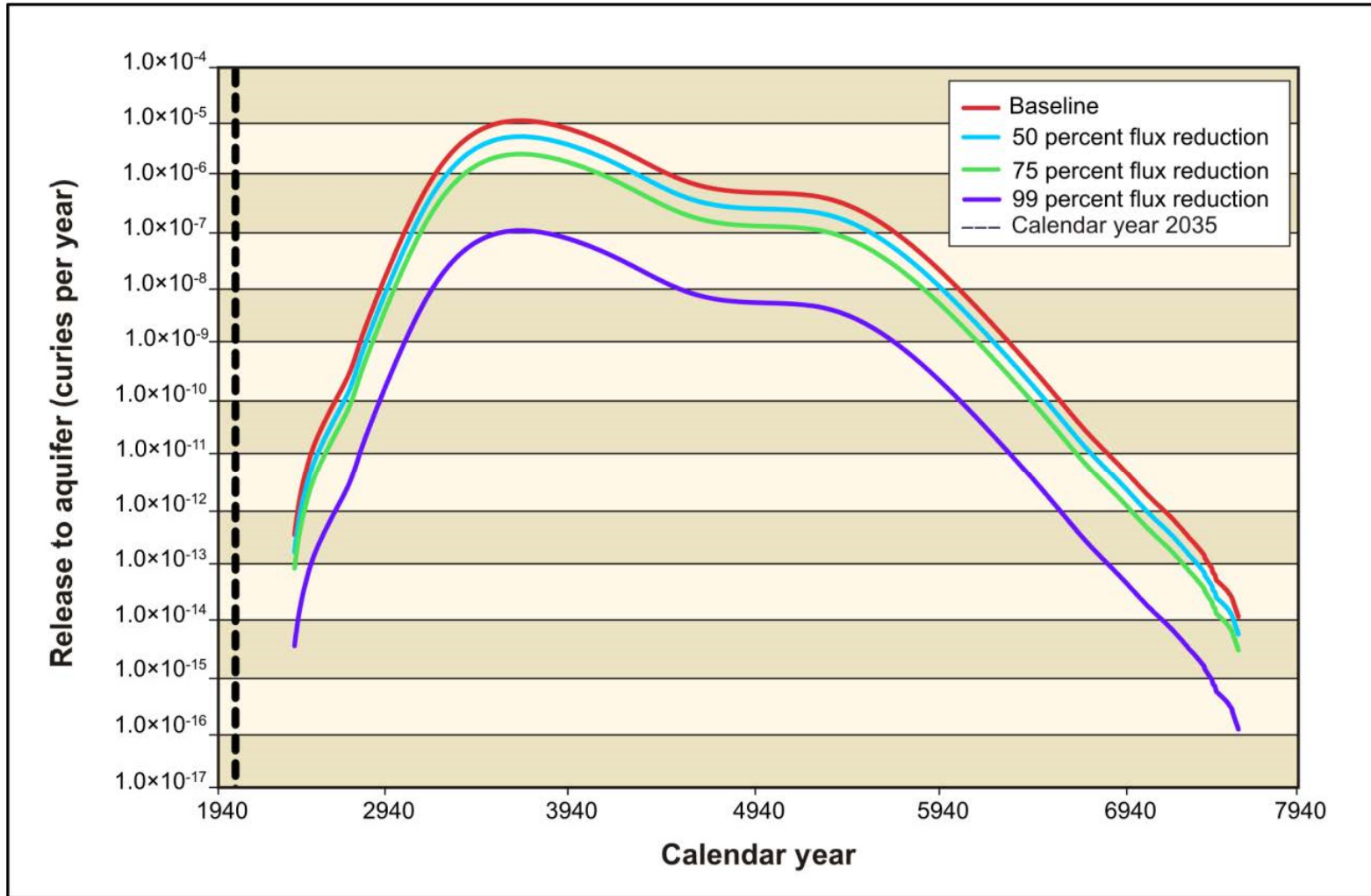
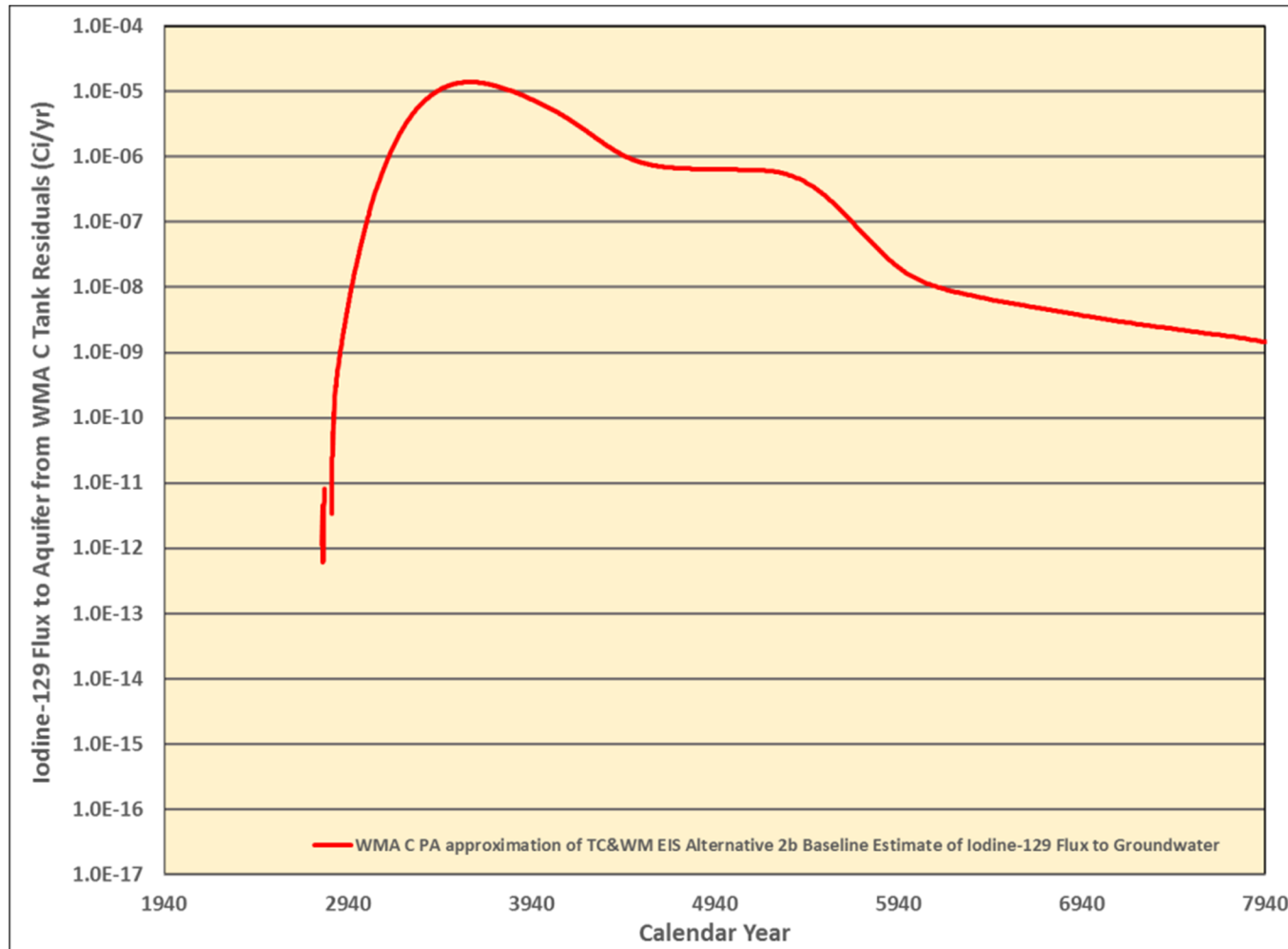


Figure U-122. Iodine-129 Flux to Aquifer Versus Time, C Tank Farm, Tank Residuals

Excerpted from Figure U-122, Appendix U of DOE/EIS-0391, "Final Tank Closure and Waste Management Environmental Impact Statement for the Hanford Site, Richland, Washington."

Figure G-6. Waste Management Area C Performance Assessment Analysis of Tank Closure and Waste Management Environmental Impact Statement Alternative 2b Model of Iodine-129 Flux from the Vadose Zone into the Aquifer.



PA = performance assessment

WMA = Waste Management Area

TC&WM EIS = Tank Closure and Waste Management Environmental Impact Statement

Reference: DOE/EIS-0391, "Final Tank Closure and Waste Management Environmental Impact Statement for the Hanford Site, Richland, Washington."

RPP-ENV-58782, Rev. 0

G.5 REFERENCES

- DOE/EIS-0391, 2012, "Final Tank Closure and Waste Management Environmental Impact Statement for the Hanford Site, Richland, Washington," U.S. Department of Energy, Office of River Protection, Richland, Washington.
Appendix M, Release to Vadose Zone
Appendix N, Vadose Zone Flow and Transport
Appendix O, Groundwater Transport Analysis
Appendix U, Supporting Information for the Long-Term Cumulative Impact Analyses
- DOE M 435.1-1, 1999, Radioactive Waste Management Manual, U.S. Department of Energy, Washington, D.C.
- DOE/ORP-2003-02, 2003, Environmental Impact Statement for Retrieval, Treatment, and Disposal of Tank Waste and Closure of Single-Shell Tanks at the Hanford Site, Richland, WA: Inventory and Source Term Data Package, Rev. 0, U.S. Department of Energy, Office of River Protection, Richland, Washington.
- Resource Conservation and Recovery Act of 1976, 42 USC 6901, et seq.

RPP-ENV-58782, Rev. 0

1
2
3
4
5
6
7
8
9
10
11

APPENDIX H

**LIST OF FEATURES, EVENTS AND PROCESSES APPLIED TO
WASTE MANAGEMENT AREA C**

RPP-ENV-58782, Rev. 0

1
2
3
4
5
6
7

This page intentionally left blank.

RPP-ENV-58782, Rev. 0

TABLE OF CONTENTS

1			
2	H.1	BACKGROUND ON FEATURES, EVENTS AND PROCESSES	
3		EVALUATION.....	H-1
4	H.2	INTRODUCTION TO SAFETY FUNCTIONS	H-2
5	H.3	SAFETY CONCEPT AND SAFETY FUNCTIONS FOR WASTE	
6		MANAGEMENT AREA C	H-3
7	H.4	INTERNATIONAL FEATURES, EVENTS, AND PROCESSES LIST WITH	
8		EVALUATIONS OF APPLICABILITY TO WASTE MANAGEMENT AREA C... H-11	
9	H.5	MAPPING SAFETY FUNCTIONS TO FEATURES, EVENTS AND	
10		PROCESSES.....	H-12
11	H.6	REFERENCES	H-88

LIST OF FIGURES

17	Figure H-1. Feature, Event, and Process Numbering Classification System.....	H-12
----	--	------

LIST OF TABLES

23	Table H-1. Safety Functions, Associated Features, Events, and Processes, and Potentially	
24	Deleterious Features, Events, and Processes Identified for the Waste	
25	Management Area C Residual Waste Performance Assessment. Details for	
26	individual Features, Events, and Processes and associated numbers identified in	
27	this table can be found in Section H.4.	H-4
28	Table H-2. Applicability of Features, Events, and Processes to Waste Management Area C	
29	Safety Functions.	H-15

RPP-ENV-58782, Rev. 0

LIST OF TERMS**Abbreviations and Acronyms**

DOE	U.S. Department of Energy
FEP	Features, Events, and Processes
IAEA	International Atomic Energy Agency
ISAM	Improvement of Safety Assessment Methodologies
WMA	Waste Management Area

RPP-ENV-58782, Rev. 0

APPENDIX H**LIST OF FEATURES, EVENTS AND PROCESSES APPLIED TO
WASTE MANAGEMENT AREA C****H.1 BACKGROUND ON FEATURES, EVENTS AND PROCESSES EVALUATION**

The use of Features, Events, and Processes (FEPs) is a well-established approach for improving the traceability and transparency of a performance assessment (PA). The intent of the use of FEPs is to identify conditions that may occur in the future that may affect the ability of the disposal system to perform successfully.

In general, the process of using FEPs consists of four steps: (1) identifying a comprehensive list of FEPs, (2) screening the comprehensive list to a manageable number, (3) describing the relationships between the FEPs, and (4) arranging them into calculational cases, or scenarios, for the safety assessment. Differences between published FEP evaluation approaches are comprised of differences between methods for one of these steps, or different ordering of the steps. For instance, the original scenario development procedure described in NUREG/CR-1667 (SAND80-1429), "Risk Methodology for Geologic Disposal of Radioactive Waste: Scenario Selection Procedure" only calls for screening the full scenarios, whereas more recent scenario development approaches emphasize screening at the FEP level (SKB Technical Report 95-22, "The Use of Interaction Matrices for Identification, Structuring, and Ranking of FEPs in a Repository System") or screening both FEPs and full scenarios (SAND94-0482, "Scenario Development for the Waste Isolation Pilot Plant: Building Confidence in the Assessment"). Despite the differences in approaches and ordering, the concepts of these four steps are the same for all scenario development procedures.

Considerable international effort has been expended to develop comprehensive FEP lists for geological (deep) disposal systems. There is only one approach that has been used for this step: collection and elicitation of expert opinion. Excellent summaries of the comprehensive FEP lists for geological disposal have been provided by Chapman et al. (SKI Report 95:26, "Systems Analysis, Scenario Construction and Consequence Analysis Definition for SITE-94") and by Guzowski and Newman (SAND93-7100, "Preliminary Identification of Potentially Disruptive Scenarios at the Greater Confinement Disposal Facility, Area 5 of the Nevada Test Site"). Chapman et al. (SKI Report 95:26) suggest that a comprehensive list of FEPs for a geological disposal system in Sweden was comprised of over 1,200 entries (SKI Technical Report 93:27, "SITE-94 Scenario Development FEP Audit List Preparation: Methodology and Presentation").

Work on formal scenario development for near-surface disposal is more recent and based heavily on the prior geological disposal literature. The International Atomic Energy Agency (IAEA) (IAEA-ISAM-1, "Safety Assessment Methodologies for Near Surface Disposal Facilities, Results of a co-ordinated research project, Volume 1: Review and enhancement of safety assessment approaches and tools") published the first comprehensive set of FEPs for near-surface disposal based on the results of the Improvement of Safety Assessment Methodologies (ISAM) coordinated research program. This FEP list was an adaptation of a

RPP-ENV-58782, Rev. 0

geological disposal comprehensive FEP list for near-surface conditions (IAEA-ISAM-1), and was audited against previously developed site-specific FEP lists for near-surface disposal [e.g., AECL-MISC-295, “Preliminary Safety Analysis Report (PSAR) for the Intrusion Resistant Underground Structure (IRUS)”], providing a good degree of confidence that the list was substantially complete and reliable. This international FEP list is attached to this report as Appendix A.

FEP approaches have also been used increasingly within the U.S. Department of Energy (DOE) Environmental Management and Tank Waste programs (e.g., “2002 LLW Repository PCSC – FEP Consideration [Phifer 2011]; FCRD-USED-2011-000297, “Features, Events and Processes for the Disposal of Low Level Radioactive Waste – FY 2011 Status Report”). Lists of Hanford-relevant FEPs have been developed [BHI-01573, “Groundwater/Vadose Zone Integration Project – The Application of Feature, Event, and Process Methodology at the Hanford Site”; WMP-22922, “Prototype Hanford Features, Events, and Processes (HFEP) Graphical User Interface”] and applied to recent PAs (WCH-520, “Performance Assessment for the Environmental Restoration Disposal Facility, Hanford Site, Washington”). The Hanford FEP lists differ in some regards from the international FEP list, mainly in being focused at a very fine level of detail, which has limited their utility in PAs.

While FEP analyses have been widely used, they have also been identified to have a number of drawbacks. In particular, as a bottom-up approach, they seek to identify all conditions of concern, without necessarily focusing on the key issues. As a result, they have in some cases led to large amounts of effort, but without a commensurate improvement in the traceability of the PA.

As a result of these issues with FEP-based analyses, in recent years there has been increasing attention given to safety function approaches in structuring PAs. Recent guidance on the conduct of PAs has de-emphasized the importance of purely FEP-based approaches, and has instead recommended a blended approach (NEA Report 6923, “Methods of Safety Assessment of Geological Disposal Facilities for Radioactive Waste, Outcomes of the NEA MeSA Initiative”). These approaches are reviewed in the next section.

H.2 INTRODUCTION TO SAFETY FUNCTIONS

The drawbacks to the FEPs process have led to a more recent emphasis in the literature on the use of an alternative approach to identifying conditions that need to be included in the PA. Increasingly, the literature on PA emphasizes the use of safety functions as either a replacement for FEP analyses or as an augmentation of FEP analyses (e.g., SKB Technical Report TR-10-45, “FEP report for the safety assessment SR-Site”; NEA Report 6923). A safety function is a feature of the system that provides a specific function that is relevant to the performance (or safety) of the facility. The set of these safety functions presents a high-level summary of the strategy by which the performance of the disposal system is assured. In addition to providing a technical approach to development of scenarios, the use of safety functions is beneficial in emphasizing the overall safety strategy with stakeholders.

RPP-ENV-58782, Rev. 0

Increasingly, PAs include both FEP evaluations as a bottom-up approach and safety functions as a top-down approach to identifying conditions that need to be evaluated in the PA (“A methodology for scenario development based on understanding of long-term evolution of geological disposal systems” [Wakasugi et al. 2012]; “Natural and Engineering Barriers – the Safety Concept Basis for LILW Repository in Vrbinja, Krško” [Virsek et al. 2014]). In this hybrid approach, FEPs are used in a more targeted manner than the traditional FEPs concept. In the hybrid approach, FEPs are identified that may affect the ability of the safety function to provide assurance of performance in the future. That is, FEPs are identified that may degrade or modify the performance of the safety function in some way. For instance, performance of an engineered cover system may be influenced by a wide variety of FEPs that would change the rate of water movement through it. These FEPs might include (for example) mechanical changes to the cover soil, changes in the vegetation on top of the cover, climate changes that lead to different precipitation patterns on top of the cover, loss of institutional control leading to onsite irrigation, and so on. Since all of these FEPs influence the system in a similar manner (i.e., changes in water flow through the cover), sensitivity analyses that vary this safety function represent an aggregated view of the potential negative effects of a suite of FEPs. In this way the PA can be organized to evaluate a large number of FEPs with fewer sensitivity cases and scenarios.

H.3 SAFETY CONCEPT AND SAFETY FUNCTIONS FOR WASTE MANAGEMENT AREA C

The safety concept is the overall approach by which a disposal system is intended to provide the performance required in regulation. The safety concept can be thought of as the set of safety functions, acting together in concert, to provide that performance. Ideally, the safety functions represent multiple and redundant barriers, so that the loss of one or some of the safety functions continues to result in adequate performance of the overall system. A set of safety functions for Waste Management Area (WMA) C are shown in Table H-1. The goal of the PA is to evaluate these safety functions, to provide reasonable assurance of performance even when some of the safety functions are lost or degraded through time or disruptive events.

A significant part of the safety concept lies in the land ownership of the Central Plateau by DOE. It is noteworthy that all of the technical calculations that are presented in a PA of WMA C are predicated on the loss of the first two safety functions: loss of institutional control of the Central Plateau by DOE, followed by loss of societal memory that the Hanford Site existed. If either or both of these safety functions remain in place, the radiological impacts of releases or residual wastes from WMA C are very low and greatly delayed in time, as shown in the TC&WM EIS analyses for tank residual wastes (DOE/EIS-0391, “Final Tank Closure and Waste Management Environmental Impact Statement for the Hanford Site, Richland, Washington”). In the assessment context of PAs conducted under DOE O 435.1, Radioactive Waste Management (see Section 2), both of these safety functions are assumed to disappear after 100 years.

Table H-1. Safety Functions, Associated Features, Events, and Processes, and Potentially Deleterious Features, Events, and Processes Identified for the Waste Management Area C Residual Waste Performance Assessment. Details for individual Features, Events, and Processes and associated numbers identified in this table can be found in Section H.4. (6 sheets)

Designation		Description	Associated FEPs	Deleterious FEPs	Associated Analyses
I1	Institutional Control	By DOE O 435.1, Radioactive Waste Management, it is assumed that control of the site will be retained for 100 years. A strong potential exists that the U.S. government will retain control of the site for a much more extended period of time. DOE O 458.1, Radiation Protection of the Public and the Environment requires that plans for management and disposal of wastes provide for institutional controls and long-term stewardship. DOE P 454.1, Use of Institutional Controls identifies how that stewardship is to be carried out.	1.1.06 1.1.09 1.1.10 1.4 (all)		Treated conservatively in all
I2	Societal memory	Societal memory is represented by records, deed restrictions, and other passive controls that would warn someone that additional care should be taken in the area. For a member of the public to come onsite to experience exposures to contamination from Waste Management Area (WMA) C, records that the Hanford Site existed would need to be forgotten or ignored. DOE O 458.1 requires record keeping that would lessen the likelihood of this occurrence. DOE P 454.1 identifies how that stewardship is to be carried out.	1.1.06 1.1.09 1.1.10 1.4 (all)		Treated conservatively in all
I3	Exposure	By DOE O 435.1, it is assumed that a post-closure well is established 100 m downgradient at the point of highest exposure. It is highly unlikely that this situation will occur, and potential wells in other locations would produce much lower impacts to a member of the public. Furthermore, even if control of the site is lost, the 100 m boundary for WMA C lies under the A Complex, and does not represent a realistic exposure point. Exposures would be more likely to occur further downgradient.	1.1 (all) 1.4 (all) 3.3 (all) 2.2.13(intruder) 2.3.03 2.3.08 2.3.09 2.3.13 2.4 (all)		Treated conservatively in all

Table H-1. Safety Functions, Associated Features, Events, and Processes, and Potentially Deleterious Features, Events, and Processes Identified for the Waste Management Area C Residual Waste Performance Assessment. Details for individual Features, Events, and Processes and associated numbers identified in this table can be found in Section H.4. (6 sheets)

Designation		Description	Associated FEPs	Deleterious FEPs	Associated Analyses
S1	Site characteristics	WMA C is a semi-arid site with low precipitation. The Central Plateau is remote from members of the public, with a substantial buffer area under U.S. Department of Energy (DOE) control. The vadose zone is thick, with long travel times in the vadose zone.	2.3.01 2.3.02 2.3.03 2.3.07 2.3.07 2.3.08 2.3.09 2.3.10 2.3.11 2.3.12 2.3.13		All
EB1	RCRA Cover (infiltration reduction)	The final design cover has not yet been established, but is believed to be able to produce very low initial flow rates. Over some period of time this function may deteriorate, with the rate of deterioration associated with a variety of processes.	1.1.02 1.1.08 1.1.12 1.2.04 1.2.07 1.3.01 1.3.02 1.3.04 1.3.06 1.3.07 1.3.08 1.4 (all) 2.1.05 2.3.01 2.3.02 2.3.07 2.3.08 2.3.10 2.3.11 2.3.12 2.3.13	1.1.08 1.1.12 1.2.04 1.2.07 2.3.08 2.3.12 2.3.13	INF0 – INF4 Treated in GoldSim [®] uncertainty analysis

Table H-1. Safety Functions, Associated Features, Events, and Processes, and Potentially Deleterious Features, Events, and Processes Identified for the Waste Management Area C Residual Waste Performance Assessment. Details for individual Features, Events, and Processes and associated numbers identified in this table can be found in Section H.4. (6 sheets)

Designation		Description	Associated FEPs	Deleterious FEPs	Associated Analyses
EB2	RCRA Cover (depth of disposal)	Limitation of types of potential inadvertent human intrusion by depth of disposal.	1.1.02 1.1.05 1.4 (all)		Intrusion
EB3	Steel Shell (permeability)	The function of the carbon steel shell to limit flow through the tank is not currently explicitly accounted for in the performance assessment. The shell is part of the overall assessment of low flow through the tank for long periods of time. Its potential eventual failure is considered as part of the generic barrier failure cases. DIF4 explores what happens if the tank behaves <i>better</i> than expected, and retains integrity for thousands of years, allowing ingrowth of progeny before releases commence.	1.1.02 2.1.05 2.1.08		DIF4
EB4	Steel Shell (chemical)	The carbon steel shell will corrode over a period of time, leaving behind corrosion products of (primarily) iron oxides. These corrosion products are highly sorptive and tend to produce reducing conditions that are highly advantageous for limiting solubilities of key radionuclides, particularly technetium.	1.1.02 2.1.05 2.1.09		None
EB5	Tank structure (structural)	The dome and walls provide structural support preventing subsidence of the closed facility.	1.1.02 1.2.03 2.1.05		No credible deleterious FEPs
EB6	Tank structure (intrusion)	The tank structure provides a barrier to intrusion.	1.1.02 1.4.03 2.1.05		Intrusion analysis
EB7	Tank structure (chemical)	The concrete of the tank acts to condition the chemistry of the waste residuals, with sorption characteristic of high pH environments.	1.1.02 2.1.05 2.1.09		Treated in GoldSim [®] uncertainty analysis GRT4 (Barrier analysis)
EB8	Tank structure (permeability)	The concrete of the tank structure is substantially intact and provides a barrier to flow into the tank.	1.1.02 1.2.03 2.1.05	1.2.03	GRT1, GRT2, GRT3

Table H-1. Safety Functions, Associated Features, Events, and Processes, and Potentially Deleterious Features, Events, and Processes Identified for the Waste Management Area C Residual Waste Performance Assessment. Details for individual Features, Events, and Processes and associated numbers identified in this table can be found in Section H.4. (6 sheets)

Designation		Description	Associated FEPs	Deleterious FEPs	Associated Analyses
EB9	Grout in tank (permeability)	The grout acts to limit water flow through the facility, making releases dominated by diffusion from the waste.	1.1.02 1.1.03 1.1.04 1.1.05 1.1.08 1.2.03 2.1.04	1.1.08 1.2.03	GRT1, GRT2, GRT3
EB10	Grout in Tank (chemical)	The grout acts to condition the chemistry of the waste residuals, with sorption characteristic of high pH environments.	1.1.02 2.1.04 2.1.09		Treated in GoldSim [®] uncertainty analysis GRT4 (Barrier analysis)
EB11	Grout in tank (structural)	The grout provides structural support preventing subsidence of the closed facility.	1.1.02 2.1.04		No credible deleterious FEPs
EB12	Grout (intrusion)	The structural strength of the grout provides a barrier to intrusion.	1.1.02 1.4.03 2.1.04 2.2.13		Intrusion analysis
EB13	Tank Base Mat (permeability)	The tank base mat, if intact, will provide a barrier that will limit flow and contaminant transport from the tank residual wastes situated at the tank bottom into the underlying vadose zone sediments.	1.1.02 2.1.05	2.1.05	GRT0 GRT1 GRT2 GRT3 (Barrier analysis)
EB14	Tank Base Mat (chemical)	The concrete pad is anticipated to continue to provide a high pH environment, with associated sorption, for an extended time in the future.	1.1.02 2.1.05 2.1.09 2.1.10		GoldSim [®] uncertainty analysis
EB15	Pipelines (permeability)	The pipelines, if intact, provide a delay to releases of waste in ancillary equipment.	2.1.06		All
AP1	Grout (air pathway)	Limitation of releases to air owing to low air permeability and long pathway to the surface.	2.1.12 2.3.07 3.1.04 3.2.09 3.2.10		Air pathway analysis

Table H-1. Safety Functions, Associated Features, Events, and Processes, and Potentially Deleterious Features, Events, and Processes Identified for the Waste Management Area C Residual Waste Performance Assessment. Details for individual Features, Events, and Processes and associated numbers identified in this table can be found in Section H.4. (6 sheets)

Designation		Description	Associated FEPs	Deleterious FEPs	Associated Analyses
WF1	Residual Waste (chemical)	The residual waste is recalcitrant by nature, providing limitations to the amount and rate of release of contamination from it upon contact with water.	2.1.01 2.1.02 2.1.12 3.1 (all) (except 3.1.06) 3.2 (all) (except 3.2.08)	2.1.1	RLS1 INV0, INV1, INV2 GoldSim [®] uncertainty
VZ1	Vadose zone thickness	The vadose zone is thick with slow rates of water flow, leading to long delay times in the vadose zone.	2.2.01 2.2.02 2.2.03 2.2.05 2.2.07 2.2.08 2.2.09 2.2.12 2.3.02 3.1.01 3.2.07	1.1.01 2.2.12	VZP0 VZP1 VZP2 VZP3 VZP4 VZP5 VZP6 VZP7 Treated in GoldSim [®] uncertainty analysis VZP9 (Barrier analysis)
VZ2	Sorption on vadose zone soils	Vadose zone soils sorb some of the contaminants of potential concern, delaying their arrival at the water table. A number of key contaminants are not believed to sorb significantly.	1.4.07 2.2.08 2.2.09 2.3.02 3.2.03 3.2.04 3.2.05 3.2.06 3.2.07	1.4.07 2.2.08 3.2.03	Treated in GoldSim [®] uncertainty analysis VZP6
VZ3	Dispersion in vadose zone	Spreading of contaminants in the vadose zone, dispersing them and decreasing concentrations.	2.2.01 2.2.02 2.2.03 2.2.05 2.2.07 2.3.02	2.2.12	Treated in GoldSim [®] uncertainty analysis VZP7

Table H-1. Safety Functions, Associated Features, Events, and Processes, and Potentially Deleterious Features, Events, and Processes Identified for the Waste Management Area C Residual Waste Performance Assessment. Details for individual Features, Events, and Processes and associated numbers identified in this table can be found in Section H.4. (6 sheets)

Designation		Description	Associated FEPs	Deleterious FEPs	Associated Analyses
SZ1	Water flow in saturated zone	Advective flow in the saturated zone leading to dilution of the contaminants.	1.2.10 1.3.01 1.3.02 1.3.03 1.3.07 1.4.10 2.2.03 2.2.05 2.2.07 2.3.03 2.3.04 3.1.01 3.2.07	1.3.01 1.3.02 1.3.03 1.3.07 2.3.03	Treated in GoldSim [®] uncertainty analysis GWP0 GWP1 GWP2 GWP3 (Barrier analysis)
SZ2	Sorption on saturated zone soils	Saturated zone soils sorb some of the contaminants of potential concern, delaying their arrival at the point of compliance. A number of key contaminants are not believed to sorb significantly.	2.2.08 2.2.09 3.2.03 3.2.04 3.2.07		Treated in GoldSim [®] uncertainty analysis
SZ3	Dispersion in saturated zone	Spreading of the plume in the saturated zone, adding dilution to the contaminant plume and lowering concentrations.	2.2.03 2.2.05 2.2.07		Treated in GoldSim [®] uncertainty analysis
SZ4	Dilution in well	Dilution caused by pumping a groundwater well to the surface where it is useable and accessible by a member of the public.	1.4.10 2.2.13 3.2.07 3.2.12 3.3.01 3.3.02 3.3.04		By groundwater protection rule, not taken into account. Groundwater concentrations at each point in space used for all analyses.

FEPs = Features, Events, and Processes

RCRA = Resource Conservation and Recovery Act of 1976

GoldSim[®] simulation software is copyrighted by GoldSim Technology Group LLC of Issaquah, Washington (see <http://www.goldsim.com>).

RPP-ENV-58782, Rev. 0

DOE O 435.1 also introduces another administrative safety function into the analysis: the point of compliance. If the first two safety functions (institutional control and societal memory) are lost, DOE O 435.1 requires an assumption that a groundwater well is installed 100 m from the disposal facility in the location of peak concentration. This assumption means that relatively little credit is given for delay and dilution in the groundwater aquifer. Even in the event that memory of the Hanford Site is lost, people would not necessarily move to the Central Plateau and use untreated groundwater as their water source. People further downgradient or people not using groundwater would necessarily be more protected than the PA calculates. The regulation, therefore, provides an additional layer of safety to the results of the analyses via this safety function.

The remaining parts of the safety concept involve the use of the engineering and geological setting to provide multiple and redundant barriers to the release and migration of residual wastes from tanks and ancillary equipment. The barriers can be divided into one of three types: hydrological safety functions, chemical safety functions, and structural safety functions. The safety concept calls for backfilling the tanks with grout, leading to a highly stable underground structure. The resulting monolith of grout contained in the tank can be assumed to maintain its ability to support the soil overburden for very long periods of time. The hydrological safety functions limit the contact of water with the residual wastes, limit that rate at which contamination can be released and transported through the environment to the compliance point, and provide dilution of contamination through dispersion and mixing with clean surrounding water. The chemical safety functions are intended to decrease the solubility and increase the sorption of key contaminants, and to provide a stable and passive chemical environment for the engineered barriers.

As discussed above, the purpose of the PA is to evaluate the safety concept to provide reasonable assurance of performance of the safety concept, even in the event that one or more of the safety functions are lost or are degraded in time. It is therefore reasonable to ask which FEPs might affect a particular safety function in a way that might degrade its function, or to cause the safety function to act differently than expected.

This approach can be used to identify a set of sensitivity analyses that can be used to explore the implications of the loss of safety functions, while at the same time exploring the implications of aggregated FEPs that might affect the safety function in similar ways. The structure of the PA for WMA C will therefore be to identify sensitivity cases and alternative models for the safety functions shown in Table H-1, and to examine what happens in the PA model when the safety function behaves differently than expected, is degraded compared to a base case, or is lost entirely. Particular attention will be given to any FEPs identified that might affect multiple safety functions simultaneously.

The safety functions identified for the WMA C post-closure period are presented in Table H-1 along with the associated FEPs and potentially deleterious FEPs. This table was generated from a workshop of senior PA experts, and represents the collective view of that group. The workshop was held in Denver April 20 – 21, 2015, with the goal of evaluating FEPs as they relate to WMA C and mapping the FEPs to safety functions. The attendee list is below.

RPP-ENV-58782, Rev. 0

1 WRPS/INTERA/Hanford

- 2 • Marcel Bergeron
- 3 • Matt Kozak
- 4 • Mike Connelly
- 5 • Alaa Aly
- 6 • Mick Apted
- 7 • Randy Arthur
- 8 • Bob Andrews

10 SRR/SRNL/ Savannah River

- 11 • Roger Seitz
- 12 • Kent Rosenberger
- 13 • Steve Hommel

15 PNNL/Hanford

- 16 • Vicky Freedman

17
18 The workshop was undertaken to evaluate which FEPs had the potential to affect safety functions
19 within the 10,000-year sensitivity and uncertainty analysis period. It therefore allowed the FEP
20 team to screen out some FEPs that may be expected to occur over extremely long time periods
21 (e.g., orogeny). The presumption in the FEP screening was that continental glaciation will not
22 occur within 10,000 years, so FEPs associated with such extreme changes were screened out.
23 All other FEPs that have a reasonable likelihood of occurrence in 10,000 years were evaluated
24 for their potential effects on the safety functions.

27 **H.4 INTERNATIONAL FEATURES, EVENTS, AND PROCESSES LIST WITH** 28 **EVALUATIONS OF APPLICABILITY TO WASTE MANAGEMENT AREA C** 29

30 This section contains an adaptation of Appendix C of IAEA-ISAM-1. The ISAM FEPs list is a
31 list of FEPs relevant to the assessment of long-term safety of near-surface disposal facilities,
32 which attempts to be comprehensive within reasonable bounds. Because these FEPs are an
33 adaptation of the FEPs used for near-surface disposal facilities, the term repository is used to
34 refer to the disposal system. It consists of 141 FEPs, each of which has an identifying number.
35 The numbers reflect a classification system, as shown in Figure H-1. At its center, the
36 classification scheme includes processes related to contaminant release, migration and exposures
37 (radionuclide and contaminant factors). The next tier are the features of the disposal system
38 (wastes, engineered and natural barriers and human behaviour) and events and processes which
39 may cause the system to evolve (environment factors). Further out, there are processes and
40 events originating outside the disposal system, but which act upon it (external factors). These
41 external factors (or external FEPs) are often considered to be scenario-generating FEPs.

42
43 Examination of the FEPs list shows a distinction between those that are descriptive of the system
44 and how it functions and those that have been included in the FEPs list because they have
45 potentially disruptive effects on the disposal system. This distinction has been used to

RPP-ENV-58782, Rev. 0

characterize how the FEPs act on WMA C safety functions, with the results documented in Section H.3.

Figure H-1. Feature, Event, and Process Numbering Classification System.

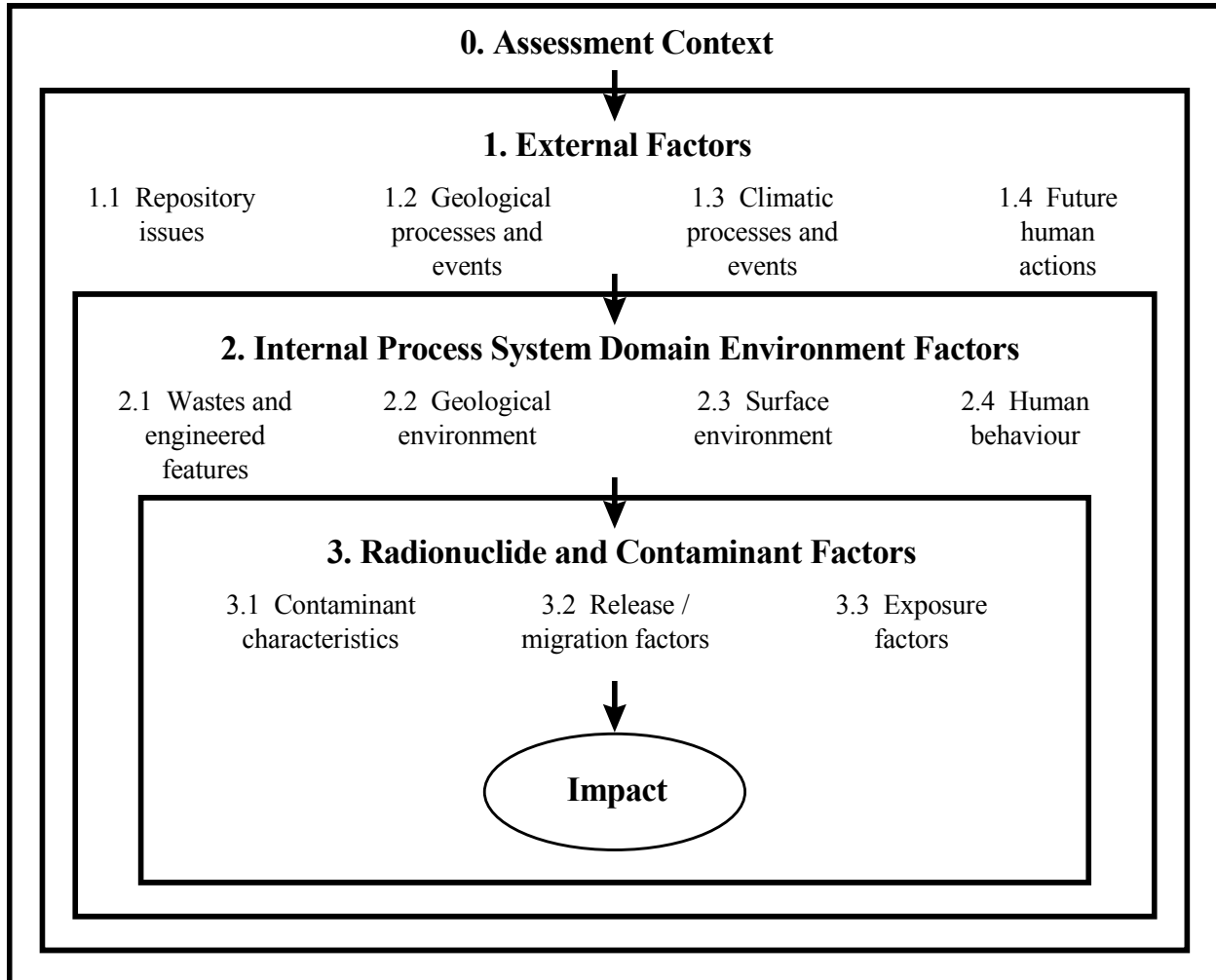


Figure excerpted from IAEA-ISAM-1, "Safety Assessment Methodologies for Near Surface Disposal Facilities, Results of a co-ordinated research project, Volume 1: Review and enhancement of safety assessment approaches and tools."

For the sake of clarity, the full list of FEPs from IAEA-ISAM-1 is included here in the same format as the original publication (refer to the list below). A new addition to the description of each FEP is a short commentary on the applicability of the FEP to the WMA C PA, and a short statement of what negative impact (if any) the FEP may have on the performance of WMA C, and how it affects safety functions.

H.5 MAPPING SAFETY FUNCTIONS TO FEATURES, EVENTS AND PROCESSES

Application of the IAEA FEPs list to the WMA C safety functions, discussed in Section H.4, leads to a mapping of applicable FEPs to each safety function. This mapping is shown in

RPP-ENV-58782, Rev. 0

1 Table H-2. A number of the FEPs have been evaluated as not applicable to WMA C, either
2 because of the geological or geographical location, because of the assessment context, or because
3 of the time frame of the analysis, which rules out FEPs requiring very long geological times for
4 their occurrence. These FEPs are denoted with N in the table (for not applicable). FEPs
5 applicable to a particular safety function are denoted with an X, whereas if the FEP is not
6 applicable to the safety function it is left blank.
7
8

RPP-ENV-58782, Rev. 0

- 1
- 2
- 3
- 4
- 5
- 6

This page intentionally left blank.

Table H-2. Applicability of Features, Events, and Processes to Waste Management Area C Safety Functions. (1 of 3 sheets)
X denotes applicable to Waste Management Area C, N denotes not applicable. See Feature, Event, and Process (FEP) list for discussion and justification.

FEP	Safety Function																											
	I1	I2	I3	S1	EB1	EB2	EB3	EB4	EB5	EB6	EB7	EB8	EB9	EB10	EB11	EB12	EB13	EB14	EB15	AP1	WF1	VZ1	VZ2	VZ3	SZ1	SZ2	SZ3	SZ4
1.1.01			X																									
1.1.02			X		X	X	X	X	X	X	X	X	X	X	X	X	X	X										
1.1.03			X																									
1.1.04			X																									
1.1.05			X			X																						
1.1.06	X	X	X																									
1.1.07			X																									
1.1.08			X		X																							
1.1.09	X	X	X																									
1.1.10	X	X	X																									
1.1.11			X																									
1.1.12			X		X																							
1.2.01	N	N	N	N	N	N	N	N	N	N	N	N	N	N	N	N	N	N	N	N	N	N	N	N	N	N	N	N
1.2.02	N	N	N	N	N	N	N	N	N	N	N	N	N	N	N	N	N	N	N	N	N	N	N	N	N	N	N	N
1.2.03									X			X	X															
1.2.04					X																							
1.2.05	N	N	N	N	N	N	N	N	N	N	N	N	N	N	N	N	N	N	N	N	N	N	N	N	N	N	N	N
1.2.06	N	N	N	N	N	N	N	N	N	N	N	N	N	N	N	N	N	N	N	N	N	N	N	N	N	N	N	N
1.2.07					X																							
1.2.08	N	N	N	N	N	N	N	N	N	N	N	N	N	N	N	N	N	N	N	N	N	N	N	N	N	N	N	N
1.2.09	N	N	N	N	N	N	N	N	N	N	N	N	N	N	N	N	N	N	N	N	N	N	N	N	N	N	N	N
1.2.10																									X			
1.3.01					X																				X			
1.3.02					X																				X			
1.3.03																									X			
1.3.04	N	N	N	N	N	N	N	N	N	N	N	N	N	N	N	N	N	N	N	N	N	N	N	N	N	N	N	N
1.3.05	N	N	N	N	N	N	N	N	N	N	N	N	N	N	N	N	N	N	N	N	N	N	N	N	N	N	N	N
1.3.06					X																							
1.3.07					X																				X			
1.3.08					X																							
1.3.09	N	N	N	N	N	N	N	N	N	N	N	N	N	N	N	N	N	N	N	N	N	N	N	N	N	N	N	N
1.3.10						X																						
1.4.01	X	X	X		X																							
1.4.02	X	X	X		X																							
1.4.03	X	X	X		X					X						X												
1.4.04	X	X	X		X																							
1.4.05	X	X	X		X																							
1.4.06	X	X	X		X																							
1.4.07	X	X	X		X																		X					
1.4.08	X	X	X		X																							
1.4.09	X	X	X		X																							
1.4.10	X	X	X		X																				X			

Table H-2. Applicability of Features, Events, and Processes to Waste Management Area C Safety Functions. (2 of 3 sheets)
X denotes applicable to Waste Management Area C, N denotes not applicable. See Feature, Event, and Process (FEP) list for discussion and justification.

FEP	Safety Function																											
	I1	I2	I3	S1	EB1	EB2	EB3	EB4	EB5	EB6	EB7	EB8	EB9	EB10	EB11	EB12	EB13	EB14	EB15	AP1	WF1	VZ1	VZ2	VZ3	SZ1	SZ2	SZ3	SZ4
1.4.11	X	X	X		X																							
1.4.12	X	X	X		X																							
1.4.13	X	X	X		X																							
1.4.14	X	X	X		X																							
1.4.15	X	X	X		X																							
2.1.01																					X							
2.1.02																					X							
2.1.03	N	N	N	N	N	N	N	N	N	N	N	N	N	N	N	N	N	N	N	N	N	N	N	N	N	N	N	N
2.1.04													X	X	X	X												
2.1.05							X	X	X	X	X	X					X	X										
2.1.06																			X									
2.1.07																												
2.1.08							X																					
2.1.09								X			X			X			X	X										
2.1.10																		X										
2.1.11	N	N	N	N	N	N	N	N	N	N	N	N	N	N	N	N	N	N	N	N	N	N	N	N	N	N	N	N
2.1.12																				X	X							
2.1.13	N	N	N	N	N	N	N	N	N	N	N	N	N	N	N	N	N	N	N	N	N	N	N	N	N	N	N	N
2.1.14	N	N	N	N	N	N	N	N	N	N	N	N	N	N	N	N	N	N	N	N	N	N	N	N	N	N	N	N
2.1.15	N	N	N	N	N	N	N	N	N	N	N	N	N	N	N	N	N	N	N	N	N	N	N	N	N	N	N	N
2.2.01																						X		X				
2.2.02																						X		X				
2.2.03																						X		X	X		X	
2.2.04	N	N	N	N	N	N	N	N	N	N	N	N	N	N	N	N	N	N	N	N	N	N	N	N	N	N	N	N
2.2.05																						X		X	X		X	
2.2.06	N	N	N	N	N	N	N	N	N	N	N	N	N	N	N	N	N	N	N	N	N	N	N	N	N	N	N	N
2.2.07																						X		X	X			
2.2.08																						X	X			X		
2.2.09																						X	X			X		
2.2.10	N	N	N	N	N	N	N	N	N	N	N	N	N	N	N	N	N	N	N	N	N	N	N	N	N	N	N	N
2.2.11	N	N	N	N	N	N	N	N	N	N	N	N	N	N	N	N	N	N	N	N	N	N	N	N	N	N	N	N
2.2.12																						X						
2.2.13			X																									X
2.3.01				X	X																							
2.3.02				X	X																	X	X	X				
2.3.03			X	X																					X			
2.3.04				X																					X			
2.3.05	N	N	N	N	N	N	N	N	N	N	N	N	N	N	N	N	N	N	N	N	N	N	N	N	N	N	N	N
2.3.06	N	N	N	N	N	N	N	N	N	N	N	N	N	N	N	N	N	N	N	N	N	N	N	N	N	N	N	N
2.3.07				X	X																	X						
2.3.08			X	X	X																							
2.3.09			X	X																								
2.3.10				X	X																							

Table H-2. Applicability of Features, Events, and Processes to Waste Management Area C Safety Functions. (3 of 3 sheets)
X denotes applicable to Waste Management Area C, N denotes not applicable. See Feature, Event, and Process (FEP) list for discussion and justification.

FEP	Safety Function																											
	I1	I2	I3	S1	EB1	EB2	EB3	EB4	EB5	EB6	EB7	EB8	EB9	EB10	EB11	EB12	EB13	EB14	EB15	AP1	WF1	VZ1	VZ2	VZ3	SZ1	SZ2	SZ3	SZ4
2.3.11				X	X																							
2.3.12				X	X																							
2.3.13			X	X	X																							
2.3.14	N	N	N	N	N	N	N	N	N	N	N	N	N	N	N	N	N	N	N	N	N	N	N	N	N	N	N	N
2.4.01			X																									
2.4.02			X																									
2.4.03			X																									
2.4.04			X																									
2.4.05			X																									
2.4.06			X																									
2.4.07			X																									
2.4.08			X																									
2.4.09			X																									
2.4.10	N	N	N	N	N	N	N	N	N	N	N	N	N	N	N	N	N	N	N	N	N	N	N	N	N	N	N	N
2.4.11	N	N	N	N	N	N	N	N	N	N	N	N	N	N	N	N	N	N	N	N	N	N	N	N	N	N	N	N
3.1.01																						X			X			
3.1.02	N	N	N	N	N	N	N	N	N	N	N	N	N	N	N	N	N	N	N	N	N	N	N	N	N	N	N	N
3.1.03																												
3.1.04																				X								
3.1.05	N	N	N	N	N	N	N	N	N	N	N	N	N	N	N	N	N	N	N	N	N	N	N	N	N	N	N	N
3.1.06	N	N	N	N	N	N	N	N	N	N	N	N	N	N	N	N	N	N	N	N	N	N	N	N	N	N	N	N
3.2.01																					X							
3.2.02																					X							
3.2.03																					X		X					
3.2.04																					X		X					
3.2.05																					X		X					
3.2.06																					X		X					
3.2.07																					X	X	X		X	X		
3.2.08	N	N	N	N	N	N	N	N	N	N	N	N	N	N	N	N	N	N	N	N	N	N	N	N	N	N	N	N
3.2.09																				X	X							
3.2.10																				X	X							
3.2.11																					X							
3.2.12																					X							
3.2.13																					X							
3.3.01			X																						X			
3.3.02			X																						X			
3.3.03			X																									
3.3.04			X																						X			
3.3.05			X																									
3.3.06			X																									
3.3.07			X																									
3.3.08			X																	X							X	

ASSESSMENT CONTEXT	0
Definition: Factors that the analyst will consider in determining the scope of the analysis. These may include factors related to regulatory requirements, definition of desired calculation end-points, requirements in a particular phase of assessment, description of the domain of concern and a description of the target groups in the assessment. Decisions at this point will affect the phenomenological scope of a particular phase of assessment, i.e. what “physical FEPs” will be included.	
Comment: <i>"Assessment Context" is a category in the International FEP List and is subdivided into individual FEPs.</i>	

Assessment endpoints	0.01
Definition: The long-term human <i>health and environmental effects or risks that may arise from the disposed wastes and repository. These FEPs include health or environmental effects of concern in an assessment (what effect and to whom/what), and health or environmental effects ruled to be of no concern.</i>	
Comment: <i>From the disposed radioactive waste to the health impact to humans, various indicators and associated criteria can be defined to serve as assessment endpoints. Which one to choose, will depend on the purpose of the assessment. The indicator most frequently considered is the radiation dose or risk to man, often represented by the annual dose rate or risk to a member of a “critical group” of potentially most exposed individuals (see FEP 0.06).</i>	
<u>Key concepts, examples, and related FEPs</u>	
Annual individual dose	Lifetime individual risk
Annual individual risk	Radionuclide concentration in the environment
Collective doses	Flux through engineered barriers
Lifetime individual dose	Flux from geosphere to biosphere
Collective effective dose	Collective risk
<u>Application to WMA C:</u> Addressed in DOE Order 435.1.	
<u>Potentially deleterious FEP:</u> Not applicable	

Timescales of concern	0.02
Definition: The time periods over which the disposed wastes and repository may present some significant human health or environmental hazard.	
Comment: <i>These may correspond to the timescale over which the safety of the disposed wastes and repository is estimated or discussed. In some countries national regulations set a limit up to which quantitative assessment is required, with more qualitative arguments to demonstrate safety being sufficient at later times.</i>	

<u>Key concepts, examples, and related FEPs</u>		
Until peak doses occur	500 – 10 000 years	0 – 500 years
> 60 000 years	10 000 – 60 000 years	
<u>Application to WMA C:</u> Addressed in DOE Order 435.1.		
<u>Potentially deleterious FEP:</u> Not applicable		

Spatial domain of concern	0.03
Definition: The domain over which the disposed wastes and repository may present some significant human health or environmental hazard.	
Comment: This may correspond to the spatial domain over which the safety of the disposed wastes and repository is estimated, or the domain which is necessary to model in order to develop an understanding of the movement of contaminants and exposures. This may be limited by the purpose of the assessment, for example if the performance of a component of the total system have to be assessed.	
<u>Key concepts, examples, and related FEPs</u>	
Description of the spatial domain of concern	
<u>Application to WMA C:</u> Addressed in DOE Order 435.1.	
<u>Potentially deleterious FEP:</u> Not applicable	

Repository assumptions	0.04
Definition: The assumptions that are made in the assessment about the construction, operation, closure and administration of the repository.	
Comment: For example, most post-closure assessments make the assumption that a repository has been successfully closed, although, in practice such decisions may be delayed or be the subject of uncertainty	
<u>Key concepts, examples, and related FEPs</u>	
Description of the construction, operation, closure and operation of the repository	Repository has been successfully closed Change in volume of disposed waste Waste emplacement configuration has change Change in repository design
<u>Application to WMA C:</u> Addressed in the performance assessment. See Sections 1-3 for a summary.	
<u>Potentially deleterious FEP:</u> Uncertainties in repository assumptions are addressed in sensitivity analyses for various safety functions. PA Maintenance is required to address changes in actual disposal relative to assumptions in the PA.	

Future human action assumptions	0.05
Definition: The assumptions made in the assessment concerning general boundary conditions for assessing future human actions.	
Comment: For example, it can be expected that human technology and society will develop over the timescales of relevance for repository safety assessment. However, this development is unpredictable. Therefore, it is usual to make some assumptions in order to constrain the range of future human activities that are considered.	
<u>Key concepts, examples, and related FEPs</u>	
<i>Only present day technologies will be considered</i> <i>Only technologies practised in the past will be considered</i> <i>Description of human society development</i> <i>Description of general human society</i> <i>The past is an accurate reflection of the future</i>	
<u>Application to WMA C:</u> Addressed in DOE Order 435.1.	
<u>Potentially deleterious FEP:</u> Not applicable	

Future human behaviour (target group) assumptions	0.06
Definition: The assumptions made concerning potentially exposed individuals or population groups that are considered in the assessment.	
Comment: Doses or risks are usually estimated for critical groups (individuals or groups) thought to be representative of the individuals or population groups that may be at highest risk or receive the highest doses as a result of the disposed wastes and repository. This is the accepted approach for assessing radiological risk or dose to members of the public resulting from a source of radioactive release to the environment. To assess the doses or risks at times in the far future, when the characteristics of potentially exposed populations are unknown, a hypothetical critical group, or groups, is/are usually defined	
<u>Key concepts, examples, and related FEPs</u>	
<i>Description of an actual critical group</i> <i>Description of a hypothetical critical group</i>	
<u>Application to WMA C:</u> Addressed in DOE Order 435.1.	
<u>Potentially deleterious FEP:</u> Not applicable DOE Order 435.1 requires evaluation at the location and time of peak concentration during the compliance period, so deleterious assumptions are part of the application of the FEP.	

Dose response assumptions	0.07
Definition: Those assumptions made in an assessment in order to convert received dose to a measure of risk to an individual or population.	

Comment: Usually this will refer to individual human dose response, e.g. by a dose-risk conversion factor where the factor is the probability of a specified health effect per unit of radiation exposure. If other organisms are considered then a risk to individual organisms or a species might be considered. The variation of a given response or human health effect (e.g. cancer incidence, cancer mortality) with the amount of radiation dose an individual or a group of individuals received is referred to as the dose-response relation. It is not possible to determine the shape of the dose response curve at low doses with any precision, because the incidence of health effects is very low. A linear dose-response relation with no dose threshold is generally assumed cautious (See ICRP 60).

Key concepts, examples, and related FEPs

None

Application to WMA C: Addressed in DOE Order 435.1.

Potentially deleterious FEP: Not applicable

Assessment purpose	0.08
Definition: The purpose for which the assessment is being undertaken.	
Comment: The aim of the assessment is likely to depend on the stage in the repository development project at which the assessment is carried out and may also affect the scope of assessment	
<u>Key concepts, examples, and related FEPs</u>	
Site selection	Demonstrate the feasibility of a disposal concept
Demonstrate regulatory compliance	Rehabilitation of contaminated site
Concept design	Public confidence
	System optimization
<u>Application to WMA C:</u> Addressed in the performance assessment. See Section 2.	
<u>Potentially deleterious FEP:</u> Not applicable	

Regulatory requirements and exclusions	0.09
Definition: The specific terms or conditions in the national regulations or guidance related to all stages of the repository that will influence the post closure safety assessment.	
Comment: Regulatory requirements and exclusions may be expressed in terms of release, dose or risk limits or targets to individuals or populations effective over a specified timescale; they may also make demands about procedures following closure of the repository. In some regulations, the long-term scenarios to be assessed are specified, or some scenarios or events are specifically ruled out of consideration.	

<u>Key concepts, examples, and related FEPs</u>		
<i>Independence of safety from control</i>	<i>Environmental protection standards</i>	<i>Multi-factor safety case</i>
<i>Optimization</i>	<i>Quality assurance</i>	<i>Radiological protection standards</i>
<i>Effects in the future</i>	<i>Quality control</i>	
<u>Application to WMA C:</u> Addressed in DOE Order 435.1.		
<u>Potentially deleterious FEP:</u> Not applicable		

Model and data issues	0.10
Definition: Model and data issues in the context of a safety assessment, refers to general (i.e. methodological) issues affecting the assessment modelling process and use of data during the process.	
Comment: A post-closure safety assessment is an attempt to quantify the exposure or risk posed by a radioactive waste disposal site to future generations of humanity and their environment. Intrinsicly, to do this one can say that the observations needed for the safety assessment of a site should be carried out for the life span of the proposed disposal facility. However, this is neither physically possible nor desirable. The only viable approach to perform a complete radiological safety assessment is to try to obtain as much observational data as possible, on a limited time scale, and then simulate the future behaviour of the disposal system through what is known as a model.	
<u>Key concepts, examples, and related FEPs</u>	
<i>Treatment of uncertainty</i>	<i>Modelling studies</i>
<i>Method of handling site data</i>	<input type="checkbox"/> <i>Model and data reduction/simplification</i>
<i>Assessment philosophy</i>	<i>Data availability</i>
	<i>Application of conservatism</i>
<u>Application to WMA C:</u> Addressed in the performance assessment. See Sections 1 – 3 for a summary.	
<u>Potentially deleterious FEP:</u> Not applicable	

EXTERNAL FACTORS	1
Definition: FEPs with causes or origin outside the disposal system domain, i.e. natural or human factors of a more global nature and their immediate effects. Included in this category are decisions related to repository design, operation and closure since these are outside the temporal boundary of the disposal system domain for post-closure assessment.	
Comment: "External Factors" is a category in the International FEP List and is divided into sub-categories.	

REPOSITORY ISSUES	1.1
Definition: Decisions on designs and waste allocation (repository type), and also events related to site investigation, operations and closure (site context).	
Comment: "Repository Issues" is a sub-category of External Factors in the International FEP List and is divided into individual FEPs.	

Site investigation	1.1.01	
Definition: FEPs related to the investigations that are carried out at a potential repository site in order to characterize the site both prior to repository excavation and during construction and operation.		
Comment: <i>Site investigation activities provide detailed site-specific performance assessment data and information necessary for the safety case to demonstrate the suitability of the site and to establish baseline conditions</i>		
<u>Key concepts, examples, and related FEPs</u>		
Geography and demography	Aquifer tests	Ecological features
Meteorology and climatology (regional and local)	Investigative boreholes	Pre-operational monitoring programme
Geology and seismology	Biosphere characteristics	Hydrogeology characteristics
Hydrology characteristics	Natural resources	Geohydrological characteristics
Geotechnical characteristics	Geochemical characteristics	Geomorphology characteristics
<u>Application to WMA C:</u> <i>Relevant to the performance assessment. See Section 4 for a discussion of site investigations.</i>		
<u>Potentially deleterious FEP:</u> <i>Drywells and boreholes may have the potential to provide relative fast paths through the vadose zone under some wetting conditions. Alternative conceptual models with preferential flow paths through the vadose zone are included in the PA.</i>		

Design, repository	1.1.02
Definition: FEPs related to the design of the repository including both the safety concept, i.e. the general features of design and how they are expected to lead to a satisfactory performance, and the more detailed engineering specification for excavation, construction and operation.	
Comment: The repository design and construction is established in a general way in the disposal concept for the repository which is based on expected host lithology characteristics, waste and backfill characteristics, construction technology, and economics. Repository design includes the principle design features that are designed to provide long-term isolation of disposed waste, minimize the need for continued active maintenance after site closure, and improve the site's natural characteristics in order to protect public health and the environment. There may, nevertheless, be a range of engineering design and construction options still open. As the repository project proceeds, and more detailed site-specific information becomes available, the range of options may be constrained and decisions will be made. At any stage, repository safety assessments may only analyse a subset of the total range of option. (See FEP 1.103).	

<u>Key concepts, examples, and related FEPs</u>	
<i>The general repository design features (e.g. host lithology, waste form, backfill, waste packages, construction technology, etc.)</i>	<i>The principle design criteria or considerations for normal and abnormal condition Operational monitoring programme</i>
<u>Application to WMA C:</u> <i>Relevant to the performance assessment. See Section 4.</i>	
<u>Potentially deleterious FEP:</u> <i>Not applicable</i>	

Construction, repository	1.1.03
Definition: FEPs related to the construction (e.g., excavation) of shafts, tunnels, disposal galleries, silos, trenches, vaults, etc. of a repository, as well as the stabilisation of these openings and installation/assembly of structural elements according to the design criteria.	
Comment: <i>Repository construction refers to the implementation of the design considerations and specifically to the construction of features of the repository necessary to provide long-term isolation of disposed waste, minimize the need for continued active maintenance after site closure, and improve the site's natural characteristics in order to protect public health and the environment. In addition, it includes the construction methods. (See FEP 1.102).</i>	
<u>Key concepts, examples, and related FEPs</u>	
<i>Drilling of borehole</i>	<i>Construction of walls, floors, mounds, layers of mounds</i>
<i>Excavation of trenches, holes, vaults</i>	<i>Site plans, engineering drawing, and construction specifications</i>
<i>Construction equipment</i>	<i>Control and diversion of water Site preparations</i>
<u>Application to WMA C:</u> <i>Relevant to the performance assessment. For WMA C this relates both to past facility construction (Section 4), and to emplacement of grout and cover.</i>	
<u>Potentially deleterious FEP:</u> <i>Potential degradation of safety functions associated with the engineered components of the system may result from failure of quality control. A range of cover performance is assumed in various sensitivity cases.</i>	

Emplacement of wastes and backfilling	1.1.04
Definition: FEPs related to the placing of wastes (usually in containers) at their final position within the repository and placing of buffer and/of backfill materials in the disposal zone.	
Comment: <i>Some waste types and inventories may require special waste emplacement arrangements to simplify the disposal practice, to ensure safety or to ensure structure stability in the repository area. The backfill material is used to refill excavated portions of the repository or any void spaces left unfilled after waste has been emplaced (see also FEP 1.1.07).</i>	

<u>Key concepts, examples, and related FEPs</u>		
Emplacement method	Filling of void spaces between the containers and in the rest of the repository	□ Covering of waste in-between containers
Waste emplacement configuration		
<u>Application to WMA C:</u> Relevant to the performance assessment with respect to the infill grout emplacement and cover emplacement.		
<u>Potentially deleterious FEP:</u> Safety functions associated with the grout and cover may be degraded by incorrect emplacement of the materials. Emplacement of grout must take due account of heat of hydration and shrinkage. A range of cover performance is assumed in various sensitivity cases.		

Closure, repository		1.1.05
Definition: FEPs related to the cessation of waste disposal operations at a site, the backfilling and sealing of boreholes type facilities, and the capping and covering of trenches, vaults, etc.		
Comment: The term closure refers to the status of, or an action directed at a disposal facility at the end of its operational life. A disposal facility is placed under permanent closure usually after completion of waste emplacement, by covering a near surface disposal facility, by backfilling and/or sealing of a borehole type facility, and termination and completion of activities in any associated structure. The intention of repository capping and sealing is to prevent infiltrating water as well as human access to the wastes. Individual sections of a repository may be closed in sequence, but closure usually refers to final closure of the whole repository, and will probably include removal of surface installations. The schedule and procedure for capping, sealing and closure may need to be considered in the assessment.		
<u>Key concepts, examples, and related FEPs</u>		
Trench/vault capping	Backfilling of boreholes	Decontamination and decommissioning plan
Site stabilisation	Removal of surface structures	Post-operational monitoring programme
Cover construction	Closure procedures	Closure compartments
<u>Application to WMA C:</u> Relevant to the performance assessment with respect to the infill grout emplacement and cover emplacement.		
<u>Potentially deleterious FEP:</u> Safety functions associated with the grout and cover may be degraded by incorrect closure. Emplacement of grout must take due account of heat of hydration and shrinkage. A range of cover performance is assumed in various sensitivity cases.		

Records and markers, repository		1.1.06
Definition: FEPs related to the retention of records of the content and nature of a repository after closure and also the placing of permanent markers at or near the site.		
Comment: It is expected that records will be kept to allow future generations to recall the existence and nature of the repository following closure. In some countries, the use of site markers has been proposed where the intention is that the location and nature of the repository might be recalled even in the event of a lapse of present-day administrative controls.		

<u>Key concepts, examples, and related FEPs</u>		
Records of the content and nature of the repository	Disposal unit and boundary markers Archive of the records	Site markers
<u>Application to WMA C:</u> Addressed as part of institutional control assumptions in DOE Order 435.1.		
<u>Potentially deleterious FEP:</u> Safety functions associated with institutional control are treated conservatively by requirements in DOE Order 435.1. Reduction of these safety functions is not credible.		
Waste allocation		1.1.07
Definition: FEPs related to the choices on allocation of wastes to the repository, including waste type(s) and amount(s).		
Comment: The waste type and waste allocation is established in a general way in the repository disposal concept. There may, however, be a number of options concerning these factors. Final decisions may not be made until the repository is operating and will be subject to regulation. In safety assessments, assumptions may need to be made about future waste arisings and future waste allocation strategies (see also FEP 1.1.04).		
<u>Key concepts, examples, and related FEPs</u>		
Waste allocation description	Future waste allocation strategies	Waste acceptance criteria for the repository
Future waste arisings	Projected inventories	
<u>Application to WMA C:</u> Not applicable for tank closure. The FEP relates to future waste arisings.		
<u>Potentially deleterious FEP:</u> Not applicable		
Quality control		1.1.08
Definition: FEPs related to quality assurance and control procedures and tests during the design, construction and operation of the repository, as well as the manufacture of the waste forms, containers and engineered features.		
Comment: It can be expected that a range of quality control measures will be applied during construction and operation of the repository, as well as to the manufacture of the waste forms, containers etc. In an assessment these may be invoked to avoid analysis of situations which, it is expected, can be prevented by quality control. There may be specific regulations governing quality control procedures, objectives and criteria.		
<u>Key concepts, examples, and related FEPs</u>		
Defects in construction of disposal system	Improper or faulty waste emplacement and backfilling	Defects during the conditioning of the waste
Defects in the construction of container		Defects in cap constructions

<u>Application to WMA C:</u> Relevant grout emplacement, and cover emplacement.	
<u>Potentially deleterious FEP:</u> Safety functions associated with grout and cover may be degraded if there is a failure of quality control. A range of cover performance is assumed in various sensitivity cases.	

Schedule and planning	1.1.09
Definition: FEPs related to the sequence of events and activities occurring during repository excavation, construction, waste emplacement and sealing.	
Comment: Relevant events may include phased construction of units and emplacement of wastes, backfilling, sealing, capping and closure of sections of the repository after wastes are emplaced, and monitoring activities to provide data on the transient behaviour of the system or to provide input to the final assessment. The sequence of events and time between events may have implications for long term performance, e.g. decline of activity and heat production from the wastes, material degradation, chemical and hydraulic changes during a prolonged “open” phase.	
<u>Key concepts, examples, and related FEPs</u>	
Phased construction of units	Phased emplacement of wastes, backfilling, sealing, capping and closure of sections of the repository
Planning of monitoring activities to provide data on the transient behaviour of the system	
<u>Application to WMA C:</u> Project timing assumed in the performance assessment is consistent with assumptions in the TC&WM EIS.	
<u>Potentially deleterious FEP:</u> Alterations in project timing have the potential to affect safety functions associated with the grout and cover. Not foreseen as a significant issue while tanks are relatively intact.	

Administrative control, repository site	1.1.10
Definition: FEPs related to measures to control events at or around the repository site, both during the operational period and after closure.	
Comment: The responsibility for administrative control of the site before closure of the repository during the construction and operational phases, and subsequently following closure of the repository may not be the same. Furthermore, the type of administrative control may vary depending on the stage in the repository lifetime.	
<u>Key concepts, examples, and related FEPs</u>	
None	
<u>Application to WMA C:</u> Addressed in multiple DOE Orders and policies. See Section 2.	
<u>Potentially deleterious FEP:</u> Safety functions associated with institutional control are treated conservatively by requirements in DOE Order 435.1. Reduction of these safety functions is not credible.	

Monitoring of repository	1.1.11
Definition: FEPs related to any monitoring that is carried out during operations or following closure of sections of, or the total, repository. This includes monitoring for operational safety and also monitoring of parameters related to the long-term safety and performance.	
Comment: <i>The extent and requirement for such monitoring activities may be determined by repository design and host lithology, regulations and public pressure.</i>	
<u>Key concepts, examples, and related FEPs</u>	
<i>Pre-operational monitoring programme</i>	<i>Post-operational monitoring programme</i>
	<i>Operational monitoring programme</i>
<u>Application to WMA C:</u> <i>Will be addressed in the performance maintenance plan.</i>	
<u>Potentially deleterious FEP:</u> <i>Not applicable, although potential preferential pathways through the vadose zone are addressed.</i>	

Accidents and unplanned events	1.1.12
Definition: FEPs related to accidents and unplanned events during construction, waste emplacement and closure, which might have an impact on long-term performance or safety.	
Comment: <i>Accidents are events that are outside the range of normal operations although the possibility that certain types of accident may occur should be anticipated in repository operational planning. Unplanned events include accidents but could also include deliberate deviations from operational plans.</i>	
<u>Key concepts, examples, and related FEPs</u>	
<i>Deviations from operations in response to an accident</i>	<i>Unexpected waste arising during operations</i>
	<i>Increase in waste delivery</i>
<i>Reduction in waste delivery</i>	<i>Unexpected geological event</i>
	<i>Earlier than anticipated container failure</i>
<i>Earlier than anticipated cap failure</i>	<i>Deliberate deviations from operational plans</i>
<u>Application to WMA C:</u> <i>Relevant to the performance assessment.</i>	
<u>Potentially deleterious FEP:</u> <i>Early degradation of cap safety function from unanticipated events; unexpected geological event may lead to early degradation of hydraulic safety functions in the engineered system. Early failure of barriers is addressed in sensitivity cases.</i>	

Retrievability	1.1.13
Definition: FEPs related to any special design, emplacement, operational or administrative measures that might be applied or considered in order to enable or ease retrieval of wastes.	
Comment: <i>Designs may specifically allow for retrieval or rule it out. In some cases, an interim period might be planned, between waste emplacement and final repository closure, during which time retrieval is possible.</i>	

<u>Key concepts, examples, and related FEPs</u>
None
<u>Application to WMA C:</u> Not relevant to the tank closure performance assessment. Waste has been retrieved to the extent practicable as documented in Retrieval Completion Certifications.
<u>Potentially deleterious FEP:</u> Not applicable

GEOLOGICAL PROCESSES AND EFFECTS	1.2
Definition: Processes arising from the wider geological setting and long-term processes	
Comment. "Geological Processes and Effects" is a sub-category of External Factors in the International FEP List and is divided into individual FEPs.	

Orogeny and related tectonic processes at plate boundaries	1.2.01
Definition: Rock deformation and translation (commonly referred to as tectonics) of this nature arises when rock masses belonging to different plates either collide against each other or slide past each other. Literally speaking, orogeny is the process of formation of mountains, often occurring over periods of a few million years, but up to several tens of millions of years.	
Comment: By present geological usage, orogeny is the process by which structures within mountain areas were formed through processes that include thrusting, folding and faulting in the lithosphere. The latter is the name given to the rigid, outermost layer of the earth, made up predominantly of solid rock which are affected by processes such as metamorphism, plutonism, and, at great depth (>10 km), by plastic folding. .	
<p>The term folding is generally used to imply the shortening of strata that results from the formation of fold structures on a broad scale, and sometimes has the connotation of general deformation of which the actual folding is only a part. A fault is a fracture in the Earth's crust accompanied by displacement of one side of the fracture relative to the other, from a few cm to several kilometres. Orogenic belts are typically characterized by compressive reverse faults as this lead to crustal shortening and duplication of geological formations. Transform faults typically occur where crustal plates slide past each other without colliding (e.g. the St. Andrea fault in California) and the relative displacement can be in the order of thousands of kilometers. Fractures and joints may be caused by compressional or tensional forces in the earth crust but do not present displacement between the rocks on each side. These forces may result in the reactivation of existing faults or, less likely, in the generation of new ones</p> <p>It is important to acknowledge that orogenic processes experience periods of quiescence alternating with periods of paroxysm and that such periods are not necessarily synchronous along the whole length of an orogenic belt.</p> <p>Implications to near-surface disposal systems: This type of movements should be considered with great care since orogenic processes can lead, in areas of active collision (e.g. Chile, Turkey, Iran, Morocco) to the propagation of fault and thrust planes up to the surface. In such events (see seismicity) extreme ground fracturing, faulting could lead to breakage of containment barriers</p>	

<u>Key Concepts, examples, and related FEPs</u>		
<i>Collision of the Earth's crustal plates</i>	<i>Faulting and folding of lithosphere: Thin skinned tectonics vs. Thick skinned tectonics</i>	<i>Granitic to granodioritic batholiths; calc-alkaline igneous activity</i>
<i>Transcurrent, strike-slip faults</i>		
<i>Thrusts: low-angle reverse faults;</i>	<i>Metamorphism, anatexis (partial melting/ migmatization), and plastic folding in the inner and deeper layer</i>	<i>Orogeny,</i>
<i>Subduction zones</i>		<i>Neotectonics</i>
<u>Application to WMA C:</u> <i>Not relevant on the time scale of the performance assessment.</i>		
<u>Potentially deleterious FEP:</u> <i>Not applicable</i>		

Anorogenic and within-plate tectonic processes (Deformation, elastic, plastic or brittle)		1.2.02
Definition: FEPs related to the physical deformation of geological structures in the interior of continental or oceanic plates in response to stress fields generated either at plate margins or in regions of anomalous stress. This includes mainly faulting and fracturing of rocks and, less frequently, also their compression and folding rocks.		
Comment. <i>The term folding is generally used for the compression of strata in the formation of fold structures on a broad scale, and sometimes has the connotation of general deformation of which the actual folding is only a part. A fault is a fracture in the Earth's crust accompanied by displacement of one side of the fracture relative to the other, from a few centimetres to a few kilometres on scale. Fractures may be caused by compressional or tensional forces in the Earth's crust. Such forces may result in the activation of existing faults and, less likely, the generation of new faults.</i>		
Implications to near-surface disposal systems: <i>Within the timescales of concern, deformation is unlikely to have an effect on near-surface disposal systems</i>		
<u>Key Concepts, examples, and related FEPs</u>		
<i>Faulting: normal, extensional faults</i>	<i>Fracturing</i>	<i>Basin and range</i>
<i>Extrusion</i>	<i>Compression of rocks</i>	<i>Continental; break- up</i>
<i>Neotectonics</i>	<i>Rifting, rift valleys</i>	<i>Uplift axes</i>
<i>Alkaline volcanism, volcanoes</i>	<i>Horst and grabens</i>	<i>Stress field</i>
<i>Dyke swarms</i>	<i>Jointing, master joints</i>	<i>Cross-fabrics</i>
<i>Fractures</i>	<i>Hot springs</i>	
<u>Application to WMA C:</u> <i>Not relevant on the time scale of the performance assessment.</i>		
<u>Potentially deleterious FEP:</u> <i>Not applicable</i>		

Seismicity	1.2.03
Definition: FEPs related to seismic events and the potential for seismic events. Rapid relative movements within the Earth's crust, usually along existing faults or geological interfaces cause a seismic event. The accompanying release of energy may result in ground movement and/or rupture, e.g. earthquakes.	
Comment: Seismic events may result in changes in the physical properties of rocks due to stress changes and induced hydrological changes. Seismic events are most common in tectonically active or volcanically active regions at crustal plate margins, less commonly they also occur in the interior of continental/oceanic plates. The seismic waves that are generated by a tectonic or volcanic disturbance of the ocean floor may result in a seismic (giant) sea wave, known as a tsunami. These may be amplified by submarine soft sediment slumps along steep continental margins. In extreme cases, soil liquefaction has been reported in areas where soils and sedimentary strata of appropriate moisture content and composition are subjected to strong seismic shaking.	
Key Concepts, examples, and related FEPs <div> <div>Change in the physical properties of rocks due to stress changes</div> <div>Faulting</div> <div>Seismic swarms</div> <div>Tsunami</div> <div>Soil liquefaction</div> <div>Hydrological changes</div> <div>Earthquakes</div> <div>Aftershocks</div> </div>	
Application to WMA C: Relevant to the performance assessment in considering the longevity of safety functions for the engineered barriers.	
Potentially deleterious FEP: The primary potential effects on the disposal system is degradation of hydraulic safety functions of the tank, grout, and base mat. Other safety functions would be unaffected. Potential for preferential pathways is considered in the sensitivity cases.	

Volcanic and magmatic activity	1.2.04
Definition: FEPs related to volcanic and magmatic activities. Magma is molten, mobile rock material, generated below the Earth's crust, which gives rise to igneous rocks when solidified. Magmatic activity occurs when there is intrusion of magma into the crust. A volcano is a vent or fissure in the Earth's surface through which molten or part-molten materials (lava) may flow, and ash and hot gases be expelled.	
Comment: The high temperatures and pressures associated with volcanic and magmatic activity may result in permanent changes in the surrounding rocks; this process is referred to as metamorphism but is not confined to volcanic and magmatic activity (see FEP 1.2.05). Intrusive magmatic activity refers to the process of emplacement of magma in pre-existing rock. Extrusive magmatic activity refers to the process whereby magma are ejected onto the surface of the Earth.	
Key Concepts, examples, and related FEPs <div> <div>Temperature and pressure rise</div> <div>Intrusive magmatic activity</div> <div>Pyroclastic explosion / flow / cloud</div> <div>Change in surrounding rocks</div> <div>Extrusive magmatic activity</div> <div>Fumaroles</div> <div>Slope tilting</div> <div>Lava flows</div> <div>Hydrothermal alteration</div> <div>CO₂ emissions</div> </div>	

<u>Application to WMA C:</u> Relevant to WMA C as potential ash fall from future volcanic events in the region.	
<u>Potentially deleterious FEP:</u> The effect of prior eruptions is included in the paleo record of infiltration. The effects of past ash fall events is therefore included in the uncertainty range in infiltration.	

Metamorphism	1.2.05
Definition: FEPs induced by the mineralogical and structural adjustment of solid rock to physical and chemical conditions, which have been imposed by the action of heat (T>200 C) and pressure at great depths (usually several kilometres) beneath the Earth's surface or near magmatic activity.	
Comment: Metamorphic processes are unlikely to be important at typical repository depths, but past metamorphic history of a host lithology may be very important to understanding its present-day characteristics.	
Implications to near-surface disposal systems: Within the timescales of concern, metamorphism is unlikely to have an effect on near-surface disposal systems.	
<u>Key Concepts, examples, and related FEPs</u>	
Metamorphic history of a host lithology	
<u>Application to WMA C:</u> Not relevant on the time scale of the performance assessment.	
<u>Potentially deleterious FEP:</u> Not applicable	

Hydrothermal activity	1.2.06
Definition: FEPs associated with high temperature groundwater, including processes such as density-driven groundwater flow and hydrothermal alteration of minerals in the rocks through which the high temperature groundwater flows.	
Comment: Groundwater temperature is determined by the large-scale geological and petrophysical properties of the rock formations (e.g. radiogenic heat formation, thermal conductivity), as well as the hydrogeological characteristics (e.g. hydraulic conductivity) of the rock and by the tectonic environment. (neotectonic deformation, extension).	
Implications to near-surface disposal systems: Within the timescales of concern, hydrothermal activity is unlikely to have an effect on typical near-surface disposal systems.	
<u>Key Concepts, examples, and related FEPs</u>	
<input type="checkbox"/> Hydrothermal synthesis Hydrothermal alterations of minerals in the rocks Scalding springs	
Density driven groundwater flow Hydrothermal metamorphism	
<u>Application to WMA C:</u> Not relevant to the WMA C geological setting.	
<u>Potentially deleterious FEP:</u> Not applicable	

Erosion and sedimentation	1.2.07	
Definition: FEPs related the large-scale (geological) removal and accumulation of rocks and sediments, with associated changes in topography and geological/hydrogeological conditions of the repository host lithology.		
Comment: Erosion is the process or group of processes whereby the earthy and rocky materials of the Earth’s crust are loosened, dissolved, or worn away, and simultaneously removed from one place to another, by natural agencies that include weathering, solution, corrosion, and transportation. Compare FEP 2.3.12, which is concerned with more local processes over shorter periods of time. Sedimentation is the act or process of forming or accumulating sediment in layers, including such processes as the separation of rock particles from the material from which the sediment is derived, the transportation of these particles to the site of deposition or settling of the particles, the chemical and other (diagenetic) changes occurring in the sediment, and the ultimate consolidation of the sediment into solid rock.		
Implications to near-surface disposal systems: Within the timescales of concern, large scale erosion and sedimentation are unlikely to have an effect on near-surface disposal systems.		
Key Concepts, examples, and related FEPs		
Change in topography, uplift	Deposition of sediment	Stream erosion
Coastal erosion	Changes in geological conditions	Changes in hydrogeological conditions
Application to WMA C: Relevant to the performance assessment in considering the longevity of safety functions for the engineered cover.		
Potentially deleterious FEP: The primary potential effects on the disposal system is degradation of the infiltration safety functions of the cover. Other safety functions would be unaffected. Potential increases in infiltration through the cover are addressed in sensitivity cases.		

Diagenesis and pedogenesis	1.2.08
Definition: The processes by which deposited sediment, at or near the Earth’s surface are formed into rocks by compaction, cementation and crystallisation, i.e. under conditions of temperature and pressure normal to the upper few kilometres of the earth’s crust.	
Comment: Diagenesis include all the chemical, physical, and biological changes, modifications, or transformations undergone by a sediment after its initial deposition, and during and after its lithification, exclusive or surficial alteration (weathering) and metamorphism. It embraces those non-destructive or reconstructive processes (e.g., consolidation, compaction, cementation, reworking, authigenesis, replacement, solution, precipitation, crystallisation, oxidation, reduction, leaching, hydration, polymerisation, adsorption, bacterial action, and formation of concretions) that occur under conditions of pressure and temperature that are normal to the surficial or outer part of the Earth’s crust.	
Pedogenesis represents the mode of origin of soils, with reference to the factors responsible for the formation of “solum”, or true soil, from unconsolidated parent material. Pedogenesis may have an effect on the behaviour of near surface disposal systems as it involves geohydrologic, atmospheric and biological processes (burrowing animals, plant roots activity/invasion) operation at or near surface on time scales of few hundred to thousands of years	
Implications to near-surface disposal systems: Within the timescales of concern, diagenesis is unlikely to have an effect on near-surface disposal systems	

<u>Key Concepts, examples, and related FEPs</u>
None
<u>Application to WMA C:</u> Not relevant to the WMA C geological setting.
<u>Potentially deleterious FEP:</u> Not applicable

Salt diapirism and dissolution	1.2.09
Definition: The long-term evolution of salt formations. Diapirism is the lateral or vertical intrusion or upwelling of either buoyant or non-buoyant rock into overlying strata (the overburden) from a source layer. Dissolution of the salt may occur where the evolving salt formation is in contact with groundwater with salt content below saturation.	
Comment: Diapirism is most commonly associated with salt formations where a salt diapir comprises a mass of salt that has flowed in a ductile manner from a source layer and pierces or intrudes into the over-lying rocks. The term can also be applied to magmatic or migmatic intrusion.	
Implications to near-surface disposal systems: Within the timescales of concern, salt diapirism and dissolution are unlikely to have an effect on near-surface disposal system.	
<u>Key Concepts, examples, and related FEPs</u>	
Diapirism	Brine pockets
<u>Application to WMA C:</u> Not relevant to the WMA C geological setting.	
<u>Potentially deleterious FEP:</u> Not applicable	

Hydrological/hydrogeological response to geological changes	1.2.10
Definition: FEPs related to changes in the hydrological or hydrogeological regime arising from the large-scale geological changes listed in FEPs 1.2.01 to 1.2.09.	
Comment: These could include changes of hydrological boundary conditions due to effects of erosion on topography, changes of hydraulic properties of saturated and unsaturated zones due to changes in rock stress or fault movements, or a change in the geochemical behaviour of the saturated and unsaturated zones. In and below low-permeability geological formations, hydrogeological conditions may evolve very slowly and often reflect past geological conditions, i.e. be in a state of disequilibrium	
<u>Key Concepts, examples, and related FEPs</u>	
Geochemical change	Changes in hydraulic properties
	Changes of hydrological boundary conditions
<u>Application to WMA C:</u> Regional scale geological changes may influence the Columbia River, which has a controlling influence on aquifer flow under the Central Plateau.	
<u>Potentially deleterious FEP:</u> Potential effects on the saturated zone flow safety functions. Variations in saturated zone flow are considered in sensitivity analyses.	

CLIMATIC PROCESSES AND EFFECTS	1.3
Definition: Processes related to global climate change and consequent regional effects.	
Comment: "Climatic Processes and Effects" is a sub-category of External Factors in the International FEP List and is divided into individual FEPs.	

Climate change, global	1.3.01	
Definition: FEPs related to the possible future, and evidence for past, long-term change of global climate. This is distinct from resulting changes that may occur at specific locations according to their regional setting and also climate fluctuations, c.f. FEP 1.3.02.		
Comment: <i>The last two million years of the Quaternary have been characterized by glacial/interglacial cycling. According to the Milankovitch Theory, the Quaternary glacial/interglacial cycles are caused by long term changes in seasonal and latitudinal distribution of incoming solar radiation which are due to the periodic variations of the Earth's orbit about the Sun (Milankovitch cycles). The direct effects are magnified by factors such as changes in ice, vegetation and cloud cover, and atmospheric composition.</i>		
<u>Key Concepts, examples, and related FEPs</u>		
Description of global climate changes	Changes in ice, vegetation and cloud cover	Isostatic movement (c.f. FEP 1.3.03)
Changes in atmospheric composition	Greenhouse effect	Glaciation (large scale)
Eustatic change (c.f. FEP 1.3.03)		
<u>Application to WMA C:</u> Climate change may affect infiltration and saturated zone flow safety functions. However, global climate changes are expressed locally in these processes. See FEP 1.3.02. See Section 3 for a discussion of the basis for long term precipitation estimation.		
<u>Potentially deleterious FEP:</u> Not relevant.		

Climate change, regional and local	1.3.02
Definition: FEPs related to the possible future changes, and evidence for past changes, of climate at the repository site. This is likely to occur in response to global climate change, but the changes will be specific to situation, and may include shorter-term fluctuations, c.f. FEP 1.3.01.	
Comment: <i>Climate is characterized by a range of factors including temperature, humidity, precipitation and pressure as well as other components of the climate system such as oceans, ice and snow, biota and the land surface. The Earth's climate varies by location and for convenience broad climate types have been distinguished in assessments, e.g. tropical, savannah, mediterranean, temperate, boreal and tundra. Climatic changes lasting only a few decades are referred to as climatic fluctuations. These are unpredictable at the current state of knowledge although historical evidence indicates the degree of past fluctuations.</i>	

<u>Key Concepts, examples, and related FEPs</u>		
Climate fluctuations Increase/decrease in precipitation)	Description of regional and local climate change	Increase/decrease in temperature
<u>Application to WMA C:</u> Climate change may affect infiltration and saturated zone flow. However, global climate changes are expressed locally in these processes. See FEP 1.3.01. See Section 3 for a discussion of the basis for long term precipitation estimation.		
<u>Potentially deleterious FEP:</u> Changes in infiltration associated with climate change are uncertain. Regional scale modelling shows either increases or decreases in future infiltration, with the magnitude of the changes within the pattern of the paleo record. The response of the aquifer system to climate change is uncertain. Climate change may potentially affect safety functions for the cover and for the saturated zone. Ranges of infiltration and aquifer flow are considered in sensitivity cases.		

Sea level change	1.3.03
Definition: FEPs related to changes in sea level, which may occur as a result of global (eustatic) change and regional geological change, e.g. isostatic movements.	
Comment: The component of sea-level change involving the interchange of water between land ice and the sea is referred to as eustatic change. As ice sheets melt so the ocean volume increases and sea levels rise. Sea level at a given location will also be affected by vertical movement of the land mass, e.g. depression and rebound due to glacial loading and unloading, referred to as isostatic change (c.f. FEP 1.3.01).	
<u>Key Concepts, examples, and related FEPs</u>	
Flooding	Saline intrusion into repository or geosphere Change in the hydrogeological regime
<u>Application to WMA C:</u> Sea level change may affect Columbia River stage, with subsequent influence on aquifer flow.	
<u>Potentially deleterious FEP:</u> Potential effect on saturated zone safety functions by alteration of the gradient.	
Periglacial effects	1.3.04
Definition: FEPs related to the physical processes and associated landforms in cold but ice-sheet-free environments. This may be at the immediate margins of former and existing glaciers and ice sheets or an environment in which frost actions is dominant.	
Comment: An important characteristic of periglacial environments is the seasonal change from winter freezing to summer thaw with large water movements and potential for erosion. The frozen subsoils are referred to as permafrost. Meltwater of the seasonal thaw is unable to percolate downwards due to permafrost and saturates the surface materials, this can result in a mass movement called solifluction (literally soil-flow). Permafrost layers may isolate the deep hydrological regime from surface hydrology, or flow may be focused at “taliks” (localized unfrozen zones, e.g. under lakes, large rivers or at regions of groundwater discharge).	
<u>Key Concepts, examples, and related FEPs</u>	
Large water movement	Strong seasonal influences Permafrost
Erosion	Soil flow (movement) – solifluction Saturation of surface materials

Application to WMA C: Not relevant on the time scale of the performance assessment. However, pollen data records provide information that extends through past glacial cycles. See Section 3.

Potentially deleterious FEP: Not applicable

Glacial and ice sheet effects, local	1.3.05
Definition: FEPs related to the effects of glaciers and ice sheets within the region of a repository, e.g. changes in the geomorphology, erosion, meltwater and hydraulic effects. This is distinct from the effect of large ice masses on global and regional climate, c.f. FEPs 1.3.01, 1.3.02.	
Comment: Erosional processes (abrasion, over-deepening) associated with glacial action, especially advancing glaciers and ice sheets, and with glacial meltwaters beneath the ice mass and at the margins, can lead to morphological changes in the environment e.g. U-shaped valleys, hanging valleys, fjords and drumlins. Depositional features associated with glaciers and ice sheets include moraines and eskers. The pressure of the ice mass on the landscape may result in significant and even depression of the regional crustal plate.	
<u>Key Concepts, examples, and related FEPs</u> <div> <div>Erosional processes (abrasion, over-deepening)</div> <div>Morphological changes (Hanging valleys, Fjords, Drumlins)</div> <div>Hydrogeological change</div> <div>Depression of the regional crustal plate</div> <div>Transportation and depositional processes and features (Moraines Eskers)</div> </div>	
<u>Application to WMA C:</u> Not relevant on the time scale of the performance assessment.	
<u>Potentially deleterious FEP:</u> Not applicable	

Warm climate effects (tropical and desert)	1.3.06
Definition: FEPs related to warm tropical and desert climates, including seasonal effects, and meteorological and geomorphological effects special to these climates.	
Comment: Regions with a tropical climate may experience extreme weather patterns (monsoons, hurricanes), that could result in flooding, storm surges, high winds etc. with implications for erosion and hydrology. The high temperatures and humidity associated with tropical climates result and soils are generally thin. In arid climates, total rainfall, erosion and recharge may be dominated by infrequent storm events.	

<u>Key Concepts, examples, and related FEPs</u>		
Extreme weather patterns	Alkali flats	Effective recharge
Monsoons	Infrequent storm events	Change in hydrological regime
Hurricanes	High rainfall	Rapid biological degradation
Flooding	High winds	Erosion
Storm surges		
<u>Application to WMA C:</u> Relevant in evaluation of the infiltration rate. See Section 3.		
<u>Potentially deleterious FEP:</u> Effects are included in estimates and uncertainties in the infiltration rate.		

Hydrological/hydrogeological response to climate changes		1.3.07
Definition: FEPs related to changes in the hydrological and hydrogeological regime, e.g. recharge, sediment load and seasonality, in response to climate change in a region.		
Comment: The hydrology and hydrogeology of a region is closely coupled to climate. Climate controls the amount of precipitation and evaporation, seasonal ice cover and thus the soil water balance, extent of soil saturation, surface runoff and groundwater recharge. Vegetation and human actions may modify these responses.		
<u>Key Concepts, examples, and related FEPs</u>		
Change in groundwater recharge	Change in regional precipitation/infiltration/evaporation	Change in surface runoff
Change in sediment load		Increase in groundwater velocity
Change in soil water balance	Change in seasonal ice cover	Creation of local ponds
<u>Application to WMA C:</u> Relevant in evaluating the infiltration rate.		
<u>Potentially deleterious FEP:</u> This FEP has the potential to affect the cover infiltration safety function. Effects of climate change on infiltration are included in the range of rates derived from the paleo record on precipitation. Potential anthropogenic effects are within the range of past climates. See Section 3.		

Ecological response to climate changes	1.3.08
Definition: FEPs related to changes in ecology, e.g. vegetation, plant and animal populations, in response to climate change in a region.	
Comment: The ecology of an environment is linked to climate. Ecological adaptation has allowed flora and fauna to survive and exploit even the most hostile of environments. For example, cacti have evolved to survive extreme heat and desiccation of the desert environment, and certain plant species complete their entire lifecycle over very short time periods following rare rain events in the desert. Some tree and plant species have evolved to survive natural events such as forest fires, and may require them to complete their lifecycle	

<u>Key Concepts, examples, and related FEPs</u>		
Desert formation	Change in animal life	Ecological adaptation
Change in vegetation		
<u>Application to WMA C:</u> Relevant in evaluating the infiltration rate.		
<u>Potentially deleterious FEP:</u> This FEP has the potential to affect the cover infiltration safety function by altering the plant community over the waste. Variation in infiltration rates are considered, barrier testing has included conditions following loss of vegetation.		

Human response to climate changes	1.3.09
Definition: FEPs related to changes in human behaviour, e.g. habits, diet, size of communities, in response to climate change in a region.	
Comment: Human response is closely linked to climate. Climate affects the abundance and availability of natural resources such as water, as well as the types of crops that can be grown. The more extreme a climate, the greater the extent of human control over these resources is necessary to maintain agricultural productivity, e.g. through the use of dams, irrigation systems, controlled agricultural environments (greenhouses).	
<u>Key Concepts, examples, and related FEPs</u>	
Change in human habits	Increase/decrease in usage of irrigation systems
Effect of climate change on food chain	Change in population density
Change in agricultural activities/products	Change in diet
<u>Application to WMA C:</u> Addressed in the exposure assessment requirements in DOE Order 435.1.	
<u>Potentially deleterious FEP:</u> Not applicable.	

Other geomorphologic changes	1.3.10
Definition: FEPs related to geomorphologic (also known as physiography) changes on a regional and local scale, i.e. the general configuration of the Earth's surface.	
Comment: Geomorphology refers to the classification, description, nature, origin and development of present landforms and their relationships to underlying structures, and of the history of geologic changes as recorded by these surface features. The term is especially applied to the generic interpretation of landforms, but has also been restricted to features produced only by erosion and deposition.	
<u>Key Concepts, examples, and related FEPs</u>	
Denudation	

Application to WMA C: Relevant in to WMA C in the morphological changes associated with adding the cover, with increased depth to the waste.

Potentially deleterious FEP: Not applicable

FUTURE HUMAN ACTIONS (ACTIVE)

1.4

Definition: Human actions and regional practices, in the post-closure period, that can potentially affect the performance of the engineered and/or geological barriers, e.g. intrusive actions, but not the passive behaviour and habits of the local population, c.f. 2.4.

Comment: Human Actions (Active)" is a sub-category of the External Factors in the International FEP List and is divided into individual FEPs.

Human influences on climate

1.4.01

Definition: FEPs related to human activities that could affect the change of climate either globally or in a region.

Comment: These activities could be intentional or unintentional, with an indirect influence more than a direct influence on the climate.

Key Concepts, examples, and related FEPs

De-forestation

Emissions of 'greenhouse' gases such as CO₂ and CH₄

Application to WMA C: Relevant in evaluating the infiltration rate. Projected anthropogenic effects on future climates may be either increases or decreases in infiltration rate.

Potentially deleterious FEP: This FEP has the potential to affect the cover infiltration safety function. Effects of climate change on infiltration are included in the range of rates derived from the paleo record on precipitation. Potential anthropogenic effects are within the range of past climates.

Motivation and knowledge issues (inadvertent/deliberate human actions)

1.4.02

Definition: FEPs related to the degree of knowledge of the existence, location and/or nature of the repository. Also, reasons for deliberate interference with, or intrusion into, a repository after closure with complete or incomplete knowledge.

Comment: Some future human actions e.g. see FEPs 1.4.03 and 1.4.04, could directly impact upon the repository performance. Many assessments distinguish between:

- inadvertent actions, which are actions taken without knowledge or awareness of the repository, and
- deliberate actions, which are actions that are taken with knowledge of the repository's existence and location, e.g. deliberate attempts to retrieve the waste, malicious intrusion and sabotage.

Intermediate cases, of intrusion with incomplete knowledge, could also occur.

<u>Key Concepts, examples, and related FEPs</u>		
Human intrusion (instigate mechanical processes Incomplete knowledge intrusion)	Deliberate actions e.g. war, sabotage, waste recovery, malicious intrusion	Inadvertent actions e.g. exploratory drilling, resource mining, archaeological intrusion
<u>Application to WMA C:</u> Not relevant for the WMA C performance assessment, since this FEP relates to probability of occurrence of inadvertent intrusion, which is not taken credit for in the assessment. Adverent intrusion is generally excluded from consideration in the international community of performance assessment.		
<u>Potentially deleterious FEP:</u> Not applicable.		

Drilling activities (human intrusion)	1.4.03	
Definition: FEPs related to any type of drilling activity near the repository.		
<i>Comment: These activities may be taken with or without knowledge of the repository and in fact is a subgroup of FEP 1.4.02.</i>		
<u>Key Concepts, examples, and related FEPs</u>		
Exploratory and/or exploitation drilling for natural resources and raw materials	Water well drilling	Drilling for hydrothermal resources
	Drilling for waste injection	Extraction of valuable components of the disposed waste
Drilling for research or site characterization studies		
<u>Application to WMA C:</u> Relevant to the intrusion scenario.		
<u>Potentially deleterious FEP:</u> Addressed in the evaluation of inadvertent intrusion.		
Mining and other underground activities (human intrusion)	1.4.04	
Definition: FEPs related to any type of mining or excavation activity carried out near the repository.		
<i>Comment: These activities may be taken with or without knowledge of the repository and in fact is a subgroup of FEP 1.4.02.</i>		

<u>Key Concepts, examples, and related FEPs</u>		
Resource mining;	Shaft construction, underground construction and tunnelling	Malicious intrusion, sabotage or war
Excavation for industry;		Injection of liquid wastes and other fluids
Geothermal energy production	Recovery of repository materials (re-use of waste)	Scientific underground investigation
Mine drillings	The presence of mine galleries - after closure	Underground nuclear testing
<u>Application to WMA C:</u> <i>Drilling activities accounted for in the drilling intrusion scenario. Other mining activities excluded based on lack of resources as WMA C. Potential for intrusive activities is also limited by depth of waste disposal and presence of intrusion barriers.</i>		
<u>Potentially deleterious FEP:</u> <i>Not applicable.</i>		

Un-intrusive site investigation	1.4.05
Definition: FEPs related to airborne, geophysical or other surface-based investigation of a repository site after repository closure	
Comment: <i>Such investigation, e.g. prospecting for geological resources, might occur after information of the location of a repository had been lost. The evidence of the repository itself, e.g. discovery of an old shaft, might itself prompt investigation, including research of historical archives.</i>	
<u>Key Concepts, examples, and related FEPs</u>	
Prospecting for geological resources	Investigation of an old shaft Research of historical archives
<u>Application to WMA C:</u> <i>Not relevant as this FEP relates to probabilities of intrusion, which are not taken credit for in the performance assessment.</i>	
<u>Potentially deleterious FEP:</u> <i>Not applicable.</i>	

Surface excavations	1.4.06
Definition: FEPs related to any type of human activities during surface excavations that can potentially affect the performance of the engineered and/or natural (geological) barriers, or the exposure pathways.	

Comment: This FEP relates to the surface environment. Strictly speaking, excavation refers to an act or process of removing soil and or rock materials from one location and transporting them to another. This may include, for example, digging, blasting, breaking, loading and hauling, which may result in direct human intrusion in the case of a near-surface repository.		
<u>Key Concepts, examples, and related FEPs</u>		
Quarrying, trenching, ploughing	Dredging of sediments in estuaries	Shallow excavations for site investigations
Digging, blasting, breaking, loading, hauling	Excavation for construction (earthworks)	Excavation for military purposes
Recycling of materials	Excavation for storage or disposal	
<u>Application to WMA C:</u> Home construction basement scenario excluded based on depth of waste disposal and presence of intrusion barriers.		
<u>Potentially deleterious FEP:</u> Not applicable.		

Pollution	1.4.07
Definition: FEPs related to any type of human activities associated with pollution that can potentially affect the performance of the engineered and/or natural (geological) barriers, or the exposure pathways.	
Comment: As used here, it refers to the alteration of the chemical composition of the surface environment in the vicinity of the repository, in such a way that the performance of the disposal system is influenced.	
<u>Key Concepts, examples, and related FEPs</u>	
Acid rain	Soil pollution
Chemical liquid waste disposal	Soil fertilization
	Groundwater pollution
<u>Application to WMA C:</u> Relevant to WMA C in potential changes to the degradation rates of the engineered barriers. Effects of past leaks on vadose zone properties.	
<u>Potentially deleterious FEP:</u> Potential effects in engineered barrier safety functions related to flow reduction. Effects of past leaks on vadose zone properties.	

Site development	1.4.08
Definition: FEPs related to any type of human activities during site development that can potentially affect the performance of the engineered and/or natural (geological) barriers, or the exposure pathways	

Comment: As used here, site development refers to alterations to the surface environment after memory of the repository has been lost. These alterations may result in direct human intrusion in the near-surface facility, or to an alteration of the host lithology or topography.		
<u>Key Concepts, examples, and related FEPs</u>		
Site occupation	Construction of roads, houses, buildings, dams, etc.	Residential, industrial, transport and road construction
Levelling of hills (e.g., airport lay out)	Human modification of the site drainage	Land reclamation/extension
<u>Application to WMA C:</u> Relevant to WMA C in potential changes to the degradation rates of the cover.		
<u>Potentially deleterious FEP:</u> Potential effects in the cover function for infiltration considered in sensitivity cases.		

Archaeology	1.4.09
Definition: FEPs related to any type of human activities associated with archaeology that can potentially affect the performance of the engineered and/or natural (geological) barriers, or the exposure pathways.	
Comment: As used here, the FEP refers to archaeological investigations in the surface environment.	
<u>Key Concepts, examples, and related FEPs</u>	
Archaeological, inadvertent human intrusion	Archaeological artefacts find during construction
<u>Application to WMA C:</u> Not relevant as this FEP relates to probabilities of intrusion, which are not taken credit for in the performance assessment.	
<u>Potentially deleterious FEP:</u> Not applicable.	

Water management (wells, reservoirs, dams)	1.4.10
Definition: FEPs related to groundwater and surface water management including water extraction, reservoirs, dams, and river management.	
Comment: Water is a valuable resource and water extraction and management schemes provide increased control over its distribution and availability through construction of dams, barrages, canals, pumping stations and pipelines. Groundwater and surface water may be extracted for human domestic use (e.g. drinking water, washing), agricultural uses (e.g. irrigation, animal consumption) and industrial uses. Extraction and management of water may affect the movement of radionuclides to and in the surface environment.	

<u>Key Concepts, examples, and related FEPs</u>		
Waterworks	Intentional artificial groundwater recharge/discharge by humans	Extraction of contaminated water from aquifer via a well
Artificial mixing of lakes		Impoundment of water for fishing/fish farming, bathing
Reservoirs	Dam, barrage, canals, pumping stations and pipeline building	Groundwater/surface water extraction for irrigation, animal consumption, drinking water, washing
Industrial usage	Desalination of water in estuaries and marines	Salt production
Human effects on water potential	Drainage systems	
Chemical liquid waste disposal		
<u>Application to WMA C:</u> Water management activities on the Columbia River have the potential to affect river stage.		
<u>Potentially deleterious FEP:</u> Potential effects on the saturated zone safety functions are consider in sensitivity cases for aquifer flow.		

Social and institutional developments	1.4.11
Definition: FEPs related to changes in social patterns and degree of local government, planning and regulation.	
Comment: The decisions made in future concerning social and institutional development may have a significant influence on the disposal system, e.g., if a change in land use is promulgated or a change in the regulatory requirements.	
<u>Key Concepts, examples, and related FEPs</u>	
Loss of archives/records, loss/degradation of societal memory	Changes in land use
Changes in planning controls and environmental legislation	Change in regulatory requirements
Demographic change and urban development	Change in institutional control
<u>Application to WMA C:</u> Excluded from consideration in DOE Order 435.1.	
<u>Potentially deleterious FEP:</u> Not applicable.	

Technological developments	1.4.12
Definition: FEPs related to future developments in human technology and changes in the capacity and motivation to implement technologies. This may include retrograde developments, e.g. loss of capacity to implement a technology.	

Comment: Of interest are those technologies that might change the capacity of man to intrude deliberately or otherwise into a repository, to cause changes that would affect the movement of contaminants, to affect the exposure or its health implications. Technological developments are likely but may not be predictable especially at longer times into the future. In most assessments, assumptions are made to limit the scope of consideration.

Key Concepts, examples, and related FEPs

Retrograde developments

Loss of capacity to implement technology

Application to WMA C: Excluded from consideration in DOE Order 435.1.

Potentially deleterious FEP: Not applicable.

Remedial actions	1.4.13
Definition: FEPs related to actions that might be taken following repository closure to remediate problems with a waste repository that, either, was not performing to the standards required, had been disrupted by some natural event or process, or had been inadvertently or deliberately damaged by human actions.	
Comment:	
<u>Key Concepts, examples, and related FEPs</u>	
None	
<u>Application to WMA C:</u> Excluded from consideration in DOE Order 435.1.	
<u>Potentially deleterious FEP:</u> Not applicable.	

Explosions and crashes	1.4.14
Definition: FEPs related to deliberate or accidental explosions and crashes such as might have some impact on a closed repository, e.g. underground nuclear testing, aircraft crash on the site, acts of war.	
Comment:	
<u>Key Concepts, examples, and related FEPs</u>	
Intrusions by war, sabotage, terrorism	Likelihood of crashes onto surface facilities, e.g. plane crashes
Underground nuclear testing	
<u>Application to WMA C:</u> Potentially relevant to the performance of the cover, but very low probability of occurrence.	
<u>Potentially deleterious FEP:</u> Potential relevance to the surface barrier safety function for infiltration. However, it is excluded from consideration based on very low probability of occurrence.	

DISPOSAL SYSTEM DOMAIN: ENVIRONMENTAL FACTORS	2
Definition: Features and processes occurring within that spatial and temporal (post-closure) domain whose principal effect is to determine the evolution of the physical, chemical, biological and human conditions of the domain that are relevant to estimating the release and migration of radionuclides and consequent exposure to man.	
Comment: "Disposal System Domain: Environmental Factors" is a category in the International FEP List and is divided into sub-categories.	

WASTES AND ENGINEERED FEATURES	2.1
Definition: Features and processes within the waste and engineered components of the disposal system. (output – source term characteristics)	
Comment: "Wastes and Engineered Features" is a sub-category of Disposal Domain:Environmental Factors in the International FEP List and is divided into individual FEPs.	
<i>Note that FEPs 2.1.01 to 2.1.06 describe the features in the disposal system, in other words, a description of the system as it is constructed, whereas FEPs 2.1.07 to 2.1.11 describe the processes or the changes in the disposal system.</i>	

Inventory, radionuclide and other material	2.1.01
Definition: FEPs related to the total content of the repository of a given type of material, substance, element, individual radionuclides, total radioactivity or inventory of toxic substances.	
Comment: The FEP often refers to content of radionuclides but the content of other materials, e.g. steels, other metals, concrete or organic materials, could be of interest.	
<u>Key Concepts, examples, and related FEPs</u>	
Radionuclide content	Concrete or organic material content
	Steel and other metal content

Waste form materials, characteristics and degradation processes	2.1.02
Definition: FEPs related to the physical, chemical, biological characteristics of the waste form at the time of disposal and as they may evolve in the repository, including FEPs which are relevant specifically as waste degradation processes.	
Comment: The waste form will usually be conditioned prior to disposal, e.g. by solidification and inclusion of grout materials. The waste form is a component of the waste package. The waste characteristics will evolve due to various processes that will be affected by the physical and chemical conditions of the repository environment. Processes that are relevant specifically as waste degradation processes, as compared to general evolution of the near field, are included in this FEP.	

<u>Key Concepts, examples, and related FEPs</u>		
Physical degradation	Ash	Activated metal
Chemical degradation	Cloves, clothing, plastics, paper wood	Sludges, evaporation residue, compacted solids, filters
Solid matrix of resin, bitumen, cement	Spent sources	
<u>Application to WMA C:</u> Relevant to the performance assessment.		
<u>Potentially deleterious FEP:</u> Uncertainties in the inventory of residual waste and its chemical and physical form. Uncertainty in the final amounts of waste in as-yet unretrieved tanks.		

Container materials, characteristics and degradation/failure processes		2.1.03
Definition: FEPs related to the physical, chemical, biological characteristics of the container at the time of disposal and as they may evolve in the repository, including FEPs that are relevant specifically as container degradation/failure processes.		
Comment: The container refers to the vessel into which the waste form is placed for handling, transportation, storage and or disposal. It is also the outer barrier protecting the waste from external intrusions. The container is a component of the waste package.		
<u>Key Concepts, examples, and related FEPs</u>		
Container degradation/failure processes	Concrete containers	Lead containers
Metal drums	Stainless steel containers	
<u>Application to WMA C:</u> Not relevant to the performance assessment. Waste is not containerized		
<u>Potentially deleterious FEP:</u> Not applicable.		

Buffer/backfill materials, characteristics and degradation processes		2.1.04
Definition: FEPs related to the physical, chemical, biological characteristics of the buffer and/or backfill at the time of disposal and as they may evolve in the repository, including FEPs that are relevant specifically as buffer/backfill degradation processes. (Effect on hydrology / flow)		
Comment: Buffer and backfill are sometimes used synonymously. In some HLW/spent fuel concepts, the term buffer is used to mean material immediately surrounding a waste container and having some chemical and/or mechanical buffering role whereas backfill is used to mean material used to fill other underground openings. However, in ILW/LLW concepts the term backfill is used to describe the material placed between waste containers, which may have a chemical role. Buffer/backfill materials may include clays, cement and mixtures of cement with aggregates, e.g. of crushed rock.		
The buffer/backfill characteristics will evolve due to various processes that will be affected by the physical and chemical conditions of the repository environment. Processes, which are relevant specifically as buffer/backfill degradation processes, as compared to general evolution of the near field, are included in this FEP.		

<u>Key Concepts, examples, and related FEPs</u>		
Buffer/backfill degradation processes Bentonite clay	Clay, cement, sand, soil	Mixture of clay and crushed rock
<u>Application to WMA C:</u> Relevant to the performance assessment as the grout infill.		
<u>Potentially deleterious FEP:</u> Uncertainty in the performance of the grout is considered in sensitivity and uncertainty analysis.		

Engineered barrier system characteristics and degradation processes		2.1.05
Definition: FEPs related to the design, physical, chemical, hydraulic etc. characteristics of the cavern/tunnel/shaft seals at the time of sealing and closure and also as they may evolve in the repository, including FEPs which are relevant specifically as cavern/tunnel/shaft seal and cap degradation processes. (Effect on hydrology / flow – change over time).		
Comment: Cavern/tunnel/shaft seal and cap failure may result from gradual degradation processes, or may be the result of a sudden event. The importance is that alternative routes for groundwater flow and radionuclide transport may be created along the various layers and tunnels and/or shafts and associated EDZ (see FEP 2.2.01).		
<u>Key Concepts, examples, and related FEPs</u>		
Engineered caps (cover) Cover degradation	Intrusion resistance caps	Cap materials: clay, concrete
<u>Application to WMA C:</u> Relevant to the performance assessment as the tank structure, base mat, and cover system.		
<u>Potentially deleterious FEP:</u> Uncertainties in the current state and long term performance of the engineered barriers is addressed in sensitivity and uncertainty analysis.		

Other engineered features materials, characteristics and degradation processes		2.1.06
Definition: FEPs related to the physical, chemical, biological characteristics of the engineered features (other than containers, buffer/backfill, caps and seals) at the time of disposal and also as they may evolve in the repository, including FEPs which are relevant specifically as degradation processes acting on the engineered features.		
Comment: Examples of other engineered features are rock bolts, shotcrete, tunnel liners, silo walls, any services and equipment not removed before closure. The engineered features, materials and characteristics will evolve due to various processes that will be affected by the physical and chemical conditions of the repository environment. Processes which are relevant specifically as degradation processes acting on the features, as compared to general evolution of the near field, are be included in this FEP.		

<u>Key Concepts, examples, and related FEPs</u>		
Trenches, holes, vaults	Reduction in flow through structures due to impermeable membrane and subsequent degradation of impermeable membrane	Cut-off walls
Walls, floors, mounds, layers of mounds		Degradation processes
Rock bolts, tunnel liners, silo walls		
<u>Application to WMA C:</u> Relevant to pipes and structures associated with ancillary equipment.		
<u>Potentially deleterious FEP:</u> Not applicable, as the ancillary equipment is treated conservatively in the base case,		

Mechanical processes and conditions (in wastes and EBS)		2.1.07
Definition: FEPs related to the mechanical processes that affect the wastes, containers, seals and other engineered features, and the overall mechanical evolution of near field with time. This includes the effects of hydraulic and mechanical loads imposed on wastes, containers and repository components by the surrounding geology.		
Comment:		
<u>Key Concepts, examples, and related FEPs</u>		
Waste and container compression	Subsidence as a result of compression of waste and cover layers	Container movement
Container collapse		Differential behaviour of joints
Buffer swelling pressure	Fracture formation in vault, backfill, joints, cover materials, host geology (local fractures)	Tunnel roof or lining collapse
Material volume changes		
<u>Application to WMA C:</u> Relevant to the performance assessment in the influence of the FEP to conditions of the base mat.		
<u>Potentially deleterious FEP:</u> Potential degradation in the current state and future evolution of the base mat hydraulic safety function which is considered in the sensitivity and uncertainty analysis.		

Hydraulic/hydrogeological processes and conditions (in wastes and EBS)		2.1.08
Definition: FEPs related to the hydraulic/hydrogeological processes that affect the wastes, containers, seals and other engineered features, and the overall hydraulic/hydrogeological evolution of near field with time. This includes the effects of hydraulic/hydrogeological influences on wastes, containers and repository components by the surrounding geology.		
Comment:		

H-54

RPP-ENV-58782, Rev. 0

<u>Key Concepts, examples, and related FEPs</u>		
Failure of drainage system	Modification of pore water by cover caused by chemical	Osmotic effects
Failure of cut-off walls	Interaction of vault material with pore water pH change	Infiltration and movement of fluids in the repository environment
Failure of cap/cover		Resaturation/desaturation of the repository or its components
Failure of the joints	Redox potential change	Water flow and contaminant transport paths within the repository
Bathtubbing	Mineralization	
Fracturing of concrete components	Modification of pore water by cover	Induced fluid effects caused by temperature change
Effect of cap+cover+backfill	Interaction of container material with pore water	-Pressure change
Influence of climate change	Matrix corrosion	-Natural convection
Influence of saline intrusion	Gas generation	-Viscosity
Gas mediated water flow	Polymer degradation (high integrity containers)	Reduction in flow through structures due to grouting
Interaction of backfill with pore water	Mineralization change	Chloride attack
pH change	Osmotic effect	Sulphate attack
Redox change	Interaction of vault materials with host groundwater	Colloid formation
Sulphate attack	Carbonation	
Effect of chelating agents		
<u>Application to WMA C:</u> Relevant to the performance assessment in the influence of the FEP to release and transport of waste from tanks and ancillary equipment.		
<u>Potentially deleterious FEP:</u> Uncertainty in the current state and future evolution of the safety functions of the waste, grout, tank, and base mat is considered in the sensitivity and uncertainty analysis		

Chemical/geochemical processes and conditions (in wastes and EBS)	2.1.09
Definition: FEPs related to the chemical/geochemical processes that affect the wastes, containers, seals and other engineered features, and the overall chemical/geochemical evolution of near field with time. This includes the effects of chemical/geochemical influences on wastes, containers and repository components by the surrounding geology.	
Comment:	

<u>Key Concepts, examples, and related FEPs</u>		
<i>Chemical interaction of backfill with pore water</i>	<i>Chemical interaction of waste with pore water</i>	<i>Induced galvanic metallic corrosion</i>
<i>pH changes</i>	<i>Metallic corrosion processes (general and pitting)</i>	<i>Polymer degradation (high integrity containers)</i>
<i>Redox changes</i>	<i>Polymer degradation (resins)</i>	<i>Chemical interaction of backfill with containers (including overpacks)</i>
<i>Sulphate attack</i>	<i>Osmotic effects</i>	<i>Induced galvanic metallic corrosion</i>
<i>Osmotic effects</i>	<i>Chemical interaction of containers (including overpacks) with pore water</i>	<i>Polymer degradation (high integrity containers)</i>
<i>Chemical interaction of vault materials with pore water</i>	<i>Metallic corrosion</i>	<i>Chemical interaction of non-radioactive waste components with radioactive waste components</i>
<i>pH changes</i>	<i>Polymer degradation (high integrity containers)</i>	<i>pH changes</i>
<i>Redox potential changes</i>	<i>Osmotic effects</i>	<i>Redox potential changes</i>
<i>Chemical interaction of vault materials with host groundwater</i>	<i>Chemical interaction of waste with containers</i>	<i>Change in chemical reaction rate caused by temperature change</i>
<i>Carbonation</i>	<i>Precipitation/dissolution reactions</i>	<i>Electrochemical processes</i>
<i>Chloride attack</i>	<i>Evolution of redox (Eh) and acidity/alkalinity (pH) etc.</i>	<i>Chemical conditioning and buffering processes</i>
<i>Sulphate attack</i>	<i>Silting/pore closure</i>	
	<i>Geochemical changes</i>	
<u>Application to WMA C:</u> <i>Relevant to the performance assessment in the influence of the FEP to release and transport of waste from tanks and ancillary equipment.</i>		
<u>Potentially deleterious FEP:</u> <i>Uncertainty in the current state and future evolution of the chemical safety functions of the waste, grout, tank, and base mat is considered in the sensitivity and uncertainty analysis.</i>		

Biological/biochemical processes and conditions (in wastes and EBS)	2.1.10
Definition: FEPs related to the biological/biochemical processes that affect the wastes, containers, seals and other engineered features, and the overall biological/biochemical evolution of near field with time. This includes the effects of biological/biochemical influences on wastes, containers and repository components by the surrounding geology.	
Comment:	

<u>Key Concepts, examples, and related FEPs</u>	
Microbial growth and poisoning	Microbial/biological effects of evolution of redox (Eh) Change in microbial caused by change in temperature and acidity/alkalinity (pH), etc.
Microbially/biologically mediated processes	
Effect of organic material	Effect of organic materials
<u>Application to WMA C:</u> Relevant to the performance assessment in the influence of the FEP to release and transport of waste from tanks and ancillary equipment.	
<u>Potentially deleterious FEP:</u> Uncertainty in the current state and future evolution of the chemical safety functions of the waste, grout, tank, and base mat is considered in the sensitivity and uncertainty analysis.	

Thermal processes and conditions (in wastes and EBS)	2.1.11
Definition: FEPs related to the thermal processes that affect the wastes, containers, seals and other engineered features, and the overall thermal evolution of the near field with time. This includes the effects of heat on wastes, containers and repository components from the surrounding geology.	
Comment:	
<u>Key Concepts, examples, and related FEPs</u>	
Temperature evolution	Chemical heat production from engineered features, e.g. concrete hydration
Differential elastic response	Change in chemical reaction rates e.g. corrosion
Non-elastic response	Temperature dependence of physical/chemical/ biological/hydraulic processes, e.g. corrosion and re-saturation
Fracture aperture changes caused by the temperature change	Fluid pressure, density viscosity changes
Change in microbial activity	Induced chemical changes caused by the temperature change
Radiogenic, chemical and biological heat production from the wastes	
<u>Application to WMA C:</u> Applicable in the performance assessment, but heat generated in residual waste for expected retrievals is negligible.	
<u>Potentially deleterious FEP:</u> Potential heat generation in tanks that retain substantial amounts of unretrievable waste, leading to effects on flow through the waste and EBS.	

Gas sources and effects (in wastes and EBS)	2.1.12
Definition: FEPs within and around the wastes, containers and engineered features resulting in the generation of gases and their subsequent effects on the repository system.	
Comment: Gas production may result from degradation and corrosion of various waste, container and engineered feature materials, as well as radiation effects. The effects of gas production may change local chemical and hydraulic conditions, and the mechanisms for radionuclide transport, i.e. gas-induced and gas-mediated transport.	

<u>Key Concepts, examples, and related FEPs</u>		
Explosion	Gas generation	Degradation of vault, overpacks or backfill (instigate mechanical processes)
Pressurisation	Corrosion	Chemical interaction of containers (including overpacks) with pore water
Radiation effects	Decomposition of organic matter (microbial)	Chemical interaction of waste with containers
		Chemical interaction of backfill with containers (including overpacks)
<u>Application to WMA C:</u> Relevant to the performance assessment in analyses of releases to the atmosphere.		
<u>Potentially deleterious FEP:</u> Not applicable.		

Radiation effects (in wastes and EBS)	2.1.13
Definition: FEPs related to the effects that result from the radiation emitted from the wastes that affect the wastes, containers, seals and other engineered features, and the overall radiogenic evolution of the near field with time.	
Comment: Examples of relevant effects are ionization, radiolytic decomposition of water (radiolysis), radiation damage to waste matrix or container materials, helium gas production due to alpha decay.	
<u>Key Concepts, examples, and related FEPs</u>	
Radiolysis	Irradiation effects on metals, concrete
Decay product gas generation	Polymer degradation (resins and high integrity containers)
	Concrete degradation
	Metallic degradation
<u>Application to WMA C:</u> Applicable in the performance assessment, but negligible.	
<u>Potentially deleterious FEP:</u> None identified..	
Nuclear criticality	2.1.14
Definition: FEPs related to the possibility and effects of spontaneous nuclear fission chain reactions within the repository.	
Comment: A chain reaction is the self-sustaining process of nuclear fission in which each neutron released from a fission triggers, on average, at least one other nuclear fission. Nuclear criticality requires a sufficient concentration and localized mass (critical mass) of fissile isotopes (e.g. U-235, Pu-239) and also presence of neutron moderating materials in a suitable geometry; a chain reaction is liable to be damped by the presence of neutron absorbing isotopes (e.g. Pu-240).	
<u>Key Concepts, examples, and related FEPs</u>	
Radiological criticality	

Application to WMA C: Not relevant to the tank closure performance assessment. Waste inventory screened for potential for criticality.

Potentially deleterious FEP: Not applicable.

Extraneous materials	2.1.15
Definition:	
Comment:	
<u>Key Concepts, examples, and related FEPs</u>	
None	
<u>Application to WMA C:</u> Not relevant.	
<u>Potentially deleterious FEP:</u> Not applicable.	

GEOLOGICAL ENVIRONMENT	2.2
Definition: The features and processes of the geological environment surrounding the repository including, for example, the hydrogeological, geomechanical and geochemical features and processes, both in pre-emplacement state and as modified by the presence of the repository and other long-term changes.	
Comment: "Geological Environment" is a sub-category in the International FEP List and is divided into individual FEPs.	
Note that FEPs 2.2.01 to 2.2.06 describe the features in the disposal system, in other words, a description of the features of the system as it is constructed, whereas FEPs 2.2.07 to 2.2.11 describe the processes or the changes in the disposal system..	

Disturbed zone, host lithology	2.2.01
Definition: FEPs related to the host lithology zone around the repository or any other underground openings that may be mechanically disturbed during construction, and the properties and characteristics as they may evolve both before and after repository closure.	
Comment: The disturbed zone may have different properties to the undisturbed host lithology, e.g. opening of fractures or change of hydraulic properties due to stress relief.	
<u>Key Concepts, examples, and related FEPs</u>	
Fracture formed by the construction Change of hydraulic properties due to stress relief	
<u>Application to WMA C:</u> Relevant as the excavation zone for the tank farm.	
<u>Potentially deleterious FEP:</u> Not applicable.	

Host lithology	2.2.02
Definition: FEPs related to the properties and characteristics of the lithology in/on which the repository is sited (excluding the zone disturbed by the construction) as they may evolve both before and after repository closure. In most cases, this FEP will be associated with the unsaturated zone.	
Comment: <i>Relevant properties include thermal and hydraulic conductivity, compressive and shear strength, porosity etc. In most cases, this FEP will be associated with the unsaturated zone (See FEP 2.2.03).</i>	
<u>Key Concepts, examples, and related FEPs</u>	
<i>Thermal and hydraulic conductivity</i>	<i>Porosity</i>
<i>Compressive and shear strength</i>	<i>Description of the host lithology</i>
<u>Application to WMA C:</u> <i>Relevant. Here host lithology is considered the H2 sand in which the facility resides.</i>	
<u>Potentially deleterious FEP:</u> <i>Uncertainties in the lithology and its properties could lead to mischaracterization of the vadose zone safety functions.</i>	
Lithological units, other	2.2.03
Definition: FEPs related to the properties and characteristics of the lithology other than the host lithology as they may evolve both before and after repository closure.	
Comment: <i>These lithological units are those that make up the region in which the repository is located. These units are identified in the geological investigations of the region. Each geological unit is characterized according to its geometry and its general physical properties and characteristics. Details concerning inhomogeneity and uncertainty associated with each unit are included in the characterization. In most cases, this FEP will be associated with the saturated zone (See FEP 2.2.02).</i>	
<u>Key Concepts, examples, and related FEPs</u>	
<i>Non-uniform stratigraphy</i>	<i>Heterogeneity</i>
	<i>Description of the lithology units</i>
<u>Application to WMA C:</u> <i>Relevant. Here “other lithological units” are those below WMA C (i.e. not the “host” lithology).</i>	
<u>Potentially deleterious FEP:</u> <i>Uncertainties in the lithology and its properties could lead to mischaracterization of the vadose zone and saturated zone safety functions.</i>	
Discontinuities, large scale (in geosphere)	2.2.04
Definition: FEPs related to the properties and characteristics of discontinuities in and between the saturated and unsaturated zones, including faults, shear zones, intrusive dykes and interfaces between different rock types.	
Comment:	

<u>Key Concepts, examples, and related FEPs</u>		
<i>Fault</i>	<i>Shear zones</i>	<i>Interfaces between different rock types</i>
<i>Intrusive dykes</i>		
<u>Application to WMA C:</u> <i>None identified.</i>		
<u>Potentially deleterious FEP:</u> <i>Not applicable.</i>		

Contaminant transport path characteristics (in geosphere)	2.2.05
Definition: FEPs related to the properties and characteristics of smaller discontinuities and features within saturated and unsaturated zones that are expected to be the main paths for contaminant transport through the geosphere, as they may evolve both before and after repository closure.	
Comment: <i>Groundwater flow and contaminant transport through rocks may occur in a variety of systems depending on the rock characteristics. Porous flow is predominantly through pores in the medium or through the interstitial spaces between small grains of materials. Fracture flow is predominantly along fractures in the rock which represent the only connected open spaces. Changes in the contaminant transport path characteristics due to the repository construction or its chemical influence etc. are included.</i>	
<u>Key Concepts, examples, and related FEPs</u>	
<i>Fracture flow</i>	<i>Fracture-matrix interaction</i>
	<i>Porous flow</i>
<u>Application to WMA C:</u> <i>Relevant and considered in sensitivity and uncertainty analysis using alternative conceptual models.</i>	
<u>Potentially deleterious FEP:</u> <i>Not applicable.</i>	

Mechanical processes and conditions (in geosphere)	2.2.06
Definition: FEPs related to the mechanical processes that affect the saturated and unsaturated zones, and the overall evolution of conditions with time. This includes the effects of changes in condition, e.g. rock stress, due to the excavation, construction and long-term presence of the repository.	
Comment:	
<u>Key Concepts, examples, and related FEPs</u>	
<i>Subsidence</i>	<i>Upliftment</i>
<u>Application to WMA C:</u> <i>Not relevant.</i>	
<u>Potentially deleterious FEP:</u> <i>None identified.</i>	

Hydraulic/hydrogeological processes and conditions (in geosphere)			2.2.07
Definition: FEPs related to the hydraulic and hydrogeological processes that affect the saturated and unsaturated zones, and the overall evolution of conditions with time. This includes the effects of changes in condition, e.g. hydraulic head, due to the excavation, construction and long-term presence of the repository.			
Comment: <i>The hydrogeological regime is the characterization of the composition and movement of water through the relevant geological formations in the repository region and the factors that control this. This requires knowledge of the recharge and discharge zones, the groundwater flow systems, saturation, and other factors that may drive the hydrogeology, such as density effects due to salinity gradients or temperature gradients. Changes of the hydrogeological regime due to the construction and/or presence of the repository are included.</i>			
<u>Key Concepts, examples, and related FEPs</u>			
Saline intrusion	Groundwater discharge to surface water, Soil, Estuary, Seas, Wells	Saturated/unsaturated conditions	
Darcy flow	Channelling and preferential flow pathways	Flow between two aquifers	
Non-Darcy flow	Aquifer(groundwater) discharge/recharge (e.g. well)	Infiltration	
Fracture flow		Flow direction	
<u>Application to WMA C:</u> Relevant and considered in sensitivity and uncertainty analysis.			
<u>Potentially deleterious FEP:</u> None identified.			

Chemical/geochemical processes and conditions (in geosphere)			2.2.08
Definition: FEPs related to the chemical and geochemical processes that affect the saturated and unsaturated zones, and the overall evolution of conditions with time. This includes the effects of changes in condition, e.g. Eh, pH, due to the excavation, construction and long-term presence of the repository.			
Comment: <i>The hydrochemical regime refers to the groundwater chemistry in the geological formations in the repository region, and the factors that control this. This requires knowledge of the groundwater chemistry including speciation, solubility, complexants, redox (reduction/oxidation) conditions, rock mineral composition and weathering processes, salinity and chemical gradients. Changes of the hydrochemical regime due to the construction and/or presence of the repository are included.</i>			
<u>Key Concepts, examples, and related FEPs</u>			
pH change	pH effects of cement on the environment, soil, etc	Effect of non-radioactive solute plume	
Redox potential changes	Mineralization changes		
<u>Application to WMA C:</u> Relevant.			
<u>Potentially deleterious FEP:</u> Potential effects of past leaks on the H2 sand below the tank farm.			

Biological/biochemical processes and conditions (in geosphere)	2.2.09
Definition: FEPs related to the biological and biochemical processes that affect the saturated and unsaturated zones, and the overall evolution of conditions with time. This includes the effects of changes in condition, e.g. microbe populations, due to the construction and long-term presence of the repository.	
Comment:	
<u>Key Concepts, examples, and related FEPs</u>	
Generating of chelating agents	Influences on redox potential
Influences on pH	Change in microbe population
Microbiology-enhanced mobility	
<u>Application to WMA C:</u> Relevant primarily in the potential effect on sorption coefficients in the geosphere.	
<u>Potentially deleterious FEP:</u> None identified.	

Thermal processes and conditions (in geosphere)	2.2.10
Definition: FEPs related to the thermal processes that affect the saturated and unsaturated zones, and the overall evolution of conditions with time. This includes the effects of changes in condition, e.g. temperature, due to the construction and long-term presence of the repository.	
Comment: Geothermal regime refers to sources of geological heat, the distribution of heat by conduction and transport (convection) in fluids, and the resulting thermal field or gradient. Changes of the geothermal regime due to the construction and/or presence of the repository are included	
<u>Key Concepts, examples, and related FEPs</u>	
Bio-heat	Chemical reactions
Change in temperature	
<u>Application to WMA C:</u> Not relevant <i>except</i> if future tank retrievals leave behind more waste than anticipated, with associated heat generation.	
<u>Potentially deleterious FEP:</u> Not applicable.	

Gas sources and effects (in geosphere)	2.2.11
Definition: FEPs related to natural gas sources and production of gas within the geosphere and also the effect of natural and repository produced gas on the geosphere, including the transport of bulk gases and the overall evolution of conditions with time.	
Comment: Gas movement in the geosphere will be determined by many factors including the rate of production, gas permeability and solubility, and the hydrostatic pressure regime.	
<u>Examples</u>	
Natural gas intrusion	

Application to WMA C: Not relevant.

Potentially deleterious FEP: Not applicable.

Undetected features (in geosphere)	2.2.12
Definition: FEPs related to natural or man-made features within the geology that may not be detected during the site investigation.	
Comment: Examples of possible undetected features are fracture zones, brine pockets or old mine workings. Some physical features of the repository environment may remain undetected during site surveys and even during pilot tunnel excavations. The nature of the geological environment will indicate the likelihood that certain types of undetected features may be present and the site investigation may be able to place bounds on the maximum size or minimum proximity to such features.	
<u>Key Concepts, examples, and related FEPs</u>	
Boreholes (drillings)	Faults, shear zones, Breccia pipes, Lava tubes, Intrusive <input type="checkbox"/> Gas or brine pockets
Mine shafts or mine galleries	dykes
<u>Application to WMA C:</u> Potentially relevant, but none identified.	
<u>Potentially deleterious FEP:</u> Potential presence of undetected major undetected feature in the vadose zone such as a clastic dike is considered as a sensitivity case.	

Geological resources	2.2.13
Definition: FEPs related to natural resources within the geosphere, particularly those that might encourage investigation or excavation at or near the repository site.	
Comment: Geological resources could include oil and gas, solid minerals, water, and geothermal resources. For a near-surface repository, quarrying of near-surface deposits, e.g. sand, gravel or clay, may be of interest	
<u>Key Concepts, examples, and related FEPs</u>	
Oil and gas	Solid minerals
Sand, gravel, clay	Water
<u>Application to WMA C:</u> Relevant, only for potential use of water resources.	
<u>Potentially deleterious FEP:</u> None identified. Water resources included in the analysis.	

SURFACE ENVIRONMENT	2.3
Definition: The features and processes within the surface environment, including near-surface aquifers and unconsolidated sediments but excluding human activities and behaviour, see 1.4 and 2.4..	
Comment: <i>Surface Environment" is a sub-category in the International FEP List and is divided into individual FEPs</i> <i>Note that FEPs 2.3.01 to 2.3.06 describe the features in the disposal system, in other words, a description of the features of the system as it is constructed, whereas FEPs 2.3.07 to 2.3.11 describe the processes or the changes in the disposal system.</i>	

Topography and morphology	2.3.01
Definition: FEPs related to the relief and shape of the surface environment and its evolution.	
Comment: <i>This FEP refers to local land form and land form changes with implications for the surface environment, e.g. plains, hills, valleys, and effects of river and glacial erosion thereon. In the long term, such changes may occur as a response to geological changes, see 1.3.</i>	
<u>Key Concepts, examples, and related FEPs</u> <div style="display: flex; justify-content: space-around; align-items: flex-start;"> <div style="text-align: left;">Land forms Plains</div> <div style="text-align: center;">Hills</div> <div style="text-align: right;">Valleys</div> </div>	
<u>Application to WMA C:</u> <i>Relevant, the closure cover changes the local topography.</i>	
<u>Potentially deleterious FEP:</u> <i>None identified.</i>	

Soil and sediment	2.3.02
Definition: FEPs related to the characteristics of the soils and sediments and their evolution.	
Comment: <i>Different soil and sediment types, e.g. characterized by particle-size distribution and organic content, will have different properties with respect erosion/deposition and contaminant sorption etc.</i>	
<u>Key Concepts, examples, and related FEPs</u> <div style="display: flex; justify-content: space-around; align-items: flex-start;"> <div style="text-align: left;">Soil and sediment development</div> <div style="text-align: center;">Soil conversion</div> </div>	
<u>Application to WMA C:</u> <i>Potentially relevant. Potential movement of sand dunes onsite. However, dune migration to the site would require regional changes in air currents.</i>	
<u>Potentially deleterious FEP:</u> <i>May cause changes in the recharge safety function considered in sensitivity and uncertainty analysis.</i>	

Aquifers and water-bearing features, near surface	2.3.03
Definition: FEPs related to the characteristics of aquifers and water-bearing features within a few metres of the land surface and their evolution.	
Comment: <i>Aquifers are water-bearing features geological units or near-surface deposits that yield significant amounts of water to wells or springs. The presence of aquifers and other water-bearing features will be determined by the geological, hydrological and climatic factors.</i>	
<u>Key Concepts, examples, and related FEPs</u>	
<i>Weathered aquifer</i>	<i>Fractured aquifer</i>
<i>Sandy aquifer</i>	<i>Description of aquifers in repository region</i>
<u>Application to WMA C:</u> <i>Relevant.</i>	
<u>Potentially deleterious FEP:</u> <i>Uncertainties in aquifer properties may lead to mischaracterization of the aquifer safety function.</i>	
Lakes, rivers, streams and springs	2.3.04
Definition: FEPs related to the characteristics of terrestrial surface water bodies and their evolution.	
Comment: <i>Streams, rivers and lakes often act as boundaries on the hydrogeological system. They usually represent a significant source of dilution for materials (including) radionuclides entering these systems, but in hot dry environments, where evaporation dominates, concentration is possible.</i>	
<u>Key Concepts, examples, and related FEPs</u>	
<i>Description of lakes, rivers, streams and springs in the repository region</i>	
<u>Application to WMA C:</u> <i>Not relevant owing to the DOE Order 435.1 assessment point. Discharges to the Columbia River are excluded from the analysis. However, the Columbia exerts an indirect influence on the system through its influence on the aquifer gradient.</i>	
<u>Potentially deleterious FEP:</u> <i>Not applicable</i>	
Coastal features	2.3.05
Definition: FEPs related to the characteristics of coasts and the near shore, and their evolution. Coastal features include headlands, bays, beaches, spits, cliffs and estuaries.	
Comment: <i>The processes operating on these features, e.g. active erosion, deposition, longshore transport, determine the development of the system and may represent a significant mechanism for dilution or accumulation of materials (including radionuclides) entering the system.</i>	

H-66

<u>Key Concepts, examples, and related FEPs</u>		
<i>Description of the coastal features in the repository region</i>	<i>Coastal surge</i>	<i>Temperature change</i>
<i>Headlands, Bays, Beaches, Spits</i>	<i>Storm</i>	<i>Recharge</i>
<i>Cliffs, Estuaries</i>	<i>tsunami</i>	<i>Bed-load processes</i>
<i>Coastal erosion</i>	<i>Groundwater discharge to estuary, shore</i>	<i>Flooding</i>
<i>Saline intrusion</i>	<i>Bioturbation</i>	<i>Plant/animal uptake/metabolism</i>
<i>Salinity changes</i>	<i>Tidal currents</i>	<i>Sand dune encroachment</i>
<i>Sedimentation</i>	<i>Sea spray</i>	<i>Coastal currents</i>
<i>Resuspension</i>	<i>Behaviour of coastal waters and marine sediment</i>	<i>Description of coastal features in vicinity of repository</i>
<i>Volatilisation</i>	<i>Estuarine changes</i>	<i>Beach development</i>
<u>Application to WMA C:</u> <i>Not relevant.</i>		
<u>Potentially deleterious FEP:</u> <i>Not applicable.</i>		

Marine features	2.3.06
Definition: FEPs related to the characteristics of seas and oceans, including the seabed, and their evolution. Marine features include oceans, ocean trenches, shallow seas, and inland seas.	
Comment: Processes operating on these features such as erosion, deposition, thermal stratification and salinity gradients, determine the development of the system and may represent a significant mechanism for dilution or accumulation of materials (including radionuclides) entering the system.	

<u>Key Concepts, examples, and related FEPs</u>		
<i>Ocean trenches, shallow seas</i>	<i>Marine sediment transport and deposition</i>	<i>Vertical mixing and isolation</i>
<i>inland seas, Oceans</i>	<i>Groundwater discharge towards sea</i>	<i>Salinity changes</i>
<i>Sedimentation</i>	<i>Sea spray</i>	<i>Plant/animal uptake/metabolism</i>
<i>Resuspension</i>	<i>Sediment transport</i>	<i>Bed-load processes</i>
<i>Volatilisation</i>	<i>Sea currents</i>	<i>Description of marine features in vicinity of repository</i>
<i>Tidal currents</i>	<i>Temperature change</i>	<i>Recharge</i>
<i>Marine currents</i>		
<u>Application to WMA C:</u> <i>Not relevant.</i>		
<u>Potentially deleterious FEP:</u> <i>Not applicable.</i>		

Atmosphere	2.3.07
Definition: FEPs related to the characteristics of the atmosphere, including capacity for transport, and their evolution.	
Comment:	
<u>Key Concepts, examples, and related FEPs</u>	
<i>Physical transport of gases</i>	<i>Chemical and photochemical reactions</i>
	<i>Aerosols and dust in the atmosphere</i>
<u>Application to WMA C:</u> <i>Relevant to the performance objectives in Order 435.1. Effects of atmospheric FEPs are also relevant in a stylized way through the infiltration rate.</i>	
<u>Potentially deleterious FEP:</u> <i>None identified.</i>	

Vegetation	2.3.08
Definition: FEPs related to the characteristics of terrestrial and aquatic vegetation both as individual plants and in mass, and their evolution.	
Comment:	
<u>Key Concepts, examples, and related FEPs</u>	
<i>Chemical changes caused by plants</i>	<i>Description of the vegetation in vicinity of repository</i>

<u>Application to WMA C:</u> Relevant to the estimation of recharge.	
<u>Potentially deleterious FEP:</u> Potential changes to vegetation may affect cover infiltration safety function (considered in sensitivity and uncertainty analysis).	

Animal populations	2.3.09
Definition: FEPs related to the characteristics of the terrestrial and aquatic animals both as individual animals and as populations, and their evolution.	
Comment:	
<u>Key Concepts, examples, and related FEPs</u>	
Animal diets	External contamination of animals
Description of the animal population in vicinity of repository	
<u>Application to WMA C:</u> Relevant. The effects of native animal populations are embedded in the assumptions regarding cover performance and general infiltration rates. Historic recharge data considers very long time frames with varying climate.	
<u>Potentially deleterious FEP:</u> None identified.	

Meteorology	2.3.10
Definition: FEPs related to the characteristics of weather and climate, and their evolution.	
Comment: Meteorology is characterized by precipitation, temperature, pressure and wind speed and direction. The variability in meteorology should be included so that extreme events such as drought, flooding, storms and snow melt are identified.	
<u>Key Concepts, examples, and related FEPs</u>	
Rainfall	Climate fluctuation
Snowfall	Dew-freezing cycles
Flooding related to high precipitation	Wet-dry cycles
Storms related to strong winds	Seasonality
Hurricanes	
High rainfall / Flooding	
Temperature	
Tsunamis	
<u>Application to WMA C:</u> Relevant to the estimation of recharge.	
<u>Potentially deleterious FEP:</u> Potential changes to climate may affect infiltration safety function are considered in sensitivity and uncertainty analysis.	

Hydrological regime and water balance (near-surface)	2.3.11
Definition: FEPs related to near-surface hydrology at a catchment scale and also soil water balance, and their evolution.	

Comment: The hydrological regime is a description of the movement of water through the surface and near-surface environment. It includes the movement of materials associated with the water such as sediments and particulate. Extremes such as drought, flooding, storms and snowmelt may be relevant.		
<u>Key Concepts, examples, and related FEPs</u>		
Surface run-off to marines/estuaries	Groundwater discharge to surface water, soils, estuaries/marines	Change in lake or reservoir levels
River flow to marines/estuaries		Alkali flats
Evaporation	Water discharge/recharge processes that effecting radionuclide content	Stream and river flow changes
Evapotranspiration		River meander
Infiltration	Stream silting	Stream flow
<u>Application to WMA C:</u> Relevant to the estimation of recharge.		
<u>Potentially deleterious FEP:</u> Potential changes in surface conditions may affect infiltration safety function are considered in sensitivity and uncertainty analysis.		

Erosion and deposition	2.3.12
Definition: FEPs related to all the erosional and depositional processes that operate in the surface environment, and their evolution.	
Comment: Relevant processes may include fluvial and glacial erosion and deposition, denudation, eolian erosion and deposition. These processes will be controlled by factors such as the climate, vegetation, topography and geomorphology.	
<u>Key Concepts, examples, and related FEPs</u>	
Deposition	Coastal erosion due to rise and fall of sea level Erosion by wave action, landslides or rockfalls
Wind erosion related to storms	(Greenhouse effect) Agriculture erosion
Erosion related to flooding	Landsliding (instigate mechanical processes) Erosion of cover
Erosion related to glaciation	Erosion (instigate mechanical processes) Weathering
<u>Application to WMA C:</u> Relevant to the estimation of recharge.	
<u>Potentially deleterious FEP:</u> Potential changes in surface conditions may affect infiltration safety function are considered in sensitivity and uncertainty analysis.	

Ecological/biological/microbial systems	2.3.13
Definition: FEPs related to living organisms and relations between populations of animals, plants and their evolution.	

Comment: Characteristics of the ecological system include the vegetation regime, and natural cycles such as forest fires or flash floods that influence the development of the ecology. The plant and animal populations occupying the surface environment are an intrinsic component of its ecology. The wide range of processes that define the ecological system regulates their behaviour and population dynamics. Human activities have significantly altered the natural ecology of most environments.		
<u>Key Concepts, examples, and related FEPs</u>		
Ecological and biological features	Chemical changes caused by micro-organisms	Chemical changes caused by plants
<u>Application to WMA C:</u> Relevant to the estimation of recharge.		
<u>Potentially deleterious FEP:</u> Potential changes in ecology may affect infiltration safety function are considered in sensitivity and uncertainty analysis.		

Animal/Plant intrusion	2.3.14
Definition: Animal and plant intrusion leading to vault or trench disruption.	
Comment:	
<u>Key Concepts, examples, and related FEPs</u>	
Seeds	Root intrusion (instigate mechanical processes)
Burrowing animals	Bio-intrusion by plants and animals
<u>Application to WMA C:</u> Not relevant. Precluded by depth of disposal. Considered in barrier design and testing.	
<u>Potentially deleterious FEP:</u> Not applicable.	

HUMAN BEHAVIOUR	2.4
Definition: The habits and characteristics of the individuals or populations, e.g. critical groups, to whom exposures are calculated, not including intrusive or other activities which will have an impact on the performance of the engineered or geological barriers, see 1.4.	
Comment: "Human Behaviour (passive)" is a sub-category in the International FEP List and is divided into individual FEPs.	

Human characteristics (physiology, metabolism)	2.4.01
Definition: FEPs related to characteristics, e.g. physiology, metabolism, of individual humans.	
Comment: Physiology refers to body and organ form and function. Metabolism refers to the chemical and biochemical reactions, which occur within an organism, or part of an organism, in connection with the production and use of energy.	

<u>Key Concepts, examples, and related FEPs</u>	
<i>Physiological and metabolism description of humans that will be the subject of the assessment</i>	
<u>Application to WMA C:</u> <i>Relevant to dose factors. Addressed in DOE orders and standards (DOE-STD-1196-2011)</i>	
<u>Potentially deleterious FEP:</u> <i>Not applicable.</i>	

Adults, children, infants and other variations	2.4.02
Definition: FEPs related to considerations of variability, in individual humans, of physiology, metabolism and habits.	
Comment: <i>Children and infants, although similar to adults, often have characteristic differences, e.g. metabolism, respiratory rates, habits (e.g. pica, ingestion of soil) which may lead to different exposure characteristics.</i>	
<u>Key Concepts, examples, and related FEPs</u>	
<i>None</i>	
<u>Application to WMA C:</u> <i>Relevant to dose factors. Addressed in DOE orders and standards (DOE-STD-1196-2011)</i>	
<u>Potentially deleterious FEP:</u> <i>Not applicable.</i>	

Diet and fluid intake	2.4.03
Definition: FEPs related to intake of food and water by individual humans and the compositions and origin of intake.	
Comment: <i>The human diet refers to the range of food products consumed by humans.</i>	
<u>Key Concepts, examples, and related FEPs</u>	
<i>Diet</i>	<i>Description of the human diet and assumptions regarding quantities/volume</i>
<u>Application to WMA C:</u> <i>Relevant to exposure factors for Order 435.1 all pathways analysis.</i>	
<u>Potentially deleterious FEP:</u> <i>Not applicable.</i>	

Habits (non-diet-related behaviour)	2.4.04
Definition: FEPs related to non-diet related behaviour of individual humans, including time spent in various environments, pursuit of activities and uses of materials.	

Comment: The human habits refer to the time spent in different environments in pursuit of different activities and other uses of materials. Agricultural practices and human factors such as culture, religion, economics and technology will influence the diet and habits. Smoking, ploughing, fishing, and swimming are examples of behaviour that might give rise to particular modes of exposure to environmental contaminants.		
<u>Key Concepts, examples, and related FEPs</u>		
Human habits	Location of shielding factors	Bathing
Resource usage	Impoundment of water	Description of human habits and behaviour
Storage of products	Fishing/fish farming	Air filtration
Ventilation		
<u>Application to WMA C:</u> Relevant to exposure factors for Order 435.1 all pathways analysis.		
<u>Potentially deleterious FEP:</u> Not applicable.		

Community characteristics	2.4.05
Definition: FEPs related to characteristics, behaviour and lifestyle of groups of humans that might be considered as target groups in an assessment.	
Comment: Relevant characteristics might be the size of a group and degree of self-sufficiency in food stuffs/diet. For example, hunter/gathering describes a subsistence lifestyle employed by nomadic or semi-nomadic groups who roam relatively large areas of land hunting wild game and/or fish, and gathering native fruits, berries, roots and nuts, to obtain their dietary requirements.	
<u>Key Concepts, examples, and related FEPs</u>	
Demographic changes	General human society description
<u>Application to WMA C:</u> Addressed in Order 435.1 guidance.	
<u>Potentially deleterious FEP:</u> Not applicable.	

Food and water processing and preparation	2.4.06
Definition: FEPs related to treatment of foodstuffs and water between raw origin and consumption.	
Comment: Once a crop is harvested or an animal slaughtered it may be subject to a variety of storage, processing and preparational activities prior to human or livestock consumption. These may change the radionuclide distribution and/or content of the product. For example, radioactive decay during storage, chemical processing, washing losses and cooking losses during food preparation.	
Water sources may be treated prior to human or livestock consumption, e.g. chemical treatment and/or filtration.	

<u>Key Concepts, examples, and related FEPs</u>	
<i>Water filtration</i>	<i>Food processing</i>
<u>Application to WMA C:</u> Relevant to exposure factors for Order 435.1 all pathways analysis.	
<u>Potentially deleterious FEP:</u> Not applicable.	

Dwellings	2.4.07
Definition: FEPs related to houses or other structures or shelter in which humans spend time.	
Comment: Dwellings are the structures which humans live in. The materials used in their construction and their location may be significant factors for determining potential radionuclide exposure pathways.	
<u>Key Concepts, examples, and related FEPs</u>	
<i>Construction of buildings, houses</i>	<i>Ventilation</i>
<i>Site occupation</i>	<i>Location and shielding factors</i>
<u>Application to WMA C:</u> Relevant to exposure factors for Order 435.1 all pathways analysis.	
<u>Potentially deleterious FEP:</u> Not applicable.	

Wild and natural land and water use	2.4.08
Definition: FEPs related to use of natural or semi-natural tracts of land and water such as forest, bush and lakes.	
Comment: Special foodstuffs and resources may be gathered from natural land and water, which may lead to significant modes of exposure.	
<u>Key Concepts, examples, and related FEPs</u>	
<i>Natural and semi-natural environments</i>	
<u>Application to WMA C:</u> Relevant to exposure factors for Order 435.1 all pathways analysis.	
<u>Potentially deleterious FEP:</u> Not applicable.	

Rural and agricultural land and water use (incl. fisheries)	2.4.09
Definition: FEPs related to use of permanently or sporadically agriculturally managed land and managed fisheries.	

Comment: An important set of processes are those related to agricultural practices, their effects on land form, hydrology and natural ecology, and also their impact in determining uptake through food chains and other exposure paths.		
<u>Key Concepts, examples, and related FEPs</u>		
Use of land for agriculture	Land use change	Fishing/ fish farming in estuaries/marines
Ploughing	Fertilization	
<u>Application to WMA C:</u> Relevant to exposure factors for Order 435.1 all pathways analysis.		
<u>Potentially deleterious FEP:</u> Not applicable.		

Urban and industrial land and water use		2.4.10
Definition: FEPs related to urban and industrial developments, including transport, and their effects on hydrology and potential contaminant pathways.		
Comment: Human populations are concentrated in urban areas in modern societies. Significant areas of land may be devoted to industrial activities. Water resources may be diverted over considerable distances to serve urban and/or industrial requirements.		
<u>Key Concepts, examples, and related FEPs</u>		
Water works	Water extraction through wells	De-salination of water
Urban and industrial environments	Water extraction for irrigation	Human water extraction
<u>Application to WMA C:</u> Not relevant to analyses conducted for exposures under Order 435.1 all pathways analysis. Subsistence farmer scenario is more conservative.		
<u>Potentially deleterious FEP:</u> Not applicable.		

Leisure and other uses of environment		2.4.11
Definition: FEPs related to leisure activities, the effects on the surface environment and implications for contaminant exposure pathways.		
Comment: Significant areas of land, water, and coastal areas may be devoted to leisure activities e.g., water bodies for recreational uses, mountains/wilderness areas for hiking and camping activities.		
<u>Key Concepts, examples, and related FEPs</u>		
Recreational land use	Impoundment of water for bathing	Beach development
<u>Application to WMA C:</u> Not relevant to analyses conducted for exposures under Order 435.1 all pathways analysis. Subsistence farmer scenario is more conservative.		
<u>Potentially deleterious FEP:</u> Not applicable.		

RADIONUCLIDE/CONTAMINANT FACTORS	3
Definition: FEPs that take place in the disposal system domain that directly affect the release and migration of radionuclides and other contaminants, or directly affect the dose to members of a critical group from given concentrations of radiotoxic and chemotoxic species in environmental media.	
Comment: "Disposal System Domain: Radionuclide Factors" is a category in the International FEP List and is divided into sub-categories..	

CONTAMINANT CHARACTERISTICS	3.1
Definition: The characteristics of the radiotoxic and chemotoxic species that might be considered in a post-closure safety assessment.	
Comment: "Contaminant Characteristics" is a sub-category in the International FEP List and is divided into individual FEPs.	

Radioactive decay and in-growth	3.1.01
Definition: Radioactivity is the spontaneous disintegration of an unstable atomic nucleus resulting in the emission of sub-atomic particles. Radioactive isotopes are known as radionuclides. Where a parent radionuclide decays to a daughter radionuclide so that the population of the daughter radionuclide increases this is known as in-growth.	
Comment: In post-closure assessment models, radioactive decay chains are often simplified, e.g. by neglecting the shorter-lived radionuclides in transport calculations, or adding dose contributions from shorter-lived radionuclides to dose factors for the longer-lived parent in dose calculations	
<u>Key Concepts, examples, and related FEPs</u>	
Production of aqueous progeny Radon emanation	
<u>Application to WMA C:</u> Relevant.	
<u>Potentially deleterious FEP:</u> Not applicable.	

Chemical/organic toxin stability	3.1.02
Definition: FEPs related to chemical stability of chemotoxic species.	
Comment:	
<u>Key Concepts, examples, and related FEPs</u>	
None	

Application to WMA C: Not relevant in this performance assessment, which is focused only on radiological exposures.

Potentially deleterious FEP: Not applicable.

Inorganic solids/solutes	3.1.03
Definition: FEPs related to the characteristics of inorganic solids/solutes that may be considered.	
Comment:	
<u>Key Concepts, examples, and related FEPs</u>	
Source terms content	
<u>Application to WMA C:</u> Relevant.	
<u>Potentially deleterious FEP:</u> None identified.	

Volatiles and potential for volatility	3.1.04
Definition: FEPs related to the characteristics of radiotoxic and chemotoxic species that are volatile or have the potential for volatility in repository or environmental conditions.	
Comment: Some radionuclides may be isotopes of gaseous elements (e.g. Kr isotopes) or may form volatile compounds. Gaseous radionuclides or species may arise from chemical or biochemical reactions, e.g. metal corrosion to yield hydrogen gas and microbial degradation of organic material to yield methane and carbon dioxide.	
<u>Key Concepts, examples, and related FEPs</u>	
None	
<u>Application to WMA C:</u> Relevant. Addressed in atmospheric release and radon release analyses.	
<u>Potentially deleterious FEP:</u> Not applicable.	

Organics and potential for organic forms	3.1.05
Definition: FEPs related to the characteristics of radiotoxic and chemotoxic species that are organic or have the potential to form organics in repository or environmental conditions.	
Comment:	

<u>Key Concepts, examples, and related FEPs</u>
<i>Source term content</i>
<u>Application to WMA C:</u> <i>Relevant, but concentrations of organic species in residual waste are low and their effects have been screened out.</i>
<u>Potentially deleterious FEP:</u> <i>Not applicable.</i>

Noble gases	3.1.06
Definition: FEPs related to the characteristics of noble gases.	
Comment: <i>Radon and thoron are special cases, see FEP 3.3.08.</i>	
<u>Key Concepts, examples, and related FEPs</u>	
<i>None</i>	
<u>Application to WMA C:</u> <i>Not relevant.</i>	
<u>Potentially deleterious FEP:</u> <i>Not applicable.</i>	

CONTAMINANT RELEASE/MIGRATION FACTORS	3.2
Definition: The processes that directly affect the release and/or migration of radionuclides in the disposal system domain.	
Comment: <i>"Release/Migration Factors" is a sub-category in the International FEP List and is divided into individual FEPs.</i>	

Dissolution, precipitation and crystallisation, contaminant	3.2.01
Definition: FEPs related to the dissolution, precipitation and crystallisation of radiotoxic and chemotoxic species under repository or environmental conditions.	
Comment: <i>Dissolution is the process by which constituents of a solid dissolve into solution. Precipitation and crystallisation are processes by which solids are formed out of liquids. Precipitation occurs when chemical species in solution react to produce a solid that does not remain in solution. Crystallisation is the process of producing pure crystals of an element, molecule or mineral from a fluid or solution undergoing a cooling process.</i>	

<u>Key Concepts, examples, and related FEPs</u>	
Chemical reactions caused by dissolution and precipitation of radionuclides	Caused by chemical interaction of backfill with pore water
Change in mineralization	Caused by chemical interaction of non-radioactive waste with radioactive waste
Caused by chemical interaction of vault material with pore water	Caused by a change in temperature
<u>Application to WMA C:</u> Relevant.	
<u>Potentially deleterious FEP:</u> Potential rapid waste dissolution may affect the safety function of the waste dissolution (considered in sensitivity and uncertainty analysis).	

Speciation and solubility, contaminant	3.2.02
Definition: FEPs related to the chemical speciation and solubility of radiotoxic and chemotoxic species in repository or environmental conditions.	
Comment: The solubility of a substance in aqueous solution is an expression of the degree to which it dissolves. Factors such as temperature and pressure affect solubility, as do the pH and redox conditions. These factors affect the chemical form and speciation of the substance. Thus different species of the same element may have different solubilities in a particular solution. Porewater and groundwater speciation and solubility are very important factors affecting the behaviour and transport of radionuclides	
<u>Key Concepts, examples, and related FEPs</u>	
Species equilibrium change caused by change in temperature	Solubility change caused by change in temperature Solubility Solubility change caused by chemical interaction between waste and pore water
<u>Application to WMA C:</u> Relevant to chemical behaviour of contaminants in residual waste.	
<u>Potentially deleterious FEP:</u> Uncertainties in chemical behaviour may affect the chemical safety functions.	

Sorption/desorption processes, contaminant	3.2.03
Definition: FEPs related to sorption/desorption of radiotoxic and chemotoxic species in repository or environmental conditions.	
Comment: Sorption describes the physico-chemical interaction of dissolved species with a solid phase. Desorption is the opposite effect. Sorption processes are very important for determining the transport of radionuclides in groundwater. Sorption is often described by a simple partition constant (K_d) which is the ratio of solid phase radionuclide concentration to that in solution. This assumes that sorption is reversible, reaches equilibrium rapidly, is independent of variations in water chemistry or mineralogy along the flow path, the solid-water ratio, or concentrations of other species. More sophisticated approaches involve the use of sorption isotherms.	

<u>Key Concepts, examples, and related FEPs</u>		
<i>Sorption</i>	<i>Effect of sorption</i>	<i>Caused by chemical interaction of non-radioactive waste with radioactive waste</i>
<i>Chemical reactions caused by adsorption or desorption</i>	<i>Caused by chemical interaction of waste with pore water</i>	<i>Sorption change caused by change in temperature</i>
<i>Anion exclusion effects</i>		
<u>Application to WMA C:</u> <i>Relevant to chemical behaviour of contaminants in residual waste.</i>		
<u>Potentially deleterious FEP:</u> <i>Uncertainties in chemical behaviour may affect the chemical safety functions (different release assumptions are considered in the sensitivity and uncertainty analysis).</i>		

Colloids, contaminant interactions and transport with		3.2.04
Definition: FEPs related to the transport of colloids and interaction of radiotoxic and chemotoxic species with colloids in repository or environmental conditions.		
Comment: <i>Colloids are particles in the nanometre to micrometre size range which can form stable suspensions in a liquid phase. Metastable solid phases are unstable thermodynamically but exist due to the very slow kinetics of their alteration into more stable products. Colloids are present in groundwater and may also be produced during degradation of the wastes or engineered barrier materials.</i>		
<i>Colloids may influence radionuclide transport in a variety of ways: retarding transport by sorption of aqueous radionuclide species and subsequent filtration; or, enhancing transport by sorption and transport with flowing groundwater</i>		
<u>Key Concepts, examples, and related FEPs</u>		
<i>Colloid formation</i>	<i>Caused by chemical interaction of backfill with pore water</i>	<i>Caused by chemical interaction of non-radioactive waste with radioactive waste</i>
<i>Caused by chemical interaction of waste with pore water</i>	<i>Colloid transport</i>	
<u>Application to WMA C:</u> <i>Potentially relevant to transport behaviour of contaminants, but considered unlikely to play a role in this environment (DOE-ORP-2008-01, page 22-12).</i>		
<u>Potentially deleterious FEP:</u> <i>Not applicable.</i>		

Chemical/complexing agents, effects on contaminant speciation/transport		3.2.05
Definition: FEPs related to the modification of speciation or transport of radiotoxic and chemotoxic species in repository or environmental conditions due to association with chemical and complexing agents.		

Comment: This FEP refers to any chemical agents that are present in the repository system and the effects that they may have on the release and migration of radionuclides from the repository environment. Chemical agents may be present in the wastes or in repository materials or introduced, e.g. from spillage during repository construction and operation, e.g. oil, hydraulic fluids, organic solvents. Chemical agents may be used during construction and operation, e.g. in drilling fluids, as additives to cements and grouts etc.

Key Concepts, examples, and related FEPs

Effects of chelating agents

Caused by chemical interaction of non-radioactive waste with radioactive waste

Caused by chemical interaction of waste with pore water

Microbial

Caused by chemical interaction of backfill with pore water

Application to WMA C: Potentially relevant to chemical safety functions, but of minimal effect owing to low concentrations of organic material in residual waste.

Potentially deleterious FEP: Potential for decrease in chemical safety functions.

Microbial/biological/plant-mediated processes, contaminant	3.2.06
Definition: FEPs related to the modification of speciation or phase change due to microbial/biological/plant activity.	
Comment: Microbial activity may facilitate chemical transformations of various kinds.	
<u>Key Concepts, examples, and related FEPs</u>	
Microbial-enhanced mobility	
<u>Application to WMA C:</u> Potentially relevant to chemical safety functions, but of minimal effect owing to low concentrations of organic material providing negligible energy source for microbes.	
<u>Potentially deleterious FEP:</u> Potential for decrease in chemical safety functions. Uncertainties in sorption are addressed in sensitivity and uncertainty analyses.	

Water-mediated transport of contaminants	3.2.07
Definition: FEPs related to transport of radiotoxic and chemotoxic species in groundwater and surface water in aqueous phase and as sediments in surface water bodies.	
Comment: Water-mediated transport of radionuclides includes all processes leading to transport of radionuclides in water. Radionuclides may travel in water as aqueous solutes (including dissolved gases), associated with colloids (see FEP 3.2.04) or, if flow conditions permit, with larger particulates/sediments.	

<u>Key Concepts, examples, and related FEPs</u>		
Multiphase transport processes	Advection, i.e. movement with the bulk movement of the fluid (in fractures, failed joints and matrix)	Percolation, i.e. movement of the fluid under gravity
Surface water aqueous transport		Transport processes between surface water and porous media
Transport by surface run-off	Molecular diffusion, i.e. random movement of individual atoms or molecules within the fluid	Isotopic dilution.
Transport in water bodies	Dispersion, i.e. the spread of spatial distribution with time due to differential advection	Mass dilution
Percolation		Discharge of radionuclides to sea
Capillary rise	Matrix diffusion, i.e. the diffusion or micro-advection of solute/colloids etc. into non-flowing pores	Fracture-matrix interaction
Groundwater transport		Discharge of radionuclides to foreshore
Infiltration	Transport of colloids	Transport of suspended sediment
Dual flow systems		
<u>Application to WMA C:</u> Relevant and addressed in the performance assessment.		
<u>Potentially deleterious FEP:</u> Not applicable.		

Solid-mediated transport of contaminants	3.2.08
Definition: FEPs related to transport of radiotoxic and chemotoxic species in solid phase, for example large-scale movements of sediments, landslide, solifluction and volcanic activity.	
Comment:	
<u>Key Concepts, examples, and related FEPs</u>	
Resuspension/deposition	Transport by suspended sediments (sedimentation)
Land slides	Erosion
Rock falls	Solid material release
Rain splash	
<u>Application to WMA C:</u> Not relevant owing to depth of disposal and facility stability.	
<u>Potentially deleterious FEP:</u> Not applicable.	

Gas-mediated transport of contaminants	3.2.09
Definition: FEPs related to transport of radiotoxic and chemotoxic species in gas or vapour phase or as fine particulate or aerosol in gas or vapour.	
Comment: <i>Radioactive gases may be generated from the wastes, e.g. C-14-labelled carbon dioxide or methane. Radioactive aerosols or particulates may be transported along with non-radioactive gases, or gases may expel contaminated groundwater ahead of them</i>	
<u>Key Concepts, examples, and related FEPs</u>	
<i>Gas mediated water flow</i>	<i>Gas phase processes</i>
<i>Gaseous release</i>	<i>Diffusion</i>
<i>Atmospheric gas transport</i>	<i>Atmospheric aerosol transport</i>
<u>Application to WMA C:</u> <i>Relevant and addressed in the performance assessment.</i>	
<u>Potentially deleterious FEP:</u> <i>None identified.</i>	

Atmospheric transport of contaminants	3.2.10
Definition: FEPs related to transport of radiotoxic and chemotoxic species in the air as gas, vapour, fine particulate or aerosol.	
Comment: <i>Radionuclides may enter the atmosphere from the surface environment as a result of a variety of processes including transpiration, suspension of radioactive dusts and particulates or as aerosols. The atmospheric system may represent a significant source of dilution for these radionuclides. It may also provide exposure pathways e.g. inhalation, immersion.</i>	
<u>Key Concepts, examples, and related FEPs</u>	
<i>Sea spray</i>	<i>Aerosol transport due to waves, wind</i>
<u>Application to WMA C:</u> <i>Relevant and addressed in the performance assessment.</i>	
<u>Potentially deleterious FEP:</u> <i>None identified.</i>	

Animal, plant and microbe mediated transport of contaminants	3.2.11
Definition: FEPs related to transport of radiotoxic and chemotoxic species as a result of animal, plant and microbial activity.	
Comment: <i>Burrowing animals, deep rooting species and movement of contaminated microbes are included</i>	

<u>Key Concepts, examples, and related FEPs</u>		
Discharge of radionuclides to soil layer (biotic intrusion)	Transport mediated by flora and fauna	Bioturbation
Animal/Plant intrusion	Uptake and desorption	Intake and emission by animals
<u>Application to WMA C:</u> Not relevant owing to depth of disposal and facility design <u>except</u> the potential for microbially mediated transport. Microbes have a potential effect on chemical safety functions (changes in sorption) but these are expected to be small owing to small concentrations of energy sources for microbes in the vadose zone.		
<u>Potentially deleterious FEP:</u> Potential changes to chemical safety functions.		

Human-action-mediated transport of contaminants	3.2.12
Definition: FEPs related to transport of radiotoxic and chemotoxic species as a direct result of human actions.	
Comment: Human-action-mediated transport of contaminants includes processes such as drilling into or excavation of the repository, the dredging of contaminated sediments from lakes, rivers and estuaries and placing them on land. Earthworks and dam construction may result in the significant movement of solid material from one part of the biosphere to another. Ploughing results in the mixing of the top layer of agricultural soil, usually on an annual basis.	
<u>Key Concepts, examples, and related FEPs</u>	
Dredging of sediments	Ploughing
	Water abstraction
<u>Application to WMA C:</u> Relevant to intrusion analyses and evaluation of all pathways exposure analysis.	
<u>Potentially deleterious FEP:</u> None identified.	

Foodchains, uptake of contaminants in	3.2.13
Definition: FEPs related to incorporation of radiotoxic and chemotoxic species into plant or animal species that are part of the possible eventual food chain to humans.	
Comment: Plants may become contaminated either as a result of direct deposition of radionuclides onto their surfaces or indirectly as a result of uptake from contaminated soils or water via the roots. Animals may become contaminated with radionuclides as a result of ingesting contaminated plants, or directly as a result of ingesting contaminated soils, sediments and water sources, or via inhalation of contaminated particulates, aerosols or gases.	
<u>Key Concepts, examples, and related FEPs</u>	
Plant/animal uptake in a marine/estuarine	Crops and natural and semi-natural flora and fauna
External contamination of animals	Internal transfer of radionuclides within animals
<u>Application to WMA C:</u> Relevant to post-intrusion analyses and evaluation of all pathways exposure analysis.	
<u>Potentially deleterious FEP:</u> None identified.	

EXPOSURE FACTORS	3.3
Definition: Processes and conditions that directly affect the dose to members of the critical group, from given concentrations of radionuclides in environmental media.	
Comment: <i>Exposure Factors" is a sub-category in the International FEP List and is divided into individual FEPs.</i>	

Drinking water, foodstuffs and drugs, contaminant concentrations in	3.3.01
Definition: FEPs related to the presence of radiotoxic and chemotoxic species in drinking water, foodstuffs or drugs that may be consumed by human.	
Comment:	
<u>Key Concepts, examples, and related FEPs</u>	
<i>Internal transfer of radionuclides within animals Crops and natural and semi-natural flora and fauna</i>	
<u>Application to WMA C:</u> <i>Relevant to and considered in exposure scenarios</i>	
<u>Potentially deleterious FEP:</u> <i>None identified.</i>	

Environmental media, contaminant concentrations in	3.3.02
Definition: FEPs related to the presence of radiotoxic and chemotoxic species in environmental media other than drinking water, foodstuffs or drugs.	
Comment: <i>The comparison of calculated contaminant concentrations in environmental media with naturally-occurring concentrations of similar species or species of similar toxic potential, may provide alternative or additional criteria for assessment less dependent on assumptions of human behaviour.</i>	
<u>Key Concepts, examples, and related FEPs</u>	
<i>None</i>	
<u>Application to WMA C:</u> <i>Relevant to and considered in exposure scenarios</i>	
<u>Potentially deleterious FEP:</u> <i>None identified.</i>	

Non-food products, contaminant concentrations in	3.3.03
Definition: FEPs related to the presence of radiotoxic and chemotoxic species in human manufactured materials or environmental materials that have special uses, e.g. clothing, building materials, peat.	

Comment: Contaminants may be concentrated in non-food products to which humans are exposed. For example, building materials, natural fibres or animal skins used in clothing, and the use of peat for fuel.
<u>Key Concepts, examples, and related FEPs</u>
None
<u>Application to WMA C:</u> Not relevant to Order 435.1 exposure scenarios
<u>Potentially deleterious FEP:</u> Not applicable.

Exposure modes	3.3.04
Definition: FEPs related to the exposure of man (or other organisms) to radiotoxic and chemotoxic species.	
Comment:	
<u>Key Concepts, examples, and related FEPs</u>	
Direct radiation from airborne plumes of radioactive materials	Immersion in contaminated water bodies
Injection through wounds	Ingestion (internal exposure) from drinking or eating contaminated water or foodstuffs
Cutaneous absorption of some species.	Inhalation (internal exposure) from inhaling gaseous or particulate radioactive materials
External exposure through water or sediment	External exposure as a result of direct irradiation from radionuclides deposited on, or present on, the ground, buildings or other objects.
Dermal exposure	
<u>Application to WMA C:</u> Relevant to and considered in exposure scenarios	
<u>Potentially deleterious FEP:</u> None identified.	

Dosimetry	3.3.05
Definition: FEPs related to the dependence between radiation or chemotoxic effect and amount and distribution of radiation or chemical agent in organs of the body.	
Comment: Dosimetry involves the estimation of radiation dose to individual organs, tissues, or the whole body, as a result of exposure to radionuclides. The radiation dose will depend on: the form of exposure, e.g. ingestion or inhalation of radionuclides leading to internal exposure or proximity to concentrations of radionuclides leading to external exposure; the metabolism of the radioelement and physico-chemical form if inhaled or ingested, which will determine the extent to which the radionuclide may be taken up and retained in body tissues; and the energy and type of radioactive emissions of the radionuclide which will affect the distribution of energy within tissues of the body.	

<u>Key Concepts, examples, and related FEPs</u>	
None	
<u>Application to WMA C:</u> Relevant to and considered in exposure scenarios	
<u>Potentially deleterious FEP:</u> None identified.	

Radiological toxicity/effects	3.3.06
Definition: FEPs related to the effect of radiation on man or other organisms.	
Comment: Radiation effects are classified as somatic (occurring in the exposed individual), genetic (occurring in the offspring of the exposed individual), stochastic (the probability of the effect is a function of dose received), non-stochastic (the severity of the effect is a function of dose received and no effect may be observed below some threshold).	
<u>Key Concepts, examples, and related FEPs</u>	
None	
<u>Application to WMA C:</u> Not relevant to dose and concentration endpoints in the Order 435.1 analysis.	
<u>Potentially deleterious FEP:</u> Not applicable.	

Non-radiological toxicity/effects	3.3.07
Definition: FEPs related to the effects of chemotoxic species on man or other organisms.	
Comment:	
<u>Key Concepts, examples, and related FEPs</u>	
None	
<u>Application to WMA C:</u> Not relevant to radiological endpoints in the Order 435.1 performance assessment. Will be addressed in complementary analyses.(Groundwater protection criteria???) – may need to include some non-rads???	
<u>Potentially deleterious FEP:</u> Not applicable.	

Radon and radon daughter exposure	3.3.08
Definition: FEPs related to exposure to radon and radon daughters.	

<p><i>Comment:</i> Radon and radon daughter exposure is considered separately to exposure to other radionuclides because the behaviour of radon and its daughter, and the modes of exposure, are different to other radionuclides.</p> <p>Radon (Rn-222) is the immediate daughter of radium (Ra-226). It is a noble gas with a half-life of about 4 days and decays through a series of very short-lived radionuclides (radon daughters), with half-lives of 27 minutes or less, to a lead isotope (Pb-210) with a half-life of 21 years. The principal mode of exposure is through the inhalation of radon daughters attached to dust particles, which may deposit in the respiratory system.</p>
<p><u>Key Concepts, examples, and related FEPs</u></p> <p>Radon emanation</p>
<p><u>Application to WMA C:</u> Relevant to the performance assessment. Evaluated as radon flux endpoint in the Order 435.1 analysis.</p> <p><u>Potentially deleterious FEP:</u> None identified.</p>

RPP-ENV-58782, Rev. 0

H.6 REFERENCES

- AECL-MISC-295, 1996, "Preliminary Safety Analysis Report (PSAR) for the Intrusion Resistant Underground Structure (IRUS)," Rev. 4, Atomic Energy of Canada, Chalk River, Ontario, Canada.
- BHI-01573, 2001, "Groundwater/Vadose Zone Integration Project – The Application of Feature, Event, and Process Methodology at the Hanford Site," Rev. 0, Bechtel Hanford, Inc., Richland, Washington.
- DOE/EIS-0391, 2012, "Final Tank Closure and Waste Management Environmental Impact Statement for the Hanford Site, Richland, Washington," U.S. Department of Energy, Washington, D.C.
- DOE O 435.1, 2001, Radioactive Waste Management, U.S. Department of Energy, Washington, D.C.
- DOE O 458.1, 2013, Radiation Protection of the Public and the Environment, U.S. Department of Energy, Office of Health, Safety and Security, Washington, D.C.
- DOE P 454.1, 2011, Use of Institutional Controls, U.S. Department of Energy, Washington, D.C.
- FCRD-USED-2011-000297, 2011, "Features, Events and Processes for the Disposal of Low Level Radioactive Waste – FY 2011 Status Report," Rev. 0, U.S. Department of Energy, Fuel Cycle Research and Development, Savannah River Site, Aiken, South Carolina.
- IAEA-ISAM-1, 2004, "Safety Assessment Methodologies for Near Surface Disposal Facilities, Results of a co-ordinated research project, Volume 1: Review and enhancement of safety assessment approaches and tools," International Atomic Energy Agency, Vienna, Austria.
- NEA Report 6923, 2012, "Methods of Safety Assessment of Geological Disposal Facilities for Radioactive Waste, Outcomes of the NEA MeSA Initiative," Nuclear Energy Agency/Organisation for Economic Co-operation and Development, Paris, France.
- NUREG/CR-1667 (SAND80-1429), 1982, "Risk Methodology for Geologic Disposal of Radioactive Waste: Scenario Selection Procedure," Sandia National Laboratories for U.S. Nuclear Regulatory Commission, Washington, D.C.
- Phifer, M., 2011, "2002 LLW Repository PCSC – FEP Consideration," Savannah River National Laboratory, Aiken, South Carolina.
- SAND93-7100, 1993, "Preliminary Identification of Potentially Disruptive Scenarios at the Greater Confinement Disposal Facility, Area 5 of the Nevada Test Site," Sandia National Laboratories, Albuquerque, New Mexico.

RPP-ENV-58782, Rev. 0

- 1 SAND94-0482, 1994, “Scenario Development for the Waste Isolation Pilot Plant: Building
2 Confidence in the Assessment,” Sandia National Laboratories, Albuquerque, New
3 Mexico.
- 4 SKB Technical Report 95-22, 1995, “The Use of Interaction Matrices for Identification,
5 Structuring, and Ranking of FEPs in a Repository System,” Swedish Nuclear Fuel and
6 Waste Management Company, Stockholm, Sweden.
- 7 SKB Technical Report TR-10-45, 2010, “FEP report for the safety assessment SR-Site,”
8 Swedish Nuclear Fuel and Waste Management Company, Stockholm, Sweden.
- 9 SKI Report 95:26, 1995, “Systems Analysis, Scenario Construction and Consequence Analysis
10 Definition for SITE-94,” Swedish Nuclear Power Inspectorate, Stockholm, Sweden.
- 11 SKI Technical Report 93:27, 1993, “SITE-94 Scenario Development FEP Audit List
12 Preparation: Methodology and Presentation,” Swedish Nuclear Power Inspectorate,
13 Stockholm, Sweden.
- 14 Virsek, S., T. Zagar, and M. W. Kozak, 2014, “Natural and Engineering Barriers – the Safety
15 Concept Basis for LILW Repository in Vrbinja, Krško,” 23rd International Conference
16 Nuclear Energy for New Europe, Portoroz, Slovenia.
- 17 Wakasugi, K., K. Ishiguro, T. Ebashi, H. Ueda, T. Koyama, H. Shiratsuchi, S. Yashio, and
18 H. Kawamura, 2012, “A methodology for scenario development based on understanding
19 of long-term evolution of geological disposal systems,” Journal of Nuclear Science and
20 Technology, Volume 49, No. 7, pp. 673–688.
- 21 WCH-520, 2013, “Performance Assessment for the Environmental Restoration Disposal Facility,
22 Hanford Site, Washington,” Rev. 1, Washington Closure Hanford, Richland, Washington.
- 23 WMP-22922, 2004, “Prototype Hanford Features, Events, and Processes (HFEP) Graphical User
24 Interface,” Rev. 0, Fluor Hanford, Inc., Richland, Washington.

25

26

RPP-ENV-58782, Rev. 0

- 1
- 2
- 3
- 4
- 5
- 6

This page intentionally left blank.

RPP-ENV-58782, Rev. 0

APPENDIX I**RESULTS OF FLOW-FIELDS DEVELOPED IN THE VADOSE ZONE FOR THE
PURPOSE OF UNCERTAINTY ANALYSIS**

RPP-ENV-58782, Rev. 0

1
2
3
4
5
6
7

This page intentionally left blank.

RPP-ENV-58782, Rev. 0

TABLE OF CONTENTS

APPENDIX I – RESULTS OF FLOW-FIELDS DEVELOPED IN THE VADOSE ZONE FOR THE PURPOSE OF UNCERTAINTY ANALYSIS	I-1
---	-----

LIST OF FIGURES

Figure I-1. Results for H1 Unit for Base Case Recharge Rates for Five Hydraulic Properties in Vadose Zone.	I-3
Figure I-2. Results for H2 Unit for Base Case Recharge Rates for Five Hydraulic Properties in Vadose Zone.	I-6
Figure I-3. Results for H3 Unit for Base Case Recharge Rates for Five Hydraulic Properties in Vadose Zone.	I-9

RPP-ENV-58782, Rev. 0

1
2
3
4
5
6
7

This page intentionally left blank.

RPP-ENV-58782, Rev. 0

APPENDIX I**RESULTS OF FLOW-FIELDS DEVELOPED IN THE VADOSE ZONE FOR THE PURPOSE OF UNCERTAINTY ANALYSIS**

The purpose of this appendix is to present information on the uncertainty range in vertical Darcy flux and volumetric moisture content in order to illustrate the range and magnitude of vertical pore water velocities over the full range of uncertainty in recharge rates. Development of vadose zone flow field and propagation of uncertainty is discussed in detail in Section 8.1.4.

The flow fields are abstracted from the three-dimensional Subsurface Transport Over Multiple Phases (STOMP)¹ modeling results as a way to efficiently evaluate the effect of uncertainty in the vadose zone flow using the GoldSim²-based system model. The flow fields are developed for five different vadose zone hydraulic properties to represent the range of vertical linear pore water velocities in the vadose zone under base case recharge conditions (Figures 8-14, 8-15, and 8-16). In order to derive the vertical pore water velocity for other recharge conditions, regression equations are developed that are used to scale the vertical Darcy flux and volumetric moisture content estimates for each of the five hydraulic properties using base case recharge rates. The regression equations for scaling vertical Darcy flux underneath 100-series tanks are presented in Table 8-10 and that for the 200-series tanks is presented in Table 8-11 for H1, H2, and H3 units. The scaling of the volumetric moisture content is simpler and presented in Table 8-12. Note that these scaling multipliers are dimensionless and are applied to values calculated under base recharge conditions, as abstracted from three-dimensional STOMP¹ model results for each of the five hydraulic properties.

The results are presented by taking the regression equations shown in Tables 8-10 and 8-12 (for 100-series tanks) and performing the calculations over the minimum and maximum recharge rates over the post-closure time period to illustrate the uncertainty range in vertical average linear pore water velocities. The results from 200-series tanks are not presented as they lead to similar uncertainty range as the 100-series tanks. Since the recharge rates are estimated for two time periods, an early post-closure time period (first 500 years while the surface cover is intact) and late post-closure time period (for the remaining time period with degraded surface cover), the uncertainties in recharge rates are different for these two time periods. As presented in Table 8-3, for the early post-closure time period, the minimum recharge rate within the WMA C area is 0.1 mm/yr and the maximum is 0.9 mm/yr with the base case recharge rate being 0.5 mm/yr. For the late post-closure time period, the minimum recharge rate is 0.5 mm/yr and the maximum is 5.2 mm/yr while the base case recharge rate is 3.5 mm/yr. The minimum and maximum recharge rates are applied in the regression equations to calculate the scaling of vertical Darcy flux and volumetric moisture content relative to those based on the base case recharge rates. From this, the vertical average linear pore water velocities are estimated at a given time by dividing the vertical Darcy flux with the volumetric moisture content value for each unit (H1, H2, and H3). Although the vertical Darcy flux and volumetric moisture content

¹ Subsurface Transport Over Multiple Phases (STOMP)[®] is copyrighted by Battelle Memorial Institute, 1996.

² GoldSim[®] simulation software is copyrighted by GoldSim Technology Group LLC of Issaquah, Washington (see <http://www.goldsim.com>).

RPP-ENV-58782, Rev. 0

for H2 and H3 are different, the scaling multipliers are the same as noted in Tables 8-10 and 8-12.

Results for each of the three units is presented below for the representative node within that unit to illustrate the uncertainty. For each unit, the time histories of vertical Darcy flux, volumetric moisture content, and vertical linear pore water velocity under base case recharge conditions are presented for each of the five hydraulic properties noted as 5th percentile, 25th percentile, 50th percentile, 75th percentile, and 95th percentile (see Section 8.1.4 for additional details). Next, the scaling multiplier calculated for vertical Darcy flux is presented based on the regression equations for the minimum and maximum recharge rate cases for each of the five hydraulic properties (percentile cases). After that, the resulting vertical linear pore water velocities are presented for each of the five hydraulic properties evaluated under minimum and maximum recharge rates. The scaling multipliers and resulting vertical velocity values do not change at late times and, therefore, the results are only presented up to 1,000 years following closure.

The variation in volumetric moisture content is not appreciable for the various recharge cases within the early post-closure time period and vary marginally after that; the scaling of volumetric moisture content is either 0.93 (for minimum recharge case) or 1.3 (for maximum recharge case) for the post-closure time period. These results are not presented separately.

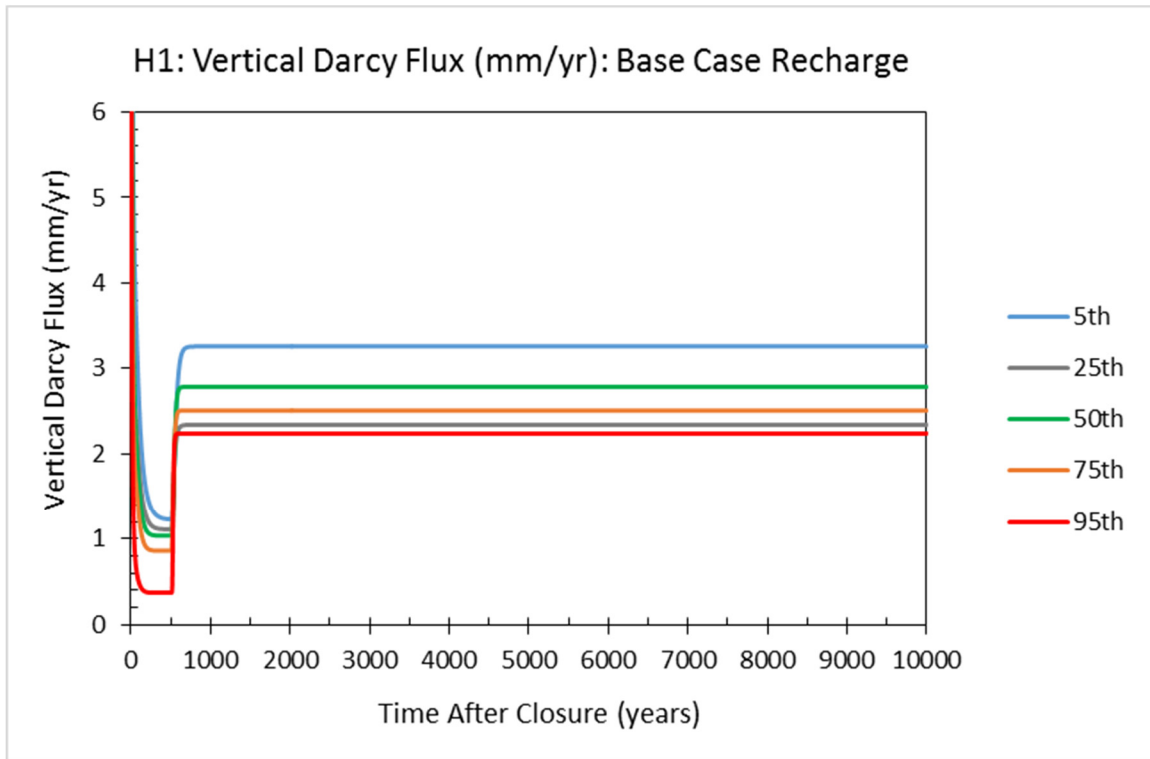
Results for H1 unit are presented in Figure I-1, while those for H2 and H3 units are presented in Figures I-2 and I-3. Figure I-1c shows the range in vertical linear pore water velocity for the H1 unit under base case recharge conditions. It represents the uncertainty range that could result from the choice of hydraulic properties alone. Figure I-1d shows the range in scaling multiplier for each of the five hydraulic properties over the minimum and maximum recharge rates while Figure 1e presents the corresponding range in vertical linear pore water velocities, which affects transport of contaminants via advection. The uncertainty range (spread) in the vertical linear pore water velocities is the largest for the 95th percentile hydraulic property (factor of 6.5) and minimum for the 25th percentile hydraulic property (factor of 2). For other hydraulic properties the range varies by factor of 3 to 3.3.

For H2 and H3 units the result are similar. The uncertainty range (spread) in the vertical linear pore water velocities is the largest for the 95th percentile hydraulic property (factor of 6.4) and minimum for the 25th percentile hydraulic property (factor of 2.5). For other hydraulic properties the range varies by factor of 3 to 4.1.

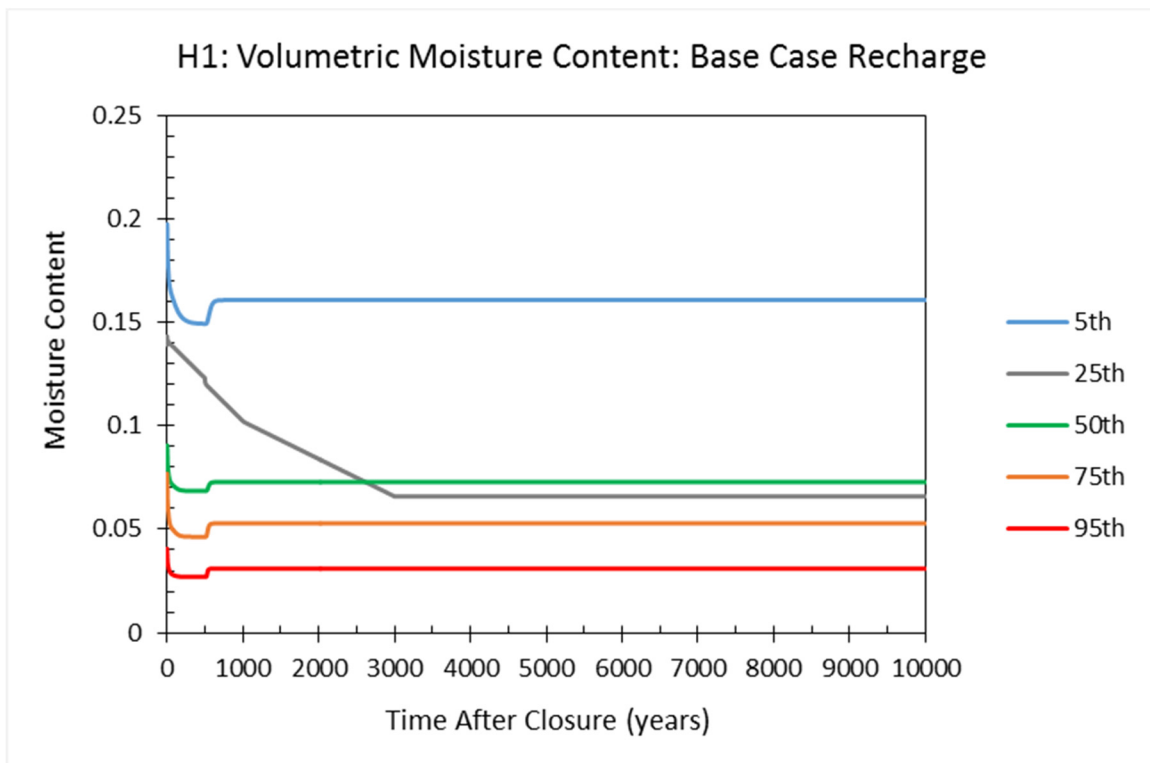
These results indicate that for realizations where 95th percentile hydraulic property is selected during uncertainty analysis, greater variance in travel times can be expected compared to other hydraulic properties (under similar recharge rate range).

RPP-ENV-58782, Rev. 0

Figure I-1. Results for H1 Unit for Base Case Recharge Rates for Five Hydraulic Properties in Vadose Zone. (1 of 3 sheets)



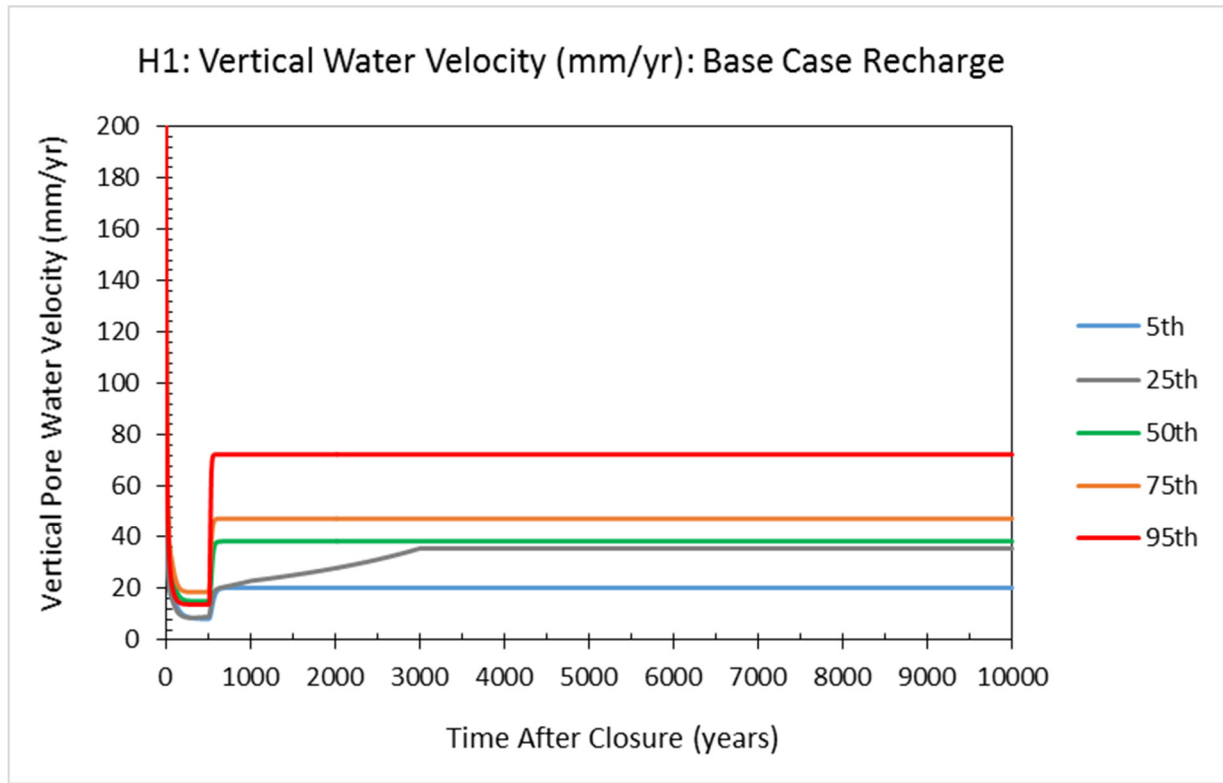
(a)



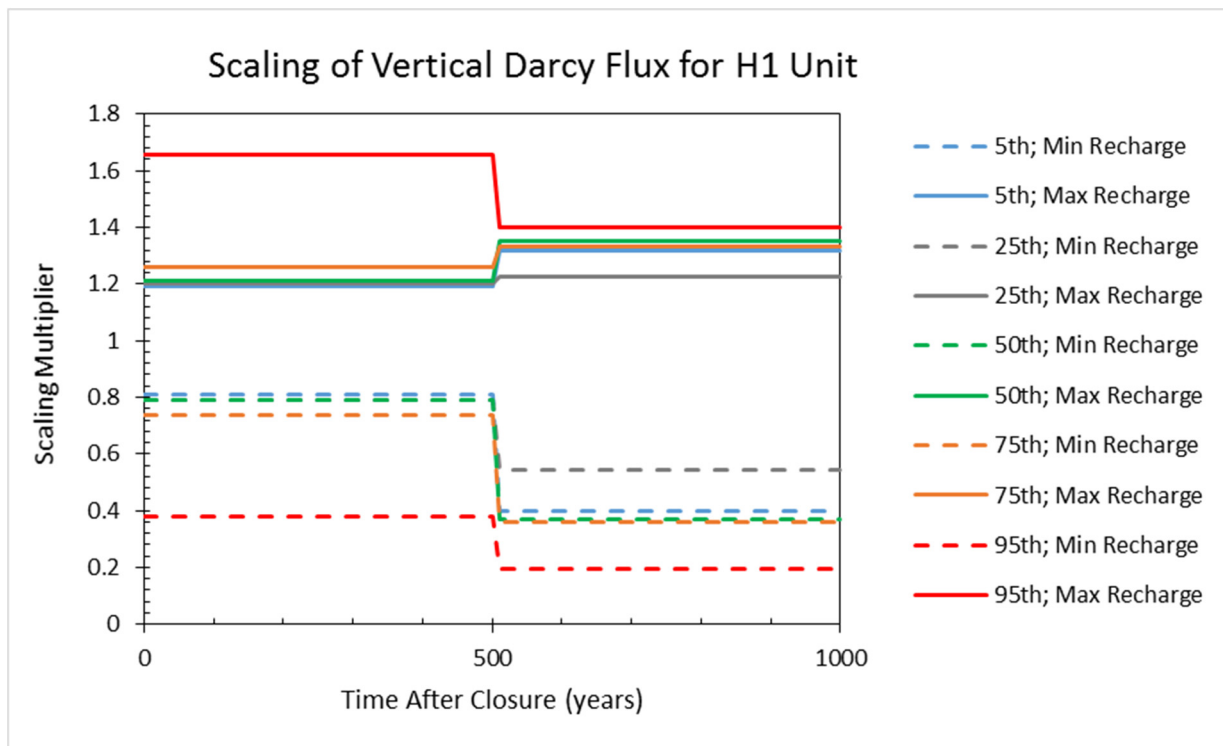
(b)

RPP-ENV-58782, Rev. 0

Figure I-1. Results for H1 Unit for Base Case Recharge Rates for Five Hydraulic Properties in Vadose Zone. (2 of 3 sheets)



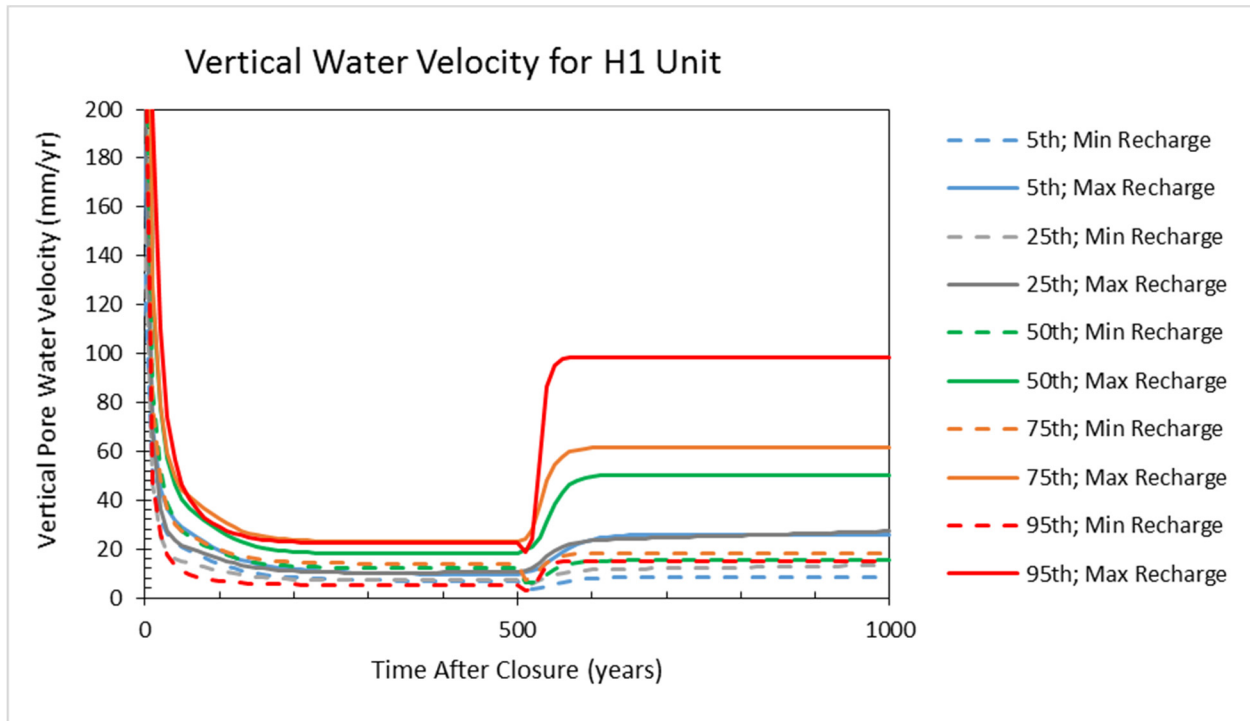
(c)



(d)

RPP-ENV-58782, Rev. 0

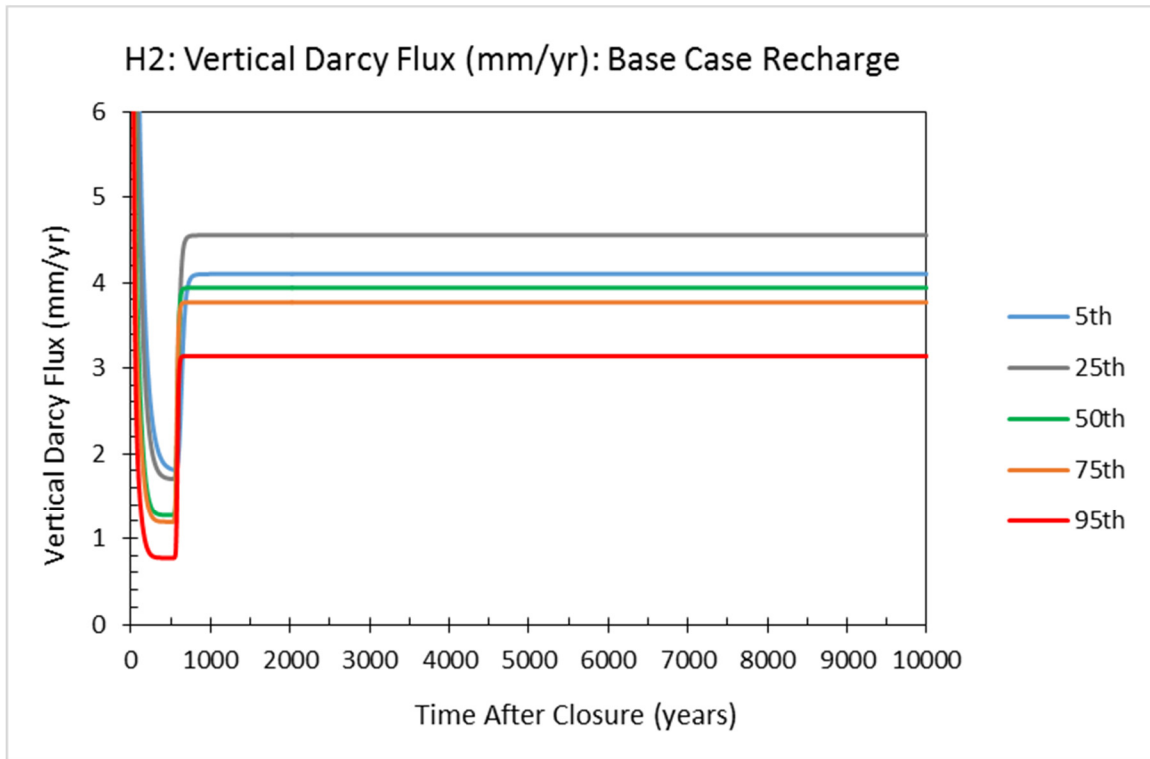
Figure I-1. Results for H1 Unit for Base Case Recharge Rates for Five Hydraulic Properties in Vadose Zone. (3 of 3 sheets)



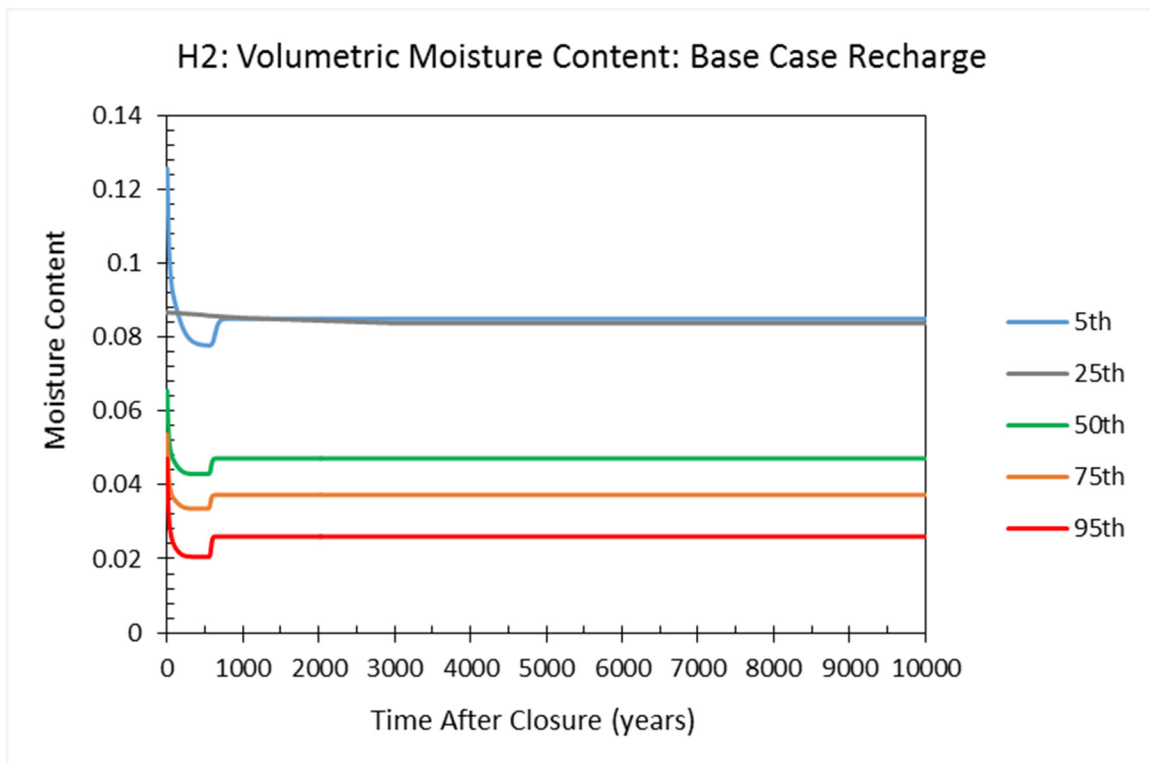
(e)

RPP-ENV-58782, Rev. 0

Figure I-2. Results for H2 Unit for Base Case Recharge Rates for Five Hydraulic Properties in Vadose Zone. (1 of 3 sheets)



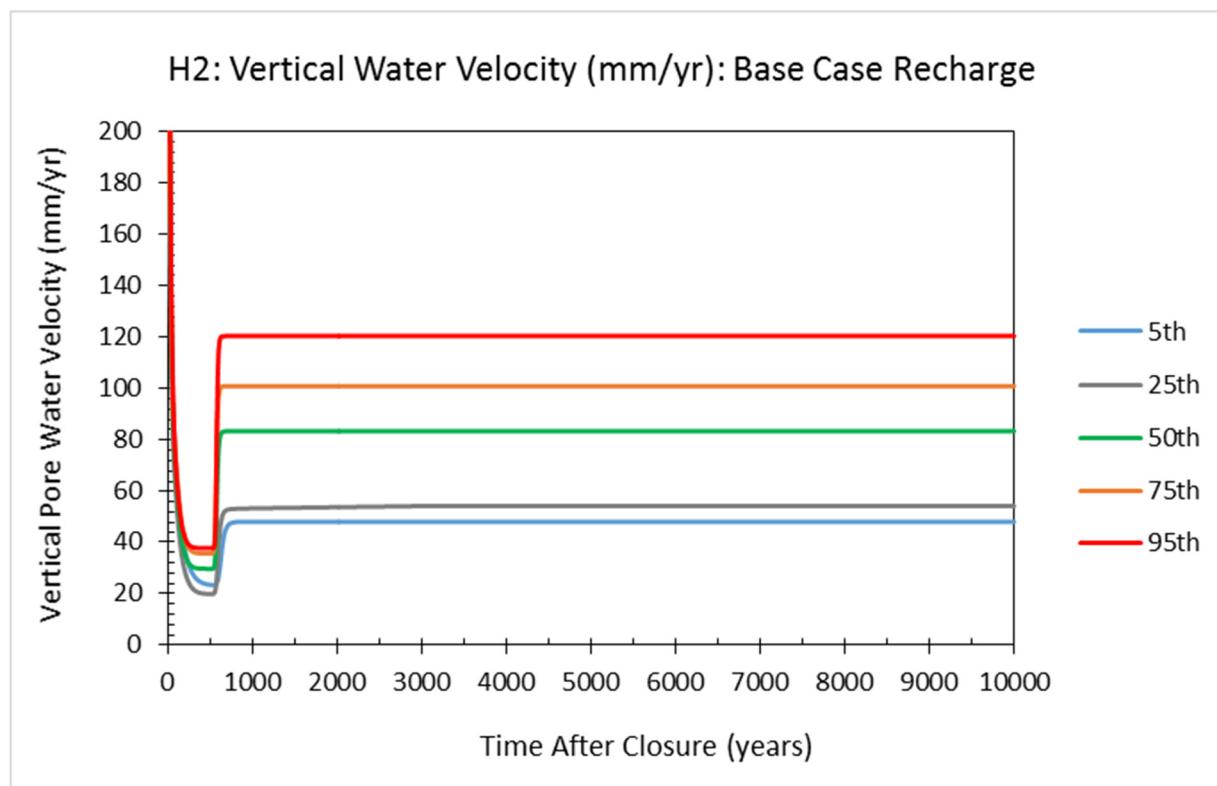
(a)



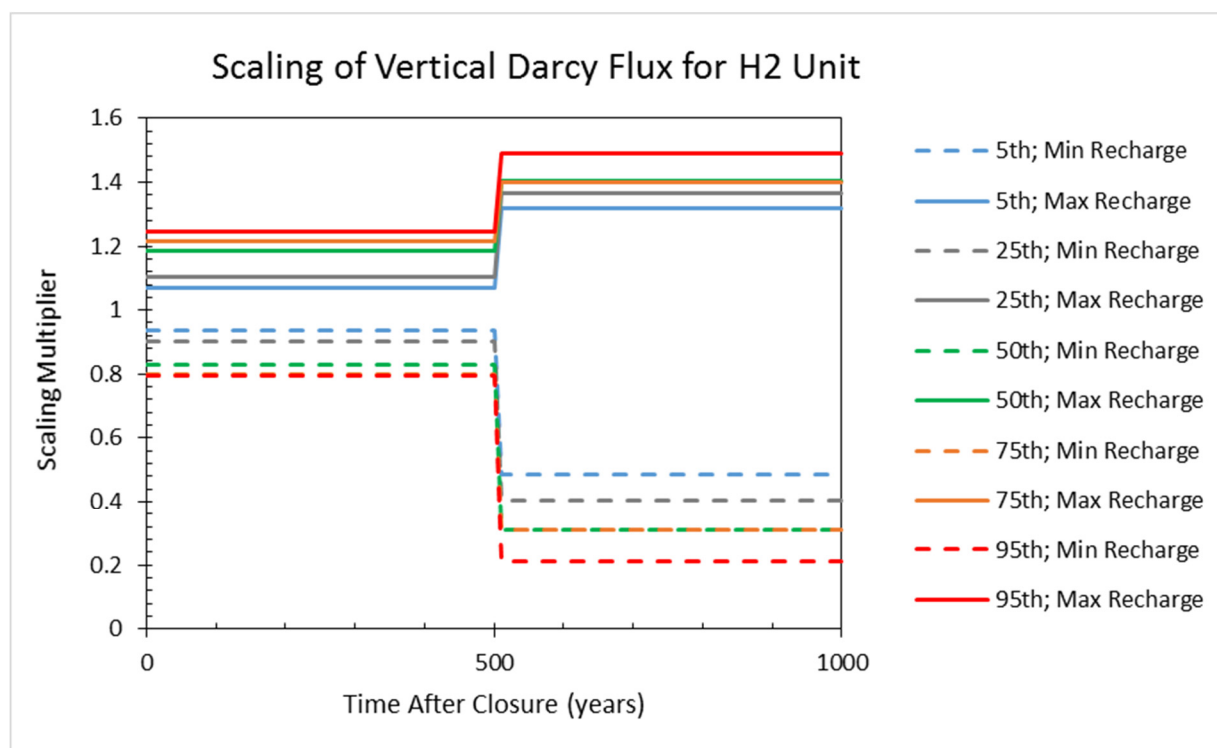
(b)

RPP-ENV-58782, Rev. 0

Figure I-2. Results for H2 Unit for Base Case Recharge Rates for Five Hydraulic Properties in Vadose Zone. (2 of 3 sheets)



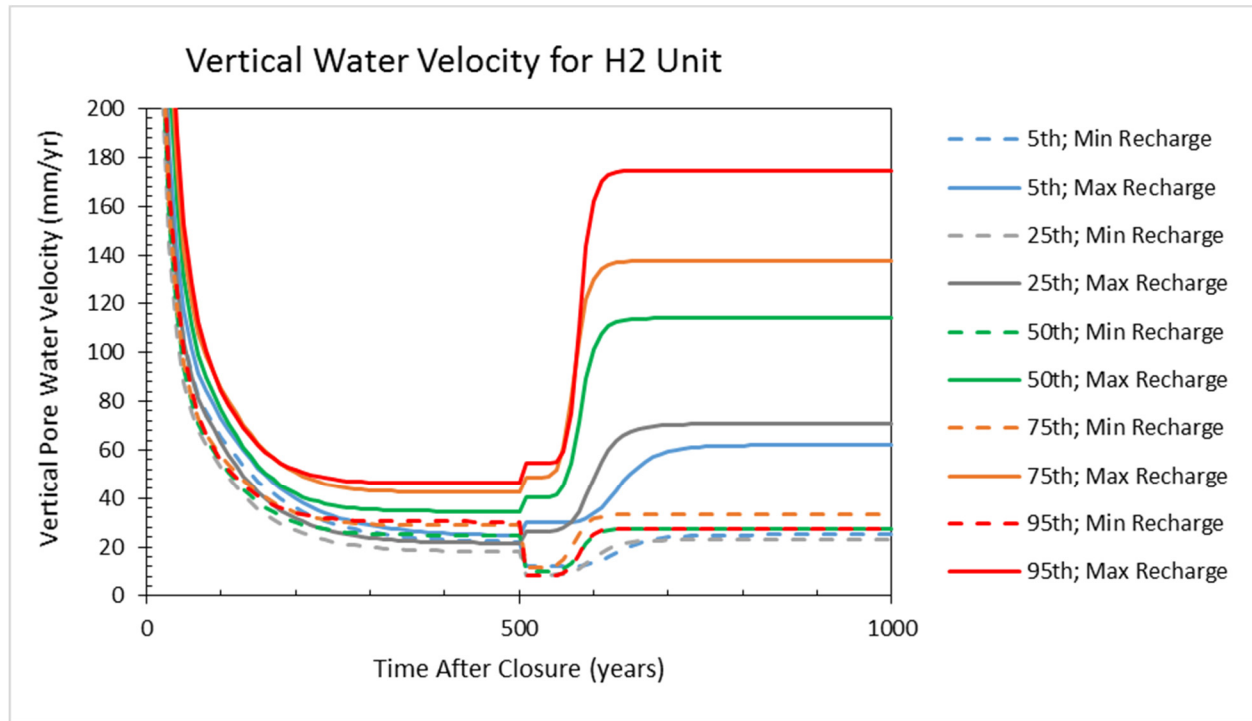
(c)



(d)

RPP-ENV-58782, Rev. 0

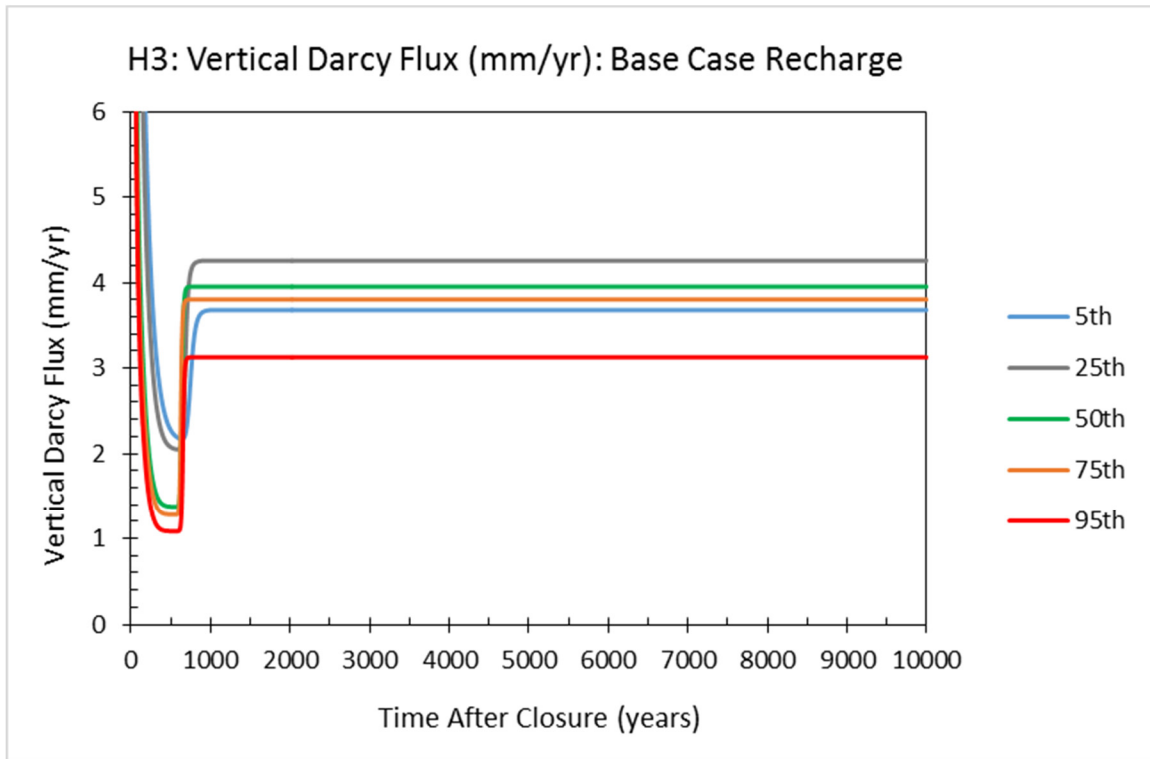
Figure I-2. Results for H2 Unit for Base Case Recharge Rates for Five Hydraulic Properties in Vadose Zone. (3 of 3 sheets)



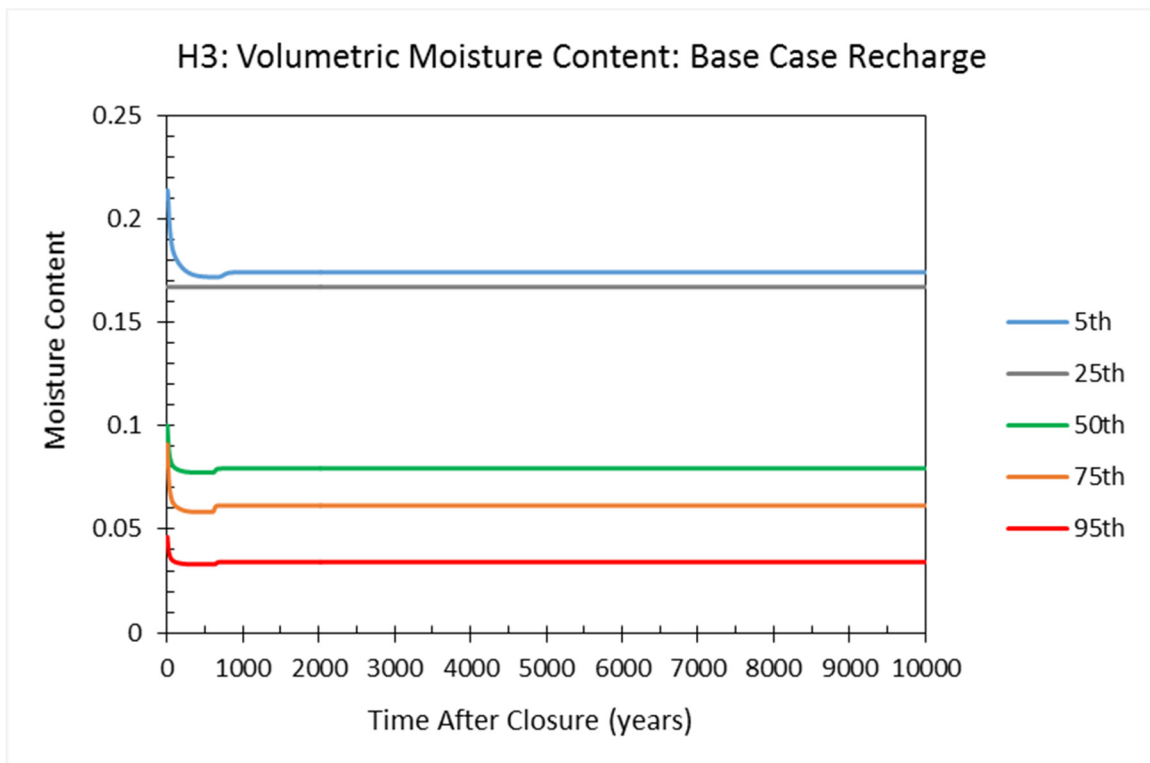
(e)

RPP-ENV-58782, Rev. 0

Figure I-3. Results for H3 Unit for Base Case Recharge Rates for Five Hydraulic Properties in Vadose Zone. (1 of 3 sheets)



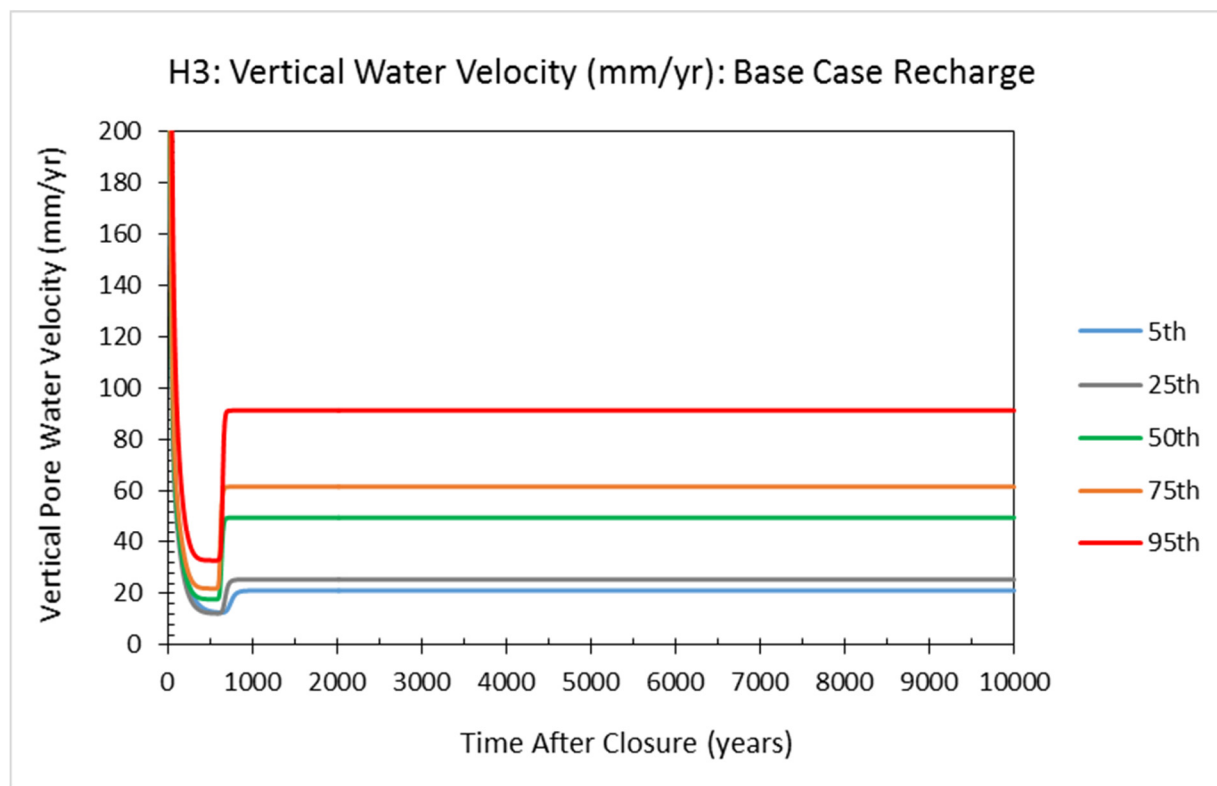
(a)



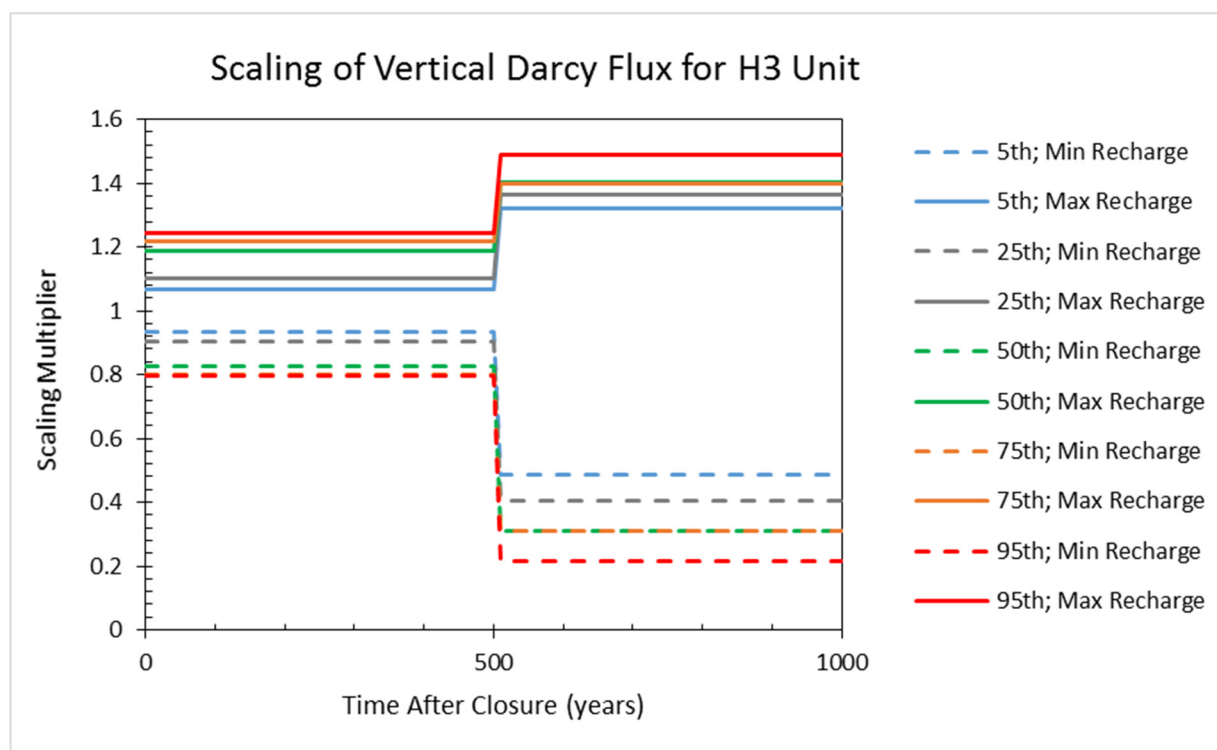
(b)

RPP-ENV-58782, Rev. 0

Figure I-3. Results for H3 Unit for Base Case Recharge Rates for Five Hydraulic Properties in Vadose Zone. (2 of 3 sheets)



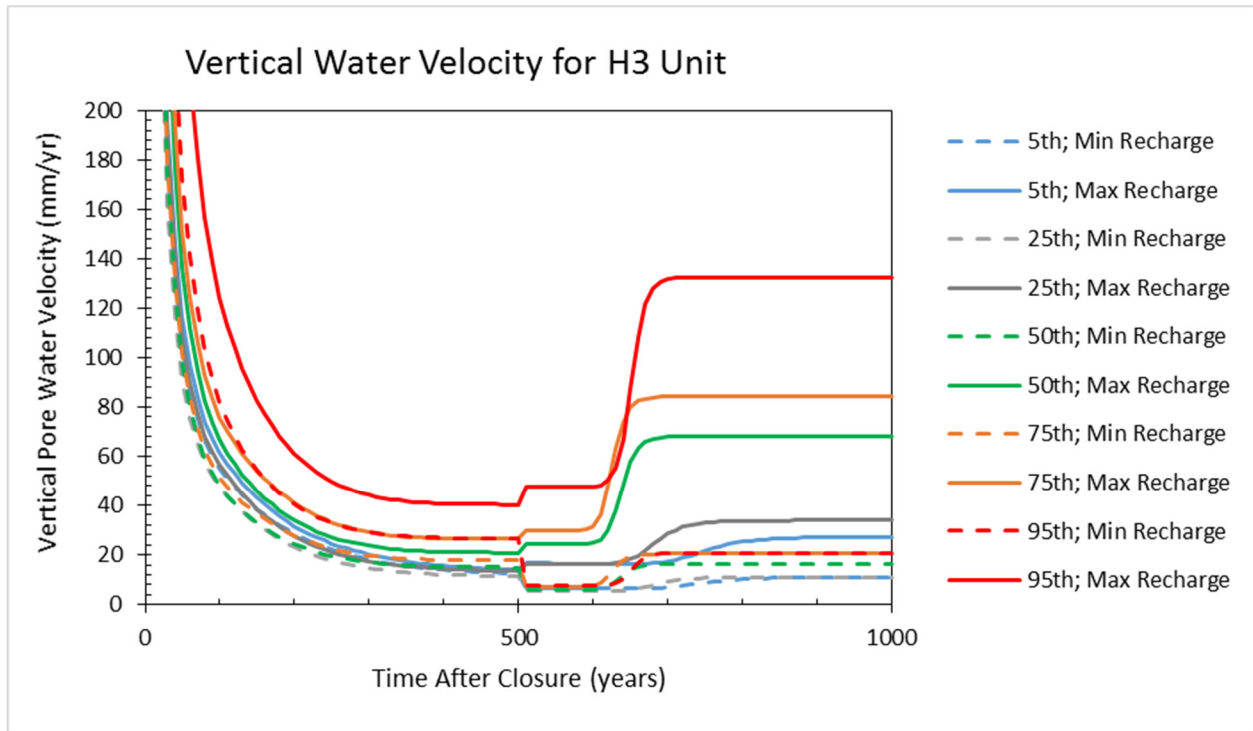
(c)



(d)

RPP-ENV-58782, Rev. 0

Figure I-3. Results for H3 Unit for Base Case Recharge Rates for Five Hydraulic Properties in Vadose Zone. (3 of 3 sheets)



(e)

RPP-ENV-58782, Rev. 0

1
2
3
4
5
6

This page intentionally left blank.